

SYNTHESIS OF ORGANIC BUILDING BLOCKS AND SYNTHETIC
STRATEGIES TOWARD ALEUTIANAMINE

Thesis by

Zachary Patrick Sercel

In Partial Fulfillment of the Requirements

for the Degree of

Doctor of Philosophy

CALIFORNIA INSTITUTE OF TECHNOLOGY

Pasadena, California

2023

(Defended May 24, 2023)

© 2023

Zachary Patrick Sercel
ORCID: 0000-0001-7977-8509

All Rights Reserved

To Betty Leifer, my grandmother

ACKNOWLEDGEMENTS

I owe a great deal of gratitude to Professor Brian Stoltz. I first met Brian about 12 years ago when I was a middle schooler seeking to learn more about chemistry. Brian was kind enough to meet with me in his office and give a brief introduction to natural product synthesis. Since then, I have been lucky to have Brian as a strong supporter of my education and am very fortunate to have been able to conduct my Ph.D. studies in his group. In addition to being an incredibly patient, supportive, and personable mentor, Brian has been extremely generous with the creative and scientific freedom he has given me, including the opportunity to spend 5 months conducting research abroad in a different field. The environment Brian has created in his group is a true realization of his vision of “the intellectual adventure of a lifetime.”

Professor Maxwell Robb has been an excellent committee chair. I really enjoyed my rotation in the Robb group during my first term of graduate school. Thank you also to Professors Sarah Reisman and Harry Gray for being wonderful committee members. The scientific and career advice that Max, Harry, and Sarah have provided has been very helpful throughout my time at Caltech. I feel fortunate to have had the opportunity to interact with such brilliant chemists. I have enjoyed hearing Harry’s stories and insight, and Sarah’s astute observations and helpful suggestions, especially during our joint group meetings, have been a huge asset.

I would also like to thank Professor Matthias Selke, who taught my sophomore organic chemistry course at Cal State LA and supervised my undergraduate thesis research. Prof. Selke’s exemplary teaching and mentorship contributed to my decision to continue studying organic chemistry. I often reflect on his memorable stories and advice.

Additionally, Dr. Richard Maddox, the late director of the Early Entrance Program at Cal State LA, had a profound impact on my life and my education. Rich's unique program enabled me to pursue my passion for chemistry 5 years earlier than I would otherwise have been able to.

I have had the privilege of collaborating with quite a few talented people on an assortment of projects in the Stoltz group. First, I would like to thank Dr. Alexander Sun. Alex mentored me for a summer when I was an undergraduate, taking the time to teach me synthetic lab technique from the ground up, which was no small investment. I also had the opportunity to work with Alex on the allylic alkylation of diazaheterocycles when I started in the group as a graduate student.

Dr. Gerit Pototschnig also served as a mentor to me as an undergraduate, specifically during my first foray into total synthesis. Gerit was a fantastic mentor and hoodmate, and her advice helped me to refine my synthetic and analytical technique. I fondly remember Gerit walking me through the (at the time, uniquely terrifying) large-scale preparation and distillation of allyl cyanofornate.

Samir Rezgui joined the aleutianamine project at an early stage. Seeing Samir tackle challenges in synthesis and reaction development has been truly inspiring. It is rare to find someone who accepts scientific challenges and curveballs with such grace, determination, and humor. I hope to be able to incorporate some of Samir's unique attitude and approach into my own science in the future. In addition to being a great project partner, Samir has been a wonderful friend and a positive influence in my life.

Hao Yu joined the synthesis the following year and quickly made a profound impact on the project through his tireless work and brilliant, creative ideas. I have really enjoyed

working with Hao and our chemistry discussions, from which I have learned a great deal. Hao is also extremely generous with the time he spends sharing his vast knowledge with the group by leading denksport exercises and informal problem sessions.

We were recently lucky to be joined on a spinoff project by Jonathan Farhi. Mentoring Jonathan in the lab has been a really enjoyable experience, and I am happy that of all the projects he could have worked on, he chose this one.

In addition, I have had the chance to collaborate with Adrian Samkian, Alex Cusumano, Youngkyu Park, Dr. Trevor Lohrey, Farbod Moghadam, and Elliot Hicks on various other projects. I am grateful to have worked with and learned from each of these project partners and am looking forward to seeing the great things they will do in the future.

I would like to thank Alex Cusumano, with whom I worked in the Spalding basement during the COVID-19 pandemic. Alex has taught me a lot about both chemistry and teamwork, in addition to being a true friend.

I have also been privileged to work with some awesome bay-mates in bay 2. Those whom I have not already mentioned include Jay Barbor, Melinda Chan, Dr. Elizabeth Goldstein, Ben Gross, Dr. Carina Jette, Dr. Sebastian Lackner, Dr. Fa Ngamnithiporn, Dr. Beau Pritchett, and Kim Sharp. It is highly motivating to be able to have conversations with such interesting and bright people every day in the lab.

In addition to Alex, I thank Alexia Kim and Tyler “TC” Casselman, the other members of our class of four. I have enjoyed getting to know each of them and chatting about the amazing chemistry that they have done.

It has been a pleasure to interact with Dr. Scott Virgil, the director of the catalysis center. The instruments expertly maintained by Scott have enabled a large portion of the

research described in this thesis. Furthermore, Scott has been very generous with his time, making himself available to chat at length about chemistry and help with challenging separations, and has provided invaluable suggestions and advice throughout the course of my graduate studies.

In the summer of 2019, I had the chance to serve as a mentor to Liz Park, an undergraduate WAVE fellow. I am grateful to Liz for the opportunity to mentor her, which I really enjoyed. She is a quick learner and demonstrated herself to be a brilliant and highly adaptive researcher.

By my count, during my time in the Stoltz lab, I have overlapped with about 100 grad students, postdocs, visiting scholars, and undergraduate researchers. Each of these people has, in some way, contributed to my professional and personal development, and there is no way that I can adequately thank all of them in these pages for the enormous impact that they have had on me. I would like to thank a few additional people in particular though: Besides my baymates, Kevin Gonzalez, Elliot Hicks, Dr. Veronica Hubble, Dr. Trevor Lohrey, Farbod Moghadam, Dr. Brendan O'Boyle, "Teacher Adrian" Samkian, and Christian Strong, among others, have been really fun to chat with and bounce ideas off of. Their suggestions have been extremely helpful, and I've enjoyed getting to know many of them outside of the lab as well.

Professor Mark Davis and the Davis research group, in addition to collaborating with us on the zeolite project, allowed me to work in their lab space during the COVID-19 pandemic when most of the lab was on a shift schedule. The generosity of the Davis group helped me get back on track after the considerable disruption caused by the pandemic.

Dr. Dave VanderVelde, Dr. Mona Shagholi, and Dr. Mike Takase maintain excellent NMR, mass spectrometry, and x-ray crystallography facilities, respectively. These facilities have been essential to this research, and advice from Dave, in particular, has greatly contributed to my practical NMR knowledge.

Professor Zeev Gross was very kind to invite me to conduct a research internship in his lab at the Technion during my fourth year. It was a great experience to live in Israel and to conduct research in a new subfield. Thanks are also due to the members of the Gross research group, especially Dr. Atif Mahammed, Marcelo Fernandez de la Mora, Arik Raslin, and Dr. Irina Saltsman, with whom I had the chance to collaborate.

Outside of the lab, Chabad at Caltech has been like a second home. I owe many thanks to the Stolik family for being so welcoming and generous. I could not imagine grad school without the friends I have met at Chabad, including Sam Davidson, Dr. Simon Mahler, Sophie Miller, Oren Mizrahi, Danielle Resheff, Will Rosencrans, Dr. Lee Rosenthal, Helen Wexler, and Michael Wollman.

The roommates with whom I have lived in various apartments during grad school have also been an invaluable source of outside perspective and insight. Thank you, Nicholas Duncan, Aidan Fenwick, and Roey Lazarovits. I have known Nicholas Duncan, in particular, for almost 10 years. His friendship has provided abundant support to me when I have needed it.

None of this journey would have been possible without the encouragement to follow my passions and the sense of scientific curiosity and wonder instilled in me from a young age by my parents, Stephanie and Pete. I am really lucky to have grown up in an environment where “do what you love” was a mantra and where I had unconditional

support for my education and career choices. I am glad that I chose to go to graduate school near my family, which has enabled me to visit home often to see my parents and my siblings, Gregory, Erin, and Jonathan. I am always proud to see the great things constantly being accomplished by my siblings. Each of them teaches me something new almost every time that I visit.

The final leg of graduate school has been so much easier thanks to the abundant love and support from my partner, Eva Zanditenas. I thank Eva for braving the distance of almost 7,500 miles so that I can do chemistry, for her unconditional willingness to lend an ear, and for helping me remain focused on what's truly important.

I gratefully acknowledge the National Science Foundation and Rose Hills Foundation for funding my Ph.D. studies.

ABSTRACT

Research in the Stoltz group is primarily focused on the total synthesis of complex, bioactive natural products and on the development of reaction methodologies to enable these synthetic endeavors. The majority of the content of this thesis focuses on permutations of this central goal.

Chapter 1 describes the development of the palladium-catalyzed decarboxylative asymmetric allylic alkylation of medicinally relevant 5- and 7-membered diazaheterocycles to afford quaternary and *gem*-disubstituted derivatives. This methodology provides a new tactic to incorporate Csp³ structural complexity into future lead compounds containing diazepane and imidazolidine moieties.

Chapter 2 discloses efforts toward the total synthesis of the cytotoxic pyrroloiminoquinone marine alkaloid aleutianamine. Key to the synthetic strategy are rapid assembly of the tricyclic pyrroloiminoquinone core in the arene oxidation state, convergent fragment coupling with a readily accessible aminothiophene derivative, and a powerful new dearomative spirocyclization. This research is ongoing.

Chapter 3 discusses preliminary attempts to improve the synthetic accessibility of minimally substituted corroles, which were conducted during a research internship in the laboratory of Prof. Zeev Gross at the Technion. During the course of this research, the first example of a β -unsubstituted free base monoazaporphyrin was isolated, and its cobalt complex was characterized by x-ray crystallography.

Finally, Appendix 8 presents a series of cationic and radical-mediated fragmentations of a derivative of (+)-3-Carene, a chiral pool material. These experiments led to the observation and mechanistic study of an unexpected rearrangement.

PUBLISHED CONTENT AND CONTRIBUTIONS

1. Sercel, Z. P.; Sun, A. W.; Stoltz, B. M. Palladium-Catalyzed Decarboxylative Asymmetric Allylic Alkylation of 1,4-diazepan-5-ones. *Org. Lett.* **2019**, *21*, 9158–9161. DOI: 10.1021/acs.orglett.9b03530

Z. P. S. participated in project design, experimental work, data acquisition and analysis, and manuscript preparation.

2. Sercel, Z. P.; Sun, A. W.; Stoltz, B. M. Synthesis of Enantioenriched *gem*-Disubstituted 4-Imidazolidinones by Palladium-Catalyzed Decarboxylative Asymmetric Allylic Alkylation. *Org. Lett.* **2021**, *23*, 6348–6351. DOI: 10.1021/acs.orglett.1c02134

Z. P. S. participated in project design, experimental work, data acquisition and analysis, and manuscript preparation.

3. Samkian, A. E.; Sercel, Z. P.; Virgil, S. C.; Stoltz, B. M. Some Unusual Transformations of a Highly Reactive α -Bromocaranone. *Tetrahedron Lett.* **2022**, *89*, 153496. DOI: 10.1016/j.tetlet.2021.153496

Z. P. S. participated in project design, experimental work, data acquisition and analysis, and manuscript preparation.

4. Moghadam, F. A.; Hicks, E. F.; Sercel, Z. P.; Cusumano, A. Q.; Bartberger, M. D.; Stoltz, B. M. Ir-Catalyzed Asymmetric Allylic Alkylation of Dialkyl Malonates Enabling the Construction of Enantioenriched All-Carbon Quaternary Centers. *J. Am. Chem. Soc.* **2022**, *144*, 7983–7987. DOI: 10.1021/jacs.2c02960

Z. P. S. participated in experimental work and data acquisition and analysis.

5. Li, C.; Lohrey, T. D.; Nguyen, P.; Min, Z.; Tang, Y.; Ge, C.; Sercel, Z. P.; McLeod, E.; Stoltz, B. M.; Su, J. Part-per-trillion trace selective gas detection using frequency locked whispering gallery mode microtoroids. *ACS Appl. Mater. Interfaces* **2022**, *14*, 42430–42440. DOI: 10.1021/acsami.2c11494

Z. P. S. participated in experimental work (synthesis).

TABLE OF CONTENTS

Dedication.....	iii
Acknowledgements.....	iv
Abstract	x
Published Content and Contributions.....	xi
Table of Contents.....	xiii
List of Figures.....	xvii
List of Schemes	xxvii
List of Tables.....	xxxi
List of Abbreviations	xxxiii
CHAPTER 1	1
<i>Palladium-Catalyzed Decarboxylative Asymmetric Allylic Alkylation of 5- and 7-Membered Diazaheterocycles</i>	
1.1	Introduction 1
1.2	Palladium-Catalyzed Decarboxylative Asymmetric Allylic Alkylation of 1,4-Diazepan-5-ones 5
1.3	Palladium-Catalyzed Decarboxylative Asymmetric Allylic Alkylation of 4-Imidazolidinones 11
1.4	Conclusion 23
1.5	Experimental Section 23
1.5.1	Materials and Methods 23
1.5.2	Experimental Procedures 25
1.5.2.1	General Procedure for Allylic Alkylation of Diazepanones 25
1.5.2.2	Synthesis of Diazepanone Allylic Alkylation Substrates 44
1.5.2.3	Derivatization of Diazepane Allylic Alkylation Products..... 62
1.5.2.4	General Procedure for Allylic Alkylation of Imidazolidinones..... 66
1.5.2.5	Synthesis of Imidazolidinone Allylic Alkylation Substrates..... 85
1.5.2.6	Derivatization of Imidazolidinone Allylic Alkylation Products.. 101
1.5.3	Determination of Enantiomeric Excess 105
1.6	References and Notes 109

APPENDIX 1 **116**
Spectra Relevant to Chapter 1

APPENDIX 2 **242**
Attempts to Effect the Allylic Alkylation of Additional Diazepanone Substrates

A2.1	Introduction	242
A2.2	Attempts to Access a 1,4-Diazepan-2-one Allylic Alkylation Substrate	243
A2.3	Attempts to Access Benzodiazepane-Derived Allylic Alkylation Substrates ..	244
A2.4	Conclusion	246
A2.5	Experimental Section	246
A2.5.1	Materials and Methods	246
A2.5.2	Experimental Procedures	247
A2.6	References and Notes	252

CHAPTER 2 **254**
Progress Toward the Total Synthesis of Aleutianamine

2.1	Introduction	254
2.2	Initial Retrosynthetic Analysis	257
2.3	Strategies Involving Enolate Arylation	258
2.4	2 nd -Generation Retrosynthesis	262
2.5	Preparation of a Versatile Tricyclic Aniline	263
2.6	Strategies for Bridged Bicycle Formation	270
2.7	3 rd -Generation Retrosynthesis.....	280
2.8	Pursuit of a Dearomative Cyclization Approach.....	281
2.9	Conclusion	295
2.10	Experimental Section	295
2.10.1	Materials and Methods	295
2.10.2	Experimental Procedures	297
2.11	References and Notes	349

APPENDIX 3 **360**
Synthetic Summary for Chapter 2

APPENDIX 4 **363**
Spectra Relevant to Chapter 2

APPENDIX 5 **447**
Additional Strategies and Tactics Toward the Total Synthesis of Aleutianamine

A5.1	Introduction	447
A5.2	Bridgehead Sulfide Installation: Model Studies	447
A5.3	Early Strategies Toward a Tricyclic Aminoindole	450
A5.4	Additional Efforts Toward Key Tetracyclic Quinolone	453
A5.5	Preliminary Evaluation of a Wacker Oxidation of Internal α,β -Unsaturated Carbonyl Compounds	457
A5.6	Alkenyl Bromide Installation Via a Functional Handle	460
A5.7	Spirocycle-First Approach to δ -Oxidized Thioimidate	462
A5.8	Experimental Section	464
A5.8.1	Materials and Methods	464
A5.8.2	Experimental Procedures	465
A5.9	References and Notes	480

CHAPTER 3 **484**
Synthetic Strategies Toward Minimally Substituted Corroles and Azaporphyrins

3.1	Introduction	484
3.2	Attempts to Improve Bilane Synthesis.....	488
3.3	Unexpected Synthesis of a Monoazaporphyrin	492
3.4	Conclusion	495
3.5	Experimental Section	496
3.5.1	Materials and Methods	496
3.5.2	Experimental Procedures	497
3.6	References and Notes	501

APPENDIX 6 **506**
Spectra Relevant to Chapter 3

APPENDIX 7 **509**
X-Ray Crystallography Reports Relevant to Chapter 3

A7.1	General Experimental Information	510
A7.2	X-Ray Crystal Structure Analysis of Cobalt Azaporphyrin 306-Co	510

APPENDIX 8 **524**
Some Unusual Transformations of a Highly Reactive α -Bromocaranone

A8.1	Introduction	524
A8.2	Synthesis and Fragmentations of a Bromocaranone	525
A8.3	Conclusion	530
A8.4	Experimental Section	530
A8.4.1	Materials and Methods	530
A8.4.2	Experimental Procedures	532
A8.5	References and Notes	544

APPENDIX 9 **547**
Notebook Cross-Reference for New Compounds

Index.....	553
About the Author	557

LIST OF FIGURES

CHAPTER 1*Palladium-Catalyzed Decarboxylative Asymmetric Allylic Alkylation of 5- and 7-Membered Diazaheterocycles*

Figure 1.1.2.	Incorporation of a <i>gem</i> -disubstituted heterocycle into linezolid	3
Figure 1.2.1.	Representative pharmaceuticals containing a diazepane-derived ring system	5
Figure 1.3.1.	Representative pharmaceuticals bearing a 4-imidazolidinone moiety	11

APPENDIX 1*Spectra Relevant to Chapter 1*

Figure A1.1.	¹ H NMR (400 MHz, CDCl ₃) of compound 20a	117
Figure A1.2.	Infrared spectrum (Thin Film, NaCl) of compound 20a	118
Figure A1.3.	¹³ C NMR (100 MHz, CDCl ₃) of compound 20a	118
Figure A1.4.	¹ H NMR (400 MHz, CDCl ₃) of compound 20b	119
Figure A1.5.	Infrared spectrum (Thin Film, NaCl) of compound 20b	120
Figure A1.6.	¹³ C NMR (100 MHz, CDCl ₃) of compound 20b	120
Figure A1.7.	¹ H NMR (400 MHz, CDCl ₃) of compound 20c	121
Figure A1.8.	Infrared spectrum (Thin Film, NaCl) of compound 20c	122
Figure A1.9.	¹³ C NMR (100 MHz, CDCl ₃) of compound 20c	122
Figure A1.10.	¹ H NMR (400 MHz, CDCl ₃) of compound 20d	123
Figure A1.11.	Infrared spectrum (Thin Film, NaCl) of compound 20d	124
Figure A1.12.	¹³ C NMR (100 MHz, CDCl ₃) of compound 20d	124
Figure A1.13.	¹ H NMR (400 MHz, CDCl ₃) of compound 20e	125
Figure A1.14.	Infrared spectrum (Thin Film, NaCl) of compound 20e	126
Figure A1.15.	¹³ C NMR (100 MHz, CDCl ₃) of compound 20e	126
Figure A1.16.	¹ H NMR (400 MHz, CDCl ₃) of compound 20f	127
Figure A1.17.	Infrared spectrum (Thin Film, NaCl) of compound 20f	128
Figure A1.18.	¹³ C NMR (100 MHz, CDCl ₃) of compound 20f	128
Figure A1.19.	¹ H NMR (400 MHz, CDCl ₃) of compound 20g	129
Figure A1.20.	Infrared spectrum (Thin Film, NaCl) of compound 20g	130
Figure A1.21.	¹³ C NMR (100 MHz, CDCl ₃) of compound 20g	130
Figure A1.22.	¹ H NMR (400 MHz, CDCl ₃) of compound 20h	131

Figure A1.23. Infrared spectrum (Thin Film, NaCl) of compound 20h	132
Figure A1.24. ¹³ C NMR (100 MHz, CDCl ₃) of compound 20h	132
Figure A1.25. ¹ H NMR (400 MHz, CDCl ₃) of compound 20i	133
Figure A1.26. Infrared spectrum (Thin Film, NaCl) of compound 20i	134
Figure A1.27. ¹³ C NMR (100 MHz, CDCl ₃) of compound 20i	134
Figure A1.28. ¹ H NMR (400 MHz, CDCl ₃) of compound 20j	135
Figure A1.29. Infrared spectrum (Thin Film, NaCl) of compound 20j	136
Figure A1.30. ¹³ C NMR (100 MHz, CDCl ₃) of compound 20j	136
Figure A1.31. ¹ H NMR (400 MHz, CDCl ₃) of compound 20k	137
Figure A1.32. Infrared spectrum (Thin Film, NaCl) of compound 20k	138
Figure A1.33. ¹³ C NMR (100 MHz, CDCl ₃) of compound 20k	138
Figure A1.34. ¹ H NMR (400 MHz, CDCl ₃) of compound 20l	139
Figure A1.35. Infrared spectrum (Thin Film, NaCl) of compound 20l	140
Figure A1.36. ¹³ C NMR (100 MHz, CDCl ₃) of compound 20l	140
Figure A1.37. ¹ H NMR (400 MHz, CDCl ₃) of compound 55	141
Figure A1.38. Infrared spectrum (Thin Film, NaCl) of compound 55	142
Figure A1.39. ¹³ C NMR (100 MHz, CDCl ₃) of compound 55	142
Figure A1.40. ¹ H NMR (400 MHz, CDCl ₃) of compound 56	143
Figure A1.41. Infrared spectrum (Thin Film, NaCl) of compound 56	144
Figure A1.42. ¹³ C NMR (100 MHz, CDCl ₃) of compound 56	144
Figure A1.43. ¹ H NMR (400 MHz, CDCl ₃) of compound 57	145
Figure A1.44. Infrared spectrum (Thin Film, NaCl) of compound 57	146
Figure A1.45. ¹³ C NMR (100 MHz, CDCl ₃) of compound 57	146
Figure A1.46. ¹ H NMR (500 MHz, CDCl ₃) of compound 18a	147
Figure A1.47. Infrared spectrum (Thin Film, NaCl) of compound 18a	148
Figure A1.48. ¹³ C NMR (125 MHz, CDCl ₃) of compound 18a	148
Figure A1.49. ¹ H NMR (400 MHz, CDCl ₃) of compound 18b	149
Figure A1.50. Infrared spectrum (Thin Film, NaCl) of compound 18b	150
Figure A1.51. ¹³ C NMR (100 MHz, CDCl ₃) of compound 18b	150
Figure A1.52. ¹ H NMR (400 MHz, CDCl ₃) of compound 18c	151
Figure A1.53. Infrared spectrum (Thin Film, NaCl) of compound 18c	152
Figure A1.54. ¹³ C NMR (100 MHz, CDCl ₃) of compound 18c	152
Figure A1.55. ¹ H NMR (400 MHz, CDCl ₃) of compound 19a	153
Figure A1.56. Infrared spectrum (Thin Film, NaCl) of compound 19a	154
Figure A1.57. ¹³ C NMR (100 MHz, CDCl ₃) of compound 19a	154

Figure A1.58. ^1H NMR (400 MHz, CDCl_3) of compound 19b	155
Figure A1.59. Infrared spectrum (Thin Film, NaCl) of compound 19b	156
Figure A1.60. ^{13}C NMR (100 MHz, CDCl_3) of compound 19b	156
Figure A1.61. ^1H NMR (400 MHz, CDCl_3) of compound 19c	157
Figure A1.62. Infrared spectrum (Thin Film, NaCl) of compound 19c	158
Figure A1.63. ^{13}C NMR (100 MHz, CDCl_3) of compound 19c	158
Figure A1.64. ^1H NMR (400 MHz, CDCl_3) of compound 19d	159
Figure A1.65. Infrared spectrum (Thin Film, NaCl) of compound 19d	160
Figure A1.66. ^{13}C NMR (100 MHz, CDCl_3) of compound 19d	160
Figure A1.67. ^1H NMR (500 MHz, CDCl_3) of compound 19e	161
Figure A1.68. Infrared spectrum (Thin Film, NaCl) of compound 19e	162
Figure A1.69. ^{13}C NMR (125 MHz, CDCl_3) of compound 19e	162
Figure A1.70. ^1H NMR (500 MHz, CDCl_3) of compound 19f	163
Figure A1.71. Infrared spectrum (Thin Film, NaCl) of compound 19f	164
Figure A1.72. ^{13}C NMR (125 MHz, CDCl_3) of compound 19f	164
Figure A1.73. ^1H NMR (400 MHz, CDCl_3) of compound 19g	165
Figure A1.74. Infrared spectrum (Thin Film, NaCl) of compound 19g	166
Figure A1.75. ^{13}C NMR (100 MHz, CDCl_3) of compound 19g	166
Figure A1.76. ^1H NMR (400 MHz, CDCl_3) of compound 19h	167
Figure A1.77. Infrared spectrum (Thin Film, NaCl) of compound 19h	168
Figure A1.78. ^{13}C NMR (100 MHz, CDCl_3) of compound 19h	168
Figure A1.79. ^1H NMR (500 MHz, CDCl_3) of compound 19i	169
Figure A1.80. Infrared spectrum (Thin Film, NaCl) of compound 19i	170
Figure A1.81. ^{13}C NMR (125 MHz, CDCl_3) of compound 19i	170
Figure A1.82. ^1H NMR (500 MHz, CDCl_3) of compound 19j	171
Figure A1.83. Infrared spectrum (Thin Film, NaCl) of compound 19j	172
Figure A1.84. ^{13}C NMR (125 MHz, CDCl_3) of compound 19j	172
Figure A1.85. ^1H NMR (400 MHz, CDCl_3) of compound 19k	173
Figure A1.86. Infrared spectrum (Thin Film, NaCl) of compound 19k	174
Figure A1.87. ^{13}C NMR (100 MHz, CDCl_3) of compound 19k	174
Figure A1.88. ^1H NMR (400 MHz, CDCl_3) of compound 19l	175
Figure A1.89. Infrared spectrum (Thin Film, NaCl) of compound 19l	176
Figure A1.90. ^{13}C NMR (100 MHz, CDCl_3) of compound 19l	176
Figure A1.91. ^1H NMR (400 MHz, CDCl_3) of compound 21	177
Figure A1.92. Infrared spectrum (Thin Film, NaCl) of compound 21	178

Figure A1.93. ^{13}C NMR (100 MHz, CDCl_3) of compound 21	178
Figure A1.94. ^1H NMR (400 MHz, CDCl_3) of compound 23	179
Figure A1.95. Infrared spectrum (Thin Film, NaCl) of compound 23	180
Figure A1.96. ^{13}C NMR (100 MHz, CDCl_3) of compound 23	180
Figure A1.97. ^1H NMR (400 MHz, CDCl_3) of compound 25	181
Figure A1.98. Infrared spectrum (Thin Film, NaCl) of compound 25	182
Figure A1.99. ^{13}C NMR (100 MHz, CDCl_3) of compound 25	182
Figure A1.100. ^1H NMR (400 MHz, DMSO-d_6 , 23.3 °C) of compound 20e	183
Figure A1.101. ^1H NMR (400 MHz, DMSO-d_6 , 80 °C) of compound 20e	184
Figure A1.102. ^{13}C NMR (100 MHz, DMSO-d_6 , 80 °C) of compound 20e	185
Figure A1.103. ^1H NMR (400 MHz, CDCl_3) of compound 35a	186
Figure A1.104. Infrared spectrum (Thin Film, NaCl) of compound 35a	187
Figure A1.105. ^{13}C NMR (100 MHz, CDCl_3) of compound 35a	187
Figure A1.106. ^1H NMR (400 MHz, CDCl_3) of compound 35b	188
Figure A1.107. Infrared spectrum (Thin Film, NaCl) of compound 35b	189
Figure A1.108. ^{13}C NMR (100 MHz, CDCl_3) of compound 35b	189
Figure A1.109. ^1H NMR (400 MHz, CDCl_3) of compound 35c	190
Figure A1.110. Infrared spectrum (Thin Film, NaCl) of compound 35c	191
Figure A1.111. ^{13}C NMR (100 MHz, CDCl_3) of compound 35c	191
Figure A1.112. ^1H NMR (400 MHz, CDCl_3) of compound 35d	192
Figure A1.113. Infrared spectrum (Thin Film, NaCl) of compound 35d	193
Figure A1.114. ^{13}C NMR (100 MHz, CDCl_3) of compound 35d	193
Figure A1.115. ^1H NMR (400 MHz, CDCl_3) of compound 35e	194
Figure A1.116. Infrared spectrum (Thin Film, NaCl) of compound 35e	195
Figure A1.117. ^{13}C NMR (100 MHz, CDCl_3) of compound 35e	195
Figure A1.118. ^1H NMR (400 MHz, CDCl_3) of compound 35f	196
Figure A1.119. Infrared spectrum (Thin Film, NaCl) of compound 35f	197
Figure A1.120. ^{13}C NMR (100 MHz, CDCl_3) of compound 35f	197
Figure A1.121. ^1H NMR (400 MHz, CDCl_3) of compound 35g	198
Figure A1.122. Infrared spectrum (Thin Film, NaCl) of compound 35g	199
Figure A1.123. ^{13}C NMR (100 MHz, CDCl_3) of compound 35g	199
Figure A1.124. ^1H NMR (400 MHz, CDCl_3) of compound 35h	200
Figure A1.125. Infrared spectrum (Thin Film, NaCl) of compound 35h	201
Figure A1.126. ^{13}C NMR (100 MHz, CDCl_3) of compound 35h	201
Figure A1.127. ^1H NMR (400 MHz, CDCl_3) of compound 35i	202

Figure A1.128. Infrared spectrum (Thin Film, NaCl) of compound 35i	203
Figure A1.129. ¹³ C NMR (100 MHz, CDCl ₃) of compound 35i	203
Figure A1.130. ¹ H NMR (400 MHz, CDCl ₃) of compound 35j	204
Figure A1.131. Infrared spectrum (Thin Film, NaCl) of compound 35j	205
Figure A1.132. ¹³ C NMR (100 MHz, CDCl ₃) of compound 35j	205
Figure A1.133. ¹ H NMR (400 MHz, CDCl ₃) of compound 35k	206
Figure A1.134. Infrared spectrum (Thin Film, NaCl) of compound 35k	207
Figure A1.135. ¹³ C NMR (100 MHz, CDCl ₃) of compound 35k	207
Figure A1.136. ¹ H NMR (400 MHz, CDCl ₃) of compound 31	208
Figure A1.137. Infrared spectrum (Thin Film, KBr) of compound 31	209
Figure A1.138. ¹³ C NMR (100 MHz, CDCl ₃) of compound 31	209
Figure A1.139. ¹ H NMR (400 MHz, CDCl ₃) of compound 32	210
Figure A1.140. Infrared spectrum (Thin Film, NaCl) of compound 32	211
Figure A1.141. ¹³ C NMR (100 MHz, CDCl ₃) of compound 32	211
Figure A1.142. ¹ H NMR (400 MHz, CDCl ₃) of compound 33	212
Figure A1.143. Infrared spectrum (Thin Film, NaCl) of compound 33	213
Figure A1.144. ¹³ C NMR (100 MHz, CDCl ₃) of compound 33	213
Figure A1.145. ¹ H NMR (400 MHz, CDCl ₃) of compound 60	214
Figure A1.146. Infrared spectrum (Thin Film, KBr) of compound 60	215
Figure A1.147. ¹³ C NMR (100 MHz, CDCl ₃) of compound 60	215
Figure A1.148. ¹ H NMR (400 MHz, CDCl ₃) of compound 34a	216
Figure A1.149. Infrared spectrum (Thin Film, NaCl) of compound 34a	217
Figure A1.150. ¹³ C NMR (100 MHz, CDCl ₃) of compound 34a	217
Figure A1.151. ¹ H NMR (400 MHz, CDCl ₃) of compound 34b	218
Figure A1.152. Infrared spectrum (Thin Film, NaCl) of compound 34b	219
Figure A1.153. ¹³ C NMR (100 MHz, CDCl ₃) of compound 34b	219
Figure A1.154. ¹ H NMR (400 MHz, CDCl ₃) of compound 34c	220
Figure A1.155. Infrared spectrum (Thin Film, NaCl) of compound 34c	221
Figure A1.156. ¹³ C NMR (100 MHz, CDCl ₃) of compound 34c	221
Figure A1.157. ¹ H NMR (400 MHz, CDCl ₃) of compound 34d	222
Figure A1.158. Infrared spectrum (Thin Film, NaCl) of compound 34d	223
Figure A1.159. ¹³ C NMR (100 MHz, CDCl ₃) of compound 34d	223
Figure A1.160. ¹ H NMR (400 MHz, CDCl ₃) of compound 34e	224
Figure A1.161. Infrared spectrum (Thin Film, NaCl) of compound 34e	225
Figure A1.162. ¹³ C NMR (100 MHz, CDCl ₃) of compound 34e	225

Figure A1.163. ^1H NMR (400 MHz, CDCl_3) of compound 34f	226
Figure A1.164. Infrared spectrum (Thin Film, NaCl) of compound 34f	227
Figure A1.165. ^{13}C NMR (100 MHz, CDCl_3) of compound 34f	227
Figure A1.166. ^1H NMR (500 MHz, CDCl_3) of compound 34g	228
Figure A1.167. Infrared spectrum (Thin Film, NaCl) of compound 34g	229
Figure A1.168. ^{13}C NMR (125 MHz, CDCl_3) of compound 34g	229
Figure A1.169. ^1H NMR (400 MHz, CDCl_3) of compound 34h	230
Figure A1.170. Infrared spectrum (Thin Film, NaCl) of compound 34h	231
Figure A1.171. ^{13}C NMR (100 MHz, CDCl_3) of compound 34h	231
Figure A1.172. ^1H NMR (400 MHz, CDCl_3) of compound 34i	232
Figure A1.173. Infrared spectrum (Thin Film, NaCl) of compound 34i	233
Figure A1.174. ^{13}C NMR (100 MHz, CDCl_3) of compound 34i	233
Figure A1.175. ^1H NMR (400 MHz, CDCl_3) of compound 34j	234
Figure A1.176. Infrared spectrum (Thin Film, NaCl) of compound 34j	235
Figure A1.177. ^{13}C NMR (100 MHz, CDCl_3) of compound 34j	235
Figure A1.178. ^1H NMR (400 MHz, CDCl_3) of compound 34k	236
Figure A1.179. Infrared spectrum (Thin Film, NaCl) of compound 34k	237
Figure A1.180. ^{13}C NMR (100 MHz, CDCl_3) of compound 34k	237
Figure A1.181. ^1H NMR (400 MHz, CDCl_3) of compound 52	238
Figure A1.182. Infrared spectrum (Thin Film, NaCl) of compound 52	239
Figure A1.183. ^{13}C NMR (100 MHz, CDCl_3) of compound 52	239
Figure A1.184. ^1H NMR (400 MHz, CDCl_3) of compound 53	240
Figure A1.185. Infrared spectrum (Thin Film, NaCl) of compound 53	241
Figure A1.186. ^{13}C NMR (100 MHz, CDCl_3) of compound 53	241

APPENDIX 2

Attempts to Effect the Allylic Alkylation of Additional Diazepanone Substrates

Figure A2.1.1. Scope of diazepanone derivatives discussed herein.....	3
---	---

APPENDIX 4

Spectra Relevant to Chapter 2

Figure A4.1. ^1H NMR (400 MHz, CDCl_3) of compound 96	364
Figure A4.2. Infrared spectrum (Thin Film, NaCl) of compound 96	365
Figure A4.3. ^{13}C NMR (100 MHz, CDCl_3) of compound 96	365

Figure A4.4. ^1H NMR (400 MHz, CDCl_3) of compound 97	366
Figure A4.5. Infrared spectrum (Thin Film, NaCl) of compound 97	367
Figure A4.6. ^{13}C NMR (100 MHz, CDCl_3) of compound 97	367
Figure A4.7. ^1H NMR (400 MHz, CDCl_3) of compound 107	368
Figure A4.8. Infrared spectrum (Thin Film, NaCl) of compound 107	369
Figure A4.9. ^{13}C NMR (100 MHz, CDCl_3) of compound 107	369
Figure A4.10. ^1H NMR (400 MHz, CDCl_3) of compound 109	370
Figure A4.11. Infrared spectrum (Thin Film, NaCl) of compound 109	371
Figure A4.12. ^{13}C NMR (100 MHz, CDCl_3) of compound 109	371
Figure A4.13. ^1H NMR (400 MHz, CDCl_3) of compound 125	372
Figure A4.14. Infrared spectrum (Thin Film, NaCl) of compound 125	373
Figure A4.15. ^{13}C NMR (100 MHz, CDCl_3) of compound 125	373
Figure A4.16. ^1H NMR (400 MHz, CDCl_3) of compound 126	374
Figure A4.17. Infrared spectrum (Thin Film, NaCl) of compound 126	375
Figure A4.18. ^{13}C NMR (100 MHz, CDCl_3) of compound 126	375
Figure A4.19. ^1H NMR (400 MHz, CDCl_3) of compound 131	376
Figure A4.20. Infrared spectrum (Thin Film, NaCl) of compound 131	377
Figure A4.21. ^{13}C NMR (100 MHz, CDCl_3) of compound 131	377
Figure A4.22. ^1H NMR (400 MHz, CDCl_3) of compound 132	378
Figure A4.23. Infrared spectrum (Thin Film, NaCl) of compound 132	379
Figure A4.24. ^{13}C NMR (100 MHz, CDCl_3) of compound 132	379
Figure A4.25. ^1H NMR (400 MHz, CDCl_3) of compound 133	380
Figure A4.26. Infrared spectrum (Thin Film, NaCl) of compound 133	381
Figure A4.27. ^{13}C NMR (100 MHz, CDCl_3) of compound 133	381
Figure A4.28. ^1H NMR (400 MHz, CDCl_3) of compound 134	382
Figure A4.29. Infrared spectrum (Thin Film, NaCl) of compound 134	383
Figure A4.30. ^{13}C NMR (100 MHz, CDCl_3) of compound 134	383
Figure A4.31. ^1H NMR (400 MHz, CDCl_3) of compound 136	384
Figure A4.32. Infrared spectrum (Thin Film, NaCl) of compound 136	385
Figure A4.33. ^{13}C NMR (100 MHz, CDCl_3) of compound 136	385
Figure A4.34. ^1H NMR (400 MHz, CDCl_3) of compound 138	386
Figure A4.35. Infrared spectrum (Thin Film, NaCl) of compound 138	387
Figure A4.36. ^{13}C NMR (100 MHz, CDCl_3) of compound 138	387
Figure A4.37. ^1H NMR (400 MHz, CDCl_3) of compound 139	388
Figure A4.38. ^{13}C NMR (100 MHz, CDCl_3) of compound 139	389

Figure A4.39. ^1H NMR (400 MHz, CDCl_3) of compound 143	390
Figure A4.40. Infrared spectrum (Thin Film, NaCl) of compound 143	391
Figure A4.41. ^{13}C NMR (100 MHz, CDCl_3) of compound 143	391
Figure A4.42. ^1H NMR (400 MHz, CDCl_3) of compound 141	392
Figure A4.43. Infrared spectrum (Thin Film, NaCl) of compound 141	393
Figure A4.44. ^{13}C NMR (100 MHz, CDCl_3) of compound 141	393
Figure A4.45. ^1H NMR (400 MHz, CDCl_3) of compound 149	394
Figure A4.46. Infrared spectrum (Thin Film, NaCl) of compound 149	395
Figure A4.47. ^{13}C NMR (100 MHz, CDCl_3) of compound 149	395
Figure A4.48. ^1H NMR (400 MHz, CDCl_3) of compound 150	396
Figure A4.49. Infrared spectrum (Thin Film, NaCl) of compound 150	397
Figure A4.50. ^{13}C NMR (100 MHz, CDCl_3) of compound 150	397
Figure A4.51. ^1H NMR (400 MHz, C_6D_6) of compound 153	398
Figure A4.52. Infrared spectrum (Thin Film, NaCl) of compound 153	399
Figure A4.53. ^{13}C NMR (100 MHz, C_6D_6) of compound 153	399
Figure A4.54. ^1H NMR (400 MHz, C_6D_6) of compound 154	400
Figure A4.55. Infrared spectrum (Thin Film, NaCl) of compound 154	401
Figure A4.56. ^{13}C NMR (100 MHz, C_6D_6) of compound 154	401
Figure A4.57. ^1H NMR (400 MHz, CDCl_3) of compound 156	402
Figure A4.58. Infrared spectrum (Thin Film, NaCl) of compound 156	403
Figure A4.59. ^{13}C NMR (100 MHz, CDCl_3) of compound 156	403
Figure A4.60. ^1H NMR (400 MHz, C_6D_6) of compound 155	404
Figure A4.61. Infrared spectrum (Thin Film, NaCl) of compound 155	405
Figure A4.62. ^{13}C NMR (100 MHz, C_6D_6) of compound 155	405
Figure A4.63. ^1H NMR (400 MHz, C_6D_6) of compound 157	406
Figure A4.64. Infrared spectrum (Thin Film, NaCl) of compound 157	407
Figure A4.65. ^{13}C NMR (100 MHz, C_6D_6) of compound 157	407
Figure A4.66. ^1H NMR (400 MHz, C_6D_6) of compound 160	408
Figure A4.67. Infrared spectrum (Thin Film, NaCl) of compound 160	409
Figure A4.68. ^{13}C NMR (100 MHz, C_6D_6) of compound 160	409
Figure A4.69. ^1H NMR (400 MHz, C_6D_6) of compound 168	410
Figure A4.70. Infrared spectrum (Thin Film, NaCl) of compound 168	411
Figure A4.71. ^{13}C NMR (100 MHz, C_6D_6) of compound 168	411
Figure A4.72. ^1H NMR (400 MHz, C_6D_6) of compound 169	412
Figure A4.73. Infrared spectrum (Thin Film, NaCl) of compound 169	413

Figure A4.74. ^{13}C NMR (100 MHz, C_6D_6) of compound 169	413
Figure A4.75. ^1H NMR (400 MHz, DMSO-d_6) of compound 214	414
Figure A4.76. Infrared spectrum (Thin Film, NaCl) of compound 214	415
Figure A4.77. ^{13}C NMR (100 MHz, DMSO-d_6) of compound 214	415
Figure A4.78. ^1H NMR (400 MHz, C_6D_6) of compound 177	416
Figure A4.79. Infrared spectrum (Thin Film, NaCl) of compound 177	417
Figure A4.80. ^{13}C NMR (100 MHz, C_6D_6) of compound 177	417
Figure A4.81. ^1H NMR (400 MHz, C_6D_6) of compound 179	418
Figure A4.82. Infrared spectrum (Thin Film, NaCl) of compound 179	419
Figure A4.83. ^{13}C NMR (100 MHz, C_6D_6) of compound 179	419
Figure A4.84. ^1H NMR (400 MHz, C_6D_6) of compound 184	420
Figure A4.85. Infrared spectrum (Thin Film, NaCl) of compound 184	421
Figure A4.86. ^{13}C NMR (100 MHz, C_6D_6) of compound 184	421
Figure A4.87. ^1H NMR (400 MHz, CDCl_3) of compound 187	422
Figure A4.88. Infrared spectrum (Thin Film, NaCl) of compound 187	423
Figure A4.89. ^{13}C NMR (100 MHz, CDCl_3) of compound 187	423
Figure A4.90. ^1H NMR (400 MHz, CDCl_3) of compound 215	424
Figure A4.91. Infrared spectrum (Thin Film, NaCl) of compound 215	425
Figure A4.92. ^{13}C NMR (100 MHz, CDCl_3) of compound 215	425
Figure A4.93. ^1H NMR (400 MHz, C_6D_6) of compound 189	426
Figure A4.94. Infrared spectrum (Thin Film, NaCl) of compound 189	427
Figure A4.95. ^{13}C NMR (100 MHz, C_6D_6) of compound 189	427
Figure A4.96. ^1H NMR (400 MHz, CD_2Cl_2) of compound 186	428
Figure A4.97. Infrared spectrum (Thin Film, NaCl) of compound 186	429
Figure A4.98. ^{13}C NMR (100 MHz, CD_2Cl_2) of compound 186	429
Figure A4.99. ^1H NMR (400 MHz, CDCl_3) of compound 190	430
Figure A4.100. Infrared spectrum (Thin Film, NaCl) of compound 190	431
Figure A4.101. ^{13}C NMR (100 MHz, CDCl_3) of compound 190	431
Figure A4.102. ^1H NMR (400 MHz, C_6D_6) of compound 185	432
Figure A4.103. Infrared spectrum (Thin Film, NaCl) of compound 185	433
Figure A4.104. ^{13}C NMR (100 MHz, C_6D_6) of compound 185	433
Figure A4.105. ^1H NMR (400 MHz, C_6D_6) of compound 192	434
Figure A4.106. Infrared spectrum (Thin Film, NaCl) of compound 192	435
Figure A4.107. ^{13}C NMR (100 MHz, C_6D_6) of compound 192	435
Figure A4.108. ^1H NMR (400 MHz, C_6D_6) of compound 198	436

Figure A4.109. Infrared spectrum (Thin Film, NaCl) of compound 198	437
Figure A4.110. ^{13}C NMR (100 MHz, C_6D_6) of compound 198	437
Figure A4.111. ^1H NMR (400 MHz, C_6D_6) of compound 195	438
Figure A4.112. Infrared spectrum (Thin Film, NaCl) of compound 195	439
Figure A4.113. ^{13}C NMR (100 MHz, C_6D_6) of compound 195	439
Figure A4.114. ^1H NMR (400 MHz, C_6D_6) of compound 201	440
Figure A4.115. Infrared spectrum (Thin Film, NaCl) of compound 201	441
Figure A4.116. ^{13}C NMR (100 MHz, C_6D_6) of compound 201	441
Figure A4.117. ^1H NMR (400 MHz, CD_3OD) of compound 206	442
Figure A4.118. Infrared spectrum (Thin Film, NaCl) of compound 206	443
Figure A4.119. ^{13}C NMR (100 MHz, CD_3OD) of compound 206	443
Figure A4.120. ^{19}F NMR (376 MHz, CD_3OD) of compound 206	444
Figure A4.121. ^1H NMR (400 MHz, C_6D_6) of compound 207	445
Figure A4.122. Infrared spectrum (Thin Film, NaCl) of compound 207	446
Figure A4.123. ^{13}C NMR (100 MHz, C_6D_6) of compound 207	446

CHAPTER 3

Synthetic Strategies Toward Minimally Substituted Corroles and Azaporphyrins

Figure 3.1.1. Introduction to the corrole ring system.....	484
Figure 3.1.2. Select milestones toward the synthesis of minimally substituted corroles.....	485
Figure 3.3.3. Comparison of the ^1H NMR spectra of azaporphyrin 306-H₂ and corrole 293	493

APPENDIX 6

Spectra Relevant to Chapter 3

Figure A6.1. ^1H NMR (400 MHz, CDCl_3) of compound 306-H₂	507
Figure A6.2. ^{19}F NMR (377 MHz, CDCl_3) of compound 306-H₂	508

APPENDIX 7

X-Ray Crystallography Reports Relevant to Chapter 3

Figure A7.2.1. X-ray crystal structure of azaporphyrin complex 306-Co	511
--	-----

LIST OF SCHEMES

CHAPTER 1

Palladium-Catalyzed Decarboxylative Asymmetric Allylic Alkylation of 5- and 7-Membered Diazaheterocycles

Scheme 1.1.1.	Development of the Pd-catalyzed decarboxylative asymmetric allylic alkylation reaction.....	2
Scheme 1.1.3.	Prior Pd-catalyzed decarboxylative asymmetric allylic alkylation of diazaheterocycles in the Stoltz group	4
Scheme 1.2.2.	Synthetic route to diazepamone-derived allyl β -amidoesters 19a-l	7
Scheme 1.2.5.	Synthesis of a suvorexant analogue.....	10
Scheme 1.3.2.	Pinza's route to imidazolidinone	12
Scheme 1.3.3.	Initial synthesis of imidazolidinone allylic alkylation substrates.....	13
Scheme 1.3.6.	Beckmann Rearrangement strategies to access 4-imidazolidinones.....	16
Scheme 1.3.7.	Attempted cyclization employing Eschenmoser's Salt as a formaldehyde equivalent	18
Scheme 1.3.9.	Cyclization of an amino alcohol with activated DMSO (Kayser)	19
Scheme 1.3.11.	Previous desulfurization of a protected thiohydantoin (Witkop)	21
Scheme 1.3.12.	Concise and high-yielding route to key allyl ester 33	21
Scheme 1.3.13.	Product transformations	22

APPENDIX 2

Attempts to Effect the Allylic Alkylation of Additional Diazepamone Substrates

Scheme A2.2.1.	Unsuccessful synthesis of a 1,4-diazepam-2-one allylic alkylation substrate	243
Scheme A2.3.1.	C-Acylation of diazepam (Wolfe)	244
Scheme A2.3.2.	Unsuccessful synthesis of a benzodiazepine allylic alkylation substrate.....	245
Scheme A2.3.3.	Unsuccessful synthesis of a tetrahydro[1,4]benzodiazepamone allylic alkylation substrate.....	245

CHAPTER 2

Progress Toward the Total Synthesis of Aleutianamine

Scheme 2.1.1.	Aleutianamine and examples of related natural products	254
Scheme 2.1.2.	Proposed biosynthetic routes to aleutianamine.....	256

Scheme 2.2.1.	Initial retrosynthetic analysis of aleutianamine	258
Scheme 2.3.2.	Corey's addition of a sulfur nucleophile to an α -bromooxime	260
Scheme 2.3.3.	Synthesis of an indole-derived aryl bromide coupling partner	261
Scheme 2.3.4.	Enolate acylation and subsequent unsuccessful bromination.....	261
Scheme 2.4.1.	Revised retrosynthetic analysis of aleutianamine	263
Scheme 2.5.1.	Attempts to reduce a pyrroloiminoquinone to aniline 120	264
Scheme 2.5.2.	Strategies envisioned for the construction of aniline 114	265
Scheme 2.5.3.	Attempted Fischer indolization of a hydrazone derivative	266
Scheme 2.5.4.	Access to desired tryptophol 126 by Fischer indolization	267
Scheme 2.5.5.	Advancement of tryptophol 126 to a protected tryptamine.....	268
Scheme 2.6.1.	Advancement of tricycle 134 to a tetracyclic quinolone.....	271
Scheme 2.6.4.	Ligands tested in entry 4 of Table 2.6.3	273
Scheme 2.6.5.	Preparation of a model Barbier addition substrate	274
Scheme 2.6.7.	Preparation of a ketal-bearing Michael acceptor.....	276
Scheme 2.6.8.	Preparation of an oxidized intramolecular Barbier addition substrate.....	276
Scheme 2.6.9.	Cyclization of bromoarene 154 and unexpected rearrangements.....	277
Scheme 2.6.10.	Attempted allylic oxidation of pentacycle 160	278
Scheme 2.6.11.	Attempted β -oxidation by a thiol conjugate addition approach.....	279
Scheme 2.7.1.	3 rd -generation retrosynthetic analysis of aleutianamine.....	281
Scheme 2.8.1.	Construction of an acetamidothiophene coupling partner	282
Scheme 2.8.2.	Fragment coupling to prepare a dearomative cyclization substrate.....	283
Scheme 2.8.3.	Known dearomative arylation and desired transformation of thiophenes.....	284
Scheme 2.8.4.	Key dearomative cyclization of aminothiophene 179	284
Scheme 2.8.5.	Attempts to access a thiolactone from acetylthioimide 184	285
Scheme 2.8.6.	Synthesis of a TFA-protected aminothiophene	286
Scheme 2.8.7.	Improved thioimide synthesis and subsequent tosylation.....	287
Scheme 2.8.8.	Successful hydrolysis of thioimide 190	287
Scheme 2.8.9.	Demonstration of the feasibility of thioaminal formation	288
Scheme 2.8.10.	Installation of the final nitrogen atom by azidation and reduction	289
Scheme 2.8.12.	Desaturation of thiolactone 185 to diene 195	291
Scheme 2.8.13.	Thioester δ -functionalization and unsuccessful downstream chemistry	292
Scheme 2.8.14.	Inefficient azidation of dienone 195	292
Scheme 2.8.15.	Benefits of an early oxidation event	293
Scheme 2.8.16.	Proof-of-concept for an oxidative strategy.....	294
Scheme 2.8.17.	Toward desired pyrroloiminoquinone 208	294

Scheme 2.8.18.	Planned completion of synthesis.....	295
----------------	--------------------------------------	-----

APPENDIX 3

Synthetic Summary for Chapter 2

Scheme A3.1.	Synthesis of tricyclic aniline 134	361
Scheme A3.2.	Synthesis of hydroxyketone 157	361
Scheme A3.3.	Synthesis of aminothiophene 188	361
Scheme A3.4.	Synthesis of thiolactol 207	362

APPENDIX 5

Additional Strategies and Tactics Toward the Total Synthesis of Aleutianamine

Scheme A5.2.1.	Planned bridgehead sulfide installation toward aleutianamine	448
Scheme A5.2.2.	A model system for bridgehead sulfide installation	449
Scheme A5.2.3.	Alternative strategy for sulfide installation.....	450
Scheme A5.3.1.	Late-stage arene amination disconnection	451
Scheme A5.3.2.	Preparation of nitroaniline 231 and failed Fischer Indolization.....	451
Scheme A5.3.3.	Intramolecular aryl C–H amination (Falck, 2016)	452
Scheme A5.3.4.	Attempts to access tricyclic aminoindoles by intramolecular C–H amination.....	453
Scheme A5.4.1.	Unexpected tosyl group migration during quinolone synthesis.....	454
Scheme A5.4.2.	Attempted preparation of N-allyl tetracycle 247	454
Scheme A5.4.3.	Evaluation of a pivaloyl indole protecting group.....	455
Scheme A5.4.4.	A julolidine desymmetrization approach to quinolone 252	455
Scheme A5.4.5.	Unsuccessful preparation of diketojulolidine 250	456
Scheme A5.5.1.	Desired enone β -oxidation and challenging Wacker oxidation of internal α,β -unsaturated carbonyl compounds.....	458
Scheme A5.6.1.	A functional handle approach to alkenyl bromide installation.....	460
Scheme A5.6.2.	Evaluation of a cyanide functional handle	461
Scheme A5.6.3.	Attempted Gewald reaction of a cyclopentadiene Diels–Alder adduct.....	462
Scheme A5.7.1.	A spirocyclization–Michael addition approach to the oxidized ring system of aleutianamine	463
Scheme A5.7.2.	Access to a 2-bromoketone electrophile.....	463
Scheme A5.7.3.	Attempts to access a spirocyclization substrate.....	464

CHAPTER 3*Synthetic Strategies Toward Minimally Substituted Corroles and Azaporphyrins*

Scheme 3.1.3.	Approaches to complexes of unsubstituted corrole 294 (Gross, 2021)	487
Scheme 3.2.1.	Evaluation of sublimation as a means for oligopyrrane separation	488
Scheme 3.2.2.	AcOH-promoted oligomerization of pyrrole and paraformaldehyde	489
Scheme 3.2.3.	A tetrapyrane from a meso-free dipyrane (Tanaka and Osuka, 2015).....	490
Scheme 3.2.4.	Attempted controlled assembly of tetrapyrane 297	491
Scheme 3.3.1.	Corrole synthesis by oxidation with $K_3Fe(CN)_6$ (Dolphin et al., 1966).....	492
Scheme 3.3.2.	Unexpected oxidation of a bilane to a monoazaporphyrin.....	493
Scheme 3.3.4.	Previous synthesis of a β -free monoazaporphyrin complex (Palmer, Gross, and Gray, 2011)	494
Scheme 3.3.5.	Metallation of monoazaporphyrin 306-H₂	495

APPENDIX 8*Some Unusual Transformations of a Highly Reactive α -Bromocaranone*

Scheme A8.1.1.	Carene and the desired transformation	524
Scheme A8.2.1.	Synthesis of a reactive α -bromocaranone	526
Scheme A8.2.3.	Radical-mediated cyclopropane fragmentation of 313	528
Scheme A8.2.4.	Proposed mechanism for the formation of racemic 321	529
Scheme A8.2.5.	Synthesis of bromide 328 and control reaction in benzene	530

LIST OF TABLES

CHAPTER 1

Palladium-Catalyzed Decarboxylative Asymmetric Allylic Alkylation of 5- and 7-Membered Diazaheterocycles

Table 1.2.3.	Reaction optimization.....	8
Table 1.2.4.	1,4-Diazepan-5-one substrate scope	9
Table 1.3.4.	Reaction optimization.....	14
Table 1.3.5.	Imidazolidinone substrate scope.....	15
Table 1.3.8.	Unsuccessful cyclization employing Eschenmoser's Salt as a formaldehyde equivalent.....	18
Table 1.3.10.	Cyclization employing activated DMSO as a methylene equivalent.....	20
Table 1.5.3.1.	Determination of enantiomeric excess.....	105
Table 1.5.3.2.	Determination of enantiomeric excess (continued).....	106
Table 1.5.3.3.	Determination of enantiomeric excess (continued).....	107
Table 1.5.3.4.	Determination of enantiomeric excess (continued).....	108

CHAPTER 2

Progress Toward the Total Synthesis of Aleutianamine

Table 2.3.1.	Investigation of the α -arylation of model vinylogous ester 96	259
Table 2.5.6.	Evaluation of the intramolecular C–N coupling of 133	269
Table 2.6.2.	Unsuccessful aza-Michael addition of aniline 134 into cyclohexenone	272
Table 2.6.3.	A model system for aza-Michael addition.....	273
Table 2.6.6.	Barbier-type addition into a model ketone.....	275
Table 2.8.11.	Conditions tested for direct desaturation of thiobutenolide 185	290

APPENDIX 5

Additional Strategies and Tactics Toward the Total Synthesis of Aleutianamine

Table A5.5.2.	Evaluation of solvents for positive control substrate 264	459
Table A5.5.3.	Evaluation of Lewis-acidic additives	459

APPENDIX 7*X-Ray Crystallography Reports Relevant to Chapter 3*

Table A7.2.2.	Crystal data and structure refinement for complex 306-Co	511
Table A7.2.3.	Fractional Atomic Coordinates ($\times 10^4$) and Equivalent Isotropic Displacement Parameters ($\text{\AA}^2 \times 10^3$) for 306-Co . $U(\text{eq})$ is defined as 1/3 of the trace of the orthogonalized U_{ij} tensor	512
Table A7.2.4.	Anisotropic Displacement Parameters ($\text{\AA}^2 \times 10^3$) for 306-Co . The Anisotropic displacement factor exponent takes the form: $-2\pi^2 [h^2 a^{*2} U_{11} + 2hka^* b^* U_{12} + \dots]$	514
Table A7.2.5.	Bond Lengths for 306-Co	516
Table A7.2.6.	Bond Angles for 306-Co	517
Table A7.2.7.	Torsion Angles for 306-Co	520
Table A7.2.8.	Hydrogen Atom Coordinates ($\text{\AA} \times 10^4$) and Isotropic Displacement Parameters ($\text{\AA}^2 \times 10^3$) for 306-Co	522

APPENDIX 8*Some Unusual Transformations of a Highly Reactive α -Bromocaranone*

Table A8.2.2.	Ag^{I} -mediated reactions of 313	527
---------------	--	-----

APPENDIX 9*Notebook Cross-Reference for New Compounds*

Table A9.1.	Notebook cross-reference for Chapter 1	548
Table A9.2.	Notebook cross-reference for Chapter 1 (continued)	549
Table A9.3.	Notebook cross-reference for Chapter 2	550
Table A9.4.	Notebook cross-reference for Chapter 2 (continued)	551
Table A9.5.	Notebook cross-reference for Appendix 2	551
Table A9.6.	Notebook cross-reference for Appendix 5	552

LIST OF ABBREVIATIONS

Å	Ångstrom
λ	wavelength
μ	micro
μ wave	microwave
$[\alpha]_D$	specific rotation at wavelength of sodium D line
[H]	reduction
[O]	oxidation
°C	degrees Celsius
Ac	acetyl
AcOH	acetic acid
An	<i>para</i> -anisoyl
APCI	atmospheric pressure chemical ionization
aq	aqueous
Ar	aryl
atm	atmosphere
Bn	benzyl
Boc	<i>tert</i> -butyloxycarbonyl
bp	boiling point
br	broad
Bu	butyl
Bz	benzoyl
c	concentration for specific rotation measurements (g/100 mL)
calc'd	calculated

CAN	ceric ammonium nitrate
cat	catalytic
cm ⁻¹	wavenumber(s)
COD	1,5-cyclooctadiene
Cp	cyclopentadienyl
CPME	cyclopentyl methyl ether
CuTC	copper(I) thiophene-2-carboxylate
Cy	cyclohexyl
d	doublet
D	deuterium
dba	dibenzylideneacetone
DBU	1,8-diazabicyclo[5.4.0]undec-7-ene
DCE	1,2-dichloroethane
DDQ	2,3-dichloro-5,6-dicyano- <i>p</i> -benzoquinone
DIAD	diisopropyl azodicarboxylate
DIBAL	diisobutylaluminum hydride
DMA	<i>N,N</i> -dimethylacetamide
DMAP	4-dimethylaminopyridine
DME	1,2-dimethoxyethane
DMF	<i>N,N</i> -dimethylformamide
DMSO	dimethyl sulfoxide
DPPA	diphenylphosphoryl azide
DPPF	1,1'-bis(diphenylphosphino)ferrocene
dr	diastereomeric ratio
e.g.	for example (Latin <i>exempli gratia</i>)
ee	enantiomeric excess
equiv	equivalent(s)

ESI	electrospray ionization
esp	$\alpha,\alpha,\alpha',\alpha'$ -tetramethyl-1,3-benzenedipropionic acid
Et	ethyl
EtOAc	ethyl acetate
FAB	fast atom bombardment
FD	field desorption
g	gram(s)
G4	fourth-generation Buchwald precatalyst
GC	gas chromatography
h	hour(s)
HFIP	1,1,1,3,3,3-hexafluoropropan-2-ol
HMDS	1,1,1,3,3,3-hexamethyldisilazane
HMPA	hexamethylphosphoramide
HPLC	high-performance liquid chromatography
HRMS	high-resolution mass spectroscopy
Hz	hertz
<i>i</i> -Bu	isobutyl
i.e.	that is (Latin id est)
IBX	2-iodoxybenzoic acid
IPA	isopropanol, 2-propanol
<i>i</i> -Pr	isopropyl
IR	infrared (spectroscopy)
<i>J</i>	coupling constant
K	Kelvin(s) (absolute temperature)
kcal	kilocalorie
L	liter; neutral ligand
LC–MS	liquid chromatography–mass spectrometry

LDA	lithium diisopropylamide
m	multiplet; milli
<i>m</i>	meta
M	metal; molar; molecular ion
<i>m/z</i>	mass to charge ratio
<i>m</i> -CPBA	<i>meta</i> -chloroperoxybenzoic acid
Me	methyl
mg	milligram(s)
MHz	megahertz
min	minute(s)
MM	mixed method
mol	mole(s)
mp	melting point
Ms	methanesulfonyl (mesyl)
MS	molecular sieves
MTBE	methyl <i>tert</i> -butyl ether
n	nano
N	normal
NBS	<i>N</i> -bromosuccinimide
<i>n</i> -Bu	butyl
NCS	<i>N</i> -chlorosuccinimide
ND	not determined
NHK	Nozaki–Hiyama–Kishi
NMP	<i>N</i> -methyl-2-pyrrolidone
NMR	nuclear magnetic resonance
NR	no reaction detected
Nu ⁻	nucleophile

<i>o</i>	ortho
<i>p</i>	para
Pd/C	palladium on carbon
PEG	polyethylene glycol
PG	protecting group
Ph	phenyl
pH	hydrogen ion concentration in aqueous solution
PHOX	phosphinooxazoline ligand
Phth	phthaloyl
PIFA	(bis(trifluoroacetoxy)iodo)benzene
Piv	pivaloyl
pmdba	bis(4-methoxybenzylidene)acetone
PPA	polyphosphoric acid
ppm	parts per million
Pr	propyl
PTSA	<i>para</i> -toluenesulfonic acid
Py	pyridine
q	quartet
R	generic for any atom or functional group
Ref.	reference
s	singlet
SFC	supercritical fluid chromatography
t	triplet
TBAF	tetrabutylammonium fluoride
TBAI	tetrabutylammonium iodide
TBHP	<i>tert</i> -butyl hydroperoxide
TBS	<i>tert</i> -butyldimethylsilyl

<i>t</i> -Bu	<i>tert</i> -butyl
Tf	trifluoromethanesulfonyl (triflyl)
TFA	trifluoroacetic acid
TFAA	trifluoroacetic anhydride
TFE	2,2,2-trifluoroethanol
THF	tetrahydrofuran
TLC	thin-layer chromatography
TMG	1,1,3,3-tetramethylguanidine
TMP	2,2,6,6-tetramethylpiperidine
TMS	trimethylsilyl
TOF	time-of-flight
TosMIC	<i>para</i> -toluenesulfonylmethyl isocyanide
<i>t_R</i>	retention time
Ts	<i>p</i> -toluenesulfonyl (tosyl)
TTMSS	tris(trimethylsilyl)silane
UV	ultraviolet
<i>v/v</i>	volume to volume
w	weak
<i>w/v</i>	weight to volume
<i>w/w</i>	weight to weight
X	anionic ligand or electronegative element

CHAPTER 1

Palladium-Catalyzed Decarboxylative Asymmetric Allylic Alkylation of 5- and 7-Membered Diazaheterocycles[†]

1.1 INTRODUCTION

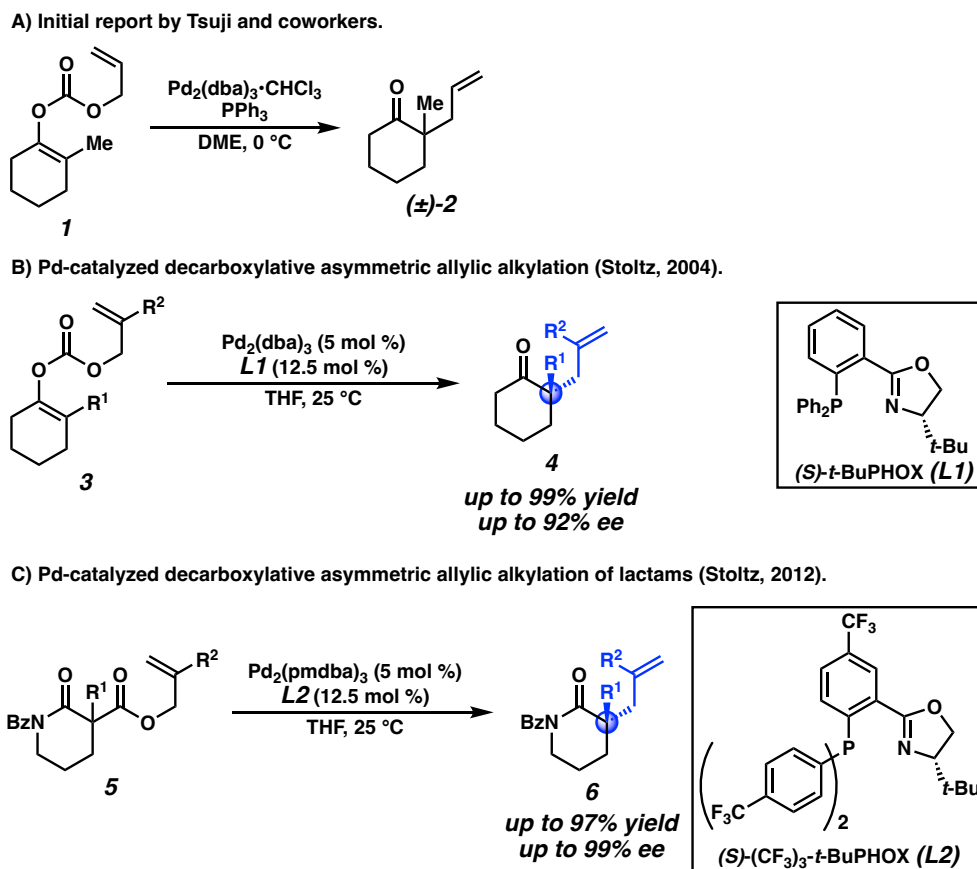
In 1983, Tsuji and coworkers reported the first example of a palladium-catalyzed decarboxylative allylic alkylation reaction (Scheme 1.1.1A).¹ Treatment of cyclohexanone-derived allyl enol carbonate **1** with catalytic Pd⁰ in the presence of triphenylphosphine provided α -quaternary ketone (\pm)-**2**. In 2004, our laboratory reported the first enantioselective example of such a palladium-catalyzed decarboxylative allylic alkylation,² employing allyl enol carbonate substrates **3** similar to those utilized in Tsuji's seminal work (Scheme 1.1.1B). The Pfaltz-type chiral ligand (*S*)-*t*-BuPHOX led to consistently high ee in this reaction.

In the following years, this chemistry has been extensively explored by our group,³ the Trost group,⁴ and others. The use of allyl β -ketoester masked enolate synthons in place of allyl enol carbonates allowed the same enantioenriched products to be obtained, but facilitated the late-stage diversification of allylic alkylation substrates by a more divergent synthetic route.^{3a} Seeking to broaden the substrate scope of the palladium-catalyzed decarboxylative asymmetric allylic alkylation beyond ketones, our group reported that this

[†]This research was conducted in collaboration with Dr. Alexander Sun. Portions of this chapter have been reproduced with permission from Sercel, Z. P.; Sun, A. W.; Stoltz, B. M. *Org. Lett.* **2019**, *21*, 9158–9161. and Sercel, Z. P.; Sun, A. W.; Stoltz, B. M. *Org. Lett.* **2021**, *23*, 6348–6351. © 2019, 2021 American Chemical Society.

method could also be used to access α -quaternary lactams **6** in excellent yield and enantioselectivity (Scheme 1.1.1C).^{3b}

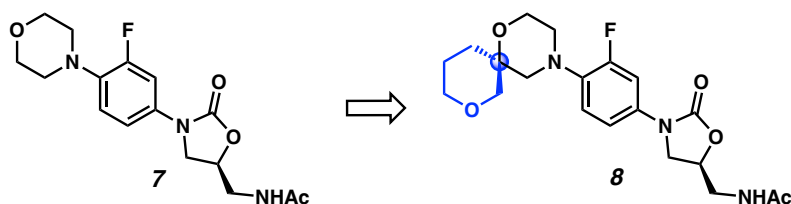
Scheme 1.1.1. Development of the Pd-catalyzed decarboxylative asymmetric allylic alkylation reaction.



In addition to simple lactams, other *gem*-disubstituted heterocycles, such as substituted morpholinones, could be accessed. Access to these heterocycles presents a notable advantage in the context of medicinal chemistry. A higher degree of saturation and the presence of sp^3 -stereogenic centers in lead molecules are correlated with greater clinical success and fewer off-target effects, which can be attributed to a greater number of accessible 3D conformers.⁵ In order to explore medicinal applications, our group reported

the incorporation of a variety of *gem*-disubstituted morpholine derivatives into the oxazolidinone antibiotic linezolid (**7**, Figure 1.1.2).⁶ Linezolid is an important treatment for antibiotic-resistant infections, but it possesses various side effects as a result of its off-target inhibition of human mitochondrial protein synthesis. Furthermore, the rapid metabolism of linezolid by oxidation of its morpholine ring necessitates frequent administration, which presents issues regarding patient-compliance with the dosing regimen.

Figure 1.1.2. Incorporation of a *gem*-disubstituted heterocycle into linezolid.

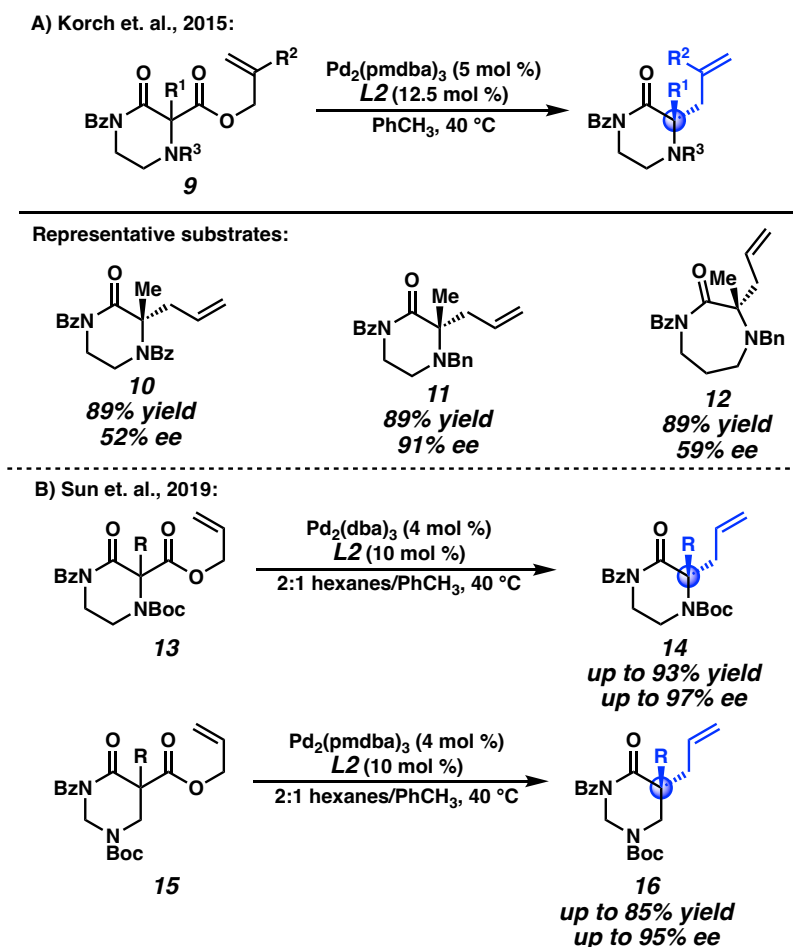


Ultimately, linezolid derivative **8** was found to be the most promising of the initial candidates, exhibiting decreased inhibition of human mitochondrial protein synthesis, although a reduction in IC_{50} against *S. aureus* ATCC 43300 was also observed.

To expand the scope of chiral heterocycles that can be prepared by palladium-catalyzed decarboxylative asymmetric allylic alkylation, our group reported the synthesis of *gem*-disubstituted piperazin-2-ones (Scheme 1.1.3A).^{3d} The choice of protecting group for the secondary amine proved key to obtaining high enantioselectivity: an electron-withdrawing benzyl group resulted in low ee (**10**), which was hypothesized to be a result of stabilization of the palladium enolate. Our group has previously reported that stabilized enolates lead to low or no enantioselectivity under our reaction conditions.⁷ These compounds are thought to favor an outer-sphere mechanism of C–C bond formation that is

not well-controlled by the PHOX ligand steric environment, in contrast to the inner-sphere mechanism favored for less stabilized enolates.

Scheme 1.1.3. *Prior Pd-catalyzed decarboxylative asymmetric allylic alkylation of diazaheterocycles in the Stoltz group.*

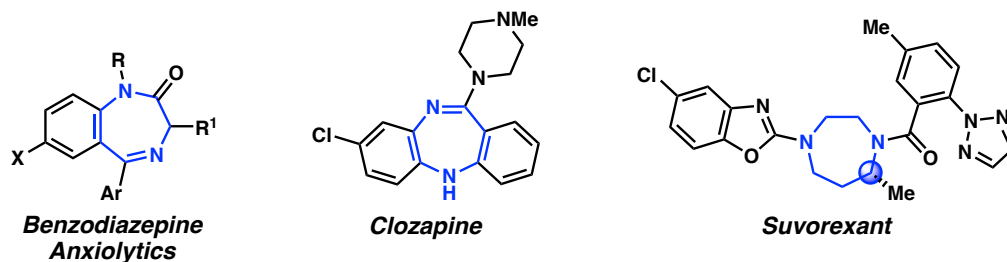


Thus, the use of a benzyl group (as in **11**) resulted in a dramatic boost in enantioselectivity. However, the presence of a basic amine presented challenges during substrate synthesis, limiting the scope of this transformation. Nevertheless, in addition to piperazinones, this report included a single example of the asymmetric allylic alkylation of a 7-membered diazepanone heterocycle (**12**), albeit in a modest 59% ee.

Recently, our group reported the use of an *N*-Boc protecting group to expand the scope of piperazin-2-ones (**14**) accessible by palladium-catalyzed decarboxylative asymmetric allylic alkylation (Scheme 1.1.3B).^{3c} The more electron-rich nature of carbamate protecting groups, in comparison with acyl groups, enabled the allylic alkylation to proceed in high ee while facilitating a more general substrate synthesis. This methodology was applied in the same report to the preparation of the isomeric enantioenriched *gem*-disubstituted tetrahydropyrimidin-4-ones (**16**).

1.2 PALLADIUM-CATALYZED DECARBOXYLATIVE ASYMMETRIC ALLYLIC ALKYLATION OF 1,4-DIAZEPAN-5-ONES

Figure 1.2.1. Representative pharmaceuticals containing a diazepane-derived ring system.

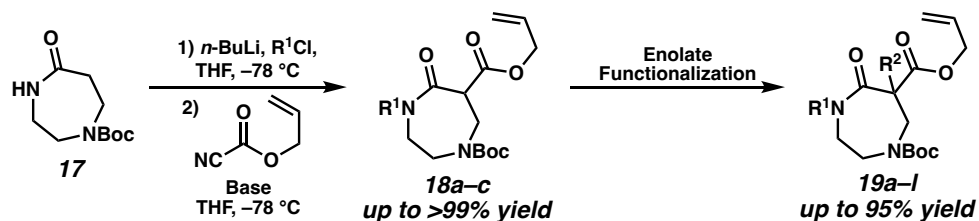


Seeking to expand the accessible chemical space of chiral *gem*-disubstituted heterocycles with potential applications in medicinal chemistry, we identified 1,4-diazepanes as an underutilized substrate class. Diazepanes are common structural motifs found in a variety of pharmaceuticals (Figure 1.2.1), including the benzodiazepine anxiolytics,⁸ the antipsychotic clozapine,⁹ and the anti-insomnia drug suvorexant.¹⁰ Notably, many of these compounds lack Csp³ complexity. Suvorexant is a notable

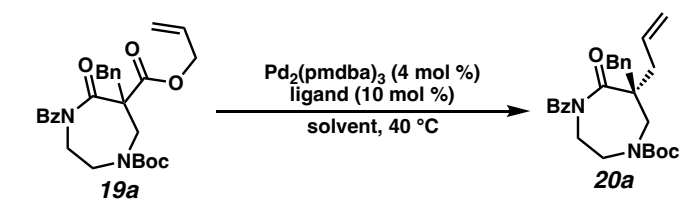
exception as the only FDA-approved drug to date bearing a stereodefined chiral center in a diazepane ring.

The lack of stereochemically complex diazepanes in the drug landscape, especially those bearing all-carbon quaternary stereocenters, is likely due to a lack of asymmetric methods available for their synthesis, leading to a reliance on kinetic resolution, either of a quaternary building block or of the diazepane itself.¹¹ The efficient and enantioselective incorporation of *gem*-disubstitution into diazepane heterocycles could enable the development of pharmaceutical agents with enhanced properties, due to the precedented benefits of increasing saturation in drug molecules.^{5,6} Furthermore, increasing substitution on the diazepane ring could potentially block metabolically labile sites, thus improving the pharmacokinetic profile of a drug candidate. Palladium-catalyzed decarboxylative asymmetric allylic alkylation represents a promising method for the synthesis of enantioenriched *gem*-disubstituted diazepane derivatives.

Starting from the commercially available *N*-Boc diazepanone **17**, substrates were readily accessible in a 3-step sequence analogous to that previously reported by our group (Scheme 1.2.2).^{3c} *N*-Acylation of **17** with an acyl chloride, followed by *C*-acylation with allyl cyanofornate, yielded allyl esters **18a–c**. It is notable that this enolate acylation proceeded smoothly despite the presence of a potential carbamate leaving group at the amide β -position. Subsequent functionalization of **18a–c** was conducted with a variety of electrophiles, providing substrates **19a–l** which bear diverse functional groups. The divergence put in place by late-stage functionalization of dicarbonyls **18** could enable rapid analoging in the context of medicinal chemistry.

Scheme 1.2.2. Synthetic route to diazepanone-derived allyl β -amidoesters **19a–l**.

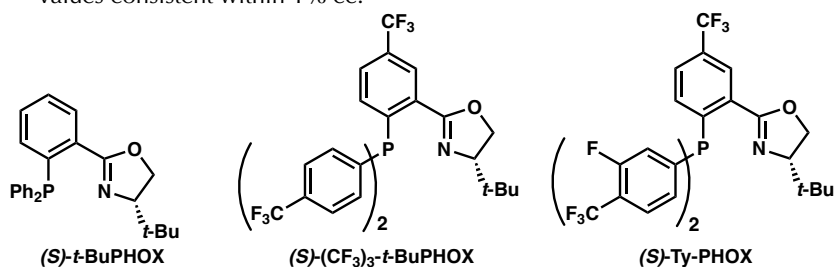
We began by examining conditions for the asymmetric allylic alkylation of diazepanone **19a** ($\text{R}^2 = \text{Bn}$), utilizing $\text{Pd}_2(\text{pmdba})_3$ as a palladium source and (*S*)- $(\text{CF}_3)_3$ -*t*-BuPHOX as a chiral ligand (Table 1.2.3). Polar solvents and toluene led to only modest ee of product **20a** (entries 1–4). In prior research by our laboratory, 2:1 hexanes/toluene proved to be an effective solvent system for achieving high ee with a variety of lactam substrates.^{3c} Indeed, compound **20a** was obtained in 87% ee under these conditions (entry 6). Finally, we were pleased to discover that an even more nonpolar solvent, methylcyclohexane,¹² further enhanced enantioselectivity, yielding **20a** in 89% ee (entry 9). Despite its lack of polarity, methylcyclohexane affords homogeneous reaction mixtures. While examining reaction conditions, we also discovered that use of the highly electron-deficient ligand (*S*)-Ty-PHOX¹³ resulted in reduced ee (entry 8). This is in contrast with previous results indicating that more electron-deficient ligands often lead to higher enantioselectivity in related systems.^{3b–c} Using a more electron-rich ligand, (*S*)-*t*-BuPHOX, also sharply decreased the ee of the product (entry 11).

Table 1.2.3. Reaction optimization.^a


entry	solvent	ligand	ee ^b (%)
1	THF	(S)-(CF ₃) ₃ - <i>t</i> -BuPHOX	20
2	1,4-dioxane	(S)-(CF ₃) ₃ - <i>t</i> -BuPHOX	38
3	MTBE	(S)-(CF ₃) ₃ - <i>t</i> -BuPHOX	70
4	PhCH ₃	(S)-(CF ₃) ₃ - <i>t</i> -BuPHOX	66
5	2:1 hexanes/benzene	(S)-(CF ₃) ₃ - <i>t</i> -BuPHOX	84
6	2:1 hexanes/PhCH ₃	(S)-(CF ₃) ₃ - <i>t</i> -BuPHOX	87 ^c
7	cyclohexane	(S)-(CF ₃) ₃ - <i>t</i> -BuPHOX	88
8	cyclohexane	(S)-Ty-PHOX	80
9	methylcyclohexane	(S)-(CF ₃) ₃ - <i>t</i> -BuPHOX	89 ^c
10	2:1 methylcyclohexane/PhCH ₃	(S)-(CF ₃) ₃ - <i>t</i> -BuPHOX	86
11	methylcyclohexane	(S)- <i>t</i> -BuPHOX	50

[a] Reaction optimization was performed on a 0.01-0.02 mmol scale.

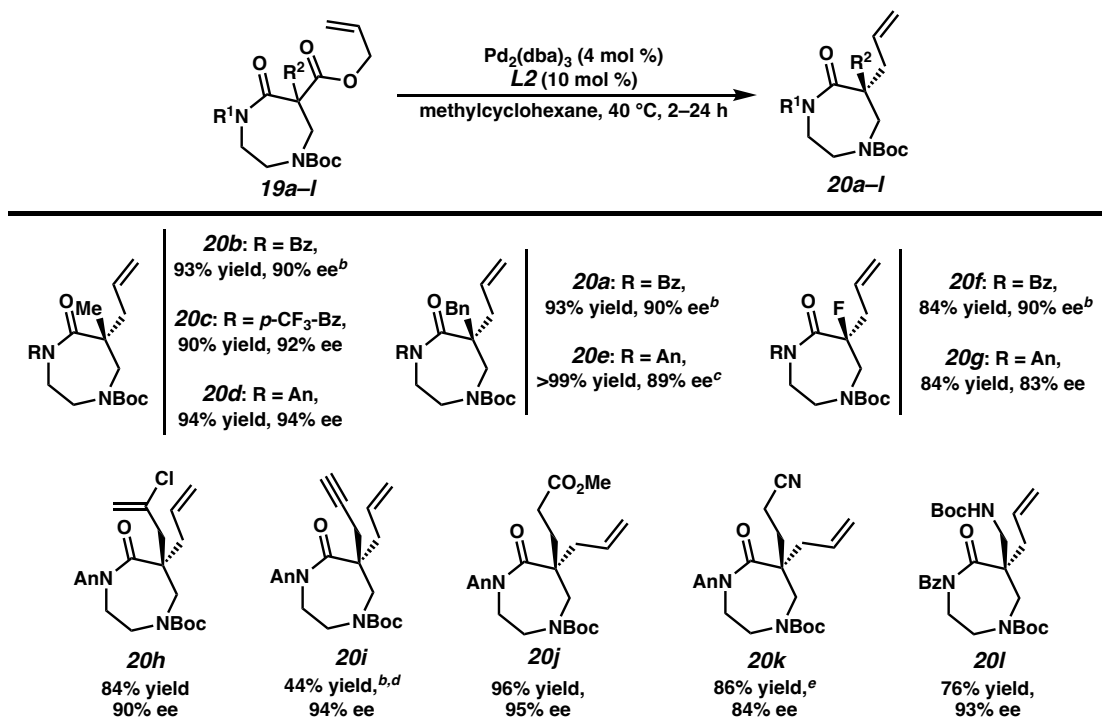
[b] Values determined by chiral SFC analysis. [c] Average over 4 trials, values consistent within 1% ee.



We then applied the optimized reaction conditions to a variety of diazepanone substrates (Table 1.2.4). First, the effect of the electronics of the lactam protecting group on the reaction outcome was investigated. Switching from a benzoyl group (**20b**) to a more electron-poor *p*-CF₃-benzoyl group (**20c**) had a minor effect on enantioselectivity. Interestingly, the use of an electron-rich *p*-anisoyl (An) group delivered product **20d** in an excellent 94% ee. It is worth noting that use of the *p*-anisoyl protecting group was not beneficial to enantioselectivity in all cases (**20a/20e**, **20f/20g**) and was often on par with the unsubstituted benzoyl group. A variety of functional groups at the quaternary carbon

were tolerated, including groups bearing an alkenyl chloride (**20h**) and a *tert*-butyl carbamate (**20i**). This method also proved reliable for the formation of tertiary alkyl fluorides (**20f**, **20g**). The low yield of propargyl lactam **20i** and the necessity for elevated reaction temperatures are also noteworthy—allylic alkylation of other α -propargyl lactams studied by our group has proceeded smoothly.^{3e} It is possible that the geometry of the diazepanone substrate promotes coordination of the alkyne to palladium, hindering the desired reactivity. Additionally, this method allowed for the preparation of benzoyl lactam **20e** on a 1 mmol scale, albeit in somewhat diminished yield and ee (see Table 1.2.4, footnote c).

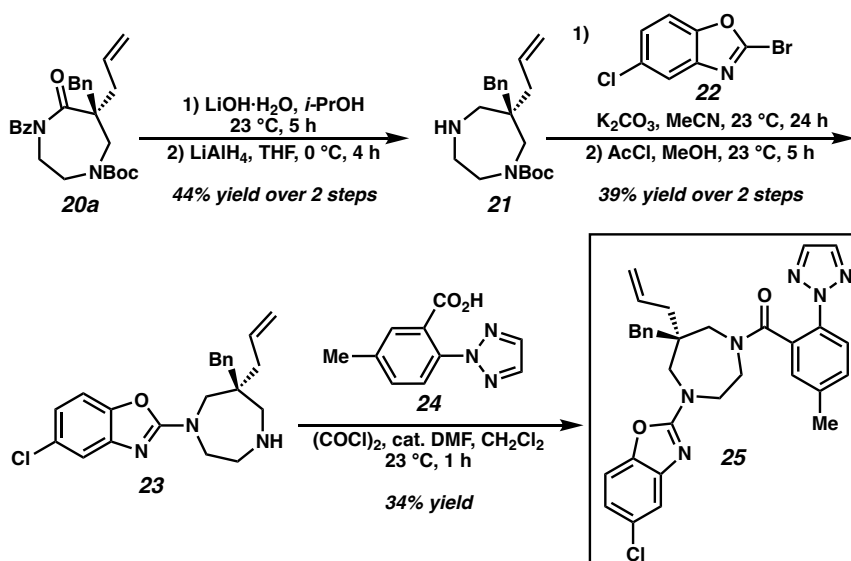
Table 1.2.4. 1,4-Diazepan-5-one substrate scope.^a



[a] Reactions were performed on a 0.1 mmol scale at a 0.014 M concentration. An = *p*-anisoyl. [b] $\text{Pd}_2(\text{pmdba})_3$ was used instead of $\text{Pd}_2(\text{dba})_3$. [c] 1 mmol scale: 82% yield, 83% ee. [d] Conducted at 50 °C for 17 h. [e] Performed in 9:1 methylcyclohexane/PhCH₃ to improve substrate solubility.

Having demonstrated the functional group tolerance of this methodology, we performed a short synthesis of an enantioenriched quaternary stereocenter-containing analogue of suvorexant, an FDA-approved sedative used to treat insomnia (Scheme 1.2.5). Diazepanone **20a** was subjected to selective debenzoylation under basic conditions, followed by reduction with LiAlH_4 to yield diazepane **21** bearing a free secondary amine. Then, nucleophilic aromatic substitution of aryl bromide **22** with **21**, followed by Boc deprotection with in situ generated HCl furnished secondary amine **23**. A final coupling with the benzoyl chloride derived from carboxylic acid **24**¹⁴ in the same pot provided target compound **25**, an analogue of suvorexant bearing an all-carbon quaternary stereocenter. The rapid synthesis of this drug analogue illustrates the ease with which *gem*-substituted diazepane units can be incorporated into pharmaceutically relevant molecules to produce new agents with potentially improved biological properties.

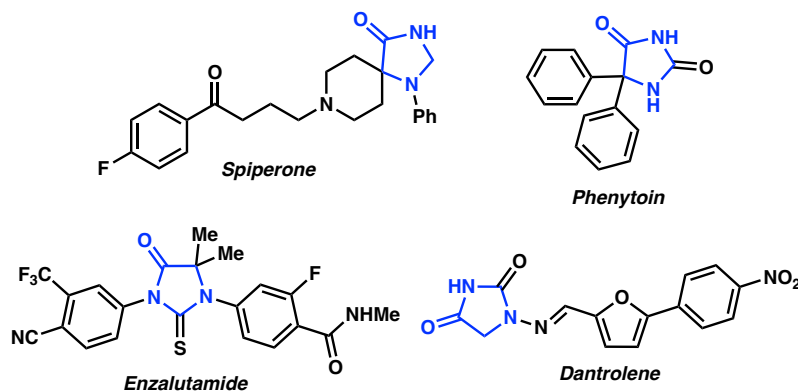
Scheme 1.2.5. Synthesis of a suvorexant analogue.



1.3 PALLADIUM-CATALYZED DECARBOXYLATIVE ASYMMETRIC ALLYLIC ALKYLATION OF 4-IMIDAZOLIDINONES

With a robust strategy for the synthesis of quaternary-substituted 7-membered diazepanones by Pd-catalyzed decarboxylative asymmetric allylic alkylation having been developed, our attention was drawn to the related 5-membered 4-imidazolidinone substrate class, which also occurs in pharmaceuticals (Figure 1.3.1). Interestingly, several of these pharmaceuticals, such as spiperone, bear a fully substituted (albeit achiral) tertiary carbon atom at the 5-position of the heterocycle.

Figure 1.3.1. Representative pharmaceuticals bearing a 4-imidazolidinone moiety.



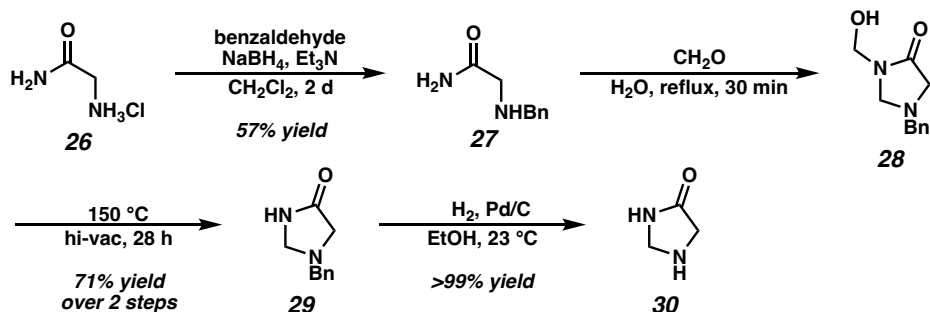
Given the prevalence of this substitution pattern, we reasoned that drug design would potentially benefit from a method that delivers chiral 4-imidazolidinones bearing fully substituted tertiary stereocenters. 4-Imidazolidinones have also been used as chiral auxiliaries in the preparation of artificial amino acids¹⁵ and have found applications in popular organic catalysts,¹⁶ but to our knowledge, preparation of these species has been largely restricted to processes involving the use of chiral pool materials or kinetic resolution.

While 4-imidazolidinone is commercially available, it is prohibitively expensive (>\$100 /g for the hydrochloride salt from Combi Blocks at the time of writing). We thus set

out to develop a scalable synthesis of imidazolidinone allylic alkylation substrates. Although these heterocycles appear trivial to prepare at first glance, the development of a practical synthetic route proved to be quite challenging.

A synthetic route to unsubstituted imidazolidinone **30** was published in 1988 by Pinza and coworkers (Scheme 1.3.2).¹⁷ Glycinamide hydrochloride (**26**) was subjected to benzylation by reductive amination with benzaldehyde to provide secondary amine **27**. Cyclization with formaldehyde proceeded rapidly, but over-addition was observed, and hemiaminal **28** was isolated. Heating under vacuum provided *N*-benzyl imidazolidinone **29** in reasonable yield. Finally, removal of the undesired benzyl protecting group by hydrogenolysis furnished 4-imidazolidinone **30** in quantitative yield.

Scheme 1.3.2. Pinza's route to imidazolidinone.^a

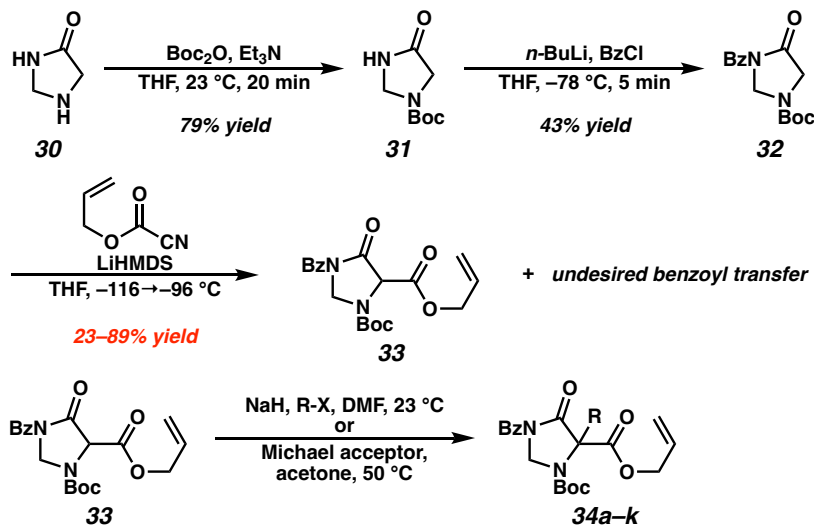


[a] Reported yields were obtained in our laboratory.

After replicating Pinza's synthesis of 4-imidazolidinone, we set out to derivatize this compound and prepare substrates for Pd-catalyzed decarboxylative asymmetric allylic alkylation (Scheme 1.3.3). Beginning with 4-imidazolidinone **30**, Boc protection proceeded smoothly to provide carbamate **31** in high yield. Subsequent benzylation with *n*-BuLi and BzCl provided fully protected heterocycle **32**, albeit in mediocre yield. Acylation of **32** proved to be challenging. The enolate of this compound is highly reactive

and nucleophilic, as evidenced by its putative intractable addition into the benzoyl protecting group of another equivalent of starting material. This pathway dominates even at $-78\text{ }^{\circ}\text{C}$, precluding the isolation of desired allyl ester **33**. Only by cooling the base solution to $-116\text{ }^{\circ}\text{C}$ and allowing the THF solvent to begin to freeze during dropwise addition of the starting material, followed by warming the enolate solution to $-96\text{ }^{\circ}\text{C}$ prior to electrophile addition, was desired product **33** produced. Unfortunately, this reaction exhibited highly variable yields, particularly when conducted on a larger scale. The yields obtained were generally in the range of 23–50%, but sometimes reached as high as 89%. Overall, key intermediate **33** could be obtained by this route in 8 steps from glycineamide hydrochloride **26** in 3–12% overall yield.

Scheme 1.3.3. Initial synthesis of imidazolidinone allylic alkylation substrates.

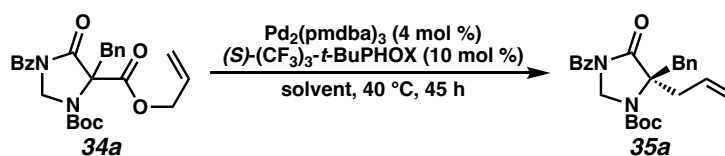


While this route suffered from excessive length and inconsistency, access to **33** nevertheless enabled us to begin evaluating the Pd-catalyzed decarboxylative asymmetric allylic alkylation of 4-imidazolidinone substrates. Treatment of **33** with NaH or K_2CO_3 and

an appropriate electrophile enabled the expedient preparation of diverse allylic alkylation substrates **34a–k**.

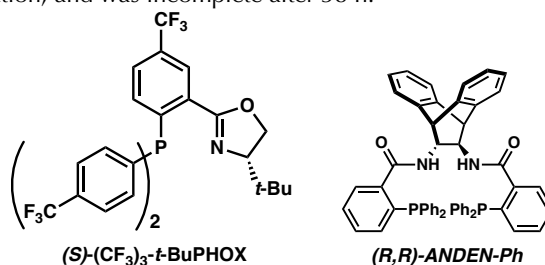
A brief solvent evaluation (Table 1.3.4) revealed that while ethereal and aromatic solvents predictably led to low to moderate enantioselectivities (entries 1–4), our group's conditions for the Pd-catalyzed decarboxylative asymmetric allylic alkylation of analogous tetrahydropyrimidin-4-ones^{3c} employing 2:1 hexanes/PhCH₃ led to 91% ee. Distinct allylic alkylation conditions developed by Trost and coworkers were also tested,^{4c} but led to low ee and sluggish reactivity (entry 6).

Table 1.3.4. Reaction optimization.^a



entry	solvent	ee ^b (%)
1	THF ^c	51
2	1,4-dioxane	68
3	benzene	89
4	PhCH ₃	87
5	2:1 hexanes/PhCH ₃	91
6 ^d	1,4-dioxane	-43

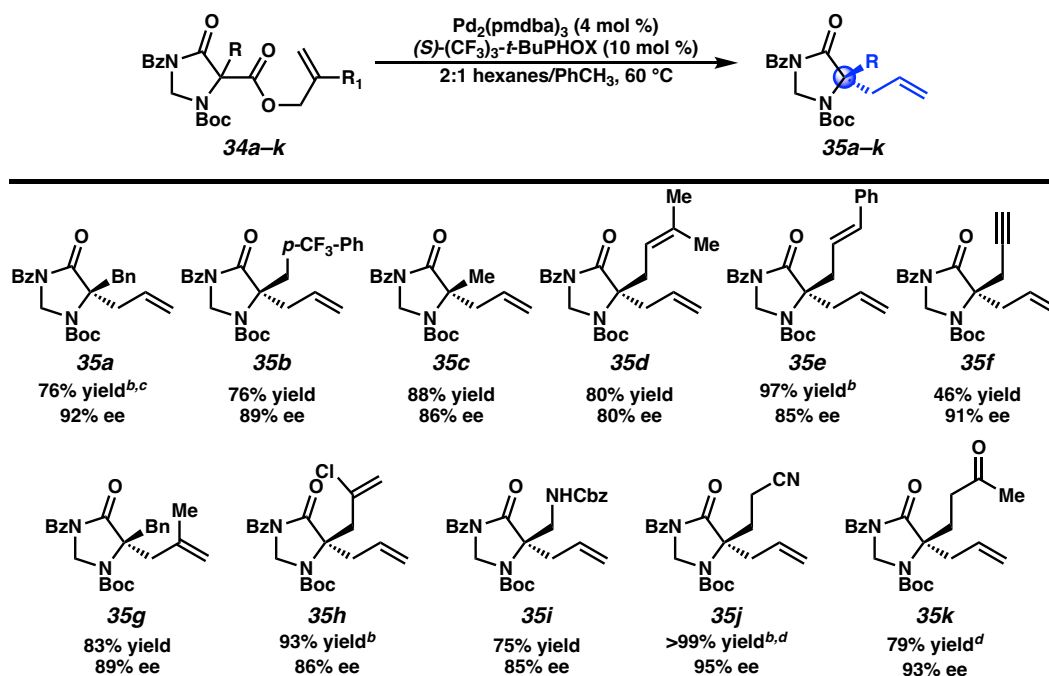
[a] Reaction optimization was performed on a 0.01 mmol scale at 0.014 M concentration. Reactions proceeded to completion unless otherwise noted. [b] Values determined by chiral SFC analysis. [c] Reaction incomplete after 45 h. [d] (*R,R*)-ANDEN-Ph Trost ligand (12 mol %) was used in place of (*S*)-(CF₃)₃-*t*-BuPHOX. Reaction was conducted at 60 °C and 0.1 M concentration, and was incomplete after 38 h.



We were pleased to discover that applying the optimal conditions from Table 1.3.4 to a variety of substrates furnished chiral *gem*-disubstituted 4-imidazolidinones **35a–k** in

high yields and levels of ee (Table 1.3.5). Various nonpolar side chains proved to be well-tolerated, such as benzyl (**35a**), *p*-trifluoromethylbenzyl (**35b**), methyl (**35c**), prenyl (**35d**), and cinnamyl (**35e**) groups. A propargyl group was also tolerated with high enantioselectivity (**35f**), albeit with a reduction in yield. We were pleased to observe that the reaction proceeded smoothly with a methyl group at the 2-position of the allyl fragment (**35g**). Lastly, several polar functional groups were also well-tolerated in the allylic alkylation (**35h–k**), including an alkenyl chloride and a carbamate. In particular, nitrile substrate **35j** was obtained in quantitative yield and an excellent 95% ee.

Table 1.3.5. Imidazolidinone substrate scope.^a



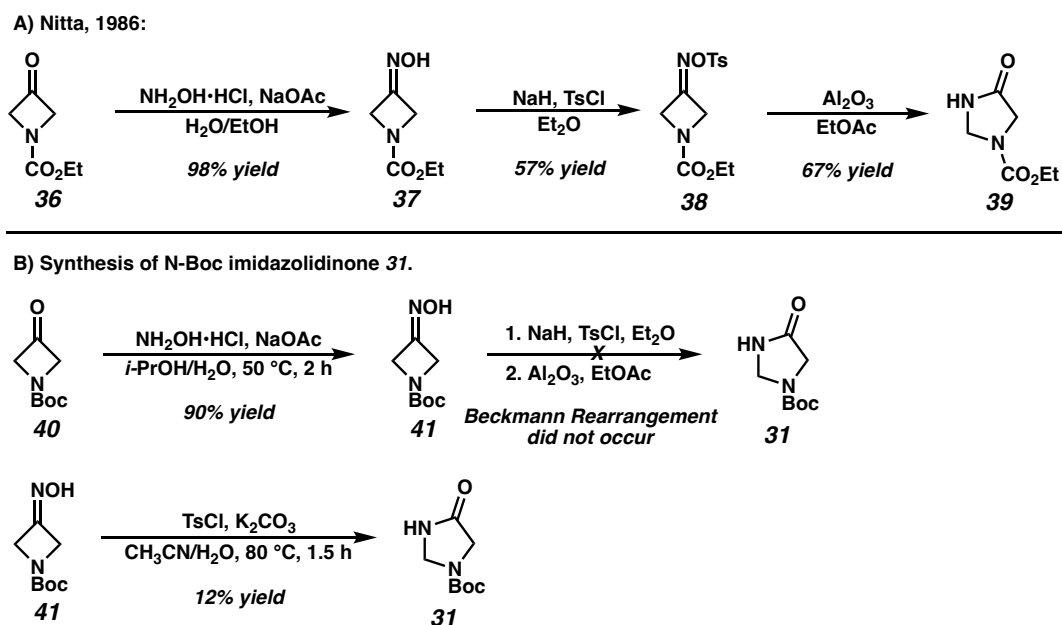
[a] Reactions were performed on a 0.1 mmol scale at 0.014 M concentration. ee values were determined by chiral SFC analysis. [b] Conducted at 40 °C. [c] 1.86 mmol scale: 86% yield, 95% ee. [d] $\text{Pd}_2(\text{dba})_3$ was used instead of $\text{Pd}_2(\text{pmdba})_3$ to facilitate product purification.

With the knowledge that 4-imidazolidinones were a competent substrate class for Pd-catalyzed decarboxylative asymmetric allylic alkylation, we set out to shorten and improve

the synthetic route to these substrates. We were aware of a synthetic route to imidazolidinones relying on the Beckmann rearrangement of 3-azetidiones (Scheme 1.3.6A) and hoped to use this strategy to prepare 1-Boc-4-imidazolidinone **31**, thereby intercepting our existing synthetic route.

Nitta and coworkers prepared *O*-tosyloxime **38** in 2 steps from carbamate **36** and found that this oxime derivative underwent a facile Beckmann rearrangement when simply passed through a column of neutral or basic alumina, yielding imidazolidinone **39**.¹⁸ Analogous oxime **41** was easily accessible from commercially available 3-azetidione **40** in 2 steps (Scheme 1.3.6B), but in our hands, a column of basic alumina was unable to affect rearrangement following tosylation. Incomplete conversion was observed under heating with basic alumina in wet acetone.

Scheme 1.3.6. Beckmann Rearrangement strategies to access 4-imidazolidinones.



We were, however, pleased to discover that free oxime **41** could undergo a 1-pot Beckmann rearrangement with TsCl and K₂CO₃ to deliver product **31** in 12% yield. This

set of conditions was found to be uniquely effective for the Beckmann Rearrangement of **41**, and unfortunately, the yield of this key step could not be increased—imidazolidinone **31** degrades under the reaction conditions. Nevertheless, the low cost of *N*-Boc-3-azetidione **40** enabled the synthetic route depicted in Scheme 1.3.6B to be harnessed to provide enough material to evaluate most of the substrate scope depicted in Table 1.3.5.

Given the poor results of a Beckmann Rearrangement strategy to access key intermediate **31**, we instead began reevaluating cyclization approaches analogous to that of Pinza.¹⁷ Direct treatment of *N*-Boc glycineamide **42** with formaldehyde resulted in no desired cyclization product. Instead, Eschenmoser's Salt, generated in situ from tetramethylmethylenediamine **43**, was envisioned to be a promising formaldehyde equivalent (Scheme 1.3.7). In the presence of an acylating agent, Eschenmoser's Salt **B** could form via loss of an amide from **A**. Nucleophilic attack by substrate **42** could produce intermediate **C**, whose only basic amine could attack another equivalent of acylating agent to provide charged species **D**. This species could eject an amide and produce *N*-acyliminium **E**, which could undergo cyclization, and following deprotonation, yield desired product **31**. Unfortunately, while putative intermediate **C** was observed by mass spectrometry, no desired product was observed under any of the conditions explored (Table 1.3.8).

Scheme 1.3.7. Attempted cyclization employing Eschenmoser's Salt as a formaldehyde equivalent.

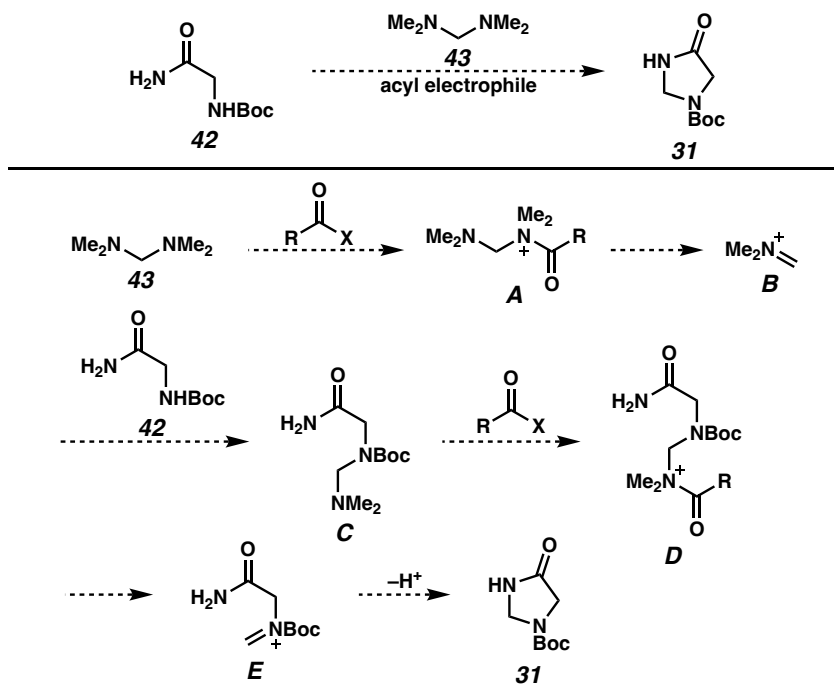
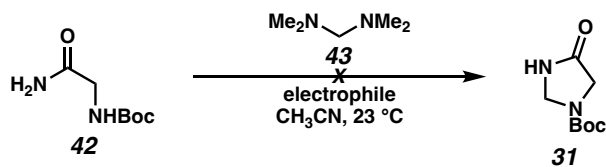


Table 1.3.8. Unsuccessful cyclization employing Eschenmoser's Salt as a formaldehyde equivalent.

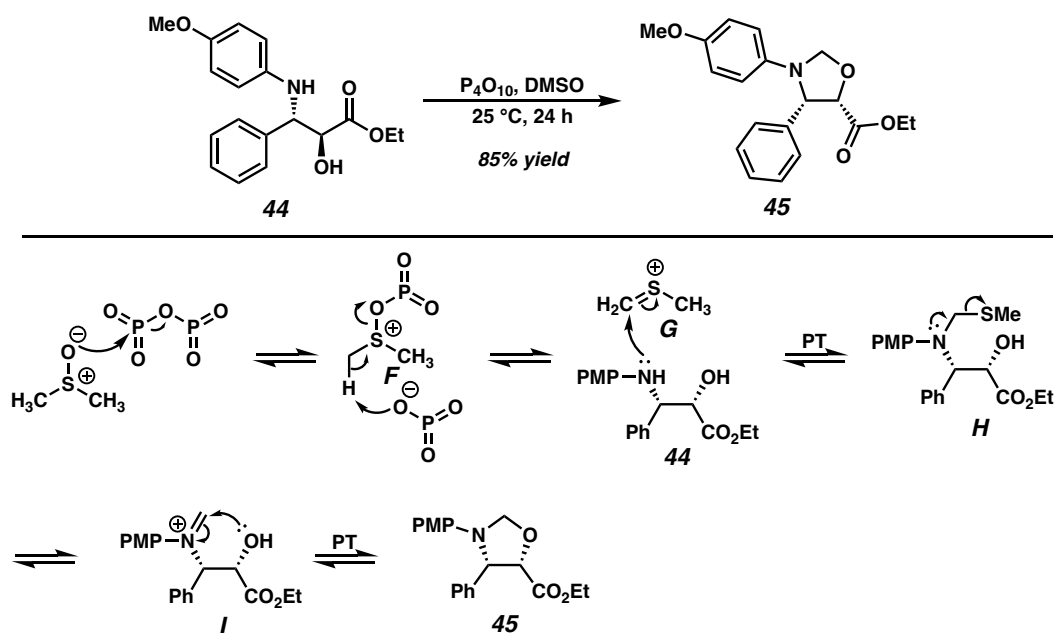


entry	conditions	% yield
1	Ac_2O (2 equiv)	0
2	AcCl (2 equiv), K_2CO_3	0
3	Ac_2O (1 equiv), <i>then</i> MeI	0
4	TFAA (2 equiv), K_2CO_3	0

Reluctant to abandon a cyclization approach to key intermediate **31**, we began to explore other formaldehyde equivalents and became aware of a report that showed promise in our system. In 2007, Kayser and coworkers disclosed that amino alcohol **44**, when

subjected to activated DMSO oxidation conditions, failed to deliver the desired 1,2-dicarbonyl product, instead furnishing oxazolidine **45** in high yield (Scheme 1.3.9).¹⁹ Phosphorous pentoxide was a uniquely effective activating agent for this transformation. Mechanistically, Kayser and coworkers propose that activation of DMSO with phosphorous pentoxide leads to intermediate **F**. Deprotonation with concomitant loss of PO_3^- provides sulfenium ion **G**, a key intermediate in the Pummerer Rearrangement and the MTM protection of alcohols.²⁰ Trapping of this ion by the aniline moiety of **44** is thought to produce methylthiomethylaniline **H**, which can eject methanethiolate, leading to iminium ion **I**. A final cyclization and proton transfer yields oxazolidine **45**.

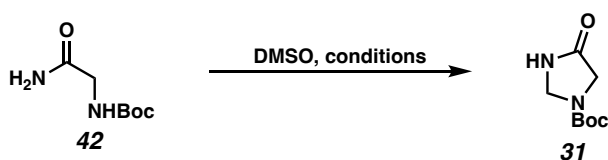
Scheme 1.3.9. Cyclization of an amino alcohol with activated DMSO (Kayser).



Hopeful that the sulfonium ion **G** derived from activated DMSO could also affect the cyclization of carbamate **42**, we subjected this compound to the conditions reported by Kayser and coworkers (Table 1.3.10) and were pleased to observe a 9% yield of product **31** (entry 1). P_4O_{10} proved to be uniquely effective in promoting this transformation. Two

sets of conditions for the α -methylenation of ketones resulted in only decomposition (entries 5, 6).^{20,21} Interestingly, Ac₂O resulted in no reaction even at 60 °C, despite its precedent as a popular DMSO activating agent for the MTM protection of alcohols (entry 3).²² Unfortunately, yields higher than 13% (entry 2) were never observed. Hence, a strategically different approach to access imidazolidinone **31** was necessitated.

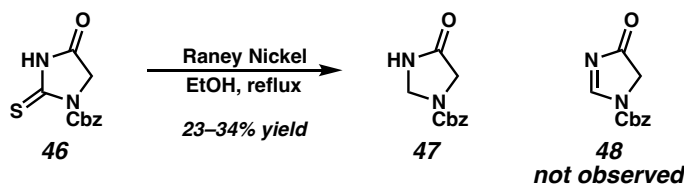
Table 1.3.10. Cyclization employing activated DMSO as a methylene equivalent.



entry	conditions	% yield
1	P ₄ O ₁₀ (2 equiv), 1.5 h, 23 °C	9
2	P ₄ O ₁₀ (1.1 equiv), 20 h, 23 °C	13
3	Ac ₂ O, 60 °C	NR
4	TFAA, NaH or Et ₃ N, 23 °C	0
5	K ₂ S ₂ O ₈ , NaOAc, 120 °C	0 (decomp)
6	PhI(OAc) ₂ , Na ₂ CO ₃ , 120 °C	0 (decomp)
7	POCl ₃ , Et ₃ N, 23 °C	trace

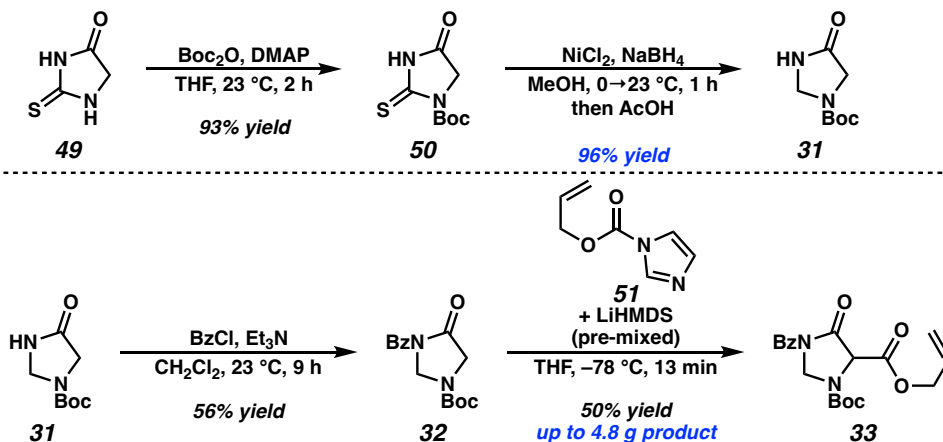
In 1957, Witkop and coworkers reported that when 2-thiohydantoin derivative **46** was subjected to desulfurization conditions with Raney Nickel, the undesired 4-imidazolidinone **47** was obtained in poor yields (Scheme 1.3.11).²³ The desired imidazolone **48** was not detected. Pinza later reported that Witkop's reaction was hard to reproduce and consistently low-yielding.¹⁷ However, aware of the success of nickel boride-promoted reductive desulfurization of other cyclic thioureas,²⁴ including aryl-substituted imidazolidinones,²⁵ we began to develop an improved route to 4-imidazolidinones from thiohydantoin (Scheme 1.3.12).

Scheme 1.3.11. Previous desulfurization of a protected thiohydantoin (Witkop).



A preceded Boc protection of inexpensive 2-thiohydantoin **49** provided carbamate **50**, which bears similarity to Witkop's substrate **46**.²⁶ Subjecting **50** to nickel boride-mediated reductive desulfurization conditions provided key 4-imidazolidinone intermediate **31**. Direct quenching of this reaction with glacial acetic acid to dissolve insoluble byproducts followed by filtration and biphasic extraction enabled the preparation of **31** in multi-gram quantities and in excellent yield, with no chromatography.

Scheme 1.3.12. Concise and high-yielding route to key allyl ester **33**.

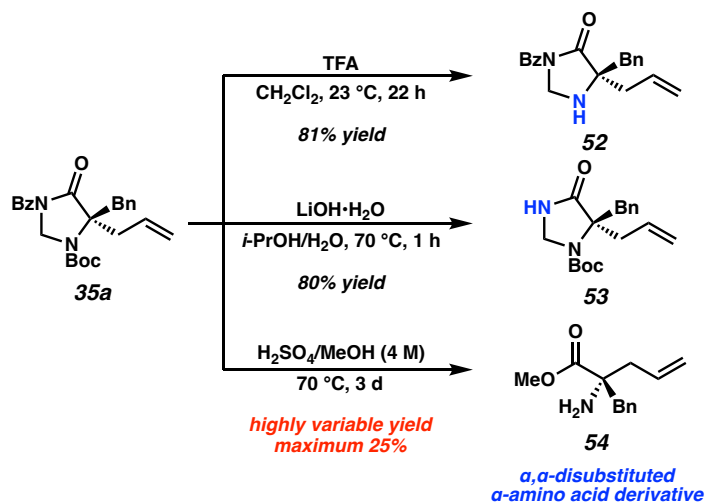


Then, yields for the benzoyl protection of free lactam **31** were improved by switching to milder conditions, providing imide **32**. Previously, acylation of **32** using LiHMDS and allyl cyanofornate proved challenging and resulted in inconsistent yields due to the high reactivity of the enolate intermediate (vide supra). It was discovered that by switching to acylimidazole electrophile **51**, the electrophile and base were stable when

pre-mixed at $-78\text{ }^{\circ}\text{C}$, and addition of starting material to the electrophile-base mixture provided target allyl ester **33** in 50% yield, which was consistent upon scale-up to produce 4.8 g of **33**. The new synthetic route depicted in Scheme 1.3.12 generates key intermediate **33** in 25% overall yield over only 4 steps.

Having demonstrated the broad functional group tolerance of the reported method, we sought to explore the feasibility of further functionalization of the 4-imidazolidinone products (Scheme 1.3.13). The selective removal of either protecting group would likely prove essential for applications in medicinal chemistry. Toward this end, treatment of chiral benzyl imidazolidinone **35a** with TFA led to facile Boc cleavage, affording free secondary amine **52**. Similarly, treatment of **35a** with lithium hydroxide readily affected benzoyl group removal, providing free lactam **53**.

Scheme 1.3.13. Product transformations.



At the outset of this research, we had planned to explore the conversion of 4-imidazolidinone allylic alkylation products **35a–k** to useful derivatives of biologically relevant and synthetically challenging α,α -disubstituted α -amino acids.²⁷ Imidazolidinones

were envisioned as surrogates for these desirable compounds based on prior examples of imidazolidinone chiral auxiliary-based strategies to access α,α -disubstituted α -amino acids,¹⁵ as well as our own group's preparation of α -quaternary substituted β -amino acids from the analogous tetrahydropyrimidinones.^{3c} Unfortunately, the presence of olefinic functionality hampered the feasibility of converting **35a–k** into amino acid derivatives due to the harsh conditions required for ring opening. Despite extensive experimentation, the highest-yielding conditions identified for the conversion of imidazolidinone **35a** to amino ester **54** (H₂SO₄/MeOH) provided highly variable results, with the maximum observed yield of **54** being only 25%.

1.4 CONCLUSION

1,4-Diazepan-5-ones and 4-imidazolidinones bearing *gem*-disubstitution were prepared in moderate to high levels of yield and enantioselectivity by palladium-catalyzed decarboxylative asymmetric allylic alkylation. Applying this methodology to these nitrogen-rich substrate classes enabled access to enantioenriched diazaheterocycles bearing diverse functionality. As illustrated by our synthesis of suvorexant analogue **25** (Scheme 1.2.5) and the demonstrated orthogonality of the imidazolidinone protecting groups (Scheme 1.3.13), the chemistry reported herein can be adapted for applications in drug design.

1.5 EXPERIMENTAL SECTION

1.5.1 MATERIALS AND METHODS

Unless otherwise stated, reactions were performed in flame-dried glassware under an argon or nitrogen atmosphere using dry, deoxygenated solvents. Solvents were dried

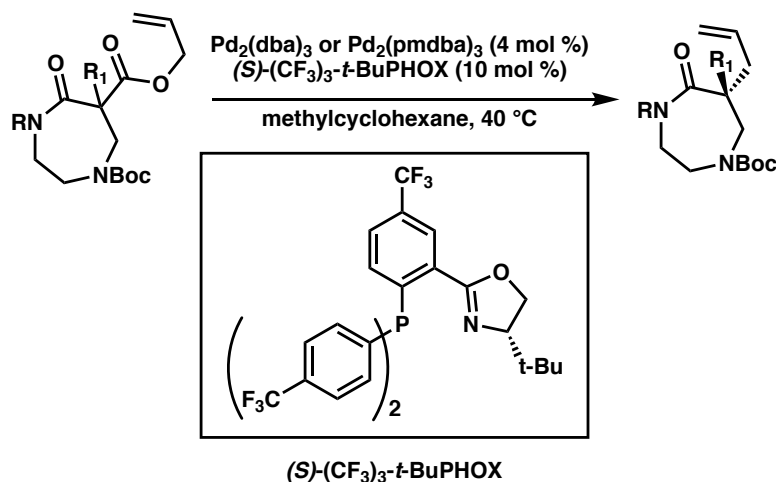
by passage through an activated alumina column under argon.²⁸ Reaction progress was monitored by thin-layer chromatography (TLC) or Agilent 1290 UHPLC-MS. TLC was performed using E. Merck silica gel 60 F254 precoated glass plates (0.25 mm) and visualized by UV fluorescence quenching or KMnO₄ staining. Silicycle SiliaFlash® P60 Academic Silica gel (particle size 40–63 nm) was used for flash chromatography. ¹H NMR spectra were recorded on Varian Inova 500 MHz, Varian 400 MHz, and Bruker 400 MHz spectrometers and are reported relative to residual CHCl₃ (δ 7.26 ppm). ¹³C NMR spectra were recorded on a Varian Inova 500 MHz spectrometer (125 MHz), a Varian 400 MHz spectrometer (100 MHz), and Bruker 400 MHz spectrometers (100 MHz) and are reported relative to CHCl₃ (δ 77.16 ppm). Data for ¹H NMR are reported as follows: chemical shift (δ ppm) (multiplicity, coupling constant (Hz), integration). Multiplicities are reported as follows: s = singlet, d = doublet, t = triplet, q = quartet, p = pentet, sept = septuplet, m = multiplet, br s = broad singlet, br d = broad doublet. Data for ¹³C NMR are reported in terms of chemical shifts (δ ppm). Some reported spectra include minor solvent impurities of water (δ 1.56 ppm), ethyl acetate (δ 4.12, 2.05, 1.26 ppm), methylene chloride (δ 5.30 ppm), acetone (δ 2.17 ppm), grease (δ 1.26, 0.86 ppm), and/or silicon grease (δ 0.07 ppm), which do not impact product assignments. Most NMR spectra are complicated by rotational isomerism about amide bonds. This behavior is illustrated by variable-temperature NMR spectra of compound **20e** in DMSO (p. 183). IR spectra were obtained by use of a Perkin Elmer Spectrum BXII spectrometer or Nicolet 6700 FTIR spectrometer using thin films deposited on NaCl or KBr plates and reported in frequency of absorption (cm⁻¹). Optical rotations were measured with a Jasco P-2000 polarimeter operating on the sodium D-line (589 nm), using a 100 mm path-length cell. Analytical SFC was performed with a Mettler

SFC supercritical CO₂ analytical chromatography system utilizing Chiralpak (AD-H, AS-H or IC) or Chiralcel (OD-H, OJ-H, or OB-H) columns (4.6 mm x 25 cm) obtained from Daicel Chemical Industries, Ltd. High resolution mass spectra (HRMS) were obtained from Agilent 6200 Series TOF with an Agilent G1978A Multimode source in electrospray ionization (ESI+), atmospheric pressure chemical ionization (APCI+), or mixed ionization mode (MM: ESI-APCI+), or from the Caltech Mass Spectrometry Laboratory using a JMS-600H High Resolution Mass Spectrometer in fast atom bombardment (FAB+) mode. Absolute stereochemistry is assigned by analogy to previous results by our group.³

Reagents were purchased from commercial sources and used as received unless otherwise stated. Ligands (*S*)-(CF₃)₃-*t*-BuPHOX and (*S*)-Ty-PHOX were prepared according to literature procedures.^{29,13}

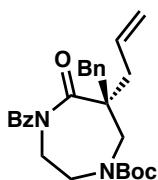
1.5.2 EXPERIMENTAL PROCEDURES

1.5.2.1 General Procedure for Allylic Alkylation of Diazepanones



In a N₂ filled glovebox, Pd₂(dba)₃ (4 mol %) or Pd₂(pmdba)₃ (4 mol %) and (*S*)-(CF₃)₃-*t*-BuPHOX (10 mol %) were suspended in methylcyclohexane (2 mL) in a 20 mL glass vial. After stirring for 20 minutes at 25 °C, the appropriate diazepanone (1.0 equiv)

and methylcyclohexane (5.2 mL, total substrate concentration 0.014 M) were added to the pre-stirred catalyst solution. The vial was then sealed and heated to 40 °C. After full consumption of starting material, as monitored by TLC, the reaction mixture was exposed to air. The crude reaction mixture was loaded directly onto a flash column and the product was isolated by silica gel flash chromatography.

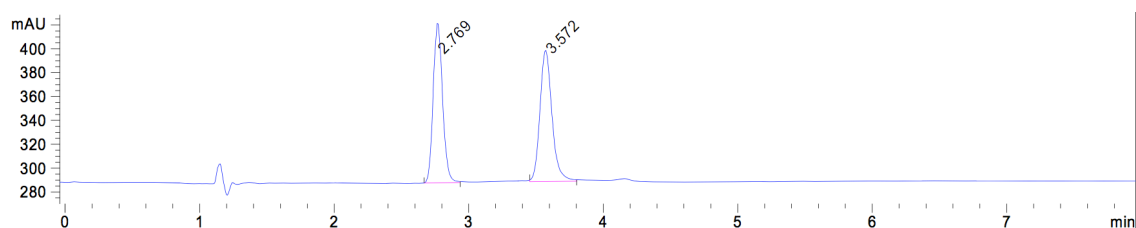
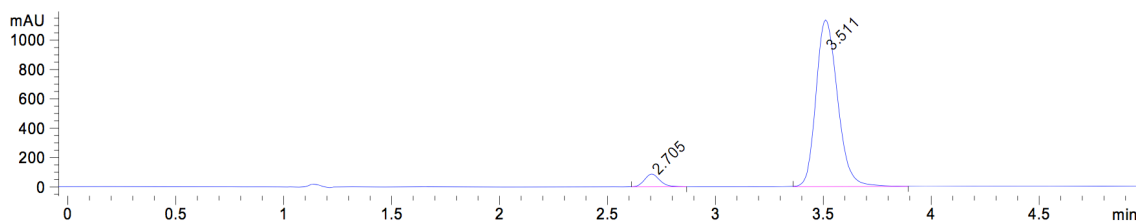


***tert*-butyl (*S*)-6-allyl-4-benzoyl-6-benzyl-5-oxo-1,4-diazepane-1-carboxylate (**20a**)**

Prepared according to the general procedure with allyl ester **19a** (51.2 mg, 0.104 mmol, 1.0 equiv), Pd₂(pmdba)₃ (4.4 mg, 0.004 mmol, 4 mol %), and (*S*)-(CF₃)₃-*t*-BuPHOX (5.9 mg, 0.01 mmol, 10 mol %). Purified by silica gel flash chromatography (15% EtOAc/hexanes) to provide benzyl diazepanone **20a** as a colorless oil (43.4 mg, 0.0967 mmol, 93% yield, 90% ee); ¹H NMR (400 MHz, CDCl₃) δ 7.56 – 7.40 (m, 3H), 7.40 – 7.32 (m, 2H), 7.32 – 7.19 (m, 3H), 7.19 – 7.00 (m, 2H), 5.88 (br s, 1H), 5.26 – 5.07 (m, 2H), 4.26 – 4.03 (m, 1H), 3.94 (d, *J* = 15.4 Hz, 1H), 3.73 (d, *J* = 42.2 Hz, 1H), 3.54 (d, *J* = 15.3 Hz, 1H), 3.40 (s, 2H), 3.09 (dd, *J* = 61.0, 13.7 Hz, 1H), 2.94 – 2.34 (m, 3H), 1.48 (s, 9H); ¹³C NMR (100 MHz, CDCl₃) δ 179.2, 174.8, 156.0, 155.4, 136.6, 136.4, 133.0, 131.5, 130.8, 128.6, 128.4, 127.8, 127.1, 120.0, 119.7, 80.8, 54.3, 53.9, 49.1, 47.4, 46.9, 42.5, 42.0, 41.5, 40.3, 28.5; IR (Neat Film, NaCl) 3062, 2975, 2928, 1693, 1682, 1601, 1452, 1415, 1392, 1365, 1322, 1283, 1246, 1156, 1044, 978, 917, 865, 728, 697 cm⁻¹; HRMS (MM: ESI-APCI): *m/z* calc'd for C₂₇H₃₃N₂O₄ [M+H]⁺: 449.2435, found 449.2429; [α]_D^{22.4}

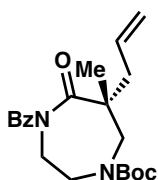
+14.19 (*c* 0.66, CHCl₃); SFC conditions: 20% IPA, 2.5 mL/min, Chiralpak AD-H column,

$\lambda = 210$ nm, t_R (min): major = 3.51, minor = 2.71.



Peak #	RetTime [min]	Type	Width [min]	Area [mAU*s]	Height [mAU]	Area %
1	2.705	BB	0.0782	428.25891	85.91843	5.1370
2	3.511	BB	0.1094	7908.53760	1133.81873	94.8630

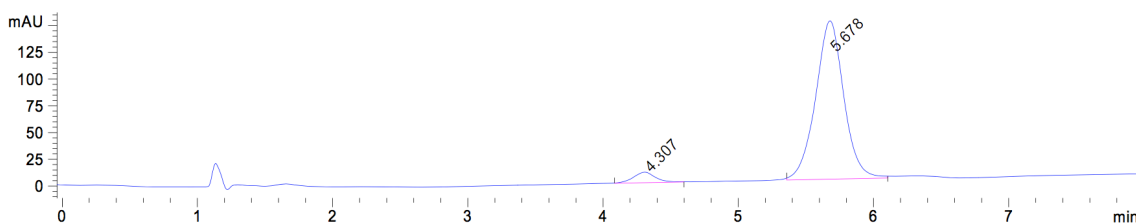
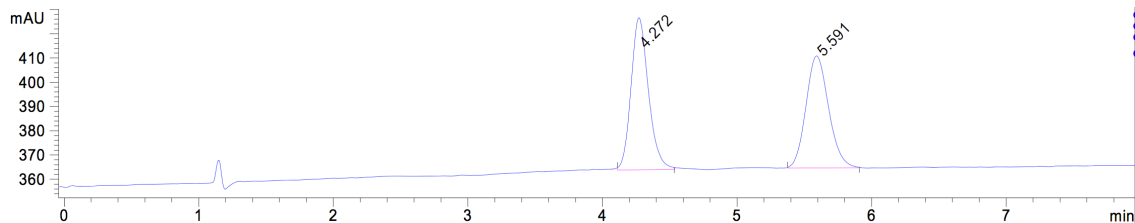
Totals : 8336.79651 1219.73716



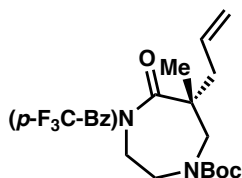
***tert*-butyl (*R*)-6-allyl-4-benzoyl-6-methyl-5-oxo-1,4-diazepane-1-carboxylate (**20b**)**

Prepared according to the general procedure with allyl ester **19b** (39.0 mg, 0.0937 mmol, 1.0 equiv), Pd₂(pmdba)₃ (4.4 mg, 0.004 mmol, 4 mol %), and (*S*)-(CF₃)₃-*t*-BuPHOX (5.9 mg, 0.01 mmol, 10 mol %). Purified by silica gel flash chromatography (20% EtOAc/hexanes) to provide methyl diazepamone **20b** as a colorless, waxy solid (32.3 mg, 0.868 mmol, 93% yield, 90% ee); ¹H NMR (400 MHz, CDCl₃) δ 7.54 – 7.43 (m, 3H), 7.43 – 7.32 (m, 2H), 5.74 (ddt, *J* = 17.1, 9.9, 7.4 Hz, 1H), 5.19 – 5.06 (m, 2H), 4.30 – 3.89 (m,

3H), 3.85 – 3.69 (m, 1H), 3.66 – 3.34 (m, 2H), 2.63 – 2.20 (m, 2H), 1.50 (s, 9H), 1.30 (s, 3H); ¹³C NMR (100 MHz, CDCl₃) δ 180.8, 174.5, 155.4, 155.0, 136.3, 132.9, 131.4, 128.3, 127.5, 119.5, 80.7, 50.9, 49.9, 47.2, 46.5, 42.5, 42.1, 41.8, 28.4, 23.5, 23.1; IR (Neat Film, NaCl) 2976, 2933, 1694, 1450, 1418, 1392, 1366, 1323, 1284, 1246, 1146, 1057, 983, 917, 868, 768, 729, 696 cm⁻¹; HRMS (MM: ESI-APCI): *m/z* calc'd for C₂₁H₂₉N₂O₄ [M+H]⁺: 373.2122, found 373.2117; [α]_D^{22.31} –12.69 (*c* 1.0, CHCl₃); SFC Conditions: 20% IPA, 2.5 mL/min, Chiralpak IC column, λ = 210 nm, *t*_R (min): minor = 4.31, major = 5.68.

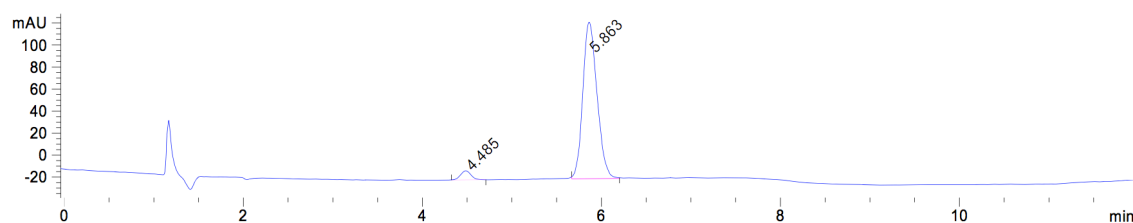
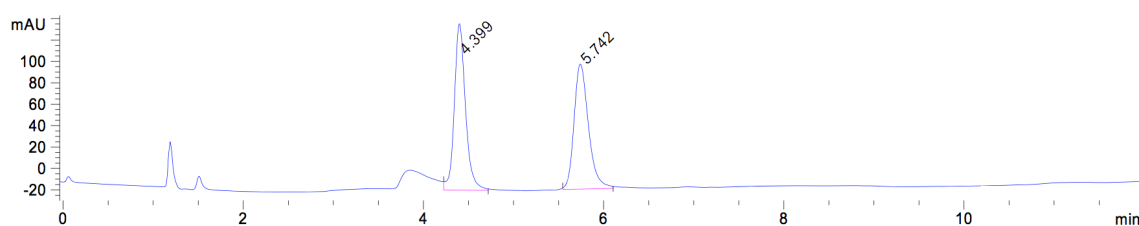


Peak #	RetTime [min]	Type	Width [min]	Area [mAU*s]	Height [mAU]	Area %
1	4.307	BB	0.1717	111.60342	9.88486	4.9364
2	5.678	BB	0.2215	2149.23340	147.92346	95.0636
Totals :				2260.83681	157.80833	

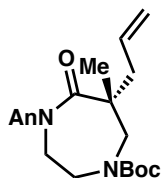


tert-butyl (R)-6-allyl-6-methyl-5-oxo-4-(4-(trifluoromethyl)benzoyl)-1,4-diazepane-1-carboxylate (20c)

Prepared according to the general procedure with allyl ester **19c** (55.3 mg, 0.114 mmol, 1.0 equiv), Pd₂(dba)₃ (4.2 mg, 4.57 μmol, 4 mol %), and (*S*)-(CF₃)₃-*t*-BuPHOX (6.7 mg, 0.011 mmol, 10 mol %). Purified by silica gel flash chromatography (20% EtOAc/hexanes) to provide methyl diazepanone **20c** as a colorless oil (45.1 mg, 0.102 mmol, 90% yield, 92% ee); ¹H NMR (400 MHz, CDCl₃) δ 7.64 (d, *J* = 8.2 Hz, 2H), 7.55 (d, *J* = 8.2 Hz, 2H), 5.71 (ddt, *J* = 17.2, 10.1, 7.4 Hz, 1H), 5.23 – 5.07 (m, 2H), 4.21 – 4.03 (m, 2H), 4.02 – 3.64 (m, 2H), 3.58 – 3.38 (m, 2H), 2.59 – 2.21 (m, 2H), 1.49 (s, 9H), 1.29 (s, 3H); ¹³C NMR (100 MHz, CDCl₃) δ 181.0, 180.8, 173.1, 155.4, 155.1, 140.0, 132.8 (q, *J*_{C-F} = 32.9 Hz), 132.7, 127.6, 125.5 (q, *J*_{C-F} = 3.7 Hz), 123.7 (q, *J*_{C-F} = 272.5 Hz), 119.9, 81.0, 50.9, 50.0, 47.2, 46.4, 42.4, 42.0, 41.8, 28.5, 23.6, 23.3; IR (Neat Film, NaCl) 3366, 3077, 2978, 2934, 1694, 1452, 1410, 1394, 1367, 1326, 1248, 1167, 1147, 1066, 1014, 984, 925, 852, 764 cm⁻¹; HRMS (MM: ESI-APCI): *m/z* calc'd for C₂₂H₃₁F₃N₃O₄ [M+NH₄]⁺: 458.2261, found 458.2250; [α]_D^{22.6} –12.32 (*c* 1.0, CHCl₃); SFC Conditions: 5% IPA, 2.5 mL/min, Chiralpak AD-H column, λ = 210 nm, t_R (min): minor = 4.49, major = 5.86.



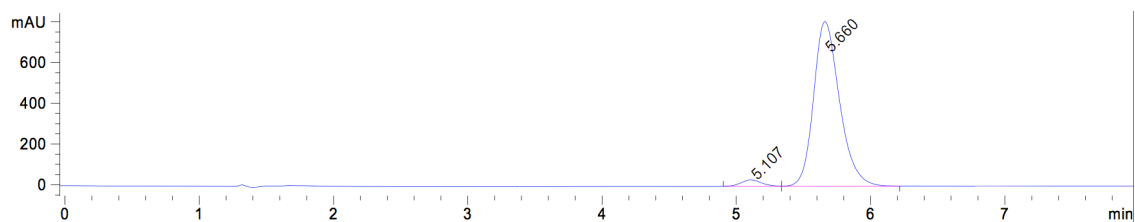
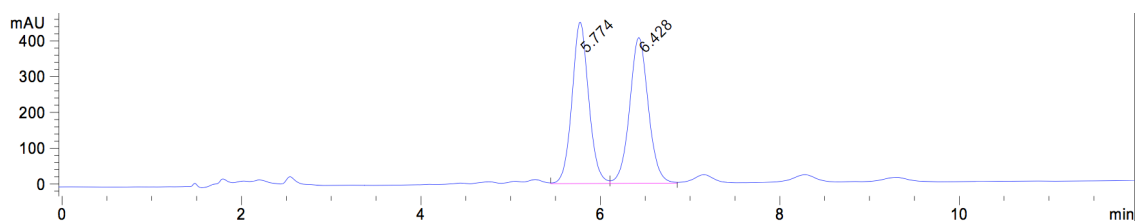
Peak #	RetTime [min]	Type	Width [min]	Area [mAU*s]	Height [mAU]	Area %
1	4.485	BB	0.1259	66.46159	8.25322	4.0582
2	5.863	BB	0.1731	1571.26794	142.02565	95.9418
Totals :				1637.72953	150.27887	



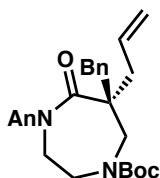
***tert*-butyl (R)-6-allyl-4-(4-methoxybenzoyl)-6-methyl-5-oxo-1,4-diazepane-1-carboxylate (20d)**

Prepared according to the general procedure with allyl ester **19d** (45.8 mg, 0.103 mmol, 1.0 equiv), Pd₂(dba)₃ (3.7 mg, 0.004 mmol, 4 mol %), and (*S*)-(CF₃)₃-*t*-BuPHOX (5.9 mg, 0.01 mmol, 10 mol %). Purified by silica gel flash chromatography (20% EtOAc/hexanes) to provide methyl diazepamone **20d** as a colorless oil (38.9 mg, 0.0966 mmol, 94% yield, 94% ee); ¹H NMR (400 MHz, CDCl₃) δ 7.62 – 7.44 (m, 2H), 6.95 – 6.75 (m, 2H), 5.76 (m, 1H), 5.26 – 4.99 (m, 2H), 4.24 – 3.87 (m, 3H), 3.83 (s, 3H), 3.75 (m, 1H), 3.59 – 3.37 (m, 2H), 2.60 – 2.25 (m, 2H), 1.49 (s, 9H), 1.31 (s, 3H); ¹³C NMR (100

MHz, CDCl₃) δ 180.7, 180.6, 174.3, 162.5, 155.4, 155.0, 133.0, 130.1, 128.1, 119.4, 113.6, 80.7, 55.4, 50.8, 49.8, 47.4, 46.6, 42.7, 42.4, 28.4, 23.5, 23.1; IR (Neat Film, NaCl) 3352, 3076, 2975, 2932, 2841, 2568, 1690, 1605, 1579, 1542, 1511, 1458, 1420, 1392, 1366, 1322, 1284, 1256, 1214, 1168, 1146, 1056, 1032, 984, 924, 868, 842, 807, 762, 743, 736, 650, 633, 621, 608 cm⁻¹; HRMS (MM: ESI-APCI): *m/z* calc'd for C₂₂H₃₁N₂O₅ [M+H]⁺: 403.2227, found 403.2225; [α]_D^{22.45} -40.51 (*c* 1.0, CHCl₃); SFC Conditions: 20% MeOH, 2.5 mL/min, Chiralpak IC column, λ = 210 nm, *t_R* (min): minor = 5.11, major = 5.66.

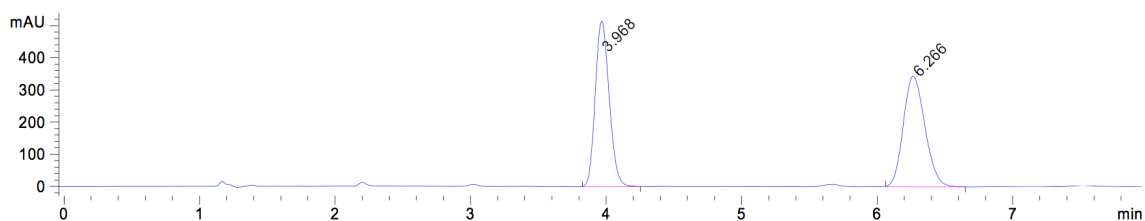


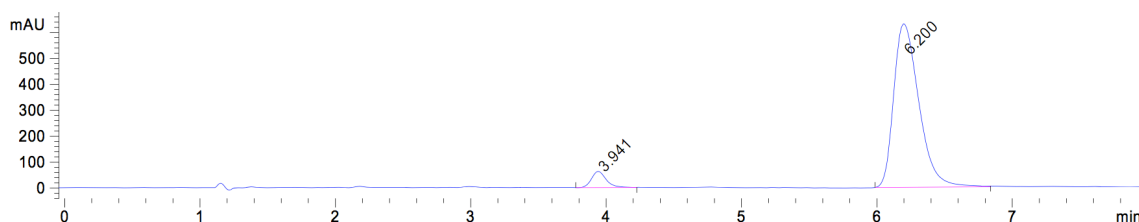
Peak #	RetTime [min]	Type	Width [min]	Area [mAU*s]	Height [mAU]	Area %
1	5.107	BV	0.1655	348.85117	32.42407	3.1027
2	5.660	VB	0.2052	1.08947e4	808.60492	96.8973
Totals :				1.12435e4	841.02899	



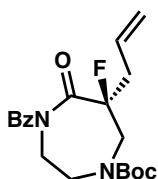
***tert*-butyl (*S*)-6-allyl-6-benzyl-4-(4-methoxybenzoyl)-5-oxo-1,4-diazepane-1-carboxylate (**20e**)**

Prepared according to the general procedure with allyl ester **19e** (52.3 mg, 0.100 mmol, 1.0 equiv), Pd₂(dba)₃ (3.7 mg, 0.004 mmol, 4 mol %), and (*S*)-(CF₃)₃-*t*-BuPHOX (5.9 mg, 0.01 mmol, 10 mol %). Purified by silica gel flash chromatography (20% EtOAc/hexanes) to provide benzyl diazepanone **20e** as a colorless oil (48.1 mg, 0.100 mmol, >99% yield, 89% ee); ¹H NMR (400 MHz, CDCl₃) δ 7.51 – 7.44 (m, 2H), 7.32 – 7.20 (m, 3H), 7.18 – 7.09 (m, 2H), 6.87 – 6.81 (m, 2H), 5.93 (br s, 1H), 5.26 – 5.12 (m, 2H), 4.09 – 3.88 (m, 2H), 3.84 (s, 3H), 3.78 – 2.41 (m, 8H), 1.48 (s, 9H); ¹³C NMR (100 MHz, CDCl₃) δ 179.0, 174.6, 162.6, 156.0, 155.4, 136.7, 133.1, 130.8, 130.5, 128.5, 128.2, 127.0, 119.9, 119.6, 113.7, 80.9, 80.7, 55.5, 54.2, 53.8, 49.1, 47.5, 47.3, 42.4, 42.0, 41.2, 40.9, 40.0, 28.5; IR (Neat Film, NaCl) 3374, 2974, 2927, 1694, 1604, 1581, 1510, 1454, 1416, 1392, 1365, 1320, 1282, 1256, 1211, 1166, 1028, 979, 925, 838, 762, 742, 705, 678, 636, 610 cm⁻¹; HRMS (MM: ESI-APCI): *m/z* calc'd for C₂₈H₃₅N₂O₅ [M+H]⁺: 479.2540, found 479.2533; [α]_D^{22.81} +19.02 (*c* 1.0, CHCl₃); SFC Conditions: 20% IPA, 2.5 mL/min, Chiralpak AD-H column, λ = 210 nm, t_R (min): minor = 3.94, major = 6.20.





Peak #	RetTime [min]	Type	Width [min]	Area [mAU*s]	Height [mAU]	Area %
1	3.941	BB	0.1159	464.67072	61.69901	5.3818
2	6.200	BB	0.1992	8169.42041	630.44366	94.6182
Totals :				8634.09113	692.14267	

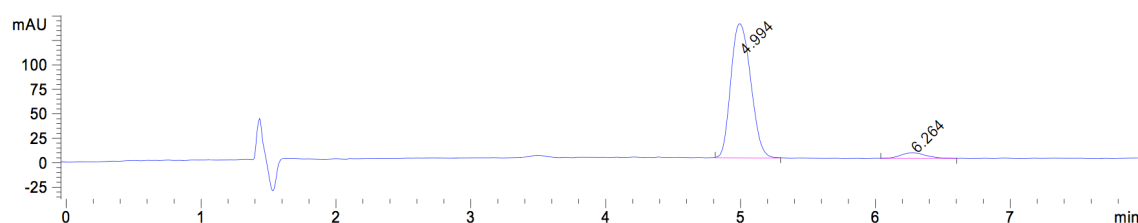
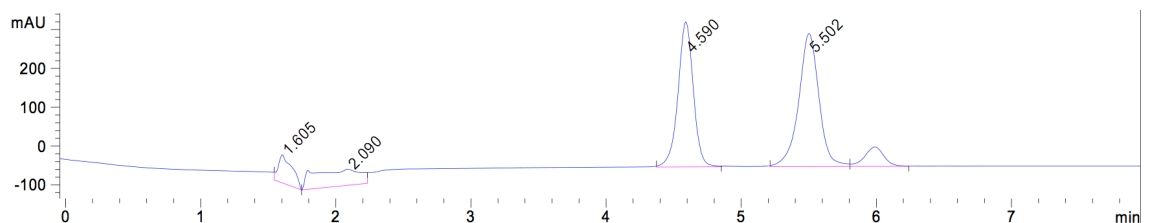


***tert*-butyl (*S*)-6-allyl-4-benzoyl-6-fluoro-5-oxo-1,4-diazepane-1-carboxylate (**20f**)**

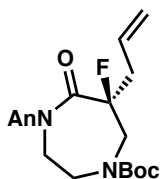
Prepared according to the general procedure with allyl ester **19f** (43.2 mg, 0.103 mmol, 1.0 equiv), Pd₂(pmdba)₃ (4.4 mg, 0.004 mmol, 4 mol %), and (*S*)-(CF₃)₃-*t*-BuPHOX (5.9 mg, 0.01 mmol, 10 mol %). Purified by silica gel flash chromatography (20% EtOAc/hexanes) to provide alkyl fluoride **20f** as a white, amorphous solid (32.6 mg, 0.0866 mmol, 84% yield, 90% ee); ¹H NMR (400 MHz, CDCl₃) δ 7.61 – 7.53 (m, 2H), 7.53 – 7.45 (m, 1H), 7.45 – 7.34 (m, 2H), 5.94 – 5.72 (m, 1H), 5.34 – 5.17 (m, 2H), 4.58 – 4.38 (m, 1H), 4.26 – 4.02 (m, 2H), 3.99 – 3.74 (m, 1H), 3.39 – 3.10 (m, 2H), 2.96 – 2.74 (m, 1H), 2.73 – 2.43 (m, 1H), 1.47 (s, 9H); ¹³C NMR (100 MHz, CDCl₃) δ 173.9, 173.9 (d, *J*_{C-F} = 26.3 Hz), 155.1, 135.2, 132.1, 130.3, 128.4, 128.2, 121.0, 97.7 (dd, *J*_{C-F} = 193.9, 47.2 Hz), 81.1, 49.8 (dd, *J*_{C-F} = 35.3, 23.1 Hz), 47.2, 46.6, 42.6, 39.7 (dd, *J*_{C-F} = 27.6, 21.9 Hz), 28.3; IR (Neat Film, NaCl) 2978, 2926, 1694, 1450, 1414, 1393, 1367, 1329, 1246, 1152, 1042, 999, 979, 926, 857, 766, 724, 694, 672, 648 cm⁻¹; HRMS (MM: ESI-APCI): *m/z* calc'd for

$C_{20}H_{29}FN_3O_4$ $[M+NH_4]^+$: 438.2035, found 438.2040; $[\alpha]_D^{22.85} +28.89$ (c 1.0, $CHCl_3$); SFC

Conditions: 10% IPA, 2.5 mL/min, Chiralcel OD-H column, $\lambda = 210$ nm, t_R (min): minor = 6.26, major = 4.99.



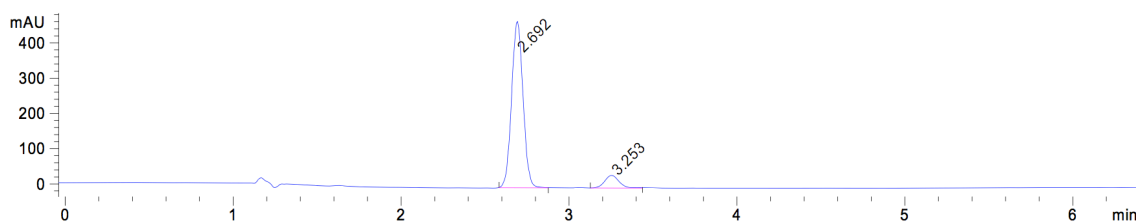
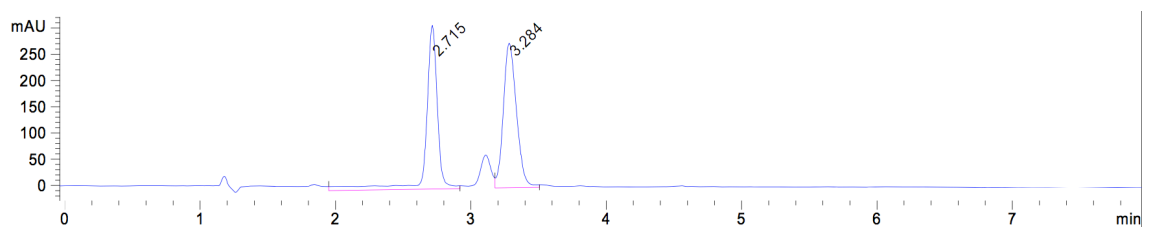
Peak #	RetTime [min]	Type	Width [min]	Area [mAU*s]	Height [mAU]	Area %
1	4.994	BB	0.1643	1412.55457	137.04532	94.8798
2	6.264	BB	0.1858	76.22813	5.63548	5.1202
Totals :				1488.78269	142.68080	



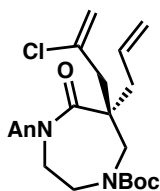
***tert*-butyl (*S*)-6-allyl-6-fluoro-4-(4-methoxybenzoyl)-5-oxo-1,4-diazepane-1-carboxylate (20g)**

Prepared according to the general procedure with allyl ester **19g** (60 mg, 0.133 mmol, 1.0 equiv), $Pd_2(dba)_3$ (4.9 mg, 0.0053 mmol, 4 mol %), and (*S*)- $(CF_3)_3$ -*t*-BuPHOX (7.9 mg, 0.013 mmol, 10 mol %). Purified by automated silica gel flash chromatography (0→50% acetone/hexanes) to provide alkyl fluoride **20g** as a colorless oil (45 mg, 0.111 mmol, 84% yield, 83% ee); 1H NMR (400 MHz, $CDCl_3$) δ 7.61 – 7.53 (m, 2H), 6.92 – 6.84

(m, 2H), 5.93 – 5.78 (m, 1H), 5.30 – 5.21 (m, 2H), 4.35 (t, $J = 16.0$ Hz, 1H), 4.22 – 4.02 (m, 2H), 3.96 – 3.85 (m, 1H), 3.84 (s, 3H), 3.40 – 3.19 (m, 2H), 2.94 – 2.78 (m, 1H), 2.71 – 2.48 (m, 1H), 1.47 (s, 9H); ^{13}C NMR (100 MHz, CDCl_3) δ 173.9, 173.7, 163.1, 155.3, 131.0, 130.6, 127.1, 121.0, 113.8, 97.8 (dd, $J_{\text{C-F}} = 193.7, 52.5$ Hz), 81.2, 55.5, 49.8 (dd, $J_{\text{C-F}} = 33.5, 23.3$ Hz), 47.5, 46.9, 43.2, 39.8 (dd, $J_{\text{C-F}} = 32.1, 21.8$ Hz), 28.3; IR (Neat Film, NaCl) 2977, 2932, 1696, 1603, 1578, 1511, 1448, 1413, 1366, 1327, 1256, 1169, 1152, 1029, 1000, 977, 923, 835, 766 cm^{-1} ; HRMS (MM: ESI-APCI): m/z calc'd for $\text{C}_{21}\text{H}_{28}\text{FN}_2\text{O}_5$ $[\text{M}+\text{H}]^+$: 407.1977, found 407.1973; $[\alpha]_{\text{D}}^{22.5} +46.99$ (c 1.7, CHCl_3); SFC conditions: 20% IPA, 2.5 mL/min, Chiralcel OD-H column, $\lambda = 210$ nm, t_{R} (min): major = 2.69, minor = 3.25.

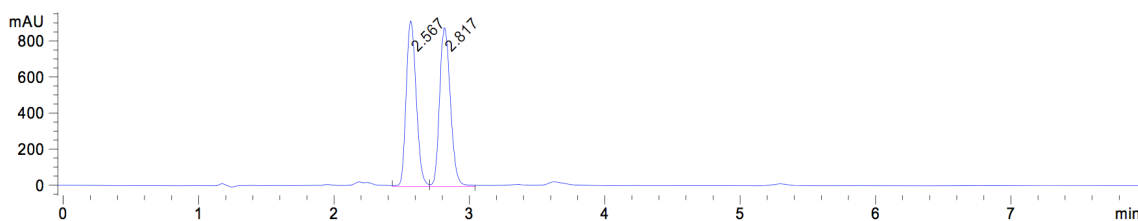


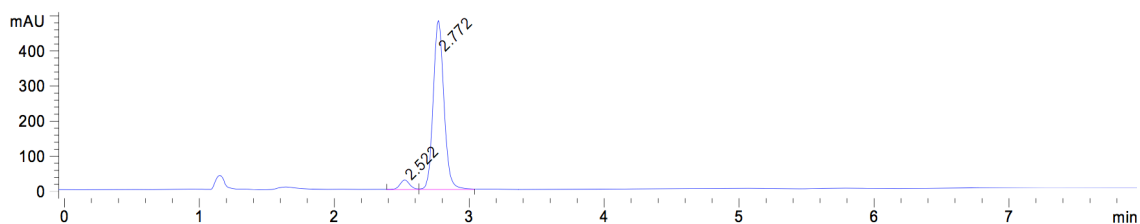
Peak #	RetTime [min]	Type	Width [min]	Area [mAU*s]	Height [mAU]	Area %
1	2.692	BB	0.0755	2233.58398	469.76068	91.4020
2	3.253	BB	0.0929	210.10995	35.55383	8.5980
Totals :				2443.69394	505.31451	



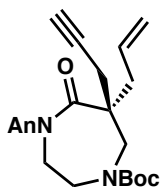
***tert*-butyl (*S*)-6-allyl-6-(2-chloroallyl)-4-(4-methoxybenzoyl)-5-oxo-1,4-diazepane-1-carboxylate (**20h**)**

Prepared according to the general procedure with allyl ester **19h** (48.1 mg, 0.0949 mmol, 1.0 equiv), Pd₂(dba)₃ (3.7 mg, 0.004 mmol, 4 mol %), and (*S*)-(CF₃)₃-*t*-BuPHOX (5.9 mg, 0.01 mmol, 10 mol %). Purified by silica gel flash chromatography (20% EtOAc/hexanes) to provide alkenyl chloride **20h** as a colorless oil (36.7 mg, 0.0793 mmol, 84% yield, 90% ee); ¹H NMR (400 MHz, CDCl₃) δ 7.55 (d, *J* = 8.8 Hz, 2H), 6.87 (d, *J* = 8.8 Hz, 2H), 5.93 – 5.71 (m, 1H), 5.36 – 5.07 (m, 4H), 4.36 – 3.84 (m, 4H), 3.83 (s, 3H), 3.82 – 3.51 (m, 2H), 3.00 – 2.33 (m, 4H), 1.50 (s, 9H); ¹³C NMR (100 MHz, CDCl₃) δ 178.2, 174.6, 162.7, 155.8, 155.2, 137.5, 132.9, 130.5, 128.3, 120.1, 118.2, 113.7, 81.1, 80.9, 55.5, 52.6, 49.2, 47.7, 47.4, 47.0, 44.5, 43.8, 42.8, 42.0, 41.8, 40.3, 28.5; IR (Neat Film, NaCl) 2976, 2930, 1694, 1631, 1604, 1580, 1510, 1456, 1421, 1393, 1366, 1320, 1282, 1256, 1212, 1167, 1150, 1030, 980, 928, 840, 765, 682, 636, 610 cm⁻¹; HRMS (MM: ESI-APCI): *m/z* calc'd for C₂₄H₃₂ClN₂O₅ [M+H]⁺: 463.1994, found 463.2005; [α]_D^{22.68} – 24.10 (*c* 0.5, CHCl₃); SFC Conditions: 20% IPA, 2.5 mL/min, Chiralpak AD-H column, λ = 210 nm, t_R (min): minor = 2.52, major = 2.77.





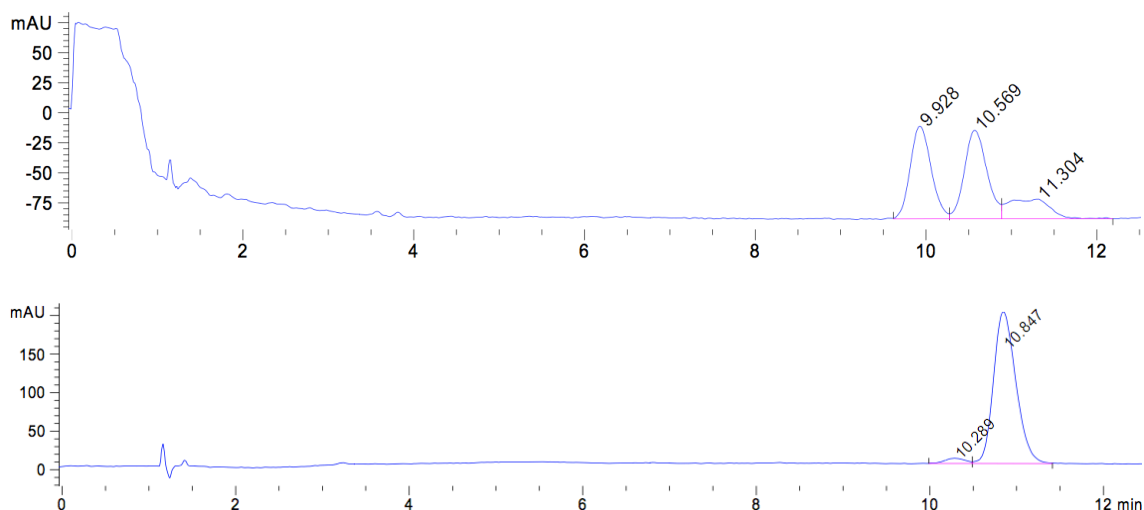
Peak #	RetTime [min]	Type	Width [min]	Area [mAU*s]	Height [mAU]	Area %
1	2.522	BV	0.0799	140.14388	27.27867	5.0016
2	2.772	VB	0.0848	2661.86450	478.89621	94.9984
Totals :				2802.00838	506.17488	



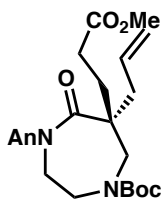
***tert*-butyl (*S*)-6-allyl-4-(4-methoxybenzoyl)-5-oxo-6-(prop-2-yn-1-yl)-1,4-diazepane-1-carboxylate (**20i**)**

Prepared according to the general procedure with allyl ester **19i** (70.0 mg, 0.149 mmol, 1.0 equiv), Pd₂(pmdba)₃ (5.4 mg, 4.9 μmol, 4 mol %), and (*S*)-(CF₃)₃-*t*-BuPHOX (8.8 mg, 0.015 mmol, 10 mol %) at 50 °C. Purification by automated silica gel flash chromatography (Teledyne ISCO, 0→40% acetone/hexanes) provided alkyne **20i** as a colorless oil (28.0 mg, 0.0656 mmol, 44% yield, 94% ee); ¹H NMR (400 MHz, CDCl₃) δ 7.59 (d, *J* = 8.2 Hz, 2H), 6.89 – 6.82 (m, 2H), 5.93 – 5.63 (m, 1H), 5.30 – 5.10 (m, 2H), 4.36 – 4.15 (m, 1H), 4.09 – 3.68 (m, 4H), 3.83 (s, 3H), 3.62 – 3.37 (m, 1H), 2.83 – 2.43 (m, 4H), 2.20 – 1.99 (m, 1H), 1.51 (s, 9H); ¹³C NMR (100 MHz, CDCl₃) δ 177.5, 174.6, 162.9, 155.6, 155.2, 132.1, 130.7, 127.9, 120.0, 113.7, 81.1, 80.9, 80.5, 72.1, 55.6, 52.7, 49.1, 46.9, 47.7, 43.0, 42.3, 39.1, 37.5, 28.5, 26.5, 25.9; IR (Neat Film, NaCl) 3283, 2972, 2922, 1692, 1603, 1511, 1454, 1418, 1365, 1322, 1255, 1169, 1031, 980, 926, 839, 766,

670 cm^{-1} ; HRMS (MM: ESI-APCI): m/z calc'd for $\text{C}_{24}\text{H}_{31}\text{N}_2\text{O}_5$ $[\text{M}+\text{H}]^+$: 427.2227, found 427.2238; $[\alpha]_{\text{D}}^{22.1} -7.69$ (c 1.0, CHCl_3); SFC conditions: 10% IPA, 2.5 mL/min, Chiralpak AD-H column, $\lambda = 210$ nm, t_{R} (min): major = 10.85, minor = 10.29.



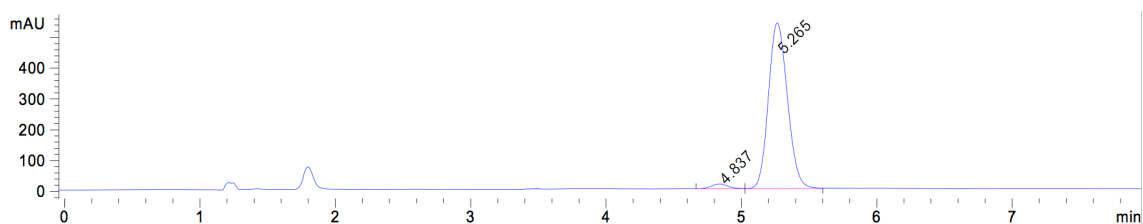
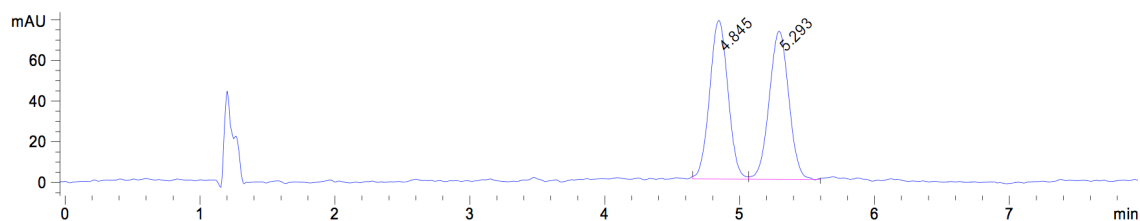
Peak #	RetTime [min]	Type	Width [min]	Area [mAU*s]	Height [mAU]	Area %
1	10.289	BV	0.2467	110.53387	6.90531	3.0290
2	10.847	VB	0.2737	3538.59668	196.86908	96.9710
Totals :				3649.13055	203.77439	



***tert*-butyl (*R*)-6-allyl-6-(3-methoxy-3-oxopropyl)-4-(4-methoxybenzoyl)-5-oxo-1,4-diazepane-1-carboxylate (**20j**)**

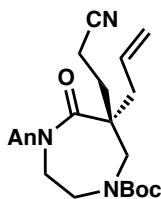
Prepared according to the general procedure with allyl ester **19j** (51.9 mg, 0.100 mmol, 1.0 equiv), $\text{Pd}_2(\text{dba})_3$ (3.7 mg, 0.004 mmol, 4 mol %), and (*S*)- $(\text{CF}_3)_3$ -*t*-BuPHOX (5.9 mg, 0.01 mmol, 10 mol %). Purified by silica gel flash chromatography (33%

EtOAc/hexanes) to provide methyl ester **20j** as a white, amorphous solid (45.8 mg, 0.0965 mmol, 96% yield, 95% ee); ^1H NMR (400 MHz, CDCl_3) δ 7.57 – 7.48 (m, 2H), 6.92 – 6.83 (m, 2H), 5.80 – 5.64 (m, 1H), 5.22 – 5.09 (m, 2H), 4.21 (ddd, $J = 15.7, 6.6, 2.1$ Hz, 1H), 4.13 – 3.85 (m, 3H), 3.83 (s, 3H), 3.62 (s, 3H), 3.51 (d, $J = 15.2$ Hz, 1H), 3.42 – 3.29 (m, 1H), 2.64 – 2.20 (m, 4H), 2.20 – 1.86 (m, 2H), 1.49 (s, 9H); ^{13}C NMR (100 MHz, CDCl_3) δ 179.2, 174.7, 173.6, 173.4, 162.7, 155.4, 155.0, 132.7, 132.5, 130.3, 128.3, 120.0, 113.8, 81.1, 80.9, 55.5, 51.8, 50.1, 48.9, 47.6, 46.8, 43.2, 42.9, 40.3, 39.7, 29.3, 28.8, 28.5; IR (Neat Film, NaCl) 2975, 2360, 1736, 1694, 1605, 1580, 1510, 1426, 1393, 1366, 1321, 1283, 1254, 1167, 1031, 980, 927, 842, 811, 762, 647, 610 cm^{-1} ; HRMS (MM: ESI-APCI): m/z calc'd for $\text{C}_{25}\text{H}_{35}\text{N}_2\text{O}_7$ $[\text{M}+\text{H}]^+$: 475.2439, found 475.2438; $[\alpha]_{\text{D}}^{22.52} +7.73$ (c 1.0, CHCl_3); SFC conditions: 15% IPA, 2.5 mL/min, Chiralcel OD-H column, $\lambda = 210$ nm, t_{R} (min): major = 5.27, minor = 4.84.



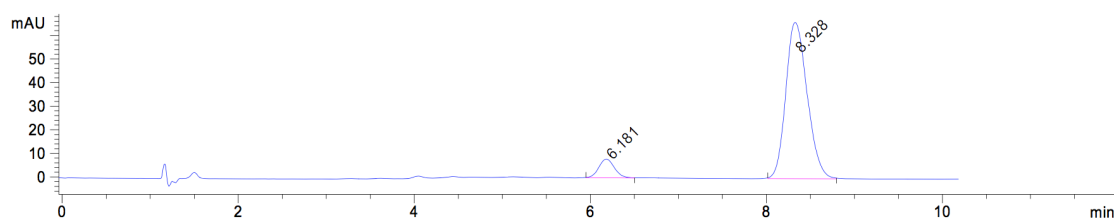
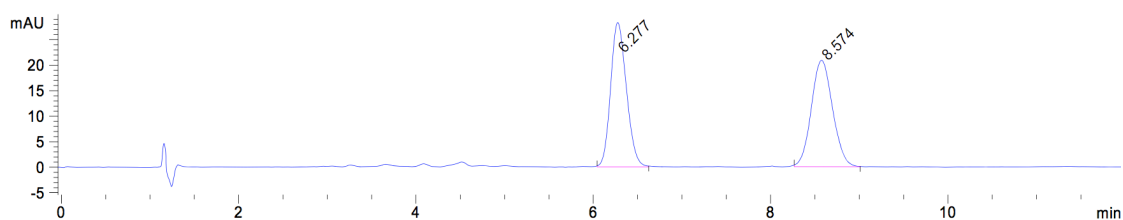
Peak #	RetTime [min]	Type	Width [min]	Area [mAU*s]	Height [mAU]	Area %
1	4.837	BV	0.1353	131.40652	15.43421	2.4390
2	5.265	VB	0.1501	5256.27393	537.28778	97.5610

Totals : 5387.68045 552.72199

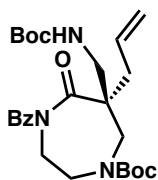


***tert*-butyl (*R*)-6-allyl-6-(2-cyanoethyl)-4-(4-methoxybenzoyl)-5-oxo-1,4-diazepane-1-carboxylate (**20k**)**

Prepared according to the general procedure with allyl ester **19k** (62.2 mg, 0.128 mmol, 1.0 equiv), Pd₂(dba)₃ (4.7 mg, 0.00512 mmol, 4 mol %), and (*S*)-(CF₃)₃-*t*-BuPHOX (7.6 mg, 0.0128 mmol, 10 mol %), using 9:1 methylcyclohexane-toluene as the reaction solvent. Purified by silica gel flash chromatography (33% EtOAc/hexanes) to provide nitrile **20k** as a white, amorphous solid (48.6 mg, 0.110 mmol, 86% yield, 84% ee); ¹H NMR (400 MHz, CDCl₃) δ 7.59 – 7.47 (m, 2H), 6.96 – 6.85 (m, 2H), 5.82 – 5.64 (m, 1H), 5.30 – 5.11 (m, 2H), 4.09 – 3.93 (m, 2H), 3.93 – 3.72 (m, 2H), 3.85 (s, 3H), 3.70 – 3.38 (m, 2H), 2.60 – 2.25 (m, 4H), 2.22 – 1.93 (m, 2H), 1.50 (s, 9H); ¹³C NMR (100 MHz, CDCl₃) δ 178.0, 174.5, 163.0, 155.6, 154.9, 131.7, 130.3, 127.9, 120.7, 119.7, 113.9, 81.4, 55.6, 52.2, 49.6, 48.0, 47.4, 46.8, 43.0, 42.6, 39.9, 39.0, 32.1, 31.5, 28.4, 12.4; IR (Neat Film, NaCl) 2975, 2931, 2361, 2246, 1690, 1604, 1579, 1510, 1456, 1419, 1366, 1321, 1256, 1168, 1148, 1031, 980, 926, 840, 811, 766, 607 cm⁻¹; HRMS (MM: ESI-APCI): *m/z* calc'd for C₂₄H₃₅N₄O₅ [M+NH₄]⁺: 459.2602, found 459.2602; [α]_D^{22.4} +9.31 (*c* 0.5, CHCl₃); SFC conditions: 20% IPA, 2.5 mL/min, Chiralcel OD-H column, λ = 310 nm, t_R (min): major = 8.33, minor = 6.18.



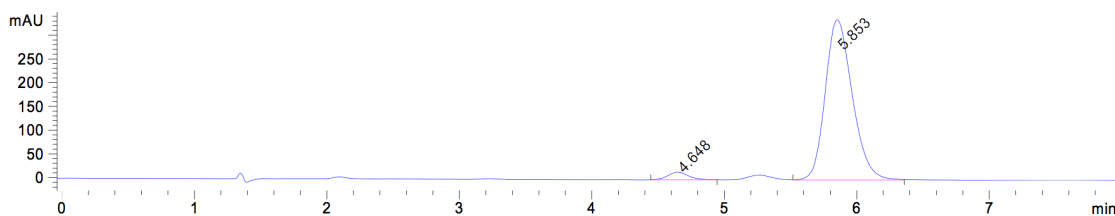
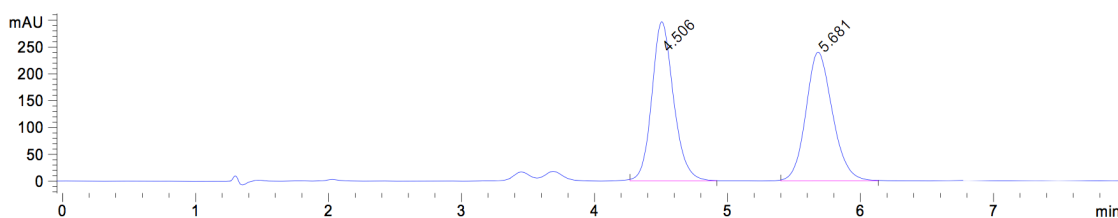
Peak #	RetTime [min]	Type	Width [min]	Area [mAU*s]	Height [mAU]	Area %
1	6.181	BB	0.1914	97.48795	7.93404	8.0193
2	8.328	BB	0.2649	1118.18079	66.25080	91.9807
Totals :				1215.66874	74.18484	



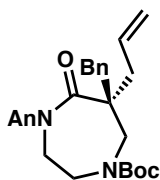
tert-butyl (S)-6-allyl-4-benzoyl-6-(((tert-butoxycarbonyl)amino)methyl)-5-oxo-1,4-diazepane-1-carboxylate (20I)

Prepared according to the general procedure with allyl ester **19I** (53 mg, 0.0997 mmol, 1.0 equiv) and Pd₂(dba)₃. Purification by automated silica gel flash chromatography (0→50% EtOAc/hexanes) provided carbamate **20I** as a white foam (37 mg, 0.0759 mmol, 76% yield, 93% ee). ¹H NMR (400 MHz, CDCl₃) δ 7.55 – 7.44 (m, 3H), 7.44 – 7.35 (m, 2H), 5.74 (ddt, *J* = 15.7, 10.5, 7.4 Hz, 1H), 5.35 (br s, 0.5H), 5.21 – 5.06 (m, 2H), 4.79 (br s, 0.5H), 4.48 – 4.28 (m, 1H), 4.14 – 3.09 (m, 7H), 2.69 – 2.18 (m, 2H), 1.50 (s, 9H), 1.44 (s, 9H); ¹³C NMR (100 MHz, CDCl₃) δ 179.3, 178.8, 174.5, 156.3, 155.9, 155.1, 136.3,

132.5, 132.1, 131.7, 128.5, 127.7, 120.1, 81.3, 81.1, 79.5, 54.8, 48.9, 47.3, 46.8, 46.3, 42.6, 41.1, 38.7, 37.1, 28.5, 28.5; IR (Neat Film, NaCl) 2977, 1687, 1502, 1422, 1391, 1365, 1322, 1282, 1245, 1168, 978, 916, 753 cm^{-1} ; HRMS (MM: ESI-APCI): m/z calc'd for $\text{C}_{26}\text{H}_{37}\text{N}_3\text{O}_6$ $[\text{M}+\text{H}]^+$: 488.2755, found 488.2747; $[\alpha]_{\text{D}}^{23.2}$ -3.70 (c 1.85, CHCl_3); SFC conditions: 20% IPA, 2.5 mL/min, Chiralpak IC column, $\lambda = 254$ nm, t_{R} (min): major = 5.85, minor = 4.65.



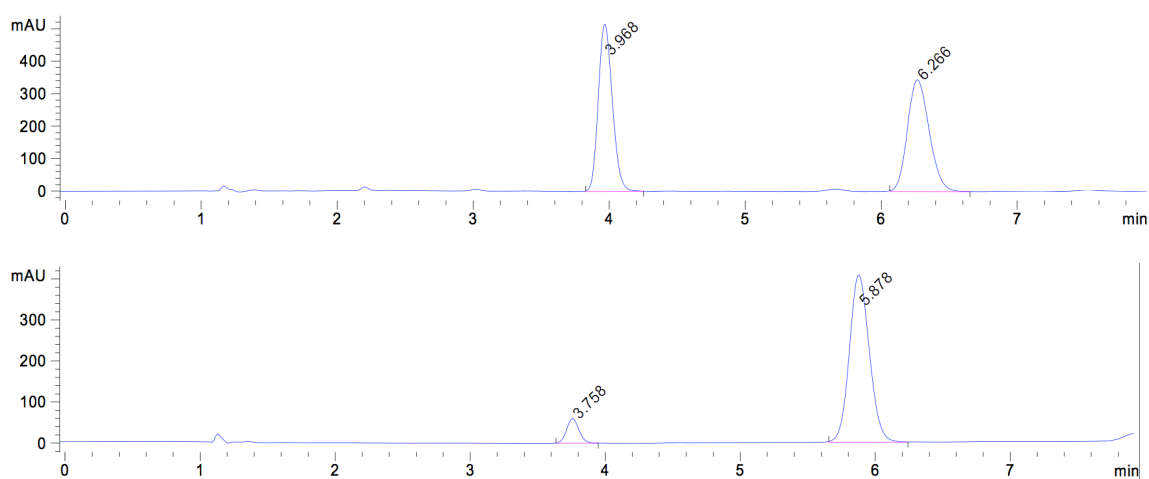
Peak #	RetTime [min]	Type	Width [min]	Area [mAU*s]	Height [mAU]	Area %
1	4.648	BB	0.1676	175.76628	16.06920	3.5426
2	5.853	VB	0.2176	4785.68066	337.25015	96.4574
Totals :				4961.44695	353.31935	



Procedure for the large-scale preparation of diazepanone 20e

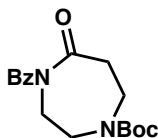
To a 500 mL Schlenk flask was added $\text{Pd}_2(\text{dba})_3$ (37 mg, 0.04 mmol, 4 mol %), (*S*)- $(\text{CF}_3)_3$ -*t*-BuPHOX (59 mg, 0.1 mmol, 10 mol %), and MeCy (20 mL). After stirring for 20

minutes at 25 °C, allyl ester **19e** (523 mg, 1.0 mmol, 1.0 equiv) and methylcyclohexane (52 mL, total substrate concentration 0.014 M) were added to the pre-stirred catalyst solution. After stirring for 23 h at 40 °C, the reaction mixture was directly loaded onto a flash column and purified by silica gel flash chromatography (20% EtOAc/hexanes) to provide benzyl diazepanone **20e** as a colorless oil (393 mg, 0.82 mmol, 82% yield, 83% ee); All characterization data matched those reported above for compound **20e**; $[\alpha]_D^{21.96} +14.757$ (*c* 1.0, CHCl₃); SFC Conditions: 20% IPA, 2.5 mL/min, Chiralpak AD-H column, $\lambda = 210$ nm, *t_R* (min): minor = 3.76, major = 5.90.



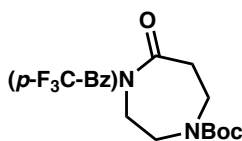
Peak #	RetTime [min]	Type	Width [min]	Area [mAU*s]	Height [mAU]	Area %
1	3.758	BB	0.0989	386.25449	60.12492	8.4266
2	5.878	BB	0.1604	4197.52441	406.90225	91.5734
Totals :				4583.77890	467.02718	

1.5.2.2 Synthesis of Diazepanone Allylic Alkylation Substrates



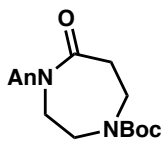
***tert*-butyl 4-benzoyl-5-oxo-1,4-diazepane-1-carboxylate (55)**

To a solution of *tert*-butyl 5-oxo-1,4-diazepane-1-carboxylate (5.00 g, 23.3 mmol, 1.0 equiv) in THF (230 mL, 0.1 M) at $-78\text{ }^{\circ}\text{C}$ was slowly added *n*-BuLi (2.18 M in hexanes, 12.8 mL, 27.9 mmol, 1.2 equiv). The opaque mixture was allowed to warm to ambient temperature until the solution became homogeneous, at which point it was again cooled to $-78\text{ }^{\circ}\text{C}$. Then, benzoyl chloride (3.52 mL, 30.3 mmol, 1.3 equiv) was added dropwise and the reaction turned light orange over several minutes. The reaction was stirred for 1 h at $-78\text{ }^{\circ}\text{C}$, then poured into saturated aqueous NH_4Cl (200 mL) and extracted with EtOAc (3 x 100 mL). The combined organic extracts were dried over Na_2SO_4 and concentrated. The crude product was purified by silica gel flash chromatography (20% acetone/hexanes) to afford benzoyl-protected lactam **55** as a white solid (7.43 g, 23.3 mmol, >99% yield); ^1H NMR (400 MHz, CDCl_3) δ 7.57 – 7.49 (m, 2H), 7.49 – 7.41 (m, 1H), 7.41 – 7.32 (m, 2H), 4.03 – 3.96 (m, 2H), 3.71 (m, 4H), 2.82 – 2.75 (m, 2H), 1.47 (s, 9H); ^{13}C NMR (100 MHz, CDCl_3) δ 175.6, 173.7, 154.5, 135.9, 131.7, 128.2, 127.9, 80.7, 47.8, 47.10, 45.4, 41.6, 41.0, 40.6, 28.3; IR (Neat Film, NaCl) 2976, 2932, 2251, 1682, 1599, 1582, 1450, 1422, 1392, 1366, 1327, 1285, 1247, 1229, 1157, 1115, 1032, 1018, 976, 954, 915, 862, 793, 769, 729, 696, 647 cm^{-1} ; HRMS (MM: ESI-APCI): m/z calc'd for $\text{C}_{17}\text{H}_{26}\text{N}_3\text{O}_4$ $[\text{M}+\text{NH}_4]^+$: 336.1918, found 336.1912.



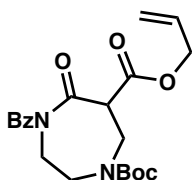
***tert*-butyl 5-oxo-4-(4-(trifluoromethyl)benzoyl)-1,4-diazepane-1-carboxylate (56)**

To a solution of *tert*-butyl 5-oxo-1,4-diazepane-1-carboxylate (500 mg, 2.33 mmol, 1 equiv) in THF (25 mL, 0.1 M) at $-78\text{ }^{\circ}\text{C}$ was slowly added *n*-BuLi (2.5 M in hexanes, 1.02 mL, 2.56 mmol, 1.1 equiv), and the reaction mixture was stirred at $-78\text{ }^{\circ}\text{C}$ for 15 min. Then, 4-trifluoromethylbenzoyl chloride (450 μL , 3.03 mmol, 1.3 equiv) was added dropwise, and the reaction was stirred for 30 min at $-78\text{ }^{\circ}\text{C}$. The reaction mixture was then poured into saturated aqueous NH_4Cl (20 mL), the layers were separated, and the aqueous layer was extracted with EtOAc (3 x 10 mL). The combined organic extracts were dried over Na_2SO_4 and concentrated under reduced pressure. The crude product was purified by silica gel flash chromatography (25% EtOAc/hexanes) to afford the title compound as a white solid (698 mg, 1.81 mmol, 77% yield); ^1H NMR (400 MHz, CDCl_3) δ 7.66 (d, $J = 8.2$ Hz, 2H), 7.60 (d, $J = 8.1$ Hz, 2H), 4.14 – 4.02 (m, 2H), 3.84 – 3.66 (m, 4H), 2.91 – 2.77 (m, 2H), 1.50 (s, 9H); ^{13}C NMR (100 MHz, CDCl_3) δ 175.7, 172.5, 154.6, 139.6, 133.0 (q, $J_{\text{C-F}} = 32.8$ Hz), 130.6, 128.0, 125.5 (q, $J_{\text{C-F}} = 3.8$ Hz), 123.7 (q, $J_{\text{C-F}} = 272.6$ Hz), 81.2, 47.7 (br), 45.3, 41.4 (br), 40.8, 28.5; IR (Neat Film, NaCl) 2981, 1689, 1455, 1422, 1367, 1326, 1301, 1249, 1230, 1159, 1127, 1066, 1028, 1015, 977, 955, 852, 832, 769 cm^{-1} ; HRMS (MM: ESI-APCI): m/z calc'd for $\text{C}_{18}\text{H}_{25}\text{F}_3\text{N}_3\text{O}_4$ $[\text{M}+\text{NH}_4]^+$: 404.1742, found 404.1797.

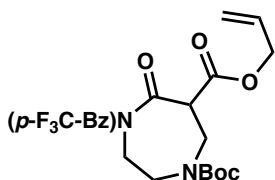


***tert*-butyl 4-(4-methoxybenzoyl)-5-oxo-1,4-diazepane-1-carboxylate (57)**

To a solution of *tert*-butyl 5-oxo-1,4-diazepane-1-carboxylate (800 mg, 3.73 mmol, 1 equiv) in THF (37 mL, 0.1 M) at $-78\text{ }^{\circ}\text{C}$ was slowly added *n*-BuLi (2.5 M in hexanes, 1.64 mL, 4.1 mmol, 1.1 equiv). The opaque mixture was allowed to warm to ambient temperature until the solution became homogeneous, at which point it was again cooled to $-78\text{ }^{\circ}\text{C}$. Then, 4-methoxybenzoyl chloride (657 μL , 4.85 mmol, 1.3 equiv) was added dropwise and the reaction was stirred for 30 min at $-78\text{ }^{\circ}\text{C}$. The reaction mixture was then poured into saturated aqueous NH_4Cl (30 mL), the layers were separated, and the aqueous layer was extracted with EtOAc (3 x 10 mL). The combined organic extracts were dried over Na_2SO_4 and concentrated under reduced pressure. The crude product was purified by automated silica gel flash chromatography (Teledyne ISCO, 0 \rightarrow 100% EtOAc/hexanes) to afford the title compound as a white solid (1.2 g, 3.44 mmol, 92% yield); ^1H NMR (400 MHz, CDCl_3) δ 7.62 – 7.54 (m, 2H), 6.93 – 6.84 (m, 2H), 4.00 – 3.93 (m, 2H), 3.83 (s, 3H), 3.78 – 3.69 (m, 4H), 2.85 – 2.78 (m, 2H), 1.48 (s, 9H); ^{13}C NMR (100 MHz, CDCl_3) δ 175.7, 173.4, 162.9, 154.6, 130.9, 130.6, 127.7, 113.7, 80.8, 55.5, 48.0, 47.4, 46.1, 41.9, 41.3, 40.8, 28.5; IR (Neat Film, NaCl) 2974, 2936, 1774, 1687, 1604, 1578, 1510, 1458, 1420, 1391, 1366, 1327, 1284, 1249, 1166, 1114, 1023, 977, 956, 916, 860, 842, 809, 767, 632 cm^{-1} ; HRMS (MM: ESI-APCI): m/z calc'd for $\text{C}_{18}\text{H}_{25}\text{N}_2\text{O}_5$ $[\text{M}+\text{H}]^+$: 349.1758, found 349.1760.

**6-allyl 1-(*tert*-butyl) 4-benzoyl-5-oxo-1,4-diazepane-1,6-dicarboxylate (18a)**

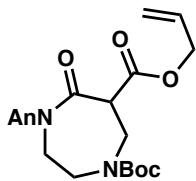
To a solution of diisopropylamine (266 μL , 1.88 mmol, 1.2 equiv) in THF (10 mL) at $-78\text{ }^\circ\text{C}$ in a flame-dried round-bottom flask was added *n*-BuLi (2.5 M in hexanes, 792 μL , 1.73 mmol, 1.1 equiv), the resulting solution was stirred at $-78\text{ }^\circ\text{C}$ for 45 min. To this solution was then added lactam **55** (500 mg, 1.57 mmol, 1.0 equiv) in THF (6 mL, 0.1 M total concentration) dropwise while stirring at $-78\text{ }^\circ\text{C}$. The reaction mixture was stirred for 75 min at $-78\text{ }^\circ\text{C}$. Allyl cyanofornate (201 μL , 1.88 mmol, 1.2 equiv) was then added dropwise at $-78\text{ }^\circ\text{C}$. After stirring for 3 h at $-78\text{ }^\circ\text{C}$, the reaction mixture was poured into saturated aqueous NH_4Cl (10 mL) and extracted with ethyl acetate (3 x 20 mL). The combined organic extracts were concentrated under reduced pressure onto silica (4 g). The silica-adsorbed crude mixture was purified by silica gel flash chromatography (20 \rightarrow 30% EtOAc/hexanes) to provide allyl ester **18a** as an off-white solid (550 mg, 1.37 mmol, 87% yield); ^1H NMR (500 MHz, CDCl_3) δ 7.65 – 7.57 (m, 2H), 7.53 – 7.45 (m, 1H), 7.42 – 7.34 (m, 2H), 5.92 (ddt, $J = 17.2, 10.4, 5.9$ Hz, 1H), 5.40 – 5.22 (m, 2H), 4.79 – 4.59 (m, 2H), 4.33 – 4.03 (m, 2H), 4.02 – 3.88 (m, 3H), 3.87 – 3.66 (m, 1H), 3.55 – 3.40 (m, 1H), 1.48 (s, 9H); ^{13}C NMR (125 MHz, CDCl_3) δ 173.7, 171.4, 167.5, 154.7, 135.3, 132.2, 131.4, 128.4, 128.4, 119.5, 81.3, 66.6, 56.0, 46.7 (br), 44.5, 43.3 (br), 28.4; IR (Neat Film, NaCl) 3374, 3062, 2977, 2934, 1746, 1694, 1600, 1582, 1450, 1419, 1393, 1367, 1327, 1246, 1156, 1037, 1020, 995, 968, 939, 857, 792, 769, 727, 695, 616 cm^{-1} ; HRMS (MM: ESI-APCI): m/z calc'd for $\text{C}_{21}\text{H}_{30}\text{N}_3\text{O}_6$ $[\text{M}+\text{NH}_4]^+$: 420.2129, found 420.2109.



6-allyl 1-(*tert*-butyl) 5-oxo-4-(4-(trifluoromethyl)benzoyl)-1,4-diazepane-1,6-dicarboxylate (18b)

To a solution of lactam **56** (500 mg, 1.29 mmol, 1.0 equiv) in THF (8 mL, 0.1 M total concentration) at $-78\text{ }^{\circ}\text{C}$ was added LiHMDS (303 mg, 1.81 mmol, 1.4 equiv) in THF (5 mL) dropwise. The resulting yellow reaction mixture was stirred for 15 min at $-78\text{ }^{\circ}\text{C}$. Then, allyl cyanoformate (166 μL , 1.55 mmol, 1.2 equiv) was added dropwise at $-78\text{ }^{\circ}\text{C}$, after which the solution slowly became colorless. After stirring for 1 h at $-78\text{ }^{\circ}\text{C}$, the reaction was poured into 2 M HCl (20 mL) and extracted with ethyl acetate (4 x 20 mL). The combined organic extracts were dried over anhydrous Na_2SO_4 and NaHCO_3 , passed through filter paper, and concentrated under reduced pressure. The crude product was purified by silica gel flash chromatography (20 \rightarrow 33% EtOAc/hexanes) to provide allyl ester **18b** as a white solid (266 mg, 0.565 mmol, 44% yield); ^1H NMR (400 MHz, CDCl_3) δ 7.69 (d, $J = 8.3$ Hz, 2H), 7.64 (d, $J = 8.4$ Hz, 2H), 5.92 (ddt, $J = 17.2, 10.4, 5.9$ Hz, 1H), 5.42 – 5.23 (m, 2H), 4.79 – 4.59 (m, 2H), 4.46 – 3.63 (m, 6H), 3.52 (m, 1H), 1.47 (s, 9H); ^{13}C NMR (100 MHz, CDCl_3) δ 172.4, 171.4, 167.4, 154.6, 138.9, 133.3 (q, $J_{\text{C-F}} = 32.6$ Hz), 131.2, 128.3, 125.4 (q, $J_{\text{C-F}} = 3.8$ Hz), 123.7 (q, $J_{\text{C-F}} = 272.5$ Hz), 119.8, 81.5, 66.8, 56.0, 47.4, 46.3, 44.2, 43.0, 28.4; IR (Neat Film, NaCl) 3377, 3083, 2980, 2935, 2463, 2358, 1928, 1798, 1747, 1694, 1652, 1619, 1584, 1513, 1455, 1414, 1394, 1368, 1327, 1246, 1156, 1131, 1067, 1034, 1016, 994, 970, 940, 879, 853, 824, 770, 723, 679, 639, 630, 612

cm⁻¹; HRMS (MM: ESI-APCI): *m/z* calc'd for C₂₂H₂₉F₃N₃O₆ [M+NH₄]⁺: 488.2003, found 488.2022.

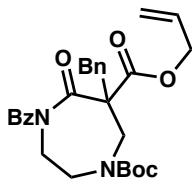


6-allyl 1-(*tert*-butyl) 4-(4-methoxybenzoyl)-5-oxo-1,4-diazepane-1,6-dicarboxylate (18c)

To a solution of lactam **57** (1.00 g, 2.87 mmol, 1.0 equiv) in THF (20 mL, 0.1 M total concentration) at -78 °C was added LiHMDS (528 mg, 3.16 mmol, 1.1 equiv) in THF (9 mL) dropwise. The resulting pale yellow reaction mixture was stirred for 15 min at -78 °C. Allyl cyanoformate (368 μL, 3.44 mmol, 1.2 equiv) was then added dropwise at -78 °C, resulting in a clear solution. After stirring for 1.5 h at -78 °C, the reaction was poured into 1 M HCl (10 mL) and diluted with ethyl acetate (20 mL). The layers were separated and the aqueous phase was extracted with ethyl acetate (3 x 30 mL). The combined organic extracts were dried over anhydrous Na₂SO₄ and NaHCO₃, filtered, and concentrated under reduced pressure onto silica. The silica-adsorbed crude mixture was purified by silica gel flash chromatography (10→20% EtOAc/hexanes) to provide allyl ester **18c** as a colorless oil (600 mg, 1.39 mmol, 48% yield); ¹H NMR (400 MHz, CDCl₃) δ 7.72 – 7.60 (m, 2H), 6.91 – 6.79 (m, 2H), 5.92 (ddt, *J* = 17.3, 10.4, 5.9 Hz, 1H), 5.42 – 5.20 (m, 2H), 4.77 – 4.56 (m, 2H), 4.40 – 3.92 (m, 4H), 3.92 – 3.62 (m, 2H), 3.82 (s, 3H), 3.58 – 3.24 (m, 1H), 1.46 (s, 9H); ¹³C NMR (100 MHz, CDCl₃) δ 173.1, 171.3, 167.6, 163.2, 154.6, 131.4, 131.2, 127.0, 119.4, 113.7, 81.1, 66.5, 55.9, 55.4, 47.7 and 46.7, 45.1, 43.3, 42.8, 28.3; IR (Neat Film, NaCl) 2977, 1746, 1693, 1603, 1578, 1511, 1454, 1419, 1392, 1366, 1324, 1255,

1168, 1025, 995, 965, 842, 766 cm^{-1} ; HRMS (MM: ESI-APCI): m/z calc'd for $\text{C}_{22}\text{H}_{28}\text{N}_2\text{O}_7$

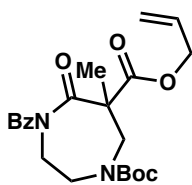
$[\text{M}+\text{H}]^+$: 433.1969, found 433.1966.



6-allyl 1-(*tert*-butyl) 4-benzoyl-6-benzyl-5-oxo-1,4-diazepane-1,6-dicarboxylate (**19a**)

To a flame-dried round bottom flask containing a solution of allyl ester **18a** (1.00 g, 2.49 mmol, 1.0 equiv) in THF (25 mL, 0.1 M) at 0 °C was added NaH (60% dispersion in mineral oil, 107 mg, 2.74 mmol, 1.1 equiv) and the mixture was stirred at 0 °C for 30 min. BnBr (1.50 mL, 12.45 mmol, 5.0 equiv) was then added dropwise and the reaction mixture was warmed to 45 °C. After 16 h, the temperature was further increased to 53 °C due to sluggish reactivity. After another 45 min of stirring at 53 °C, the reaction mixture was cooled to 23 °C and poured into saturated aqueous NH_4Cl (25 mL), the layers were separated, and the aqueous layer was extracted with ethyl acetate (3 x 10 mL). The combined organic extracts were dried over anhydrous Na_2SO_4 , filtered, and concentrated under reduced pressure. The crude product was purified by silica gel flash chromatography (20% EtOAc/hexanes) to provide the title compound as a colorless foam (922 mg, 1.87 mmol, 75% yield); ^1H NMR (400 MHz, CDCl_3) δ 7.68 (d, $J = 7.6$ Hz, 2H), 7.55 – 7.46 (m, 1H), 7.37 (t, $J = 7.7$ Hz, 2H), 7.31 – 7.25 (m, 3H), 7.24 – 7.12 (m, 2H), 5.86 (tq, $J = 22.8$, 6.5 Hz, 1H), 5.42 – 5.26 (m, 2H), 4.71 – 4.55 (m, 2H), 4.22 (dd, $J = 75.3$, 15.5 Hz, 1H), 4.05 – 3.57 (m, 4H), 3.57 – 3.36 (m, 2H), 3.22 (dd, $J = 68.5$, 13.7 Hz, 1H), 1.45 (s, 9H); ^{13}C NMR (100 MHz, CDCl_3) δ (174.4, 174.0, 172.2, 172.0, 170.8, 170.2, 155.5, 155.0, 135.7, 135.6, 135.5, 132.0, 131.1, 130.9, 130.8, 130.6, 128.5, 128.5, 128.3, 127.5, 127.4,

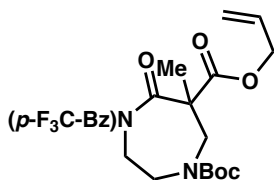
120.6, 120.2, 81.2, 81.0, 67.0, 66.9, 62.6, 62.2, 47.3, 46.7, 46.2, 45.8, 42.4, 42.1, 42.0, 28.5; IR (Neat Film, NaCl) 3063, 3030, 2977, 2933, 1694, 1601, 1583, 1495, 1450, 1416, 1393, 1366, 1325, 1280, 1247, 1154, 1132, 1092, 1041, 1023, 980, 939, 868, 796, 768, 728, 703, 662 cm^{-1} ; HRMS (MM: ESI-APCI): m/z calc'd for $\text{C}_{24}\text{H}_{25}\text{N}_2\text{O}_6$ $[\text{M}-t\text{Bu}+2\text{H}]^+$: 437.1707, found 437.1697.



6-allyl 1-(*tert*-butyl) 4-benzoyl-6-methyl-5-oxo-1,4-diazepane-1,6-dicarboxylate (19b)

To a solution of allyl ester **18a** (240 mg, 0.596 mmol, 1.0 equiv) in THF (6 mL, 0.1 M) at 0 °C was added 60 % NaH (26 mg, 0.657 mmol, 1.1 equiv). The solution was stirred at 0 °C for 40 min, after which MeI (186 μL , 2.98 mmol, 5.0 equiv) was added rapidly. The reaction was heated to 45 °C and stirred for 16 h, cooled to 23 °C, poured into saturated aqueous NH_4Cl (5 mL), and extracted with EtOAc (3 x 3 mL). The combined organic extracts were dried over Na_2SO_4 and concentrated onto silica gel. The silica-adsorbed crude product was purified by silica gel flash chromatography (20% EtOAc/hexanes) to afford the title compound as a light yellow oil (200 mg, 0.480 mmol, 81% yield). ^1H NMR (400 MHz, CDCl_3) δ 7.78 – 7.63 (m, 2H), 7.58 – 7.43 (m, 1H), 7.38 (t, $J = 7.6$ Hz, 2H), 5.96 (ddt, $J = 16.6, 10.4, 6.0$ Hz, 1H), 5.49 – 5.26 (m, 2H), 4.85 – 4.64 (m, 2H), 4.46 – 4.22 (m, 1H), 4.10 (br d, $J = 14.8$ Hz, 1H), 3.86 – 3.42 (m, 4H), 1.57 (s, 3H), 1.45 (s, 9H); ^{13}C NMR (100 MHz, CDCl_3) δ 174.5 174.1, 173.0, 171.7, 155.1, 154.9, 135.7, 132.0, 131.2, 128.3, 128.2, 120.2, 81.1, 66.9, 57.7, 49.8, 49.0, 47.1, 46.0, 43.2, 28.4, 23.6; IR (Neat Film, NaCl) 2977, 1693, 1449, 1416, 1366, 1325, 1281, 1249, 1139, 1104, 1047, 983, 938, 768, 727,

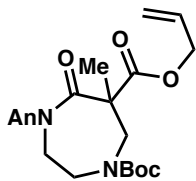
694 cm^{-1} ; HRMS (MM: ESI-APCI): m/z calc'd for $\text{C}_{22}\text{H}_{29}\text{N}_2\text{O}_6$ $[\text{M}+\text{H}]^+$: 417.2020, found 417.2010.



6-allyl 1-(*tert*-butyl) 6-methyl-5-oxo-4-(4-(trifluoromethyl)benzoyl)-1,4-diazepane-1,6-dicarboxylate (19c)

To a suspension of allyl ester **18b** (150 mg, 0.319 mmol, 1.0 equiv) and Cs_2CO_3 (208 mg, 0.638 mmol, 2.0 equiv) in acetonitrile (3.2 mL, 0.1 M) was added MeI (99 μL , 1.59 mmol, 5.0 equiv) at 23 $^\circ\text{C}$. The reaction was heated to 45 $^\circ\text{C}$ and stirred for 5 h, then cooled to 23 $^\circ\text{C}$, poured into saturated aqueous NH_4Cl (6 mL), and extracted with EtOAc (3 x 3 mL). The combined organic extracts were dried over anhydrous Na_2SO_4 , filtered, and concentrated under reduced pressure. The crude product was purified by silica gel flash chromatography (15% EtOAc/petroleum ether) to provide the title compound as a colorless oil (146 mg, 0.301 mmol, 95% yield); ^1H NMR (400 MHz, CDCl_3) δ 7.75 (d, $J = 8.1$ Hz, 2H), 7.63 (d, $J = 8.1$ Hz, 2H), 5.97 (ddt, $J = 17.3, 10.3, 6.1$ Hz, 1H), 5.48 – 5.29 (m, 2H), 4.84 – 4.68 (m, 2H), 4.49 – 4.30 (m, 1H), 4.18 – 3.98 (m, 1H), 3.90 – 3.39 (m, 4H), 1.57 (s, 3H), 1.45 (s, 9H); ^{13}C NMR (100 MHz, CDCl_3) δ 173.2, 172.7, 171.7, 154.9, 139.2, 133.1 (q, $J_{\text{C-F}} = 32.5$ Hz), 131.1, 128.2, 125.4, 123.8 (q, $J_{\text{C-F}} = 272.7$ Hz), 120.5, 81.3, 67.0, 57.7, 49.7, 49.0, 46.9, 45.8, 43.1, 42.9, 28.4, 23.7; IR (Neat Film, NaCl) 3384, 3083, 2979, 2937, 1698, 1619, 1584, 1514, 1478, 1453, 1416, 1394, 1367, 1326, 1285, 1250, 1207, 1166, 1136, 1110, 1066, 1022, 1012, 985, 938, 855, 832, 817, 790, 769, 740, 722, 680 cm^{-1}

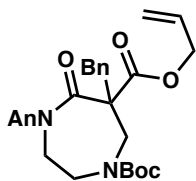
¹; HRMS (MM: ESI-APCI): *m/z* calc'd for C₂₃H₂₈F₃N₂O₆ [M+H]⁺: 485.1894, found 485.1907.



6-allyl 1-(tert-butyl) 4-(4-methoxybenzoyl)-6-methyl-5-oxo-1,4-diazepane-1,6-dicarboxylate (19d)

To a suspension of allyl ester **18c** (200 mg, 0.462 mmol, 1.0 equiv), Cs₂CO₃ (301 mg, 0.925 mmol, 2.0 equiv) in acetonitrile (4.6 mL, 0.1 M) was added MeI (143 μL, 2.31 mmol, 5.0 equiv) at 23 °C. The reaction was heated to 45 °C and stirred for 40 min, then cooled to 23 °C, poured into saturated aqueous NH₄Cl (10 mL), and extracted with EtOAc (3 x 5 mL). The combined organic extracts were dried over anhydrous Na₂SO₄, filtered, and concentrated under reduced pressure. The crude product was purified by automated silica gel flash chromatography (Teledyne ISCO, 0→90% EtOAc/hexanes) to provide the title compound as a colorless oil (70 mg, 0.157 mmol, 34% yield). ¹H NMR (400 MHz, CDCl₃) δ 7.75 – 7.65 (m, 2H), 6.90 – 6.82 (m, 2H), 5.96 (ddt, *J* = 17.3, 10.4, 6.0 Hz, 1H), 5.44 – 5.29 (m, 2H), 4.77 – 4.66 (m, 2H), 4.27 – 4.15 (m, 1H), 4.14 – 4.04 (m, 1H), 3.83 (s, 3H), 3.80 – 3.70 (m, 1H), 3.67 – 3.58 (m, 2H), 3.56 – 3.46 (m, 1H), 1.57 (s, 3H), 1.44 (s, 9H); ¹³C NMR (100 MHz, CDCl₃) δ 174.0, 173.6, 172.9, 172.0, 171.8, 162.9, 155.2, 154.9, 131.2, 131.2, 131.0, 127.6, 120.1, 120.0, 113.6, 81.0, 66.8, 57.5, 55.5, 49.6, 48.9, 47.2, 46.1, 43.7, 28.4, 23.7; IR (Neat Film, NaCl) 2974, 2937, 1698, 1604, 1578, 1511, 1453, 1416, 1392, 1366, 1324, 1280, 1256, 1169, 1139, 1103, 1031, 1001, 983, 929, 840, 768, 733 cm⁻¹; HRMS (MM: ESI-APCI): *m/z* calc'd for C₂₃H₃₁N₂O₇

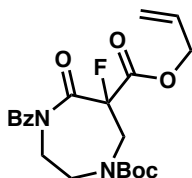
[M+H]⁺: 447.2126, found 447.2128.



6-allyl 1-(*tert*-butyl) 6-benzyl-4-(4-methoxybenzoyl)-5-oxo-1,4-diazepane-1,6-dicarboxylate (19e)

To a flame-dried round bottom flask containing a solution of allyl ester **18c** (300 mg, 0.694 mmol, 1.0 equiv) in THF (7 mL, 0.1 M) at 0 °C was added NaH (60% dispersion in mineral oil, 38 mg, 0.972 mmol, 1.4 equiv) and the mixture was stirred at 0 °C for 15 min and then allowed to warm to 23 °C over 15 min. BnBr (412 μL, 3.47 mmol, 5.0 equiv) was then added dropwise and the reaction mixture was heated to 50 °C. After stirring for 8 h, the reaction mixture was allowed to cool to 23 °C and poured into saturated aqueous NH₄Cl (5 mL), the layers were separated, and the aqueous phase was extracted with ethyl acetate (3 x 2 mL). The combined organic extracts were dried over anhydrous Na₂SO₄, filtered, and concentrated under reduced pressure. The crude product was purified by silica gel flash chromatography (20% EtOAc/hexanes) to provide the title compound as a colorless foam (303 mg, 0.580 mmol, 84% yield); ¹H NMR (500 MHz, CDCl₃) δ 7.72 (d, J = 8.5 Hz, 2H), 7.31 – 7.12 (m, 5H), 6.90 – 6.80 (m, 2H), 5.95 – 5.75 (m, 1H), 5.41 – 5.26 (m, 2H), 4.69 – 4.54 (m, 2H), 4.21 – 4.05 (m, 1H), 4.02 – 3.86 (m, 2H), 3.83 (s, 3H), 3.78 – 3.62 (m, 2H), 3.56 – 3.49 (m, 1H), 3.43 – 3.10 (m, 2H), 1.45 (s, 9H); ¹³C NMR (125 MHz, CDCl₃) δ 173.7, 173.4, 172.0, 171.7, 170.8, 170.2, 162.9, 155.4, 154.8, 135.7, 135.6, 131.1, 130.9, 130.7, 130.5, 128.5, 128.3, 128.2, 127.5, 127.3, 127.0, 120.2, 119.9, 113.5,

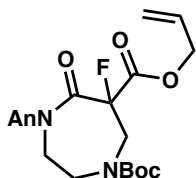
80.9, 80.7, 66.6, 62.4, 62.0, 55.3, 47.1, 46.8, 46.0, 45.8, 42.8, 42.5, 41.9, 28.3; IR (Neat Film, NaCl) 2976, 2359, 1698, 1604, 1512, 1455, 1416, 1366, 1324, 1258, 1155, 1028, 979, 840, 741, 703, 671, 634 cm^{-1} ; HRMS (MM: ESI-APCI): m/z calc'd for $\text{C}_{29}\text{H}_{35}\text{N}_2\text{O}_7$ $[\text{M}+\text{H}]^+$: 523.2439, found 523.2446.



6-allyl 1-(*tert*-butyl) 4-benzoyl-6-fluoro-5-oxo-1,4-diazepane-1,6-dicarboxylate (19f)

To a 20 mL vial containing allyl ester **18a** (250 mg, 0.621 mmol, 1.0 equiv) in THF (7.4 mL, 0.1 M) at 23 °C was added NaH (60% dispersion in mineral oil, 27.3 mg, 0.683 mmol, 1.1 equiv). After stirring for 12 min, Selectfluor™ (264 mg, 0.745 mmol, 1.2 equiv) was added in a single portion, and the reaction mixture was warmed to 50 °C and stirred for 24 h, after which starting material remained as judged by TLC. Additional Selectfluor™ (264 mg, 0.745 mmol, 1.2 equiv) was then added, and the reaction mixture was stirred for an additional 8 h at 50 °C. The reaction mixture was allowed to cool to 23 °C and water (5 mL) was added. The layers were separated and the aqueous layer was extracted with EtOAc (3 x 5 mL). The combined organic extracts were dried over anhydrous Na_2SO_4 , concentrated under reduced pressure, and purified by silica gel flash chromatography (25% EtOAc/hexanes) to provide the title compound (167 mg, 0.397 mmol, 64% yield); ^1H NMR (500 MHz, CDCl_3) δ 7.64 – 7.56 (m, 2H), 7.52 – 7.43 (m, 1H), 7.36 (t, $J = 7.7$ Hz, 2H), 5.99 – 5.80 (m, 1H), 5.43 – 5.19 (m, 2H), 4.83 – 4.56 (m, 2H), 4.52 – 4.17 (m, 3H), 4.03 – 3.56 (m, 2H), 3.27 – 3.08 (m, 1H), 1.47 (s, 9H); ^{13}C NMR (125 MHz, CDCl_3) δ 173.1, 169.6, 169.4, 164.8, 164.6, 154.9, 134.3, 132.5, 130.7, 128.5, 128.4, 119.7, 95.7 (d, $J =$

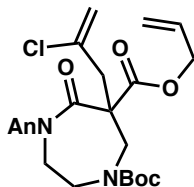
204.8 Hz), 81.5, 67.2, 47.6 (dd, $J_{C-F} = 137.5, 24.1$ Hz), 47.3, 46.4, 42.8, 28.3; IR (Neat Film, NaCl) 2978, 2926, 1694, 1450, 1414, 1393, 1367, 1329, 1246, 1152, 1042, 999, 979, 926, 857, 766, 724, 694, 672, 648 cm^{-1} ; HRMS (MM: ESI-APCI): m/z calc'd for $\text{C}_{21}\text{H}_{29}\text{FN}_3\text{O}_6$ $[\text{M}+\text{NH}_4]^+$: 438.2035, found 438.2040.



6-allyl 1-(tert-butyl) 6-fluoro-4-(4-methoxybenzoyl)-5-oxo-1,4-diazepane-1,6-dicarboxylate (19g)

To a 20 mL vial containing allyl ester **18c** (320 mg, 0.740 mmol, 1.0 equiv) and NaH (60% dispersion in mineral oil, 32.5 mg, 0.814 mmol, 1.1 equiv) was added THF (7.4 mL, 0.1 M) at 23 °C. After stirring for 30 min, Selectfluor™ (315 mg, 0.889 mmol, 1.2 equiv) was added in a single portion, and the reaction mixture was warmed to 50 °C and stirred for 5 h. The crude reaction mixture was then concentrated under reduced pressure and purified by silica gel flash chromatography (30% acetone/hexanes) to provide the title compound (290 mg, 0.644 mmol, 87% yield); ^1H NMR (400 MHz, CDCl_3) δ 7.66 – 7.58 (m, 2H), 6.90 – 6.82 (m, 2H), 5.91 (ddt, $J = 16.3, 10.9, 5.7$ Hz, 1H), 5.43 – 5.21 (m, 2H), 4.84 – 4.40 (m, 3H), 4.40 – 4.16 (m, 2H), 4.00 – 3.86 (m, 1H), 3.82 (s, 3H), 3.77 – 3.56 (m, 1H), 3.22 – 3.09 (m, 1H), 1.47 (s, 9H); ^{13}C NMR (100 MHz, CDCl_3) δ 172.6, 169.6 (dd, $J_{C-F} = 48.2, 25.4$ Hz), 164.9 (d, $J_{C-F} = 25.8$ Hz), 163.4, 155.0, 131.3, 130.8, 126.1, 119.8, 113.9, 95.7 (dd, $J_{C-F} = 205.6, 14.6$ Hz), 81.5, 67.3, 55.5, 47.5 (dd, $J_{C-F} = 109.0, 23.7$ Hz), 47.2 (d, $J_{C-F} = 92.2$ Hz), 43.4, 28.3; IR (Neat Film, NaCl) 2976, 2936, 2844, 1759, 1698, 1603, 1578, 1512, 1449, 1414, 1367, 1327, 1258, 1168, 1151, 1076, 1030, 997, 977,

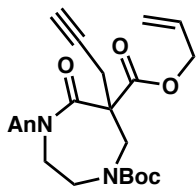
942, 929, 841, 817, 770, 760, 730, 698 cm^{-1} ; HRMS (MM: ESI-APCI): m/z calc'd for $\text{C}_{22}\text{H}_{28}\text{FN}_2\text{O}_7$ $[\text{M}+\text{H}]^+$: 451.1875, found 451.1877.



6-allyl 1-(*tert*-butyl) 6-(2-chloroallyl)-4-(4-methoxybenzoyl)-5-oxo-1,4-diazepane-1,6-dicarboxylate (19h)

To a suspension of allyl ester **18c** (300 mg, 0.694 mmol, 1.0 equiv) and Cs_2CO_3 (453 mg, 1.39 mmol, 2.0 equiv) in acetonitrile (7 mL, 0.1 M) was added 2,3-dichloropropene (320 μL , 3.47 mmol, 5.0 equiv) at 23 $^\circ\text{C}$. The reaction mixture was heated to 50 $^\circ\text{C}$ and stirred for 19 h, after which starting material remained as judged by TLC. Tetrabutylammonium iodide (25.6 mg, 0.0694 mmol, 0.1 equiv) was added and the reaction mixture was stirred at 50 $^\circ\text{C}$ for an additional 9 h, then allowed to cool to 23 $^\circ\text{C}$. The mixture was filtered through a cotton plug and concentrated under reduced pressure. The crude product was purified by silica gel flash chromatography (20% EtOAc/petroleum ether) to provide the title compound as a colorless oil (196 mg, 0.387 mmol, 56% yield); ^1H NMR (400 MHz, CDCl_3) δ 7.71 (d, $J = 8.8$ Hz, 2H), 6.85 (d, $J = 8.9$ Hz, 2H), 6.12 – 5.94 (m, 1H), 5.60 – 5.25 (m, 4H), 4.78 (qdt, $J = 12.8, 6.0, 1.2$ Hz, 2H), 4.25 (br t, $J = 13.9$ Hz, 1H), 4.17 – 3.87 (m, 3H), 3.84 (s, 3H), 3.76 – 3.51 (m, 1H), 3.48 – 3.30 (m, 1H), 3.29 – 2.99 (m, 2H), 1.43 (d, $J = 16.9$ Hz, 9H); ^{13}C NMR (100 MHz, CDCl_3) δ 173.9, 173.3, 170.3, 163.1, 155.9, 155.1, 137.0, 136.7, 131.1, 127.2, 120.6, 120.3, 119.4, 118.4, 113.6, 81.4, 81.0, 67.5, 60.0, 55.5, 47.1, 45.9, 46.0, 45.2, 45.6, 44.7, 43.1, 42.8, 28.4; IR (Neat Film, NaCl) 3356, 3080, 2977, 2933, 2841, 2568, 2254, 1700, 1629, 1605, 1579, 1512,

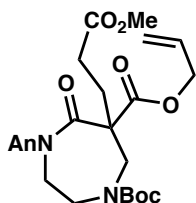
1456, 1417, 1393, 1367, 1326, 1281, 1257, 1217, 1196, 1153, 1029, 988, 910, 842, 811, 780, 757, 732, 668, 634, 621 cm^{-1} ; HRMS (MM: ESI-APCI): m/z calc'd for $\text{C}_{25}\text{H}_{32}\text{ClN}_2\text{O}_7$ $[\text{M}+\text{H}]^+$: 507.1893, found 507.1902.



6-allyl 1-(tert-butyl) 4-(4-methoxybenzoyl)-5-oxo-6-(prop-2-yn-1-yl)-1,4-diazepane-1,6-dicarboxylate (19i)

To a solution of allyl ester **18c** (250 mg, 0.578 mmol, 1.0 equiv) in THF (5.8 mL, 0.1 M) was added NaH (60% dispersion in mineral oil, 25 mg, 0.636 mmol, 1.1 equiv) at 0 °C. After stirring for 30 min at 0 °C, propargyl bromide (80% wt/wt in toluene, 125 μL , 1.16 mmol, 2.0 equiv) was added at 0 °C. The reaction mixture was heated to 50 °C and stirred for 16 h. The mixture was allowed to cool to 23 °C, quenched with aqueous NaHCO_3 (10 mL) and extracted with EtOAc (3 x 5 mL). The combined organic extracts were dried over anhydrous Na_2SO_4 , filtered, and concentrated under reduced pressure. The crude product was purified by automated silica gel flash chromatography (Teledyne ISCO, 0 \rightarrow 50% acetone/hexanes) to provide propargyl allyl ester **19i** as a colorless oil (220 mg, 0.468 mmol, 81% yield). ^1H NMR (500 MHz, CDCl_3) δ 7.73 – 7.59 (m, 2H), 6.84 (d, J = 8.6 Hz, 2H), 5.99 (ddt, J = 17.3, 10.4, 6.0 Hz, 1H), 5.54 – 5.27 (m, 2H), 4.85 – 4.69 (m, 2H), 4.33 – 3.85 (m, 4H), 3.82 (s, 3H), 3.76 – 3.56 (m, 1H), 3.56 – 3.39 (m, 1H), 3.14 – 2.90 (m, 2H), 2.08 (s, 1H), 1.42 (d, J = 14.3 Hz, 9H); ^{13}C NMR (125 MHz, CDCl_3) δ 173.7, 173.2, 170.5, 170.3, 169.7, 169.3, 163.0, 155.6, 154.9, 131.2, 131.0, 127.1, 120.3, 120.0, 113.6, 81.1, 81.0, 78.9, 78.6, 72.3, 67.3, 60.7, 60.4, 55.5, 47.1, 46.5, 46.2, 46.0, 43.0, 28.3,

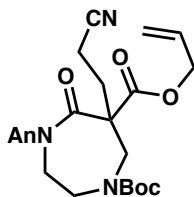
27.0, 26.9; IR (Neat Film, NaCl) 3280, 2975, 2936, 1737, 1694, 1604, 1579, 1547, 1512, 1454, 1416, 1393, 1366, 1326, 1280, 1258, 1156, 1134, 1030, 994, 980, 841, 778, 770, 737, 706, 677, 634, 622 cm^{-1} ; HRMS (MM: ESI-APCI): m/z calc'd for $\text{C}_{25}\text{H}_{31}\text{N}_2\text{O}_7$ $[\text{M}+\text{H}]^+$: 471.2126, found 471.2130.



6-allyl 1-(*tert*-butyl) 6-(3-methoxy-3-oxopropyl)-4-(4-methoxybenzoyl)-5-oxo-1,4-diazepane-1,6-dicarboxylate (19j)

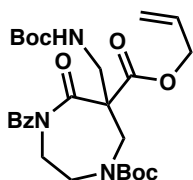
To a 20 mL vial containing allyl ester **18c** (300 mg, 0.694 mmol, 1.0 equiv) and K_2CO_3 (480 mg, 3.47 mmol, 5.0 equiv) was added acetone (2.8 mL, 0.25 M) and methyl acrylate (126 μL , 1.39 mmol, 2.0 equiv) at 23 $^\circ\text{C}$. The vessel was sealed and heated to 50 $^\circ\text{C}$. After stirring for 5 h, additional methyl acrylate (126 μL , 1.39 mmol, 2.0 equiv) was added and the reaction was stirred for an additional 14 h. The reaction mixture was then filtered through a plug of cotton, concentrated under reduced pressure, and purified by silica gel flash chromatography (33% EtOAc/petroleum ether) to provide diester **19j** as a colorless, waxy solid (185 mg, 0.357 mmol, 51% yield); ^1H NMR (500 MHz, CDCl_3) δ 7.77 – 7.65 (m, 2H), 6.92 – 6.79 (m, 2H), 5.96 (ddt, $J = 17.2, 10.3, 6.1$ Hz, 1H), 5.48 – 5.27 (m, 2H), 4.82 – 4.63 (m, 2H), 4.32 – 3.84 (m, 3H), 3.83 (s, 3H), 3.81 – 3.66 (m, 1H), 3.62 (s, 3H), 3.58 – 3.40 (m, 2H), 2.56 – 2.13 (m, 4H), 1.44 (s, 9H); ^{13}C NMR (125 MHz, CDCl_3) δ 173.8, 173.5, 173.0, 171.9, 170.9, 170.6, 163.0, 155.1, 154.8, 131.1, 131.0, 127.5, 120.6, 113.6, 81.2, 67.0, 60.4, 55.5, 51.7, 48.7, 47.8, 47.0, 46.0, 43.4, 31.4, 29.8, 28.3; IR

(Neat Film, NaCl) 3354, 2976, 2843, 2568, 2255, 2044, 1694, 1605, 1579, 1556, 1513, 1416, 1393, 1367, 1260, 1168, 1030, 982, 916, 843, 811, 782, 766, 732, 648, 634 cm^{-1} ; HRMS (MM: ESI-APCI): m/z calc'd for $\text{C}_{26}\text{H}_{38}\text{N}_3\text{O}_9$ $[\text{M}+\text{NH}_4]^+$: 536.2603, found 536.2603.



6-allyl 1-(tert-butyl) 6-(2-cyanoethyl)-4-(4-methoxybenzoyl)-5-oxo-1,4-diazepane-1,6-dicarboxylate (19k)

To a 20 mL vial containing allyl ester **18c** (300 mg, 0.694 mmol, 1.0 equiv) and K_2CO_3 (480 mg, 3.47 mmol, 5.0 equiv) was added acetone (2.8 mL, 0.25 M) and acrylonitrile (182 μL , 2.78 mmol, 4.0 equiv) at 23 $^\circ\text{C}$. The vessel was sealed and heated to 50 $^\circ\text{C}$. After 17 h of stirring, the reaction mixture was filtered through a plug of cotton, concentrated under reduced pressure, and purified by silica gel flash chromatography (33% EtOAc/petroleum ether) to provide **19k** as a colorless foam (176 mg, 0.362 mmol, 52% yield); ^1H NMR (400 MHz, CDCl_3) δ 7.74 (d, J = 8.8 Hz, 2H), 6.89 (d, J = 8.9 Hz, 2H), 6.01 (ddt, J = 16.7, 10.3, 6.3 Hz, 1H), 5.51 – 5.36 (m, 2H), 4.89 – 4.75 (m, 2H), 4.32 – 3.88 (m, 3H), 3.86 (s, 3H), 3.84 – 3.34 (m, 3H), 2.71 – 2.09 (m, 4H), 1.53 – 1.34 (m, 9H); ^{13}C NMR (100 MHz, CDCl_3) δ 170.8, 170.3, 163.2, 155.3, 131.0, 130.6, 127.1, 121.4, 121.1, 119.1, 113.7, 81.4, 67.5, 60.2, 55.5, 47.5, 46.8, 43.6, 32.9, 28.3, 13.6; IR (Neat Film, NaCl) 2975, 2934, 2250, 1694, 1605, 1579, 1512, 1455, 1419, 1393, 1367, 1326, 1255, 1164, 1031, 1000, 979, 941, 916, 842, 813, 781, 762, 733, 648, 634 cm^{-1} ; HRMS (MM: ESI-APCI): m/z calc'd for $\text{C}_{25}\text{H}_{35}\text{N}_4\text{O}_7$ $[\text{M}+\text{NH}_4]^+$: 503.2500, found 503.2505.

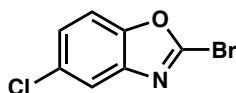


6-allyl 1-(*tert*-butyl) 4-benzoyl-6-(((*tert*-butoxycarbonyl)amino)methyl)-5-oxo-1,4-diazepane-1,6-dicarboxylate (19I)

A solution of allyl ester **18a** (200 mg, 0.497 mmol, 1.0 equiv) and *tert*-butyl ((phenylsulfonyl)methyl)carbamate^{30,31} (162 mg, 0.597 mmol, 1.2 equiv) in CH₂Cl₂ (2.5 mL, 0.2 M) at 23 °C was stirred for 5 min, after which time Cs₂CO₃ (405 mg, 1.24 mmol, 2.5 equiv) was added at the same temperature. After an additional 30 min of stirring, saturated aqueous NH₄Cl (1 mL) was added, and the biphasic mixture was vigorously stirred for 20 min. The layers were separated, and the aqueous phase was extracted with CH₂Cl₂ (3 x 3 mL). The combined organic extracts were dried over anhydrous Na₂SO₄, filtered, and concentrated under reduced pressure onto silica gel (2 g). The silica-adsorbed crude reaction mixture was purified by automated silica gel flash chromatography (Teledyne ISCO, 10→40% acetone/hexanes) to provide carbamate **19I** as a white foam (200 mg, 0.376 mmol, 76% yield): ¹H NMR (400 MHz, CDCl₃) δ 7.83 – 7.71 (m, 2H), 7.59 – 7.46 (m, 1H), 7.46 – 7.36 (m, 2H), 6.00 (ddt, *J* = 16.6, 10.3, 6.1 Hz, 1H), 5.51 – 5.25 (m, 2H), 5.17 (br s, 1H), 4.79 – 4.64 (m, 2H), 4.48 – 4.23 (m, 1H), 4.14 – 3.20 (m, 7H), 1.44 (s, 9H), 1.42 (s, 9H); ¹³C NMR (100 MHz, CDCl₃) δ 174.1, 173.8, 172.7, 170.1, 169.6, 156.0, 155.2, 154.7, 135.5, 132.2, 131.4, 128.5, 128.4, 120.2, 81.4, 79.6, 67.4, 62.7, 47.1, 46.8, 45.9, 43.2, 28.5, 28.4; IR (Neat Film, NaCl) 3457, 2977, 2934, 2253, 1704, 1600, 1503, 1450, 1417, 1392, 1367, 1325, 1283, 1248, 1158, 1042, 980, 913, 860, 767, 729, 693, 663 cm⁻¹; HRMS (MM: ESI-APCI): *m/z* calc'd for C₂₇H₃₈N₃O₈ [M+H]⁺: 532.2653,

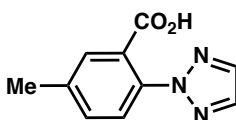
found 532.2664.

1.5.2.3 Derivatization of Diazepane Allylic Alkylation Products



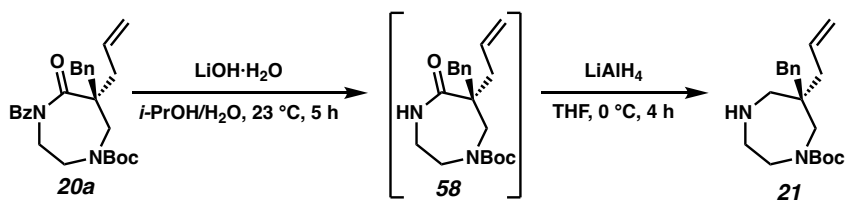
2-bromo-5-chlorobenzo[d]oxazole (22)

Prepared according to the literature procedure by Mangion and coworkers¹⁴ and used directly in the synthesis of **23**.



5-methyl-2-(2H-1,2,3-triazol-2-yl)benzoic acid (24)

Prepared according to the literature procedure by Mangion and coworkers.¹⁴ All characterization data matched those reported in the literature.



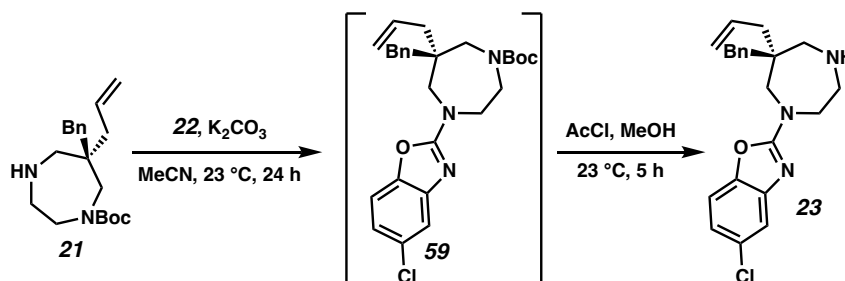
tert-butyl (*S*)-6-allyl-6-benzyl-5-oxo-1,4-diazepane-1-carboxylate (58)

To a flask containing benzoyl-protected diazepanone **20a** (460 mg, 1.03 mmol, 1.0 equiv) was added isopropyl alcohol (100 mL, 0.01 M) and water (10 mL), followed by LiOH·H₂O (61 mg, 1.45 mmol, 1.5 equiv) at 23 °C. After stirring for 4 h at 23 °C, the isopropyl alcohol was removed under reduced pressure and the resulting aqueous mixture extracted with EtOAc (4 x 50 mL). The combined organic extracts were dried with sodium

sulfate, filtered, and concentrated under reduced pressure to yield a crude oil (400 mg) that was used without further purification.

***tert*-butyl (*R*)-6-allyl-6-benzyl-1,4-diazepane-1-carboxylate (21)**

Crude lactam **58** (350 mg [theoretical maximum 310 mg lactam], 0.903 mmol, 1 equiv) was dissolved in THF (10.2 mL, 0.1 M) and cooled to 0 °C. LiAlH₄ (77 mg, 2.03 mmol, 2.25 equiv) was then added, and the reaction mixture was stirred at 0 °C for 4 h, over the course of which an additional 3.37 equiv (116 mg, 3.05 mmol) of LiAlH₄ were added in total (77 mg, followed by 39 mg, at equal intervals). The reaction mixture was then diluted with diethyl ether (10 mL) and water (300 μL) was added. After gas generation subsided, 15% aqueous NaOH (300 μL) was added, followed by additional water (900 μL). After stirring at 0 °C for 15 min, anhydrous MgSO₄ was added, and the mixture was stirred for an additional 10 min, whereafter it was filtered through celite and concentrated under reduced pressure. Purification by automated silica gel flash chromatography (Teledyne ISCO, 0→20% MeOH/CH₂Cl₂) provided the product as a light yellow oil (130 mg, 0.393 mmol, 44% yield); ¹H NMR (400 MHz, CDCl₃) δ 7.40 – 7.14 (m, 5H), 6.01 (dq, *J* = 17.1, 7.8 Hz, 1H), 5.18 (d, *J* = 15.9 Hz, 2H), 3.67 – 3.30 (m, 4H), 2.97 (m, 2H), 2.88 – 2.48 (m, 4H), 2.30 – 2.06 (m, 3H), 1.50 (s, 9H); ¹³C NMR (100 MHz, CDCl₃) δ 155.8, 138.1, 134.6, 130.7, 128.0, 126.2, 118.2, 79.8, 79.5, 57.9, 57.2, 55.3, 54.2, 50.9, 49.8, 49.3, 43.5, 41.3, 39.8, 39.4, 28.5; IR (Neat Film, NaCl) 3357, 3066, 3028, 2976, 2928, 1694, 1602, 1464, 1455, 1416, 1391, 1365, 1334, 1302, 1248, 1166, 1031, 996, 952, 912, 866, 771, 733, 703, 685, 672, 659, 644, 612 cm⁻¹; HRMS (MM: ESI-APCI): *m/z* calc'd for C₂₀H₃₁N₂O₂ [M+H]⁺: 331.2380, found 331.2399; [α]_D^{22.24} –6.496 (c 2.0, CHCl₃).



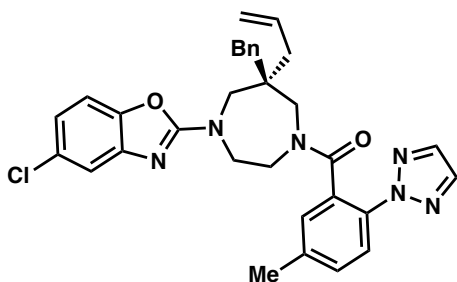
***tert*-butyl (*R*)-6-allyl-6-benzyl-4-(5-chlorobenzo[*d*]oxazol-2-yl)-1,4-diazepane-1-carboxylate (**59**)**

To a 1-dram vial containing diazepane **21** (9.5 mg, 0.0287 mmol, 1.0 equiv), aryl bromide **22** (10.0 mg, 0.0431 mmol, 1.5 equiv), and K₂CO₃ (7.9 mg, 0.0574 mmol, 2 equiv) was added MeCN (0.3 mL, 0.1 M) at 23 °C. After stirring for 24 h at 23 °C, saturated aqueous NH₄Cl (1 mL) was added, and the mixture was extracted with EtOAc (3 x 1 mL). The combined organic extracts were dried over anhydrous Na₂SO₄ and concentrated under reduced pressure. The crude material (15.4 mg) thus obtained was carried forward without further purification.

(*S*)-2-(6-allyl-6-benzyl-1,4-diazepan-1-yl)-5-chlorobenzo[*d*]oxazole (23**)**

Crude carbamate **59** was dissolved in MeOH (0.3 mL, 0.1 M) and AcCl (20.5 μL, 0.288 mmol, 10 equiv) was added at 23 °C. After stirring for 5 h at 23 °C, the reaction mixture was concentrated under reduced pressure and purified by silica gel flash chromatography (66% EtOAc/benzene + 1% Et₃N) to provide **23** as a beige, amorphous solid (4.3 mg, 0.0113 mmol, 39% yield from **21**) of sufficient purity for use in the next reaction, however, further purification was possible by silica gel flash chromatography with 2% Et₃N in Et₂O; ¹H NMR (400 MHz, CDCl₃) δ 7.34 – 7.27 (m, 3H), 7.25 – 7.17 (m, 3H), 7.12 (d, *J* = 8.4 Hz, 1H), 6.94 (dd, *J* = 8.4, 2.3 Hz, 1H), 5.99 (ddt, *J* = 14.5, 10.4, 7.2

Hz, 1H), 5.30 (d, $J = 3.1$ Hz, 1H), 5.20 – 5.10 (m, 1H), 3.87 – 3.61 (m, 3H), 3.15 – 3.00 (m, 2H), 2.90 – 2.66 (m, 3H), 2.57 (d, $J = 13.9$ Hz, 1H), 2.22 – 2.10 (m, 3H); ^{13}C NMR (100 MHz, CDCl_3) δ 147.5, 137.8, 134.1, 130.8, 129.4, 128.2, 126.4, 120.1, 118.8, 116.2, 109.2, 57.8, 56.5, 53.3, 49.2, 43.8, 41.3, 39.8; IR (Neat Film, NaCl) 2922, 1638, 1570, 1458, 1249, 1167, 921, 792, 710 cm^{-1} ; HRMS (MM: ESI-APCI): m/z calc'd for $\text{C}_{22}\text{H}_{25}\text{ClN}_3\text{O}$ $[\text{M}+\text{H}]^+$: 382.1681, found 382.1695; $[\alpha]_{\text{D}}^{21.89} +7.524$ (c 0.07, CHCl_3).

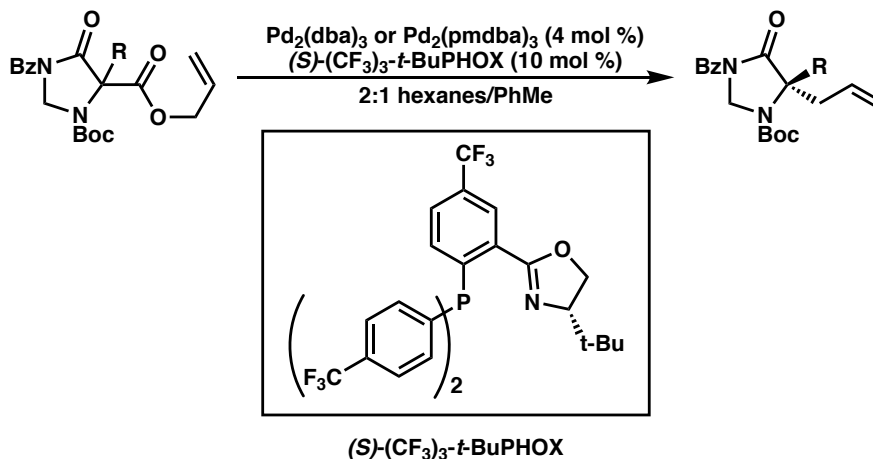


(R)-6-allyl-6-benzyl-4-(5-chlorobenzo[*d*]oxazol-2-yl)-1,4-diazepan-1-yl(5-methyl-2-(2H-1,2,3-triazol-2-yl)phenyl)methanone (25)

To a vial containing carboxylic acid **24** (35 mg, 0.172 mmol, 1.0 equiv) in CH_2Cl_2 (1.8 mL) at 23 °C was added DMF (4 μL , 0.0517 mmol, 0.3 equiv) and oxalyl chloride (18 μL , 0.207 mmol, 1.2 equiv). After stirring for 1 h, Et_3N (48 μL , 0.344 mmol, 2.0 equiv) was added, followed by amine **23** (60 mg, 0.155 mmol, 0.9 equiv) in CH_2Cl_2 (1.8 mL, 0.05 M total concentration). After stirring for an additional 1 h at 23 °C, the reaction mixture was quenched with saturated aqueous NaHCO_3 (3 mL), the layers were separated, and the aqueous layer was extracted with CH_2Cl_2 (3 x 2 mL). The combined organic extracts were dried over anhydrous Na_2SO_4 , concentrated under reduced pressure, and purified by automated silica gel flash chromatography (Teledyne ISCO, 0→40% Et_2O /hexanes) to provide amide **25** as a beige oil (29.6 mg, 0.0522 mmol, 34% yield); ^1H NMR (400 MHz,

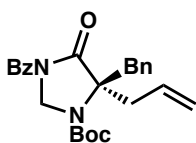
CDCl₃) δ 7.73 (s, 1H), 7.55 (s, 1H), 7.34 – 7.27 (m, 6H), 7.20 – 7.09 (m, 3H), 7.04 – 6.92 (m, 2H), 6.11 (ddt, *J* = 17.6, 10.4, 7.3 Hz, 1H), 5.26 – 5.12 (m, 2H), 4.24 – 4.07 (m, 1H), 3.96 (dd, *J* = 17.1, 14.4 Hz, 1H), 3.90 – 3.75 (m, 1H), 3.70 – 3.40 (m, 4H), 3.38 – 3.12 (m, 2H), 2.99 – 2.80 (m, 2H), 2.43 – 2.38 (m, 2H), 2.38 – 2.33 (m, 2H); ¹³C NMR (100 MHz, CDCl₃) δ 170.7, 170.5, 170.0, 163.0, 147.2, 144.4, 138.7, 138.6, 138.5, 136.9, 135.9, 135.8, 135.8, 135.7, 135.7, 135.6, 135.6, 134.2, 133.9, 133.8, 133.6, 133.5, 133.2, 132.9, 130.9, 130.8, 130.6, 130.6, 130.4, 130.4, 129.9, 129.5, 129.5, 129.0, 129.0, 128.3, 128.3, 128.2, 128.2, 128.2, 128.1, 128.1, 126.6, 126.6, 122.2, 122.0, 121.9, 120.5, 120.5, 119.2, 119.1, 119.0, 116.3, 116.3, 109.3, 109.2, 56.2, 56.1, 55.5, 54.3, 52.9, 52.2, 49.5, 49.3, 49.2, 48.9, 47.6, 45.0, 43.5, 43.1, 42.4, 42.2, 42.0, 41.8, 39.5, 39.5, 37.6, 21.0, 21.0, 20.9; IR (Neat Film, NaCl) 3431, 2923, 2854, 2356, 1644, 1634, 1574, 1568, 1538, 1505, 1462, 1454, 1428, 1372, 1308, 1251, 1216, 1172, 1054, 952, 921, 852, 822, 794, 737, 704 cm⁻¹; HRMS (MM: ESI-APCI): *m/z* calc'd for C₃₂H₃₂ClN₆O₂ [M+H]⁺: 567.2270, found 567.2294; [α]_D^{22.24} +41.90 (c 1.0, CHCl₃).

1.5.2.4 General Procedure for Allylic Alkylation of Imidazolidinones



In a N₂ filled glovebox, Pd₂(dba)₃ (4 mol %) or Pd₂(pmdba)₃ (4 mol %) and (S)-

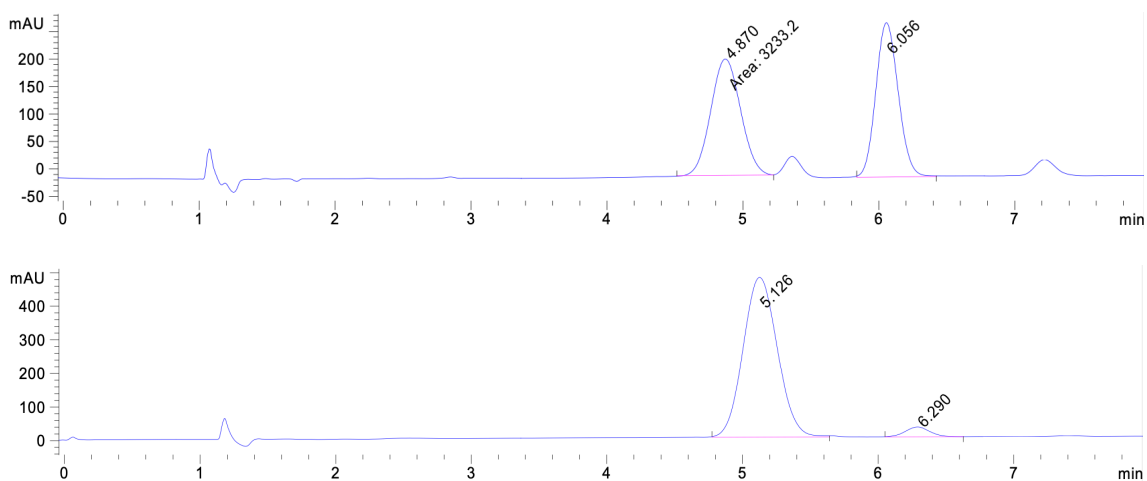
(CF₃)₃-*t*-BuPHOX (10 mol %) were suspended in 2:1 hexanes:PhMe (2 mL) in a 20 mL glass vial. After stirring for 20 minutes at 25 °C, the appropriate imidazolidinone (1.0 equiv) and 2:1 hexanes:PhMe (5.1 mL, total substrate concentration 0.014 M) were added to the pre-stirred catalyst solution. The vial was then sealed and heated to the appropriate temperature in a heating block. After full consumption of starting material, as monitored by TLC, the reaction mixture was exposed to air. The crude reaction mixture was loaded directly onto a flash column and the product was isolated by silica gel flash chromatography.



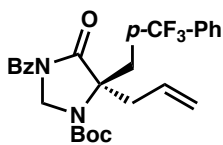
***tert*-butyl (*R*)-5-allyl-3-benzoyl-5-benzyl-4-oxoimidazolidine-1-carboxylate (**35a**)**

Prepared according to the general procedure with allyl ester **34a** (49.0 mg, 0.105 mmol, 1.0 equiv), Pd₂(pmdba)₃ (4.4 mg, 0.004 mmol, 4 mol %), and (*S*)-(CF₃)₃-*t*-BuPHOX (5.9 mg, 0.01 mmol, 10 mol %) at 40 °C for 50 h. Purified by silica gel flash chromatography (10% EtOAc/hexanes) to provide benzyl imidazolidinone **35a** as a colorless oil (33.7 mg, 0.0801 mmol, 76% yield, 92% ee); ¹H NMR (400 MHz, CDCl₃; compound exists as a 2:1 mixture of rotamers. For fully resolved peaks, the major rotamer is denoted by *, and the minor rotamer by #) δ 7.52 (dtd, *J* = 9.6, 6.5, 2.5 Hz, 1H), 7.44 – 7.30 (m, 4H), 7.31 – 7.23 (m, 3H), 7.12 (ddt, *J* = 8.8, 7.2, 2.0 Hz, 2H), 5.77 – 5.56 (m, 1H), 5.27 – 5.13 (m, 2H), 4.93 (d, *J* = 7.6 Hz, 1H[#]), 4.85 (d, *J* = 7.4 Hz, 1H*), 4.31 (d, *J* = 7.6 Hz, 1H[#]), 4.18 (d, *J* = 7.4 Hz, 1H*), 3.62 (d, *J* = 13.4 Hz, 1H*), 3.40 (d, *J* = 13.5 Hz, 1H[#]), 3.27 (dd, *J* = 13.6, 7.7 Hz, 1H*), 3.02 (dd, *J* = 13.8, 7.4 Hz, 1H[#]), 2.95 (dd, *J* = 13.5, 4.4

Hz, 1H), 2.69 – 2.52 (m, 1H), 1.65 (s, 9H[#]), 1.54 (s, 9H*); ¹³C NMR (100 MHz, CDCl₃) δ 171.5, 171.4, 168.4, 168.1, 152.6, 151.9, 135.9, 135.3, 133.3, 133.3, 132.6, 132.5, 131.9, 131.5, 130.0, 129.9, 128.9, 128.9, 128.8, 128.6, 127.9, 127.9, 127.8, 127.6, 120.6, 120.5, 82.2, 81.3, 71.5, 71.1, 61.3, 61.3, 41.7, 40.9, 40.6, 39.7, 28.8, 28.5; IR (Neat Film, NaCl) 2927, 1758, 1707, 1390, 1368, 1295, 1167, 702, 660 cm⁻¹; HRMS (MM: ESI-APCI): *m/z* calc'd for C₂₅H₂₉N₂O₄ [M+H]⁺: 421.2122, found 421.2108; [α]_D^{21.7} +19.50 (*c* 1.0, CHCl₃); SFC (AD-H, IPA/CO₂ = 7/93, flow rate = 2.5 mL/min, λ = 210 nm) *t*_R = 5.13 min (major), 6.29 min (minor).



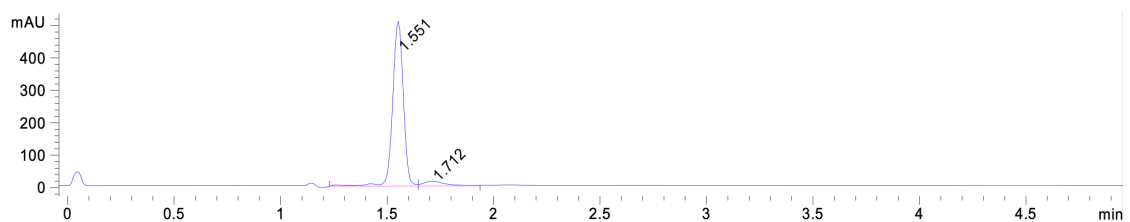
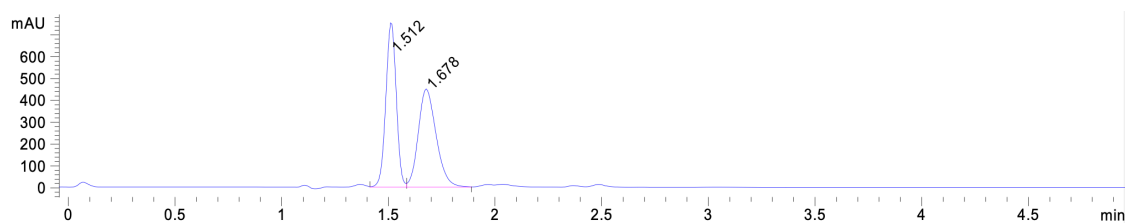
Peak #	RetTime [min]	Type	Width [min]	Area [mAU*s]	Height [mAU]	Area %
1	5.126	BB	0.2769	8353.69336	475.74954	95.8254
2	6.290	BB	0.1943	363.92191	29.01324	4.1746
Totals :				8717.61526	504.76278	



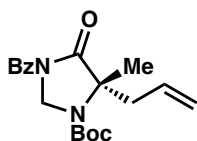
***tert*-butyl (*R*)-5-allyl-3-benzoyl-4-oxo-5-(4-(trifluoromethyl)benzyl)imidazolidine-1-carboxylate (**35b**)**

Prepared according to the general procedure with allyl ester **34b** (53.8 mg, 0.101 mmol, 1.0 equiv), Pd₂(pmdba)₃ (4.4 mg, 0.004 mmol, 4 mol %), and (*S*)-(CF₃)₃-*t*-BuPHOX (5.9 mg, 0.01 mmol, 10 mol %) at 60 °C for 23 h. Purified by silica gel flash chromatography (10% EtOAc/hexanes) to provide 4-trifluorobenzyl imidazolidinone **35b** as a colorless oil (37.7 mg, 0.0772 mmol, 76% yield, 89% ee); ¹H NMR (400 MHz, CDCl₃; compound exists as a 3:1 mixture of rotamers. For fully resolved peaks, the major rotamer is denoted by *, and the minor rotamer by #) δ 7.60 – 7.52 (m, 3H), 7.47 – 7.37 (m, 3H), 7.36 – 7.22 (m, 3H), 5.82 – 5.59 (m, 1H), 5.31 – 5.19 (m, 2H), 4.96 (d, *J* = 7.7 Hz, 1H[#]), 4.89 (d, *J* = 7.5 Hz, 1H*), 4.42 (d, *J* = 7.7 Hz, 1H[#]), 4.34 (d, *J* = 7.5 Hz, 1H*), 3.72 (d, *J* = 13.4 Hz, 1H*), 3.48 (d, *J* = 13.5 Hz, 1H[#]), 3.29 (ddt, *J* = 13.7, 7.8, 1.0 Hz, 1H), 3.05 (dd, *J* = 13.3, 1.8 Hz, 1H), 2.72 – 2.55 (m, 1H), 1.67 (s, 9H[#]), 1.56 (s, 9H*); ¹³C NMR (100 MHz, CDCl₃) δ 171.1, 171.1, 168.3, 168.0, 152.5, 152.0, 140.2, 139.6, 133.1, 133.1, 132.8, 132.8, 131.5, 131.1, 130.4, 130.4, 130.0, 129.7, 128.9, 128.0, 128.0, 125.7, 125.7, 125.6, 125.5, 125.5, 125.4, 125.4, 122.9, 121.1, 121.0, 82.5, 81.7, 71.3, 70.9, 61.4, 61.4, 41.4, 41.1, 40.3, 39.9, 28.8, 28.5; IR (Neat Film, NaCl) 2977, 1754, 1707, 1391, 1369, 1326, 1294, 1263, 1226, 1165, 1126, 1068, 1019, 858, 700, 662 cm⁻¹; HRMS (MM: ESI-APCI): *m/z* calc'd for C₂₆H₃₁F₃N₃O₄ [M+NH₄]⁺: 506.2261, found 506.2254; [α]_D^{21.5} +25.45 (*c* 1.0, CHCl₃); SFC (OJ-H, IPA/CO₂ = 10/90, flow rate = 2.5 mL/min, λ = 254 nm) t_R = 1.55 min (major),

1.71 min (minor).



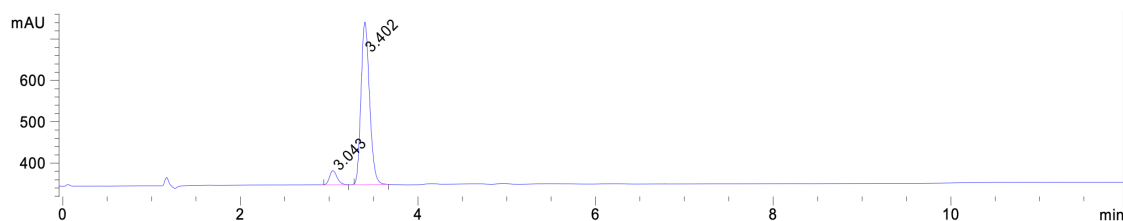
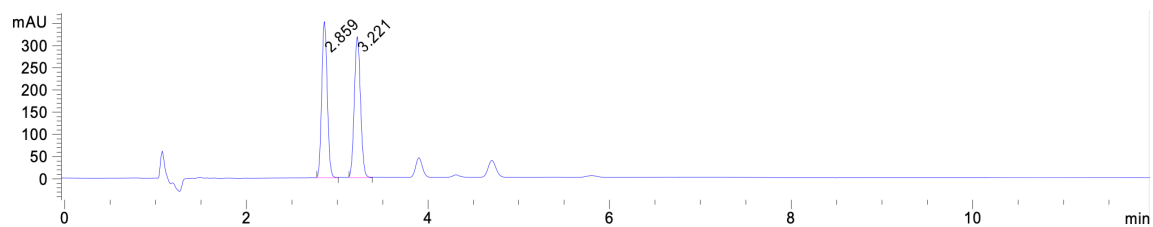
Peak #	RetTime [min]	Type	Width [min]	Area [mAU*s]	Height [mAU]	Area %
1	1.551	BV	0.0572	1769.47620	501.62180	94.5252
2	1.712	VB	0.1027	102.48551	14.44985	5.4748
Totals :				1871.96171	516.07164	



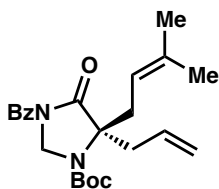
***tert*-butyl (*S*)-5-allyl-3-benzoyl-5-methyl-4-oxoimidazolidine-1-carboxylate (**35c**)**

Prepared according to the general procedure with allyl ester **34c** (40.7 mg, 0.105 mmol, 1.0 equiv), Pd₂(pmdba)₃ (4.4 mg, 0.004 mmol, 4 mol %), and (*S*)-(CF₃)₃-*t*-BuPHOX (5.9 mg, 0.01 mmol, 10 mol %) at 60 °C for 19 h. Purified by silica gel flash chromatography (15% EtOAc/hexanes) to provide methyl imidazolidinone **35c** as a colorless oil (31.3 mg, 0.0909 mmol, 88% yield, 86% ee); ¹H NMR (400 MHz, CDCl₃; compound exists as a 4:3 mixture of rotamers. For fully resolved peaks, the major rotamer is denoted by *, and the minor rotamer by #) δ 7.65 – 7.50 (m, 3H), 7.43 (t, *J* = 7.6 Hz, 2H),

5.70 (ddt, $J = 17.3, 9.9, 7.5$ Hz, 1H), 5.25 – 5.13 (m, 3H), 5.07 (dd, $J = 13.8, 7.7$ Hz, 1H), 3.16 (dd, $J = 13.7, 7.8$ Hz, 1H*), 2.90 (dd, $J = 13.8, 7.2$ Hz, 1H#), 2.56 – 2.38 (m, 1H), 1.63 – 1.48 (m, 12H); ^{13}C NMR (100 MHz, CDCl_3) δ 172.7, 168.8, 168.6, 152.8, 151.7, 133.3, 132.7, 132.1, 131.9, 129.1, 128.1, 120.5, 81.8, 81.3, 66.2, 65.8, 60.9, 60.8, 41.3, 40.0, 28.6, 28.5, 23.6, 22.7; IR (Neat Film, NaCl) 3076, 2977, 2931, 1759, 1702, 1602, 1477, 1450, 1388, 1368, 1297, 1263, 1227, 1168, 1124, 1059, 998, 965, 928, 906, 879, 859, 823, 792, 774, 733, 704, 662, 614 cm^{-1} ; HRMS (MM: ESI-APCI): m/z calc'd for $\text{C}_{19}\text{H}_{25}\text{N}_2\text{O}_4$ $[\text{M}+\text{H}]^+$: 345.1809, found 345.1805; $[\alpha]_{\text{D}}^{21.6} +4.82$ (c 1.0, CHCl_3); SFC (AD-H, IPA/ CO_2 = 7/93, flow rate = 2.5 mL/min, $\lambda = 210$ nm) $t_{\text{R}} = 3.40$ min (major), 3.04 min (minor).

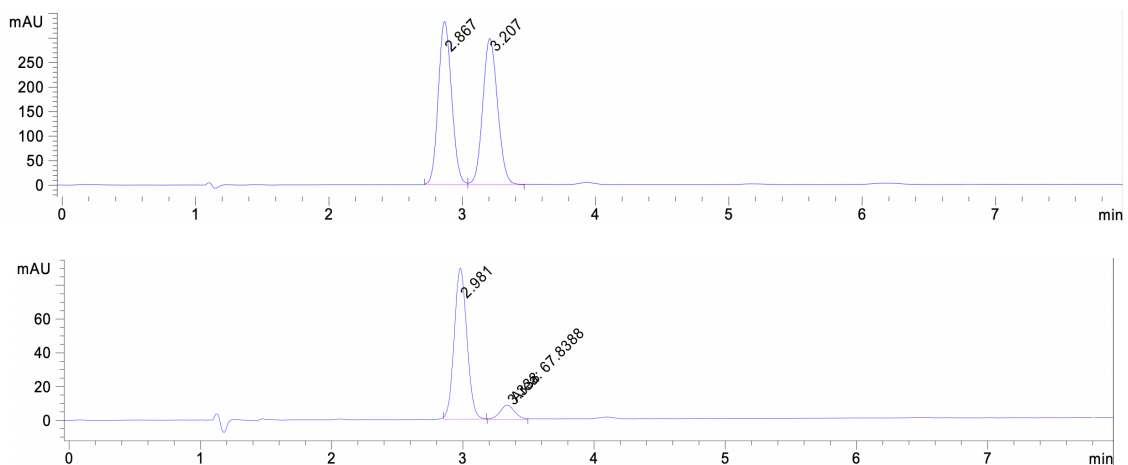


Peak #	RetTime [min]	Type	Width [min]	Area [mAU*s]	Height [mAU]	Area %
1	3.043	BB	0.0891	202.17691	34.15617	7.1007
2	3.402	BB	0.1066	2645.11890	392.73572	92.8993
Totals :				2847.29581	426.89189	

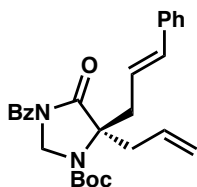


***tert*-butyl (*R*)-5-allyl-3-benzoyl-5-(3-methylbut-2-en-1-yl)-4-oxoimidazolidine-1-carboxylate (**35d**)**

Prepared according to the general procedure with allyl ester **34d** (42.2 mg, 0.0954 mmol, 1.0 equiv), Pd₂(pmdba)₃ (4.4 mg, 0.004 mmol, 4 mol %), and (*S*)-(CF₃)₃-*t*-BuPHOX (5.9 mg, 0.01 mmol, 10 mol %) at 60 °C for 24 h. Purified by silica gel flash chromatography (10% EtOAc/hexanes) to provide prenyl imidazolidinone **35d** as a colorless oil (30.3 mg, 0.0760 mmol, 80% yield, 80% ee); ¹H NMR (400 MHz, CDCl₃; compound exists as a 3:2 mixture of rotamers. For fully resolved peaks, the major rotamer is denoted by *, and the minor rotamer by #) δ 7.62 – 7.50 (m, 3H), 7.42 (td, *J* = 7.7, 4.8 Hz, 2H), 5.75 – 5.58 (m, 1H), 5.24 – 4.96 (m, 5H), 3.17 (dd, *J* = 13.6, 7.8 Hz, 1H*), 3.06 (dd, *J* = 14.3, 7.9 Hz, 1H*), 2.90 (dd, *J* = 13.8, 7.2 Hz, 1H#), 2.78 (dd, *J* = 14.4, 6.9 Hz, 1H#), 2.58 – 2.36 (m, 2H), 1.73 (d, *J* = 1.5 Hz, 3H), 1.64 (d, *J* = 1.4 Hz, 3H), 1.56 (s, 9H#), 1.51 (s, 9H*); ¹³C NMR (100 MHz, CDCl₃) δ 172.1, 168.7, 168.5, 152.7, 151.7, 137.3, 137.2, 133.3, 132.7, 132.7, 132.1, 131.7, 129.1, 129.1, 128.0, 128.0, 120.4, 120.3, 117.3, 117.0, 81.8, 81.2, 70.4, 70.0, 61.7, 61.6, 40.6, 39.4, 35.3, 34.3, 28.6, 28.5, 26.4, 26.3, 18.3, 18.2; IR (Neat Film, NaCl) 2976, 1758, 1702, 1449, 1396, 1368, 1305, 1264, 1223, 1168, 1143, 924, 858, 772, 702, 665 cm⁻¹; HRMS (MM: ESI-APCI): *m/z* calc'd for C₂₃H₃₀N₂O₄ [M+H]⁺: 399.2278, found 399.2275; [α]_D^{21.7} –3.75 (*c* 1.0, CHCl₃); SFC (OJ-H, IPA/CO₂ = 1/99, flow rate = 2.5 mL/min, λ = 254 nm) t_R = 2.98 min (major), 3.34 min (minor).



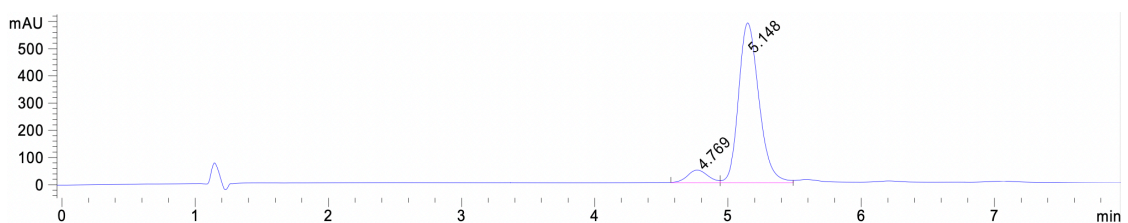
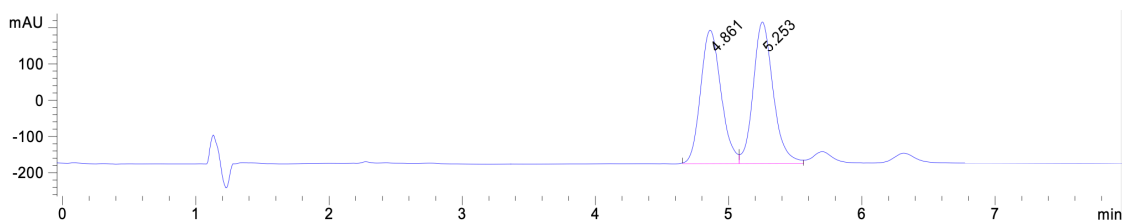
Peak #	RetTime [min]	Type	Width [min]	Area [mAU*s]	Height [mAU]	Area %
1	2.981	BB R	0.1067	602.06128	89.25969	89.8733
2	3.338	MM T	0.1314	67.83878	8.60667	10.1267
Totals :				669.90005	97.86636	



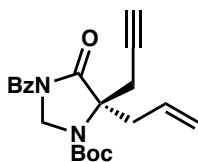
tert-butyl (R)-5-allyl-3-benzoyl-5-cinnamyl-4-oxoimidazolidine-1-carboxylate (35e)

Prepared according to the general procedure with allyl ester **34e** (47.6 mg, 0.0970 mmol, 1.0 equiv), Pd₂(pmdba)₃ (4.4 mg, 0.004 mmol, 4 mol %), and (*S*)-(CF₃)₃-*t*-BuPHOX (5.9 mg, 0.01 mmol, 10 mol %) at 40 °C for 48 h. Purified by silica gel flash chromatography (10% EtOAc/hexanes) to provide cinnamyl imidazolidinone **35e** as a colorless oil (41.9 mg, 0.0938 mmol, 97% yield, 85% ee); ¹H NMR (400 MHz, CDCl₃; compound exists as a 1.8:1 mixture of rotamers. For fully resolved peaks, the major rotamer is denoted by *, and the minor rotamer by #) δ 7.61 – 7.48 (m, 3H), 7.42 – 7.35 (m, 2H), 7.35 – 7.29 (m, 4H), 7.25 (dtd, *J* = 6.6, 3.5, 1.5 Hz, 1H), 6.60 – 6.48 (m, 1H), 6.14 – 6.00

(m, 1H), 5.79 – 5.64 (m, 1H), 5.27 – 5.17 (m, 2H), 5.17 – 4.99 (m, 2H), 3.30 (ddd, $J = 13.7, 7.6, 1.3$ Hz, 1H*), 3.18 (dd, $J = 13.6, 7.8$ Hz, 1H*), 3.05 (ddd, $J = 13.8, 6.8, 1.4$ Hz, 1H#), 2.93 (dd, $J = 13.8, 7.4$ Hz, 1H#), 2.71 – 2.45 (m, 2H), 1.62 (s, 9H#), 1.53 (s, 9H*); ^{13}C NMR (100 MHz, CDCl_3) δ 171.8, 168.6, 168.4, 152.7, 151.8, 137.0, 136.7, 135.6, 135.5, 133.2, 132.8, 132.7, 131.8, 131.4, 129.1, 129.1, 128.9, 128.8, 128.0, 128.0, 127.9, 126.4, 126.3, 122.8, 122.3, 120.8, 120.7, 82.0, 81.4, 70.4, 70.0, 61.6, 61.6, 40.7, 40.1, 39.5, 38.9, 28.7, 28.5; IR (Neat Film, NaCl) 2974, 1755, 1703, 1398, 1296, 1172, 703 cm^{-1} ; HRMS (MM: ESI-APCI): m/z calc'd for $\text{C}_{27}\text{H}_{34}\text{N}_3\text{O}_4$ $[\text{M}+\text{NH}_4]^+$: 464.2544, found 464.2521; $[\alpha]_{\text{D}}^{21.6} +30.48$ (c 1.0, CHCl_3); SFC (AD-H, IPA/ $\text{CO}_2 = 10/90$, flow rate = 2.5 mL/min, $\lambda = 210$ nm) $t_{\text{R}} = 5.15$ min (major), 4.77 min (minor).

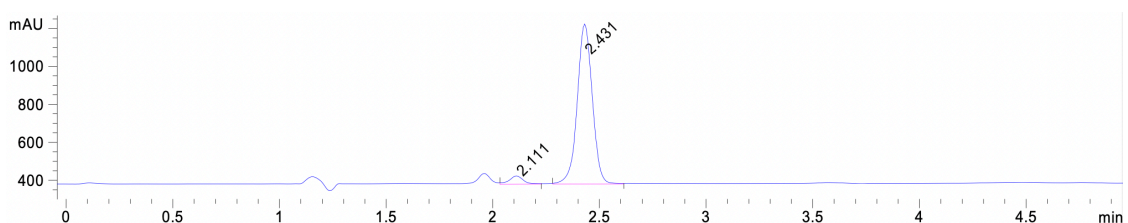
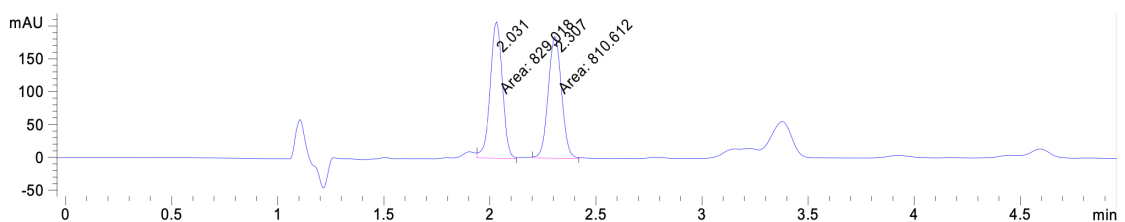


Peak #	RetTime [min]	Type	Width [min]	Area [mAU*s]	Height [mAU]	Area %
1	4.769	BV	0.1642	491.00110	46.11145	7.2964
2	5.148	VV	0.1641	6238.37354	586.57178	92.7036
Totals :				6729.37463	632.68322	

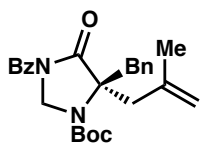


***tert*-butyl (*R*)-5-allyl-3-benzoyl-4-oxo-5-(prop-2-yn-1-yl)imidazolidine-1-carboxylate (35f)**

Prepared according to the general procedure with allyl ester **34f** (43.8 mg, 0.106 mmol, 1.0 equiv), Pd₂(pmdba)₃ (4.7 mg, 0.00425 mmol, 4 mol %), and (*S*)-(CF₃)₃-*t*-BuPHOX (6.3 mg, 0.0106 mmol, 10 mol %) at 60 °C for 45 h. Purified by silica gel flash chromatography (20% EtOAc/hexanes) to provide propargyl imidazolidinone **35f** as a colorless oil (18.1 mg, 0.0491 mmol, 46% yield, 91% ee); ¹H NMR (400 MHz, CDCl₃; compound exists as a 1.8:1 mixture of rotamers. For fully resolved peaks, the major rotamer is denoted by *, and the minor rotamer by #) δ 7.75 – 7.61 (m, 2H), 7.60 – 7.50 (m, 1H), 7.49 – 7.38 (m, 2H), 5.81 – 5.59 (m, 1H), 5.32 – 5.03 (m, 4H), 3.39 – 2.75 (m, 2H), 2.66 (dd, *J* = 16.7, 2.6 Hz, 1H[#]), 2.59 (dd, *J* = 16.7, 2.6 Hz, 1H*), 2.52 – 2.36 (m, 1H), 2.09 (t, *J* = 2.6 Hz, 1H[#]), 2.06 (t, *J* = 2.6 Hz, 1H*), 1.57 (s, 9H[#]), 1.53 (s, 9H*); ¹³C NMR (100 MHz, CDCl₃) δ 171.0, 170.9, 168.6, 168.4, 152.4, 151.8, 133.1, 132.8, 132.8, 131.4, 131.1, 129.3, 129.2, 128.1, 128.1, 121.0, 120.9, 116.2, 82.2, 81.7, 79.1, 78.3, 72.0, 71.3, 69.6, 69.1, 62.2, 62.1, 40.1, 39.9, 38.7, 38.6, 28.6, 28.5, 28.5, 27.2, 25.9; IR (Neat Film, NaCl) 3276, 2980, 2930, 1760, 1704, 1642, 1602, 1478, 1449, 1392, 1369, 1306, 1266, 1228, 1172, 1091, 1015, 928, 878, 857, 768, 739, 704, 664 cm⁻¹; HRMS (MM: ESI-APCI): *m/z* calc'd for C₂₁H₂₈N₃O₄ [M+NH₄]⁺: 386.2074, found 386.2066; [α]_D^{21.4} -14.43 (*c* 1.0, CHCl₃); SFC (OJ-H, IPA/CO₂ = 7/93, flow rate = 2.5 mL/min, λ = 210 nm) t_R = 2.43 min (major), 2.11 min (minor).



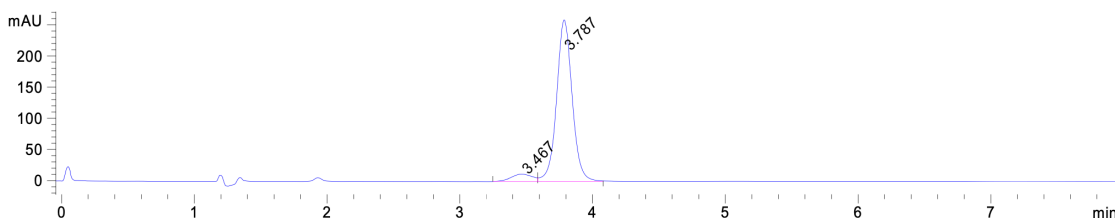
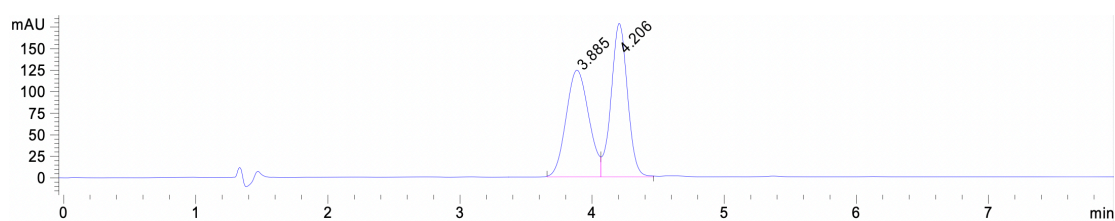
Peak #	RetTime [min]	Type	Width [min]	Area [mAU*s]	Height [mAU]	Area %
1	2.111	VB	0.0701	201.94838	43.56282	4.6637
2	2.431	BB	0.0775	4128.23242	838.20636	95.3363
Totals :				4330.18080	881.76918	



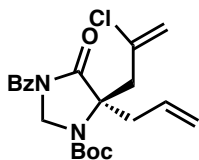
***tert*-butyl (*R*)-3-benzoyl-5-benzyl-5-(2-methylallyl)-4-oxoimidazolidine-1-carboxylate (35g)**

Prepared according to the general procedure with allyl ester **34g** (48.1 mg, 0.101 mmol, 1.0 equiv), Pd₂(pmdba)₃ (4.4 mg, 0.004 mmol, 4 mol %), and (*S*)-(CF₃)₃-*t*-BuPHOX (5.9 mg, 0.01 mmol, 10 mol %) at 60 °C for 26 h. Purified by silica gel flash chromatography (10% EtOAc/hexanes) to provide benzyl imidazolidinone **35g** as a colorless oil (36.4 mg, 0.0838 mmol, 83% yield, 89% ee); ¹H NMR (400 MHz, CDCl₃; compound exists as a 2.5:1 mixture of rotamers. For fully resolved peaks, the major rotamer is denoted by *, and the minor rotamer by #) δ 7.57 – 7.48 (m, 1H), 7.40 (d, *J* = 4.4 Hz, 3H), 7.35 – 7.22 (m, 4H), 7.16 – 7.08 (m, 2H), 4.98 – 4.75 (m, 3H), 4.36 (d, *J* = 7.7 Hz,

1H[#]), 4.21 (d, *J* = 7.5 Hz, 1H^{*}), 3.66 (d, *J* = 13.3 Hz, 1H^{*}), 3.45 (d, *J* = 13.4 Hz, 1H[#]), 3.22 (d, *J* = 13.5 Hz, 1H^{*}), 3.01 – 2.88 (m, 1H), 2.62 (d, *J* = 13.7 Hz, 1H[#]), 2.56 (d, *J* = 13.5 Hz, 1H^{*}), 1.72 (s, 3H), 1.66 (s, 9H[#]), 1.54 (s, 9H^{*}); ¹³C NMR (100 MHz, CDCl₃) δ 171.5, 171.3, 168.5, 168.2, 152.6, 152.0, 140.7, 140.3, 135.8, 135.2, 133.5, 133.4, 132.5, 132.5, 130.0, 130.0, 128.9, 128.8, 128.6, 127.9, 127.9, 127.8, 127.6, 116.6, 116.4, 82.3, 81.3, 71.6, 71.1, 61.2, 61.1, 43.6, 42.5, 42.2, 41.1, 28.8, 28.6, 23.9, 23.8; IR (Neat Film, NaCl) 2974, 1755, 1708, 1450, 1397, 1368, 1295, 1216, 1171, 1141, 1076, 901, 703 cm⁻¹; HRMS (MM: ESI-APCI): *m/z* calc'd for C₂₆H₃₀N₂NaO₄ [M+Na]⁺: 457.2098, found 457.2083; [α]_D^{21.8} +26.68 (*c* 1.5, CHCl₃); SFC (OD-H, IPA/CO₂ = 10/90, flow rate = 2.5 mL/min, λ = 254 nm) t_R = 3.79 min (major), 3.47 min (minor).

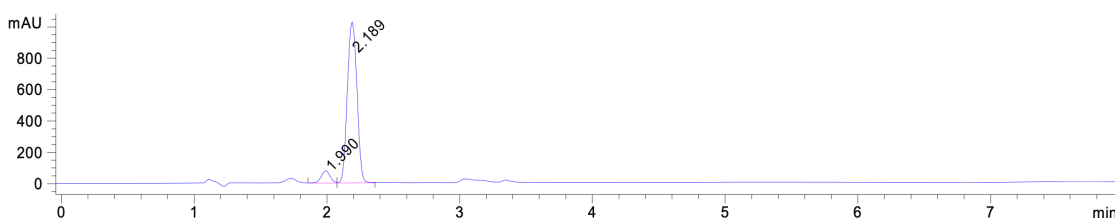
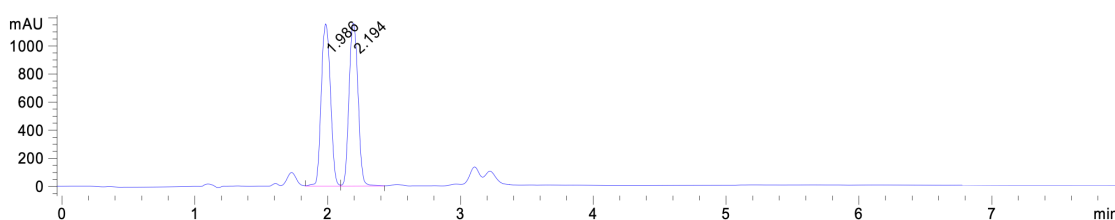


Peak #	RetTime [min]	Type	Width [min]	Area [mAU*s]	Height [mAU]	Area %
1	3.467	BV	0.1666	127.29535	11.72836	5.6929
2	3.787	VB	0.1232	2108.72607	258.53174	94.3071
Totals :				2236.02142	270.26010	



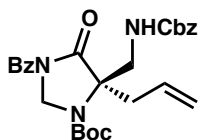
***tert*-butyl (*R*)-5-allyl-3-benzoyl-5-(2-chloroallyl)-4-oxoimidazolidine-1-carboxylate
(35h)**

Prepared according to the general procedure with allyl ester **34h** (44.6 mg, 0.0994 mmol, 1.0 equiv), Pd₂(pmdba)₃ (4.4 mg, 0.004 mmol, 4 mol %), and (*S*)-(CF₃)₃-*t*-BuPHOX (5.9 mg, 0.01 mmol, 10 mol %) at 40 °C for 5.5 h. Purified by silica gel flash chromatography (10% EtOAc/hexanes) to provide alkenyl chloride **35h** as a colorless oil (37.4 mg, 0.0924 mmol, 93% yield, 86% ee); ¹H NMR (400 MHz, CDCl₃; compound exists as a 2.7:1 mixture of rotamers. For fully resolved peaks, the major rotamer is denoted by *, and the minor rotamer by #) δ 7.64 (ddt, *J* = 8.5, 2.9, 1.7 Hz, 2H), 7.55 (ddt, *J* = 7.6, 6.9, 1.3 Hz, 1H), 7.46 – 7.38 (m, 2H), 5.75 – 5.60 (m, 1H), 5.38 – 5.28 (m, 2H), 5.27 – 5.08 (m, 4H), 3.40 (d, *J* = 14.3 Hz, 1H), 3.20 – 3.06 (m, 1H), 2.94 – 2.76 (m, 1H), 2.54 – 2.38 (m, 1H), 1.57 (s, 9H[#]), 1.50 (s, 9H^{*}); ¹³C NMR (100 MHz, CDCl₃) δ 170.9, 170.9, 168.4, 168.1, 152.2, 151.6, 136.7, 136.7, 133.2, 133.2, 132.6, 132.6, 131.1, 130.7, 129.0, 129.0, 127.9, 121.1, 121.0, 117.9, 117.8, 82.0, 81.3, 68.8, 68.6, 61.6, 61.5, 44.8, 44.1, 41.0, 39.6, 28.5, 28.3; IR (Neat Film, NaCl) 2976, 1758, 1707, 1394, 1368, 1295, 1266, 1140, 704 cm⁻¹; HRMS (MM: ESI-APCI): *m/z* calc'd for C₂₁H₂₉ClN₃O₄ [M+NH₄]⁺: 422.1841, found 422.1825. [α]_D^{21.7} -3.52 (*c* 1.0, CHCl₃); SFC (OJ-H, IPA/CO₂ = 7/93, flow rate = 2.5 mL/min, λ = 210 nm) t_R = 2.19 min (major), 1.99 min (minor).



Peak #	RetTime [min]	Type	Width [min]	Area [mAU*s]	Height [mAU]	Area %
1	1.990	VV	0.0762	376.84677	78.24028	6.7893
2	2.189	VB	0.0829	5173.75439	1024.01025	93.2107

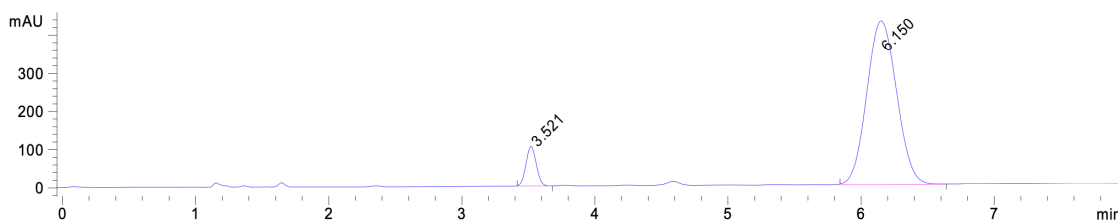
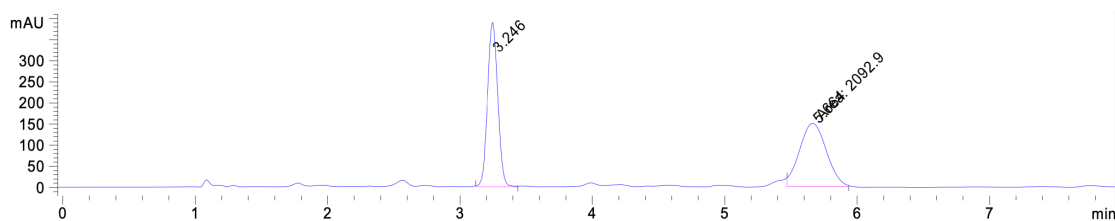
Totals : 5550.60117 1102.25053



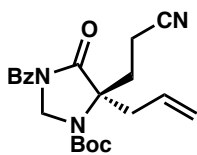
tert-butyl (R)-5-allyl-3-benzoyl-5-(((benzyloxy)carbonyl)amino)methyl-4-oxoimidazolidine-1-carboxylate (35i)

Prepared according to the general procedure with allyl ester **34i** (53.7 mg, 0.0100 mmol, 1.0 equiv), Pd₂(dba)₃ (3.7 mg, 0.004 mmol, 4 mol %), and (*S*)-(CF₃)₃-*t*-BuPHOX (5.9 mg, 0.01 mmol, 10 mol %) at 40 °C for 22 h. Purified by silica gel flash chromatography (25% EtOAc/hexanes) to provide carbamate **35i** as a colorless foam (37.2 mg, 0.0754 mmol, 75% yield, 85% ee); ¹H NMR (400 MHz, CDCl₃; compound exists as a 2:1 mixture of rotamers. For fully resolved peaks, the major rotamer is denoted by *, and the minor rotamer by #) δ 7.73 – 7.59 (m, 2H), 7.55 (td, *J* = 7.3, 1.4 Hz, 1H), 7.42 (q, *J* =

7.4 Hz, 2H), 7.36 – 7.27 (m, 5H), 5.75 – 5.55 (m, 1H), 5.26 – 4.97 (m, 6H), 3.80 – 3.62 (m, 2H), 3.02 (dd, $J = 13.5, 8.0$ Hz, 1H*), 2.85 (dd, $J = 13.7, 7.3$ Hz, 1H#), 2.51 (dd, $J = 13.8, 7.5$ Hz, 1H#), 2.41 (dd, $J = 13.5, 7.0$ Hz, 1H*), 1.58 (s, 9H#), 1.50 (s, 9H*); ^{13}C NMR (100 MHz, CDCl_3) δ 171.2, 170.8, 168.5, 168.2, 156.4, 156.3, 152.4, 152.2, 136.5, 136.2, 133.1, 133.0, 132.8, 132.7, 131.0, 130.7, 129.3, 129.2, 128.7, 128.4, 128.3, 128.0, 121.2, 82.6, 81.8, 69.5, 67.3, 67.2, 61.6, 61.5, 45.7, 45.5, 37.9, 37.1, 28.6, 28.4; IR (Neat Film, NaCl) 3347, 2977, 1704, 1519, 1449, 1392, 1369, 1304, 1166, 1073, 927, 858, 733, 698, 662 cm^{-1} ; HRMS (MM: ESI-APCI): m/z calc'd for $\text{C}_{27}\text{H}_{31}\text{N}_3\text{NaO}_6$ $[\text{M}+\text{Na}]^+$: 516.2105, found 516.2087; $[\alpha]_{\text{D}}^{21.8} -18.93$ (c 1.0, CHCl_3); SFC (AD-H, IPA/ $\text{CO}_2 = 20/80$, flow rate = 2.5 mL/min, $\lambda = 210$ nm) $t_{\text{R}} = 6.15$ min (major), 3.52 min (minor).

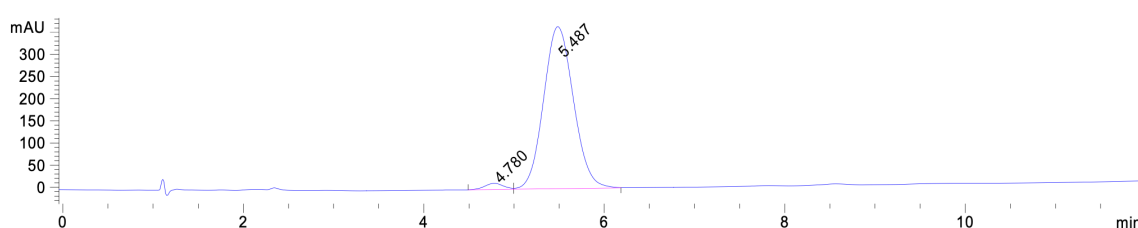
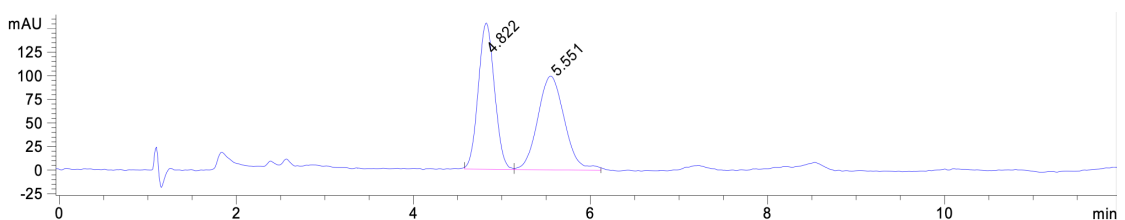


Peak #	RetTime [min]	Type	Width [min]	Area [mAU*s]	Height [mAU]	Area %
1	3.521	BB	0.0826	555.56512	103.55190	7.6912
2	6.150	BB	0.2457	6667.77832	428.14005	92.3088
Totals :				7223.34344	531.69194	

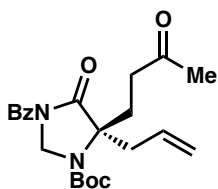


***tert*-butyl (*S*)-5-allyl-3-benzoyl-5-(2-cyanoethyl)-4-oxoimidazolidine-1-carboxylate
(**35j**)**

Prepared according to the general procedure with allyl ester **34j** (41.4 mg, 0.0970 mmol, 1.0 equiv), Pd₂(dba)₃ (3.7 mg, 0.004 mmol, 4 mol %), and (*S*)-(CF₃)₃-*t*-BuPHOX (5.9 mg, 0.01 mmol, 10 mol %) at 40 °C for 22 h. Purified by silica gel flash chromatography (20% EtOAc/hexanes) to provide nitrile **35j** as a colorless oil (37.2 mg, 0.0970 mmol, >99% yield, 95% ee); ¹H NMR (400 MHz, CDCl₃; compound exists as a 2.5:1 mixture of rotamers. For fully resolved peaks, the major rotamer is denoted by *, and the minor rotamer by #) δ 7.69 – 7.61 (m, 2H), 7.61 – 7.54 (m, 1H), 7.49 – 7.38 (m, 2H), 5.74 – 5.60 (m, 1H), 5.30 – 5.18 (m, 3H), 5.17 – 5.06 (m, 1H), 3.11 (dd, *J* = 13.6, 8.1 Hz, 1H*), 2.86 (dd, *J* = 13.7, 7.4 Hz, 1H#), 2.63 (dt, *J* = 13.8, 6.8 Hz, 1H*), 2.53 – 2.14 (m, 4H), 1.57 (s, 9H#), 1.53 (s, 9H*); ¹³C NMR (100 MHz, CDCl₃) δ 170.7, 170.6, 168.2, 168.0, 152.2, 151.9, 133.0, 132.9, 132.8, 132.7, 130.5, 130.1, 129.0, 129.0, 128.0, 121.7, 121.6, 118.4, 118.2, 82.7, 82.1, 68.6, 68.3, 61.5, 61.5, 41.1, 39.7, 31.6, 30.4, 28.5, 28.3, 12.9, 12.7; IR (Neat Film, NaCl) 2976, 1756, 1705, 1390, 1295, 1164, 704 cm⁻¹; HRMS (MM: ESI-APCI): *m/z* calc'd for C₂₁H₂₉N₄O₄ [M+NH₄]⁺: 401.2183, found 401.2182; [α]_D^{21.7} –33.24 (c 1.0, CHCl₃); SFC (IC, IPA/CO₂ = 15/85, flow rate = 2.5 mL/min, λ = 210 nm) t_R = 5.49 min (major), 4.78 min (minor).



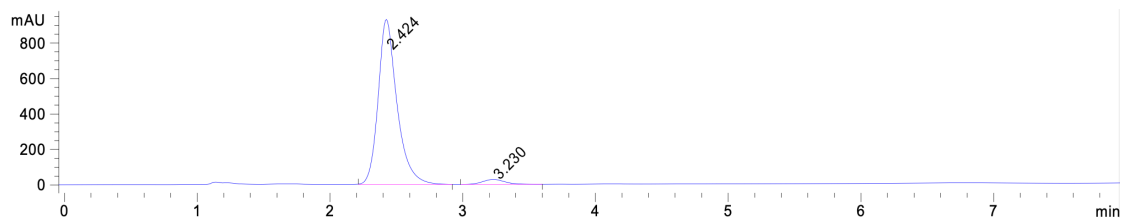
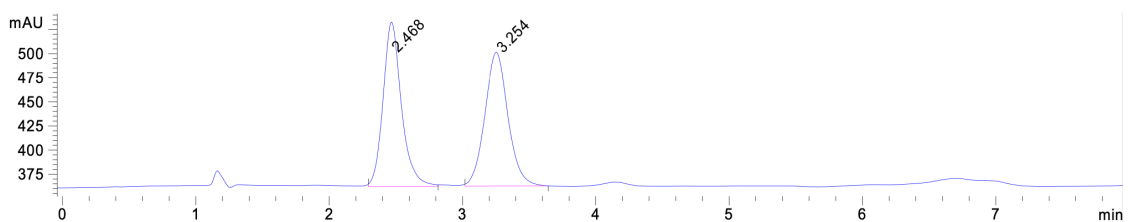
Peak #	RetTime [min]	Type	Width [min]	Area [mAU*s]	Height [mAU]	Area %
1	4.780	BV	0.2240	201.12321	13.96798	2.3301
2	5.487	VB	0.3566	8430.33691	366.18921	97.6699
Totals :				8631.46013	380.15718	



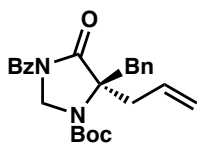
***tert*-butyl (*S*)-5-allyl-3-benzoyl-4-oxo-5-(3-oxobutyl)imidazolidine-1-carboxylate (35k)**

Prepared according to the general procedure with allyl ester **34k** (44.4 mg, 0.010 mmol, 1.0 equiv), Pd₂(dba)₃ (3.7 mg, 0.004 mmol, 4 mol %), and (*S*)-(CF₃)₃-*t*-BuPHOX (5.9 mg, 0.01 mmol, 10 mol %) at 60 °C for 19 h. Purified by silica gel flash chromatography (25% EtOAc/hexanes) to provide ketone **35k** as a colorless oil (31.4 mg, 0.0784 mmol, 79% yield, 93% ee); ¹H NMR (400 MHz, CDCl₃; compound exists as a 1.3:1 mixture of rotamers. For fully resolved peaks, the major rotamer is denoted by *, and the minor rotamer by #) δ 7.67 – 7.60 (m, 2H), 7.59 – 7.52 (m, 1H), 7.44 (t, *J* = 7.7 Hz, 2H),

5.76 – 5.60 (m, 1H), 5.25 – 5.17 (m, 2H), 5.13 – 5.02 (m, 2H), 3.15 (dd, $J = 13.6, 8.0$ Hz, 1H*), 2.89 (dd, $J = 13.8, 7.2$ Hz, 1H#), 2.59 – 2.27 (m, 4H), 2.21 – 2.00 (m, 4H), 1.54 (s, 9H#), 1.51 (s, 9H*); ^{13}C NMR (100 MHz, CDCl_3) δ 207.3, 206.6, 171.7, 171.6, 168.6, 168.3, 152.6, 151.7, 133.2, 133.1, 132.8, 132.7, 131.5, 131.2, 129.1, 129.1, 128.1, 121.0, 121.0, 82.3, 81.6, 69.0, 68.7, 61.5, 61.4, 41.2, 39.6, 39.0, 38.2, 30.5, 30.1, 29.6, 28.5, 28.5; IR (Neat Film, NaCl) 2974, 1755, 1708, 1450, 1397, 1368, 1295, 1216, 1171, 1141, 1076, 901, 703 cm^{-1} ; HRMS (MM: ESI-APCI): m/z calc'd for $\text{C}_{22}\text{H}_{32}\text{N}_3\text{O}_5$ $[\text{M}+\text{NH}_4]^+$: 418.2336, found 418.2347; $[\alpha]_{\text{D}}^{21.7} +3.65$ (c 1.0, CHCl_3); SFC (IC, IPA/ $\text{CO}_2 = 20/80$, flow rate = 2.5 mL/min, $\lambda = 210$ nm) $t_{\text{R}} = 2.42$ min (major), 3.23 min (minor).

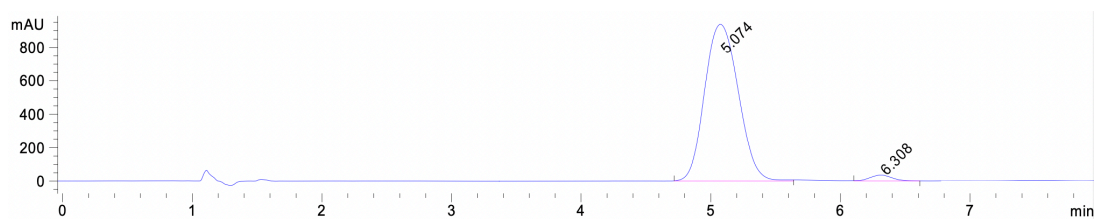
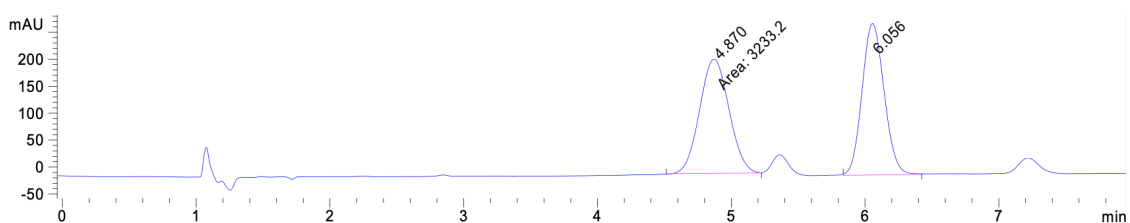


Peak #	RetTime [min]	Type	Width [min]	Area [mAU*s]	Height [mAU]	Area %
1	2.424	BB	0.1476	9197.75391	927.91022	96.5494
2	3.230	BB	0.1735	328.72174	28.72386	3.4506
Totals :				9526.47565	956.63408	



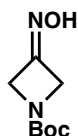
Procedure for the large-scale preparation of compound **35a**

In a N₂ filled glovebox, Pd₂(pmdba)₃ (82 mg, 0.0744 mmol, 4 mol %) and (*S*)-(CF₃)₃-*t*-BuPHOX (110 mg, 0.186 mmol, 10 mol %) were suspended in 2:1 hexanes:PhMe (45 mL) in a 500 mL Schlenk flask. After stirring for 20 minutes at 25 °C, imidazolidinone **34a** (864 mg, 1.86 mmol, 1.0 equiv) and 2:1 hexanes:PhMe (90 mL, total substrate concentration 0.014 M) were added to the pre-stirred catalyst solution. The flask was then sealed and heated at 40 °C in an oil bath for 64 h. The reaction mixture was then cooled to 23 °C and exposed to air. The crude reaction mixture was loaded directly onto a flash column and the product was isolated by silica gel flash chromatography (10% EtOAc/hexanes) to provide **35a** as a colorless oil (674 mg, 1.60 mmol, 86% yield, 95% ee); All characterization data matched those reported above for compound **35a**; [α]_D^{22.1} +21.69 (*c* 1.0, CHCl₃); SFC (AD-H, IPA/CO₂ = 7/93, flow rate = 2.5 mL/min, λ = 210 nm) *t*_R = 5.07 min (major), 6.31 min (minor).



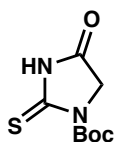
Peak #	RetTime [min]	Type	Width [min]	Area [mAU*s]	Height [mAU]	Area %
1	5.074	BB	0.2908	1.69582e4	938.43024	97.6531
2	6.308	BB	0.1790	407.56235	35.22752	2.3469
Totals :				1.73657e4	973.65776	

1.5.2.5 Synthesis of Imidazolidinone Allylic Alkylation Substrates



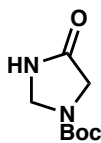
***tert*-butyl 3-(hydroxyimino)azetidine-1-carboxylate (41)**

Prepared from *tert*-butyl 3-oxoazetidine-1-carboxylate according to the literature procedure of Xiang, Yang, and coworkers, substituting *i*-PrOH for MeOH.³² All characterization data matched those reported in the literature.



***tert*-butyl 4-oxo-2-thioxoimidazolidine-1-carboxylate (50)**

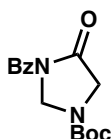
Prepared from 2-thiohydantoin according to the literature procedure of Tatibouët under an atmosphere of air.²⁶ All characterization data matched those reported in the literature.



tert-butyl 4-oxoimidazolidine-1-carboxylate (31)

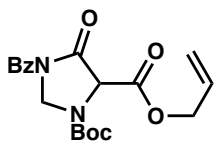
Compound **50** (10.43 g, 48.23 mmol, 1.0 equiv) and anhydrous NiCl₂ (31.25 g, 241.1 mmol, 5.0 equiv) were added to a round-bottom flask, MeOH (dried by distillation over 3 Å molecular sieves, 480 mL, 0.1 M) was added, and the mixture was subjected to rapid magnetic stirring to form a suspension. This suspension was cooled to 0 °C in an ice bath, and NaBH₄ (27.37 g, 723.4 mmol, 15 equiv) was added portionwise. Care should be taken, as this step is highly exothermic and results in the rapid generation of a large volume of gas. Following complete addition of NaBH₄, the reaction mixture was removed from the ice bath and allowed to warm to 23 °C. After 1 h of stirring, glacial acetic acid (10 mL) was added, and the reaction mixture was filtered through a plug of celite under pressurized air. A steel rod was periodically used to break up the plug of nickel salts and accelerate filtration. The resulting bright green solution was concentrated under reduced pressure. The resulting solids were dissolved in a mixture of deionized water (500 mL), EtOAc (300 mL), and glacial acetic acid (20 mL). The organic phase was separated, and the aqueous phase was extracted with ethyl acetate (4x200 mL). The combined organic phases were washed with a solution of NaHCO₃ and NaCl (100 mL, equal parts saturated NaHCO₃ and NaCl solutions), dried over Na₂SO₄, and concentrated under reduced pressure to afford the title compound as an off-white solid (8.58 g, 46.08 mmol, 96% yield) of sufficient purity for use in the next step; an analytically pure sample could be obtained by silica gel flash chromatography (90% EtOAc/hexanes); ¹H NMR (400 MHz, CDCl₃) δ 7.25 – 7.01 (m,

1H), 4.78 (d, $J = 11.6$ Hz, 2H), 3.89 (d, $J = 15.2$ Hz, 2H), 1.48 (s, 9H); ^{13}C NMR (100 MHz, CDCl_3) δ 172.3, 153.1, 152.7, 81.2, 59.1, 58.9, 47.6, 47.1, 28.4; IR (Neat Film, KBr) 3213, 3120, 2978, 2934, 1714, 1456, 1414, 1366, 1326, 1294, 1257, 1171, 1128, 1080, 898, 855, 771, 700, 575, 491, 461 cm^{-1} ; HRMS (FAB+): m/z calc'd for $\text{C}_8\text{H}_{15}\text{N}_2\text{O}_3$ $[\text{M}+\text{H}]^+$: 187.1083, found 187.1086.



***tert*-butyl 3-benzoyl-4-oxoimidazolidine-1-carboxylate (32)**

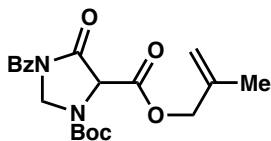
To a solution of **31** (8.58 g, 46.08 mmol, 1.0 equiv) in CH_2Cl_2 (400 mL, 0.12 M) at 23 °C was added Et_3N (11.6 mL, 82.94 mmol, 1.8 equiv) followed by BzCl (8.03 mL, 69.12 mmol, 1.5 equiv). After 9 h of stirring, the reaction mixture was washed with water (200 mL) and brine (100 mL) and the combined aqueous washes were extracted with CH_2Cl_2 (2x50 mL). The combined organic phases were dried over Na_2SO_4 and concentrated under reduced pressure. The crude product was purified by silica gel flash chromatography (25% EtOAc /hexanes) to afford the title compound as a white solid (7.47 g, 25.73 mmol, 56% yield); ^1H NMR (400 MHz, CDCl_3) δ 7.68 – 7.60 (m, 2H), 7.59 – 7.52 (m, 1H), 7.49 – 7.39 (m, 2H), 5.29 (s, 2H), 4.17 (s, 2H), 1.51 (s, 9H); ^{13}C NMR (100 MHz, CDCl_3) δ 168.6, 167.5, 152.6, 133.1, 132.8, 129.2, 128.1, 81.9, 61.8, 49.9, 49.4, 28.4; IR (Neat Film, NaCl) 2980, 1763, 1708, 1477, 1448, 1411, 1368, 1305, 1212, 1163, 1127, 895, 858, 768, 727, 704, 662 cm^{-1} ; HRMS (MM: ESI-APCI): m/z calc'd for $\text{C}_{15}\text{H}_{22}\text{N}_3\text{O}_4$ $[\text{M}+\text{NH}_4]^+$: 308.1600, found 308.1605.



5-allyl 1-(*tert*-butyl) 3-benzoyl-4-oxoimidazolidine-1,5-dicarboxylate (**33**)

To a solution of LiHMDS (9.43 g, 56.38 mmol, 2.2 equiv) in THF (150 mL) at -78 °C in a flame-dried round-bottom flask was added allyl *1H*-imidazole-1-carboxylate³³ (4.68 g, 30.76 mmol, 1.2 equiv) by syringe with rapid stirring. Immediately thereafter, a solution of imidazolidinone **32** (7.44 g, 25.63 mmol, 1.0 equiv) in THF (100 mL, 0.1 M total concentration) was added over 15 min by cannula while stirring at -78 °C. After an additional 13 min of stirring, the reaction mixture was poured into 1 N aqueous HCl (200 mL) and extracted with ethyl acetate (3 x 50 mL). The combined organic extracts were dried over a mixture of NaHCO₃ and Na₂SO₄ and concentrated under reduced pressure. The crude product was purified by silica gel flash chromatography (20→35% Et₂O/hexanes) to provide allyl ester **33** as a viscous oil that solidified upon standing to form a white solid (4.80 g, 12.82 mmol, 50% yield); ¹H NMR (400 MHz, CDCl₃; compound exists as a 1.1:1 mixture of rotamers. For fully resolved peaks, the major rotamer is denoted by *, and the minor rotamer by #) δ 7.61 (dd, J = 8.3, 1.3 Hz, 2H), 7.56 (t, J = 7.5 Hz, 1H), 7.42 (t, J = 7.8 Hz, 2H), 5.98 – 5.80 (m, 1H), 5.43 – 5.18 (m, 4H), 4.96 (s, 1H[#]), 4.88 (s, 1H*), 4.81 – 4.62 (m, 2H), 1.52 (s, 9H[#]), 1.46 (s, 9H*); ¹³C NMR (100 MHz, CDCl₃) δ 168.4, 168.2, 165.7, 165.6, 163.5, 163.2, 152.1, 151.9, 133.0, 132.6, 131.0, 130.9, 129.2, 128.1, 119.8, 119.2, 82.8, 82.6, 67.2, 63.5, 63.0, 61.5, 28.3, 28.2; IR (Neat Film, NaCl) 2977, 1748, 1716, 1449, 1405, 1369, 1302, 1250, 1167, 1135, 987, 939, 770, 725, 696, 668

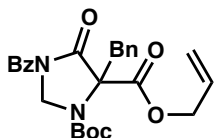
cm⁻¹; HRMS (MM: ESI-APCI): *m/z* calc'd for C₁₉H₂₆N₃O₆ [M+NH₄]⁺: 392.1816, found 392.1822.



1-(*tert*-butyl) 5-(2-methylallyl) 3-benzoyl-4-oxoimidazolidine-1,5-dicarboxylate (**60**)

To a solution of methallyl *1H*-imidazole-1-carboxylate³⁴ (286 mg, 1.72 mmol, 2 equiv) in THF (5.2 mL) at -78 °C in a flame-dried round-bottom flask was added LiHMDS solution (1 M in THF, 1.89 mL, 1.89 mmol, 2.2 equiv) by syringe. Immediately thereafter, a solution of imidazolidinone **32** (250 mg, 0.861 mmol, 1.0 equiv) in THF (3.4 mL, 0.1 M total concentration) was added dropwise by syringe with rapid stirring at -78 °C. After an additional 10 min of stirring, the reaction mixture was poured into 1 N aqueous HCl (20 mL) and extracted with ethyl acetate (4 x 15 mL). The combined organic extracts were dried over a mixture of NaHCO₃ and Na₂SO₄ and concentrated under reduced pressure. The crude product was purified by silica gel flash chromatography (40% Et₂O/hexanes) to provide methallyl ester **60** as a viscous oil that solidified upon standing to form a white solid (149 mg, 0.384 mmol, 45% yield); ¹H NMR (400 MHz, CDCl₃; compound exists as a 1:1 mixture of rotamers. Fully resolved rotamer peaks are denoted by *) δ 7.65 – 7.59 (m, 2H), 7.59 – 7.53 (m, 1H), 7.43 (t, *J* = 7.8 Hz, 2H), 5.48 – 5.27 (m, 2H), 5.06 – 4.84 (m, 3H), 4.75 – 4.51 (m, 2H), 1.75 (s, 3H), 1.52 (s, 9H*), 1.46 (s, 9H*); ¹³C NMR (100 MHz, CDCl₃) δ 168.5, 168.3, 165.7, 165.6, 163.5, 163.3, 152.1, 151.9, 138.9, 138.8, 133.0, 132.7, 132.7, 129.2, 128.2, 114.5, 114.1, 82.8, 82.7, 69.8, 63.5, 63.1, 61.5, 28.4, 28.3, 19.6, 19.5, 19.5, 19.5; IR (Neat Film, KBr) 3064, 2978, 2934, 1772, 1750, 1716, 1602, 1583, 1477,

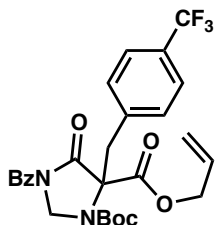
1449, 1406, 1369, 1303, 1251, 1170, 1137, 1085, 1027, 1000, 964, 908, 858, 787, 770, 726, 699, 665, 629, 591, 519, 411 cm^{-1} ; HRMS (MM: ESI-APCI): m/z calc'd for $\text{C}_{27}\text{H}_{30}\text{N}_2\text{NaO}_6$ $[\text{M}+\text{Na}]^+$: 411.1527, found 411.1544;



5-allyl 1-(*tert*-butyl) 3-benzoyl-5-benzyl-4-oxoimidazolidine-1,5-dicarboxylate (**34a**)

To a solution of lactam **33** (500 mg, 1.34 mmol, 1.0 equiv) in DMF (13.4 mL, 0.1 M) at 23 °C was added NaH (60% dispersion in mineral oil, 64 mg, 1.60 mmol, 1.2 equiv). The reaction mixture was stirred for 25 min, resulting in a bright yellow solution. BnBr (477 μL , 4.02 mmol, 3.0 equiv) was then added and the reaction mixture was stirred at 23 °C for 55 min. The reaction mixture was poured into water (20 mL) and extracted with ethyl acetate (4x15 mL). The combined organic extracts were washed with saturated aq. LiCl (2x10 mL), dried over anhydrous Na_2SO_4 , and concentrated under reduced pressure. The crude product was purified by silica gel flash chromatography (7.5 \rightarrow 15% acetone/hexanes) to provide the title compound as a colorless oil (291 mg, 0.626 mmol, 47% yield); ^1H NMR (400 MHz, CDCl_3 ; compound exists as a 1.2:1 mixture of rotamers. For fully resolved peaks, the major rotamer is denoted by *, and the minor rotamer by #) δ 7.59 – 7.49 (m, 1H), 7.47 – 7.26 (m, 7H), 7.21 – 7.14 (m, 2H), 6.02 – 5.80 (m, 1H), 5.42 – 5.26 (m, 2H), 5.24 (d, $J = 7.1$ Hz, 1H*), 5.16 (d, $J = 7.0$ Hz, 1H#), 4.83 – 4.61 (m, 2H), 4.46 (d, $J = 7.2$ Hz, 1H#), 4.40 (d, $J = 7.0$ Hz, 1H*), 3.86 – 3.50 (m, 2H), 1.56 (s, 9H#), 1.56 (s, 9H*); ^{13}C NMR (100 MHz, CDCl_3) δ 168.2, 168.0, 166.7, 166.6, 166.2, 166.1, 152.0, 151.8, 134.7, 134.1, 132.8, 132.8, 132.6, 132.6, 131.2, 130.9, 130.3, 130.2, 128.9,

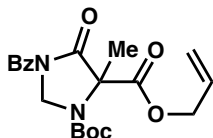
128.9, 128.8, 128.6, 128.0, 127.9, 127.9, 127.7, 119.7, 119.1, 82.9, 82.4, 72.9, 72.8, 67.2, 67.2, 61.2, 61.2, 38.0, 37.1, 28.4, 28.3; IR (Neat Film, NaCl) 2977, 1771, 1712, 1602, 1450, 1393, 1294, 1230, 1147, 1075, 1010, 768, 701 cm^{-1} ; HRMS (MM: ESI-APCI): m/z calc'd for $\text{C}_{26}\text{H}_{32}\text{N}_3\text{O}_6$ $[\text{M}+\text{NH}_4]^+$: 482.2286, found 482.2284.



5-allyl 1-(*tert*-butyl) 3-benzoyl-4-oxo-5-(4-(trifluoromethyl)benzyl)imidazolidine-1,5-dicarboxylate (34b)

To a solution of lactam **33** (128.4 mg, 0.343 mmol, 1.0 equiv) in DMF (3.4 mL, 0.1 M) at 23 °C was added NaH (60% dispersion in mineral oil, 16.5 mg, 0.412 mmol, 1.2 equiv). The reaction mixture was stirred for 15 min, resulting in a bright yellow solution. 4-trifluoromethylbenzyl bromide (159 μL , 1.03 mmol, 3.0 equiv) was then added and the reaction mixture was stirred at 23 °C for 35 min. The reaction mixture was poured into water (5 mL) and extracted with ethyl acetate (4x5 mL). The combined organic extracts were washed with saturated aq. LiCl (2x3 mL), dried over anhydrous Na_2SO_4 , and concentrated under reduced pressure. The crude product was purified by silica gel flash chromatography (15% EtOAc/hexanes) to provide the title compound as a colorless oil (122 mg, 0.229 mmol, 67% yield); ^1H NMR (400 MHz, CDCl_3) δ 7.64 – 7.51 (m, 3H), 7.44 – 7.27 (m, 6H), 5.99 – 5.84 (m, 1H), 5.43 – 5.15 (m, 3H), 4.84 – 4.63 (m, 2H), 4.55 (dd, $J = 7.2, 2.8$ Hz, 1H), 3.92 – 3.59 (m, 2H), 1.56 (s, 9H); ^{13}C NMR (100 MHz, CDCl_3) δ 168.3, 168.0, 166.6, 166.5, 165.9, 165.7, 152.4, 152.0, 139.2, 138.6, 133.1, 132.6, 131.2,

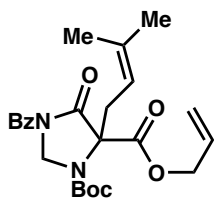
130.8, 130.3, 129.9, 129.0, 128.2, 128.1, 125.8, 125.7, 125.6, 125.5, 120.1, 119.5, 83.4, 82.9, 72.8, 72.7, 67.5, 67.5, 61.5, 61.4, 37.8, 37.0, 28.5, 28.4; IR (Neat Film, NaCl) 2977, 1772, 1710, 1389, 1325, 1291, 1228, 1164, 1068, 1019, 857, 697, 665 cm^{-1} ; HRMS (MM: ESI-APCI): m/z calc'd for $\text{C}_{27}\text{H}_{31}\text{F}_3\text{N}_3\text{O}_6$ $[\text{M}+\text{NH}_4]^+$: 550.2159, found 550.2139.



5-allyl 1-(*tert*-butyl) 3-benzoyl-5-methyl-4-oxoimidazolidine-1,5-dicarboxylate (**34c**)

To a suspension of NaH (60% dispersion in mineral oil, 32 mg, 0.801 mmol, 1.2 equiv) in THF (6.7 mL, 0.1 M) at -78 °C was added lactam **33** (250 mg, 0.668 mmol, 1.0 equiv). The reaction mixture was warmed to 0 °C and stirred for 45 min, resulting in a bright yellow solution. MeI (208 μL , 3.34 mmol, 5.0 equiv) was then added and the reaction mixture was stirred at 23 °C for 2 h. The reaction mixture was poured into saturated aq. NaHCO_3 (10 mL) and extracted with ethyl acetate (3x6 mL). The combined organic extracts were dried over anhydrous Na_2SO_4 and concentrated under reduced pressure. The crude product was purified by automated silica gel flash chromatography (Telodyne ISCO, 0 \rightarrow 50% acetone/hexanes) to provide the title compound as a colorless oil (90 mg, 0.232 mmol, 35% yield); ^1H NMR (400 MHz, CDCl_3 ; compound exists as a 1.2:1 mixture of rotamers. For fully resolved peaks, the major rotamer is denoted by *, and the minor rotamer by #) δ 7.63 – 7.52 (m, 3H), 7.42 (t, $J = 7.6$ Hz, 2H), 5.96 – 5.80 (m, 1H), 5.41 – 5.19 (m, 4H), 4.75 – 4.57 (m, 2H), 1.83 (s, 3H#), 1.78 (s, 3H*), 1.50 (s, 9H#), 1.46 (s, 9H*); ^{13}C NMR (100 MHz, CDCl_3) δ 168.6, 168.4, 167.5, 167.2, 152.3, 152.2, 133.0, 132.7, 131.3, 131.0, 129.1, 128.1, 119.6, 119.1, 82.6, 82.4, 68.4, 68.2, 67.1, 61.1, 61.0, 28.4, 28.2,

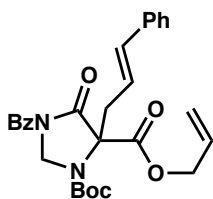
20.5, 19.9; IR (Neat Film, NaCl) 2979, 1773, 1740, 1714, 1602, 1477, 1450, 1386, 1370, 1305, 1244, 1162, 1124, 1067, 913, 859, 770, 732, 702, 667 cm^{-1} ; HRMS (MM: ESI-APCI): m/z calc'd for $\text{C}_{20}\text{H}_{28}\text{N}_3\text{O}_6$ $[\text{M}+\text{NH}_4]^+$: 406.1973, found 406.1975.



5-allyl 1-(*tert*-butyl) 3-benzoyl-5-(3-methylbut-2-en-1-yl)-4-oxoimidazolidine-1,5-dicarboxylate (34d)

To a solution of lactam **33** (300 mg, 0.801 mmol, 1.0 equiv) in DMF (8 mL, 0.1 M) at 23 °C was added NaH (60% dispersion in mineral oil, 38.5 mg, 0.962 mmol, 1.2 equiv). The reaction mixture was stirred for 13 min, resulting in a bright yellow solution. Prenyl bromide (280 μL , 2.40 mmol, 3.0 equiv) was then added and the reaction mixture was stirred at 23 °C for 1 h. The reaction mixture was poured into water (20 mL) and extracted with ethyl acetate (4x15 mL). The combined organic extracts were washed with saturated aq. LiCl (2x10 mL), dried over anhydrous Na_2SO_4 , and concentrated under reduced pressure. The crude product was purified by silica gel flash chromatography (15% EtOAc/hexanes) to provide the title compound as a colorless oil (230 mg, 0.520 mmol, 65% yield); ^1H NMR (400 MHz, CDCl_3 ; compound exists as a 1.1:1 mixture of rotamers. For fully resolved peaks, the major rotamer is denoted by *, and the minor rotamer by #) δ 7.61 – 7.51 (m, 3H), 7.45 – 7.37 (m, 2H), 5.98 – 5.76 (m, 1H), 5.43 – 5.19 (m, 3H), 5.16 – 4.99 (m, 2H), 4.77 – 4.52 (m, 2H), 3.26 – 2.93 (m, 2H), 1.77 (s, 3H), 1.67 (d, $J = 1.4$ Hz, 3H*), 1.66 (d, $J = 1.5$ Hz, 3H#), 1.51 (s, 9H#), 1.47 (s, 9H*); ^{13}C NMR (100 MHz, CDCl_3) δ 168.6, 168.4, 166.9, 166.9, 166.8, 166.7, 152.1, 152.1, 138.5, 138.4, 133.0, 132.8, 131.4,

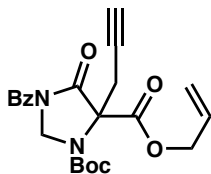
131.0, 129.1, 129.1, 128.1, 128.1, 119.6, 119.1, 116.1, 115.8, 82.6, 82.3, 72.1, 72.0, 67.1, 67.0, 61.7, 31.7, 30.8, 28.4, 28.3, 26.4, 26.3, 18.3, 18.2; IR (Neat Film, NaCl) 2978, 2931, 1771, 1746, 1713, 1601, 1450, 1388, 1293, 1228, 1167, 1030, 993, 940, 859, 792, 772, 701, 665 cm^{-1} ; HRMS (MM: ESI-APCI): m/z calc'd for $\text{C}_{24}\text{H}_{30}\text{N}_2\text{NaO}_6$ $[\text{M}+\text{Na}]^+$: 465.1996, found 465.1984;



5-allyl 1-(*tert*-butyl) 3-benzoyl-5-cinnamyl-4-oxoimidazolidine-1,5-dicarboxylate (34e)

To a solution of lactam **33** (157.2 mg, 0.420 mmol, 1.0 equiv) in DMF (4.2 mL, 0.1 M) at 23 °C was added NaH (60% dispersion in mineral oil, 20.2 mg, 0.504 mmol, 1.2 equiv). The reaction mixture was stirred for 14 min, resulting in a bright yellow solution. Cinnamyl bromide (186 μL , 1.26 mmol, 3.0 equiv) was then added and the reaction mixture was stirred at 23 °C for 20 min. The reaction mixture was poured into water (10 mL) and extracted with ethyl acetate (4x6 mL). The combined organic extracts were washed with saturated aq. LiCl (2x5 mL), dried over anhydrous Na_2SO_4 , and concentrated under reduced pressure. The crude product was purified by silica gel flash chromatography (15% EtOAc/hexanes) to provide the title compound as a colorless oil (154 mg, 0.314 mmol, 75% yield); ^1H NMR (400 MHz, CDCl_3 ; compound exists as a 1.1:1 mixture of rotamers. For fully resolved peaks, the major rotamer is denoted by *, and the minor rotamer by #) δ 7.55 – 7.49 (m, 3H), 7.41 – 7.30 (m, 6H), 7.28 – 7.24 (m, 1H), 6.61 (dd, $J = 15.9, 2.9$ Hz,

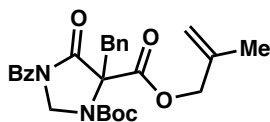
1H), 6.16 – 6.02 (m, 1H), 5.98 – 5.82 (m, 1H), 5.42 – 5.12 (m, 4H), 4.81 – 4.58 (m, 2H), 3.53 – 3.42 (m, 1H*), 3.29 (ddd, $J = 14.3, 6.5, 1.5$ Hz, 1H[#]), 3.23 – 3.10 (m, 1H), 1.54 (s, 9H*), 1.52 (s, 9H[#]); ¹³C NMR (100 MHz, CDCl₃) δ 168.6, 168.3, 166.7, 166.7, 166.5, 166.2, 152.3, 152.2, 136.8, 136.5, 136.4, 136.3, 133.0, 133.0, 132.7, 131.3, 131.0, 129.2, 128.9, 128.8, 128.2, 128.1, 128.1, 128.0, 126.4, 121.7, 121.2, 119.8, 119.2, 82.9, 82.6, 72.3, 72.1, 67.2, 61.7, 36.5, 35.6, 29.8, 28.4, 28.4; IR (Neat Film, NaCl) 2975, 1772, 1709, 1388, 1290, 1226, 1168, 752, 694 cm⁻¹; HRMS (MM: ESI-APCI): m/z calc'd for C₂₈H₃₄N₃O₆ [M+NH₄]⁺: 508.2442, found 508.2426.



5-allyl 1-(*tert*-butyl) 3-benzoyl-4-oxo-5-(prop-2-yn-1-yl)imidazolidine-1,5-dicarboxylate (34f)

To a solution of lactam **33** (250 mg, 0.668 mmol, 1.0 equiv) in THF (6.7 mL, 0.1 M) at 23 °C was added NaH (60% dispersion in mineral oil, 32 mg, 0.801 mmol, 1.2 equiv). The reaction mixture was stirred for 15 min, resulting in a bright yellow solution. Propargyl bromide (80% in PhMe, 252 μ L, 2.67 mmol, 4.0 equiv) was then added and the reaction mixture was stirred at 23 °C for 1 h. The reaction mixture was poured into saturated aq. NaHCO₃ (10 mL) and extracted with ethyl acetate (3x6 mL). The combined organic extracts were dried over anhydrous Na₂SO₄ and concentrated under reduced pressure. The crude product was purified by automated silica gel flash chromatography (Telodyne ISCO, 0→30% acetone/hexanes) to provide the title compound as a colorless oil (158 mg, 0.383 mmol, 57% yield); ¹H NMR (400 MHz, CDCl₃; compound exists as a 1:1 mixture of

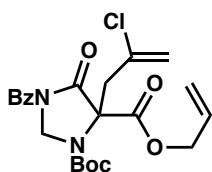
rotamers. Fully resolved rotamer peaks are denoted by *) δ 7.72 – 7.63 (m, 2H), 7.59 – 7.52 (m, 1H), 7.48 – 7.37 (m, 2H), 5.96 – 5.75 (m, 1H), 5.44 (d, $J = 7.1$ Hz, 1H*), 5.40 (d, $J = 6.9$ Hz, 1H*), 5.36 – 5.20 (m, 3H), 4.76 – 4.53 (m, 2H), 3.46 (dd, $J = 17.2, 2.7$ Hz, 1H*), 3.27 (dd, $J = 17.3, 2.7$ Hz, 1H*), 3.23 – 3.15 (m, 1H), 2.12 (dt, $J = 5.4, 2.6$ Hz, 1H), 1.52 (s, 9H*), 1.47 (s, 9H*); ^{13}C NMR (100 MHz, CDCl_3) δ 168.4, 168.1, 165.9, 165.8, 165.6, 165.6, 151.9, 151.5, 133.0, 132.5, 131.0, 130.7, 129.2, 128.1, 119.9, 119.3, 82.9, 82.7, 78.2, 77.5, 72.3, 71.8, 71.1, 70.8, 67.3, 67.3, 62.0, 28.3, 28.2, 24.2, 23.3; IR (Neat Film, NaCl) 3280, 2977, 1771, 1747, 1714, 1602, 1450, 1392, 1370, 1296, 1229, 1152, 1059, 1019, 858, 790, 770, 740, 701, 665 cm^{-1} ; HRMS (MM: ESI-APCI): m/z calc'd for $\text{C}_{22}\text{H}_{28}\text{N}_3\text{O}_6$ $[\text{M}+\text{NH}_4]^+$: 430.1973, found 430.1969.



1-(*tert*-butyl) 5-(2-methylallyl) 3-benzoyl-5-benzyl-4-oxoimidazolidine-1,5-dicarboxylate (34g)

To a solution of lactam **60** (76.1 mg, 0.196 mmol, 1.0 equiv) in THF (2 mL, 0.1 M) at 23 °C was added NaH (60% dispersion in mineral oil, 9.4 mg, 0.235 mmol, 1.2 equiv). The reaction mixture was stirred for 5 min, resulting in a bright yellow solution. BnBr (93 μL , 0.784 mmol, 4.0 equiv) was then added and the reaction mixture was stirred at 23 °C for 5 h. The reaction mixture was poured into saturated aq. NaHCO_3 (5 mL) and extracted with ethyl acetate (4x3 mL). The combined organic extracts were dried over anhydrous Na_2SO_4 and concentrated under reduced pressure. The crude product was purified by silica gel flash chromatography (15% EtOAc/hexanes) to provide the title compound as a colorless oil (50.6 mg, 0.106 mmol, 54% yield); ^1H NMR (500 MHz, CDCl_3 ; compound

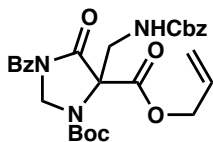
exists as a 4:3 mixture of rotamers. For fully resolved peaks, the major rotamer is denoted by *, and the minor rotamer by #) δ 7.58 – 7.51 (m, 1H), 7.43 – 7.36 (m, 3H), 7.36 – 7.29 (m, 4H), 7.20 – 7.15 (m, 2H), 5.24 (d, $J = 7.2$ Hz, 1H[#]), 5.16 (d, $J = 7.1$ Hz, 1H*), 5.03 – 4.94 (m, 2H), 4.76 – 4.56 (m, 2H), 4.48 (d, $J = 7.2$ Hz, 1H[#]), 4.41 (d, $J = 7.0$ Hz, 1H*), 3.84 (d, $J = 14.0$ Hz, 1H*), 3.63 (d, $J = 14.1$ Hz, 1H[#]), 3.59 – 3.54 (m, 1H), 1.77 (s, 3H), 1.57 (s, 9H[#]), 1.56 (s, 9H*); ^{13}C NMR (125 MHz, CDCl_3) δ 168.2, 168.0, 166.6, 166.6, 166.2, 166.1, 152.0, 151.8, 139.1, 138.6, 134.7, 134.1, 132.8, 132.8, 132.6, 130.2, 128.9, 128.9, 128.8, 128.6, 128.0, 127.9, 127.9, 127.7, 114.4, 114.0, 82.9, 82.4, 72.9, 69.9, 69.8, 61.3, 61.2, 37.9, 37.1, 28.4, 28.3, 19.6, 19.5; IR (Neat Film, NaCl) 2977, 1770, 1714, 1453, 1392, 1294, 1223, 1168, 1075, 1008, 857, 703, 665 cm^{-1} ; HRMS (MM: ESI-APCI): m/z calc'd for $\text{C}_{27}\text{H}_{34}\text{N}_3\text{O}_6$ $[\text{M}+\text{NH}_4]^+$: 496.2442, found 496.2423.



5-allyl 1-(*tert*-butyl) 3-benzoyl-5-(2-chloroallyl)-4-oxoimidazolidine-1,5-dicarboxylate (34h)

To a vial containing lactam **33** (250 mg, 0.668 mmol, 1.0 equiv), NaH (60% dispersion in mineral oil, 32 mg, 0.802 mmol, 1.2 equiv), and TBAI (25 mg, 0.0668 mmol, 0.1 equiv) was added THF (6.7 mL, 0.1 M) at 23 °C. The reaction mixture was stirred for 20 min, resulting in a bright yellow solution. 2,3-dichloropropene (246 μL , 2.67 mmol, 4.0 equiv) was then added and the reaction mixture was stirred at 23 °C for 27 h. The mixture was then heated to 40 °C using a heating block and stirred for an additional 4 h, then poured into saturated aq. NaHCO_3 (10 mL) and extracted with ethyl acetate (4x5 mL). The

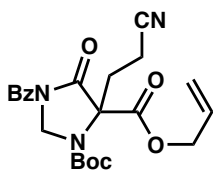
combined organic extracts were dried over anhydrous Na₂SO₄ and concentrated under reduced pressure. The crude product was purified by silica gel flash chromatography (15% EtOAc/hexanes) to provide the title compound as a colorless oil (163.9 mg, 0.365 mmol, 55% yield); ¹H NMR (400 MHz, CDCl₃; compound exists as a 1.2:1 mixture of rotamers. For fully resolved peaks, the major rotamer is denoted by *, and the minor rotamer by #) δ 7.66 – 7.61 (m, 2H), 7.59 – 7.53 (m, 1H), 7.46 – 7.39 (m, 2H), 5.97 – 5.80 (m, 1H), 5.48 – 5.19 (m, 6H), 4.81 – 4.56 (m, 2H), 3.67 (d, *J* = 14.8 Hz, 1H*), 3.43 (d, *J* = 14.9 Hz, 1H#), 3.36 – 3.23 (m, 1H), 1.50 (s, 9H*), 1.47 (s, 9H#); ¹³C NMR (100 MHz, CDCl₃) δ 168.3, 168.1, 166.5, 166.4, 166.0, 165.8, 151.9, 151.6, 136.0, 135.9, 132.9, 132.8, 132.6, 132.6, 131.0, 130.7, 129.1, 128.0, 120.0, 119.3, 118.4, 82.8, 82.5, 70.6, 70.6, 67.4, 67.3, 61.6, 61.5, 41.5, 41.0, 31.0, 28.2; IR (Neat Film, NaCl) 3062, 2980, 2931, 2909, 2360, 1770, 1747, 1714, 1694, 1651, 1634, 1602, 1583, 1477, 1450, 1392, 1370, 1322, 1295, 1231, 1172, 1145, 1099, 1050, 1013, 989, 936, 888, 857, 792, 769, 724, 703, 682, 665, 634 cm⁻¹; HRMS (MM: ESI-APCI): *m/z* calc'd for C₂₂H₂₉ClN₃O₆ [M+NH₄]⁺: 466.1739, found 466.1750.



5-allyl 1-(*tert*-butyl) 3-benzoyl-5-(((benzyloxy)carbonyl)amino)methyl)-4-oxoimidazolidine-1,5-dicarboxylate (34i)

To a vial containing lactam **33** (199 mg, 0.532 mmol, 1.0 equiv), and benzyl ((phenylsulfonyl)methyl)carbamate³¹ (195 mg, 0.638 mmol, 1.2 equiv) was added CH₂Cl₂ (2.7 mL, 0.2 M). Cs₂CO₃ (433 mg, 1.33 mmol, 2.5 equiv) was then added in a single portion

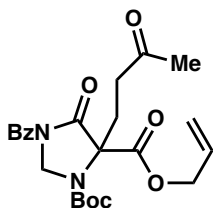
and the reaction mixture was stirred at 23 °C for 4 h. Saturated aq. NH₄Cl (3 mL) was then added, and the resulting mixture was stirred vigorously for 30 min. The layers were then separated, and the aqueous layer was extracted with CH₂Cl₂ (3 x 3 mL). The combined organic extracts were dried over anhydrous Na₂SO₄ and concentrated under reduced pressure. The crude product was purified by silica gel flash chromatography (20% EtOAc/hexanes) to provide the title compound as a colorless oil (149 mg, 0.341 mmol, 64% yield); ¹H NMR (400 MHz, CDCl₃) δ 7.82 – 7.58 (m, 2H), 7.54 (td, *J* = 7.0, 1.6 Hz, 1H), 7.40 (q, *J* = 7.9 Hz, 2H), 7.32 (q, *J* = 2.3 Hz, 5H), 5.99 – 5.73 (m, 1H), 5.46 – 4.82 (m, 7H), 4.76 – 4.53 (m, 2H), 4.17 – 3.95 (m, 2H), 1.49 (d, *J* = 5.9 Hz, 9H); ¹³C NMR (100 MHz, CDCl₃) δ 168.4, 168.1, 166.2, 166.1, 165.5, 165.1, 156.8, 156.6, 152.5, 151.8, 136.4, 136.2, 132.9, 132.9, 132.6, 132.5, 131.0, 130.7, 129.4, 129.3, 128.7, 128.6, 128.4, 128.3, 128.2, 128.0, 120.0, 119.3, 83.1, 82.8, 71.2, 70.7, 67.2, 67.2, 67.1, 61.5, 61.3, 43.2, 43.0, 29.8, 28.3, 28.2; IR (Neat Film, NaCl) 3380, 3066, 2978, 1714, 1601, 1519, 1454, 1393, 1304, 1166, 1068, 989, 941, 855, 737, 698, 666 cm⁻¹; HRMS (MM: ESI-APCI): *m/z* calc'd for C₂₈H₃₁N₃NaO₈ [M+Na]⁺: 560.2003, found 560.1998.



5-allyl 1-(*tert*-butyl) 3-benzoyl-5-(2-cyanoethyl)-4-oxoimidazolidine-1,5-dicarboxylate (34j)

To a vial containing lactam **33** (250 mg, 0.668 mmol, 1.0 equiv) and K₂CO₃ (462 mg, 3.34 mmol, 5 equiv) were added acetone (2.7 mL, 0.25 M) and acrylonitrile (175 μL, 2.67 mmol, 4 equiv). The vial was sealed and the reaction mixture was heated to 50 °C

using a heating block, stirred for 20 h, and allowed to cool to 23 °C. The crude mixture was filtered through cotton and concentrated under reduced pressure. The product was purified by silica gel flash chromatography (25% EtOAc/hexanes) to provide the title compound as a colorless oil (94.6 mg, 0.221 mmol, 33% yield); ¹H NMR (400 MHz, CDCl₃; compound exists as a 1.7:1 mixture of rotamers. For fully resolved peaks, the major rotamer is denoted by *, and the minor rotamer by #) δ 7.70 – 7.61 (m, 2H), 7.61 – 7.54 (m, 1H), 7.44 (t, *J* = 7.7 Hz, 2H), 5.96 – 5.78 (m, 1H), 5.48 – 5.21 (m, 4H), 4.78 – 4.56 (m, 2H), 2.94 – 2.59 (m, 2H), 2.53 – 2.34 (m, 2H), 1.52 (s, 9H*), 1.47 (s, 9H#); ¹³C NMR (100 MHz, CDCl₃) δ 168.4, 168.1, 166.4, 165.5, 165.3, 152.9, 152.2, 133.1, 132.6, 130.9, 130.6, 129.3, 128.2, 120.4, 119.7, 118.5, 118.2, 83.7, 83.4, 70.9, 70.8, 67.6, 67.6, 61.8, 61.8, 28.3, 28.3, 27.6, 12.7, 12.5; IR (Neat Film, NaCl) 3065, 2979, 2936, 2343, 2249, 1770, 1745, 1714, 1698, 1651, 1602, 1582, 1477, 1449, 1386, 1372, 1301, 1245, 1225, 1173, 1154, 1114, 1081, 1048, 1028, 994, 939, 894, 858, 845, 793, 781, 770, 733, 701, 672, 664, 621 cm⁻¹; HRMS (MM: ESI-APCI): *m/z* calc'd for C₂₂H₂₉N₄O₆ [M+NH₄]⁺: 445.2082, found 445.2085.

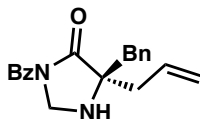


**5-allyl 1-(tert-butyl) 3-benzoyl-4-oxo-5-(3-oxobutyl)imidazolidine-1,5-dicarboxylate
(34k)**

To a vial containing lactam **33** (250 mg, 0.668 mmol, 1.0 equiv) and K₂CO₃ (462 mg, 3.34 mmol, 5 equiv) were added acetone (3 mL, 0.25 M) and methyl vinyl ketone (223

μL , 2.67 mmol, 4 equiv). The vial was sealed, and the reaction mixture was heated to 50 °C using a heating block, stirred for 6 h, and allowed to cool to 23 °C. The crude mixture was filtered through cotton and concentrated under reduced pressure. The product was purified by silica gel flash chromatography (33% EtOAc/hexanes) to provide the title compound as a colorless oil (228 mg, 0.513 mmol, 77% yield); ^1H NMR (400 MHz, CDCl_3 ; compound exists as a 1.1:1 mixture of rotamers. For fully resolved peaks, the major rotamer is denoted by *, and the minor rotamer by #) δ 7.62 (d, $J = 7.7$ Hz, 2H), 7.55 – 7.48 (m, 1H), 7.39 (t, $J = 7.7$ Hz, 2H), 5.95 – 5.75 (m, 1H), 5.41 – 5.05 (m, 4H), 4.73 – 4.52 (m, 2H), 2.75 – 2.35 (m, 4H), 2.11 (d, $J = 3.0$ Hz, 3H), 1.47 (s, 9H*), 1.43 (s, 9H#); ^{13}C NMR (100 MHz, CDCl_3) δ 207.5, 206.7, 168.4, 168.2, 166.9, 166.8, 166.4, 166.2, 152.5, 152.2, 132.8, 132.8, 132.7, 132.7, 131.1, 130.8, 129.1, 128.0, 119.7, 119.1, 82.9, 82.6, 70.9, 67.1, 67.1, 61.4, 61.3, 38.5, 37.8, 29.8, 29.4, 28.2, 28.1, 27.8, 26.9; IR (Neat Film, NaCl) 3074, 2977, 2931, 1757, 1703, 1642, 1602, 1583, 1478, 1448, 1393, 1368, 1304, 1226, 1168, 1091, 1061, 999, 970, 928, 880, 858, 826, 795, 768, 731, 701, 664 cm^{-1} ; HRMS (MM: ESI-APCI): m/z calc'd for $\text{C}_{23}\text{H}_{32}\text{N}_3\text{O}_7$ $[\text{M}+\text{NH}_4]^+$: 462.2235, found 462.2251.

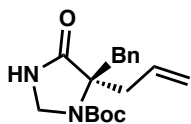
1.5.2.6 Derivatization of Imidazolidinone Allylic Alkylation Products



(*R*)-5-allyl-3-benzoyl-5-benzylimidazolidin-4-one (52)

To a solution of benzyl imidazolidinone **35a** (15 mg, 0.0357 mmol, 1.0 equiv) in CH_2Cl_2 (0.36 mL, 0.1 M) was added trifluoroacetic acid (41 μL , 0.536 mmol, 15 equiv), and the reaction mixture was stirred in a sealed vial at 23 °C for 22 h. The resulting solution was concentrated under reduced pressure and the residue taken up in Et_2O (0.5 mL),

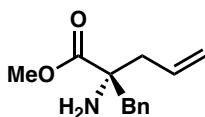
washed with 5% aq. K_2CO_3 (1 mL), dried with Na_2SO_4 , and concentrated under reduced pressure. The crude product was purified by silica gel flash chromatography (33% EtOAc/hexanes) to provide free amine **52** as a white solid (9.3 mg, 0.0290 mmol, 81% yield); 1H NMR (400 MHz, $CDCl_3$) δ 7.58 – 7.49 (m, 3H), 7.46 – 7.40 (m, 2H), 7.38 – 7.29 (m, 3H), 7.29 – 7.22 (m, 2H), 5.85 (dddd, $J = 17.0, 10.2, 8.6, 6.2$ Hz, 1H), 5.31 – 5.17 (m, 2H), 4.71 (d, $J = 9.6$ Hz, 1H), 4.32 (d, $J = 9.6$ Hz, 1H), 3.15 (d, $J = 13.6$ Hz, 1H), 2.76 (d, $J = 13.6$ Hz, 1H), 2.63 (ddt, $J = 14.0, 6.1, 1.4$ Hz, 1H), 2.32 (ddt, $J = 13.9, 8.5, 0.9$ Hz, 1H), 2.21 (s, 1H); ^{13}C NMR (100 MHz, $CDCl_3$) δ 176.0, 169.7, 135.6, 133.4, 132.5, 132.1, 130.5, 129.3, 128.8, 128.0, 127.6, 120.9, 68.4, 61.9, 42.1, 41.1; IR (Neat Film, NaCl) 2921, 1743, 1674, 1494, 1449, 1380, 1306, 1235, 922, 796, 732, 700 cm^{-1} ; HRMS (MM: ESI-APCI): m/z calc'd for $C_{20}H_{21}N_2O_2$ $[M+H]^+$: 321.1598, found 321.1590; $[\alpha]_D^{21.7} +69.27$ (c 0.5, $CHCl_3$).



tert-butyl (R)-5-allyl-5-benzyl-4-oxoimidazolidine-1-carboxylate (53)

To a solution of benzyl imidazolidinone **35a** (15 mg, 0.0357 mmol, 1.0 equiv) in 50% MeOH/ H_2O (0.36 mL, 0.1 M) was added $LiOH \cdot H_2O$ (22 mg, 0.536 mmol, 15 equiv) and the reaction mixture was heated with stirring in a sealed vial at 70 $^{\circ}C$ for 1 h using a heating block. MeOH was removed under reduced pressure and the solution was diluted with H_2O (0.5 mL) and extracted with ethyl acetate (4 x 0.5 mL). The combined organic extracts were dried over Na_2SO_4 and concentrated under reduced pressure. The crude product was purified by silica gel flash chromatography (40% EtOAc/hexanes) to provide

free lactam **53** as a colorless film (9.0 mg, 0.0284 mmol, 80% yield); ^1H NMR (400 MHz, CDCl_3 ; compound exists as a 1.1:1 mixture of rotamers. For fully resolved peaks, the major rotamer is denoted by *, and the minor rotamer by #) δ 7.26 – 7.12 (m, 5H), 6.38 (d, $J = 32.9$ Hz, 1H), 5.74 – 5.53 (m, 1H), 5.24 – 5.04 (m, 2H), 4.41 (d, $J = 5.5$ Hz, $1\text{H}^\#$), 4.32 (d, $J = 5.4$ Hz, 1H^*), 3.79 (d, $J = 5.5$ Hz, $1\text{H}^\#$), 3.68 (d, $J = 5.3$ Hz, 1H^*), 3.50 (d, $J = 13.3$ Hz, 1H^*), 3.27 (d, $J = 13.4$ Hz, $1\text{H}^\#$), 3.16 (dd, $J = 13.6, 8.4$ Hz, $1\text{H}^\#$), 3.01 (dd, $J = 13.3, 1.7$ Hz, 1H), 2.93 (dd, $J = 13.8, 8.2$ Hz, 1H^*), 2.71 – 2.54 (m, 1H), 1.64 (s, $9\text{H}^\#$), 1.49 (s, 9H^*); ^{13}C NMR (100 MHz, CDCl_3) δ 174.4, 174.2, 152.9, 151.9, 136.5, 135.9, 132.4, 132.0, 130.0, 129.9, 128.5, 128.3, 127.1, 126.9, 119.7, 119.6, 81.7, 80.5, 68.6, 68.4, 58.1, 57.9, 41.1, 40.0, 38.8, 28.8, 28.5; IR (Neat Film, NaCl) 3242, 2976, 2930, 1708, 1454, 1402, 1368, 1341, 1257, 1174, 1143, 1078, 996, 920, 768, 702 cm^{-1} ; HRMS (MM: ESI-APCI): m/z calc'd for $\text{C}_{18}\text{H}_{25}\text{N}_2\text{O}_3$ $[\text{M}+\text{H}]^+$: 317.1860, found 317.1852; $[\alpha]_{\text{D}}^{21.8} -67.38$ (c 0.5, CHCl_3).



methyl (*R*)-2-amino-2-benzylpent-4-enoate (**54**)

To a solution of benzyl imidazolidinone **35a** (10 mg, 0.0238 mmol, 1.0 equiv) in MeOH (0.4 mL, 0.06 M) was added concentrated H_2SO_4 (85 μL). The reaction vessel was sealed, and the reaction mixture was stirred at 70 $^\circ\text{C}$ in a heating block for 3 days. Care should be taken, as gas pressure is generated over the course of the reaction. The crude mixture was then added to saturated aq. NaHCO_3 (10 mL, gas evolution) and extracted with ethyl acetate (4 x 4 mL). The combined organic extracts were dried with Na_2SO_4 and concentrated under reduced pressure. The crude product was purified by silica gel flash

chromatography (20% EtOAc/hexanes + 0.1% Et₃N) to provide amino ester **11** as a colorless film (1.3 mg, 0.00593 mmol, 25% yield). ¹H NMR (500 MHz, CDCl₃) δ 7.31 – 7.26 (m, 2H), 7.26 – 7.22 (m, 1H), 7.18 – 7.08 (m, 2H), 5.77 – 5.64 (m, 1H), 5.24 – 5.11 (m, 2H), 3.71 (s, 3H), 3.19 (d, *J* = 13.2 Hz, 1H), 2.80 (dd, *J* = 13.2, 6.9 Hz, 1H), 2.73 (ddt, *J* = 13.3, 6.4, 1.3 Hz, 1H), 2.33 (dd, *J* = 13.5, 8.4 Hz, 1H). All characterization data matched those reported in the literature.³⁵

1.5.3 DETERMINATION OF ENANTIOMERIC EXCESS

Table 1.5.3.1. Determination of enantiomeric excess.

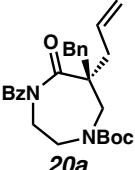
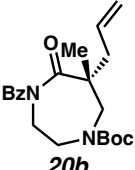
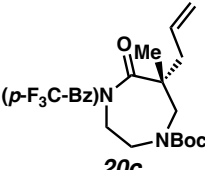
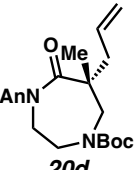
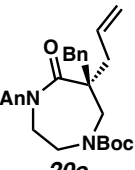
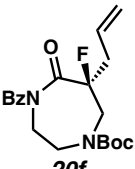
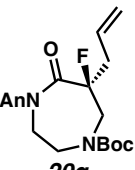
entry	compound	assay conditions	t_R of major isomer (min)	t_R of minor isomer (min)	% ee
1	 20a	SFC Chiralpak AD-H 20% IPA isocratic, 2.5 mL/min	3.51	2.71	90
2	 20b	SFC Chiralpak IC 20% IPA isocratic, 2.5 mL/min	5.68	4.31	90
3	 20c	SFC Chiralpak AD-H 5% IPA isocratic, 2.5 mL/min	5.86	4.49	92
4	 20d	SFC Chiralpak IC 20% MeOH isocratic, 2.5 mL/min	5.66	5.11	94
5	 20e	SFC Chiralpak AD-H 20% IPA isocratic, 2.5 mL/min	6.20	3.94	89
6	 20f	SFC Chiralpak AD-H 20% IPA isocratic, 2.5 mL/min	4.99	6.26	90
7	 20g	SFC Chiralcel OD-H 20% IPA isocratic, 2.5 mL/min	2.69	3.25	83

Table 1.5.3.2. Determination of enantiomeric excess (continued).

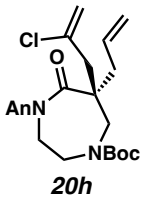
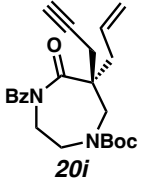
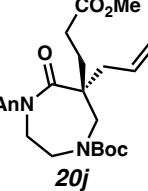
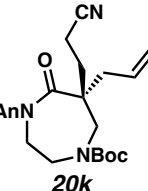
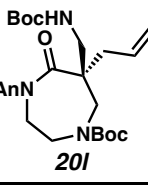
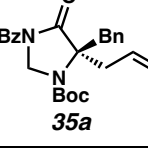
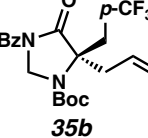
entry	compound	assay conditions	t_R of major isomer (min)	t_R of minor isomer (min)	% ee
8	 20h	SFC Chiralpak AD-H 20% IPA isocratic, 2.5 mL/min	2.77	2.52	90
9	 20i	SFC Chiralpak AD-H 10% IPA isocratic, 2.5 mL/min	10.85	10.29	94
10	 20j	SFC Chiralcel OD-H 15% IPA isocratic, 2.5 mL/min	5.27	4.84	95
11	 20k	SFC Chiralcel OD-H 20% IPA isocratic, 2.5 mL/min	8.33	6.18	84
12	 20l	SFC Chiralpak IC 20% IPA isocratic, 2.5 mL/min	5.85	4.65	93
13	 35a	SFC Chiralpak AD-H 7% IPA isocratic, 2.5 mL/min	5.13	6.29	92
14	 35b	SFC Chiralcel OJ-H 10% IPA isocratic, 2.5 mL/min	1.55	1.71	89

Table 1.5.3.3. Determination of enantiomeric excess (continued).

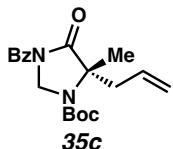
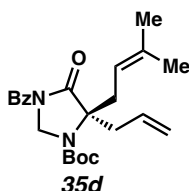
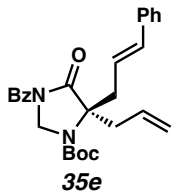
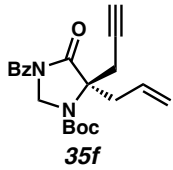
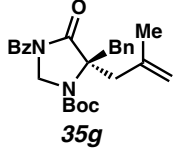
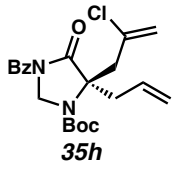
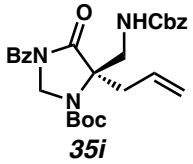
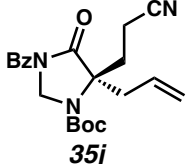
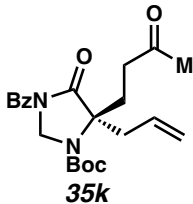
entry	compound	assay conditions	t_R of major isomer (min)	t_R of minor isomer (min)	% ee
15	 35c	SFC Chiralpak AD-H 7% IPA isocratic, 2.5 mL/min	3.40	3.04	86
16	 35d	SFC Chiralpak OJ-H 1% IPA isocratic, 2.5 mL/min	2.98	3.34	80
17	 35e	SFC Chiralpak AD-H 10% IPA isocratic, 2.5 mL/min	5.15	4.77	85
18	 35f	SFC Chiralcel OJ-H 7% IPA isocratic, 2.5 mL/min	2.43	2.11	91
19	 35g	SFC Chiralcel OD-H 10% IPA isocratic, 2.5 mL/min	3.79	3.47	89
20	 35h	SFC Chiralcel OJ-H 7% IPA isocratic, 2.5 mL/min	2.19	1.99	86

Table 1.5.3.4. Determination of enantiomeric excess (continued).

entry	compound	assay conditions	t_R of major isomer (min)	t_R of minor isomer (min)	% ee
21	 35i	SFC Chiralpak AD-H 20% IPA isocratic, 2.5 mL/min	6.15	3.52	85
22	 35j	SFC Chiralpak IC 15% IPA isocratic, 2.5 mL/min	5.49	4.78	95
23	 35k	SFC Chiralpak IC 20% IPA isocratic, 2.5 mL/min	2.42	3.23	93

1.6 REFERENCES AND NOTES

- (1) Tsuji, J.; Minami, I.; Shimizu, I. Palladium-catalyzed allylation of ketones and aldehydes via allyl enol carbonates. *Tetrahedron Lett.* **1983**, *24*, 1793–1796.
- (2) Behenna, D. C.; Stoltz, B. M. The Enantioselective Tsuji Allylation. *J. Am. Chem. Soc.* **2004**, *126*, 15044–15045.
- (3) a) Mohr, J. T.; Behenna, D. C.; Harned, A. M.; Stoltz, B. M. Deracemization of Quaternary Stereocenters by Pd-Catalyzed Enantioconvergent Decarboxylative Allylation of Racemic β -Ketoesters. *Angew. Chem. Int. Ed.* **2005**, *44*, 6924–6927.
b) Behenna, D. C.; Liu, Y.; Yurino, T.; Kim, J.; White, D. E.; Virgil, S. C.; Stoltz, B. M. Enantioselective construction of quaternary *N*-heterocycles by palladium-catalysed decarboxylative allylic alkylation of lactams. *Nat. Chem.* **2012**, *4*, 130–133. c) Bennett, N. B.; Duquette, D. C.; Kim, J.; Liu, W.; Marziale, A. N.; Behenna, D. C.; Virgil, S. C.; Stoltz, B. M. Expanding Insight into Asymmetric Palladium-Catalyzed Allylic Alkylation of *N*-Heterocyclic Molecules and Cyclic Ketones. *Chem. Eur. J.* **2013**, *19*, 4414–4418. d) Korch, K. M.; Eidamshaus, C.; Behenna, D. C.; Nam, S.; Horne, D.; Stoltz, B. M. Enantioselective Synthesis of α -Secondary and α -Tertiary Piperazin-2-ones and Piperazines by Catalytic Asymmetric Allylic Alkylation. *Angew. Chem. Int. Ed.* **2015**, *54*, 179–183. e) Sun, A. W.; Hess, S. N.; Stoltz, B. M. Enantioselective synthesis of *gem*-disubstituted *N*-Boc diazaheterocycles via decarboxylative asymmetric allylic alkylation. *Chem. Sci.* **2019**, *10*, 788–792. f) Cusumano, A. Q.; Stoltz, B. M.; Goddard, A. W.

- Reaction Mechanism, Origins of Enantioselectivity, and Reactivity Trends in Asymmetric Allylic Alkylation: A Comprehensive Quantum Mechanics Investigation of a C(sp³)-C(sp³) Cross-Coupling. *J. Am. Chem. Soc.* **2020**, *142*, 13917–13933.
- (4) a) Trost, B. M.; Xu, J. Regio- and Enantioselective Pd-Catalyzed Allylic Alkylation of Ketones through Allyl Enol Carbonates. *J. Am. Chem. Soc.* **2005**, *127*, 2846–2847. b) Trost, B. M.; Bream, R. N.; Xu, J. Asymmetric Allylic Alkylation of Cyclic Vinylogous Esters and Thioesters by Pd-Catalyzed Decarboxylation of Enol Carbonate and β-Ketoester Substrates. *Angew. Chem. Int. Ed.* **2006**, *45*, 3109–3112. c) Trost, B. M.; Nagaraju, A.; Wang, F.; Zuo, Z.; Xu, J.; Hull, K. L. Palladium-Catalyzed Decarboxylative Asymmetric Allylic Alkylation of Dihydroquinolinones. *Org. Lett.* **2019**, *21*, 1784–1788. d) James, J.; Jackson, M.; Guiry, P. J. Palladium-Catalyzed Decarboxylative Asymmetric Allylic Alkylation: Development, Mechanistic Understanding and Recent Advances. *Adv. Synth. Catal.* **2019**, *361*, 3016–3049.
- (5) a) Lovering, F.; Bikker, J.; Humblet, C. Escape from Flatland: Increasing Saturation as an Approach to Improving Clinical Success. *J. Med. Chem.* **2009**, *52*, 6752–6756. b) Lovering, F. Escape from Flatland 2: complexity and promiscuity. *Med. Chem. Commun.* **2013**, *4*, 515–519.
- (6) Sun, A. W.; Bulterys, P. L.; Bartberger, M. D.; Jorth, P. A.; O’Boyle, B. M.; Virgil, S. C.; Miller, J. F.; Stoltz, B. M. Incorporation of a chiral *gem*-disubstituted

nitrogen heterocycle yields an oxazolidinone antibiotic with reduced mitochondrial toxicity. *Bioorg. Med. Chem. Lett.* **2019**, *29*, 2686–2689.

- (7) Behenna, D. C. et. al. Enantioselective Decarboxylative Alkylation Reactions: Catalyst Development, Substrate Scope, and Mechanistic Studies. *Chem. Eur. J.* **2011**, *17*, 14199–14223.
- (8) Gates, M. New synthesis of diazepam. *J. Org. Chem.* **1980**, *45*, 1675–1681.
- (9) Trynieszewski, M.; Bujok, R.; Cmoch, P.; Gańczarczyk, R.; Kulszewicz-Bajer, I.; Wróbel, Z. Direct Reductive Cyclocondensation of the Nitro Group with the Amido Group: Key Role of the Iminophosphorane Intermediate in the Synthesis of 1,4-Dibenzodiazepine Derivatives. *J. Org. Chem.* **2019**, *84*, 2277–2286.
- (10) Coleman, P. J.; Gotter, A. L.; Herring, W. J.; Winrow, C. J.; Renger, J. J. The Discovery of Suvorexant, the First Orexin Receptor Drug for Insomnia. *Annu. Rev. Pharmacol. Toxicol.* **2017**, *57*, 509–533.
- (11) a) Knabe, J.; Bender, S. 1,5-Benzodiazepine, 1. Mitt.: Racemate und Enantiomere von 3,3-Dialkyl-1,5-benzodiazepin-2,4-dionen: Synthese, Konfiguration und enantiomere Reinheit. *Arch. Pharm.* **1993**, *326*, 551–558. b) Cao, S. X.; Feher, V.; Ichikawa, T.; Jones, B.; Kaldor, S. W.; Kiryanov, A. A.; Lam, B.; Liu, Y.; McBride, C.; Natalia, S. R.; Nie, Z.; Stafford, J. A. Polo-Like Kinase Inhibitors. U.S. Patent 8318727, 2009. c) Barlind, J. G.; et al. Identification and design of a novel series of MGAT2 inhibitors. *Bioorg. Med. Chem. Lett.* **2013**, *23*, 2721–2726.

- (12) Dong, D. C.; Winnik, M. A. The Py scale of solvent polarities. *Can. J. Chem.* **1984**, *62*, 2560–2565.
- (13) Alexy, E. J.; Fulton, T. J.; Zhang, H.; Stoltz, B. M. Palladium-catalyzed enantioselective decarboxylative allylic alkylation of fully substituted N-acyl indole-derived enol carbonates. *Chem. Sci.* **2019**, *10*, 5996–6000.
- (14) Mangion, I. K.; Sherry, B. D.; Yin, J.; Fleitz, F. J. Enantioselective Synthesis of a Dual Orexin Receptor Antagonist. *Org. Lett.* **2012**, *14*, 3458–3461.
- (15) Representative publications: a) Seebach, D.; Juaristi, E.; Miller, D. D.; Schickli, C.; Weber, T. Addition of Chiral Glycine, Methionine, and Vinylglycine Enolate Derivatives to Aldehydes and Ketones in the Preparation of Enantiomerically Pure α -Amino- β -hydroxy Acids. *Helv. Chim. Acta* **1987**, *70*, 237–261. b) Wang, X.; Frutos, R. P.; Zhang, L.; Sun, X.; Xu, Y.; Wirth, T.; Nicola, T.; Nummy, L. J.; Krishnamurthy, D.; Busacca, C. A.; Yee, N.; Senanayake, C. H. Asymmetric Synthesis of LFA-1 Inhibitor BIRT2584 on Metric Ton Scale. *Org. Process Res. Dev.* **2011**, *15*, 1185–1191. c) Leonard, D. J.; Ward, J. W.; Clayden, J. Asymmetric α -arylation of amino acids. *Nature* **2018**, *562*, 105–109. d) Abas, H.; Mas-Roselló, J.; Amer, M. M.; Durand, D. J.; Groleau, R. R.; Fey, N.; Clayden, J. Asymmetric and Geometry-Selective α -Alkenylation of α -Amino Acids. *Angew. Chem. Int. Ed.* **2019**, *58*, 2418–2422.
- (16) Cozzi, P. G.; Gualandi, A.; Mengozzi, L.; Wilson, C. M. Imidazolidinones as Asymmetric Organocatalysts. In *Sustainable Catalysis: Without Metals or Other*

Endangered Elements, Part 2; North, M., Ed.; Royal Society of Chemistry: Cambridge, 2016; 164–195.

- (17) Pfeiffer, U.; Riccaboni, M. T.; Erba, R.; Pinza, M. A short synthesis of 4-imidazolidinone. *Liebigs Ann. Chem.* **1988**, 993–995.
- (18) Nitta, Y.; Yamaguchi, T.; Tanaka, T. First Synthesis of 4-Imidazolidinone. *Heterocycles* **1986**, *24*, 25–28.
- (19) Wang, J.; Rochon, F. D.; Yang, Y.; Hua, L.; Kayser, M. M. Synthesis of oxazolidines using DMSO/P₄O₁₀ as a formaldehyde equivalent. *Tetrahedron: Asymmetry* **2007**, *18*, 1115–1123.
- (20) Liu, Y.; Ji, P.; Xu, J.; Hu, Y.; Liu, Q.; Luo, W.; Guo, C. Transition Metal-Free α -Csp³-H Methylenation of Ketones to Form C=C Bond Using Dimethyl Sulfoxide as Carbon Source. *J. Org. Chem.* **2017**, *82*, 7159–7164.
- (21) Pothikumar, R.; Sujatha, C.; Namitharan, K. Transition-Metal-Free In Situ Generation of Terminal Alkenes: Synthesis of Multisubstituted Acrylamidines via Tandem sp³ C–H Olefination/sp² C–H Arylation Reactions. *ACS Catal.* **2017**, *7*, 7783–7787.
- (22) Pojer, P. M.; Angyal, S. J. Methylthiomethyl ethers: Their use in the protection and methylation of hydroxyl groups. *Aust. J. Chem.* **1978**, *31*, 1031–1040.
- (23) Freter, K.; Rabinowitz, J. C.; Witkop, B. Labile Stoffwechselprodukte V. Zur Biogenese Des Formiminoglycins Aus 4(5H)-Imidazolone. *Liebigs Ann. Chem.* **1957**, *607*, 174–187.

- (24) Khurana, J. M.; Kukreja, G. Nickel boride mediated reductive desulfurization of 2-thioxo-4(3*H*)-quinazolinones: A new synthesis of quinazolin-4(3*H*)-ones and 2,3-dihydro-4(1*H*)-quinazolinones. *J. Heterocyclic Chem.* **2003**, *40*, 677–679.
- (25) Khurana, J. M.; Agrawal, A.; Bansal, G. 5,5-diaryl and 5-alkyl-3-phenyl-4-imidazolidones: A novel synthesis. *J. Heterocyclic Chem.* **2009**, *46*, 1007–1010.
- (26) Gosling, S.; Rollin, P.; Tatibouët, A. Thiohydantoins: Selective N- and S-Functionalization for Liebeskind-Srogl Reaction Study *Synthesis* **2011**, 3649–3660.
- (27) Recent reviews: a) Vogt, H.; Bräse, S. Recent approaches towards the asymmetric synthesis of α,α -disubstituted α -amino acids. *Org. Biomol. Chem.* **2007**, *5*, 406–430. b) Bera, K.; Namboothiri, I. N. N. Asymmetric Synthesis of Quaternary α -Amino Acids and Their Phosphonate Analogues. *Asian J. Org. Chem.* **2014**, *3*, 1234–1260. c) Metz, A. E.; Kozlowski, M. C. Recent Advances in Asymmetric Catalytic Methods for the Formation of Acyclic α,α -Disubstituted α -Amino Acids. *J. Org. Chem.* **2015**, *80*, 1–7. d) Cativiela, C.; Ordóñez, M.; Viveros-Ceballos, J. L. Stereoselective synthesis of acyclic α,α -disubstituted α -amino acids derivatives from amino acids templates. *Tetrahedron* **2020**, *76*, 130875.
- (28) Pangborn, A. M.; Giardello, M. A.; Grubbs, R. H.; Rosen, R. K.; Timmers, F. J. Safe and Convenient Procedure for Solvent Purification. *Organometallics* **1996**, *15*, 1518–1520.

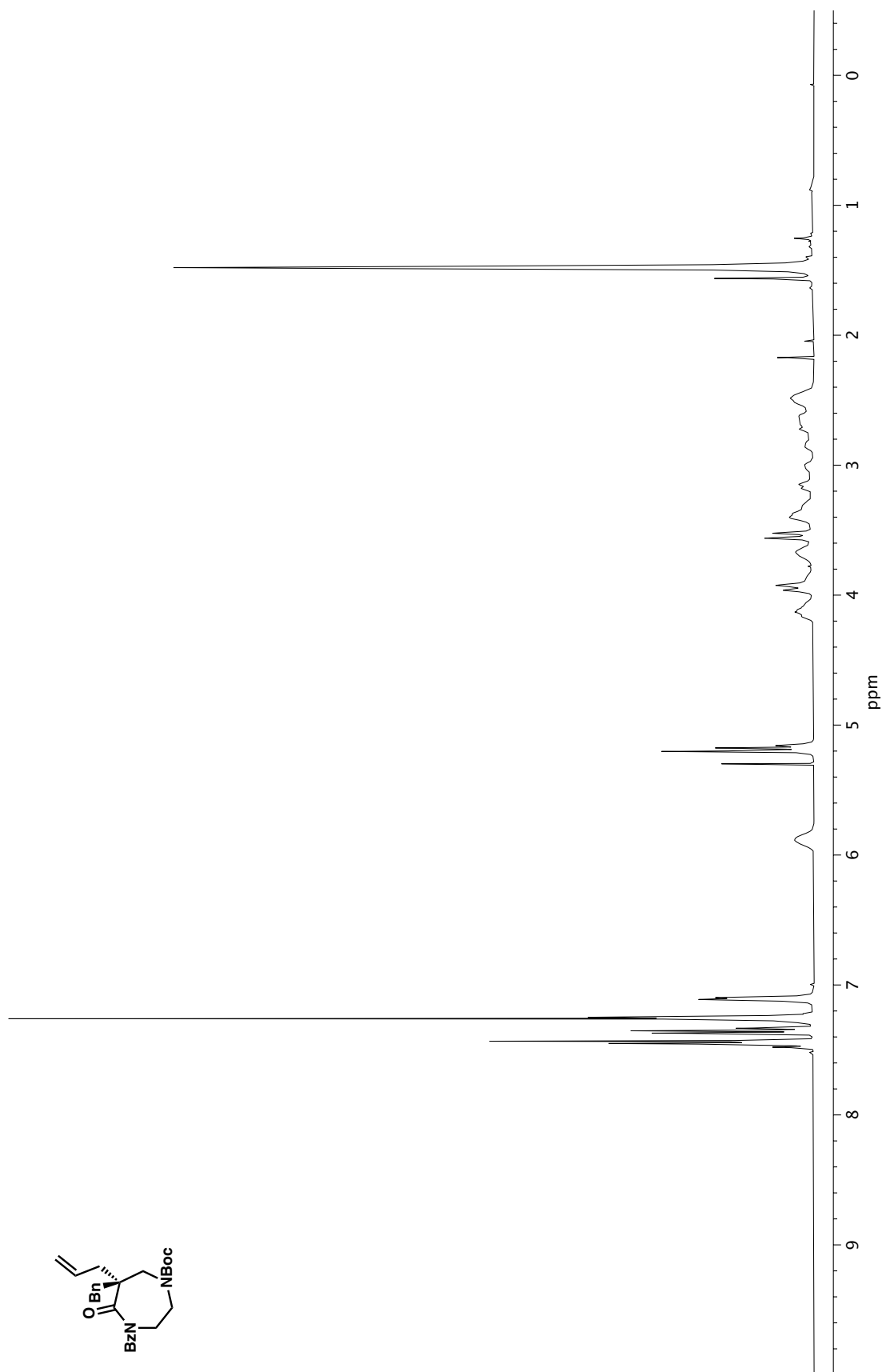
- (29) McDougal, N. T.; Streuff, J.; Mukherjee, H.; Virgil, S. C.; Stoltz, B. M. Rapid synthesis of an electron-deficient t-BuPHOX ligand: cross-coupling of aryl bromides with secondary phosphine oxides. *Tetrahedron Lett.* **2010**, *51*, 5550–5554.
- (30) Klepacz, A.; Zwierzak, A. An expeditious one-pot synthesis of diethyl N-Boc-1-aminoalkylphosphonates. *Tetrahedron Lett.* **2002**, *43*, 1079–1080.
- (31) Sikriwal, D.; Kant, R.; Maulik, P. R.; Dikshit, D. K. A short formal synthesis of three epimers of penmacric acid. *Tetrahedron* **2010**, *66*, 6167–6173.
- (32) Jia, P.; Hu, Y.; Ye, Z.; Li, X.; Xiang, H.; Yang, H. *O*-Perfluoropyridin-4-yl Oximes: Iminyl Radical Precursors for Photo- or Thermal-Induced N–O Cleavage in C(sp²)–C(sp³) Bond Formation. *J. Org. Chem.* **2020**, *85*, 3538–3547.
- (33) Trost, B. M.; Xu, J. The *O*-Acylation of Ketone Enolates by Allyl 1H-Imidazole-1-carboxylate Mediated with Boron Trifluoride Etherate – A Convenient Procedure for the Synthesis of Substituted Allyl Enol Carbonates. *J. Org. Chem.* **2007**, *72*, 9372–9375.
- (34) Heller, S. T.; Schultz, E. E.; Sarpong, R. Chemoselective N-Acylation of Indoles and Oxazolidinones with Carbonylazoles. *Angew. Chem. Int. Ed.* **2012**, *51*, 8304–8308.
- (35) Wei, L.; Xu, S.; Zhu, Q.; Che, C.; Wang, C. Synergistic Cu/Pd Catalysis for Enantioselective Allylic Alkylation of Aldimine Esters: Access to α,α -Disubstituted α -Amino Acids. *Angew. Chem. Int. Ed.* **2017**, *56*, 12312–12316.

APPENDIX 1

Spectra Relevant to Chapter 1:

Palladium-Catalyzed Decarboxylative Asymmetric Allylic Alkylation of

5- and 7-Membered Diazaheterocycles

Figure A1.1. ¹H NMR (400 MHz, CDCl₃) of compound 20a.

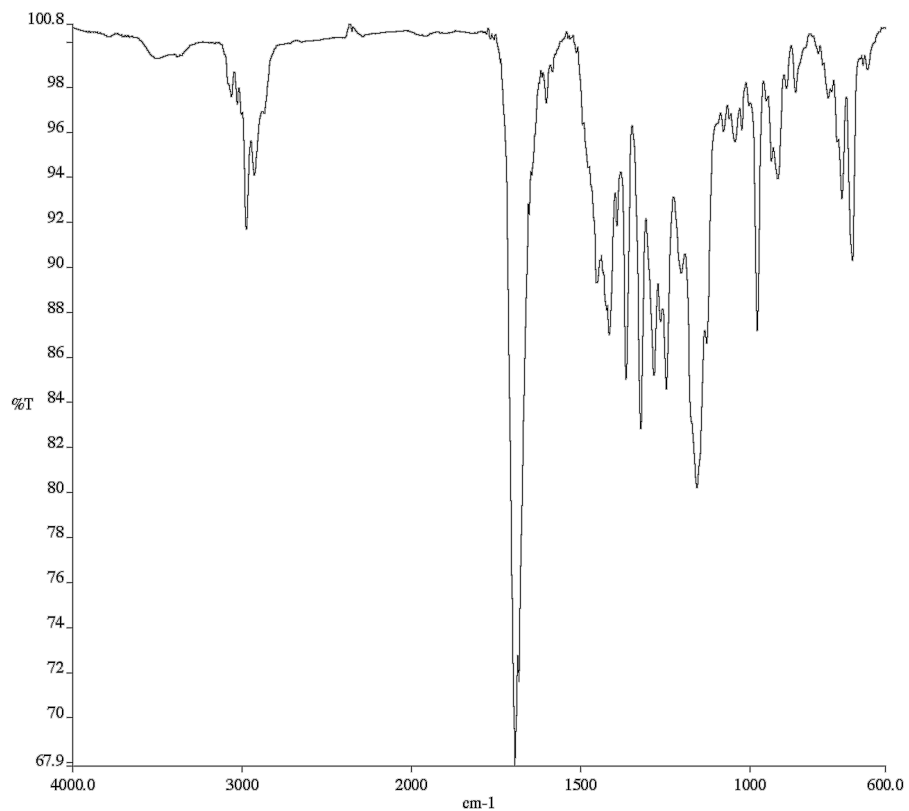


Figure A1.2. Infrared spectrum (Thin Film, NaCl) of compound **20a**.

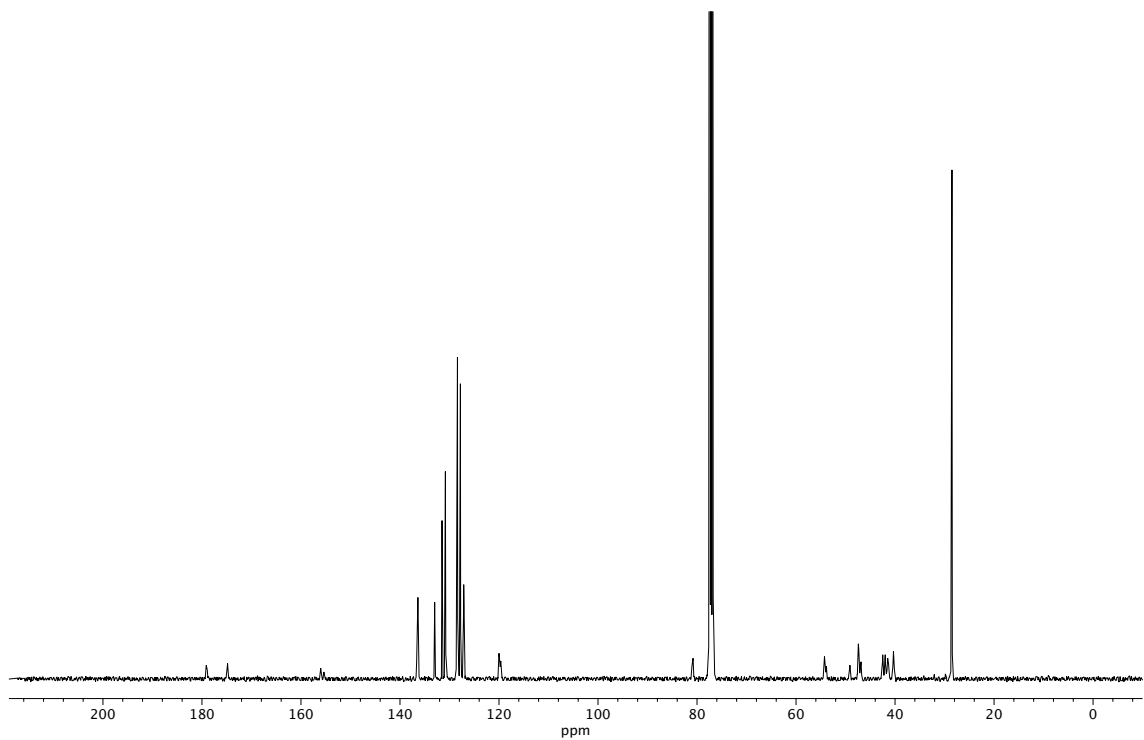
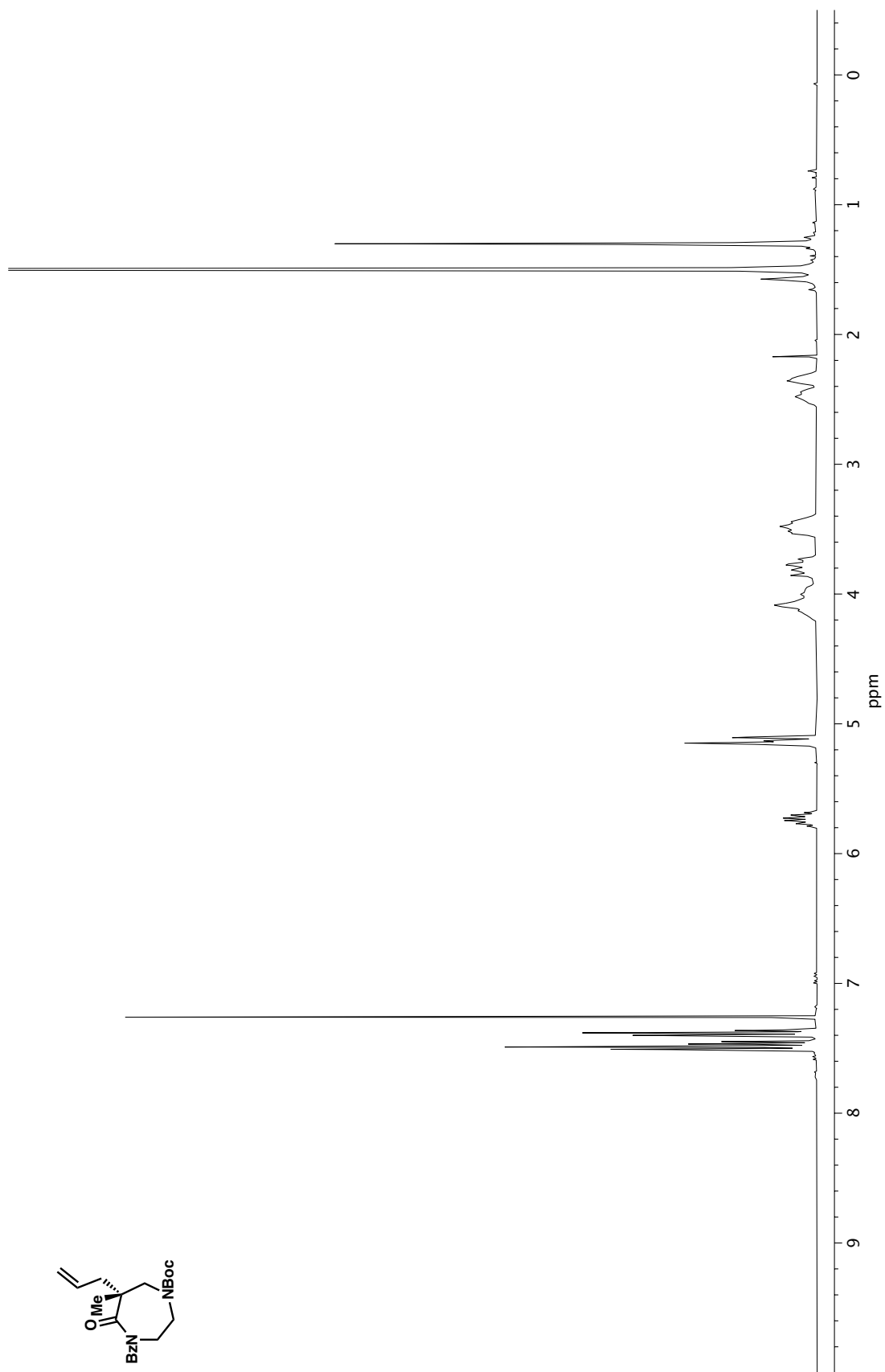


Figure A1.3. ¹³C NMR (100 MHz, CDCl₃) of compound **20a**.

Figure A1.4. ^1H NMR (400 MHz, CDCl_3) of compound **20b**.

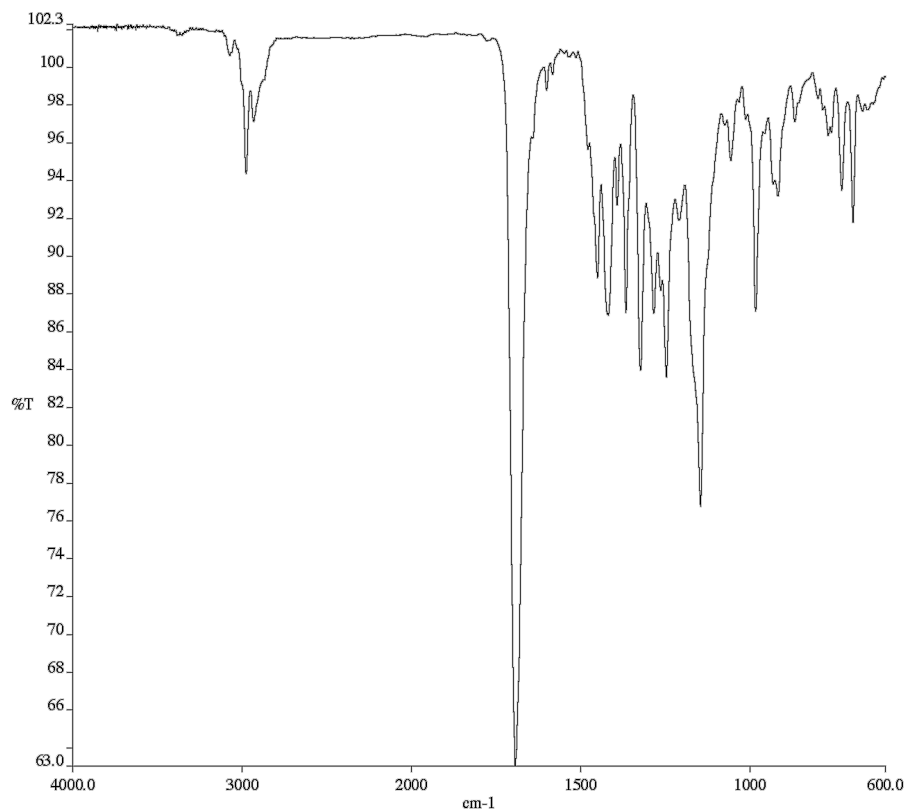


Figure A1.5. Infrared spectrum (Thin Film, NaCl) of compound **20b**.

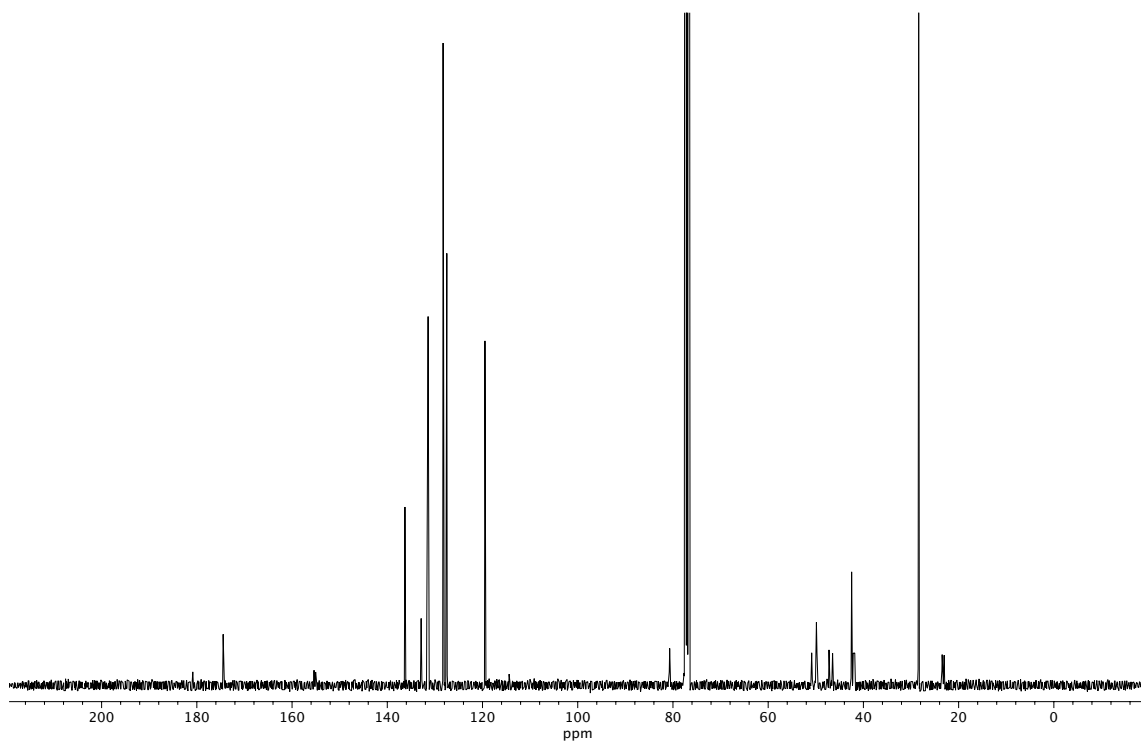
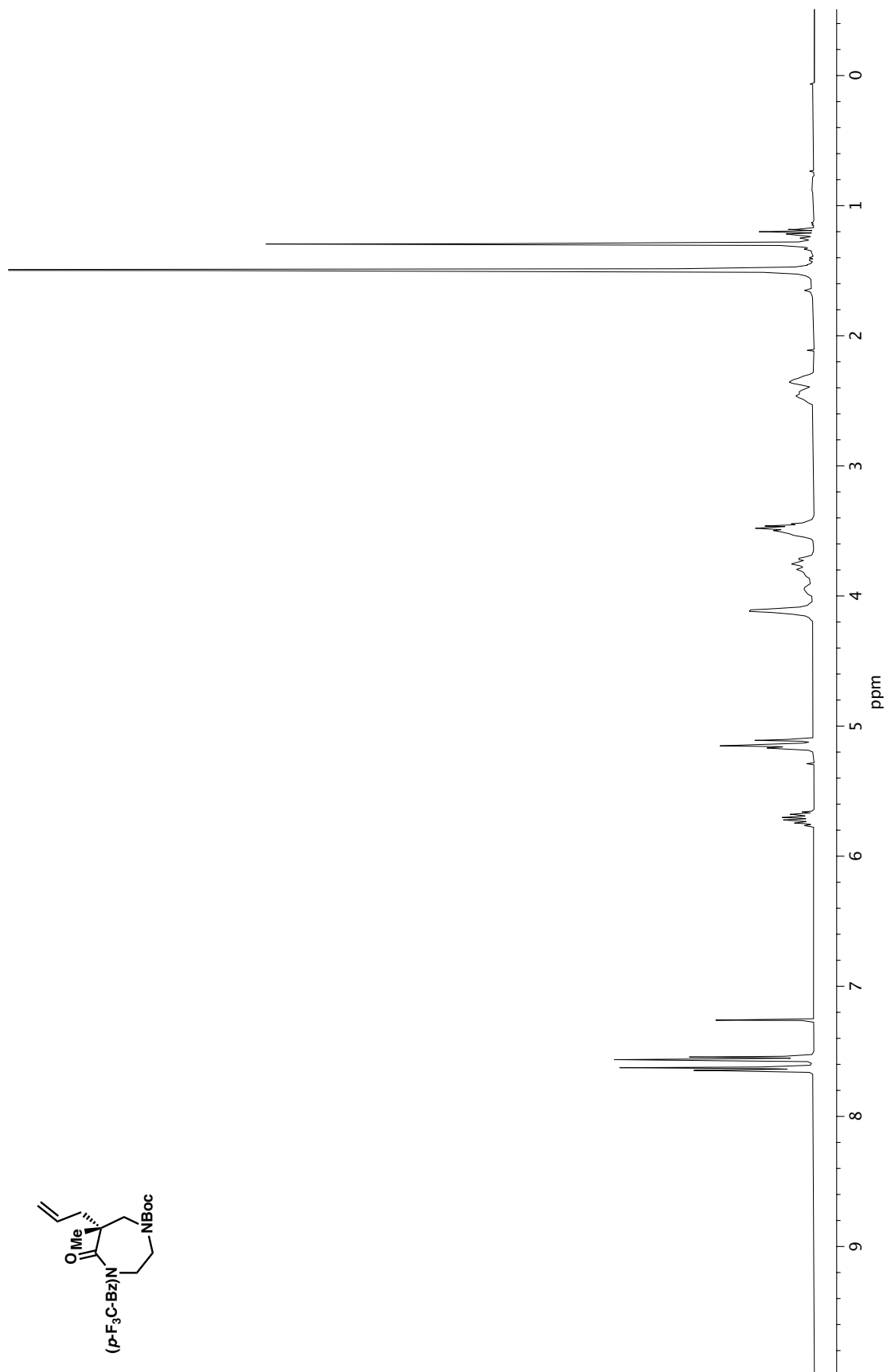


Figure A1.6. ¹³C NMR (100 MHz, CDCl₃) of compound **20b**.



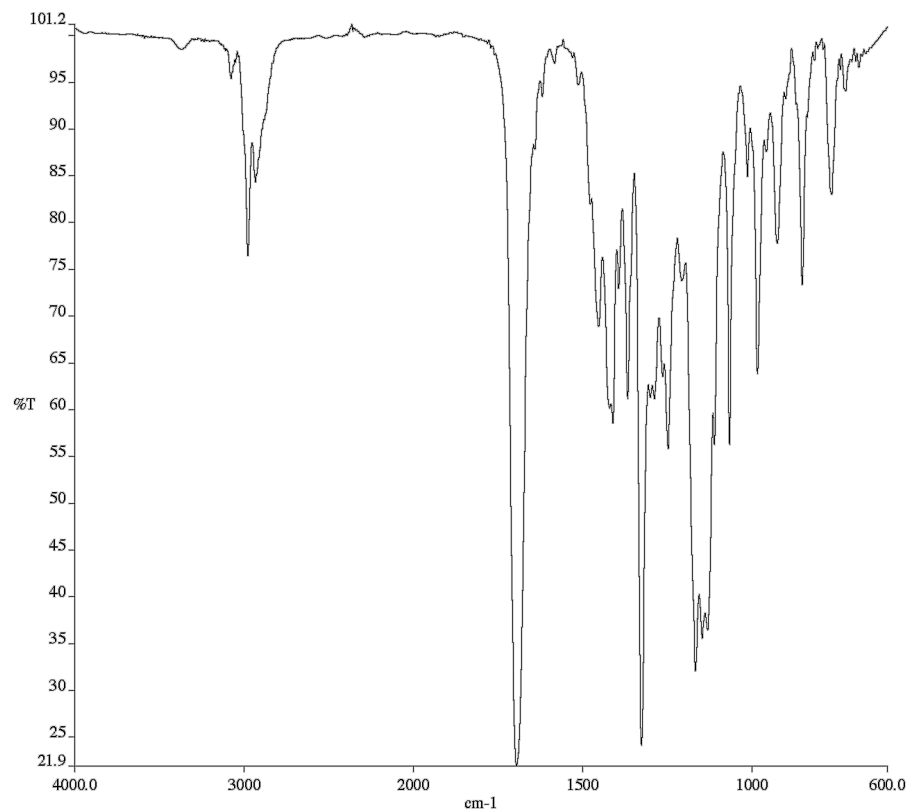


Figure A1.8. Infrared spectrum (Thin Film, NaCl) of compound **20c**.

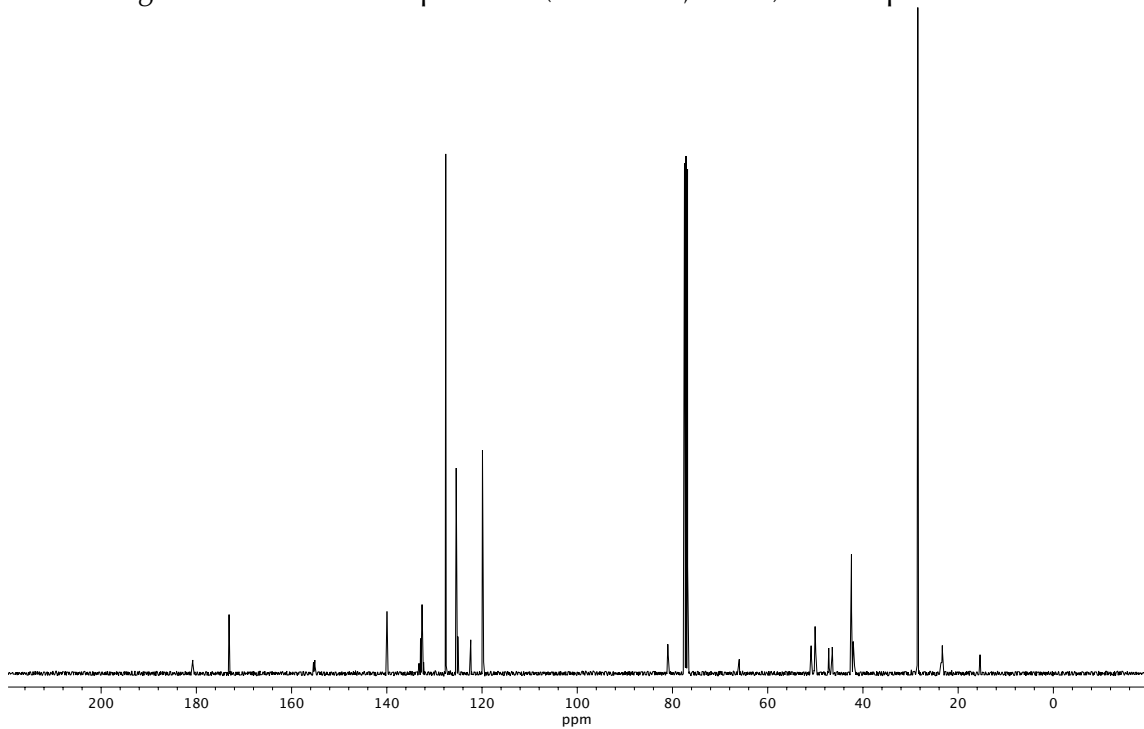
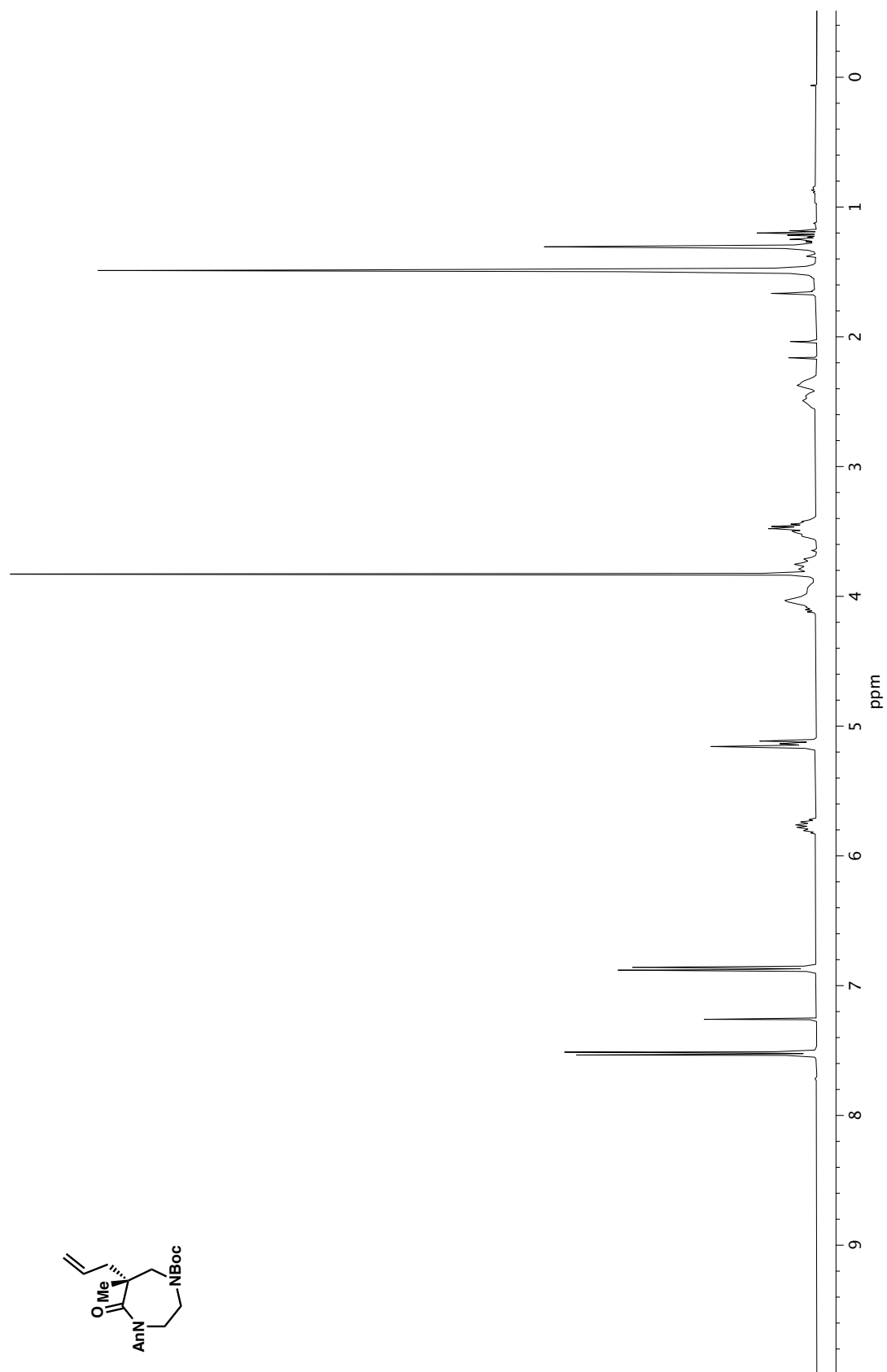


Figure A1.9. ¹³C NMR (100 MHz, CDCl₃) of compound **20c**.

Figure A1.10. ^1H NMR (400 MHz, CDCl_3) of compound **20d**.

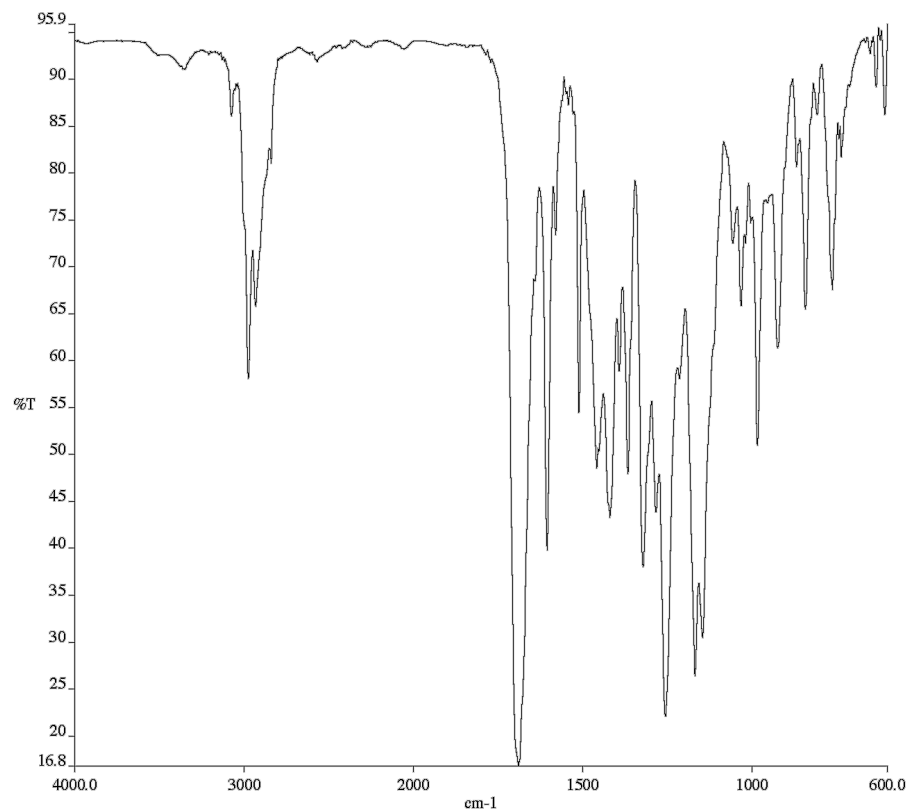


Figure A1.11. Infrared spectrum (Thin Film, NaCl) of compound **20d**.

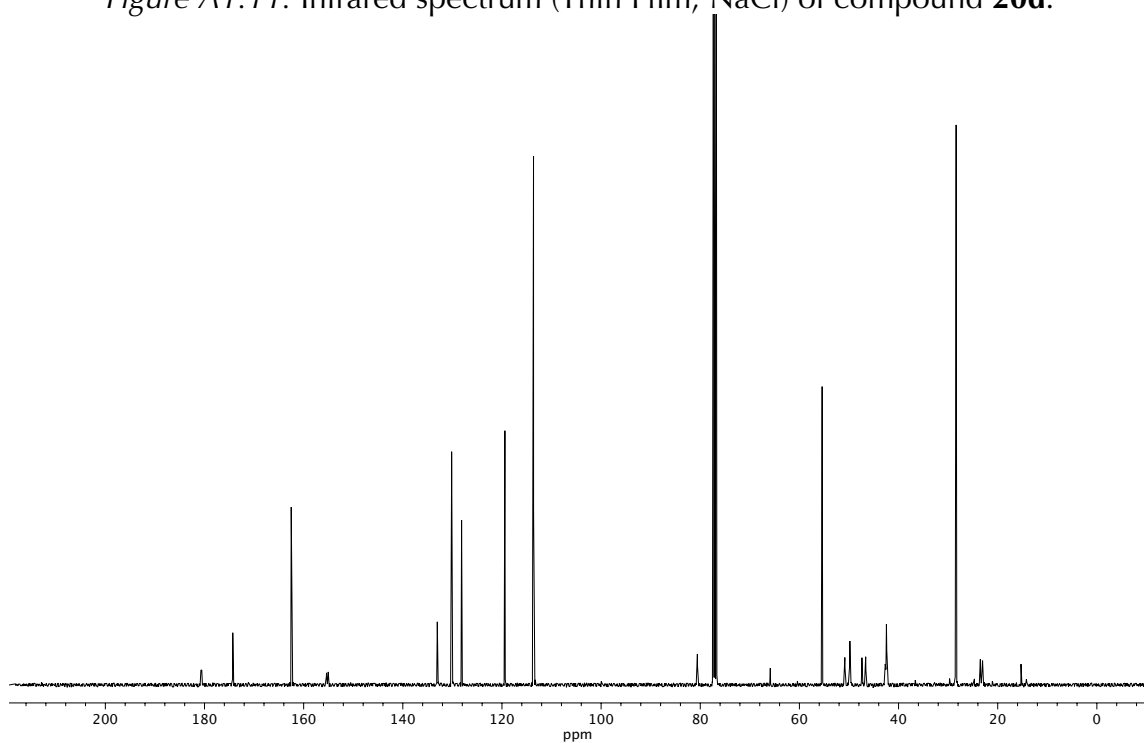
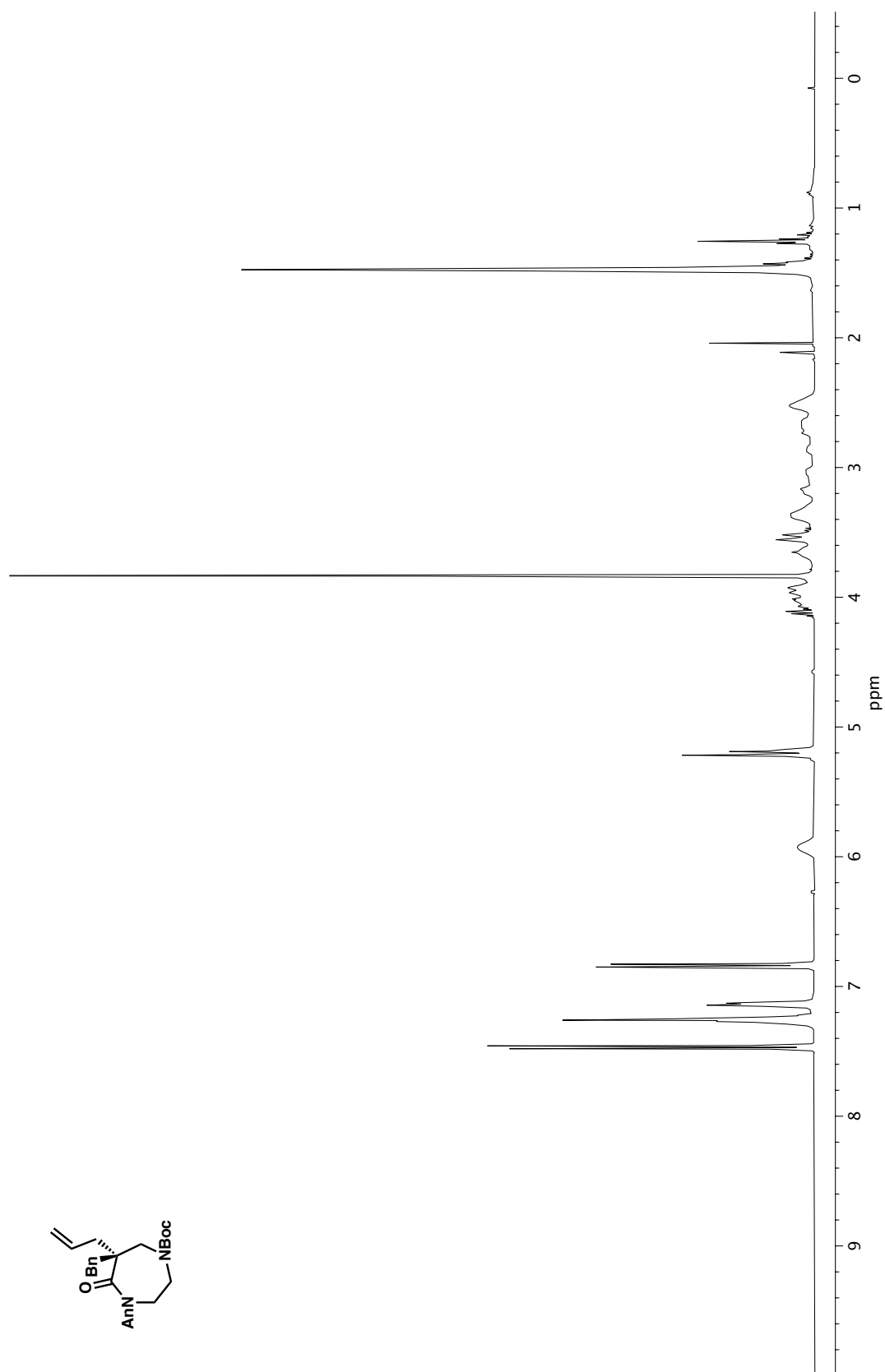


Figure A1.12. ¹³C NMR (100 MHz, CDCl₃) of compound **20d**.

Figure A1.13. ¹H NMR (400 MHz, CDCl₃) of compound **20e**.

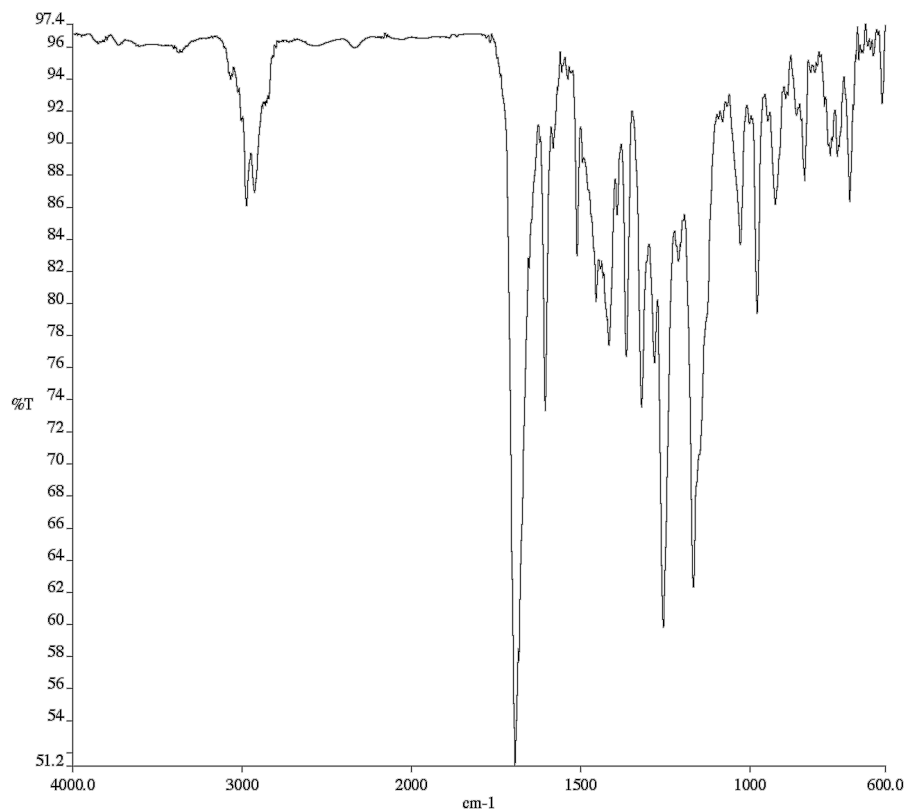


Figure A1.14. Infrared spectrum (Thin Film, NaCl) of compound **20e**.

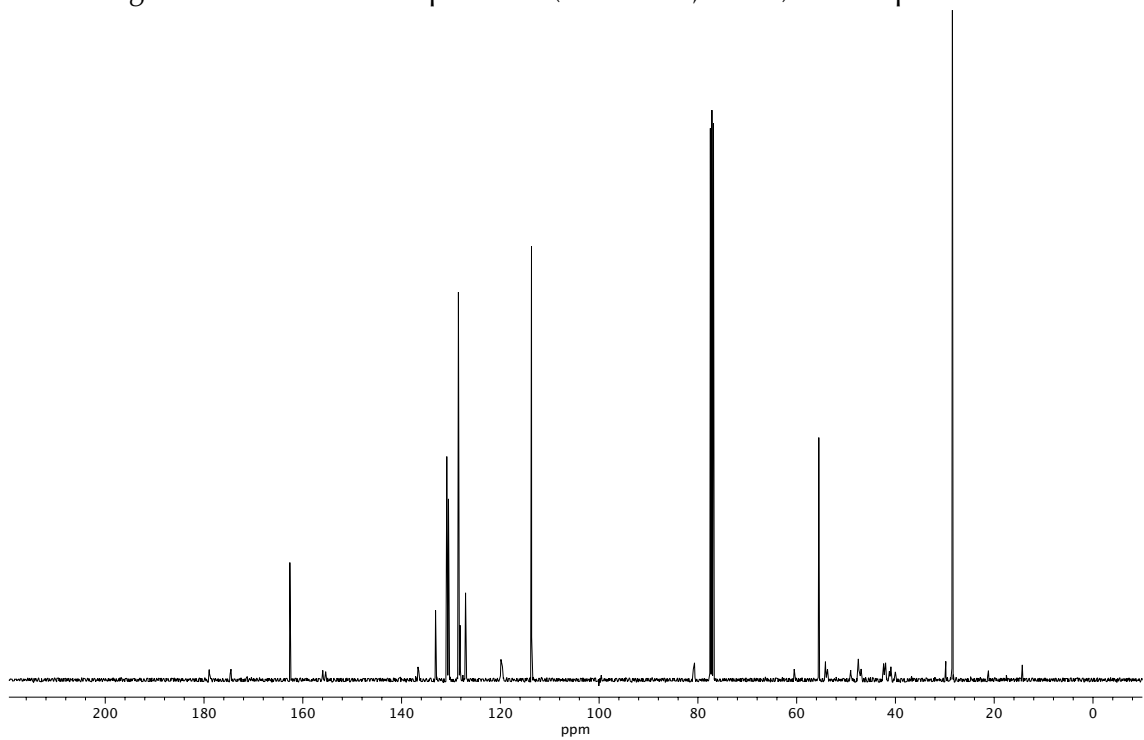
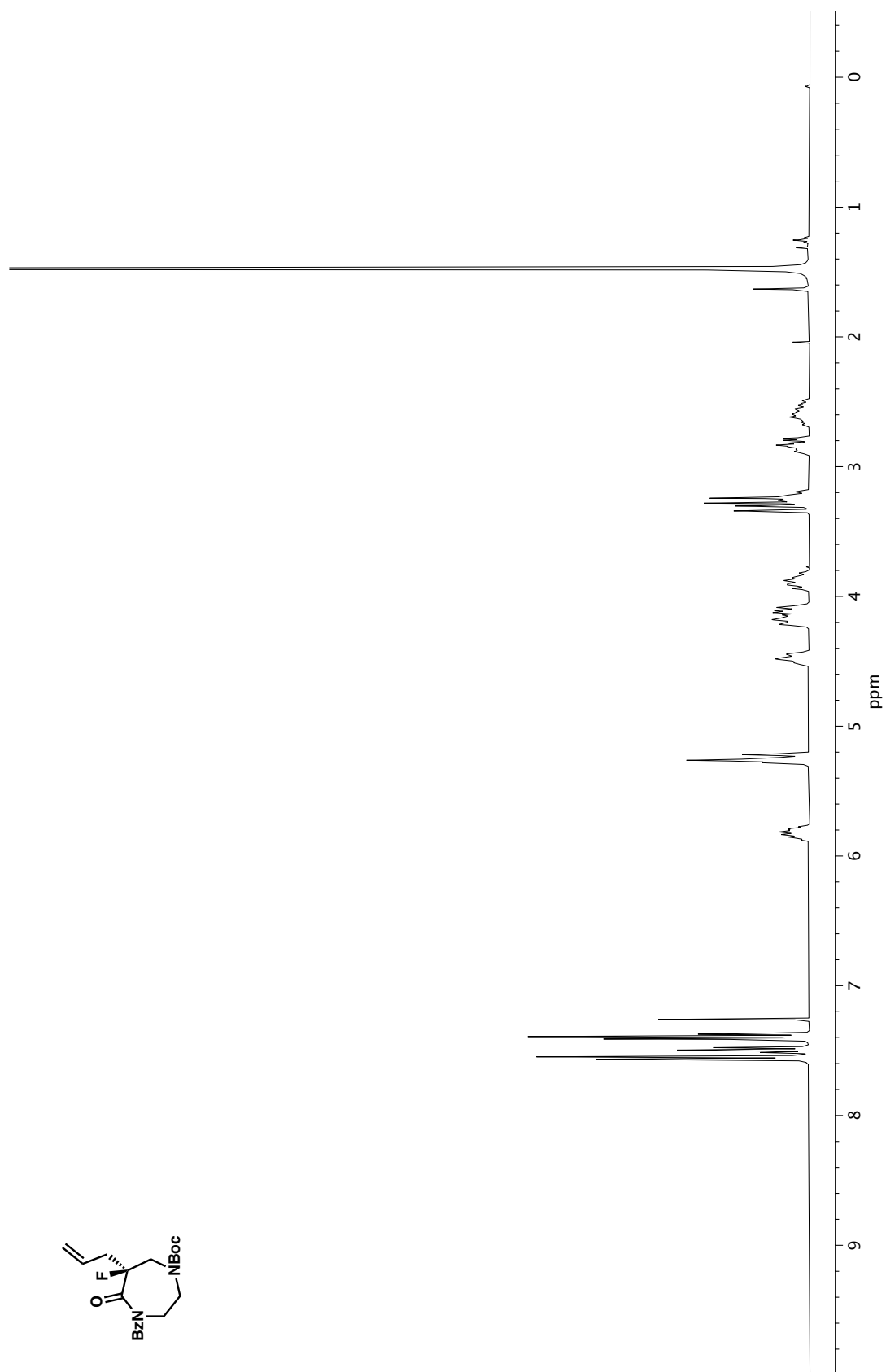


Figure A1.15. ¹³C NMR (100 MHz, CDCl₃) of compound **20e**.

Figure A1.16. ¹H NMR (400 MHz, CDCl₃) of compound 20f.

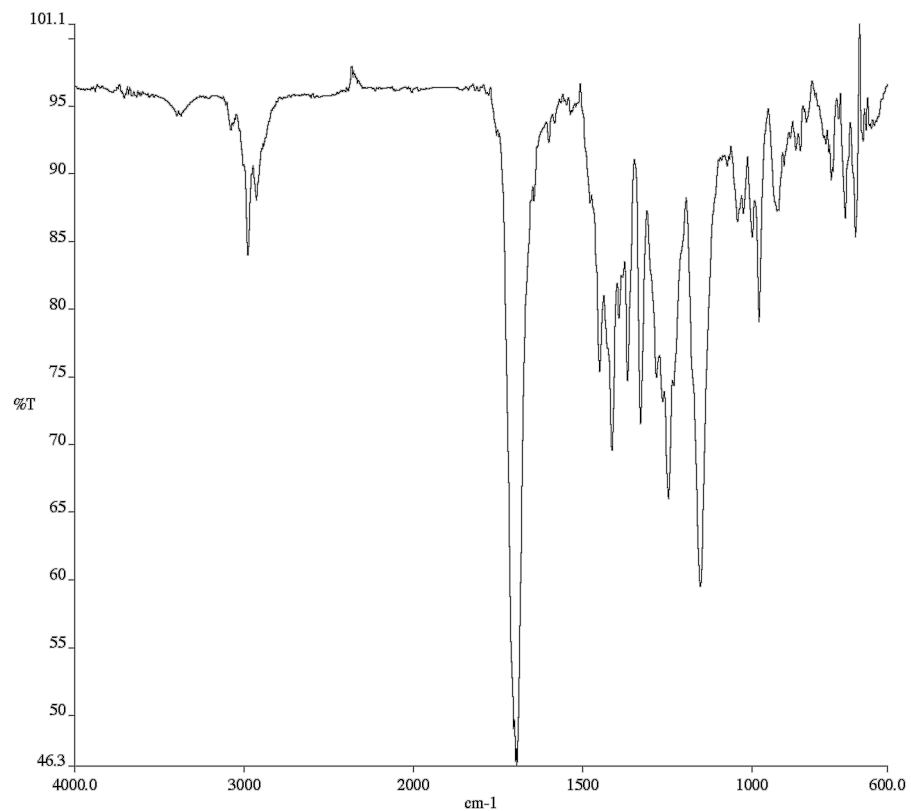


Figure A1.17. Infrared spectrum (Thin Film, NaCl) of compound **20f**.

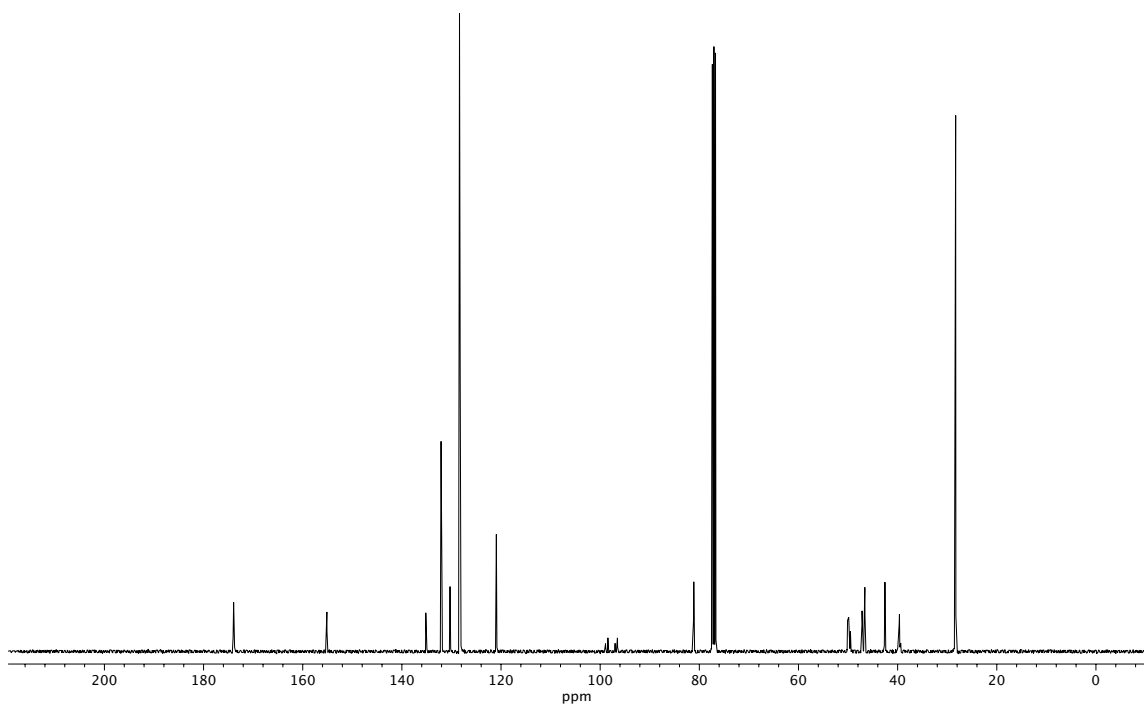
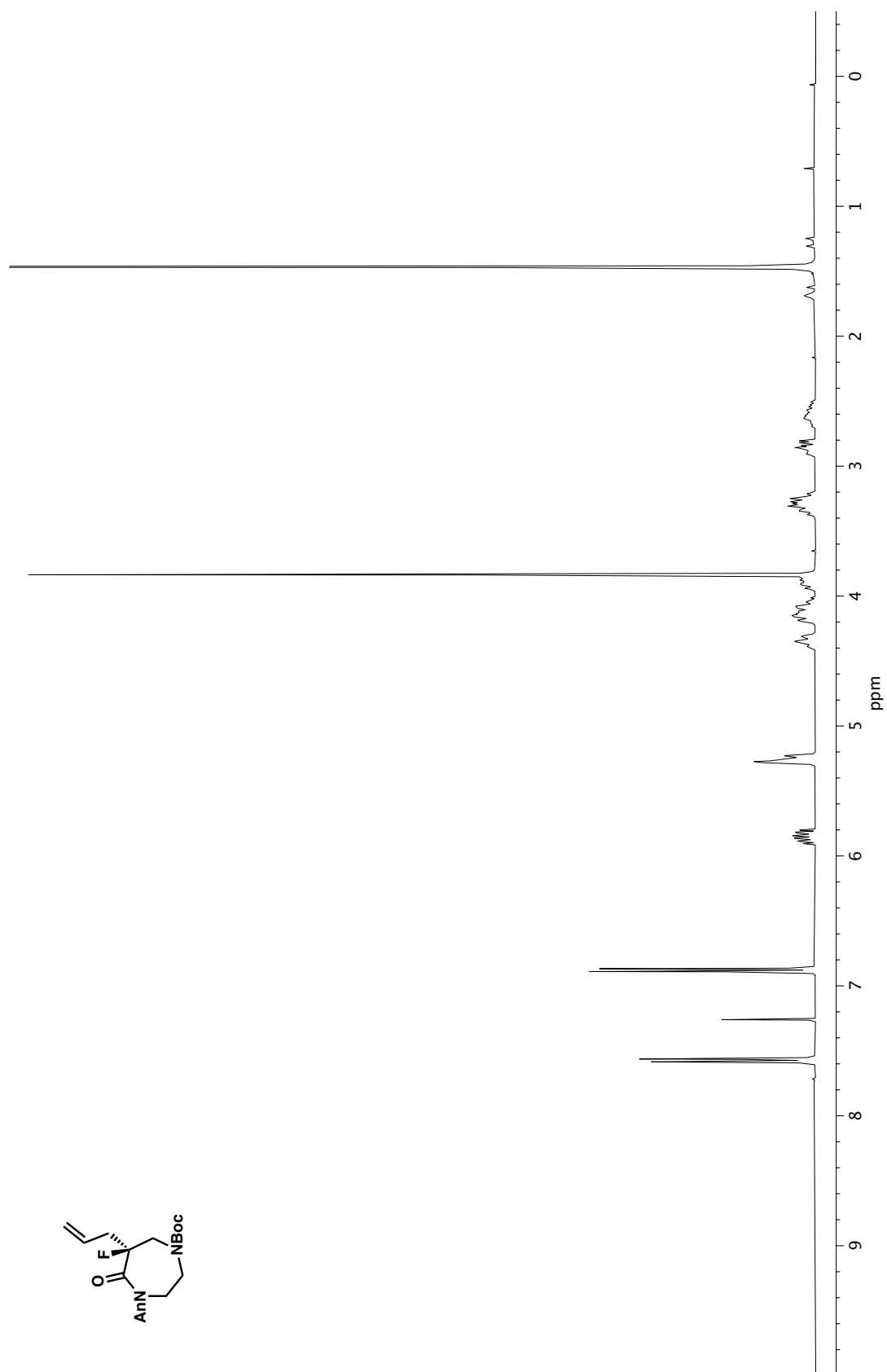


Figure A1.18. ¹³C NMR (100 MHz, CDCl₃) of compound **20f**.

Figure A1.19. ^1H NMR (400 MHz, CDCl_3) of compound **20g**.

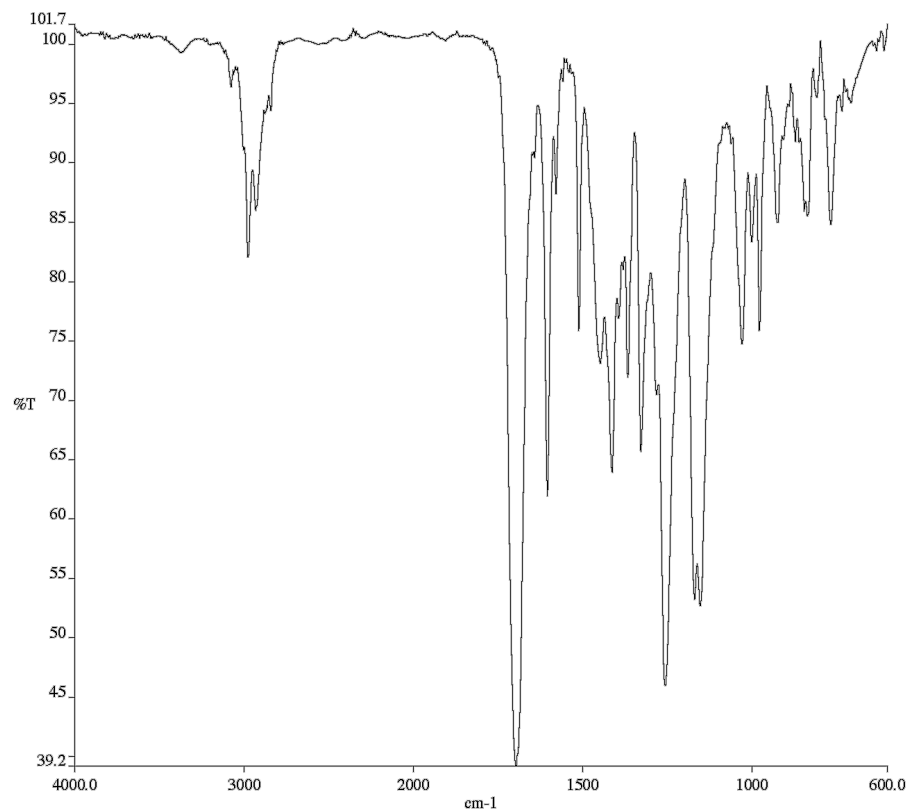


Figure A1.20. Infrared spectrum (Thin Film, NaCl) of compound **20g**.

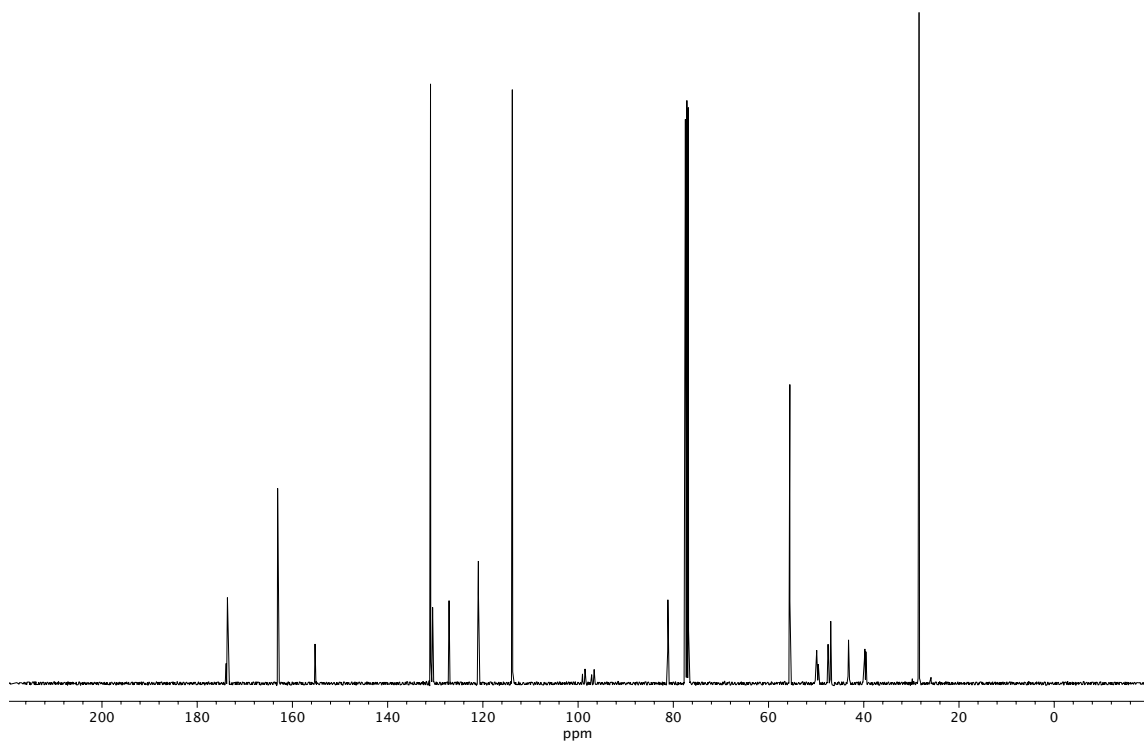


Figure A1.21. ¹³C NMR (100 MHz, CDCl₃) of compound **20g**.

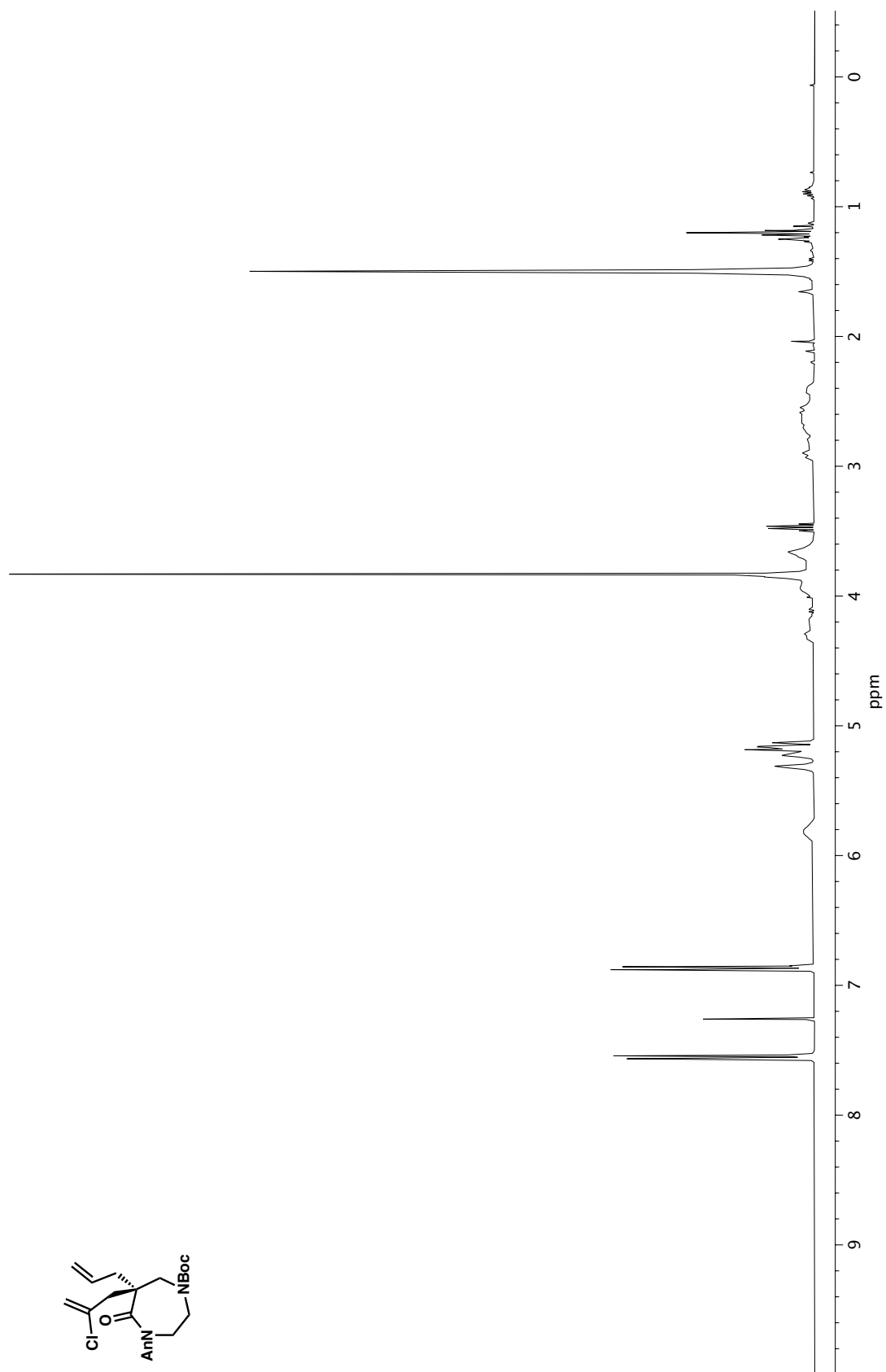


Figure A1.22. ^1H NMR (400 MHz, CDCl_3) of compound **20h**.

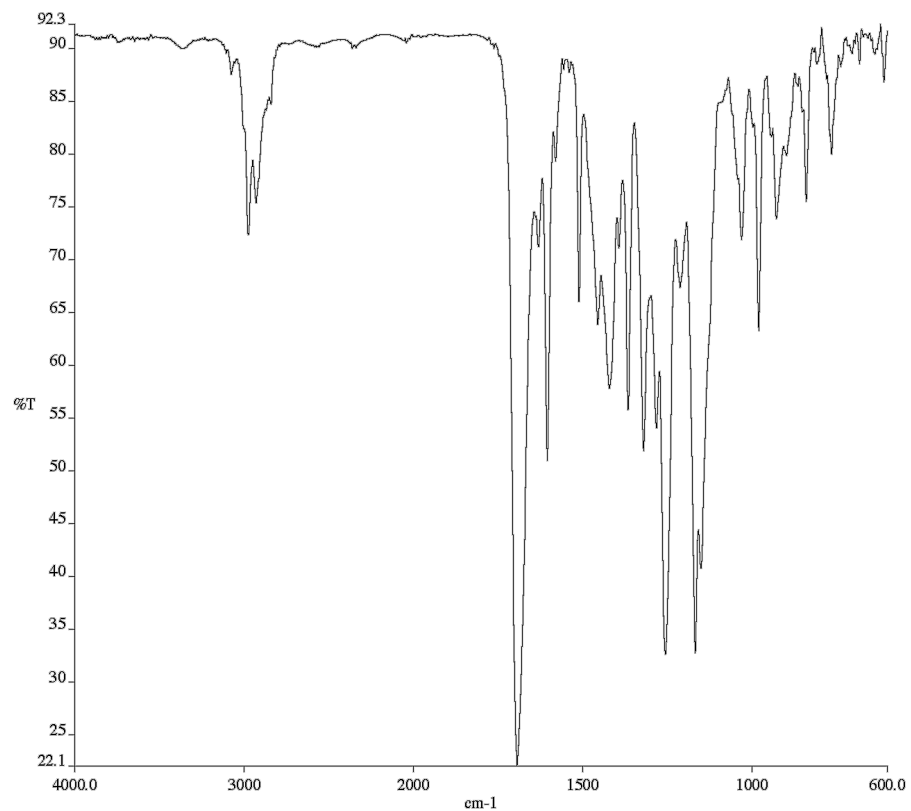


Figure A1.23. Infrared spectrum (Thin Film, NaCl) of compound **20h**.

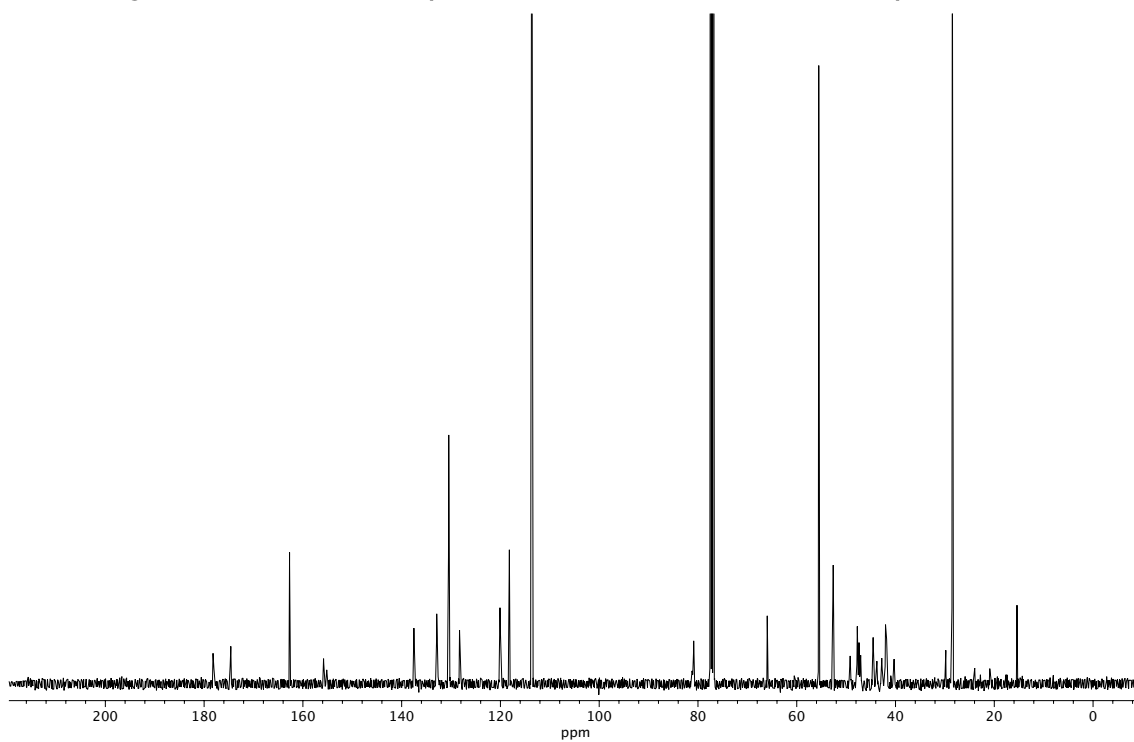
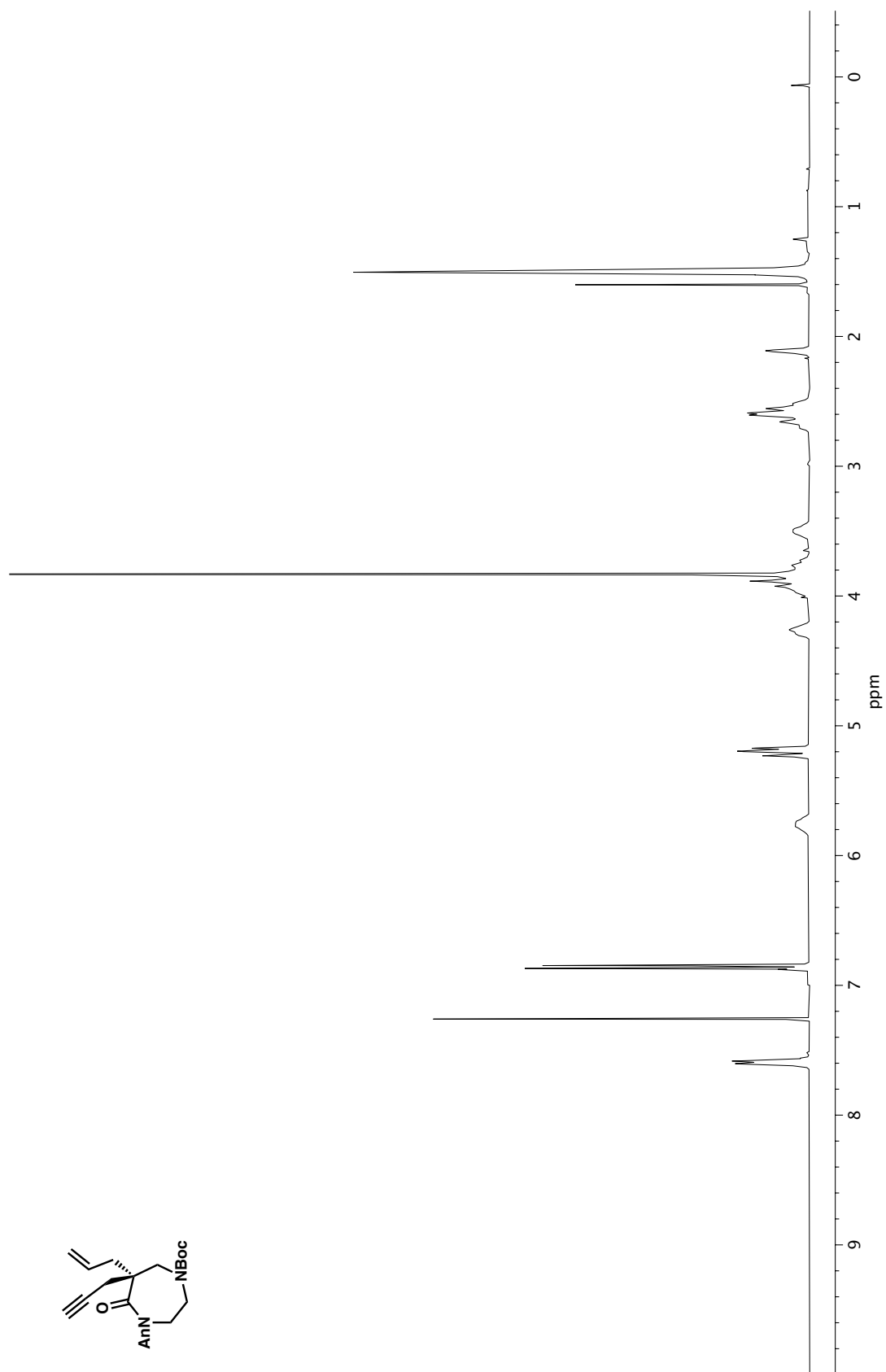


Figure A1.24. ¹³C NMR (100 MHz, CDCl₃) of compound **20h**.

Figure A1.25. ^1H NMR (400 MHz, CDCl_3) of compound **20i**.

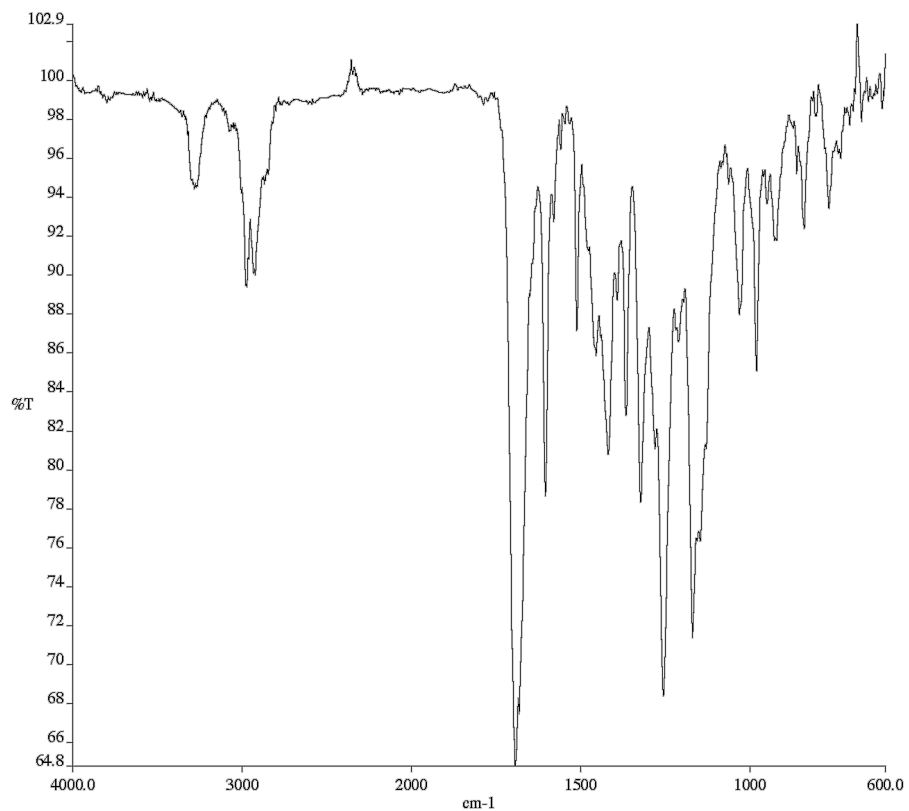


Figure A1.26. Infrared spectrum (Thin Film, NaCl) of compound **20i**.

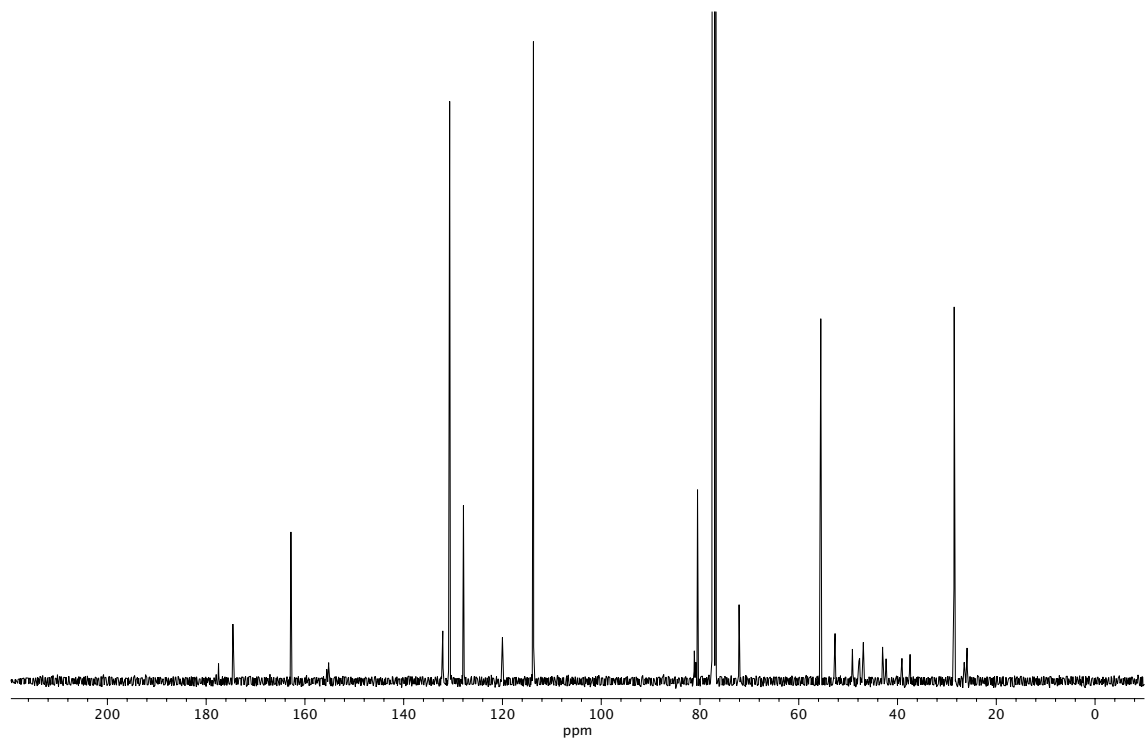
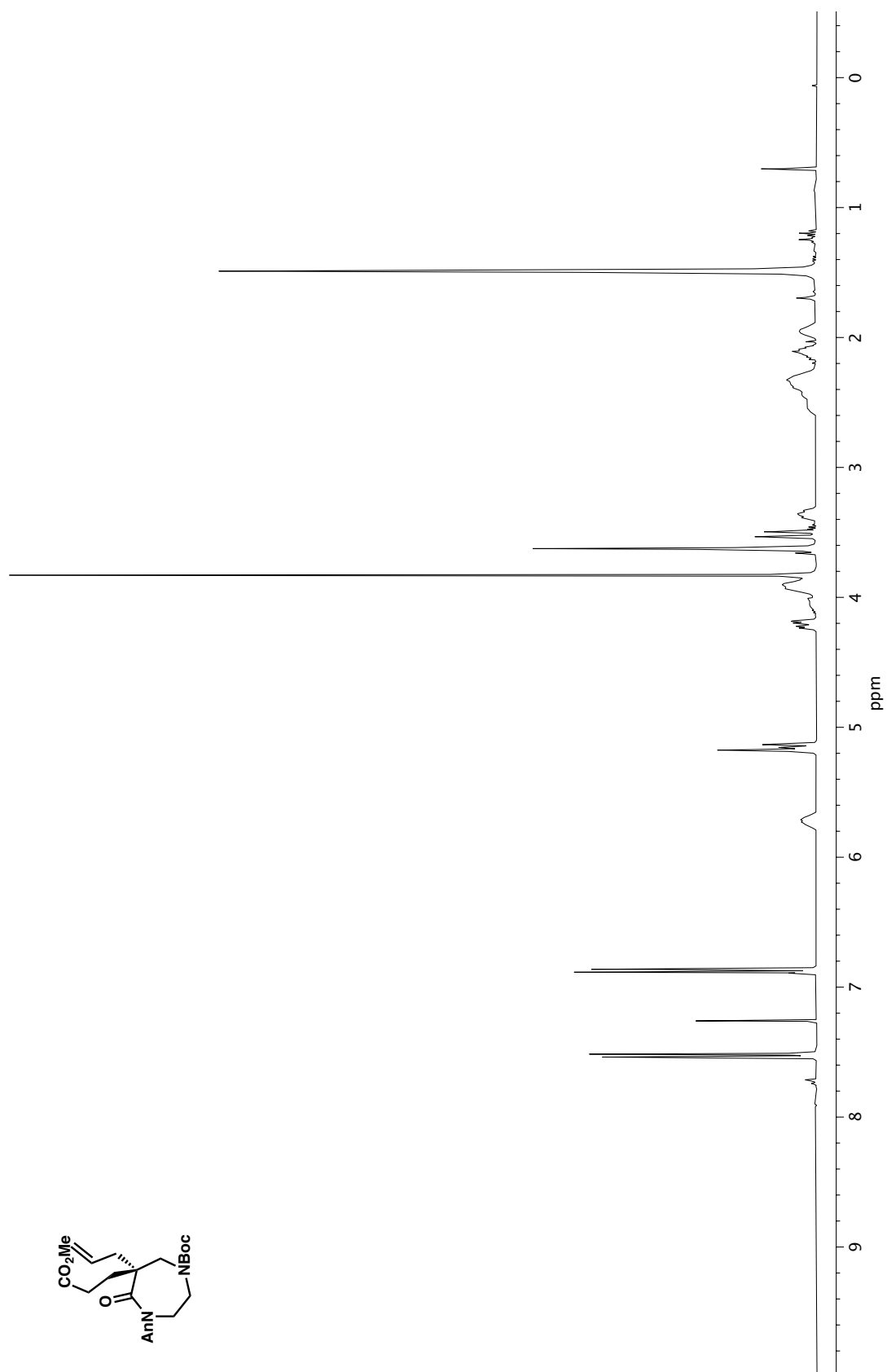


Figure A1.27. ¹³C NMR (100 MHz, CDCl₃) of compound **20i**.

Figure A1.28. ¹H NMR (400 MHz, CDCl₃) of compound 20j.

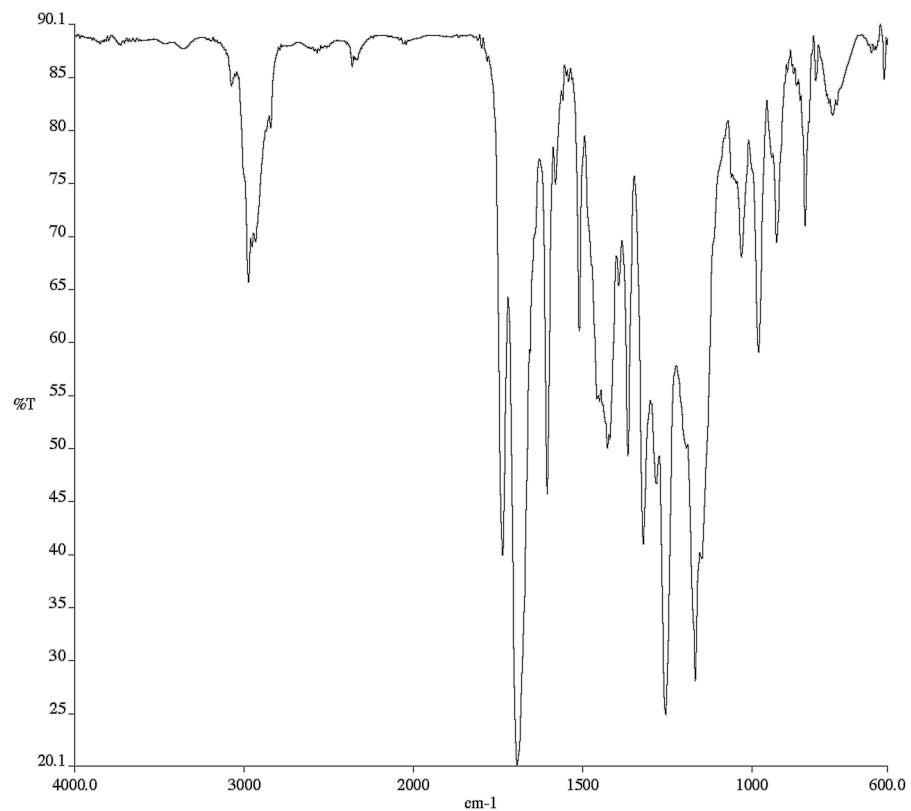


Figure A1.29. Infrared spectrum (Thin Film, NaCl) of compound **20j**.

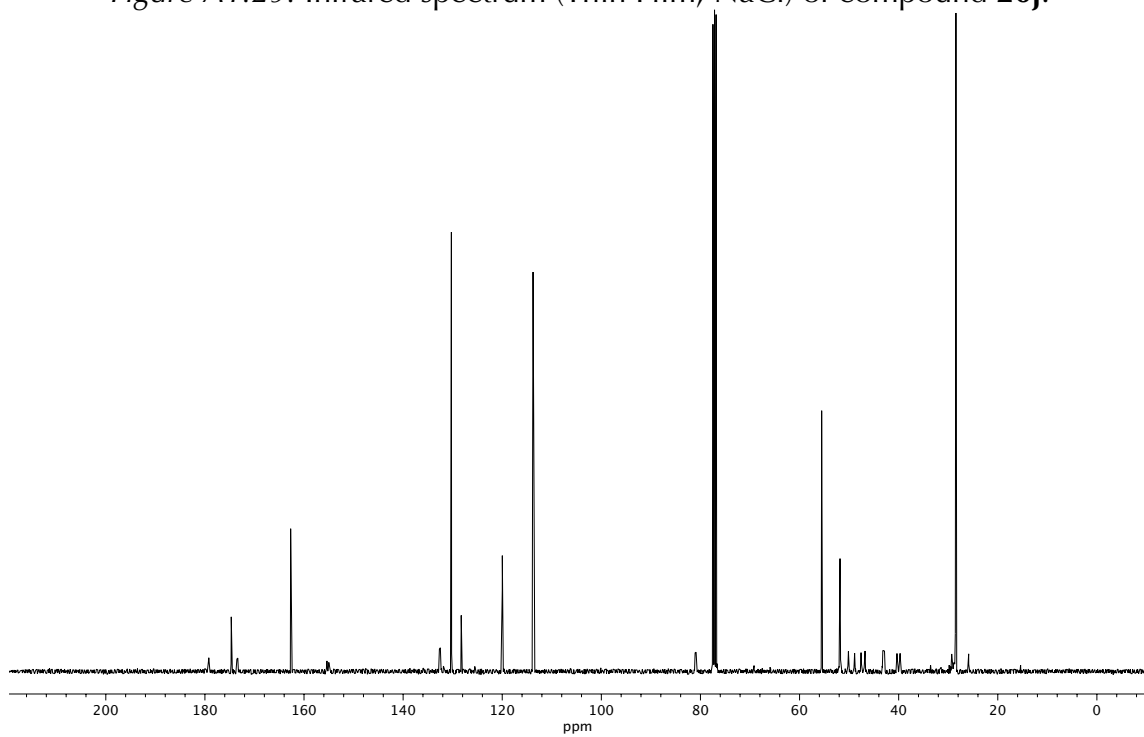


Figure A1.30. ¹³C NMR (100 MHz, CDCl₃) of compound **20j**.

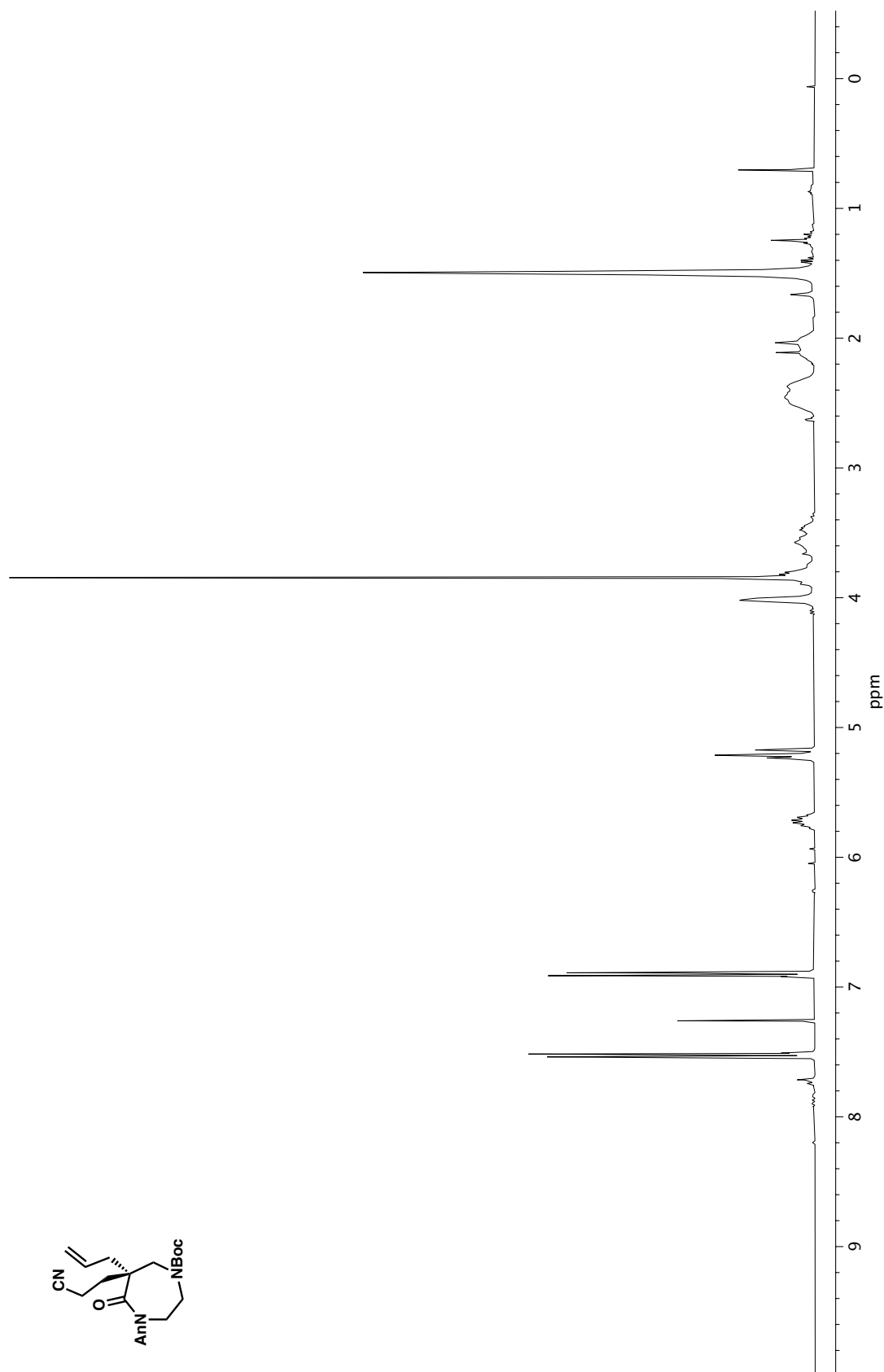


Figure A1.31. ^1H NMR (400 MHz, CDCl_3) of compound **20k**.

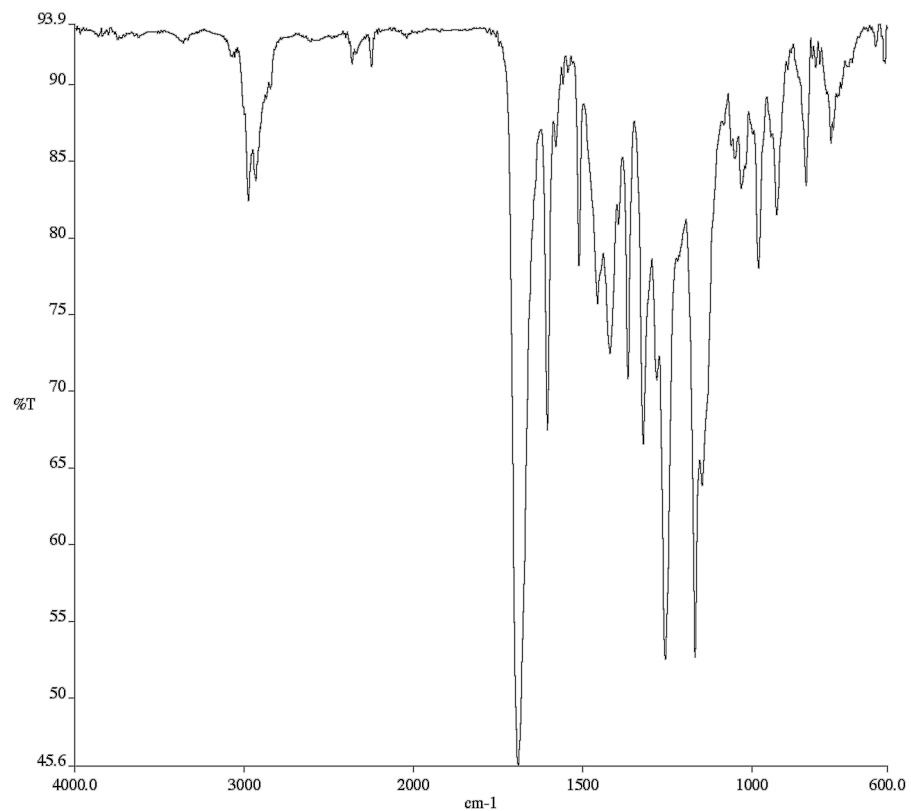


Figure A1.32. Infrared spectrum (Thin Film, NaCl) of compound **20k**.

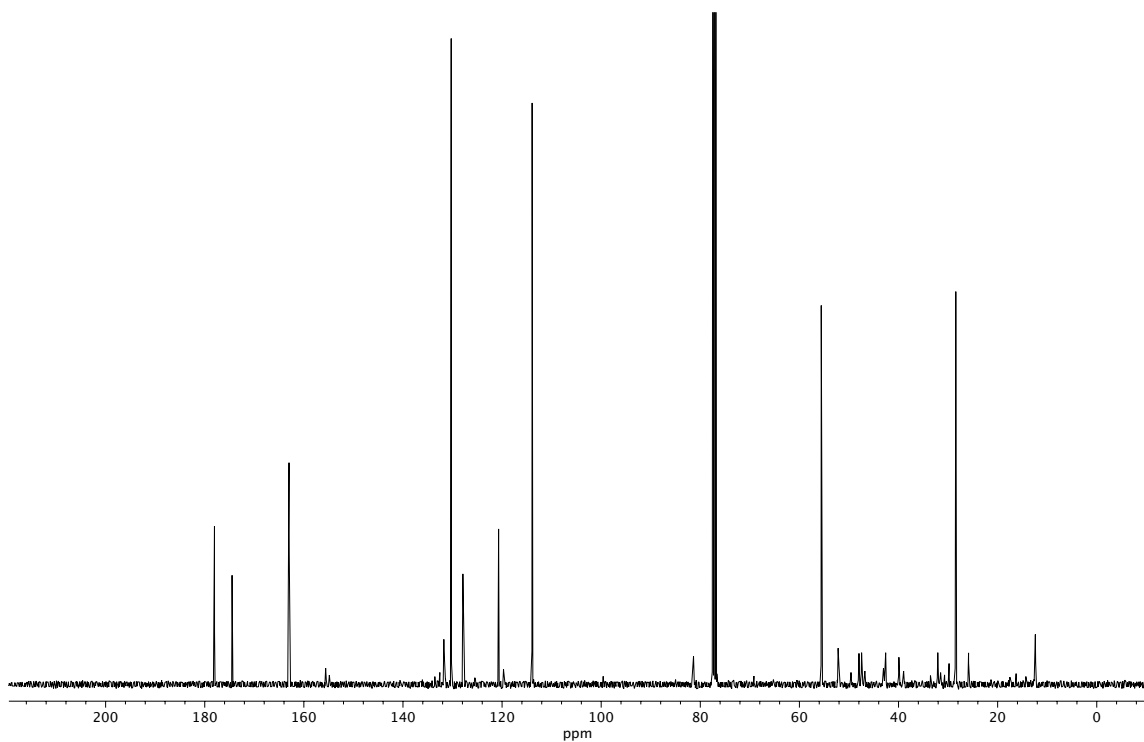


Figure A1.33. ¹³C NMR (100 MHz, CDCl₃) of compound **20k**.

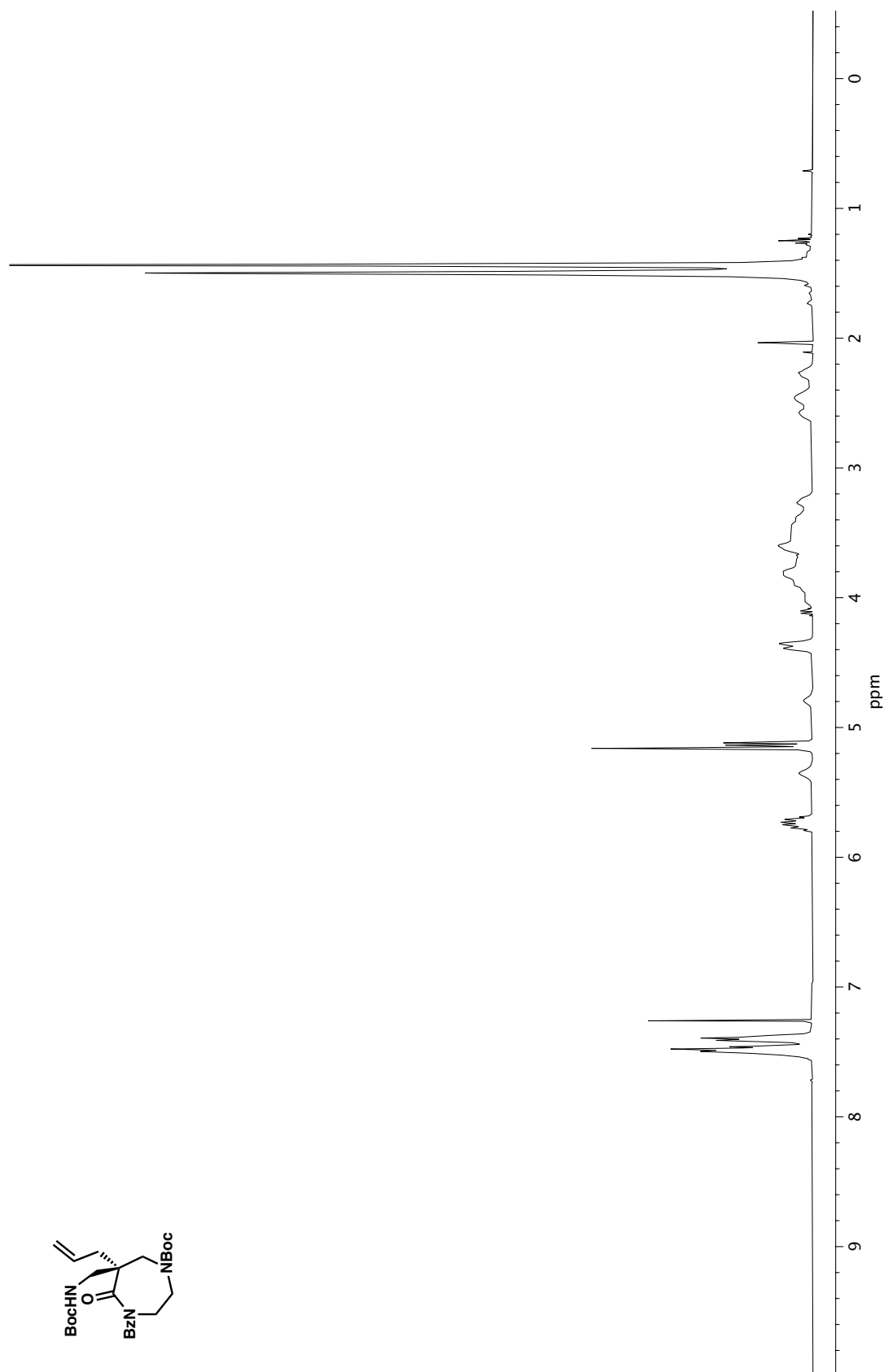


Figure A1.34. ¹H NMR (400 MHz, CDCl₃) of compound **20I**.

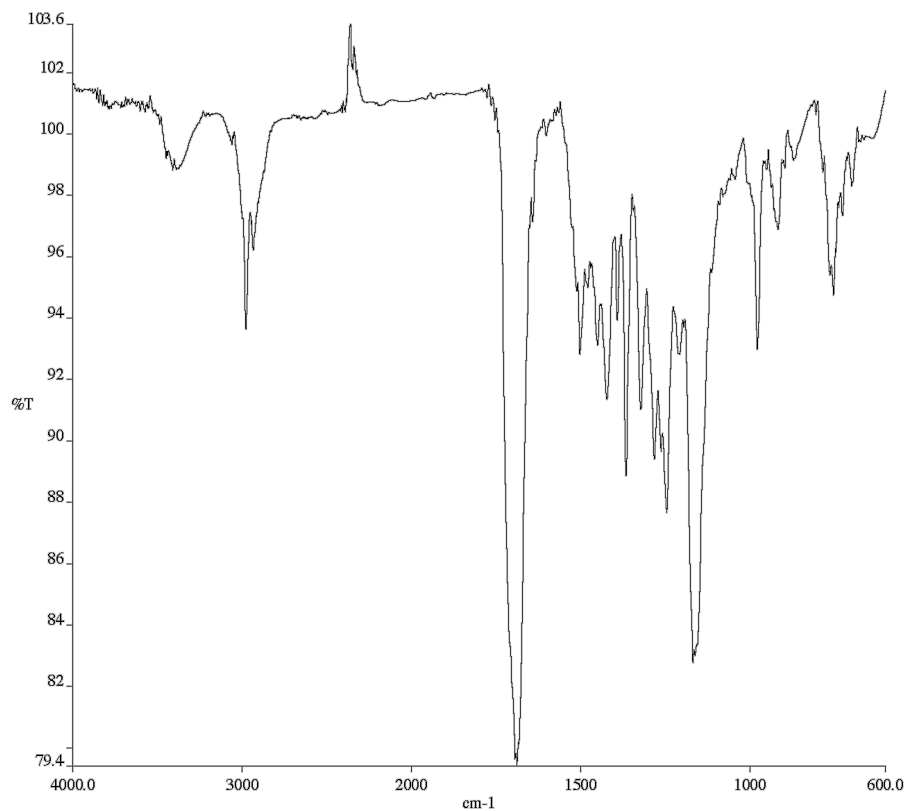


Figure A1.35. Infrared spectrum (Thin Film, NaCl) of compound **20I**.

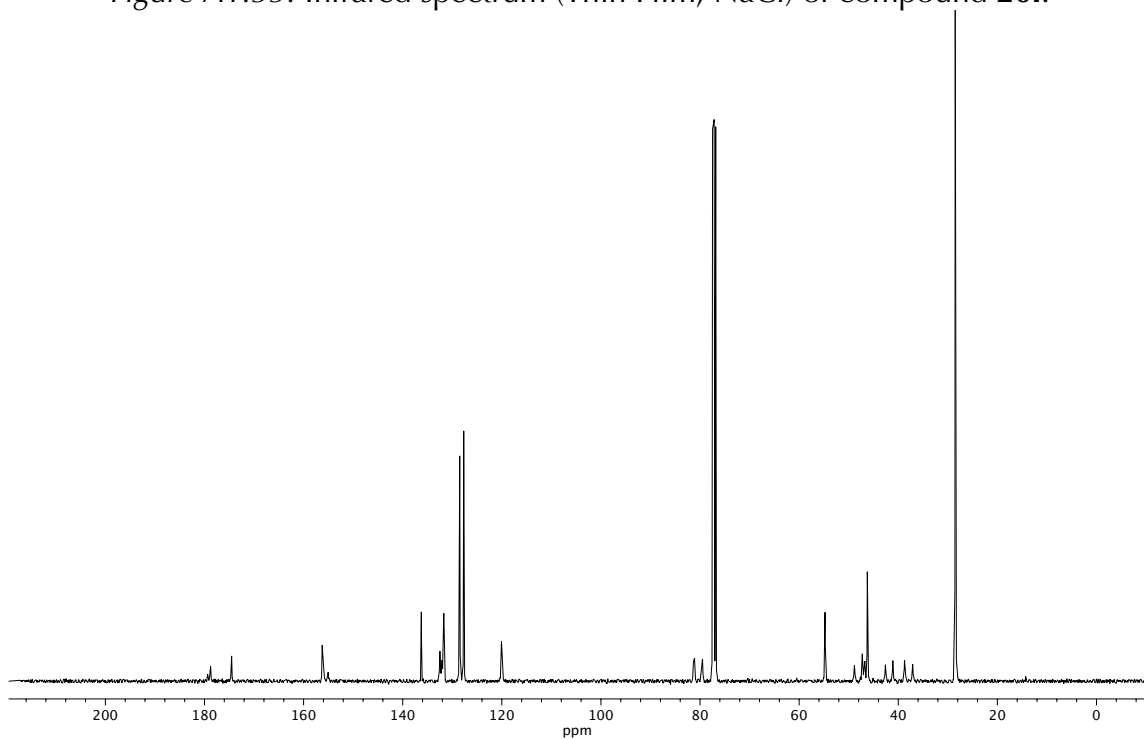


Figure A1.36. ¹³C NMR (100 MHz, CDCl₃) of compound **20I**.

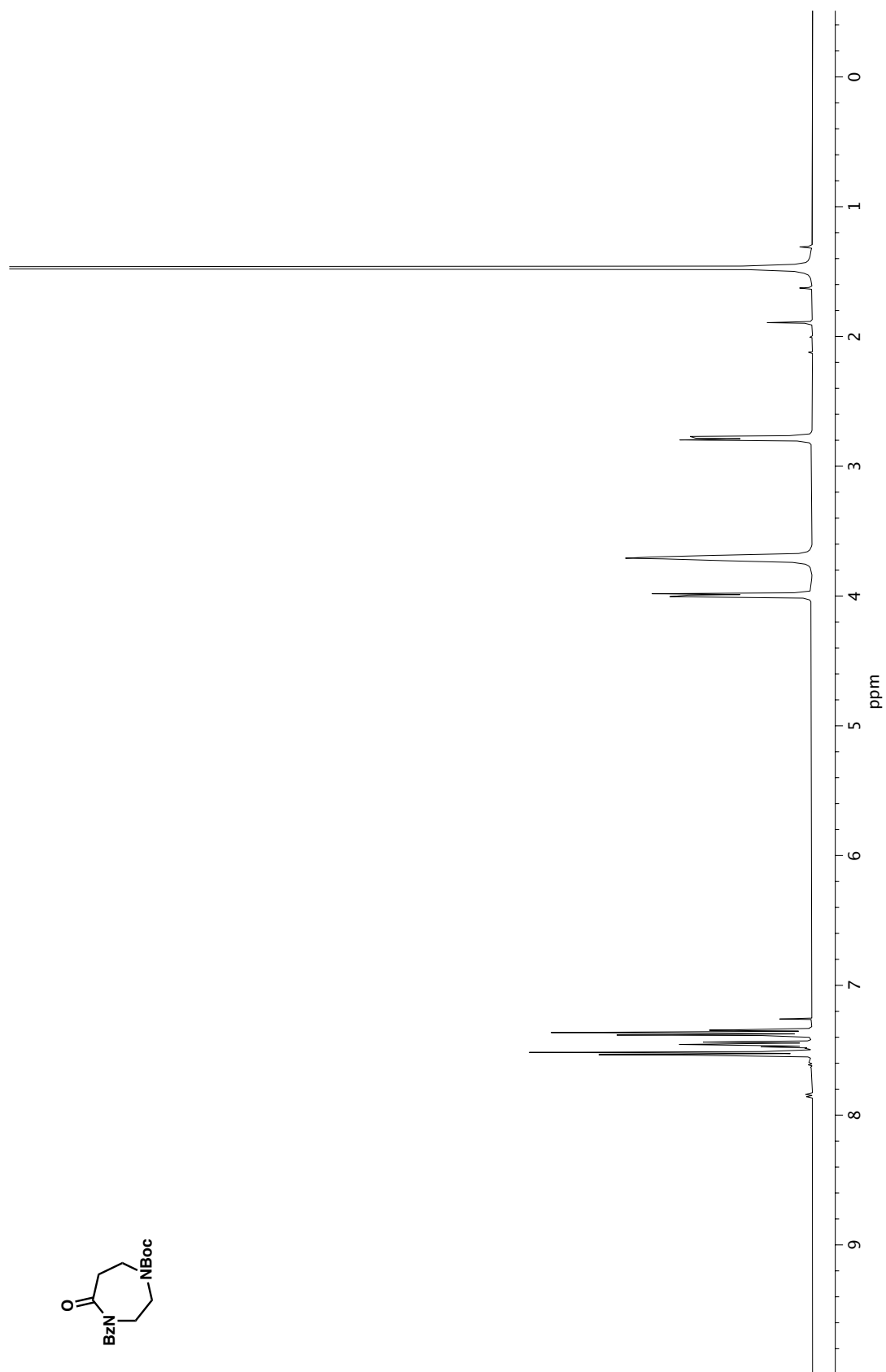


Figure A1.37. ¹H NMR (400 MHz, CDCl₃) of compound 55.

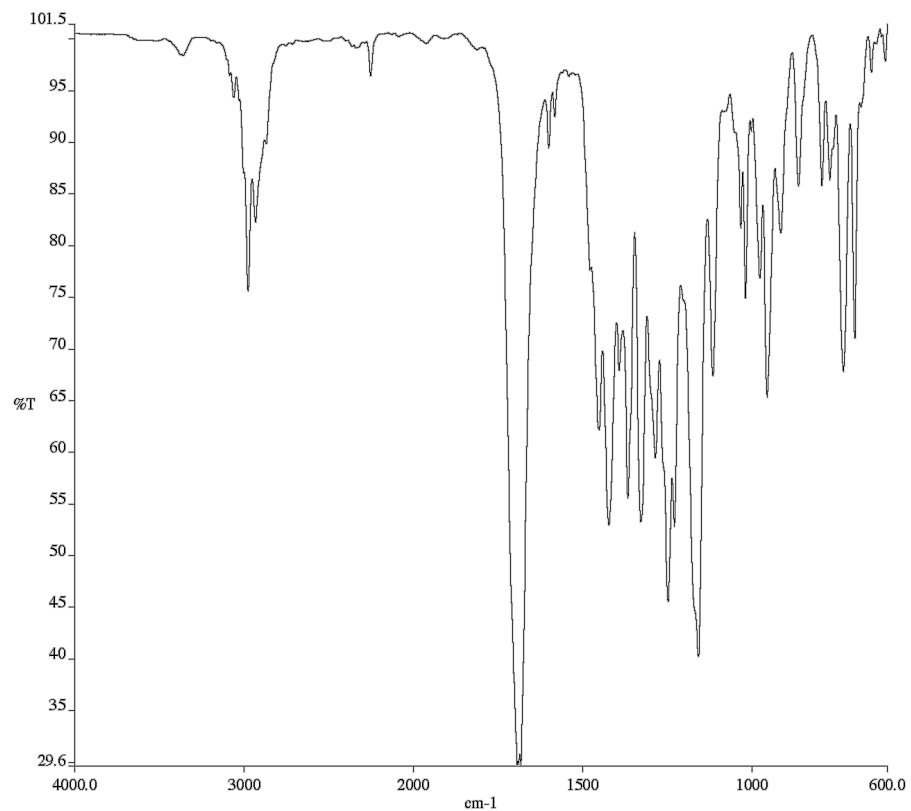


Figure A1.38. Infrared spectrum (Thin Film, NaCl) of compound **55**.

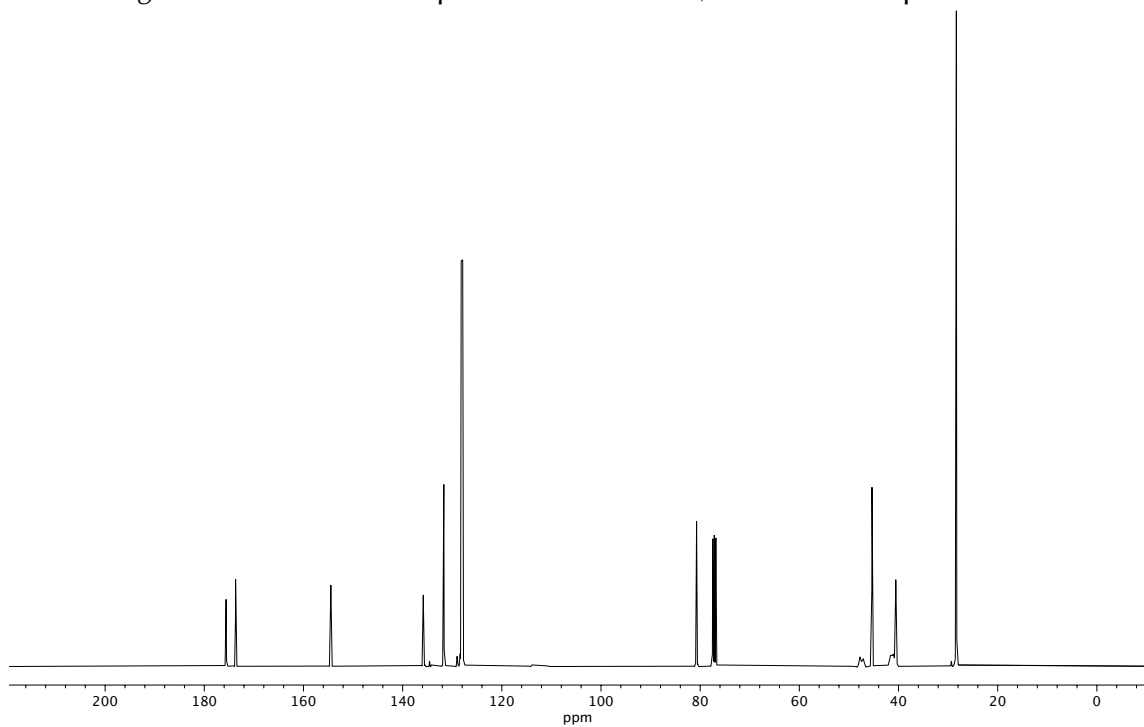


Figure A1.39. ¹³C NMR (100 MHz, CDCl₃) of compound **55**.

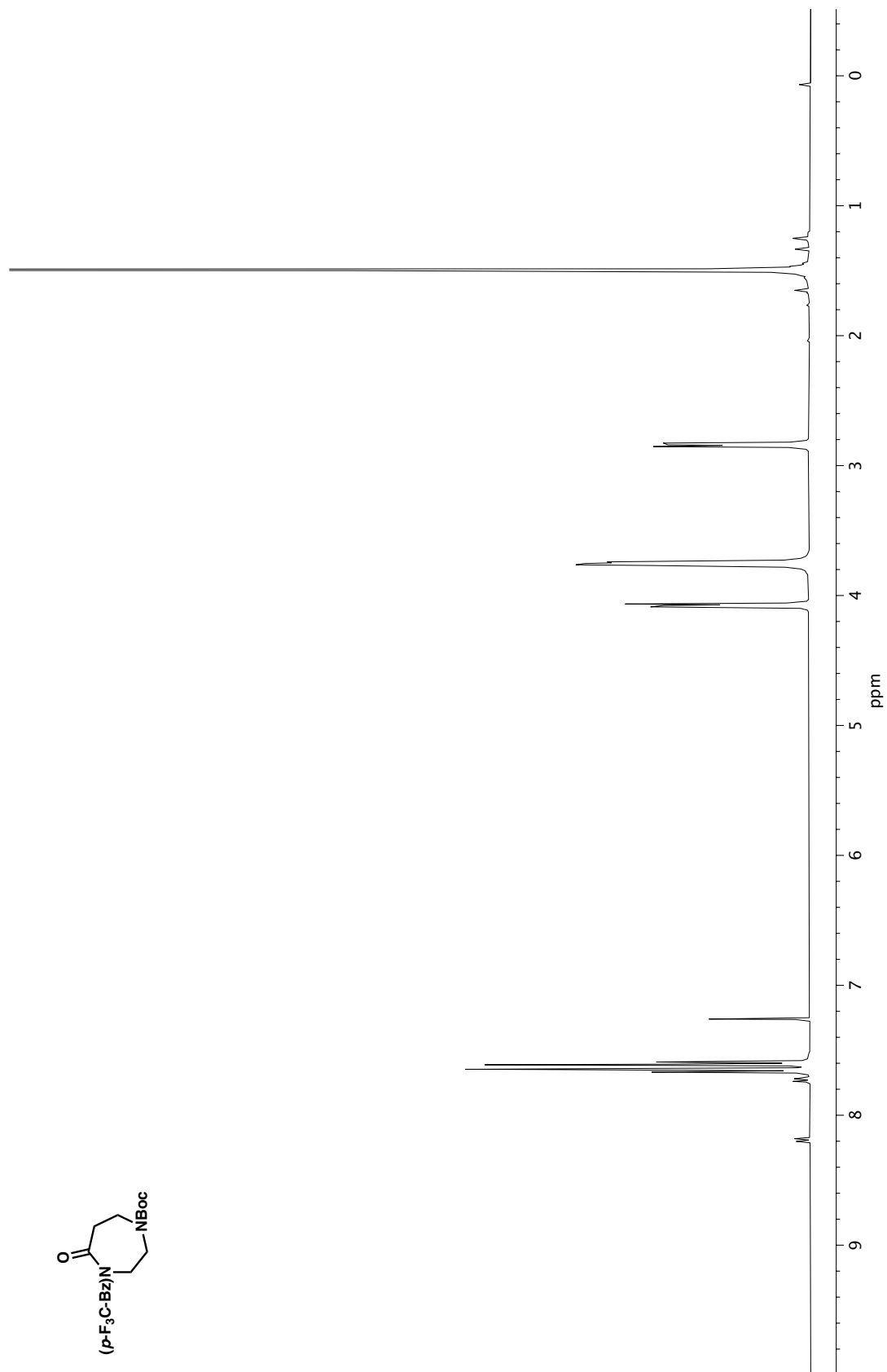


Figure A1.40. ¹H NMR (400 MHz, CDCl₃) of compound 56.

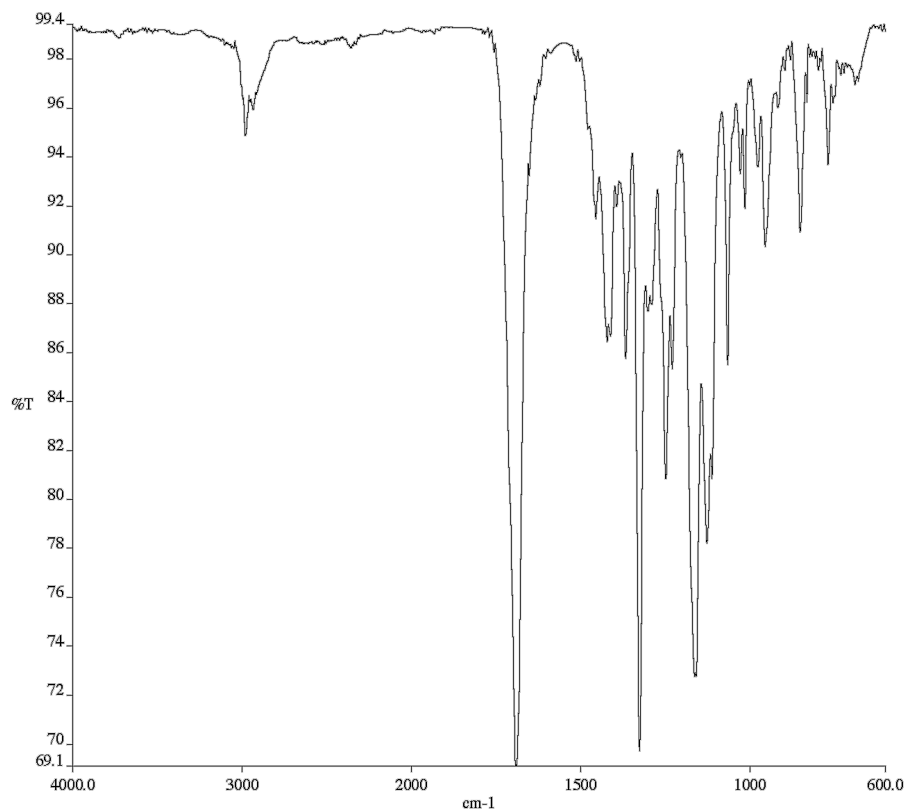


Figure A1.41. Infrared spectrum (Thin Film, NaCl) of compound **56**.

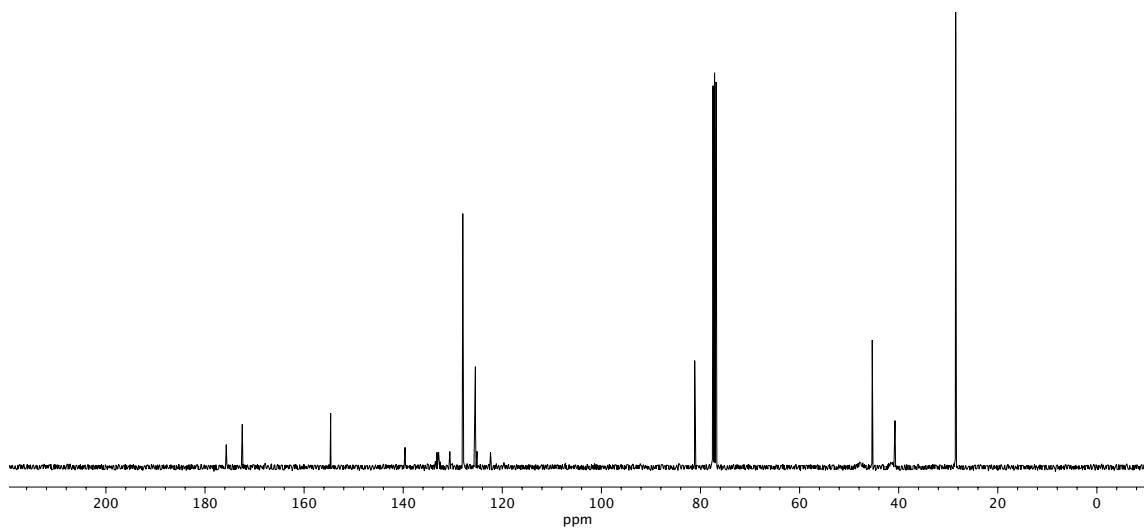
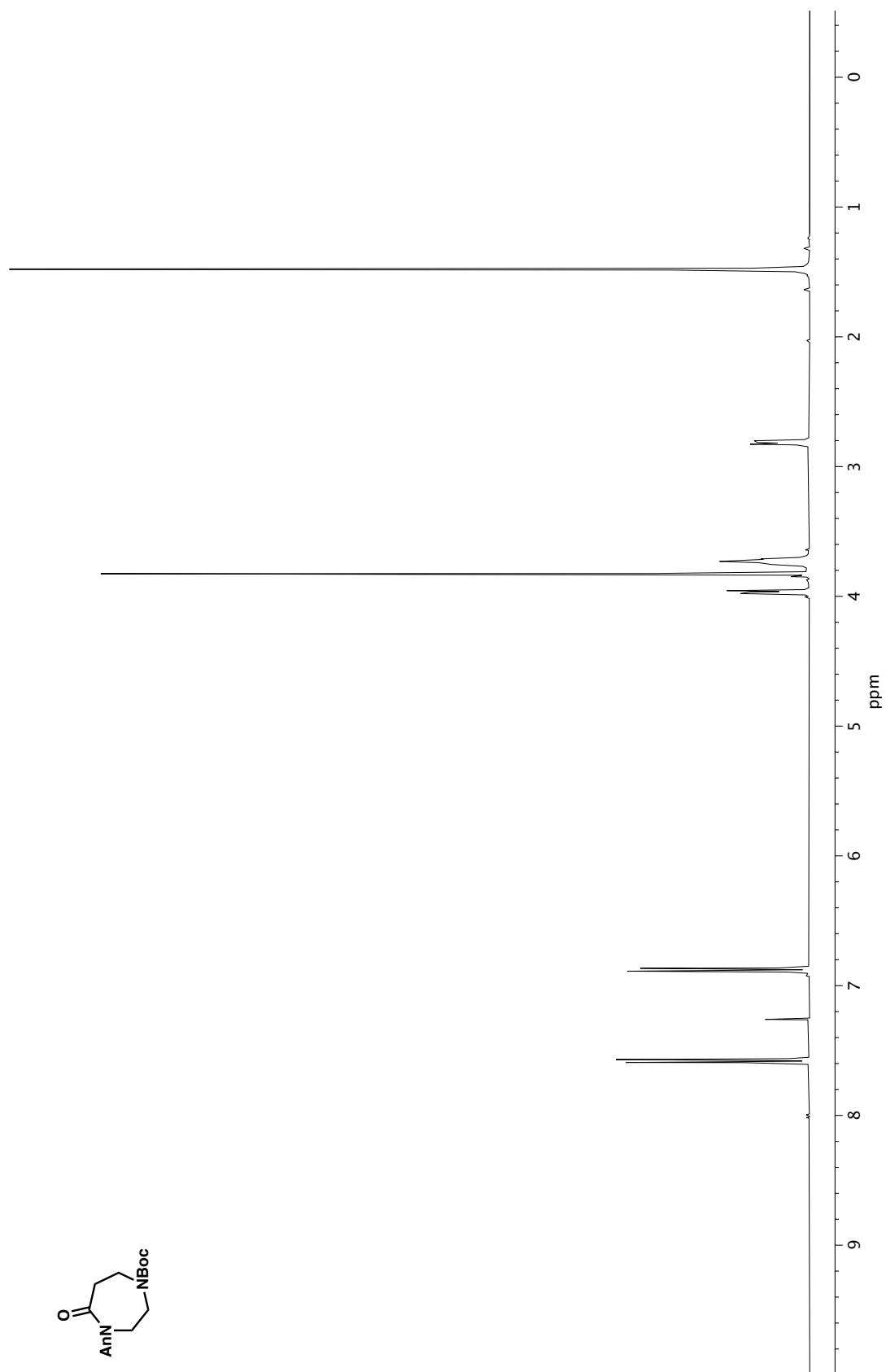


Figure A1.42. ¹³C NMR (100 MHz, CDCl₃) of compound **56**.

Figure A1.43. ¹H NMR (400 MHz, CDCl₃) of compound 57.

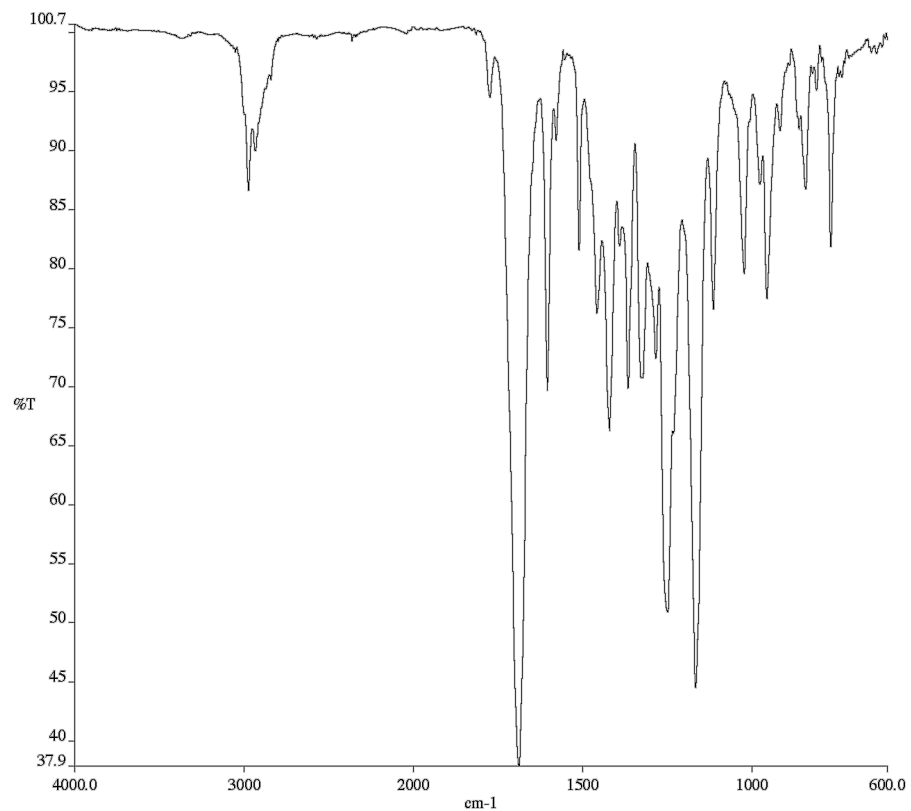


Figure A1.44. Infrared spectrum (Thin Film, NaCl) of compound **57**.

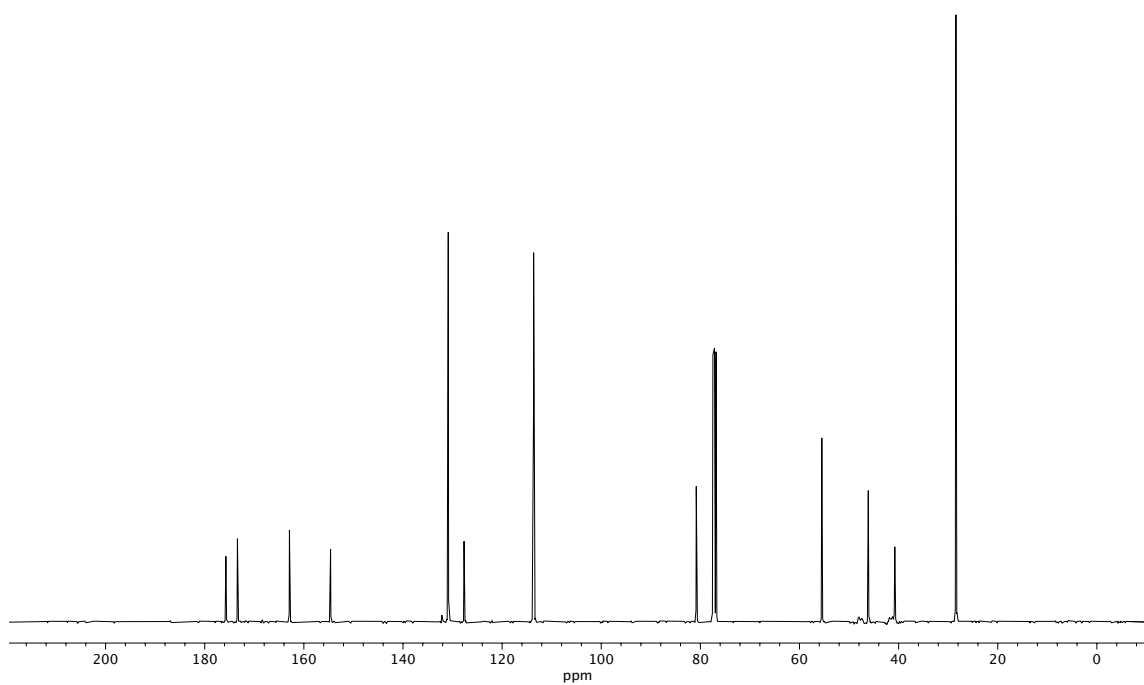
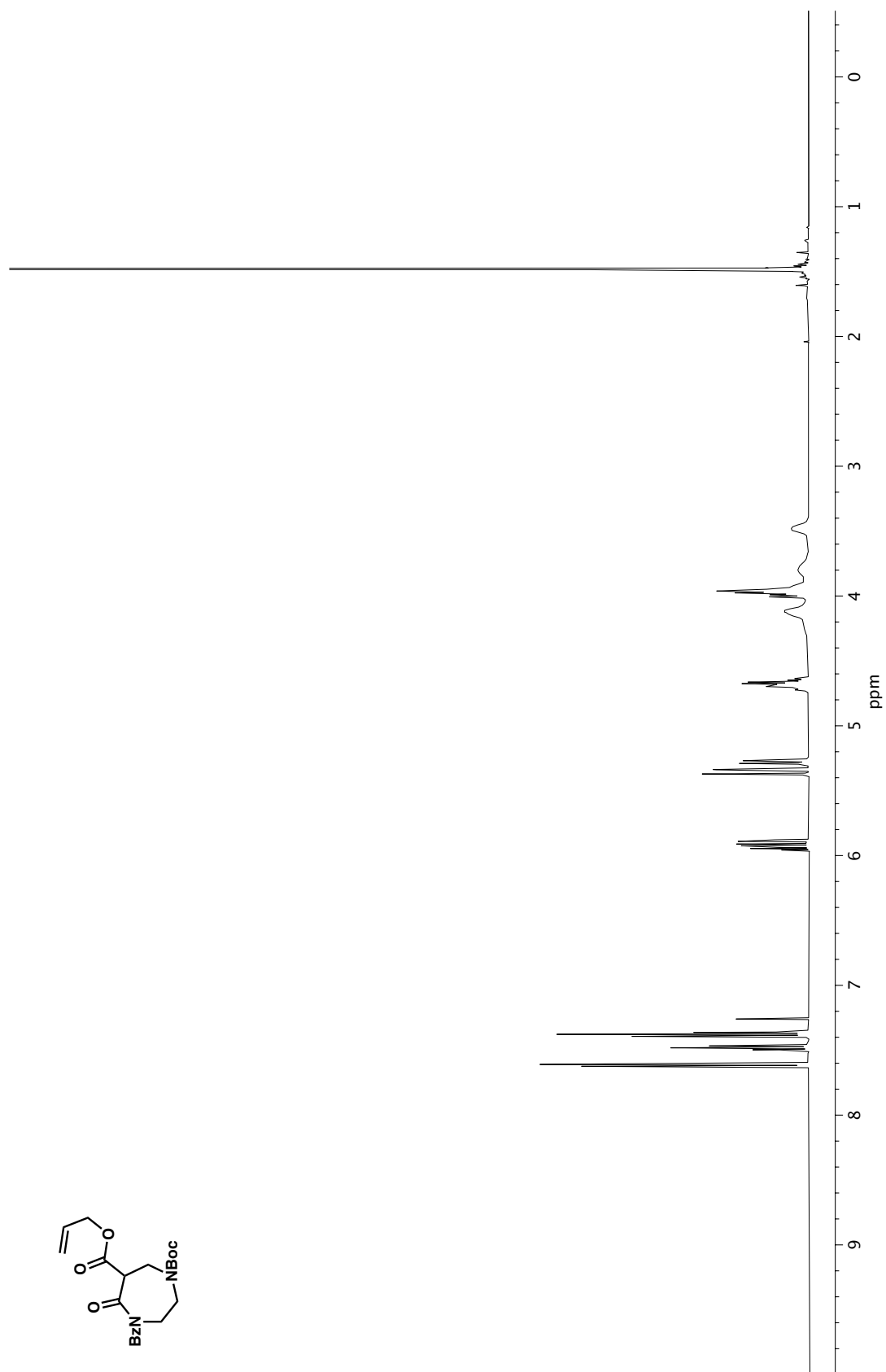


Figure A1.45. ¹³C NMR (100 MHz, CDCl₃) of compound **57**.

Figure A1.46. ¹H NMR (500 MHz, CDCl₃) of compound **18a**.

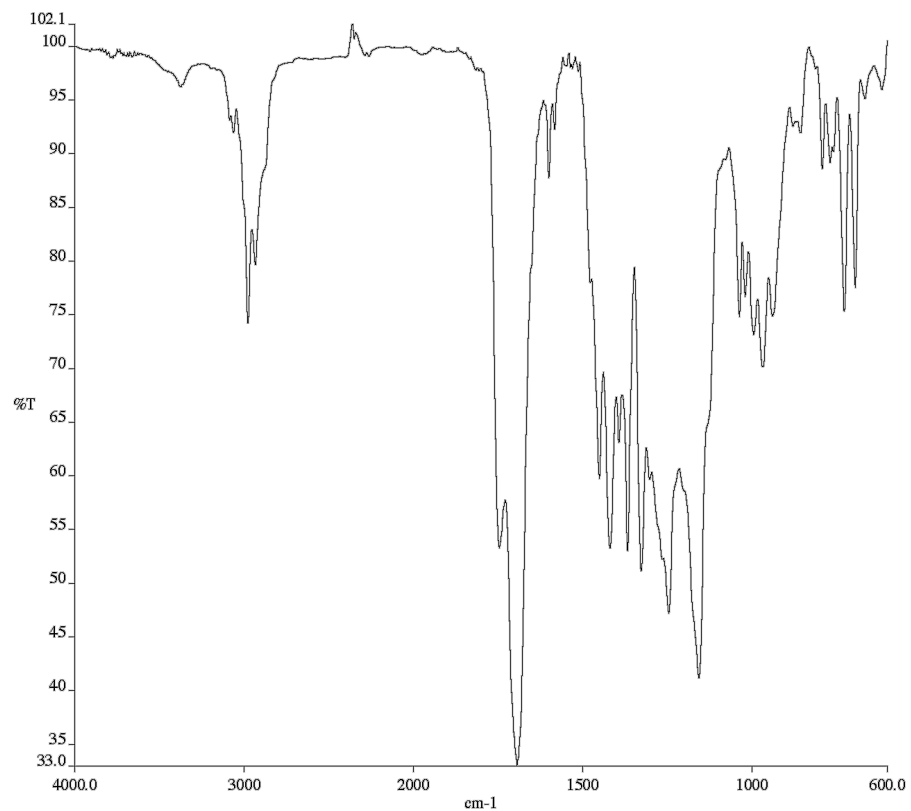


Figure A1.47. Infrared spectrum (Thin Film, NaCl) of compound **18a**.

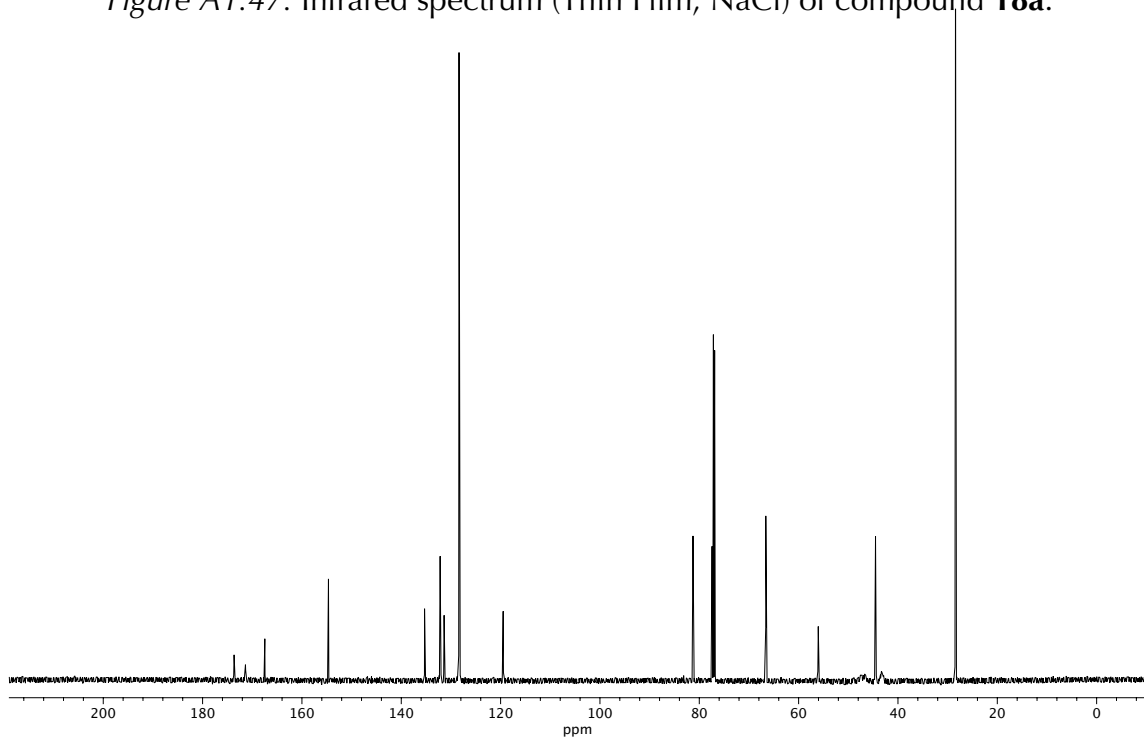
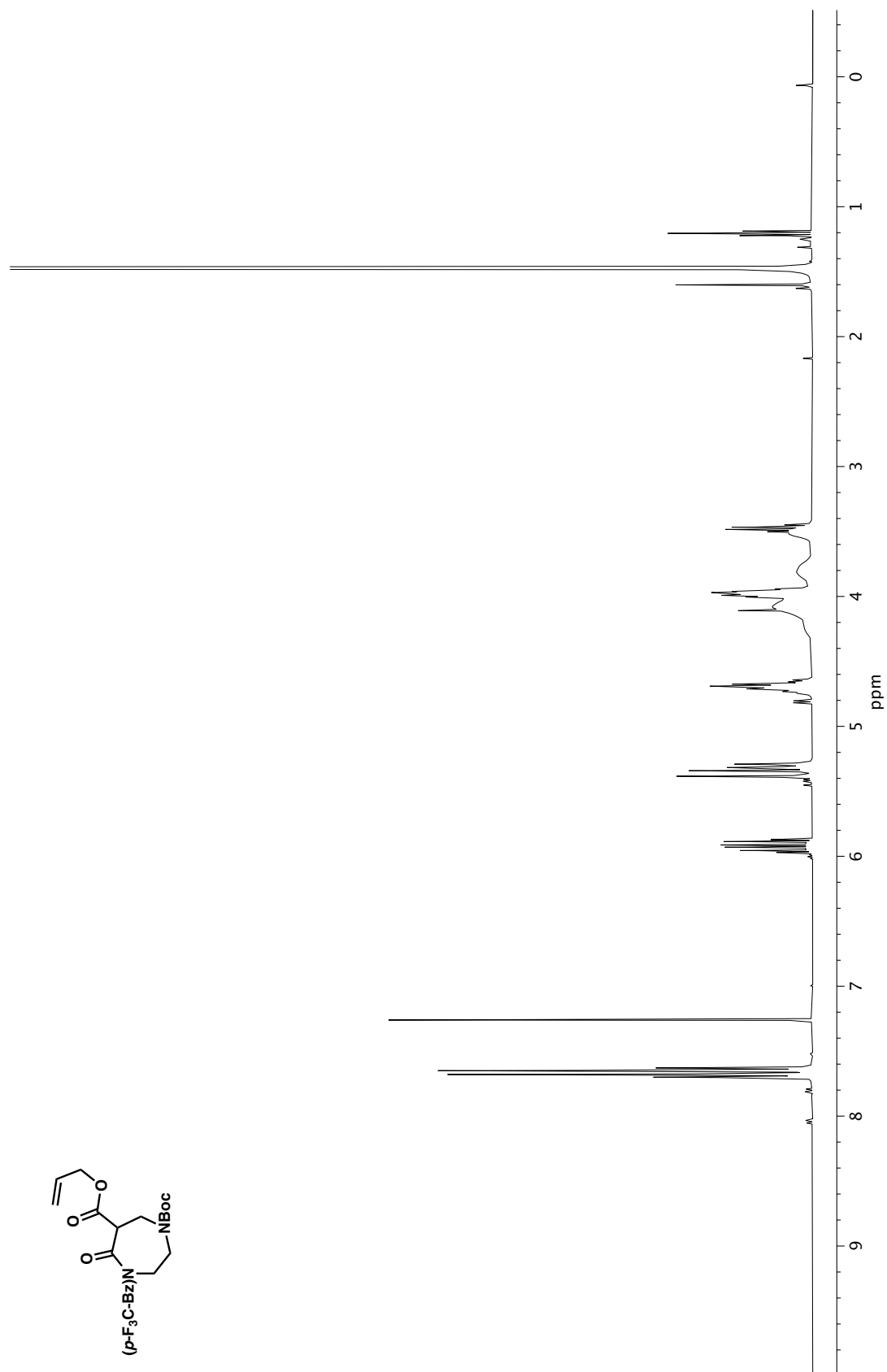


Figure A1.48. ¹³C NMR (125 MHz, CDCl₃) of compound **18a**.

Figure A1.49. ¹H NMR (400 MHz, CDCl₃) of compound **18b**.

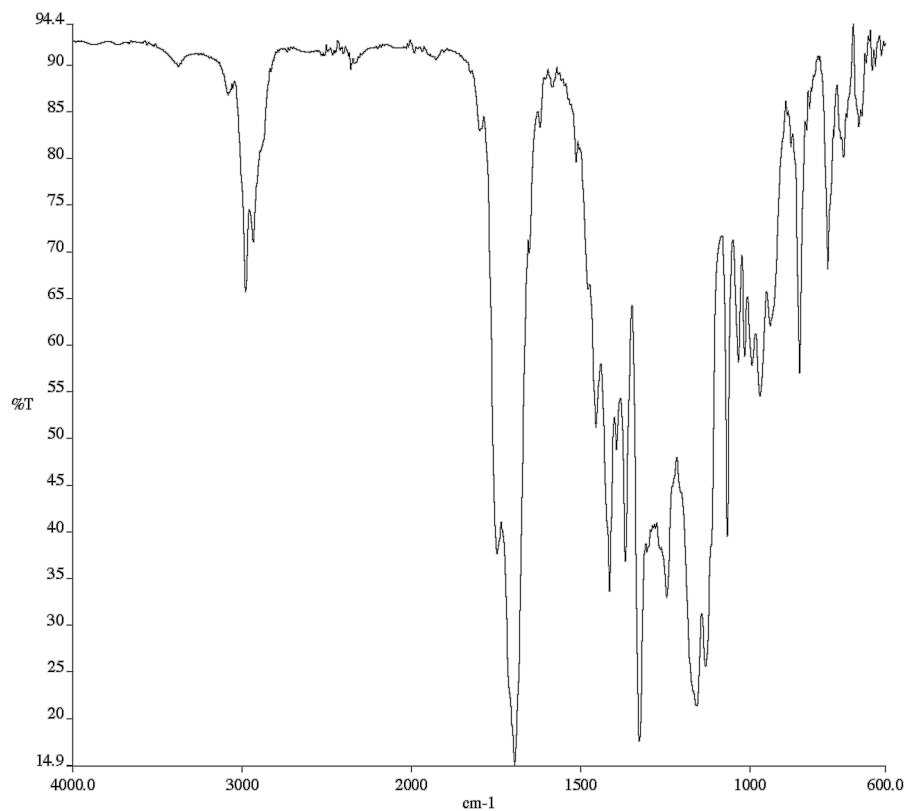


Figure A1.50. Infrared spectrum (Thin Film, NaCl) of compound **18b**.

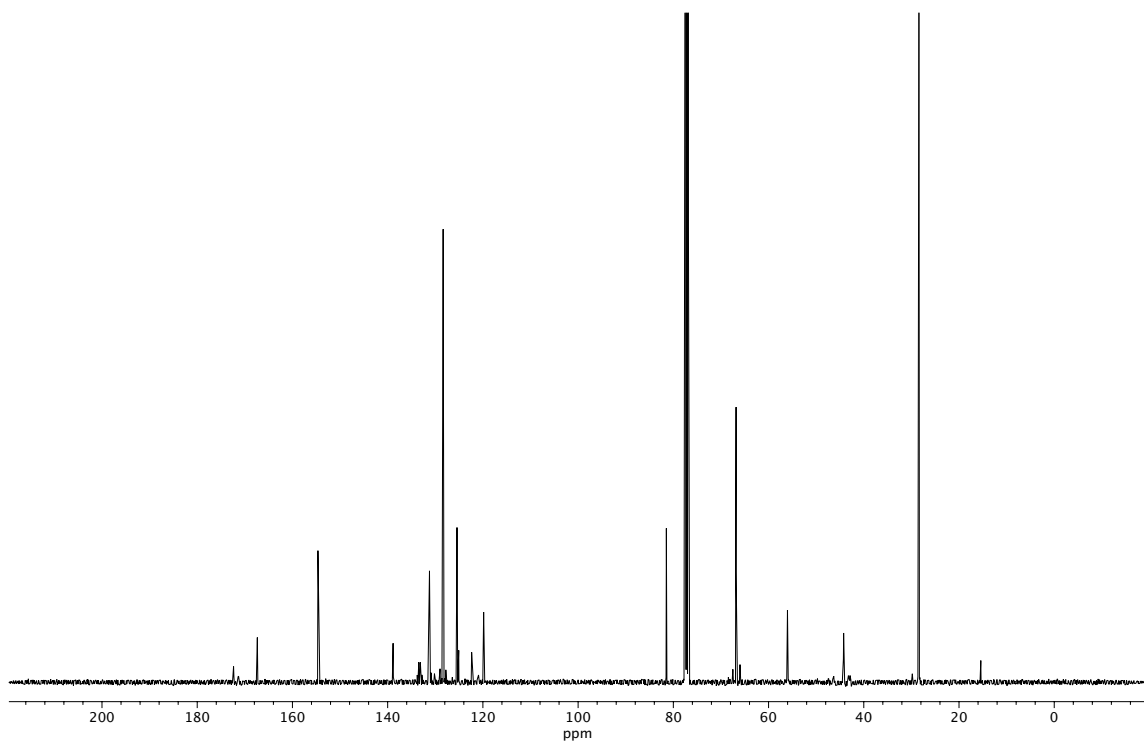
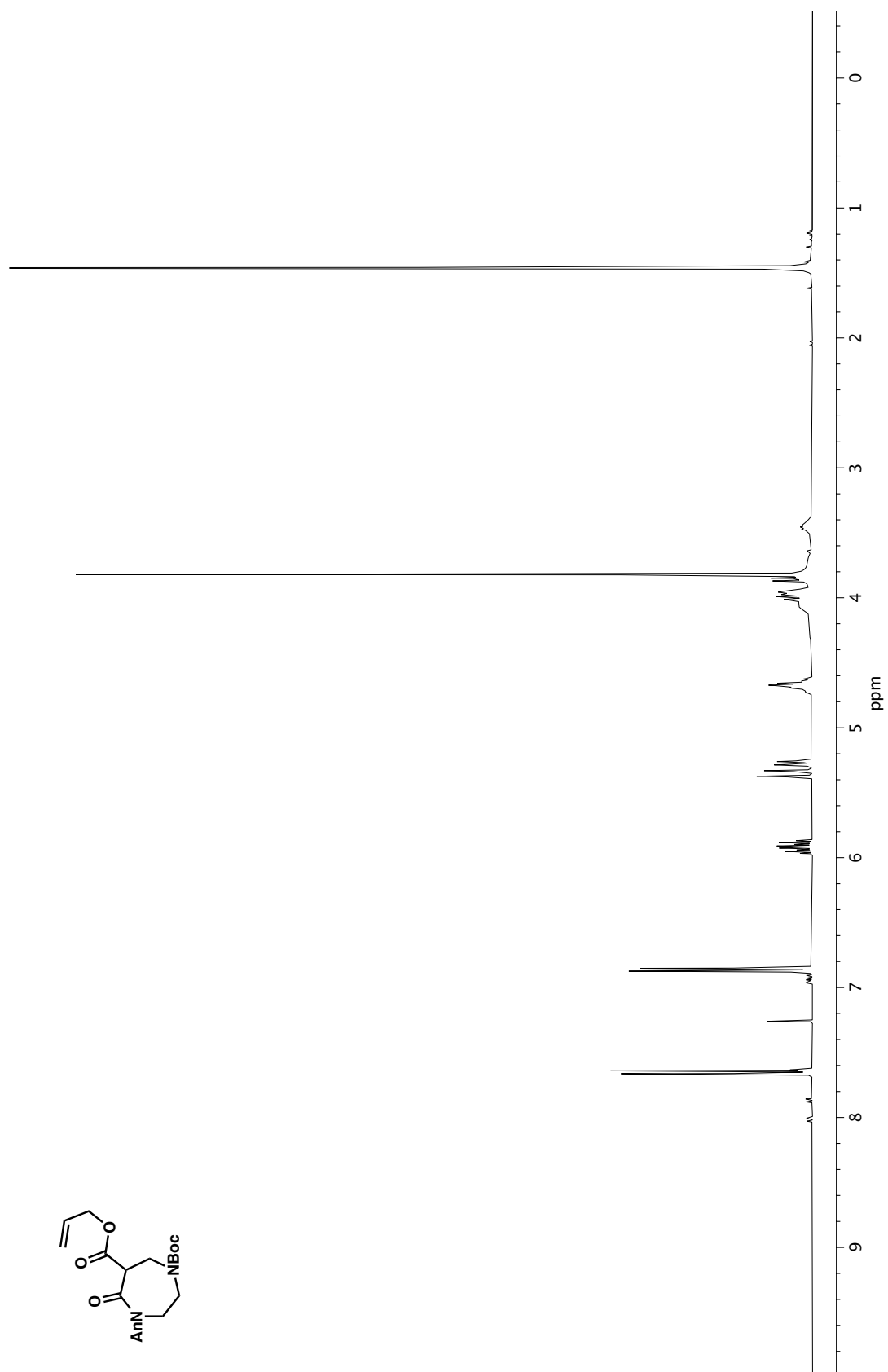


Figure A1.51. ¹³C NMR (100 MHz, CDCl₃) of compound **18b**.

Figure A1.52. ^1H NMR (400 MHz, CDCl_3) of compound **18c**.

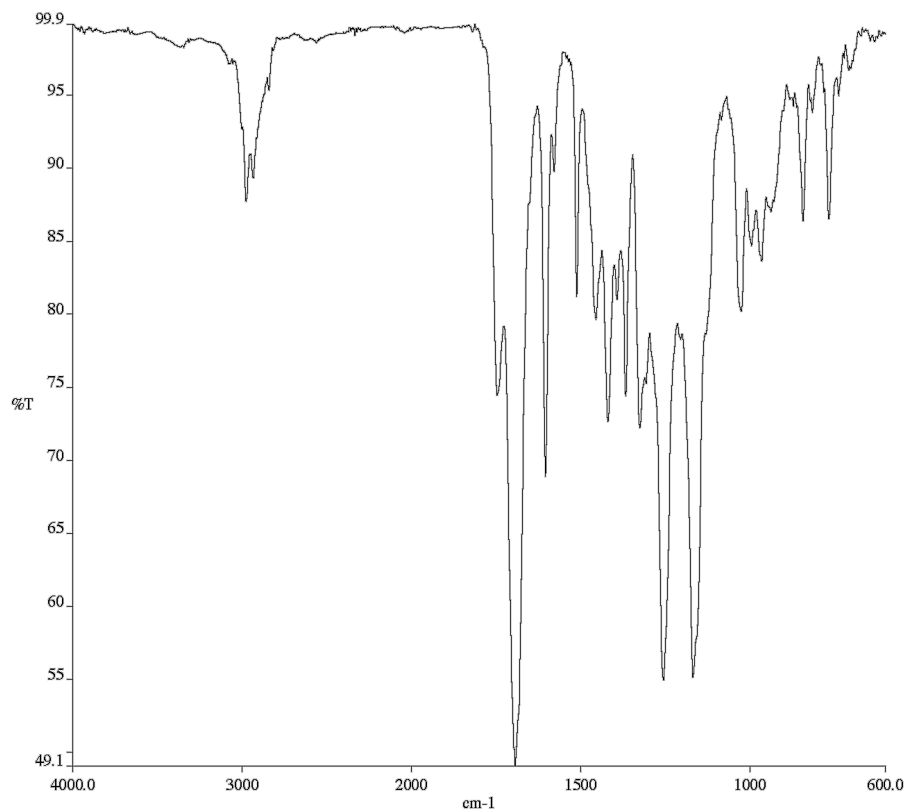


Figure A1.53. Infrared spectrum (Thin Film, NaCl) of compound **18c**.

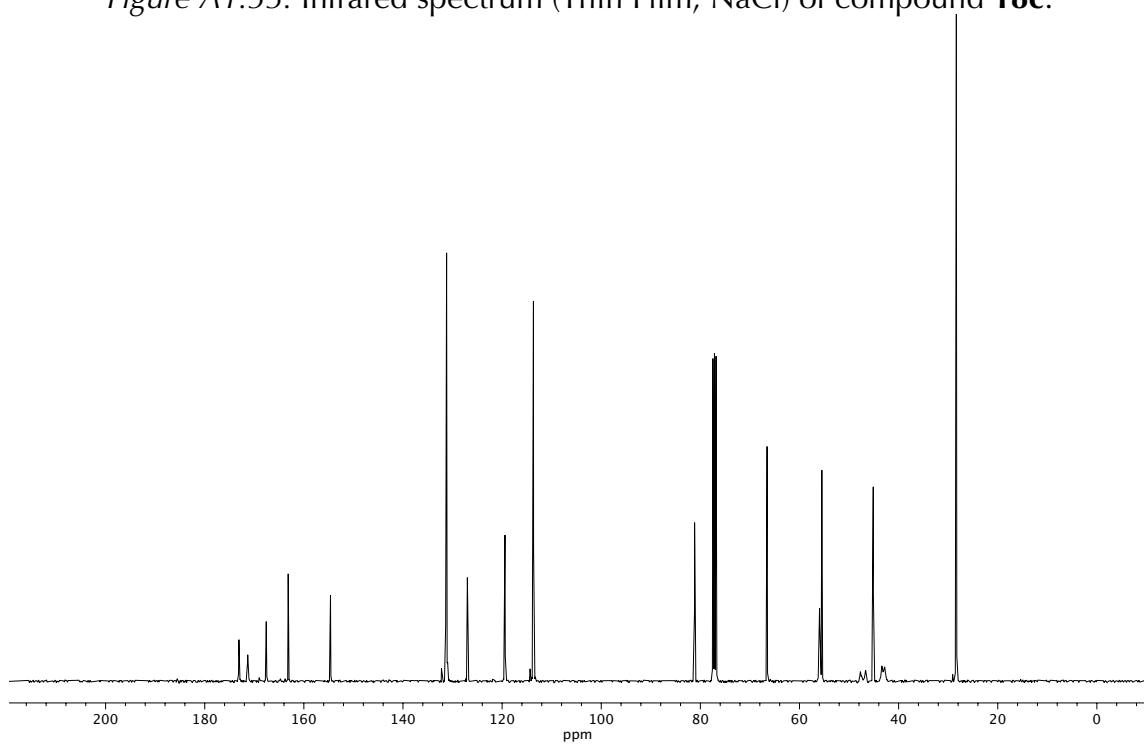


Figure A1.54. ^{13}C NMR (100 MHz, CDCl_3) of compound **18c**.

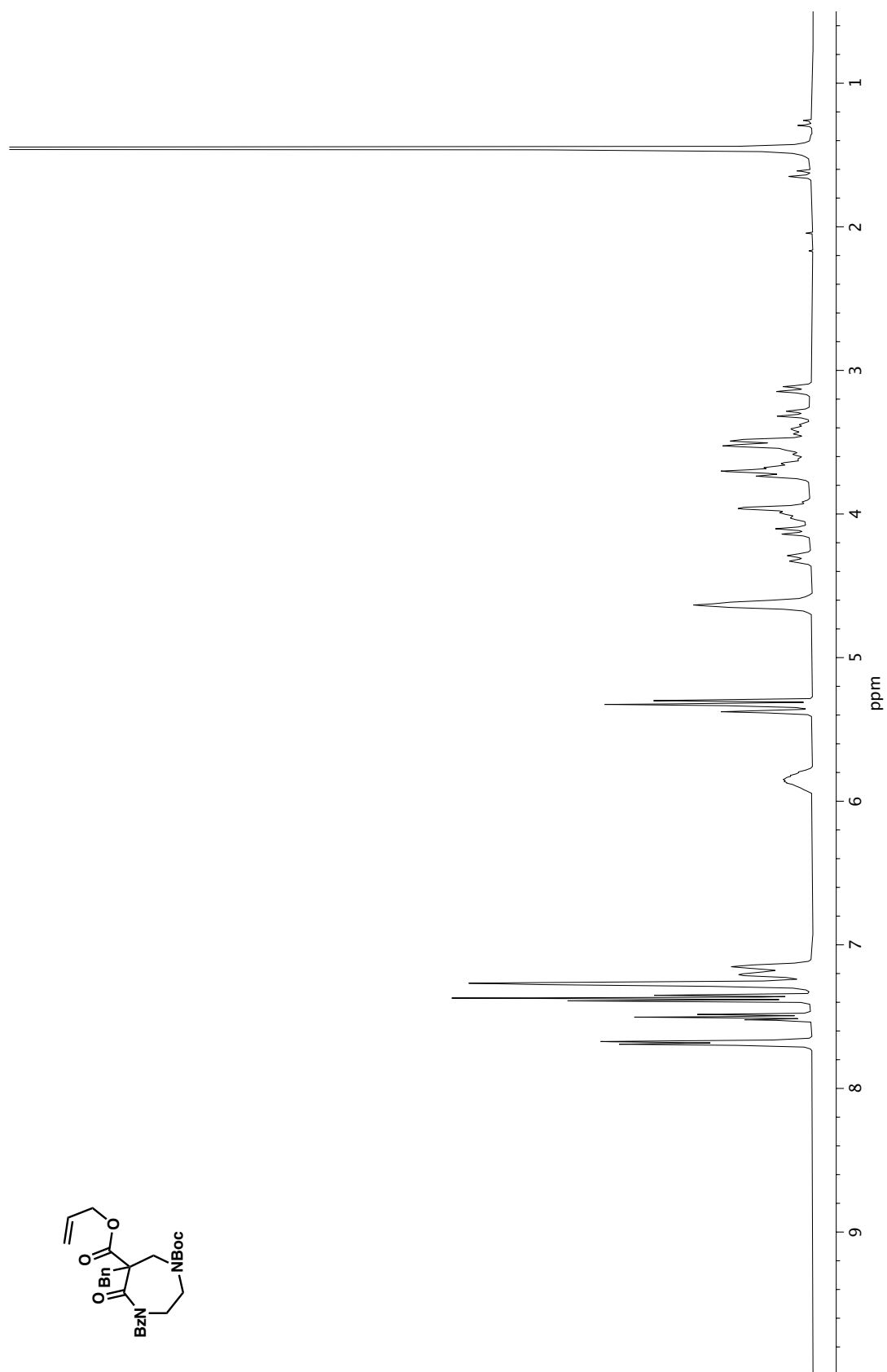


Figure A1.55. ¹H NMR (400 MHz, CDCl₃) of compound **19a**.

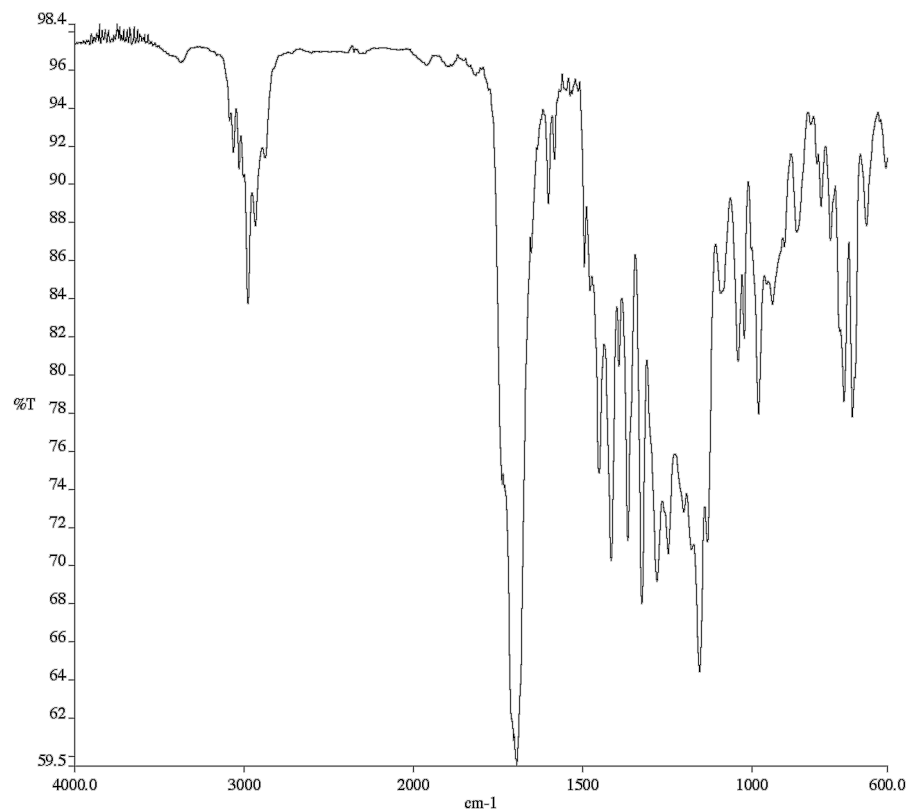


Figure A1.56. Infrared spectrum (Thin Film, NaCl) of compound **19a**.

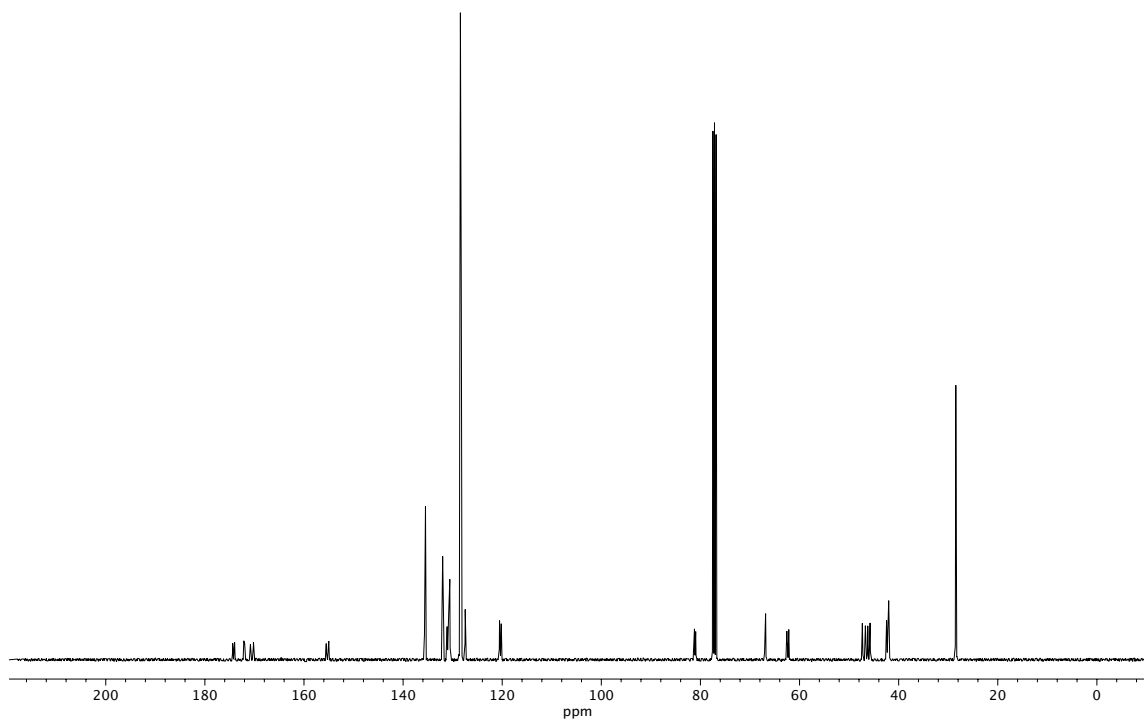


Figure A1.57. ¹³C NMR (100 MHz, CDCl₃) of compound **19a**.

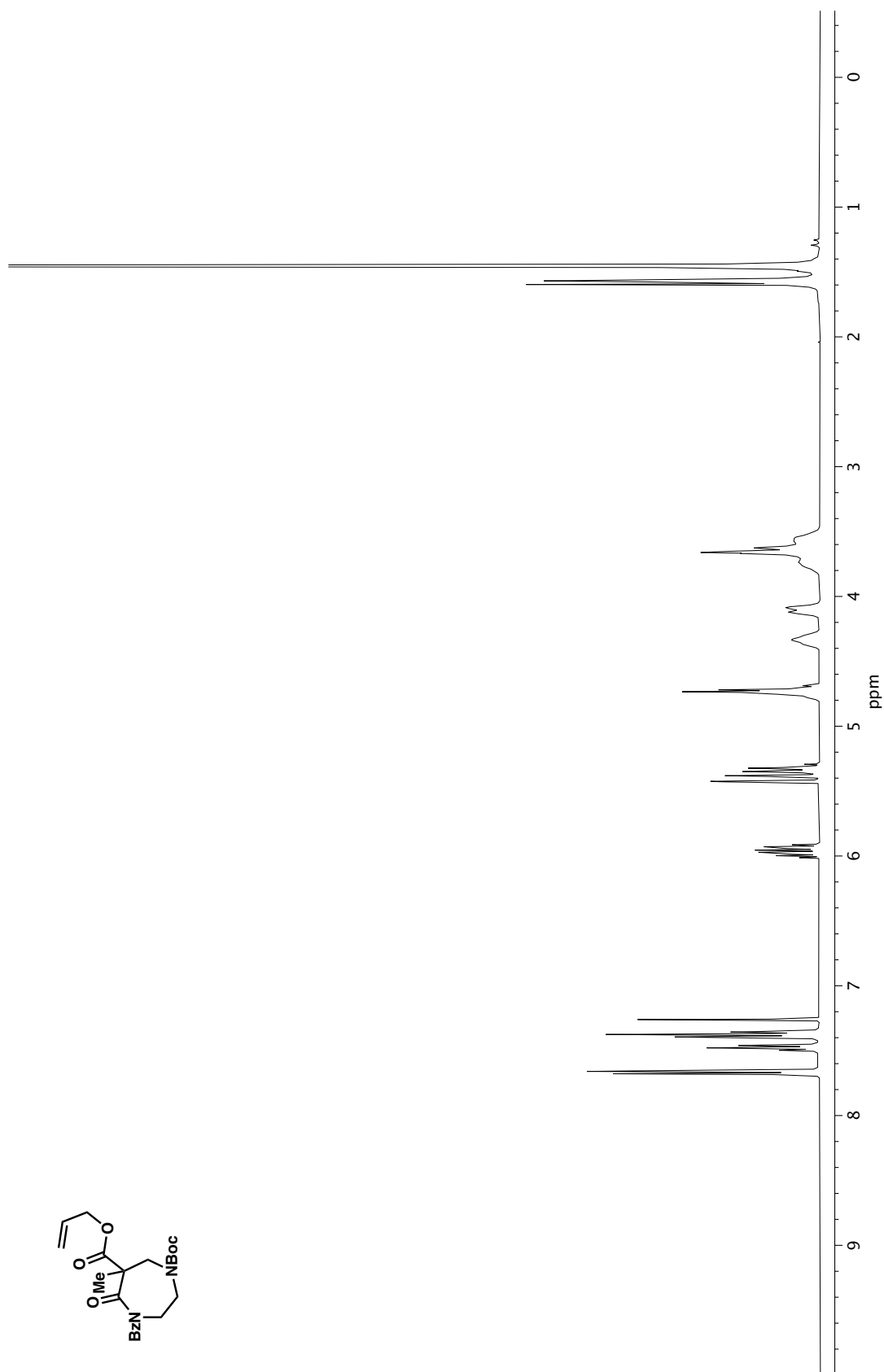


Figure A1.58. ¹H NMR (400 MHz, CDCl₃) of compound **19b**.

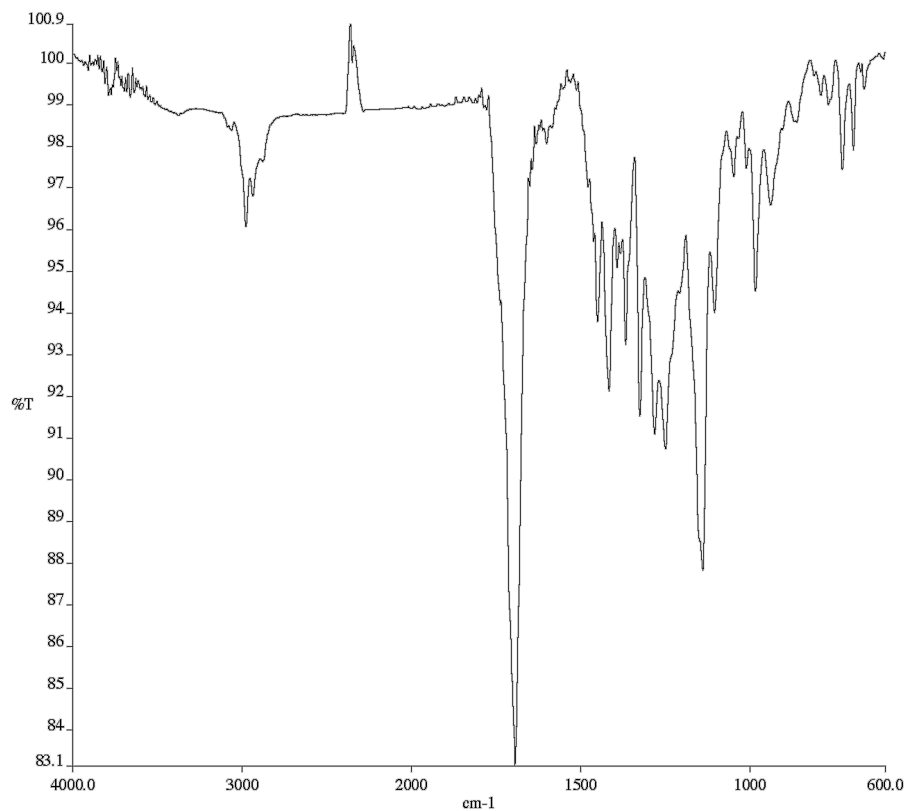


Figure A1.59. Infrared spectrum (Thin Film, NaCl) of compound **19b**.

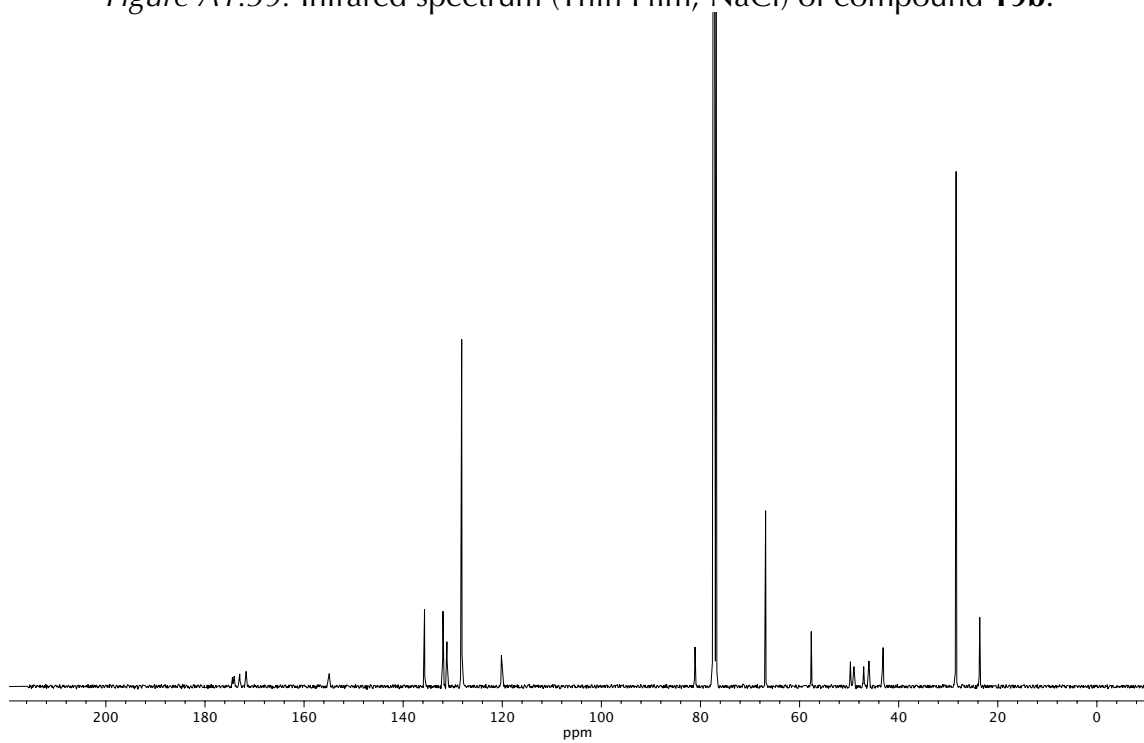
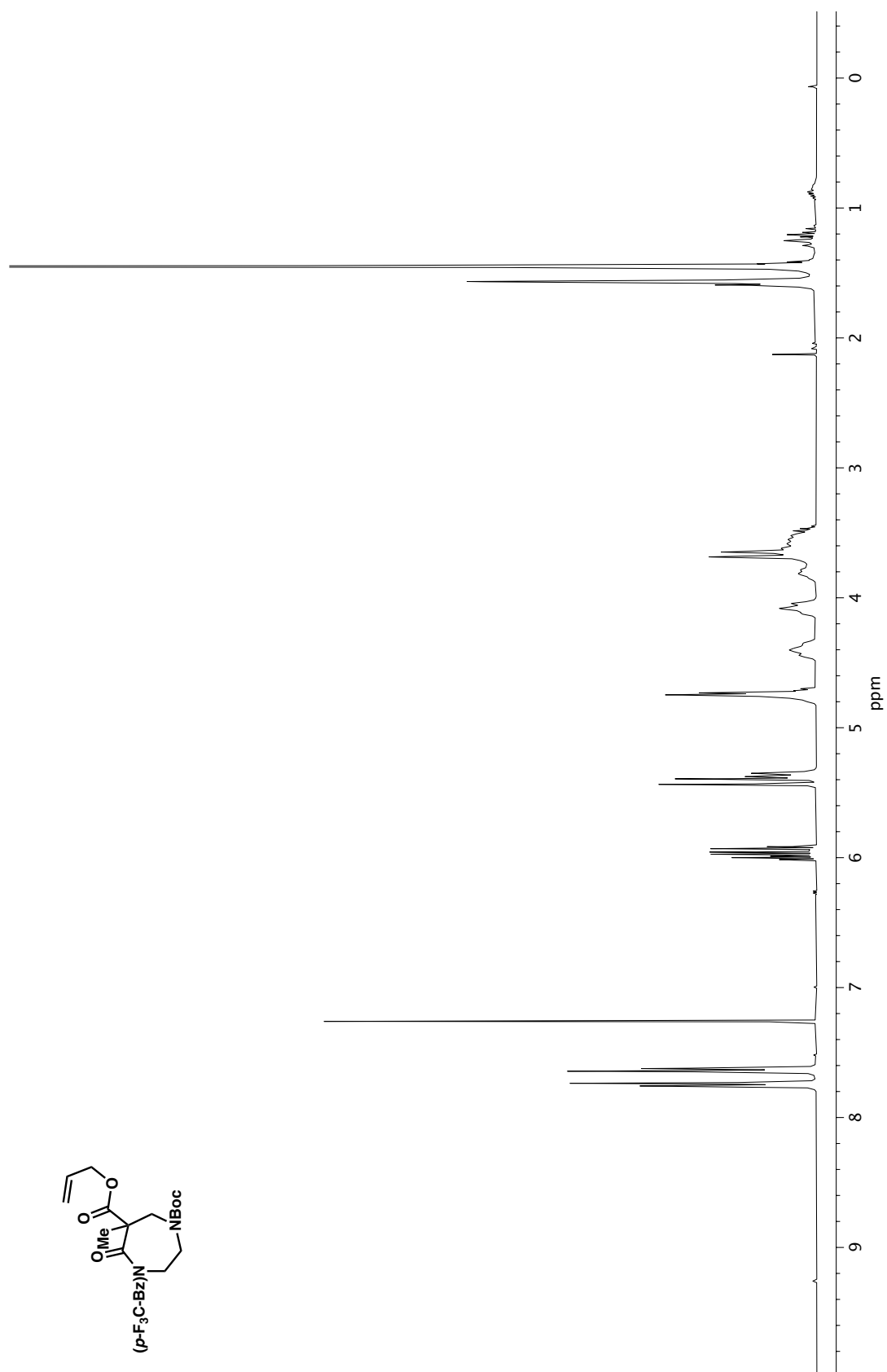


Figure A1.60. ¹³C NMR (100 MHz, CDCl₃) of compound **19b**.

Figure A1.61. ¹H NMR (400 MHz, CDCl₃) of compound **19c**.

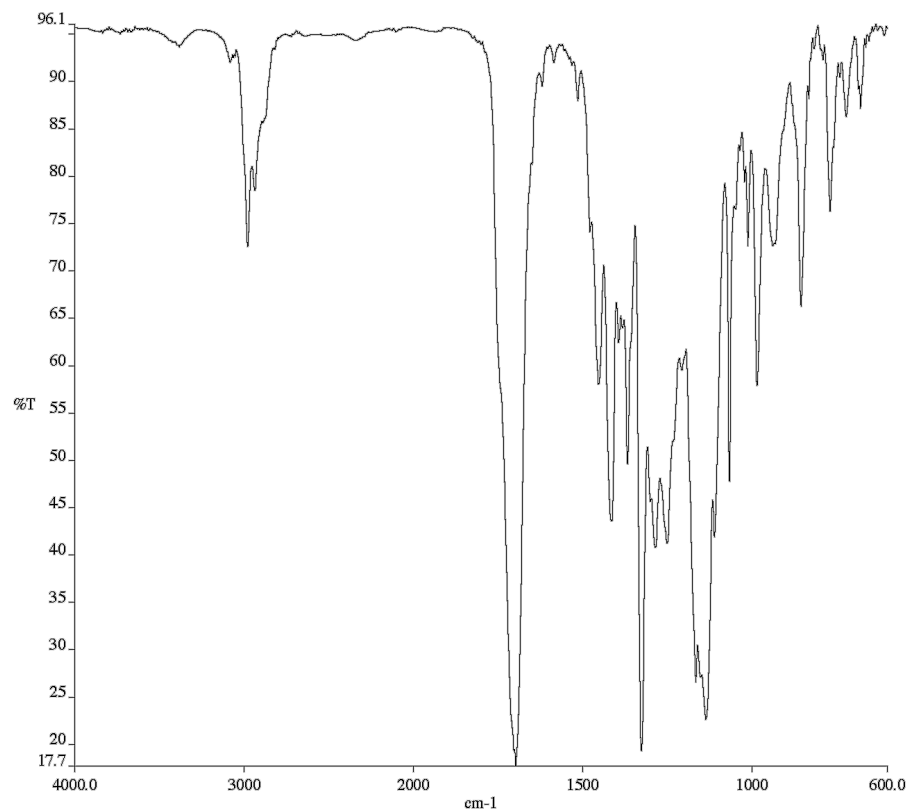


Figure A1.62. Infrared spectrum (Thin Film, NaCl) of compound **19c**.

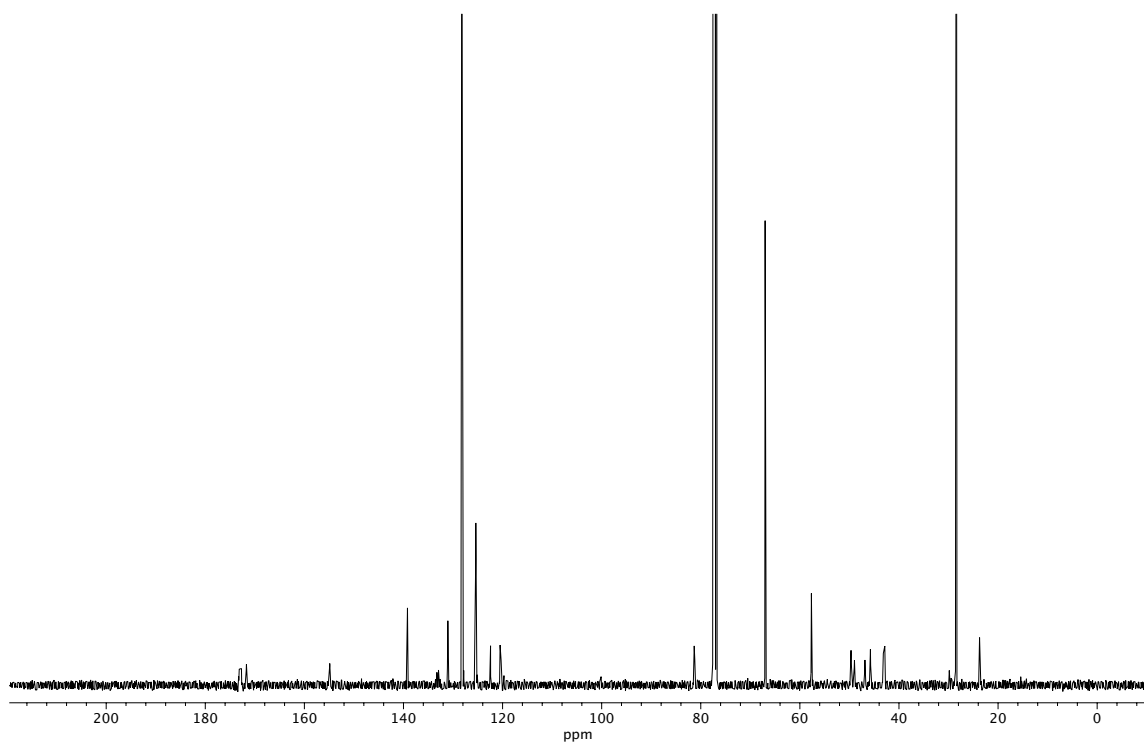
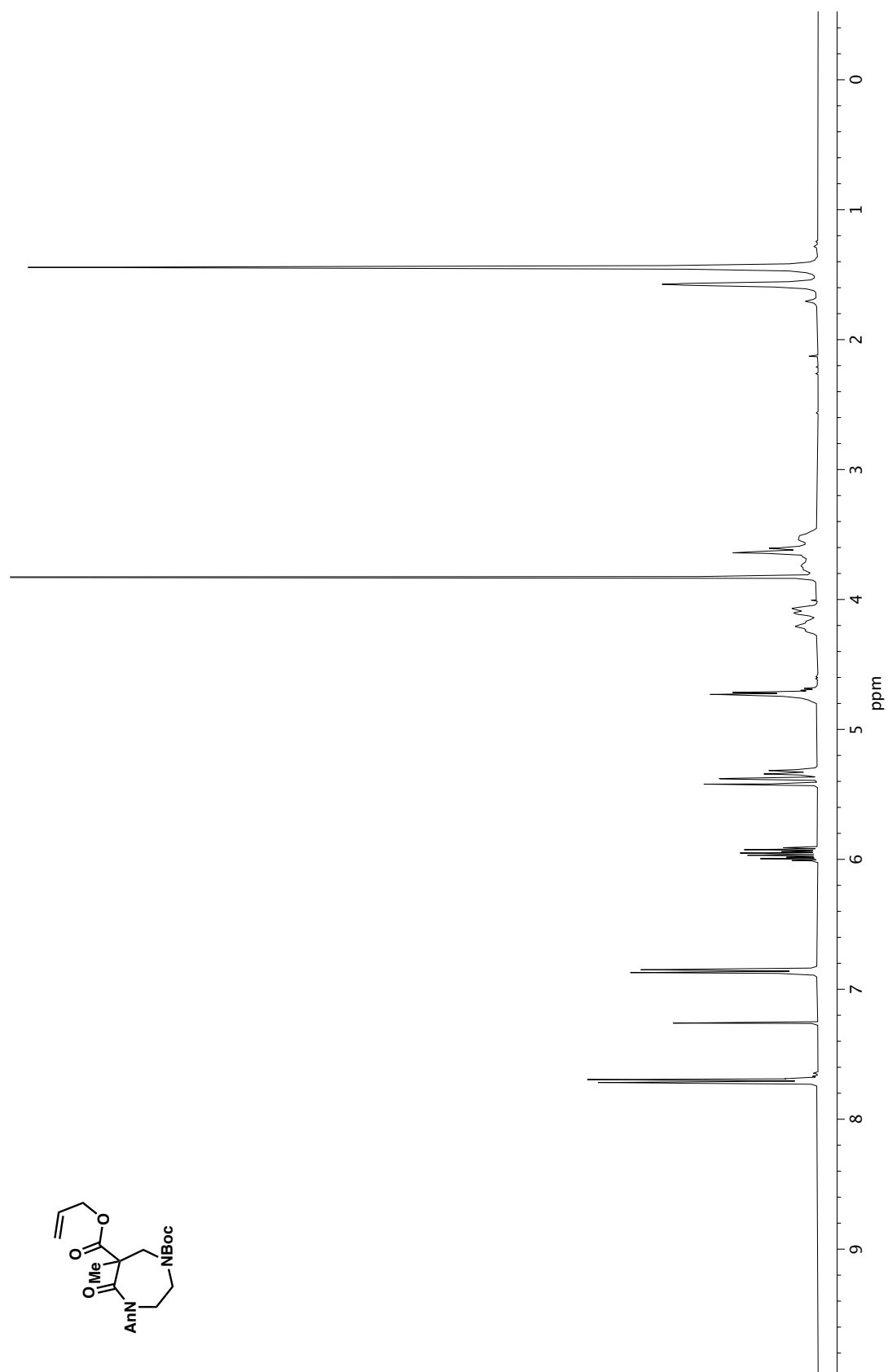


Figure A1.63. ¹³C NMR (100 MHz, CDCl₃) of compound **19c**.

Figure A1.64. ^1H NMR (400 MHz, CDCl_3) of compound **19d**.

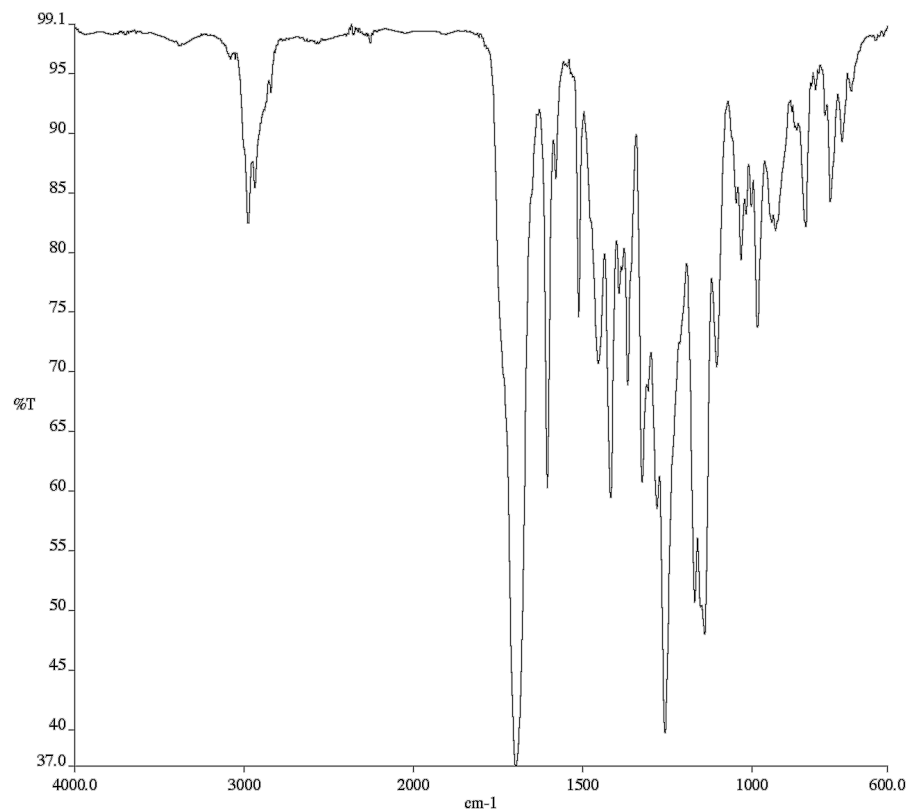


Figure A1.65. Infrared spectrum (Thin Film, NaCl) of compound **19d**.

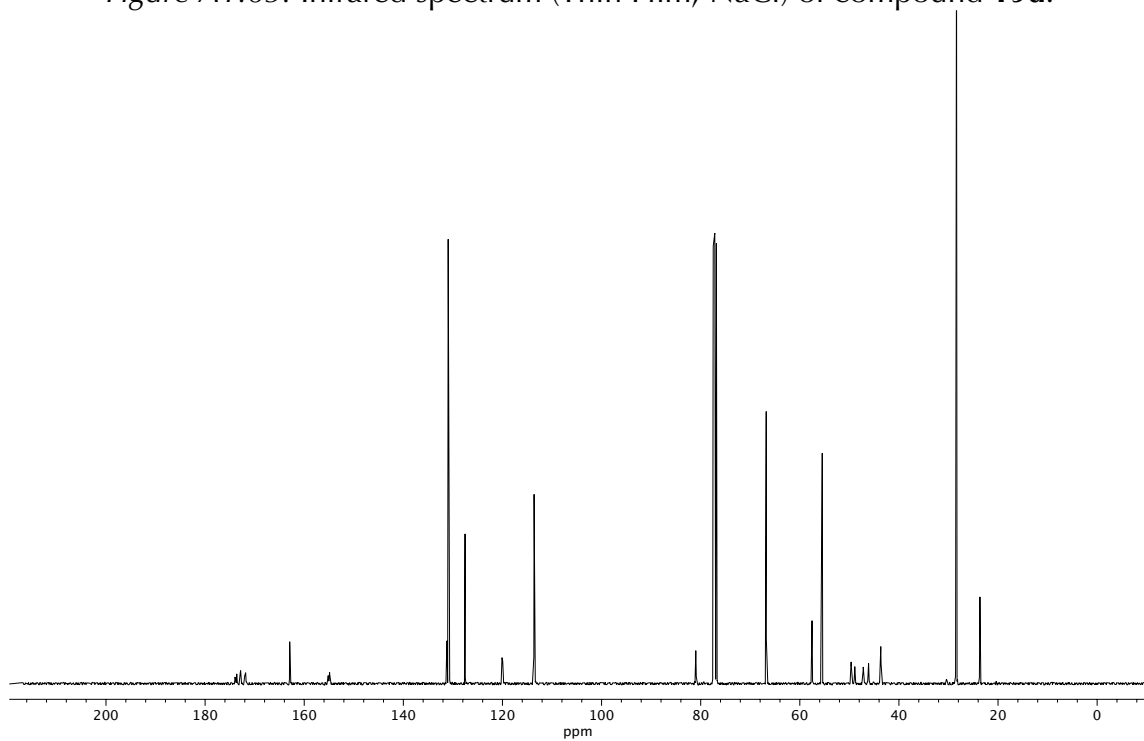
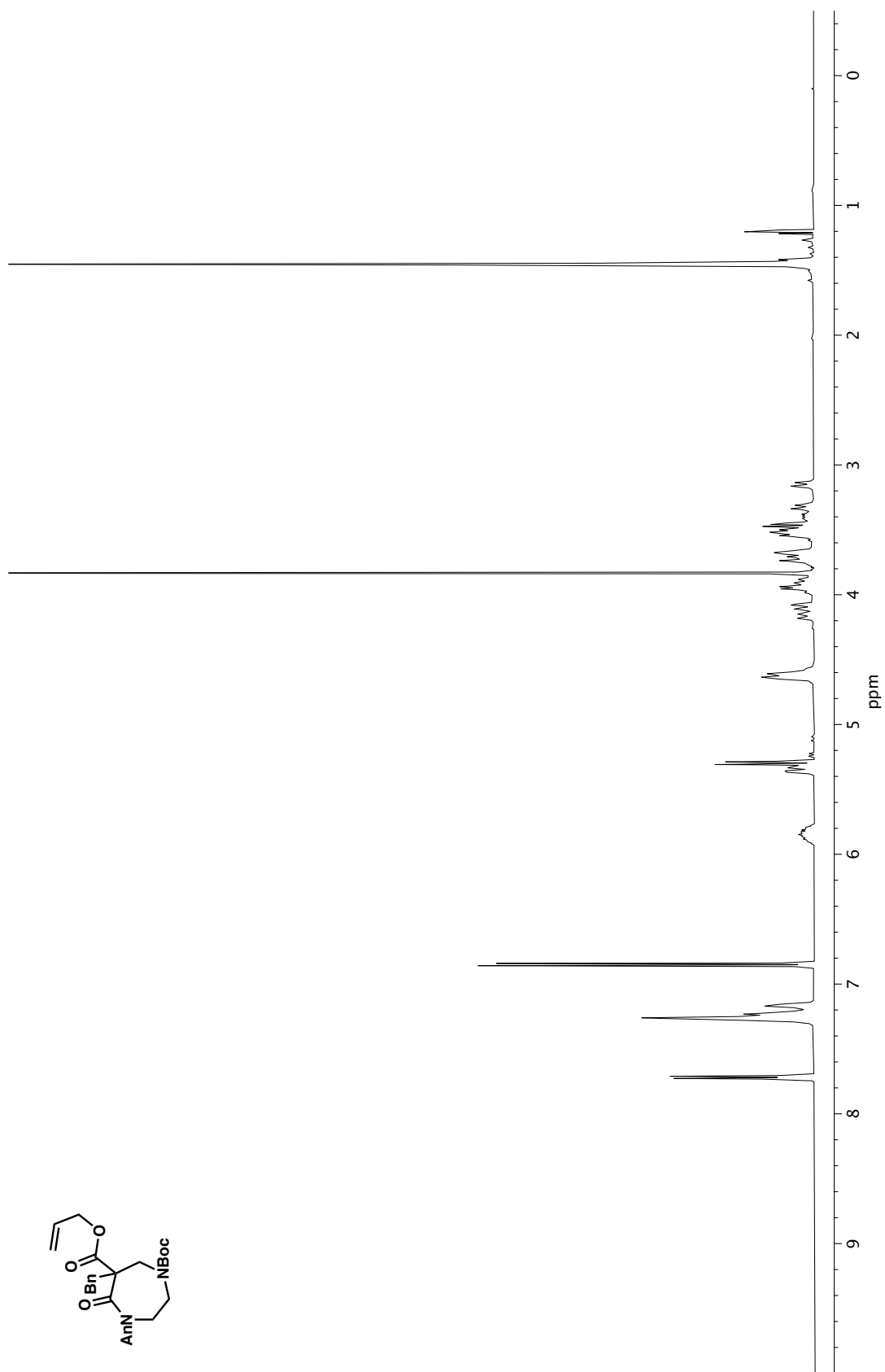


Figure A1.66. ¹³C NMR (100 MHz, CDCl₃) of compound **19d**.

Figure A1.67. ¹H NMR (500 MHz, CDCl₃) of compound **19e**.

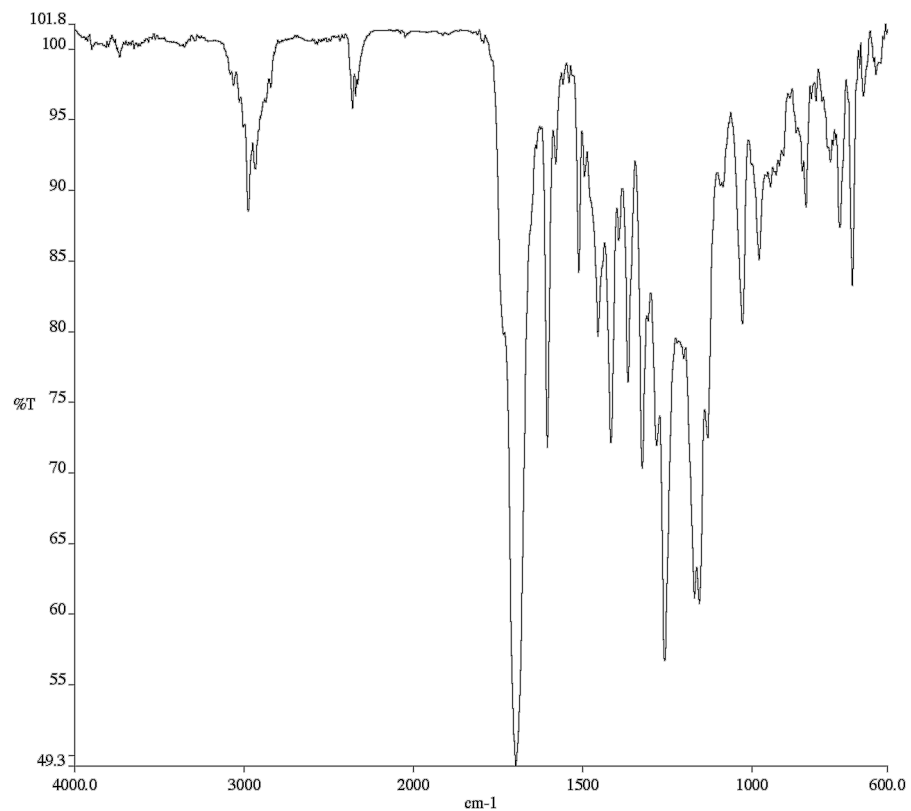


Figure A1.68. Infrared spectrum (Thin Film, NaCl) of compound **19e**.

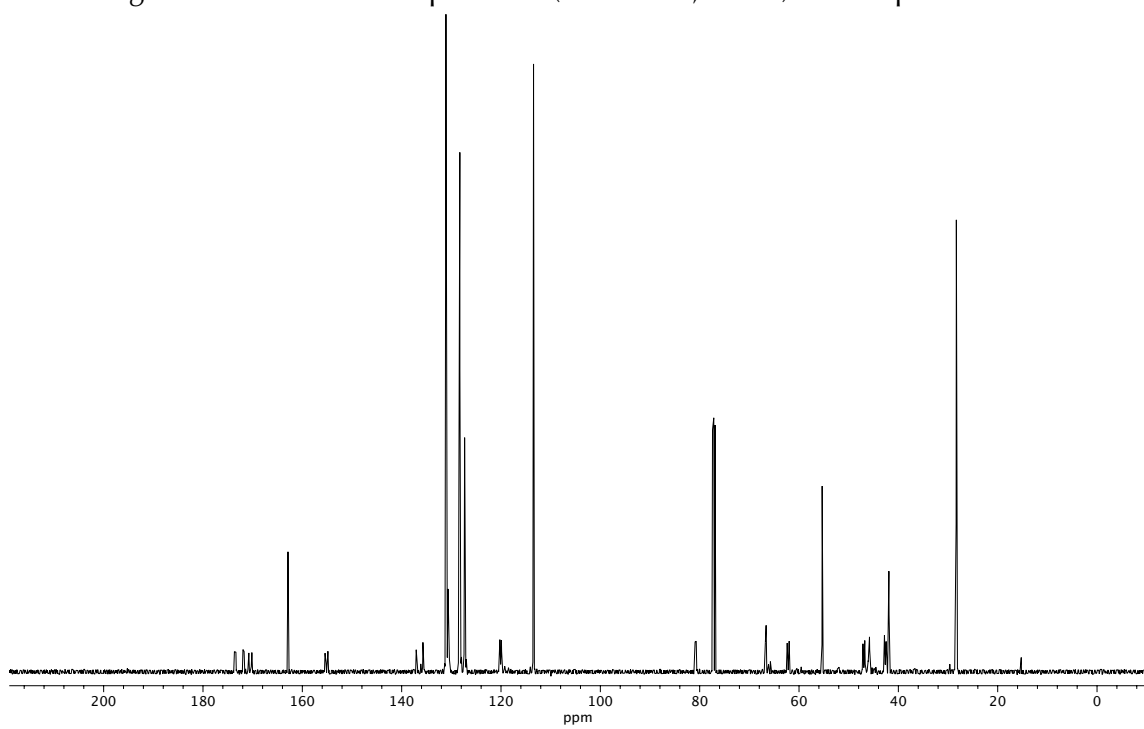
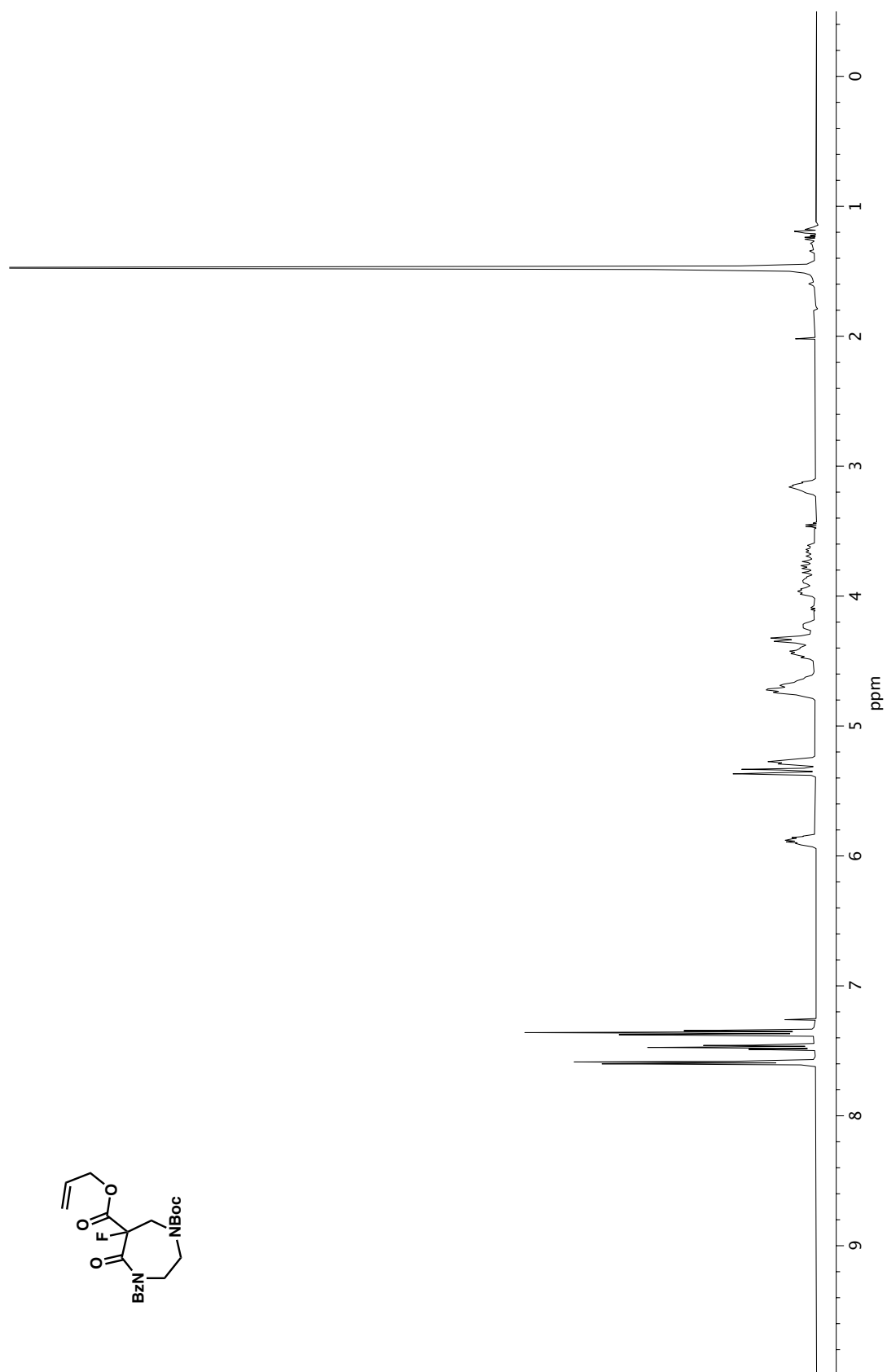


Figure A1.69. ¹³C NMR (125 MHz, CDCl₃) of compound **19e**.

Figure A1.70. ¹H NMR (500 MHz, CDCl₃) of compound **19f**.

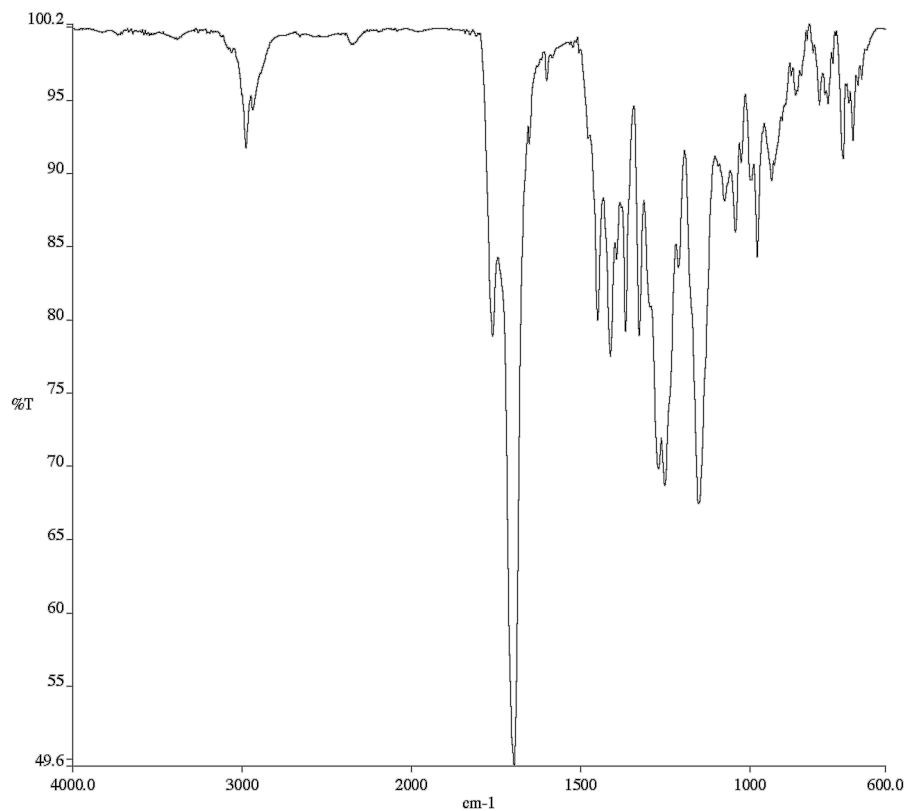


Figure A1.71. Infrared spectrum (Thin Film, NaCl) of compound **19f**.

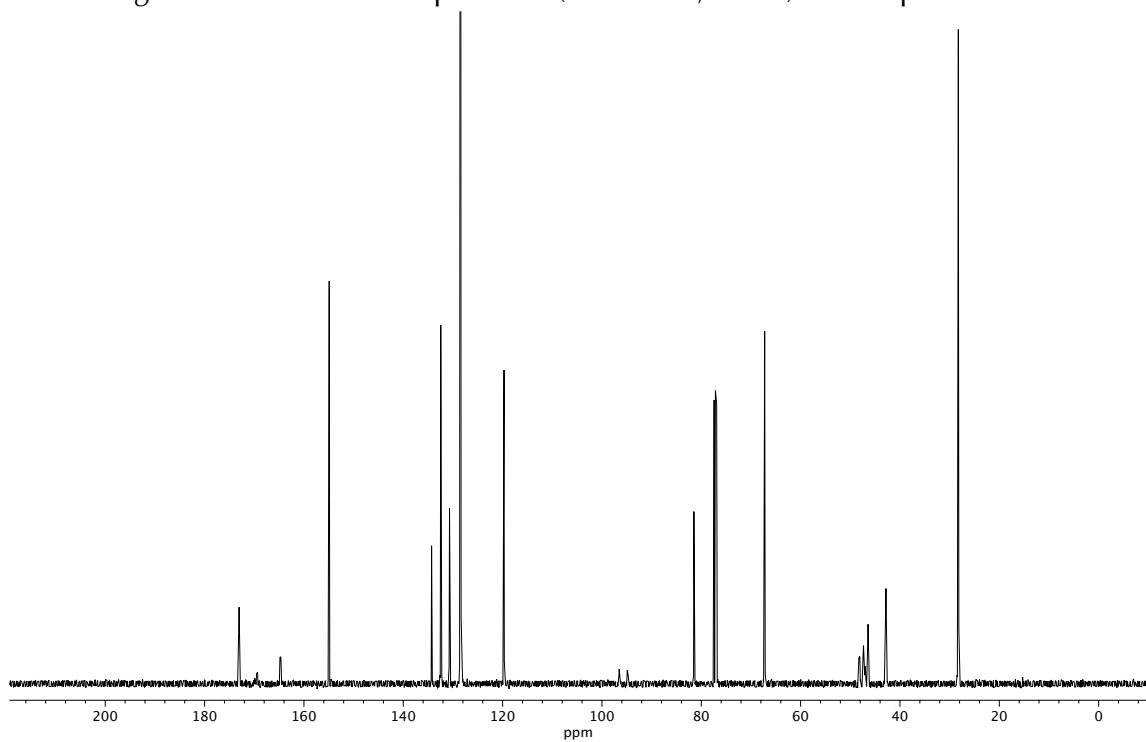
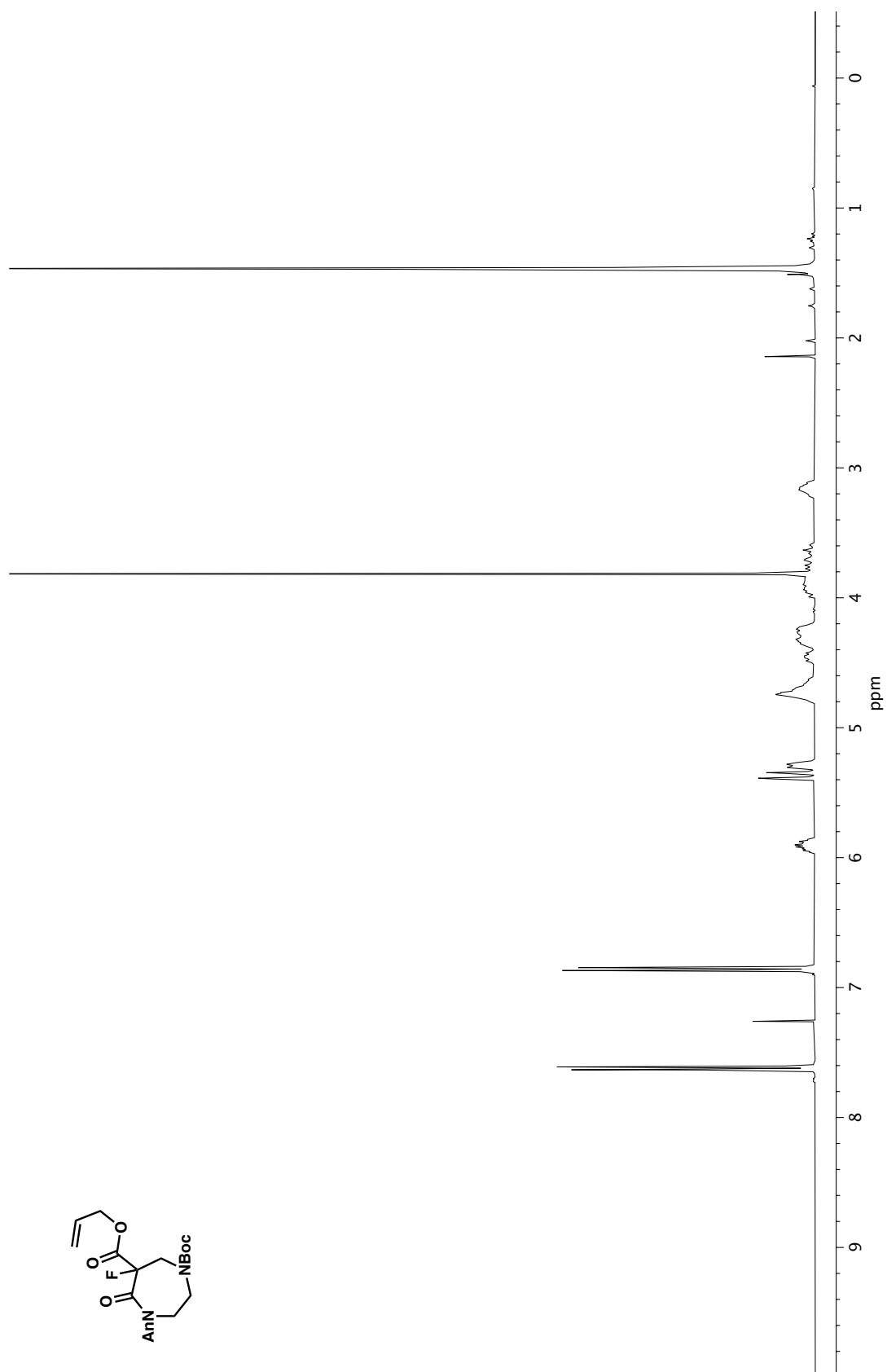


Figure A1.72. ¹³C NMR (125 MHz, CDCl₃) of compound **19f**.

Figure A1.73. ¹H NMR (400 MHz, CDCl₃) of compound **19g**.

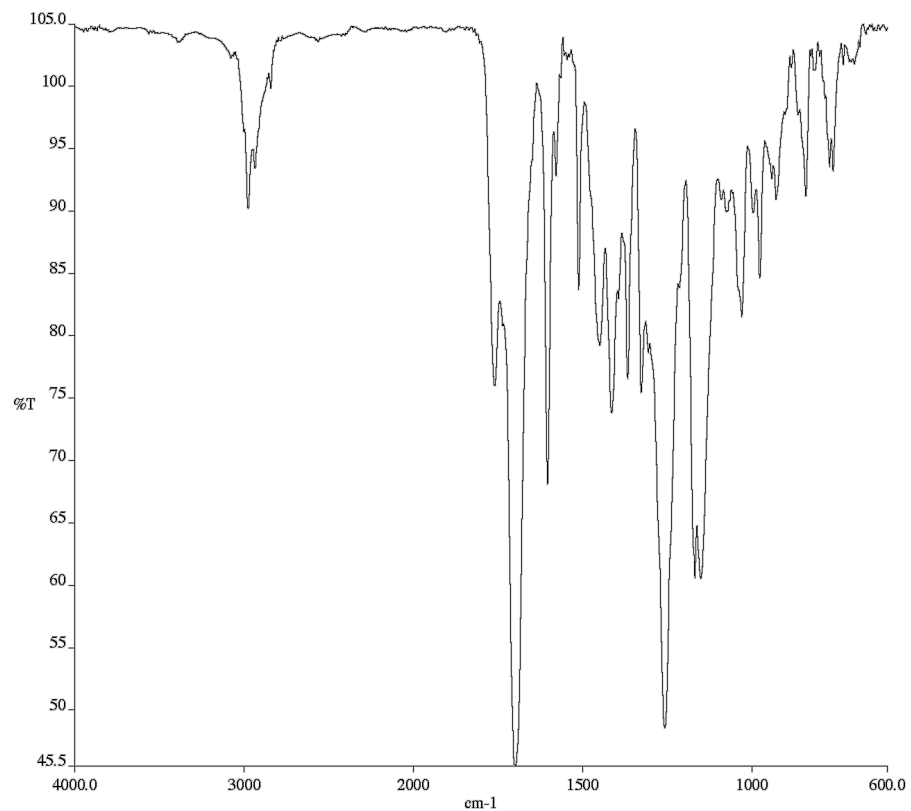


Figure A1.74. Infrared spectrum (Thin Film, NaCl) of compound **19g**.

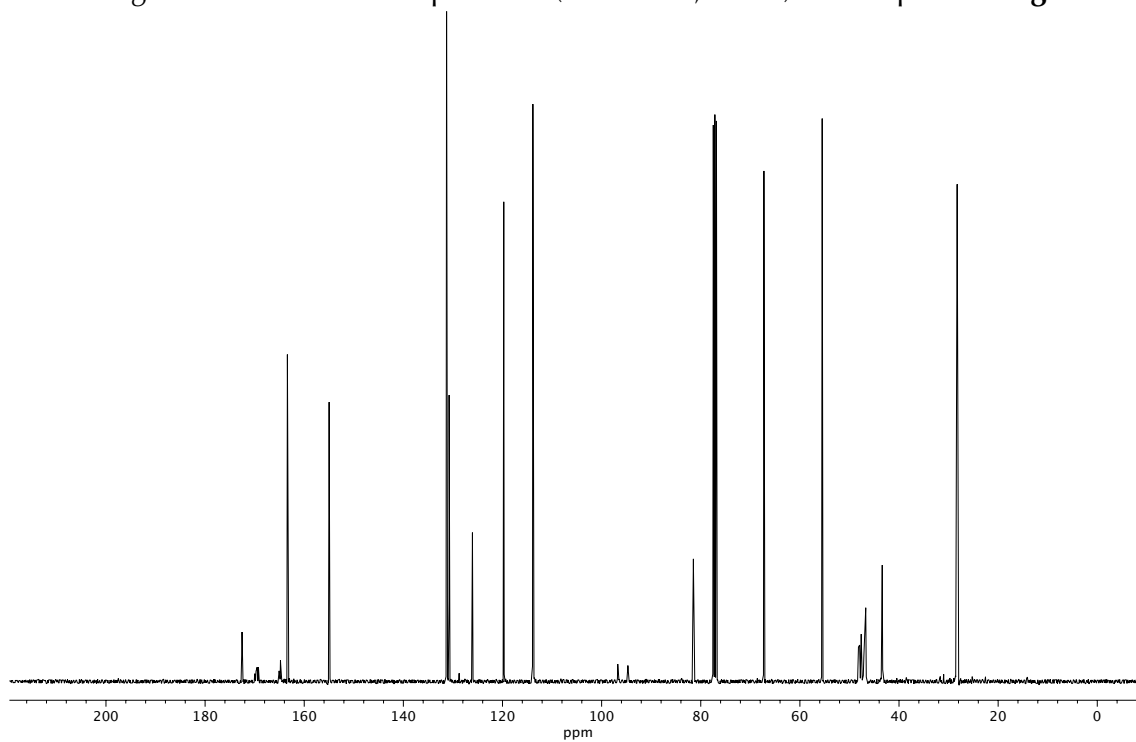
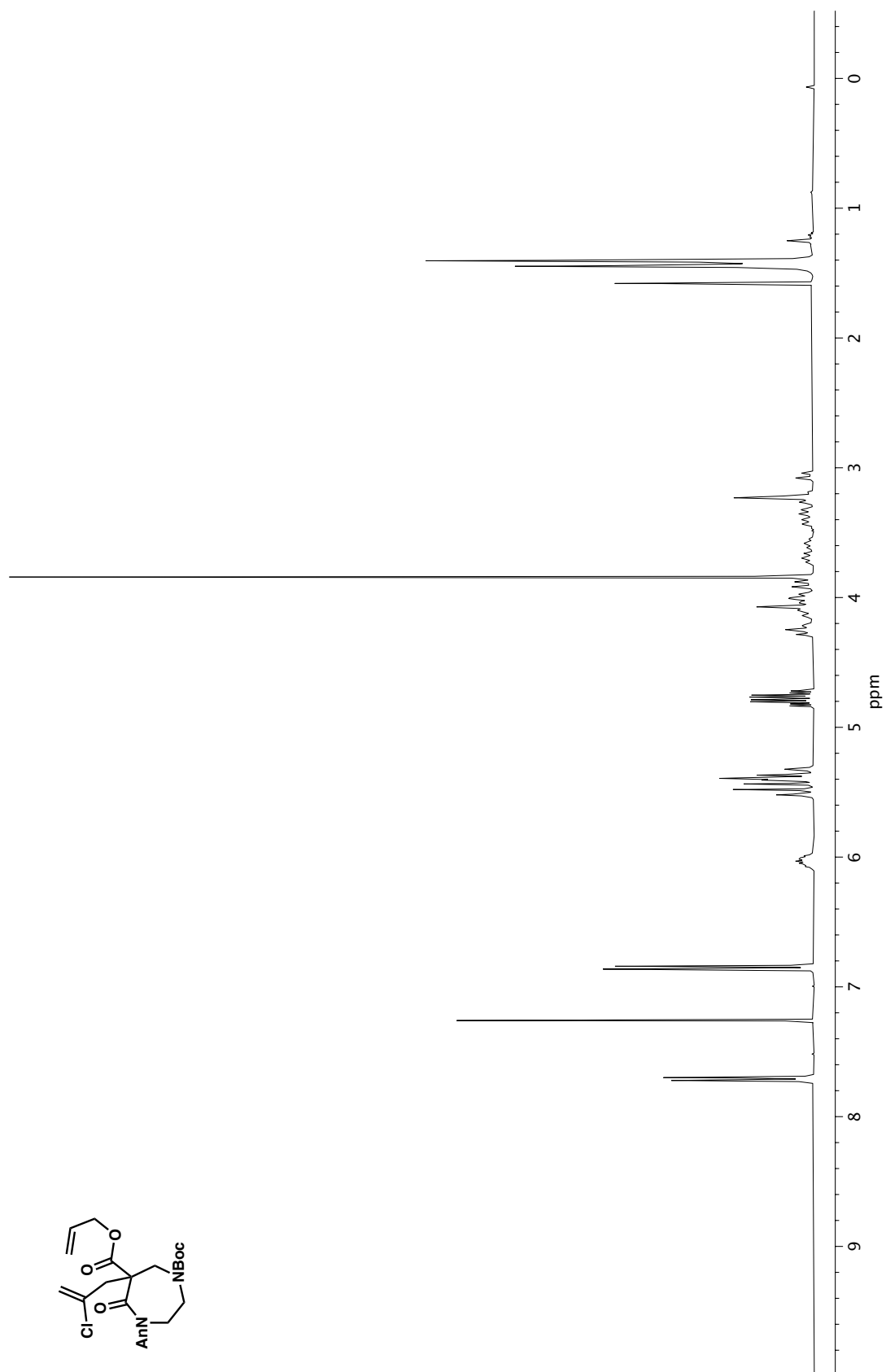


Figure A1.75. ¹³C NMR (100 MHz, CDCl₃) of compound **19g**.

Figure A1.76. ¹H NMR (400 MHz, CDCl₃) of compound **19h**.

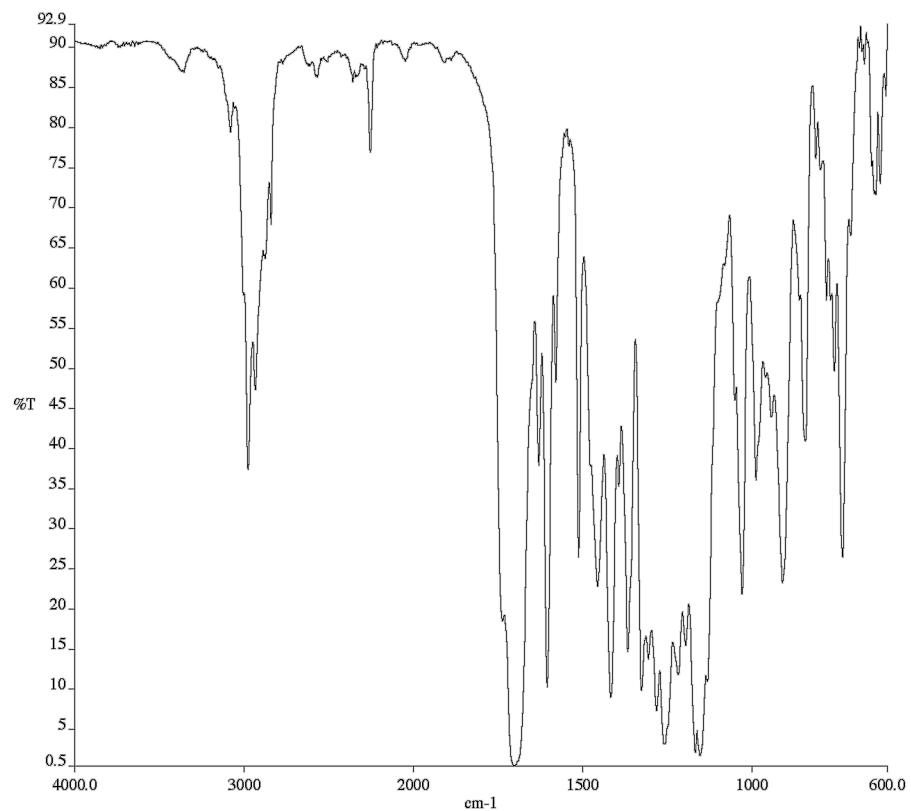


Figure A1.77. Infrared spectrum (Thin Film, NaCl) of compound **19h**.

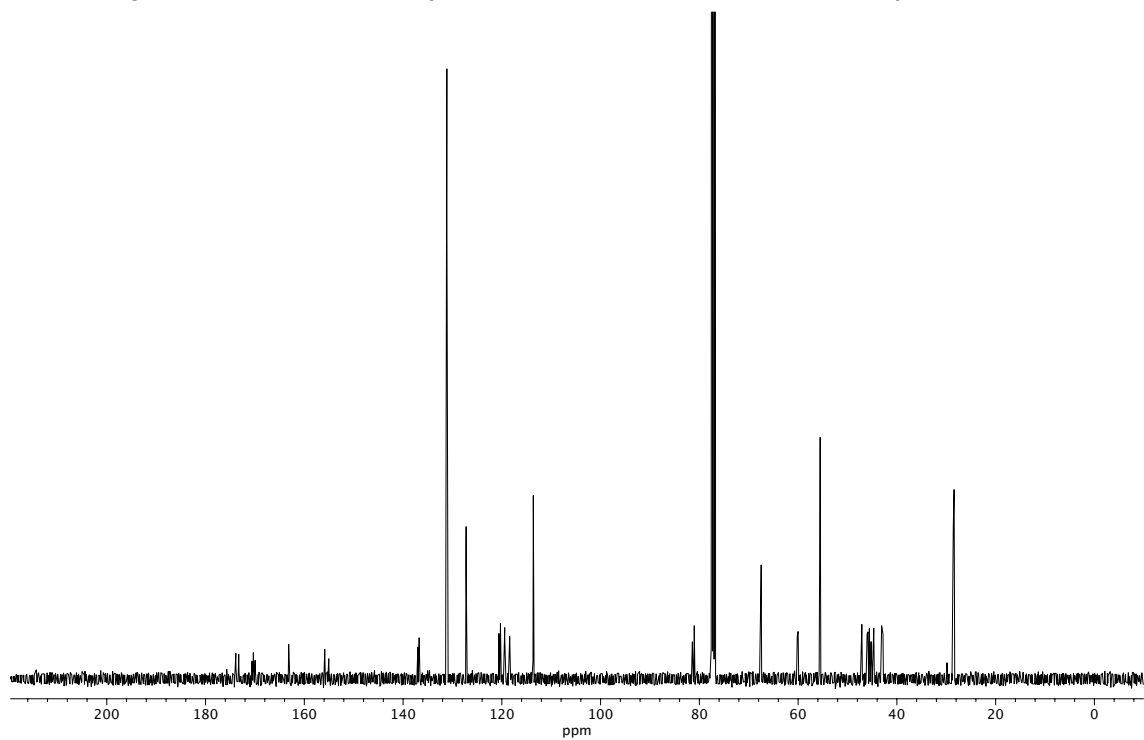
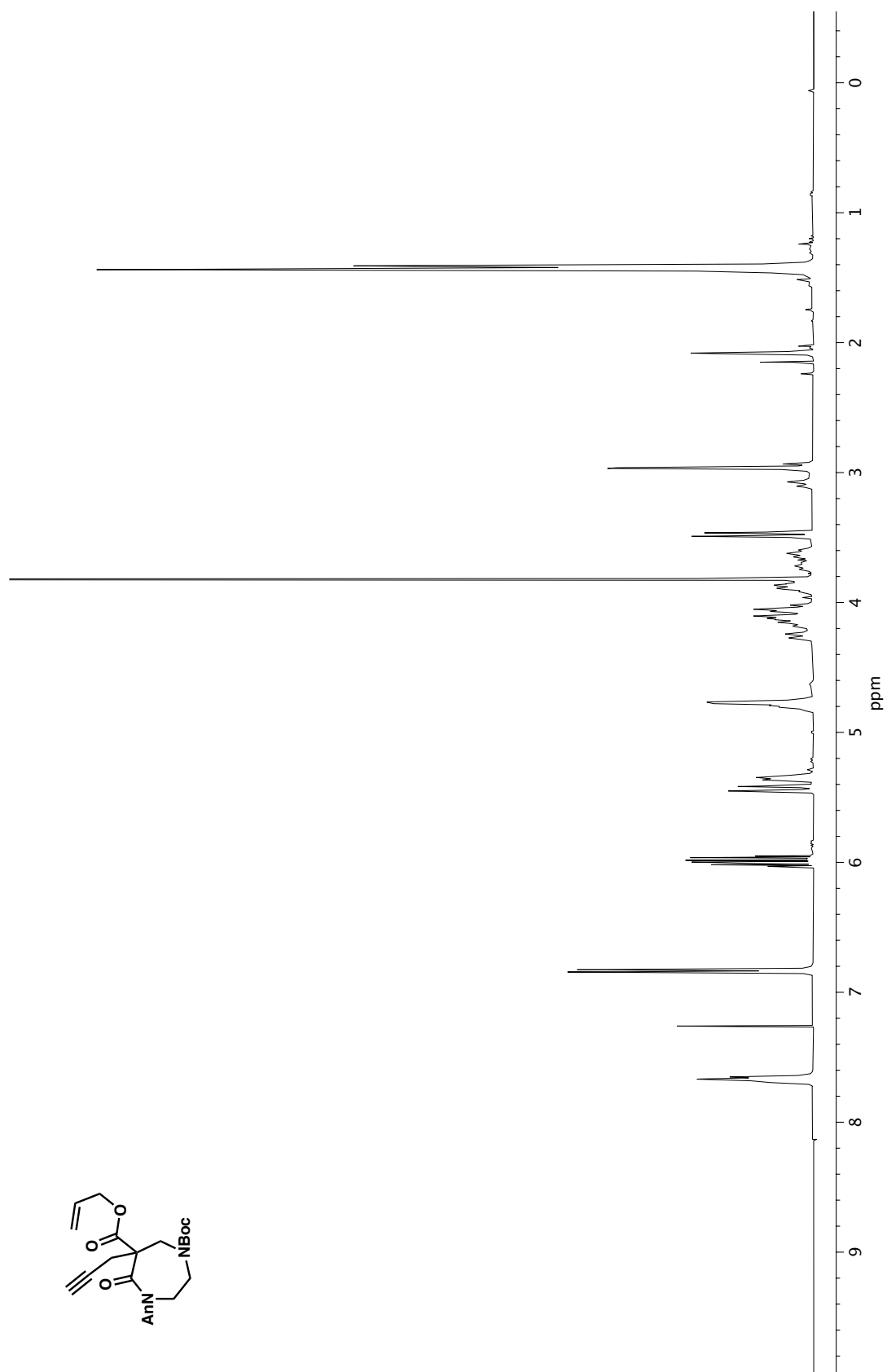


Figure A1.78. ¹³C NMR (100 MHz, CDCl₃) of compound **19h**.

Figure A1.79. ^1H NMR (500 MHz, CDCl_3) of compound **19i**.

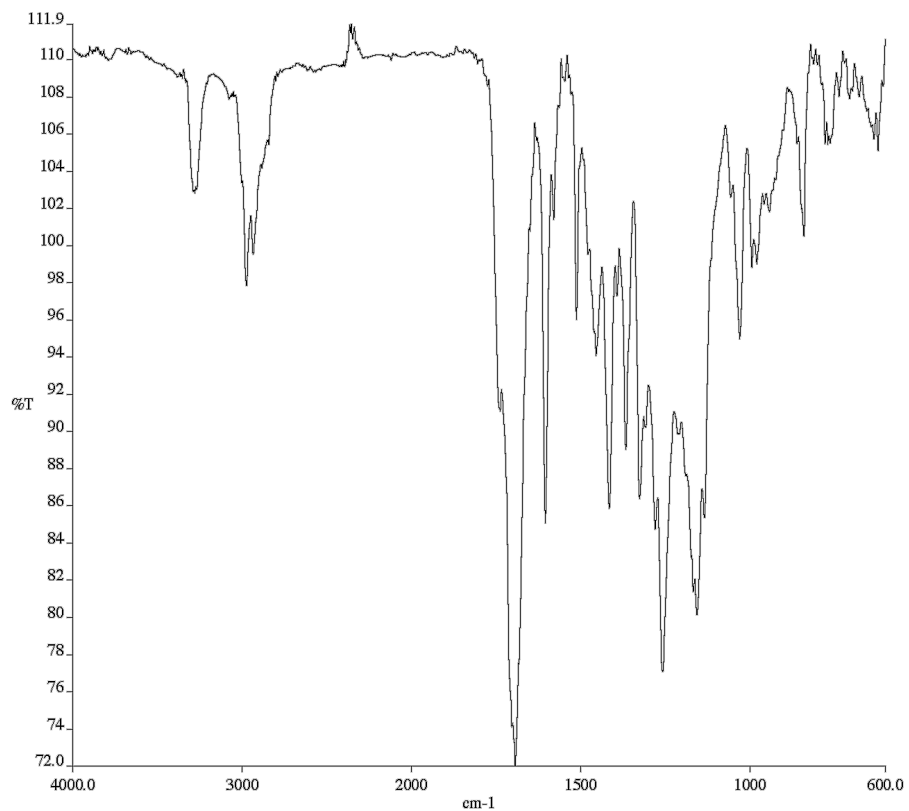


Figure A1.80. Infrared spectrum (Thin Film, NaCl) of compound **19i**.

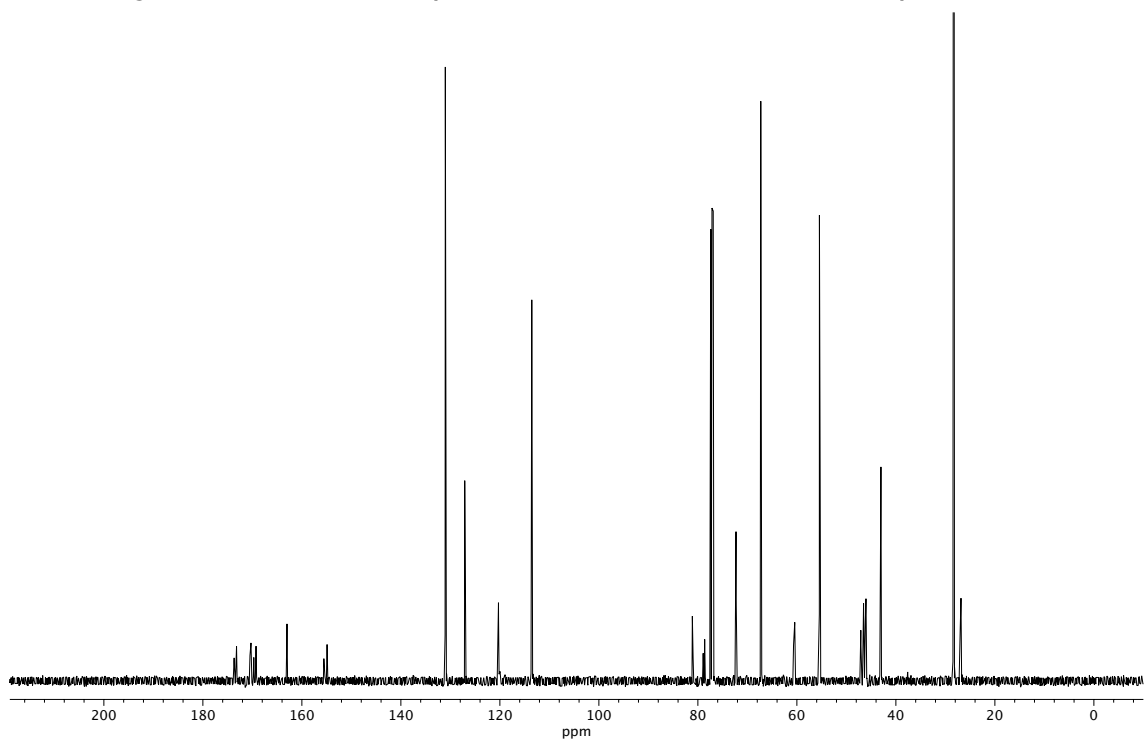
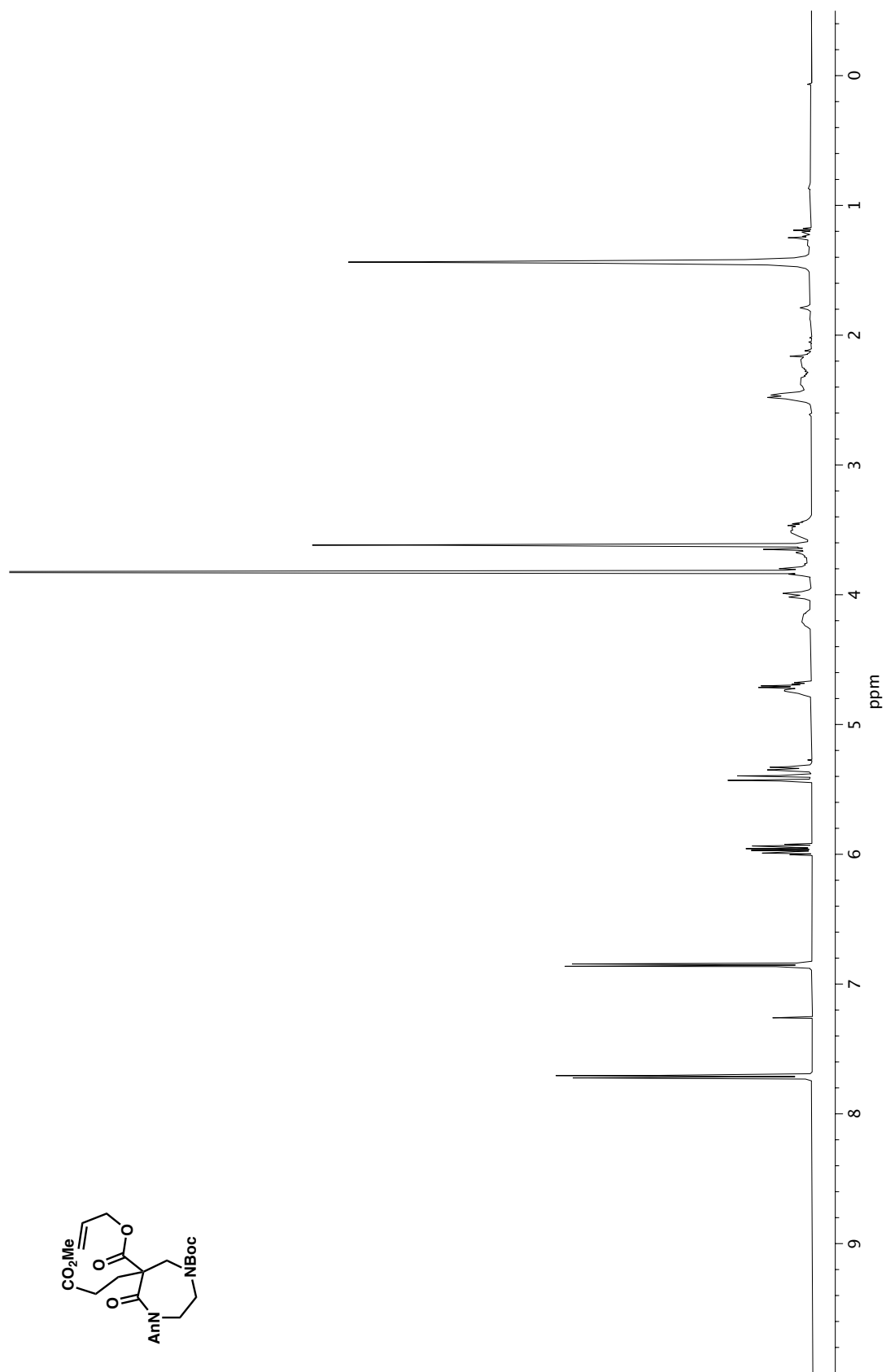


Figure A1.81. ¹³C NMR (125 MHz, CDCl₃) of compound **19i**.

Figure A1.82. ¹H NMR (500 MHz, CDCl₃) of compound **19j**.

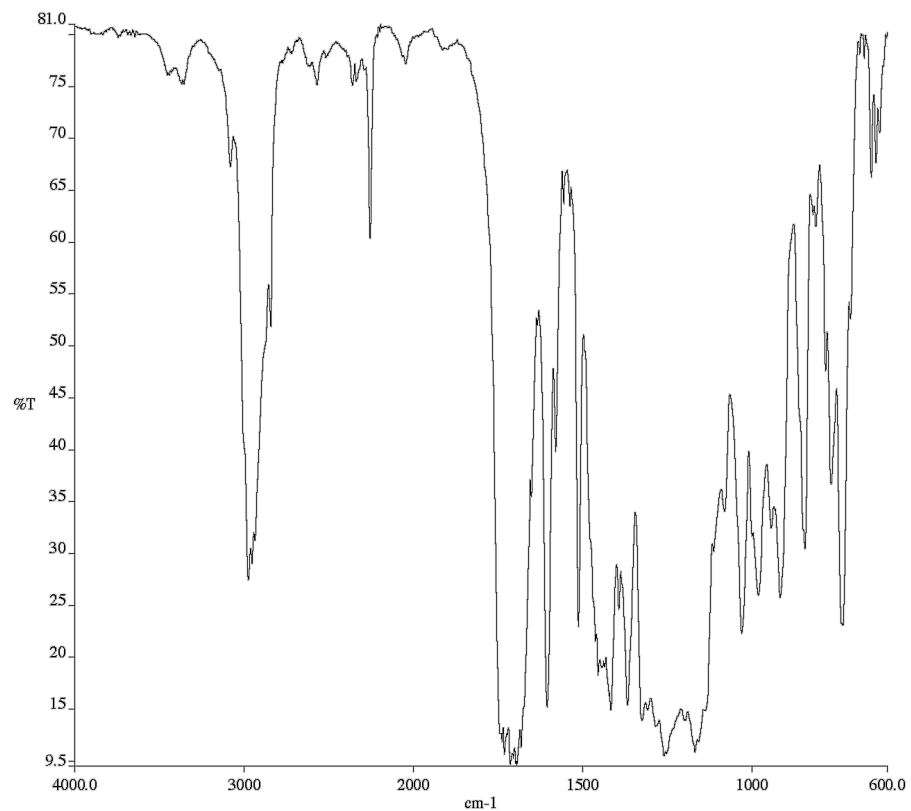


Figure A1.83. Infrared spectrum (Thin Film, NaCl) of compound **19j**.

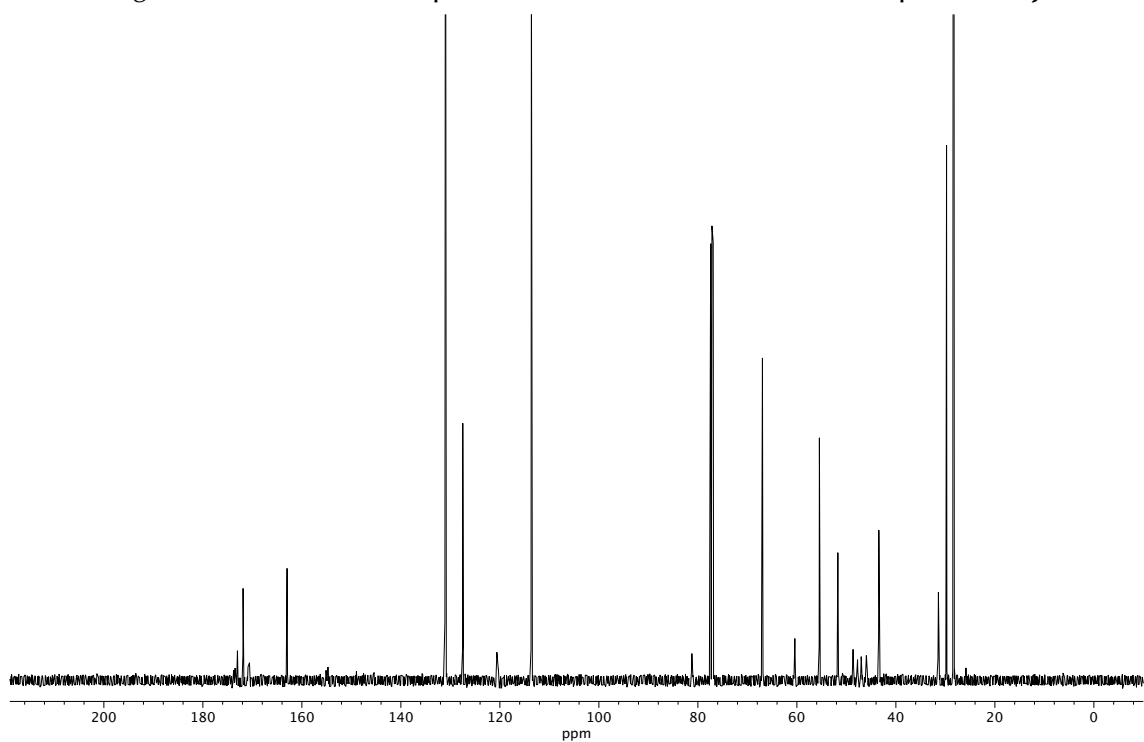
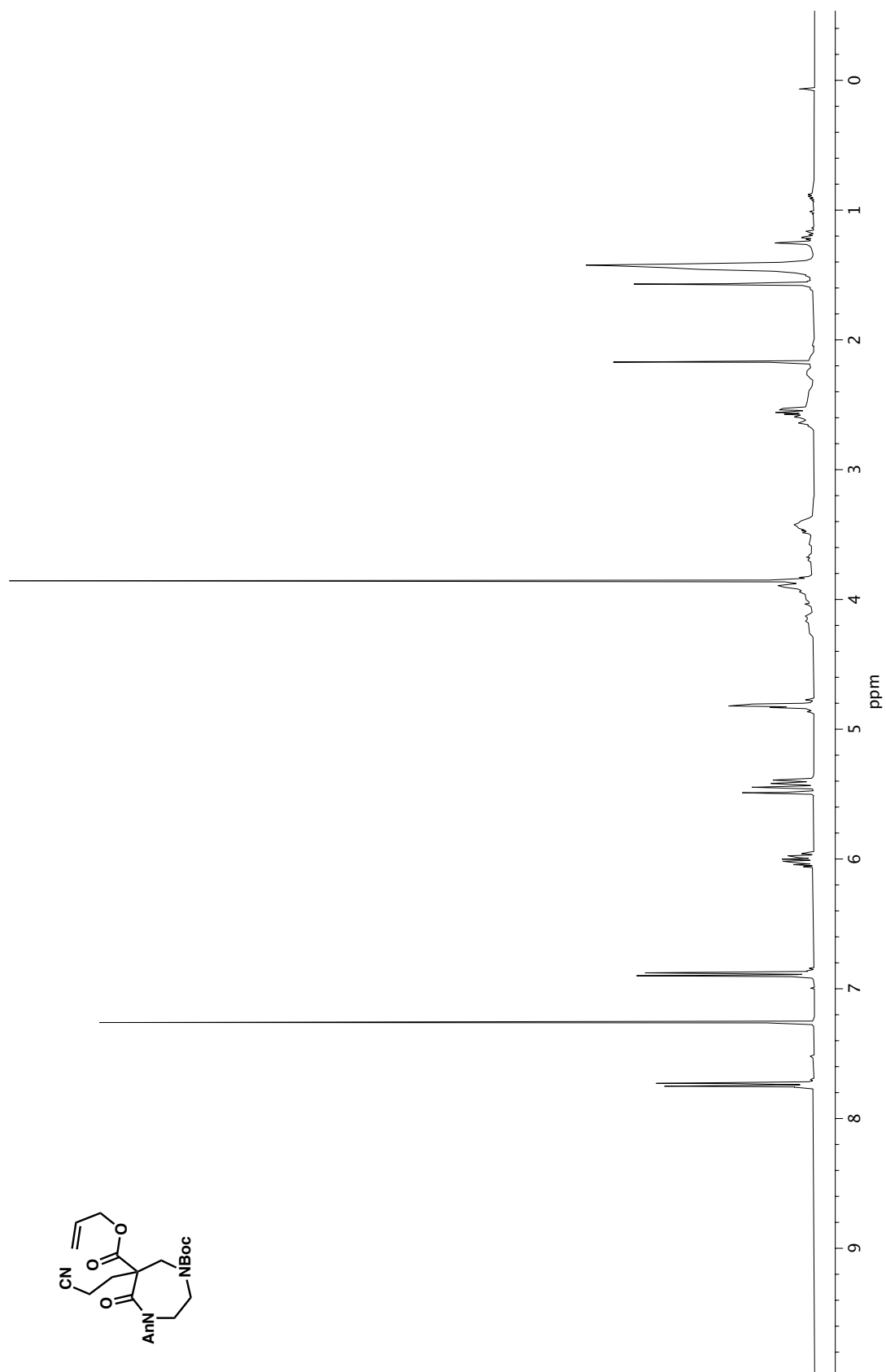


Figure A1.84. ¹³C NMR (125 MHz, CDCl₃) of compound **19j**.

Figure A1.85. ^1H NMR (400 MHz, CDCl_3) of compound **19k**.

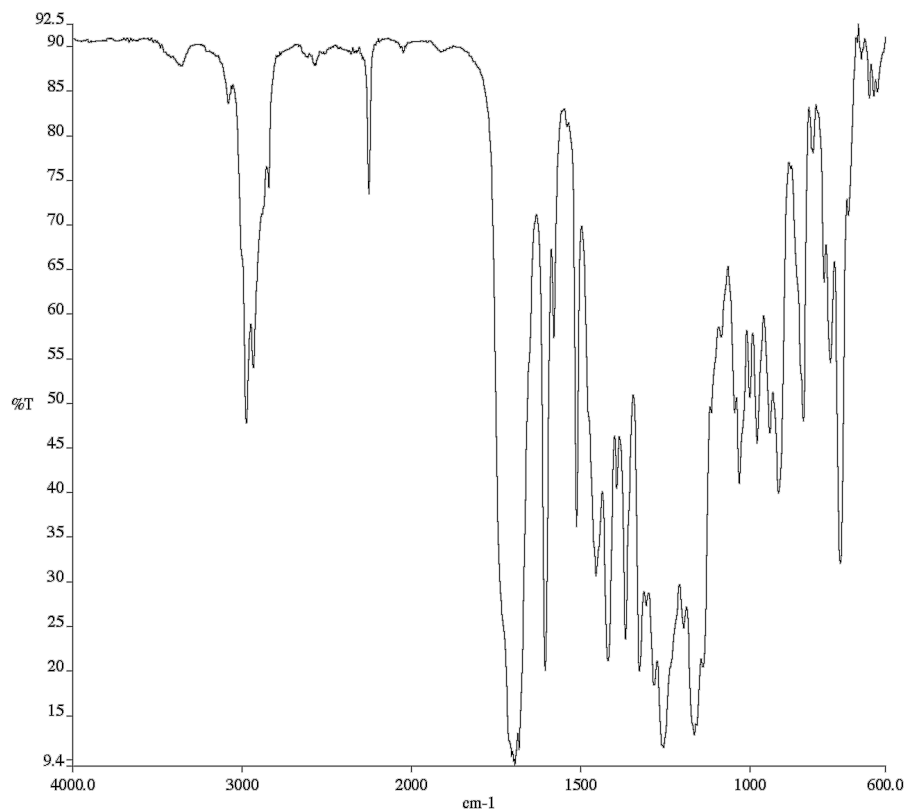


Figure A1.86. Infrared spectrum (Thin Film, NaCl) of compound **19k**.

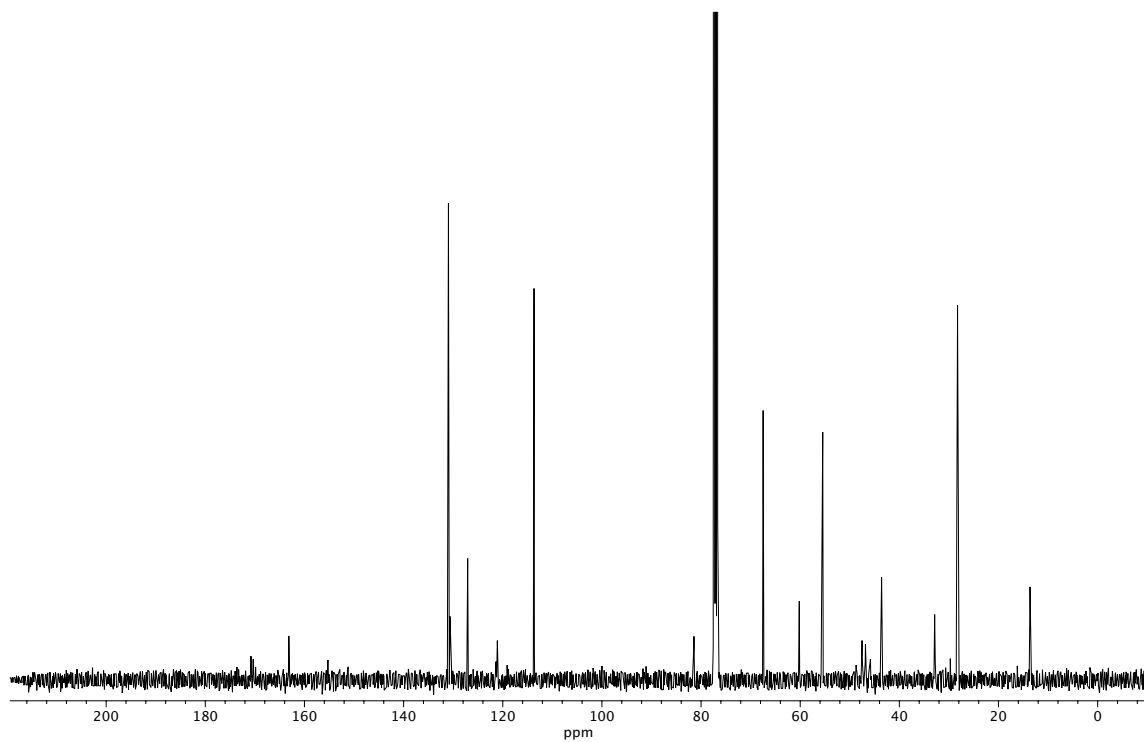
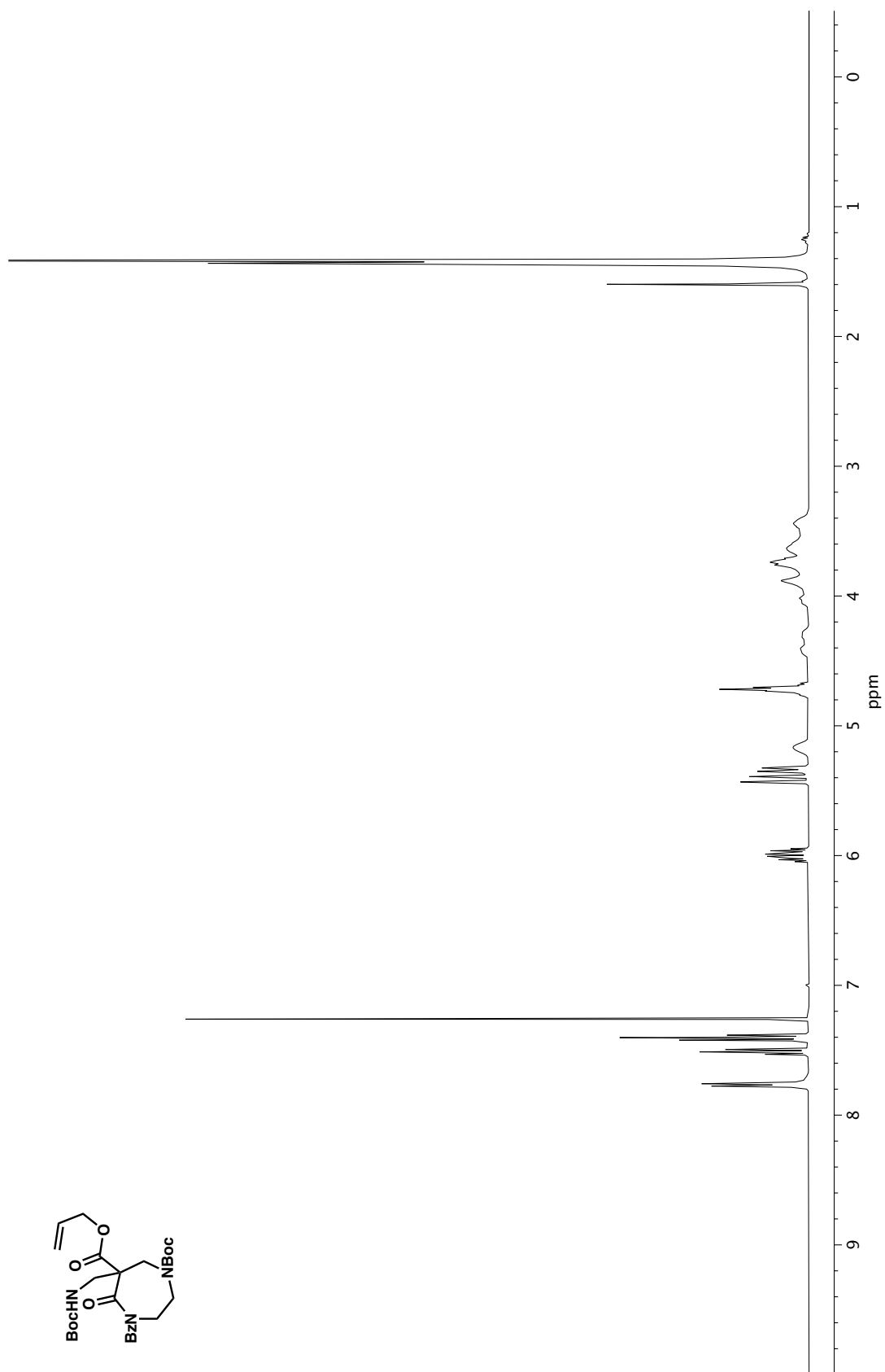


Figure A1.87. ¹³C NMR (100 MHz, CDCl₃) of compound **19k**.

Figure A1.88. ^1H NMR (400 MHz, CDCl_3) of compound **19I**.

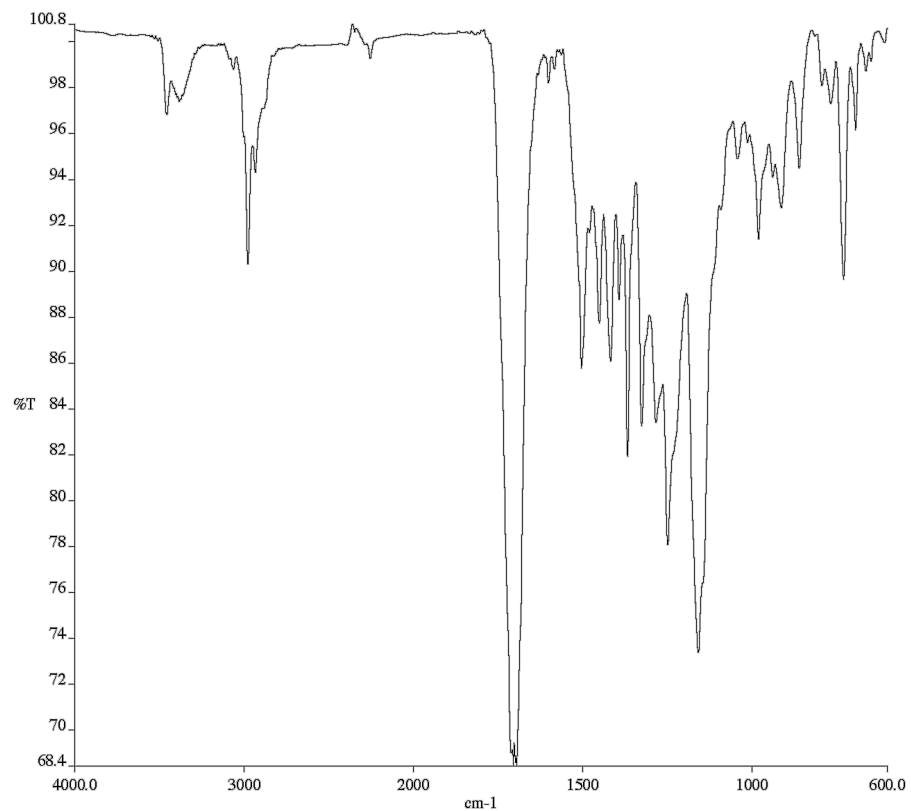


Figure A1.89. Infrared spectrum (Thin Film, NaCl) of compound **19I**.

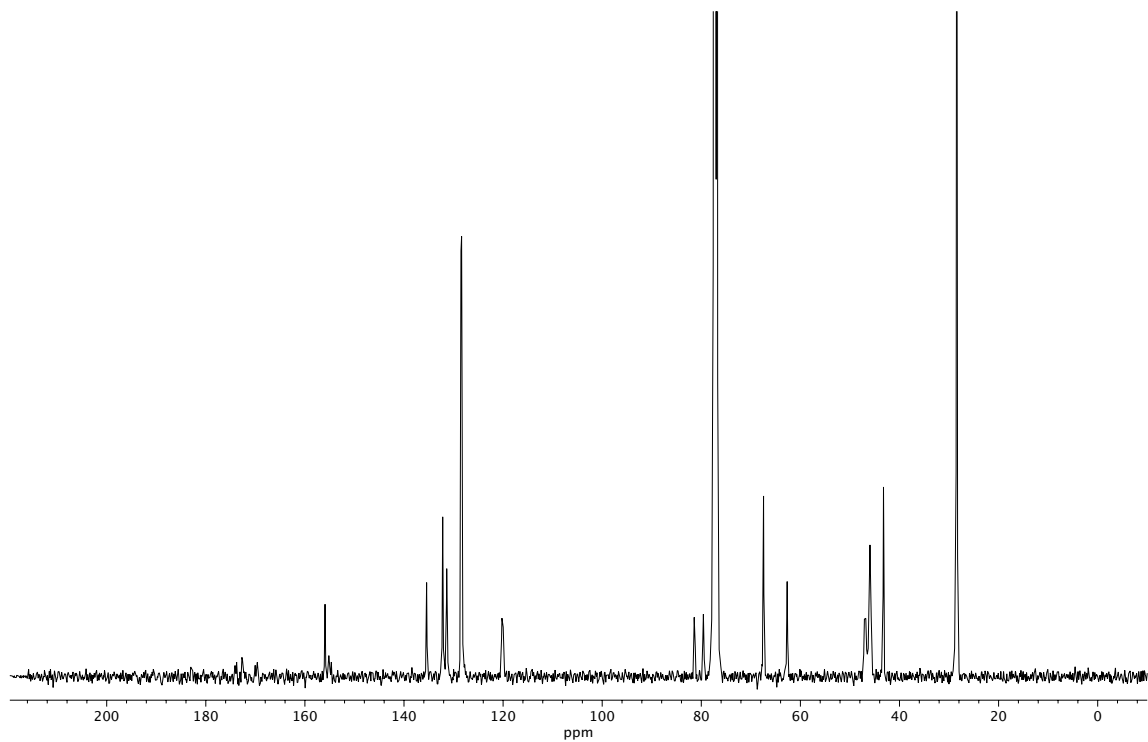


Figure A1.90. ¹³C NMR (100 MHz, CDCl₃) of compound **19I**.

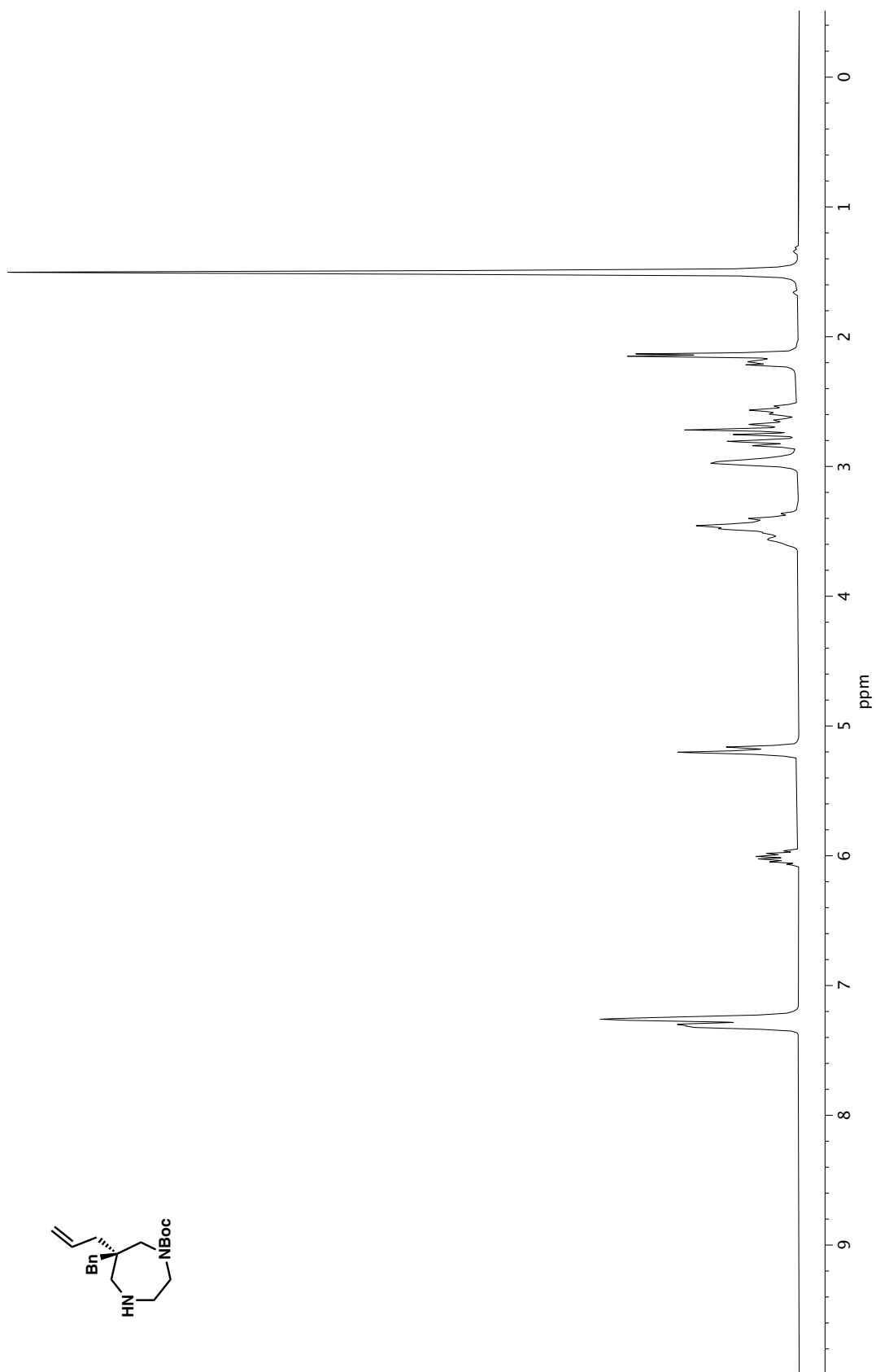


Figure A1.91. ^1H NMR (400 MHz, CDCl_3) of compound **21**.

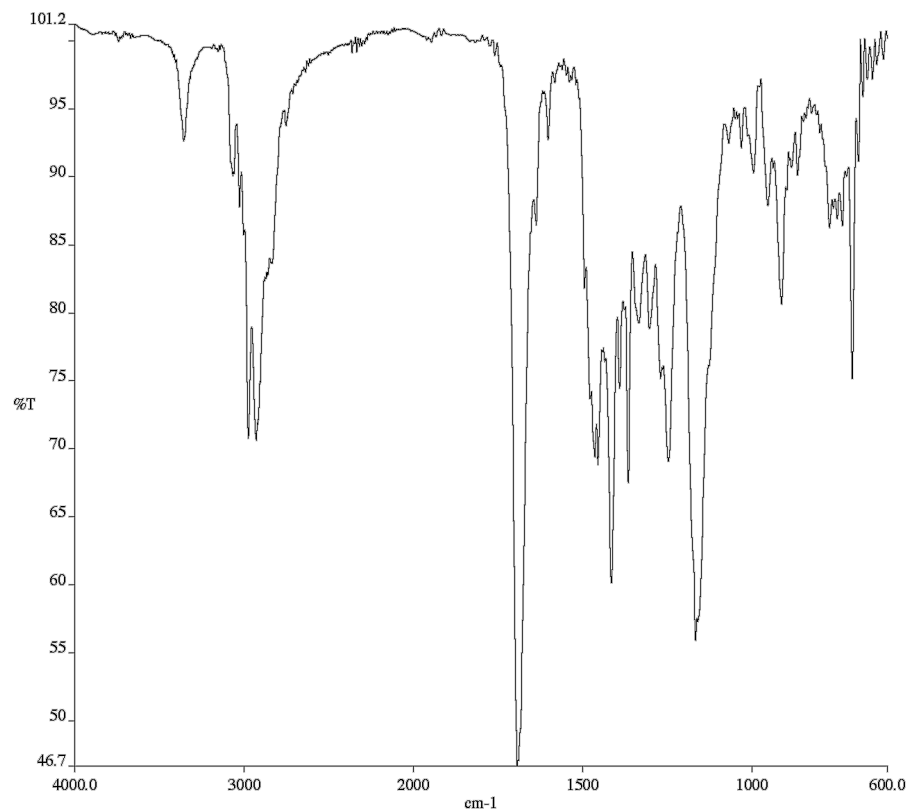


Figure A1.92. Infrared spectrum (Thin Film, NaCl) of compound **21**.

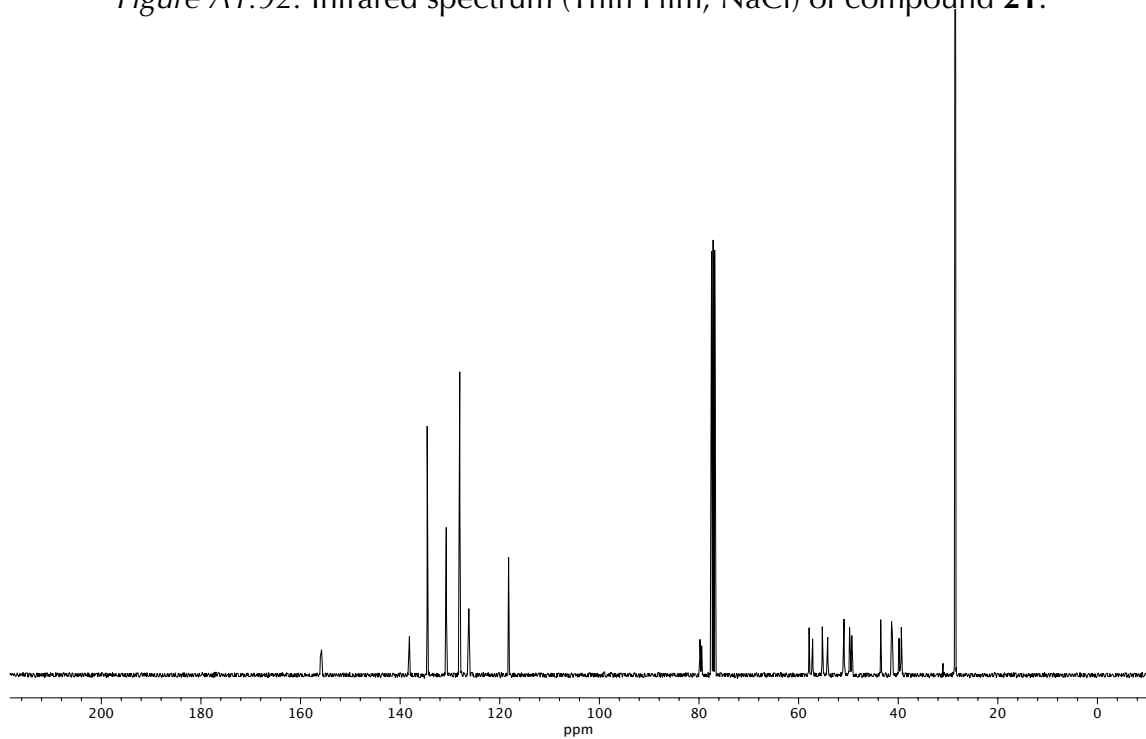
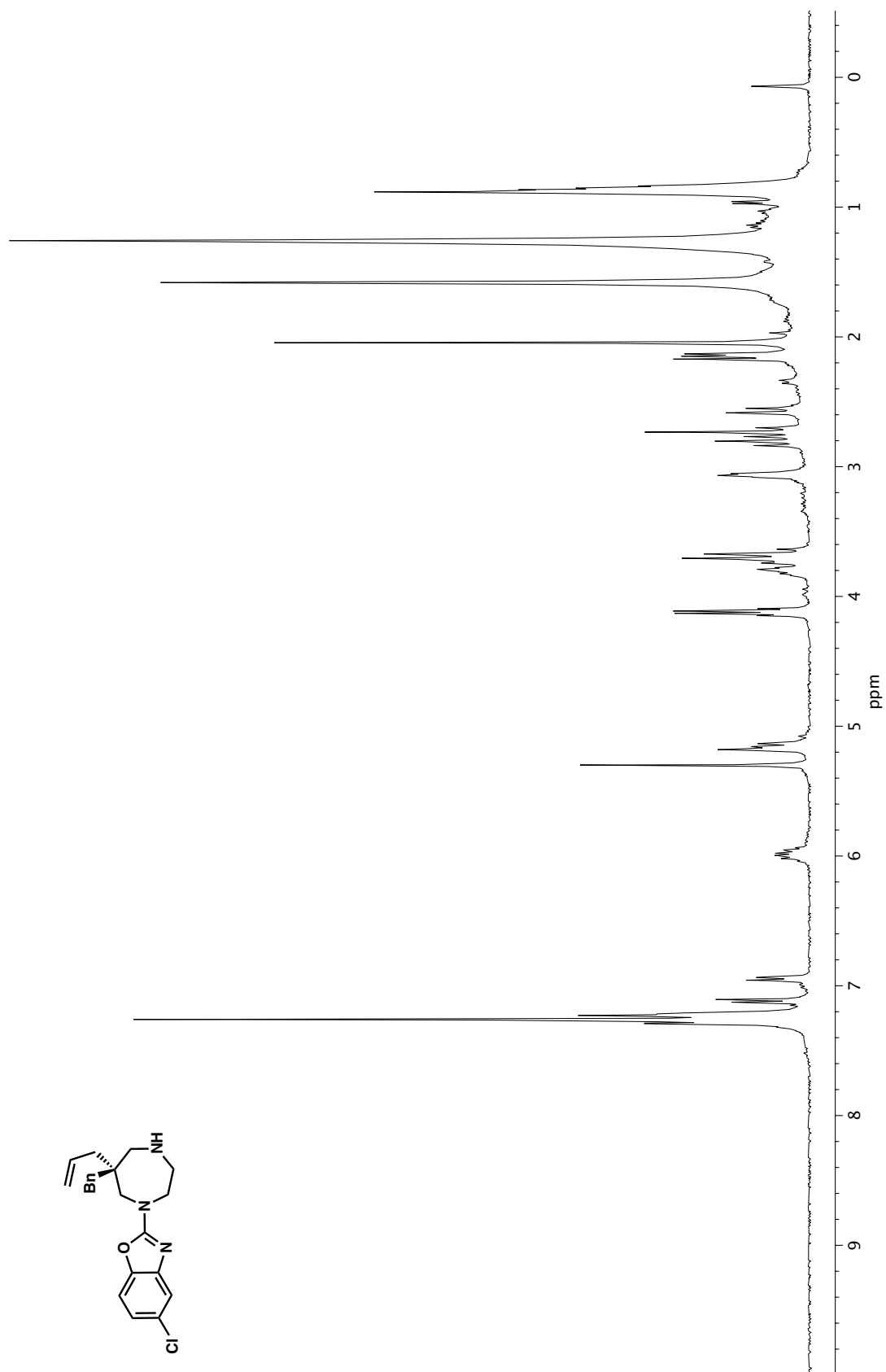


Figure A1.93. ¹³C NMR (100 MHz, CDCl₃) of compound **21**.

Figure A1.94. ¹H NMR (400 MHz, CDCl₃) of compound 23.

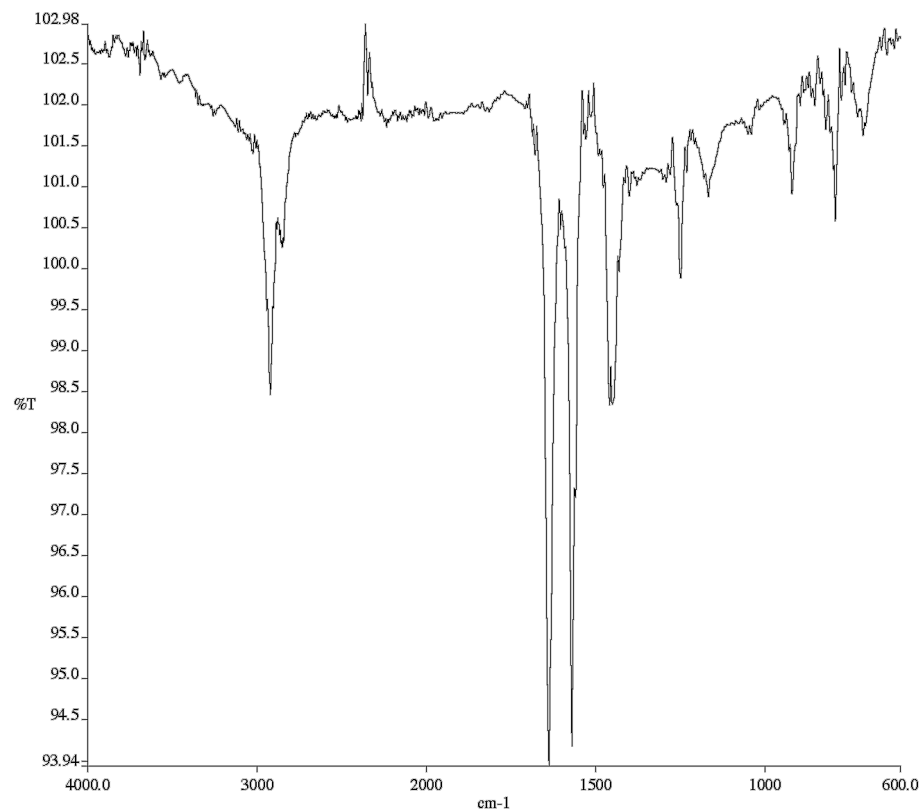


Figure A1.95. Infrared spectrum (Thin Film, NaCl) of compound **23**.

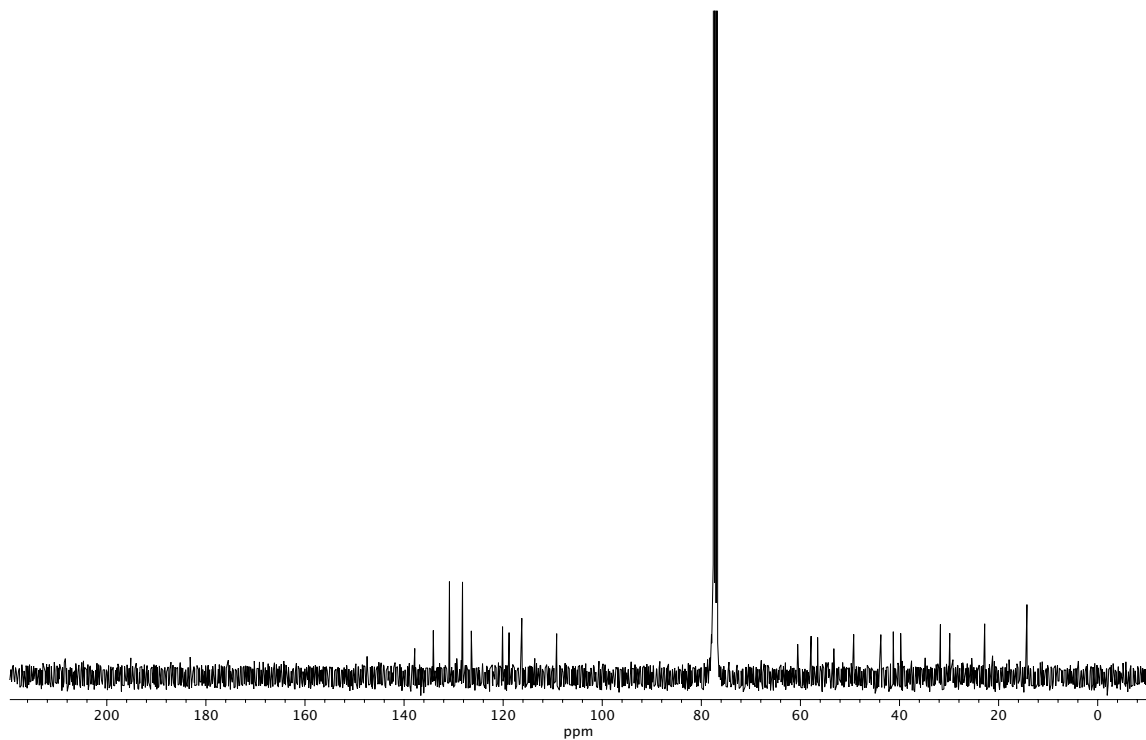
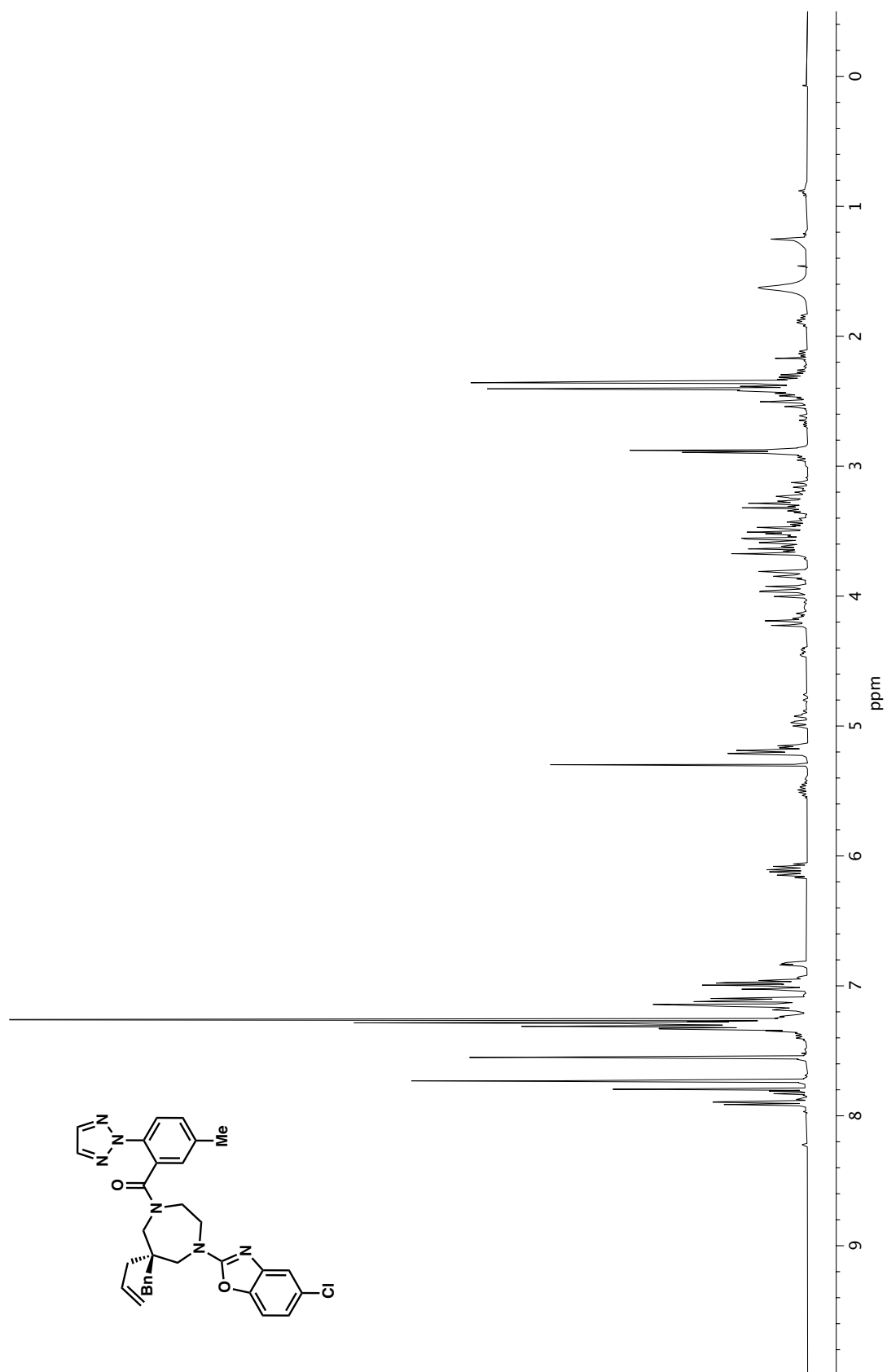


Figure A1.96. ¹³C NMR (100 MHz, CDCl₃) of compound **23**.

Figure A1.97. ¹H NMR (400 MHz, CDCl₃) of compound 25.

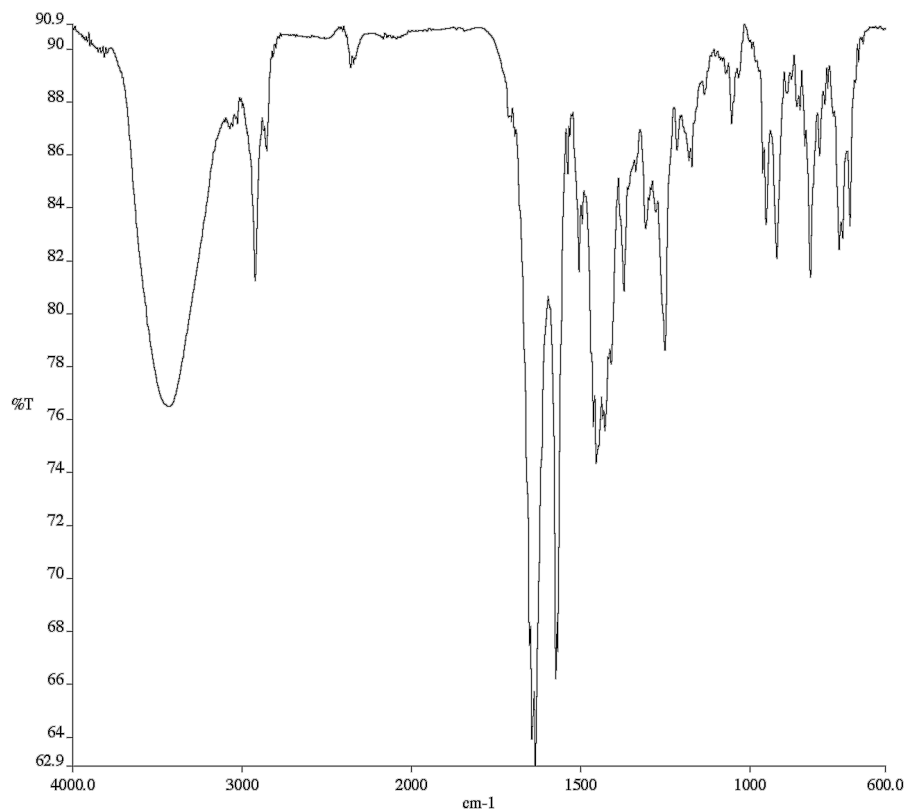


Figure A1.98. Infrared spectrum (Thin Film, NaCl) of compound **25**.

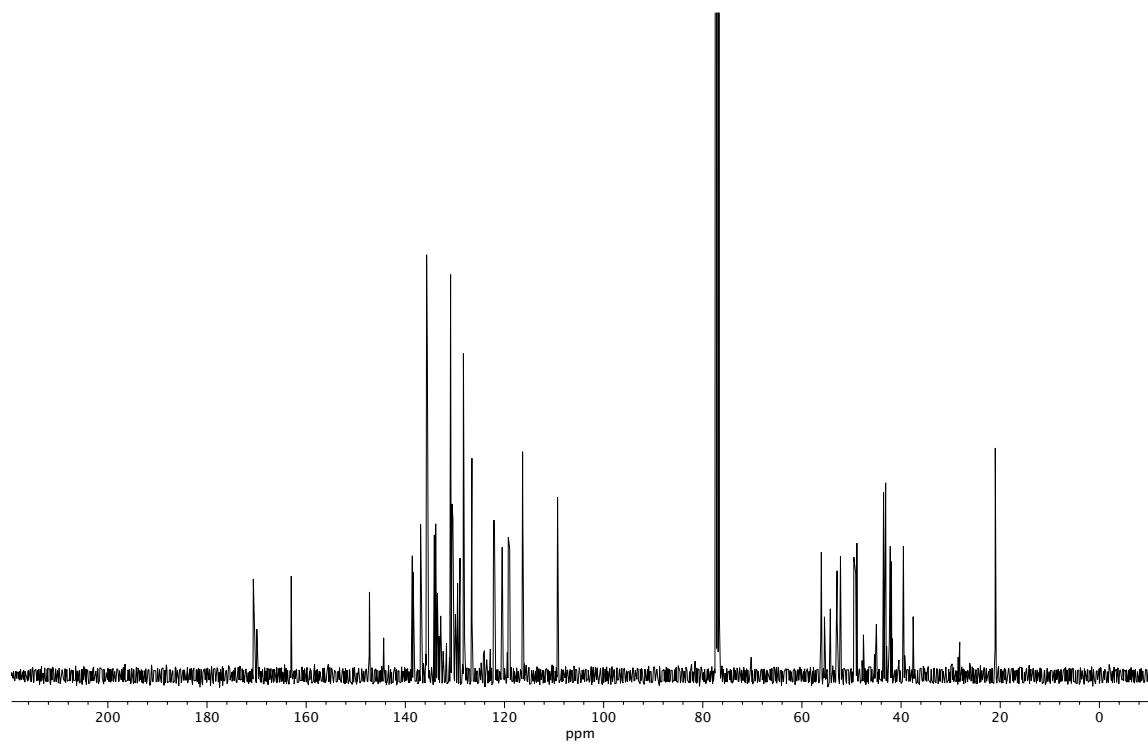
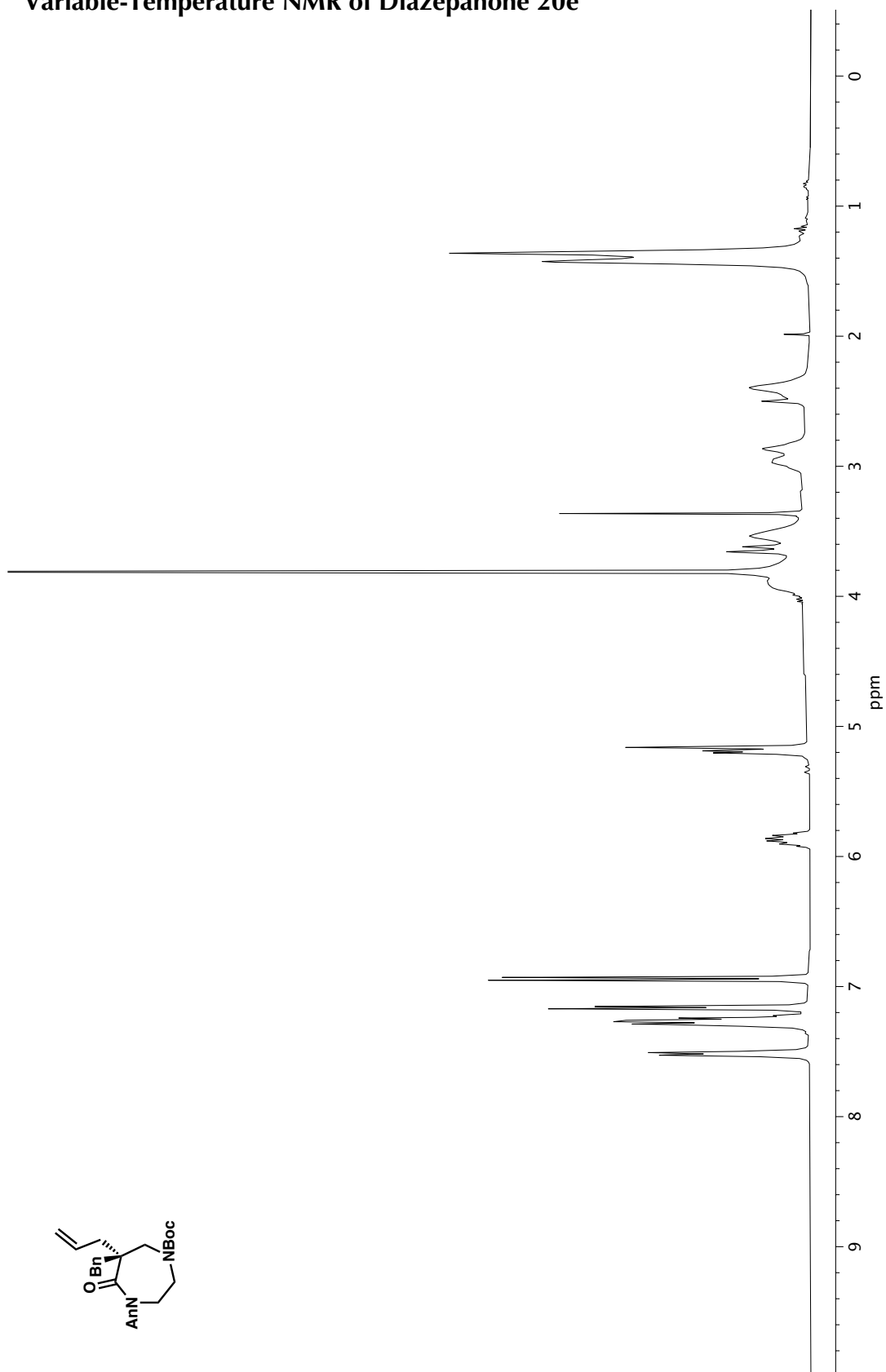
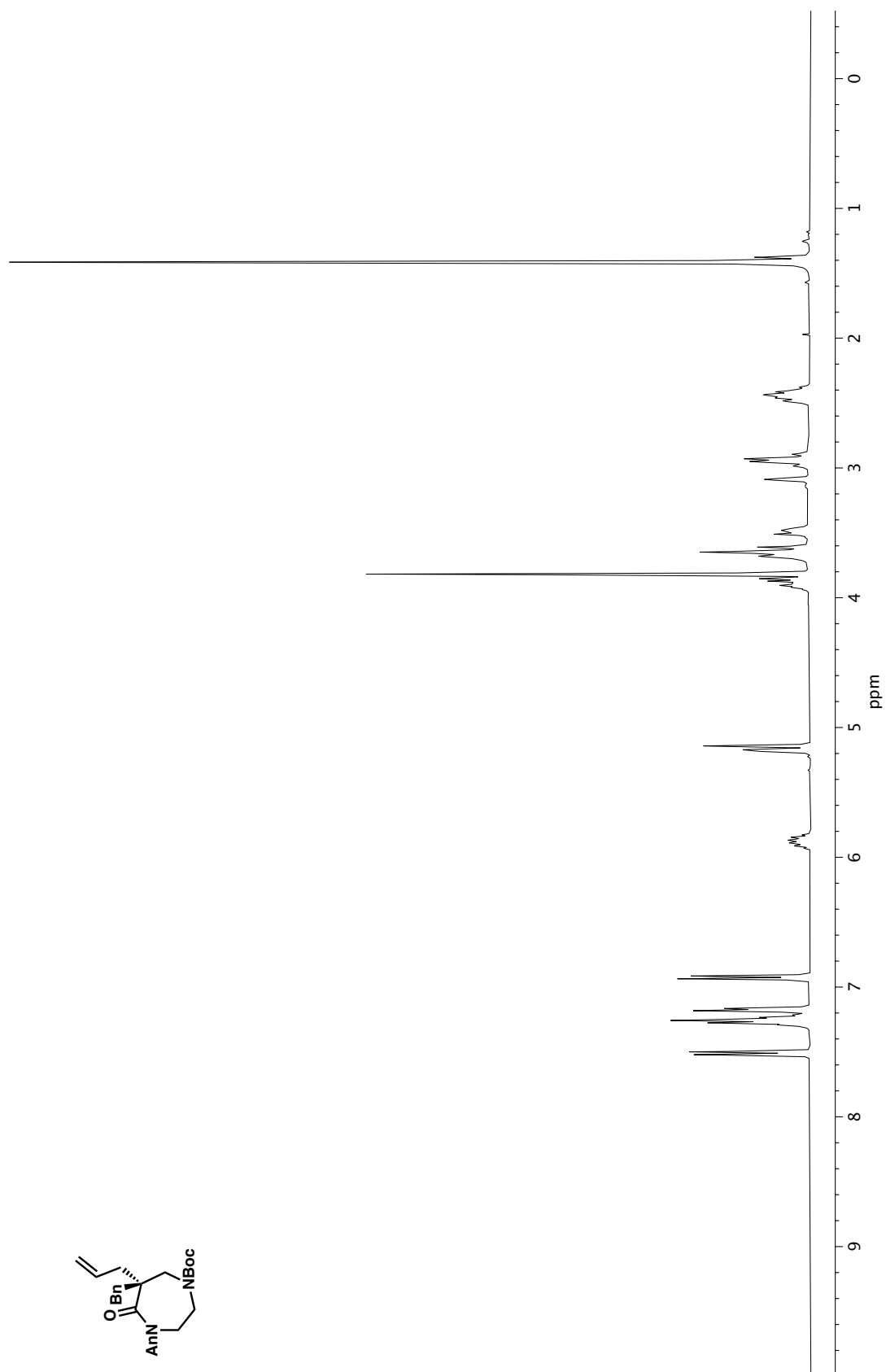


Figure A1.99. ¹³C NMR (100 MHz, CDCl₃) of compound **25**.

Variable-Temperature NMR of Diazepanone **20e**Figure A1.100. ¹H NMR (400 MHz, DMSO-d₆, 23.3 °C) of compound **20e**.

Figure A1.101. ¹H NMR (400 MHz, DMSO-*d*₆, 80 °C) of compound **20e**.

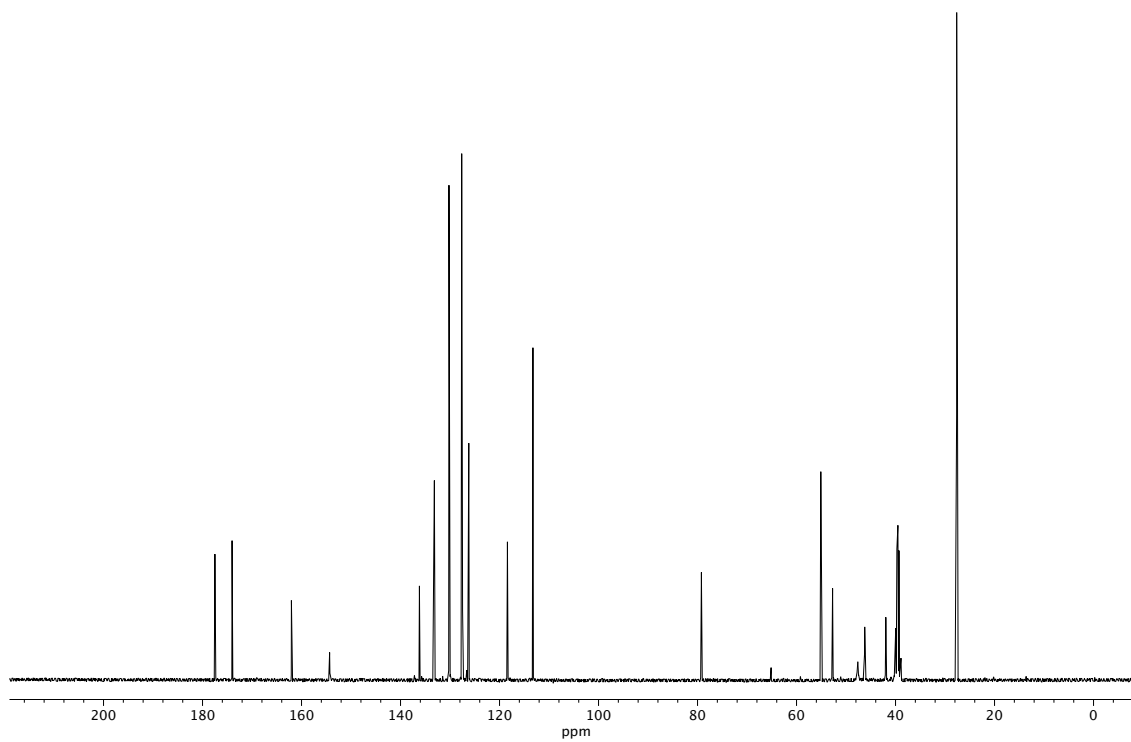
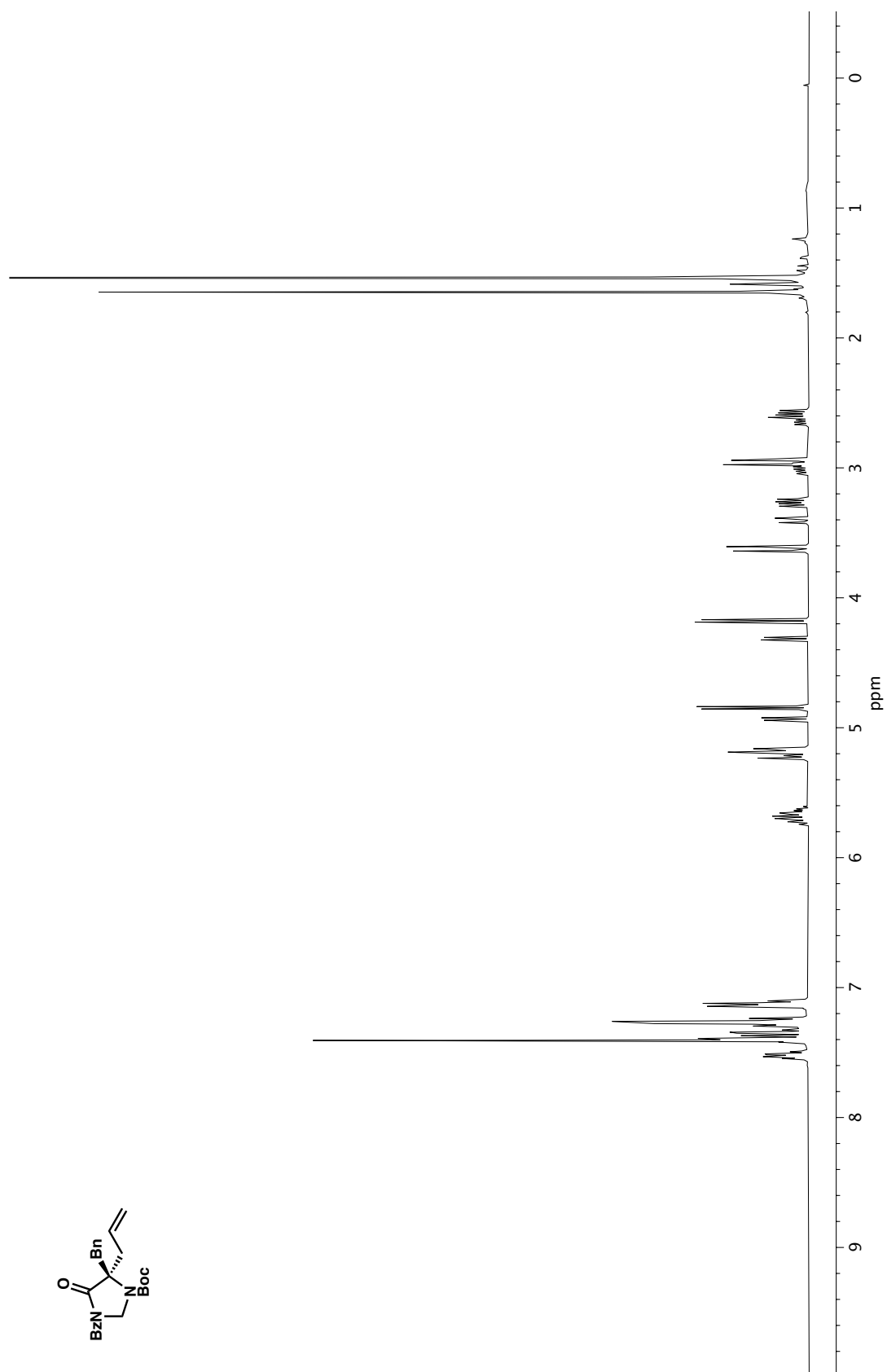


Figure A1.102. ^{13}C NMR (100 MHz, $\text{DMSO-}d_6$, 80 °C) of compound **20e**.

Figure A1.103. ¹H NMR (400 MHz, CDCl₃) of compound 35a.

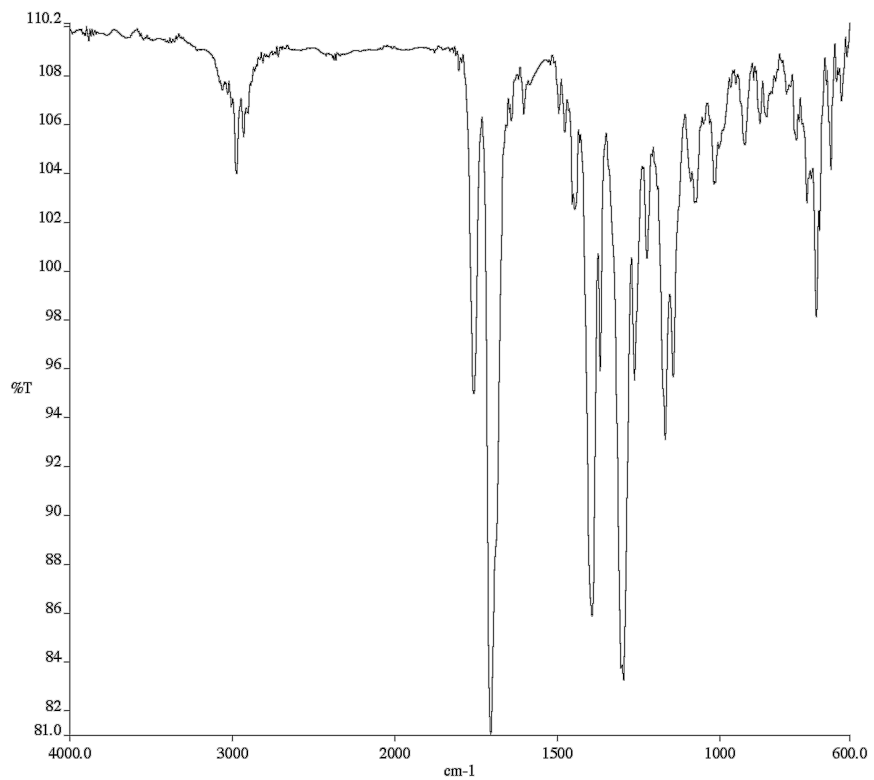


Figure A1.104. Infrared spectrum (Thin Film, NaCl) of compound **35a**.

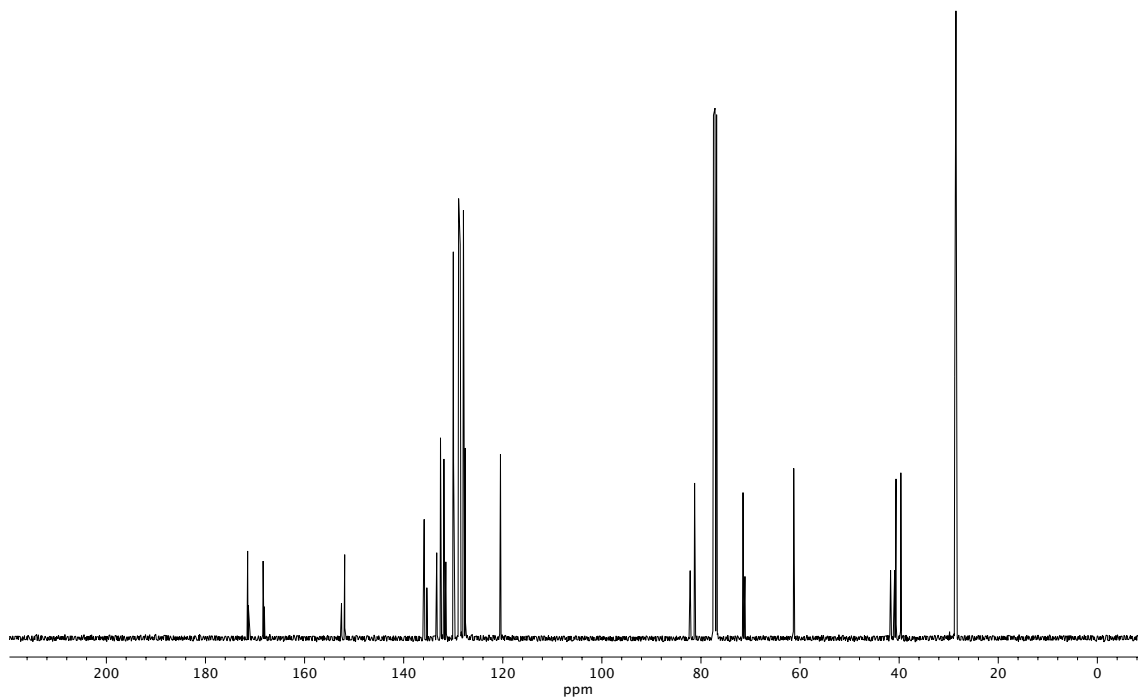
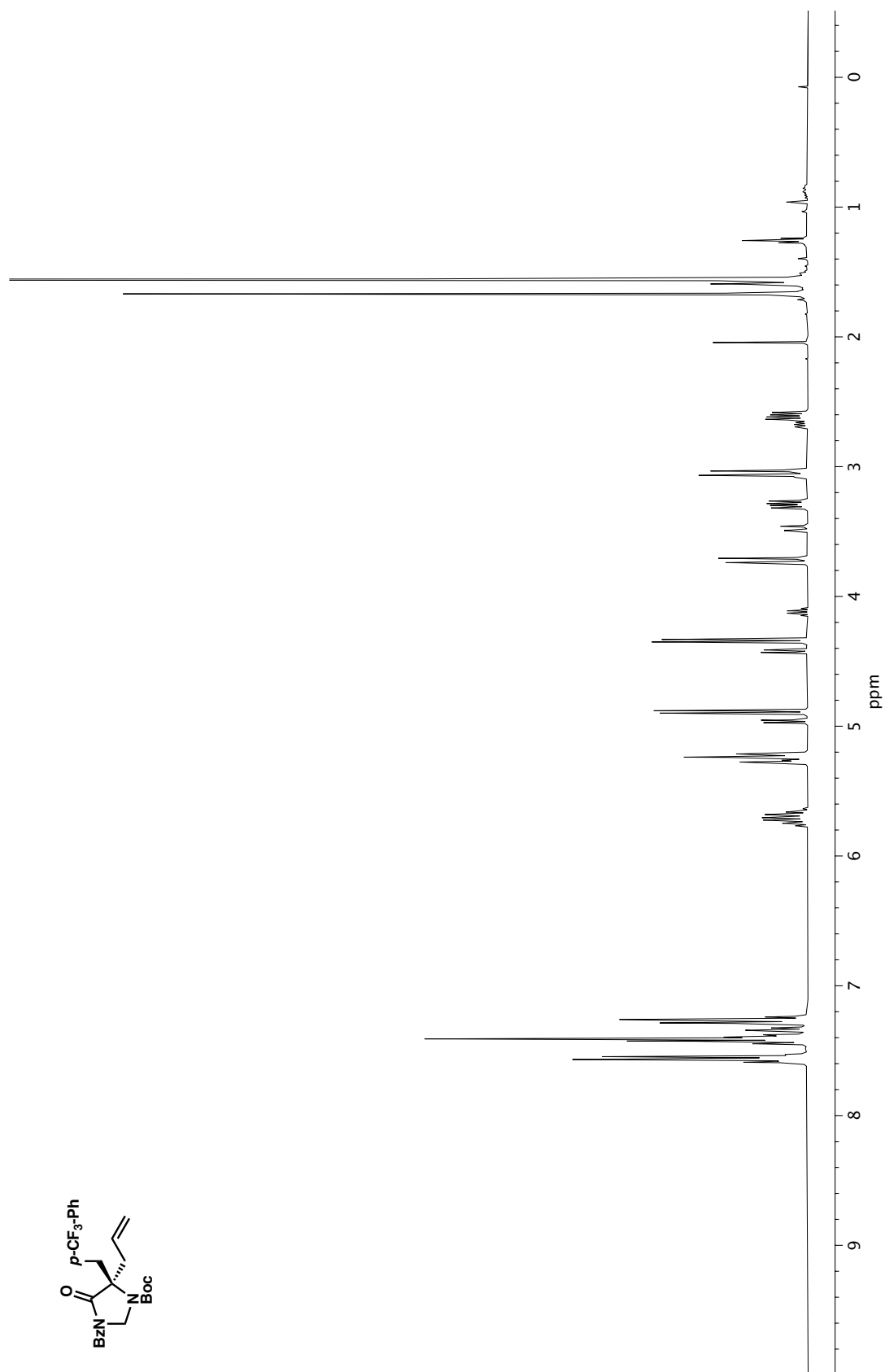


Figure A1.105. ¹³C NMR (100 MHz, CDCl₃) of compound **35a**.

Figure A1.106. ^1H NMR (400 MHz, CDCl_3) of compound **35b**.

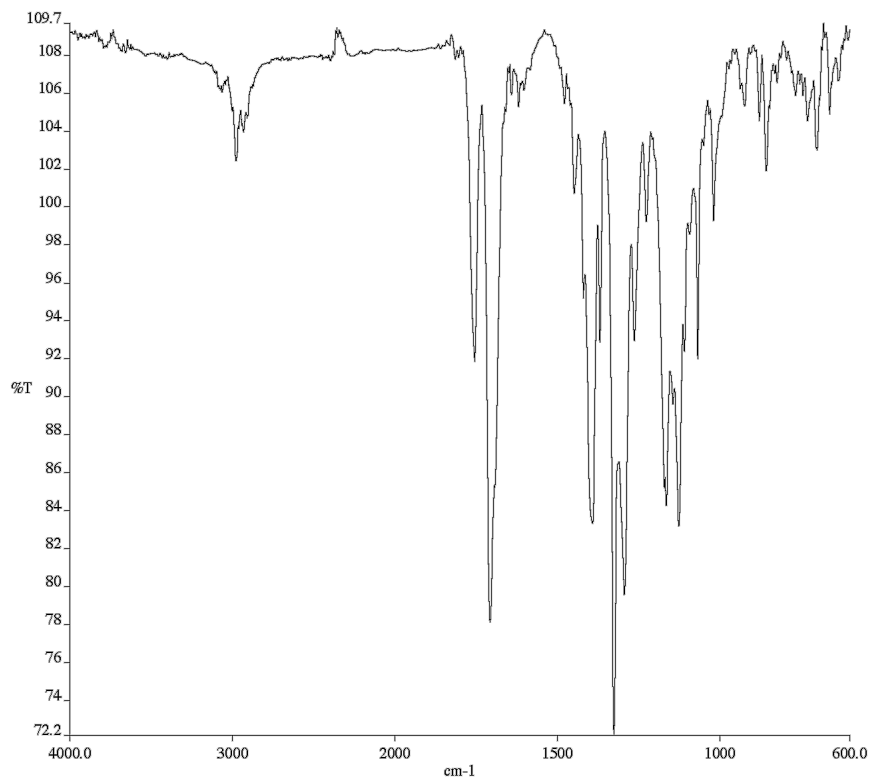


Figure A1.107. Infrared spectrum (Thin Film, NaCl) of compound **35b**.

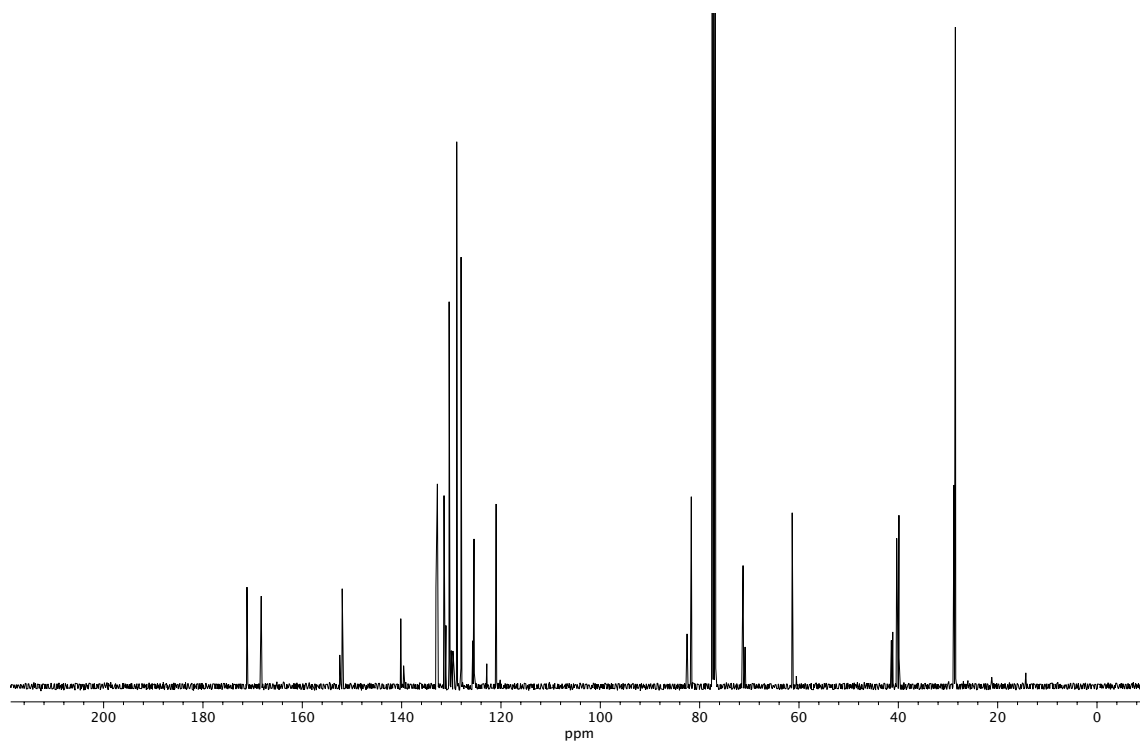


Figure A1.108. ¹³C NMR (100 MHz, CDCl₃) of compound **35b**.

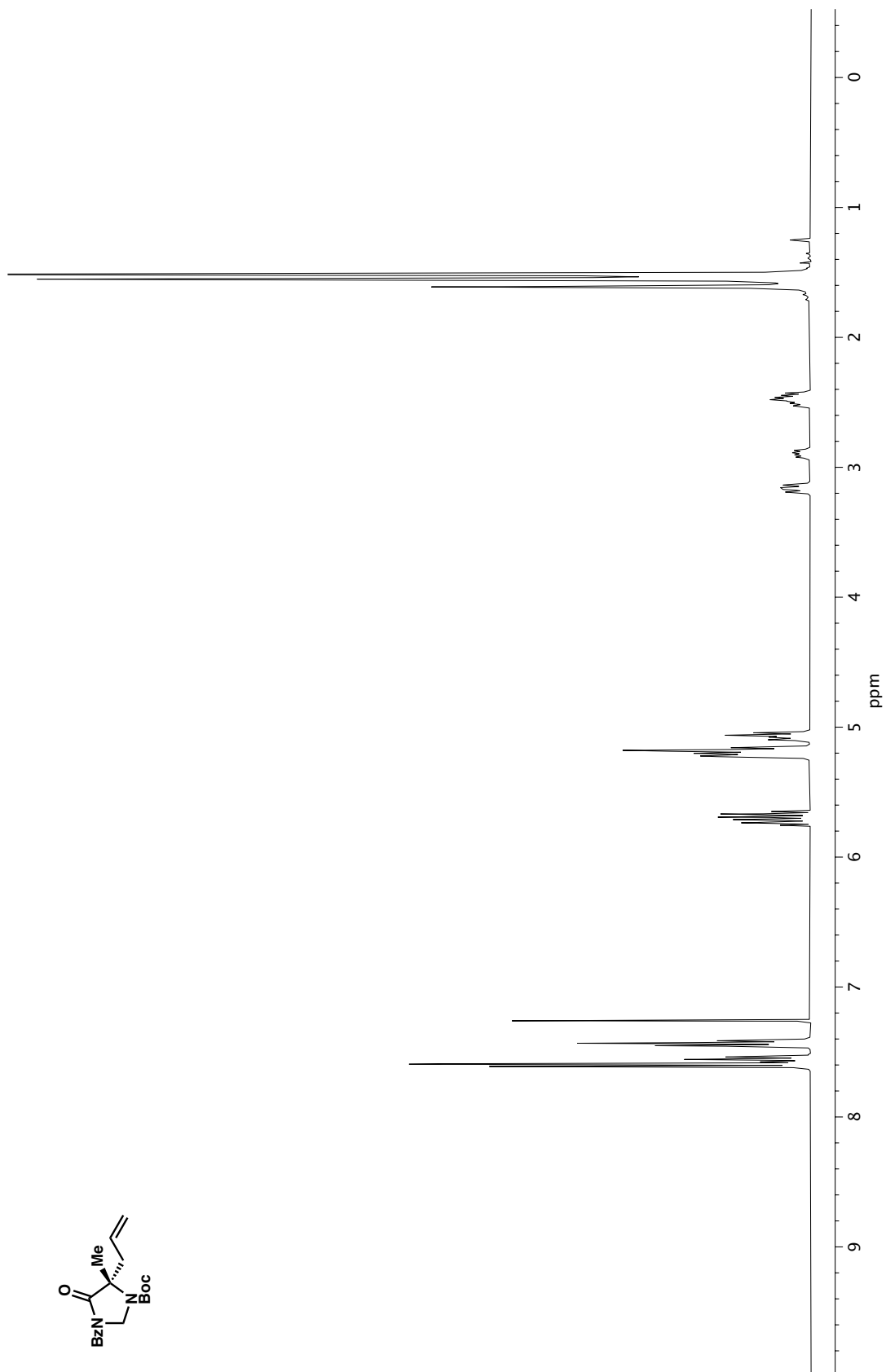


Figure A1.109. ^1H NMR (400 MHz, CDCl_3) of compound **35c**.

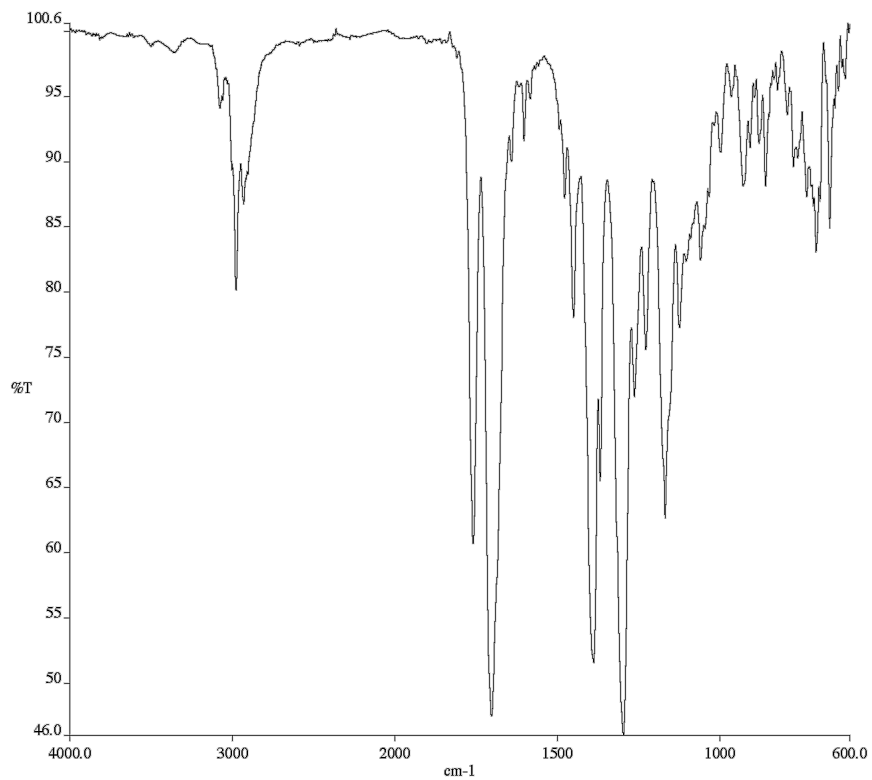


Figure A1.110. Infrared spectrum (Thin Film, NaCl) of compound **35c**.

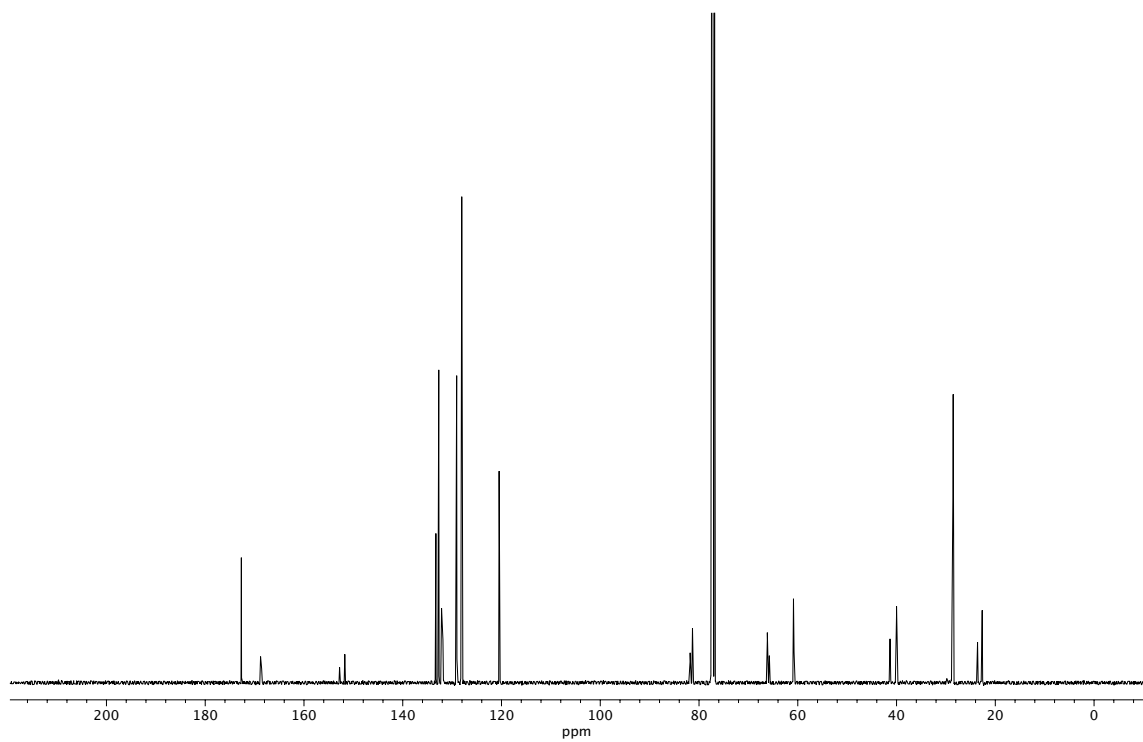
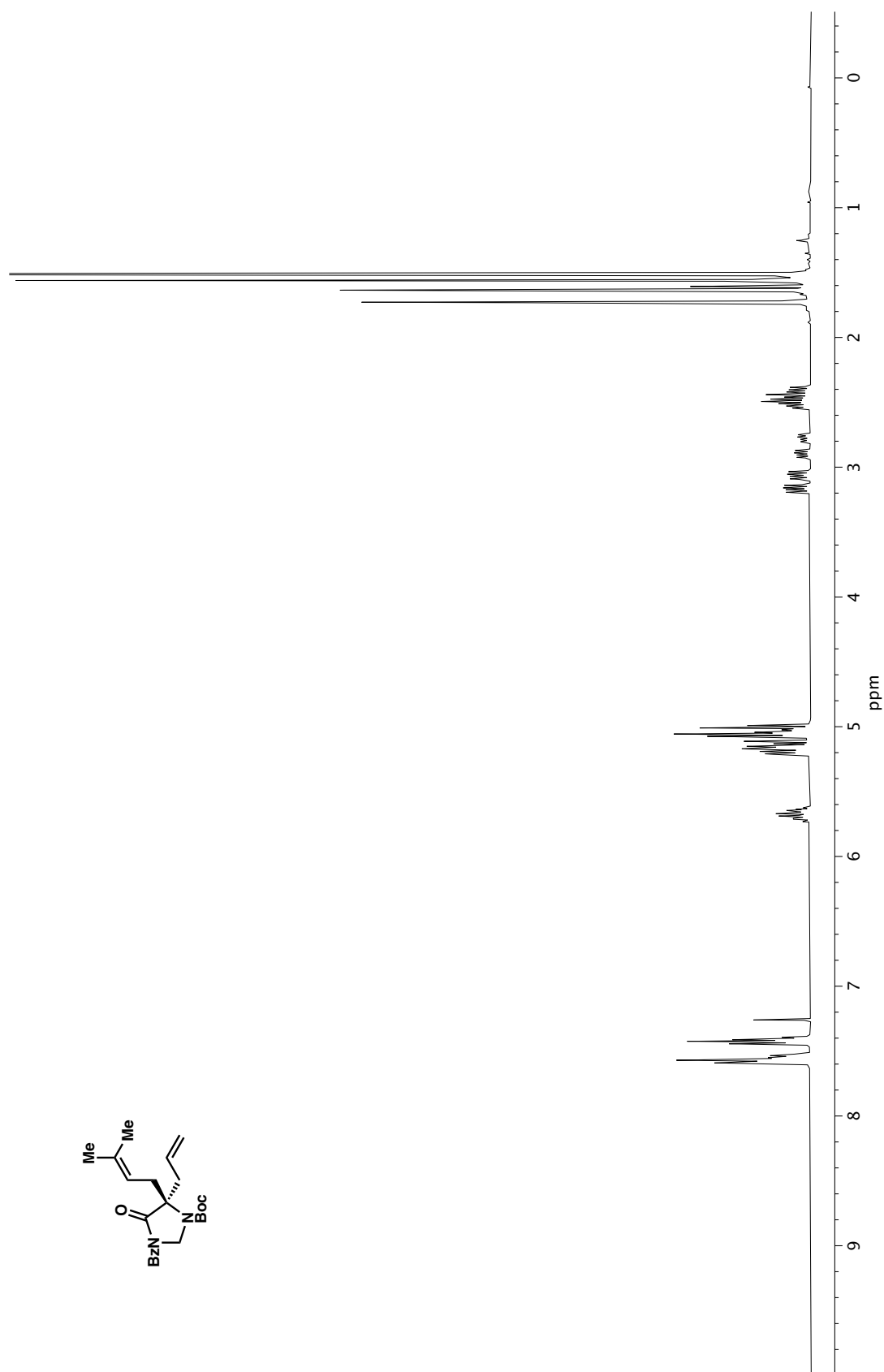


Figure A1.111. ^{13}C NMR (100 MHz, CDCl_3) of compound **35c**.

Figure A1.112. ¹H NMR (400 MHz, CDCl₃) of compound 35d.

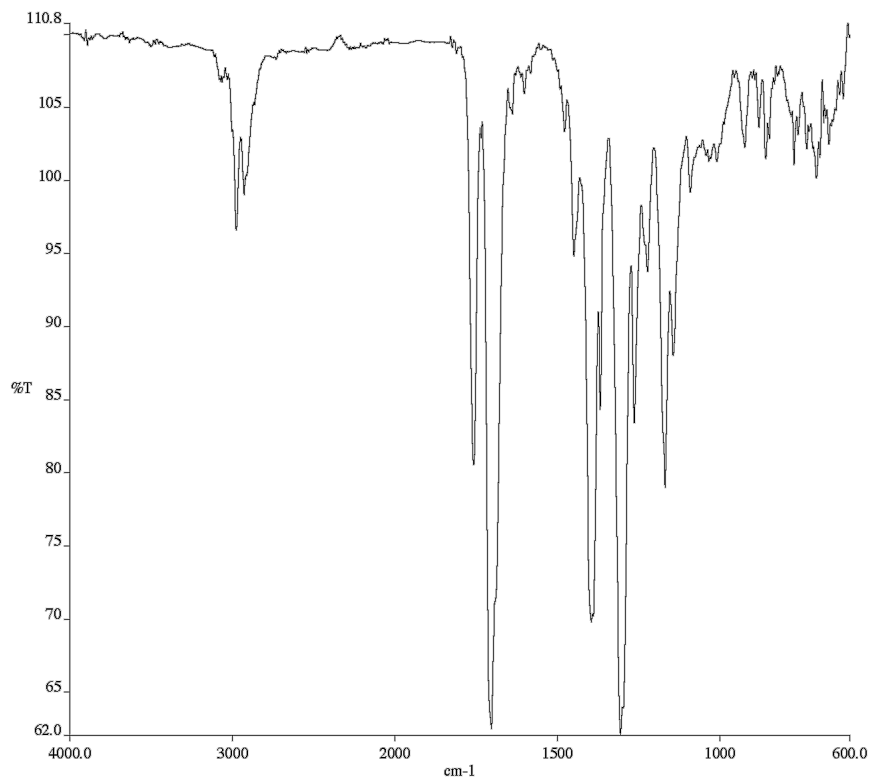


Figure A1.113. Infrared spectrum (Thin Film, NaCl) of compound **35d**.

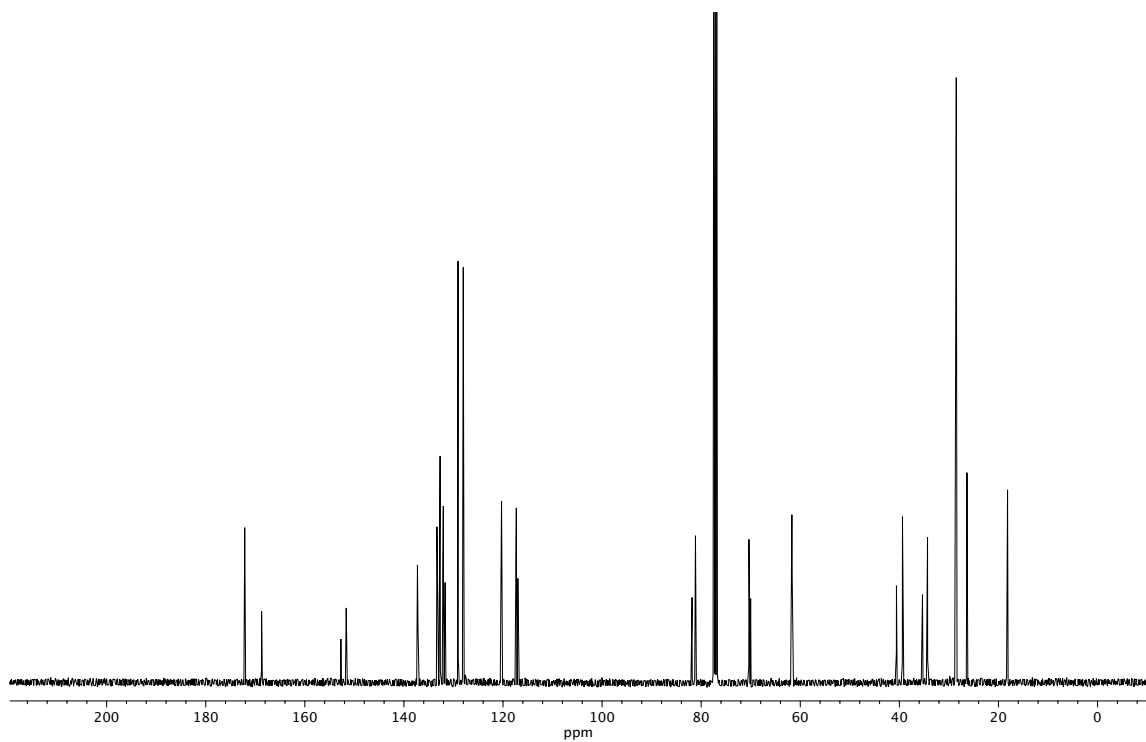


Figure A1.114. ¹³C NMR (100 MHz, CDCl₃) of compound **35d**.

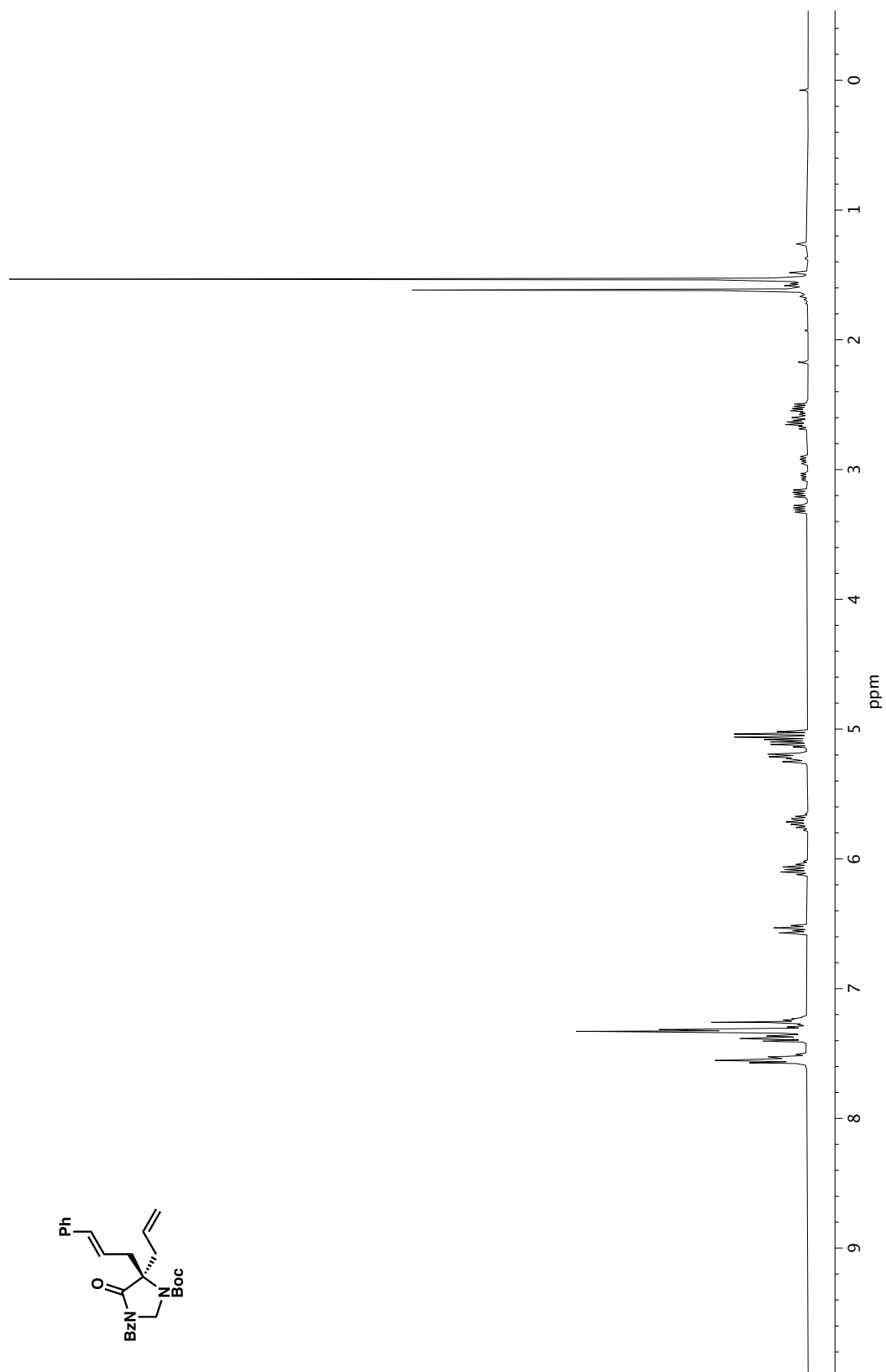


Figure A1.115. ^1H NMR (400 MHz, CDCl_3) of compound **35e**.

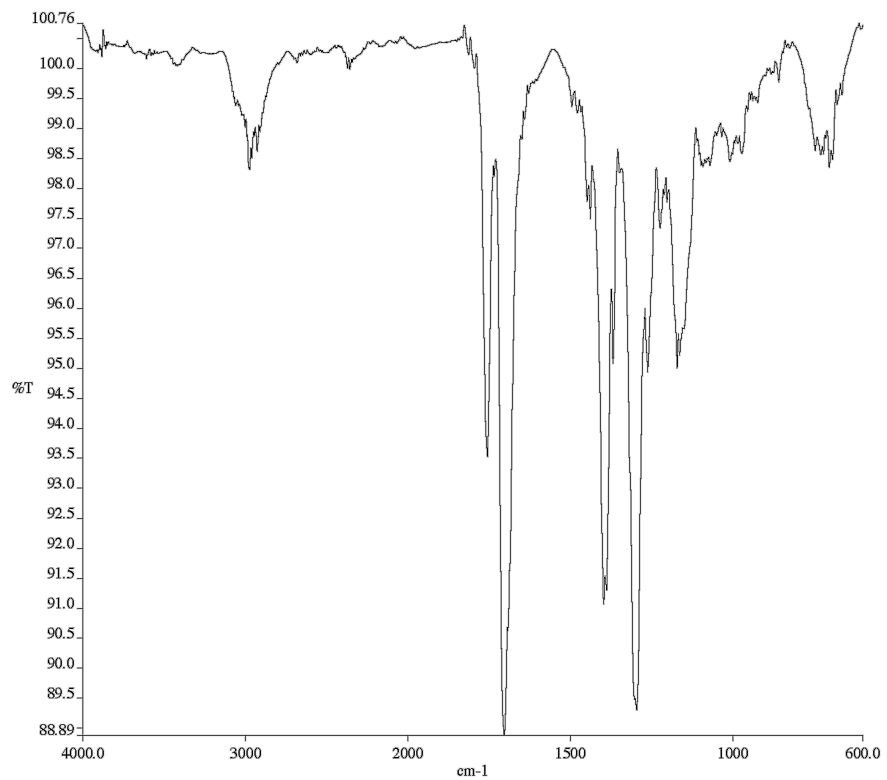


Figure A1.116. Infrared spectrum (Thin Film, NaCl) of compound **35e**.

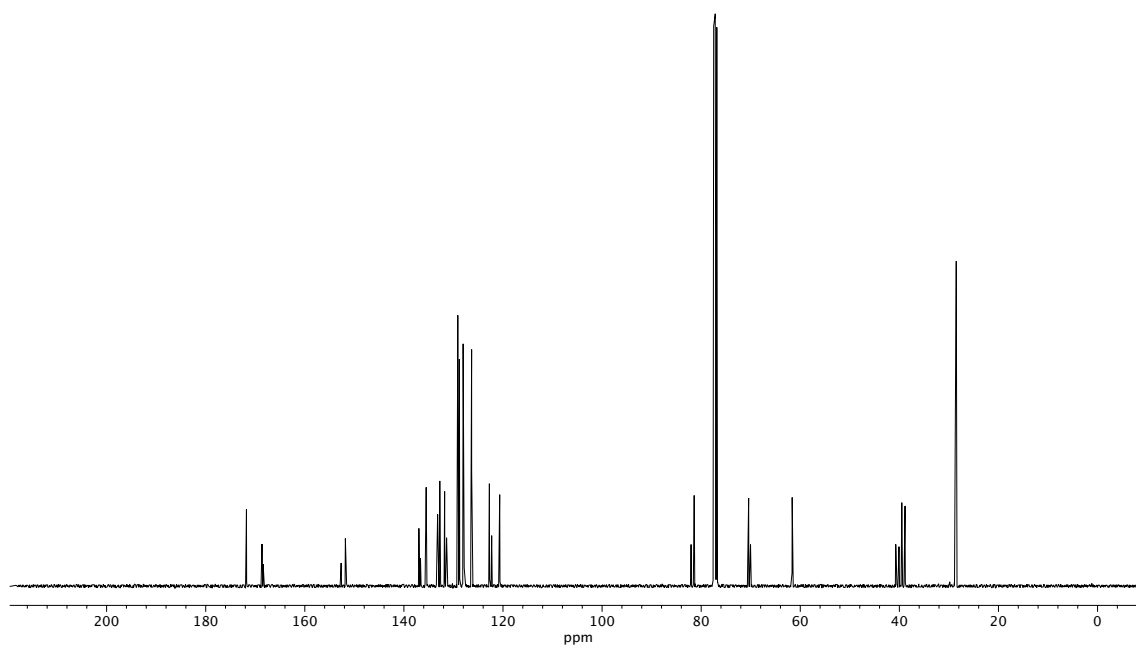


Figure A1.117. ¹³C NMR (100 MHz, CDCl₃) of compound **35e**.

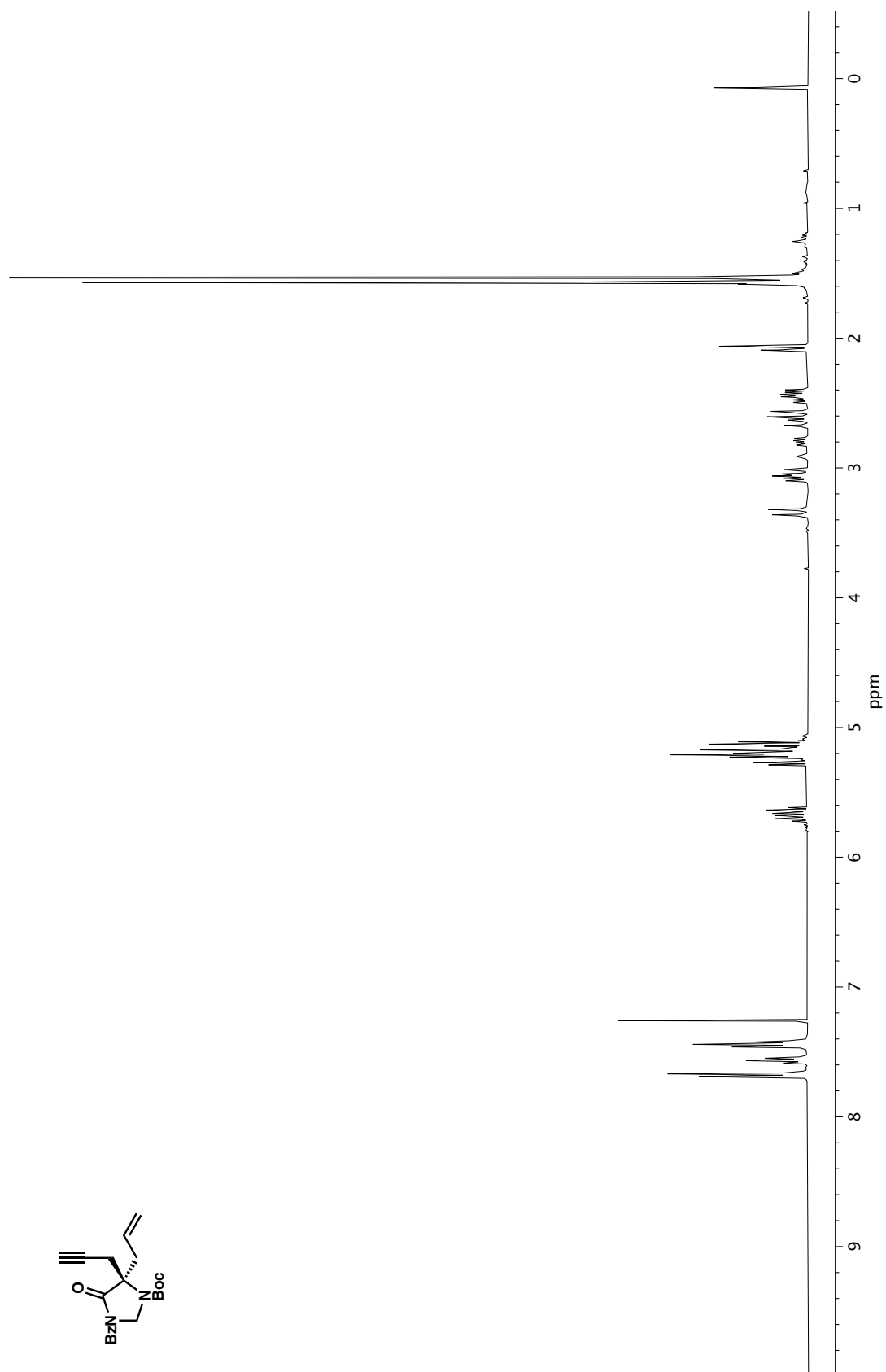


Figure A1.118. ¹H NMR (400 MHz, CDCl₃) of compound 35f.

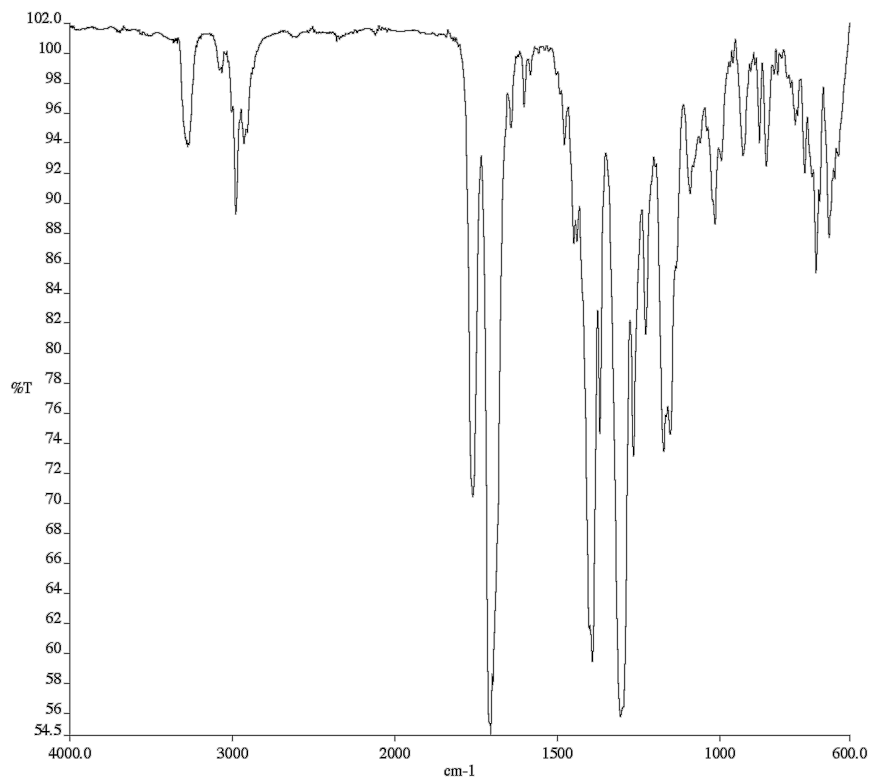


Figure A1.119. Infrared spectrum (Thin Film, NaCl) of compound **35f**.

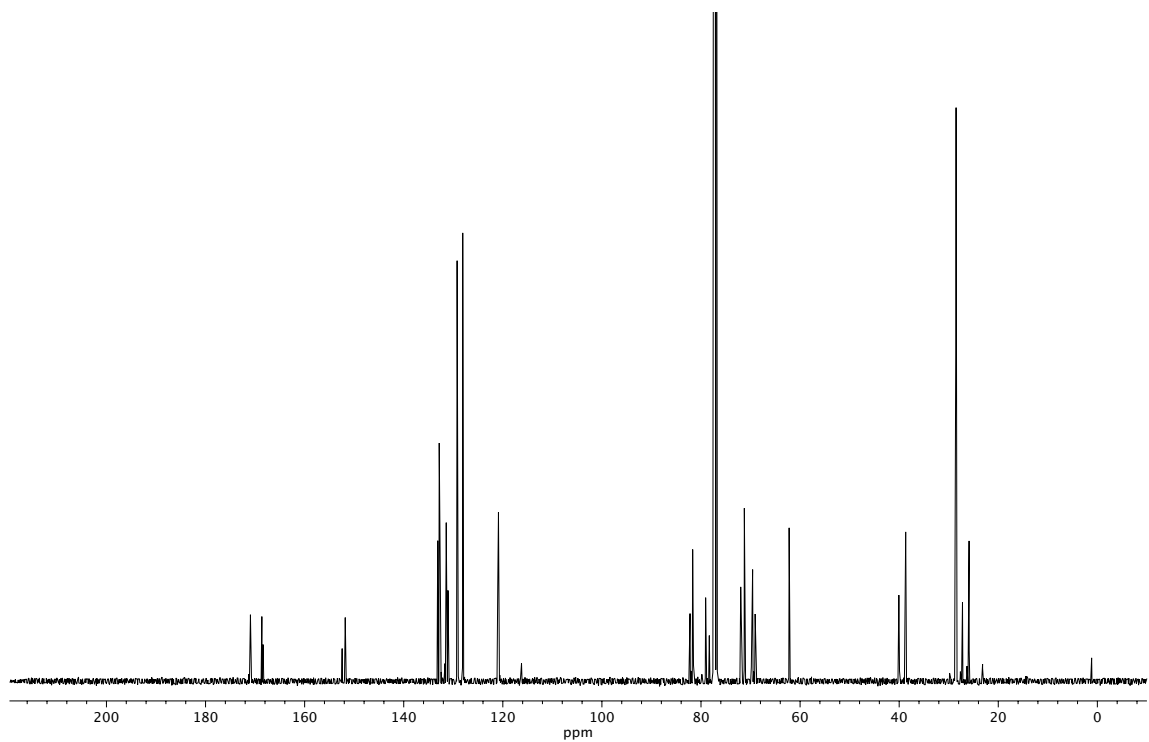
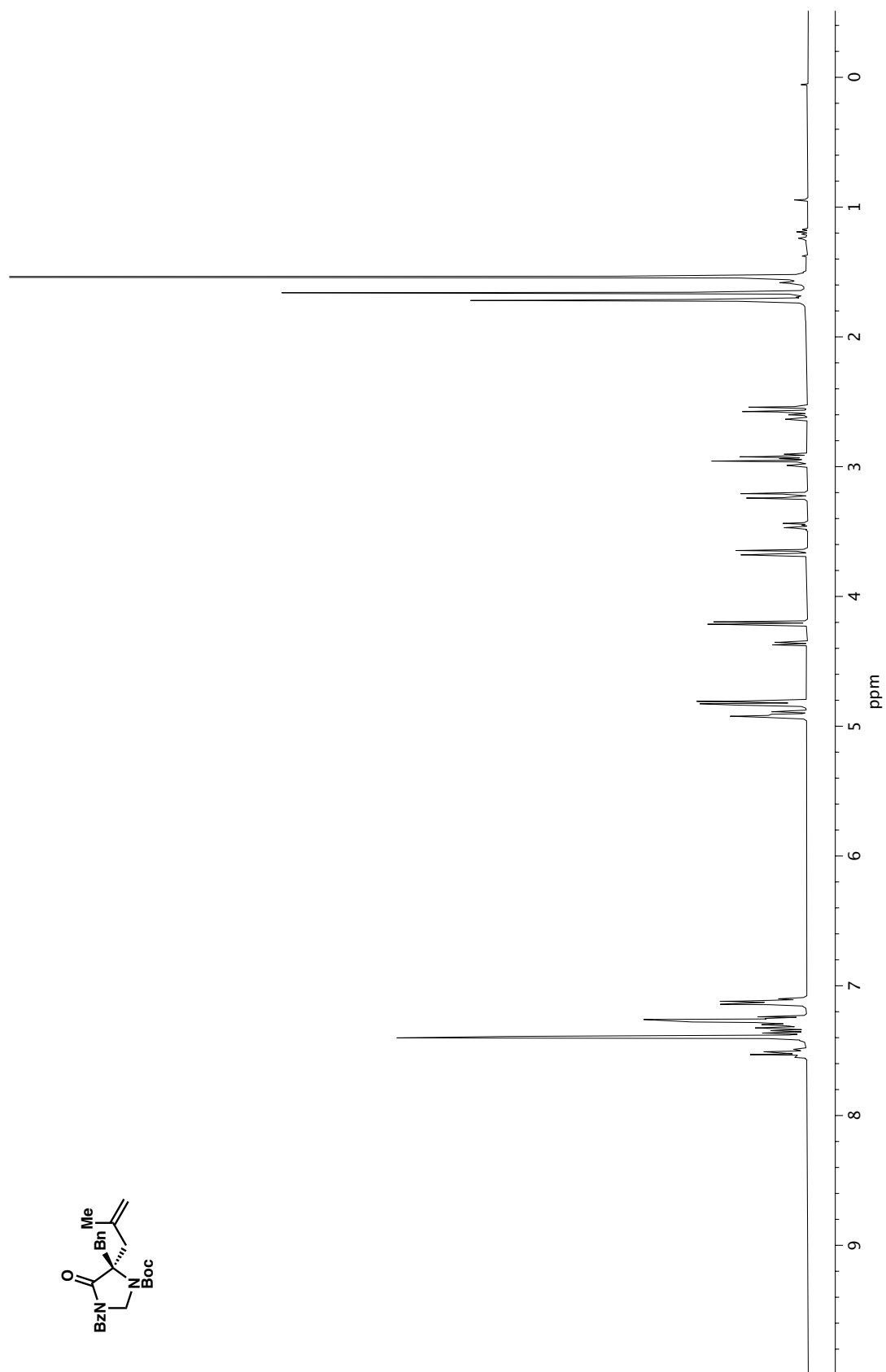


Figure A1.120. ¹³C NMR (100 MHz, CDCl₃) of compound **35f**.

Figure A1.121. ^1H NMR (400 MHz, CDCl_3) of compound 35g.

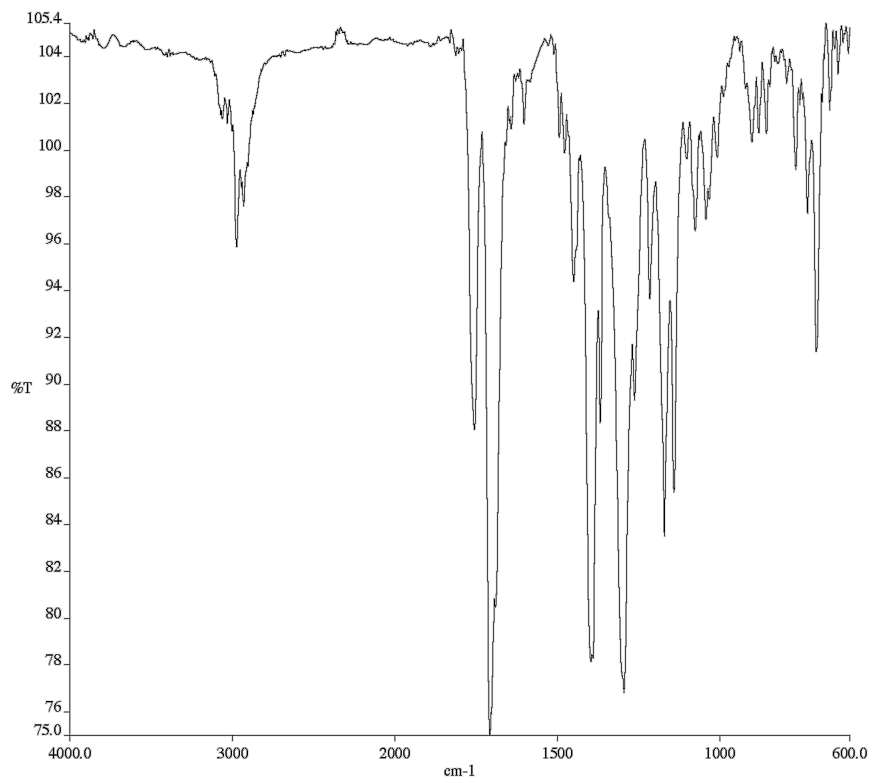


Figure A1.122. Infrared spectrum (Thin Film, NaCl) of compound **35g**.

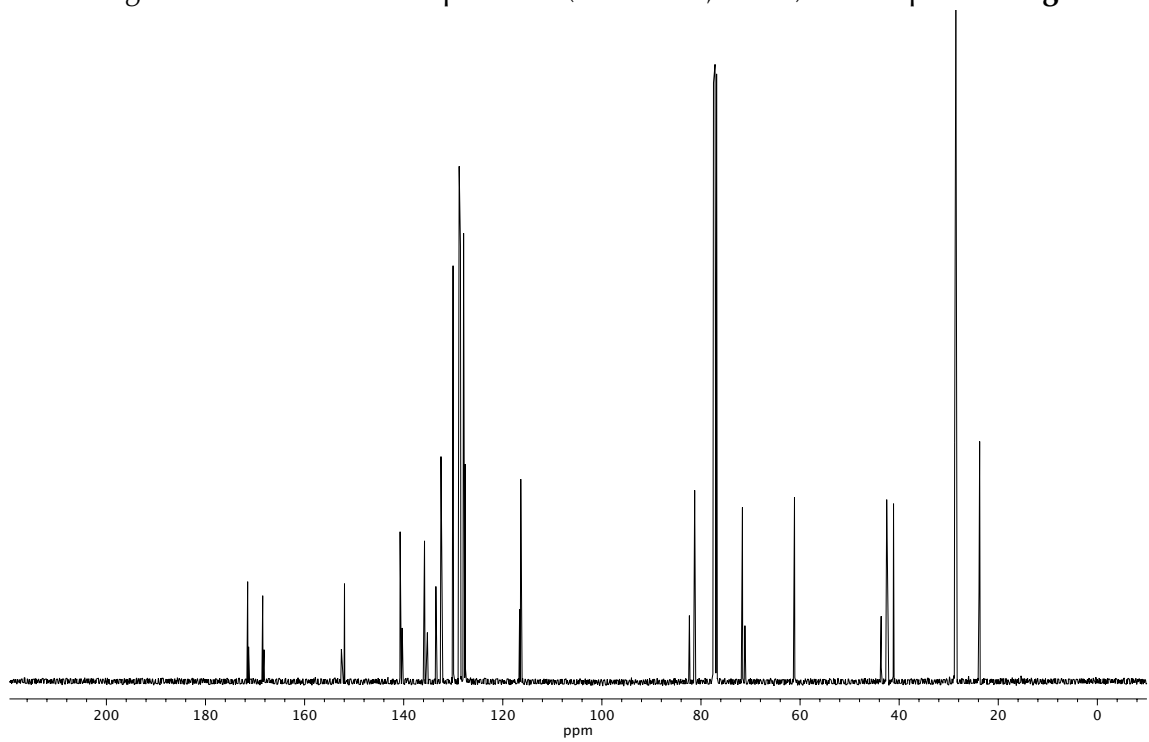


Figure A1.123. ¹³C NMR (100 MHz, CDCl₃) of compound **35g**.

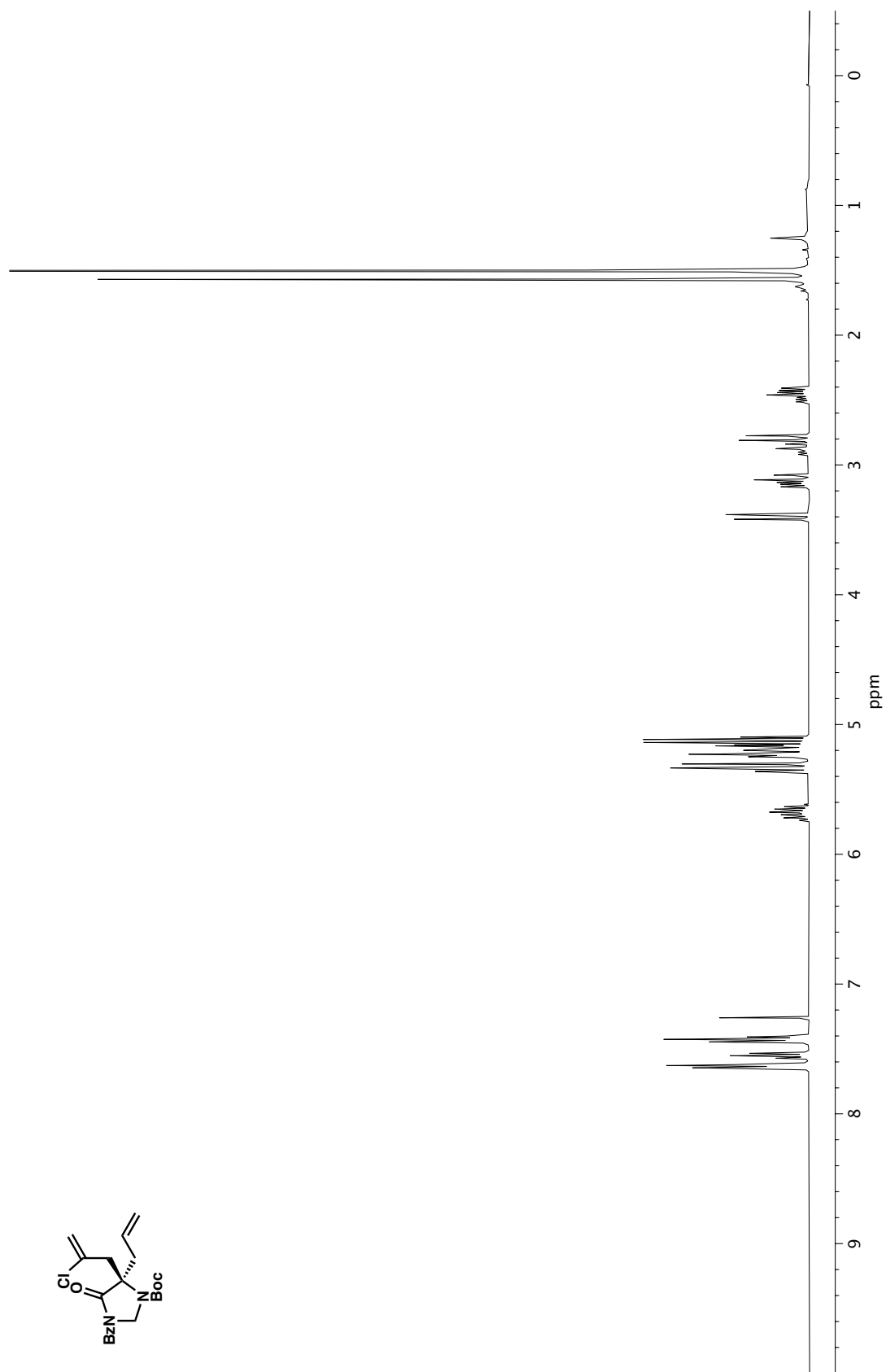


Figure A1.124. ¹H NMR (400 MHz, CDCl₃) of compound **35h**.

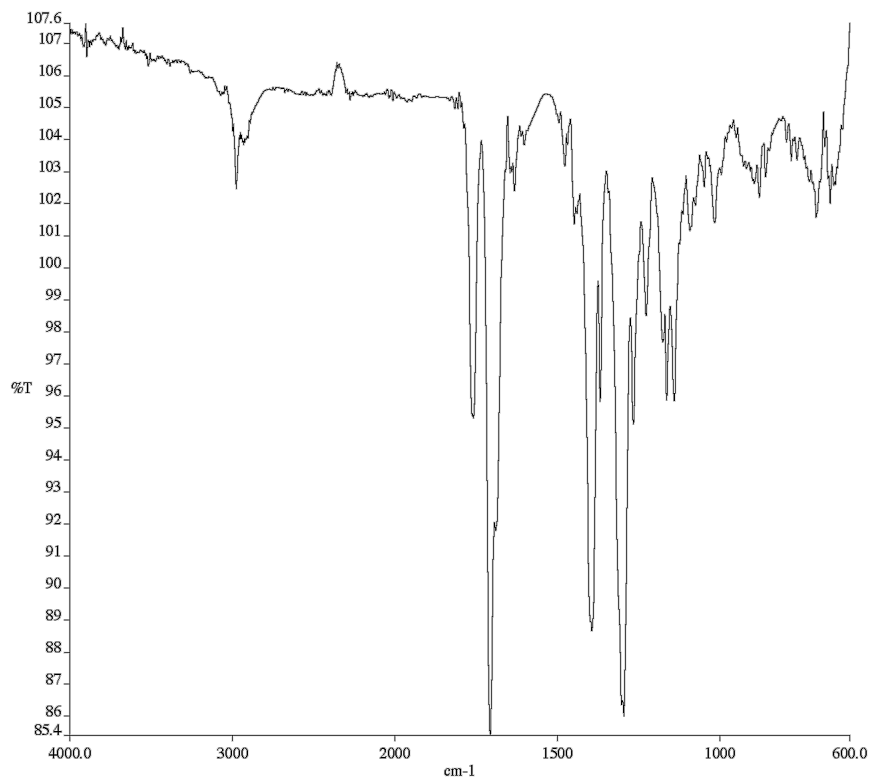


Figure A1.125. Infrared spectrum (Thin Film, NaCl) of compound **35h**.

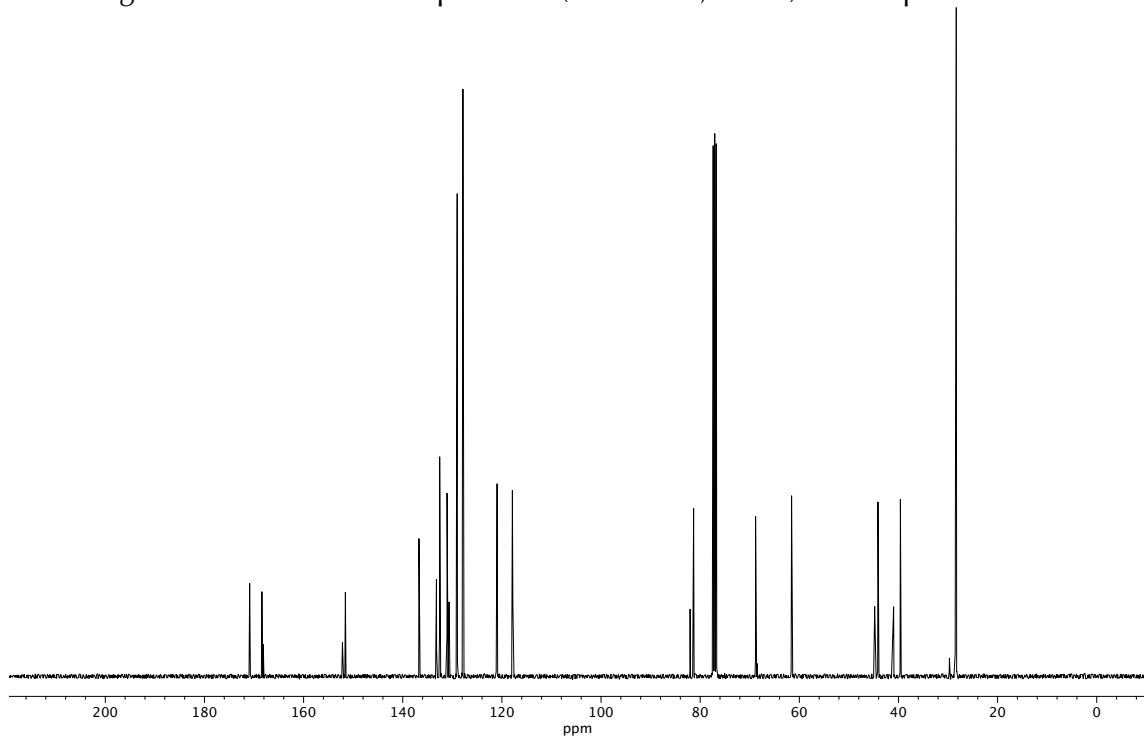
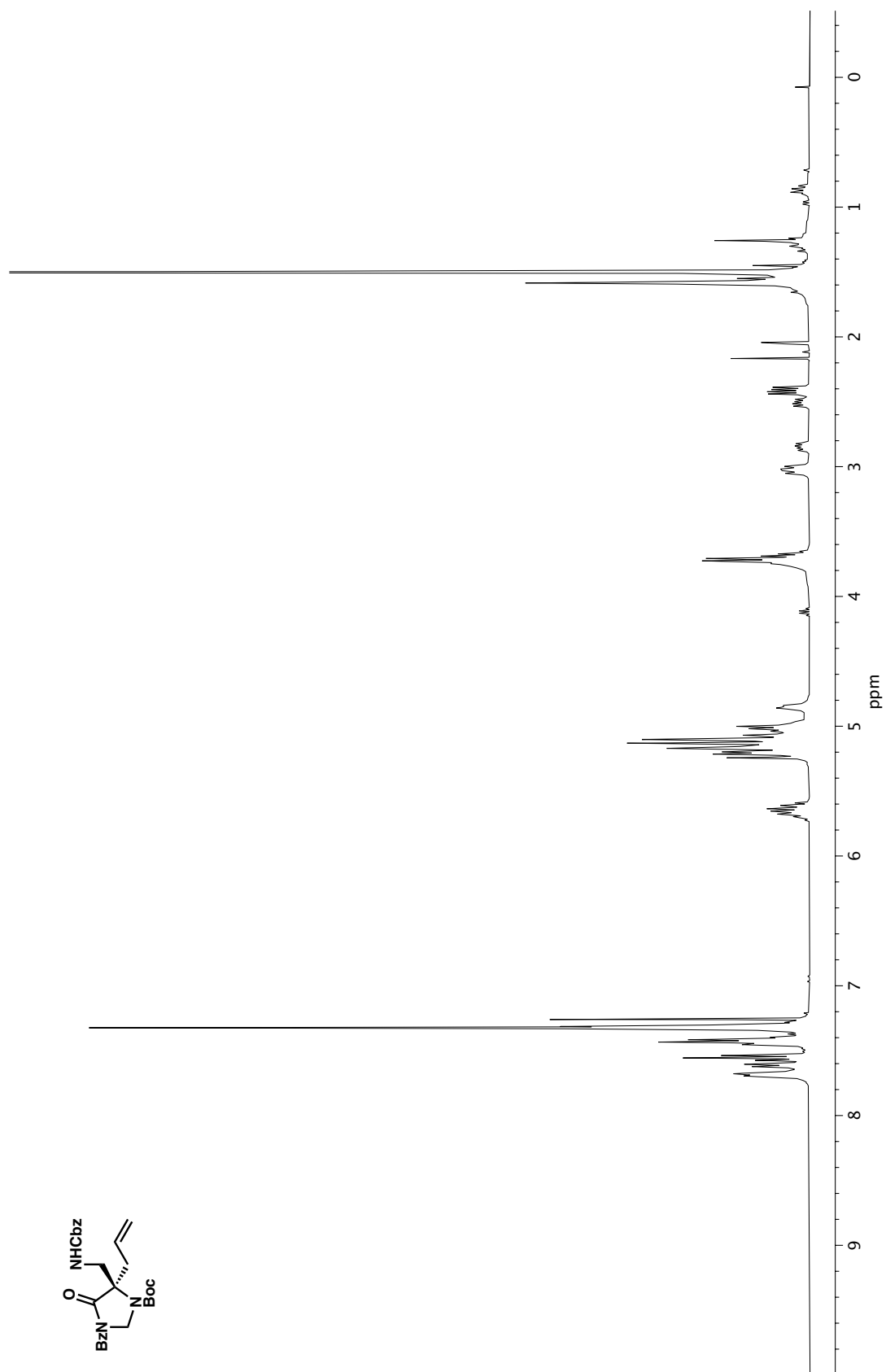


Figure A1.126. ¹³C NMR (100 MHz, CDCl₃) of compound **35h**.

Figure A1.127. ¹H NMR (400 MHz, CDCl₃) of compound 35i.

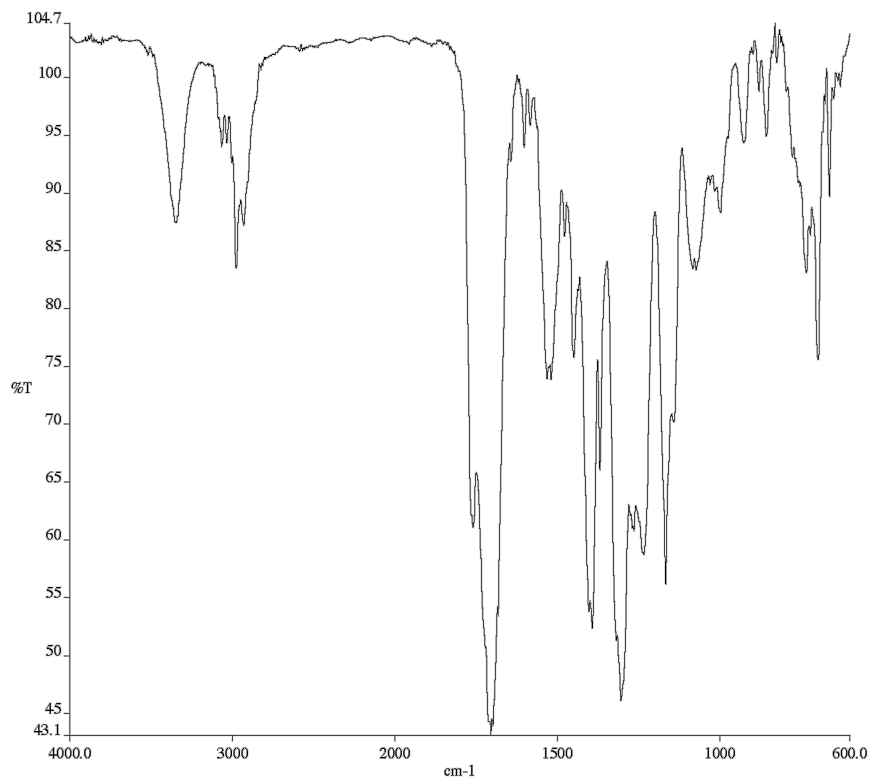


Figure A1.128. Infrared spectrum (Thin Film, NaCl) of compound **35i**.

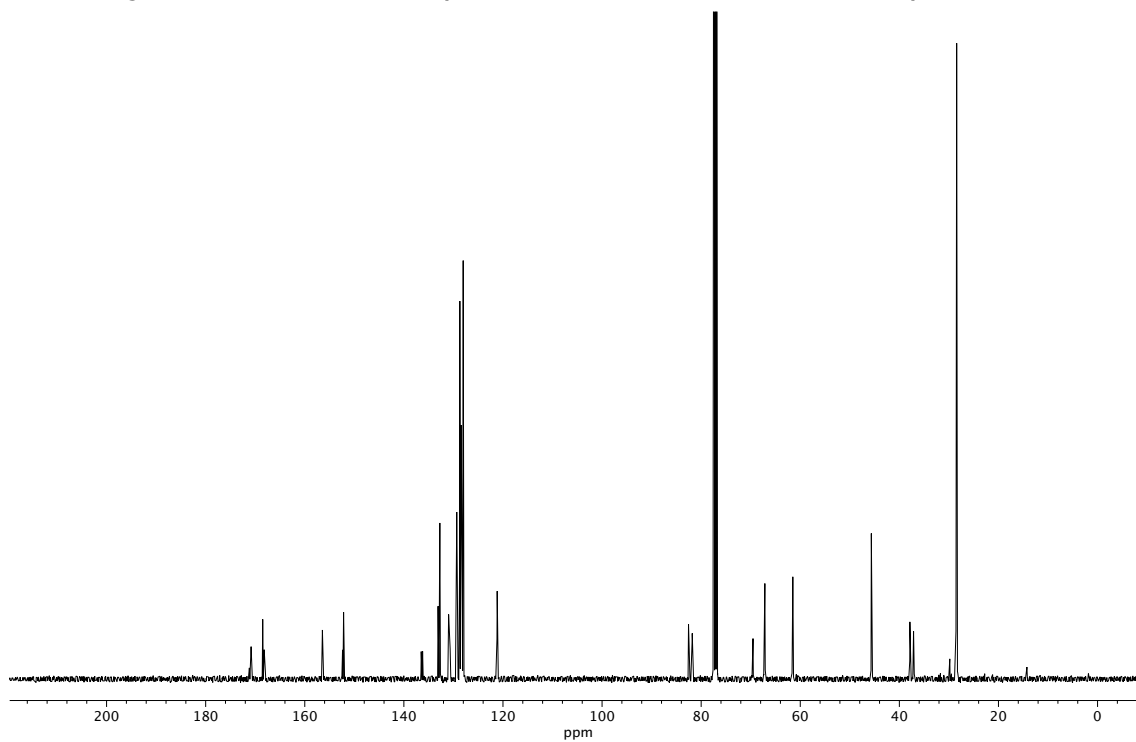
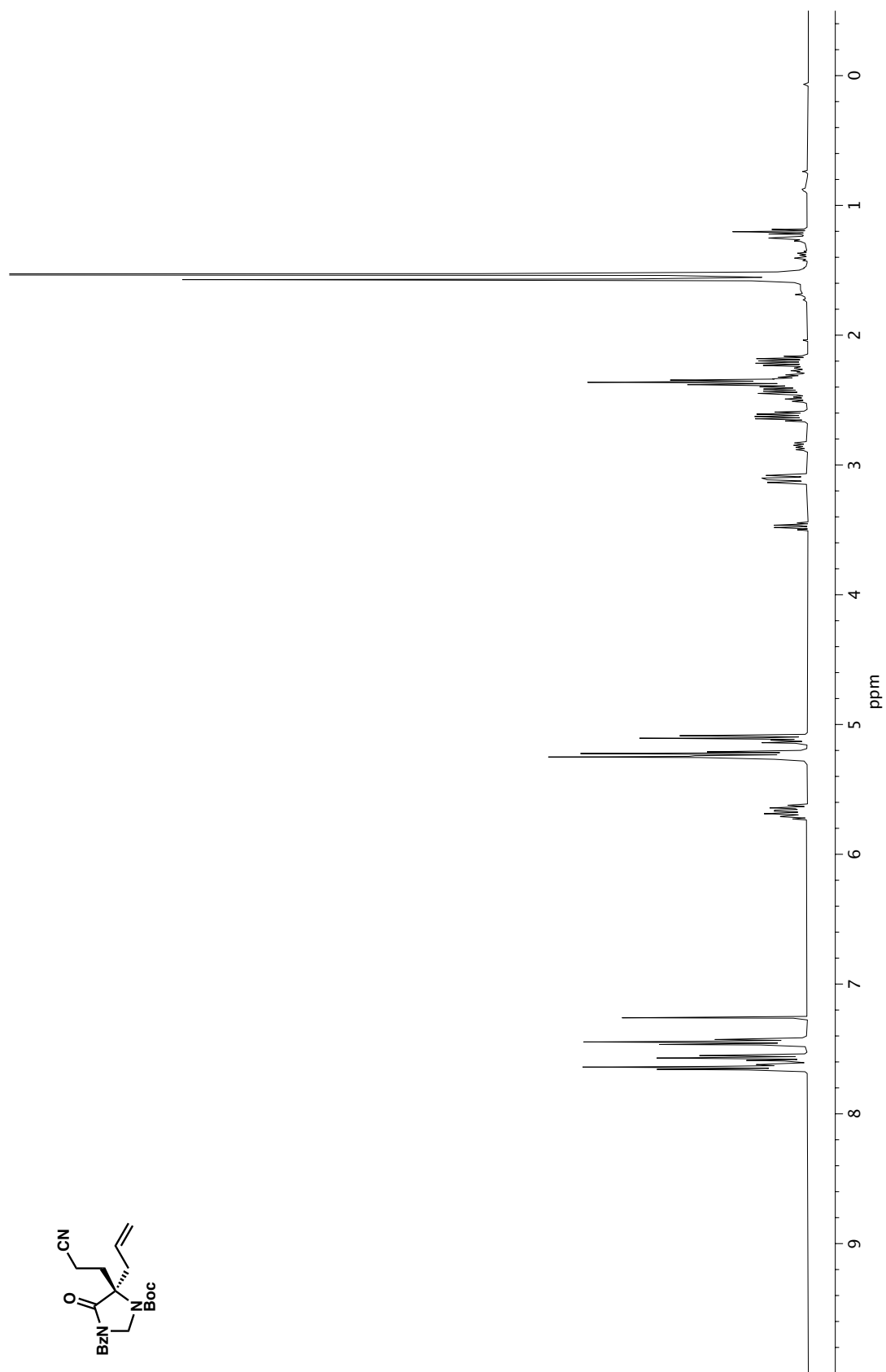


Figure A1.129. ¹³C NMR (100 MHz, CDCl₃) of compound **35i**.

Figure A1.130. ¹H NMR (400 MHz, CDCl₃) of compound 35j.

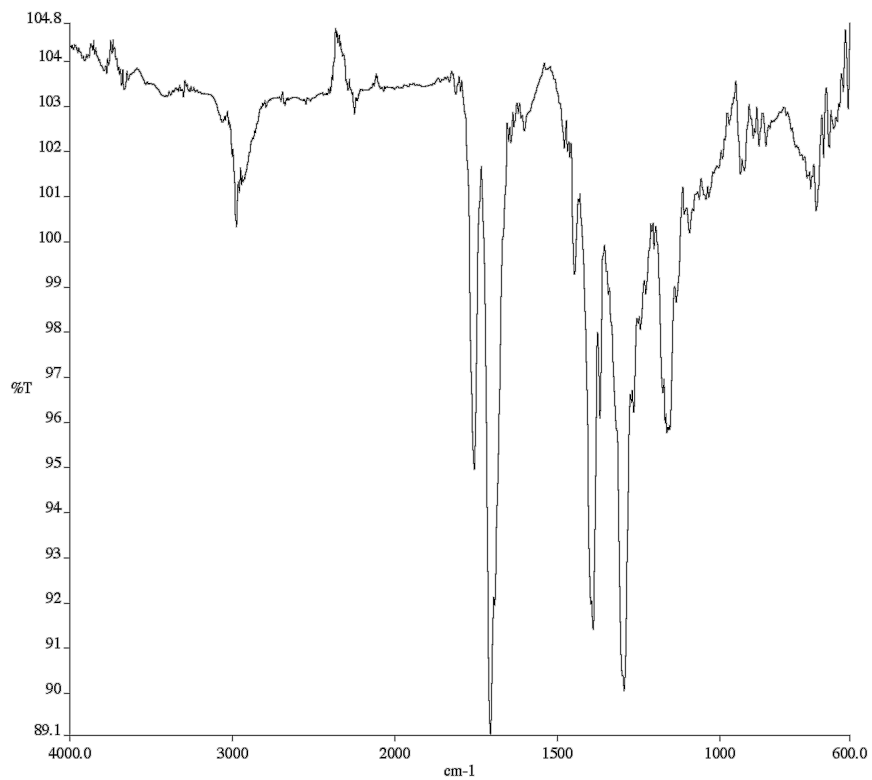


Figure A1.131. Infrared spectrum (Thin Film, NaCl) of compound **35j**.

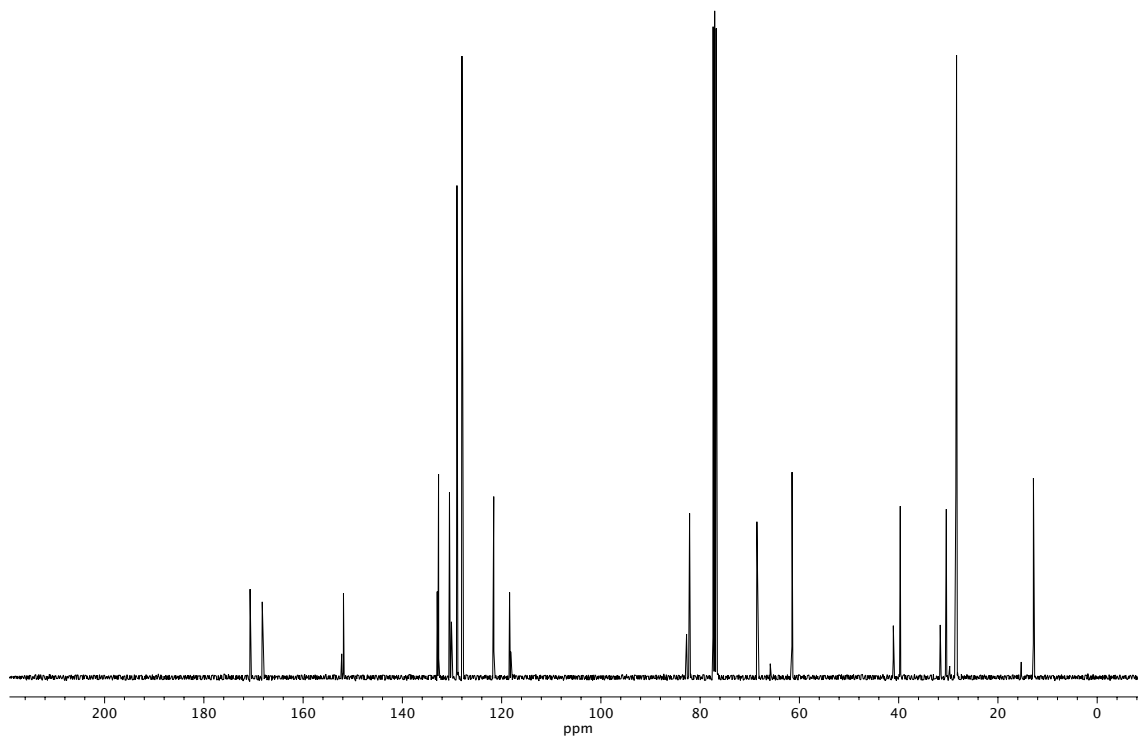


Figure A1.132. ¹³C NMR (100 MHz, CDCl₃) of compound **35j**.

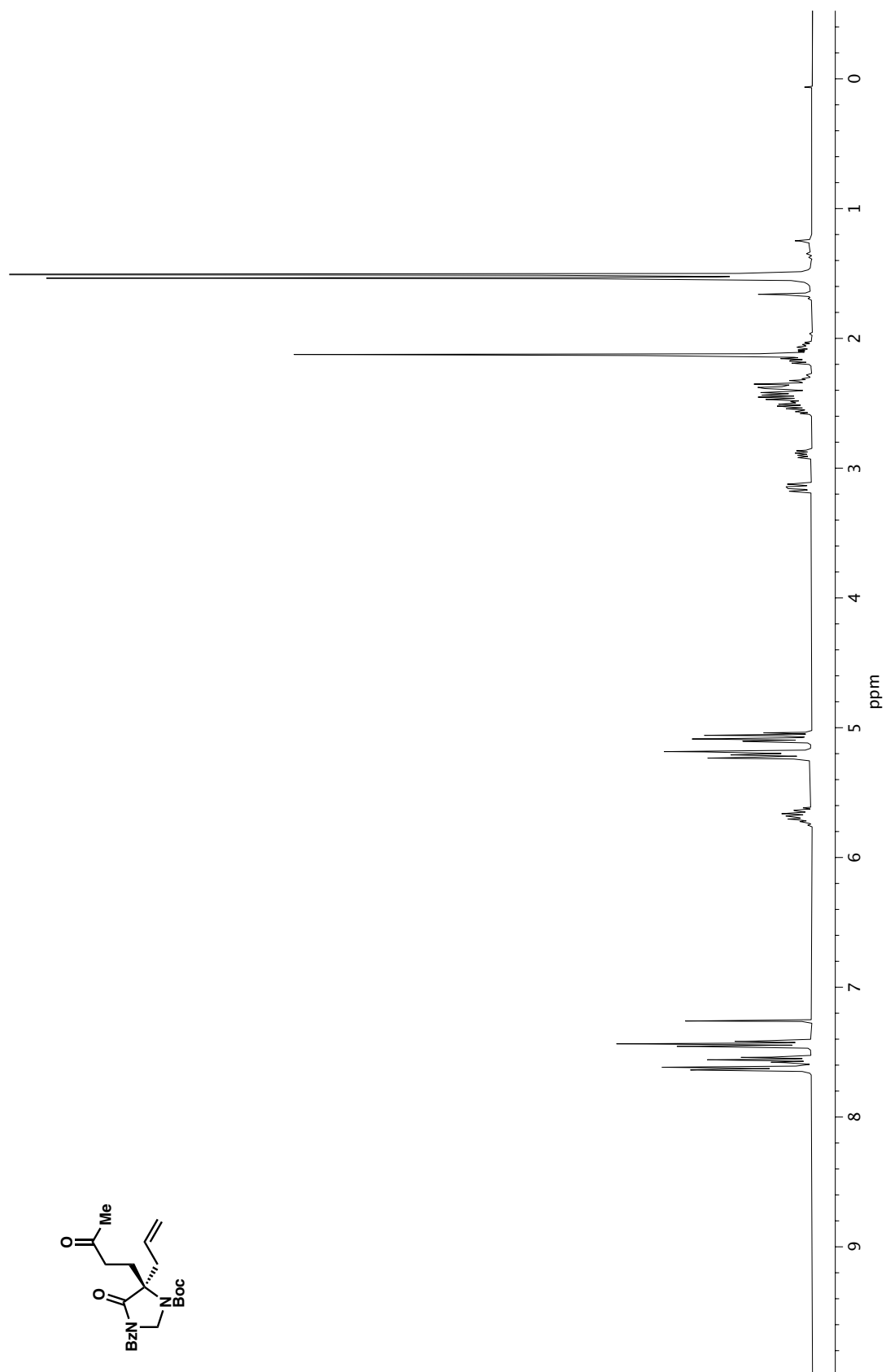


Figure A1.133. ¹H NMR (400 MHz, CDCl₃) of compound 35k.

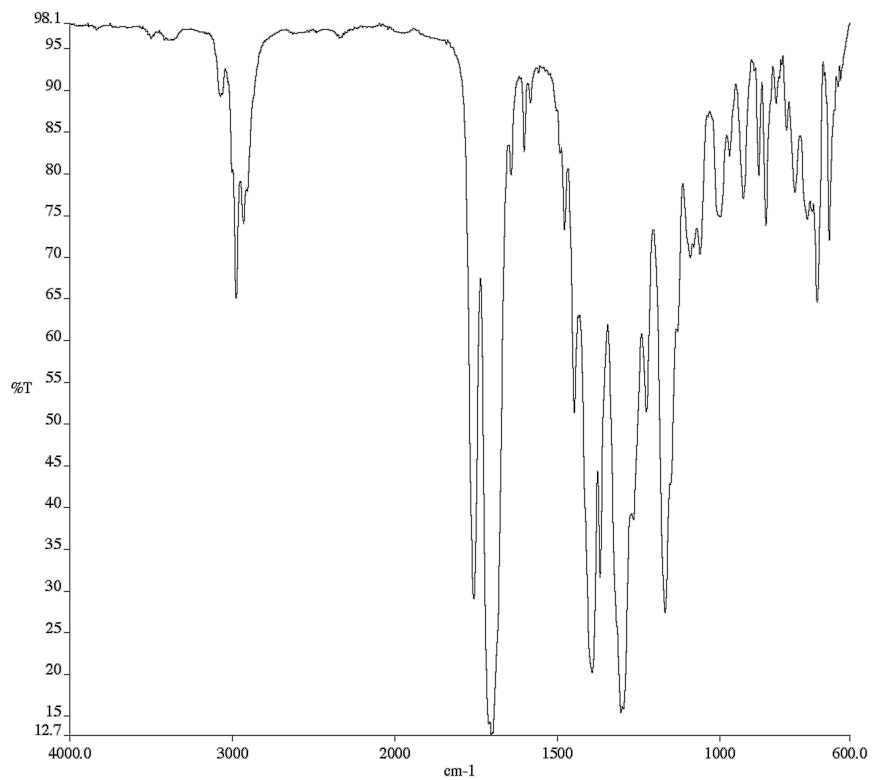


Figure A1.134. Infrared spectrum (Thin Film, NaCl) of compound **35k**.

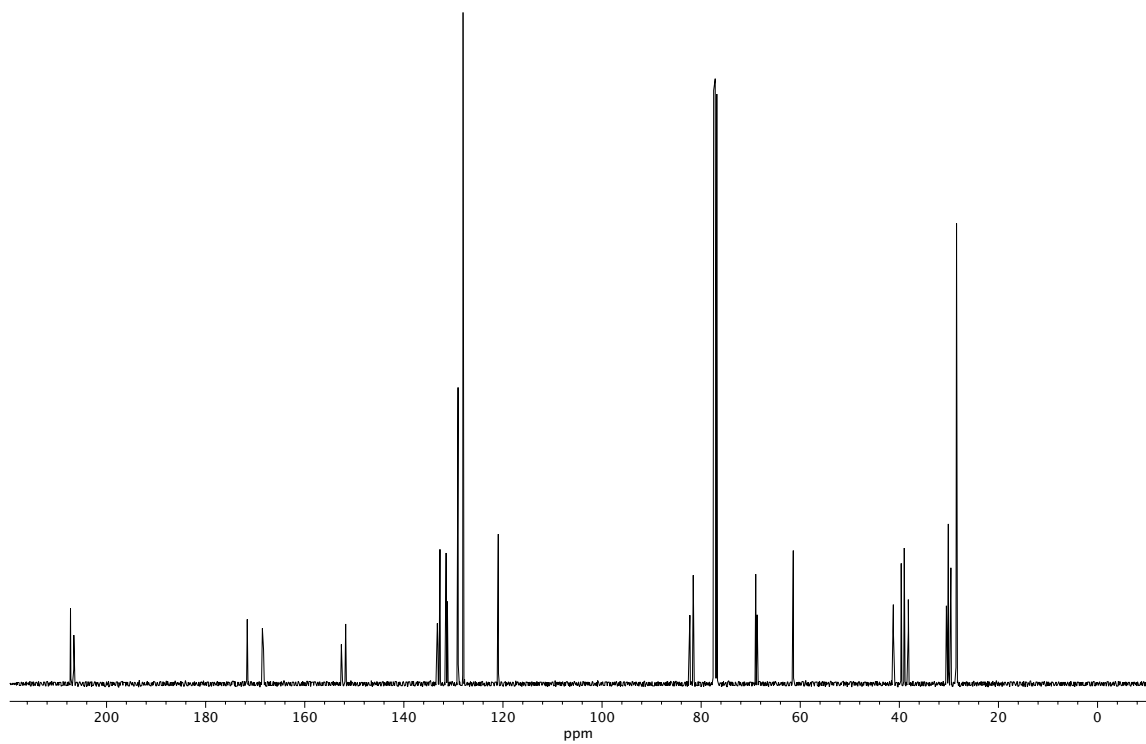


Figure A1.135. ¹³C NMR (100 MHz, CDCl₃) of compound **35k**.

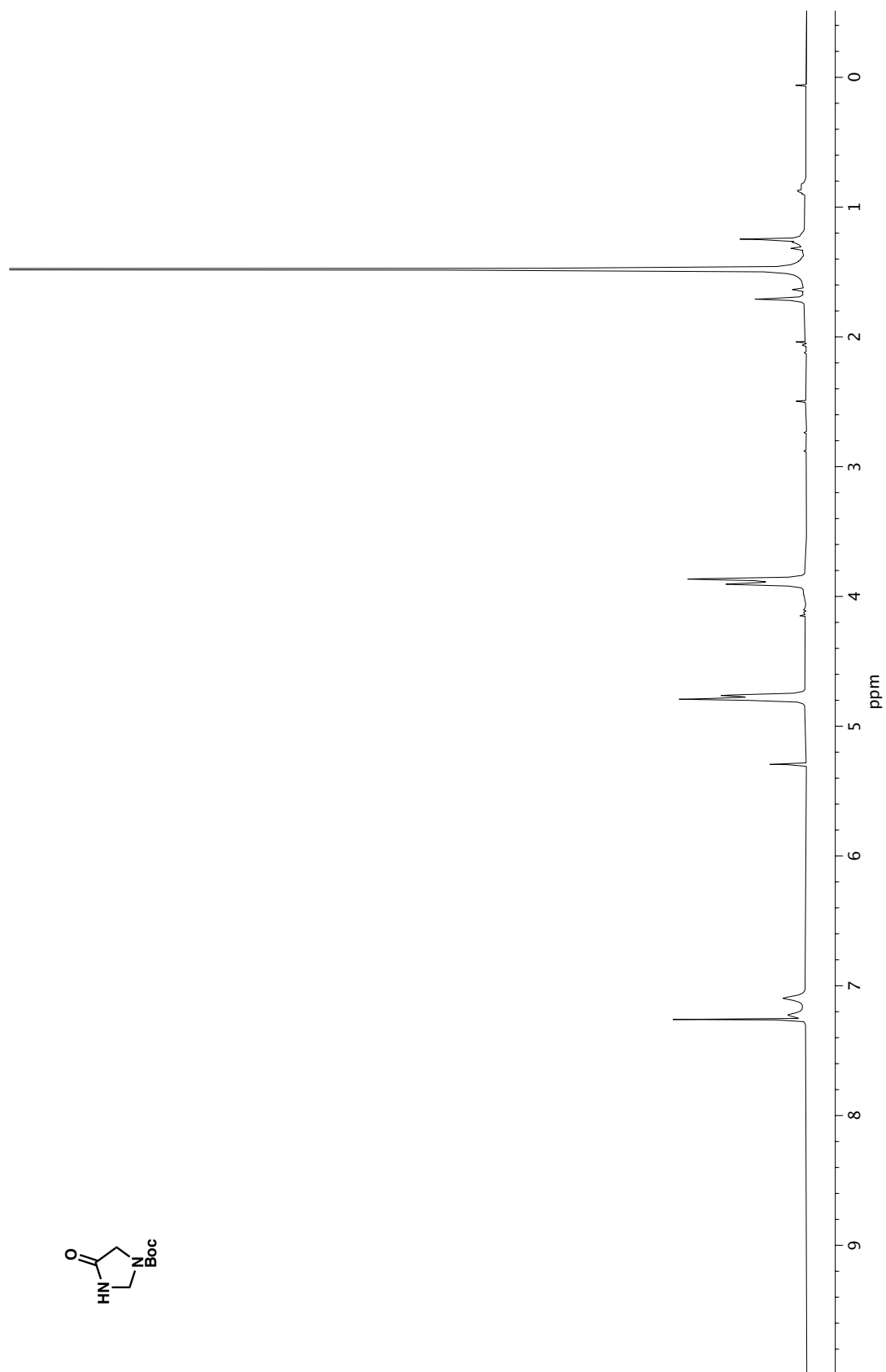


Figure A1.136. ¹H NMR (400 MHz, CDCl₃) of compound 31.

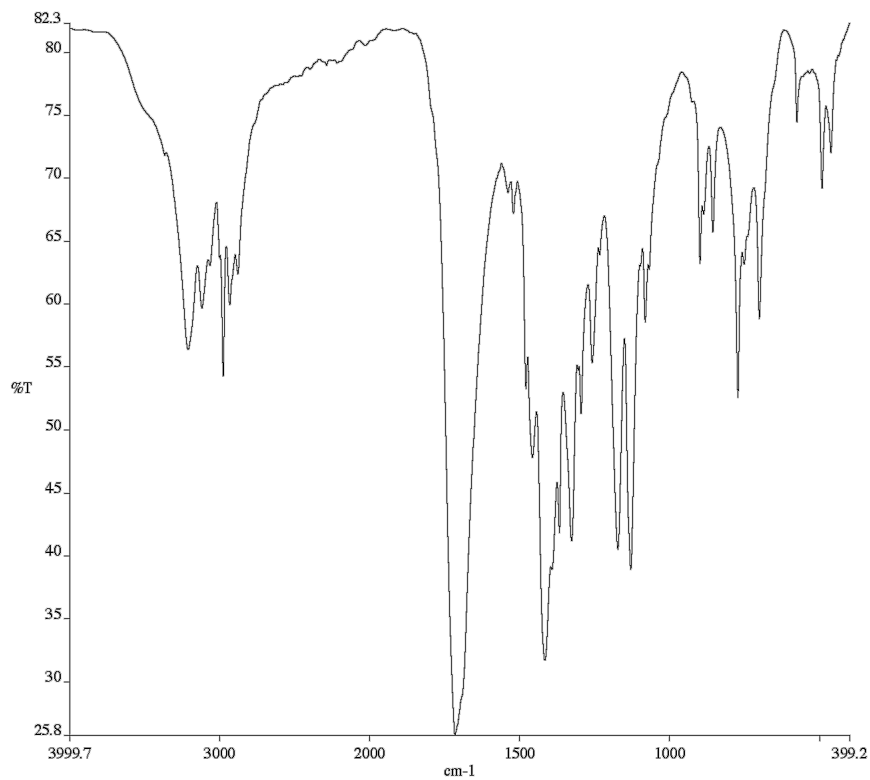


Figure A1.137. Infrared spectrum (Thin Film, KBr) of compound **31**.

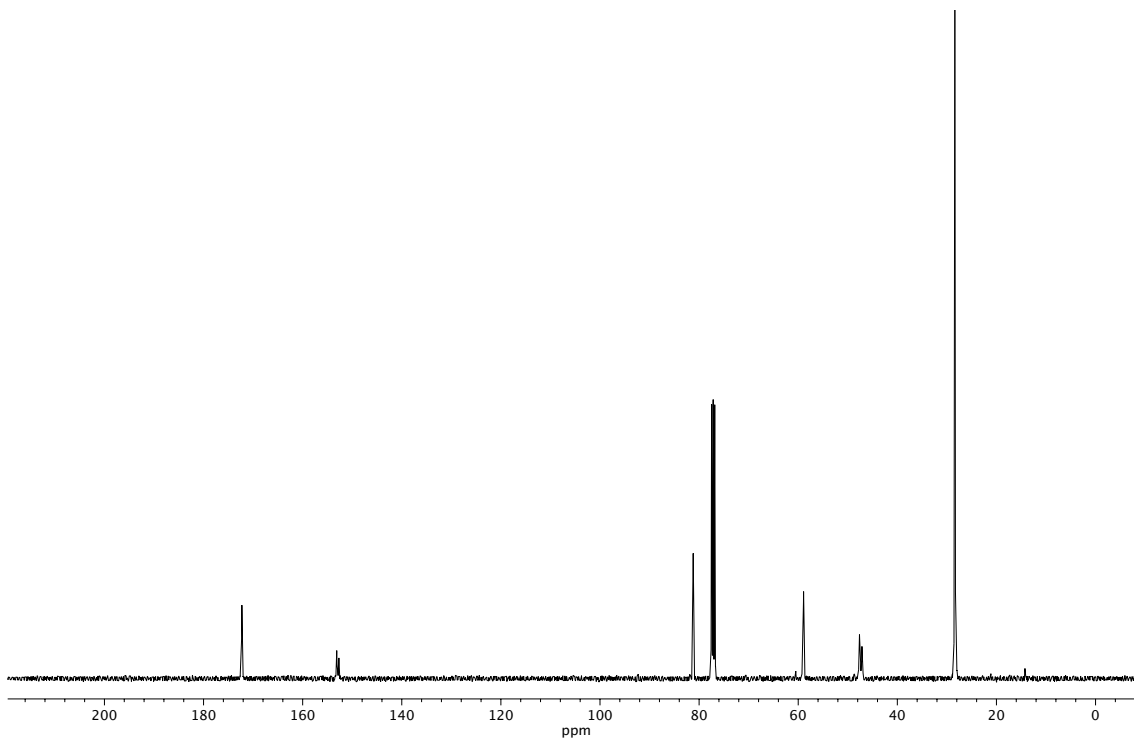
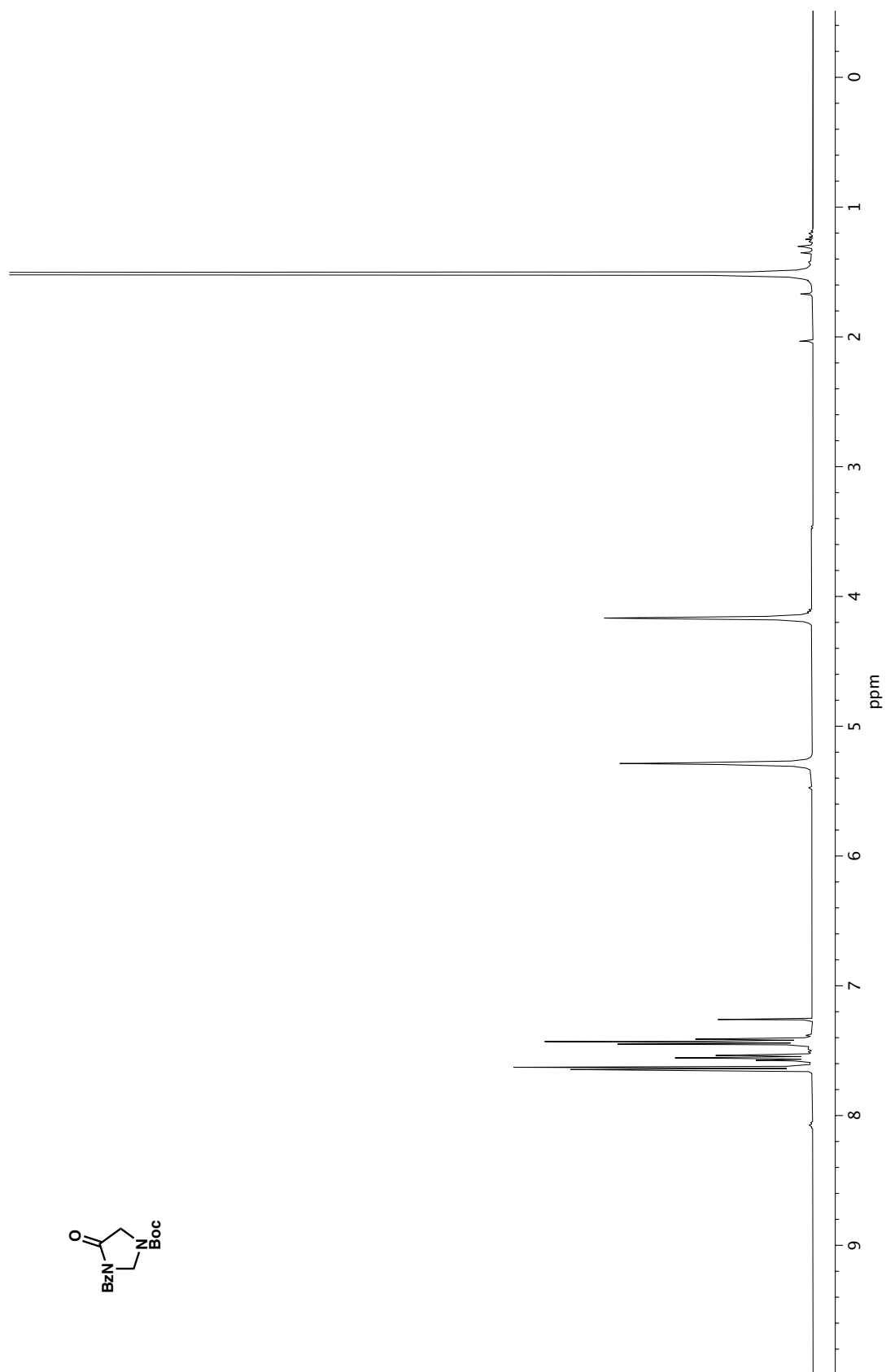


Figure A1.138. ¹³C NMR (100 MHz, CDCl₃) of compound **31**.

Figure A1.139. ^1H NMR (400 MHz, CDCl_3) of compound **32**.

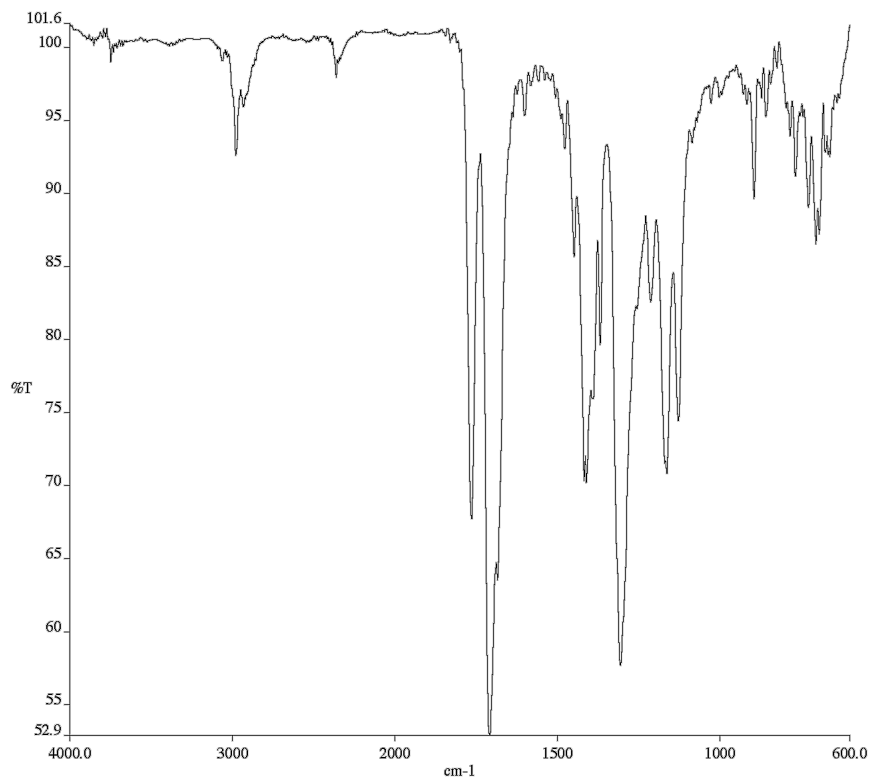


Figure A1.140. Infrared spectrum (Thin Film, NaCl) of compound **32**.

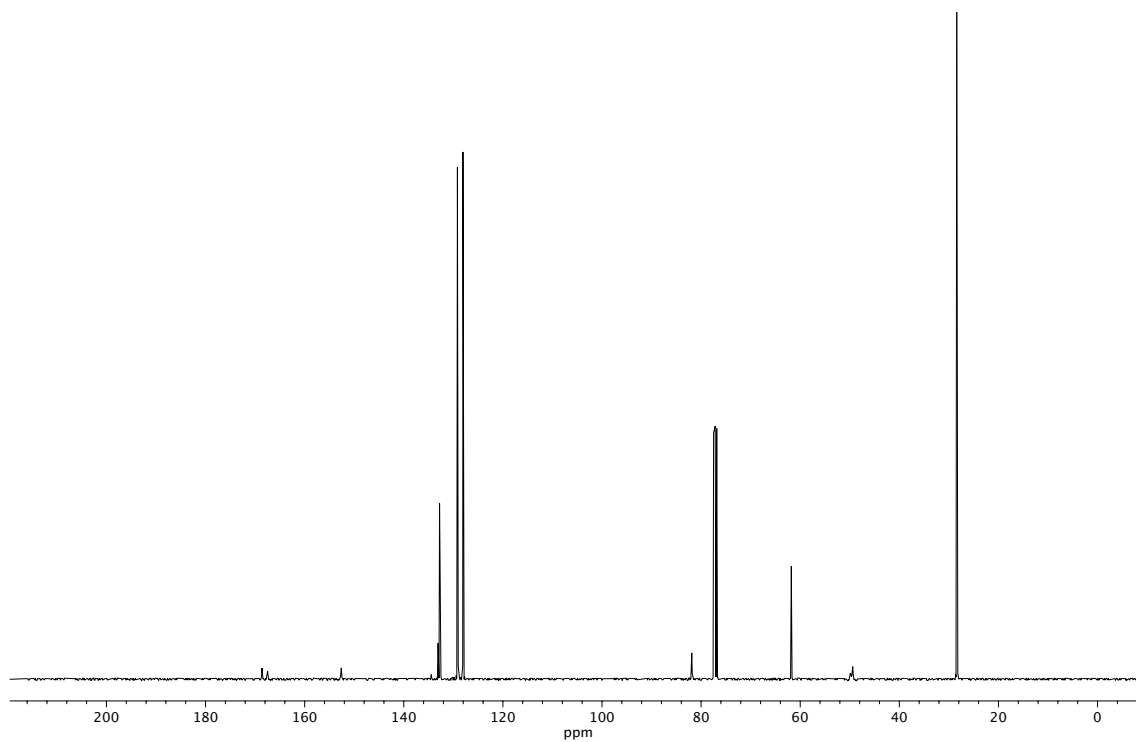
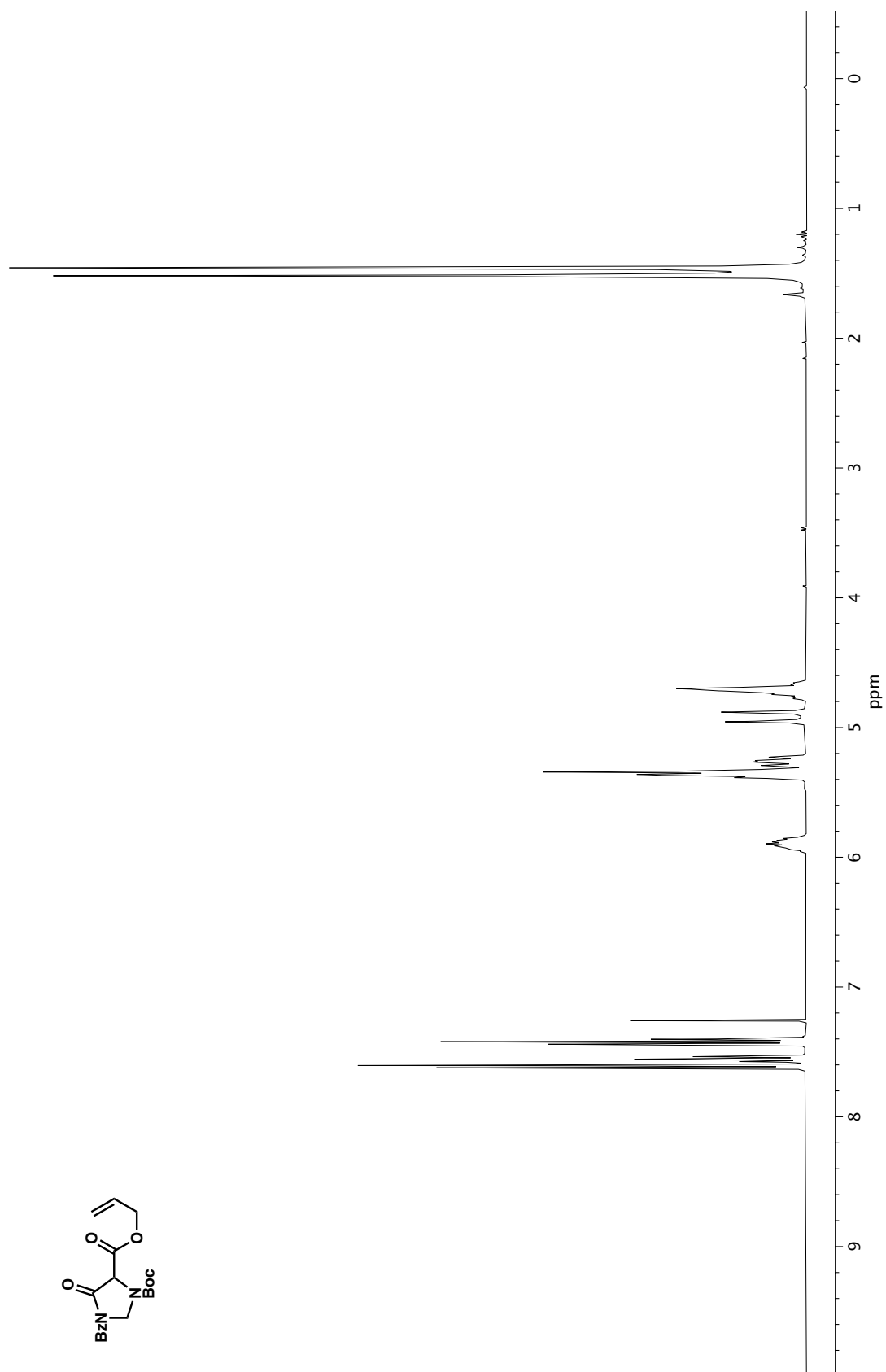


Figure A1.141. ¹³C NMR (100 MHz, CDCl₃) of compound **32**.

Figure A1.142. ^1H NMR (400 MHz, CDCl_3) of compound 33.

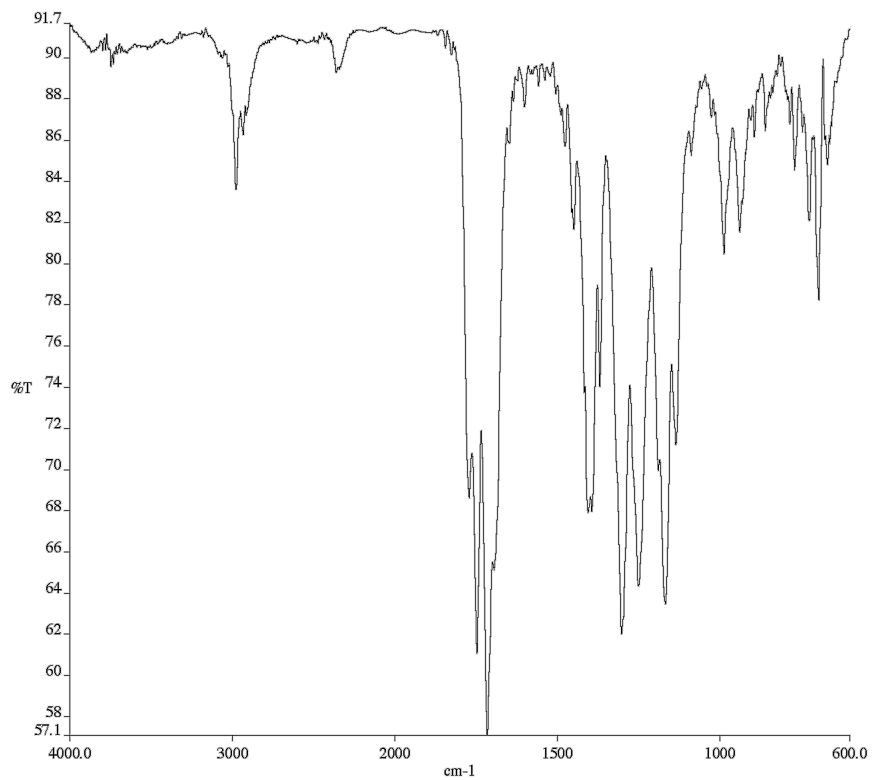


Figure A1.143. Infrared spectrum (Thin Film, NaCl) of compound **33**.

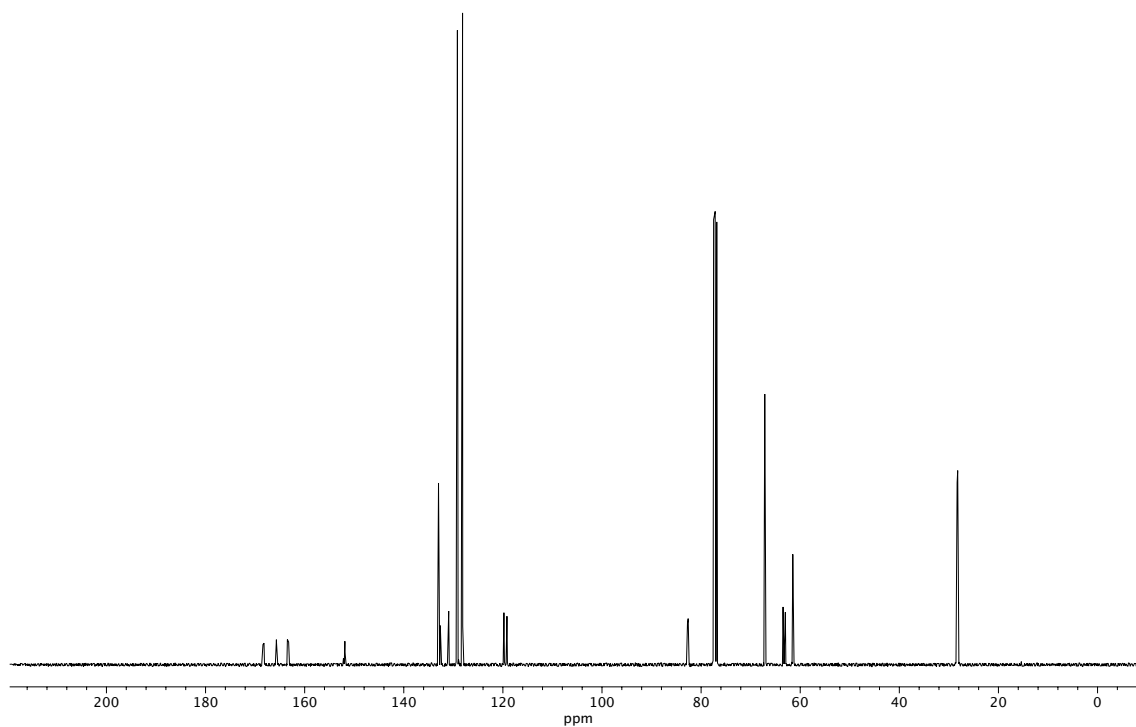
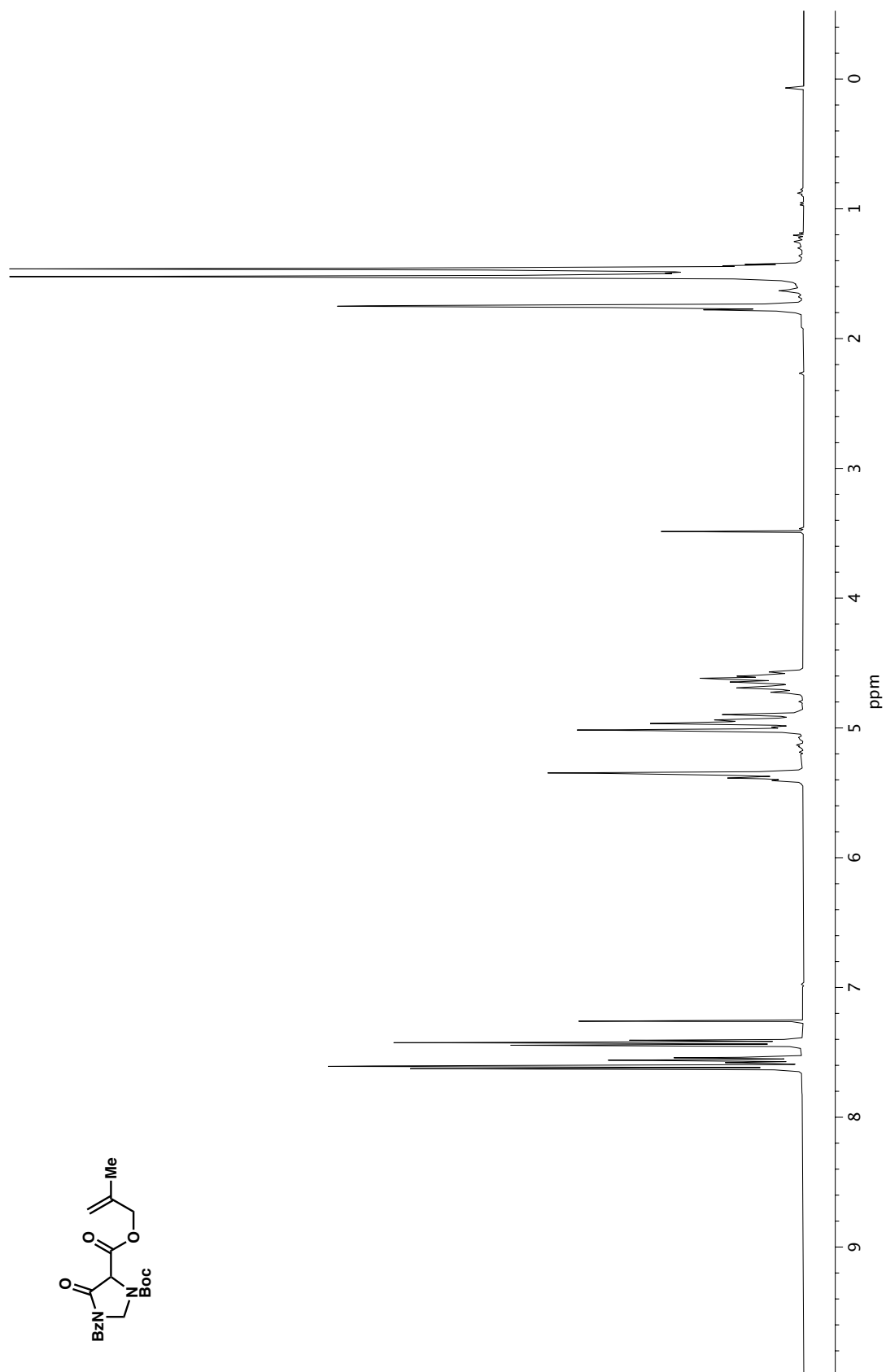


Figure A1.144. ¹³C NMR (100 MHz, CDCl₃) of compound **33**.

Figure A1.145. ^1H NMR (400 MHz, CDCl_3) of compound **60**.

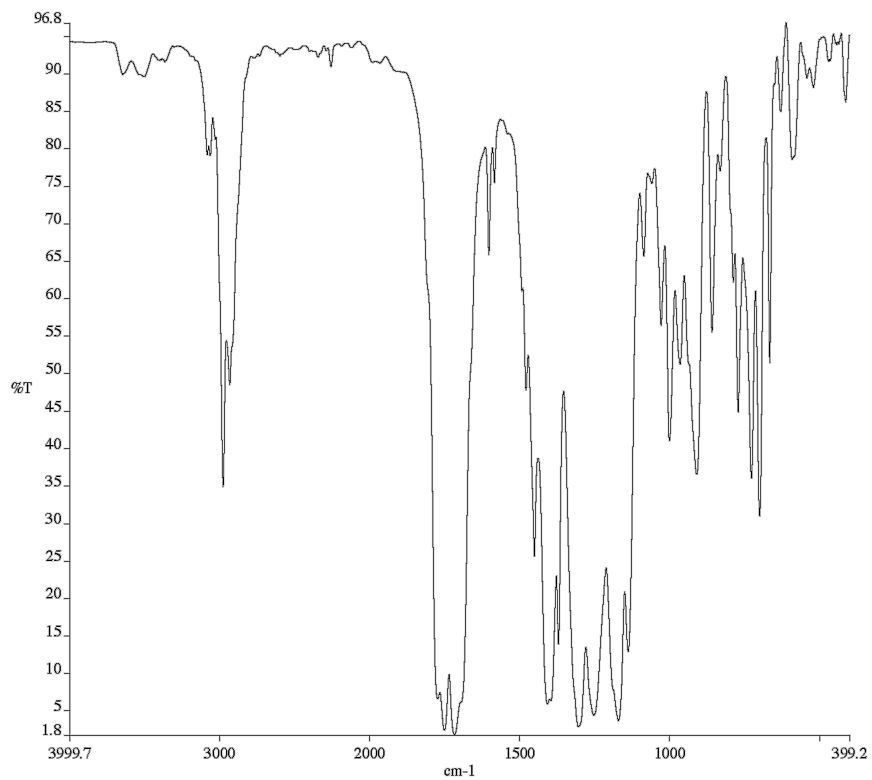


Figure A1.146. Infrared spectrum (Thin Film, KBr) of compound **60**.

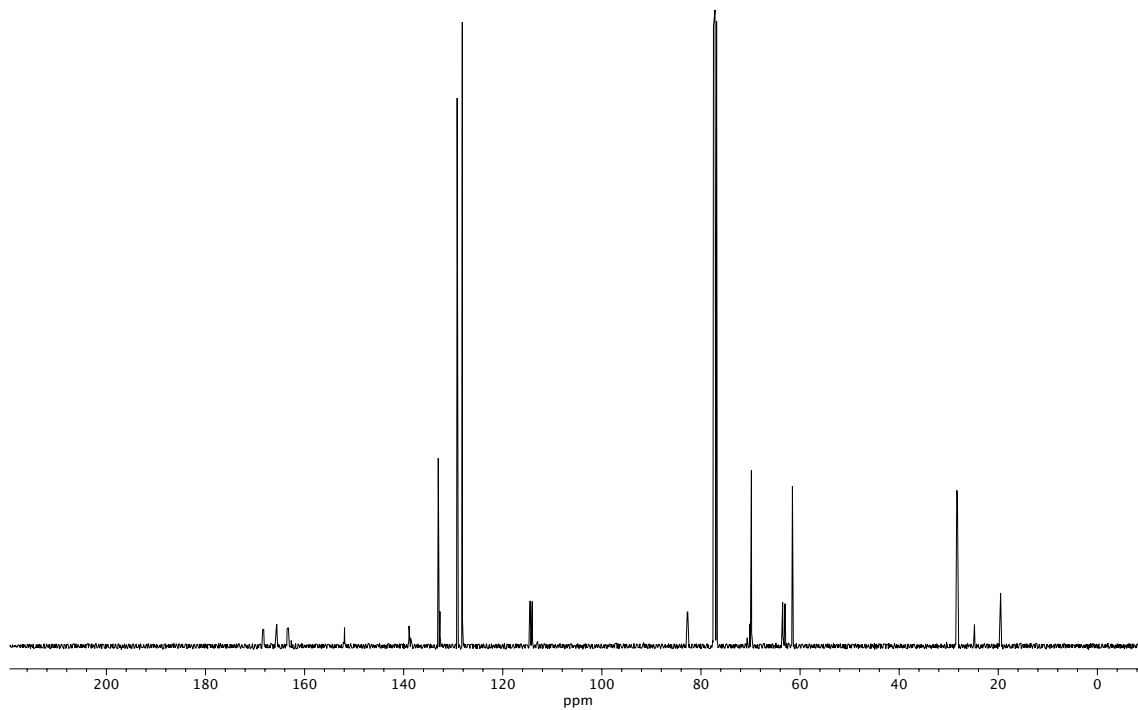


Figure A1.147. ¹³C NMR (100 MHz, CDCl₃) of compound **60**.

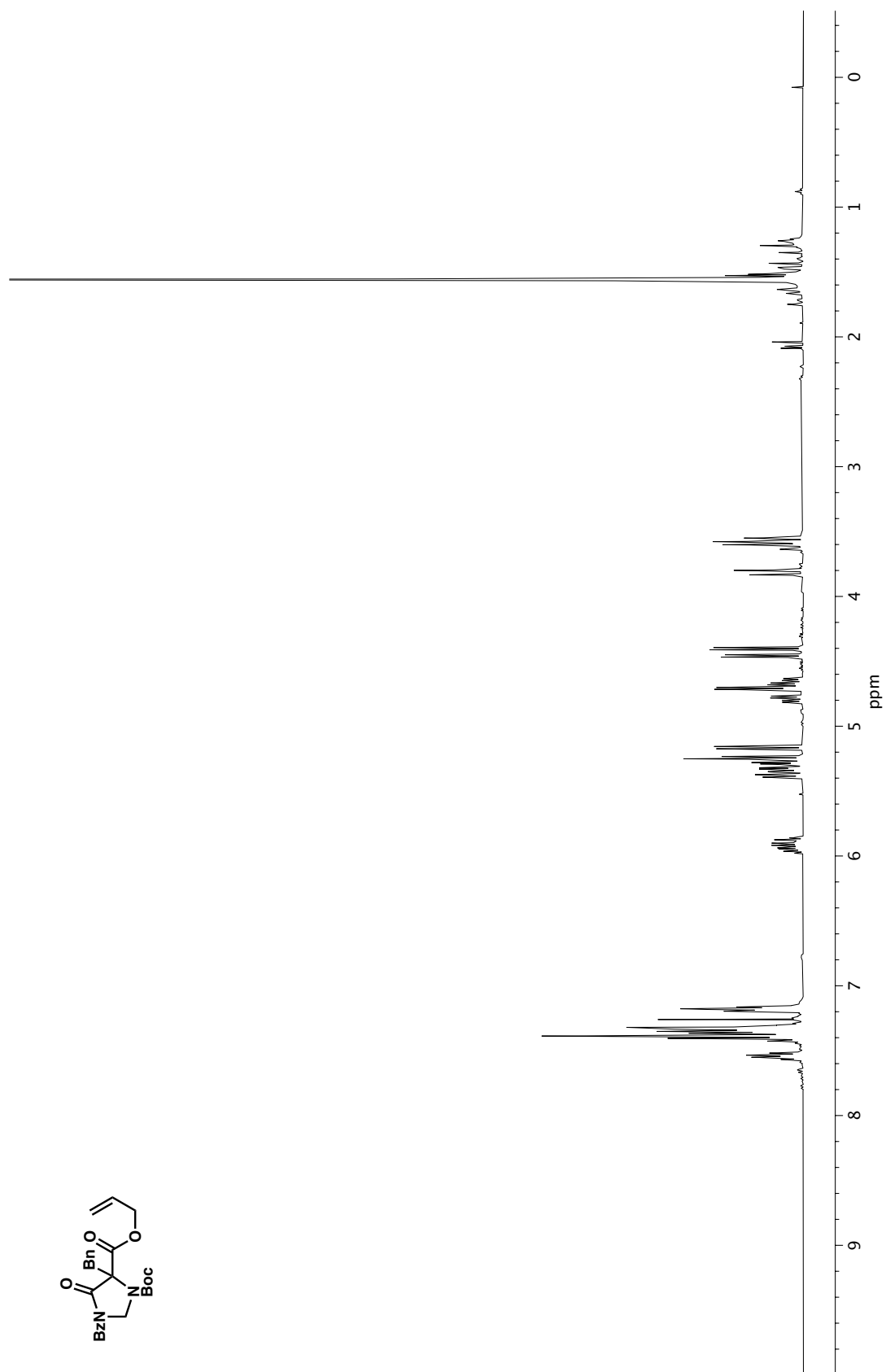


Figure A1.148. ^1H NMR (400 MHz, CDCl_3) of compound **34a**.

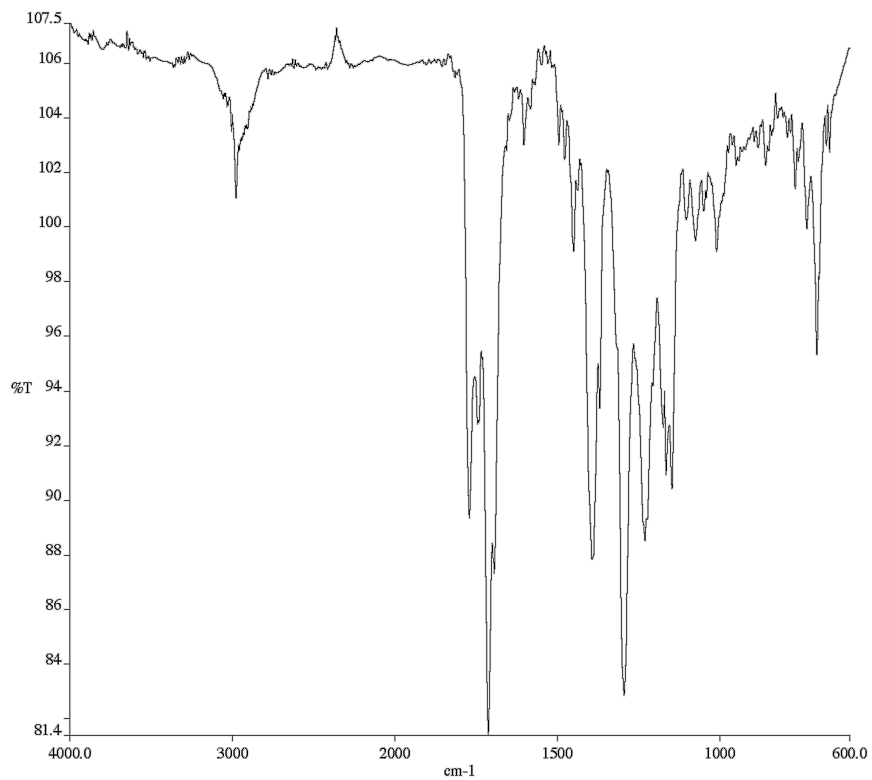


Figure A1.149. Infrared spectrum (Thin Film, NaCl) of compound **34a**.

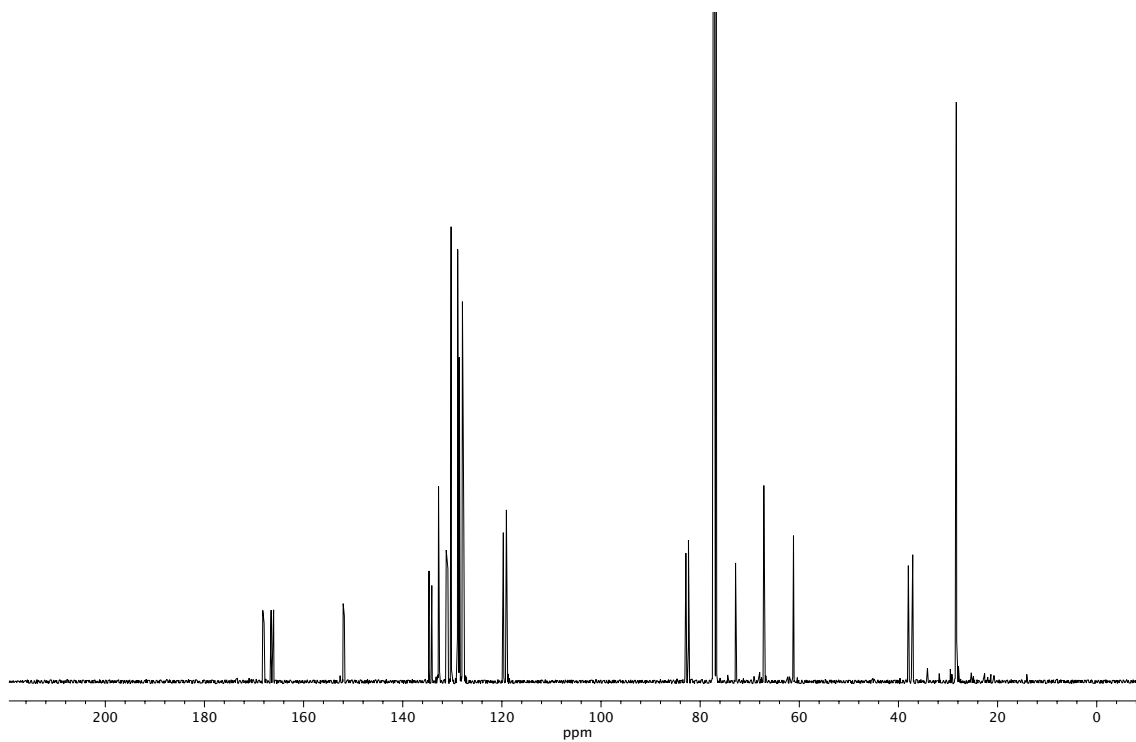
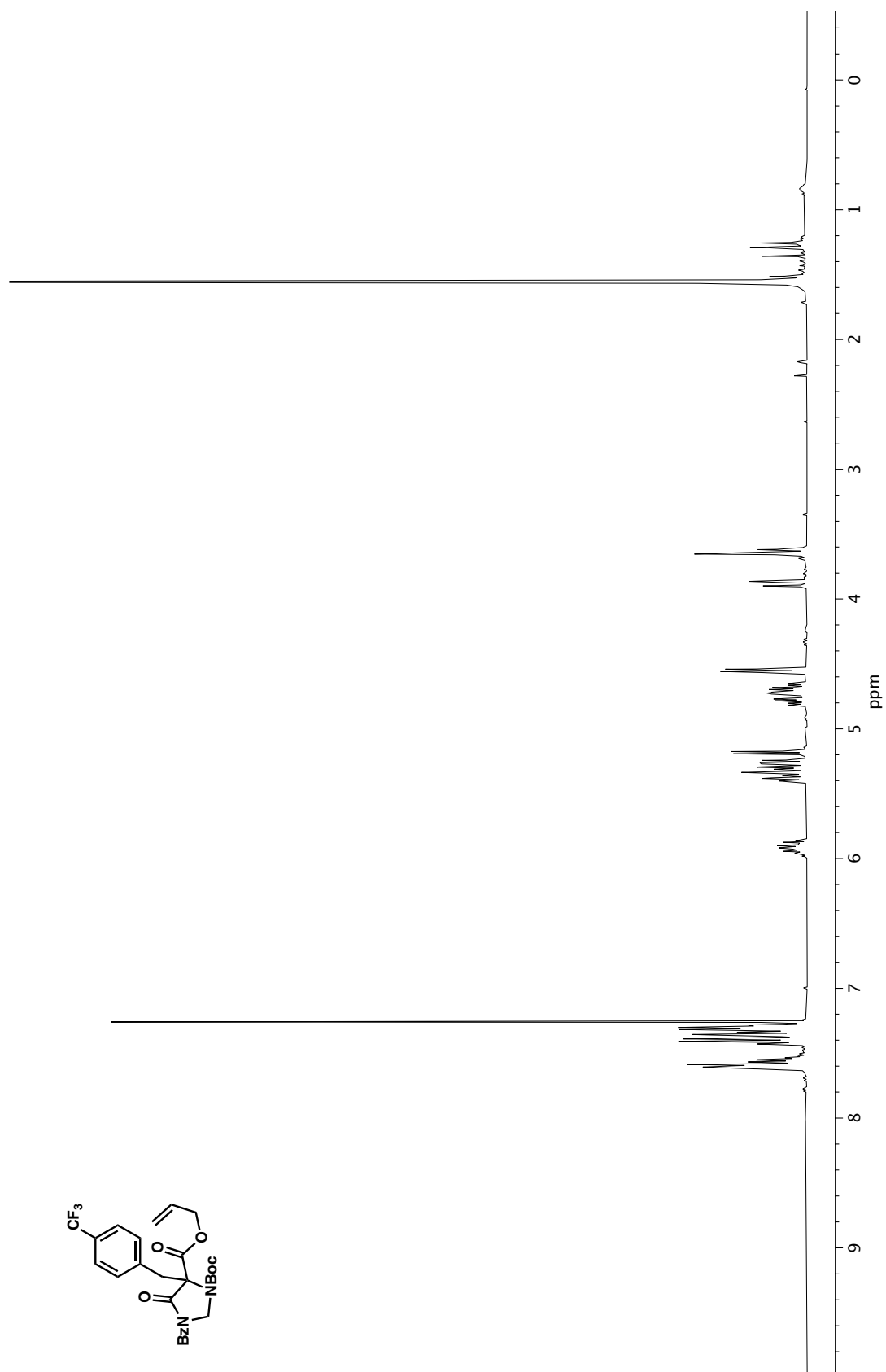


Figure A1.150. ¹³C NMR (100 MHz, CDCl₃) of compound **34a**.

Figure A1.151. ^1H NMR (400 MHz, CDCl_3) of compound **34b**.

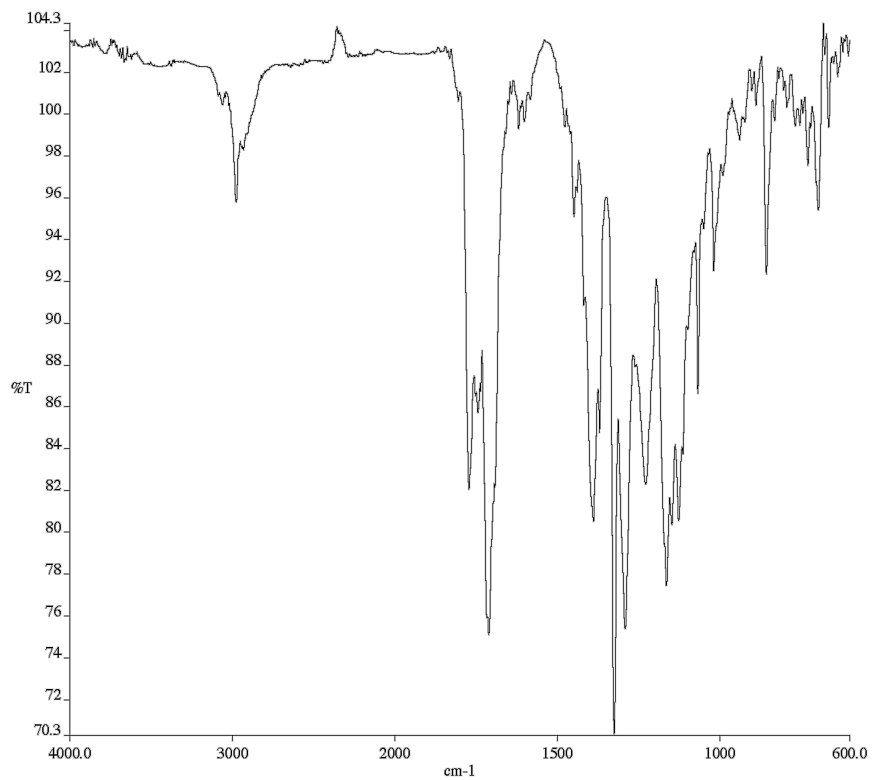


Figure A1.152. Infrared spectrum (Thin Film, NaCl) of compound **34b**.

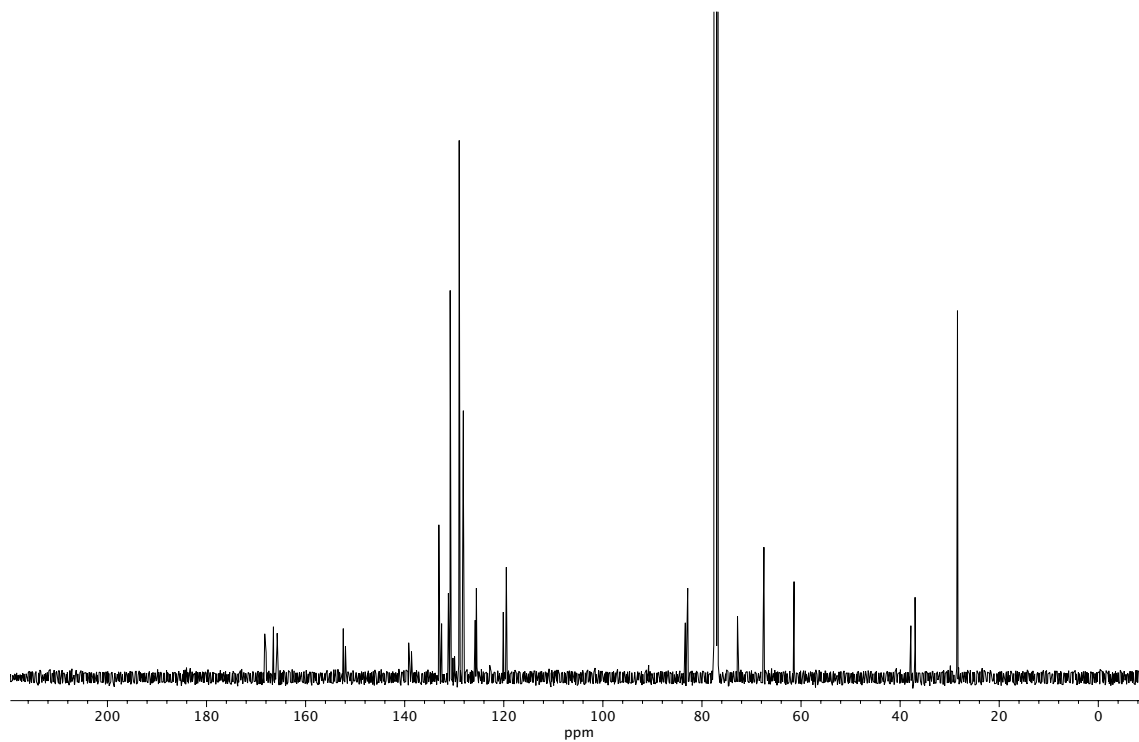


Figure A1.153. ¹³C NMR (100 MHz, CDCl₃) of compound **34b**.

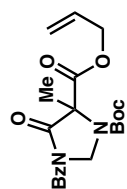
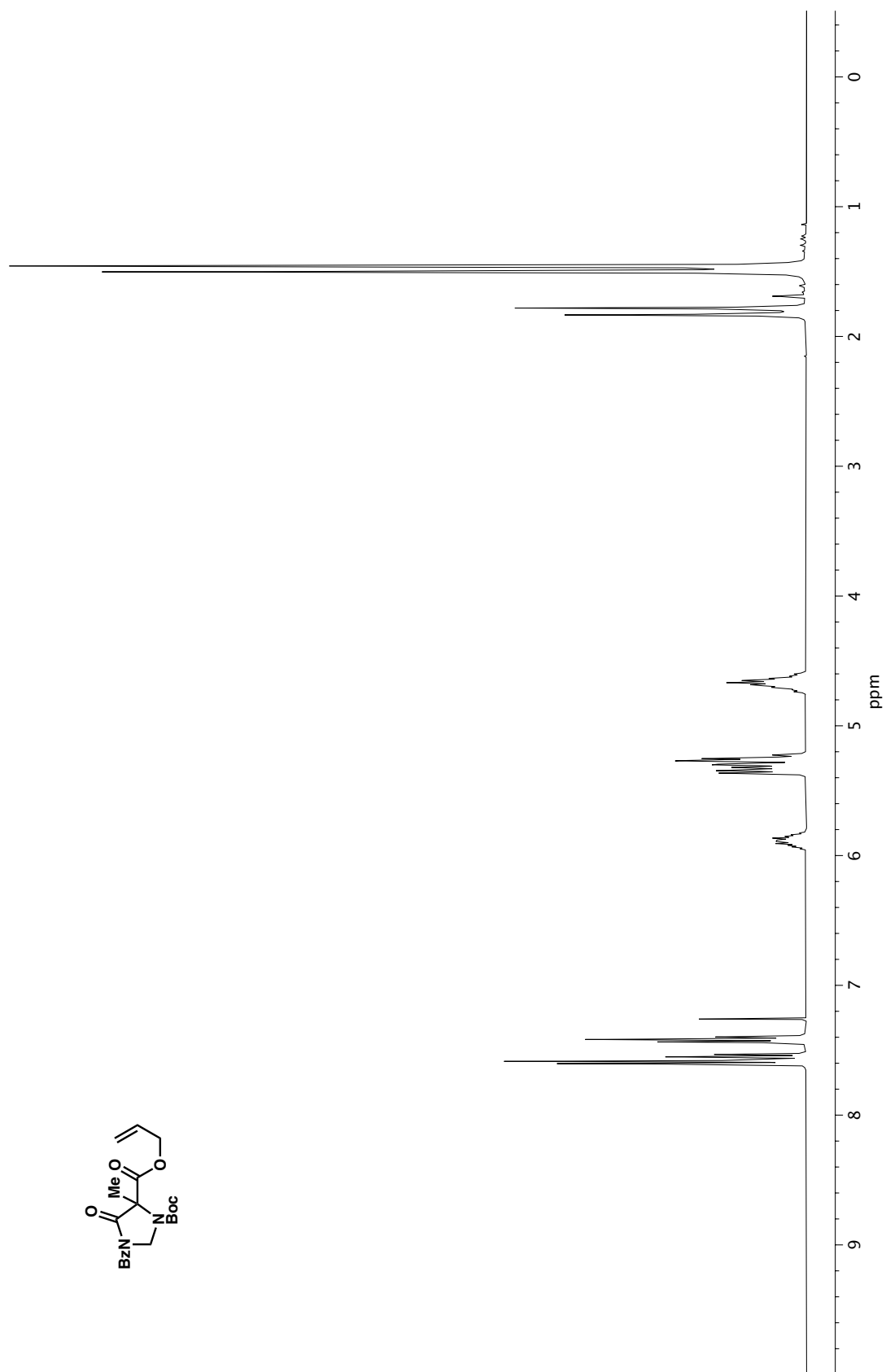


Figure A1.154. ^1H NMR (400 MHz, CDCl_3) of compound **34c**.

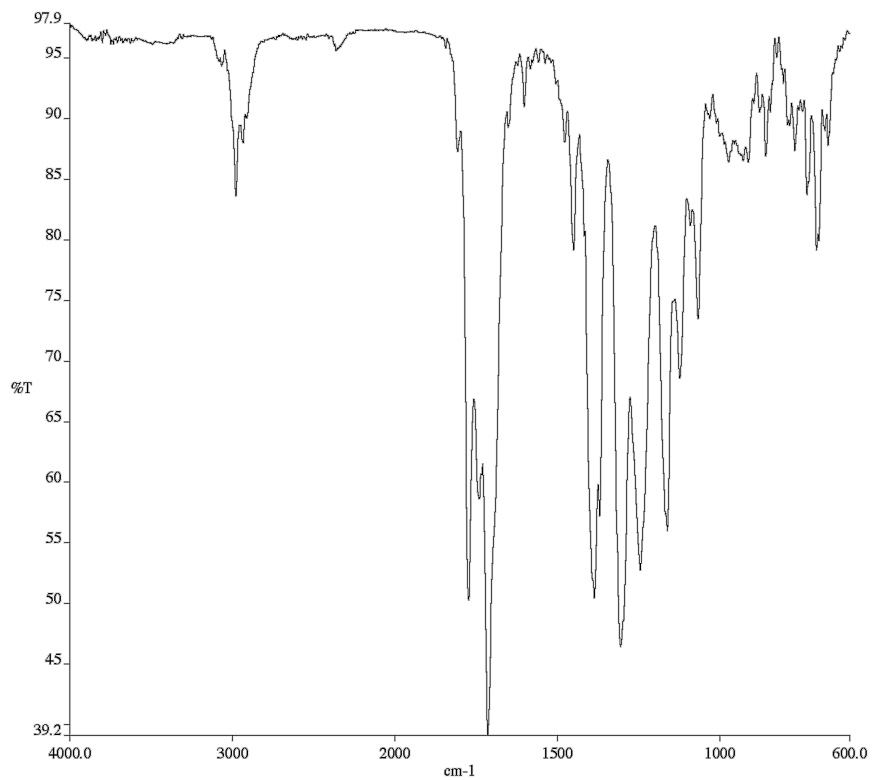


Figure A1.155. Infrared spectrum (Thin Film, NaCl) of compound **34c**.

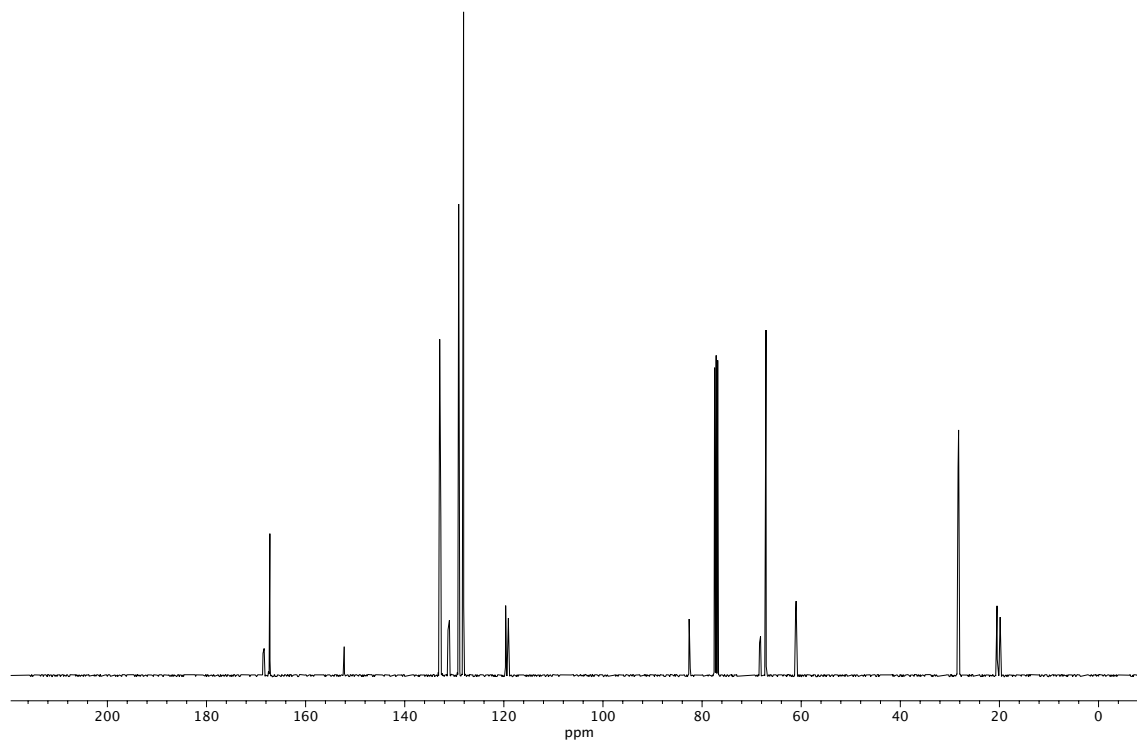


Figure A1.156. ¹³C NMR (100 MHz, CDCl₃) of compound **34c**.

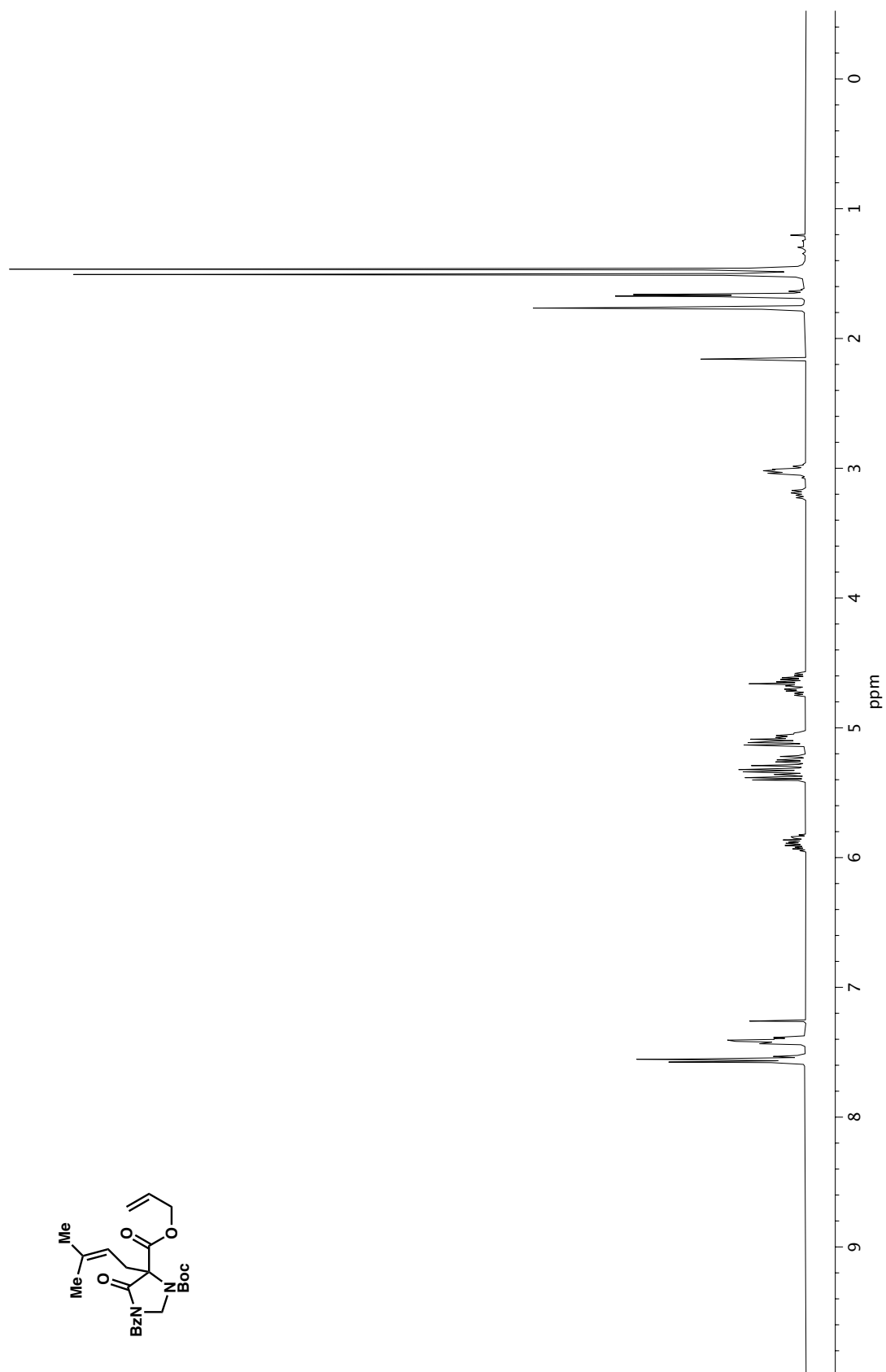


Figure A1.157. ^1H NMR (400 MHz, CDCl_3) of compound **34d**.

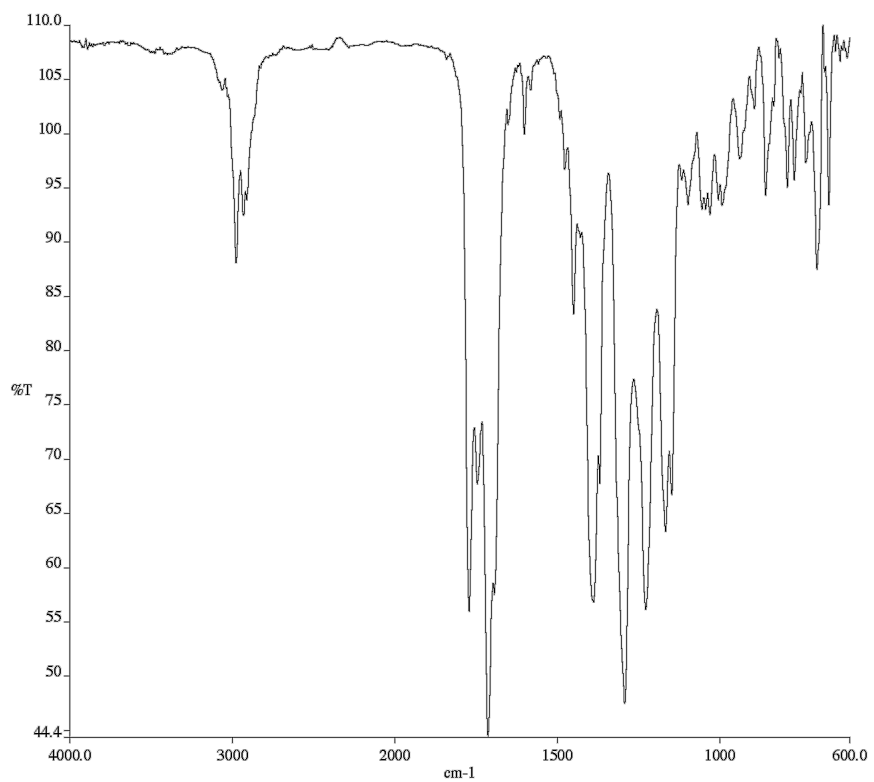


Figure A1.158. Infrared spectrum (Thin Film, NaCl) of compound **34d**.

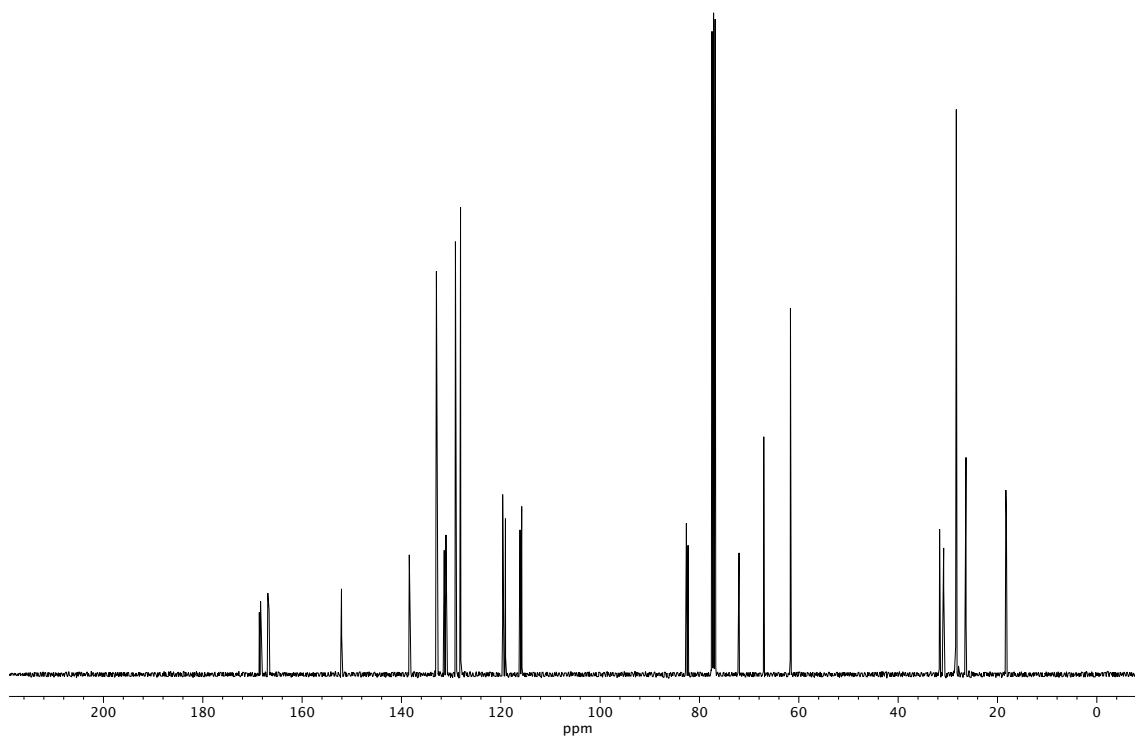
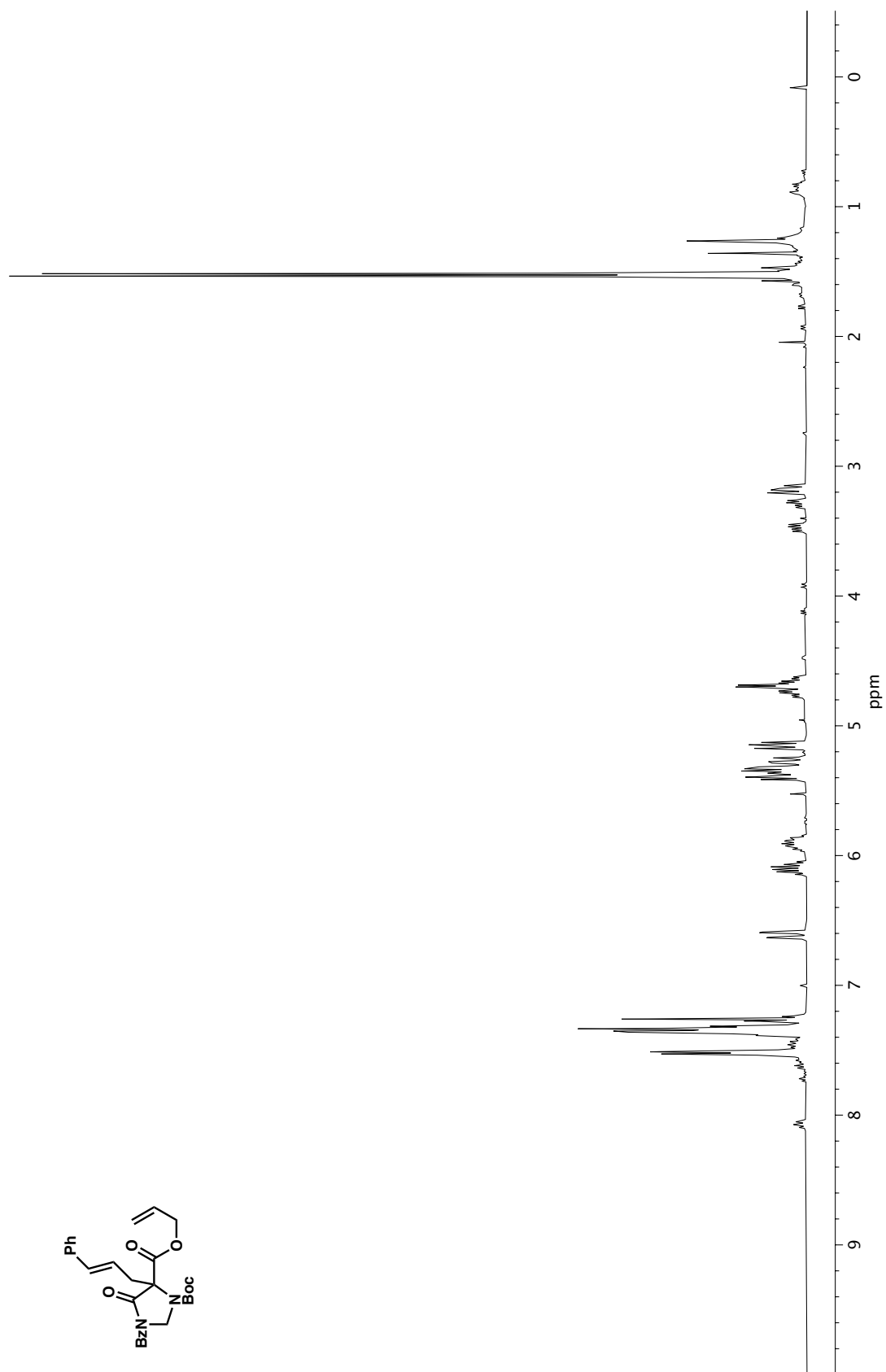


Figure A1.159. ¹³C NMR (100 MHz, CDCl₃) of compound **34d**.

Figure A1.160. ^1H NMR (400 MHz, CDCl_3) of compound **34e**.

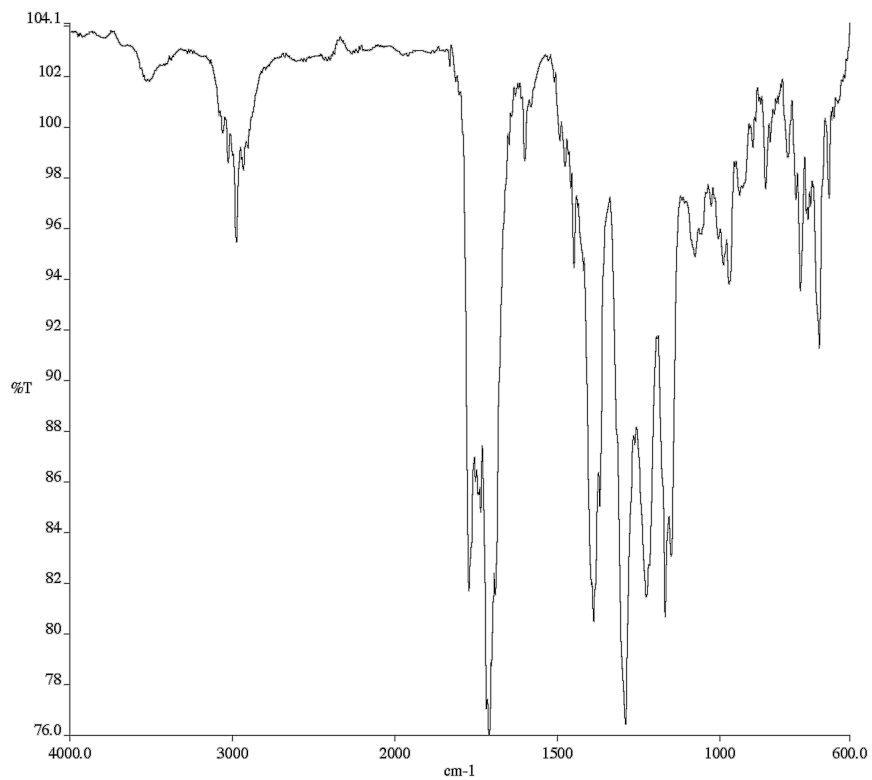


Figure A1.161. Infrared spectrum (Thin Film, NaCl) of compound **34e**.

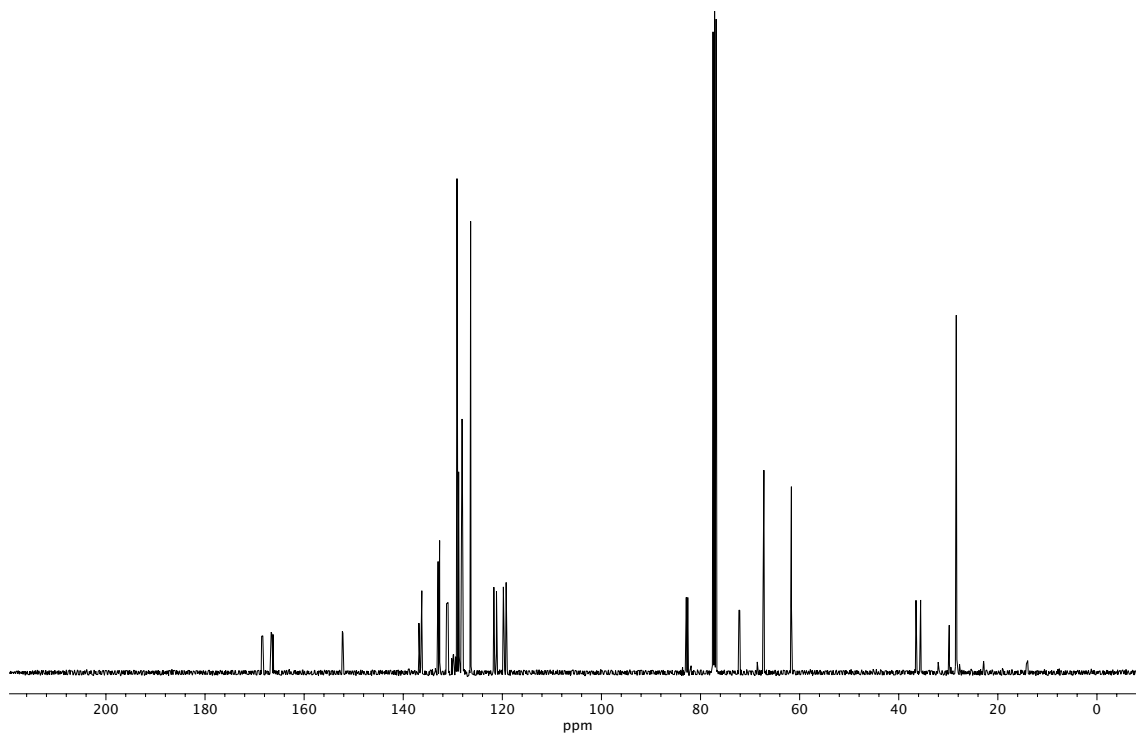


Figure A1.162. ¹³C NMR (100 MHz, CDCl₃) of compound **34e**.

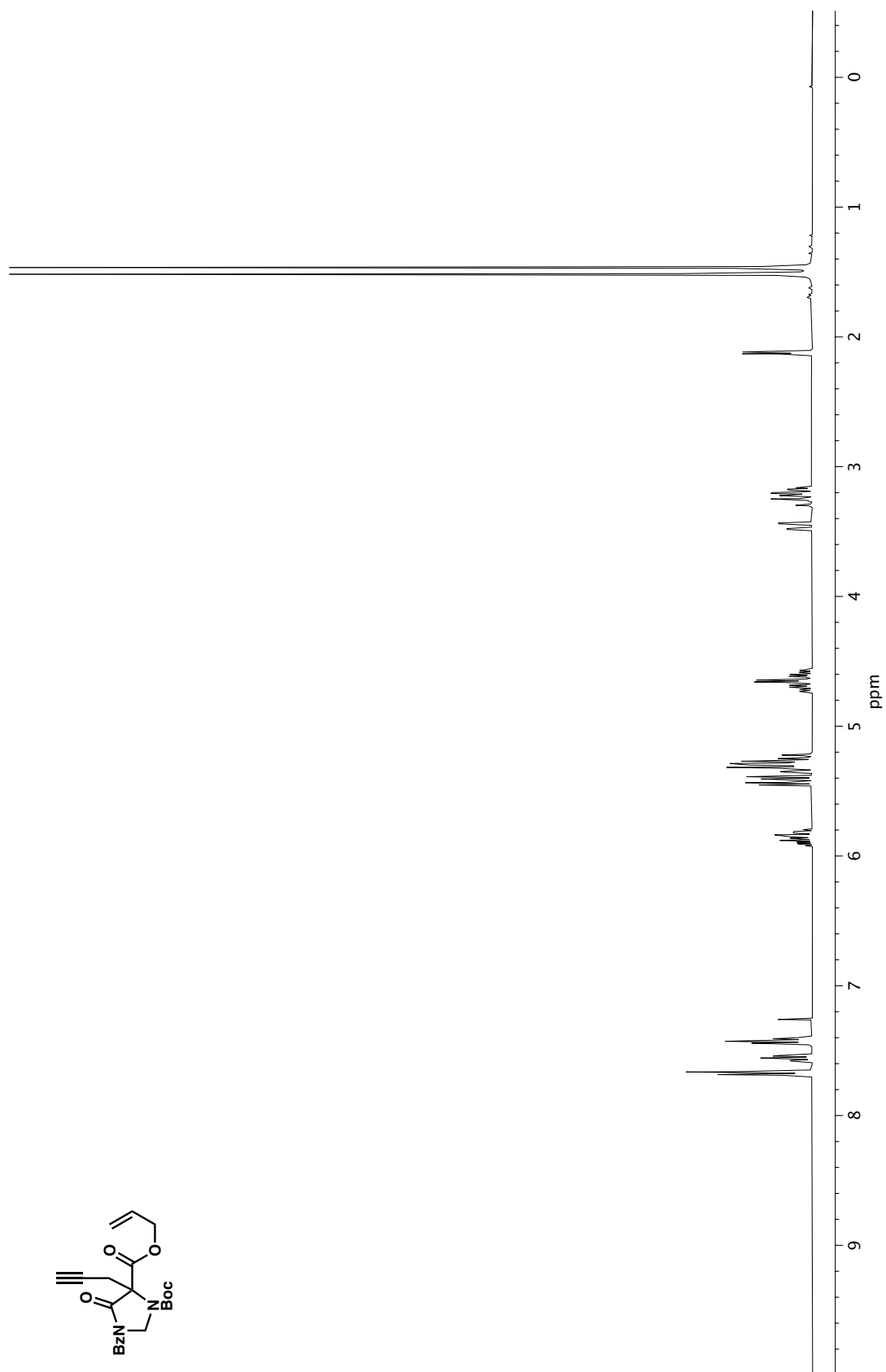


Figure A1.163. ¹H NMR (400 MHz, CDCl₃) of compound 34f.

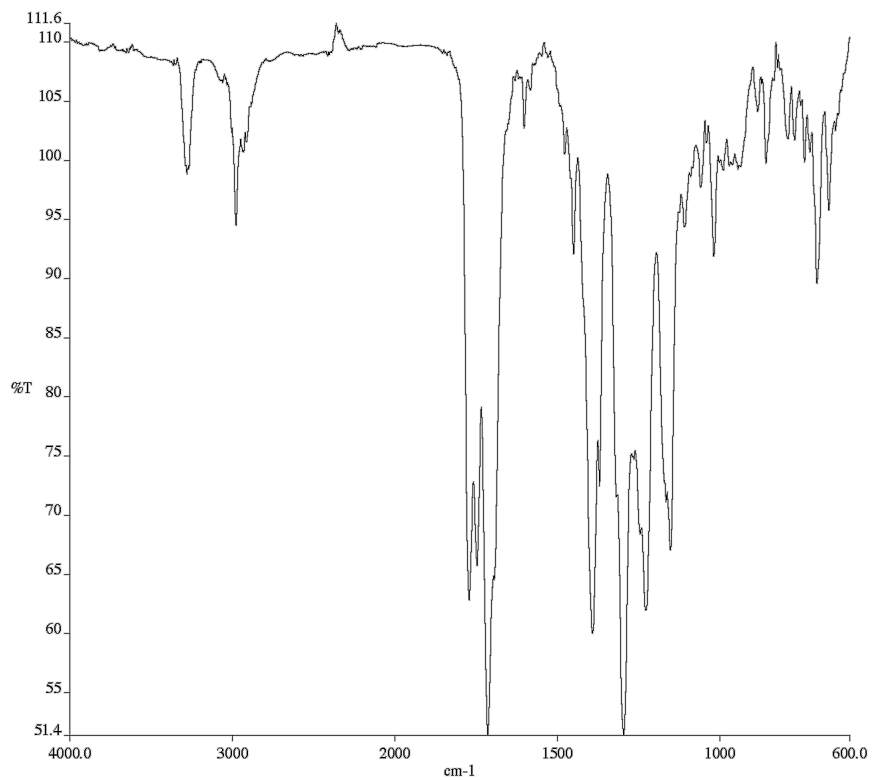


Figure A1.164. Infrared spectrum (Thin Film, NaCl) of compound **34f**.

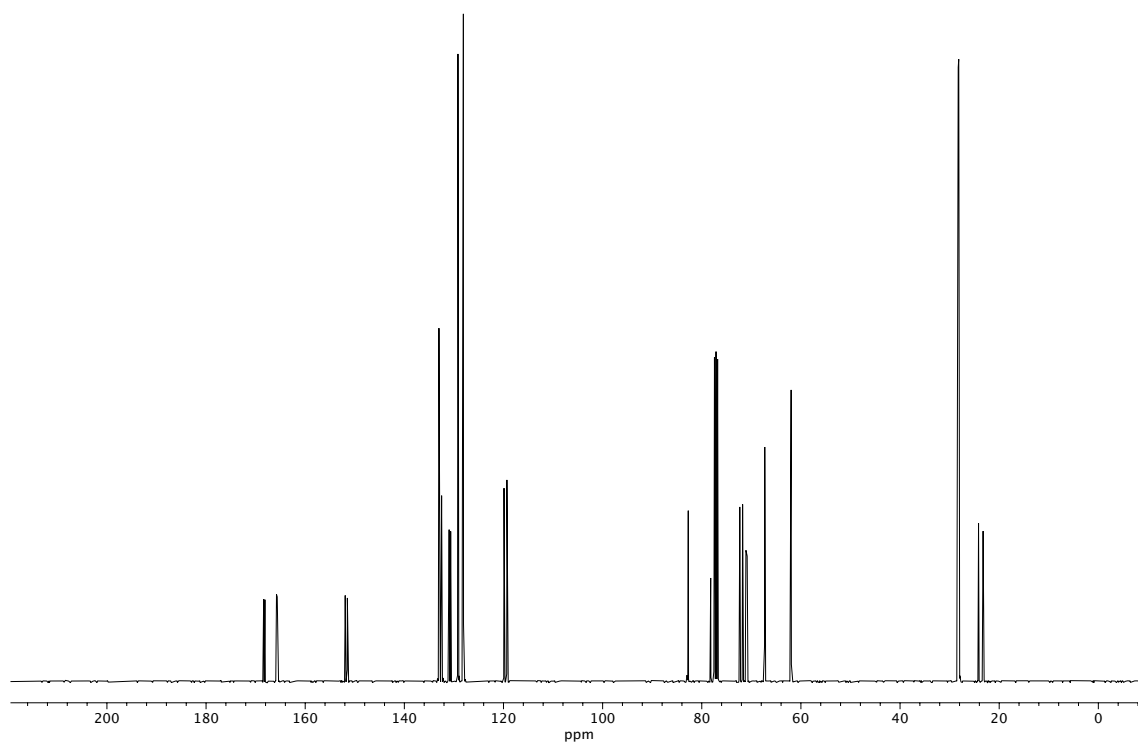
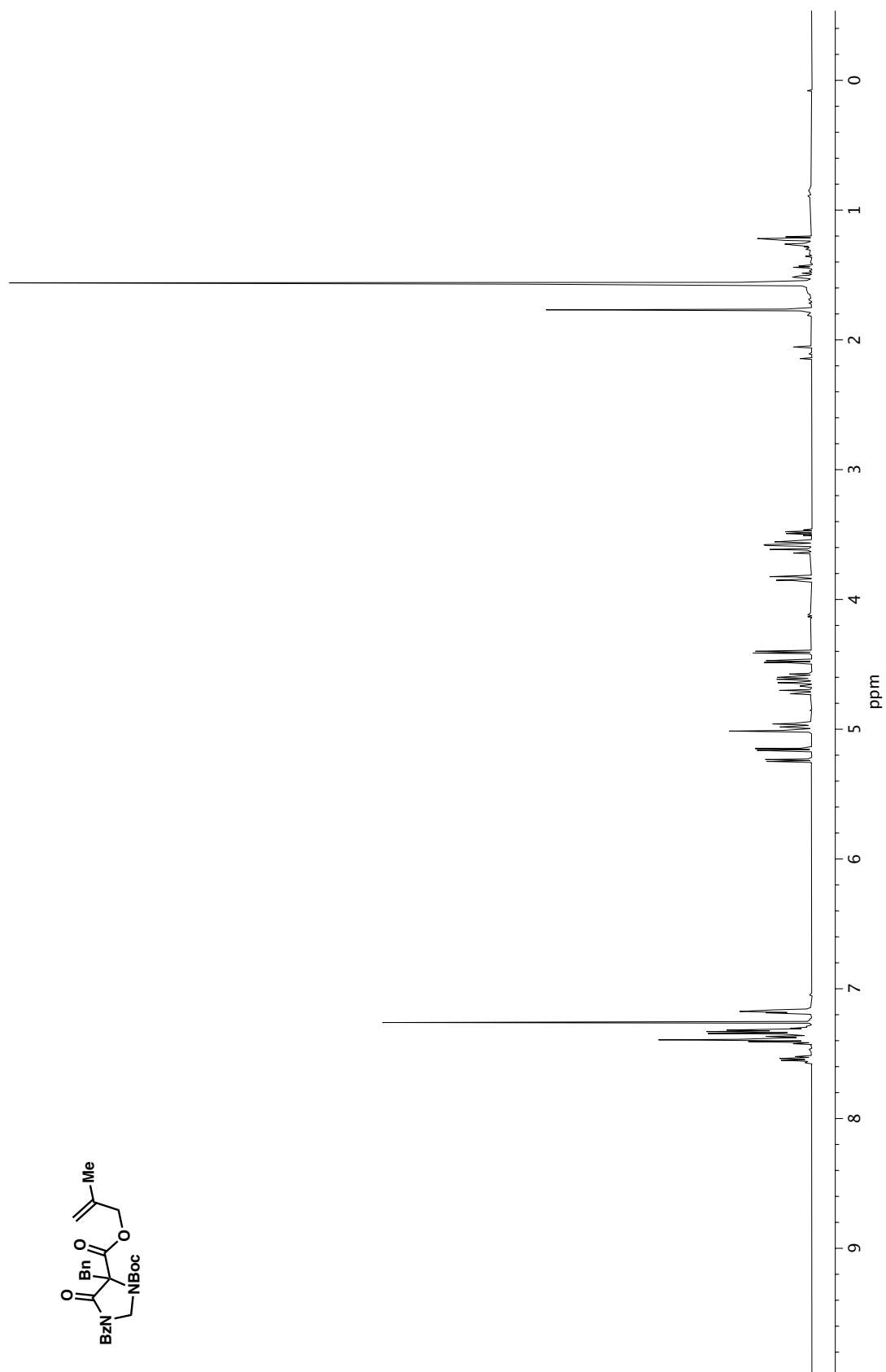


Figure A1.165. ¹³C NMR (100 MHz, CDCl₃) of compound **34f**.

Figure A1.166. ^1H NMR (500 MHz, CDCl_3) of compound **34g**.

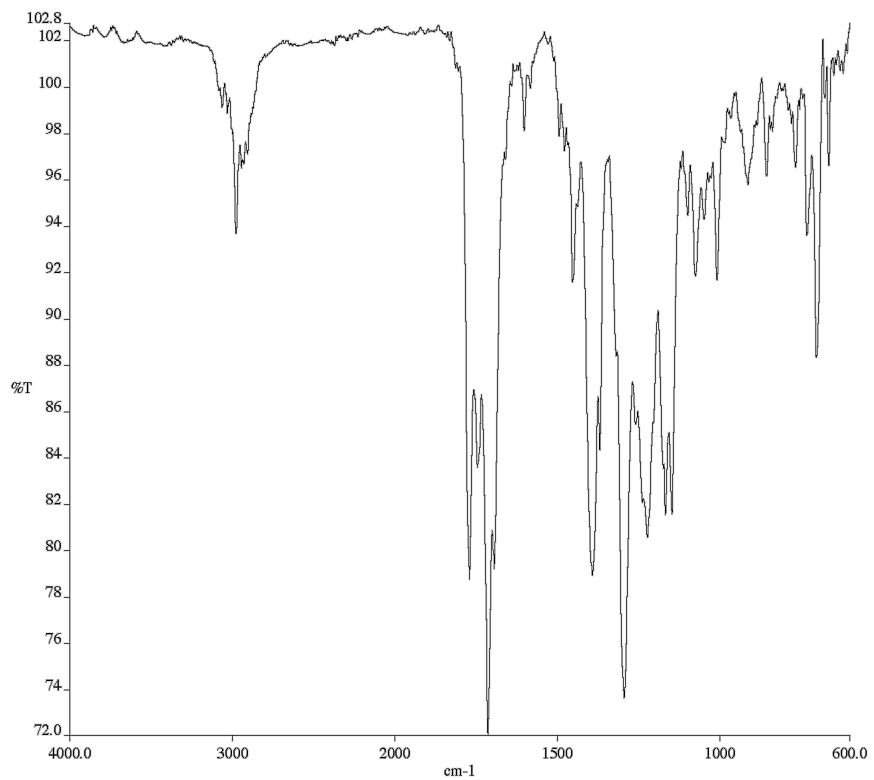


Figure A1.167. Infrared spectrum (Thin Film, NaCl) of compound **34g**.

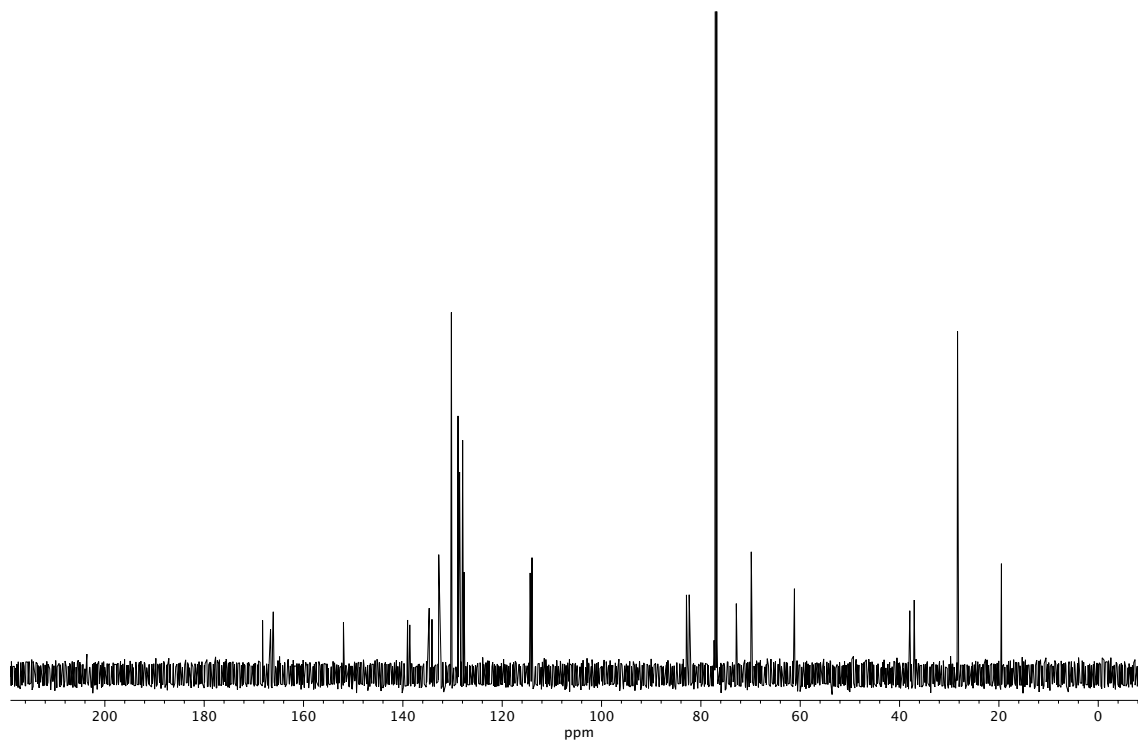
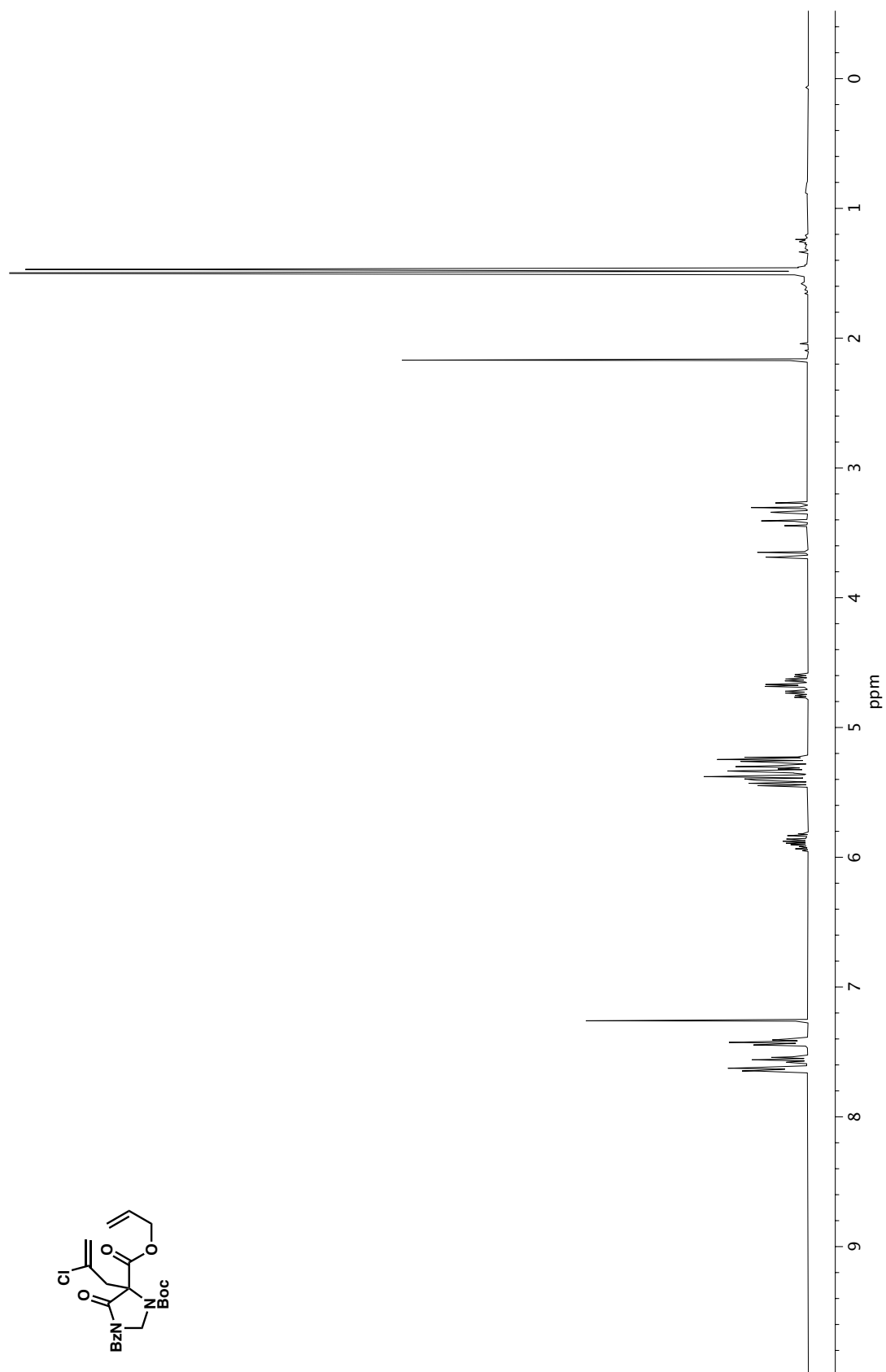


Figure A1.168. ¹³C NMR (125 MHz, CDCl₃) of compound **34g**.

Figure A1.169. ^1H NMR (400 MHz, CDCl_3) of compound **34h**.

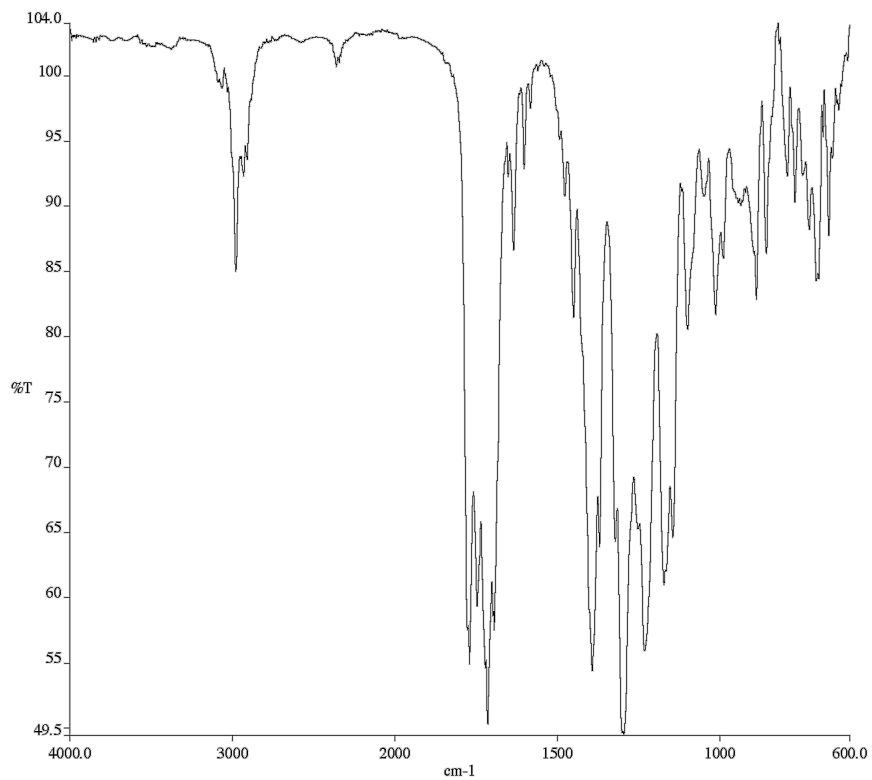


Figure A1.170. Infrared spectrum (Thin Film, NaCl) of compound **34h**.

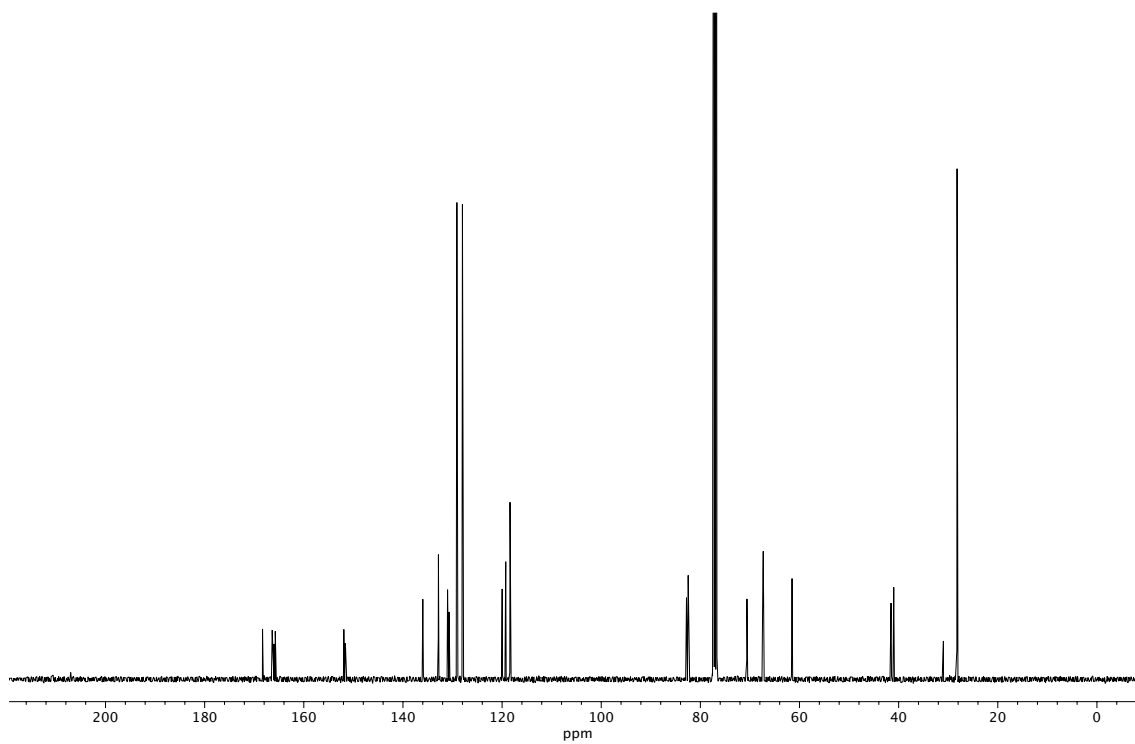


Figure A1.171. ¹³C NMR (100 MHz, CDCl₃) of compound **34h**.

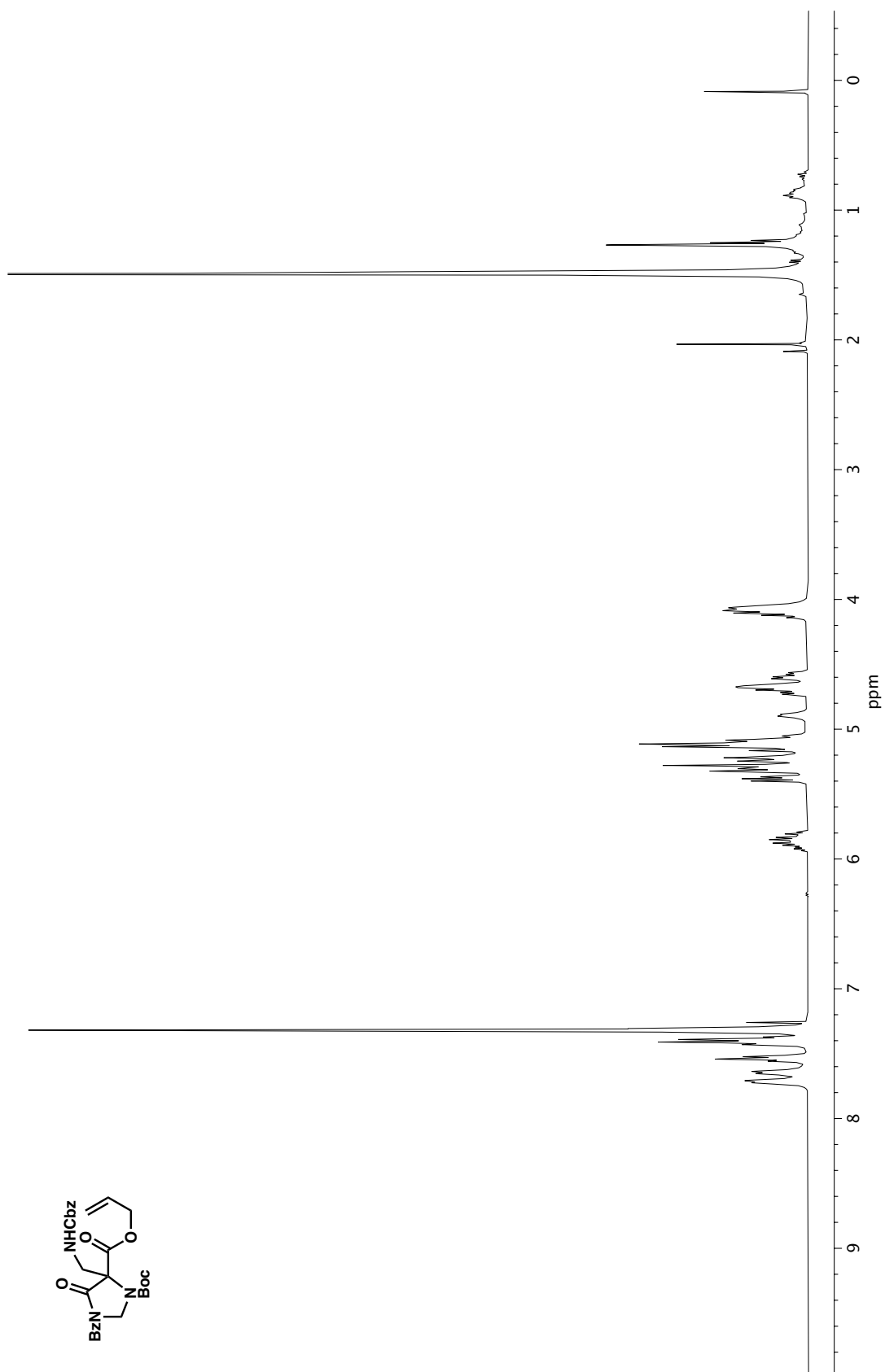


Figure A1.172. ¹H NMR (400 MHz, CDCl₃) of compound **34i**.

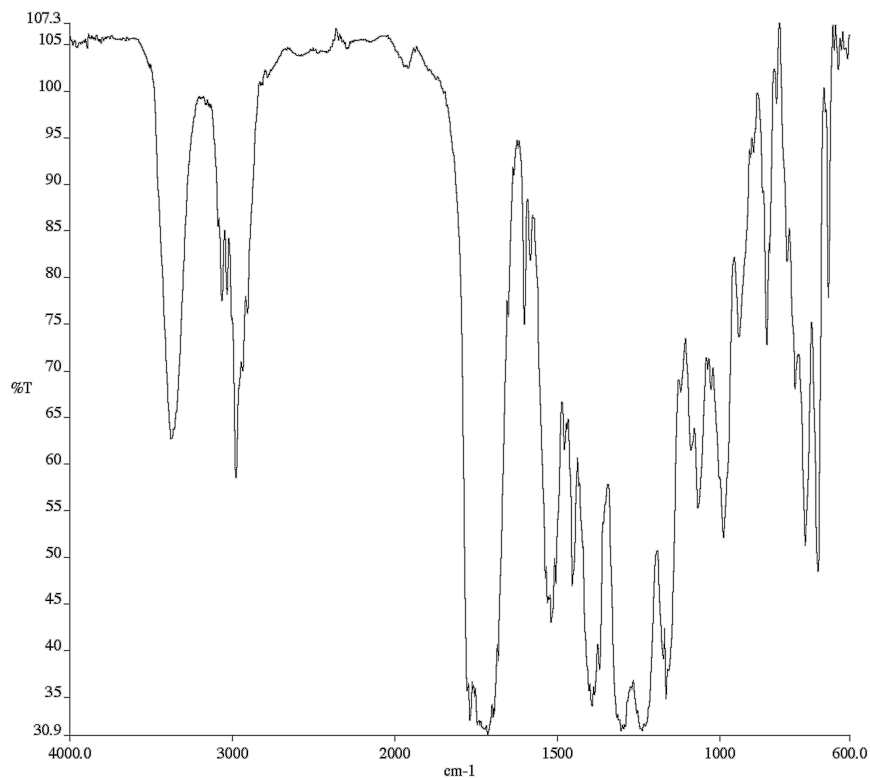


Figure A1.173. Infrared spectrum (Thin Film, NaCl) of compound **34i**.

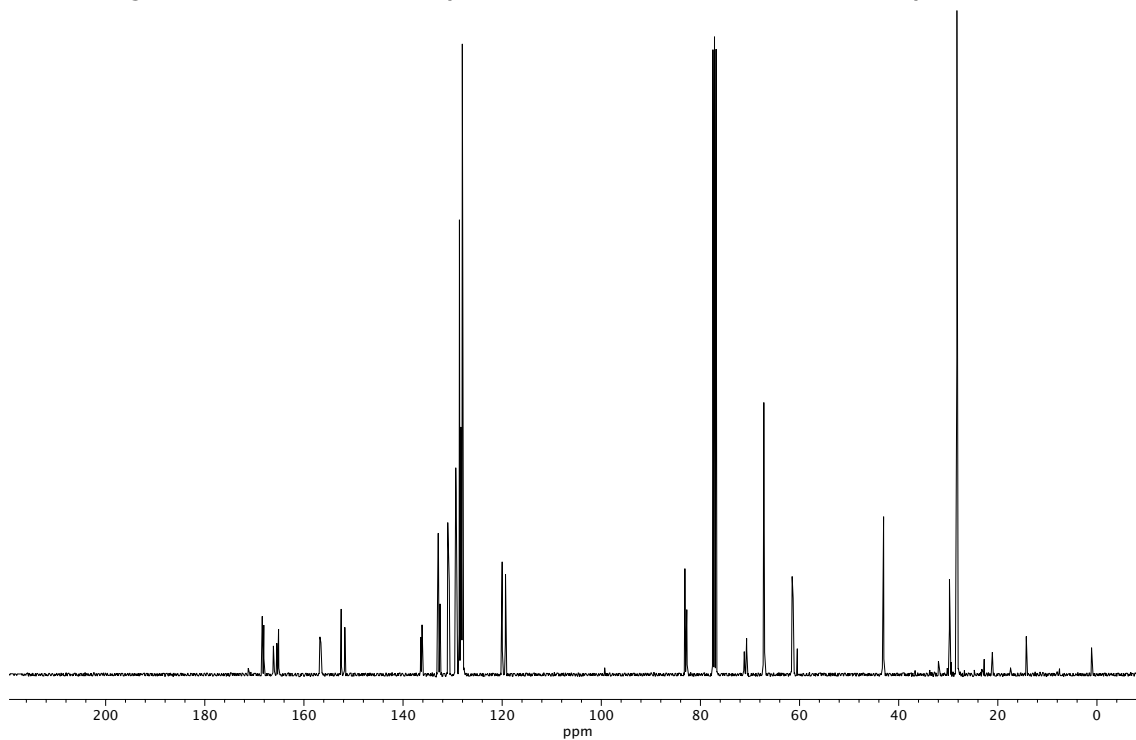
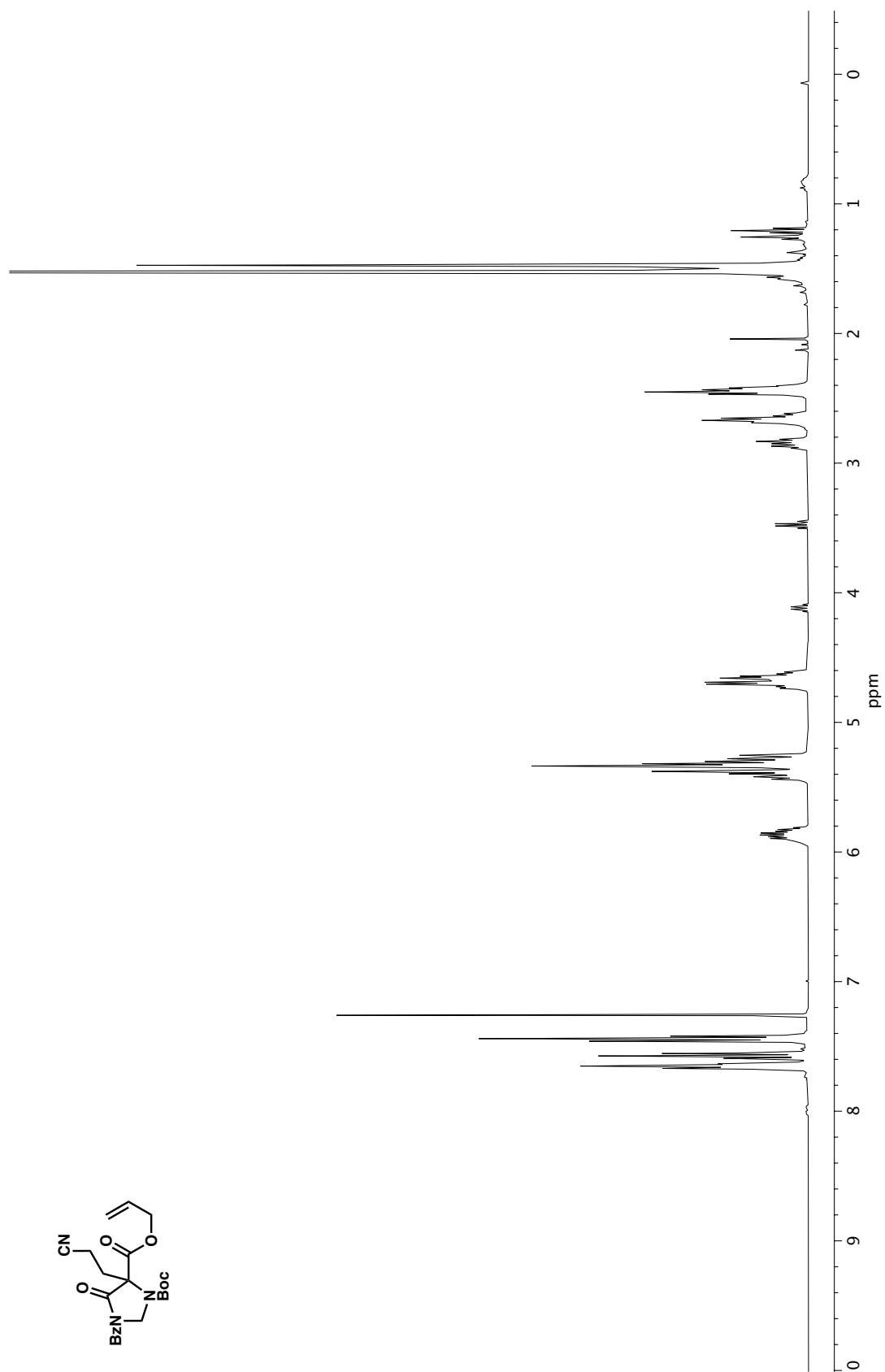


Figure A1.174. ¹³C NMR (100 MHz, CDCl₃) of compound **34i**.

Figure A1.175. ¹H NMR (400 MHz, CDCl₃) of compound 34j.

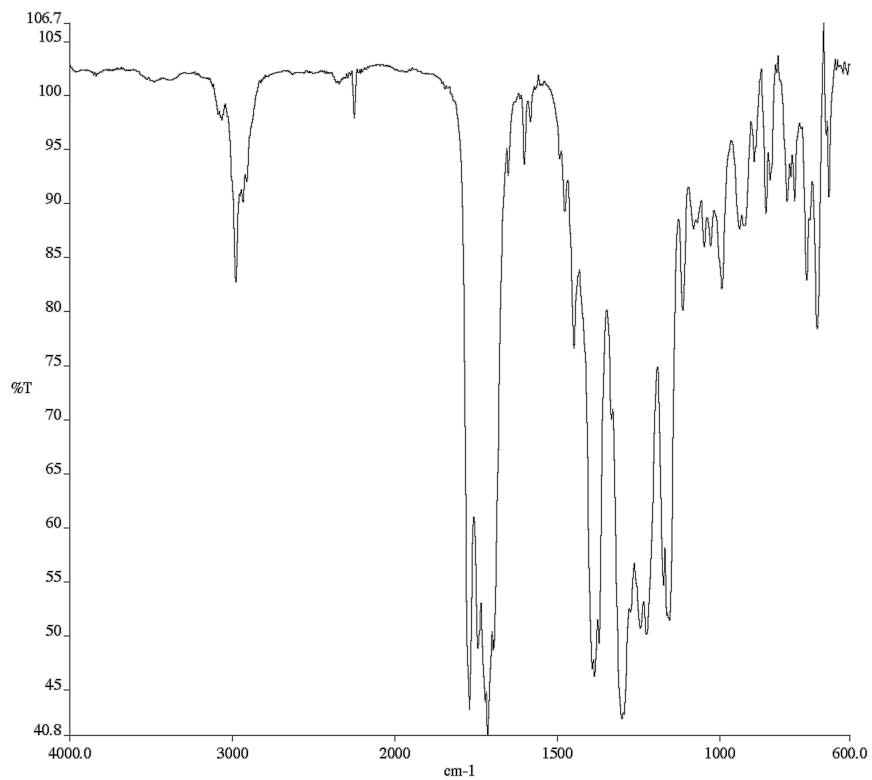


Figure A1.176. Infrared spectrum (Thin Film, NaCl) of compound **34j**.

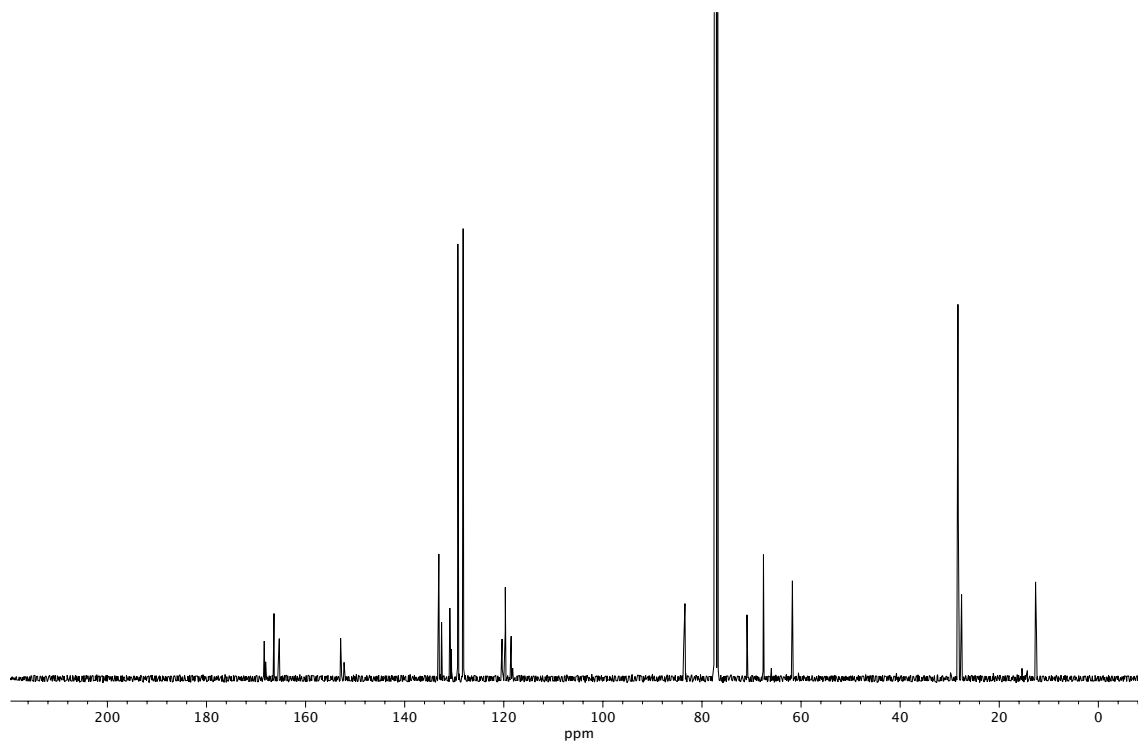


Figure A1.177. ¹³C NMR (100 MHz, CDCl₃) of compound **34j**.

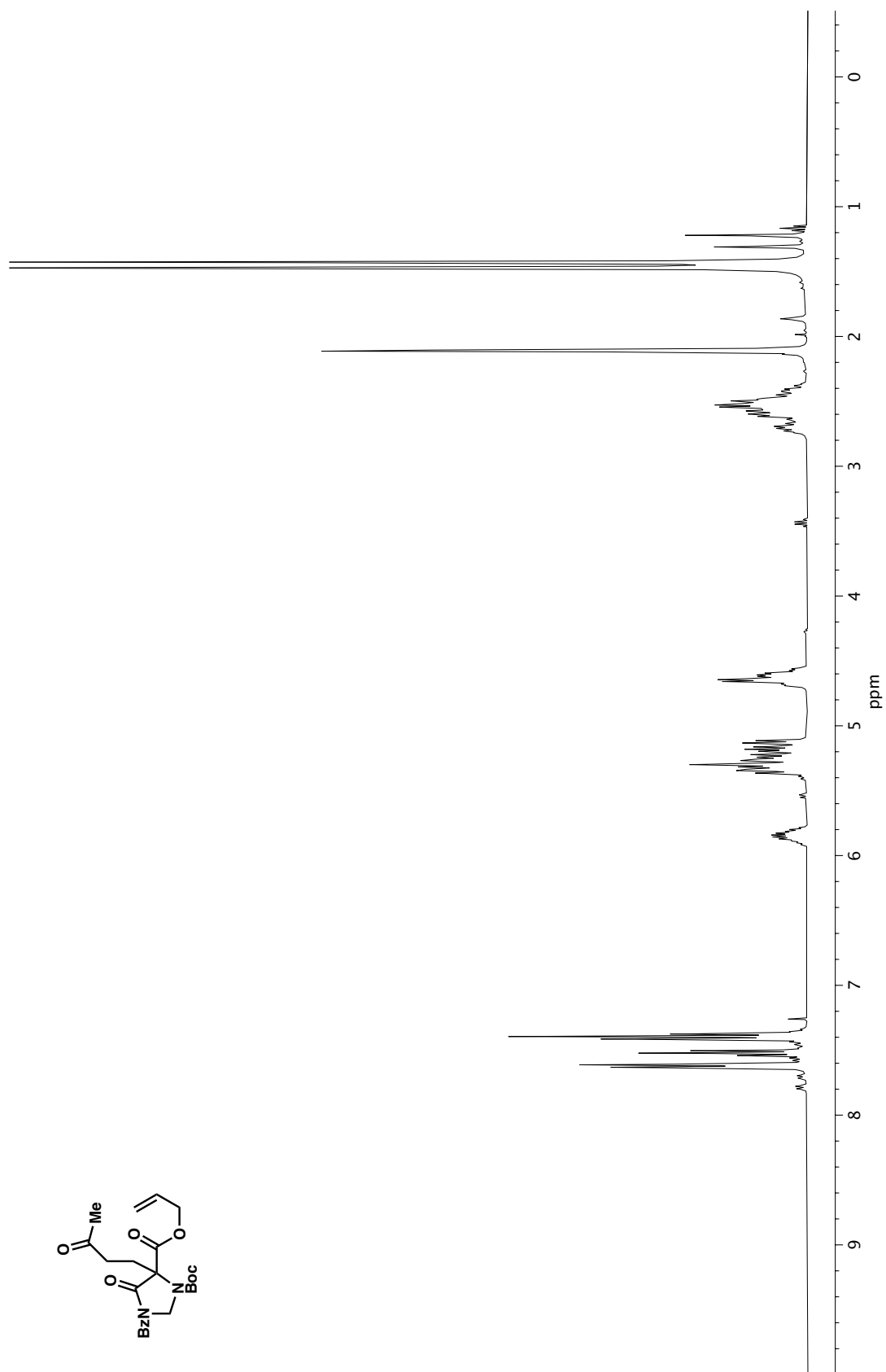


Figure A1.178. ¹H NMR (400 MHz, CDCl₃) of compound 34k.

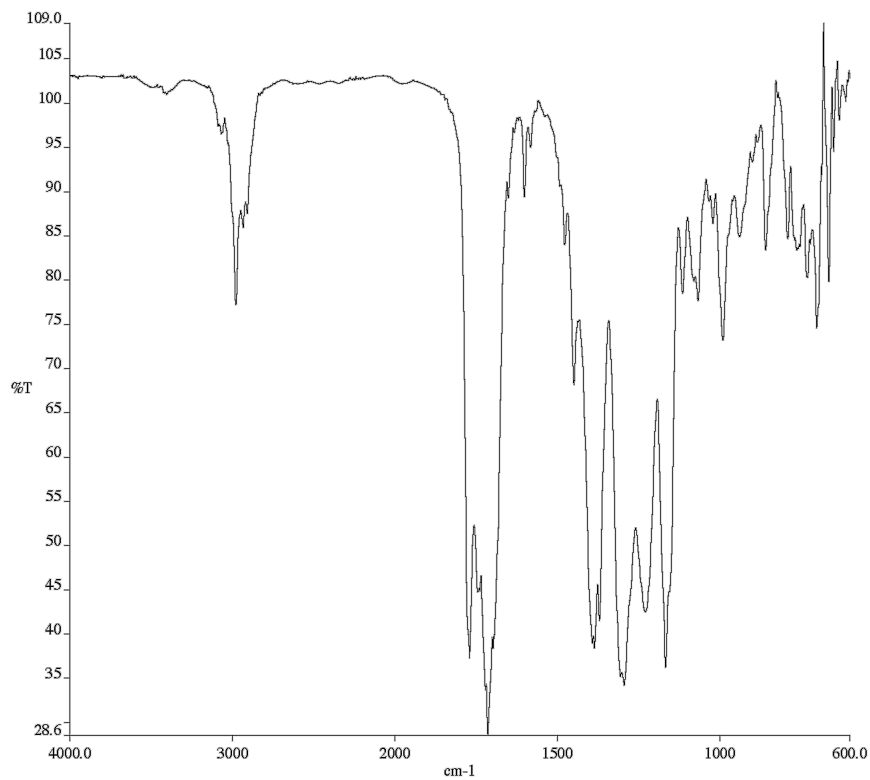


Figure A1.179. Infrared spectrum (Thin Film, NaCl) of compound **34k**.

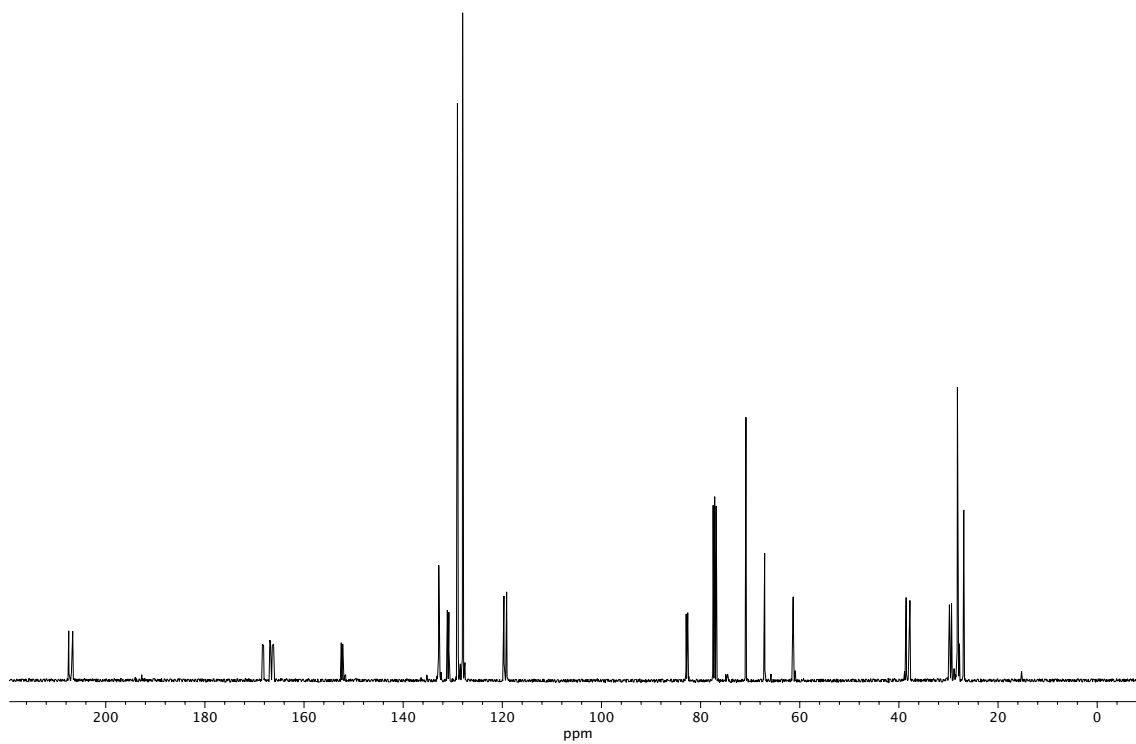
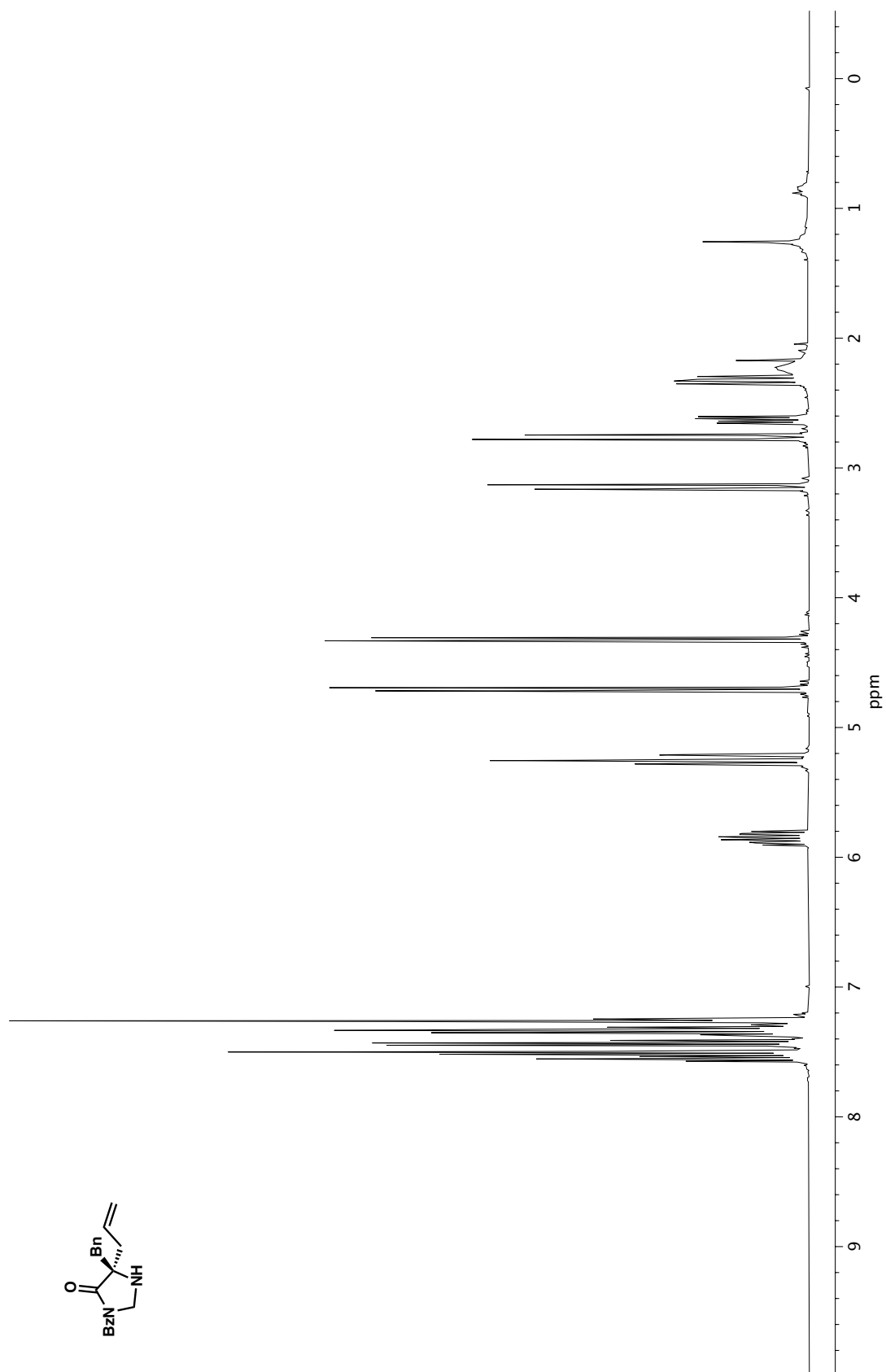


Figure A1.180. ¹³C NMR (100 MHz, CDCl₃) of compound **34k**.

Figure A1.181. ^1H NMR (400 MHz, CDCl_3) of compound 52.

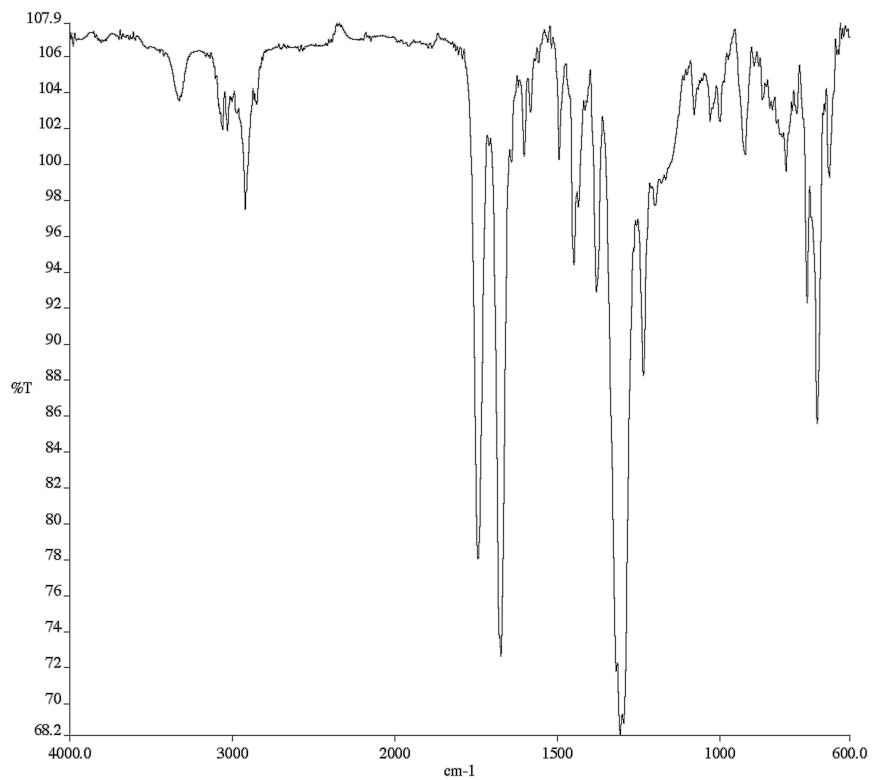


Figure A1.182. Infrared spectrum (Thin Film, NaCl) of compound **52**.

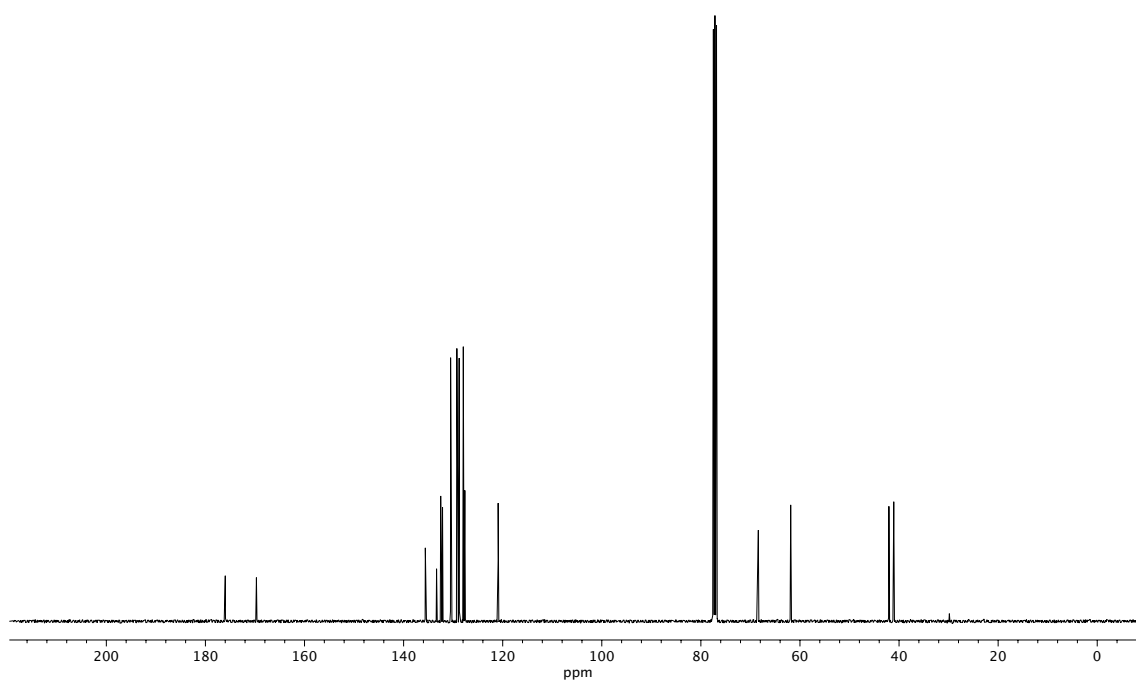
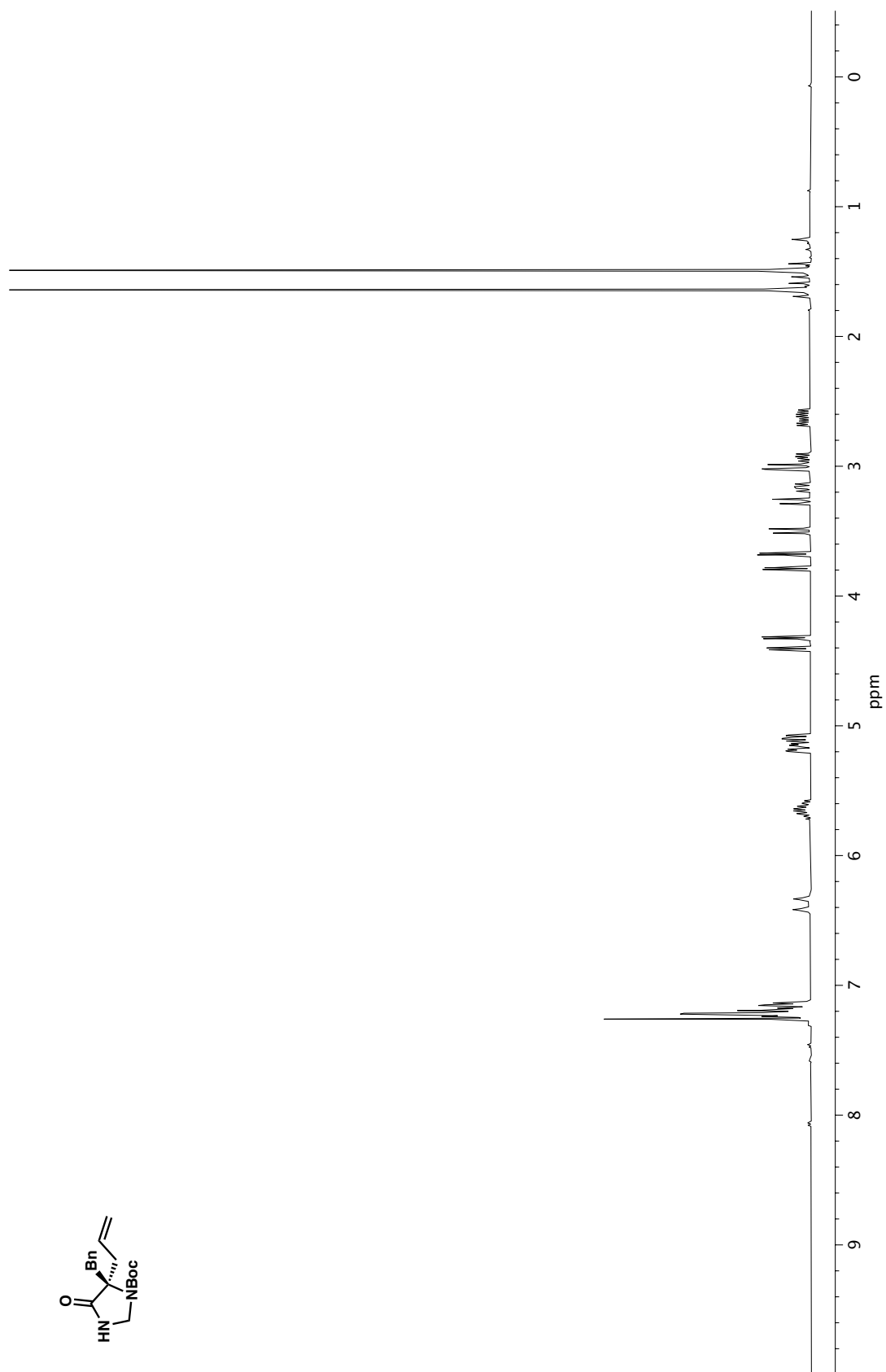


Figure A1.183. ¹³C NMR (100 MHz, CDCl₃) of compound **52**.

Figure A1.184. ^1H NMR (400 MHz, CDCl_3) of compound 53.

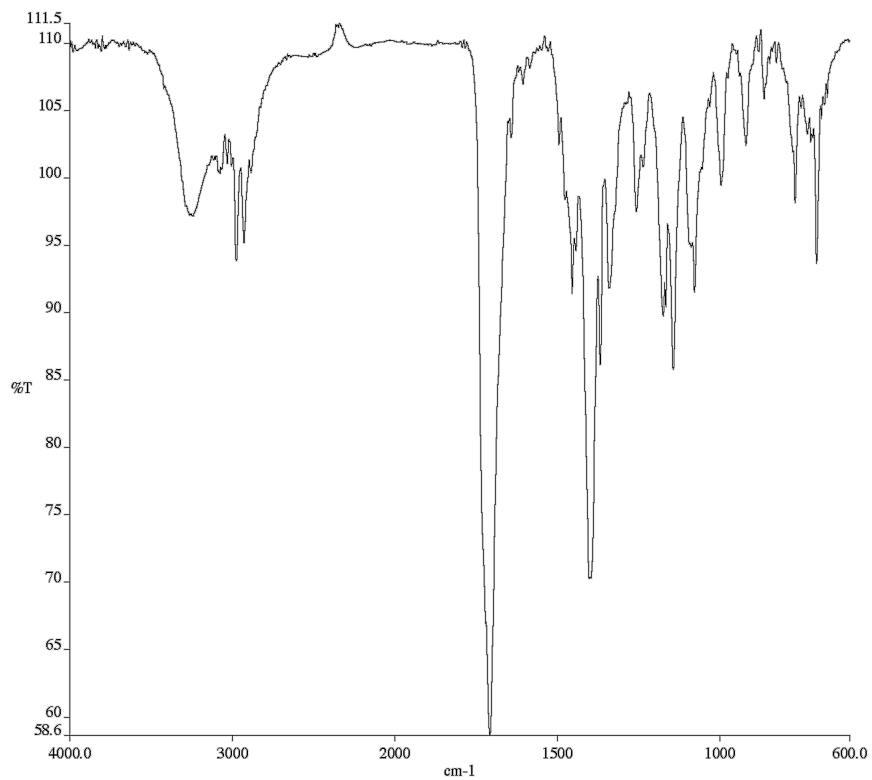


Figure A1.185. Infrared spectrum (Thin Film, NaCl) of compound **53**.

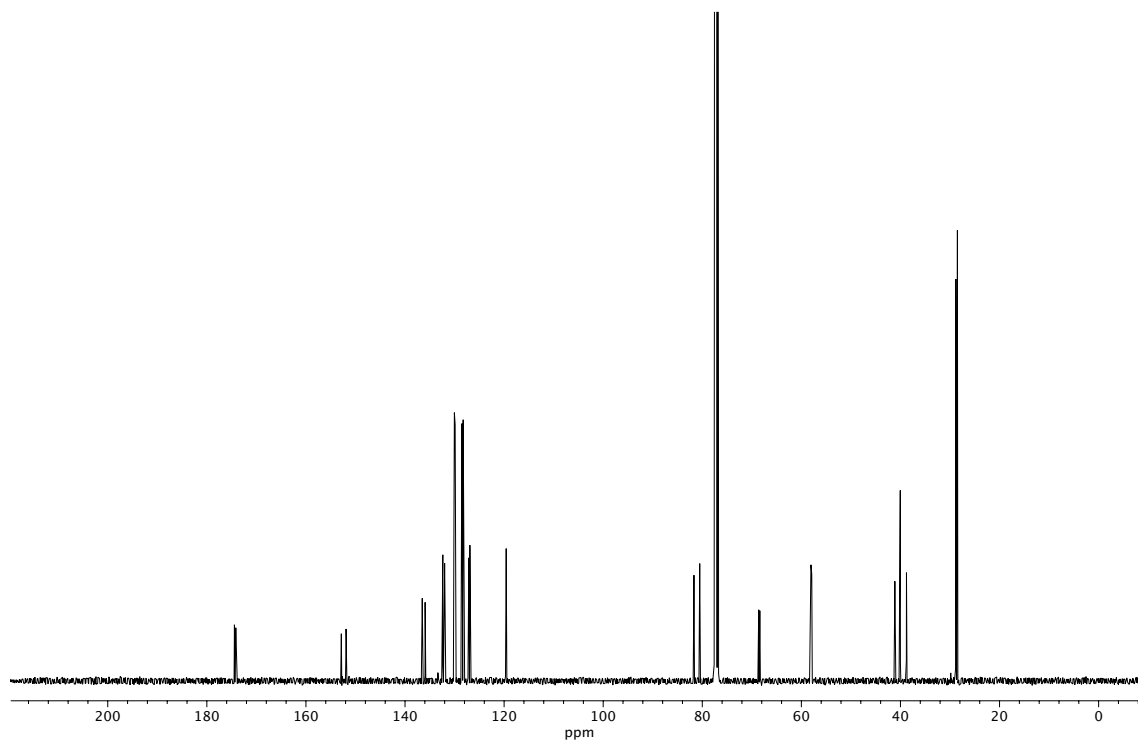


Figure A1.186. ^{13}C NMR (100 MHz, CDCl_3) of compound **53**.

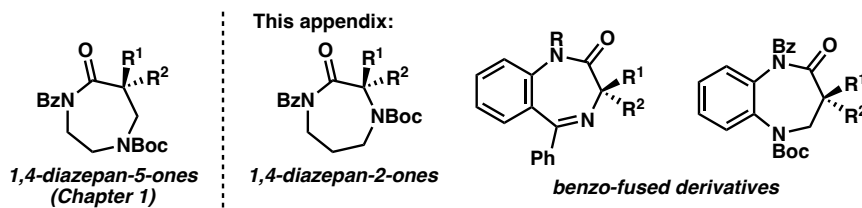
APPENDIX 2

Attempts to Effect the Allylic Alkylation of Additional Diazepanone Substrates[†]

A2.1 INTRODUCTION

Having developed a tolerant Pd-catalyzed decarboxylative asymmetric allylic alkylation approach to enantioenriched *gem*-disubstituted 1,4-diazepan-5-ones (Chapter 1), we sought to apply this methodology to structurally related diazepane heterocycles (Figure A2.1.1).

Figure A2.1.1. Scope of diazepanone derivatives discussed herein.



We had hoped to revisit the allylic alkylation of isomeric 1,4-diazepan-2-ones. Our group had previously reported a single example of the allylic alkylation of a 1,4-diazepan-2-one substrate bearing an *N*-benzyl amine protecting group, which resulted in a modest 59% ee.¹ Additionally, the allylic alkylation of benzo-fused derivatives of both 1,4-

[†]This research was conducted in collaboration with Dr. Alexander Sun.

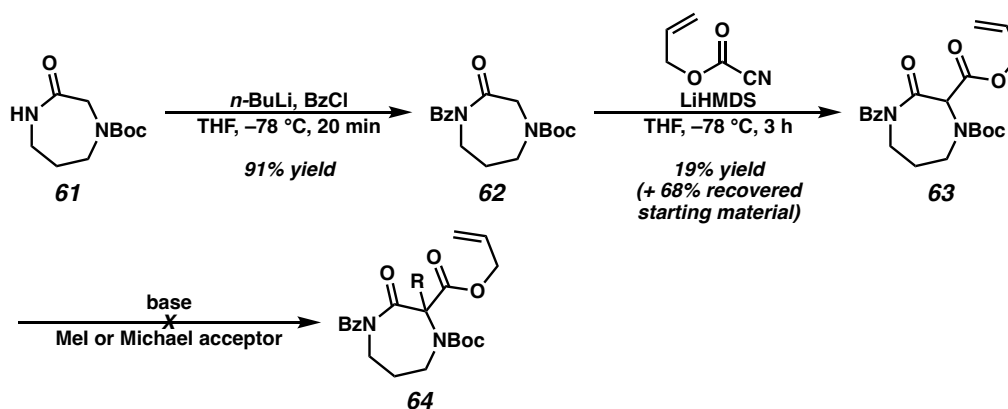
diazepan-5-ones and 1,4-diazepan-2-ones is a desirable transformation, as both of these motifs have found medicinal applications.²

A2.2 ATTEMPTS TO ACCESS A 1,4-DIAZEPAN-2-ONE ALLYLIC ALKYLATION SUBSTRATE

Compared to our group's previous isolated example of a *N*-benzyl 1,4-diazepan-2-one substrate, replacement of the *N*-benzyl group with an *N*-Boc group was expected to ease substrate synthesis. Thus, synthesis of this related substrate was attempted by a method analogous to the synthesis of 1,4-diazepan-5-ones **19a–l** (see Chapter 1, Scheme 1.2.2).

Commercial Boc-protected 1,4-diazepan-2-one **61** smoothly underwent deprotonation with *n*-BuLi and benzylation to afford protected diazepanone **62** (Scheme A2.2.1). *C*-acylation under our standard conditions resulted in a mixture of 1,3-dicarbonyl **63** and unreacted starting material.

Scheme A2.2.1. Unsuccessful synthesis of a 1,4-diazepan-2-one allylic alkylation substrate.



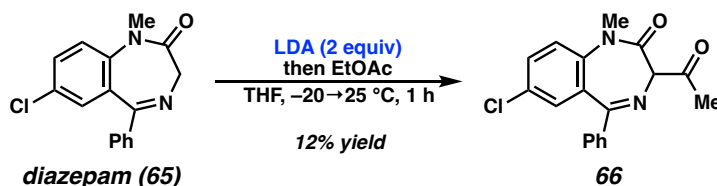
Unfortunately, all attempts to prepare allylic alkylation substrates **64** were unsuccessful in our hands, resulting in either no reaction or putative *O*-alkylation to provide

products which hydrolyzed back to **63** upon aqueous workup. Direct alkylation of **62** also resulted in putative *O*-alkylation. This behavior may be due to the proximity of the bulky *tert*-butyl carbamate to the nucleophilic enolate carbon, coupled with the substrate geometry. This undesired reactivity stands in stark contrast to the facile preparation of analogous piperazin-2-ones **13** (Chapter 1).³

A2.3 ATTEMPTS TO ACCESS BENZODIAZEPANE-DERIVED ALLYLIC ALKYLATION SUBSTRATES

Seeking to remove the steric bulk of the Boc protecting group while maintaining medicinal relevance, we reasoned that close derivatives of the benzodiazepine anxiolytics could themselves be competent substrates for Pd-catalyzed decarboxylative asymmetric allylic alkylation. In 1981, Wolfe and coworkers reported that the FDA-approved anxiolytic diazepam (**65**) could be lithiated with 2 equivalents of LDA and acylated by treatment with ethyl acetate to provide dicarbonyl **66**, albeit in poor yield (Scheme A2.3.1).⁴ Treatment of diazepam with fewer than 2 equivalents of LDA resulted in incomplete deprotonation—the enolate may be destabilized by antiaromaticity.

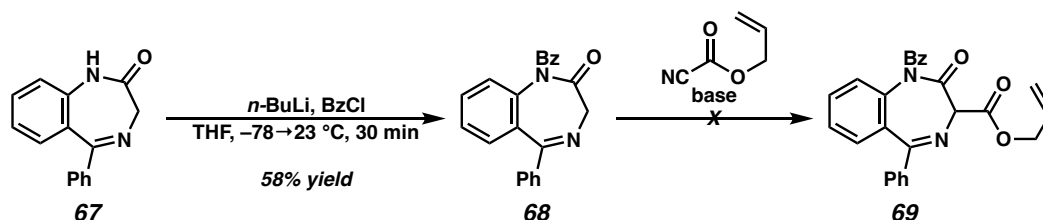
Scheme A2.3.1. *C*-Acylation of diazepam (Wolfe).



While conjugated enolates generally result in poor enantioselectivity in our group's Pd-catalyzed decarboxylative asymmetric allylic alkylation,⁵ we were interested in testing whether the destabilized enolate of a benzodiazepine would result in a higher ee. Toward this end, benzodiazepine **67** was prepared in two steps by a literature procedure (Scheme

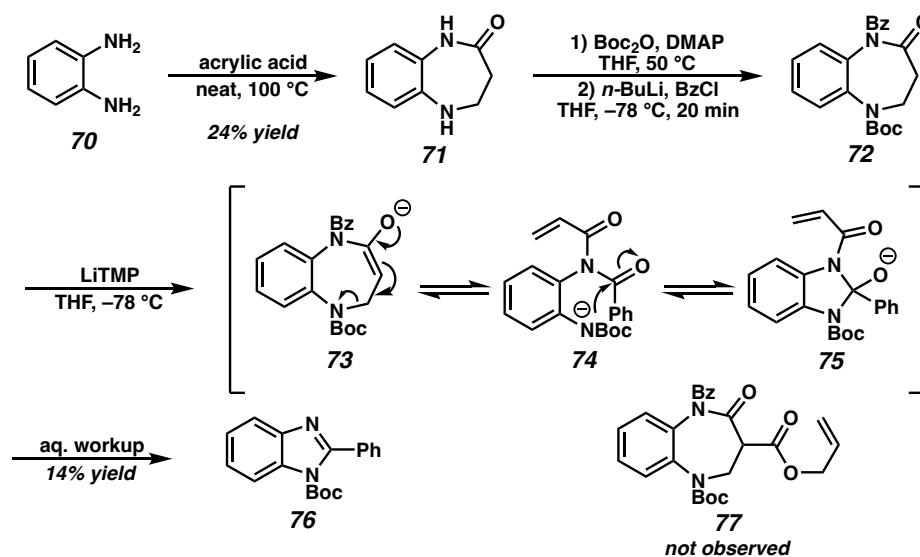
A2.3.2).⁶ This compound was subjected to routine benzylation to yield protected benzodiazepine **68**, but 1,3-dicarbonyl **69** was not observed under any of the acylation conditions tested. The use of LDA or LiHMDS as a base led to unidentified decomposition products, while LiTMP resulted in recovery of starting material.

Scheme A2.3.2. *Unsuccessful synthesis of a benzodiazepine allylic alkylation substrate.*



Finally, isomeric tetrahydrobenzodiazepanones **71** were evaluated as a potential substrate class due to their demonstrated applications in medicinal chemistry (Scheme A2.3.3).^{2b}

Scheme A2.3.3. *Unsuccessful synthesis of a tetrahydro[1,4]benzodiazepanone allylic alkylation substrate.*



Treatment of 1,2-phenylenediamine **70** with acrylic acid provided cyclized product **71**,⁷ and both nitrogen atoms could be protected over two steps to furnish carbamate **72**. However, ester **77** was discovered not to be accessible by enolate acylation of **72**. Instead, the highly fluorescent benzimidazole side-product **76** was isolated in 14% yield. This material probably arises from β -elimination of the carbamate from enolate **73**, facilitated by the altered electronics of the aniline moiety. The resulting intermediate **74** can then undergo 5-*exo*-trig ring closure with the *N*-benzoyl group, leading to intermediate alkoxide **75**. Finally, during aqueous workup, aromatization with loss of acrylate provides the observed product **76**.

A2.4 CONCLUSION

Attempts were made to prepare several additional diazepane-derived allylic alkylation substrates but were unsuccessful. In two cases (1,4-diazepan-2-ones and benzodiazepines), the necessary prefunctionalization of the enolate was thwarted by steric or electronic factors. In the third case (benzo-fused 1,4-diazepan-5-ones), an unexpected fragmentation of the ring system precluded the synthesis of allylic alkylation substrates.

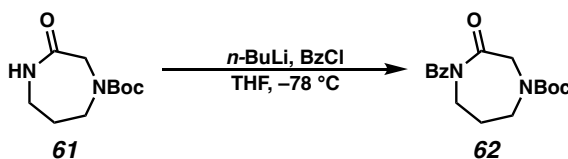
A2.5 EXPERIMENTAL SECTION

A2.5.1 MATERIALS AND METHODS

Unless otherwise stated, reactions were performed in flame-dried glassware under an argon or nitrogen atmosphere using dry, deoxygenated solvents. Solvents were dried by passage through an activated alumina column under argon.⁸ Reaction progress was monitored by thin-layer chromatography (TLC) or Agilent 1290 UHPLC-MS. TLC was performed using E. Merck silica gel 60 F254 precoated glass plates (0.25 mm) and visualized by UV fluorescence quenching or KMnO₄ staining. Silicycle SiliaFlash® P60

Academic Silica gel (particle size 40–63 nm) was used for flash chromatography. ^1H NMR spectra were recorded on Varian Inova 500 MHz and Bruker 400 MHz spectrometers and are reported relative to residual CHCl_3 (δ 7.26 ppm). ^{13}C NMR spectra were recorded on a Bruker 400 MHz spectrometer (100 MHz) and are reported relative to CHCl_3 (δ 77.16 ppm). Data for ^1H NMR are reported as follows: chemical shift (δ ppm) (multiplicity, coupling constant (Hz), integration). Multiplicities are reported as follows: s = singlet, d = doublet, t = triplet, q = quartet, p = pentet, sept = septuplet, m = multiplet, br s = broad singlet, br d = broad doublet. Many NMR spectra are complicated by rotational isomerism about amide bonds. Reagents were purchased from commercial sources and used as received unless otherwise stated.

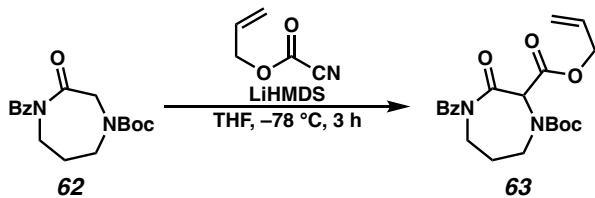
A2.5.2 EXPERIMENTAL PROCEDURES



tert-butyl 4-benzoyl-3-oxo-1,4-diazepane-1-carboxylate (**62**)

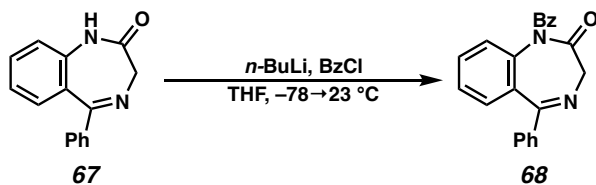
To a flame-dried round bottom flask containing lactam **61** (300 mg, 1.40 mmol, 1.0 equiv) was added THF (14 mL). The flask was cooled to $-78\text{ }^\circ\text{C}$ and $n\text{-BuLi}$ (2.5 M in hexanes, 0.59 mL, 1.47 mmol, 1.05 equiv) was added dropwise with stirring. Immediately following addition, BzCl (211 μL , 1.82 mmol, 1.3 equiv) was added dropwise. The reaction mixture was stirred at $-78\text{ }^\circ\text{C}$ for 20 min, whereafter it was quenched with saturated aq. NaHCO_3 . The resulting suspension was extracted with EtOAc (3x). The combined organic extracts were dried over Na_2SO_4 , concentrated under reduced pressure, and purified by silica gel flash chromatography (40% EtOAc /hexanes) to afford the title compound (403 mg, 1.27 mmol, 91% yield); ^1H NMR (500 MHz, CDCl_3) δ 7.65 – 7.53 (m, 2H), 7.52 –

7.43 (m, 1H), 7.42 – 7.33 (m, 2H), 4.21 (s, 2H), 4.17 – 4.03 (m, 2H), 3.81 – 3.61 (m, 2H), 2.01 – 1.88 (m, 2H), 1.55 (d, $J = 8.2$ Hz, 9H).



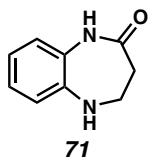
2-allyl 1-(*tert*-butyl) 4-benzoyl-3-oxo-1,4-diazepane-1,2-dicarboxylate (**63**)

To a flame-dried 20 mL glass vial were added imide **62** (150 mg, 0.471 mmol, 1.0 equiv) and THF (3 mL). The vial was cooled to -78 °C and a freshly prepared solution of LiHMDS (87 mg, 0.52 mmol, 1.1 equiv) in THF (1.7 mL) was added dropwise with stirring. The reaction mixture was stirred at -78 °C for 25 min, after which allyl cyanoformate (65 μ L, 0.61 mmol, 1.3 equiv) was added dropwise. After 1 h at -78 °C, additional allyl cyanoformate (50 μ L, 0.47 mmol, 1.0 equiv) was added. Following an additional 2 h of stirring, the reaction mixture was quenched by addition to 2 N aq. HCl. The solution was extracted with EtOAc (3x). Na_2SO_4 was added to the aqueous layer to accelerate separation between the phases. The combined organic extracts were dried over a mixture of Na_2SO_4 and NaHCO_3 and concentrated under reduced pressure. The crude product was purified by silica gel flash chromatography (33% EtOAc/hexanes) to afford recovered starting imide **62** (102 mg, 0.320 mmol, 68%) and the title compound as a white solid (35.7 mg, 0.0887 mmol, 19% yield); ^1H NMR (500 MHz, CDCl_3) δ 7.58 (d, $J = 7.8$ Hz, 2H), 7.54 – 7.44 (m, 1H), 7.42 – 7.35 (m, 2H), 5.91 (ddq, $J = 16.4, 11.5, 5.6$ Hz, 1H), 5.77 (s, 1H, first rotamer), 5.56 (s, 1H, second rotamer), 5.40 – 5.32 (m, 1H), 5.27 (t, $J = 10.7$ Hz, 1H), 4.78 – 4.67 (m, 2H), 4.40 – 4.15 (m, 1H), 4.15 – 3.77 (m, 2H), 3.32 – 3.13 (m, 1H), 2.05 – 1.92 (m, 2H), 1.52 (d, $J = 16.1$ Hz, 9H).



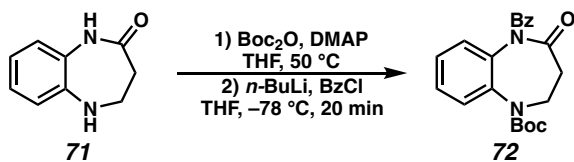
1-benzoyl-5-phenyl-1,3-dihydro-2H-benzo[e][1,4]diazepin-2-one (**68**)

To a flame-dried 100 mL round bottom flask were added benzodiazepine **67**⁶ (462 mg, 1.96 mmol, 1.0 equiv) and THF (20 mL). The flask was cooled to -78 °C and $n\text{-BuLi}$ (2.5 M in hexanes, 0.86 mL, 2.15 mmol, 1.1 equiv) was added dropwise. Immediately following addition, BzCl (296 μL , 2.55 mmol, 1.3 equiv) was added dropwise. The cooling bath was then removed, and the flask was allowed to warm to 23 °C over 30 min. Then, the reaction mixture was quenched with saturated aq. NH_4Cl , and the resulting suspension was extracted with EtOAc (3x). The combined organic extracts were dried over Na_2SO_4 and concentrated under reduced pressure. The crude product was combined with material from an earlier 0.212 mmol batch and purified by silica gel flash chromatography (33% EtOAc/hexanes) to afford the title compound as a pastel yellow solid (427 mg, 1.25 mmol, 58% combined yield); ^1H NMR (400 MHz, CDCl_3) δ 7.76 – 7.62 (m, 4H), 7.55 – 7.42 (m, 6H), 7.41 – 7.29 (m, 4H), 4.87 (d, $J = 11.0$ Hz, 1H), 4.02 (d, $J = 11.1$ Hz, 1H).



1,3,4,5-tetrahydro-2H-benzo[b][1,4]diazepin-2-one (**71**)

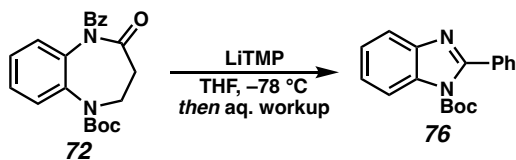
Prepared according to a patent procedure.⁷ All characterization data matched those reported in the patent.



***tert*-butyl 5-benzoyl-4-oxo-2,3,4,5-tetrahydro-1*H*-benzo[*b*][1,4]diazepine-1-carboxylate (72)**

To a flame-dried 500 mL round bottom flask were added benzodiazepanone **71** (5 g, 31 mmol, 1.0 equiv), Boc₂O (7.39 g, 33.9 mmol, 1.1 equiv), and THF (310 mL). The reaction mixture was stirred at 50 °C for 5 h, after which TLC analysis indicated no conversion. DMAP (379 mg, 3.1 mmol, 0.1 equiv) was then added, followed by additional Boc₂O (3.9 g, 18 mmol, 0.6 equiv). Following cessation of reaction conversion as judged by TLC analysis, the reaction mixture was concentrated under reduced pressure and purified by automated silica gel flash chromatography (Teledyne ISCO, 0→20→100% acetone/CH₂Cl₂) to provide an intermediate carbamate containing an isomeric impurity.

6.3 g (24.0 mmol, 1.0 equiv) of this intermediate were dissolved in THF (130 mL) in a flame-dried 250 mL round bottom flask. The flask was cooled to –78 °C and *n*-BuLi (2.5 M in hexanes, 11.5 mL, 28.8 mmol, 1.2 equiv) was added dropwise with stirring. After 5 min, BzCl (3.6 mL, 31.0 mmol, 1.3 equiv) was added dropwise. After an additional 20 min at –78 °C, the reaction mixture was quenched with aq. NaH₂PO₄ and extracted with EtOAc (3x). The combined organic extracts were dried over Na₂SO₄, concentrated under reduced pressure, and purified by automated silica gel flash chromatography (Teledyne ISCO, 0→100% EtOAc/hexanes) to afford the title compound. ¹H NMR (400 MHz, CDCl₃) δ 7.82 (dd, *J* = 8.1, 1.3 Hz, 1H), 7.69 – 7.64 (m, 2H), 7.50 – 7.45 (m, 1H), 7.43 – 7.38 (m, 2H), 7.30 (ddd, *J* = 8.2, 6.8, 2.1 Hz, 1H), 7.20 – 7.13 (m, 2H), 3.70 (t, *J* = 4.6 Hz, 2H), 3.01 (t, *J* = 4.6 Hz, 2H), 1.20 (s, 9H).



***tert*-butyl 2-phenyl-1*H*-benzo[*d*]imidazole-1-carboxylate**

To a flame-dried 1-dram glass vial were added THF (0.4 mL) and TMP (27.5 μ L, 0.163 mmol, 1.2 equiv). The vial was cooled to -78 $^{\circ}$ C and *n*-BuLi (2.5 M in hexanes, 65.2 μ L, 0.163 mmol, 1.2 equiv) was added. The vial was then warmed to 0 $^{\circ}$ C in an ice bath.

To a second flame-dried 1-dram glass vial were added benzodiazepanone **72** (50 mg, 0.136 mmol, 1.0 equiv) and THF (1 mL). The vial was cooled to -78 $^{\circ}$ C and the freshly prepared LiTMP solution was added dropwise. The reaction mixture was stirred for 15 min at -78 $^{\circ}$ C, whereafter allyl cyanofornate (18.9 μ L, 0.177 mmol, 1.3 equiv) was added. After an additional hour of stirring, the reaction mixture was quenched with saturated aq. NH_4Cl and extracted with EtOAc (3x). The combined organic extracts were dried over Na_2SO_4 and concentrated under reduced pressure. The crude product was combined with material from a second 0.136 mmol scale reaction conducted with LDA in place of LiTMP and purified by silica gel flash chromatography (15% EtOAc/hexanes) to provide the title compound as a fluorescent yellow film (11 mg, 0.037 mmol, 14% combined yield); ^1H NMR (400 MHz, CDCl_3) δ 8.07 – 8.02 (m, 1H), 7.82 – 7.77 (m, 1H), 7.66 – 7.60 (m, 2H), 7.50 – 7.44 (m, 3H), 7.42 – 7.35 (m, 2H), 1.40 (s, 9H); ^{13}C NMR (100 MHz, CDCl_3) δ 154.0, 148.7, 142.7, 134.0, 132.6, 129.7, 129.3, 128.1, 125.1, 124.6, 120.3, 114.8, 85.4, 27.7.

A2.6 REFERENCES AND NOTES

- (1) Korch, K. M.; Eidamshaus, C.; Behenna, D. C.; Nam, S.; Horne, D.; Stoltz, B. M. Enantioselective Synthesis of α -Secondary and α -Tertiary Piperazin-2-ones and Piperazines by Catalytic Asymmetric Allylic Alkylation. *Angew. Chem. Int. Ed.* **2015**, *54*, 179–183.
- (2) a) Gates, M. New synthesis of diazepam. *J. Org. Chem.* **1980**, *45*, 1675–1681. b) Hussener, T.; Hübner, H.; Gmeiner, P.; Troschütz, R. Clozapine derived 2,3-dihydro-1*H*-1,4- and 1,5-benzodiazepines with D4 receptor selectivity: synthesis and biological testing. *Bioorg. Med. Chem.* **2004**, *12*, 2625–2637.
- (3) Sun, A. W.; Hess, S. N.; Stoltz, B. M. Enantioselective synthesis of *gem*-disubstituted *N*-Boc diazaheterocycles *via* decarboxylative asymmetric allylic alkylation. *Chem. Sci.* **2019**, *10*, 788–792.
- (4) Reitter, B. E.; Sachdeva, Y. P.; Wolfe, J. F. Metalation of diazepam and use of the resulting carbanion intermediate in a new synthesis of 3-substituted diazepam derivatives. *J. Org. Chem.* **1981**, *46*, 3945–3949.
- (5) Behenna, D. C. et. al. Enantioselective Decarboxylative Alkylation Reactions: Catalyst Development, Substrate Scope, and Mechanistic Studies. *Chem. Eur. J.* **2011**, *17*, 14199–14223.
- (6) Bock, M. G.; DiPardo, R. M.; Evans, B. E.; Rittle, K. E.; Veber, D. F.; Freidinger, R. M.; Hirshfield, J.; Springer, J. P. Synthesis and resolution of 3-amino-1,3-dihydro-5-phenyl-2*H*-1,4-benzodiazepin-2-ones. *J. Org. Chem.* **1987**, *52*, 3232–3239.

- (7) Albright, J. D.; Reich, M. F.; Sum, F.; Santos, E. G. D. Tricyclic diazepine vasopressin antagonists and oxytocin antagonists. US Patent US5733905A, March 31, 1998.
- (8) Pangborn, A. M.; Giardello, M. A.; Grubbs, R. H.; Rosen, R. K.; Timmers, F. J. Safe and Convenient Procedure for Solvent Purification. *Organometallics* **1996**, *15*, 1518–1520.

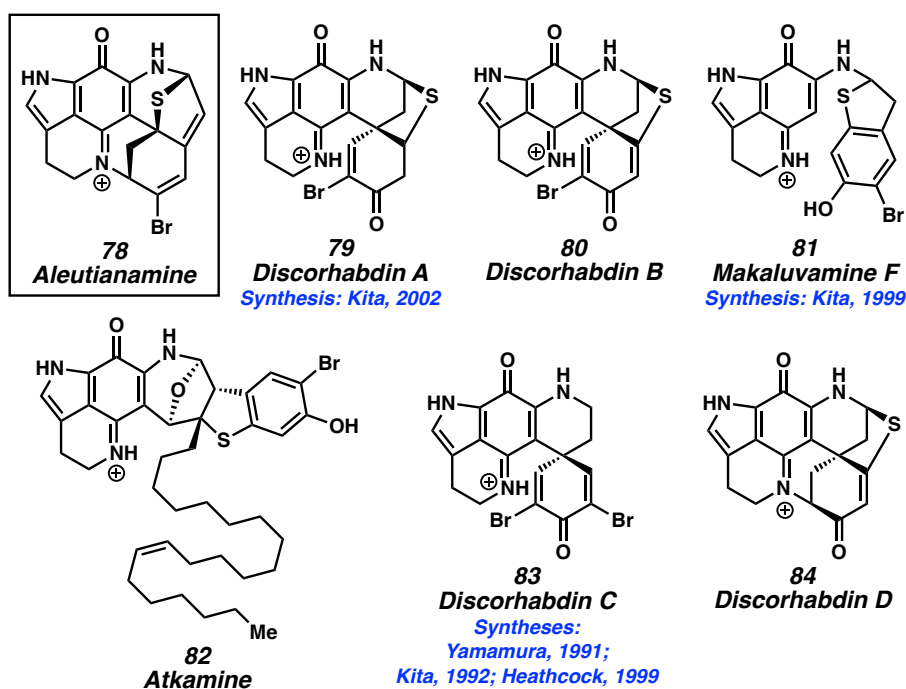
CHAPTER 2

Progress Toward the Total Synthesis of Aleutianamine[†]

2.1 INTRODUCTION

In 2019, Hamann and coworkers reported the isolation of the pyrroloiminoquinone alkaloid aleutianamine (**78**, Scheme 2.1.1) from the sea sponge *Latrunculia (Latrunculia) austini* found off the coast of the Aleutian Islands.¹

Scheme 2.1.1. Aleutianamine and examples of related natural products.



[†]This research was performed in collaboration with Samir Rezgui and Hao Yu and is ongoing. Portions of this chapter are reproduced from a grant proposal submitted to the NSF.

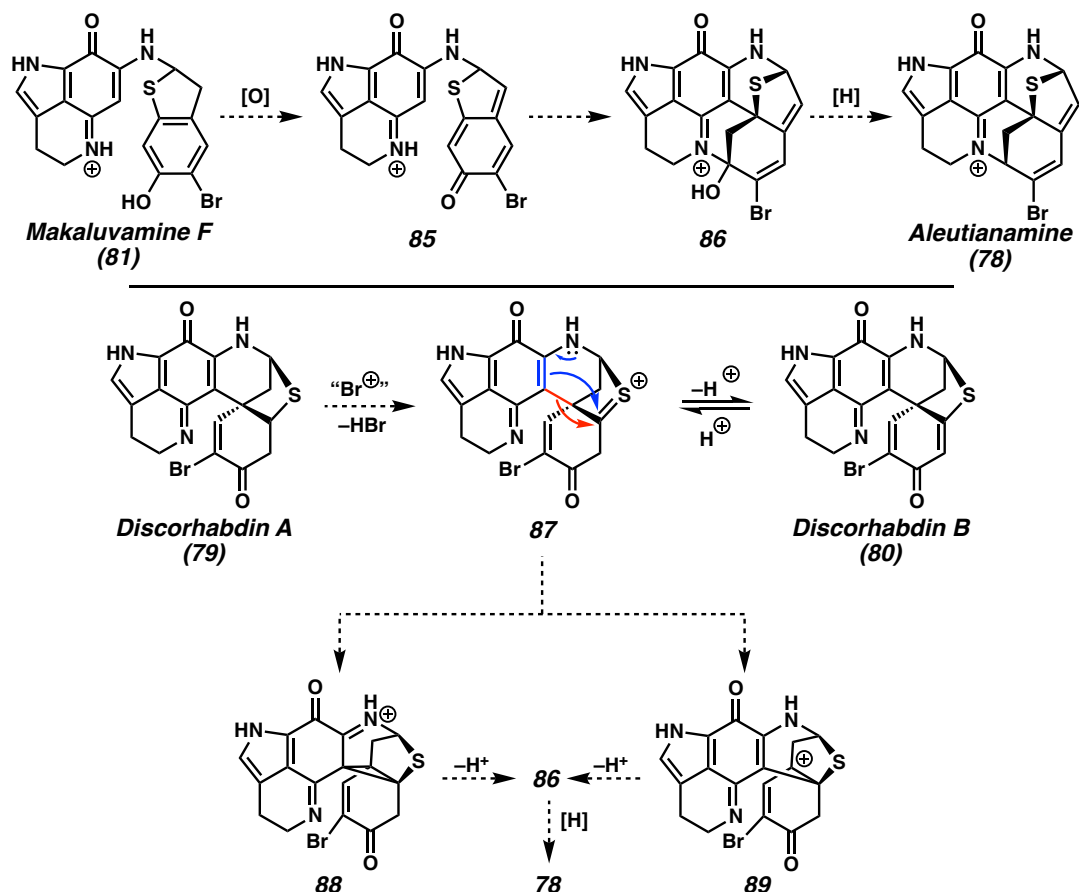
This compound was found to possess potent cytotoxicity against several human solid tumor cell lines, with exceptional selectivity for pancreatic cancer (25 nM IC₅₀ against PANC-1). The structure of aleutianamine was elucidated by a combination of spectroscopic and density functional theory methods. Structurally, aleutianamine bears a highly fused heptacyclic ring system, which consists of a planar pyrroloiminoquinone unit, a bridged [3.3.1]bicycle, and another bridging thioaminal linkage. The pyrroloiminoquinone moiety of aleutianamine is shared with related natural products including the discorhabdins and makaluvamines. Specifically, discorhabdins A (**79**) and B (**80**) are proposed to have a biosynthetic relationship to aleutianamine (*vide infra*), as they also share the alkenyl bromide and thioaminal linkage. Makaluvamine F (**81**), which bears a tethered aryl bromide, may also be a biosynthetic precursor. Aleutianamine also bears some structural resemblance to atkamine (**82**) and other discorhabdins (e.g **83**, **84**). Pyrroloiminoquinones have been longstanding targets for total synthesis.^{2,3}

The congested tertiary sulfide at C(5) of aleutianamine is a unique structural motif and presents a considerable synthetic challenge. The multi-bridged ring system of the natural product bears two stereocenters in addition to the tertiary sulfide and is highly strained due to extensive unsaturation. The unusual structure of aleutianamine, coupled with its potent biological activity, makes this compound an attractive synthetic target of considerable challenge.

Aleutianamine is proposed to biosynthetically arise from makaluvamine F (**81**) by oxidation to *p*-quinone methide **85**, which could then cyclize to hemiaminal **86** (Scheme 2.1.2).¹ Reduction would lead to aleutianamine (**78**). Alternatively, either *S*-bromination of discorhabdin A (**79**) followed by HBr elimination or protonation of discorhabdin B (**80**)

would lead to sulfenium intermediate **87**. Then, enamine-like reactivity (blue) would lead to cyclopropane **88**, or a σ -bond shift (red) would afford tertiary carbocation **89**. Both **88** and **89** could finally undergo an elimination reaction, which following cyclization would lead to common intermediate **86**, one biosynthetic step away from aleutianamine (**78**).

Scheme 2.1.2. Proposed biosynthetic routes to aleutianamine.

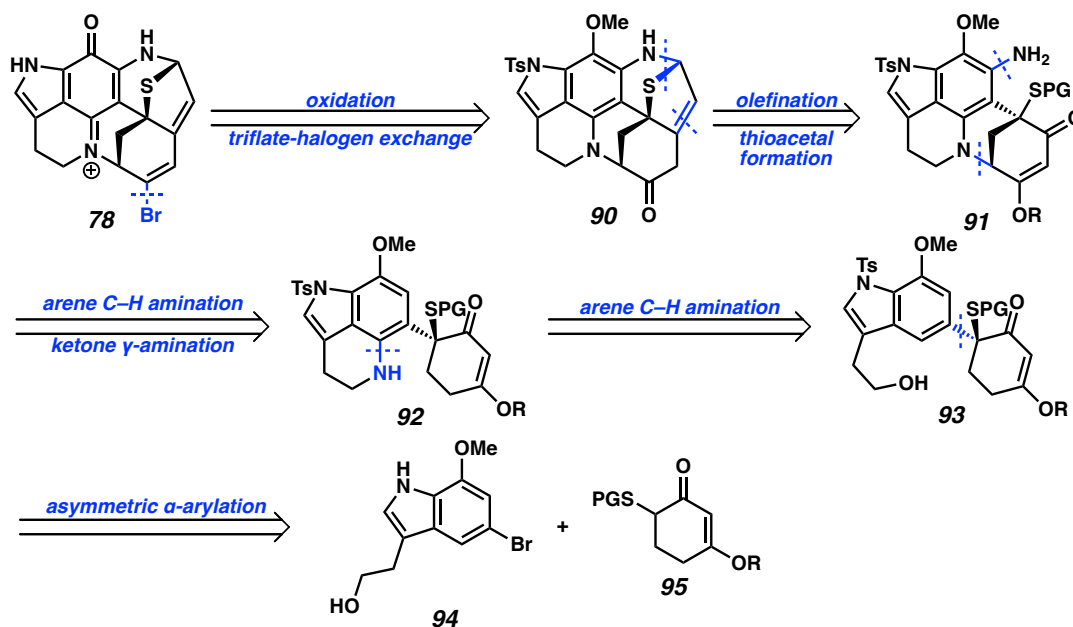


We set out to develop a synthetic route to aleutianamine that was orthogonal to these biosynthetic proposals, as this exercise was expected to provide a unique opportunity for organic methods development and would lead to new strategies that could be applied to the synthesis of other pyrroloiminoquinone alkaloids.

2.2 INITIAL RETROSYNTHETIC ANALYSIS

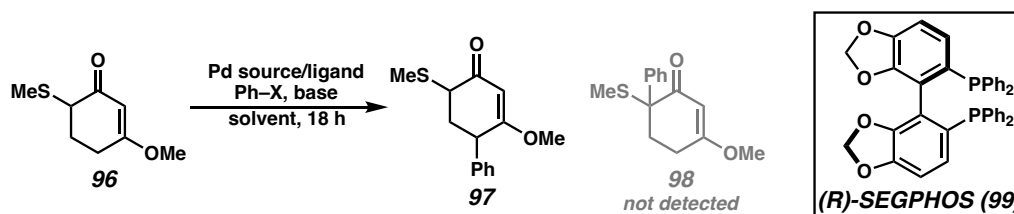
In designing a total synthesis of aleutianamine, we recognized the need to orchestrate the introduction of reactive functional groups to minimize the potential for deleterious reactivity. The alkenyl bromide was identified as one such reactive moiety, and the introduction of this functional group was therefore planned for the latest possible stage. Additionally, while syntheses of the related discorhabdins have often involved early oxidation of an arene precursor to the quinone oxidation state,² we imagined that delaying this oxidation would enable more diverse strategies for functionalizing the 6-membered core.

Thus, retrosynthetically, aleutianamine (**78**) was expected to arise from keto-arene **90** by arene oxidation, enol triflate formation, and late stage triflate-halogen exchange.⁴ An olefination of vinylogous ester **91** followed by intramolecular thioaminal formation could produce **90**. Primary aniline **91** could be disconnected by arene C–H amination—the relatively late-stage introduction of this electron-donating group would render earlier arene intermediates more stable and more easily accessible, although we recognized that the requisite amination would present a challenge. Additionally, we planned to construct the remaining bridged bicycle at this stage by a formal γ -amination of the vinylogous ester, inspired by a related sequence used to access *Securinega* alkaloids.⁵ These disconnections lead back to secondary aniline **92**. The aryl C–N bond could be disconnected by a second C–H amination, now intramolecular, and tryptophol precursor **93** could be prepared by an asymmetric α -arylation of vinylogous ester **95** with aryl bromide **94**.

Scheme 2.2.1. Initial retrosynthetic analysis of aleutianamine.

2.3 STRATEGIES INVOLVING ENOLATE ARYLATION

As the α -arylation of α -thioketone **95** is unprecedented, this transformation was first investigated in the context of a model system using α -thioketone **96** (Table 2.3.1). Despite the variation of solvent, palladium source, aryl halide, and base, formation of desired α -arylated product **98** was never observed. Instead, γ -arylated product **97** was isolated in low yields. The use of (*R*)-SEGPHOS (**99**) as a ligand shut down the formation of **97**.⁶ As vinylogous esters have been previously arylated to form quaternary centers under conditions similar to those tested,⁷ we hypothesize that the sulfide moiety of **96** inhibits the desired reaction.

Table 2.3.1. Investigation of the α -arylation of model vinylogous ester **96**.^a

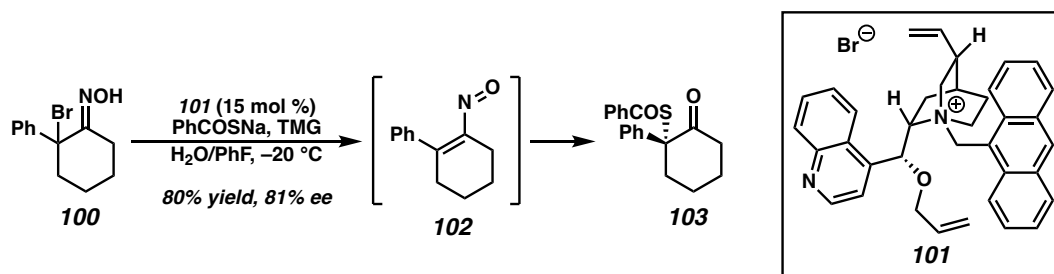
entry	solvent	temp (°C)	Pd source	added ligand	Ph-X	base	% SM	% 97
1	1,4-dioxane	80	Pd(Pt-Bu ₃) ₂	—	PhBr	NaHMDS	34	16
2	1,4-dioxane	80	Pd(Pt-Bu ₃) ₂	—	PhBr ^b	NaHMDS	31	10
3	1,4-dioxane	60	Pd(Pt-Bu ₃) ₂	—	PhBr	NaHMDS	19	6.5
4	1,4-dioxane	100	Pd(Pt-Bu ₃) ₂	—	PhBr	NaHMDS	19	6.3
5	1,4-dioxane	80	Pd(Pt-Bu ₃) ₂	—	PhBr	LiHMDS	28	11
6	1,4-dioxane	80	Pd(Pt-Bu ₃) ₂	—	PhBr	LDA	26	21
7	1,4-dioxane	80	Pd(Pt-Bu ₃) ₂	—	PhBr	KHMDS	5.7	1
8	1,4-dioxane	80	Pd(Pt-Bu ₃) ₂	—	PhBr	NaH	4.9	1.6
9	PhCH ₃	60	Pd(dba) ₂	99	PhOTf	NaOt-Bu ^c	ND	0
10	PhCH ₃	60	Pd(dba) ₂	99	PhOTf	LDA	ND	0
11	1,4-dioxane	80	Pd(Pt-Bu ₃) ₂	—	PhOTf	LDA	ND	0
12	1,4-dioxane	80	Pd(Pt-Bu ₃) ₂	—	PhCl	LDA	ND	0
13	1,4-dioxane	80	Pd(Pt-Bu ₃) ₂	—	PhI	LDA	11	15
14	PhCH ₃	60	Pd(dba) ₂	99	PhBr	NaOt-Bu ^c	ND	0
15	PhCH ₃	60	Pd(dba) ₂	99	PhBr	LDA	ND	0
16	PhCH ₃	80	Pd(Pt-Bu ₃) ₂	—	PhBr	LDA	29	9.4
17	2:1 hexanes/PhCH ₃	80	Pd(Pt-Bu ₃) ₂	—	PhBr	LDA	22	8
18	DMF	80	Pd(Pt-Bu ₃) ₂	—	PhBr	LDA	27	3.3
19	2-MeTHF	80	Pd(Pt-Bu ₃) ₂	—	PhBr	LDA	27	12
20	<i>n</i> -Bu ₂ O	80	Pd(Pt-Bu ₃) ₂	—	PhBr	LDA	15	trace
21	CPME	80	Pd(Pt-Bu ₃) ₂	—	PhBr	LDA	21	6.9
22	1,4-dioxane	80	Pd(dba) ₂	99	PhBr	LDA	ND	0
23	1,4-dioxane	80	Pd(dba) ₂	Pt-Bu ₃ ^d	PhBr	LDA	28	13

[a] Unless otherwise indicated, reactions were conducted at 0.1 M concentration with 1 equiv **96**, 1 equiv Ar-X, 1 equiv base, and 10 mol % Pd. Reactions with (*R*)-SEGPHOS were conducted with 12 mol % ligand. All yields were determined by ¹H NMR analysis with 1,3,5-trimethoxybenzene as an internal standard. [b] 3 equiv PhBr. [c] 2 equiv NaOt-Bu. ^d 20 mol %.

In order to circumvent the deleterious effect of the sulfur atom on α -arylation, an alternative order of events involving sulfide installation subsequent to α -arylation was envisioned. Corey reported an enantioselective phase transfer-catalyzed addition of nucleophiles to α -bromooximes,⁸ including an example of the addition of a sulfur nucleophile (Scheme 2.3.2). Treatment of oxime **100** with base led to intermediate

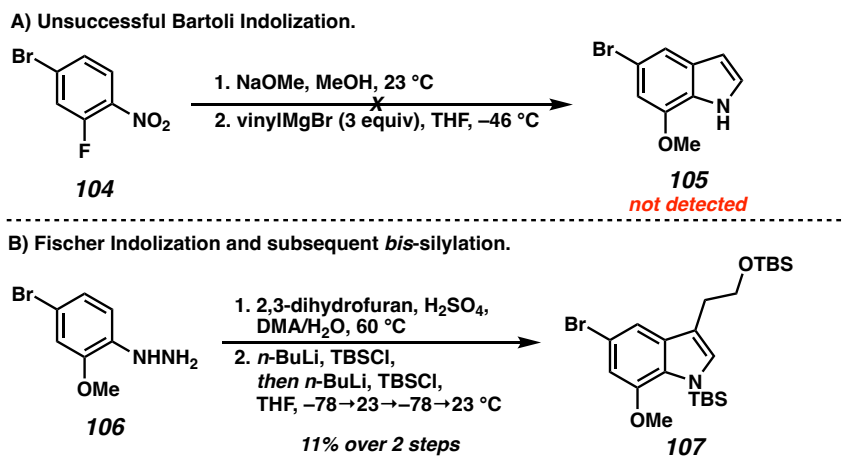
unsaturated nitrosamine **102**, which underwent addition of PhCOS^- catalyzed by chiral ammonium salt **101** to afford enantioenriched α -thio ketone **103**.

Scheme 2.3.2. Corey's addition of a sulfur nucleophile to an α -bromooxime.

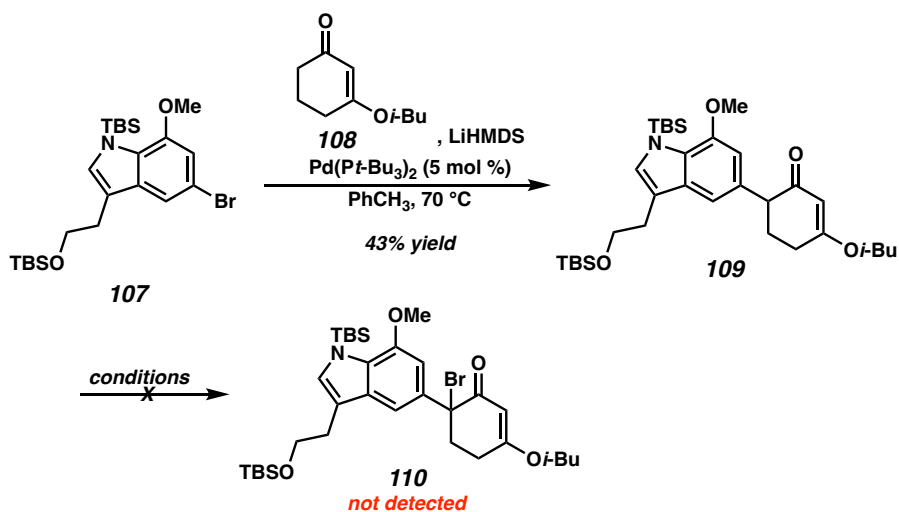


An appropriate tryptophol-derived aryl bromide was necessary for the α -arylation reaction toward a substrate to which Corey's chemistry could be applied. The Bartoli indolization was first examined as a method to prepare indole **105**, which could potentially be advanced to a tryptamine (Scheme 2.3.3A). Aryl fluoride **104** underwent a precedented $\text{S}_{\text{N}}\text{Ar}$ reaction with NaOMe ,⁹ but subjection of the product to Bartoli indolization conditions led only to nonspecific decomposition despite its similarity to known substrates.¹⁰

Instead, known arylhydrazine **106**¹¹ underwent a Fischer indolization with 2,3-dihydrofuran,¹² and subsequent *bis*-silylation by repeated deprotonation and silyl chloride addition afforded fully protected aryl bromide **107**.

Scheme 2.3.3. Synthesis of an indole-derived aryl bromide coupling partner.

Satisfyingly, treatment of aryl bromide **107** with known vinylogous ester **108**,¹³ base, and Pd(*P**t*-Bu)₃)₂ led to the formation of α -arylated product **109** in 43% yield (Scheme 2.3.4).¹⁴ The silyl-protected indole was found to be optimal for this transformation—a tosyl indole led to a complex reaction profile, while a Boc-protected indole led to acylation of the enolate of vinylogous ester **108**. Unfortunately, α -bromination of arylated ketone **109** could not be effected under any conditions tested, with aromatized or γ -brominated products being isolated.

Scheme 2.3.4. Enolate acylation and subsequent unsuccessful bromination.

As access to bromoketone **110** would be necessary in order to install the sulfide by Corey's method, the synthetic plan depicted in Scheme 2.2.1 was abandoned at this relatively early stage. The challenges encountered with Pd-catalyzed arylation of sulfide-containing substrate **96** and the facile nature of the aromatization of the cyclohexenone moiety of **109**, did, however, inform later synthetic plans—the sulfide installation was delayed to a later stage, and care was taken to introduce/construct the 6-membered carbocycle in a lower oxidation state to prevent aromatization.

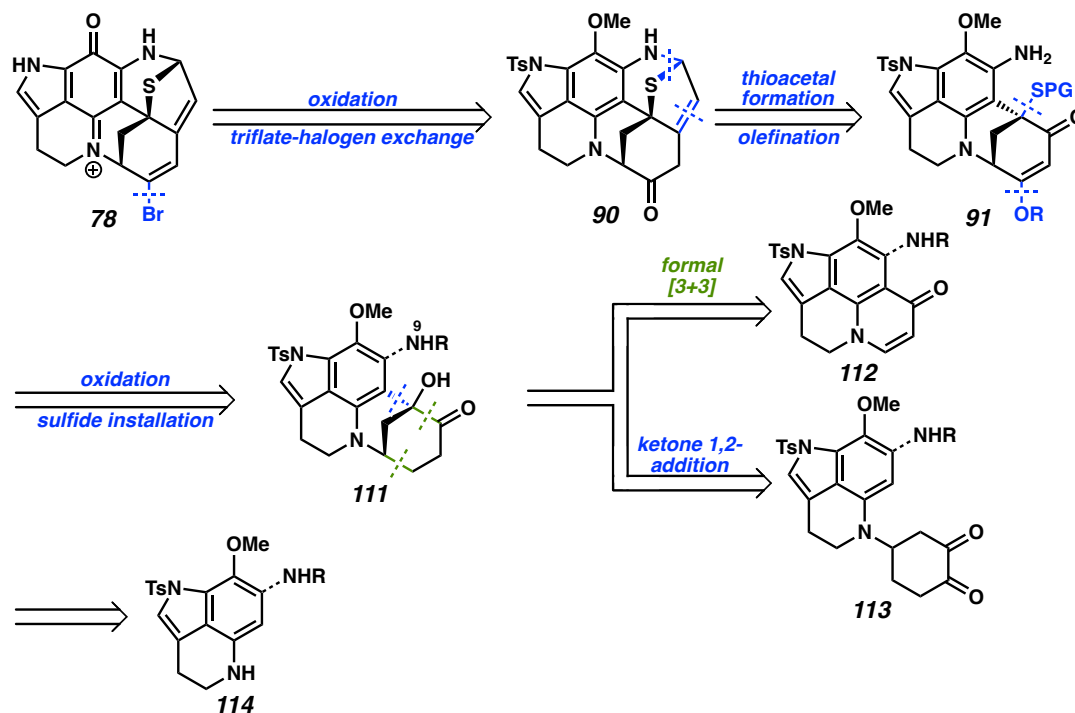
2.4 2ND-GENERATION RETROSYNTHESIS

At this stage, a revised retrosynthetic analysis of aleutianamine that would circumvent the issues encountered with enolate arylation strategies was envisioned (Scheme 2.4.1). As in the first retrosynthesis, aleutianamine was planned to arise from keto-arene **90**, which could be prepared by olefination of vinylogous ester **91** and thioaminal formation. In contrast to the earlier synthetic plan, however, vinylogous ester **91** was disconnected to saturated hydroxyketone **111** by sulfide installation via bridgehead carbocation chemistry (demonstrated in a model system, see Appendix 5) and oxidation. This approach would enable a wider array of strategies for construction of the bridged bicycle, including methods that would not tolerate a sulfide. Additionally, as the feasibility of installing N(9) (aleutianamine numbering), the protected aniline group of pentacycle **111**, by late-stage arene amination was uncertain, strategies involving precursors both with and without this nitrogen atom were investigated.

The bridged bicyclic ketone of pentacycle **111** could be traced back either to 4-quinolone **112** by a formal [3+3] cycloaddition approach,¹⁵ or to a protected derivative of

1,2-diketone **113** by halogenation and an intramolecular Barbier–type addition. Both of these intermediates would arise from tricyclic aniline **114**.

Scheme 2.4.1. Revised retrosynthetic analysis of aleutianamine.



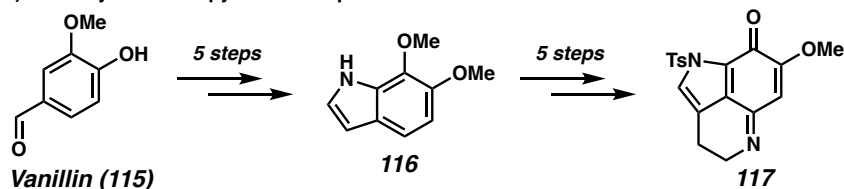
2.5 PREPARATION OF A VERSATILE TRICYCLIC ANILINE

As aniline **114** is essentially a reduced and protected variant of tricyclic pyrroloiminoquinones already well-studied in the discorhabdin and makaluvamine literature,^{2,3} we set out to intercept a pyrroloiminoquinone intermediate and study its reduction. Methoxypyrroloiminoquinone **117** was prepared by the method of Kita from vanillin (**115**) via dimethoxyindole **116** (Scheme 2.5.1A).^{2b} Unfortunately, addition of phthalimide to afford derivative **118**, which would obviate later aniline protection, was unsuccessful (Scheme 2.5.1B). Instead, a substitution reaction with ammonium chloride afforded known aminopyrroloiminoquinone **119**, previously accessed by White.¹⁶ While addition of NaBH₄ did lead to rapid disappearance of the deep purple color of **119**, selective

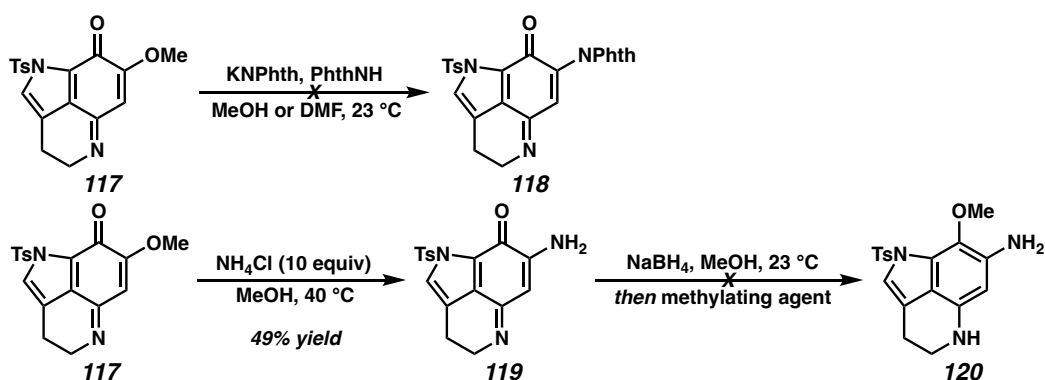
methylation of the resulting putative phenoxide could not be effected, and the reduced intermediate was not stable to air.

Scheme 2.5.1. Attempts to reduce a pyrroloiminoquinone to aniline **120**.

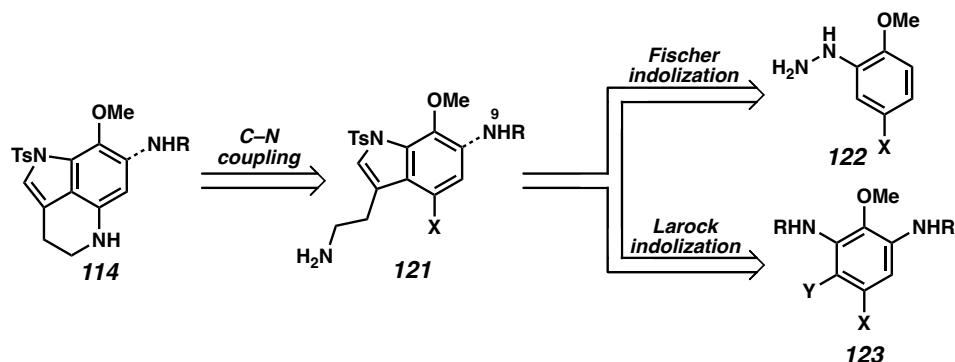
A) Kita's synthesis of pyrroloiminoquinone intermediate **117**.



B) Attempts to access a reduced dianiline from pyrroloiminoquinone **117**.

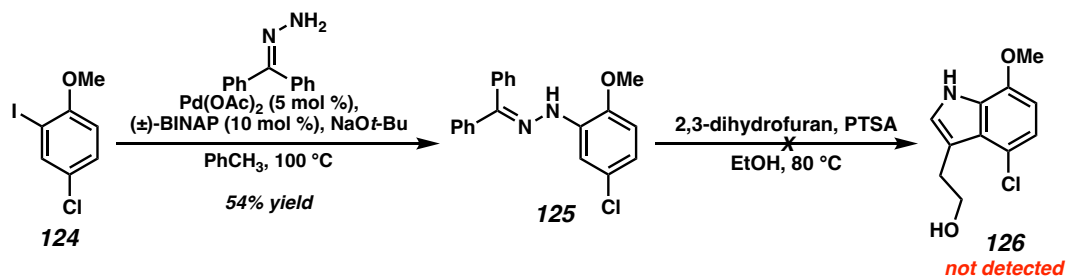


Due to the challenges associated with reducing known pyrroloiminoquinone **119** to a stable arene intermediate, we instead opted to develop a strategically unique synthesis of tricyclic aniline **114** (Scheme 2.5.2). Instead of the risky C–H amination proposed in our first retrosynthesis (i.e., **93**→**92**), the secondary aniline could arise from an intramolecular C–N cross coupling of a halogenated tryptamine **121**. This tryptamine would be prepared by either Fischer indolization of arylhydrazine **122** or Larock indolization of dianiline derivative **123**. Early experiments revealed that the preparation of a Fischer indolization substrate bearing the additional N(9) was impractical, so this transformation was only explored in the context of *des*-amino arene **122**.

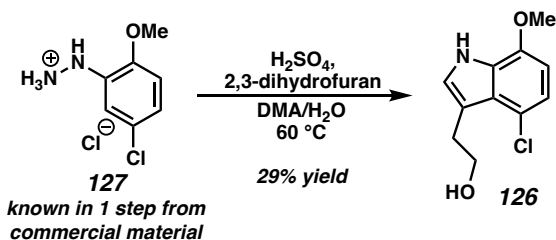
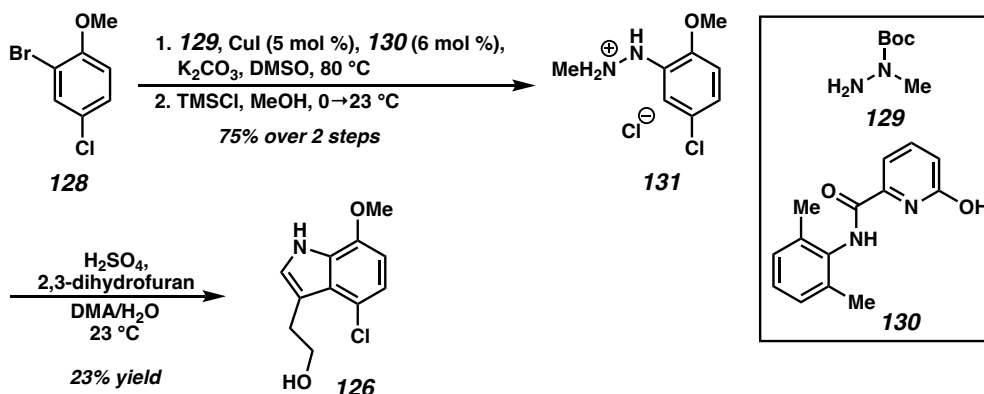
Scheme 2.5.2. Strategies envisioned for the construction of aniline **114**.

Investigation of the Larock indolization of **123** led to the development of a powerful cascade cyclization that afforded a derivative of tricycle **114** in a single step. While the advancement of the resulting dianiline intermediate did not bear fruit in the context of the total synthesis of aleutianamine, efforts are ongoing to employ this Larock cascade in the syntheses of other pyrroloiminoquinone alkaloids. This research is outside the scope of this thesis chapter.

An arylhydrazine substrate for Fischer indolization toward tricycle **114** was first prepared by Pd-catalyzed Buchwald–Hartwig coupling of aryl iodide **124** with benzophenone hydrazone under Eilbracht's conditions (Scheme 2.5.3),¹⁷ as this strategy would circumvent the intermediacy of a potentially explosive arenediazonium salt. The Fischer indolization of benzophenone arylhydrazones was reported by Buchwald,¹⁸ but treatment of hydrazone **125** with 2,3-dihydrofuran and acid led to nonspecific decomposition. Desired tryptophol **126** was not detected. Indeed, Buchwald and coworkers noted that the C(2)-unsubstituted indoles derived from aldehydes were unstable under their reaction conditions.^{18b}

Scheme 2.5.3. Attempted Fischer indolization of a hydrazone derivative.

Fischer indolization was instead performed on a free arylhydrazine (Scheme 2.5.4A). Hydrochloride salt **127** was available in 1 step (diazotization and reduction) by a patent procedure.¹⁹ Satisfyingly, treatment with 2,3-dihydrofuran and excess acid in a mixture of water and dimethylacetamide afforded desired tryptophol product **126**. While the 29% yield of tryptophol **126** from **127** could not be increased, our attention was drawn to Schmidt's report that terminal methylation of arylhydrazines could facilitate Fischer indolization (Scheme 2.5.4B).²⁰ Copper-catalyzed cross coupling of aryl bromide **128** with hydrazine derivative **129** was accomplished under the conditions developed by Singer and successfully employed by Schmidt using ligand **130**,²¹ and Boc cleavage yielded methylated arylhydrazine salt **131**. Interestingly, while the Fischer indolization of **131** now proceeded to afford tryptophol **126** at ambient temperature, the yield of the product was not improved. Moving forward, we opted to continue employing the classical Fischer indolization of arylhydrazine salt **127**, since no chromatography was required in this sequence prior to indolization. Thus, despite the low indolization yield, tryptophol **126** could be prepared in the multigram quantities necessary for synthetic route development.

Scheme 2.5.4. Access to desired tryptophol **126** by Fischer indolization.**A) Successful Fischer indolization with 2,3-dihydrofuran.****B) Low-temperature Fischer indolization of an *N*-methyl substrate.**

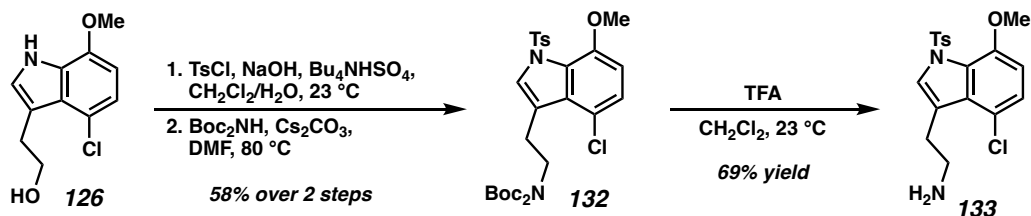
Advancement of tryptophol **126** to a derivative of key tricyclic aniline **114** would require protection of the indole and conversion of the tryptophol to a tryptamine (Scheme 2.5.5A). Simultaneous tosylation of the indole and primary alcohol was followed by S_N2 displacement of the primary tosylate with Boc₂NH to afford protected tryptamine **132**. Biphasic tosylation conditions with a tetrabutylammonium phase transfer catalyst were uniquely effective for the *bis*-tosylation of **126**; NaH in THF led to monotosylation of the indole while Et₃N and DMAP in CH₂Cl₂ led to monotosylation of the alcohol. Other sets of conditions tested led only to nonspecific decomposition. Treatment of imide **132** with TFA led to deprotection to afford free tryptamine **133**.

While this sequence enabled access to sufficient quantities of **133** for the investigation of downstream chemistry, the yield of the *bis*-tosylation step was inconsistent and dropped sharply at a higher scale. An improved sequence to access tryptamine **133** was

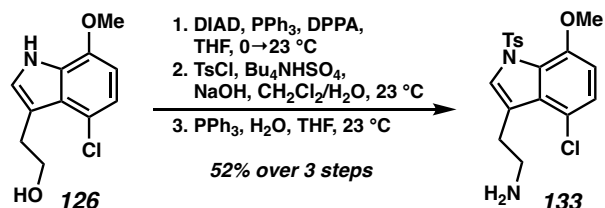
therefore developed (Scheme 2.5.5B). Azidation of tryptophol **126** by a Mitsunobu reaction provided an intermediate azide, the indole was tosylated under biphasic conditions, and a final Staudinger reduction provided primary amine **133** in moderate yield over 3 steps.

Scheme 2.5.5. Advancement of tryptophol **126** to a protected tryptamine.

A) Initial advancement to a primary tryptamine.



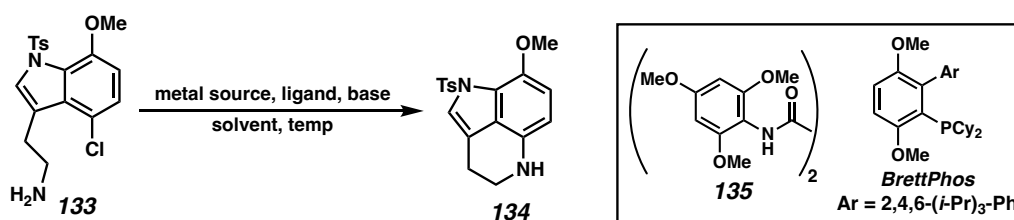
B) Improved sequence to access a primary tryptamine.



Conditions for the intramolecular C–N coupling of the amine and aryl chloride of **133** were then evaluated (Table 2.5.6). The array of methods at our disposal was limited by the challenge associated with oxidative addition into an aryl chloride rather than a more reactive aryl bromide or iodide. Buchwald–Hartwig coupling using LiHMDS as a base provided only trace product (entry 1).²² Other nickel-²³ or copper-catalyzed²⁴ methods failed to deliver an appreciable quantity of the desired product (entries 2/3). Control experiments revealed that heating tryptamine **133** with NaO*t*-Bu led to detosylation, while heating with LiHMDS led to tosyl group migration to the primary amine. Optimization efforts were thereafter limited to the use of weak bases. Buchwald–Hartwig coupling in dioxane using either K₃PO₄ or Cs₂CO₃ as the base led to slow formation of tricycle **134**, but the sluggish nature of the reactions (a likely result of low inorganic base solubility in

dioxane) precluded their use (entries 4/5). Satisfyingly, the copper-catalyzed Ullman-type coupling of aryl chlorides developed by Ma afforded **134** in 51% yield with the use of oxalamide ligand **135** (entry 6).²⁵

Table 2.5.6. Evaluation of the intramolecular C–N coupling of **133**.^a



entry	solvent	temp (°C)	reagents	% yield
1	1,4-dioxane	100	Pd(OAc) ₂ (2 mol %), BrettPhos (4 mol %), LiHMDS	trace
2	PhCH ₃	100	Ni(COD) ₂ (5 mol %), DPPF (10 mol %), NaOt-Bu	—
3	NMP	120	Cu ₂ O (5 mol %), NaOt-Bu	trace
4	1,4-dioxane	100	BrettPhos Pd G4 (2 mol %), BrettPhos (2 mol %), K ₃ PO ₄	ND ^b
5	1,4-dioxane	100	BrettPhos Pd G4 (2 mol %), BrettPhos (2 mol %), Cs ₂ CO ₃	ND ^b
6	DMSO	120	CuI (5 mol %), 135 (10 mol %), K ₃ PO ₄	51 ^c
7	1,4-dioxane	100	BrettPhos Pd G4 (4 mol %), BrettPhos (4 mol %), K ₃ PO ₄ , 18-C-6	33
8	<i>t</i> -BuOH	70	BrettPhos Pd G4 (2 mol %), BrettPhos (2 mol %), K ₃ PO ₄	—
9	<i>t</i> -BuOH	100	BrettPhos Pd G4 (2 mol %), BrettPhos (2 mol %), K ₃ PO ₄	63
10	<i>t</i> -BuOH	100	BrettPhos Pd G4 (2 mol %), BrettPhos (2 mol %), Cs ₂ CO ₃	60
11	<i>t</i> -BuOH	100	BrettPhos Pd G4 (5 mol %), BrettPhos (5 mol %), K ₃ PO ₄	90

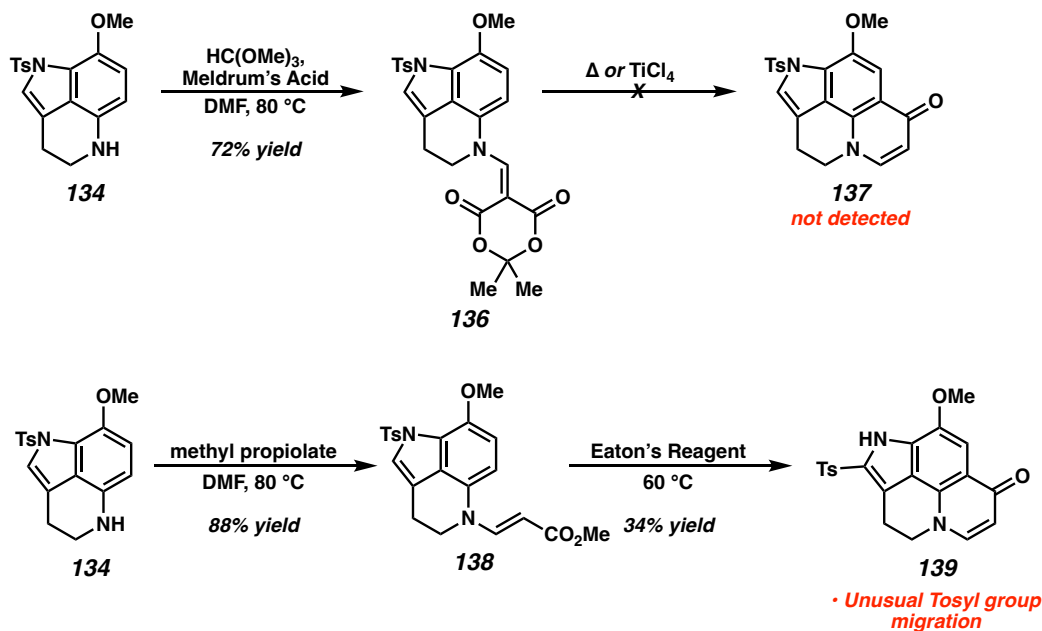
[a] All reported yields are isolated yields unless otherwise noted. [b] Slight conversion to the desired product was observed by LC–MS analysis of the crude reaction mixture after 18 h, but the reactions were not driven to completion. [c] Yield on a 0.396 mmol scale. Yield decreased to 38% on a 1.50 mmol scale.

Unfortunately, this yield decreased at higher scales, so optimization efforts were continued. Addition of 18-crown-6 to a Buchwald–Hartwig coupling employing K₃PO₄ did accelerate the reaction, but **134** was obtained in only 33% yield (entry 7). Instead, to improve base solubility, *t*-BuOH was tested as a solvent. The reaction did not proceed at 70 °C (entry 8) but conducting the coupling at 100 °C in a sealed tube afforded **134** in synthetically useful yields (entries 9/10), with K₃PO₄ slightly outcompeting Cs₂CO₃ as a base. Raising the palladium loading to 5 mol % improved the consistency of the reaction and increased the yield to 90%.

2.6 STRATEGIES FOR BRIDGED BICYCLE FORMATION

Now enabled by a scalable route to tricyclic aniline **134**, the formation of the bridged [3.3.1]bicycle of the natural product was investigated. First, we set out to advance aniline **134** to a tetracyclic quinolone that could undergo a formal [3+3] cycloaddition (Scheme 2.6.1). Aniline **134** was condensed with trimethyl orthoformate and Meldrum's Acid to yield bright yellow adduct **136**. The cyclization of related adducts by pyrolysis is known to afford 4-quinolones.²⁶ Pyrolysis of **136** led only to nonspecific decomposition, while treatment with TiCl₄ led to inefficient reversion to aniline **134**.

Aniline **134** was instead heated with methyl propiolate, inducing an aza-Michael reaction to yield “push-pull” olefin **138** in high yield. Ultimately, cyclization did proceed in Eaton's Reagent at 60 °C, but concomitant migration of the indole tosyl group to the C(2) position was observed and the product was only isolated in 34% yield. To our knowledge, the migration of a tosyl group from an indole nitrogen to C(2) is not precedented. Other indole protecting groups that were expected to be less likely to migrate were briefly evaluated (see Appendix 5). A Piv group spontaneously migrated to the primary amine of the Piv-protected derivative of **133**, while an *N*-allyl indole derivative of “push-pull” olefin **138** did not survive the harsh conditions of the cyclization. This formal [3+3] approach was therefore abandoned in favor of a ketone 1,2-addition strategy for the construction of the [3.3.1]bicycle.

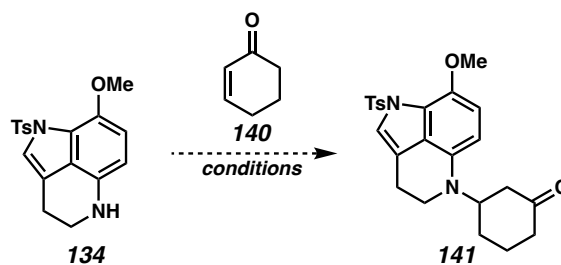
Scheme 2.6.1. Advancement of tricycle **134** to a tetracyclic quinolone.

Early model studies revealed that assembly of a 1,2-diketone system and Friedel–Crafts-type addition of the arene into one of the ketones was not feasible. A strategy involving intramolecular Barbier-type addition was therefore pursued. This strategy would necessitate tethering a 6-membered ketone to the aniline nitrogen. The aza-Michael reaction was identified as an optimal tactic for this C–N bond formation.

Reports of the aza-Michael addition of secondary anilines into α,β -unsaturated carbonyl compounds bearing β -substitution are relatively scarce. Cyclohexene (**140**) was used as a model enone for this addition, as it was anticipated that some optimization would be necessary. While heating aniline **134** with enone **140** in DCE did lead to trace product (by LC–MS analysis), we were unable to drive this reaction to a higher degree of conversion (Table 2.6.2, entry 1). The addition of Lewis acids also failed to promote the reaction (entries 2–4). While HFIP is known to promote the addition of anilines into acyclic Michael acceptors,²⁷ it did not effect the coupling of **134** and **140** (entry 5). A set of DMAP-

catalyzed conditions utilized for aza-Michael additions of indoline also failed to promote the desired reaction (entry 6).²⁸

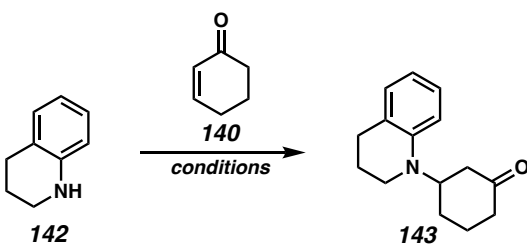
Table 2.6.2. Unsuccessful aza-Michael addition of aniline **134** into cyclohexenone.^a



entry	solvent	temp (°C)	additive	equiv enone	result
1	DCE	80	N/A	10	trace ^b
2	CH ₂ Cl ₂	23	BF ₃ ·OEt ₂	5	trace ^b
3	CH ₂ Cl ₂ /Et ₂ O	23	Cu(OTf) ₂ (20 mol %)	5	decomp
4	CH ₂ Cl ₂	23	TiCl ₄	5	trace
5	HFIP	60	N/A	5	NR
6	MeCN	23	DMAP	5	NR

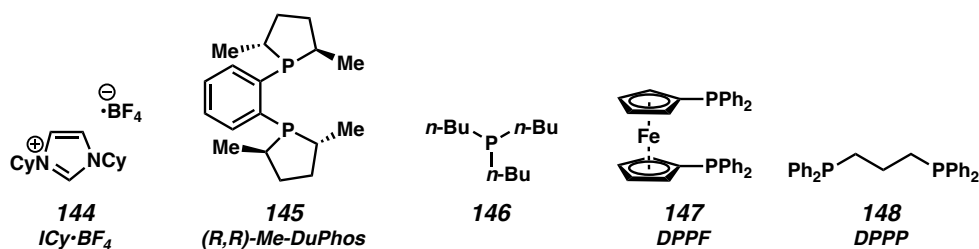
[a] Reaction outcomes were determined by LC–MS analysis. [b] Reaction led to a complex mixture containing unreacted **134** and nonspecific decomposition products.

Realizing that additional optimization would be necessary, we directed our efforts to a model system, utilizing tetrahydroquinoline (**142**) as a nucleophile in order to preserve valuable material (Table 2.6.3). Conducting the reaction at elevated temperature in aqueous Na₂CO₃ led to only slight conversion but did enable the isolation and characterization of an authentic standard of product **143** in 4% yield (entry 1). Interestingly, heating **142** and **140** in AcOH, with or without a Cu^I additive, led to the formation of a different major product (entries 2/3). This product was not fully characterized, although LC–MS analysis indicated that it may be an isomer of desired product **143**. Lee reported an aza-Michael addition of anilines to acyclic Michael acceptors catalyzed by CuCl and NHC or phosphine ligands.²⁹ Although 5 ligands were tested (entry 4, **144–148**, Scheme 2.6.4), no reactivity was observed in the system at hand.

Table 2.6.3. A model system for aza-Michael addition.^a


entry	solvent	temp (°C)	additive	equiv enone	result
1	H ₂ O	80	Na ₂ CO ₃	1	4% yield ^b
2	AcOH	75	N/A	2.5	unidentified major pdt
3	AcOH	75	CuCl	2.5	unidentified major pdt
4 ^c	PhCH ₃	23	CuCl, 144–148, KO ^t -Bu	1	NR
5	PEG400	50	RuCl ₃ (5 mol %)	1	trace
6	Et ₃ N/HOAc	23	N/A	5	41% yield ^b

[a] Reaction outcomes were determined by LC–MS analysis unless otherwise noted. [b] Isolated yields. [c] 7 mol % CuCl, 7 mol % ligand, 14 mol % KO^t-Bu.

Scheme 2.6.4. Ligands tested in entry 4 of Table 2.6.3.

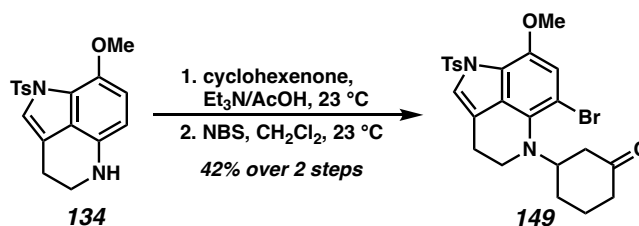
The RuCl₃-catalyzed reaction conditions reported by Wang led to only trace product (entry 5). Finally, to our delight, when **142** and **140** were combined in a mixture of triethylamine and acetic acid, as described for basic amines and primary anilines by Verma et al., the desired tertiary aniline **143** was obtained in 41% isolated yield (entry 6).³⁰

Intriguingly, this model aza-Michael addition appeared qualitatively to proceed to a higher degree of conversion at lower reaction temperatures, and an excess of cyclohexenone was necessary to drive the reaction forward. Around the same time that these experiments were conducted, a report was published by Condakes detailing the

equilibrium nature of related aza-Michael additions of π -excessive heterocycles into β -substituted unsaturated esters catalyzed by base.³¹ The reactions reported by Condakes appear to exhibit a similar thermodynamic profile to the formation of **143** — increasing the reaction temperature led to a more reactant-favored equilibrium.

The ionic liquid-promoted aza-Michael reaction to form model compound **143** translated well to tricycle **134** (Scheme 2.6.5). Aza-Michael reaction with cyclohexenone was followed by selective *ortho*-bromination of the aniline with NBS to afford model cyclization substrate **149**.

Scheme 2.6.5. Preparation of a model Barbier addition substrate.



With model substrate **149** in hand, we evaluated conditions for a Barbier-type addition of the aryl bromide into the cyclic ketone (Table 2.6.6). Lithium-halogen exchange did not provide the desired tertiary alcohol **150**—we hypothesize that the generated aryllithium species could be protonated intramolecularly to form an enolate (entry 1). Formation of an aryl Grignard species could not be effected (entries 2–3). While the Nozaki–Hiyama–Kishi reaction is generally selective for addition into aldehydes, the use of forcing reaction conditions was anticipated to provide an opportunity to achieve the desired ketone addition. Subjecting bromide **149** to standard NHK conditions at elevated temperature led to the formation of trace amounts of desired alcohol **150**, but primarily led to *retro*-aza-Michael fragmentation to tricycle **134** with accompanying protodebromination (entry 4). The use of neocuproine as a ligand for nickel was hypothesized to promote

reactivity under milder conditions,³² but only protodebromination was observed in this case (entry 5). Switching the catalyst from nickel to palladium and employing a stoichiometric variant of Yamamoto's conditions for the intramolecular addition of aryl bromides to ketones resulted, satisfyingly, in the formation of desired alcohol **150** (entry 6).³³ This reaction was then conducted at a larger scale with catalytic palladium (entry 7)—while the low yield obtained suggests poor or no catalyst turnover despite the addition of 1-hexanol (used by Yamamoto as a stoichiometric reductant), a sufficient quantity of **150** was obtained to confirm the structure of the product. We therefore decided to move forward with a Pd-mediated approach to construction of the azabicyclononane moiety and set out to prepare an analogue of cyclization substrate **149** in a higher oxidation state.

Table 2.6.6. Barbier-type addition into a model ketone.^a

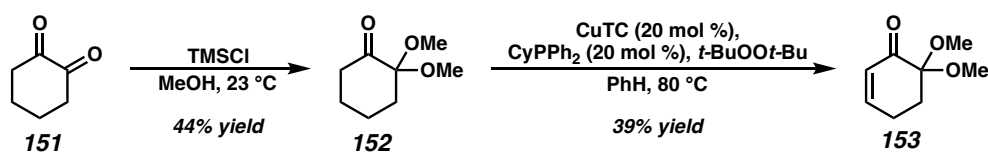
entry	conditions	result
1	<i>t</i> -BuLi, THF, -95 °C	partial protodebromination
2	<i>i</i> -PrMgCl·LiCl, THF, -78 °C	no Mg–Br exchange
3	Mg ⁰ , THF, 50 °C	NR
4	NiCl ₂ (0.4 equiv), CrCl ₂ , DMF, 125 °C	150 (trace) + 134 (major)
5	NiCl ₂ (0.4 equiv), CrCl ₂ , neocuproine, DMF, 23 °C	141 (major)
6	Pd(OAc) ₂ (1 equiv), PCy ₃ (2 equiv), K ₂ CO ₃ , DMF, 135 °C	150 (major)
7	Pd(OAc) ₂ (0.3 equiv), PCy ₃ (0.4 equiv), K ₂ CO ₃ , 1-hexanol, DMF, 135 °C	150 (17% yield) + 134 (29% yield) ^b

[a] Reaction outcomes were determined by LC–MS analysis unless otherwise noted. [b] Isolated yields.

An additional functional handle could be introduced in the desired oxidation state as a ketal, which would obviate later redox manipulations. Toward this aim, 1,2-dione **151** was subjected to known monoketalization (Scheme 2.6.7).³⁴ Subsequent desaturation of ketone **152** was complicated by the propensity of desired enone **153** to undergo

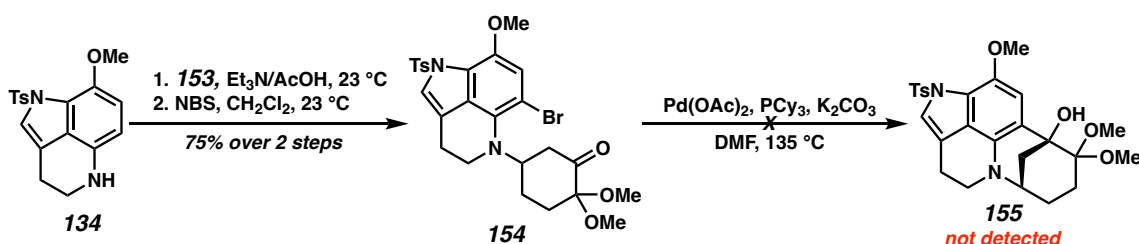
aromatization by elimination of methanol. While IBX oxidation, selenide installation and selenoxide elimination, and Saegusa–Ito oxidation all failed to deliver the desired enone, the copper-catalyzed method developed by Dong provided enone **153** in modest yield.³⁵ Desaturation with *N*-*t*-butylbenzenesulfinimidoyl chloride also provided the desired product, but Dong's conditions were favored due to the ready availability of the reagents.

Scheme 2.6.7. Preparation of a ketal-bearing Michael acceptor.



Subsequent aza-Michael addition of aniline **134** and bromination proceeded smoothly to afford Barbier addition substrate **154** (Scheme 2.6.8). Unfortunately, Yamamoto's conditions failed to provide tertiary alcohol **155** despite the successful application of this method toward the cyclization of model substrate **149**.

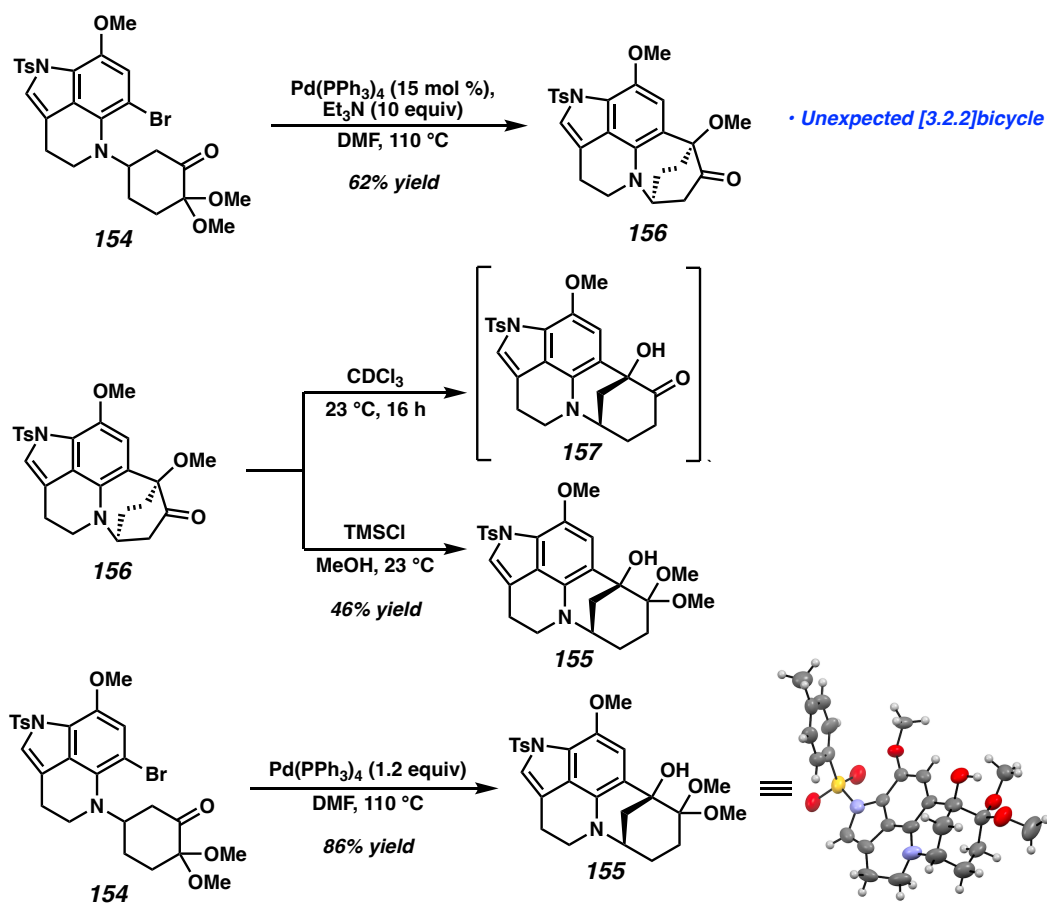
Scheme 2.6.8. Preparation of an oxidized intramolecular Barbier addition substrate.



While several additional sets of Ni-catalyzed conditions were tested, providing only trace cyclized product,³⁶ the simple conditions developed by Reissig for Pd-catalyzed addition of aryl iodides to ketones led to efficient cyclization of aryl bromide **154** (Scheme 2.6.9).³⁷ Interestingly, however, the major product of this cyclization was found to be azabicyclo[3.2.2]nonane **156**, arising from formal addition of the arene to the ketal instead of the ketone. It is uncertain if this addition occurs directly to the ketal or if **156** is formed

by addition of an arylpalladium species to the ketone with concomitant semipinacol rearrangement of a [3.2.1]bicycle. In any case, allowing ketone **156** to stand overnight in CDCl_3 (likely containing catalytic acid formed by decomposition, and conceivably containing at least 1 equivalent of water) effected complete rearrangement to desired bicyclic ketone **157** bearing a bridgehead alcohol. Alternatively, rearrangement of **156** to bicyclic ketal **155** was promoted by acidic methanol. Finally, employing a stoichiometric quantity of $\text{Pd}(\text{PPh}_3)_4$ in the Barbier-type addition rather than using Et_3N as a stoichiometric reductant directly afforded bicyclic ketal **155**, the initially anticipated product. The structure of **155** was confirmed by x-ray crystallography.

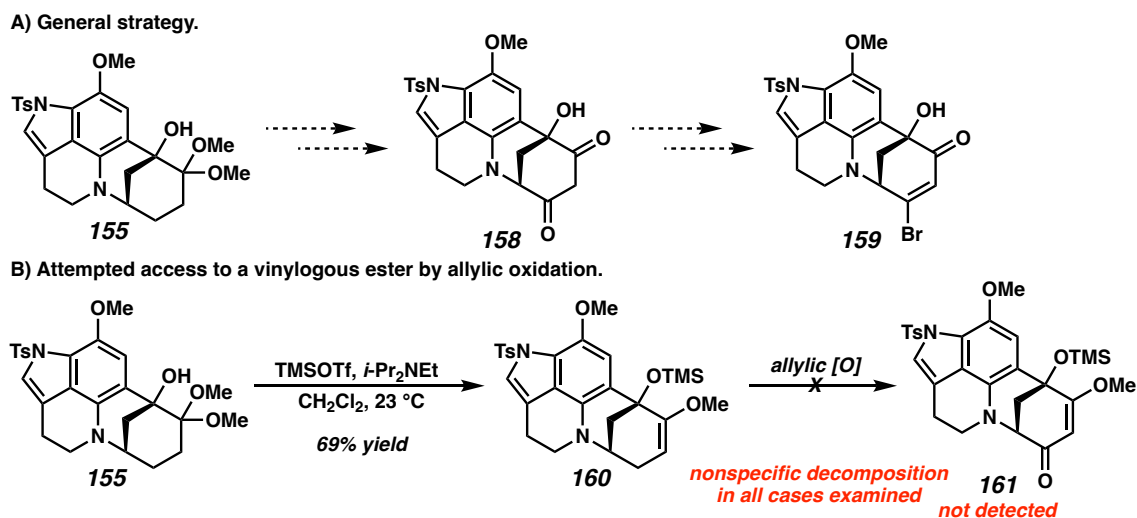
Scheme 2.6.9. Cyclization of bromoarene **154** and unexpected rearrangements.



With desired pentacyclic intermediate **155** in hand, strategies were evaluated for the installation of the 1,3-dicarbonyl equivalent (e.g., **158**, Scheme 2.6.10A) that would be required for eventual formation of the alkenyl bromide of aleutianamine. In general, elaboration of a saturated ketone or enone to a 1,3-dicarbonyl equivalent is challenging to perform directly, with Wacker-type oxidations failing in all but the simplest cases (see Appendix 5 for preliminary evaluation of a relevant oxidation).

We first imagined that a vinylogous ester could be installed by allylic oxidation of an enol ether (Scheme 2.6.10B).³⁸ Thus, ketal **155** was treated with TMSOTf and *i*-Pr₂NEt, leading to silylation of the tertiary alcohol and elimination of the ketal to afford methyl enol ether **160**. Unfortunately, under selenium- or hypervalent iodine-mediated allylic oxidation conditions, nonspecific decomposition was observed with no detectable trace of the desired compound **161**.

Scheme 2.6.10. Attempted allylic oxidation of pentacycle **160**.

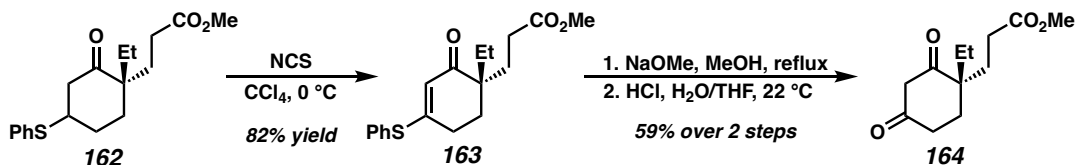


Another demonstrated, albeit lengthier strategy to accomplish the desired transformation involves desaturation of a ketone followed by thiol conjugate addition and further desaturation to a vinylogous thioester, another 1,3-diketone equivalent. Precedent

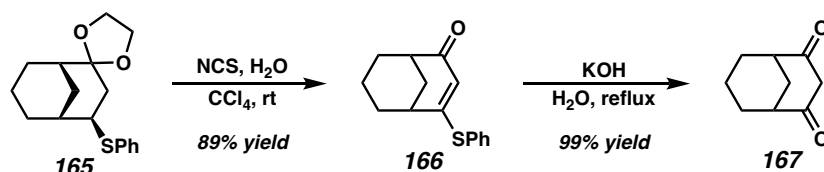
for this sequence was reported by d'Angelo (Scheme 2.6.11A), wherein sulfide **162** was converted to vinylogous thioester **163** with NCS, and subsequent treatment with NaOMe and acidic hydrolysis afforded 1,3-diketone **164**.³⁹ Similarly, Kakisawa reported the desaturation of sulfide **165** with concomitant ketal hydrolysis (Scheme 2.6.11B).⁴⁰ The product **166** underwent direct alkaline hydrolysis to diketone **167**. In our system, ketal **155** underwent hydrolysis to the ketone under biphasic conditions, double silylation to afford an intermediate TMS enol ether that was surprisingly stable to silica, and Saegusa–Ito oxidation to afford enone **168** (Scheme 2.6.11C).

Scheme 2.6.11. Attempted β -oxidation by a thiol conjugate addition approach.

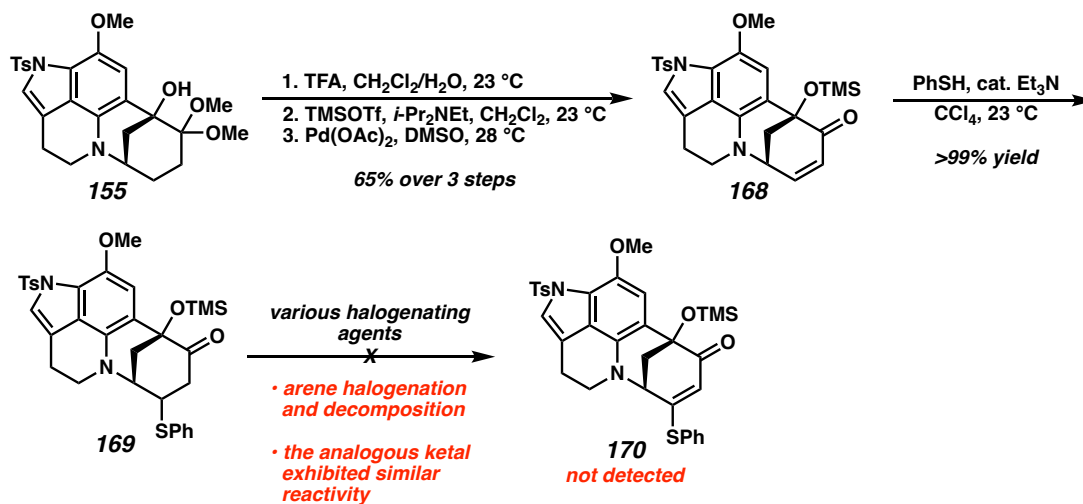
A) Precedent for desaturation of a β -thio ketone and subsequent solvolysis (d'Angelo, 1994).



B) Precedent for an analogous transformation of a ketal (Kakisawa, 1987).



C) Efforts to prepare a vinylogous thioester by a 1,4-addition/oxidation sequence.



Conjugate addition of PhSH afforded sulfide **169**. Unfortunately, treatment of **169** or the derived ethylene ketal with various halogenating reagents did not effect the necessary desaturation to vinylogous thioester **170**, unlike in the systems of d'Angelo and Kakisawa.

While the evaluation of further reaction conditions could indeed lead to a synthetically useful derivative of 1,3-dicarbonyl **158**, at this point, we had several concerns about the synthetic route leading up to sulfide **169**. Namely, the route was highly linear, proceeding in a longest linear sequence of 13 steps. Although the feasibility of bridgehead sulfide installation had been demonstrated in a model system (see Appendix 5), we realized that the plan to subject a late-stage intermediate to the harsh carbocation chemistry necessary for this transformation bore excessive risk. Additionally, having already required 13 steps to access an intermediate lacking both the bridgehead sulfide and the alkenyl bromide of the natural product, the synthetic sequence would probably become inelegantly lengthy over the course of the installation of these challenging motifs. We therefore conceived of a 3rd-generation retrosynthetic analysis of aleutianamine.

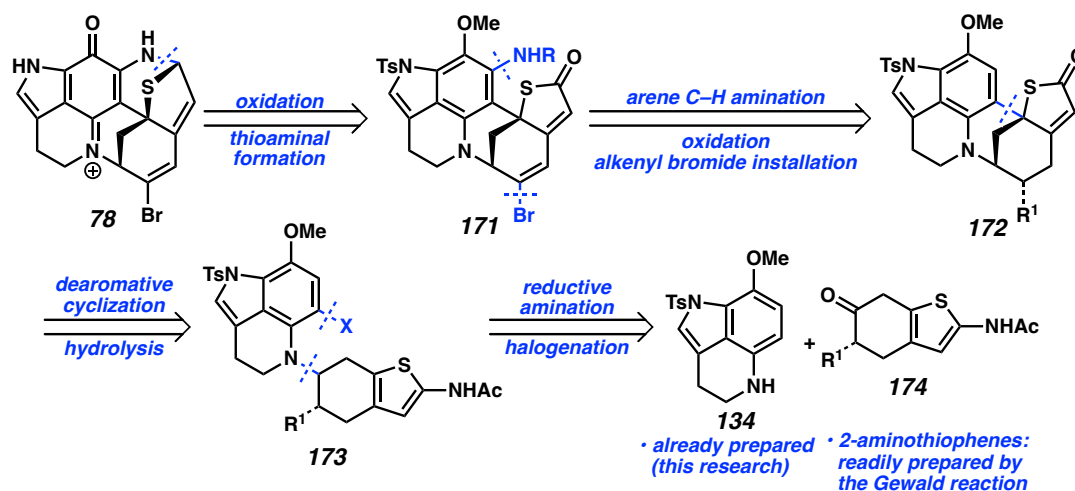
2.7 3rd-GENERATION RETROSYNTHESIS

An ideal synthesis of aleutianamine would: 1) be convergent and enable rapid assembly of structural complexity, 2) provide a robust strategy for the construction of the tertiary bridgehead sulfide moiety of the natural product, and 3) take advantage of the scalable early-stage chemistry already developed during our previous synthetic efforts.

A retrosynthetic analysis that would meet all of these requirements could, like our previous strategies, invoke a late-stage arene oxidation, but now, aleutianamine would be tracked back to doubly unsaturated thiolactone **171**, which could undergo reduction and ring closure (Scheme 2.7.1).

Structural simplification of hexacycle **171** by disconnection of the acyclic aniline and alkenyl bromide leads back to thiobutenolide precursor **172**—while we aimed to install the bromide in a selective fashion, carrying a functional handle R^1 through the synthetic sequence was envisioned as an alternative strategy. From this point, in a highly simplifying disconnection, **172** could arise from haloarene **173** by an unprecedented cyclization reaction involving dearomatization of the thiophene ring. This cyclization would establish the full carbon skeleton of the natural product as well as the bridgehead sulfide in a single step. Tertiary aniline **173** would arise from a convergent fragment coupling of tricyclic aniline **134** and keto-thiophene **174** by reductive amination followed by arene halogenation. Rapid access to material to test the key cyclization step would be facilitated by the access to tricycle **134** already enabled by our previous synthetic efforts and by facile preparation of 2-aminothiophenes by the Gewald reaction.

Scheme 2.7.1. 3rd-generation retrosynthetic analysis of aleutianamine.

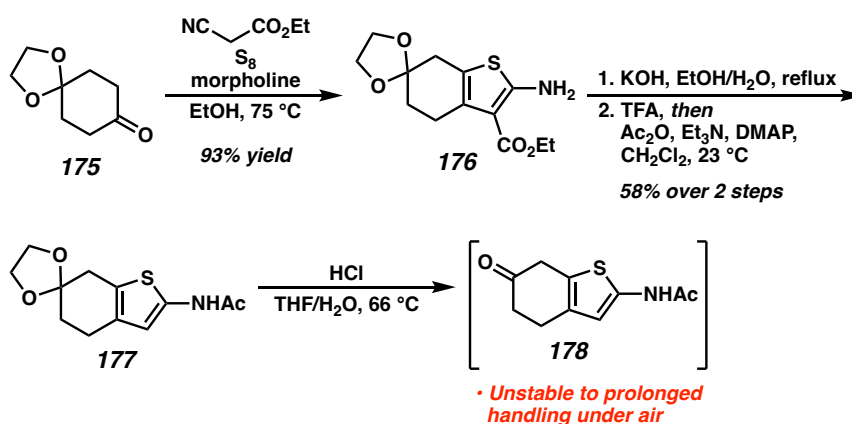


2.8 PURSUIT OF A DEAROMATIVE CYCLIZATION APPROACH

To realize this new synthetic plan, we developed an expedient synthesis of a thiophene coupling partner (Scheme 2.8.1). Monoketal **175** smoothly underwent the

Gewald aminothiophene synthesis in the presence of ethyl cyanoacetate to afford 2-aminothiophene **176** under published conditions.⁴¹ Saponification and TFA-promoted decarboxylation then served to remove the ester group, and the resulting amine was readily acetylated to provide amide **177**. Finally, the ketal could undergo acidic hydrolysis to provide desired ketone **178**. As ketone **178** was found to undergo oxidation in air, this compound was prepared just prior to use or stored in the glovebox. Syntheses of analogues of **178** bearing functional handles for alkenyl bromide installation were also attempted (see Appendix 5), but each functional handle tested presented its own synthetic obstacles and these approaches were eventually abandoned in favor of planned late-stage alkenyl bromide installation.

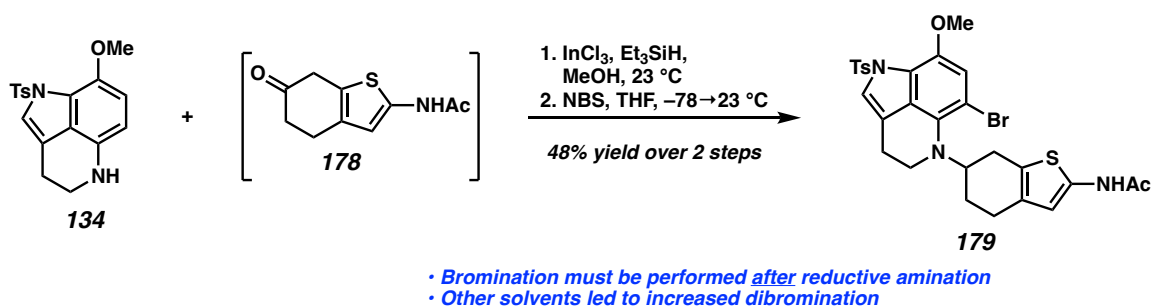
Scheme 2.8.1. Construction of an acetamidothiophene coupling partner.



Now with access to both fragments, the key reductive amination was tested. While the potentially low nucleophilicity of secondary aniline **134** was an initial concern, we were please to observe that the InCl₃/Et₃SiH system reported by Yang smoothly promoted reductive amination between aniline **134** and ketone **178** (Scheme 2.8.2).⁴² Subsequent bromination at the aniline *ortho*-position was initially challenging due to competitive bromination at the C(3)-position of the thiophene and the formation of dibrominated

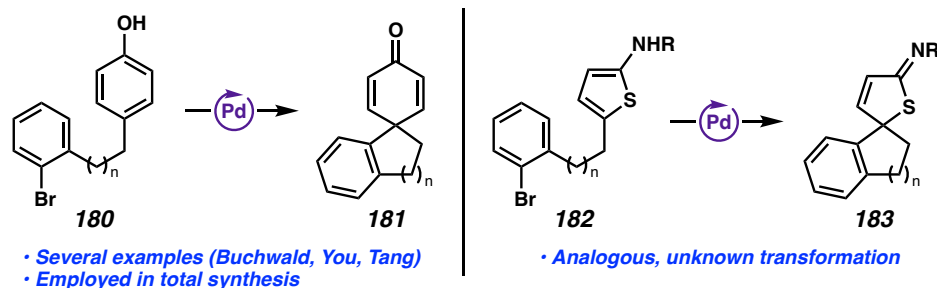
products prior to complete consumption of the starting material. The use of THF as the reaction solvent was crucial to maximally (albeit not completely) suppress this undesired reactivity, allowing for the preparation of key bromoarene cyclization substrate **179**. Note that bromination of tricycle **134** prior to coupling completely shut down the reductive amination.

Scheme 2.8.2. Fragment coupling to prepare a dearomative cyclization substrate.



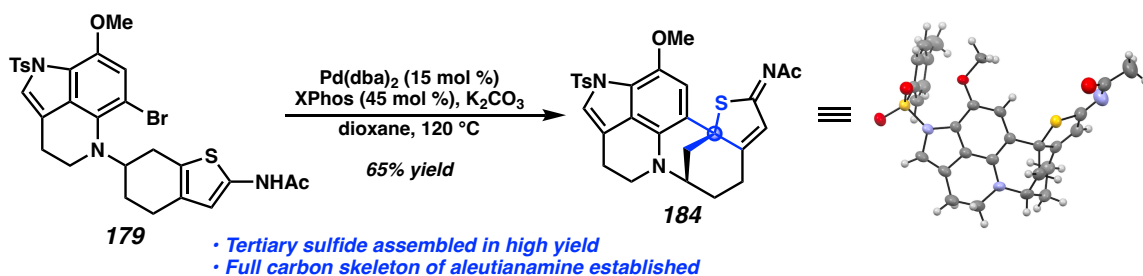
While Pd-catalyzed dearomative Heck-type transformations of furans have been reported,⁴³ related transformations of thiophenes are scarce and have not been performed by transition metal catalysis. A possible explanation for the lack of reports of thiophene dearomatization by Heck-type reactivity is the high degree of aromaticity of thiophenes compared to other π -excessive heterocycles.⁴⁴ We therefore opted to model the desired transformation on reported dearomative intramolecular arylations of phenols **180**, which lead to ketones **181** (Scheme 2.8.3). Buchwald's initial report of this transformation has inspired further development by other groups⁴⁵ and synthetic applications.⁴⁶ Examples exist of related dearomative transformations of anilines, albeit with a limited scope.⁴⁷ Based on this combined precedent, we envisioned that the dearomative arylation of aminothiophenes **182** to access thioimidates **183** would be feasible, driven by deprotonation of the aminothiophene to render the heterocycle more electron-rich and by the formation of an additional C=N π -bond.

Scheme 2.8.3. Known dearomative arylation and desired transformation of thiophenes.



Indeed, gratifyingly, treatment of brominated acetamide **179** with Pd⁰, ligand, and base under conditions derived from those used by Buchwald for the dearomative arylation of phenols provided desired cyclized thioimide **184** on the first attempt with protodebromination as the primary side product (Scheme 2.8.4).^{45a} The successful application of this transformation completes the carbon skeleton of the natural product.

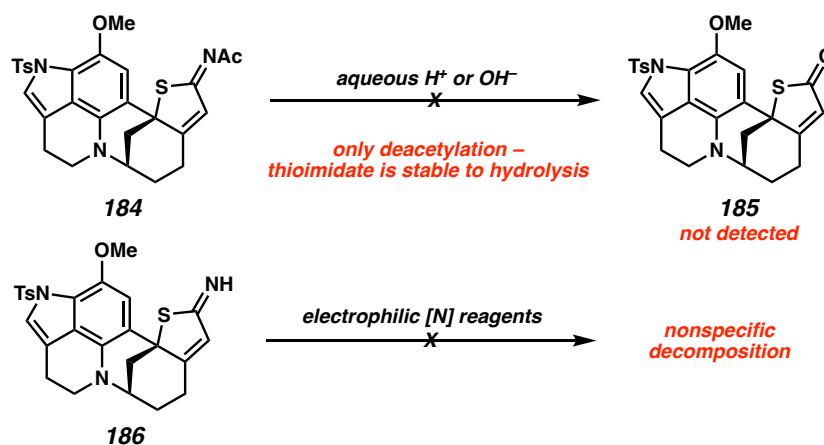
Scheme 2.8.4. Key dearomative cyclization of aminothiophene **179**.



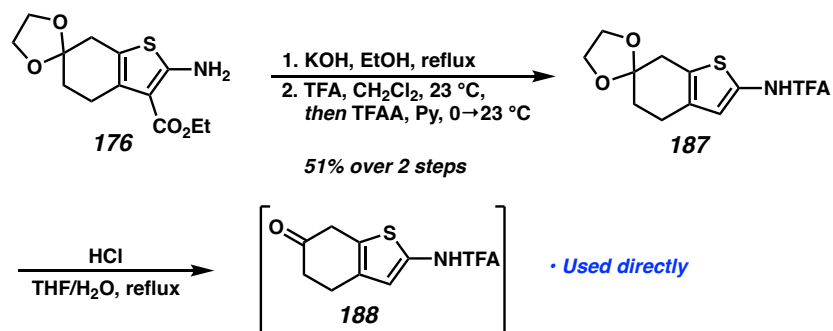
Following the preparation of thioimide **184**, experiments were conducted to effect C–H amination and subsequent closure of the final ring of the natural product. While amination could occur, albeit in low yield, ring closure was unsuccessful. Furthermore, a path toward alkenyl bromide installation from thioimide **184** was unclear. Our efforts therefore shifted to hydrolysis of the thioimide to the corresponding thiolactone.

Interestingly, attempts to effect acidic or basic hydrolysis of acetylthioimide **184** to thiolactone **185** led only to deacetylation with no further reactivity (Scheme 2.8.5). Under acidic conditions, prolonged heating led to nonspecific decomposition after deacetylation. This behavior was rather surprising given the generally facile hydrolysis of imines. Deacetylated thioimide **186** (prepared independently, vide infra) was exposed to several electrophilic nitrogen sources in an attempt to render the nitrogen a better leaving group, unsuccessfully.

Scheme 2.8.5. Attempts to access a thiolactone from acetylthioimide **184**.



We imagined that a derivative of thioimide **184** bearing a more electron-withdrawing thioimide protecting group could be more hydrolytically labile. Furthermore, a more electron-poor 2-aminothiophene might be less prone to undesired competitive bromination. Therefore, following hydrolysis of Gewald product **176**, the resulting acid was decarboxylated and treated with TFAA and base in the same pot, leading to TFA-protected aminothiophene **187** (Scheme 2.8.6). Ketal removal provided an intermediate ketone (**188**) that was used directly in the following step to prevent oxidation.

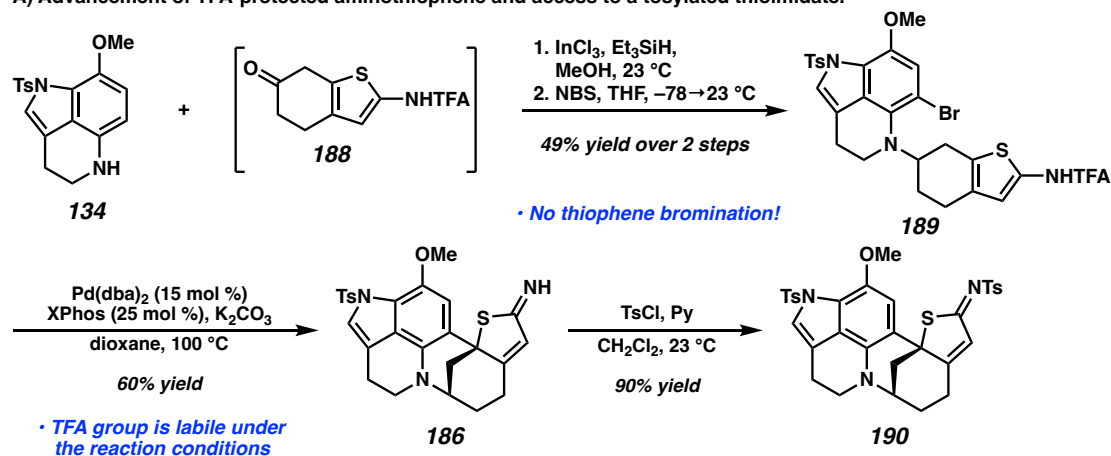
Scheme 2.8.6. Synthesis of a TFA-protected aminothiophene.

Coupling of tricycle **134** and ketone **188** proceeded smoothly by reductive amination, and bromination provided cyclization substrate **189** (Scheme 2.8.7A). *Ortho*-brominated product **189** was the only product isolated from the reaction mixture, with the more electron-deficient TFA-protected aminothiophene not undergoing competitive bromination. Satisfyingly, **189** underwent dearomative cyclization under the conditions applied earlier to acetyl-protected substrate **179**, but the product isolated was free thioimide **186**—TFA cleavage appears to be effected under the reaction conditions, possibly due to adventitious water originating from the hygroscopic base. It was thus clear that the TFA group would not facilitate hydrolysis. Instead, free thioimide **186** was sulfonylated with TsCl to provide tosyl-protected derivative **190**.

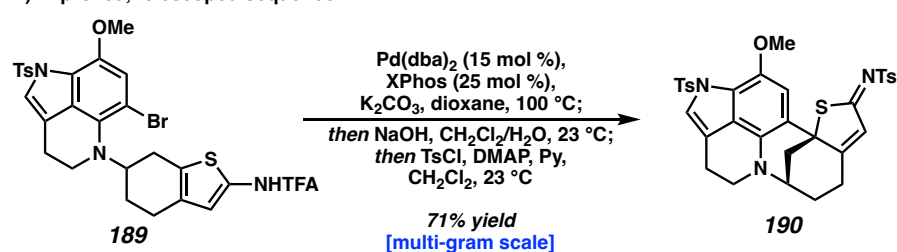
While this improved synthetic sequence was sufficient to access useful quantities of **190**, we hypothesized that the yield of polar thioimide **186** was reduced during chromatographic purification. To circumvent this purification, the dearomative cyclization and protection steps were combined (Scheme 2.8.7B). For consistency, the product of the dearomative cyclization was stirred with alkali prior to tosylation, as TFA cleavage was not always complete after the cyclization. To date, this step has enabled the preparation of up to 2.66 g of tosylthioimide **190** in a single batch.

Scheme 2.8.7. Improved thioimide synthesis and subsequent tosylation.

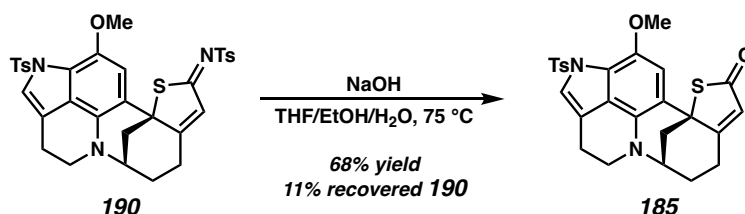
A) Advancement of TFA-protected aminothiophene and access to a tosylated thioimide.



B) Improved, telescoped sequence.

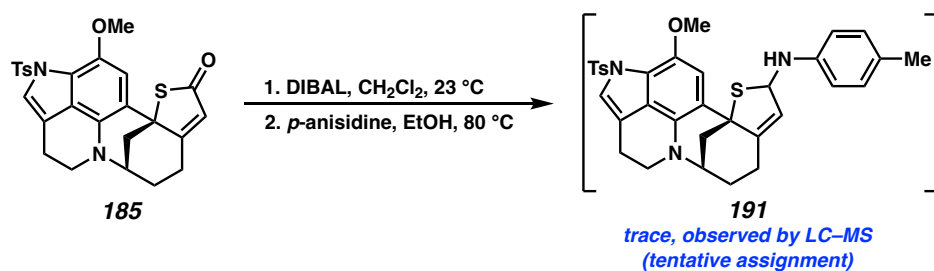


Subjecting tosylthioimide **190** to basic hydrolysis led to desired thiolactone **185** in 68% yield with 11% recovered starting material (Scheme 2.8.8). Notably, the yield of **185** varied significantly depending on the solvent ratio (excluding THF led to inconsistent results due to low solubility), temperature (a low yield was obtained at 60°C , with LC–MS evidence for partial hydrolysis products that did not convert to **185** upon further subjection to alkali), and air exposure (the electron-rich arene appears to undergo nonspecific decomposition by an oxidative pathway).

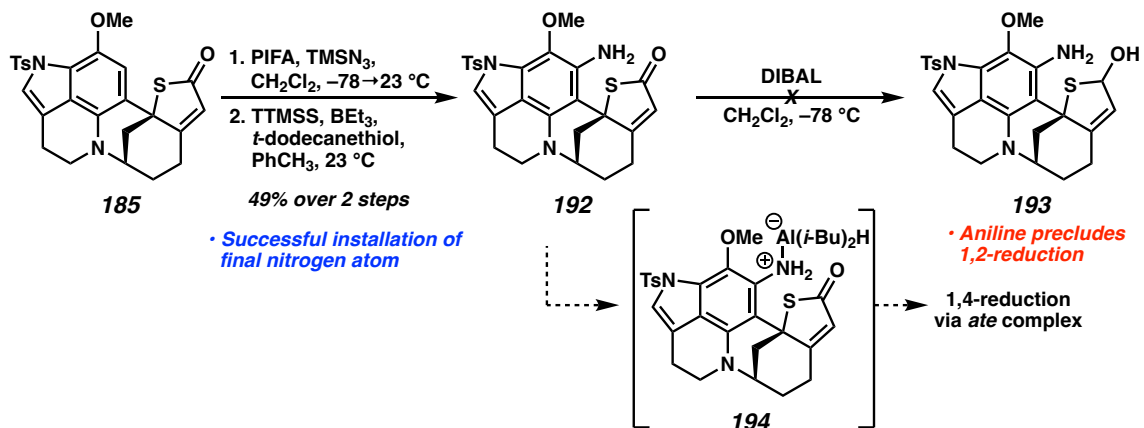
Scheme 2.8.8. Successful hydrolysis of thioimide **190**.

Prior to studying alkenyl bromide installation or arene amination, a test reaction was conducted to determine the feasibility of condensation to form the thioaminal moiety of the natural product (Scheme 2.8.9). Thiolactone **185** was treated with DIBAL to afford an intermediate thiolactol as a mixture of diastereomers. Heating this intermediate with *p*-anisidine, a model aniline, formed a trace amount of putative thioaminal **191**, as detected by LC–MS.

Scheme 2.8.9. Demonstration of the feasibility of thioaminal formation.



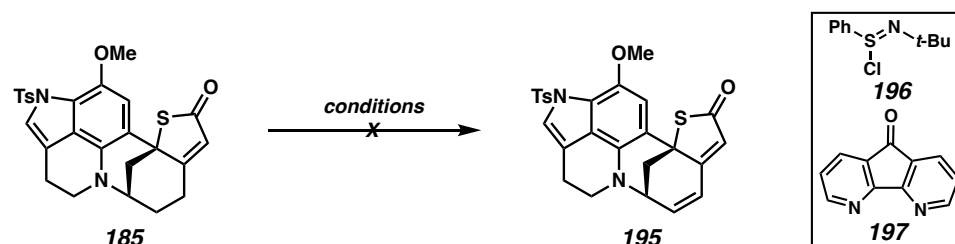
Following this promising result, installation of the final nitrogen atom of the natural product was attempted (Scheme 2.8.10). Reactions of thioimide **184** studied at an earlier stage indicated that a modified version of Kita's oxidative arene azidation conditions were uniquely effective for installation of the nitrogen atom at the desired position *ortho* to the methoxy group.⁴⁸ These conditions were found to be applicable to thiolactone **185**, and reduction of the aryl azide under silane-mediated radical conditions⁴⁹ afforded desired aniline **192**.⁵⁰ Unfortunately, treatment of aniline **192** with DIBAL failed to provide the desired thiolactol **193**: Evidently, the aniline can form *ate* complex **194**, which preferentially leads to 1,4-reduction.

Scheme 2.8.10. Installation of the final nitrogen atom by azidation and reduction.

While further optimization may enable access to thiolactol **193**, we instead directed our efforts to further desaturation of the thiolactone and installation of the alkenyl bromide. Direct desaturation of thiobutenolide **185** to the doubly unsaturated derivative **195** was explored under a variety of reaction conditions (Table 2.8.11). IBX led to nonspecific decomposition (entry 1), while *N*-*t*-butylbenzenesulfinimidoyl chloride (**196**) failed to effect desaturation (entry 2). Dong's Cu-catalyzed conditions provided very little reactivity with only trace product formation (entry 3), perhaps unsurprisingly due to the proposed involvement of a 6-membered transition state in this reaction, which would not be possible for vinylogous desaturation.³⁵ Newhouse's Pd-catalyzed conditions provided some conversion, but the reaction stalled (entry 4).⁵¹ A control experiment with Pd(OAc)₂ revealed that the [Pd(allyl)Cl₂] precatalyst is necessary for this reaction (entry 5), but the use of stoichiometric [Pd(allyl)Cl₂] led to a mixture of putative allylation products (entry 6). Stahl reported a method for mono-desaturation of cyclic ketones, finding during optimization that Pd(TFA)₂ in DMSO led to high amounts of doubly unsaturated (aromatized) product.⁵² While these conditions did lead to trace quantities of desired diene **195** (entry 7), useful levels of conversion were not achieved even after prolonged stirring.

Stahl's Pd/diazafluorenone (**197**) conditions,⁵³ reported to lead to rapid aromatization of cyclohexanone, did not lead to any reactivity (entry 8).

Table 2.8.11. Conditions tested for direct desaturation of thiobutenolide **185**.

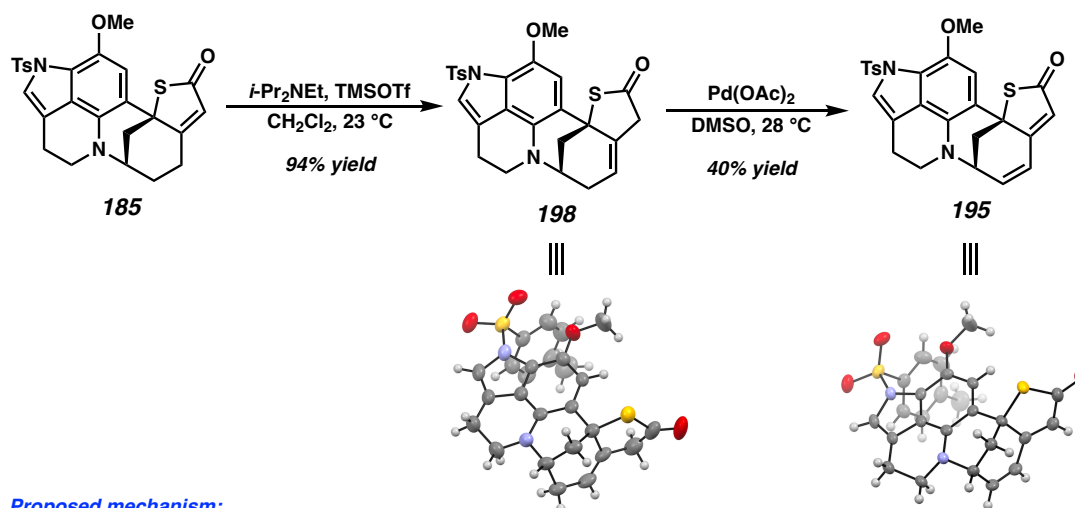


entry	conditions	result
1	IBX, MeCN, 50 °C	decomp
2	LiHMDS, 196 , THF, -78→23 °C	SM + decomp
3	CuTC, CyPPh ₂ , (<i>t</i> -BuO) ₂ , PhH, 80 °C	trace product
4	LiTMP, ZnCl ₂ , [Pd(allyl)Cl] ₂ (5 mol %), allyl acetate, THF, -40→28 °C	stalled
5	LiTMP, ZnCl ₂ , Pd(OAc) ₂ , THF, -40→28 °C	NR
6	LiTMP, ZnCl ₂ , [Pd(allyl)Cl] ₂ (1.1 equiv), THF, -40→28 °C	putative allylation
7	Pd(TFA) ₂ (1 equiv), DMSO, 80 °C	trace product
8	Pd(TFA) ₂ (20 mol %), 197 (20 mol %), O ₂ , DMSO, 80 °C	NR

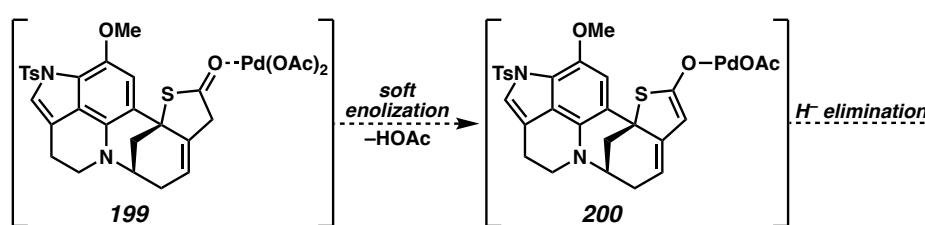
Diene **195** can, fortunately, be accessed by a 2-step oxidation protocol (Scheme 2.8.12). Soft enolization with *i*-Pr₂NEt and TMSOTf leads to an unstable silyl ketene thioacetal. Upon workup and chromatography, this intermediate appears to undergo protonation at the α -carbon, affording deconjugated olefin **198**. Then, treatment with stoichiometric Pd(OAc)₂ provides desired diene **195** in modest yield. This desaturation likely proceeds by initial coordination of the palladium to the carbonyl, as in intermediate **199**. Soft enolization would be enabled by the acidic nature of the ketone α -position, leading to extended palladium enolate **200**. A hydride elimination would provide the desired product. Support for this proposed mechanism is provided by the failure of thiobutenolide **185** to directly afford diene **195** upon treatment with Pd(OAc)₂—acidified α -protons are likely necessary for formation of palladium enolate **200**. Unfortunately, we have been unable to render the desaturation of deconjugated ketone **198** catalytic. Further

efforts will be made in the future to circumvent the requirement of this process for stoichiometric palladium.

Scheme 2.8.12. Desaturation of thiolactone **185** to diene **195**.



Proposed mechanism:



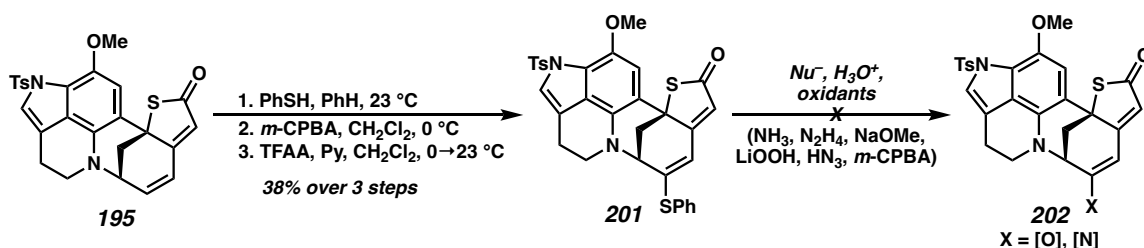
Control experiment:



Toward the desired alkenyl bromide, diene **195** underwent conjugate addition of thiophenol followed by oxidation to the sulfoxide and Pummerer rearrangement to afford doubly vinylogous dithiocarbonate **201** (Scheme 2.8.13). We imagined that hydrolysis to the doubly vinylogous acid could enable bromide installation by $[\text{COBr}]_2/\text{DMF}$ ⁵⁴ or by triflate formation and triflate-halogen exchange,⁴ or that access to a vinylogous amide could enable bromide installation by radical chemistry.⁵⁵ To our dismay, **201** was

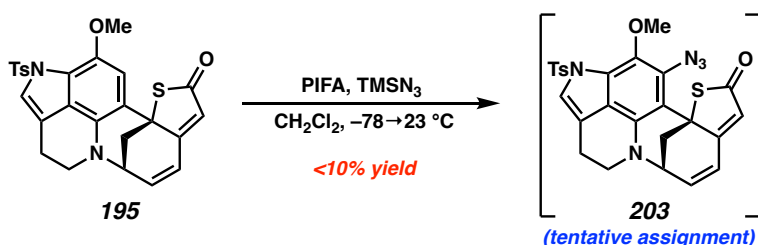
recalcitrant to sulfide displacement by a variety of nucleophiles, and the phenyl sulfide did not undergo selective oxidation to render it a better leaving group.

Scheme 2.8.13. Thioester δ -functionalization and unsuccessful downstream chemistry.



Around the same time, we discovered that unlike thiobutenolide **185**, diene **195** was not an efficient substrate for oxidative arene azidation (Scheme 2.8.14). Putative aryl azide **203** was detected in the reaction mixture by LC–MS, but a low yield was obtained upon isolation. As desaturation of the thiobutenolide following azidation may present a functional group compatibility challenge, we reevaluated the synthetic plan for arene amination and bromide installation.

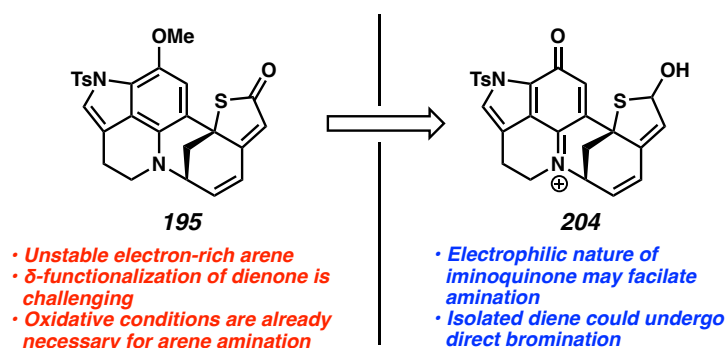
Scheme 2.8.14. Inefficient azidation of dienone **195**.



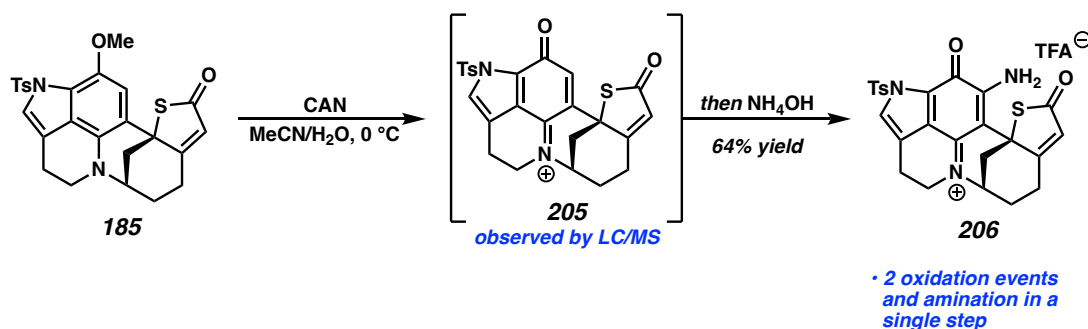
Throughout the synthetic sequence leading up to **195**, most intermediates were found to be somewhat oxidatively unstable, especially in the presence of acid, undergoing discoloration in air and decomposition in CDCl₃. This behavior hinted that arene **195** may be readily oxidized to the corresponding pyrroloiminoquinone. While conducting the

synthetic sequence in the arene oxidation state enabled aniline alkylation by reductive amination, dearomative thiophene functionalization, and subsequent transformations, we realized that it could be beneficial to oxidize the arene to the quinone oxidation state prior to installation of the final nitrogen atom and the alkenyl bromide (Scheme 2.8.15). The electrophilic nature of pyrroloiminoquinone **204** could facilitate direct amination and circumvent the low-yielding azidation step. Additionally, the thiolactone could be reduced to a thiolactol, altering the diene electronics and potentially enabling direct bromination at the desired position. Although the exploration of backup strategies for earlier installation of the alkenyl bromide is ongoing, we have begun to explore this strategy.

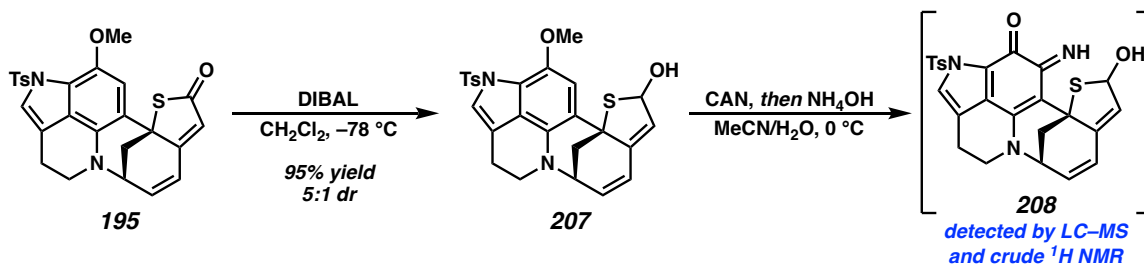
Scheme 2.8.15. Benefits of an early oxidation event.



To evaluate the key arene oxidation, thiolactone **185** was subjected to the CAN-mediated conditions described by White (Scheme 2.8.16).¹⁶ Addition of CAN to the substrate led to rapid formation of orange putative cationic pyrroloiminoquinone **205**. This intermediate was not isolated; instead, gratifyingly, addition of aqueous ammonia led to purple, aminated pyrroloiminoquinone **206**, isolated as the TFA salt after HPLC purification. The second oxidation event after ammonia addition is likely mediated by atmospheric oxygen.

Scheme 2.8.16. Proof-of-concept for an oxidative strategy.

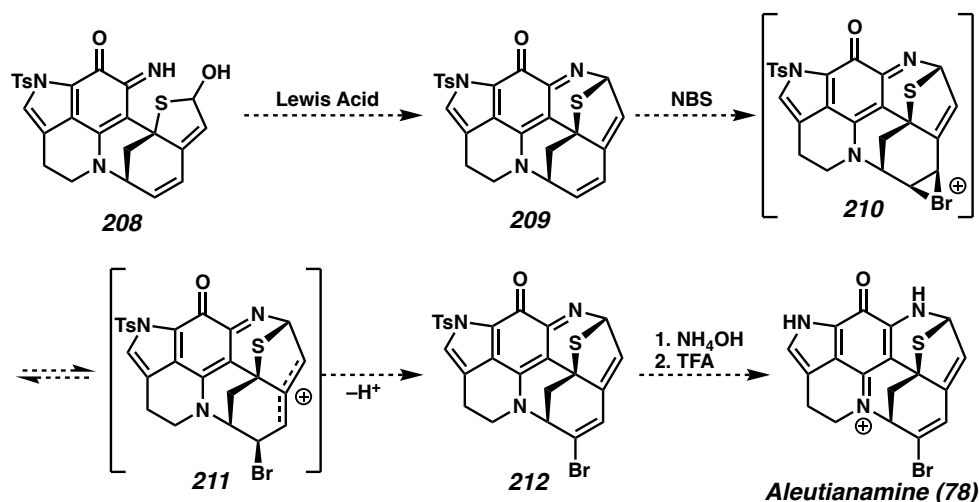
To translate this promising result to a synthetically relevant system, desaturated thiobutenolide **195** was treated with DIBAL, which led to the formation of thiolactol **207** as a 5:1 mixture of diastereomers (inseparable on silica gel) (Scheme 2.8.17). Oxidation of **207** with CAN and ammonia addition did indeed lead to putative desired pyrroloiminoquinone **208**. Efforts to isolate this intermediate and effect its cyclization are ongoing.

Scheme 2.8.17. Toward desired pyrroloiminoquinone **208**.

We plan to treat **208** with a Lewis acid to effect dehydrative cyclization to heptacycle **209** (Scheme 2.8.18). Bromination will then be attempted with NBS—the electron-poor nature of the pyrroloiminoquinone and additional electron-withdrawing effect of the tosyl protecting group should favor bromination of the diene instead of the pyrrole moiety. If desired bromonium ion **210** forms, elimination from the more stable allylic carbocation **211** should afford alkenyl bromide **212** with the necessary

regioselectivity. Finally, detosylation of the electron-poor heterocycle by mild ammonia-mediated conditions¹⁶ and formation of the TFA salt could provide aleutianamine (**78**).

Scheme 2.8.18. *Planned completion of synthesis.*



2.9 CONCLUSION

Efforts toward the first total synthesis of the marine alkaloid aleutianamine have been conducted. Our strategy has evolved through three distinct major synthetic plans. To date, a hexacyclic intermediate bearing the entire carbon skeleton and all three nitrogen atoms of aleutianamine has been prepared by a strategy involving Pd-catalyzed dearomative spirocyclization of an aminothiophene intermediate. Efforts to advance this intermediate to the natural product are ongoing.

2.10 EXPERIMENTAL SECTION

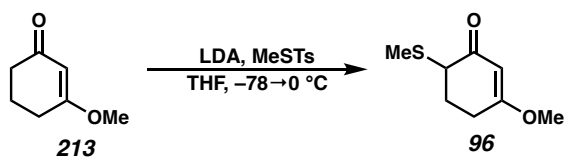
2.10.1 MATERIALS AND METHODS

Unless otherwise stated, reactions were performed in flame-dried glassware under an argon or nitrogen atmosphere using dry, deoxygenated solvents. Solvents were dried by passage through an activated alumina column under argon.⁵⁶ NBS was recrystallized from boiling water prior to use, amines and TMSCl were distilled under nitrogen prior to use,

and K_2CO_3 was flame-dried under vacuum and stored in a nitrogen-filled glovebox prior to use. All other reagents were purchased from commercial sources and used as received unless otherwise indicated. Reaction progress was monitored by thin-layer chromatography (TLC) or Agilent 1290 UHPLC-MS. TLC was performed using E. Merck silica gel 60 F254 precoated glass plates (0.25 mm) and visualized by UV fluorescence quenching or $KMnO_4$ staining. Silicycle SiliaFlash® P60 Academic Silica gel (particle size 40–63 nm) was used for flash chromatography. Preparative HPLC was performed on an Agilent 1100 Series HPLC system using a 9.4 x 250 mm Agilent Eclipse XDB-C18 column, or on an Agilent 1200 Series HPLC system using a 9.4 x 250 mm Agilent Zorbax Rx-SIL column. 1H NMR spectra were recorded on Varian Inova 500 MHz, Varian 600 MHz, and Bruker 400 MHz spectrometers and are reported relative to residual $CHCl_3$ (δ 7.26 ppm), C_6D_6 (δ 7.16 ppm), $DMSO-d_6$ (δ 2.50 ppm), CD_2Cl_2 (δ 5.32 ppm), or CD_3OD (δ 3.31 ppm). ^{13}C NMR spectra were recorded on a Bruker 400 MHz spectrometer (100 MHz) and are reported relative to $CHCl_3$ (δ 77.16 ppm), C_6D_6 (δ 128.06 ppm), $DMSO-d_6$ (δ 39.52 ppm), CD_2Cl_2 (δ 53.84 ppm), or CD_3OD (δ 49.00 ppm). Data for 1H NMR are reported as follows: chemical shift (δ ppm) (multiplicity, coupling constant (Hz), integration). Multiplicities are reported as follows: s = singlet, d = doublet, t = triplet, q = quartet, p = pentet, sept = septuplet, m = multiplet, br s = broad singlet, br d = broad doublet. Data for ^{13}C NMR are reported in terms of chemical shifts (δ ppm). Some reported spectra include minor solvent impurities of water, ethyl acetate, diethyl ether, methylene chloride, acetone, grease, and/or silicon grease, which do not impact product assignments. IR spectra were obtained by use of a Perkin Elmer Spectrum BXII spectrometer using thin films deposited on NaCl plates and reported in frequency of absorption (cm^{-1}). High resolution

mass spectra (HRMS) were obtained from an Agilent 6230 LC/TOF with an Agilent Jet Stream ion source in electrospray ionization (ESI+ or ESI-) mode, or from the Caltech Mass Spectrometry Laboratory using a JEOL JMS-T2000GC AccuTOF™ GC-Alpha in field desorption (FD+) mode.

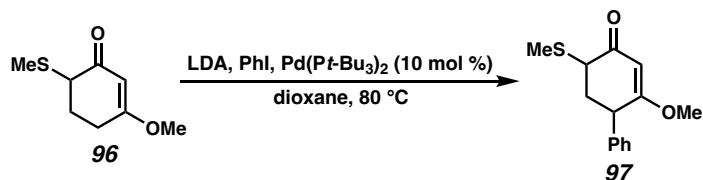
2.10.2 EXPERIMENTAL PROCEDURES



3-methoxy-6-(methylthio)cyclohex-2-en-1-one (96)

To a 20 mL glass vial equipped with a septum cap were added THF (8 mL) and *i*-Pr₂NH (0.29 mL, 2.1 mmol, 1.3 equiv). The solution was cooled to -78 °C and *n*-BuLi (2.5 M in hexanes, 0.76 mL, 1.9 mmol, 1.2 equiv) was added slowly with stirring. The mixture was then allowed to warm to 23 °C and cooled back to -78 °C. A solution of 3-methoxycyclohex-2-en-1-one (**213**, 200 mg, 1.59 mmol, 1.0 equiv)⁵⁷ in THF (1 mL) was then added dropwise and the resulting light-yellow solution was stirred at -78 °C for 5 min. Subsequently, a solution of methyl thiosylate⁵⁸ (384 mg, 1.90 mmol, 1.2 equiv) in THF (1 mL) was added slowly. After stirring for an additional 5 min at -78 °C, the reaction mixture was warmed to 0 °C in an ice bath, resulting in a pink, milky suspension. Saturated aq. NH₄Cl (5 mL) was then added, and the resulting biphasic suspension was extracted with EtOAc. The combined organic phases were dried over Na₂SO₄ and concentrated under reduced pressure. The crude product was purified by silica gel flash chromatography (33% EtOAc/hexanes) to afford the title compound as a yellow solid (210 mg, 1.22 mmol, 77% yield); ¹H NMR (400 MHz, CDCl₃) δ 5.29 (d, *J* = 0.97 Hz, 1H), 3.69 (s, 3H), 3.25 (t, *J* = 4.3 Hz, 1H), 2.75 – 2.61 (m, 1H), 2.40 – 2.24 (m, 2H), 2.16 (s, 3H), 2.16 – 2.06 (m, 1H);

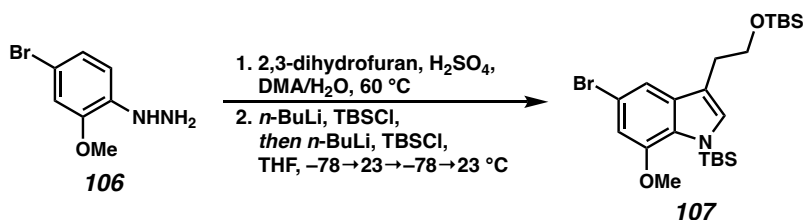
^{13}C NMR (100 MHz, CDCl_3) δ 195.5, 177.2, 100.0, 55.8, 48.4, 27.1, 26.0, 14.6; IR (Neat Film, NaCl) 2920, 2851, 1651, 1607, 1446, 1381, 1317, 1228, 1185, 1075, 1002, 837, 786 cm^{-1} ; HRMS (ESI+): m/z calc'd for $\text{C}_8\text{H}_{13}\text{O}_2\text{S}$ $[\text{M}+\text{H}]^+$: 173.0631, found 173.0629.



6-methoxy-3-(methylthio)-2,3-dihydro-[1,1'-biphenyl]-4(1H)-one (97)

To a 20 mL glass vial in a nitrogen-filled glovebox were added $\text{Pd}(t\text{-Bu}_3)_2$ (15 mg, 0.029 mmol, 10 mol %) and 1,4-dioxane (1.5 mL). The mixture was stirred at 28 °C to dissolve the palladium complex. PhI (32.5 μL , 0.290 mmol, 1.0 equiv) was then added rapidly. Separately, a solution of sulfide **96** (50 mg, 0.290 mmol, 1.0 equiv) in 1,4-dioxane (1 mL) was prepared in a 1-dram glass vial. Solid LDA (31 mg, 0.290 mmol, 1.0 equiv) was then added and the mixture was shaken to effect dissolution. The resulting enolate solution was then added to the 20 mL vial containing the Pd/PhI mixture, and additional dioxane (0.4 mL) was used to quantitatively transfer the enolate. The vial was sealed with a PTFE-lined cap, removed from the glovebox, and stirred at 80 °C in a metal heating block for 20 h. The reaction mixture was allowed to cool to 23 °C, saturated aq. NaHCO_3 (5 mL) was added, and the biphasic mixture was extracted with Et_2O (4x3 mL). The combined organic phases were dried over Na_2SO_4 and concentrated under reduced pressure. The crude product was purified by silica gel flash chromatography (33% EtOAc /hexanes) to afford the title compound as a yellow solid (12.1 mg, 0.0487 mmol, 17% yield); ^1H NMR (400 MHz, CDCl_3) δ 7.37 – 7.31 (m, 2H), 7.31 – 7.27 (m, 1H), 7.20 – 7.13 (m, 2H), 5.53 (d, J = 1.1 Hz, 1H), 3.96 (dd, J = 8.5, 5.6 Hz, 1H), 3.67 (s, 3H), 3.33 (t, J = 5.1 Hz, 1H),

2.46 – 2.34 (m, 2H), 2.18 (s, 3H); ^{13}C NMR (100 MHz, CDCl_3) δ 195.5, 177.1, 140.1, 128.9, 128.2, 127.4, 101.8, 56.3, 47.6, 43.4, 37.1, 14.7; IR (Neat Film, NaCl) 3027, 2918, 1651, 1602, 1454, 1358, 1220, 1076, 1011, 838, 750, 704 cm^{-1} ; HRMS (ESI⁺): m/z calc'd for $\text{C}_{14}\text{H}_{17}\text{O}_2\text{S}$ $[\text{M}+\text{H}]^+$: 249.0944, found 249.0942.

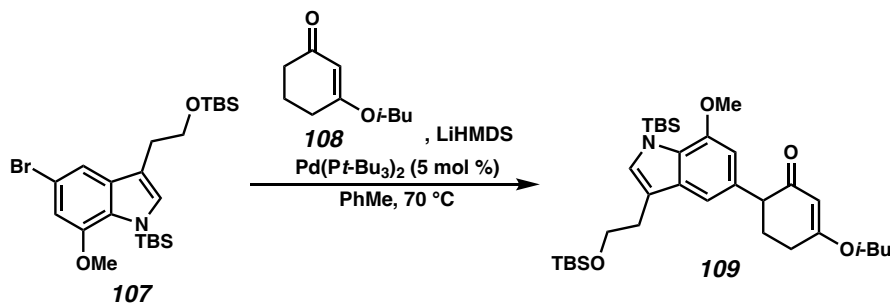


Silyl indole 107

To a 20 mL glass vial was added (4-bromo-2-methoxyphenyl)hydrazine¹¹ (**106**, 832 mg, 3.83 mmol, 1.0 equiv), DMA (5 mL), deionized water (3.6 mL), and 25% (v/v) aq. H₂SO₄ (1.85 mL, 8.62 mmol, 2.25 equiv). 2,3-dihydrofuran (290 μL , 3.83 mmol, 1.0 equiv) was then added and the vial was sealed and heated to 60 °C in a metal heating block. After 4 h of stirring at 60 °C, the reaction mixture was transferred to a separatory funnel containing 1:1 saturated aq. NaHCO₃/brine. The resulting suspension was extracted with EtOAc (4x5 mL). The combined organic extracts were washed with water, dried over Na₂SO₄, and concentrated under reduced pressure. The crude product was purified by silica gel flash chromatography (50% EtOAc/hexanes) to afford an intermediate tryptophol as a viscous brown oil (351 mg, 1.30 mmol, 34% yield); ^1H NMR (400 MHz, CDCl_3) δ 8.27 (br s, 1H), 7.36 (dd, J = 1.5, 0.6 Hz, 1H), 7.05 (d, J = 2.2 Hz, 1H), 6.75 (d, J = 1.5 Hz, 1H), 3.94 (s, 3H), 3.88 (t, J = 6.3 Hz, 2H), 2.96 (td, J = 6.3, 0.8 Hz, 2H).

The intermediate tryptophol (320 mg, 1.18 mmol, 1.0 equiv) was transferred to a 20 mL glass vial. Traces of water were azeotropically removed by addition of three portions of benzene followed by rotary evaporation, the headspace of the vial was evacuated and

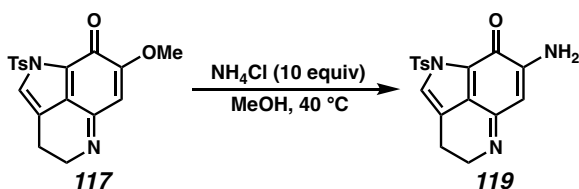
flushed with nitrogen, and THF (10 mL) was added. The solution was cooled to $-78\text{ }^{\circ}\text{C}$. *n*-BuLi (2.5 M in hexanes, 0.47 mL, 1.18 mmol, 1.0 equiv) was added slowly and the reaction mixture was subsequently allowed to warm to $23\text{ }^{\circ}\text{C}$. Then, TBSCl (187 mg, 1.24 mmol, 1.05 equiv) in THF (1 mL) was added and the reaction mixture was allowed to stir at $23\text{ }^{\circ}\text{C}$ for 15 min. After cooling back to $-78\text{ }^{\circ}\text{C}$, additional *n*-BuLi (2.5 M in hexanes, 0.47 mL, 1.18 mmol, 1.0 equiv) was added slowly and the reaction mixture was subsequently allowed to warm back to $23\text{ }^{\circ}\text{C}$. Additional TBSCl (187 mg, 1.24 mmol, 1.05 equiv) in THF (1 mL) was then added. After an additional 1 h of stirring, the reaction mixture was concentrated under reduced pressure and purified by silica gel flash chromatography (5% EtOAc/hexanes) to afford the title compound as a colorless oil (183 mg, 0.367 mmol, 31% yield); ^1H NMR (400 MHz, CDCl_3) δ 7.31 (d, $J = 1.7\text{ Hz}$, 1H), 7.04 (s, 1H), 6.69 (d, $J = 1.7\text{ Hz}$, 1H), 3.87 (s, 3H), 3.83 (t, $J = 7.0\text{ Hz}$, 2H), 2.87 (td, $J = 7.0, 0.9\text{ Hz}$, 2H), 0.89 (s, 9H), 0.85 (s, 9H), 0.51 (s, 6H), 0.01 (s, 6H); ^{13}C NMR (100 MHz, CDCl_3) δ 147.6, 134.6, 131.1, 129.9, 115.0, 114.4, 112.8, 105.6, 63.7, 54.5, 29.0, 26.9, 26.1, 19.7, 18.5, -1.5 , -5.2 ; IR (Neat Film, NaCl) 2927, 2856, 1572, 1462, 1367, 1300, 1254, 1104, 992, 911, 824, 683 cm^{-1} ; HRMS (ESI+): m/z calc'd for $\text{C}_{23}\text{H}_{41}\text{BrNO}_2\text{Si}_2$ $[\text{M}+\text{H}]^+$: 498.1854, found 498.1844.



Vinylogous ester **109**

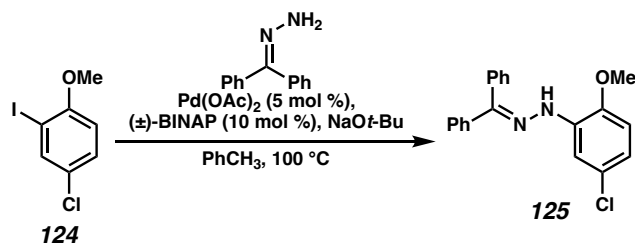
To a 20 mL glass vial were added silyl indole **107** (173 mg, 0.347 mmol, 1.0 equiv) and 3-isobutoxycyclohex-2-en-1-one¹³ (**108**, 58 mg, 0.347 mmol, 1.0 equiv). Traces of water were azeotropically removed by addition of three portions of benzene followed by rotary evaporation and the vial was transferred to a nitrogen-filled glovebox. Pd(*t*-Bu₃)₂ (8.9 mg, 0.0174 mmol, 5 mol %) was added followed by PhCH₃ (3.5 mL). A solution of LiHMDS (116 mg, 0.694 mmol, 2.0 equiv) in PhCH₃ (1 mL) was added dropwise with manual swirling. Additional PhCH₃ (0.2 mL) was used to quantitatively transfer the remaining base. The vial was sealed with a PTFE-lined cap, removed from the glovebox, and heated to 70 °C in a metal heating block for 75 min. The reaction mixture was subsequently cooled to 23 °C and saturated aq. NH₄Cl (5 mL) was added. The layers were separated, and the aqueous layer was extracted with EtOAc (3x2 mL). The combined organic phases were washed with water, dried over Na₂SO₄, and concentrated under reduced pressure. The crude product was purified by silica gel flash chromatography (20% EtOAc/hexanes) to afford the title compound as a colorless film (87.5 mg, 0.149 mmol, 43% yield); ¹H NMR (400 MHz, CDCl₃) δ 7.02 (s, 1H), 6.98 (s, 1H), 6.44 (s, 1H), 5.54 (s, 1H), 3.86 (s, 3H), 3.86 – 3.82 (m, 2H), 3.66 (d, *J* = 6.5 Hz, 2H), 3.64 – 3.58 (m, 1H), 2.91 (t, *J* = 7.3 Hz, 2H), 2.55 (t, *J* = 6.1 Hz, 2H), 2.33 (q, *J* = 6.6 Hz, 2H), 2.11 – 2.02 (m, 1H), 1.00 (d, *J* = 6.7 Hz, 6H), 0.91 (s, 9H), 0.90 (s, 9H), 0.51 (s, 6H), 0.05 (s, 6H); ¹³C NMR

(100 MHz, CDCl₃) δ 200.2, 177.6, 147.1, 133.3, 131.8, 130.2, 130.1, 114.8, 110.7, 103.4, 102.7, 74.9, 63.8, 54.0, 52.4, 29.9, 29.2, 28.3, 27.8, 26.9, 26.1, 19.6, 19.2, 18.4, -1.5, -5.1; IR (Neat Film, NaCl) 2927, 2856, 1654, 1609, 1469, 1382, 1313, 1252, 1177, 1098, 994, 910, 838, 682 cm⁻¹; HRMS (ESI⁺): *m/z* calc'd for C₃₃H₅₆NO₄Si₂ [M+H]⁺: 586.3742, found 586.3752.



Pyrroloiminoquinone **119**

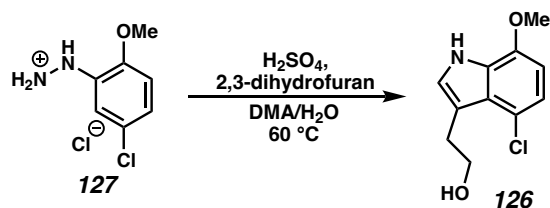
Conditions for the preparation of **119** were adapted from a procedure for the synthesis of a related compound by Tokuyama.⁵⁹ To a 1-dram glass vial containing pyrroloiminoquinone **117**^{2c} (24.8 mg, 0.0696 mmol, 1.0 equiv) and NH₄Cl (37 mg, 0.696 mmol, 10 equiv) was added degassed MeOH (2.3 mL). The vial was sealed with a PTFE-lined cap and stirred at 23 °C for 21 h. The reaction mixture was concentrated under reduced pressure and purified by silica gel flash chromatography (10% MeOH/CH₂Cl₂) to afford the title compound as a dark purple solid (11.6 mg, 0.0340 mmol, 49% yield). All characterization data matched those reported by White and coworkers.¹⁶



Arylhydrazone **125**

Conditions for the synthesis of **125** were adapted from those reported for a related compound by Eilbracht.¹⁷ To a 20 mL glass vial in a nitrogen-filled glovebox were added $\text{Pd}(\text{OAc})_2$ (17 mg, 0.075 mmol, 5 mol %), *rac*-BINAP (93 mg, 0.15 mmol, 10 mol %), and PhCH_3 (3.5 mL). The vial was sealed with a PTFE-lined cap and heated to $100\text{ }^\circ\text{C}$ in a metal block for 5 min, followed by cooling to $28\text{ }^\circ\text{C}$. To a separate 20 mL glass vial in the glovebox were added aryl iodide **124** (403 mg, 1.50 mmol, 1.0 equiv), $\text{NaO}t\text{-Bu}$ (202 mg, 2.10 mmol, 1.4 equiv), and PhCH_3 (0.8 mL). The Pd/BINAP solution was then added to the aryl iodide/base mixture, the vial was sealed and removed from the glovebox, and the reaction mixture was stirred at $100\text{ }^\circ\text{C}$ in a metal heating block for 14 h. The vial was then allowed to cool to $23\text{ }^\circ\text{C}$. The resulting dark orange suspension was diluted with Et_2O (3 mL), filtered through a short SiO_2 plug with EtOAc , and concentrated under reduced pressure. The crude product was purified by silica gel flash chromatography (10% Et_2O /hexanes, dry-loaded with Celite) to afford the title compound as a light-yellow solid (273 mg, 0.811 mmol, 54% yield); ^1H NMR (400 MHz, CDCl_3) δ 7.95 (s, 1H), 7.66 – 7.48 (m, 6H), 7.38 – 7.28 (m, 5H), 6.73 (dd, $J = 8.5, 2.6$ Hz, 1H), 6.64 (d, $J = 8.5$ Hz, 1H), 3.66 (s, 3H); ^{13}C NMR (100 MHz, CDCl_3) δ 146.1, 144.0, 138.2, 135.1, 132.8, 129.6, 129.3, 128.9, 128.3, 128.2, 126.9, 126.7, 118.3, 112.3, 110.8, 55.8; IR (Neat Film, NaCl) 3345,

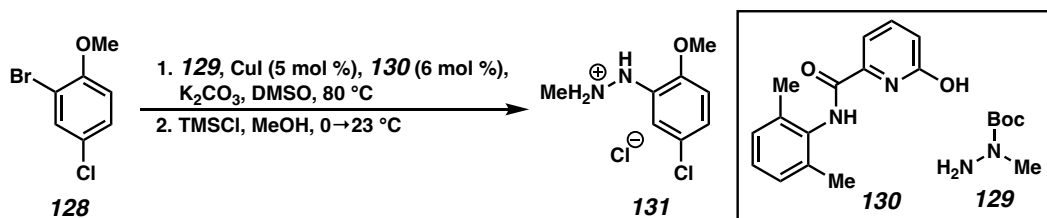
3057, 2937, 2835, 2352, 1598, 1514, 1422, 1322, 1254, 1217, 1133, 1026, 857, 767, 695 cm^{-1} ; HRMS (ESI+): m/z calc'd for $\text{C}_{20}\text{H}_{18}\text{ClN}_2\text{O}$ $[\text{M}+\text{H}]^+$: 337.1102, found 337.1099.



Tryptophol 126

To a 250 mL round bottom flask were added (5-chloro-2-methoxyphenyl)hydrazine hydrochloride¹⁹ (**127**, 8.60 g, 41.1 mmol, 1.0 equiv), DMA (65 mL), H₂O (65 mL), and 25% (v/v) aq. H₂SO₄ (11.0 mL, 51.4 mmol, 1.25 equiv). 2,3-dihydrofuran (3.42 mL, 45.2 mmol, 1.1 equiv) was added slowly with stirring, resulting in a slow color change to yellow, whereafter the flask was equipped with an air-cooled reflux condenser and heated to 60 °C in an oil bath for 6 h. The reaction mixture was then allowed to cool to 23 °C and transferred to a separatory funnel containing 1:1 saturated aq. NaHCO₃/brine (250 mL). The mixture was then extracted with EtOAc (4x100 mL), and the combined organic extracts were washed with water, dried over Na₂SO₄, and concentrated under reduced pressure. The crude product was purified by silica gel flash chromatography (60% EtOAc/hexanes) to afford the title compound as a thick, red-brown syrup that slowly crystallized upon storage at -20 °C (2.66 g, 11.79 mmol, 29% yield); ¹H NMR (400 MHz, CDCl₃) δ 8.54 (br s, 1H), 7.00 (d, *J* = 2.2 Hz, 1H), 6.96 (d, *J* = 8.2 Hz, 1H), 6.50 (d, *J* = 8.2 Hz, 1H), 3.94 (t, *J* = 6.4 Hz, 2H), 3.91 (s, 3H), 3.23 (td, *J* = 6.4, 0.8 Hz, 2H); ¹³C NMR (100 MHz, CDCl₃) δ 145.2, 128.4, 124.8, 123.8, 120.2, 118.2, 113.1, 102.4, 63.7, 55.7, 29.5; IR (Neat Film, NaCl) 3416, 2935, 2580, 1786, 1703, 1626, 1571, 1494, 1452, 1339, 1230, 1115, 1052, 937, 789,

736, 694, 628 cm^{-1} ; HRMS (FD⁺): m/z calc'd for $\text{C}_{11}\text{H}_{13}\text{ClNO}_2$ $[\text{M}+\text{H}]^+$: 225.0557, found 225.0552.

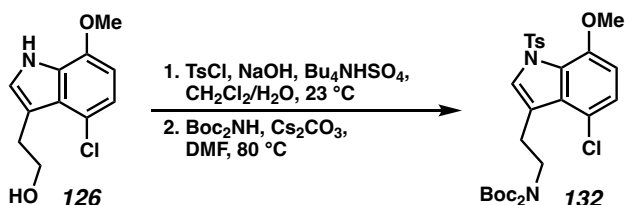


N-methylarylhydrazine hydrochloride **131**

Conditions for the synthesis of **131** were adapted from those reported for related compounds by Schmidt.²⁰ To a 20 mL glass vial in a nitrogen-filled glovebox were added CuI (34 mg, 0.179 mmol, 5 mol %), hydroxypicolinamide ligand **130**²¹ (53 mg, 0.22 mmol, 6 mol %), K_2CO_3 (762 mg, 5.51 mmol, 1.5 equiv), aryl bromide **128** (0.50 mL, 3.67 mmol, 1.0 equiv), and carbamate **129** (0.68 mL, 4.59 mmol, 1.25 equiv), followed by DMSO (3.7 mL). The vial was sealed with a PTFE cap and removed from the glovebox. The reaction mixture was stirred at 80 °C for 17 h, whereafter the resulting gray suspension was filtered through a Celite plug with EtOAc and transferred to a separatory funnel containing pH 7 phosphate buffer (20 mL). The layers were shaken and separated, the aqueous phase was extracted with EtOAc (10 mL), and the combined organic phases were washed with water, then brine, and finally dried over Na_2SO_4 . The crude product was purified by silica gel flash chromatography (15% EtOAc/hexanes) to afford an intermediate aryl carbamate as an off-white solid (902 mg, 3.15 mmol, 86% yield); ^1H NMR (500 MHz, CDCl_3) δ 6.77 (dd, $J = 8.5, 2.4$ Hz, 1H), 6.70 (d, $J = 8.5$ Hz, 1H), 6.65 (d, $J = 2.5$ Hz, 1H), 6.44 (br s, 1H), 3.83 (s, 3H), 3.23 (s, 3H), 1.45 (s, 9H).

This intermediate carbamate (900 mg, 3.15 mmol, 1.0 equiv) was added to a 20 mL glass vial, followed by MeOH (1.8 mL). Upon complete dissolution of the intermediate

compound, the solution was cooled to 0 °C and the headspace of the vial was purged with nitrogen. TMSCl (0.64 mL, 5.05 mmol, 1.60 equiv) was added dropwise over 6 min, whereafter the reaction mixture was allowed to warm to 23 °C. After stirring for 19 h, PhCH₃ (3.6 mL) was added, and the solvent was removed under reduced pressure. The resulting solid was suspended in additional PhCH₃ (5 mL) and placed in a –20 °C freezer for 2 h. The solid was collected by vacuum filtration, washed with PhCH₃, and dried under high vacuum to afford the title compound as a beige solid (612 mg, 2.74 mmol, 87% yield); ¹H NMR (400 MHz, DMSO-d₆) δ 11.31 (br s, 2H), 8.07 (br s, 1H), 7.39 (q, *J* = 1.1 Hz, 1H), 7.02 (d, *J* = 1.3 Hz, 2H), 3.82 (s, 3H), 2.78 (s, 3H); ¹³C NMR (100 MHz, DMSO-d₆) δ 147.1, 133.5, 124.3, 122.1, 115.5, 112.6, 56.0, 34.0; IR (Neat Film, NaCl) 3180, 3028, 2928, 2653, 2469, 2350, 2244, 2093, 1919, 1822, 1695, 1587, 1494, 1414, 1336, 1220, 1126, 1022, 952, 874, 792, 748, 670 cm⁻¹; HRMS (ESI+): *m/z* calc'd for C₈H₁₂ClN₂O [M+H]⁺: 187.0633, found 187.0627.



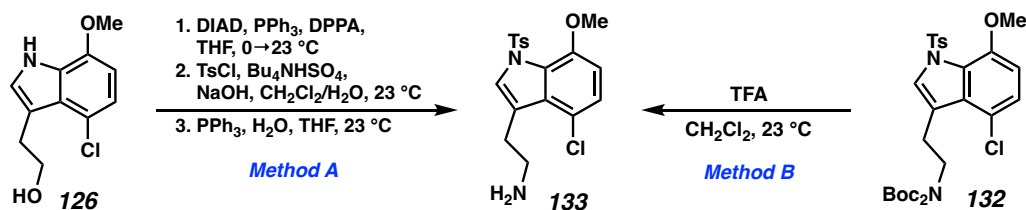
Protected tryptamine 132

To a 50 mL round bottom flask under air were added tryptophol **126** (500 mg, 2.22 mmol, 1.0 equiv), Bu₄NHSO₄ (75 mg, 0.222 mmol, 10 mol %), and CH₂Cl₂ (9 mL), followed by 50% w/v aq. NaOH (2 mL). After stirring for 5 min, TsCl (1.69 g, 8.88 mmol, 4.0 equiv) was added in a single portion. The reaction mixture was subjected to vigorous magnetic stirring for 20 min, then diluted with H₂O (15 mL) and CH₂Cl₂ (10 mL). The layers were separated, and the aqueous phase was extracted with CH₂Cl₂ (3x10 mL). The

combined organic phases were washed with brine, dried over Na₂SO₄, and concentrated under reduced pressure. The crude product was purified by silica gel flash chromatography (33% EtOAc/hexanes) to afford an intermediate tosylate as an orange solid (0.80 g, 1.50 mmol, 67% yield); ¹H NMR (500 MHz, CDCl₃) δ 7.73 – 7.64 (m, 4H), 7.62 (s, 1H), 7.28 (d, *J* = 8.0 Hz, 2H), 7.17 (d, *J* = 8.0 Hz, 2H), 6.98 (d, *J* = 8.5 Hz, 1H), 6.54 (d, *J* = 8.5 Hz, 1H), 4.36 (t, *J* = 6.6 Hz, 2H), 3.65 (s, 3H), 3.28 (t, *J* = 6.6 Hz, 2H), 2.41 (s, 3H), 2.35 (s, 3H).

This intermediate (0.80 g, 1.50 mmol, 1.0 equiv) was transferred to a 20 mL glass vial. Traces of water were azeotropically removed by addition of three portions of benzene followed by rotary evaporation. Boc₂NH (391 mg, 1.8 mmol, 1.2 equiv) and Cs₂CO₃ (586 mg, 1.8 mmol, 1.2 equiv) were added, and the headspace of the vial was evacuated and backfilled with nitrogen. DMF (7.5 mL) was added, and the reaction mixture was stirred at 23 °C for 11 h, after which TLC analysis indicated no conversion. The vial was sealed with a PTFE cap and stirred vigorously at 80 °C in a metal heating block for 2 h, after which TLC analysis indicated complete consumption of the starting material. The reaction mixture was cooled to 23 °C, diluted with H₂O (50 mL), and extracted with EtOAc (4x15 mL). The combined organic extracts were washed twice with water, dried over Na₂SO₄, and concentrated under reduced pressure. The crude product was purified by silica gel flash chromatography (25% EtOAc/hexanes) to afford the title compound as a peach solid (751 mg, 1.30 mmol, 87% yield); ¹H NMR (400 MHz, CDCl₃) δ 7.73 – 7.66 (m, 2H), 7.62 (s, 1H), 7.26 (dd, *J* = 7.4, 1.4 Hz, 2H), 7.05 (d, *J* = 8.5 Hz, 1H), 6.56 (d, *J* = 8.5 Hz, 1H), 4.00 (t, *J* = 6.8 Hz, 2H), 3.62 (s, 3H), 3.28 – 3.18 (m, 2H), 2.39 (s, 3H), 1.38 (s, 18H); ¹³C NMR (100 MHz, CDCl₃) δ 152.5, 146.5, 144.3, 137.4, 129.9, 129.5, 128.1, 127.3, 126.3, 124.5,

118.7, 117.1, 107.6, 82.3, 55.9, 46.7, 28.0, 25.7, 21.7; IR (Neat Film, NaCl) 3120, 2978, 1740, 1698, 1574, 1488, 1368, 1250, 1173, 1000, 854, 813, 661 cm^{-1} ; HRMS (ESI+): m/z calc'd for $\text{C}_{28}\text{H}_{35}\text{ClN}_2\text{NaO}_7\text{S}$ $[\text{M}+\text{Na}]^+$: 601.1746, found 601.1758.



Tryptamine 133

Method A:

To a 250 mL round bottom flask was added tryptophol **126** (3.36 g, 14.89 mmol, 1.0 equiv). Traces of water were azeotropically removed by addition of three portions of benzene followed by rotary evaporation. PPh_3 (4.69 g, 17.87 mmol, 1.2 equiv) was added, and the headspace of the flask was evacuated and backfilled with nitrogen. THF (60 mL) was added, and the reaction mixture was cooled to 0°C . Then, DIAD (3.52 mL, 17.87 mmol, 1.2 equiv) was added dropwise over 4 min. The reaction mixture was stirred at 0°C for an additional 15 min, after which DPPA (3.85 mL, 17.87 mmol, 1.2 equiv) was added rapidly and the reaction mixture was allowed to warm to 23°C . The reaction mixture became cloudy over several minutes. TLC analysis after 16 h indicated a high degree of conversion to product. Stirring for another 24 h led to no change in the reaction profile by TLC analysis. The reaction mixture was concentrated under reduced pressure and purified by automated silica gel flash chromatography (Teledyne ISCO, $0 \rightarrow 40\%$ EtOAc/hexanes) to afford an intermediate azide as an orange-brown solid (2.50 g, 9.97 mmol, 67% yield); ^1H NMR (500 MHz, CDCl_3) δ 8.32 (br s, 1H), 7.06 (d, $J = 2.4$ Hz, 1H), 6.97 (d, $J = 8.2$

Hz, 1H), 6.53 (d, $J = 8.2$ Hz, 1H), 3.94 (s, 3H), 3.59 (t, $J = 7.1$ Hz, 2H), 3.27 (td, $J = 7.1$, 0.8 Hz, 2H).

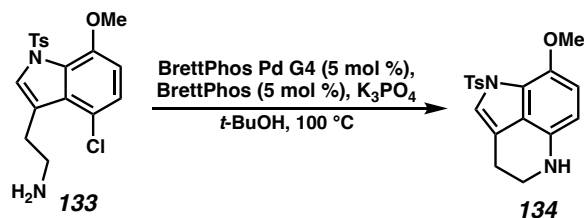
To a 250 mL round bottom flask under air were added this intermediate azide (5.11 g, 20.4 mmol, 1.0 equiv), CH₂Cl₂ (41 mL), and Bu₄NHSO₄ (69 mg, 0.204 mmol, 1 mol %), followed by 50% w/v aq. NaOH (14 mL). After stirring for 5 min, TsCl (7.78 g, 40.8 mmol, 2.0 equiv) was added in a single portion. The reaction mixture was subjected to vigorous magnetic stirring for 10 min, then diluted with H₂O (100 mL) and CH₂Cl₂ (30 mL). The layers were separated, and the aqueous phase was extracted with CH₂Cl₂ (3x50 mL). The combined organic phases were washed with brine, dried over Na₂SO₄, and concentrated under reduced pressure. The crude product was purified by automated silica gel flash chromatography (Teledyne ISCO, 0→45% EtOAc/hexanes) to afford an intermediate tosyl indole as a white solid (6.77 g, 16.7 mmol, 82% yield); ¹H NMR (400 MHz, CDCl₃) δ 7.74 (t, $J = 1.0$ Hz, 1H), 7.73 – 7.67 (m, 2H), 7.30 – 7.26 (m, 2H), 7.08 (d, $J = 8.5$ Hz, 1H), 6.58 (d, $J = 8.5$ Hz, 1H), 3.64 (s, 3H), 3.65 – 3.59 (m, 2H), 3.26 (td, $J = 7.1$, 0.9 Hz, 2H), 2.40 (s, 3H).

To a 500 mL round bottom flask under air were added this intermediate tosyl indole (11.73 g, 28.97 mmol, 1.0 equiv), PPh₃ (9.88 g, 37.66 mmol, 1.3 equiv), and THF (190 mL). The reaction mixture was stirred at 23 °C for 15 h, whereafter deionized water (9.5 mL) was added. After an additional 30 h, the reaction mixture was concentrated under reduced pressure and purified by silica gel flash chromatography (10% MeOH/CH₂Cl₂ + 1% Et₃N) to afford the title compound as a white solid (10.41 g, 27.48 mmol, 95% yield); ¹H NMR (400 MHz, CDCl₃) δ 7.72 – 7.65 (m, 3H), 7.29 – 7.23 (m, 2H), 7.05 (d, $J = 8.5$ Hz, 1H), 6.56 (d, $J = 8.5$ Hz, 1H), 3.62 (s, 3H), 3.14 – 3.00 (m, 4H), 2.39 (s, 3H); ¹³C NMR

(100 MHz, CDCl₃) δ 146.5, 144.4, 137.4, 129.7, 129.5, 127.4, 127.2, 126.5, 124.6, 118.5, 118.1, 107.5, 55.8, 42.9, 30.7, 21.7; IR (Neat Film, NaCl) 2938, 2686, 2595, 2515, 2363, 1574, 1487, 1366, 1290, 1237, 1171, 1092, 1052, 997, 937, 809, 662 cm⁻¹; HRMS (ESI⁺): *m/z* calc'd for C₁₈H₂₀ClN₂O₃S [M+H]⁺: 379.0878, found 379.0877.

Method B:

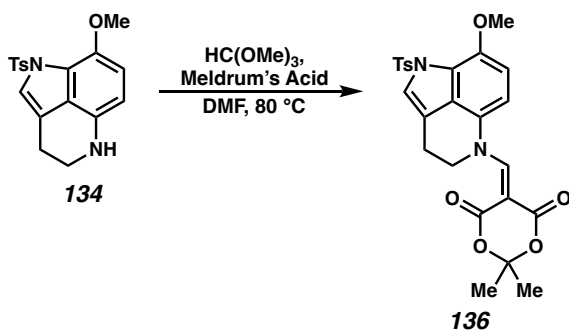
To a 50 mL round bottom flask under air were added imide **132** (750 mg, 1.30 mmol, 1.0 equiv), CH₂Cl₂ (13 mL), and TFA (1.5 mL, 19.4 mmol, 15 equiv). The reaction mixture was stirred at 23 °C for 11 h, then transferred to a separatory funnel containing aq. K₂CO₃ (20 mL). The funnel was shaken, the layers were separated, and the aqueous phase was extracted with CH₂Cl₂ (3x10 mL). The combined organic phases were dried over Na₂SO₄ and concentrated under reduced pressure. The crude product was purified by silica gel flash chromatography (10% MeOH/CH₂Cl₂ + 1% Et₃N) to afford the title compound as a white solid (341 mg, 0.90 mmol, 69% yield). For characterization data, see above.



Tricycle 134

A 20 mL glass vial containing tryptamine **133** (1.0 g, 2.64 mmol, 1.0 equiv) was brought into a nitrogen-filled glovebox. To this vial were added BrettPhos Pd G4 (121 mg, 0.132 mmol, 5 mol %), BrettPhos (71 mg, 0.132 mmol, 5 mol %), and K₃PO₄ (784 mg, 3.70 mmol, 1.4 equiv), followed by *t*-BuOH (6.6 mL). The vial was sealed with a PTFE-lined cap, removed from the glovebox, and stirred at 100 °C in a metal heating block. After 3 days, the reaction mixture was partitioned between CH₂Cl₂ and water and the layers were

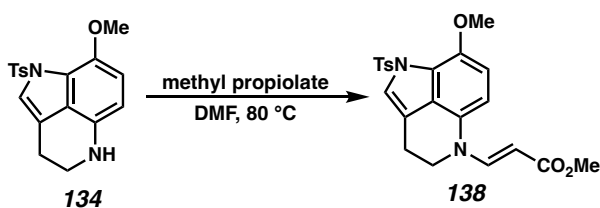
separated. The aqueous phase was extracted with CH_2Cl_2 (3x), and the combined organic phases were concentrated under reduced pressure. The crude product was purified by silica gel flash chromatography (40% EtOAc/hexanes) to afford the title compound as a beige foam (816 mg, 2.38 mmol, 90% yield); ^1H NMR (400 MHz, CDCl_3) δ 7.83 – 7.76 (m, 2H), 7.33 (d, $J = 1.4$ Hz, 1H), 7.25 – 7.20 (m, 2H), 6.56 (d, $J = 8.1$ Hz, 1H), 6.27 (d, $J = 8.1$ Hz, 1H), 3.70 (s, 3H), 3.37 (t, $J = 5.9$ Hz, 2H), 2.91 (ddd, $J = 6.9, 5.5, 1.4$ Hz, 2H), 2.36 (s, 3H); ^{13}C NMR (100 MHz, CDCl_3) δ 144.1, 140.5, 137.1, 135.8, 129.4, 127.7, 124.0, 122.6, 120.2, 115.2, 110.7, 105.0, 57.5, 43.0, 22.8, 21.7; IR (Neat Film, NaCl) 3384, 2956, 2834, 1595, 1512, 1421, 1356, 1260, 1170, 1103, 1035, 977, 937, 795, 664 cm^{-1} ; HRMS (ESI+): m/z calc'd for $\text{C}_{18}\text{H}_{19}\text{N}_2\text{O}_3\text{S}$ $[\text{M}+\text{H}]^+$: 343.1111, found 343.1127.



Diester 136

To a $\frac{1}{2}$ dram vial were added tricyclic **134** (10 mg, 0.0292 mmol, 1 equiv) and Meldrum's acid (5.0 mg, 0.035 mmol, 1.2 equiv). The headspace of the vial was evacuated and backfilled with nitrogen. Then, DMF (0.06 mL) and trimethyl orthoformate (6.4 μL , 0.0584 mmol, 2 equiv) were added. The vial was sealed with a PTFE-lined cap and stirred at $80\text{ }^\circ\text{C}$ in a metal heating block. Upon heating, the reaction mixture slowly turned from beige to yellow to dark red. After 2 h, the reaction mixture was allowed to cool to $23\text{ }^\circ\text{C}$, diluted with H_2O (1 mL), and extracted with EtOAc (5x0.5 mL). The combined organic

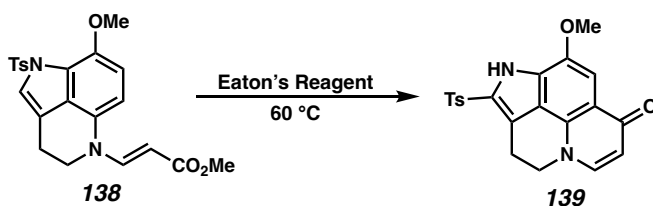
phases were washed with water (2x0.5 mL), dried over Na₂SO₄, and concentrated under reduced pressure. The crude product was purified by silica gel flash chromatography (50% EtOAc/hexanes) to afford the title compound as an intensely yellow foam (10.5 mg, 0.0211 mmol, 72% yield); ¹H NMR (400 MHz, CDCl₃) δ 8.63 (s, 1H), 7.82 – 7.76 (m, 2H), 7.57 (t, *J* = 1.3 Hz, 1H), 7.30 – 7.27 (m, 2H), 6.95 (d, *J* = 8.4 Hz, 1H), 6.67 (d, *J* = 8.4 Hz, 1H), 4.23 (t, *J* = 6.1 Hz, 2H), 3.80 (s, 3H), 3.17 – 3.06 (m, 2H), 2.40 (s, 3H), 1.78 (s, 6H); ¹³C NMR (100 MHz, CDCl₃) δ 165.9, 160.9, 154.7, 146.7, 144.9, 136.5, 129.7, 127.9, 127.8, 125.6, 123.3, 122.8, 112.7, 111.9, 107.9, 103.5, 88.4, 56.2, 52.3, 27.1, 22.6, 21.8; IR (Neat Film, NaCl) 2939, 1688, 1567, 1511, 1438, 1359, 1278, 1190, 1108, 967, 785, 660 cm⁻¹; HRMS (ESI⁺): *m/z* calc'd for C₂₅H₂₄N₂NaO₇S [M+Na]⁺: 519.1196, found 519.1192.



“Push-pull” olefin **138**

To a 1-dram glass vial were added tricyclic **134** (43.5 mg, 0.127 mmol, 1.0 equiv), DMF (0.25 mL), and methyl propiolate (113 μL, 1.27 mmol, 10 equiv). The vial was sealed with a PTFE-lined cap and stirred at 80 °C in a metal heating block for 15 h. The reaction mixture was then diluted with water (2 mL) and extracted with EtOAc (5x0.5 mL). The combined organic extracts were washed with water, dried over Na₂SO₄, and concentrated under reduced pressure. The crude product was purified by automated silica gel flash chromatography (Teledyne ISCO, 0→100% EtOAc/hexanes) to afford the title compound as a yellow foam (47.6 mg, 0.112 mmol, 88% yield); ¹H NMR (400 MHz, CDCl₃) δ 8.05 (d, *J* = 13.3 Hz, 1H), 7.82 – 7.73 (m, 2H), 7.46 (t, *J* = 1.4 Hz, 1H), 7.28 – 7.24 (m, 2H),

6.81 (d, $J = 8.4$ Hz, 1H), 6.65 (d, $J = 8.4$ Hz, 1H), 5.17 (d, $J = 13.3$ Hz, 1H), 3.75 (s, 3H), 3.72 (s, 3H), 3.72 – 3.68 (m, 2H), 3.02 (td, $J = 6.1, 1.4$ Hz, 2H), 2.39 (s, 3H); ^{13}C NMR (100 MHz, CDCl_3) δ 169.8, 145.0, 144.4, 143.3, 136.7, 129.4, 129.1, 127.7, 124.0, 123.2, 121.6, 113.0, 108.9, 107.7, 90.0, 56.5, 51.0, 44.9, 21.8, 21.6; IR (Neat Film, NaCl) 2948, 1695, 1605, 1511, 1440, 1359, 1275, 1171, 1108, 998, 801, 662 cm^{-1} ; HRMS (ESI+): m/z calc'd for $\text{C}_{22}\text{H}_{23}\text{N}_2\text{O}_5\text{S}$ $[\text{M}+\text{H}]^+$: 427.1322, found 427.1322.

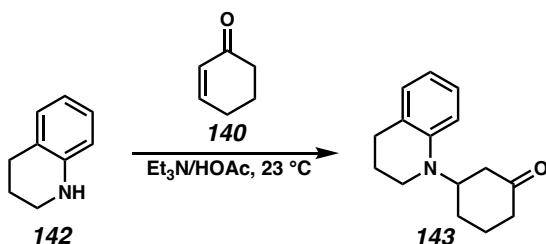


Quinolone 139

To a 1-dram glass vial were added ester **138** (25.6 mg, 0.060 mmol, 1.0 equiv) and Eaton's reagent (0.6 mL). The vial was sealed with a PTFE-lined cap and stirred at 60 °C in a metal heating block for 2 h. The reaction mixture was then quenched with saturated aqueous K_2CO_3 . The resulting solution was extracted with 1:1 EtOAc/ CH_2Cl_2 (2x3 mL) and CH_2Cl_2 (2x3 mL). The combined organic extracts were dried over Na_2SO_4 and concentrated under reduced pressure. The crude product was purified by silica gel flash chromatography (10% MeOH/ CH_2Cl_2) to afford the title compound as a light brown solid (8.1 mg, 0.0205 mmol, 34% yield); ^1H NMR (400 MHz, CD_2Cl_2) δ 10.05 (br s, 1H), 7.93 – 7.84 (m, 2H), 7.51 (d, $J = 7.5$ Hz, 1H), 7.37 – 7.31 (m, 3H), 6.29 (d, $J = 7.5$ Hz, 1H), 4.27 (t, $J = 6.6$ Hz, 2H), 3.93 (s, 3H), 3.50 (t, $J = 6.6$ Hz, 2H), 2.38 (s, 3H); ^{13}C NMR (100 MHz, CD_2Cl_2) δ 176.9, 145.4, 145.2, 139.2, 139.0, 130.9, 130.5, 128.2, 127.8, 127.5, 120.1, 118.9, 116.1, 112.3, 100.1, 56.4, 50.4, 22.5, 21.7; An IR spectrum could not be

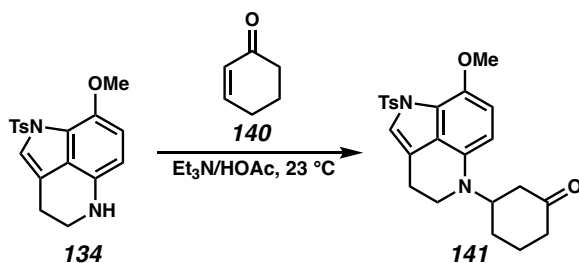
obtained due to the difficulty associated with depositing a thin film of this compound;

HRMS (ESI+): m/z calc'd for $C_{21}H_{19}N_2O_4S$ $[M+H]^+$: 395.1060, found 395.1067.



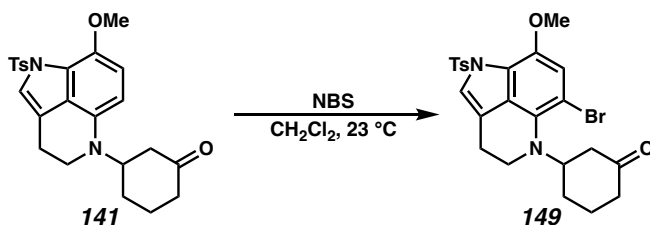
Model aza-Michael adduct 143

To a 1-dram glass vial under air were added 1:1 (v/v) $Et_3N/HOAc$ (0.65 mL), tetrahydroquinoline (**142**, 0.07 mL, 0.52 mmol, 1.0 equiv), and cyclohexenone (**140**, 0.25 mL, 2.58 mmol, 5.0 equiv). After stirring at $23\text{ }^\circ\text{C}$ for 19 h, the reaction mixture was diluted with water (7 mL), extracted with $EtOAc$ (3x3 mL), dried over Na_2SO_4 , and concentrated under reduced pressure. The crude product was purified by automated silica gel flash chromatography (Teledyne ISCO, 0→50% $EtOAc$ /hexanes) to afford the title compound as a colorless oil that crystallized upon standing to form a white solid (49.1 mg, 0.214 mmol, 41% yield); 1H NMR (400 MHz, $CDCl_3$) δ 7.09 – 7.01 (m, 1H), 7.01 – 6.93 (m, 1H), 6.68 – 6.57 (m, 2H), 4.09 – 3.95 (m, 1H), 3.29 (ddd, $J = 11.5, 7.4, 4.3$ Hz, 1H), 3.19 (ddd, $J = 11.2, 7.1, 4.3$ Hz, 1H), 2.75 (t, $J = 6.4$ Hz, 2H), 2.62 – 2.54 (m, 2H), 2.49 – 2.38 (m, 1H), 2.29 (td, $J = 13.9, 6.4$ Hz, 1H), 2.16 – 2.08 (m, 1H), 2.03 (dddd, $J = 11.8, 8.2, 4.3, 2.3$ Hz, 1H), 2.00 – 1.84 (m, 3H), 1.72 – 1.57 (m, 1H); ^{13}C NMR (100 MHz, $CDCl_3$) δ 210.0, 144.6, 129.5, 127.3, 123.6, 116.4, 110.9, 56.2, 45.1, 41.6, 41.1, 28.8, 28.4, 22.7, 22.6; IR (Neat Film, NaCl) 2939, 2861, 1709, 1601, 1496, 1456, 1303, 1271, 1219, 1192, 1058, 745 cm^{-1} ; HRMS (ESI+): m/z calc'd for $C_{15}H_{20}NO$ $[M+H]^+$: 230.1539, found 230.1546.



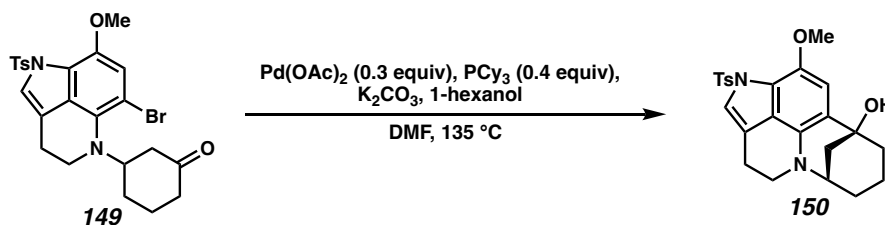
Aza-Michael adduct **141**

To a 1/2-dram glass vial under air were added tricycle **134** (40 mg, 0.117 mmol, 1.0 equiv), 1:1 (v/v) Et₃N/HOAc (0.23 mL), and cyclohexenone (**140**, 0.11 mL, 1.17 mmol, 10 equiv). After stirring at 23 °C for 30 h, the reaction mixture was quenched with saturated aq. NaHCO₃ (7 mL). The resulting suspension was extracted with EtOAc (3x2 mL), dried over Na₂SO₄, and concentrated under reduced pressure. The crude product was purified by automated silica gel flash chromatography (Teledyne ISCO, 40→100% Et₂O/hexanes) to afford the title compound as a beige foam (30 mg, 0.0684 mmol, 58% yield); ¹H NMR (400 MHz, CDCl₃) δ 7.82 – 7.73 (m, 2H), 7.33 (d, *J* = 1.4 Hz, 1H), 7.23 (d, *J* = 8.1 Hz, 2H), 6.58 (d, *J* = 8.3 Hz, 1H), 6.25 (d, *J* = 8.3 Hz, 1H), 3.92 (tt, *J* = 11.8, 4.0 Hz, 1H), 3.69 (s, 3H), 3.36 – 3.28 (m, 1H), 3.20 – 3.12 (m, 1H), 2.98 – 2.91 (m, 2H), 2.61 (ddt, *J* = 13.3, 4.3, 1.9 Hz, 1H), 2.58 – 2.50 (m, 1H), 2.44 (ddq, *J* = 14.3, 4.3, 2.0 Hz, 1H), 2.36 (s, 3H), 2.29 (td, *J* = 13.8, 6.3 Hz, 1H), 2.17 – 2.02 (m, 2H), 1.90 (qd, *J* = 12.5, 3.5 Hz, 1H), 1.66 (tdt, *J* = 12.4, 8.4, 3.6 Hz, 1H); ¹³C NMR (100 MHz, CDCl₃) δ 209.9, 144.2, 140.2, 137.1, 135.5, 129.4, 127.7, 124.1, 123.2, 119.8, 115.2, 110.2, 102.9, 57.2, 55.8, 44.7, 41.9, 41.2, 28.5, 23.3, 22.8, 21.7; IR (Neat Film, NaCl) 2936, 2835, 1709, 1596, 1509, 1357, 1281, 1171, 1106, 914, 780, 733, 661 cm⁻¹; HRMS (ESI⁺): *m/z* calc'd for C₂₄H₂₇N₂O₄S [M+H]⁺: 439.1686, found 439.1692.



Bromoarene 149

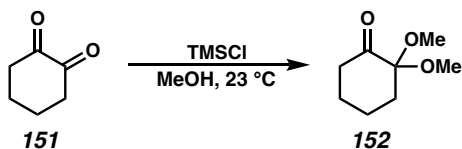
To a 1-dram glass vial under air were added tertiary aniline **141** (21.8 mg, 0.0497 mmol, 1.0 equiv) and CH₂Cl₂ (2 mL). Recrystallized NBS (9.3 mg, 0.0522 mmol, 1.05 equiv) was added rapidly with stirring, resulting in a brown color. After 15 mins, the reaction mixture was concentrated under reduced pressure and purified by silica gel flash chromatography (40% EtOAc/hexanes) to afford the title compound as a beige foam (18.8 mg, 0.0363 mmol, 73% yield); ¹H NMR (400 MHz, CDCl₃) δ 7.78 – 7.73 (m, 2H), 7.41 (t, *J* = 1.4 Hz, 1H), 7.28 – 7.23 (m, 2H), 6.77 (s, 1H), 3.88 (tdd, *J* = 12.0, 4.9, 3.6 Hz, 1H), 3.71 (s, 3H), 3.43 – 3.29 (m, 2H), 2.84 – 2.70 (m, 2H), 2.67 – 2.53 (m, 2H), 2.38 (s, 3H), 2.38 – 2.32 (m, 1H), 2.23 (td, *J* = 14.0, 6.5 Hz, 1H), 2.11 (dtd, *J* = 11.3, 3.2, 1.8 Hz, 1H), 2.04 – 1.98 (m, 1H), 1.86 (qd, *J* = 12.4, 3.6 Hz, 1H), 1.49 (qt, *J* = 13.4, 4.0 Hz, 1H); ¹³C NMR (100 MHz, CDCl₃) δ 209.9, 144.5, 142.7, 136.8, 133.3, 129.6, 127.7, 127.3, 122.3, 122.2, 114.5, 113.4, 106.2, 61.5, 56.7, 48.0, 43.0, 40.9, 30.8, 22.5, 22.2, 21.8; IR (Neat Film, NaCl) 2939, 2863, 1709, 1596, 1490, 1439, 1344, 1284, 1229, 1174, 1111, 1032, 993, 804, 735, 665, 608 cm⁻¹; HRMS (ESI⁺): *m/z* calc'd for C₂₄H₂₆BrN₂O₄S [M+H]⁺: 517.0791, found 517.0806.



Tertiary alcohol **150**

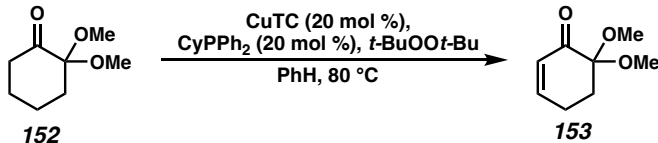
To a 1-dram glass vial was added bromoarene **149** (12 mg, 0.0232 mmol, 1.0 equiv). Traces of water were azeotropically removed by addition of three portions of benzene followed by rotary evaporation. The vial was transferred to a nitrogen-filled glovebox. K₂CO₃ (6.4 mg, 0.0464 mmol, 2 equiv), Pd(OAc)₂ (1.4 mg, 0.00624 mmol, 0.3 equiv), and PCy₃ (2.6 mg, 0.00927 mmol, 0.4 equiv) were added to the vial. Then, DMF (1.15 mL) and 1-hexanol (14 μL, 0.116 mmol, 5.0 equiv) were added, the vial was sealed with a PTFE-lined cap and removed from the glovebox, and the reaction mixture was stirred at 135 °C in a metal heating block. After 25 h, the reaction mixture was allowed to cool to 23 °C, diluted with water (10 mL), and extracted with EtOAc (4x3 mL). The combined organic extracts were washed with water (2x3 mL), dried over Na₂SO₄, and concentrated under reduced pressure. The crude product was purified by silica gel flash chromatography (50% EtOAc/hexanes) to afford tricycle **134** (2.3 mg, 0.00672 mmol, 29% yield) and the title compound as a brown film (1.7 mg, 0.00388 mmol, 17% yield); ¹H NMR (400 MHz, CDCl₃) δ 7.83 – 7.79 (m, 2H), 7.29 (t, *J* = 1.5 Hz, 1H), 7.25 – 7.21 (m, 2H), 6.74 (s, 1H), 3.71 (d, *J* = 1.9 Hz, 3H), 3.60 – 3.56 (m, 1H), 3.28 – 3.19 (m, 1H), 3.18 – 3.08 (m, 1H), 2.99 – 2.94 (m, 2H), 2.37 (s, 3H), 2.20 – 2.13 (m, 1H), 2.09 (d, *J* = 2.7 Hz, 1H), 1.95 (dd, *J* = 11.7, 2.9 Hz, 1H), 1.74 – 1.69 (m, 2H), 1.36 (tdd, *J* = 13.8, 4.9, 2.7 Hz, 1H), 1.11 (dtt, *J* = 17.5, 6.4, 3.4 Hz, 1H); ¹³C NMR (100 MHz, CDCl₃) δ 144.1, 139.5, 137.2, 133.2, 129.4, 129.4, 127.9, 122.9, 120.8, 120.2, 114.6, 105.8, 70.0, 57.5, 56.1, 47.0,

40.8, 40.8, 29.0, 23.2, 21.7, 20.4; IR (Neat Film, NaCl) 3385, 2930, 2851, 1596, 1505, 1450, 1404, 1360, 1286, 1225, 1170, 1105, 978, 814, 735, 662 cm^{-1} ; HRMS (ESI⁺): m/z calc'd for $\text{C}_{24}\text{H}_{27}\text{N}_2\text{O}_4\text{S}$ $[\text{M}+\text{H}]^+$: 439.1686, found 439.1689.



Ketal **152**

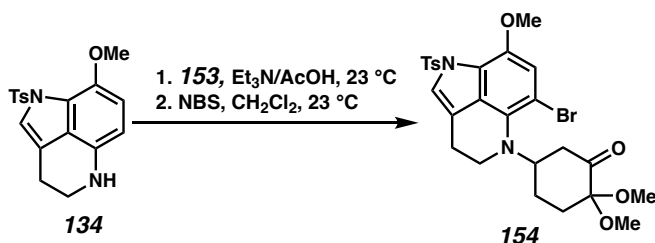
Prepared according to the procedure of Caubere starting with 1.0 g (8.92 mmol) of dione **151**.³⁴ Purification by silica gel flash chromatography (20% EtOAc/hexanes, fractions were analyzed by TLC with DNP staining) afforded ketal **152** as a colorless, fragrant oil (619 mg, 3.91 mmol, 44% yield). All characterization data matched those reported in the literature.³⁴



Enone **153**

Conditions for the synthesis of **153** were adapted from those reported for related compounds by Dong.³⁵ To a 20 mL glass vial in a nitrogen-filled glovebox were added CuTC (24 mg, 0.126 mmol, 20 mol %), CyPPh₂ (34 mg, 0.126 mmol, 20 mol %), benzene (6.3 mL), and a magnetic stir bar. The vial was sealed with a septum cap and removed from the glovebox. Ketal **152** (100 mg, 0.632 mmol, 1.0 equiv) and di-*tert*-butyl peroxide (0.17 mL, 0.948 mmol, 1.5 equiv) were added by injection. The reaction mixture was then heated to 80 °C in a metal heating block, resulting in a deep green solution. After 23 h, the reaction mixture was allowed to cool to 23 °C, concentrated under reduced pressure, and purified

by silica gel flash chromatography (33% EtOAc/hexanes) to afford the title compound as a colorless oil (38.1 mg, 0.244 mmol, 39% yield); ^1H NMR (400 MHz, C_6D_6) δ 6.2 – 6.1 (m, 1H), 5.8 (dtd, $J = 10.0, 2.0, 0.9$ Hz, 1H), 3.1 (d, $J = 1.0$ Hz, 6H), 1.9 – 1.8 (m, 2H), 1.8 – 1.7 (m, 2H); ^{13}C NMR (100 MHz, C_6D_6) δ 192.1, 148.9, 128.1, 97.0, 49.6, 31.1, 24.6; IR (Neat Film, NaCl) 2940, 2834, 1694, 1623, 1437, 1388, 1310, 1231, 1160, 1117, 1060, 916, 850, 801 cm^{-1} ; HRMS (ESI $^+$): m/z calc'd for $\text{C}_8\text{H}_{12}\text{NaO}_3$ $[\text{M}+\text{Na}]^+$: 179.0679, found 179.0678.

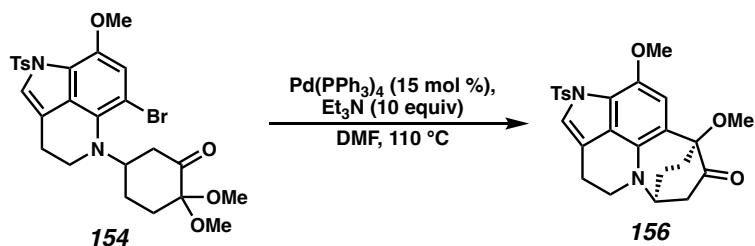


Bromoarene **154**

To a 1-dram glass vial under air were added tricyclic amine **134** (50 mg, 0.146 mmol, 1.0 equiv), enone **153** (114 mg, 0.730 mmol, 5.0 equiv), and 1:1 (v/v) $\text{Et}_3\text{N}/\text{HOAc}$ (0.15 mL). The reaction mixture was stirred at $23\text{ }^\circ\text{C}$ for 21 h, then partitioned between water and EtOAc. The layers were separated, and the aqueous phase was extracted with EtOAc (3x). The combined organic phases were washed with brine, dried over Na_2SO_4 , and concentrated under reduced pressure. The crude product was purified by silica gel flash chromatography (80% $\text{Et}_2\text{O}/\text{hexanes}$) to afford an intermediate tertiary aniline as a beige foam (59 mg, 0.118 mmol, 81% yield); ^1H NMR (400 MHz, CDCl_3) δ 7.81 – 7.76 (m, 2H), 7.33 (t, $J = 1.4$ Hz, 1H), 7.25 – 7.21 (m, 2H), 6.58 (d, $J = 8.3$ Hz, 1H), 6.27 – 6.21 (m, 1H), 3.90 (tt, $J = 11.8, 3.7$ Hz, 1H), 3.69 (s, 3H), 3.41 – 3.37 (m, 1H), 3.36 (s, 3H), 3.22 (s, 3H), 3.15 (dt, $J = 11.2, 6.3$ Hz, 1H), 2.98 – 2.87 (m, 3H), 2.61 (ddd, $J = 12.0, 3.9, 2.3$ Hz, 1H),

2.41 (dt, $J = 14.3, 3.7$ Hz, 1H), 2.37 (s, 3H), 2.17 (qd, $J = 13.1, 4.0$ Hz, 1H), 1.95 – 1.85 (m, 1H), 1.60 – 1.55 (m, 1H).

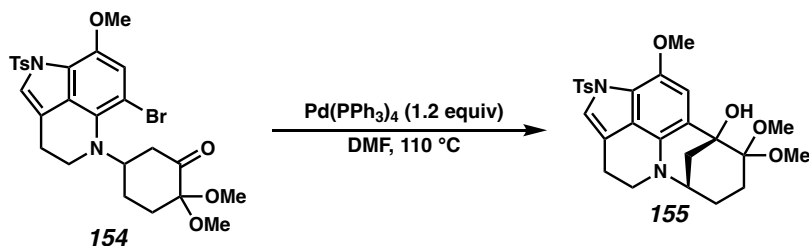
To a sample of this intermediate aniline (19.5 mg, 0.0391 mmol, 1.0 equiv) also containing secondary aniline **134** as a major impurity (7.6 mg, 0.0222 mmol) in a 1-dram glass vial was added CH_2Cl_2 (2.5 mL). Recrystallized NBS (11 mg, 0.0613 mmol, 1.0 equiv w.r.t. combined total aniline) was added rapidly with stirring, resulting in a brown color. After 10 mins, the reaction mixture was concentrated under reduced pressure and purified by silica gel flash chromatography (80% Et_2O /hexanes) to afford the title compound as an off-white foam (21.1 mg, 0.0365 mmol, 93% yield); ^1H NMR (400 MHz, C_6D_6) δ 7.84 – 7.78 (m, 2H), 7.47 (t, $J = 1.5$ Hz, 1H), 6.70 (s, 1H), 6.66 – 6.60 (m, 2H), 3.99 (tt, $J = 12.4, 4.0$ Hz, 1H), 3.28 (s, 3H), 3.18 (s, 3H), 2.97 (s, 3H), 2.96 – 2.91 (m, 1H), 2.88 (ddd, $J = 6.6, 5.3, 2.8$ Hz, 2H), 2.77 (ddd, $J = 11.7, 4.2, 2.2$ Hz, 1H), 2.23 – 2.10 (m, 2H), 1.94 (dt, $J = 14.5, 3.4$ Hz, 1H), 1.86 – 1.76 (m, 1H), 1.75 (s, 3H), 1.57 (dq, $J = 13.0, 3.4$ Hz, 1H), 1.18 (td, $J = 14.0, 4.0$ Hz, 1H); ^{13}C NMR (100 MHz, C_6D_6) δ 202.6, 144.0, 143.1, 137.9, 133.8, 129.4, 127.4, 123.0, 122.5, 114.8, 114.1, 106.2, 100.9, 62.0, 56.3, 49.9, 48.5, 45.8, 42.8, 30.6, 27.4, 22.2, 21.1; IR (Neat Film, NaCl) 2936, 2835, 1732, 1692, 1597, 1490, 1360, 1285, 1222, 1172, 1111, 1057, 992, 933, 806, 666 cm^{-1} ; HRMS (ESI+): m/z calc'd for $\text{C}_{26}\text{H}_{30}\text{BrN}_2\text{O}_6\text{S}$ $[\text{M}+\text{H}]^+$: 577.1002, found 577.1015.



Aza[3.2.2]bicyclononene 156

To a flame-dried 1-dram glass vial was added bromoarene **154** (5 mg, 0.00866 mmol, 1.0 equiv) as a stock solution in benzene. Traces of water were azeotropically removed by addition of two additional portions of benzene followed by rotary evaporation. The vial was transferred to a nitrogen-filled glovebox and $\text{Pd(PPh}_3)_4$ (1.5 mg, 0.0013 mmol, 15 mol %), DMF (0.22 mL), and Et_3N (12 μL , 0.0866 mmol, 10 equiv) were added. The vial was sealed with a PTFE-lined cap, removed from the glovebox, and stirred at 110 °C in a metal heating block for 18 h. The reaction mixture was diluted with water (2 mL) and extracted with EtOAc (4x0.5 mL). The combined organic extracts were washed with water, dried over Na_2SO_4 , and concentrated under reduced pressure. The crude product was purified by preparative TLC on basic alumina (60% EtOAc/hexanes) to afford the title compound as a beige film (2.5 mg, 0.00536 mmol, 62% yield); ^1H NMR (400 MHz, CDCl_3) δ 7.76 (d, $J = 8.1$ Hz, 2H), 7.32 (d, $J = 1.3$ Hz, 1H), 7.22 (d, $J = 8.0$ Hz, 2H), 6.84 (s, 1H), 3.68 (d, $J = 1.0$ Hz, 3H), 3.56 – 3.50 (m, 1H), 3.43 (d, $J = 1.1$ Hz, 3H), 3.32 (qdd, $J = 11.1, 6.7, 5.1$ Hz, 2H), 3.01 – 2.86 (m, 3H), 2.71 – 2.62 (m, 1H), 2.55 (td, $J = 11.6, 4.7$ Hz, 1H), 2.42 (dd, $J = 10.0, 4.9$ Hz, 1H), 2.37 (s, 3H), 2.32 (dd, $J = 5.2, 2.6$ Hz, 1H), 2.04 – 1.95 (m, 1H); ^{13}C NMR (100 MHz, CDCl_3) δ 204.3, 144.2, 140.7, 137.0, 132.0, 129.4, 127.8, 124.0, 123.6, 120.3, 116.8, 115.0, 106.6, 82.8, 56.8, 56.6, 51.9, 51.8, 44.2, 31.2, 26.3, 23.5, 21.7; IR (Neat Film, NaCl) 2926, 2851, 1727, 1494, 1366, 1285, 1171, 1108,

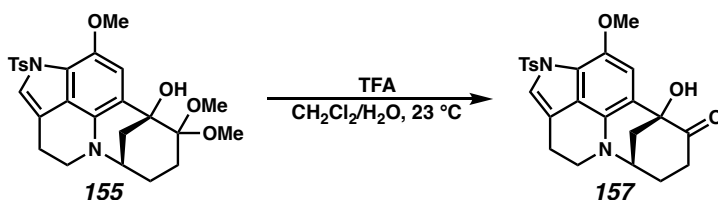
1019, 807, 670 cm^{-1} ; HRMS (ESI⁺): m/z calc'd for $\text{C}_{25}\text{H}_{27}\text{N}_2\text{O}_5\text{S}$ $[\text{M}+\text{H}]^+$: 467.1635, found 467.1636.



Bicyclic ketal **155**

To a 1-dram glass vial was added bromoarene **154** (53.7 mg, 0.0930 mmol, 1.0 equiv). Traces of water were azeotropically removed by addition of three portions of benzene followed by rotary evaporation. The vial was transferred to a nitrogen-filled glovebox, and $\text{Pd}(\text{PPh}_3)_4$ (125 mg, 0.108 mmol, 1.16 equiv) and DMF (2.4 mL) were added. The vial was sealed with a PTFE-lined cap, removed from the glovebox, and heated to $110\text{ }^\circ\text{C}$ in a metal heating block. After stirring for 17 h, the reaction mixture was allowed to cool to $23\text{ }^\circ\text{C}$, diluted with water and brine, and extracted with EtOAc (3x). The combined organic extracts were dried over Na_2SO_4 , concentrated under reduced pressure, and purified by silica gel flash chromatography (45% EtOAc/hexanes) to afford the desired product as a beige film (40 mg, 0.0802 mmol, 86% yield); ^1H NMR (400 MHz, C_6D_6) δ 7.97 – 7.91 (m, 2H), 7.47 (s, 1H), 7.19 (s, 1H), 6.62 – 6.57 (m, 2H), 3.63 (s, 3H), 3.34 (s, 3H), 3.04 (s, 3H), 2.99 (q, $J = 2.4$ Hz, 1H), 2.79 (td, $J = 9.8, 4.1$ Hz, 1H), 2.65 (ddd, $J = 15.2, 4.8, 1.8$ Hz, 1H), 2.58 – 2.46 (m, 2H), 2.11 (dd, $J = 11.8, 2.9$ Hz, 1H), 1.98 (ddd, $J = 11.9, 3.5, 2.2$ Hz, 1H), 1.73 (s, 3H), 1.59 – 1.50 (m, 2H), 1.28 – 1.11 (m, 2H); ^{13}C NMR (100 MHz, C_6D_6) δ 143.4, 139.6, 138.1, 133.7, 129.4, 124.3, 121.1, 120.3, 118.0, 114.9, 110.5, 102.7, 75.7, 58.2, 54.7, 51.3, 48.8, 46.7, 38.2, 27.4, 27.0, 23.3, 21.1 (an additional

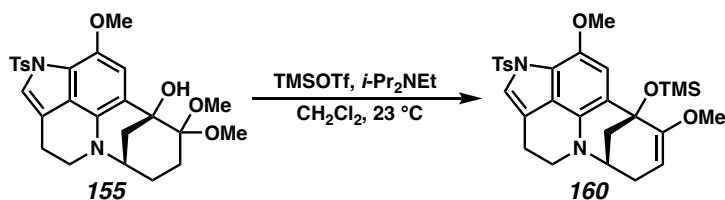
^{13}C resonance associated with the tosyl group is likely obscured by the solvent signal); IR (Neat Film, NaCl) 2934, 2832, 1504, 1451, 1406, 1360, 1283, 1227, 1169, 1103, 967, 913, 813, 663 cm^{-1} ; HRMS (ESI⁺): m/z calc'd for $\text{C}_{26}\text{H}_{31}\text{N}_2\text{O}_6\text{S}$ $[\text{M}+\text{H}]^+$: 499.1897, found 499.1890.



α -Hydroxyketone **157**

To a 1-dram glass vial under air were added ketal **155** (10 mg, 0.020 mmol, 1.0 equiv), CH_2Cl_2 (1 mL), water (0.1 mL), and TFA (6.0 μL , 0.078 mmol, 3.9 equiv). The reaction mixture was stirred at $23\text{ }^\circ\text{C}$ for 40 min, then neutralized with saturated aq. NaHCO_3 (1 mL) and stirred for an additional 10 min. The layers were separated, and the aqueous phase was extracted with CH_2Cl_2 (3x0.5 mL). The combined organic phases were dried over Na_2SO_4 and concentrated under reduced pressure to afford the title compound as a beige film (9.0 mg, 0.020 mmol, >99% yield); ^1H NMR (400 MHz, C_6D_6) δ 7.72 – 7.67 (m, 2H), 7.29 (t, $J = 1.3$ Hz, 1H), 6.66 (s, 1H), 6.44 – 6.36 (m, 2H), 4.55 (s, 1H), 3.20 (s, 3H), 2.61 (td, $J = 3.6, 1.8$ Hz, 1H), 2.55 – 2.46 (m, 1H), 2.45 – 2.33 (m, 1H), 2.32 – 2.23 (m, 2H), 2.15 (dt, $J = 12.5, 3.4$ Hz, 1H), 1.89 – 1.72 (m, 2H), 1.52 (s, 3H), 1.47 (dd, $J = 12.4, 2.8$ Hz, 2H), 0.84 (tdd, $J = 13.8, 6.0, 2.8$ Hz, 1H); ^{13}C NMR (100 MHz, C_6D_6) δ 209.9, 143.7, 140.4, 138.0, 133.2, 129.4, 124.3, 121.8, 120.9, 116.3, 114.2, 107.0, 75.9, 57.2, 54.6, 46.8, 39.6, 33.5, 32.3, 23.1, 21.1 (an additional ^{13}C resonance associated with the tosyl group is obscured by the solvent signal); IR (Neat Film, NaCl) 3466, 2925, 2853,

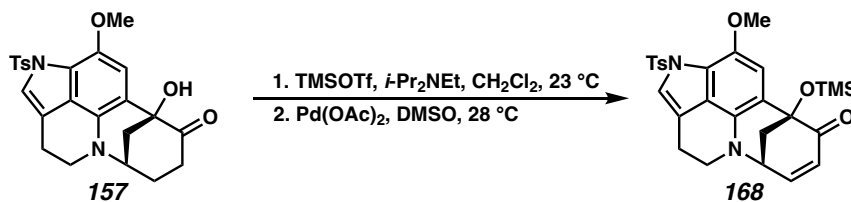
1712, 1596, 1505, 1462, 1435, 1367, 1285, 1223, 1171, 1105, 1010, 970, 892, 816, 735, 665 cm^{-1} ; HRMS (ESI+): m/z calc'd for $\text{C}_{24}\text{H}_{25}\text{N}_2\text{O}_5\text{S}$ $[\text{M}+\text{H}]^+$: 453.1479, found 453.1472.



Methyl enol ether 160

To a 1-dram glass vial was added ketal **155** (5 mg, 0.010 mmol, 1.0 equiv). Traces of water were azeotropically removed by addition of three portions of benzene followed by rotary evaporation. The headspace of the vial was evacuated and backfilled with nitrogen. CH_2Cl_2 (1 mL) and *i*- Pr_2NEt (27 μL , 0.16 mmol, 16 equiv) were added, followed by the addition of TMSOTf (18 μL , 0.10 mmol, 10 equiv). The reaction mixture was stirred at 23 $^\circ\text{C}$ for 30 min, then quenched with aq. NaOH (0.3 mL). The layers were separated, and the aqueous phase was extracted with CH_2Cl_2 (1x). The combined organic phases were dried over Na_2SO_4 and concentrated under reduced pressure. The crude product was purified by preparative TLC on silica gel (50% EtOAc/hexanes) to afford the title compound as a beige film (3.7 mg, 0.00687 mmol, 69% yield); ^1H NMR (400 MHz, C_6D_6) δ 7.94 – 7.87 (m, 2H), 7.40 (t, $J = 1.7$ Hz, 1H), 7.27 (s, 1H), 6.58 (d, $J = 8.2$ Hz, 2H), 4.15 (dd, $J = 4.9, 2.4$ Hz, 1H), 3.63 (s, 3H), 3.20 (dt, $J = 4.6, 2.9$ Hz, 1H), 2.94 (s, 3H), 2.91 – 2.84 (m, 1H), 2.68 – 2.55 (m, 2H), 2.53 – 2.43 (m, 1H), 2.20 – 1.99 (m, 4H), 1.73 (s, 3H), 0.29 (s, 9H); ^{13}C NMR (100 MHz, C_6D_6) δ 159.3, 143.2, 139.5, 138.2, 131.5, 129.3, 123.8, 121.5, 121.4, 120.3, 114.8, 109.0, 90.9, 71.6, 58.3, 54.1, 53.6, 47.3, 38.5, 30.3, 23.2, 21.1, 2.1 (an additional ^{13}C resonance associated with the tosyl group is likely obscured by the solvent signal); IR (Neat Film, NaCl) 2932, 2834, 1657, 1597, 1505, 1463, 1406, 1361,

1285, 1249, 1172, 1104, 1024, 932, 843, 682 cm^{-1} ; HRMS (ESI⁺): m/z calc'd for $\text{C}_{28}\text{H}_{35}\text{N}_2\text{O}_5\text{SSi}$ $[\text{M}+\text{H}]^+$: 539.2030, found 539.2028.

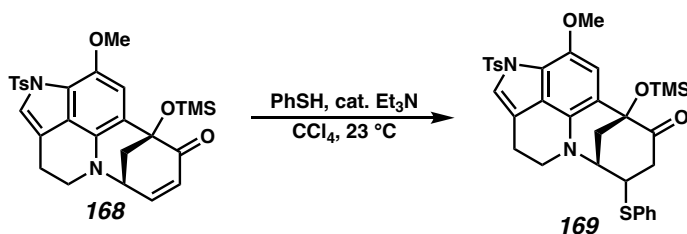


Enone 168

To a 1-dram glass vial was added ketone **157** (9 mg, 0.020 mmol, 1.0 equiv). Traces of water were azeotropically removed by addition of three portions of benzene followed by rotary evaporation. The headspace of the vial was evacuated and backfilled with nitrogen. CH₂Cl₂ (0.5 mL) and *i*-Pr₂NEt (40 μL , 0.23 mmol, 11 equiv) were added, followed by the addition of TMSOTf (28 μL , 0.15 mmol, 7.5 equiv). The reaction mixture was stirred at 23 °C for 1 h, after which LC–MS analysis indicated incomplete conversion. Additional *i*-Pr₂NEt (14 μL , 0.080 mmol, 4 equiv) and TMSOTf (10 μL , 0.055 mmol, 2.8 equiv) were therefore added, and stirring was continued for an additional 40 min, after which LC–MS analysis indicated complete conversion. The reaction mixture was loaded directly onto a silica gel preparative TLC plate. Elution with 25% EtOAc/hexanes afforded a silyl enol ether that was used directly in the following step.

This intermediate was transferred to a 20 mL glass vial and brought into a nitrogen-filled glovebox. Pd(OAc)₂ (9 mg, 0.040 mmol, 2.0 equiv) and DMSO (1.2 mL) were added. The reaction mixture was stirred at 28 °C for 4 days, whereafter the vial was removed from the glovebox and the reaction mixture diluted with water and extracted with CH₂Cl₂ (4x). The combined organic extracts were washed with 1 M aq. LiCl, dried over Na₂SO₄, and concentrated under reduced pressure. The crude product was purified by preparative TLC

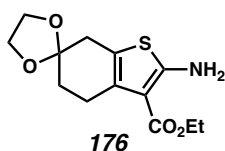
on silica gel (70% EtOAc/hexanes) to afford the title compound as a yellow solid (7 mg, 0.013 mmol, 65% yield over 2 steps); ^1H NMR (400 MHz, C_6D_6) δ 7.87 – 7.78 (m, 2H), 7.47 (d, $J = 1.6$ Hz, 1H), 7.04 (s, 1H), 6.57 (d, $J = 8.0$ Hz, 2H), 5.87 (d, $J = 9.9$ Hz, 1H), 5.81 (ddd, $J = 10.0, 5.1, 1.8$ Hz, 1H), 3.43 (s, 3H), 3.32 (td, $J = 4.4, 2.8$ Hz, 1H), 2.65 – 2.57 (m, 2H), 2.41 – 2.29 (m, 1H), 2.23 (ddd, $J = 12.0, 2.7, 1.8$ Hz, 1H), 2.15 – 1.99 (m, 2H), 1.71 (s, 3H), 0.37 (s, 9H); ^{13}C NMR (100 MHz, C_6D_6) δ 196.0, 143.7, 142.0, 141.0, 137.9, 130.8, 129.6, 129.4, 124.5, 123.0, 121.1, 115.7, 114.0, 107.3, 77.0, 56.8, 54.6, 47.2, 38.6, 23.1, 21.1, 2.7 (an additional ^{13}C resonance associated with the tosyl group is likely obscured by the solvent signal); IR (Neat Film, NaCl) 2925, 2854, 1693, 1504, 1463, 1352, 1263, 1173, 1107, 1024, 963, 932, 844, 759, 666 cm^{-1} ; HRMS (ESI $^+$): m/z calc'd for $\text{C}_{27}\text{H}_{31}\text{N}_2\text{O}_5\text{SSi}$ $[\text{M}+\text{H}]^+$: 523.1717, found 523.1718.



Phenyl sulfide **169**

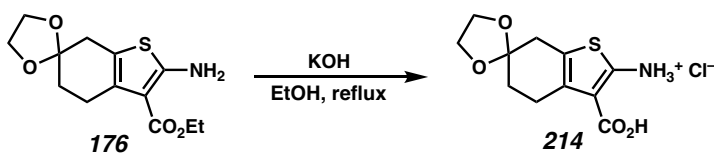
To a 1-dram glass vial was added enone **168** (12.4 mg, 0.024 mmol, 1.0 equiv), CCl₄ (0.1 mL), thiophenol (6 μL , 0.059 mmol, 2.5 equiv), and Et₃N (2.0 μL , 0.014 mmol, 0.6 equiv). The reaction mixture was stirred at 23 °C for 35 min, during which time the yellow color of the starting material disappeared. The reaction mixture was loaded directly onto a silica gel preparative TLC plate. Elution with 40% EtOAc/hexanes afforded the title compound as a colorless film (15.6 mg, 0.024 mmol, >99% yield); ^1H NMR (400 MHz, C_6D_6) δ 7.92 – 7.86 (m, 2H), 7.49 (d, $J = 1.3$ Hz, 1H), 7.30 – 7.25 (m, 2H), 7.02 – 6.87 (m, 4H), 6.63 – 6.58 (m, 2H), 3.67 (dq, $J = 6.1, 2.1$ Hz, 1H), 3.46 (s, 3H), 3.31 (dt, $J = 4.9, 2.3$

Hz, 1H), 2.94 (dd, $J = 12.5, 2.9$ Hz, 1H), 2.72 – 2.61 (m, 1H), 2.56 – 2.42 (m, 4H), 2.37 (dt, $J = 15.8, 1.8$ Hz, 1H), 2.09 (ddd, $J = 12.5, 3.4, 2.3$ Hz, 1H), 1.72 (s, 3H), 0.51 (s, 9H); ^{13}C NMR (100 MHz, C_6D_6) δ 204.7, 143.8, 140.7, 137.9, 134.1, 132.7, 131.2, 129.5, 129.4, 127.9, 124.3, 121.8, 121.0, 117.3, 114.0, 107.4, 79.4, 58.3, 57.2, 50.2, 46.8, 40.2, 35.2, 23.1, 21.1, 3.0 (an additional ^{13}C resonance associated with the tosyl group is likely obscured by the solvent signal); IR (Neat Film, NaCl) 2934, 2847, 1725, 1502, 1358, 1285, 1249, 1172, 1106, 963, 845, 665 cm^{-1} ; HRMS (ESI+): m/z calc'd for $\text{C}_{33}\text{H}_{37}\text{N}_2\text{O}_5\text{S}_2\text{Si}$ $[\text{M}+\text{H}]^+$: 633.1908, found 633.1895.



Aminothiophene 176

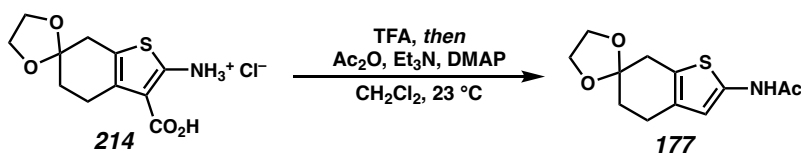
Prepared according to the procedure of Andersen, Møller, and coworkers from 1,4-cyclohexandione monoethylene ketal (**175**).⁴¹ All characterization data matched those reported in the literature.



Amino acid hydrochloride 214

To a 350 mL glass pressure vessel under air were added aminothiophene **176** (22.2 g, 78.35 mmol, 1.0 equiv), KOH (17.6 g, 313.4 mmol, 4.0 equiv), EtOH (165 mL), and water (33 mL). The flask was sealed, and the reaction mixture was stirred at 75 °C in an oil bath for 12 h. The reaction mixture was subsequently transferred to an Erlenmeyer flask and cooled to 0 °C in an ice bath. The solution was acidified with 1 N aq. HCl (375 mL),

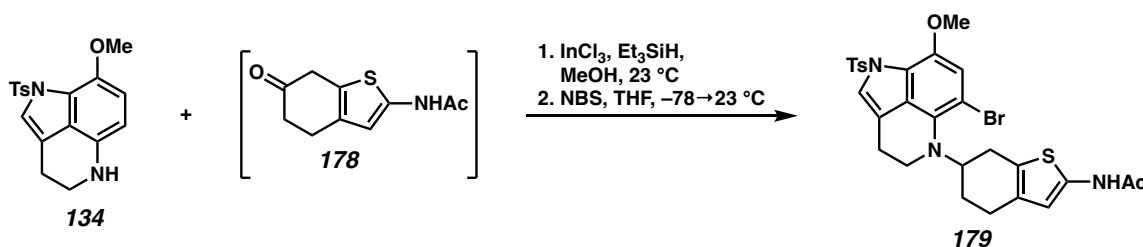
resulting in the formation of a thick precipitate. The product was collected by vacuum filtration and washed with water. The resulting clay-like material was transferred to a round bottom flask with MeOH. The solvent was removed under reduced pressure and the product was dried under high vacuum to afford the title compound as a cream-colored powder (17.95 g, 61.53 mmol, 79% yield assuming complete conversion to hydrochloride); ^1H NMR (400 MHz, DMSO) δ 11.81 (br s, 1H), 7.20 (br s, 2H), 3.90 (s, 4H), 2.72 (t, J = 6.4 Hz, 2H), 2.59 (s, 2H), 1.75 (t, J = 6.5 Hz, 2H); ^{13}C NMR (100 MHz, DMSO) δ 166.7, 163.4, 130.9, 112.4, 107.6, 102.6, 63.9, 34.3, 31.0, 25.1; IR (Neat Film, NaCl) 3409, 2890, 1635, 1580, 1474, 1451, 1353, 1294, 1267, 1105, 1054, 1036, 926, 642 cm^{-1} ; HRMS (ESI $^-$): m/z calc'd for $\text{C}_{11}\text{H}_{12}\text{NO}_4\text{S}$ $[\text{M}-\text{H}]^-$: 254.0493, found 254.0494.



Acetamidothiophene 177

To a 500 mL round bottom flask containing hydrochloride salt **214** (10.78 g, 37.0 mmol, 1.0 equiv) were added CH_2Cl_2 (186 mL) and TFA (8.6 mL, 111 mmol, 3.0 equiv). After stirring for 2 h at 23 $^\circ\text{C}$, DMAP (230 mg, 1.86 mmol, 5 mol %) and Et_3N (26 mL, 185 mmol, 5.0 equiv) were added rapidly, followed by acetic anhydride (5.25 mL, 56.0 mmol, 1.5 equiv). After an additional 4 h, the reaction mixture was concentrated under reduced pressure and purified by silica gel flash chromatography (35% acetone/hexanes) to afford a crude product. Repurification by silica gel flash chromatography (30% acetone/hexanes) provided the title compound as a cream-colored solid (6.95 g, 27.4 mmol, 74% yield); ^1H NMR (400 MHz, C_6D_6) δ 6.64 (br s, 1H), 6.14 (s, 1H), 3.52 – 3.40 (m, 4H), 2.85 (s, 2H), 2.74 (tt, J = 6.5, 1.6 Hz, 2H), 1.86 (t, J = 6.5 Hz, 2H), 1.39 (s, 3H); ^{13}C NMR

(100 MHz, C₆D₆) δ 165.7, 137.5, 130.9, 125.4, 111.7, 108.9, 64.5, 35.1, 34.9, 32.5, 32.4, 24.4, 22.7; IR (Neat Film, NaCl) 3260, 3089, 3046, 2931, 2892, 1650, 1583, 1434, 1370, 1301, 1263, 1114, 1060, 986, 946, 837, 737 cm⁻¹; HRMS (ESI⁺): *m/z* calc'd for C₁₂H₁₆NO₃S [M+H]⁺: 254.0845, found 254.0847.



Bromoarene 179

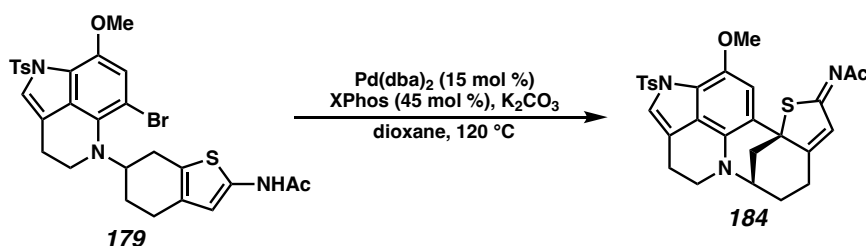
To a 40 mL glass vial were added ketal **177** (500 mg, 1.97 mmol, 1.0 equiv). The vial was sealed with a PTFE/silicone septum, and the headspace was evacuated and backfilled with nitrogen. THF (13 mL) and 4 N aq. HCl (1.98 mL, 7.92 mmol, 4.0 equiv) were added and the vial was sealed and stirred at 66 °C in a metal heating block. After 1.5 h, the reaction mixture was allowed to cool to 23 °C, neutralized with saturated aq. NaHCO₃, and extracted with CH₂Cl₂ (3x). The combined organic extracts were concentrated under reduced pressure and dried under high vacuum with a P₄O₁₀ trap to remove water, providing 420 mg of crude ketone **178** containing ~10% of an unknown impurity, but that was sufficiently pure to use in the next step.

To a 20 mL glass vial were added tricycle **134** (182 mg, 0.532 mmol, 1.0 equiv), the crude ketone prepared from ketal **177** (144 mg, 0.692 mmol, 1.3 equiv assuming a pure compound), and InCl₃ (235 mg, 1.06 mmol, 2.0 equiv). The headspace of the vial was evacuated and backfilled with nitrogen. Dry MeOH (3.6 mL) and triethylsilane (0.26 mL, 1.6 mmol, 3.0 equiv) were added by syringe and the reaction mixture was allowed to stir

at 23 °C for 19 h. At this point, additional triethylsilane (0.26 mL, 1.6 mmol, 3.0 equiv) was added. After 2 more days, additional triethylsilane (0.26 mL, 1.6 mmol, 3.0 equiv) and intermediate ketone **178** (50 mg, 0.24 mmol, 0.45 equiv assuming a pure compound) were added. After stirring for an additional 21 h at 23 °C, the reaction mixture was diluted with saturated aq. NaHCO₃ and extracted with CH₂Cl₂ (3x). The combined organic extracts were dried over Na₂SO₄, concentrated under reduced pressure, and purified by silica gel flash chromatography (35% acetone/hexanes) to afford an intermediate tertiary aniline as an off-white foam (231 mg, 0.431 mmol, 81% yield); ¹H NMR (400 MHz, C₆D₆) δ 7.95 – 7.87 (m, 2H), 7.48 (s, 1H), 6.64 (d, *J* = 8.1 Hz, 2H), 6.50 (d, *J* = 8.3 Hz, 1H), 6.19 (s, 1H), 6.04 (d, *J* = 8.4 Hz, 1H), 3.90 – 3.74 (m, 1H), 3.56 (s, 3H), 2.79 – 2.61 (m, 3H), 2.57 – 2.40 (m, 5H), 1.73 (s, 3H), 1.71 – 1.64 (m, 1H), 1.62 – 1.56 (m, 1H), 1.55 (s, 3H).

To a 50 mL round bottom flask was added this intermediate tertiary aniline (103.4 mg, 0.193 mmol, 1.0 equiv), and the headspace of the flask was evacuated and backfilled with nitrogen. THF (5 mL) was added, and the flask was cooled to –78 °C. Subsequently, a solution of NBS (34.3 mg, 0.193 mmol, 1.0 equiv) was added by syringe pump over a period of 1 h with rapid stirring. After completion of the addition, the cooling bath was removed, and the reaction mixture was allowed to warm to 23 °C. The reaction mixture was concentrated under reduced pressure and purified by silica gel flash chromatography (30% acetone/hexanes) to afford the title compound as an off-white foam of sufficient purity for use in the next step (70 mg, 0.114 mmol, 59% yield); a nearly pure sample for analysis was obtained by preparative HPLC (SiO₂ column, 30→100% acetone/hexanes over 18 min at 12 mL/min). ¹H NMR (400 MHz, C₆D₆) δ 7.86 – 7.80 (m, 2H), 7.52 (s, 1H), 7.35 (s, 1H), 6.75 (s, 1H), 6.65 (d, *J* = 8.1 Hz, 2H), 6.28 (s, 1H), 4.24 (ddq, *J* = 13.9, 7.9,

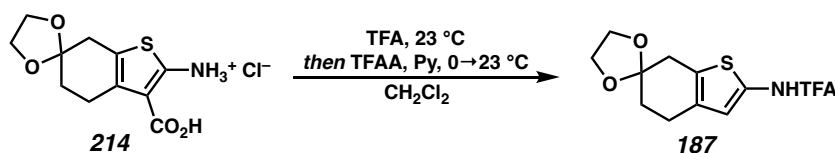
2.6 Hz, 1H), 3.21 (s, 3H), 3.05 – 2.91 (m, 2H), 2.86 (ddd, $J = 13.9, 7.8, 4.9$ Hz, 1H), 2.72 (ddd, $J = 14.5, 11.3, 2.4$ Hz, 1H), 2.55 – 2.36 (m, 2H), 2.35 – 2.18 (m, 2H), 1.87 – 1.69 (m, 1H), 1.76 (s, 3H), 1.59 – 1.49 (m, 1H), 1.56 (s, 3H); ^{13}C NMR (100 MHz, C_6D_6) δ 166.1, 144.0, 142.8, 137.9, 137.6, 134.8, 131.1, 129.5, 128.0, 127.7, 126.8, 123.1, 122.3, 115.4, 114.3, 112.2, 106.1, 59.9, 56.4, 43.1, 29.6, 28.8, 26.3, 22.8, 22.6, 21.1. Additional peaks in the ^1H NMR spectrum at 1.60 ppm and in the ^{13}C NMR spectrum at 29.2 and 176.8 ppm arise from an unknown impurity; correlations to the resonances of bromoarene **179** are not observed in a $^1\text{H}/^{13}\text{C}$ HMBC experiment; IR (Neat Film, NaCl) 3256, 2932, 2842, 1713, 1582, 1487, 1347, 1288, 1228, 1169, 1112, 804, 684 cm^{-1} ; HRMS (ESI $^+$): m/z calc'd for $\text{C}_{28}\text{H}_{29}\text{BrN}_3\text{O}_4\text{S}_2$ $[\text{M}+\text{H}]^+$: 614.0777, found 614.0786.



Thioimidate **184**

To a 1-dram glass vial in a nitrogen-filled glovebox were added bromoarene **179** (18 mg, 0.0293 mmol, 1.0 equiv), 1,4-dioxane (0.3 mL), and K_2CO_3 (6.1 mg, 0.0441 mmol, 1.5 equiv). $\text{Pd}(\text{dba})_2$ (2.5 mg, 0.0043 mmol, 0.15 equiv) and XPhos (3.5 mg, 0.0132 mmol, 0.45 equiv) were added as a stock solution in 1,4-dioxane (0.44 mL, prestirred for 10 min at $28\text{ }^\circ\text{C}$). The vial was sealed with a PTFE-lined cap, removed from the glovebox, and stirred at $120\text{ }^\circ\text{C}$ in a metal heating block for 6 h. Then, the reaction mixture was allowed to cool to $23\text{ }^\circ\text{C}$ and concentrated under reduced pressure. The crude product was purified by preparative TLC on silica gel (100% EtOAc) to afford the title compound as a brown

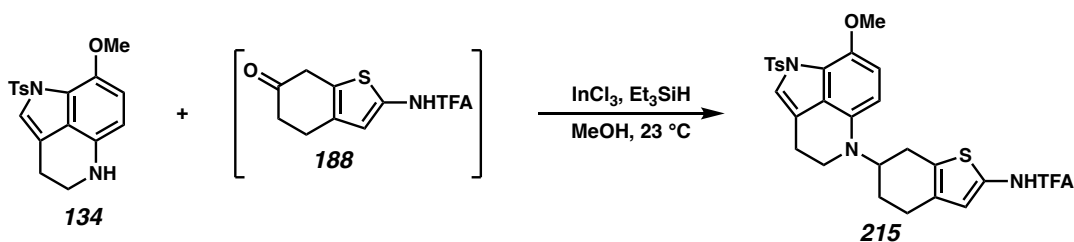
solid (11.2 mg of material containing 10 wt % EtOAc by ^1H NMR analysis, 0.0189 mmol, 65% yield); ^1H NMR (400 MHz, C_6D_6) δ 7.87 – 7.82 (m, 2H), 7.47 (s, 1H), 6.86 (s, 1H), 6.62 – 6.56 (m, 2H), 6.11 (d, $J = 1.4$ Hz, 1H), 3.24 (s, 3H), 2.74 (p, $J = 2.9$ Hz, 1H), 2.72 – 2.55 (m, 2H), 2.51 – 2.42 (m, 2H), 2.38 (dt, $J = 12.3, 2.7$ Hz, 1H), 2.33 (s, 3H), 1.91 (dt, $J = 13.9, 6.5$ Hz, 1H), 1.72 (s, 3H), 1.69 – 1.58 (m, 3H), 0.84 – 0.70 (m, 1H); ^{13}C NMR (100 MHz, C_6D_6) δ 184.5, 183.6, 175.0, 143.8, 140.1, 137.9, 133.4, 129.4, 124.3, 123.2, 121.9, 120.9, 114.4, 112.4, 109.1, 63.5, 57.2, 52.9, 47.1, 40.3, 31.5, 27.6, 25.1, 23.0, 21.1 (an additional ^{13}C resonance associated with the tosyl group is likely obscured by the solvent signal); IR (Neat Film, NaCl) 2924, 1665, 1503, 1362, 1285, 1234, 1172, 1106, 1004, 672 cm^{-1} ; HRMS (ESI+): m/z calc'd for $\text{C}_{28}\text{H}_{28}\text{N}_3\text{O}_4\text{S}_2$ $[\text{M}+\text{H}]^+$: 534.1516, found 534.1524.



Trifluoroacetamidothiophene 187

To a 500 mL round bottom flask was added hydrochloride salt **214** (14.29 g, 48.98 mmol, 1.0 equiv). Traces of water were azeotropically removed by addition of three portions of benzene followed by rotary evaporation. Then, the headspace of the flask was evacuated and backfilled with nitrogen, and CH_2Cl_2 (150 mL) and TFA (11.2 mL, 146.9 mmol, 3.0 equiv) were added. After 15 min, additional CH_2Cl_2 (50 mL) was added to reduce the viscosity of the mixture. The reaction mixture was stirred for 2.5 h at 23 $^\circ\text{C}$, whereafter it was cooled to 0 $^\circ\text{C}$ in an ice bath and pyridine (19.7 mL, 244.9 mmol, 5.0 equiv) was added rapidly. TFAA (10.2 mL, 73.47 mmol, 1.5 equiv) was then added, and the ice bath was removed. After stirring for an additional 16 h at 23 $^\circ\text{C}$, silica gel was

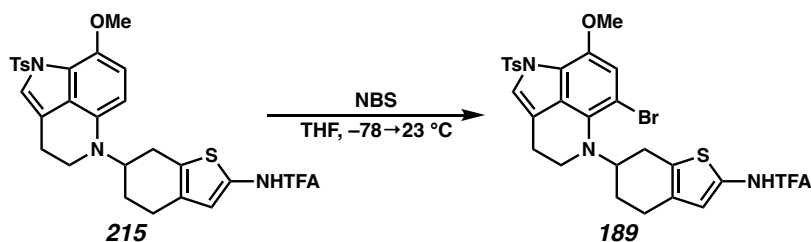
added, and the reaction mixture was concentrated under reduced pressure and purified by silica gel flash chromatography (33% EtOAc/hexanes) to afford the title compound as an orange solid (9.67 g, 31.47 mmol, 64% yield); ^1H NMR (400 MHz, CDCl_3) δ 8.72 (s, 1H), 6.59 (s, 1H), 4.06 – 3.98 (m, 4H), 2.91 (d, $J = 1.5$ Hz, 2H), 2.74 (tt, $J = 6.5, 1.6$ Hz, 2H), 1.94 (t, $J = 6.5$ Hz, 2H); ^{13}C NMR (100 MHz, CDCl_3) δ 154.2, 153.8, 153.4, 153.0, 133.4, 131.8, 127.9, 120.1, 117.2, 116.1, 114.4, 111.5, 108.5, 64.8, 34.9, 31.7, 24.0; IR (Neat Film, NaCl) 3248, 3097, 2894, 1713, 1589, 1434, 1362, 1250, 1169, 1060, 946, 905, 842, 739 cm^{-1} ; HRMS (ESI $^+$): m/z calc'd for $\text{C}_{12}\text{H}_{13}\text{F}_3\text{NO}_3\text{S}$ $[\text{M}+\text{H}]^+$: 308.0563, found 308.0561.



Tertiary aniline **215**

To a 100 mL round bottom flask containing thiophene-ketal **187** (1.64 g, 5.34 mmol, 1.5 equiv) under nitrogen and equipped with a reflux condenser were added THF (27 mL) and 4 N aq. HCl (5.3 mL, 21.2 mmol, 4.0 equiv w.r.t. ketal). The reaction mixture was heated to reflux and stirred for 1.5 h, then allowed to cool to $23\text{ }^\circ\text{C}$ and quenched with saturated aq. NaHCO_3 (100 mL). The resulting mixture was extracted with CH_2Cl_2 (3x40 mL). The combined organic extracts were washed with brine, and the brine phase was back-extracted once with CH_2Cl_2 . The combined organic phases were dried over a mixture of Na_2SO_4 and MgSO_4 and concentrated under reduced pressure to afford crude ketone **188** as an orange solid that was used directly without further purification.

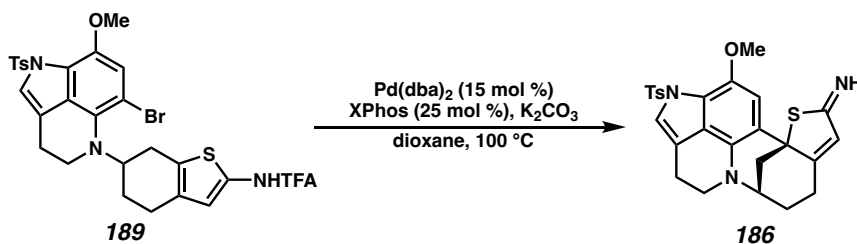
To a 50 mL round bottom flask were added tricyclic aniline **134** (1.22 g, 3.56 mmol, 1.0 equiv), the crude ketone resulting from hydrolysis of ketal **187** (5.34 mmol assuming pure compound), and InCl_3 (1.57 g, 7.12 mmol, 2.0 equiv). The headspace of the flask was evacuated and backfilled with nitrogen. MeOH (12 mL) and Et_3SiH (5.7 mL, 35.6 mmol, 10 equiv) were added and the reaction mixture was stirred at 23 °C for 24 h, whereafter it was transferred to a separatory funnel containing saturated aq. NaHCO_3 (200 mL). The resulting suspension was extracted with CH_2Cl_2 (3x70 mL). The combined organic extracts (still containing a significant quantity of water and indium salts) were dried over Na_2SO_4 , concentrated under reduced pressure, and purified by automated silica gel flash chromatography (Teledyne ISCO, 0→60% EtOAc/hexanes) to afford the title compound as a golden-colored foam of sufficient purity for use in the next step (1.80 g, 3.05 mmol, 86% yield). A sample for analysis was obtained by preparative TLC on silica gel (33% EtOAc/hexanes); ^1H NMR (400 MHz, CDCl_3) δ 8.40 (br s, 1H), 7.82 – 7.75 (m, 2H), 7.34 (t, $J = 1.5$ Hz, 1H), 7.26 – 7.21 (m, 2H), 6.60 (s, 1H), 6.58 (d, $J = 8.3$ Hz, 1H), 6.30 (d, $J = 8.8$ Hz, 1H), 4.15 – 4.01 (m, 1H), 3.68 (s, 3H), 3.33 (dt, $J = 11.0, 5.4$ Hz, 1H), 3.21 (dt, $J = 11.5, 6.2$ Hz, 1H), 2.99 – 2.92 (m, 3H), 2.91 – 2.66 (m, 3H), 2.37 (s, 3H), 2.07 – 1.98 (m, 2H); ^{13}C NMR (100 MHz, CDCl_3) δ 153.8, 153.4, 144.2, 140.0, 137.1, 136.3, 133.2, 132.4, 129.5, 129.4, 127.7, 124.2, 123.2, 119.7, 117.2, 116.5, 115.4, 114.4, 110.3, 102.7, 57.3, 53.5, 42.2, 27.0, 26.0, 25.9, 23.5, 21.7; IR (Neat Film, NaCl) 3281, 3126, 3058, 2935, 2841, 1714, 1588, 1510, 1442, 1356, 1251, 1169, 1108, 1056, 996, 903, 739, 663 cm^{-1} ; HRMS (ESI+): m/z calc'd for $\text{C}_{28}\text{H}_{27}\text{F}_3\text{N}_3\text{O}_4\text{S}_2$ $[\text{M}+\text{H}]^+$: 590.1390, found 590.1404.



Bromoarene 189

To a 250 mL round bottom flask was added tertiary aniline **215** (1.78 g, 3.02 mmol, 1.0 equiv). Traces of water were azeotropically removed by addition of three portions of benzene followed by rotary evaporation, and the headspace of the flask was evacuated and backfilled with nitrogen. The starting material was taken up in THF (50 mL), and the flask was cooled to $-78\text{ }^{\circ}\text{C}$ and protected from light. A solution of NBS (484 mg, 2.72 mmol, 0.9 equiv) in THF (50 mL) was added as a slow stream with rapid stirring. Following addition, the reaction mixture was allowed to stir at $-78\text{ }^{\circ}\text{C}$ for 5 additional min, whereafter the cooling bath was removed and the reaction mixture allowed to warm to $23\text{ }^{\circ}\text{C}$. The reaction mixture was concentrated under reduced pressure and purified by automated silica gel flash chromatography (Teledyne ISCO, 0 \rightarrow 50% EtOAc/hexanes) to afford the title compound as a brown foam (1.16 g, 1.74 mmol, 57% yield from tertiary aniline **215** or 64% from NBS); ^1H NMR (400 MHz, C_6D_6) δ 7.86 – 7.80 (m, 2H), 7.54 (t, $J = 1.5$ Hz, 1H), 6.75 (s, 1H), 6.67 – 6.57 (m, 2H), 6.01 (s, 1H), 4.17 (dddd, $J = 13.7, 11.3, 5.3, 2.6$ Hz, 1H), 3.19 (s, 3H), 2.99 – 2.75 (m, 3H), 2.58 (tdd, $J = 11.7, 3.9, 2.0$ Hz, 1H), 2.36 – 2.09 (m, 4H), 1.80 – 1.71 (m, 1H), 1.76 (s, 3H), 1.45 (tdd, $J = 12.2, 10.7, 6.7$ Hz, 1H); ^{13}C NMR (100 MHz, C_6D_6) δ 153.6, 153.2, 144.1, 143.0, 137.8, 134.6, 133.6, 131.9, 129.6, 129.5, 128.0, 127.7, 123.1, 122.4, 117.7, 116.6, 116.2, 115.2, 114.2, 106.2, 59.5, 56.3, 43.0, 29.5, 28.5, 26.0, 22.6, 21.1; IR (Neat Film, NaCl) 3295, 2931, 1714, 1588, 1490, 1438, 1347,

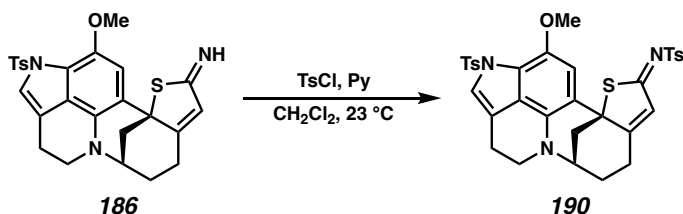
1251, 1172, 1111, 908, 804, 737, 665 cm^{-1} ; HRMS (ESI+): m/z calc'd for $\text{C}_{28}\text{H}_{26}\text{BrF}_3\text{N}_3\text{O}_4\text{S}_2$ $[\text{M}+\text{H}]^+$: 668.0495, found 668.0502.



Thioimidate **186**

To a 40 mL glass vial was added bromoarene **189** (331 mg, 0.495 mmol, 1.0 equiv). Traces of water were azeotropically removed by addition of three portions of benzene followed by rotary evaporation and the vial was transferred to a nitrogen-filled glovebox. Solid K_2CO_3 (96 mg, 0.695 mmol, 1.4 equiv) was added to the vial. In a separate vial, a stock solution of $\text{Pd}(\text{dba})_2$ (46.2 mg) and XPhos (64.2 mg) in 1,4-dioxane (13.3 mL) was prepared and stirred at 28°C for 10 min. Then, 12.4 mL of this solution were transferred to the vial containing bromoarene **189** (for 43 mg $\text{Pd}(\text{dba})_2$ [0.0748 mmol, 15 mol %] and 59.1 mg XPhos [0.124 mmol, 25 mol %]). The vial was sealed with a PTFE/silicone septum cap, removed from the glovebox, and stirred at 100°C for 6 h. The reaction mixture was then allowed to cool to 23°C and passed through a PTFE syringe filter, which was subsequently rinsed with EtOAc. The solution was concentrated under reduced pressure and purified by silica gel flash chromatography (100% EtOAc \rightarrow 100% acetone) to afford the title compound as an off-white solid (145 mg, 0.295 mmol, 60% yield); ^1H NMR (400 MHz, CD_2Cl_2) δ 7.81 – 7.72 (m, 2H), 7.32 – 7.24 (m, 3H), 6.81 (s, 1H), 5.78 (d, $J = 1.7$ Hz, 1H), 3.64 (s, 3H), 3.59 (p, $J = 2.7$ Hz, 1H), 3.35 (ddd, $J = 11.1, 9.7, 5.7$ Hz, 1H), 3.25 (ddd, $J = 11.1, 4.8, 3.5$ Hz, 1H), 3.04 – 2.94 (m, 2H), 2.65 (dt, $J = 12.5, 2.9$ Hz, 1H), 2.54

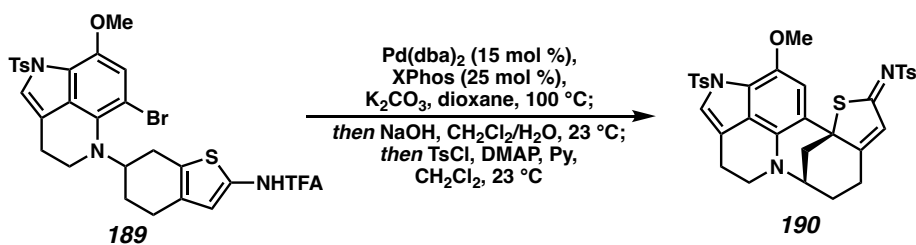
–2.47 (m, 1H), 2.40 (qd, $J = 5.3, 3.1$ Hz, 1H), 2.37 (s, 3H), 2.33 (dd, $J = 12.5, 2.9$ Hz, 1H), 2.06 – 1.97 (m, 1H), 1.61 (tdd, $J = 13.7, 5.3, 2.9$ Hz, 1H); ^{13}C NMR (100 MHz, CD_2Cl_2) δ 178.5, 168.3, 144.9, 139.3, 137.2, 133.5, 129.7, 128.0, 123.5, 122.3, 121.7, 120.6, 115.2, 114.5, 109.1, 63.5, 57.4, 47.6, 41.9, 31.9, 24.8, 23.2, 21.7 (the bridgehead methine ^{13}C resonance is obscured by the solvent peak); IR (Neat Film, NaCl) 2925, 2851, 1595, 1503, 1462, 1349, 1284, 1226, 1174, 1106, 1011, 898, 808, 738, 704, 672 cm^{-1} ; HRMS (ESI+): m/z calc'd for $\text{C}_{26}\text{H}_{26}\text{N}_3\text{O}_3\text{S}_2$ $[\text{M}+\text{H}]^+$: 492.1410, found 492.1416.



N-tosylthioimide 190

To a 1-dram glass vial containing TsCl (16 mg, 0.0814 mmol, 2.0 equiv) under nitrogen was added thioimide **186** (20 mg, 0.0407 mmol, 1.0 equiv) as a stock solution in CH_2Cl_2 (1 mL), followed by pyridine (10 μL , 0.122 mmol, 3.0 equiv). The reaction mixture was stirred at 23 $^\circ\text{C}$ for 3 days, after which it was concentrated under reduced pressure and purified by silica gel flash chromatography (50% EtOAc/hexanes) to afford the title compound as an orange film (23.7 mg, 0.0367 mmol, 90% yield); ^1H NMR (400 MHz, CDCl_3) δ 7.93 (d, $J = 8.1$ Hz, 2H), 7.83 – 7.74 (m, 2H), 7.36 – 7.28 (m, 3H), 7.28 – 7.22 (m, 2H), 6.49 (s, 1H), 5.97 (d, $J = 1.6$ Hz, 1H), 3.65 – 3.61 (m, 1H), 3.59 (s, 3H), 3.37 (dt, $J = 10.9, 7.6$ Hz, 1H), 3.27 (dt, $J = 11.1, 4.2$ Hz, 1H), 3.06 – 2.97 (m, 2H), 2.83 (dt, $J = 12.6, 2.8$ Hz, 1H), 2.68 – 2.58 (m, 1H), 2.49 – 2.44 (m, 1H), 2.43 (s, 3H), 2.38 (s, 3H), 2.21 – 2.04 (m, 2H), 1.59 – 1.51 (m, 1H); ^{13}C NMR (100 MHz, CDCl_3) δ 184.5, 175.3, 144.4, 144.0, 139.4, 137.3, 136.9, 133.1, 129.6, 129.5, 127.9, 127.6, 123.6, 122.7, 121.6,

120.7, 114.2, 111.1, 107.8, 65.4, 57.2, 53.0, 47.4, 40.4, 31.7, 25.4, 23.0, 21.7; IR (Neat Film, NaCl) 2924, 2850, 1596, 1519, 1449, 1286, 1228, 1167, 1107, 1010, 867, 813, 734, 664 cm^{-1} ; HRMS (ESI⁺): m/z calc'd for $\text{C}_{33}\text{H}_{32}\text{N}_3\text{O}_5\text{S}_3$ $[\text{M}+\text{H}]^+$: 646.1499, found 646.1500.



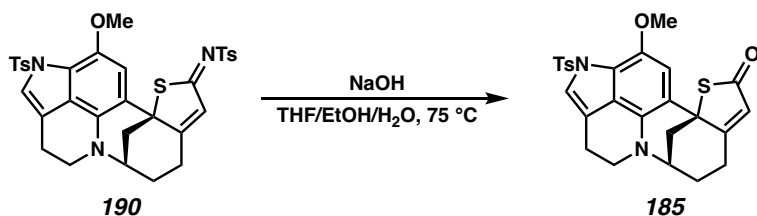
Procedure for the direct preparation of *N*-tosylthioimide **190** from bromoarene **189**

To a 500 mL Schlenk bomb in a nitrogen-filled glovebox was added bromoarene **189** (3.88 g, 5.80 mmol, 1.0 equiv) as a solution in a minimal amount of benzene. The benzene was removed under reduced pressure, and K_2CO_3 (1.12 g, 8.12 mmol, 1.4 equiv) and 1,4-dioxane (110 mL) were added. In a separate vial, $\text{Pd}(\text{dba})_2$ (500 mg, 0.870 mmol, 15 mol %) and XPhos (691 mg, 1.45 mmol, 25 mol %) were combined. 1,4-dioxane (35 mL) was added and the mixture was stirred at 28 °C for 10 min. Then, the Pd/ligand solution was transferred by pipette to the Schlenk bomb. The vessel was sealed, removed from the glovebox, and stirred at 100 °C for 7 h. The reaction mixture was allowed to cool to 23 °C, filtered through a Celite plug with EtOAc, and concentrated under reduced pressure.

The residue was taken up in CH_2Cl_2 (70 mL). 1 N aq. NaOH was added, and the biphasic mixture was subjected to vigorous magnetic stirring for 1 h. The layers were separated, and the aqueous phase was extracted with CH_2Cl_2 (3x20 mL). The combined

organic phases were dried over Na_2SO_4 and concentrated under reduced pressure in a 500 mL round bottom flask.

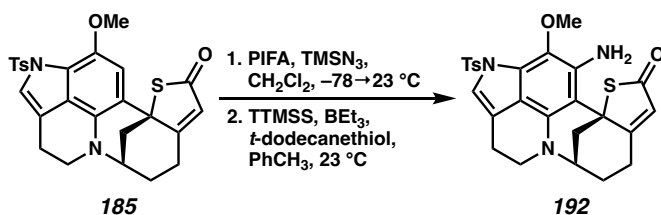
Traces of water were azeotropically removed by addition of three portions of PhCH_3 followed by rotary evaporation. DMAP (71 mg, 0.58 mmol, 10 mol %) was added and the headspace of the flask was evacuated and backfilled with nitrogen. CH_2Cl_2 (115 mL) was added, followed by pyridine (1.4 mL, 17.4 mmol, 3.0 equiv). TsCl (2.21 g, 11.6 mmol, 2.0 equiv) was added in a single portion under a stream of nitrogen. The reaction mixture was stirred at 23 °C for 58 h, then concentrated under reduced pressure. The crude product was purified by automated silica gel flash chromatography (Teledyne ISCO, 0→40→75% EtOAc/hexanes) to afford *N*-tosylthioimidate **190** as an orange foam that crystallized upon standing (2.66 g, 4.12 mmol, 71% yield). For characterization data, see above.



Thiolactone 185

To a 20 mL glass vial containing thioimidate **190** (200 mg, 0.310 mmol, 1.0 equiv) under nitrogen were added THF (2.5 mL), a degassed mixture of water (2 mL) and ethanol (10 mL), and 2 N aq. NaOH (0.62 mL, 1.24 mmol, 4.0 equiv). The vial was opened and sealed with a PTFE/silicone septum under a stream of argon. The reaction mixture was stirred at 80 °C at 490 rpm in a metal heating block for 25 min, after which the solution was nearly homogenous. The vial was immediately removed from the heating block and allowed to cool to approximately 35 °C, at which point the reaction mixture was quenched

with glacial acetic acid (0.3 mL) and diluted with water (40 mL), leading to the formation of a beige precipitate. The suspension was extracted with EtOAc (4x30 mL), and the combined organic phases were dried over Na₂SO₄ concentrated under reduced pressure. The crude product was purified by silica gel flash chromatography (2.5% EtOAc/CH₂Cl₂) to afford recovered thioimidate **190** (23.5 mg of material containing 10 wt % TsNH₂ by ¹H NMR analysis, 0.0328 mmol, 11% yield) and the title compound (104 mg, 0.211 mmol, 68% yield); ¹H NMR (400 MHz, C₆D₆) δ 7.86 (d, *J* = 8.2 Hz, 2H), 7.47 (d, *J* = 1.6 Hz, 1H), 6.89 (t, *J* = 1.3 Hz, 1H), 6.67 – 6.59 (m, 2H), 5.50 (d, *J* = 1.7 Hz, 1H), 3.32 (s, 3H), 2.87 – 2.78 (m, 1H), 2.78 – 2.59 (m, 2H), 2.59 – 2.45 (m, 2H), 2.40 (dt, *J* = 12.4, 2.8 Hz, 1H), 1.91 – 1.81 (m, 1H), 1.81 – 1.76 (m, 1H), 1.74 (s, 3H), 1.73 – 1.66 (m, 1H), 1.66 – 1.56 (m, 1H), 0.97 – 0.81 (m, 1H); ¹³C NMR (100 MHz, C₆D₆) δ 196.3, 177.3, 143.9, 140.0, 137.8, 133.5, 129.4, 124.2, 121.9, 121.7, 121.0, 114.6, 112.8, 108.9, 60.8, 60.8, 57.0, 53.0, 47.1, 40.9, 31.4, 24.8, 23.0, 21.1 (an additional ¹³C resonance associated with the tosyl group is likely obscured by the solvent signal); IR (Neat Film, NaCl) 2931, 2851, 1682, 1504, 1348, 1284, 1227, 1169, 1107, 1011, 897, 851, 814, 738, 662 cm⁻¹; HRMS (ESI⁺): *m/z* calc'd for C₂₆H₂₅N₂O₄S₂ [M+H]⁺: 493.1250, found 493.1251.



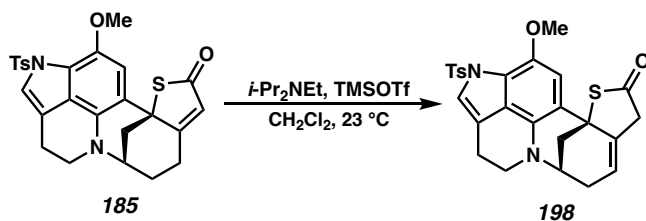
Primary aniline **192**

To a 1-dram glass vial containing thiolactone **185** (22.6 mg, 0.0459 mmol, 1.0 equiv) under nitrogen were added CH₂Cl₂ (2.3 mL) and TMSN₃ (30 μL, 0.23 mmol, 5.0 equiv). The reaction mixture was cooled to –78 °C and a solution of PIFA (18.8 mg, 0.0437

mmol, 0.95 equiv) in CH_2Cl_2 (0.5 mL) was added dropwise. After stirring for 10 min at $-78\text{ }^\circ\text{C}$, the reaction mixture was allowed to warm to $23\text{ }^\circ\text{C}$, concentrated under reduced pressure, and purified by preparative TLC on silica gel (90% Et_2O /hexanes, eluted twice) to afford an intermediate aryl azide as a brown film (15.3 mg, 0.0287 mmol, 62% yield); ^1H NMR (600 MHz, C_6D_6) δ 7.95 – 7.91 (m, 2H), 7.34 (s, 1H), 6.56 (d, $J = 8.2$ Hz, 2H), 5.66 (d, $J = 1.6$ Hz, 1H), 3.81 (s, 3H), 2.61 – 2.56 (m, 2H), 2.53 – 2.46 (m, 1H), 2.41 – 2.32 (m, 2H), 2.24 (dt, $J = 12.7, 2.8$ Hz, 1H), 1.82 – 1.77 (m, 1H), 1.63 (dd, $J = 12.7, 3.1$ Hz, 1H), 1.58 (s, 3H), 1.54 – 1.43 (m, 2H), 0.79 (tdd, $J = 13.0, 5.7, 3.2$ Hz, 1H).

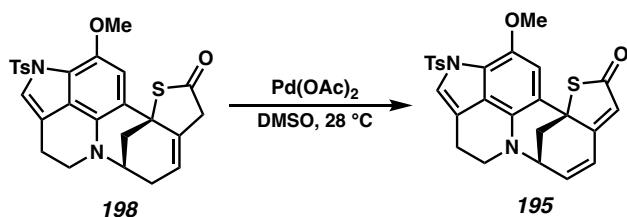
To a $\frac{1}{2}$ -dram glass vial under air was added this intermediate aryl azide (7.3 mg, 0.0137 mmol, 1.0 equiv) as a stock solution in CH_2Cl_2 . The solvent was removed by blowing a stream of nitrogen over the surface of the solution. Then, PhCH_3 (0.36 mL), tris(trimethylsilyl)silane (21 μL , 0.0684 mmol, 5.0 equiv), *tert*-dodecanethiol (1.6 μL , 0.0069 mmol, 0.5 equiv), and triethylborane (1 M in hexanes, 41 μL , 0.0411 mmol, 3.0 equiv) were added under air. After 5 min, the reaction mixture was concentrated under reduced pressure and purified by preparative TLC on silica gel (100% EtOAc) to afford the title compound as a brown film (5.5 mg, 0.0108 mmol, 79% yield); ^1H NMR (400 MHz, C_6D_6) δ 8.02 – 7.97 (m, 2H), 7.26 (d, $J = 1.6$ Hz, 1H), 6.59 – 6.54 (m, 2H), 5.60 (d, $J = 1.5$ Hz, 1H), 4.53 (s, 2H), 3.77 (s, 3H), 2.63 – 2.50 (m, 3H), 2.42 – 2.34 (m, 3H), 1.75 – 1.67 (m, 2H), 1.65 (s, 3H), 1.58 – 1.53 (m, 2H), 0.75 – 0.63 (m, 1H); ^{13}C NMR (100 MHz, C_6D_6) δ 194.9, 175.9, 143.9, 139.9, 136.8, 136.6, 129.6, 127.5, 127.2, 122.7, 117.8, 116.5, 112.2, 100.0, 60.3, 60.3, 52.8, 48.0, 44.0, 30.9, 25.2, 22.9, 21.0 (an additional ^{13}C resonance associated with the tosyl group is likely obscured by the solvent signal); IR (Neat Film, NaCl) 3440, 3347, 2921, 2854, 1682, 1486, 1367, 1294, 1177, 1136, 1094, 967, 828, 738,

683 cm^{-1} ; HRMS (ESI⁺): m/z calc'd for $\text{C}_{26}\text{H}_{26}\text{N}_3\text{O}_4\text{S}_2$ $[\text{M}+\text{H}]^+$: 508.1359, found 508.1374.



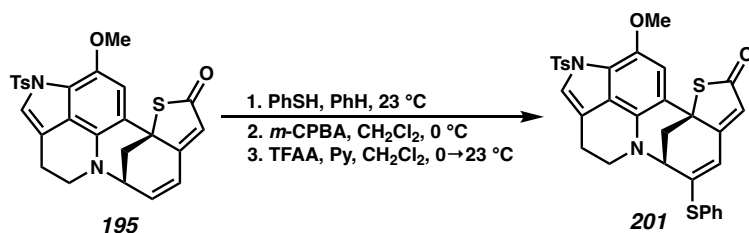
Deconjugated olefin **198**

To a 1-dram glass vial was added thiolactone **185** (50 mg, 0.102 mmol, 1.0 equiv). Traces of water were azeotropically removed by addition of three portions of benzene followed by rotary evaporation, and the headspace of the vial was evacuated and flushed with nitrogen. The starting material was taken up in CH_2Cl_2 (1 mL), and $i\text{-Pr}_2\text{NEt}$ (0.18 mL, 1.02 mmol, 10 equiv) and TMSOTf (0.13 μL , 0.714 mmol, 7.0 equiv) were injected. The reaction mixture was stirred at 23 $^\circ\text{C}$ for 20 h, then loaded directly onto a silica gel flash column and eluted (hexanes \rightarrow 30% EtOAc/hexanes) to afford the title compound as a beige solid containing starting material as a minor impurity (47.3 mg, 0.0960 mmol, 94% yield); ^1H NMR (400 MHz, C_6D_6) δ 7.92 – 7.85 (m, 2H), 7.43 (s, 1H), 7.04 (s, 1H), 6.62 (d, $J = 8.2$ Hz, 2H), 4.83 (q, $J = 3.2$ Hz, 1H), 3.46 (s, 3H), 3.12 – 3.00 (m, 2H), 2.77 – 2.67 (m, 1H), 2.66 – 2.49 (m, 3H), 2.48 – 2.39 (m, 1H), 2.07 (dd, $J = 11.7, 3.8$ Hz, 1H), 1.96 – 1.86 (m, 2H), 1.78 (q, $J = 3.9$ Hz, 1H), 1.72 (s, 3H); ^{13}C NMR (100 MHz, C_6D_6) δ 202.0, 143.8, 139.6, 139.0, 137.9, 131.5, 129.4, 124.1, 121.9, 120.8, 119.0, 116.4, 114.6, 109.0, 58.1, 56.3, 52.2, 47.3, 45.8, 35.6, 31.4, 22.9, 21.1 (an additional ^{13}C resonance associated with the tosyl group is likely obscured by the solvent signal); IR (Neat Film, NaCl) 2928, 2836, 1713, 1596, 1504, 1361, 1285, 1172, 1108, 895, 811, 731, 667, 616 cm^{-1} ; HRMS (ESI⁺): m/z calc'd for $\text{C}_{26}\text{H}_{25}\text{N}_2\text{O}_4\text{S}_2$ $[\text{M}+\text{H}]^+$: 493.1250, found 493.1248.



Diene 195

To a 20 mL glass vial was added deconjugated thiolactone **198** (19.9 mg, 0.0404 mmol, 1.0 equiv). Traces of water were azeotropically removed by addition of three portions of benzene followed by rotary evaporation, the vial was transferred to a nitrogen-filled glovebox, and Pd(OAc)₂ (9.5 mg, 0.0424 mmol, 1.05 equiv) and DMSO (2.4 mL) were added. The vial was sealed with a PTFE/silicone septum and stirred at 28 °C for 24 h, then removed from the glovebox and stirred at 23 °C for an additional 24 h. Then, the reaction mixture was diluted with water (30 mL) and extracted with EtOAc (4x15 mL). The combined organic extracts were washed with brine (2x15 mL), dried over Na₂SO₄, and concentrated under reduced pressure. The crude product was purified by preparative TLC (100% Et₂O, eluted twice) to afford the title compound as a bright orange film (8.0 mg, 0.0163 mmol, 40% yield); ¹H NMR (400 MHz, C₆D₆) δ 7.83 – 7.78 (m, 2H), 7.44 (d, *J* = 1.6 Hz, 1H), 6.92 (s, 1H), 6.62 – 6.53 (m, 2H), 5.87 (ddd, *J* = 9.7, 1.9, 0.9 Hz, 1H), 5.52 (s, 1H), 5.46 – 5.38 (m, 1H), 3.29 (s, 3H), 3.19 (dtt, *J* = 4.7, 3.3, 2.0 Hz, 1H), 2.67 – 2.55 (m, 3H), 2.40 – 2.32 (m, 2H), 1.93 (dd, *J* = 12.3, 3.9 Hz, 1H), 1.71 (s, 3H); ¹³C NMR (100 MHz, C₆D₆) δ 196.1, 171.8, 143.8, 141.3, 137.8, 132.8, 131.8, 129.4, 128.0, 125.1, 124.1, 123.4, 121.6, 121.2, 114.3, 113.6, 108.7, 58.2, 56.8, 53.0, 47.9, 37.6, 23.0, 21.1; IR (Neat Film, NaCl) 3060, 2934, 2841, 1681, 1622, 1504, 1347, 1287, 1226, 1177, 1106, 1016, 967, 898, 856, 813, 732, 662, 623 cm⁻¹; HRMS (ESI⁺): *m/z* calc'd for C₂₆H₂₃N₂O₄S₂ [M+H]⁺: 491.1094, found 491.1098.



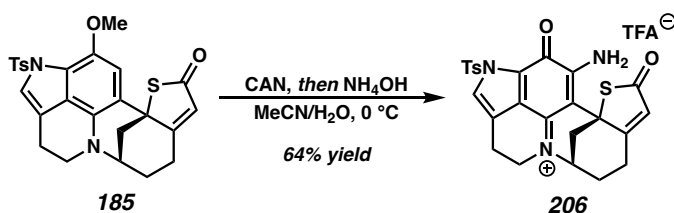
Doubly vinylogous dithiocarbonate **201**

To a ½-dram glass vial containing diene **195** (5.0 mg, 0.0102 mmol, 1.0 equiv) under nitrogen were added benzene (0.2 mL), thiophenol (5.2 μL, 0.051 mmol, 5.0 equiv), and Et₃N (14.2 μL, 0.102 mmol, 10 equiv). The reaction mixture was stirred at 23 °C for 75 min, whereafter it was loaded directly onto a silica gel flash column. Elution (10 → 25% EtOAc/hexanes) provided an intermediate sulfide as a colorless film (4.7 mg, 0.00782 mmol, 77% yield); ¹H NMR (600 MHz, C₆D₆) δ 7.86 (d, *J* = 8.0 Hz, 2H), 7.47 (s, 1H), 7.21 (d, *J* = 7.6 Hz, 2H), 7.04 – 6.94 (m, 3H), 6.90 (s, 1H), 6.62 (d, *J* = 8.0 Hz, 2H), 5.66 (d, *J* = 1.7 Hz, 1H), 3.62 – 3.52 (m, 1H), 3.31 (s, 3H), 3.14 (q, *J* = 3.1 Hz, 1H), 2.79 (dd, *J* = 12.8, 2.8 Hz, 1H), 2.67 – 2.60 (m, 1H), 2.51 – 2.38 (m, 3H), 2.33 (d, *J* = 14.8 Hz, 1H), 2.19 (dt, *J* = 12.5, 2.4 Hz, 1H), 2.10 (ddd, *J* = 14.8, 6.0, 1.8 Hz, 1H), 1.72 (s, 3H).

To a 1-dram glass vial containing this intermediate sulfide (3.2 mg, 0.00533 mmol, 1.0 equiv) under nitrogen was added CH₂Cl₂ (133 μL), and the vial was cooled to 0 °C in an ice bath. *m*-CPBA (77 wt %, 1.2 mg, 0.00535 mmol, 1.0 equiv) was added dropwise as a solution in CH₂Cl₂ (133 μL) and the reaction mixture was allowed to stir at 0 °C for 100 min. The solution was then diluted with EtOAc (1 mL), washed with saturated aq. K₂CO₃ (3x), dried over Na₂SO₄, and concentrated to provide a crude sulfoxide that was used directly in the next step.

To a ½-dram glass vial was added the crude sulfoxide as a solution in dry CH₂Cl₂ (0.25 mL). The vial was cooled to 0 °C, and pyridine (7.0 μL, 0.087 mmol, 16 equiv) and

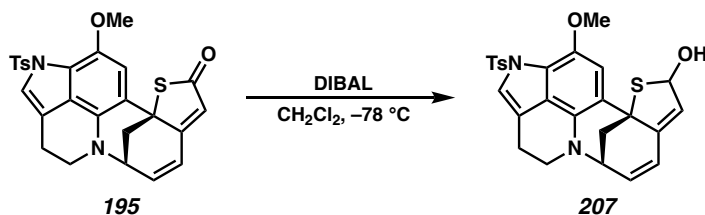
TFAA (7.5 μL , 0.054 mmol, 10 equiv) were added. The reaction mixture was stirred for 5 min at 0 $^{\circ}\text{C}$, then allowed to warm to 23 $^{\circ}\text{C}$ and stirred for an additional 14 h. MeOH (7 μL) was then added to quench excess TFAA, and the reaction mixture was loaded directly onto a silica gel flash column and eluted (25% EtOAc/hexanes). The product was combined with the product of another reaction conducted on a 0.0118 mmol scale to provide the title compound as an orange-red film (5.0 mg, 0.00835 mmol, 49% combined yield); ^1H NMR (400 MHz, C_6D_6) δ 7.83 – 7.76 (m, 2H), 7.47 (d, J = 1.7 Hz, 1H), 7.08 – 7.01 (m, 2H), 6.96 – 6.86 (m, 4H), 6.55 (d, J = 8.1 Hz, 2H), 5.80 (s, 1H), 5.11 (s, 1H), 3.54 (t, J = 3.2 Hz, 1H), 3.46 (td, J = 11.6, 3.9 Hz, 1H), 3.25 (s, 3H), 2.93 (ddd, J = 11.1, 4.9, 2.6 Hz, 1H), 2.68 – 2.57 (m, 1H), 2.53 (dt, J = 15.6, 3.3 Hz, 1H), 2.34 (dd, J = 12.2, 2.6 Hz, 1H), 2.00 (dd, J = 12.3, 3.8 Hz, 1H), 1.72 (s, 3H); ^{13}C NMR (100 MHz, C_6D_6) δ 195.4, 171.3, 145.0, 143.7, 141.4, 137.8, 134.4, 130.1, 129.8, 129.6, 129.3, 124.2, 123.0, 121.3, 118.5, 118.4, 114.3, 112.9, 108.8, 57.1, 56.8, 56.8, 50.1, 37.8, 23.2, 21.1 (2 additional aryl ^{13}C resonances are likely obscured by the solvent signal); IR (Neat Film, NaCl) 2924, 2853, 1678, 1593, 1503, 1348, 1281, 1173, 1108, 1022, 897, 810, 675 cm^{-1} ; HRMS (ESI $^{+}$): m/z calc'd for $\text{C}_{32}\text{H}_{27}\text{N}_2\text{O}_4\text{S}_3$ $[\text{M}+\text{H}]^{+}$: 599.1127, found 599.1120.



Pyrroloiminoquinone **206**

To a 1-dram glass vial containing thiolactone **185** (7.0 mg, 0.014 mmol, 1.0 equiv) was added MeCN (0.42 mL). The solution was cooled to 0 $^{\circ}\text{C}$ and CAN (15.6 mg, 0.0284 mmol, 2.0 equiv) was added dropwise as a solution in water (0.28 mL). The solution

became deep purple during addition, and the color rapidly faded to bright orange upon completion of the addition. After stirring for 3 min at 0 °C, concentrated aq. NH₄OH (50 μL) was added rapidly, leading to a dark purple color and a brown precipitate. The reaction mixture was stirred for an additional 30 min at 0 °C, then diluted with water (1 mL) and extracted with EtOAc (3x0.5 mL). The combined organic extracts were dried over Na₂SO₄ and concentrated under reduced pressure. The crude product was purified by preparative HPLC (C₁₈ column, 40→100% MeCN/H₂O with 0.1% TFA over 10 min at 5 mL/min) to afford the title compound as a purple film (5.3 mg, 0.0090 mmol, 64% yield); ¹H NMR (400 MHz, CD₃OD) δ 8.14 – 8.07 (m, 2H), 7.94 (t, *J* = 1.0 Hz, 1H), 7.49 – 7.40 (m, 2H), 6.19 (d, *J* = 1.3 Hz, 1H), 4.31 – 4.20 (m, 2H), 3.99 (ddd, *J* = 13.9, 5.9, 4.3 Hz, 1H), 3.17 – 3.09 (m, 2H), 2.97 (dt, *J* = 13.1, 2.8 Hz, 1H), 2.85 (dd, *J* = 13.6, 4.7 Hz, 1H), 2.56 – 2.46 (m, 2H), 2.44 (s, 3H), 2.34 (dd, *J* = 13.1, 2.5 Hz, 1H), 2.07 – 1.93 (m, 1H); ¹³C NMR (100 MHz, CD₃OD) δ 194.0, 173.7, 164.9, 155.0, 150.1, 147.4, 133.2, 129.8, 128.9, 128.5, 127.4, 124.3, 122.6, 118.3, 94.2, 57.7, 56.6, 51.5, 42.2, 31.5, 23.4, 20.3, 18.3; ¹⁹F NMR (376 MHz, CD₃OD) δ –77.2 (s); IR (Neat Film, NaCl) 3416, 3296, 3146, 2955, 1728, 1693, 1607, 1556, 1510, 1438, 1407, 1379, 1338, 1292, 1195, 1179, 1168, 1141, 1123, 1093, 1068, 991, 955, 785, 706, 666, 642, 626 cm⁻¹; HRMS (ESI⁺): *m/z* calc'd for C₂₅H₂₂N₃O₄S₂ [M+H]⁺: 492.1046, found 492.1057.



Thiolactol 207

To a 1-dram glass vial was added diene **195** (2.0 mg, 0.00408 mmol, 1.0 equiv). Traces of water were azeotropically removed by addition of three portions of benzene followed by rotary evaporation, the headspace of the vial was evacuated and flushed with nitrogen, and the starting material was taken up in CH_2Cl_2 (200 μL). The vial was cooled to $-78\text{ }^\circ\text{C}$, and freshly prepared DIBAL solution (0.4 M in CH_2Cl_2 , 0.10 mL, 0.040 mmol, 10 equiv) was added dropwise. A dark brown color initially formed and slowly faded to yield a colorless solution. After 5 min, 0.5 mL saturated aq. Rochelle's salt was injected at $-78\text{ }^\circ\text{C}$. The cooling bath was then removed at the mixture stirred vigorously at $23\text{ }^\circ\text{C}$ for 30 min. The layers were separated, and the aqueous phase was extracted with EtOAc (3x). The combined organic phases were dried over Na_2SO_4 and concentrated under reduced pressure to provide the title compound as a 5:1 mixture of diastereomers of sufficient purity for use in the next step (1.9 mg, 0.00386 mmol, 95% yield); ^1H NMR (400 MHz, C_6D_6) δ 7.91 – 7.86 (m, 2H), 7.57 (s, 1H), 7.45 (s, 1H), 6.59 (dd, $J = 8.3, 4.3$ Hz, 2H), 6.03 (d, $J = 9.8$ Hz, 1H, major diastereomer), 5.98 (d, $J = 9.8$ Hz, 1H, minor diastereomer), 5.84 – 5.79 (m, 1H), 5.55 – 5.45 (m, 1H), 5.25 (d, $J = 3.2$ Hz, 1H, major diastereomer), 5.16 (d, $J = 2.1$ Hz, 1H, minor diastereomer), 3.64 (s, 3H), 3.35 (ddd, $J = 5.1, 3.9, 2.3$ Hz, 1H), 2.73 – 2.62 (m, 3H), 2.55 (dt, $J = 12.0, 1.7$ Hz, 1H), 2.46 – 2.36 (m, 1H), 2.02 (dd, $J = 12.0, 3.9$ Hz, 1H), 1.95 – 1.84 (m, 1H), 1.71 (s, 3H); ^{13}C NMR (100 MHz, C_6D_6) δ 151.2, 143.5, 141.1, 138.1, 130.7, 129.4, 129.4, 129.0, 125.6, 124.0, 123.1, 122.5, 120.9, 119.4, 115.0, 112.1,

84.1, 59.6, 57.2, 53.9, 48.1, 38.8, 23.1, 21.1; IR (Neat Film, NaCl) 2927, 2856, 1684, 1500, 1460, 1361, 1285, 1225, 1173, 1107, 970, 897, 813, 755, 663 cm^{-1} ; HRMS (ESI+): m/z calc'd for $\text{C}_{26}\text{H}_{25}\text{N}_2\text{O}_4\text{S}_2$ $[\text{M}+\text{H}]^+$: 493.1250, found 493.1250.

2.11 REFERENCES AND NOTES

- (1) Zou, Y.; Wang, X.; Sims, J.; Wang, B.; Pandey, P.; Welsh, C. L.; Stone, R. P.; Avery, M. A.; Doerksen, R. J.; Ferreira, D.; Anklin, C.; Valeriote, F. A.; Kelly, M.; Hamann, M. T. Computationally Assisted Discovery and Assignment of a Highly Strained and PANC-1 Selective Alkaloid from Alaska's Deep Ocean. *J. Am. Chem. Soc.* **2019**, *141*, 4338–4344.
- (2) a) Tohma, H.; Harayama, Y.; Hashizume, M.; Iwata, M.; Egi, M.; Kita, Y. Synthetic Studies on the Sulfur-Cross-Linked Core of Antitumor Marine Alkaloid, Discorhabdins: Total Synthesis of Discorhabdin A. *Angew. Chem. Int. Ed.* **2002**, *41*, 348–350. b) Tohma, H.; Harayama, Y.; Hashizume, M.; Iwata, M.; Kiyono, Y.; Egi, M.; Kita, Y. The First Total Synthesis of Discorhabdin A. *J. Am. Chem. Soc.* **2003**, *125*, 11235–11240. c) Kita, Y.; Egi, M.; Tohma, H. Total synthesis of sulfur-containing pyrroloiminoquinone marine product, (\pm)-makaluvamine F using hypervalent iodine(III)-induced reactions. *Chem. Commun.* **1999**, 143–144. d) Nishiyama, S.; Cheng, J.; Tao, X.; Yamamura, S. Synthetic studies on novel sulfur-containing alkaloids, prianosins and discorhabdins: total synthesis of discorhabdin C. *Tetrahedron Lett.* **1991**, *32*, 4151–4154. e) Kita, Y.; Tohma, H.; Inagaki, M.; Hatanaka, K.; Yakura, T. Total synthesis of discorhabdin C: a general aza spiro dienone formation from O-silylated phenol derivatives using a hypervalent iodine reagent. *J. Am. Chem. Soc.* **1992**, *114*, 2175–2180. f) Aubart, K. M.; Heathcock, C. H. A Biomimetic Approach to the Discorhabdin Alkaloids: Total Syntheses of Discorhabdins C and E and Dethiadiscorhabdin D. *J. Org. Chem.* **1999**, *64*, 16–22.

- (3) For a review on pyrroloiminoquinone alkaloids and their synthesis, see: Hu, J.; Fan, H.; Xiong, J.; Wu, S. Discorhabdins and Pyrroloiminoquinone-Related Alkaloids. *Chem. Rev.* **2011**, *111*, 5465–5491.
- (4) Hofstra, J. L.; Poremba, K. E.; Shimozone, A. M.; Reisman, S. E. Nickel-Catalyzed Conversion of Enol Triflates into Alkenyl Halides. *Angew. Chem. Int. Ed.* **2019**, *58*, 14901–14905.
- (5) Horii, Z.; Hanaoka, M.; Yamawaki, Y.; Tamura, Y.; Saito, S.; Shigematsu, N.; Kotera, K.; Yoshikawa, H.; Sato, Y.; Nakai, H.; Sugimoto, N. The total synthesis of securinine and virosecurinine. *Tetrahedron* **1967**, *23*, 1165–1174.
- (6) SEGPPOS was previously used to effect enantioselective α -arylation of sterically similar substrates: Liao, X.; Weng, Z.; Hartwig, J. F. Enantioselective α -Arylation of Ketones with Aryl Triflates Catalyzed by Difluorophos Complexes of Palladium and Nickel. *J. Am. Chem. Soc.* **2008**, *130*, 195–200.
- (7) Johnson, T.; Pultar, F.; Menke, F.; Lautens, M. Palladium-Catalyzed α -Arylation of Vinylogous Esters for the Synthesis of γ,γ -Disubstituted Cyclohexenones. *Org. Lett.* **2016**, *18*, 6488–6491.
- (8) Gomes, R. D.; Corey, E. J. A Method for the Catalytic Enantioselective Synthesis of Chiral α -Azido and α -Amino Ketones from Racemic α -Bromo Ketones, and Its Generalization to the Formation of Bonds to C, O, and S. *J. Am. Chem. Soc.* **2019**, *141*, 20058–20061.
- (9) Drescher, K.; Haupt, A.; Unger, L.; Turner, S. C.; Braje, W.; Grandel, R.; Henry, C.; Backfisch, G.; Beyerbach, A.; Lubisch, W. Heterocyclic compounds suitable

- for treating disorders that respond to modulation of the dopamine D3 receptor. US Patent 7851463B2, December 14, 2010.
- (10) Boyd, E. M.; Sperry, J. Synthetic studies towards dendridine A: synthesis of *hemi-dendridine A* acetate by Fischer indolization. *Tetrahedron Lett.* **2012**, *53*, 3623–3626.
- (11) Koike, T.; Hoashi, Y.; Tomata, Y. Heterocyclic Compound and Use Thereof. US Patent Application 20120142672A1, June 7, 2012.
- (12) Conditions derived from: Lombardo, V. M.; Thomas, C. D.; Scheidt, K. A. A Tandem Isomerization/Prins Strategy: Iridium(III)/Brønsted Acid Cooperative Catalysis. *Angew. Chem. Int. Ed.* **2013**, *52*, 12910–12914.
- (13) Liu, Y.; Liniger, M.; McFadden, R. M.; Roizen, J. L.; Malette, J.; Reeves, C. M.; Behenna, D. C.; Seto, M.; Kim, J.; Mohr, J. T.; Virgil, S. C.; Stoltz, B. M. Formal total syntheses of classic natural product target molecules via palladium-catalyzed enantioselective alkylation. *Beilstein J. Org. Chem.* **2014**, *10*, 2501–2512.
- (14) Informed by the conditions reported by Lautens and coworkers in ref 7.
- (15) Bichovski, P.; Haas, T. M.; Kratzert, D.; Streuff, J. Synthesis of Bridged Benzazocines and Benzoxocines by a Titanium-Catalyzed Double-Reductive Umpolung Strategy. *Chem. Eur. J.* **2015**, *21*, 2339–2342.
- (16) White, J. D.; Yager, K. M.; Yakura, T. Synthetic Studies of the Pyrroloquinoline Nucleus of the Makaluvamine Alkaloids. Synthesis of the Topoisomerase II Inhibitor Makaluvamine D. *J. Am. Chem. Soc.* **1994**, *116*, 1831–1838.

- (17) Köhling, P.; Schmidt, A. M.; Eilbracht, P. Tandem Hydroformylation/Fischer Indole Synthesis: A Novel and Convenient Approach to Indoles from Olefins. *Org. Lett.* **2003**, *5*, 3213–3216.
- (18) a) Wagaw, S.; Yang, B. H.; Buchwald, S. L. A Palladium-Catalyzed Strategy for the Preparation of Indoles: A Novel Entry into the Fischer Indole Synthesis. *J. Am. Chem. Soc.* **1998**, *120*, 6621–6622. b) Wagaw, S.; Yang, B. H.; Buchwald, S. L. A Palladium-Catalyzed Method for the Preparation of Indoles via the Fischer Indole Synthesis. *J. Am. Chem. Soc.* **1999**, *121*, 10251–10263.
- (19) Thibeault, C.; Clark, C. G.; DeLucca, I.; Hu, C. H.; Jeon, Y.; Lam, P. Y. S.; Qiao, J. X.; Yang, W.; Wang, Y.; Wang, T. C. 7-hydroxy-spiropiperidine indoliny1 antagonists of p2y1 receptor. U.S. Patent 9428504B2, August 30, 2016.
- (20) Schmidt, M. A. Effect of Terminal Alkylation of Aryl and Heteroaryl Hydrazines in the Fischer Indole Synthesis. *J. Org. Chem.* **2022**, *87*, 1941–1960.
- (21) Bernhardson, D. J.; Widlicka, D. W.; Singer, R. A. Cu-Catalyzed Couplings of Heteroaryl Primary Amines and (Hetero)aryl Bromides with 6-Hydroxypicolinamide Ligands. *Org. Process Res. Dev.* **2019**, *23*, 1538–1551.
- (22) Maiti, D.; Fors, B. P.; Henderson, J. L.; Nakamura, Y.; Buchwald, S. L. Palladium-catalyzed coupling of functionalized primary and secondary amines with aryl and heteroaryl halides: two ligands suffice in most cases. *Chem. Sci.* **2011**, *2*, 57–68.
- (23) Wolfe, J. P.; Buchwald, S. L. Nickel-Catalyzed Amination of Aryl Chlorides. *J. Am. Chem. Soc.* **1997**, *119*, 6054–6058.

- (24) Xu, H.; Wolf, C. Copper catalyzed coupling of aryl chlorides, bromides and iodides with amines and amides. *Chem. Commun.* **2009**, 1715–1717.
- (25) Zhou, W.; Fan, M.; Yin, J.; Jiang, Y.; Ma, D. CuI/Oxalic Diamide Catalyzed Coupling Reaction of (Hetero)Aryl Chlorides and Amines. *J. Am. Chem. Soc.* **2015**, *137*, 11942–11945.
- (26) Cassis, R.; Tapia, R.; Valderrama, J. A. Synthesis of 4(1H)-Quinolones by Thermolysis of Arylaminomethylene Meldrum's Acid Derivatives. *Synth. Comm.* **1985**, *15*, 125–133.
- (27) De, K.; Legros, J.; Crousse, B.; Bonnet-Delpon, D. Solvent-Promoted and -Controlled Aza-Michael Reaction with Aromatic Amines. *J. Org. Chem.* **2009**, *74*, 6260–6265.
- (28) Bayindir, S.; Erdogan, E.; Kilic, H.; Saracoglu, N. An Efficient Synthesis of New Aza-Substituted Indoles via Michael-Type Addition. *Synlett* **2010**, 1455–1458.
- (29) Kim, S.; Kang, S.; Kim, G.; Lee, Y. Copper-Catalyzed Aza-Michael Addition of Aromatic Amines or Aromatic Aza-Heterocycles to α,β -Unsaturated Olefins. *J. Org. Chem.* **2016**, *81*, 4048–4057.
- (30) Verma, A. K.; Attri, P.; Chopra, V.; Tiwari, R. K.; Chandra, R. Triethylammonium acetate (TEAA): a recyclable inexpensive ionic liquid promotes the chemoselective aza- and thia-Michael reactions. *Monatsh. Chem.* **2008**, *139*, 1041–1047.

- (31) Gupta, A.; Condakes, M. L. Thermodynamic Understanding of an Aza-Michael Reaction Enables Five-Step Synthesis of the Potent Integrin Inhibitor MK-0429. *J. Org. Chem.* **2021**, *86*, 17523–17527.
- (32) Namba, K.; Cui, S.; Wang, J.; Kishi, Y. A New Method for Translating the Asymmetric Ni/Cr-Mediated Coupling Reactions from Stoichiometric to Catalytic. *Org. Lett.* **2005**, *7*, 5417–5419.
- (33) Quan, L. G.; Lamrani, M.; Yamamoto, Y. Intramolecular Nucleophilic Addition of Aryl Bromides to Ketones Catalyzed by Palladium. *J. Am. Chem. Soc.* **2000**, *122*, 4827–4828.
- (34) Gregoire, B.; Carre, M. C.; Caubere, P. Arynic condensation of ketone enolates. 17. New general access to benzocyclobutene derivatives. *J. Org. Chem.* **1986**, *51*, 1419–1427.
- (35) Chen, M.; Dong, G. Copper-Catalyzed Desaturation of Lactones, Lactams, and Ketones under pH-Neutral Conditions. *J. Am. Chem. Soc.* **2019**, *141*, 14889–14897.
- (36) a) Zhou, P.; Xu, T. Nickel-catalyzed intramolecular desymmetrization addition of aryl halides to 1,3-diketones. *Chem. Commun.* **2020**, *56*, 8194–8197. b) Li, Y.; Li, W.; Tian, J.; Huang, G.; Lv, H. Nickel-Catalyzed Asymmetric Addition of Aromatic Halides to Ketones: Highly Enantioselective Synthesis of Chiral 2,3-Dihydrobenzofurans Containing a Tertiary Alcohol. *Org. Lett.* **2020**, *22*, 5353–5357.

- (37) Saadi, J.; Bentz, C.; Redies, K.; Lentz, D.; Zimmer, R.; Reissig, H.
Stereoselective synthesis of tricyclic compounds by intramolecular palladium-catalyzed addition of aryl iodides to carbonyl groups. *Beilstein J. Org. Chem.* **2016**, *12*, 1236–1242.
- (38) Select examples: a) Yu, J.; Wu, H.; Corey, E. J. Pd(OH)₂/C-Mediated Selective Oxidation of Silyl Enol Ethers by *tert*-Butylhydroperoxide, a Useful Method for the Conversion of Ketones to α,β -Enones or β -Silyloxy- α,β -enones. *Org. Lett.* **2005**, *7*, 1415–1417. b) Sparling, B. A.; Moebius, D. C.; Shair, M. D. Enantioselective Total Synthesis of Hyperforin. *J. Am. Chem. Soc.* **2013**, *135*, 644–647. c) Tucker, J. K.; Shair, M. D. Catalytic Allylic Oxidation to Generate Vinylogous Acyl Sulfonates from Vinyl Sulfonates. *Org. Lett.* **2019**, *21*, 2473–2476.
- (39) Desmaële, D.; d'Angelo, J. Stereocontrolled Elaboration of Quaternary Carbon Centers through the Asymmetric Michael Reaction Using Chiral Imines: Enantioselective Synthesis of (+)-Aspidospermidine. *J. Org. Chem.* **1994**, *59*, 2292–2303.
- (40) Inouye, Y.; Kojima, T.; Owada, J.; Kakisawa, H. Preparation of Bicyclo[3.3.1]nonane-2,4-dione Derivatives. *Bull. Chem. Soc. Jpn.* **1987**, *60*, 4369–4375.
- (41) Andersen, H. S.; Olsen, O. H.; Iversen, L. F.; Sørensen, A. L. P.; Mortensen, S. B.; Christensen, M. S.; Branner, S.; Hansen, T. K.; Lau, J. F.; Jeppesen, L.; Moran, E. J.; Su, J.; Bakir, F.; Judge, L.; Shahbaz, M.; Collins, T.; Vo, T.; Newman, M. J.;

- Ripka, W. C.; Møller, N. P. H. Discovery and SAR of a Novel Selective and Orally Bioavailable Nonpeptide Classical Competitive Inhibitor Class of Protein-Tyrosine Phosphatase 1B. *J. Med. Chem.* **2002**, *45*, 4443–4459.
- (42) Lee, O.; Law, K.; Ho, C.; Yang, D. Highly Chemoselective Reductive Amination of Carbonyl Compounds Promoted by InCl₃/Et₃SiH/MeOH System. *J. Org. Chem.* **2008**, *73*, 8829–8837.
- (43) a) Liu, J.; Xu, X.; Li, J.; Liu, B.; Jiang, H.; Yin, B. Palladium-catalyzed dearomatizing 2,5-alkoxyarylation of furan rings: diastereospecific access to spirooxindoles. *Chem. Commun.* **2016**, *52*, 9550–9553. b) Li, J.; Peng, H.; Wang, F.; Wang, X.; Jiang, H.; Yin, B. 2,5-Oxyarylation of Furans: Synthesis of Spiroacetals via Palladium-Catalyzed Aerobic Oxidative Coupling of Boronic Acids with α -Hydroxyalkylfurans. *Org. Lett.* **2016**, *18*, 3226–3229. c) For an example of a similar transformation of naphthalenes, see: Yang, P.; Zheng, C.; Nie, Y.; You, S. Palladium-catalyzed dearomative 1,4-difunctionalization of naphthalenes. *Chem. Sci.* **2020**, *11*, 6830–6835.
- (44) Wertjes, W. C.; Southgate, E. H.; Sarlah, D. Recent advances in chemical dearomatization of nonactivated arenes. *Chem. Soc. Rev.* **2018**, *47*, 7996–8017.
- (45) a) Rousseaux, S.; García-Fortanet, J.; Sanchez, M. A. D. A.; Buchwald, S. L. Palladium(0)-Catalyzed Arylative Dearomatization of Phenols. *J. Am. Chem. Soc.* **2011**, *133*, 9282–9285. b) Xu, R.; Gu, Q.; Wu, W.; Zhao, Z.; You, S. Construction of Erythrinane Skeleton via Pd(0)-Catalyzed Intramolecular Dearomatization of *para*-Aminophenols. *J. Am. Chem. Soc.* **2014**, *136*,

- 15469–15472. c) Du, K.; Guo, P.; Chen, Y.; Cao, Z.; Wang, Z.; Tang, W. Enantioselective Palladium-Catalyzed Dearomative Cyclization for the Efficient Synthesis of Terpenes and Steroids. *Angew. Chem. Int. Ed.* **2015**, *54*, 3033–3037.
- (46) Representative example: Zhao, G.; Xu, G.; Qian, C.; Tang, W. Efficient Enantioselective Syntheses of (+)-Dalesconol A and B. *J. Am. Chem. Soc.* **2017**, *139*, 3360–3363.
- (47) a) Bedford, R. B.; Butts, C. P.; Haddow, M. F.; Osborne, R.; Sankey, R. F. Reactive 4a-alkyl-4aH carbazoles by catalytic dearomatisation, and their unusual dimerisation and dealkylation reactions. *Chem. Commun.* **2009**, 4832–4834. b) García-Fortanet, J.; Kessler, F.; Buchwald, S. L. Palladium-Catalyzed Asymmetric Dearomatization of Naphthalene Derivatives. *J. Am. Chem. Soc.* **2009**, *131*, 6676–6677.
- (48) a) Kita, Y.; Tohma, H.; Inagaki, M.; Hatanaka, K.; Yakura, T. A novel oxidative azidation of aromatic compounds with hypervalent iodine reagent, phenyliodine(III) bis(trifluoroacetate) (PIFA) and trimethylsilyl azide. *Tetrahedron Lett.* **1991**, *32*, 4321–4324. b) Kita, Y.; Tohma, H.; Hatanaka, K.; Takada, T.; Fujita, S.; Mitoh, S.; Sakurai, H.; Oka, S. Hypervalent Iodine-Induced Nucleophilic Substitution of para-Substituted Phenol Ethers. Generation of Cation Radicals as Reactive Intermediates. *J. Am. Chem. Soc.* **1994**, *116*, 3684–3691.
- (49) Benati, L.; Bencivenni, G.; Leardini, R.; Minozzi, M.; Nanni, D.; Scialpi, R.; Spagnolo, P.; Zanardi, G. Radical Reduction of Aromatic Azides to Amines with Triethylsilane. *J. Org. Chem.* **2006**, *71*, 5822–5825.

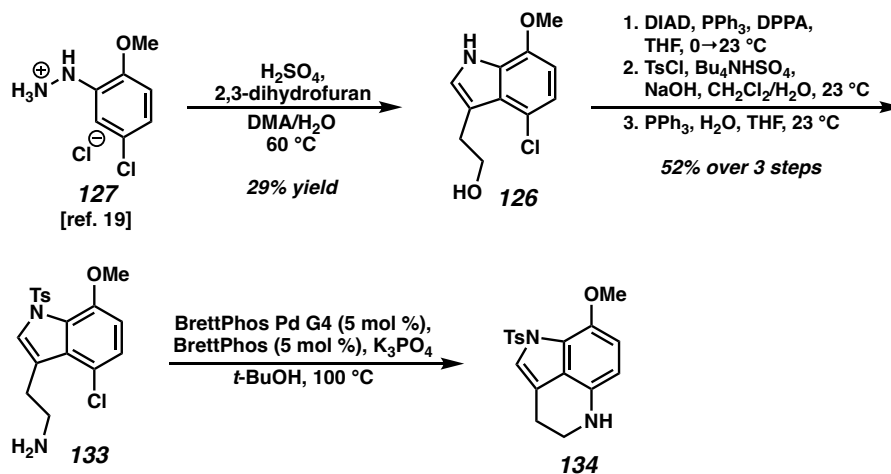
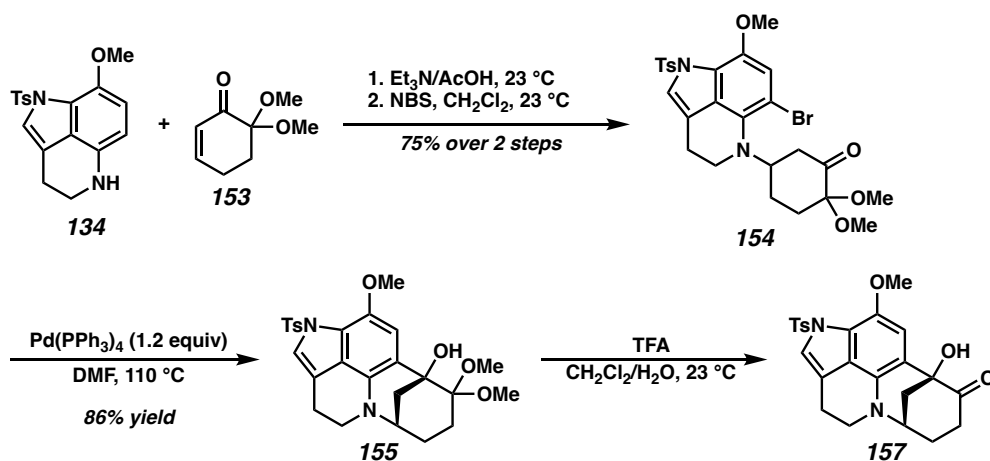
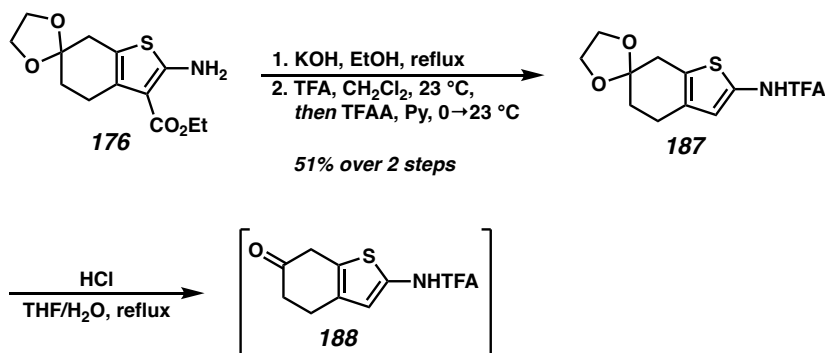
- (50) More classical Staudinger reduction conditions failed to promote the desired reduction in our hands.
- (51) Chen, Y.; Romaine, J. P.; Newhouse, T. R. Palladium-Catalyzed α,β -Dehydrogenation of Esters and Nitriles. *J. Am. Chem. Soc.* **2015**, *137*, 5875–5878.
- (52) Diao, T.; Stahl, S. Synthesis of Cyclic Enones via Direct Palladium-Catalyzed Aerobic Dehydrogenation of Ketones. *J. Am. Chem. Soc.* **2011**, *133*, 14566–14569.
- (53) Diao, T.; Wadzinski, T. J.; Stahl, S. S. Direct aerobic α,β -dehydrogenation of aldehydes and ketones with a Pd(TFA)₂/4,5-diazafluorenone catalyst. *Chem. Sci.* **2012**, *3*, 887.
- (54) Yang, M.; Yin, F.; Fujino, H.; Snyder, S. A. The Total Synthesis of Chalcitrin. *J. Am. Chem. Soc.* **2019**, *141*, 4515–4520.
- (55) Dherange, B. D.; Yuan, M.; Kelly, C. B.; Reiher, C. A.; Grosanu, C.; Berger, K. J.; Gutierrez, O.; Levin, M. D. Direct Deaminative Functionalization. *J. Am. Chem. Soc.* **2023**, *145*, 17–24.
- (56) Pangborn, A. M.; Giardello, M. A.; Grubbs, R. H.; Rosen, R. K.; Timmers, F. J. Safe and Convenient Procedure for Solvent Purification. *Organometallics* **1996**, *15*, 1518–1520.
- (57) Clerici, A.; Pastori, N.; Porta, O. Mild acetalisation of mono and dicarbonyl compounds catalysed by titanium tetrachloride. Facile synthesis of β -keto enol ethers. *Tetrahedron* **2001**, *57*, 217–225.

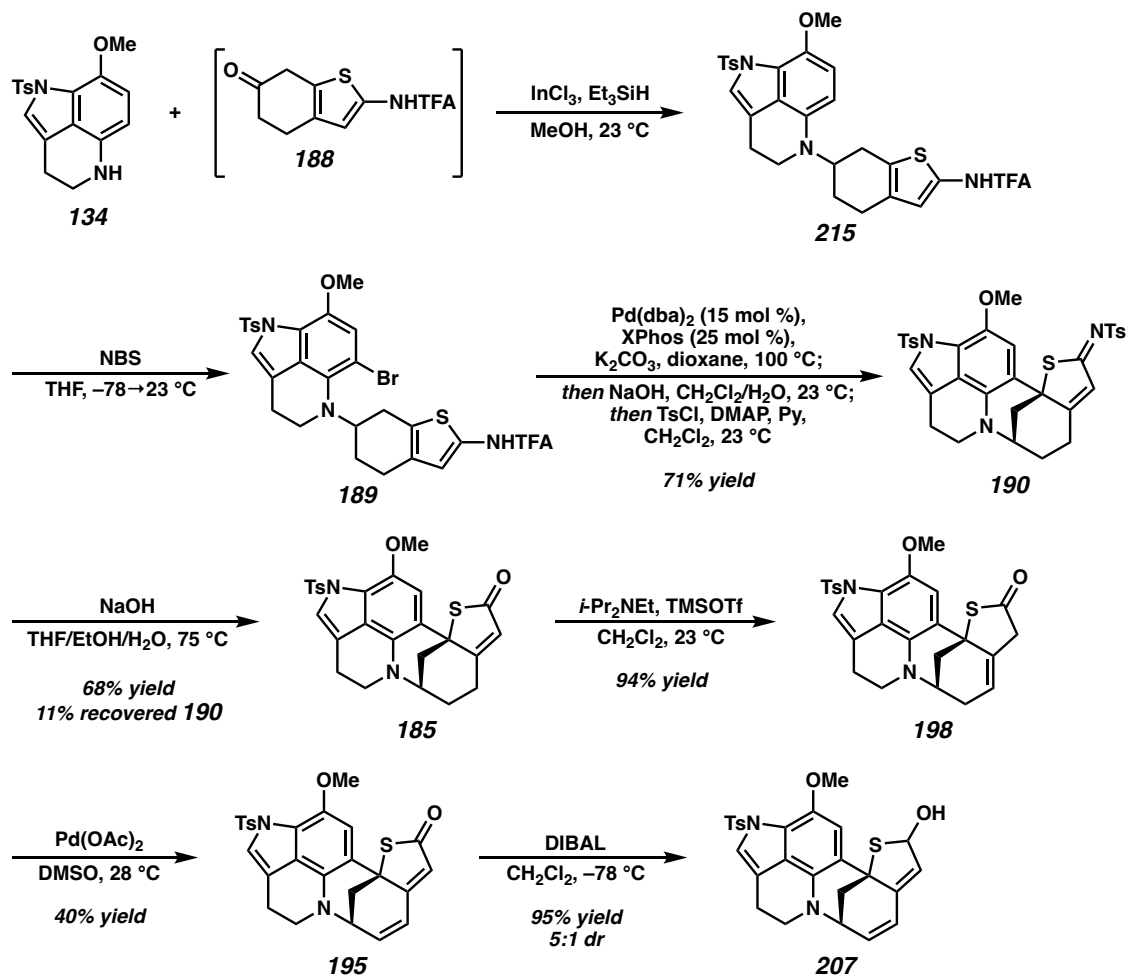
- (58) Fujiki, K.; Tanifuji, N.; Sasaki, Y.; Yokoyama, T. New and Facile Synthesis of Thiosulfonates from Sulfinate/Disulfide/I₂ System. *Synthesis* **2002**, 343–348.
- (59) Oshiyama, T.; Satoh, T.; Okano, K.; Tokuyama, H. Total synthesis of makaluvamine A/D, damirone B, batzelline C, makaluvone, and isobatzelline C featuring one-pot benzyne-mediated cyclization/functionalization. *Tetrahedron* **2012**, *68*, 9376–9383.

APPENDIX 3

Synthetic Summary for Chapter 2:

Progress Toward the Total Synthesis of Aleutianamine

Scheme A3.1. Synthesis of tricyclic aniline 134.**Scheme A3.2. Synthesis of hydroxyketone 157.****Scheme A3.3. Synthesis of aminothiophene 188.**

Scheme A3.3. Synthesis of thiolactol **207**.

APPENDIX 4

Spectra Relevant to Chapter 2:

Progress Toward the Total Synthesis of Aleutianamine

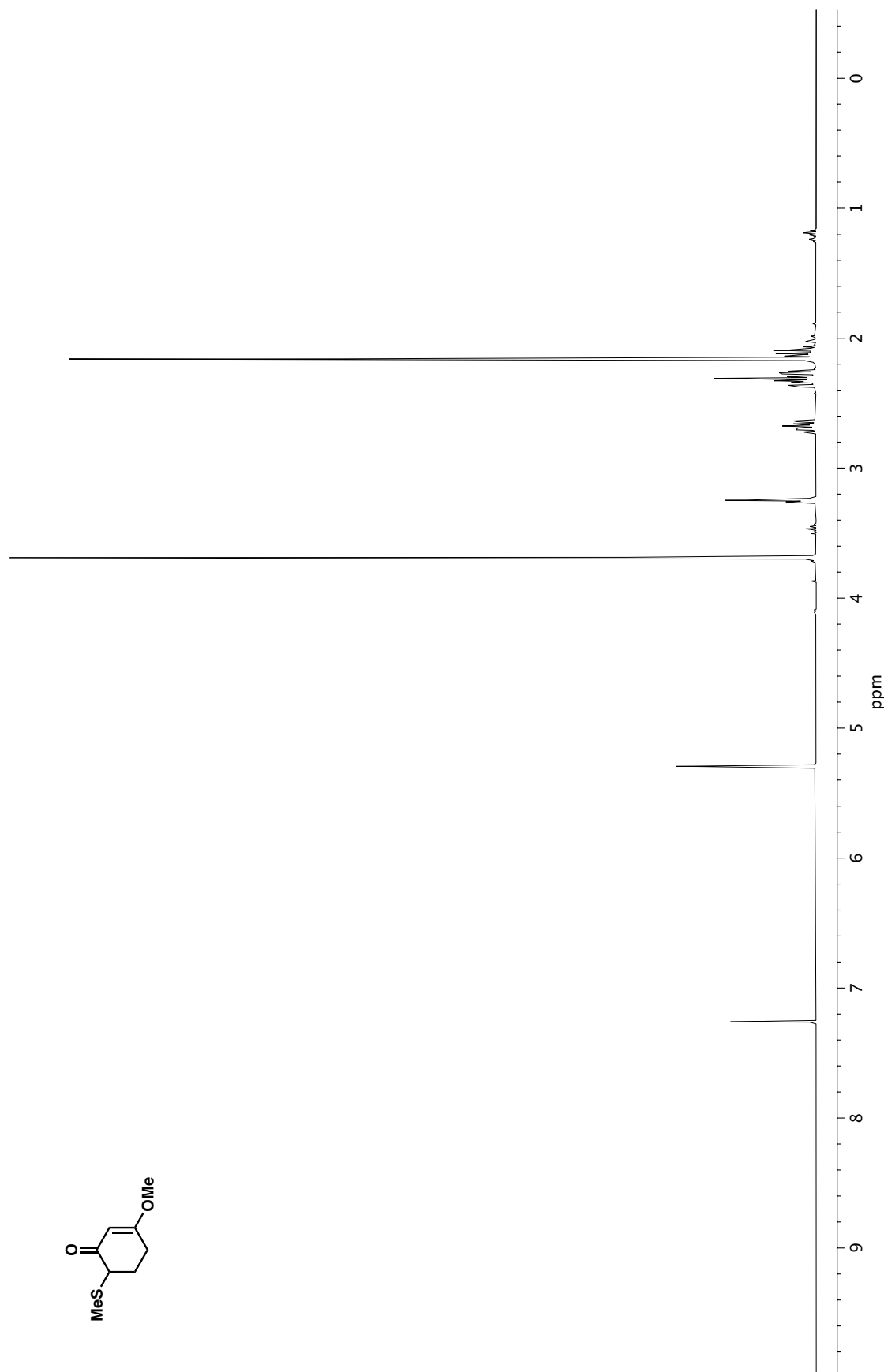


Figure A4.1. ^1H NMR (400 MHz, CDCl_3) of compound **96**.

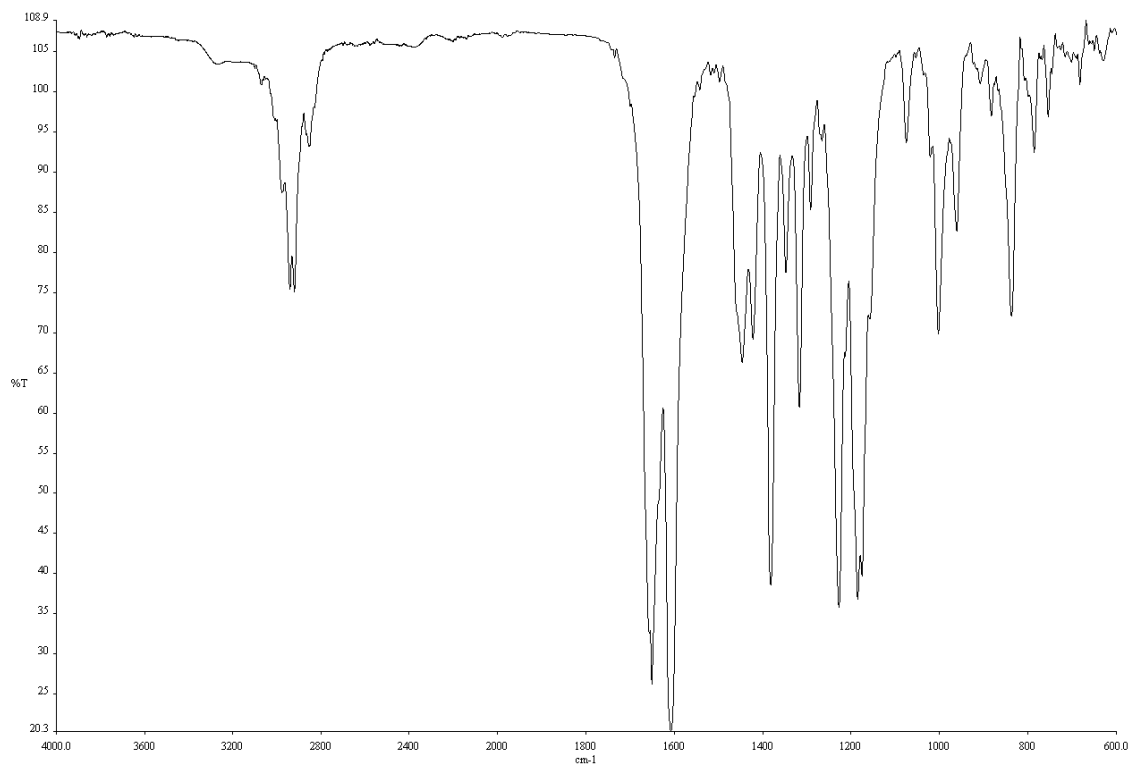


Figure A4.2. Infrared spectrum (Thin Film, NaCl) of compound **96**.

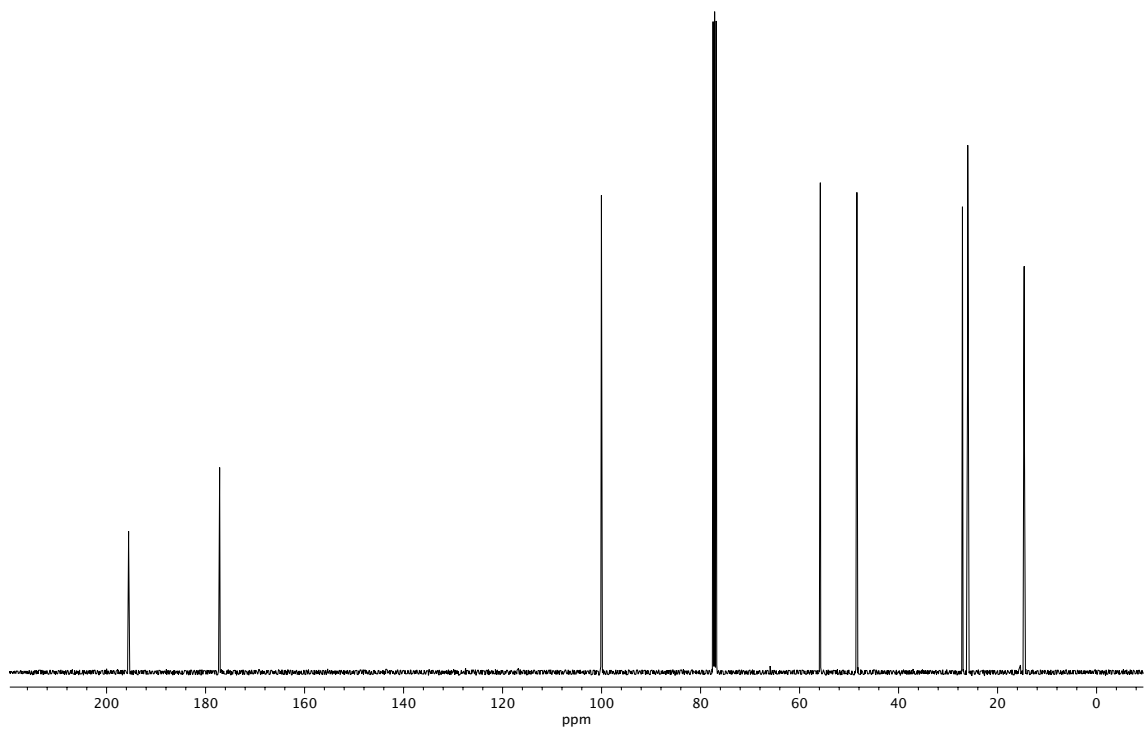
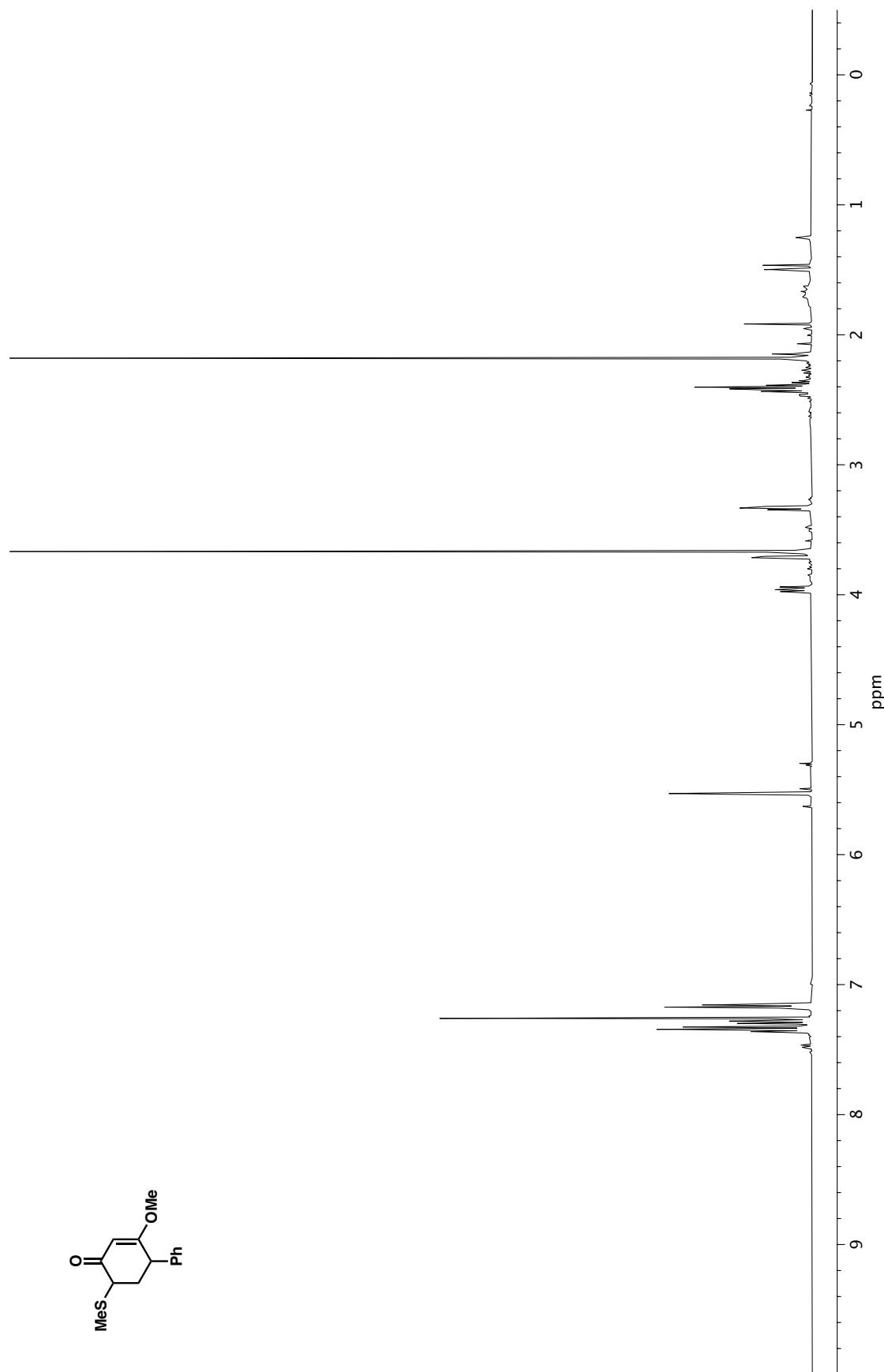


Figure A4.3. ^{13}C NMR (100 MHz, CDCl_3) of compound **96**.



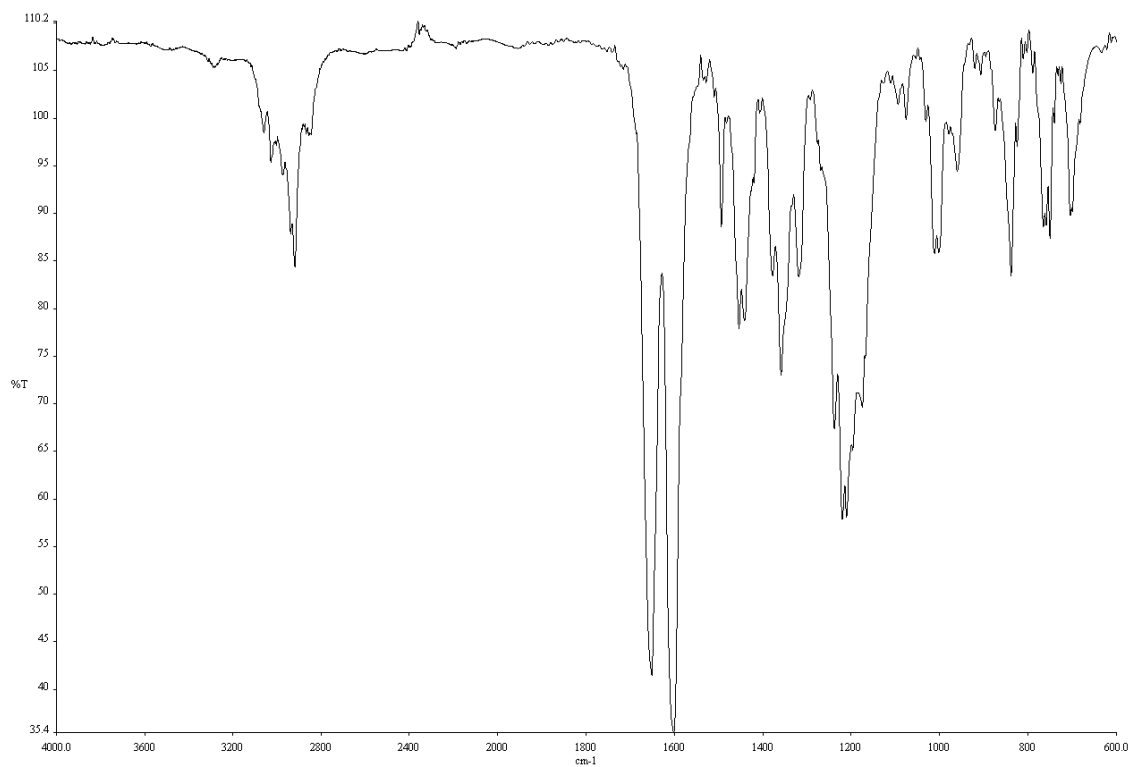


Figure A4.5. Infrared spectrum (Thin Film, NaCl) of compound **97**.

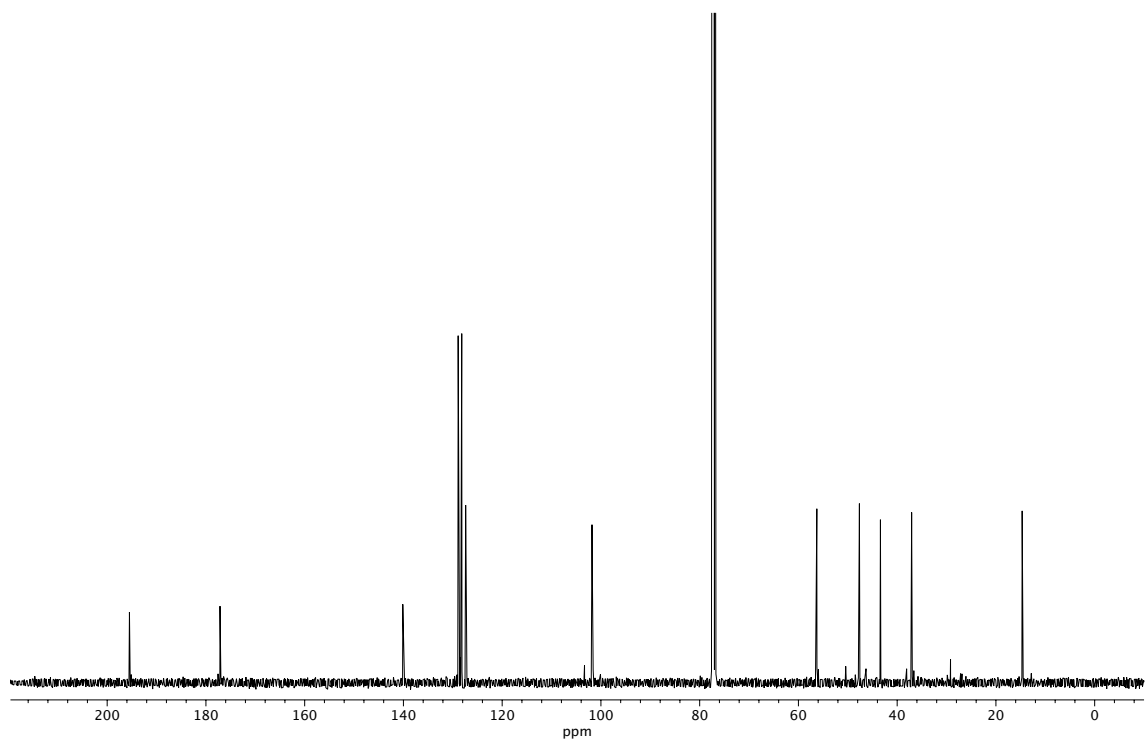
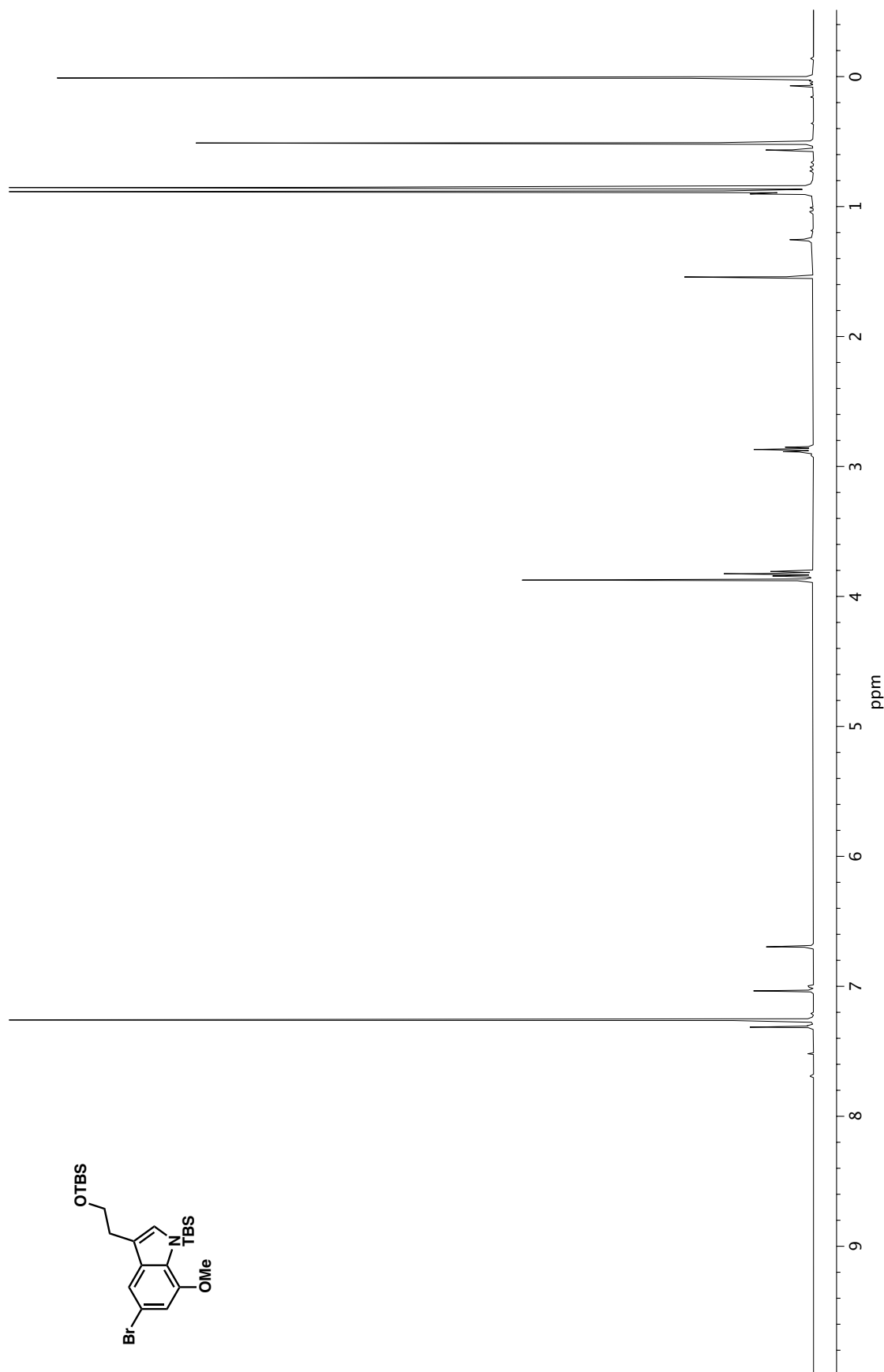


Figure A4.6. ¹³C NMR (100 MHz, CDCl₃) of compound **97**.



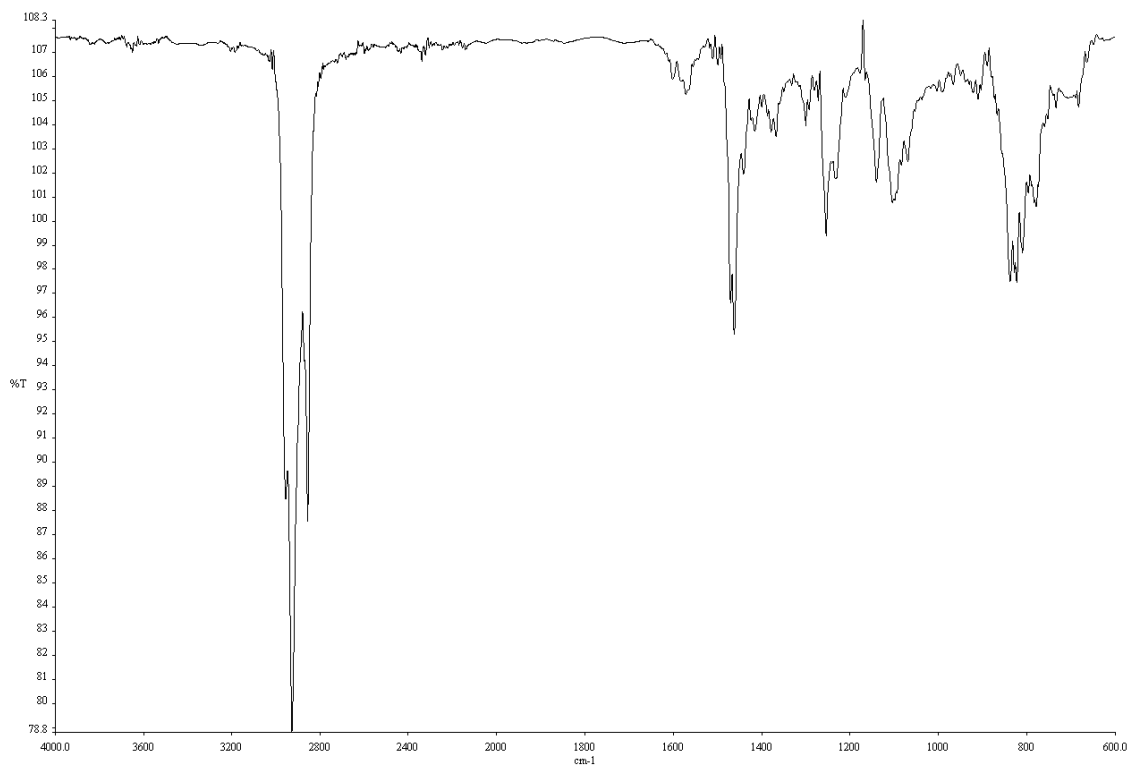


Figure A4.8. Infrared spectrum (Thin Film, NaCl) of compound **107**.

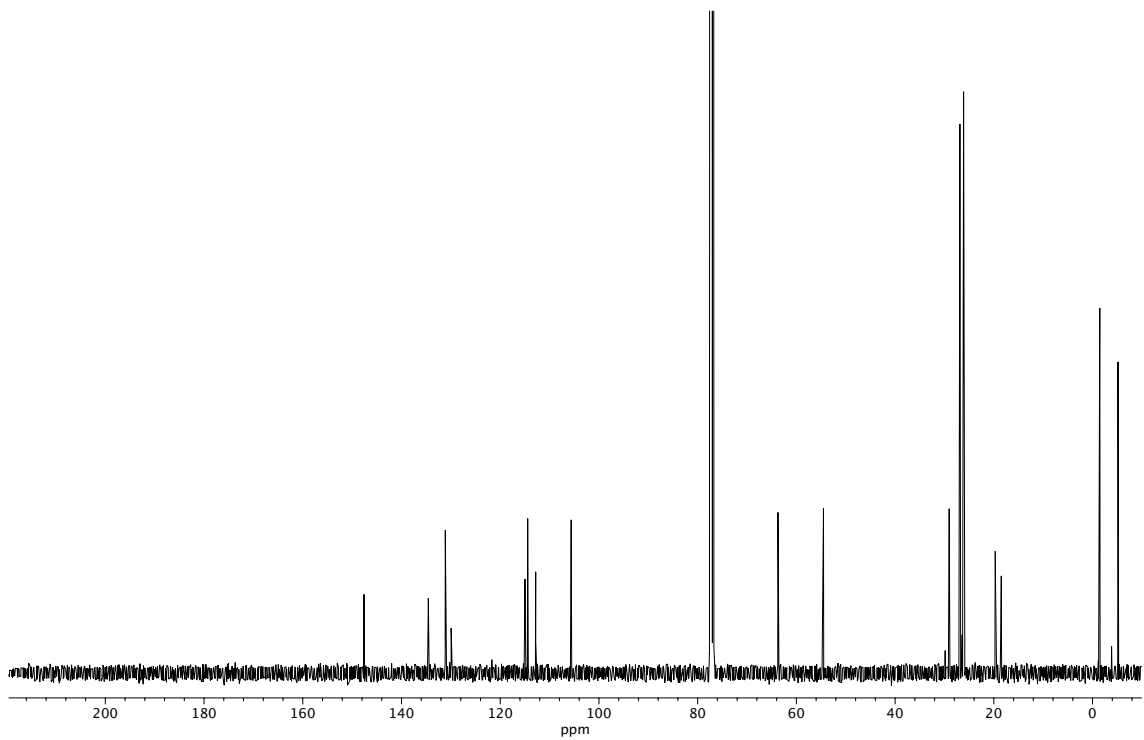
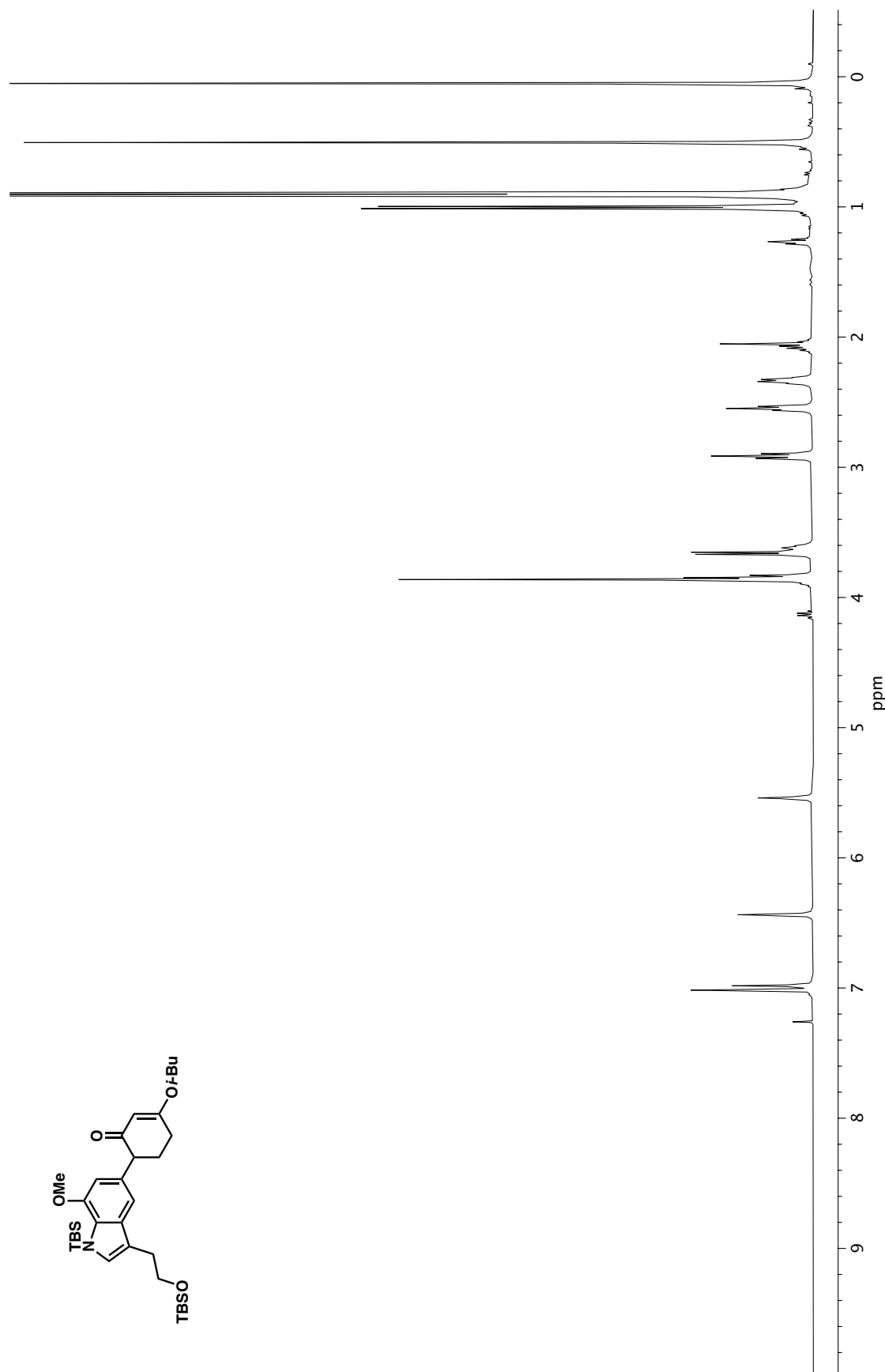


Figure A4.9. ^{13}C NMR (100 MHz, CDCl_3) of compound **107**.

Figure A4.10. $^1\text{H NMR}$ (400 MHz, CDCl_3) of compound **109**.

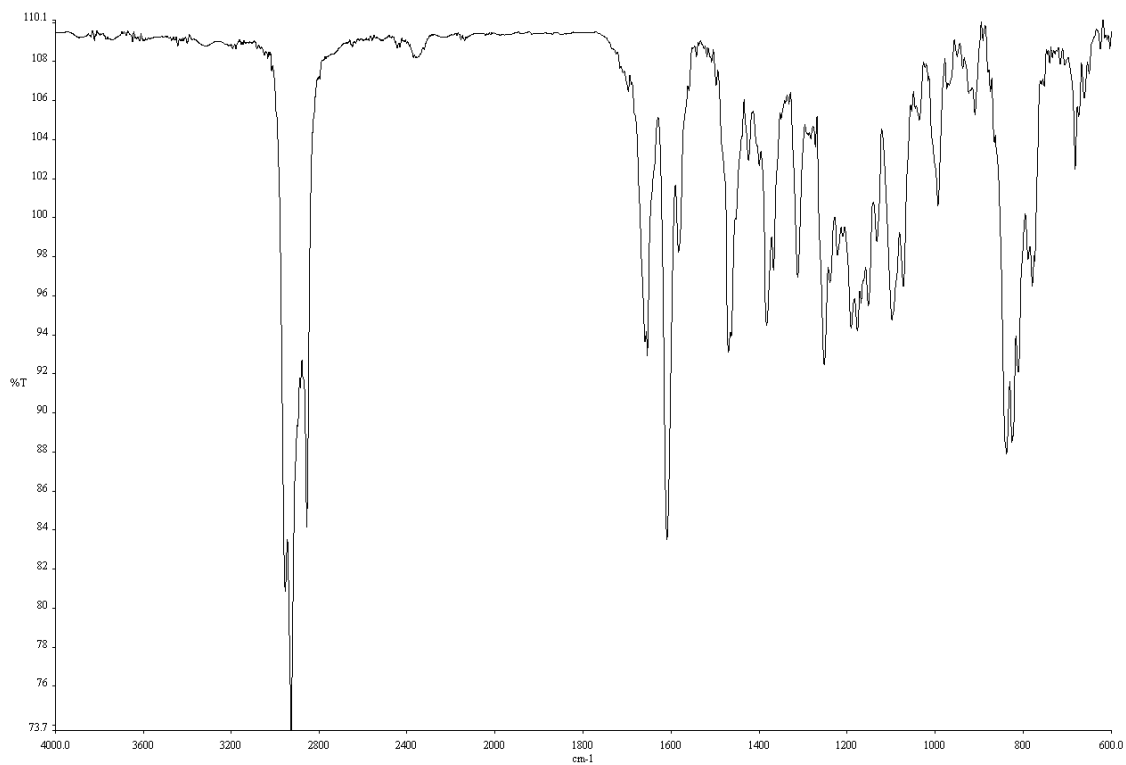


Figure A4.11. Infrared spectrum (Thin Film, NaCl) of compound **109**.

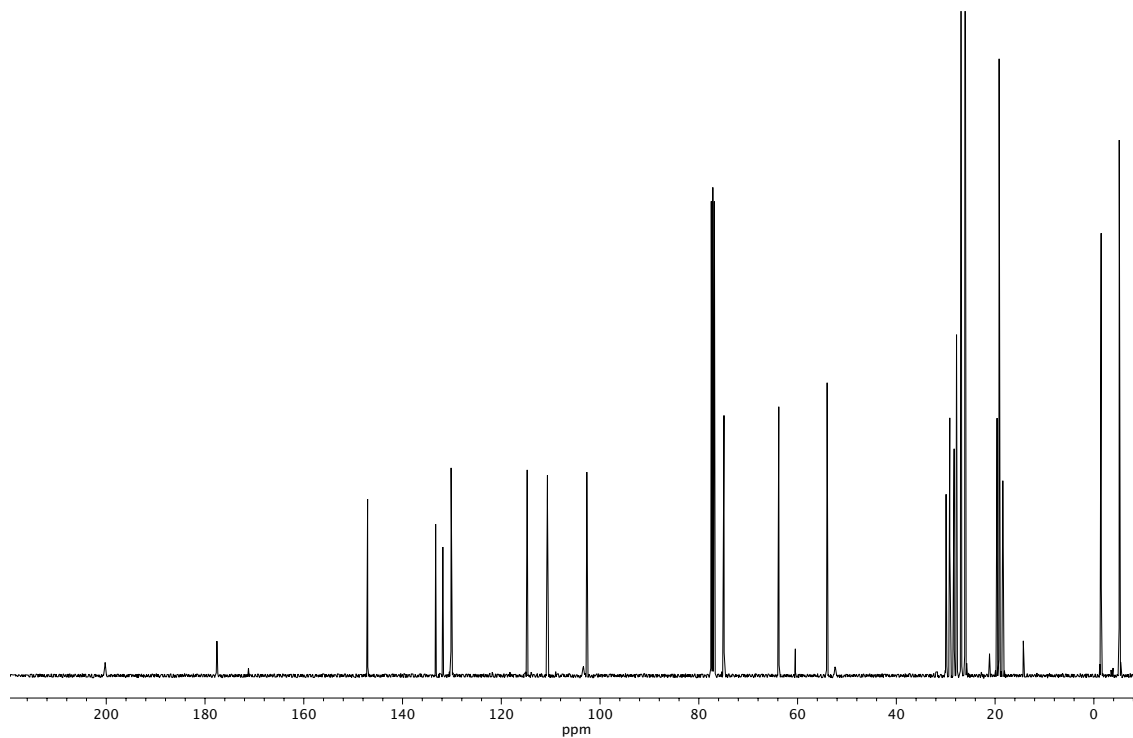
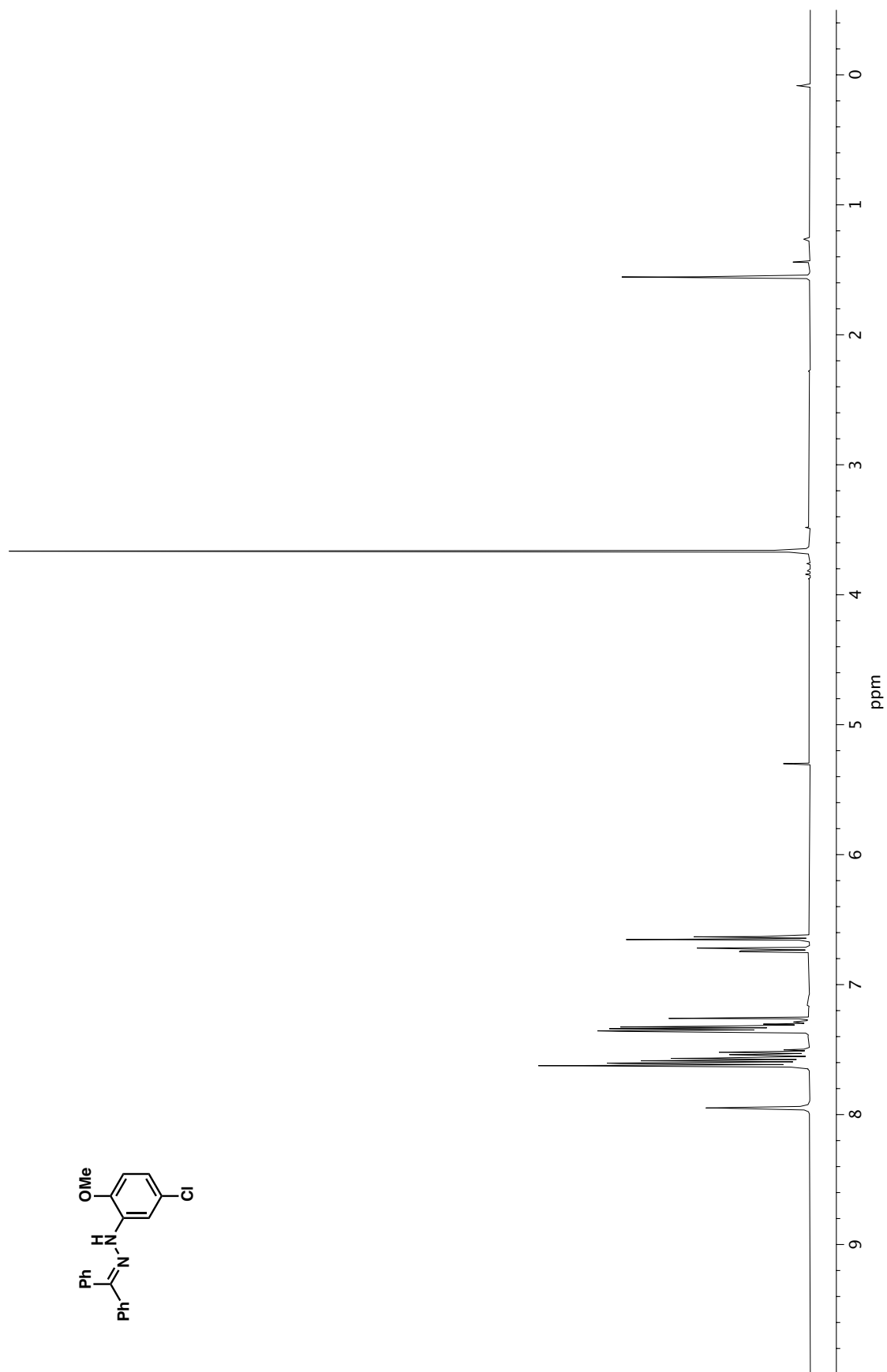


Figure A4.12. ¹³C NMR (100 MHz, CDCl₃) of compound **109**.

Figure A4.13. ¹H NMR (400 MHz, CDCl₃) of compound **125**.

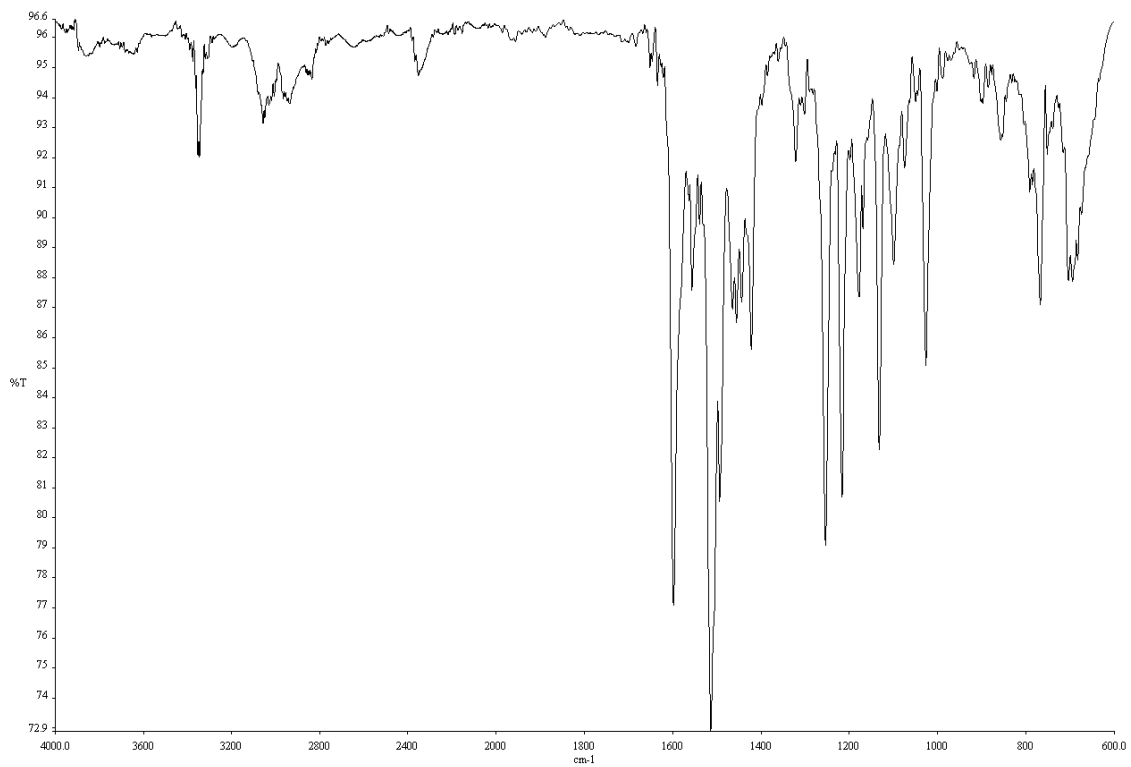


Figure A4.14. Infrared spectrum (Thin Film, NaCl) of compound **125**.

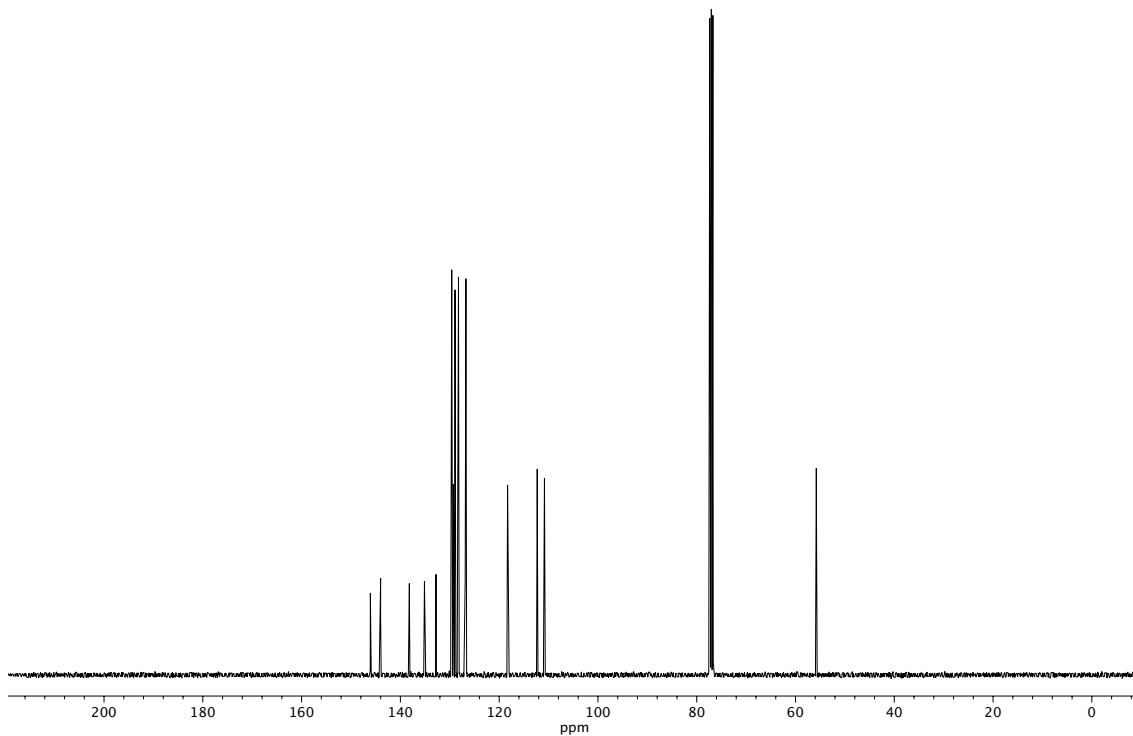
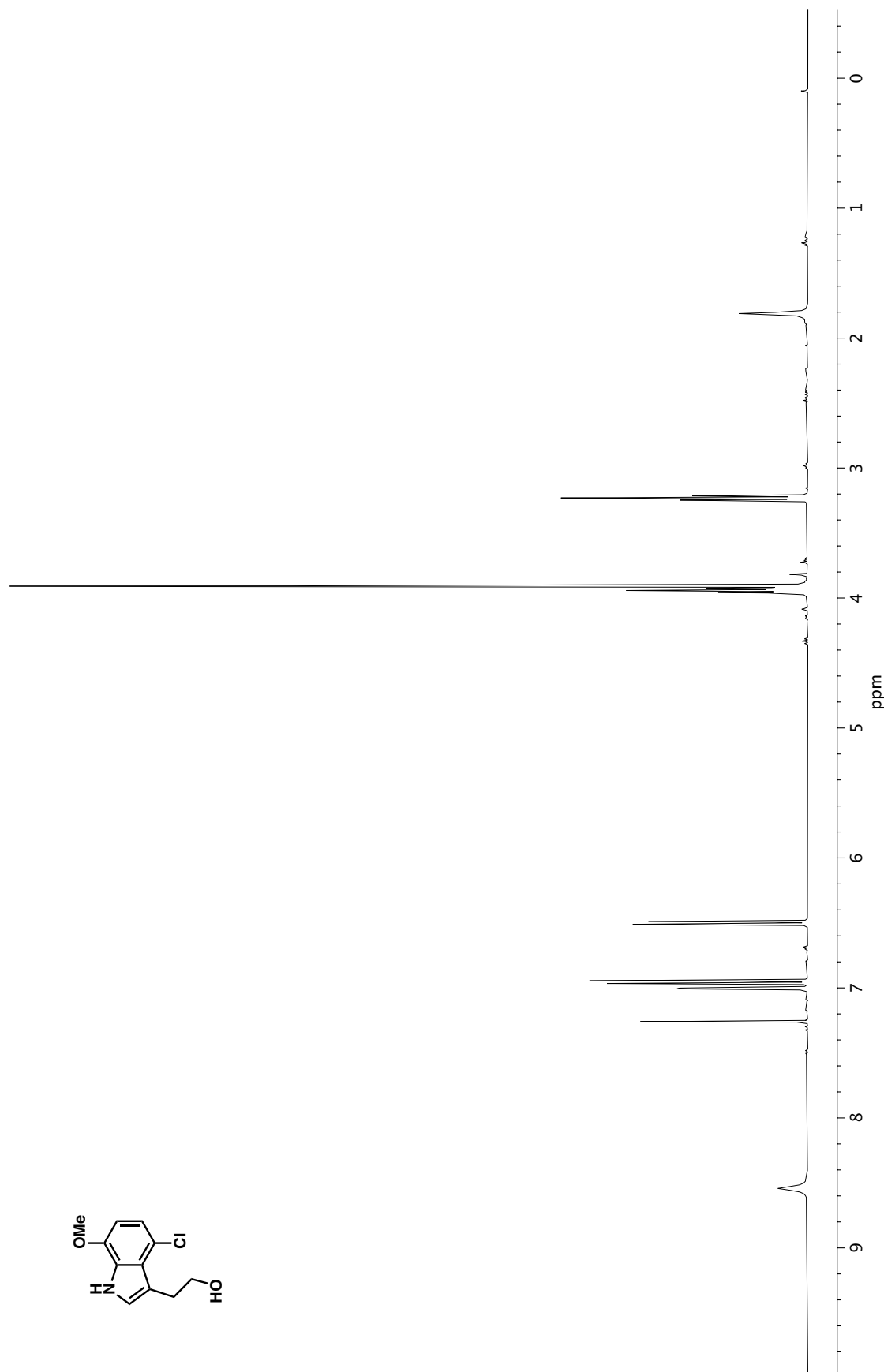


Figure A4.15. ¹³C NMR (100 MHz, CDCl₃) of compound **125**.

Figure A4.16. ¹H NMR (400 MHz, CDCl₃) of compound **126**.

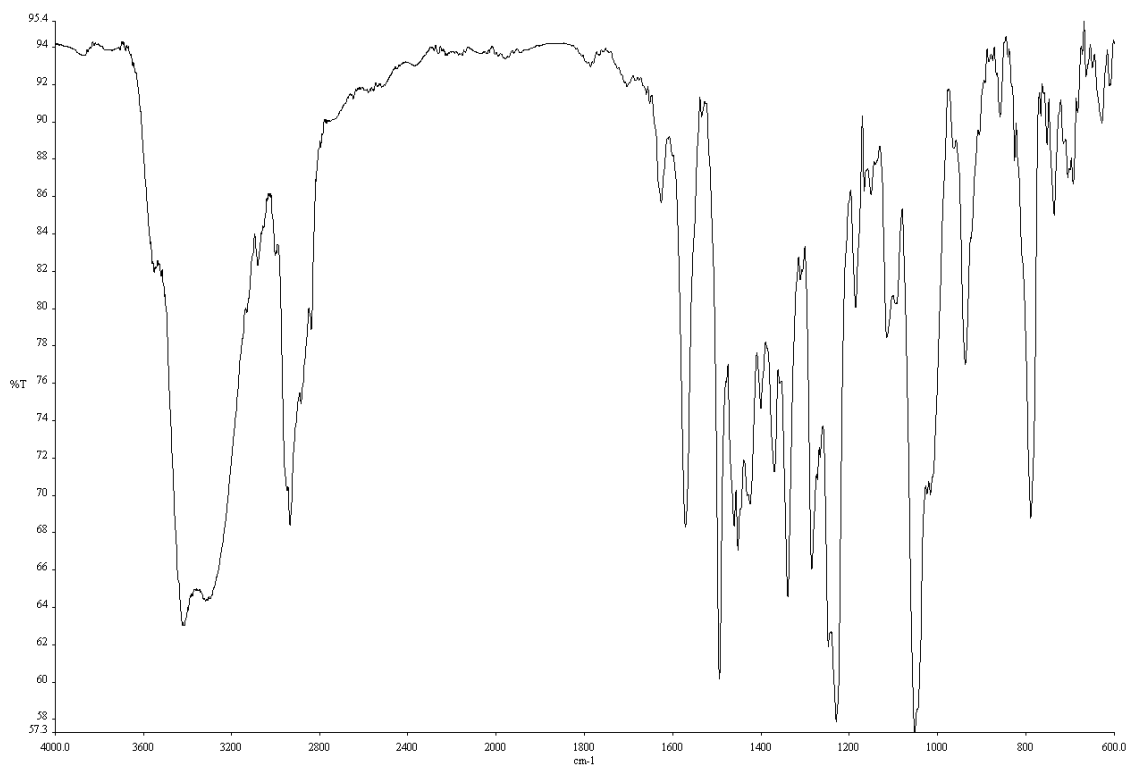


Figure A4.17. Infrared spectrum (Thin Film, NaCl) of compound **126**.

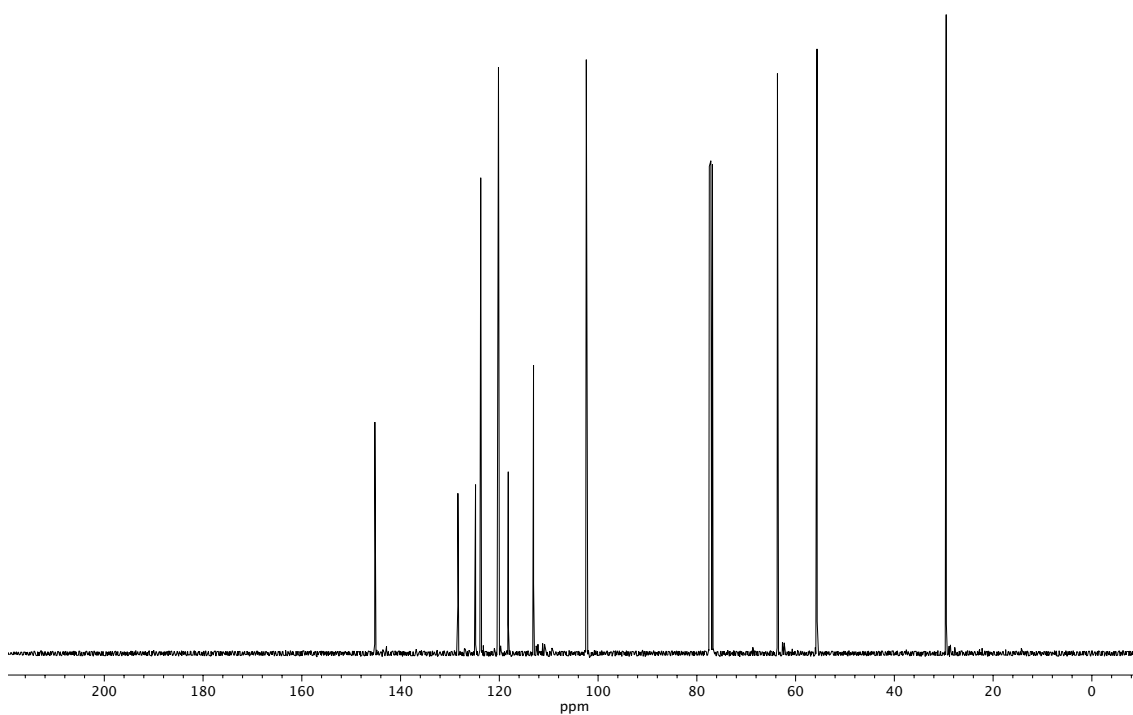
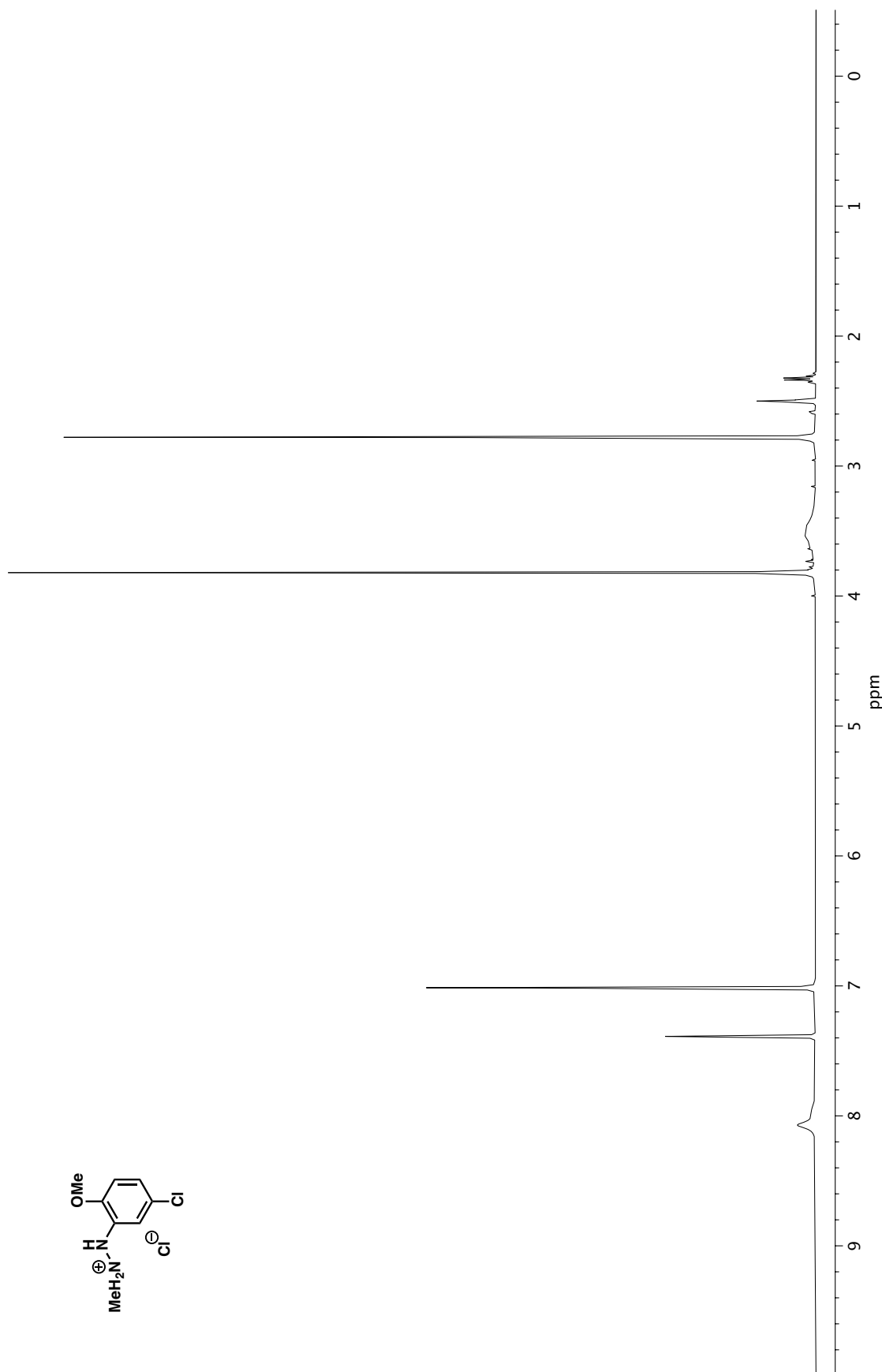


Figure A4.18. ^{13}C NMR (100 MHz, CDCl_3) of compound **126**.

Figure A4.19. ^1H NMR (400 MHz, DMSO-d_6) of compound **131**.

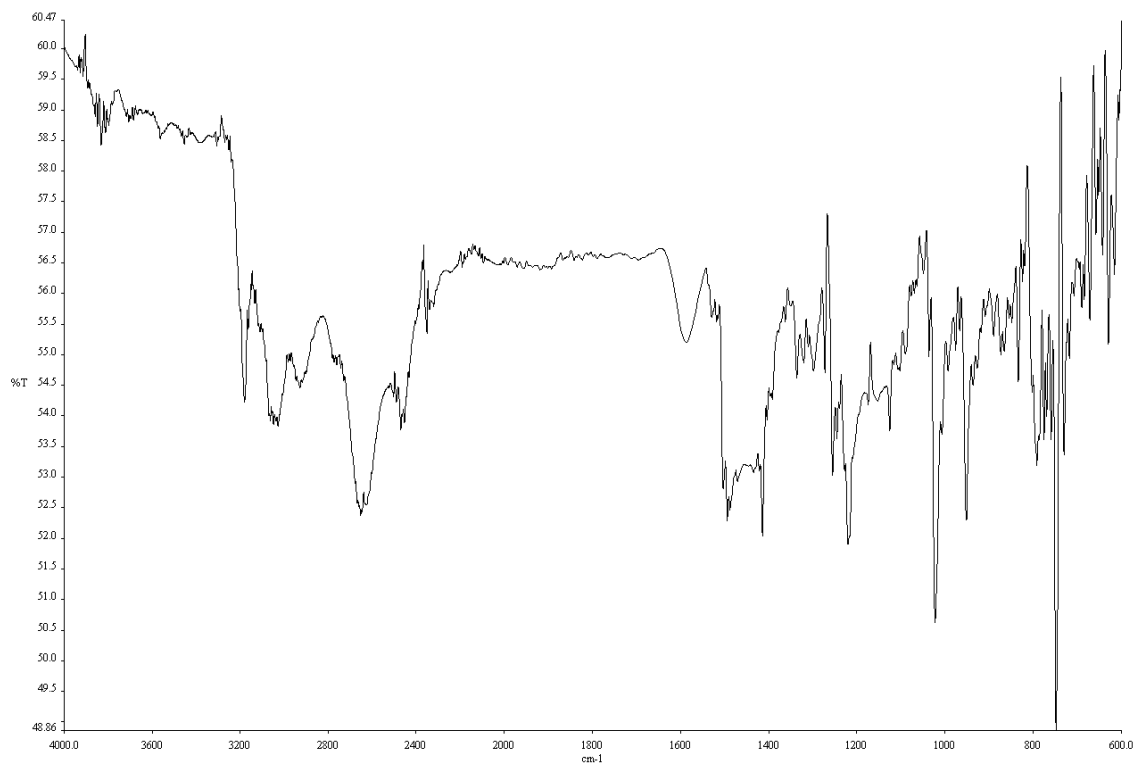


Figure A4.20. Infrared spectrum (Thin Film, NaCl) of compound **131**.

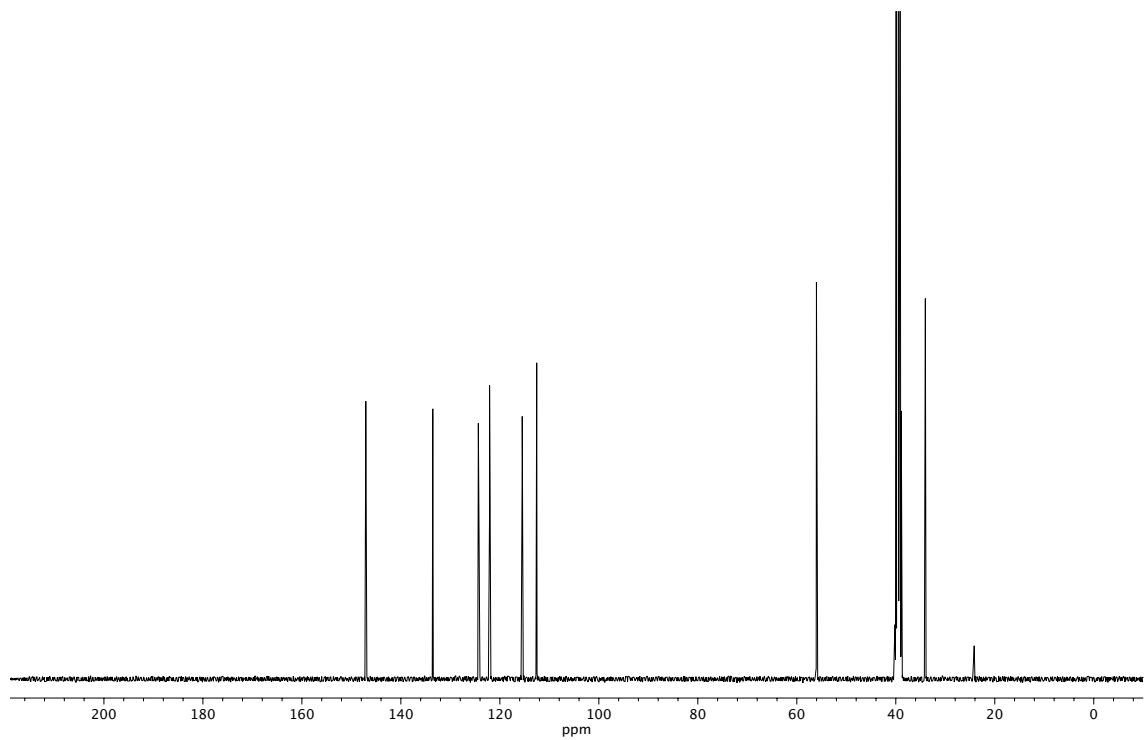
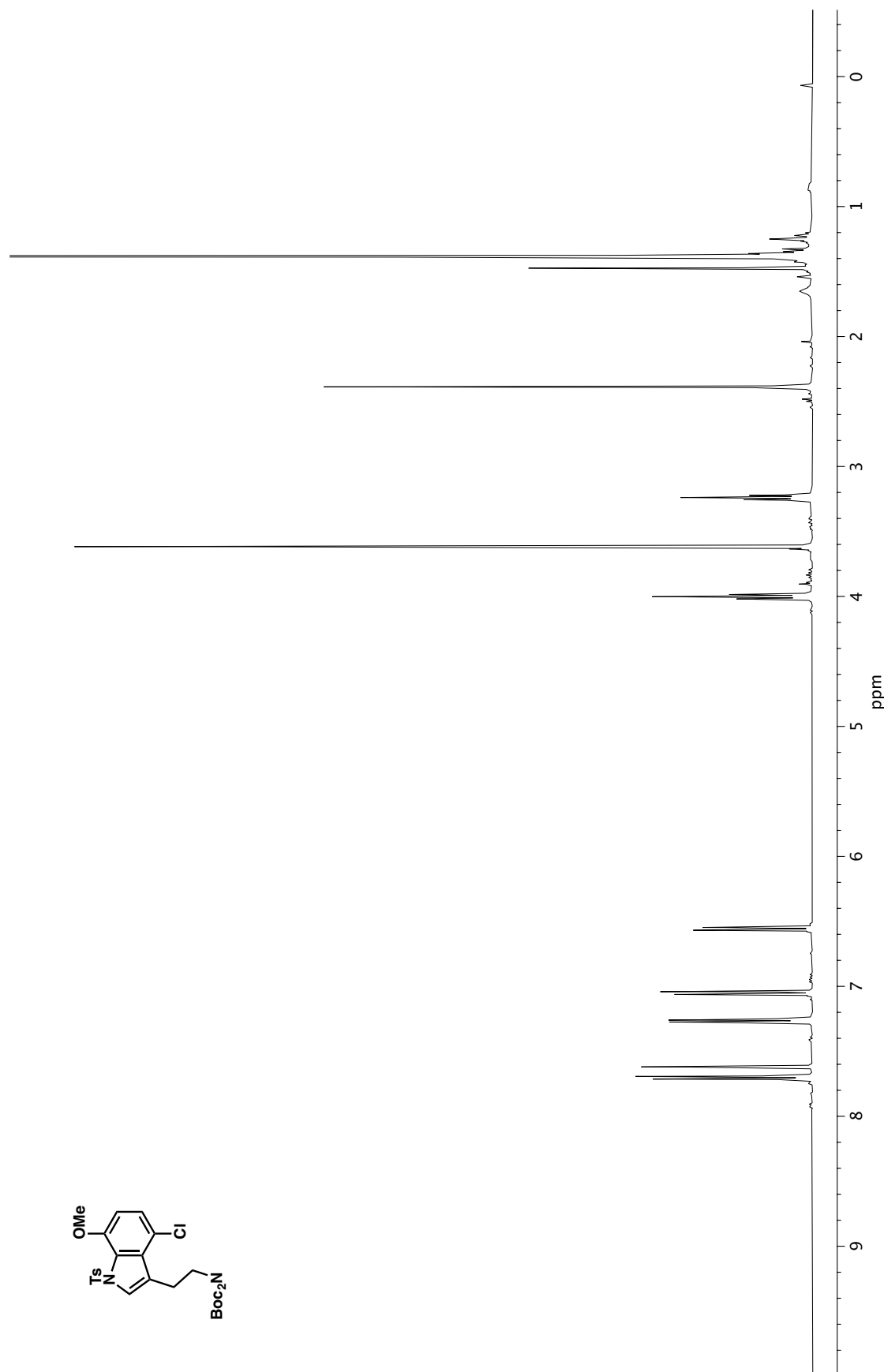


Figure A4.21. ¹³C NMR (100 MHz, DMSO-d₆) of compound **131**.

Figure A4.22. ¹H NMR (400 MHz, CDCl₃) of compound **132**.

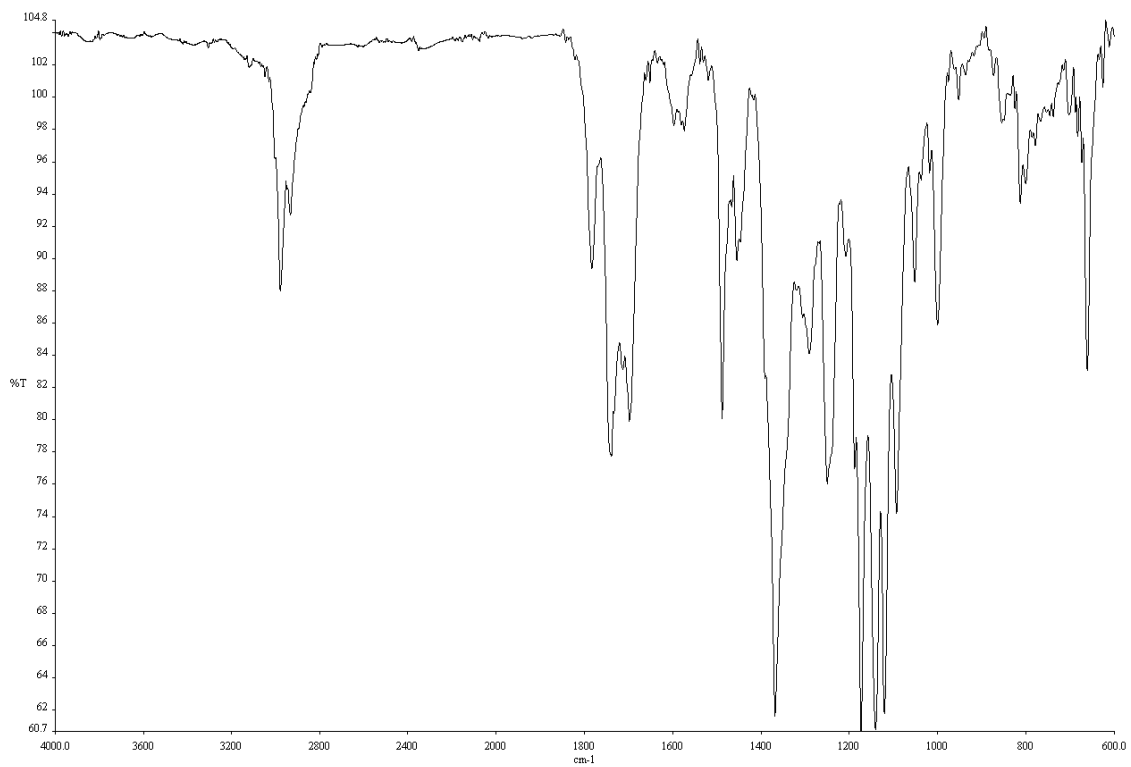


Figure A4.23. Infrared spectrum (Thin Film, NaCl) of compound **132**.

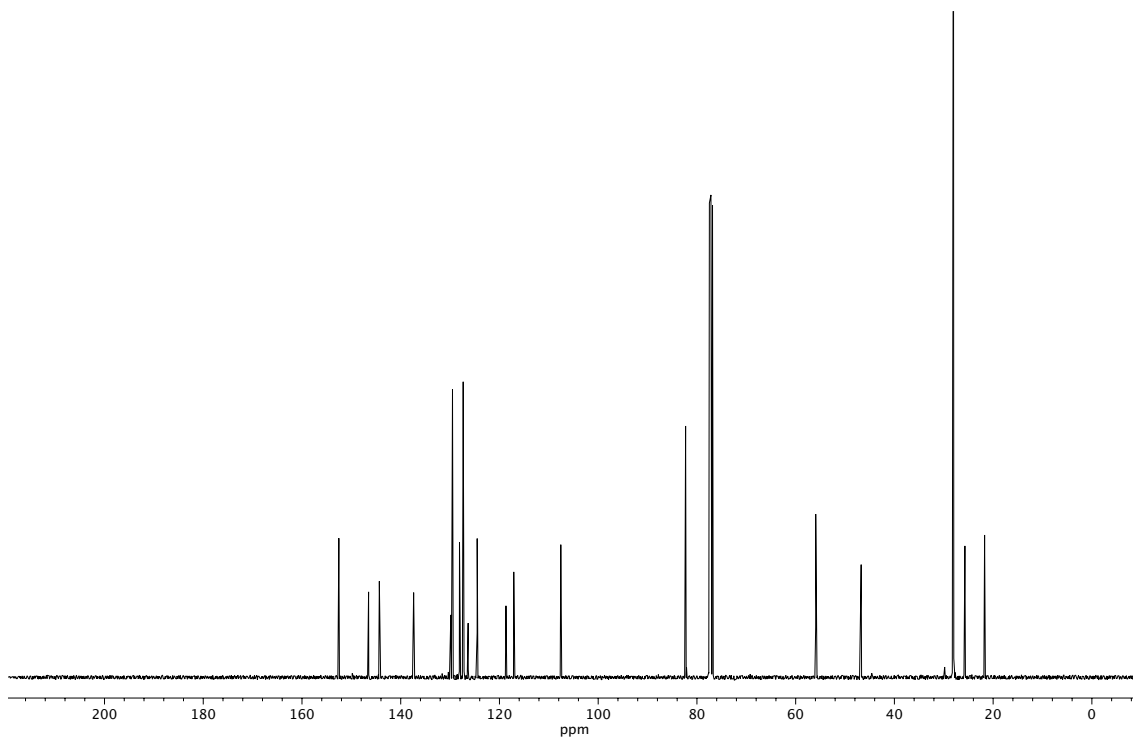
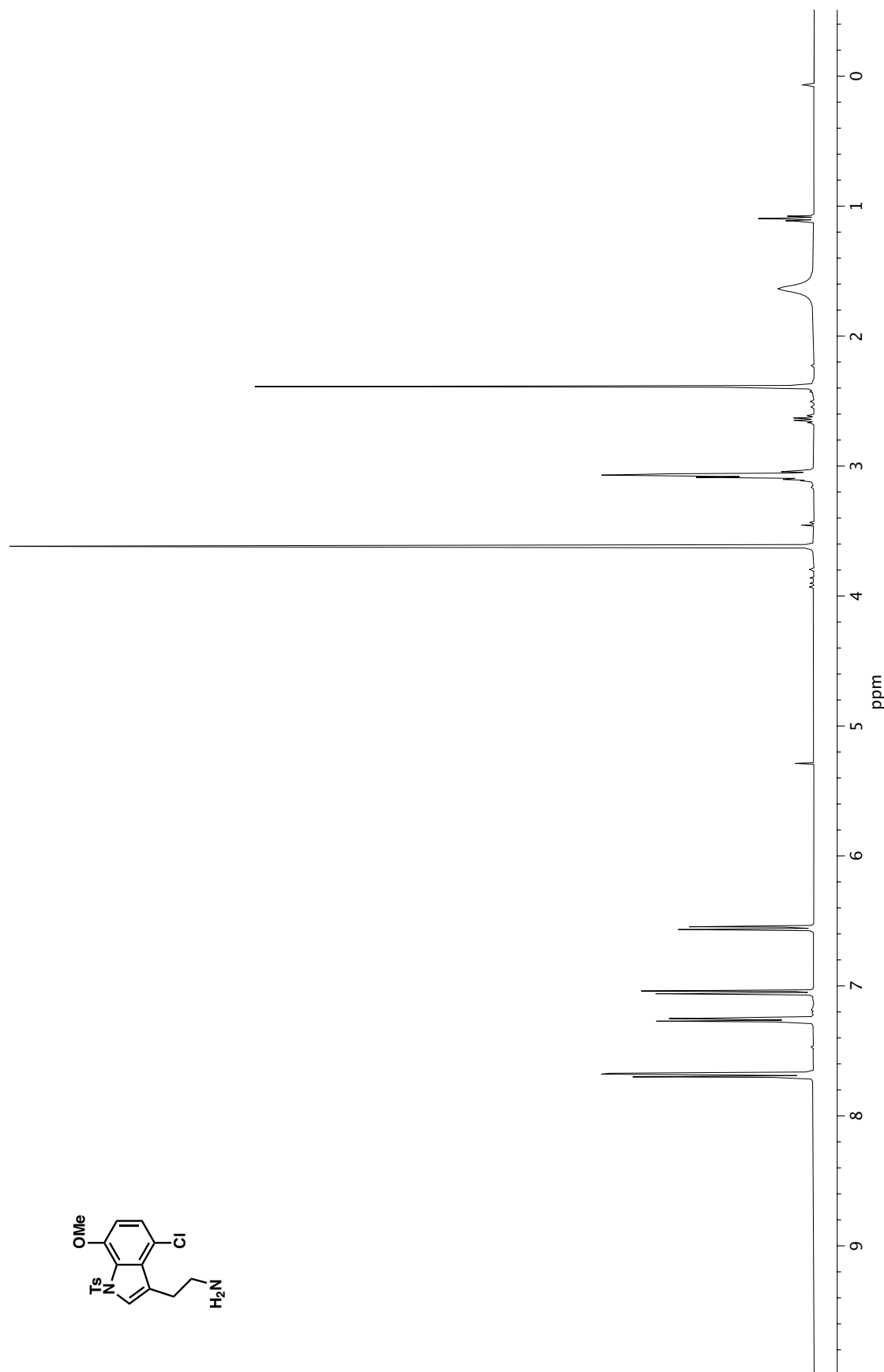


Figure A4.24. ^{13}C NMR (100 MHz, CDCl_3) of compound **132**.

Figure A4.2.5. ¹H NMR (400 MHz, CDCl₃) of compound **133**.

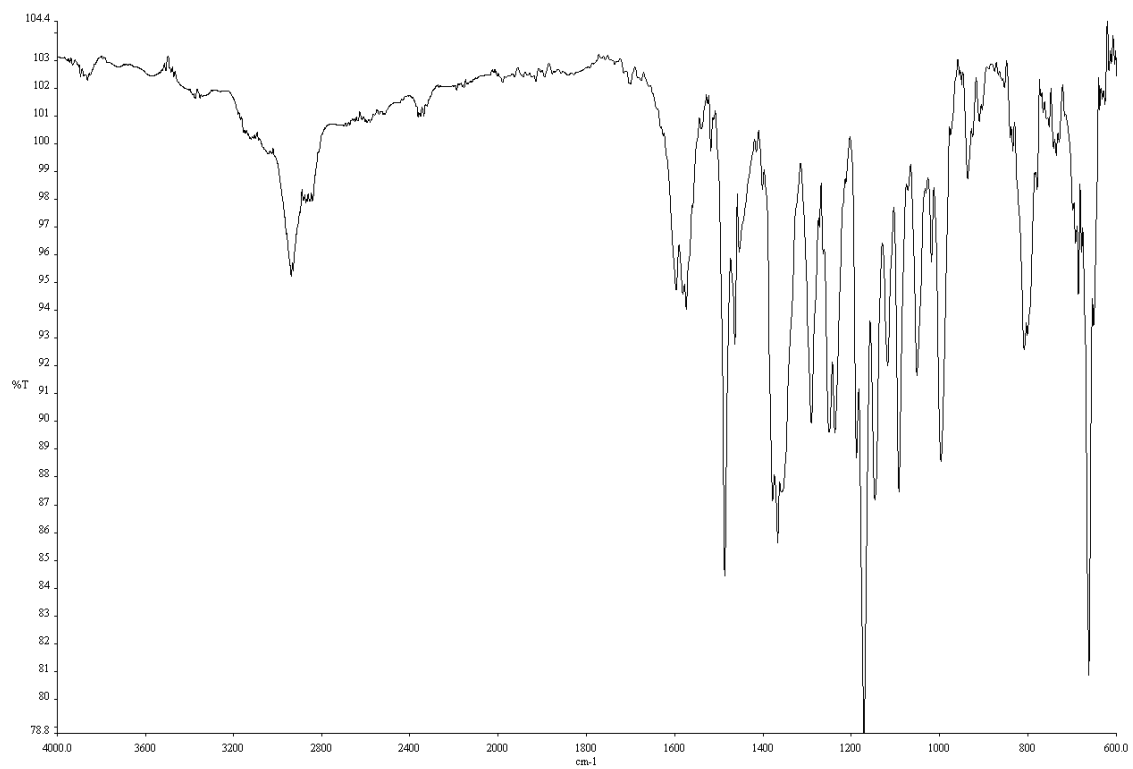


Figure A4.26. Infrared spectrum (Thin Film, NaCl) of compound **133**.

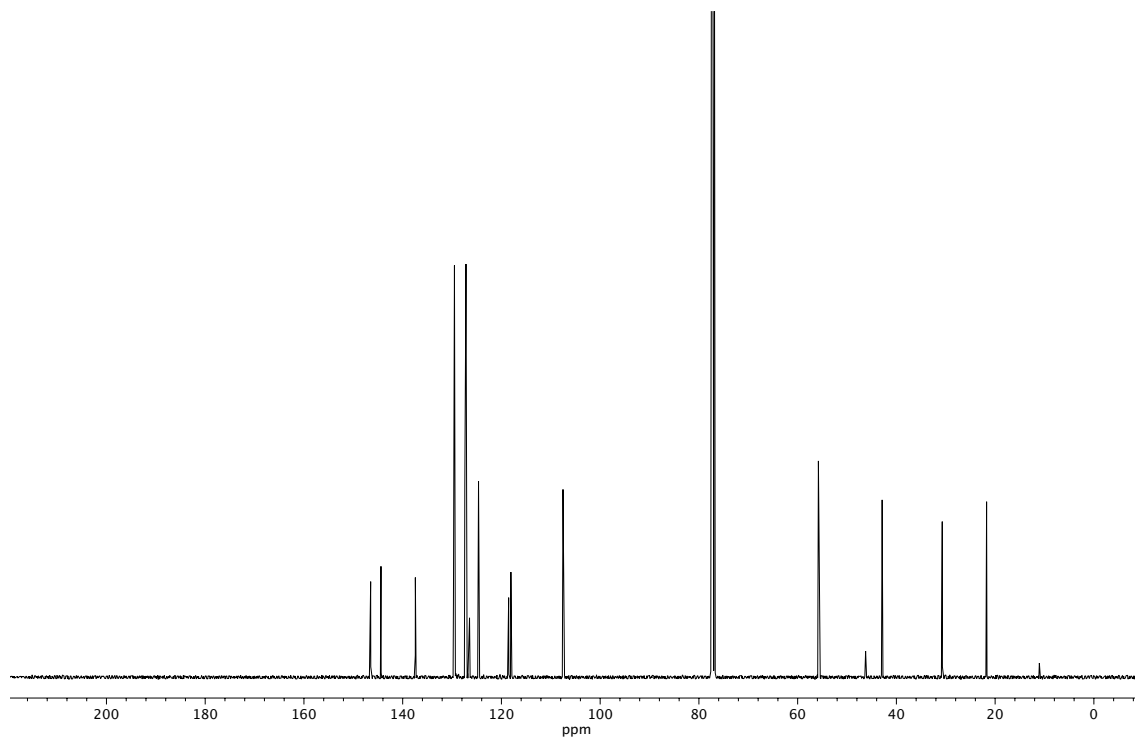


Figure A4.27. ^{13}C NMR (100 MHz, CDCl_3) of compound **133**.

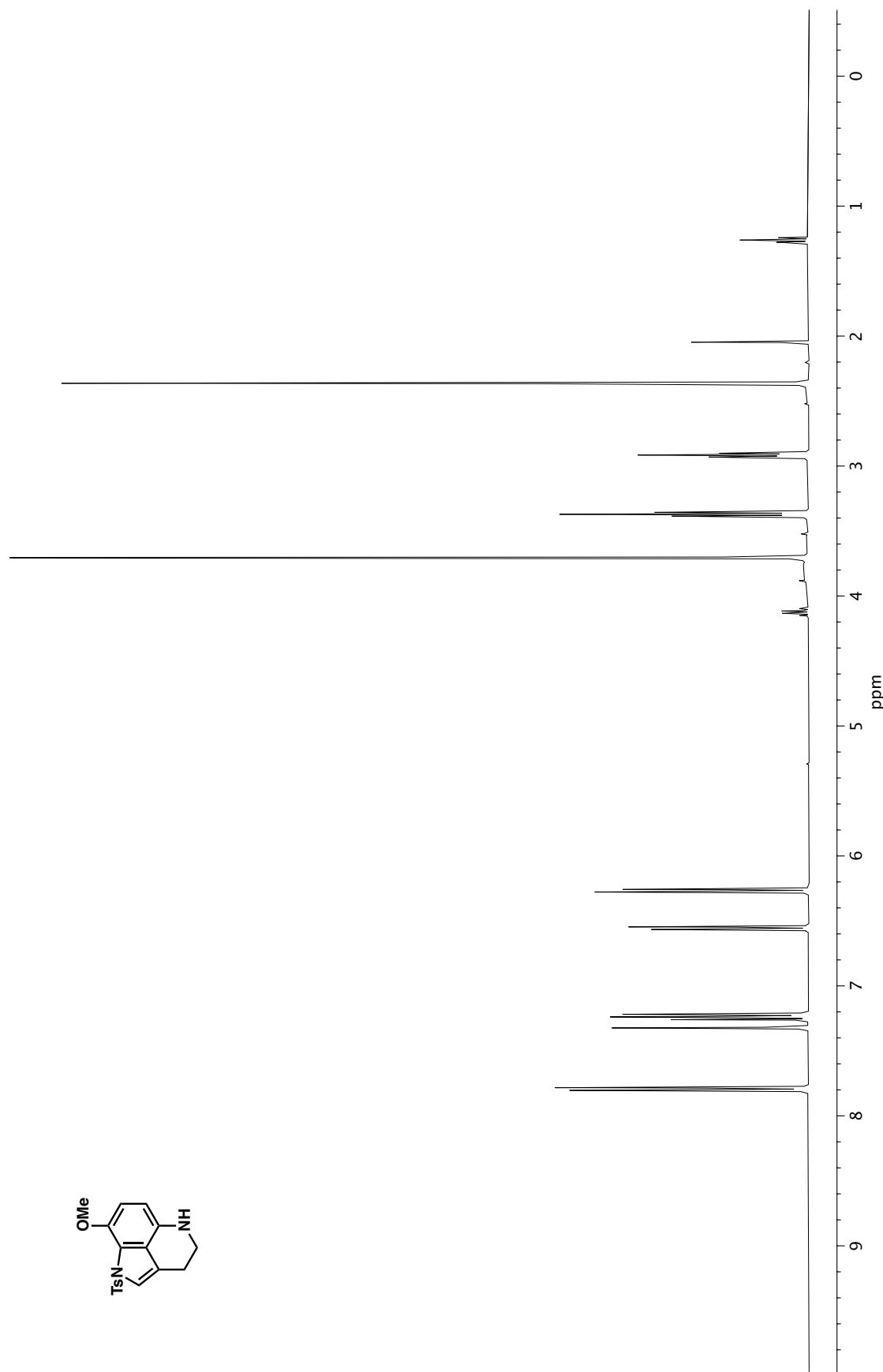


Figure A4.28. ^1H NMR (400 MHz, CDCl_3) of compound **134**.

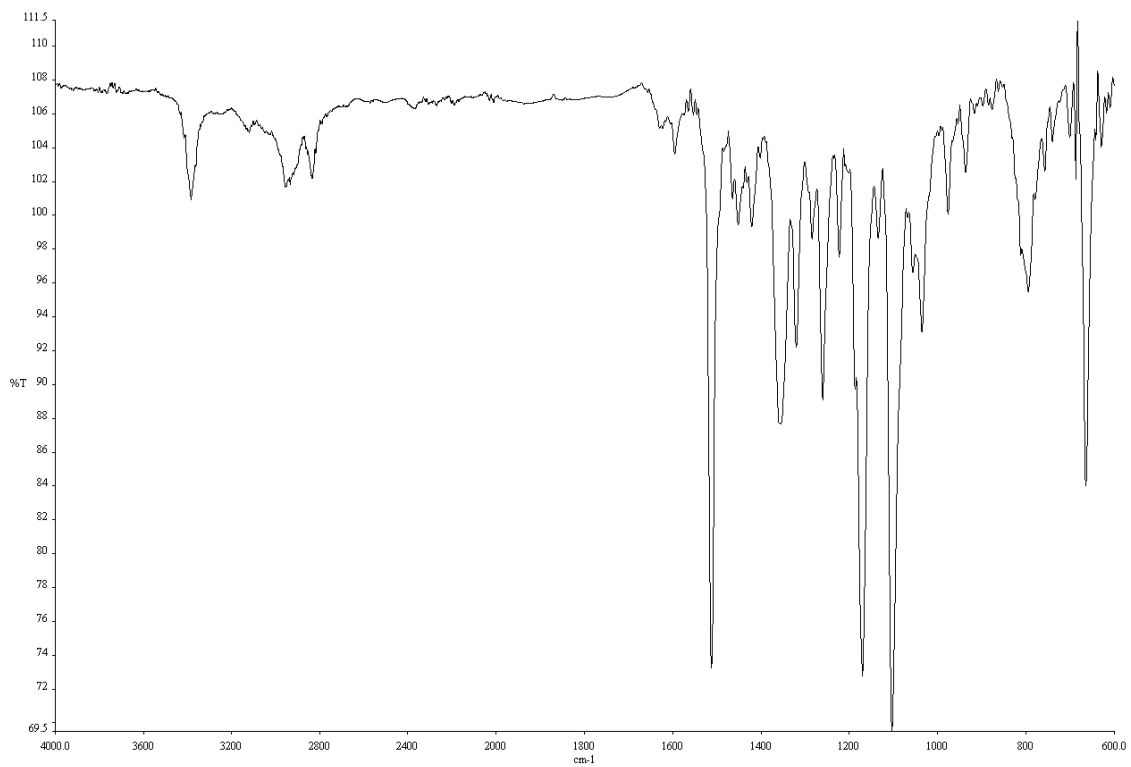


Figure A4.29. Infrared spectrum (Thin Film, NaCl) of compound **134**.

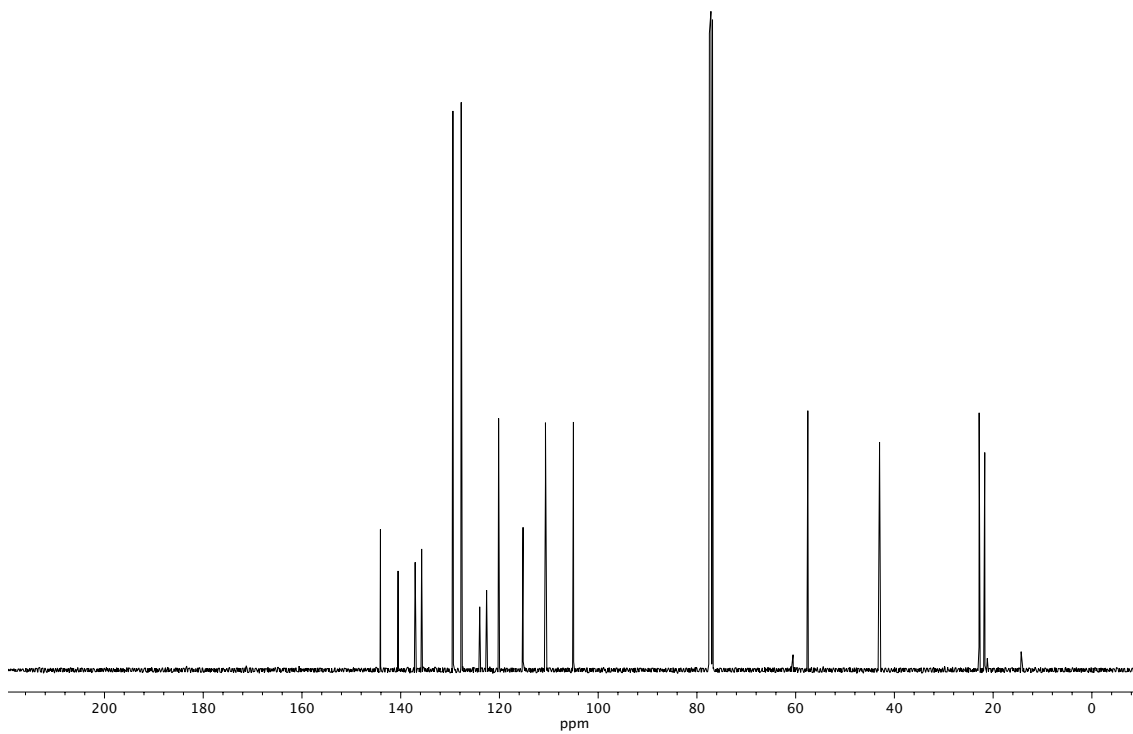
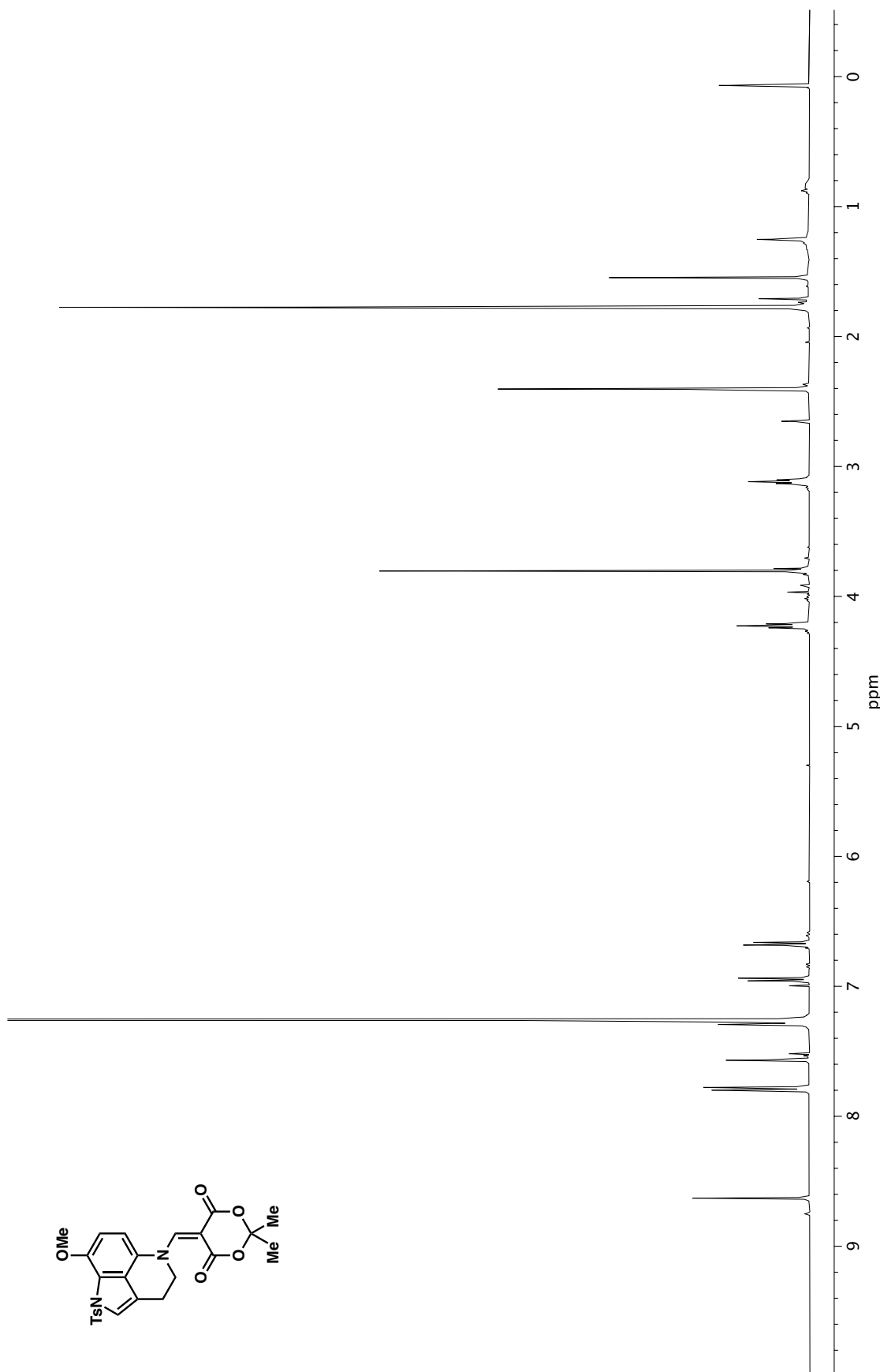


Figure A4.30. ^{13}C NMR (100 MHz, CDCl_3) of compound **134**.



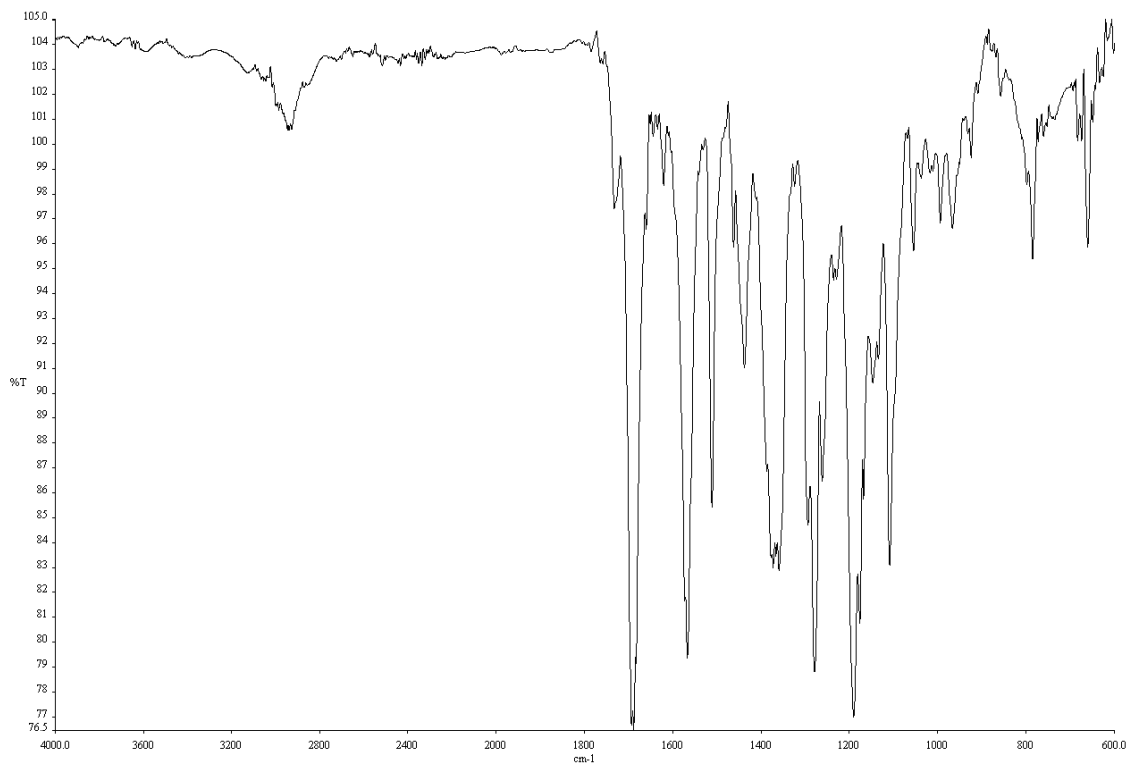


Figure A4.32. Infrared spectrum (Thin Film, NaCl) of compound **136**.

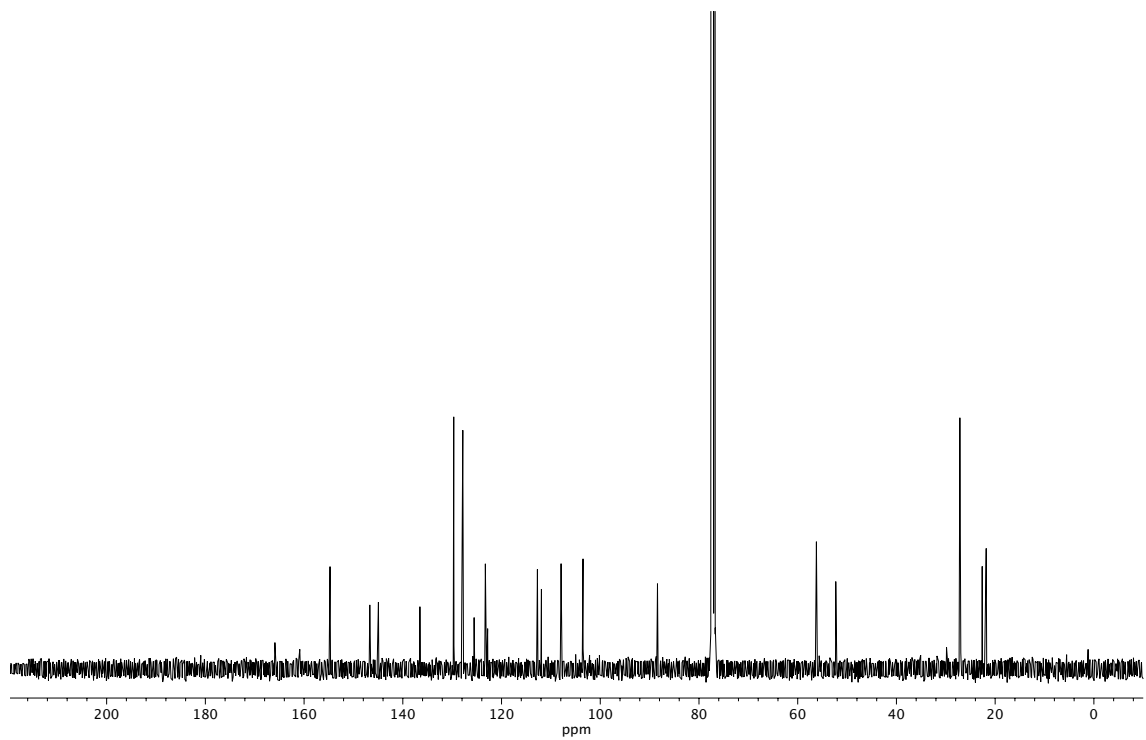
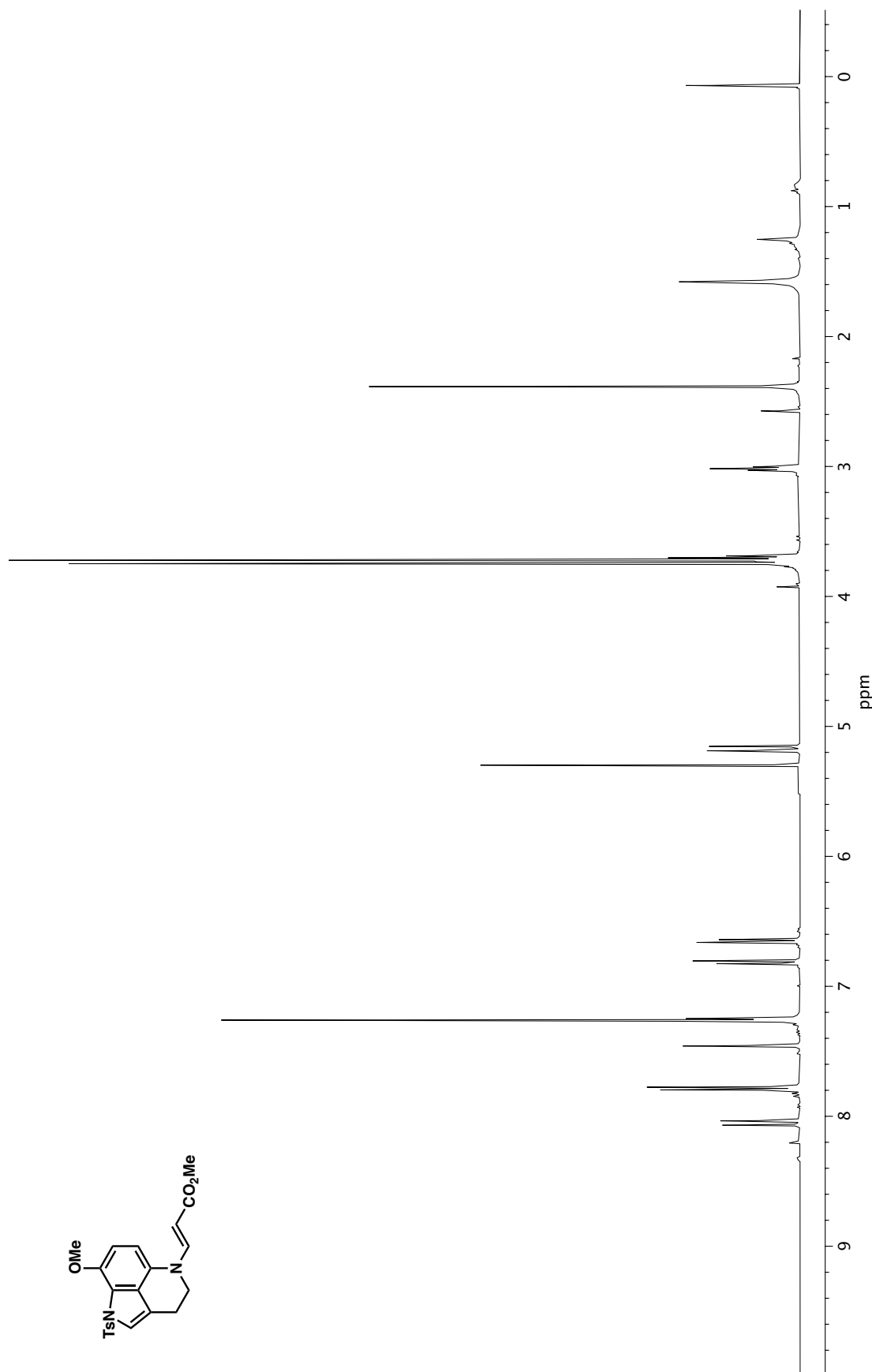


Figure A4.33. ¹³C NMR (100 MHz, CDCl₃) of compound **136**.

Figure A4.34. ¹H NMR (400 MHz, CDCl₃) of compound **138**.

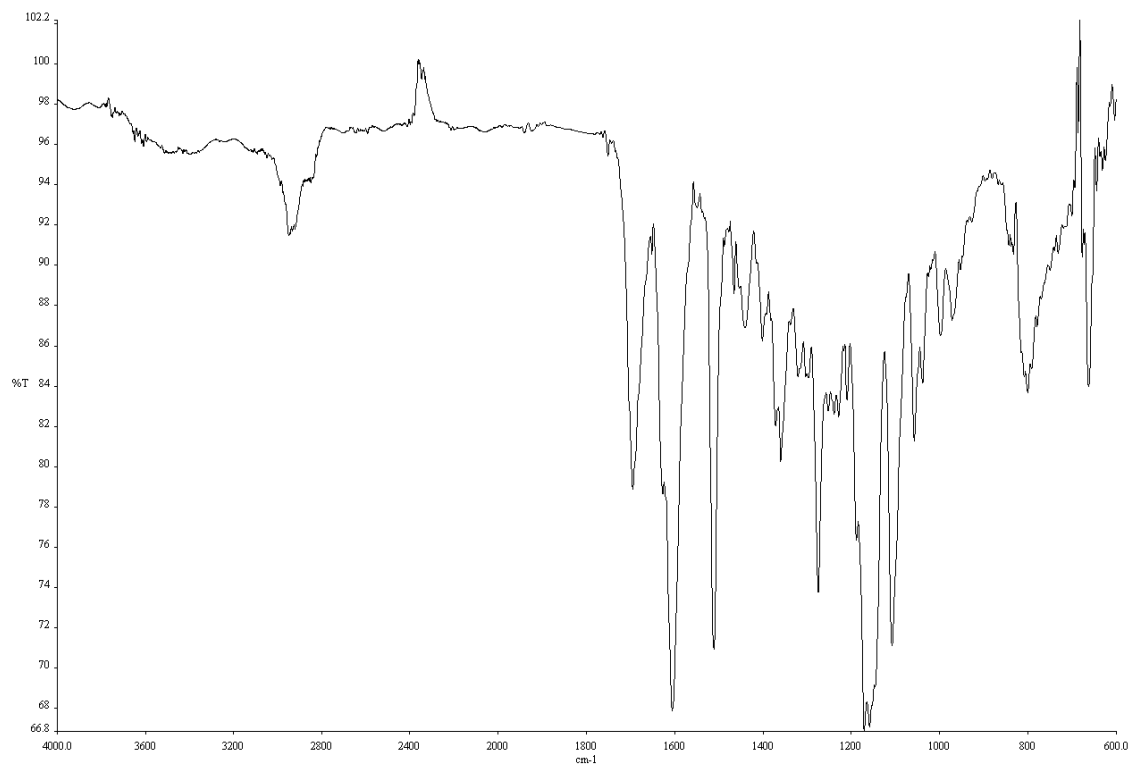


Figure A4.35. Infrared spectrum (Thin Film, NaCl) of compound **138**.

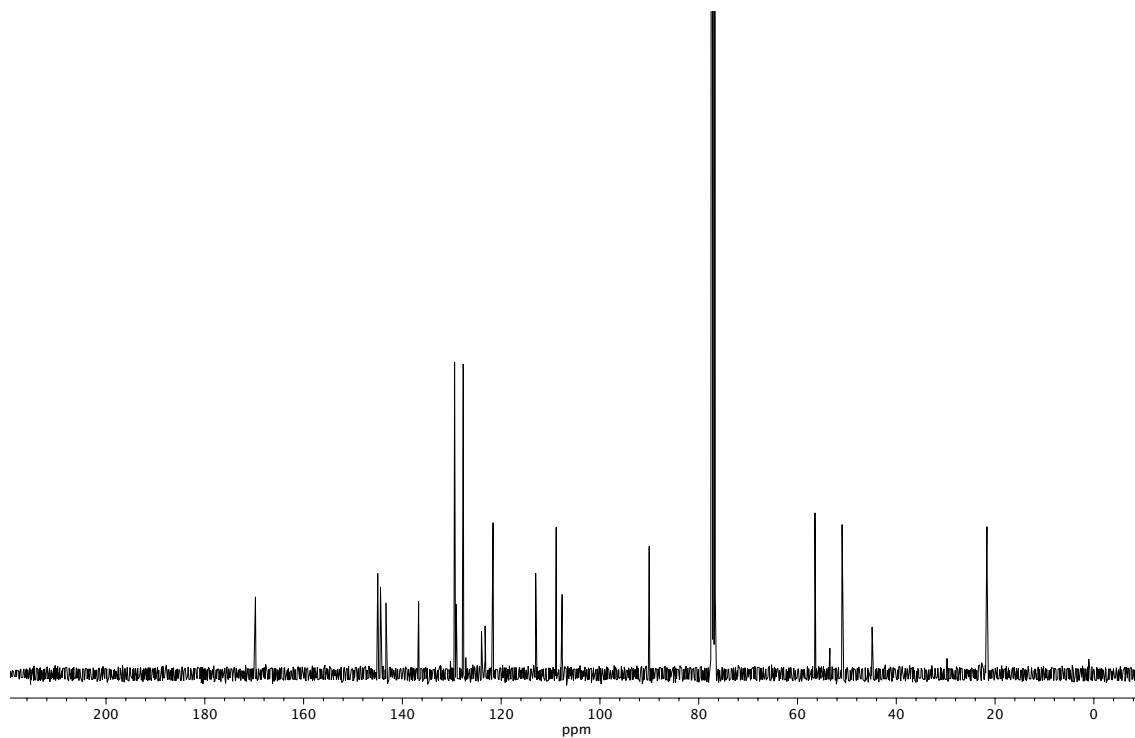
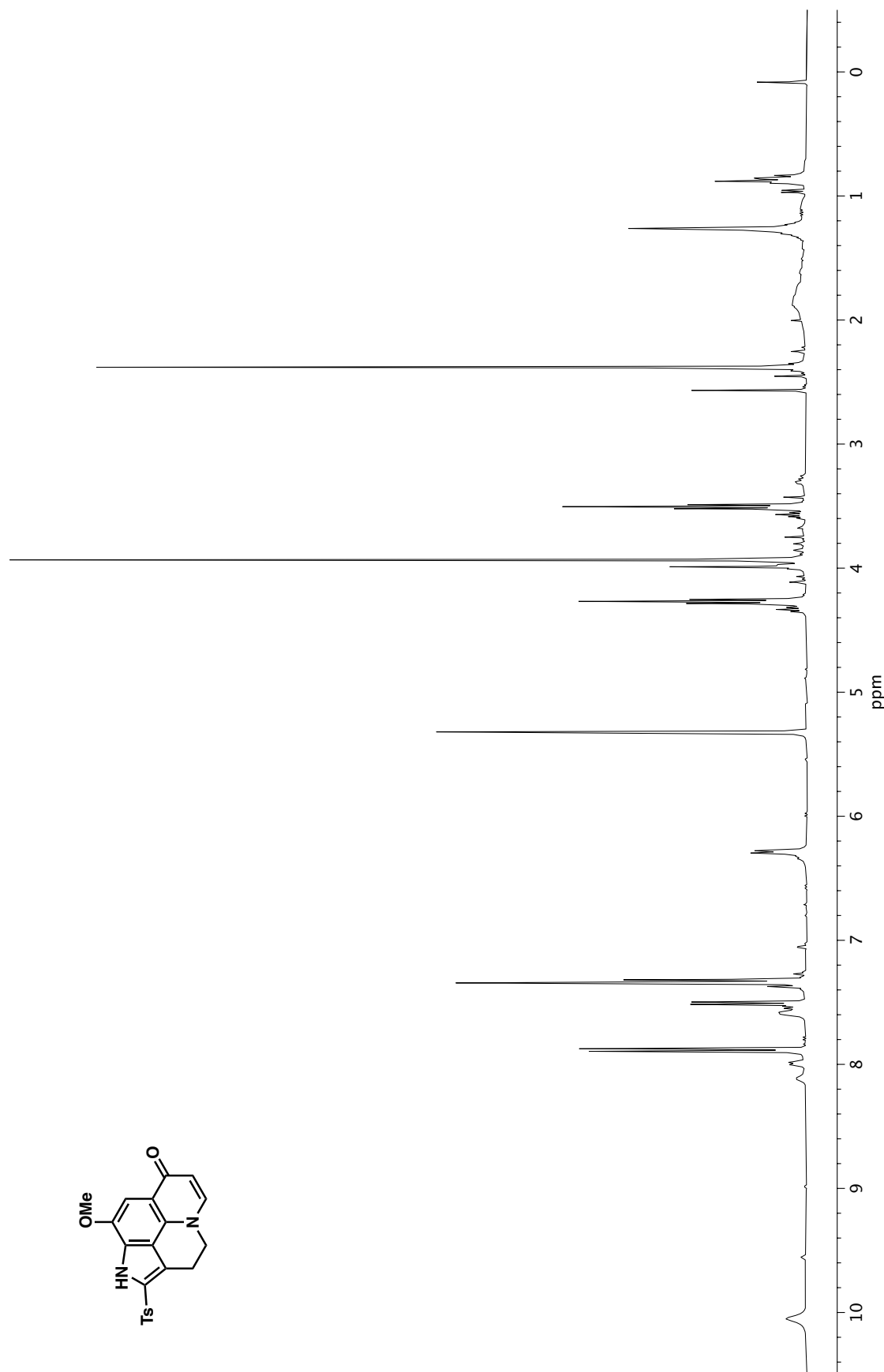


Figure A4.36. ^{13}C NMR (100 MHz, CDCl_3) of compound **138**.



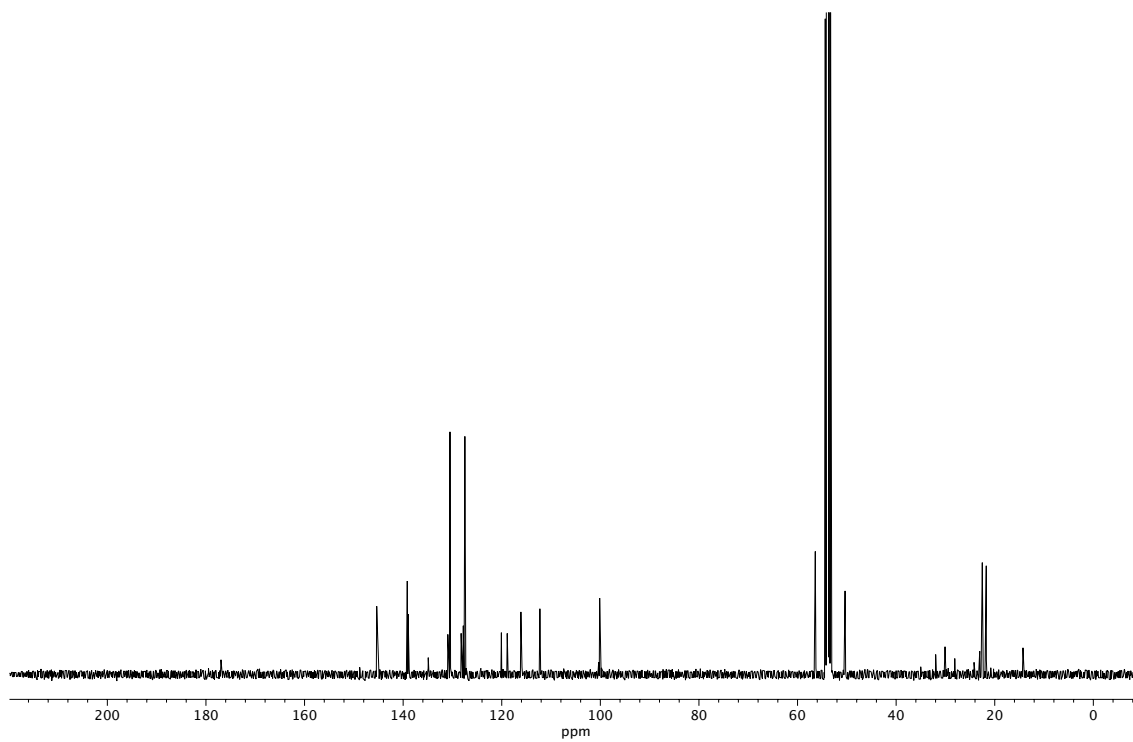
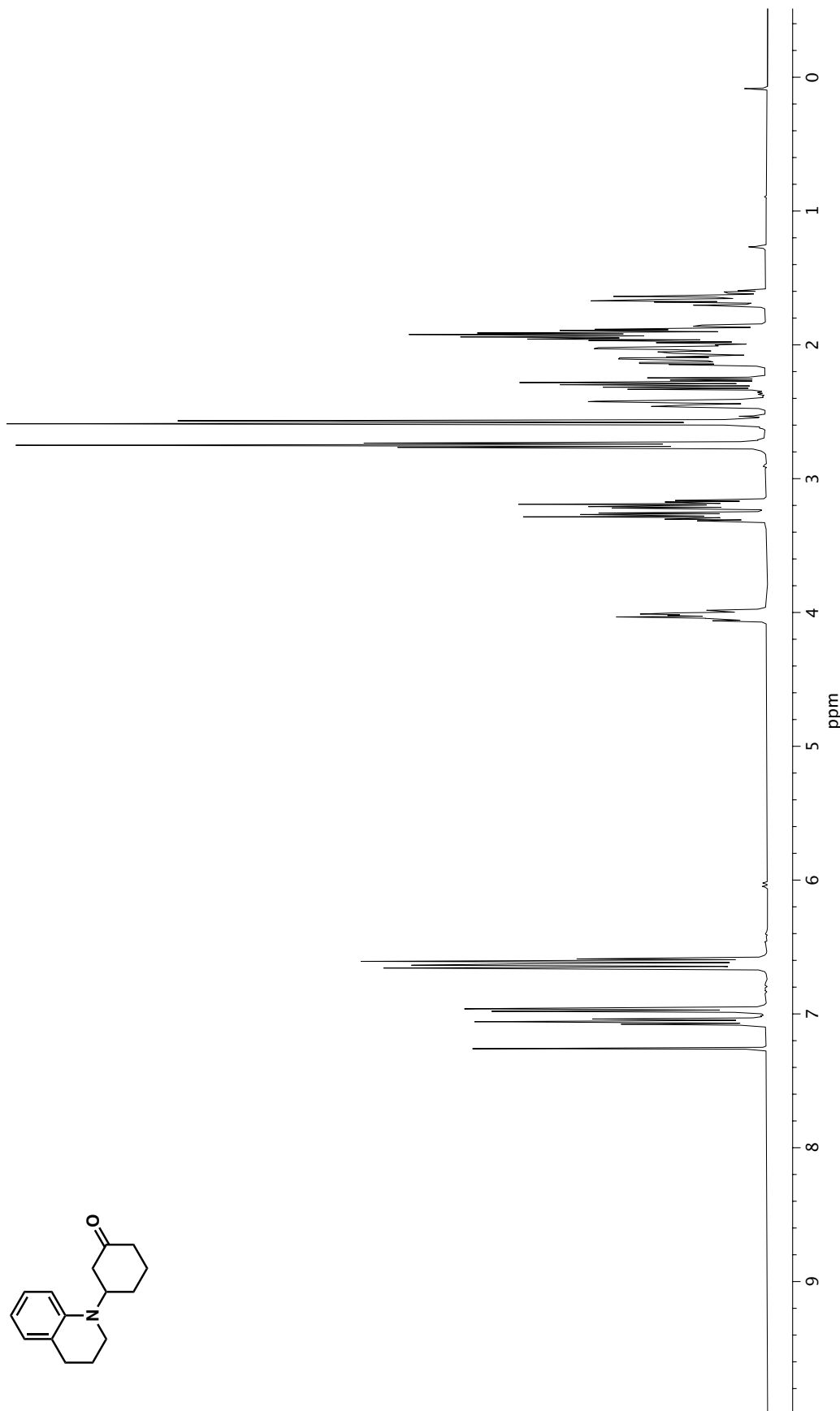


Figure A4.38. ^{13}C NMR (100 MHz, CD_2Cl_2) of compound **139**.

Figure A4.39. ^1H NMR (400 MHz, CDCl_3) of compound **143**.

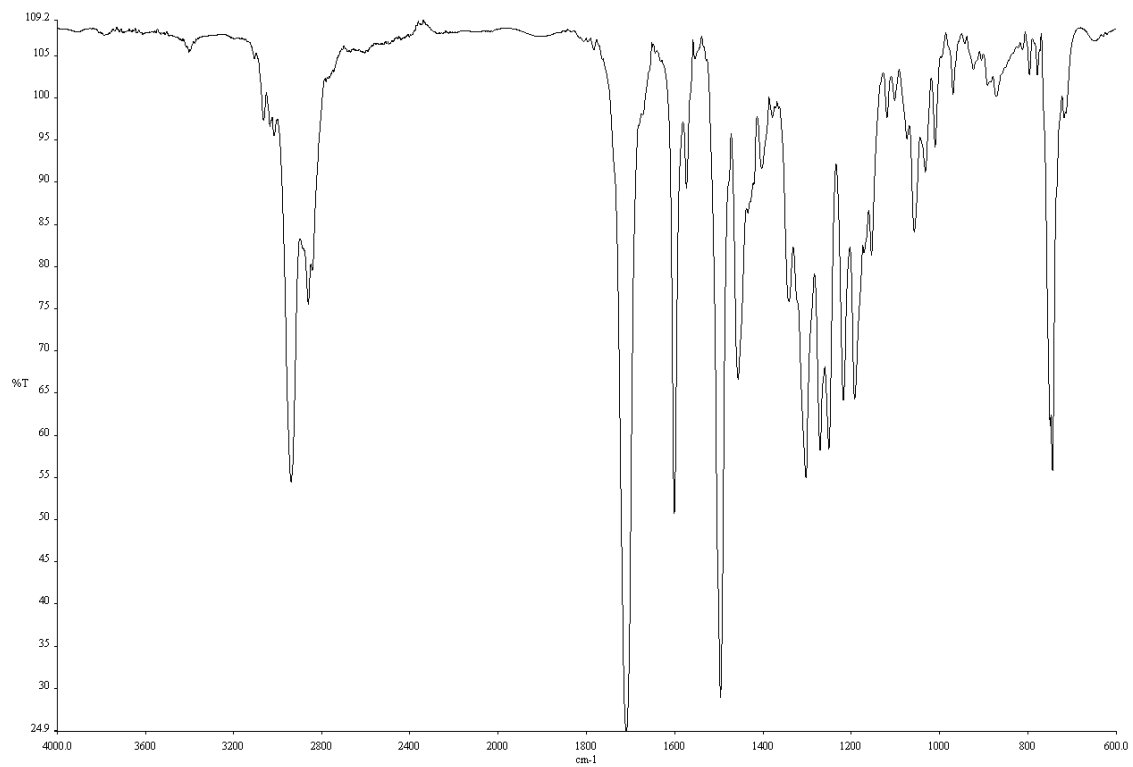


Figure A4.40. Infrared spectrum (Thin Film, NaCl) of compound **143**.

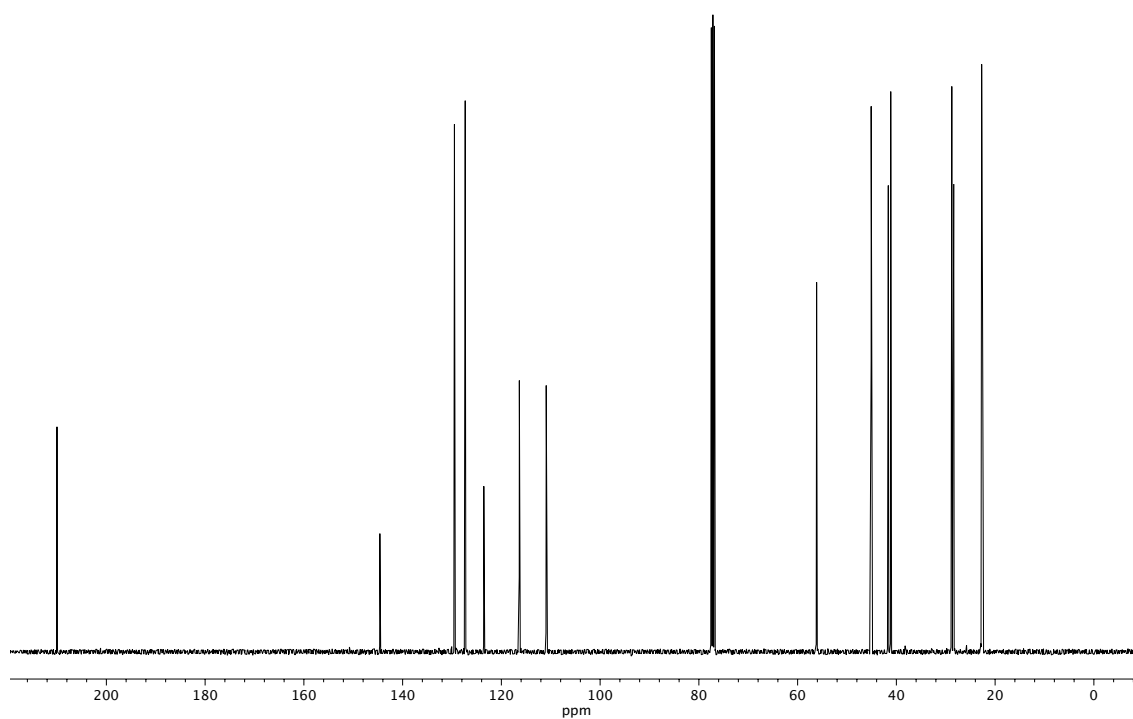
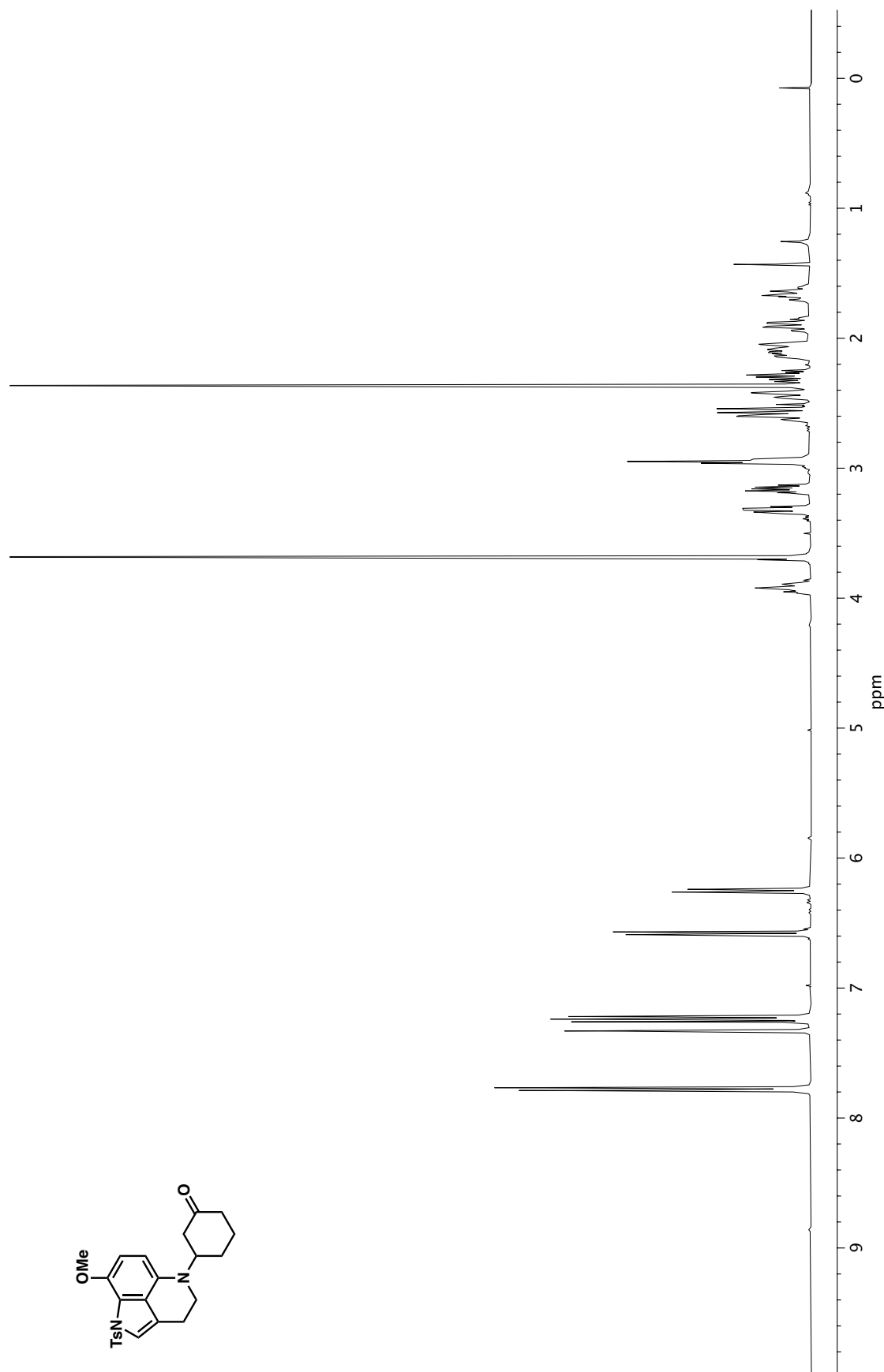


Figure A4.41. ^{13}C NMR (100 MHz, CDCl_3) of compound **143**.

Figure A4.42. ¹H NMR (400 MHz, CDCl₃) of compound **141**.

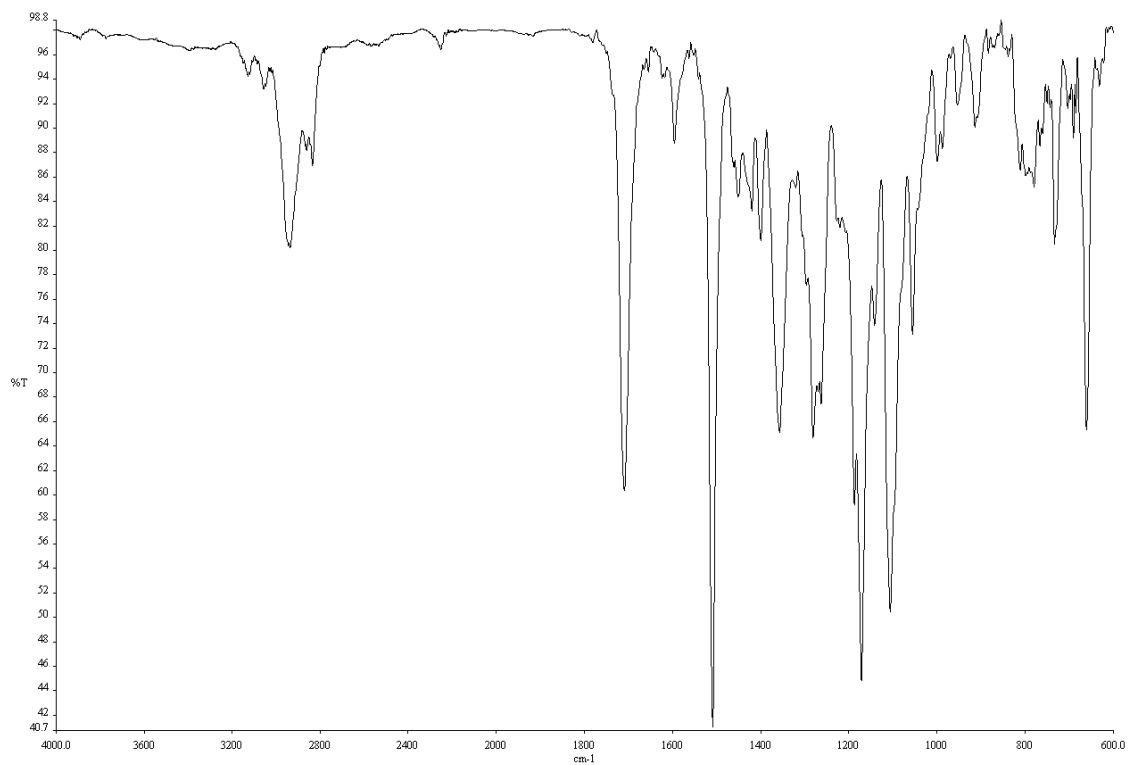


Figure A4.43. Infrared spectrum (Thin Film, NaCl) of compound **141**.

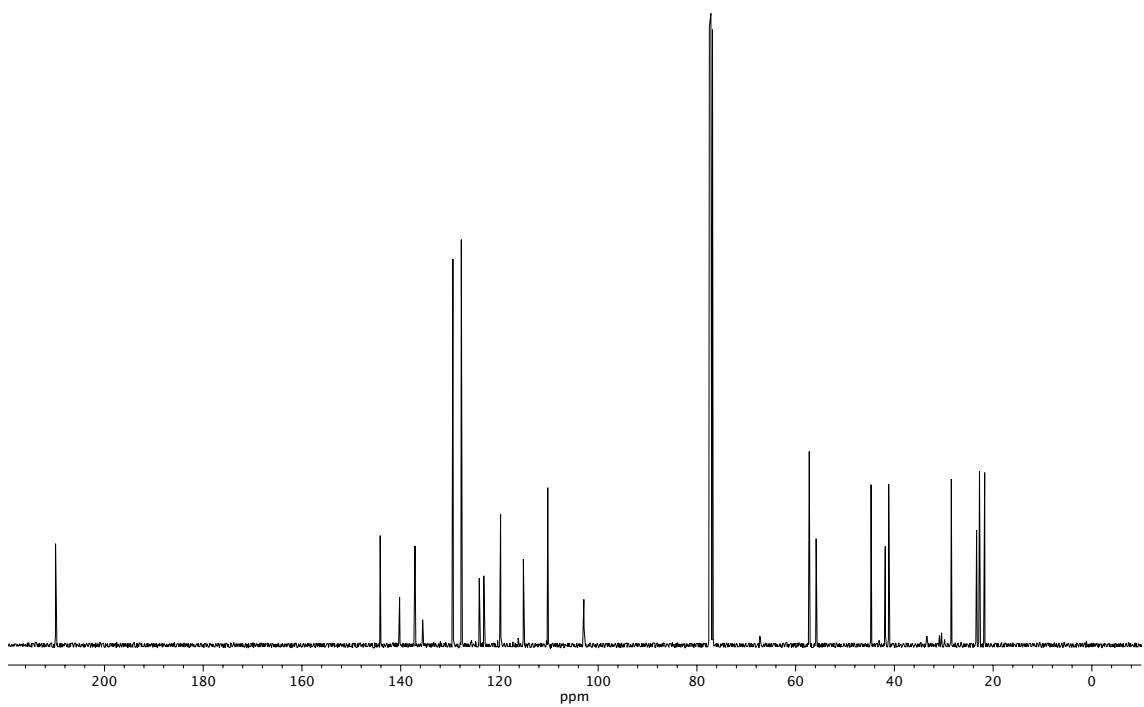
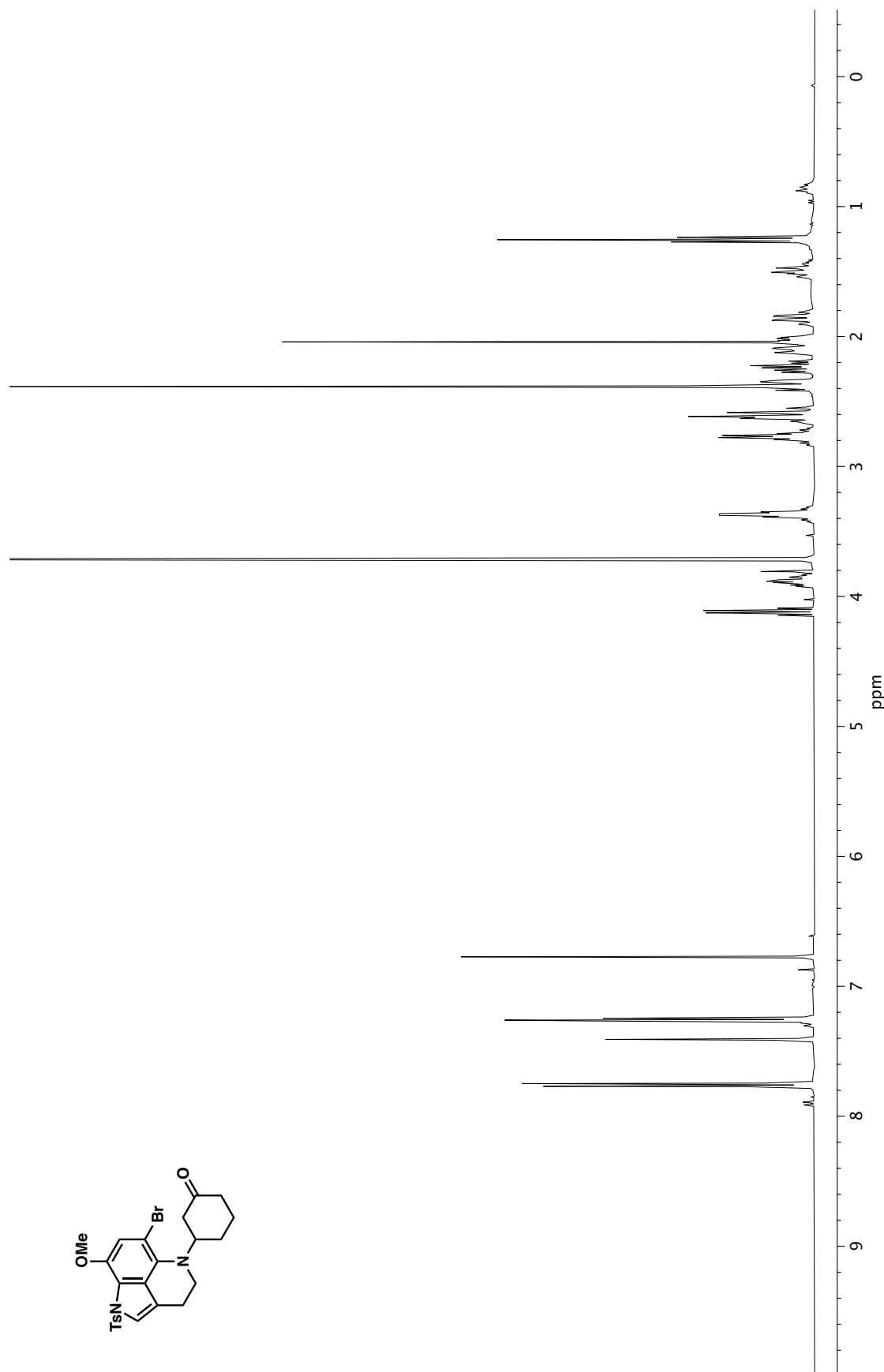


Figure A4.44. ¹³C NMR (100 MHz, CDCl₃) of compound **141**.

Figure A4.45. ¹H NMR (400 MHz, CDCl₃) of compound **149**.

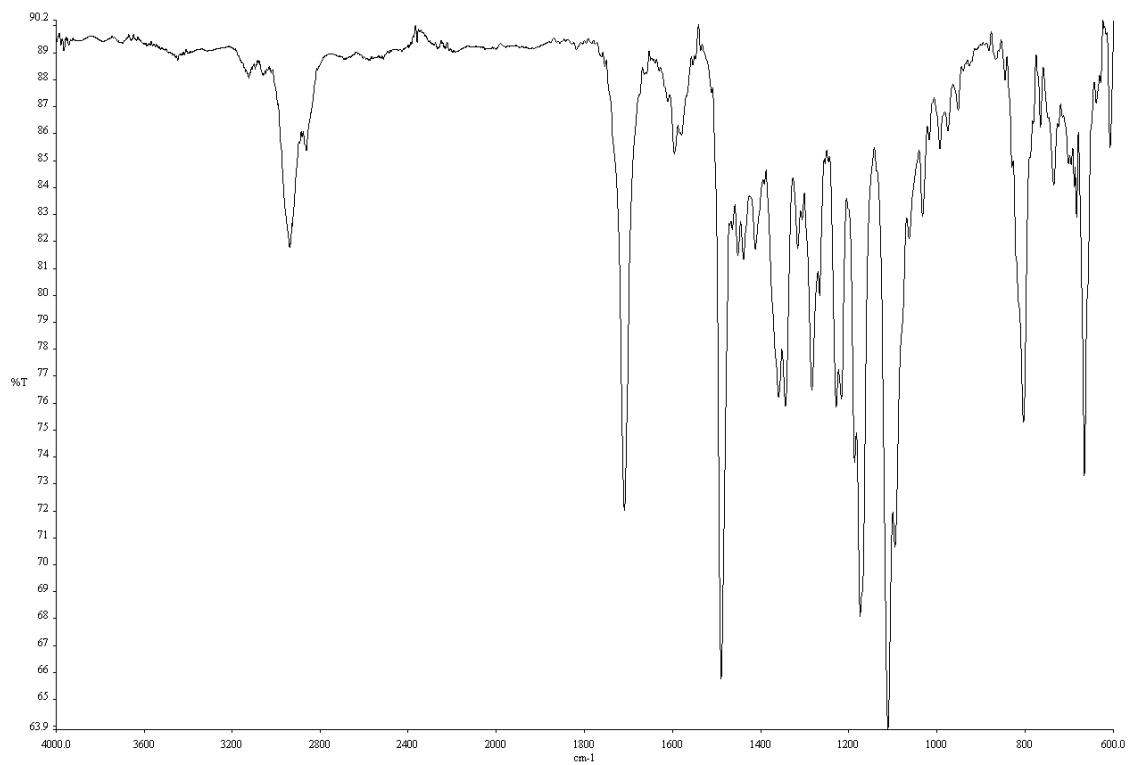


Figure A4.46. Infrared spectrum (Thin Film, NaCl) of compound **149**.

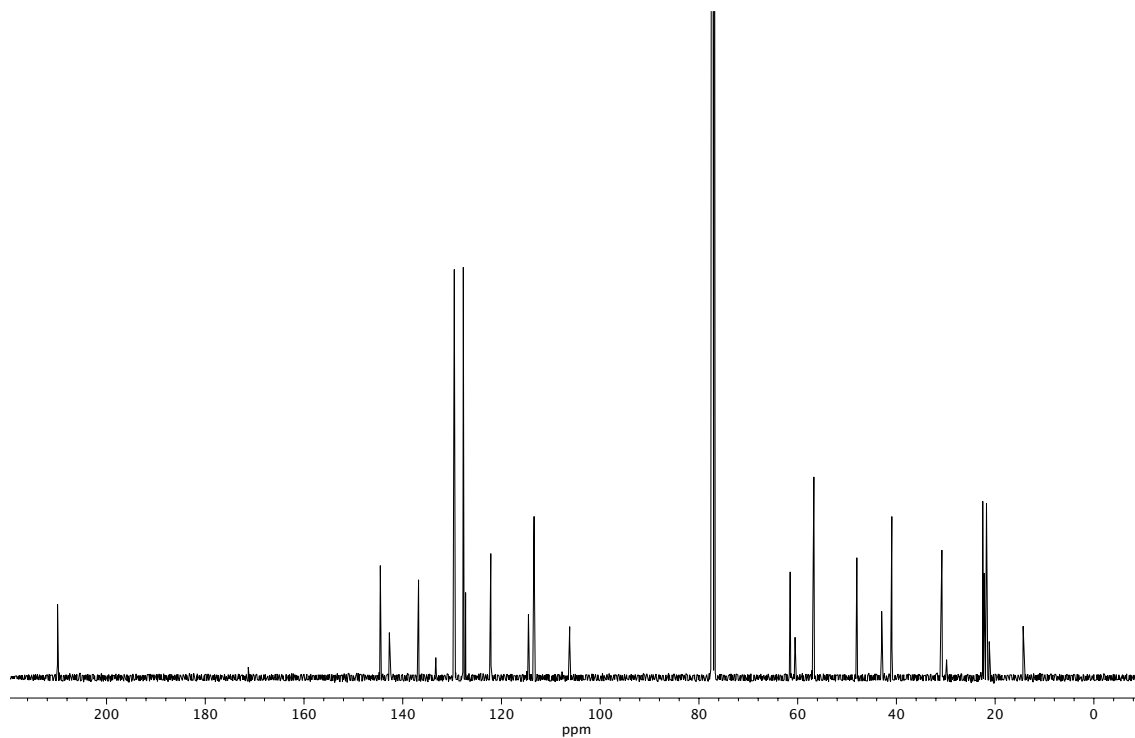
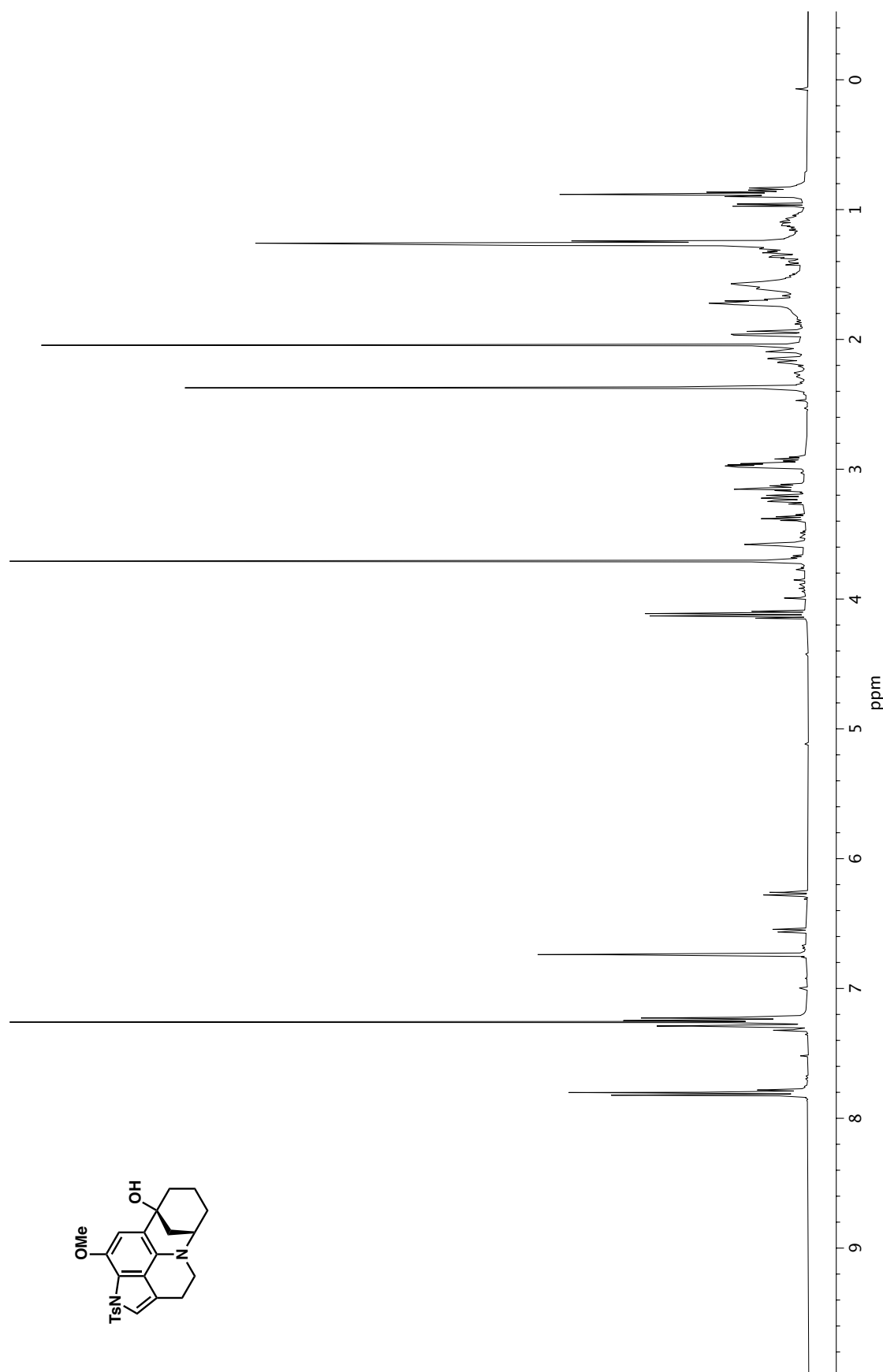


Figure A4.47. ^{13}C NMR (100 MHz, CDCl_3) of compound **149**.

Figure A4.48. ¹H NMR (400 MHz, CDCl₃) of compound **150**.

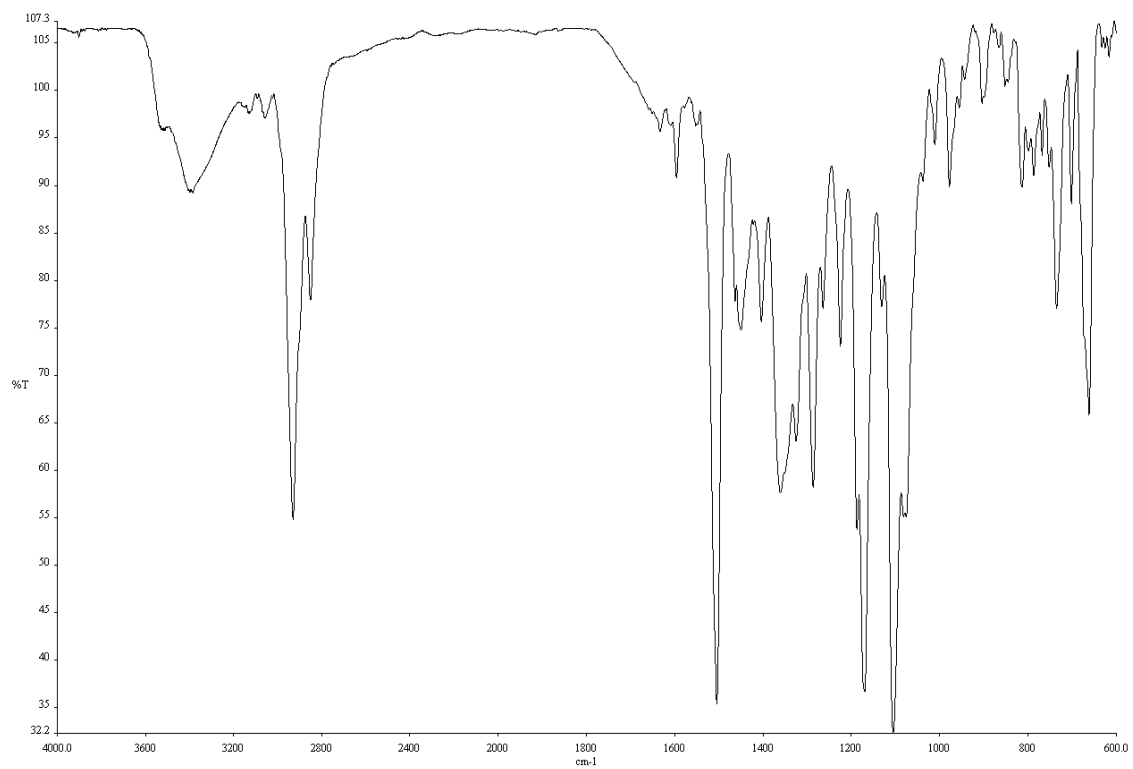


Figure A4.49. Infrared spectrum (Thin Film, NaCl) of compound **150**.

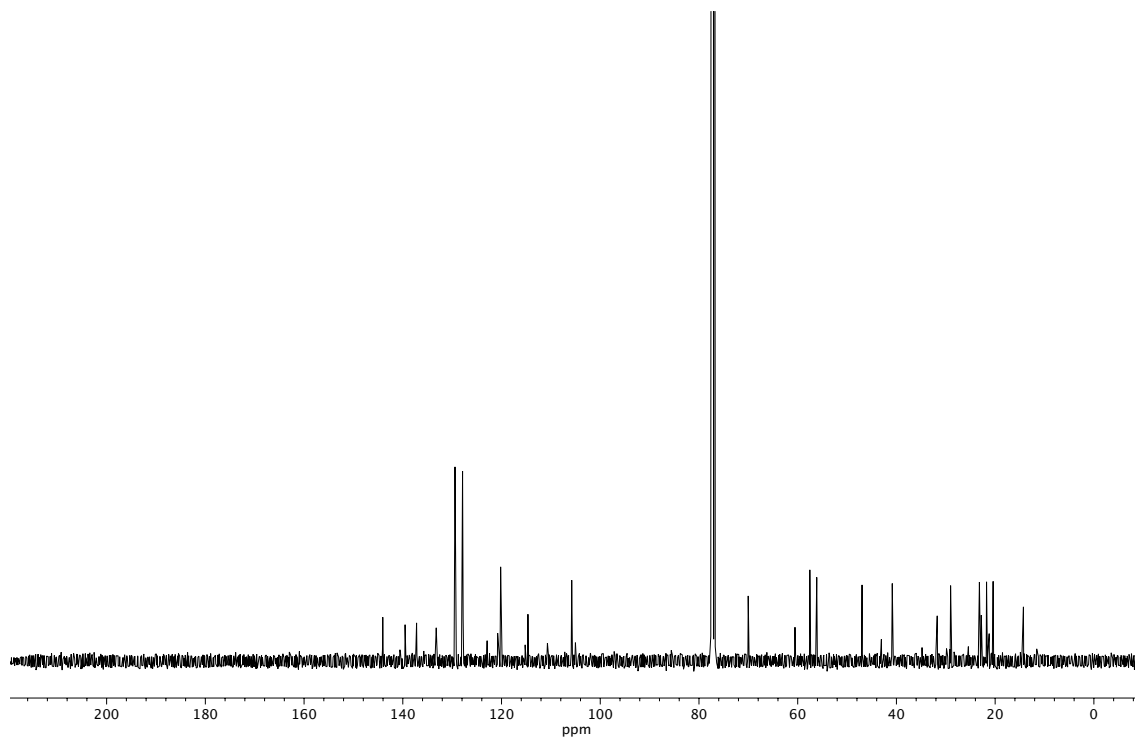


Figure A4.50. ¹³C NMR (100 MHz, CDCl₃) of compound **150**.

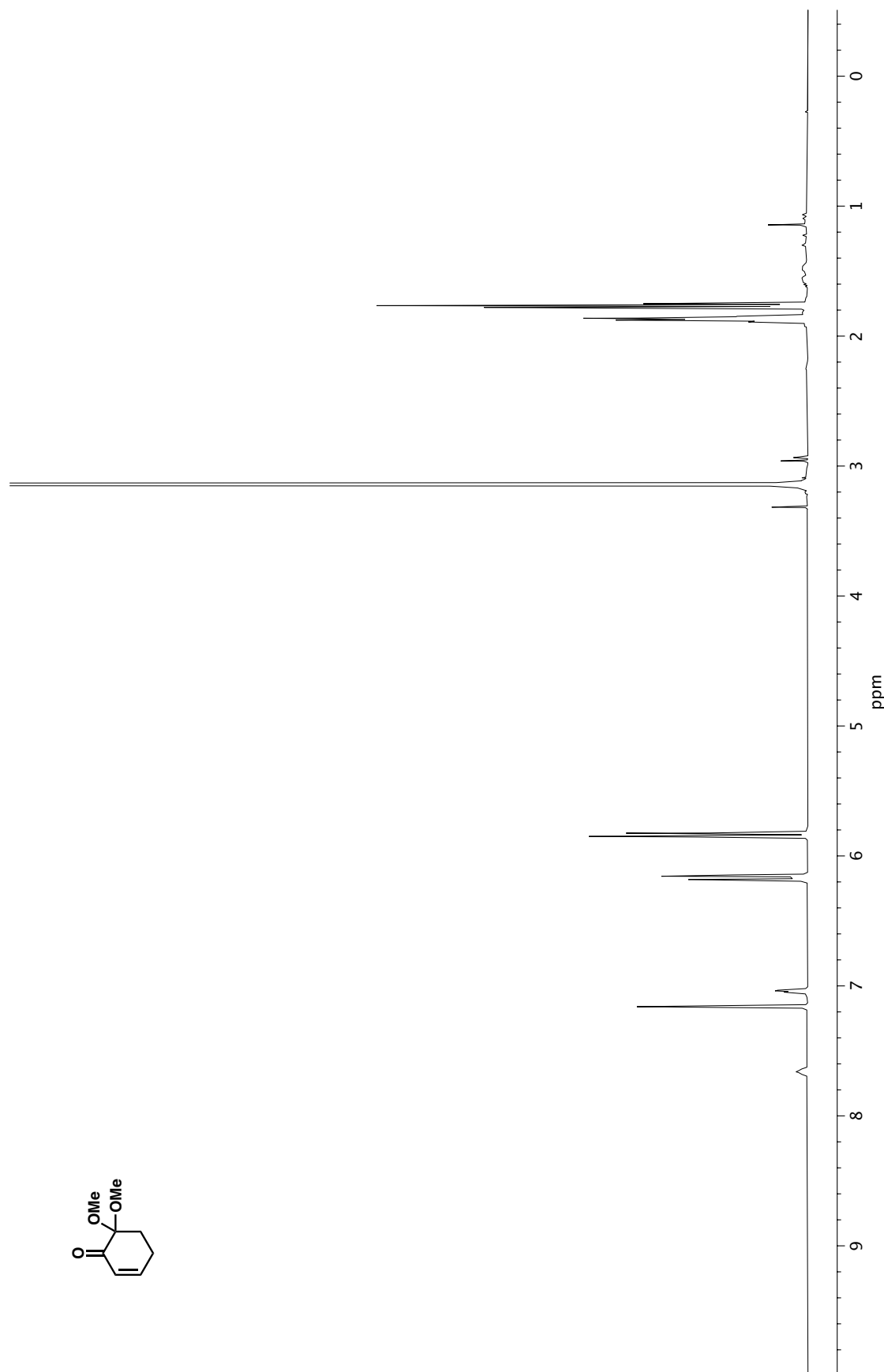


Figure A4.51. ^1H NMR (400 MHz, C_6D_6) of compound 153.

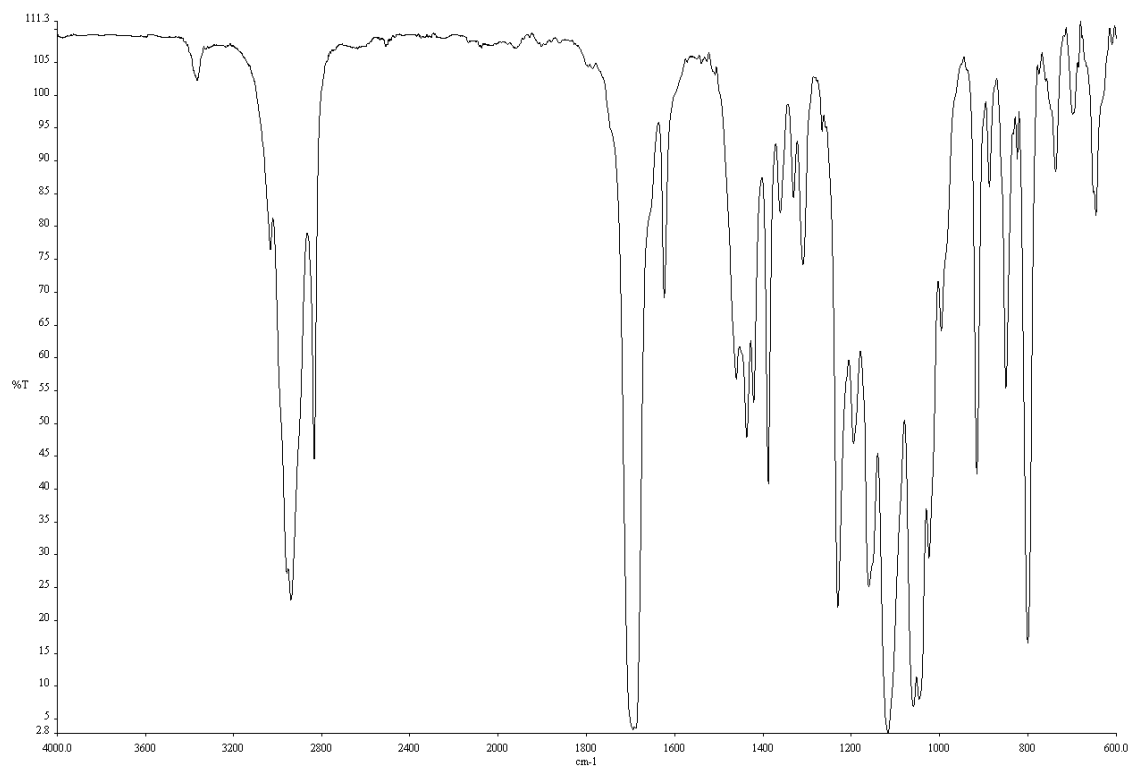


Figure A4.52. Infrared spectrum (Thin Film, NaCl) of compound **153**.

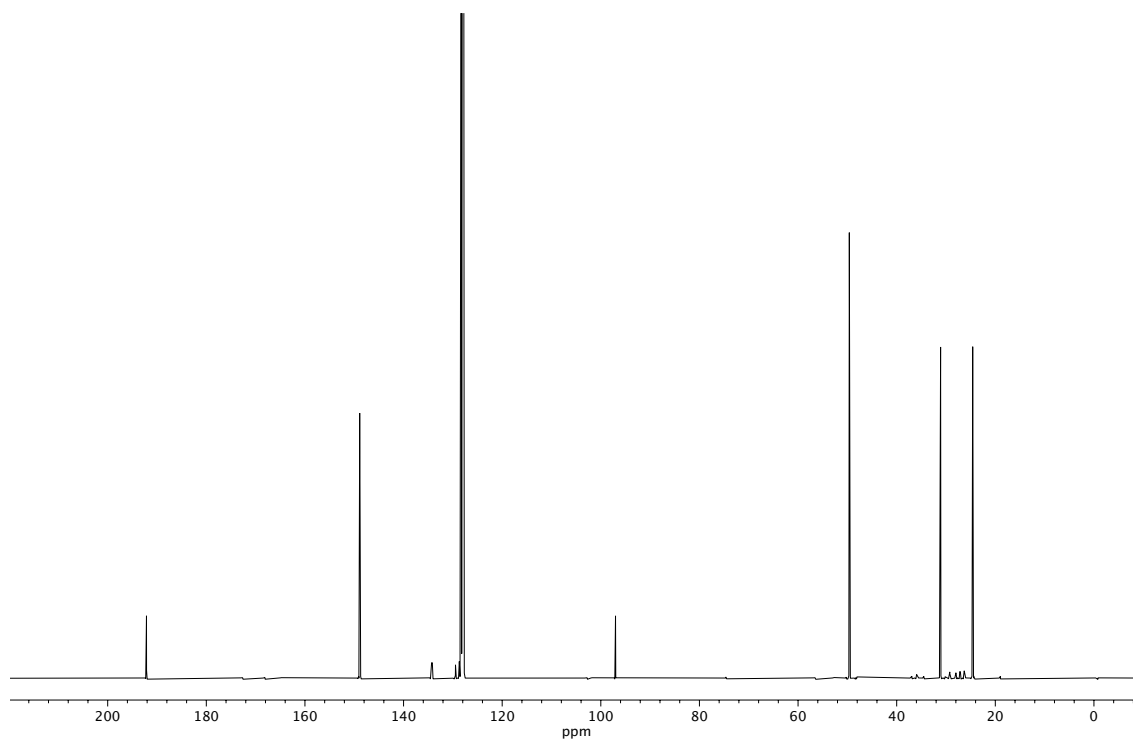


Figure A4.53. ¹³C NMR (100 MHz, C₆D₆) of compound **153**.

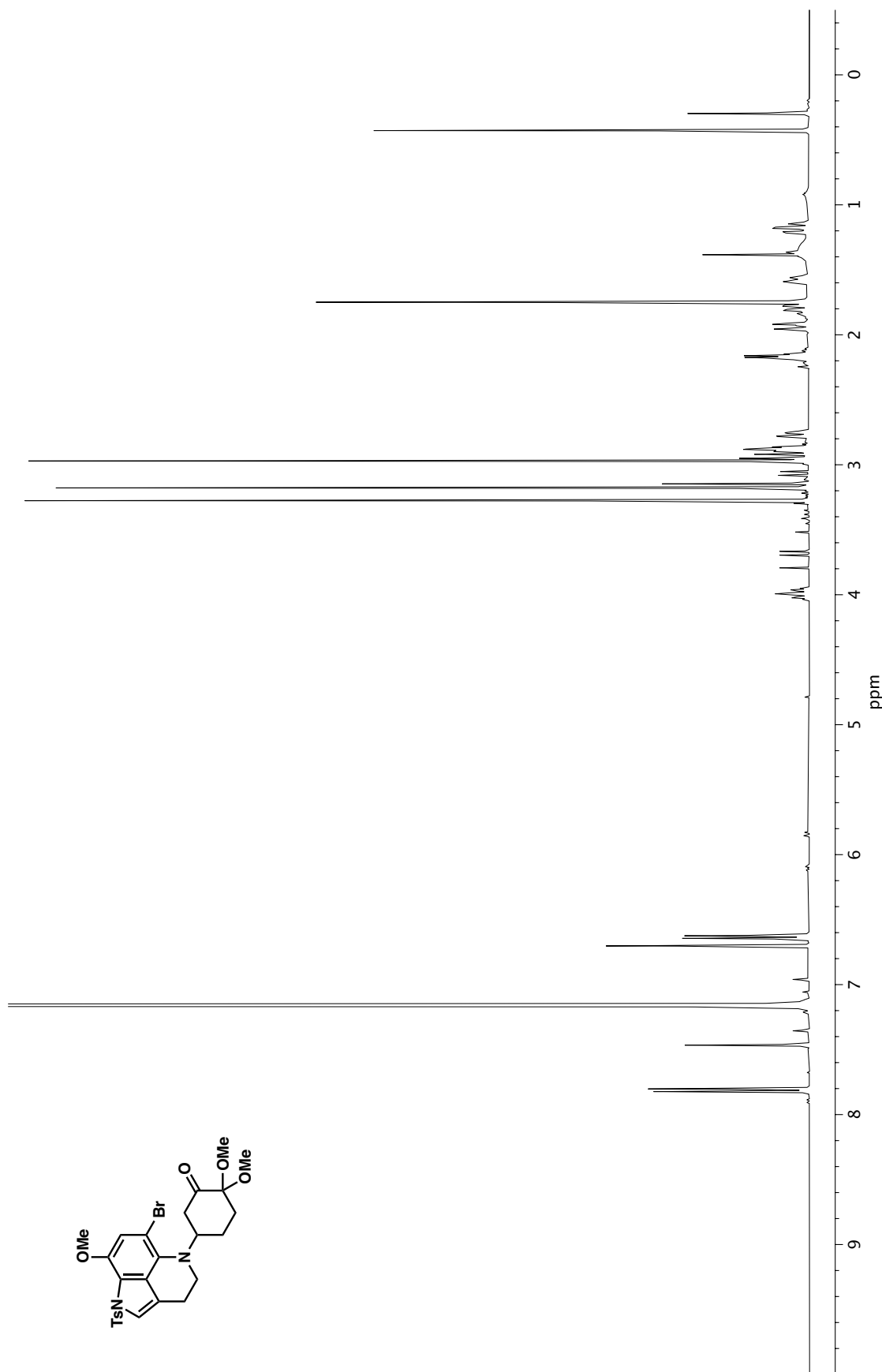


Figure A4.54. ^1H NMR (400 MHz, C_6D_6) of compound 154.

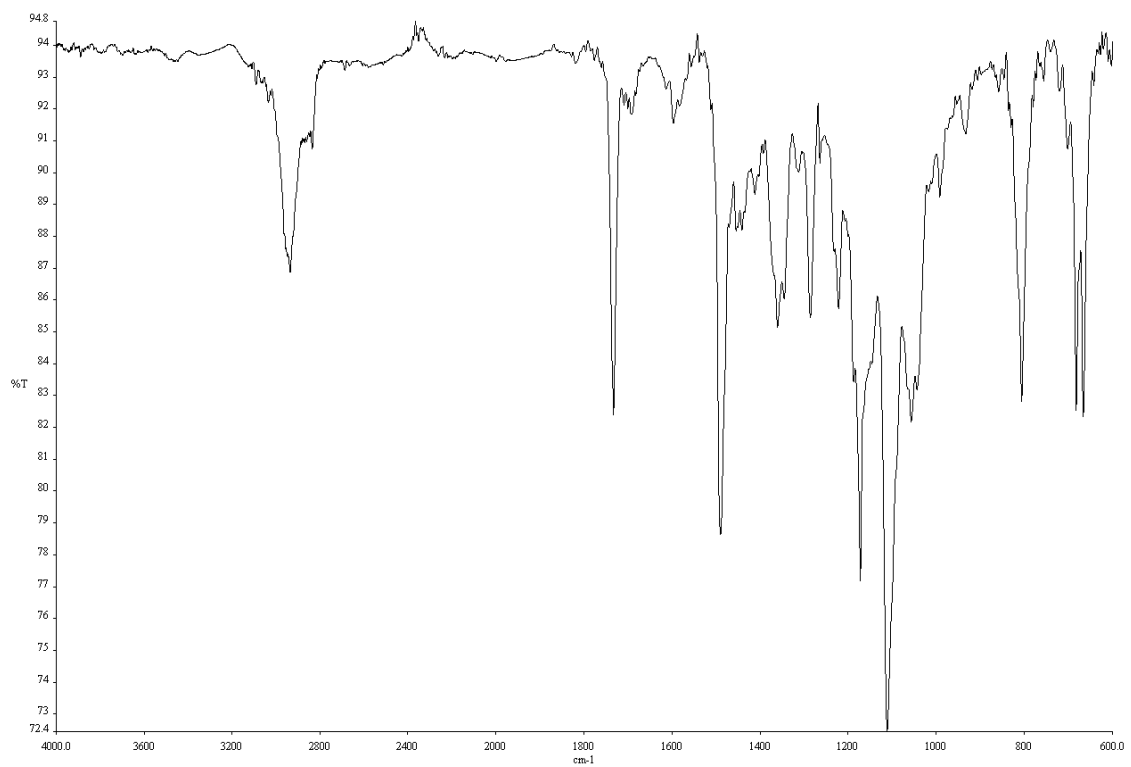


Figure A4.55. Infrared spectrum (Thin Film, NaCl) of compound **154**.

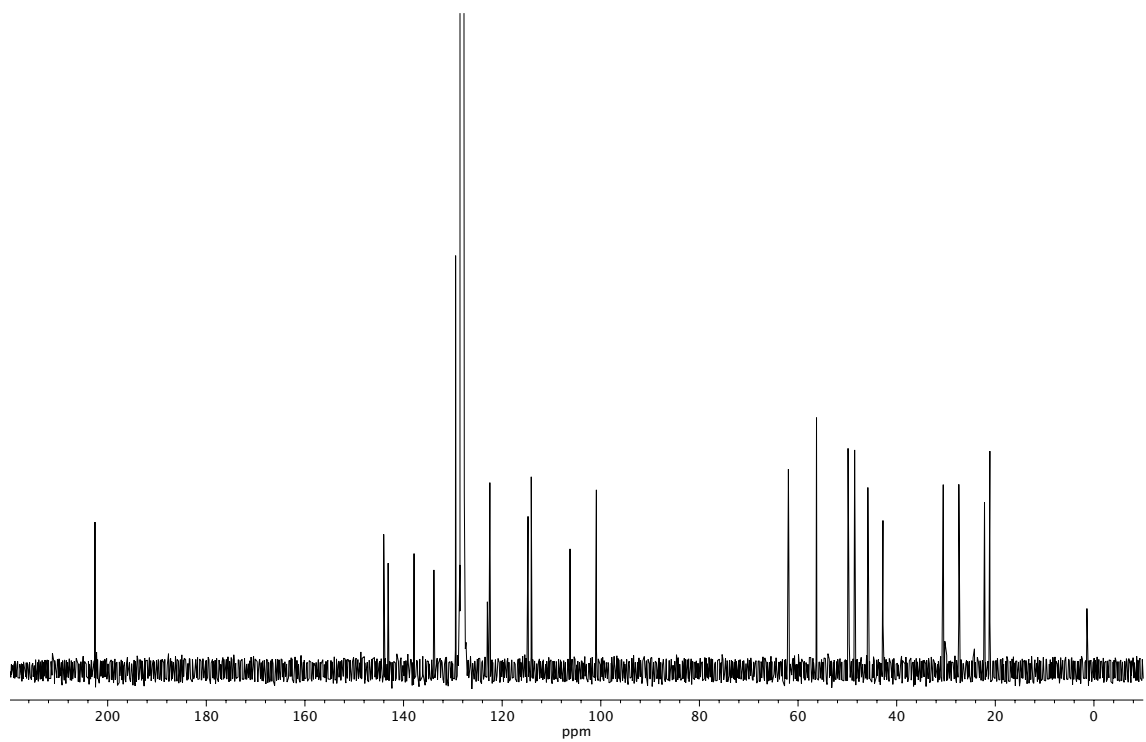
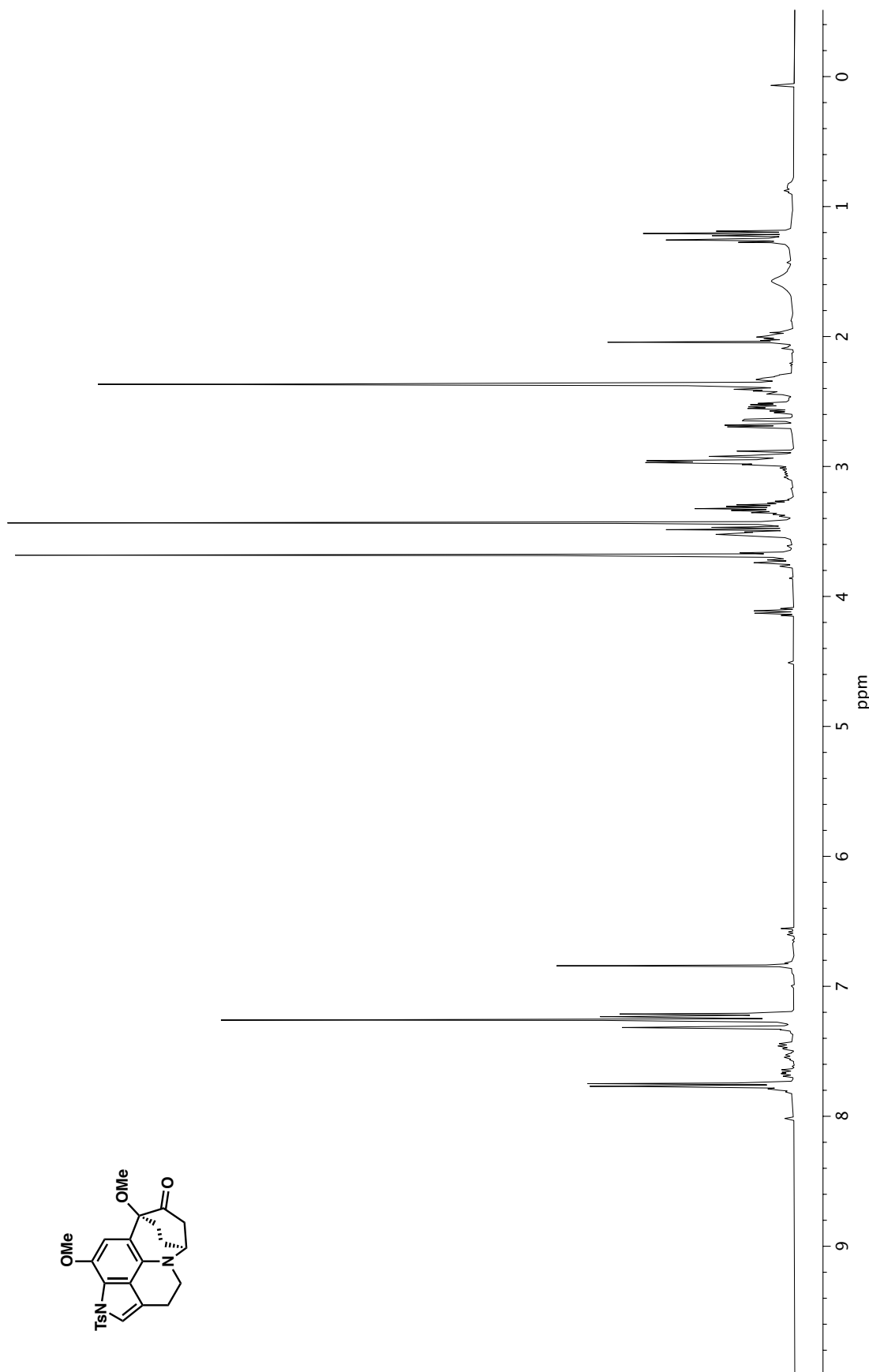


Figure A4.56. ^{13}C NMR (100 MHz, C_6D_6) of compound **154**.



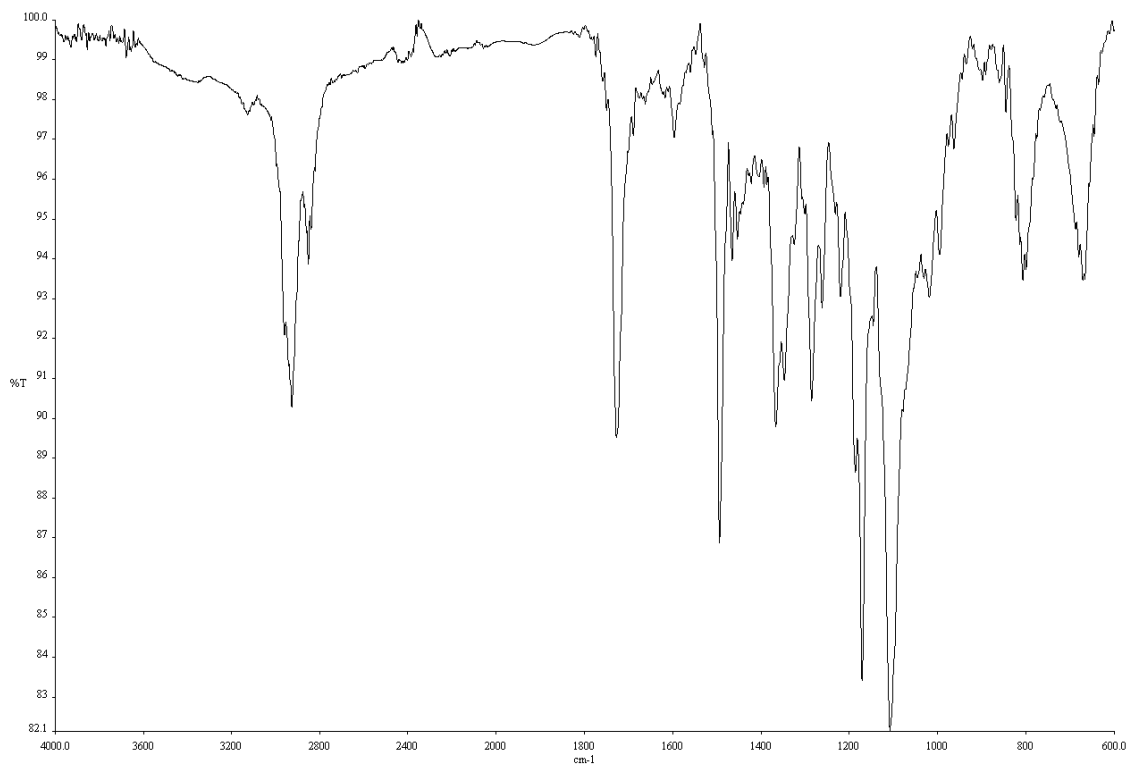


Figure A4.58. Infrared spectrum (Thin Film, NaCl) of compound **156**.

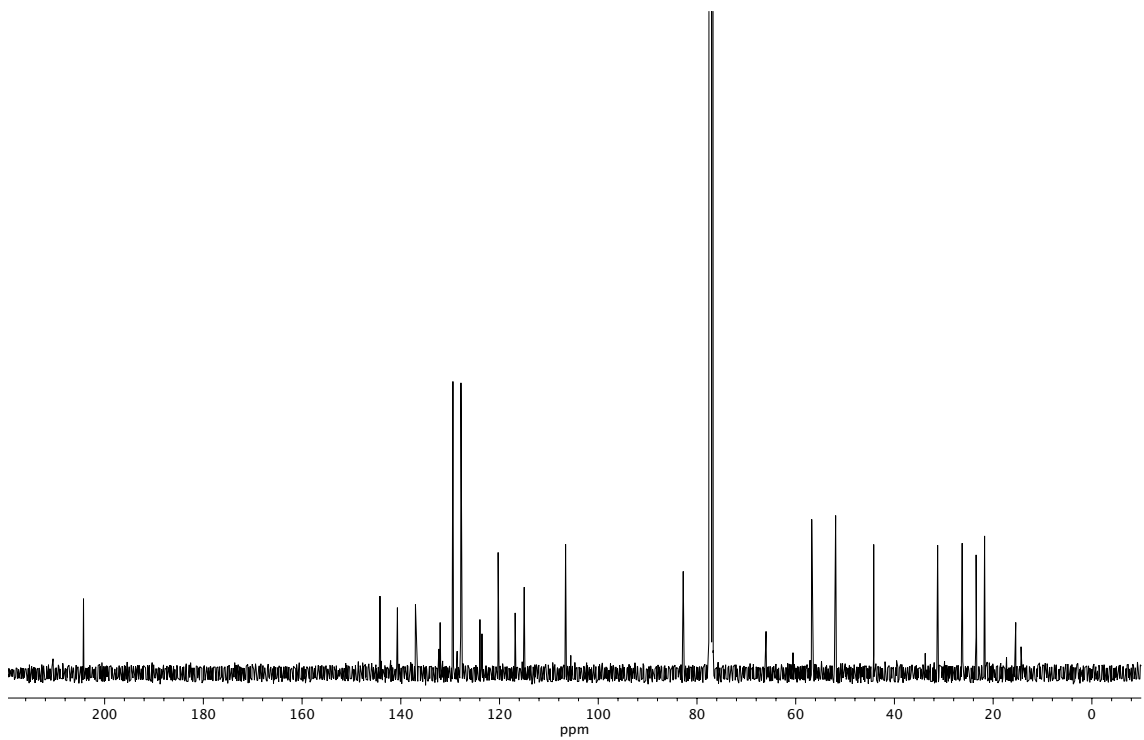


Figure A4.59. ^{13}C NMR (100 MHz, CDCl_3) of compound **156**.

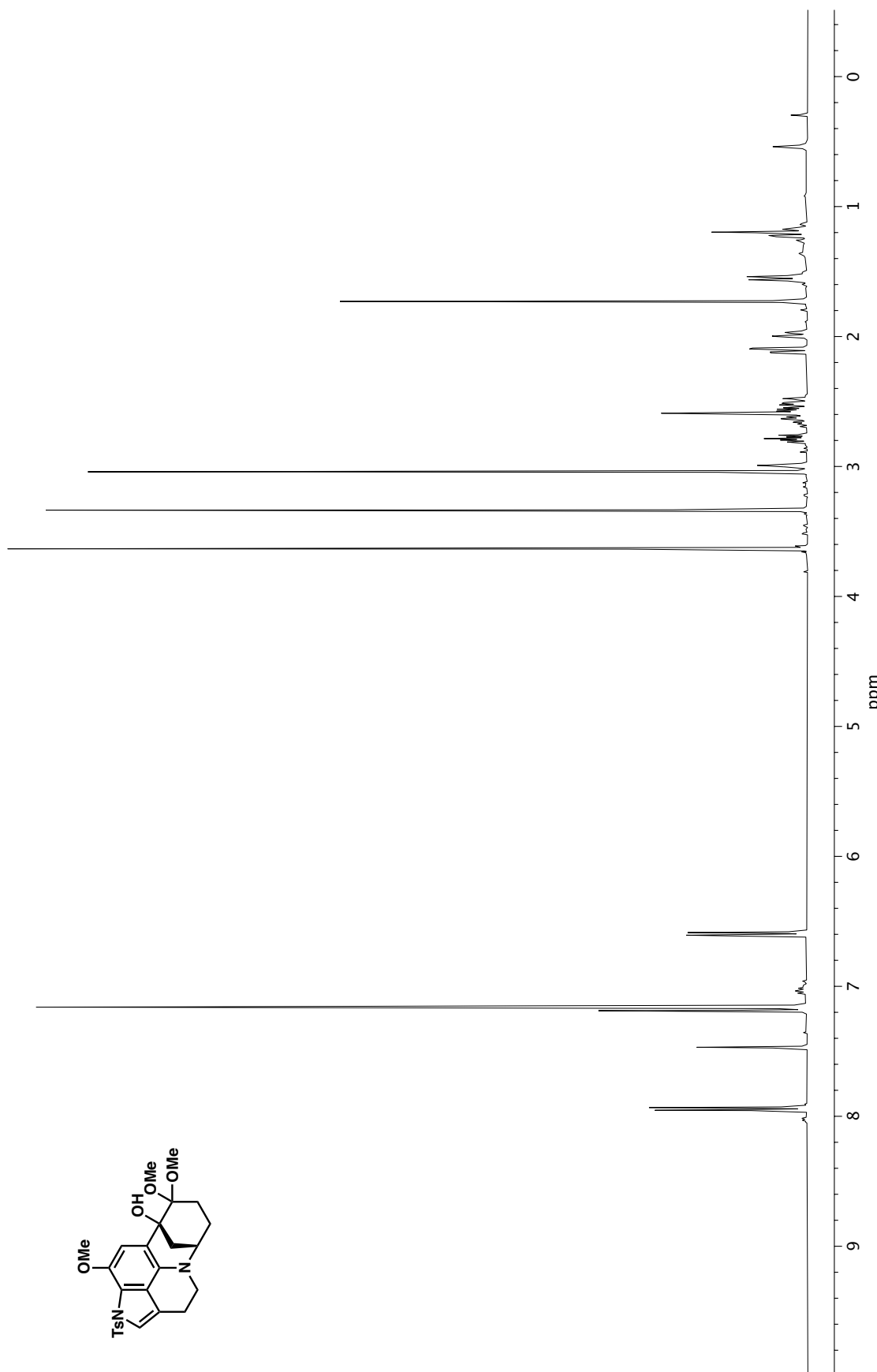


Figure A4.60. ^1H NMR (400 MHz, C_6D_6) of compound **155**.

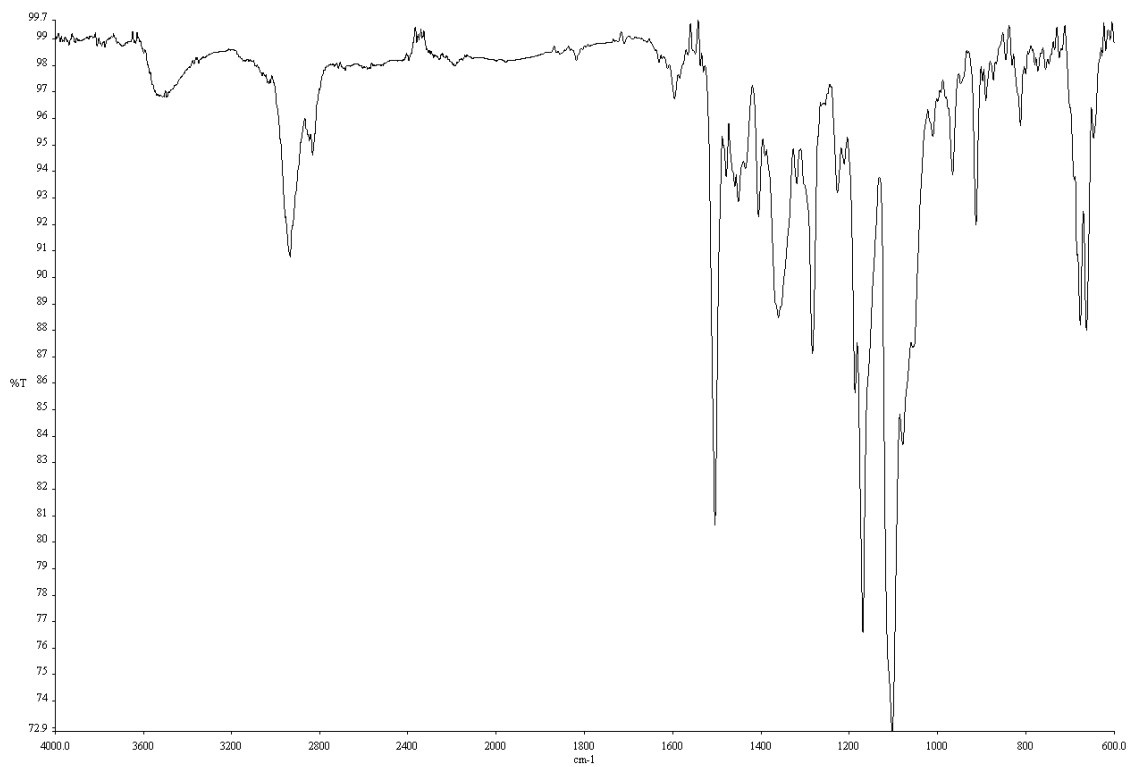


Figure A4.61. Infrared spectrum (Thin Film, NaCl) of compound **155**.

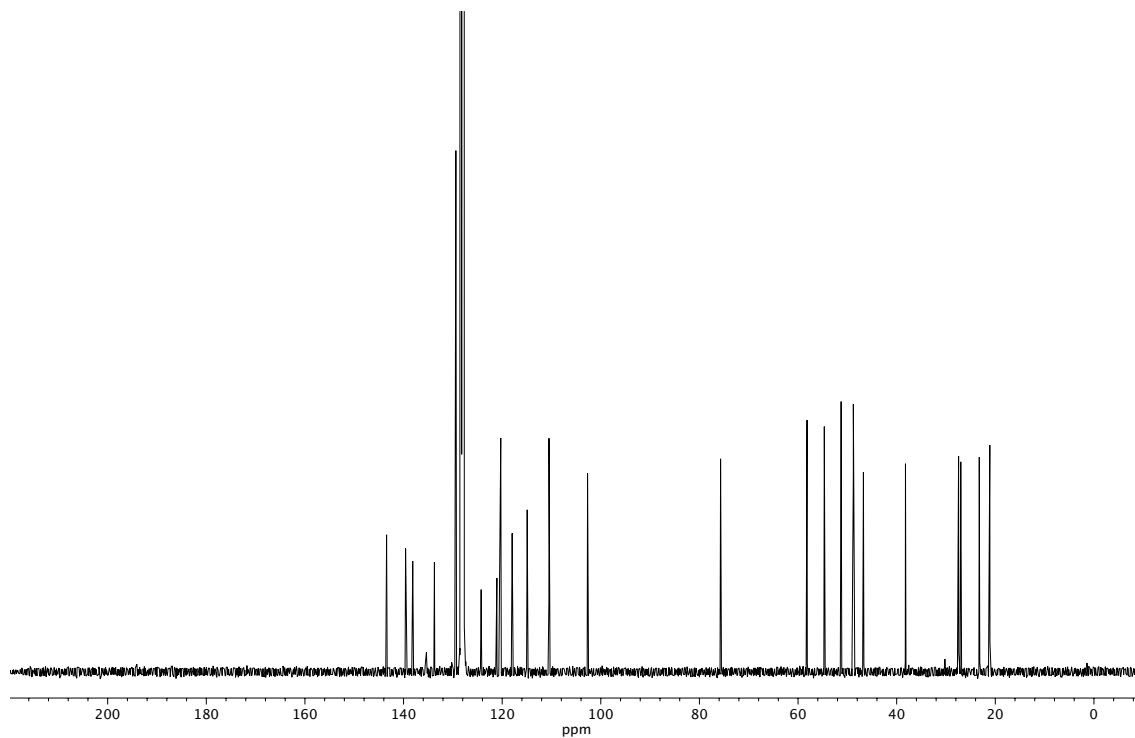
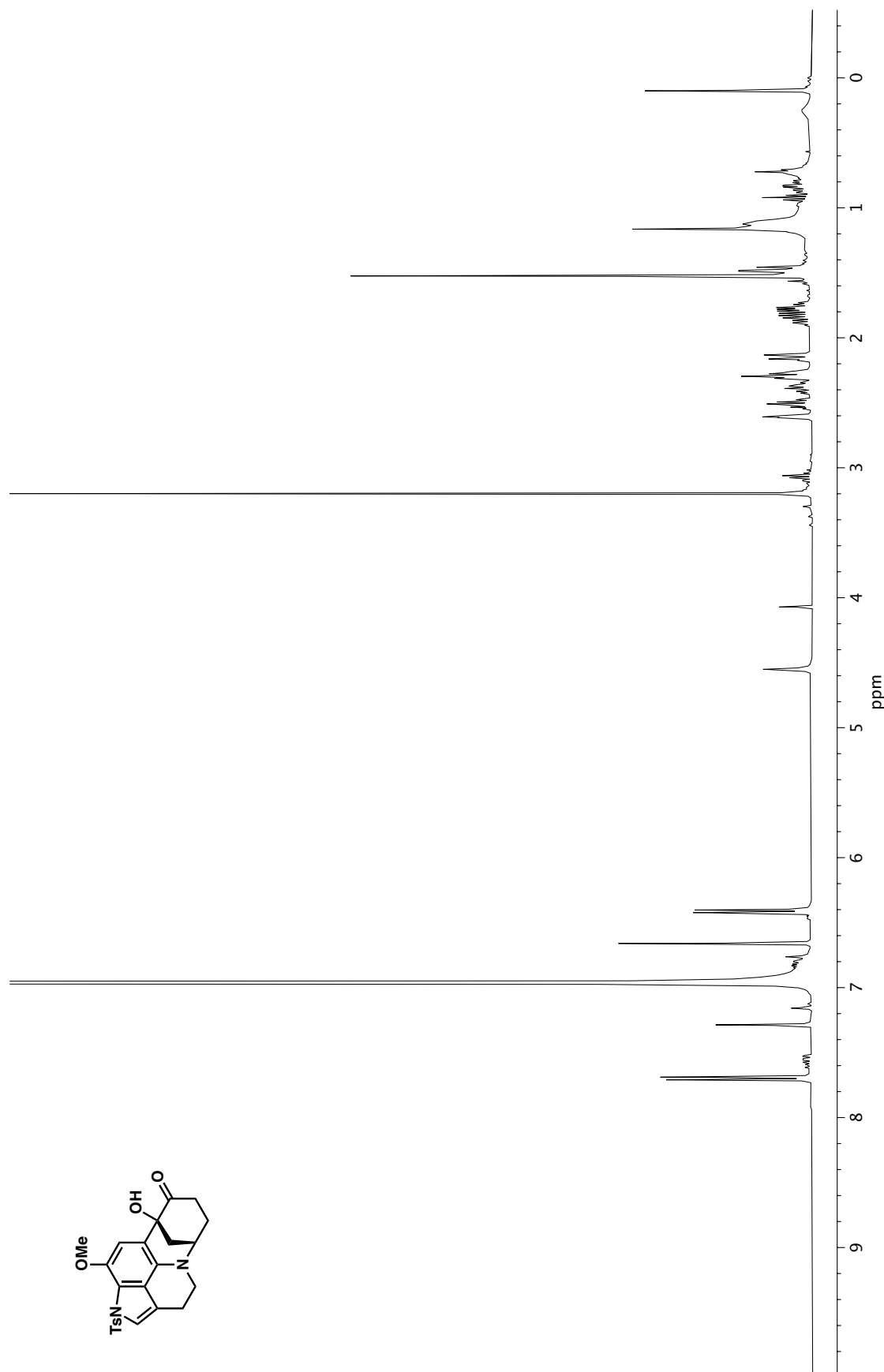


Figure A4.62. ^{13}C NMR (100 MHz, C_6D_6) of compound **155**.

Figure A4.63. ¹H NMR (400 MHz, C₆D₆) of compound **157**.

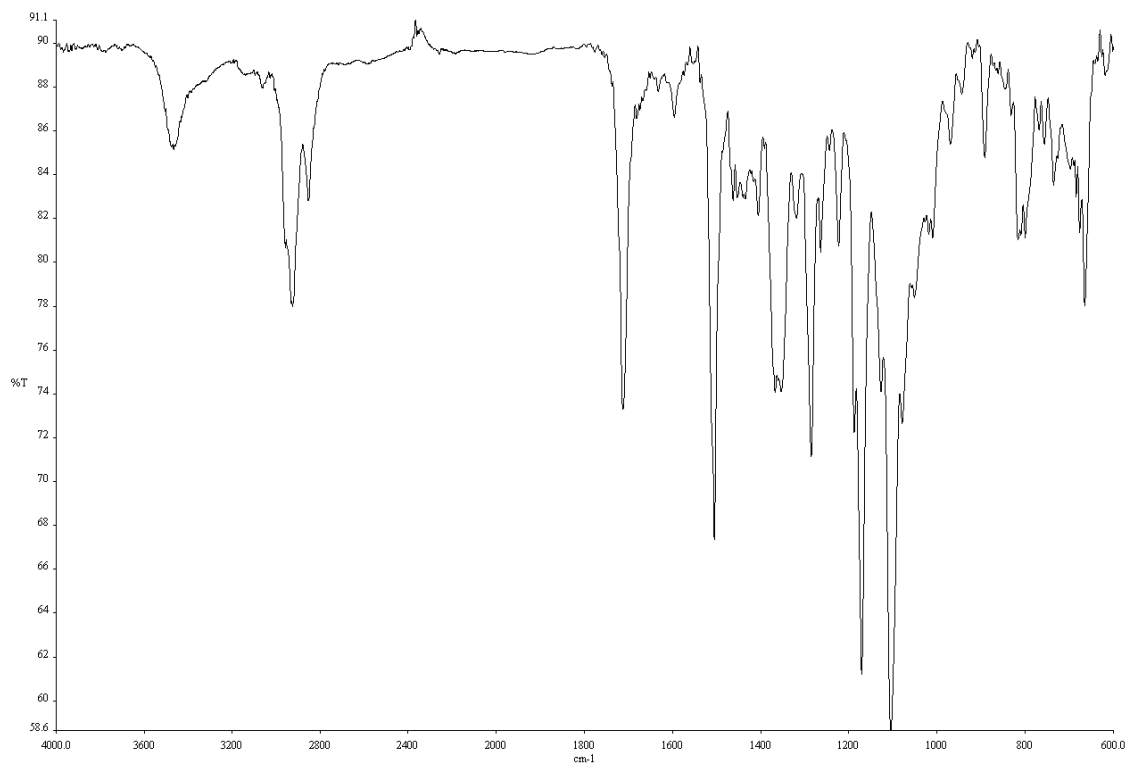


Figure A4.64. Infrared spectrum (Thin Film, NaCl) of compound **157**.

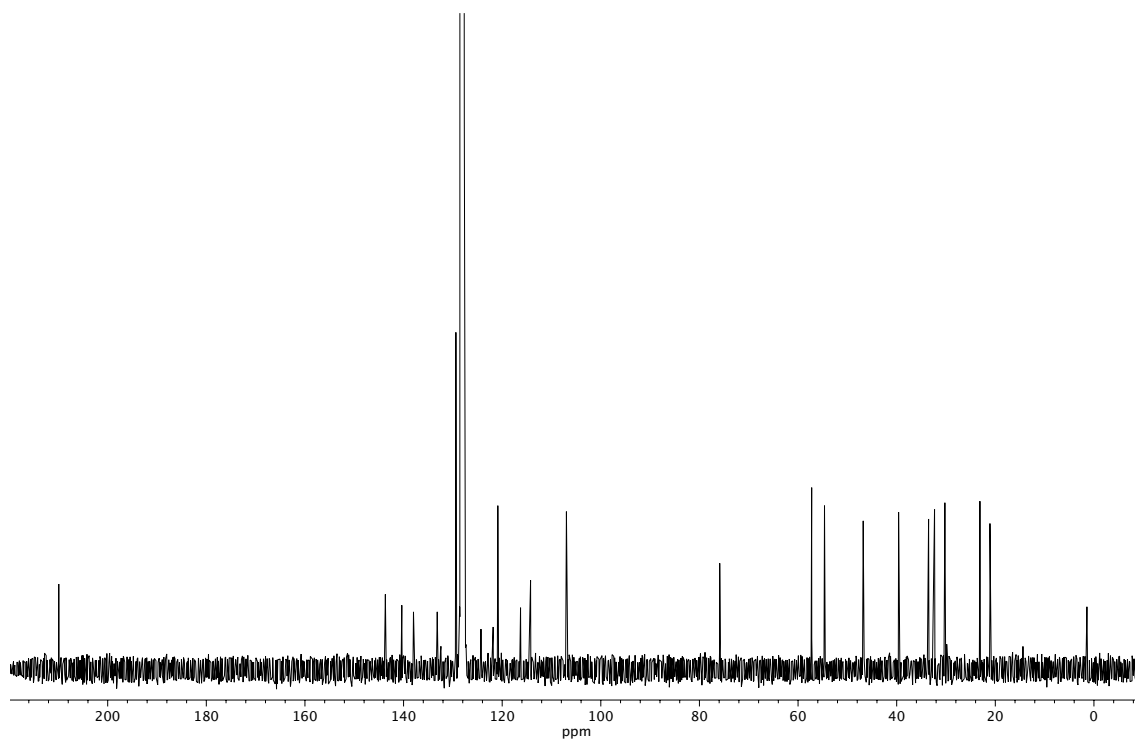
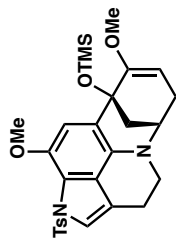
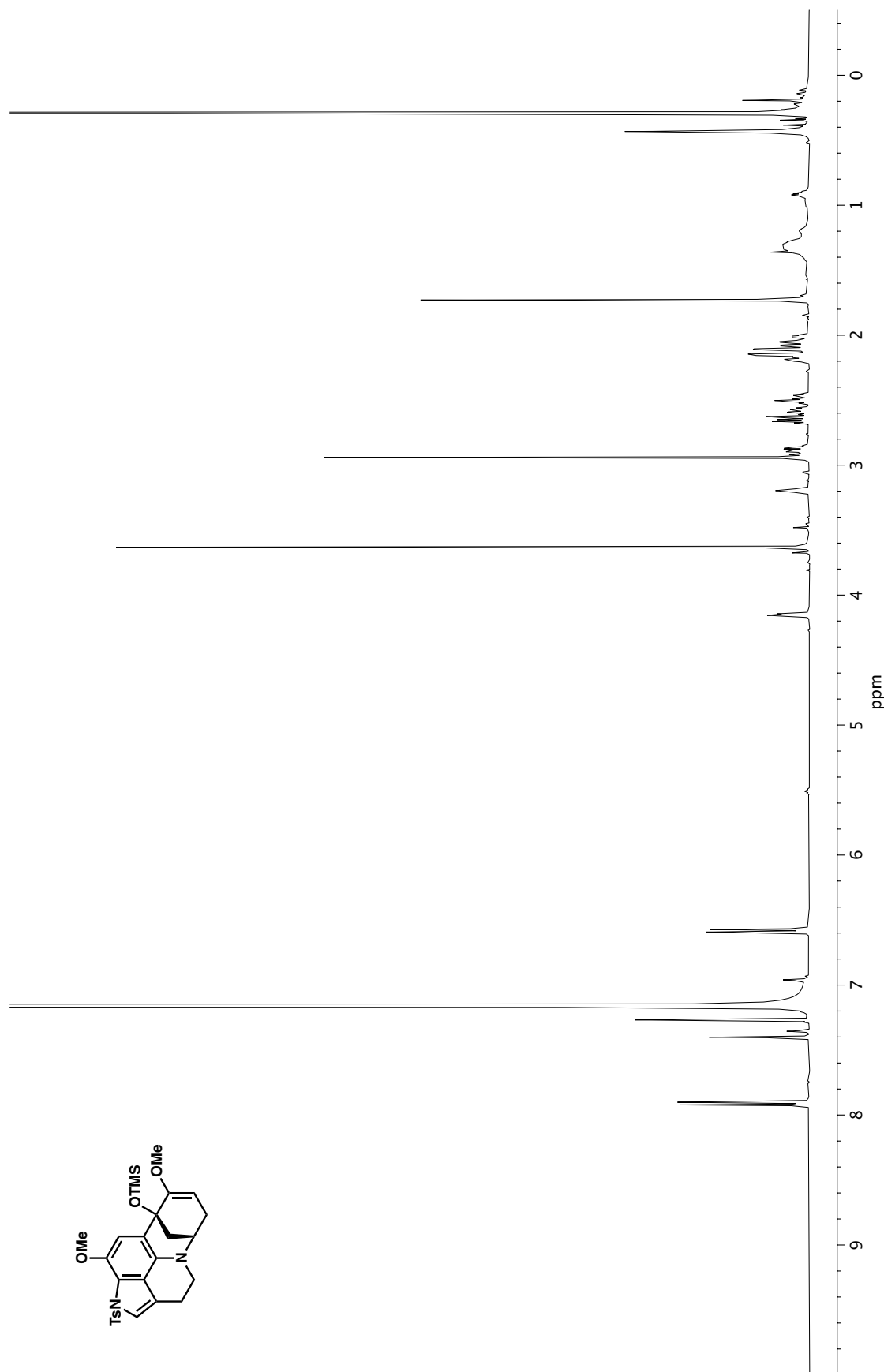


Figure A4.65. ^{13}C NMR (100 MHz, C_6D_6) of compound **157**.



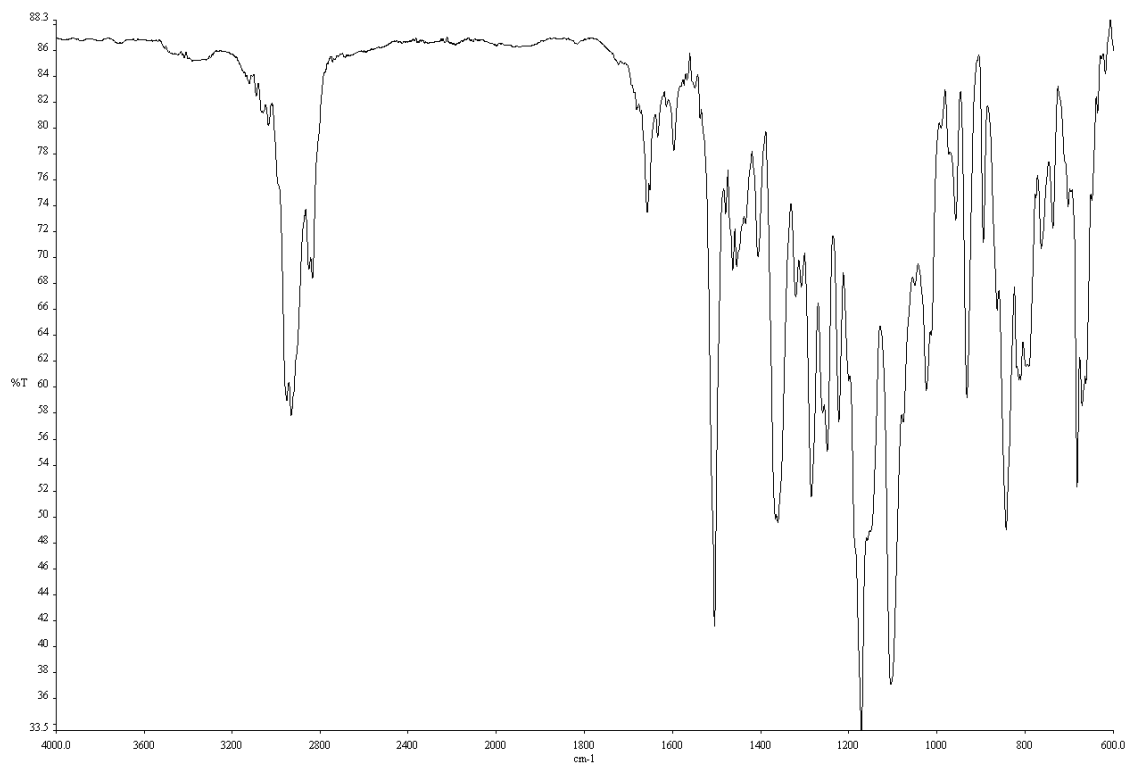


Figure A4.67. Infrared spectrum (Thin Film, NaCl) of compound **160**.

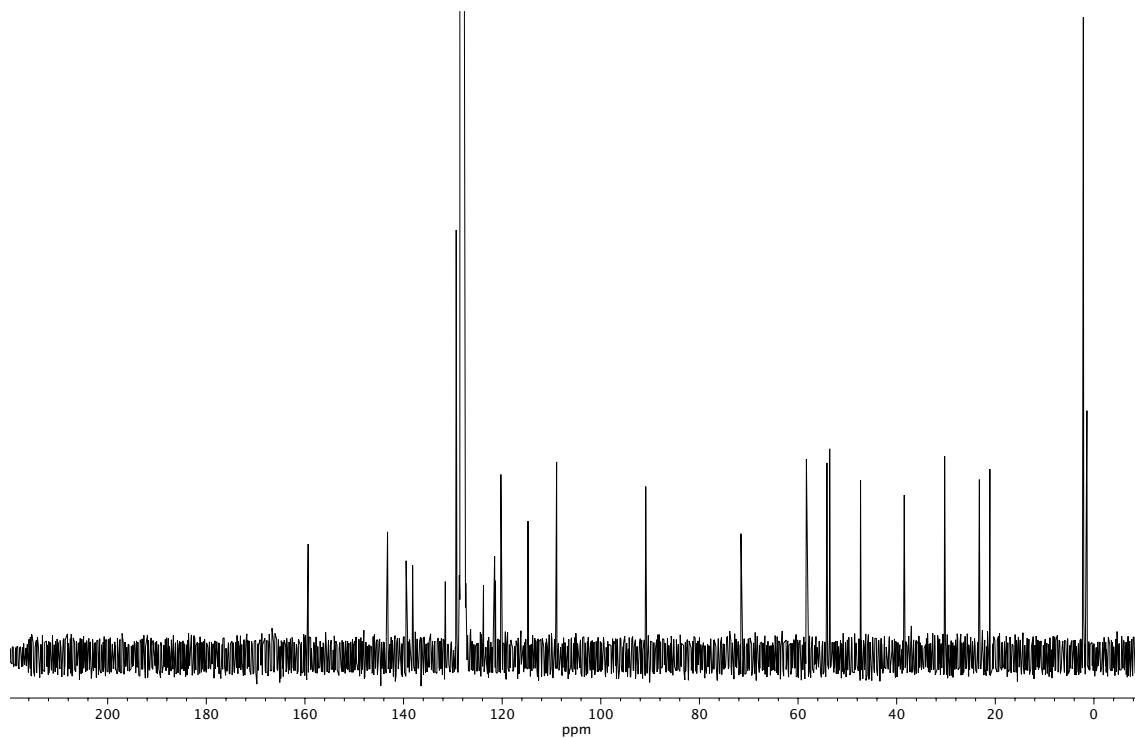


Figure A4.68. ¹³C NMR (100 MHz, C₆D₆) of compound **160**.

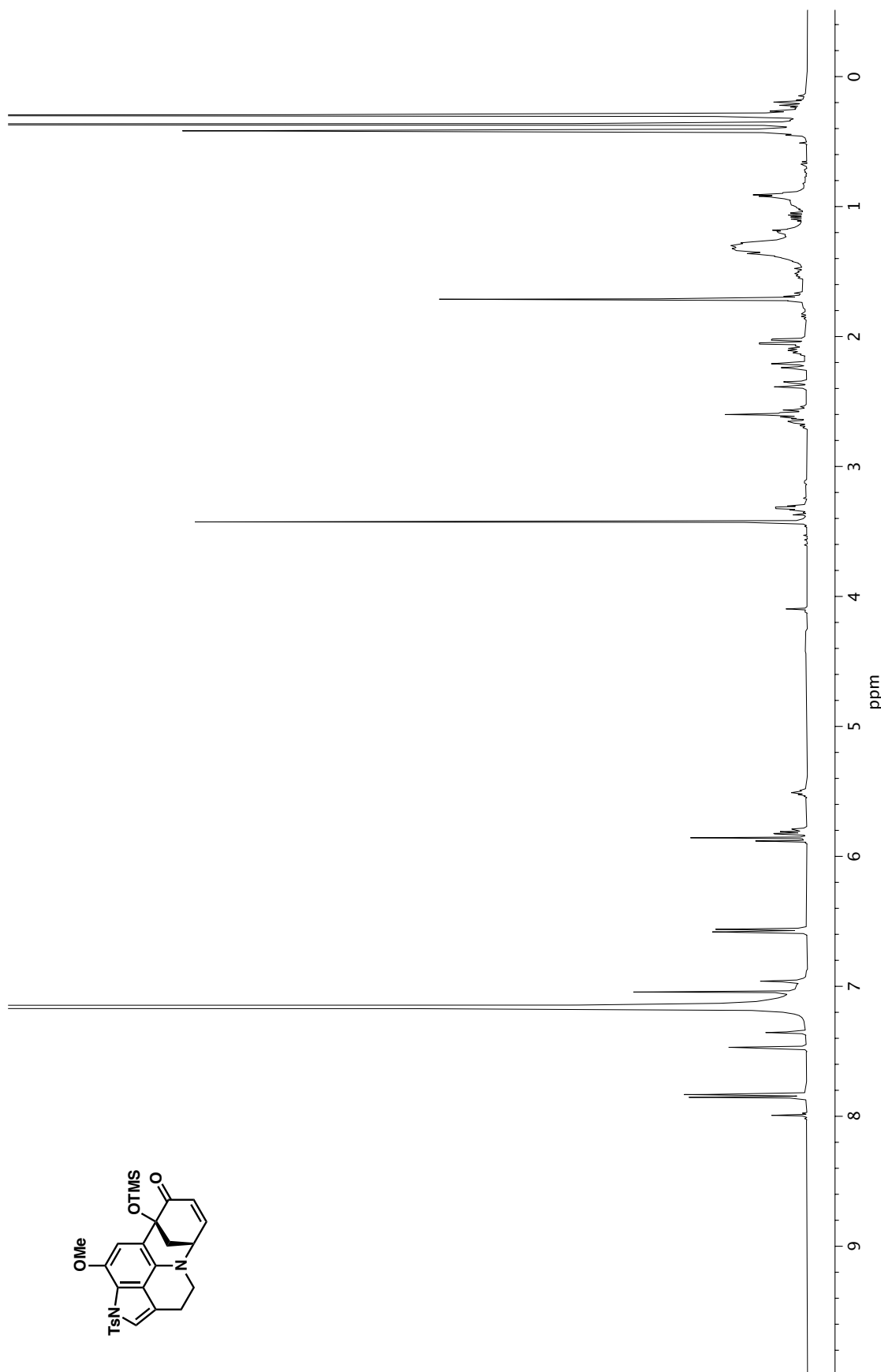


Figure A4.69. ¹H NMR (400 MHz, C₆D₆) of compound **168**.

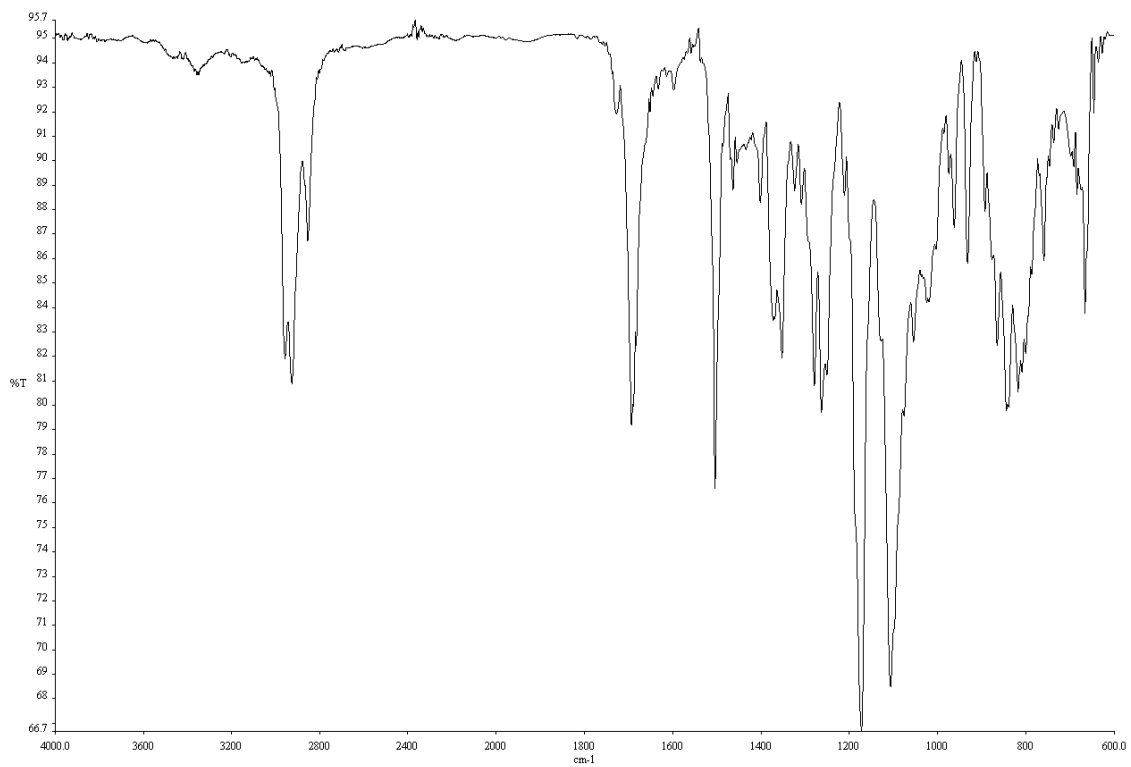


Figure A4.70. Infrared spectrum (Thin Film, NaCl) of compound **168**.

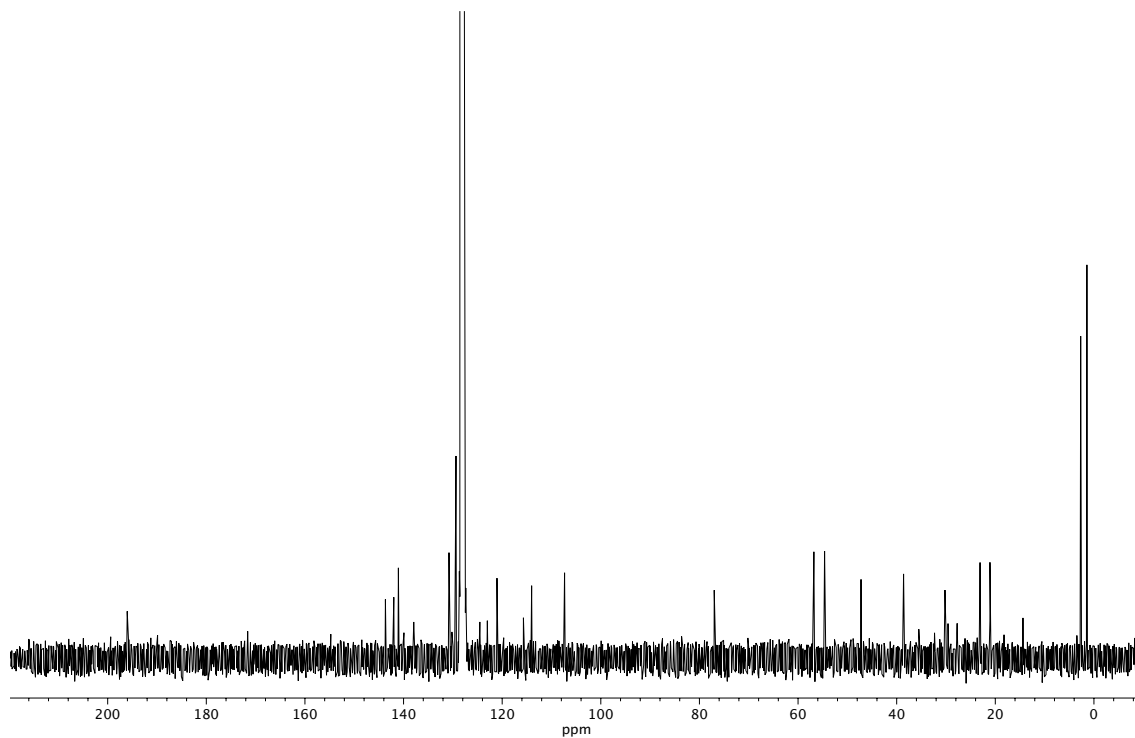


Figure A4.71. ¹³C NMR (100 MHz, C₆D₆) of compound **168**.

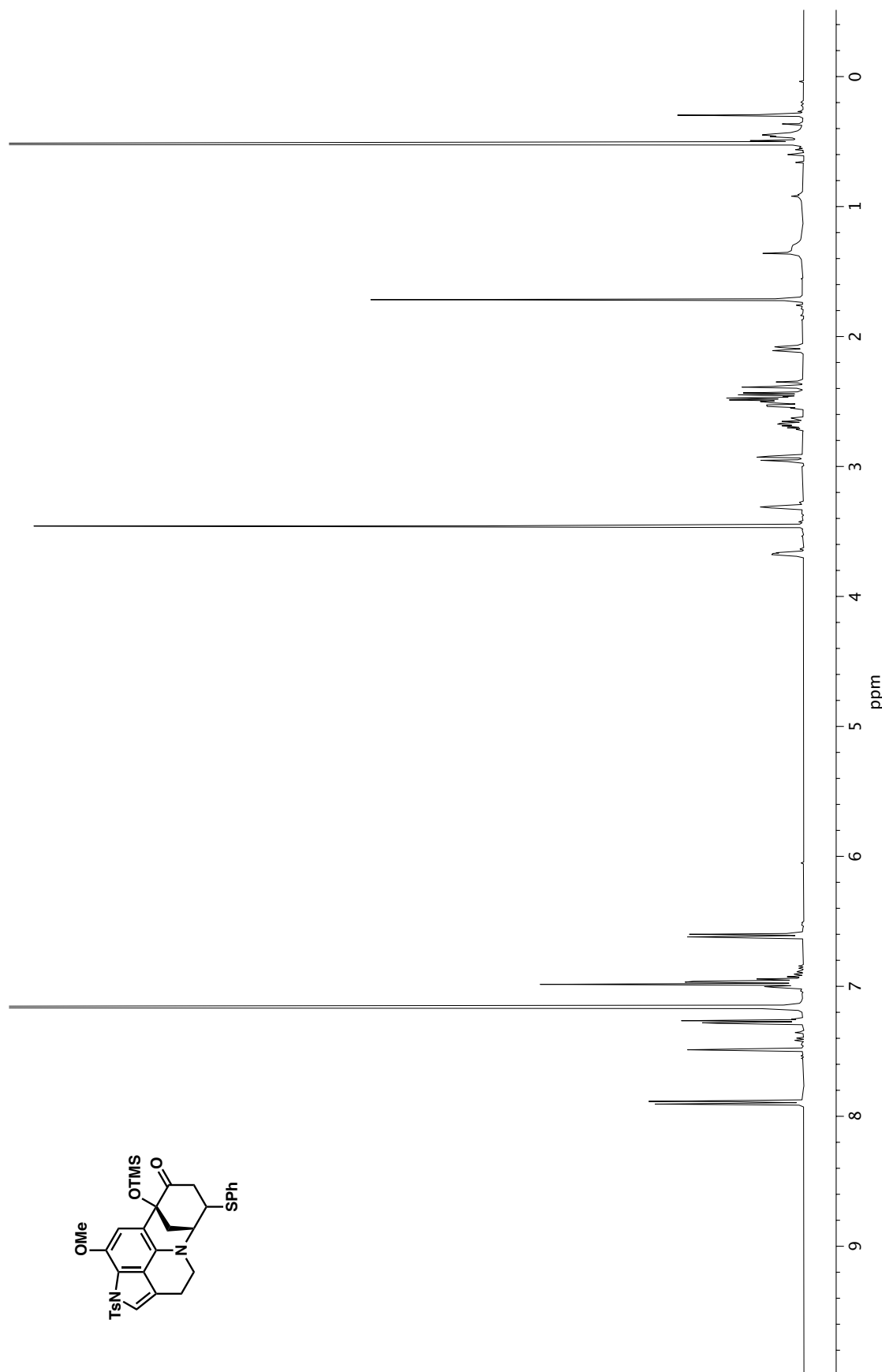


Figure A4.72. ¹H NMR (400 MHz, C₆D₆) of compound **169**.

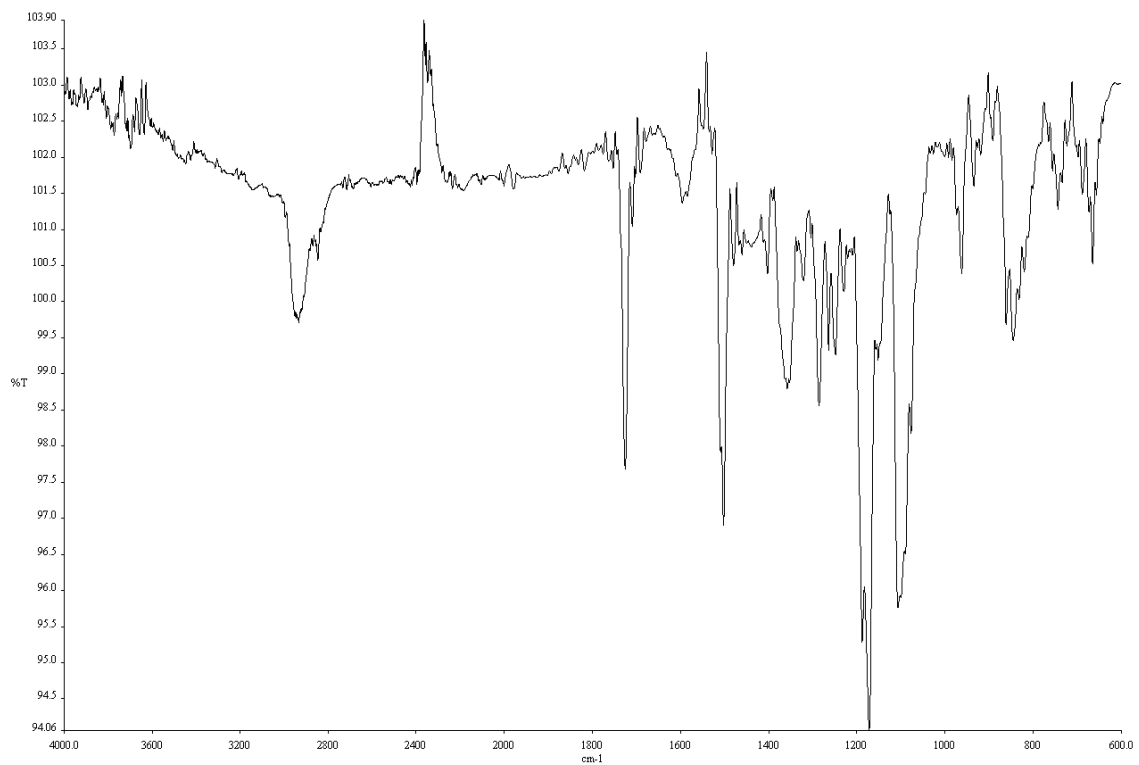


Figure A4.73. Infrared spectrum (Thin Film, NaCl) of compound **169**.

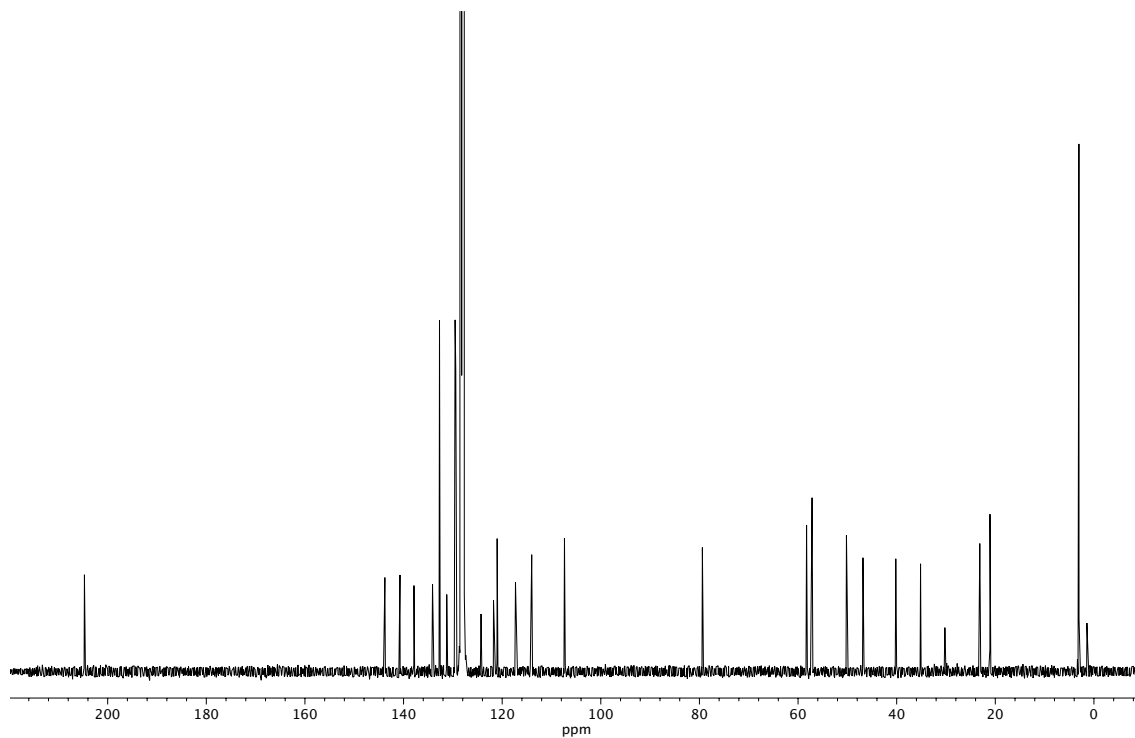


Figure A4.74. ^{13}C NMR (100 MHz, C_6D_6) of compound **169**.

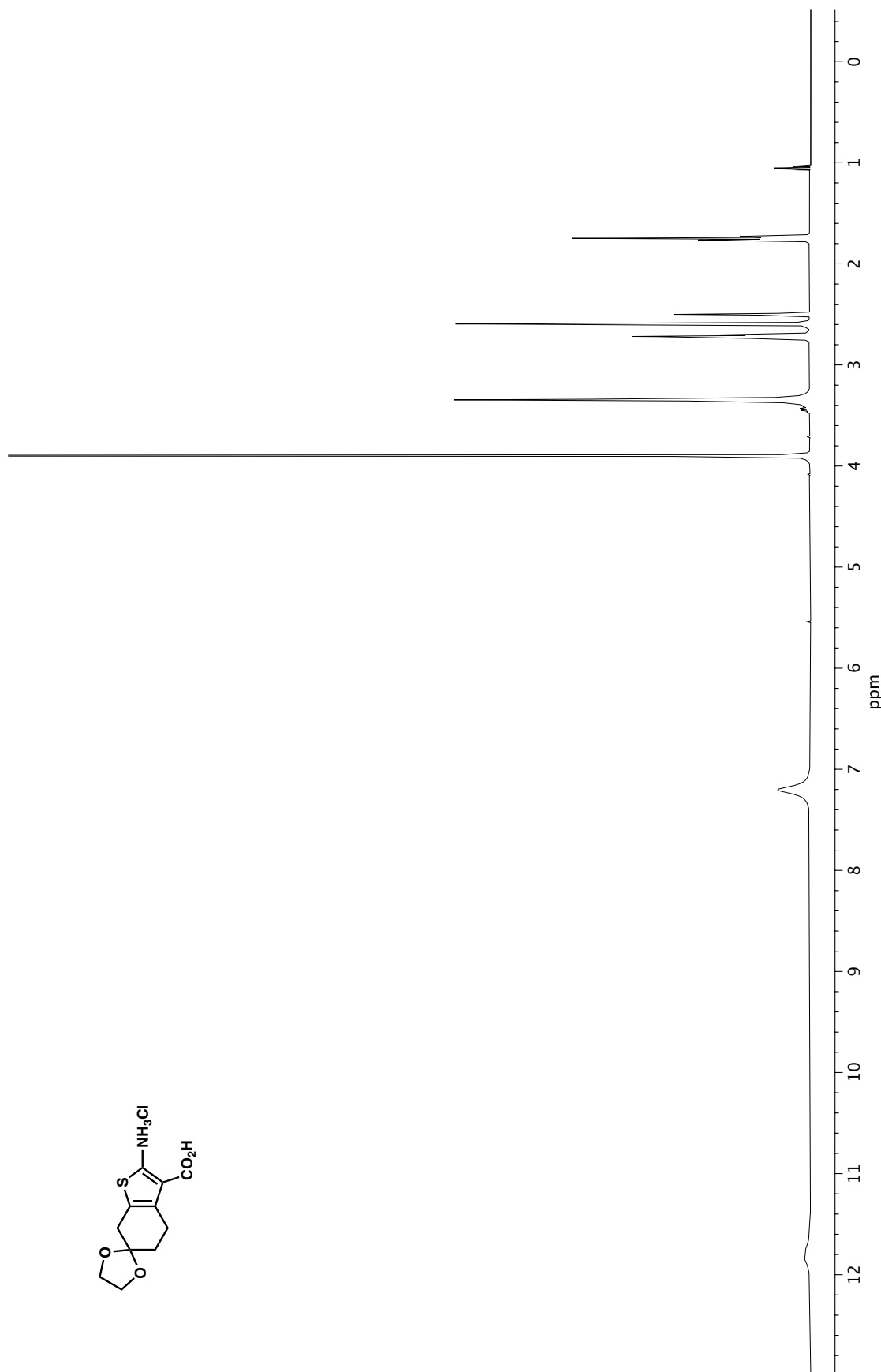


Figure A4.75. ^1H NMR (400 MHz, DMSO-d_6) of compound 214.

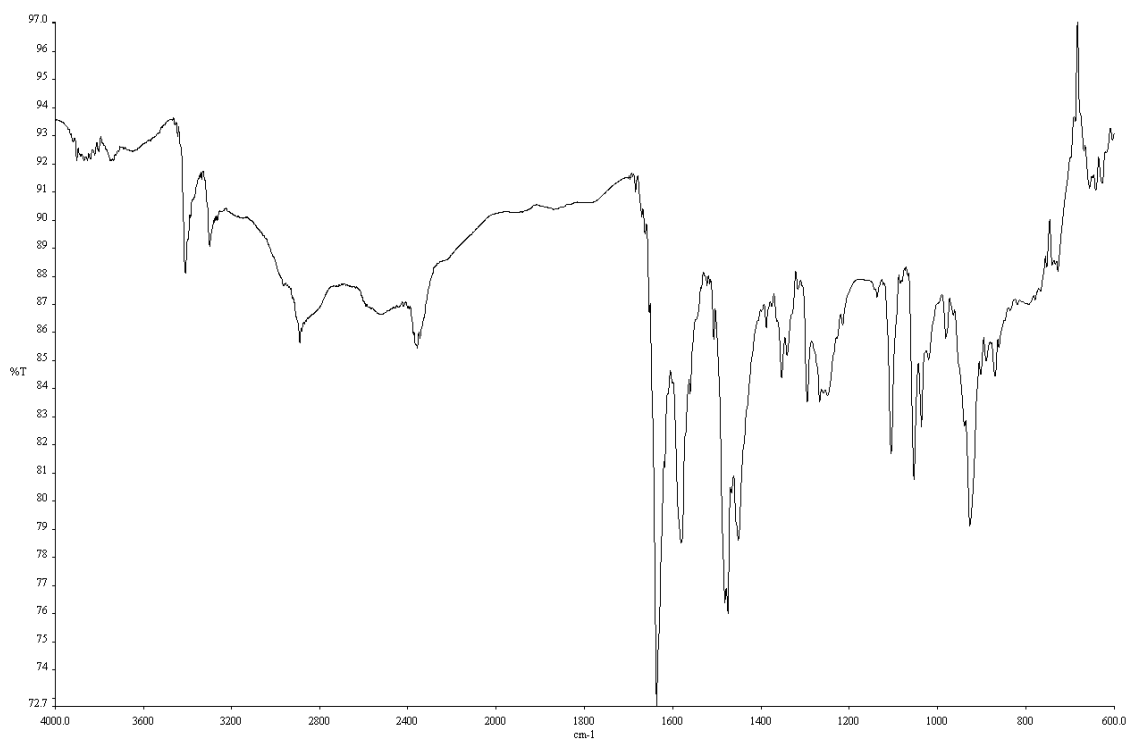


Figure A4.76. Infrared spectrum (Thin Film, NaCl) of compound **214**.

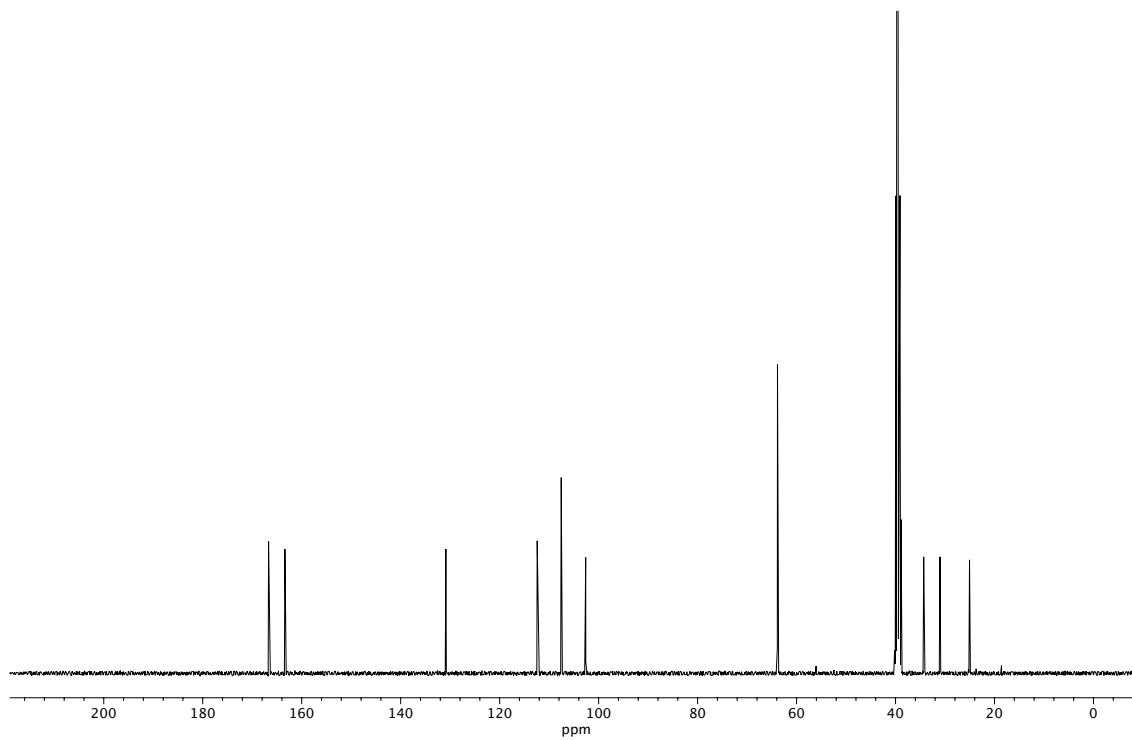


Figure A4.77. ¹³C NMR (100 MHz, DMSO-d₆) of compound **214**.

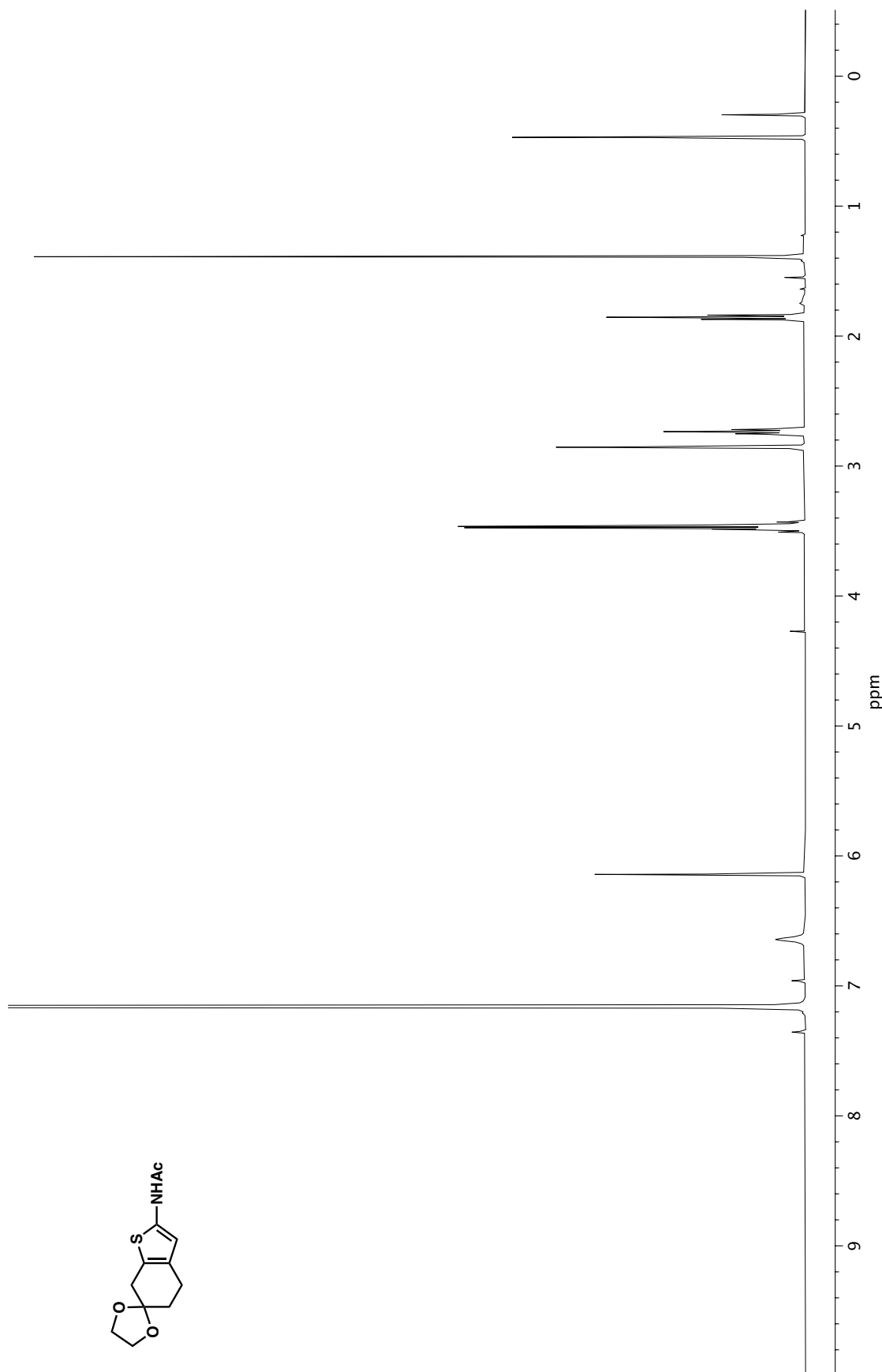


Figure A4.78. ^1H NMR (400 MHz, C_6D_6) of compound **177**.

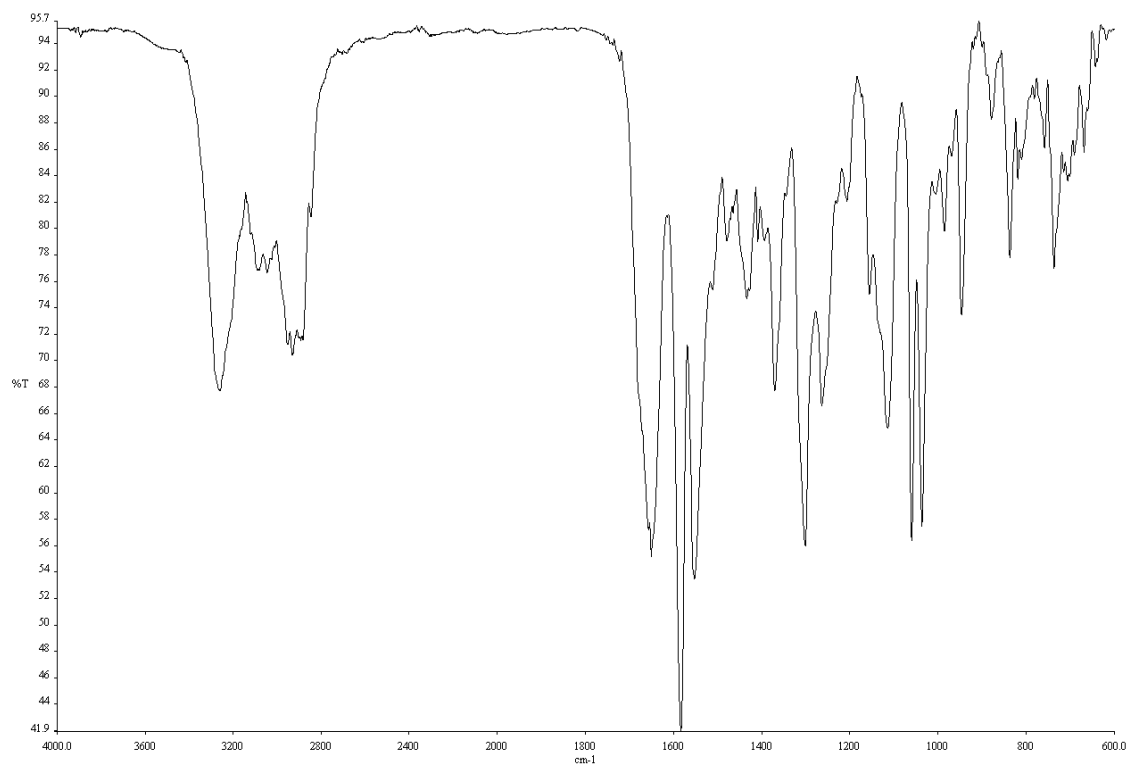


Figure A4.79. Infrared spectrum (Thin Film, NaCl) of compound **177**.

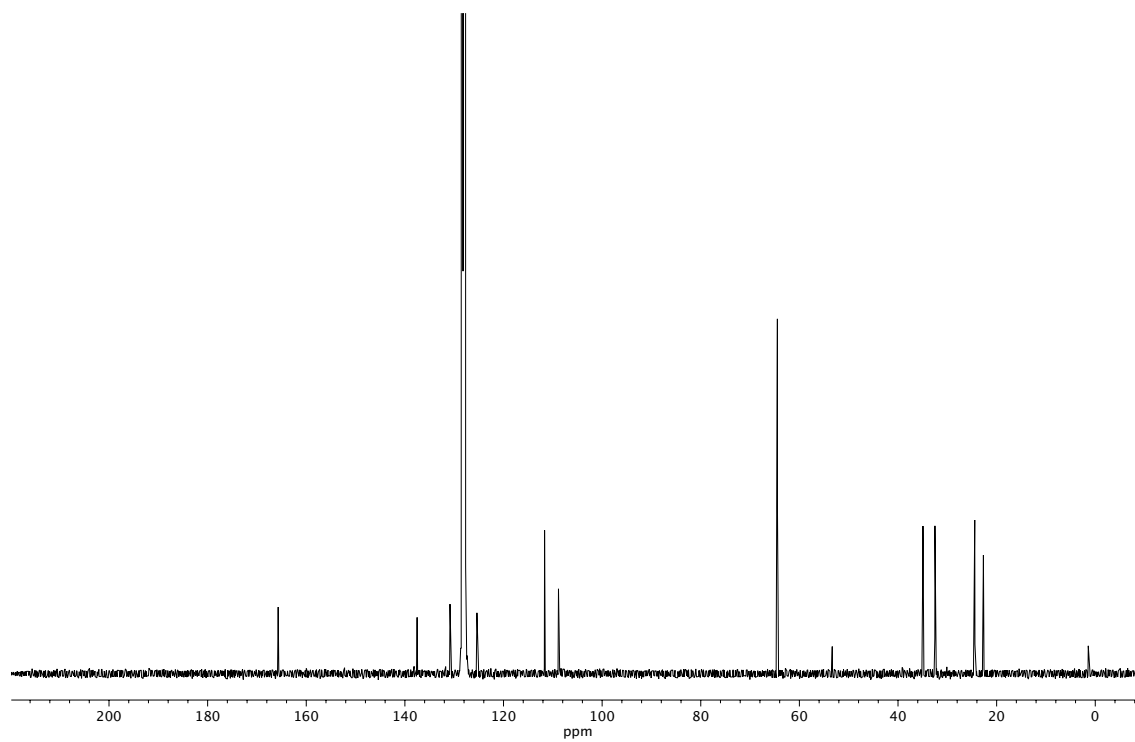
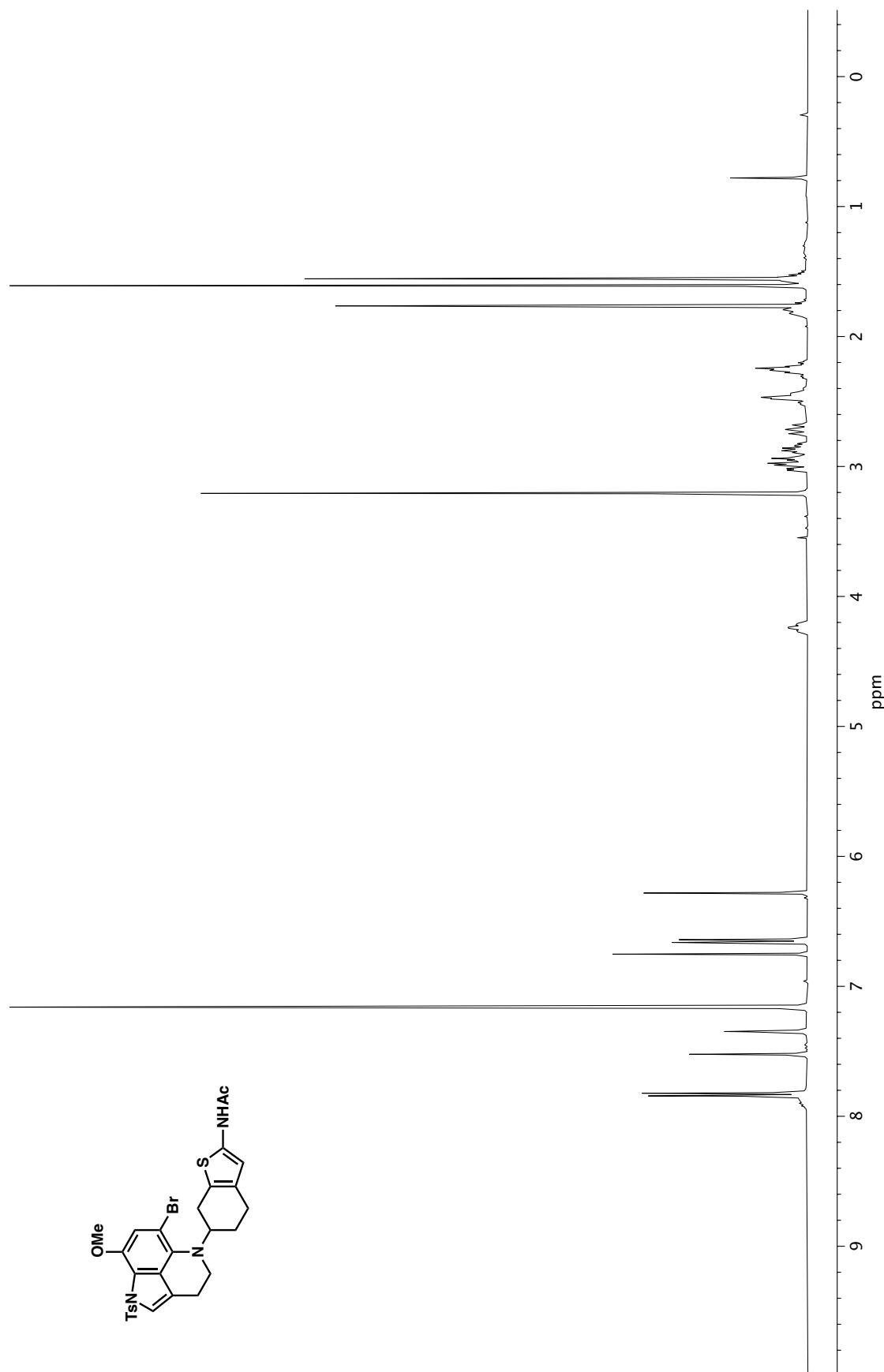


Figure A4.80. ¹³C NMR (100 MHz, C₆D₆) of compound **177**.

Figure A4.81. ^1H NMR (400 MHz, C_6D_6) of compound 179.

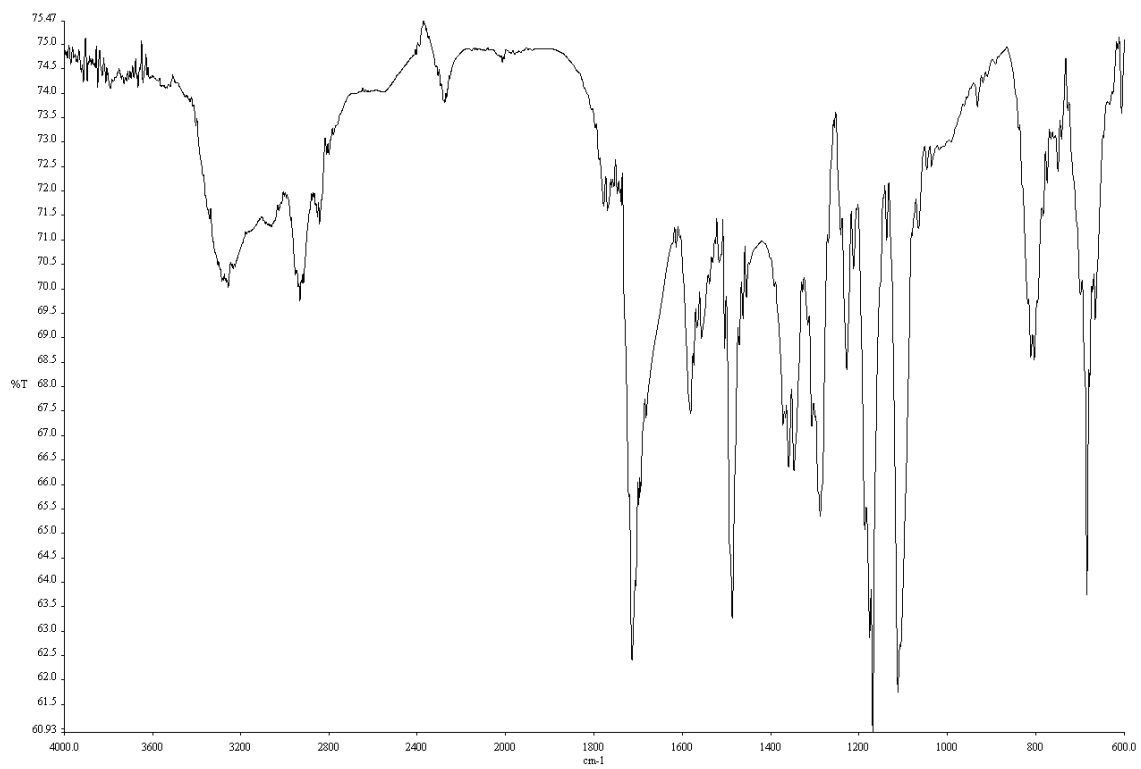


Figure A4.82. Infrared spectrum (Thin Film, NaCl) of compound **179**.

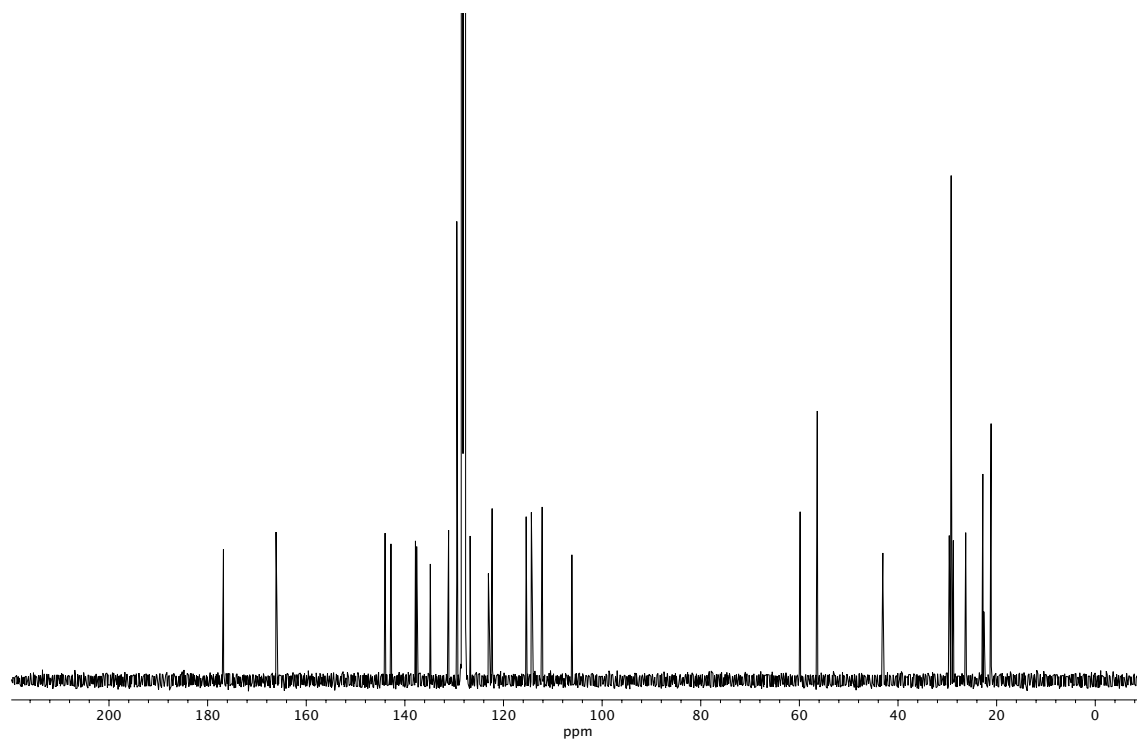


Figure A4.83. ¹³C NMR (100 MHz, C₆D₆) of compound **179**.

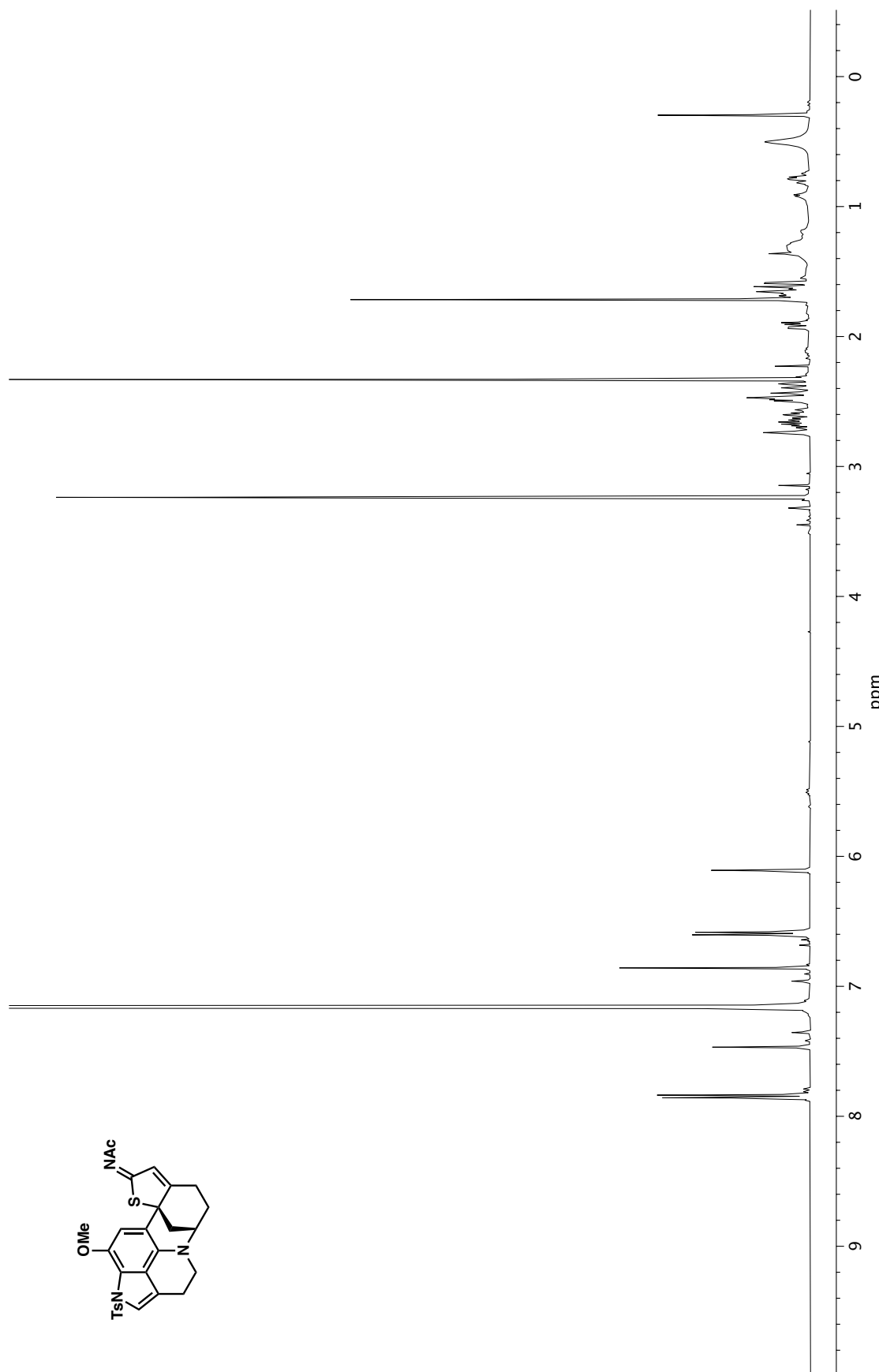


Figure A4.84. ^1H NMR (400 MHz, C_6D_6) of compound 184.

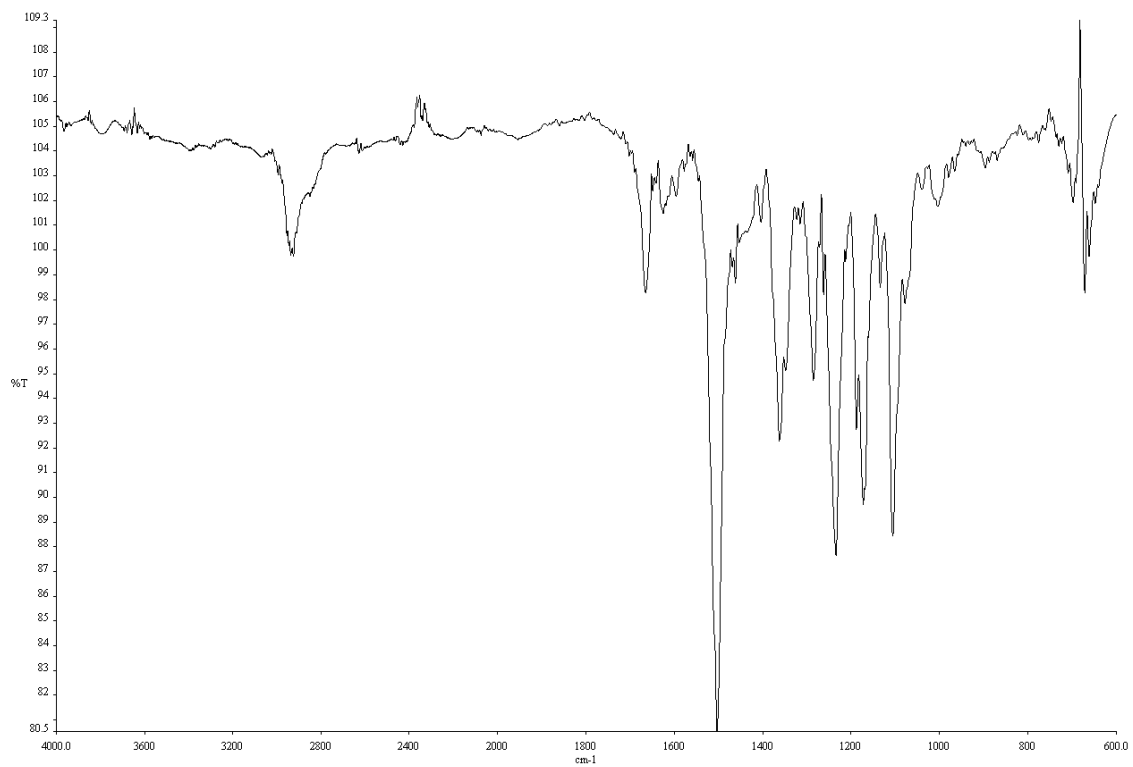


Figure A4.85. Infrared spectrum (Thin Film, NaCl) of compound **184**.

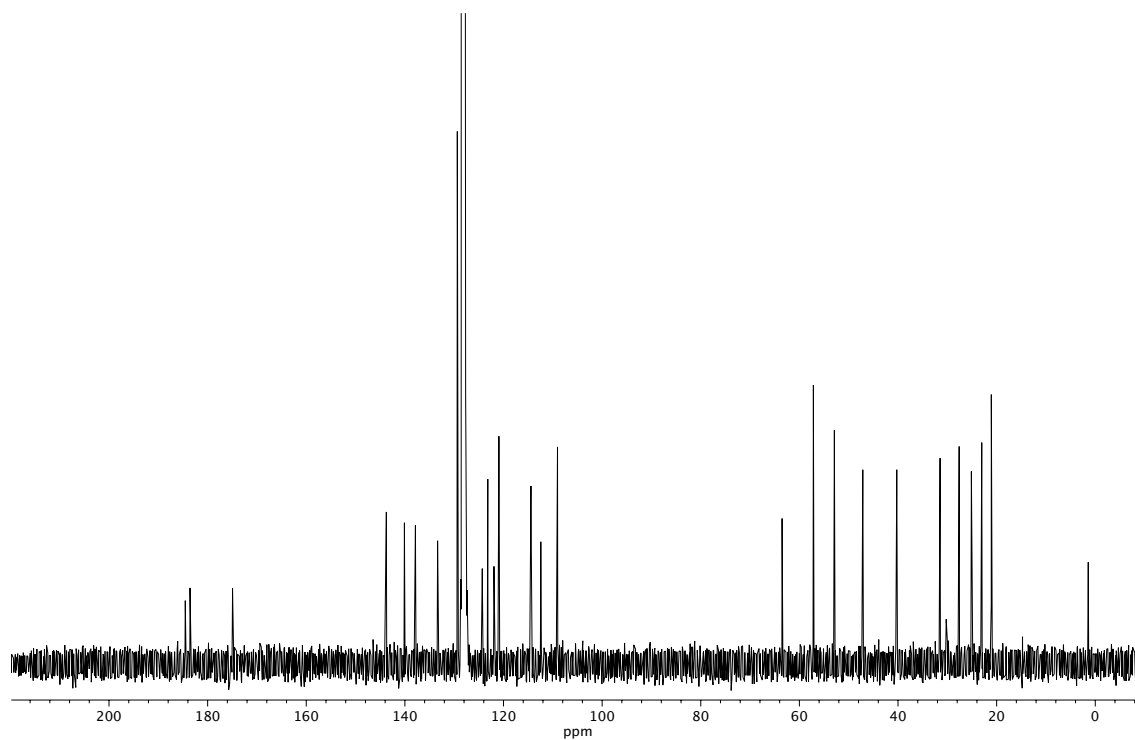


Figure A4.86. ¹³C NMR (100 MHz, C₆D₆) of compound **184**.

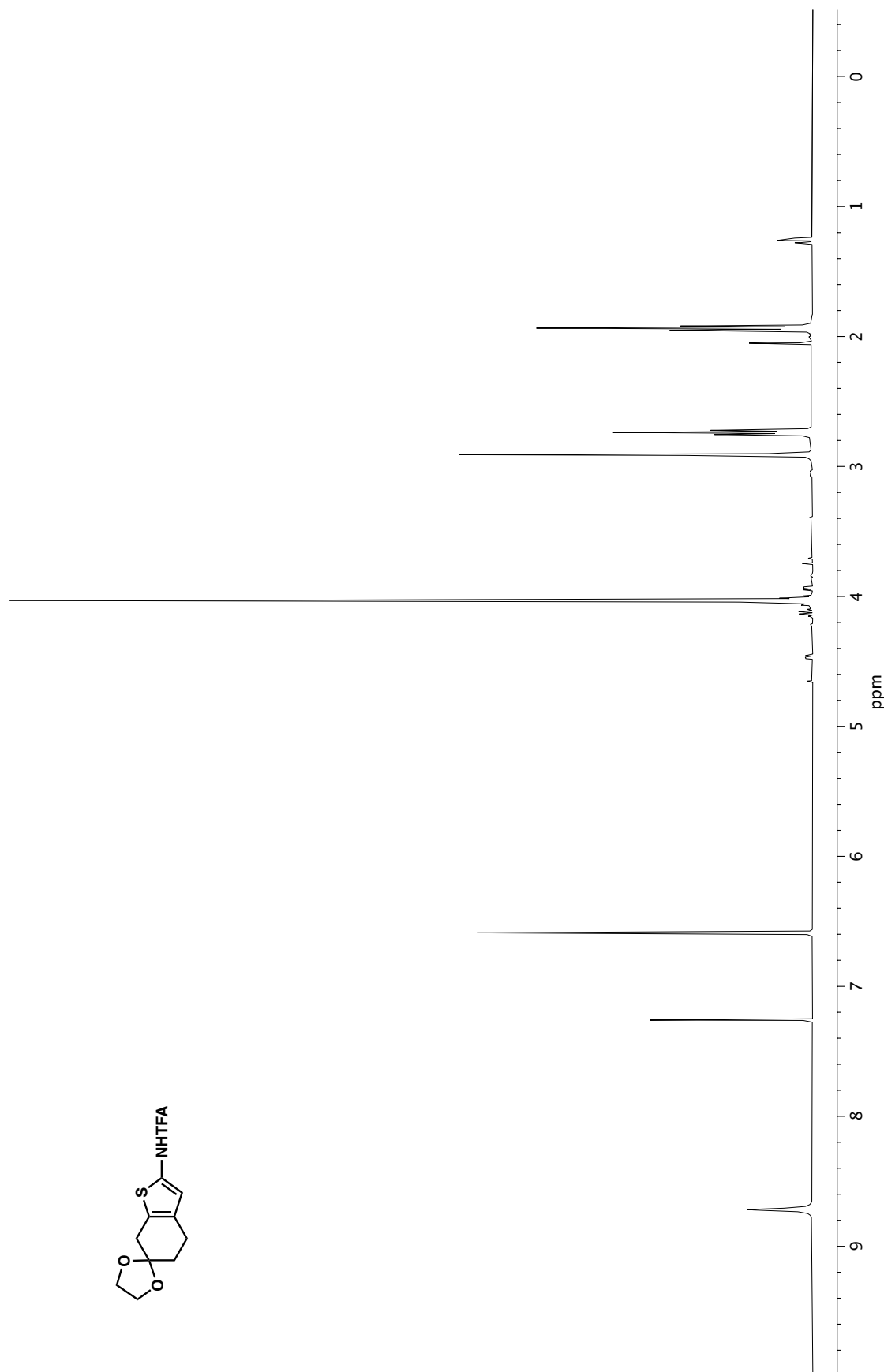


Figure A4.87. ^1H NMR (400 MHz, CDCl_3) of compound **187**.

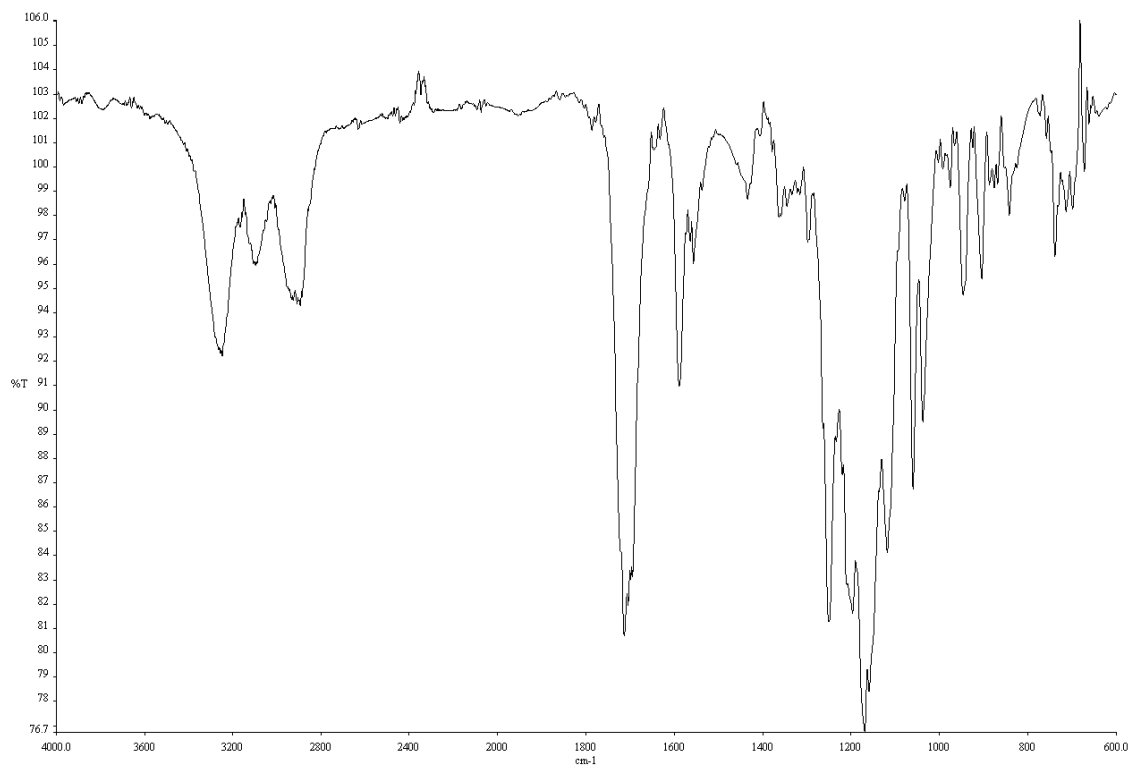


Figure A4.88. Infrared spectrum (Thin Film, NaCl) of compound **187**.

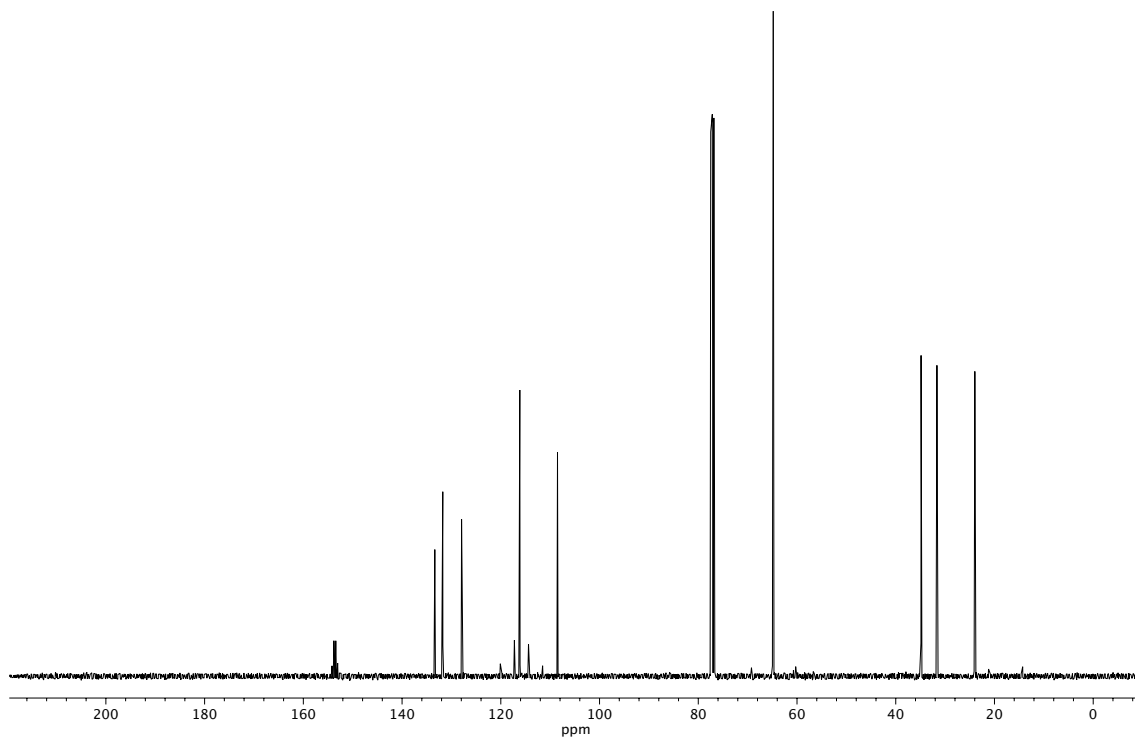
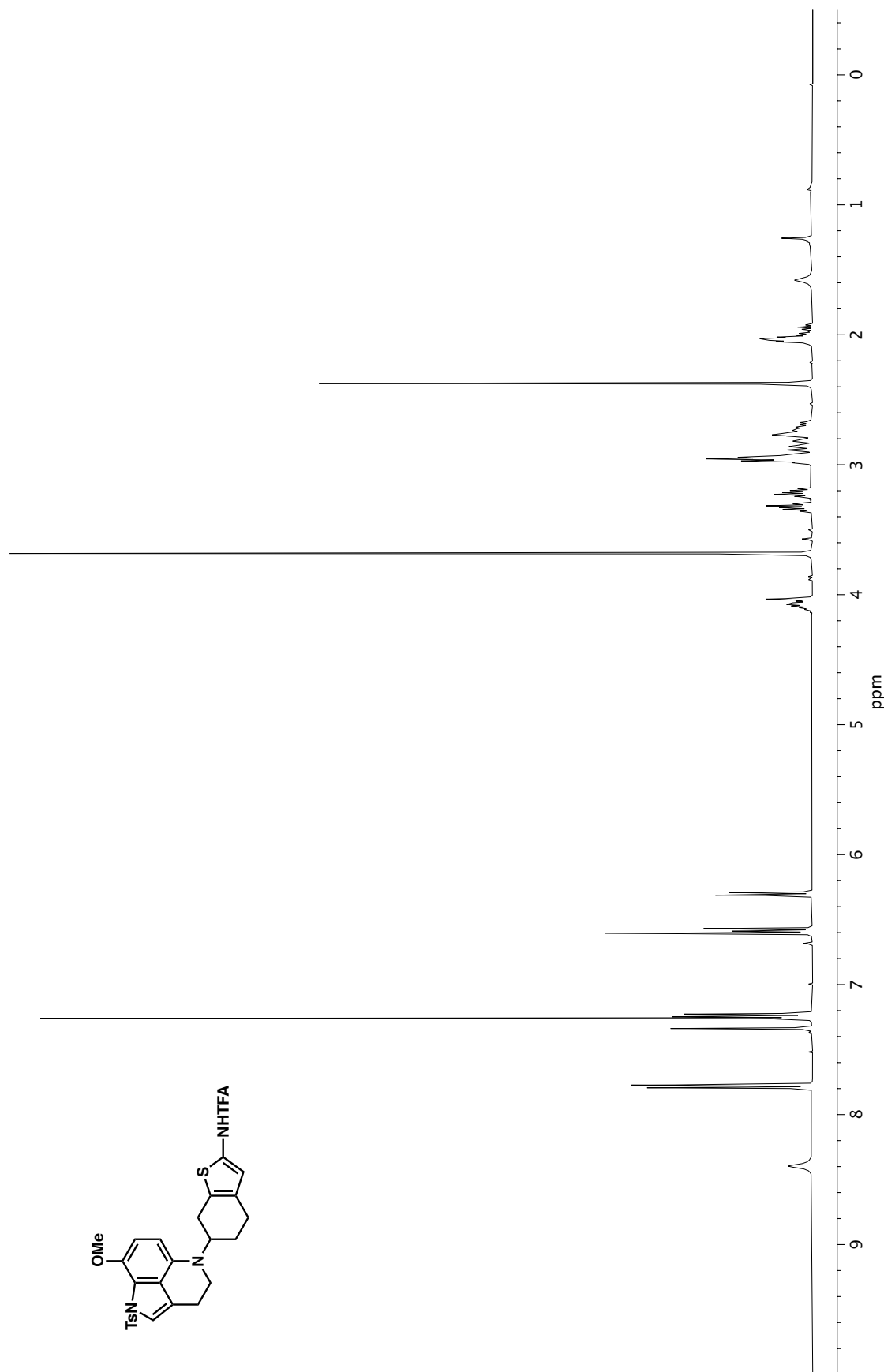


Figure A4.89. ¹³C NMR (100 MHz, CDCl₃) of compound **187**.

Figure A4.90. $^1\text{H NMR}$ (400 MHz, CDCl_3) of compound 215.

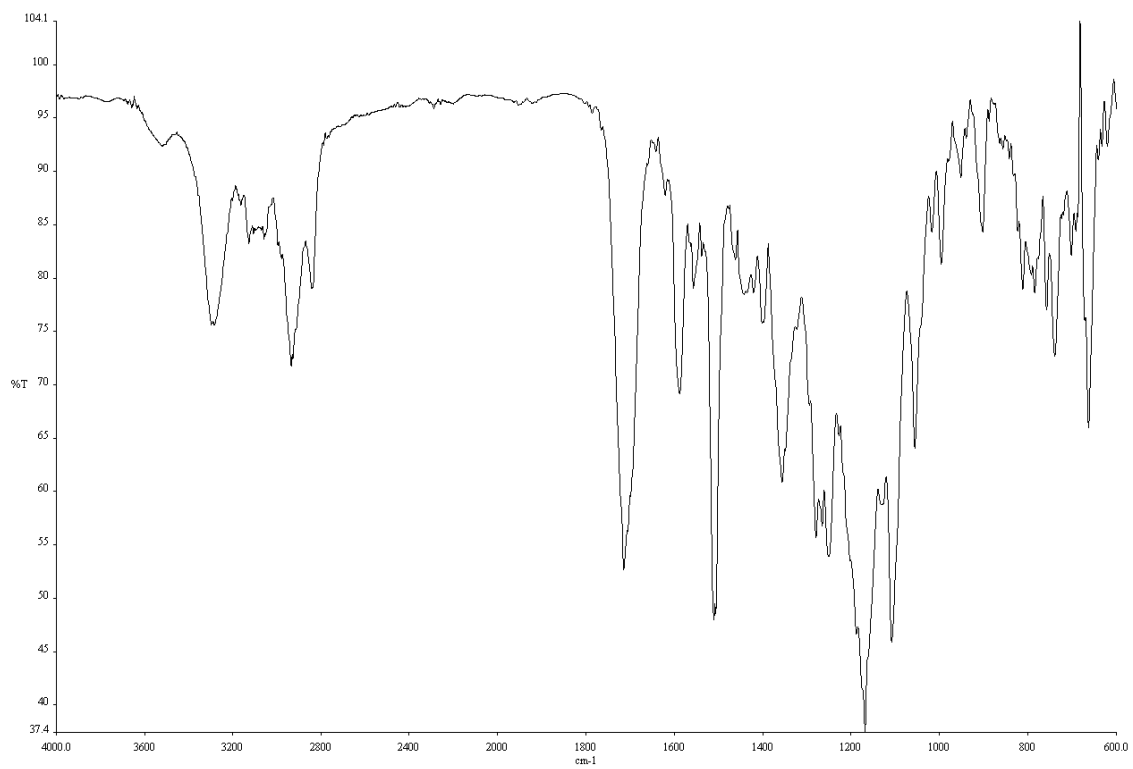


Figure A4.91. Infrared spectrum (Thin Film, NaCl) of compound **215**.

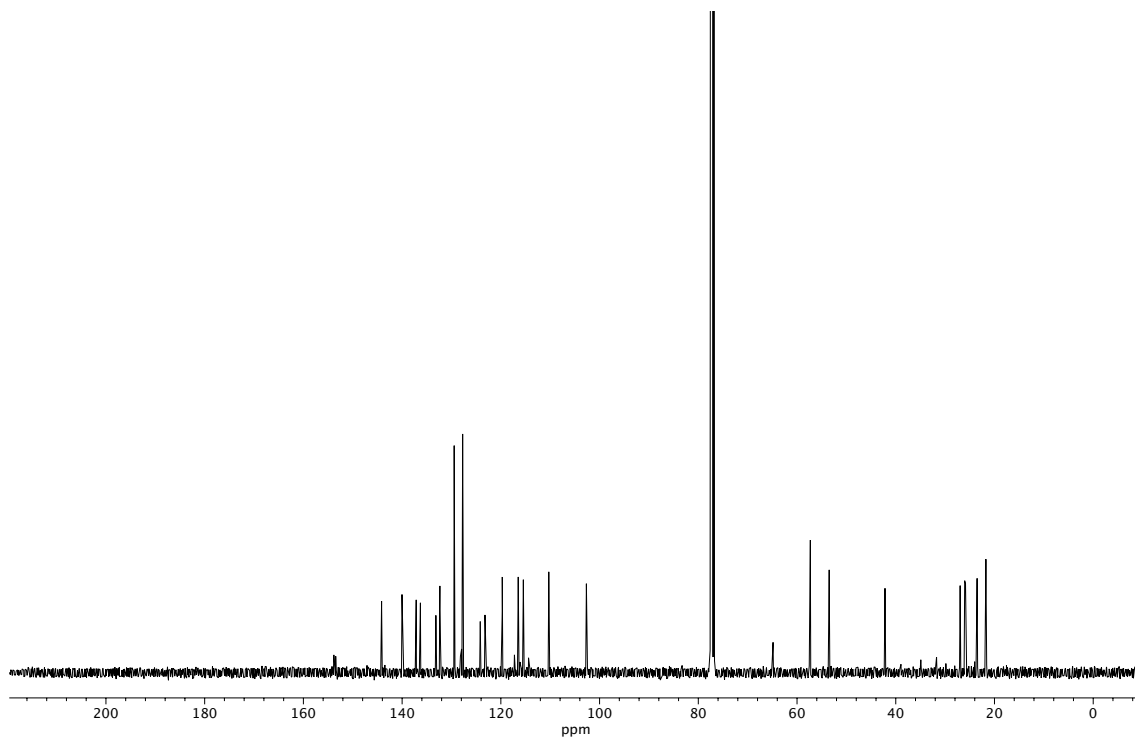
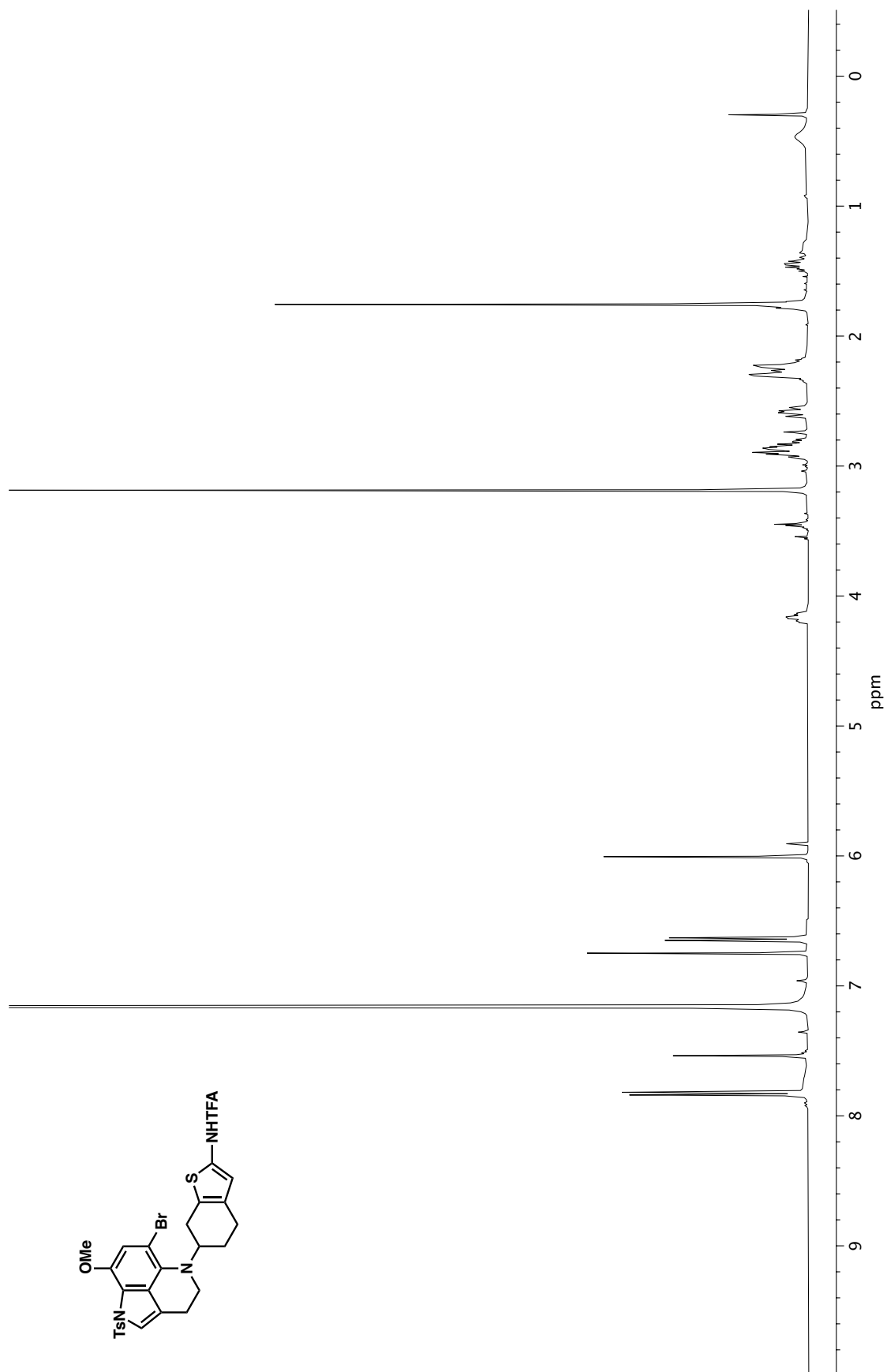


Figure A4.92. ^{13}C NMR (100 MHz, CDCl_3) of compound **215**.

Figure A4.93. ^1H NMR (400 MHz, C_6D_6) of compound **189**.

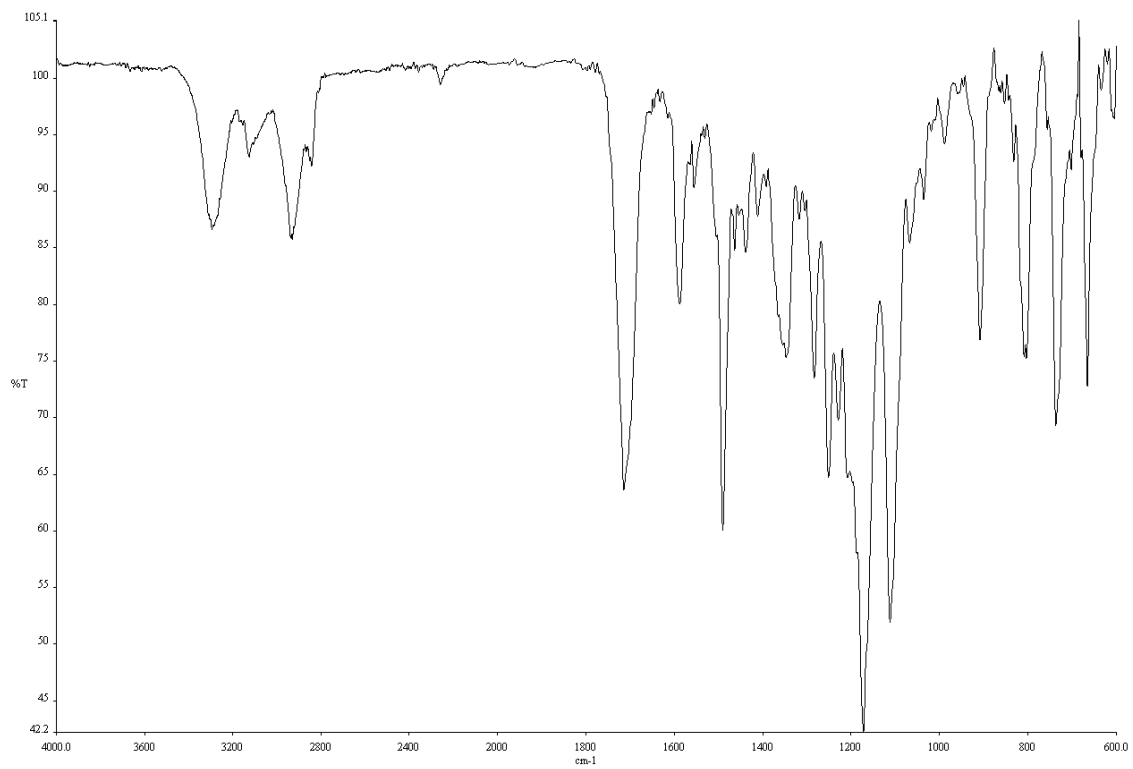


Figure A4.94. Infrared spectrum (Thin Film, NaCl) of compound **189**.

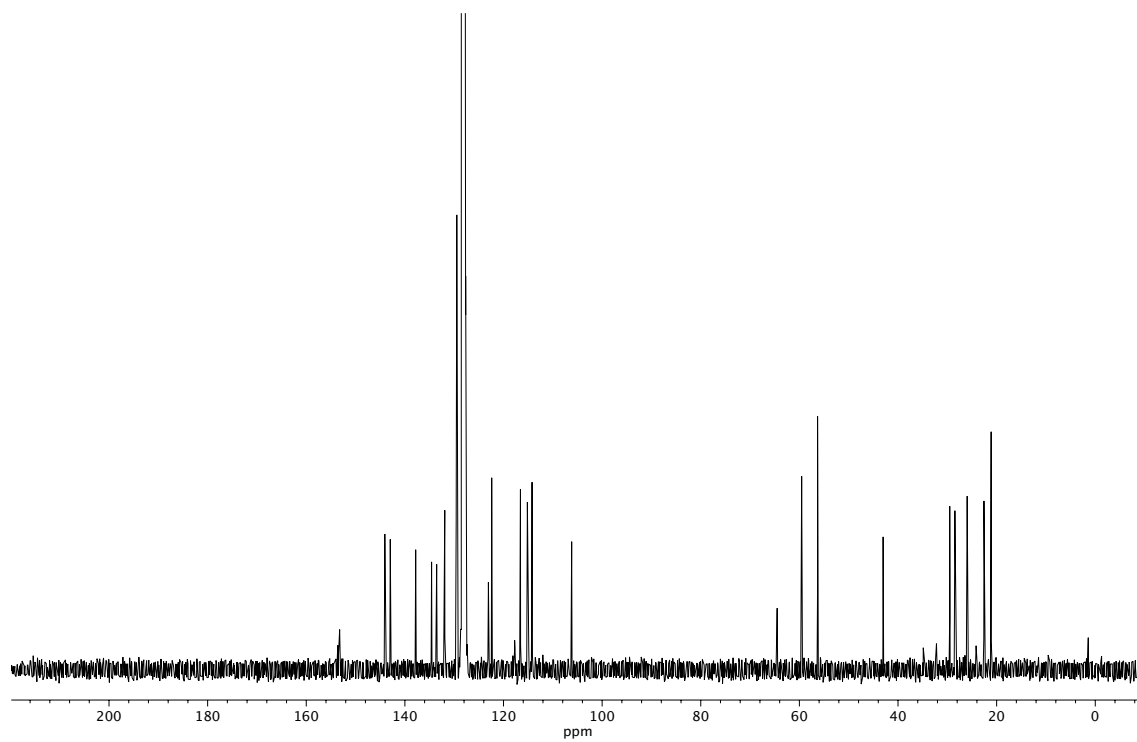
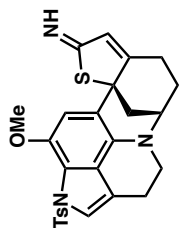
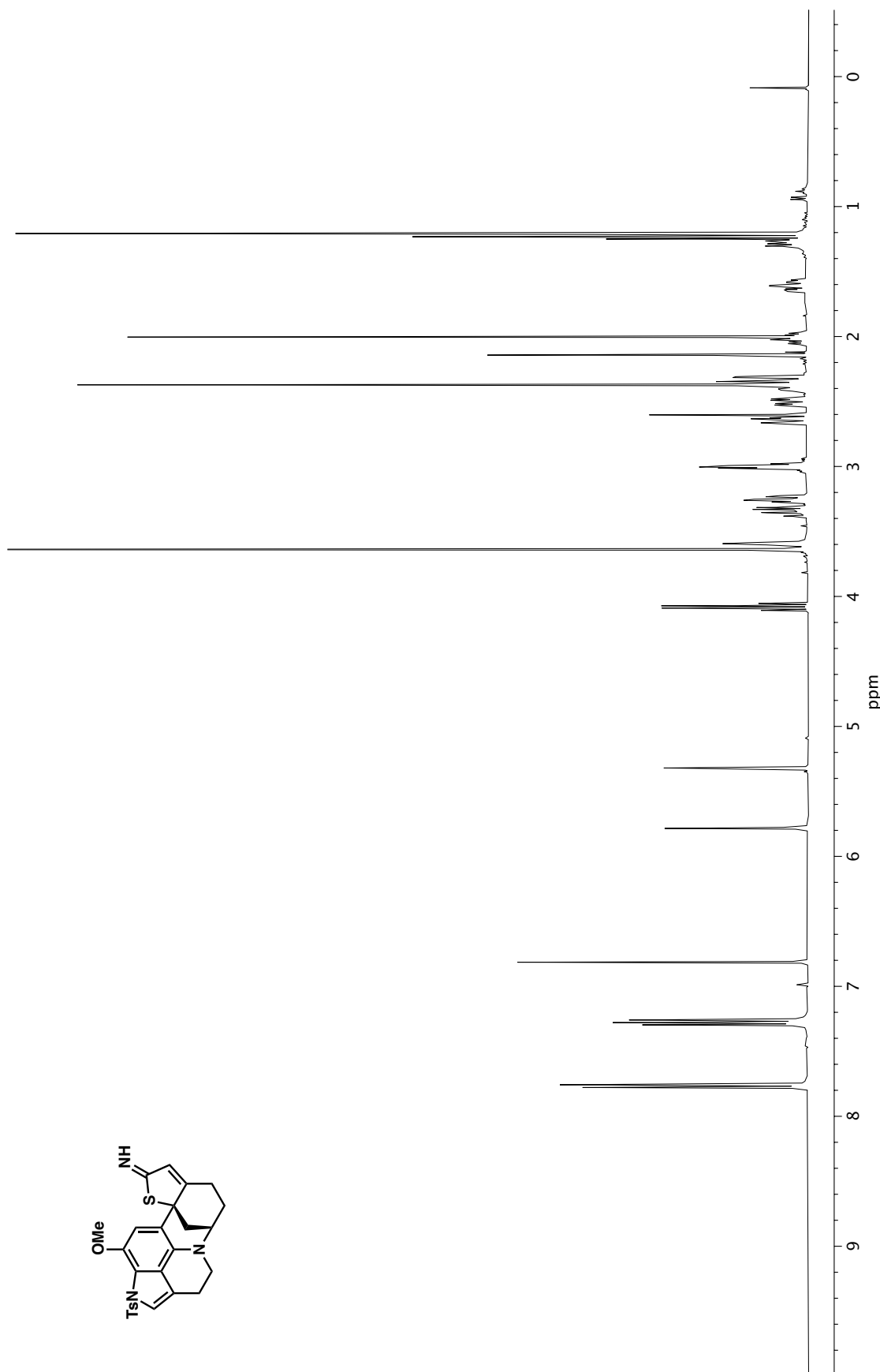


Figure A4.95. ¹³C NMR (100 MHz, C₆D₆) of compound **189**.



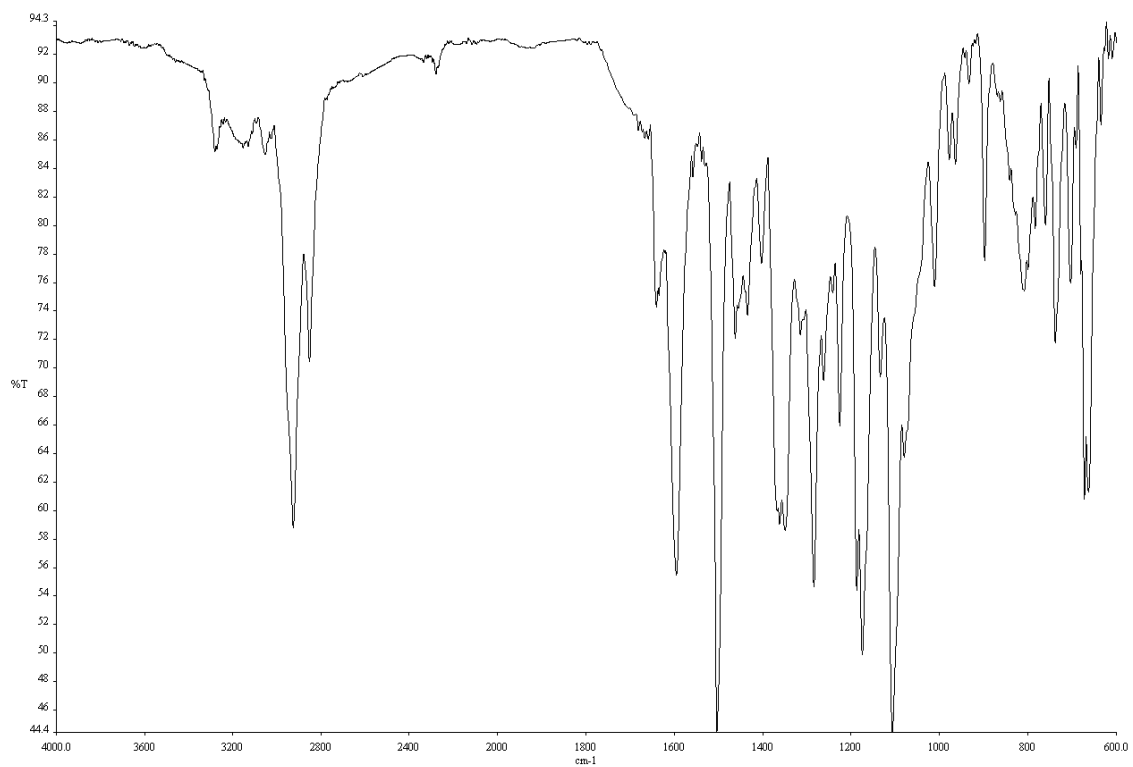


Figure A4.97. Infrared spectrum (Thin Film, NaCl) of compound **186**.

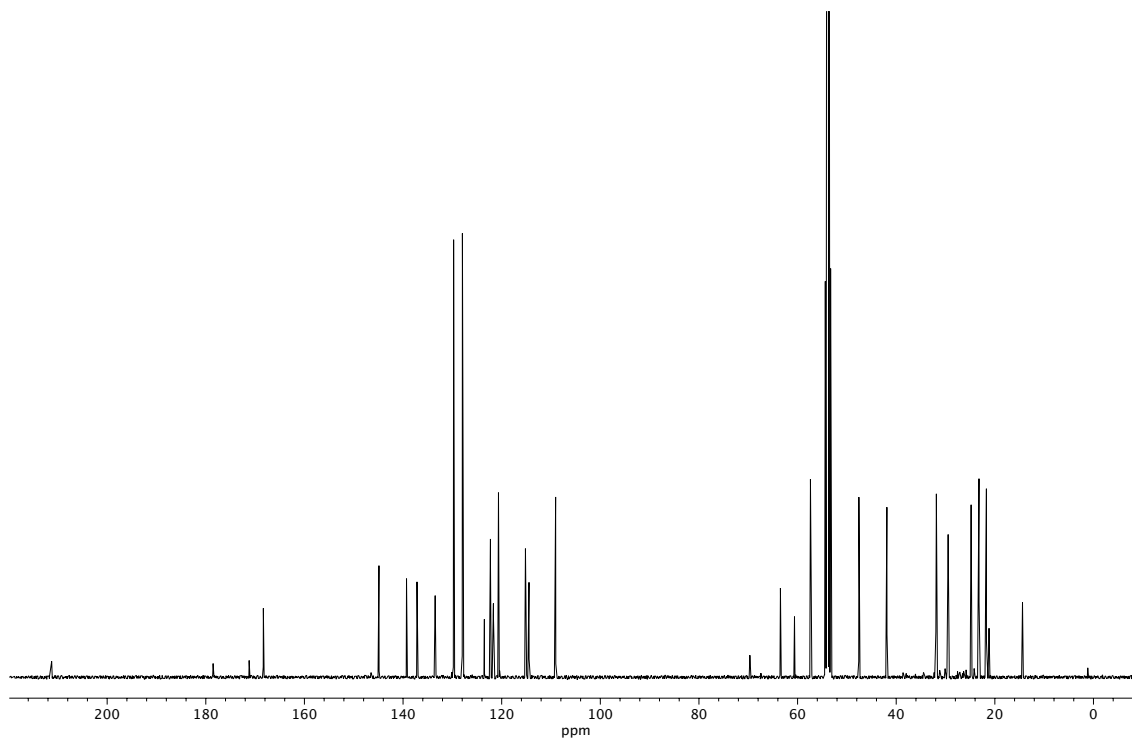
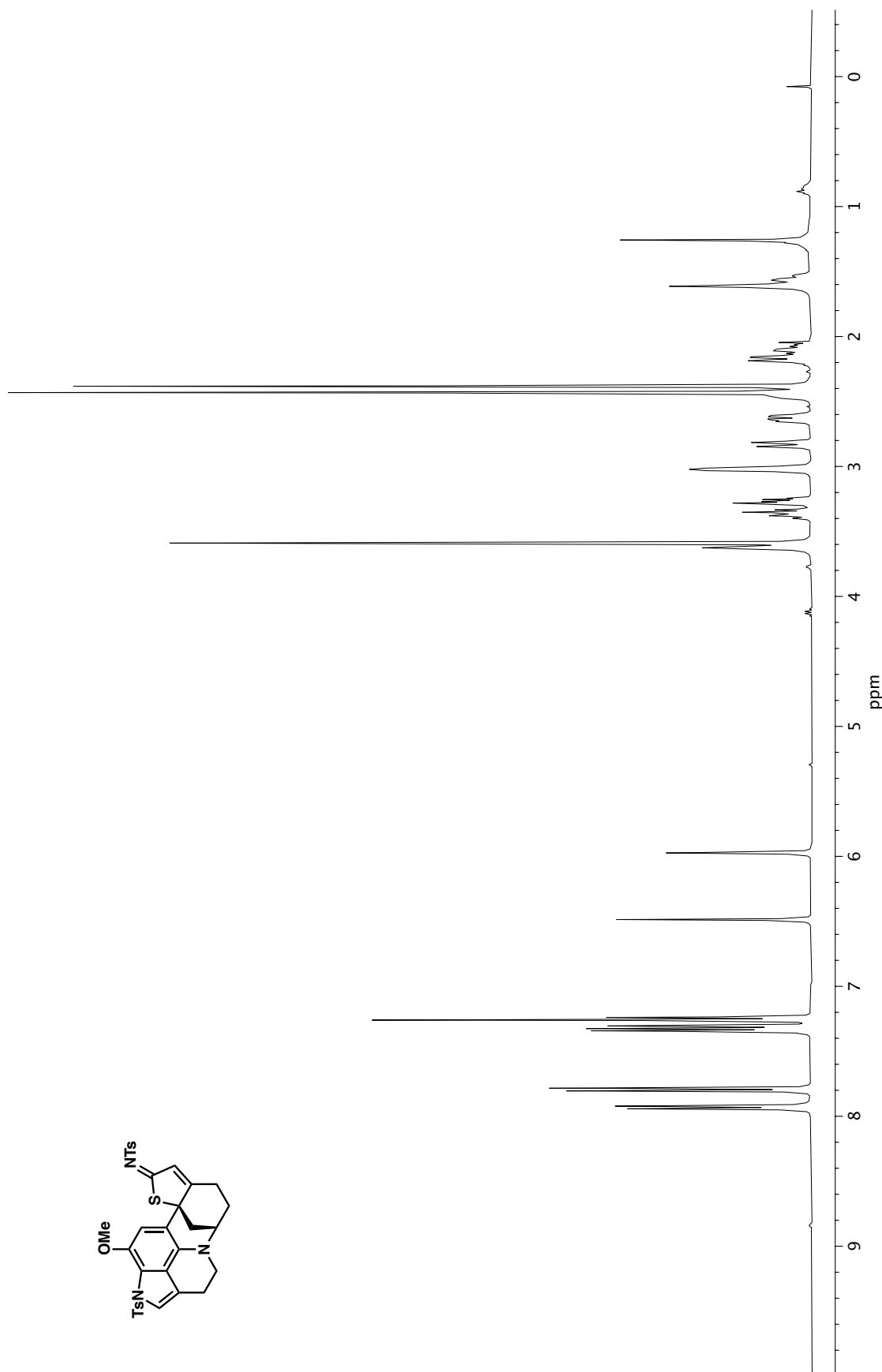


Figure A4.98. ^{13}C NMR (100 MHz, CD_2Cl_2) of compound **186**.



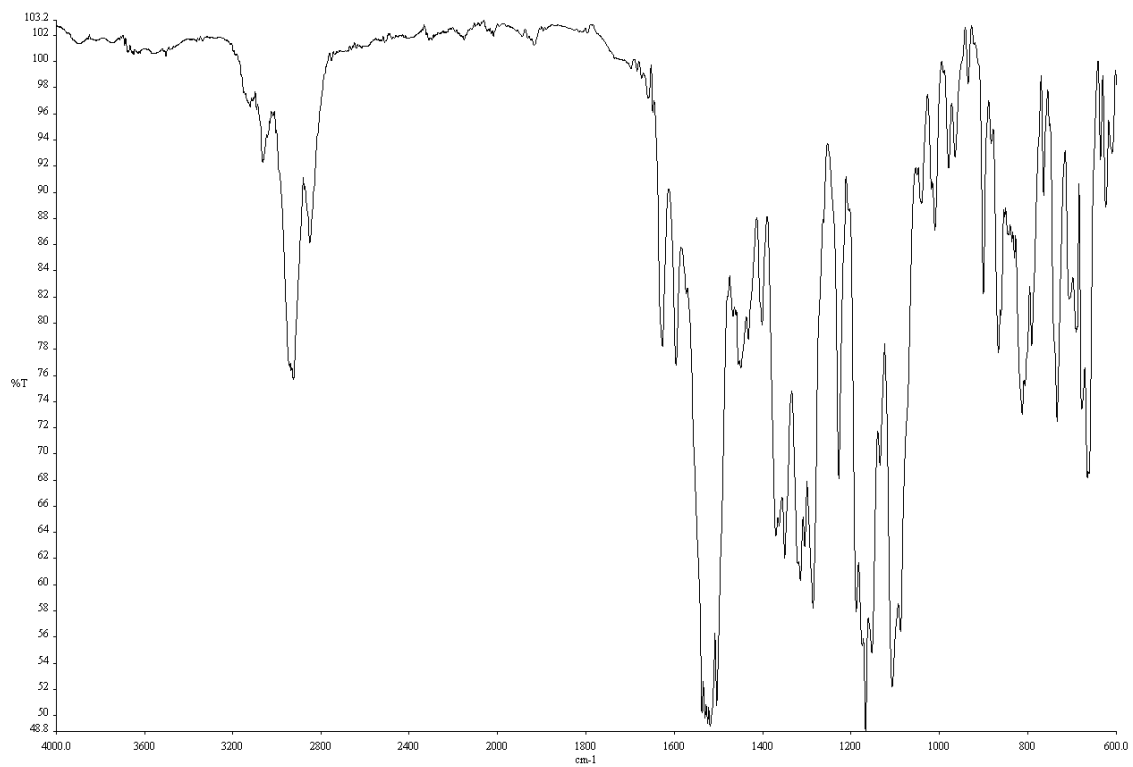


Figure A4.100. Infrared spectrum (Thin Film, NaCl) of compound **190**.

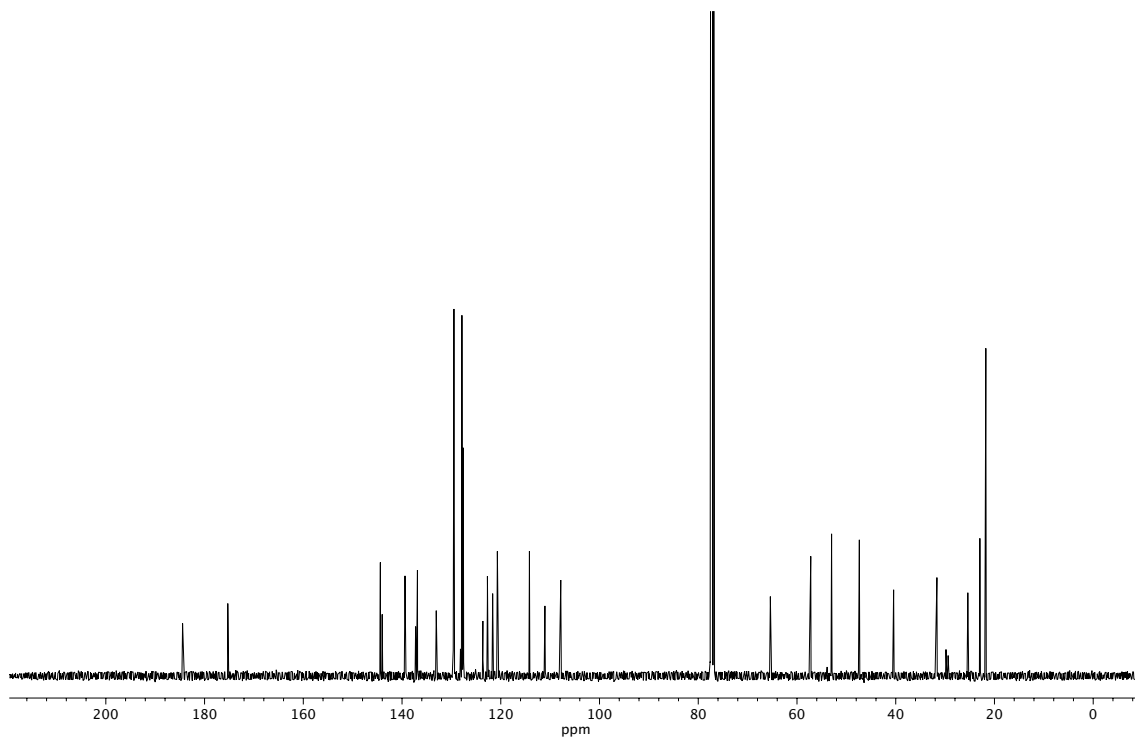


Figure A4.101. ¹³C NMR (100 MHz, CDCl₃) of compound **190**.

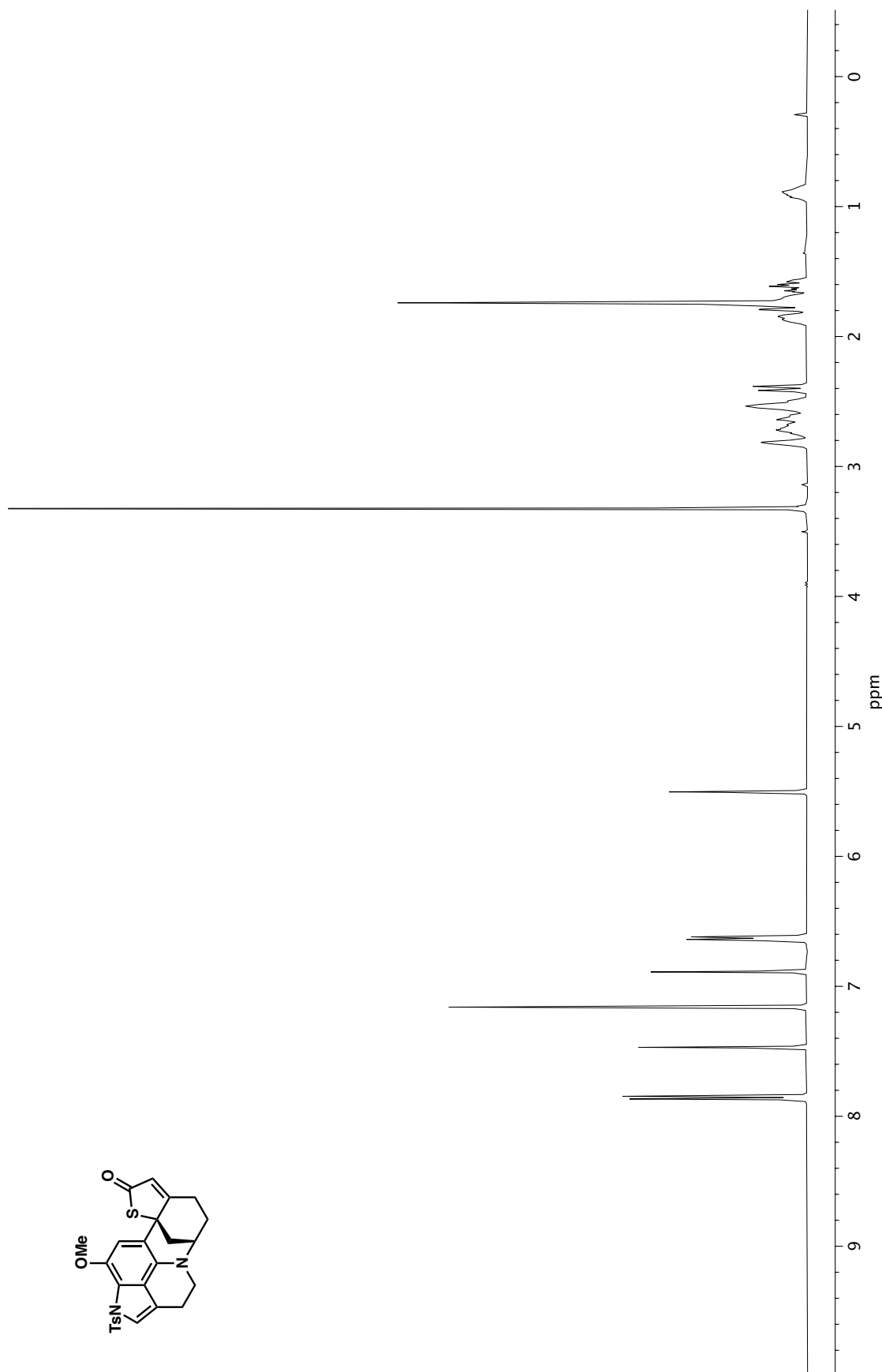


Figure A4.102. ^1H NMR (400 MHz, C_6D_6) of compound **185**.

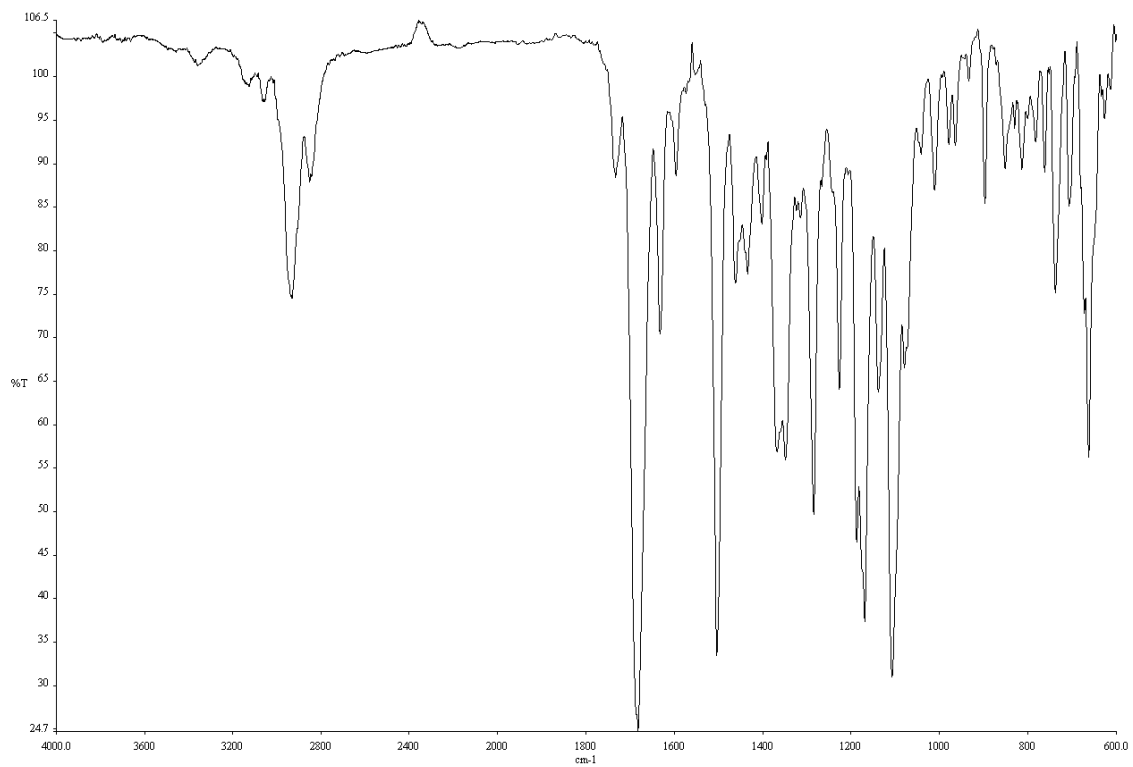


Figure A4.103. Infrared spectrum (Thin Film, NaCl) of compound **185**.

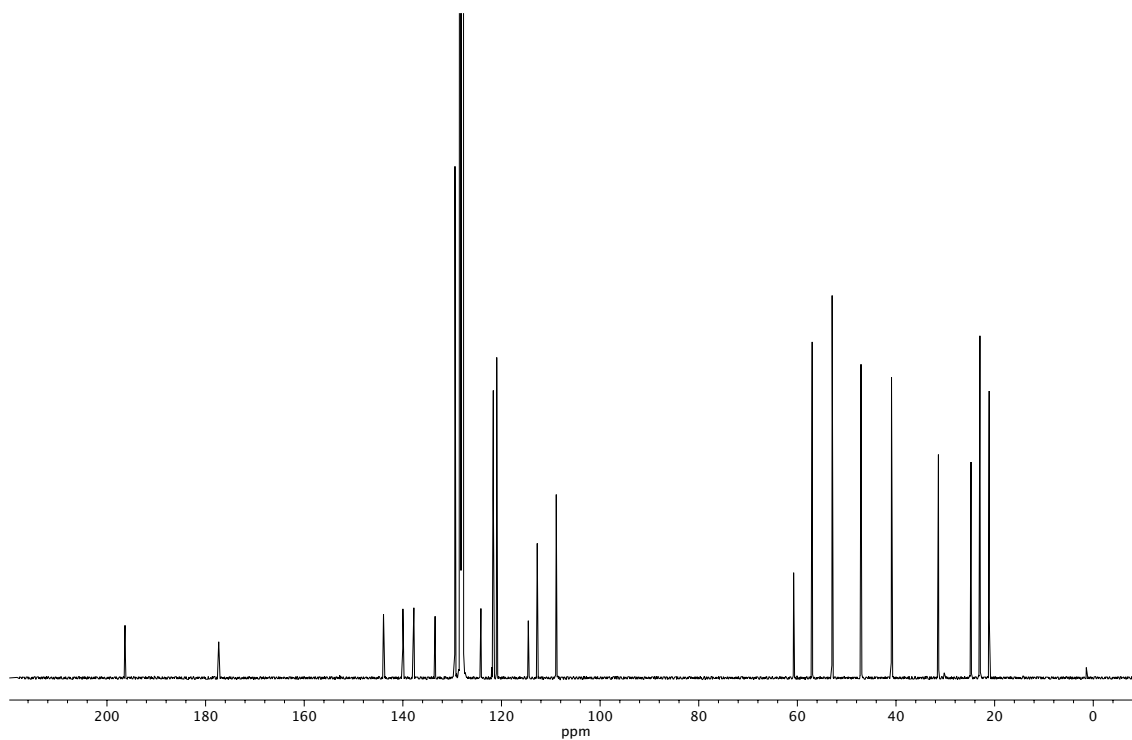
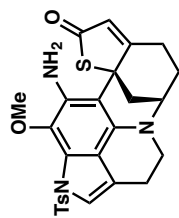
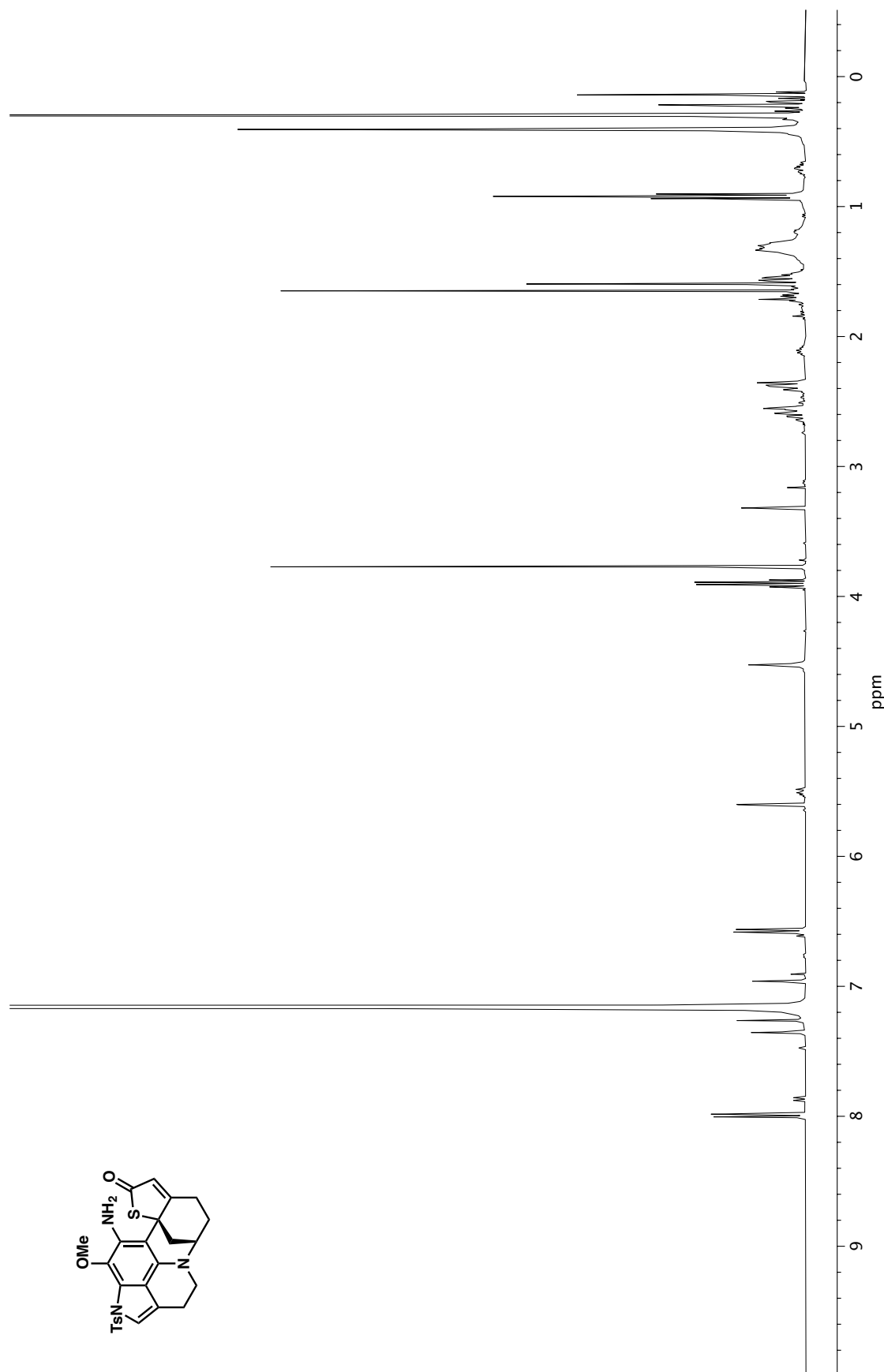


Figure A4.104. ¹³C NMR (100 MHz, C₆D₆) of compound **185**.



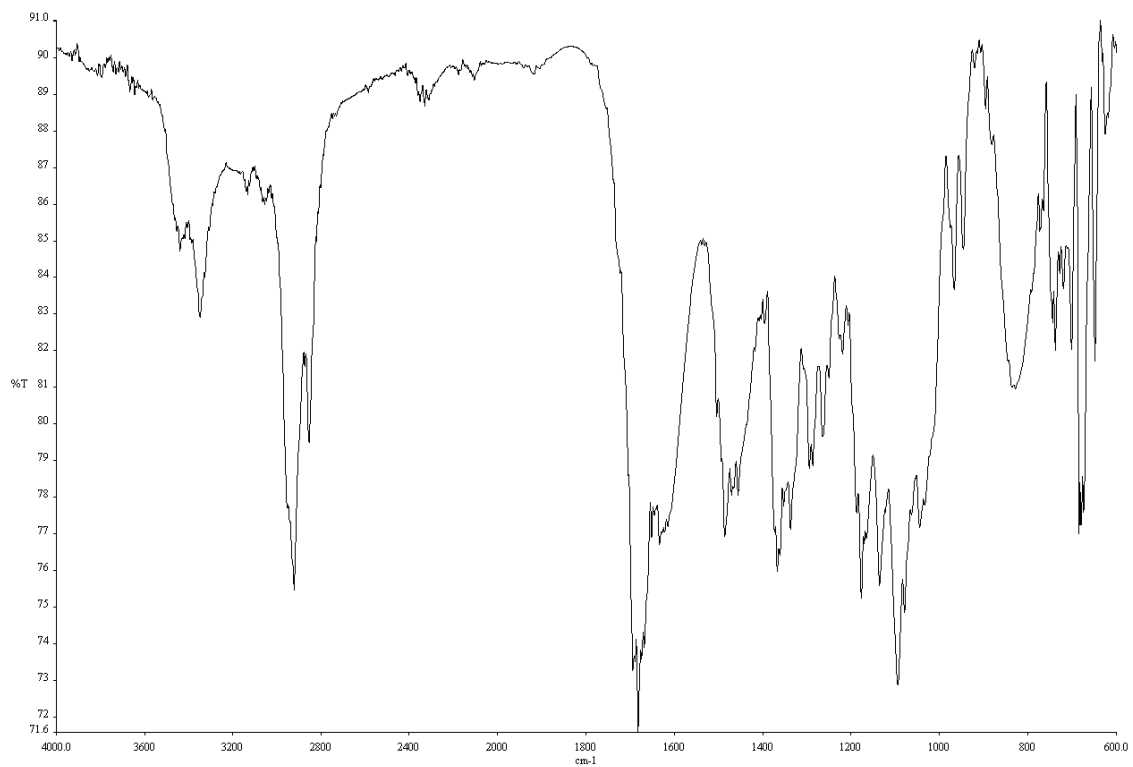


Figure A4.106. Infrared spectrum (Thin Film, NaCl) of compound **192**.

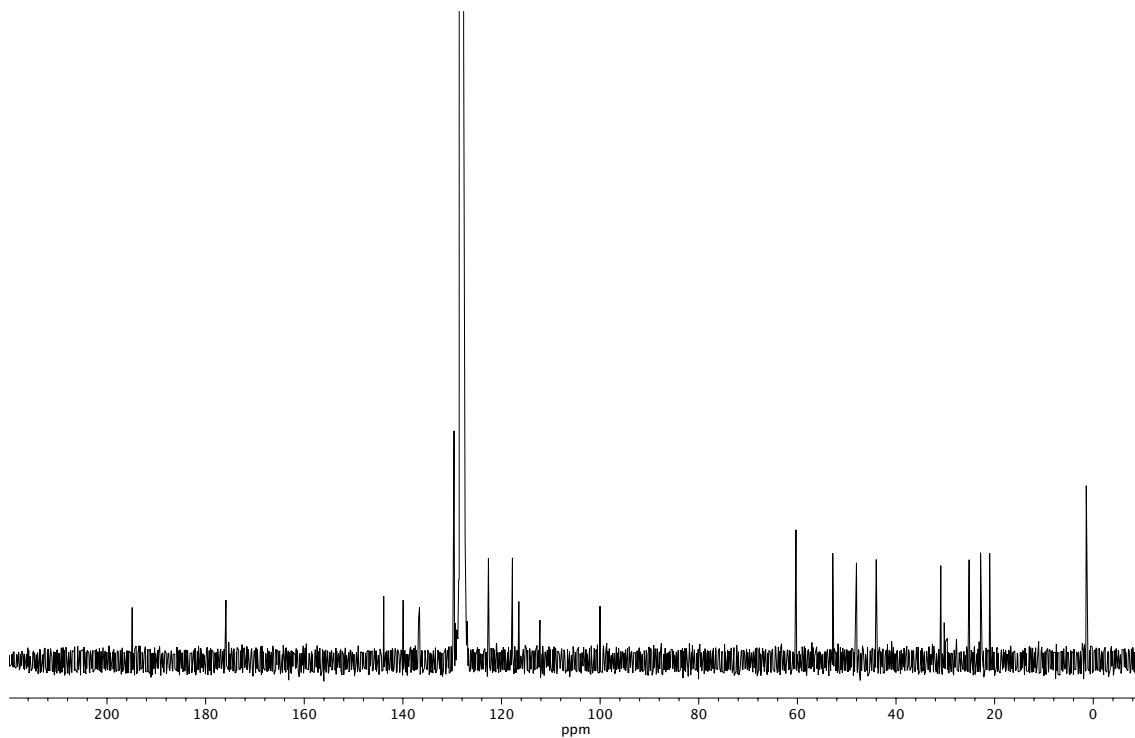
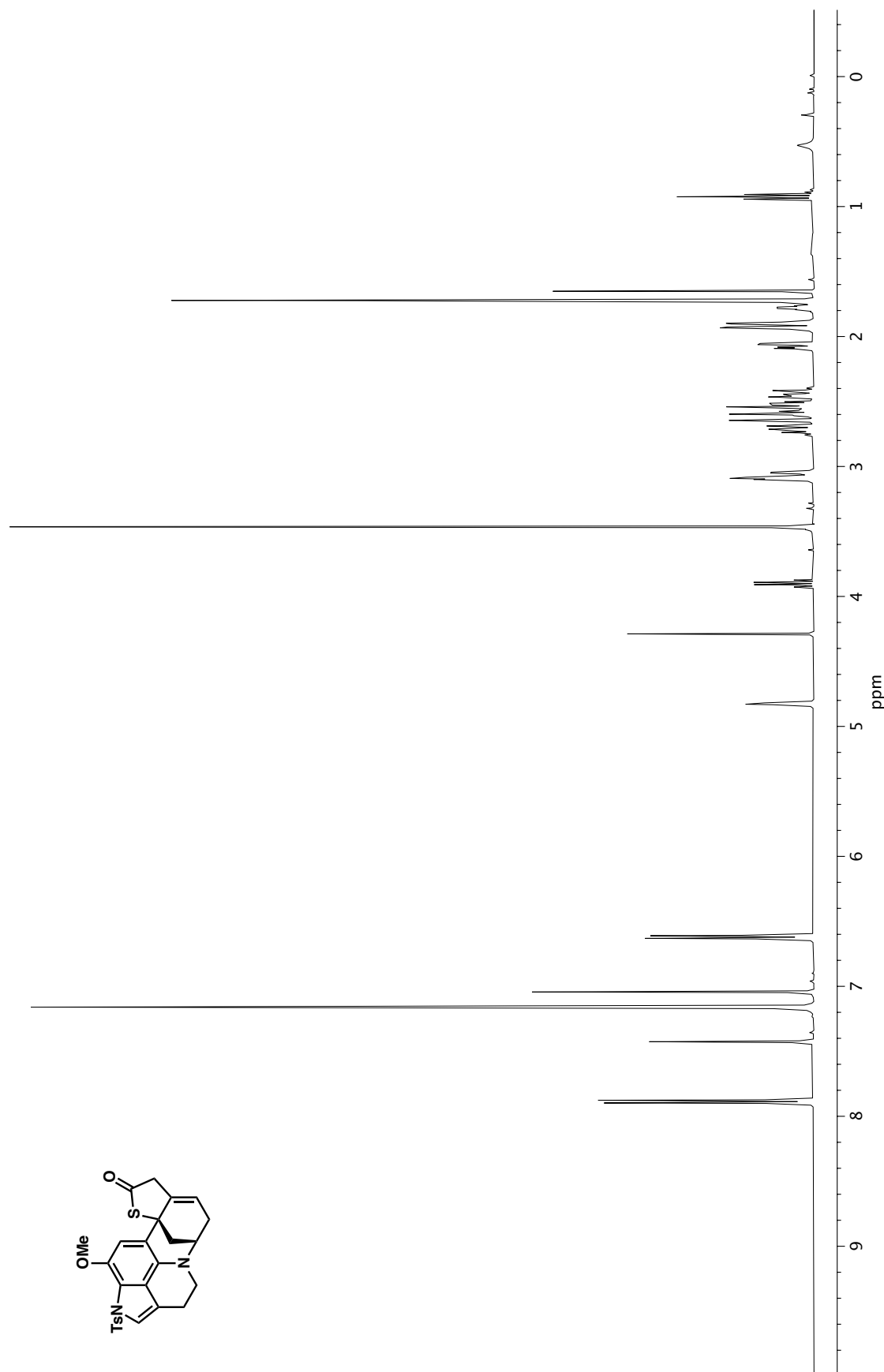


Figure A4.107. ^{13}C NMR (100 MHz, C_6D_6) of compound **192**.

Figure A4.108. ^1H NMR (400 MHz, C_6D_6) of compound **198**.

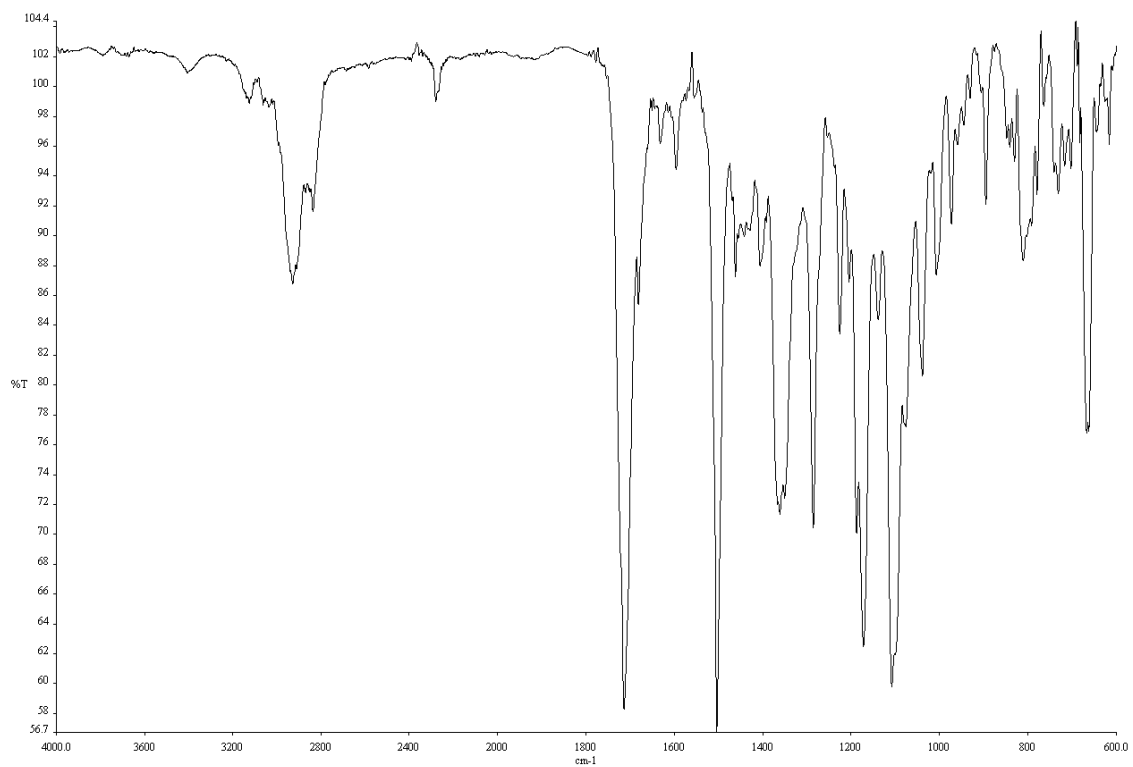


Figure A4.109. Infrared spectrum (Thin Film, NaCl) of compound **198**.

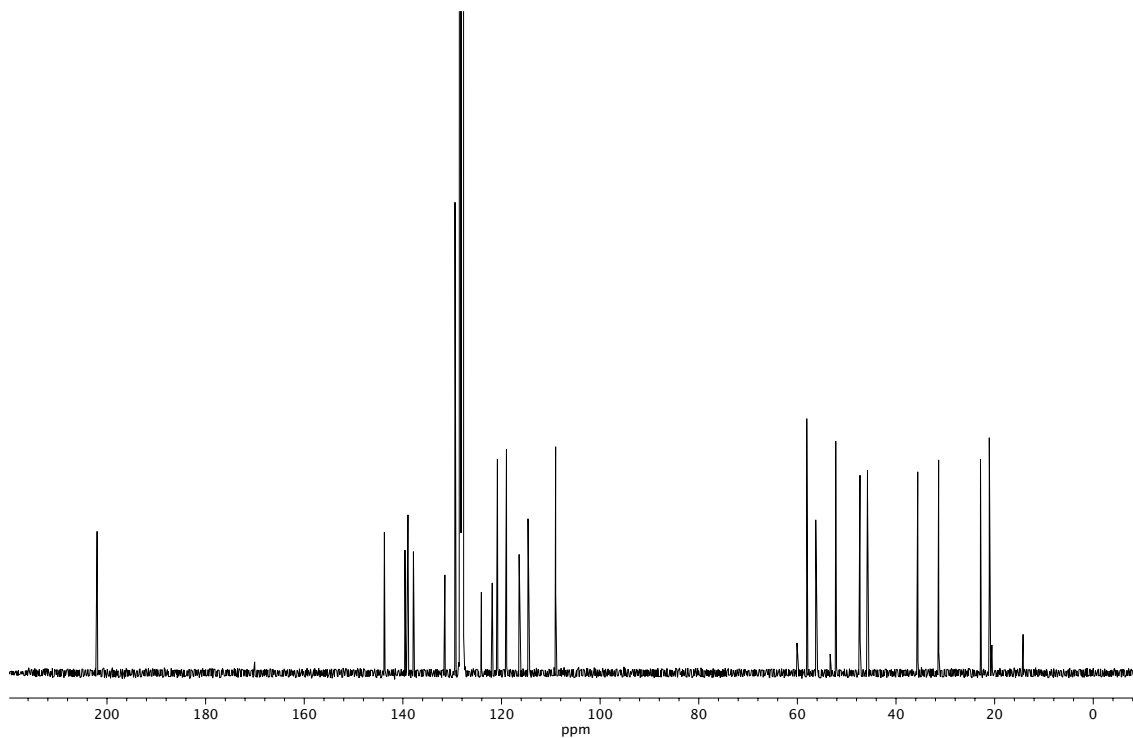


Figure A4.110. ^{13}C NMR (100 MHz, C_6D_6) of compound **198**.

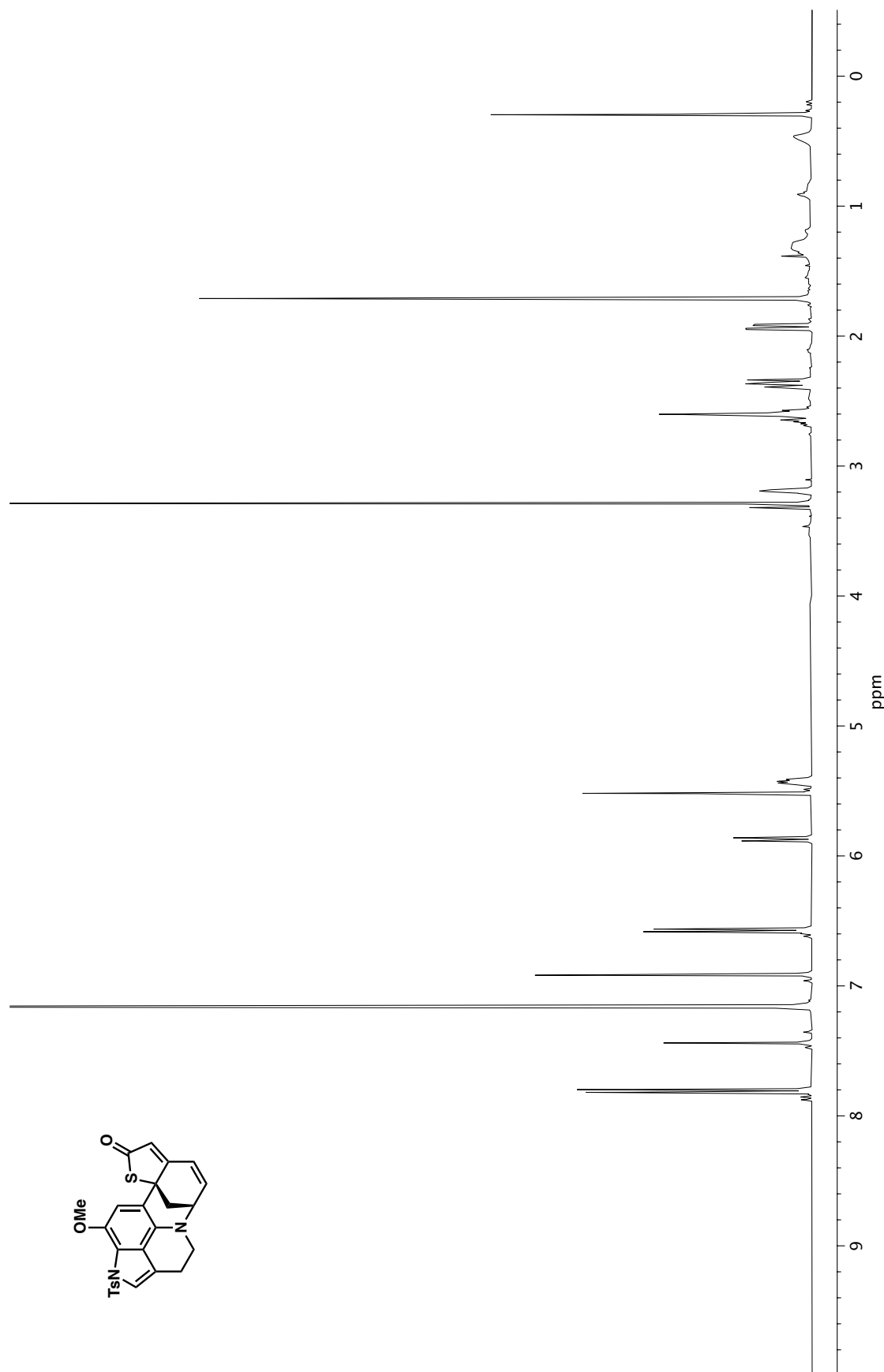


Figure A4.111. ^1H NMR (400 MHz, C_6D_6) of compound **195**.

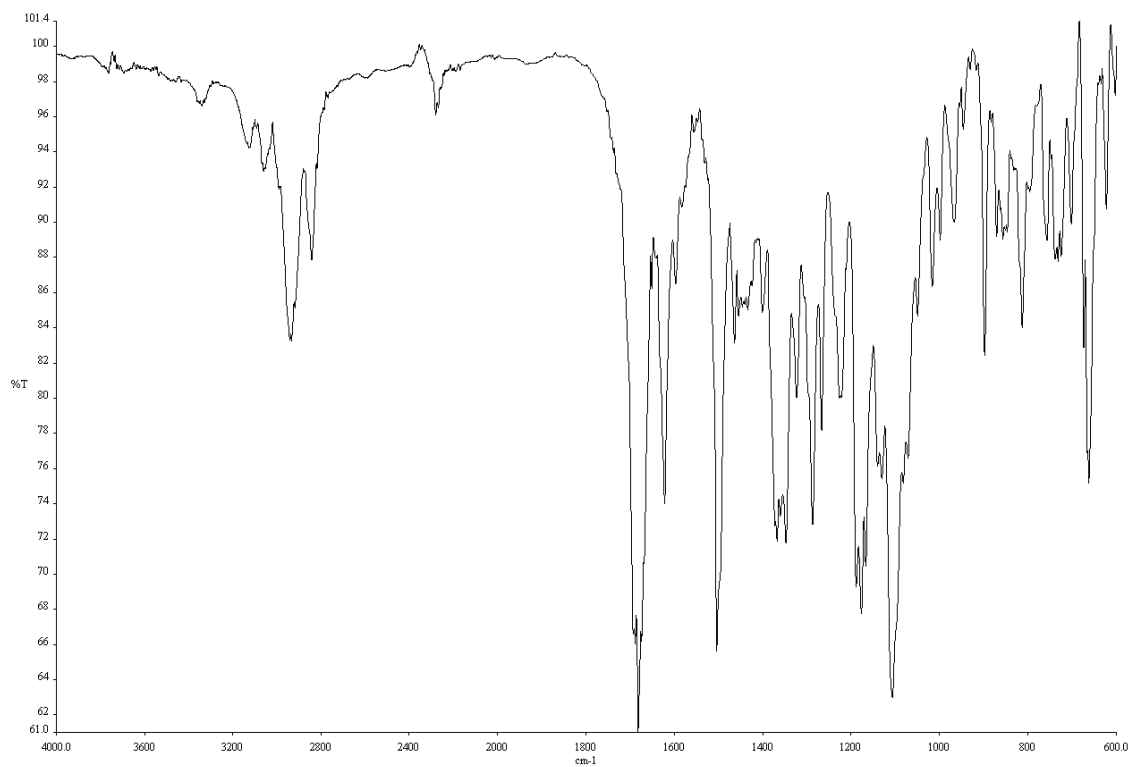


Figure A4.112. Infrared spectrum (Thin Film, NaCl) of compound **195**.

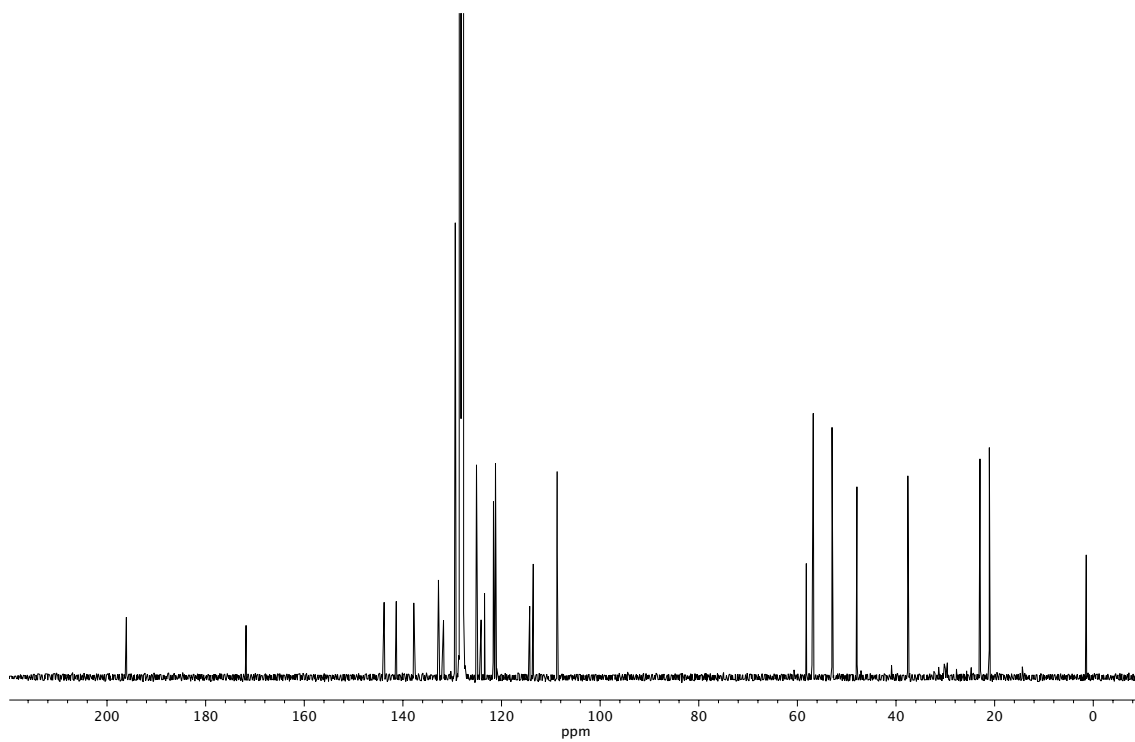


Figure A4.113. ¹³C NMR (100 MHz, C₆D₆) of compound **195**.

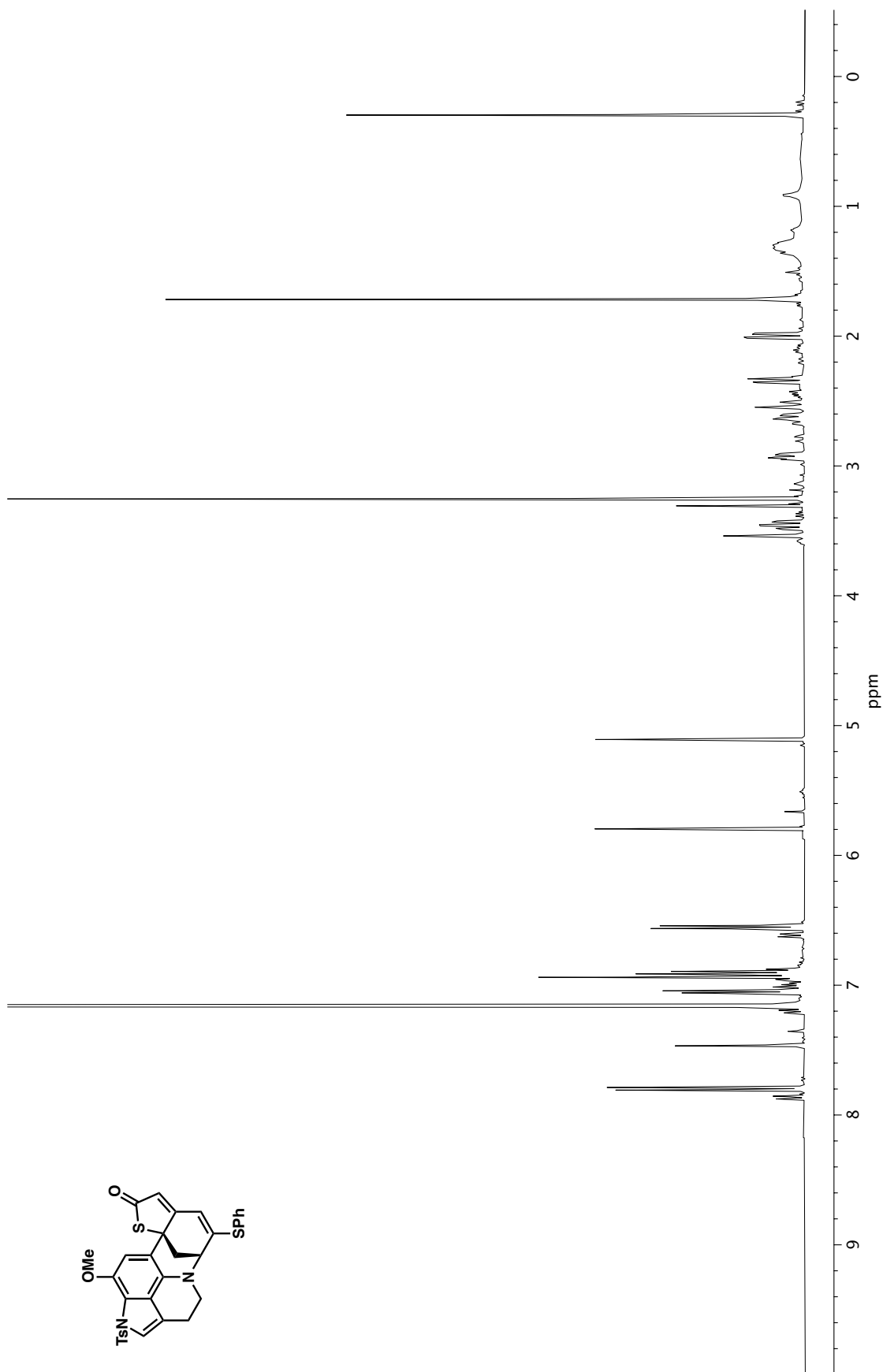


Figure A4.114. ^1H NMR (400 MHz, C_6D_6) of compound **201**.

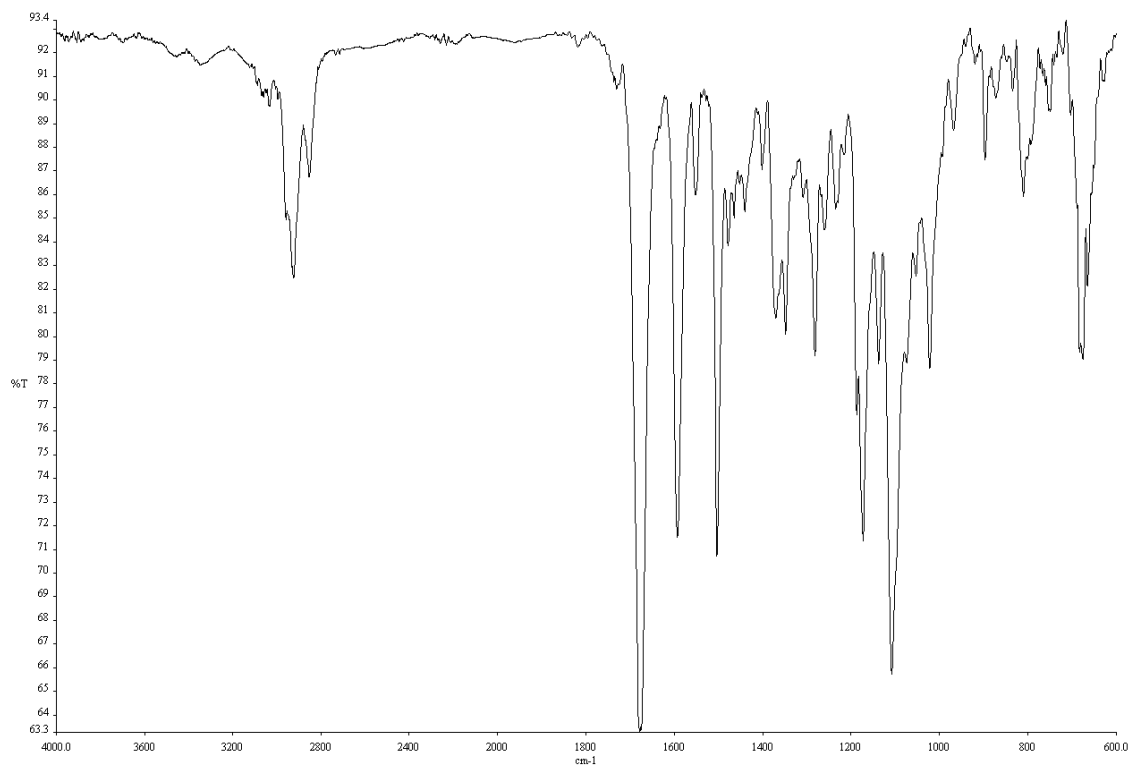


Figure A4.115. Infrared spectrum (Thin Film, NaCl) of compound **201**.

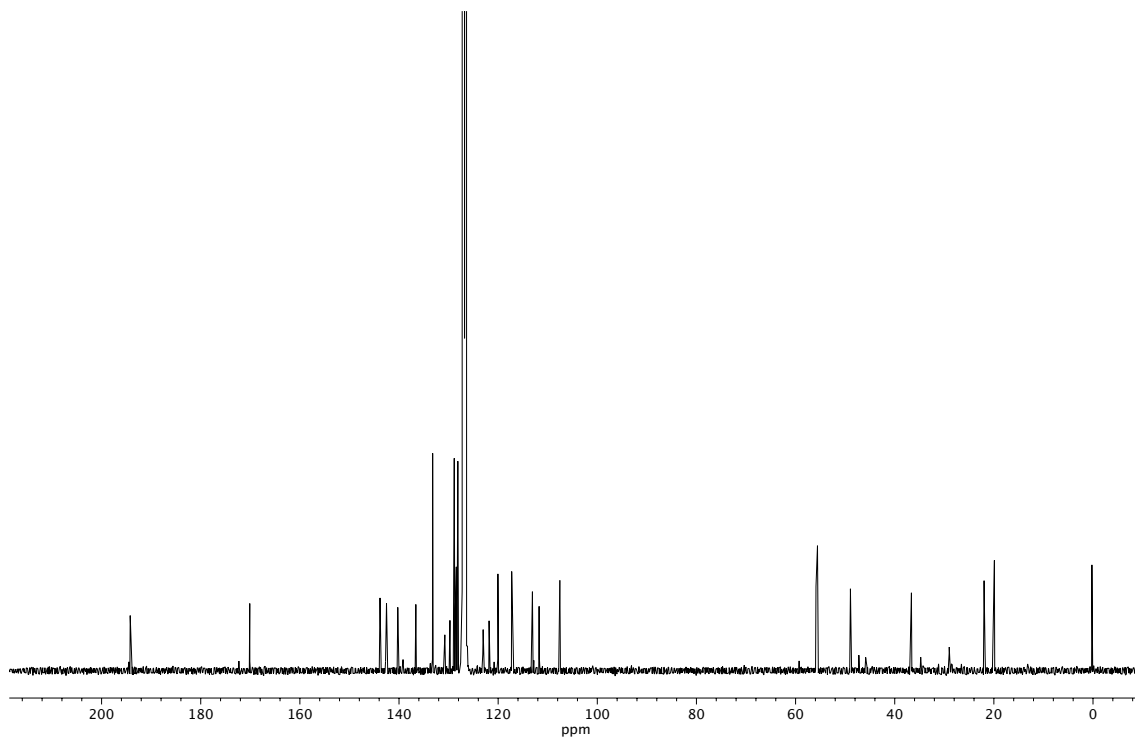
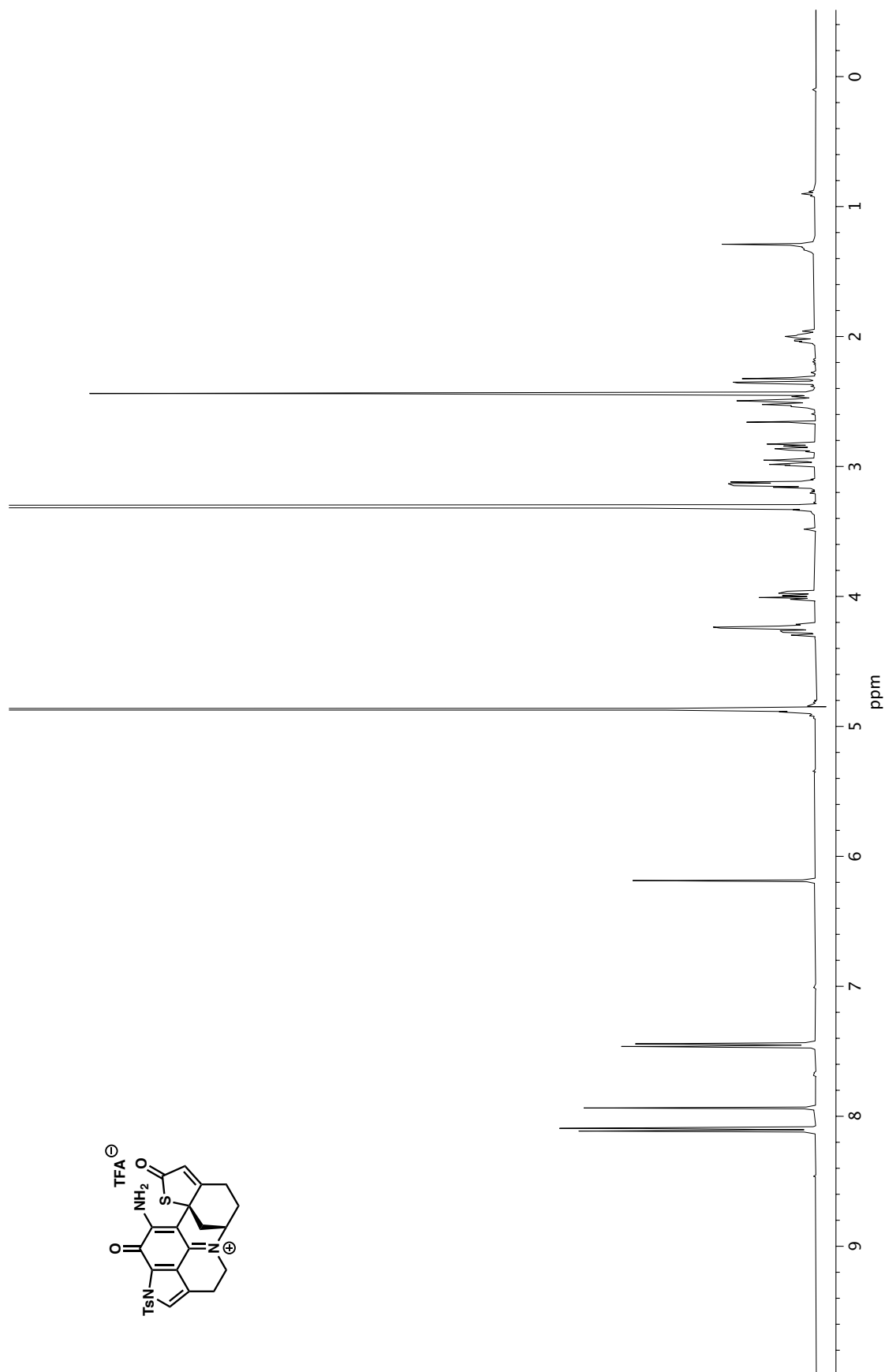


Figure A4.116. ¹³C NMR (100 MHz, C₆D₆) of compound **201**.

Figure A4.117. ^1H NMR (400 MHz, CD_3OD) of compound **206**.

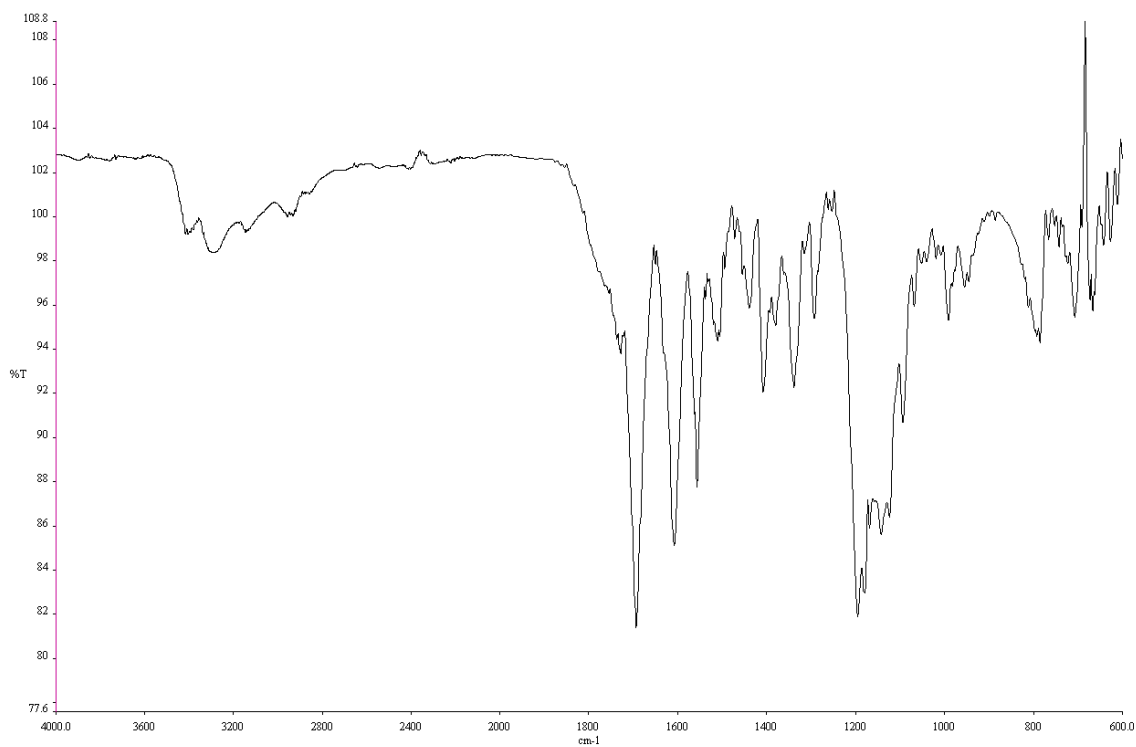


Figure A4.118. Infrared spectrum (Thin Film, NaCl) of compound **206**.

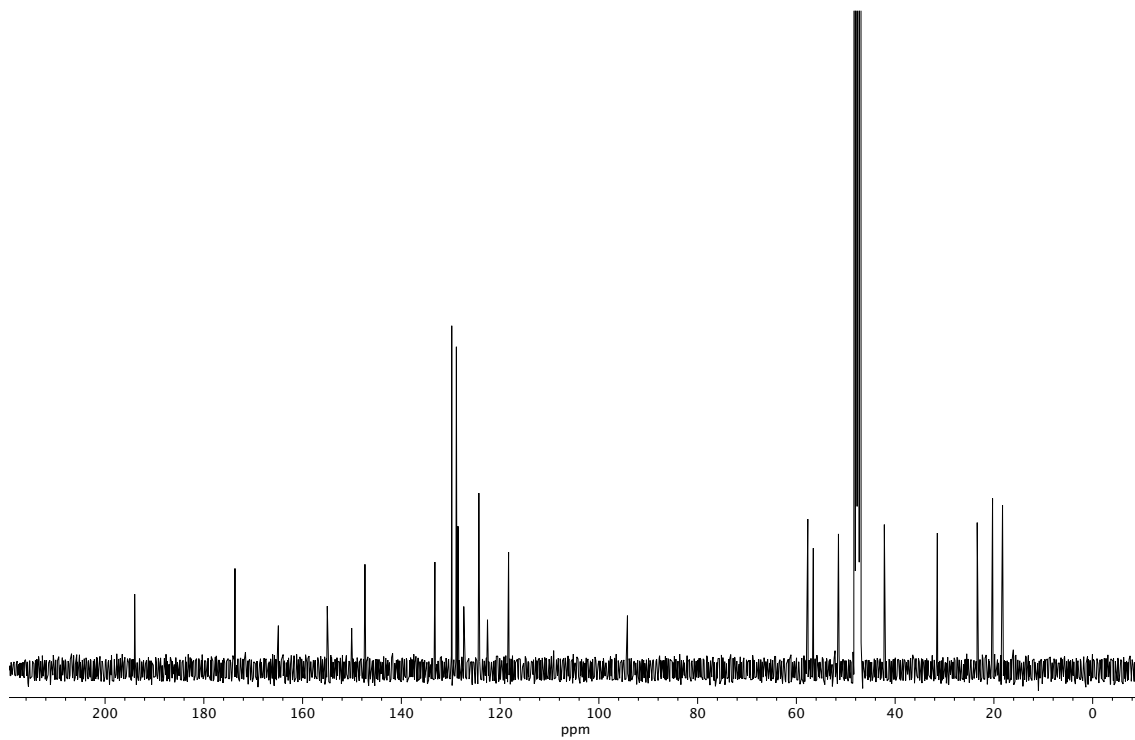


Figure A4.119. ¹³C NMR (100 MHz, CD₃OD) of compound **206**.

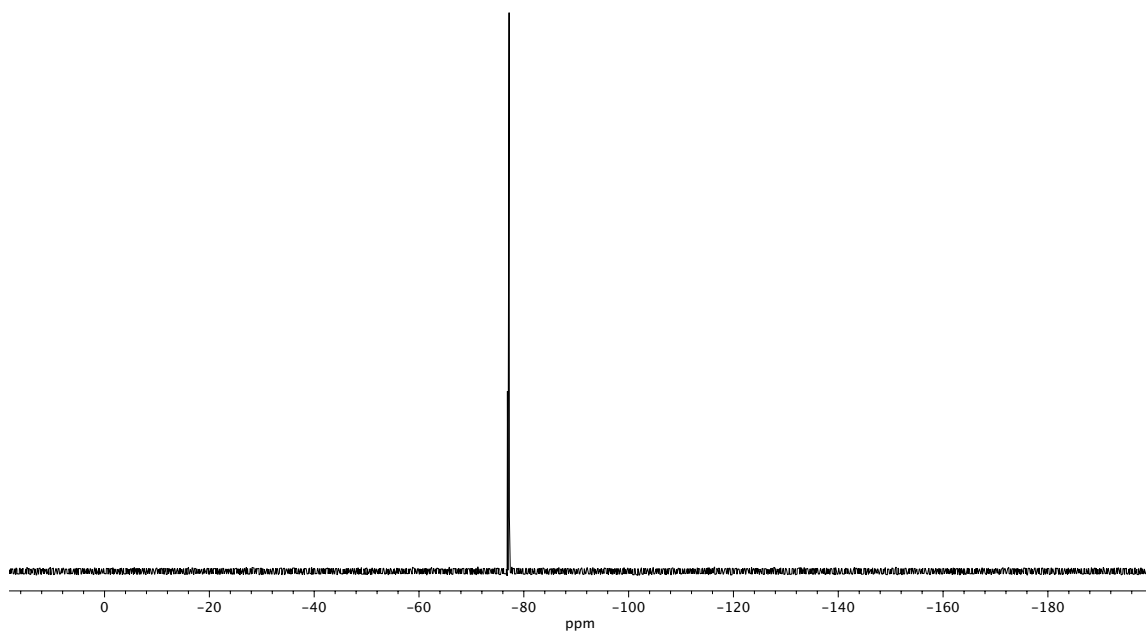
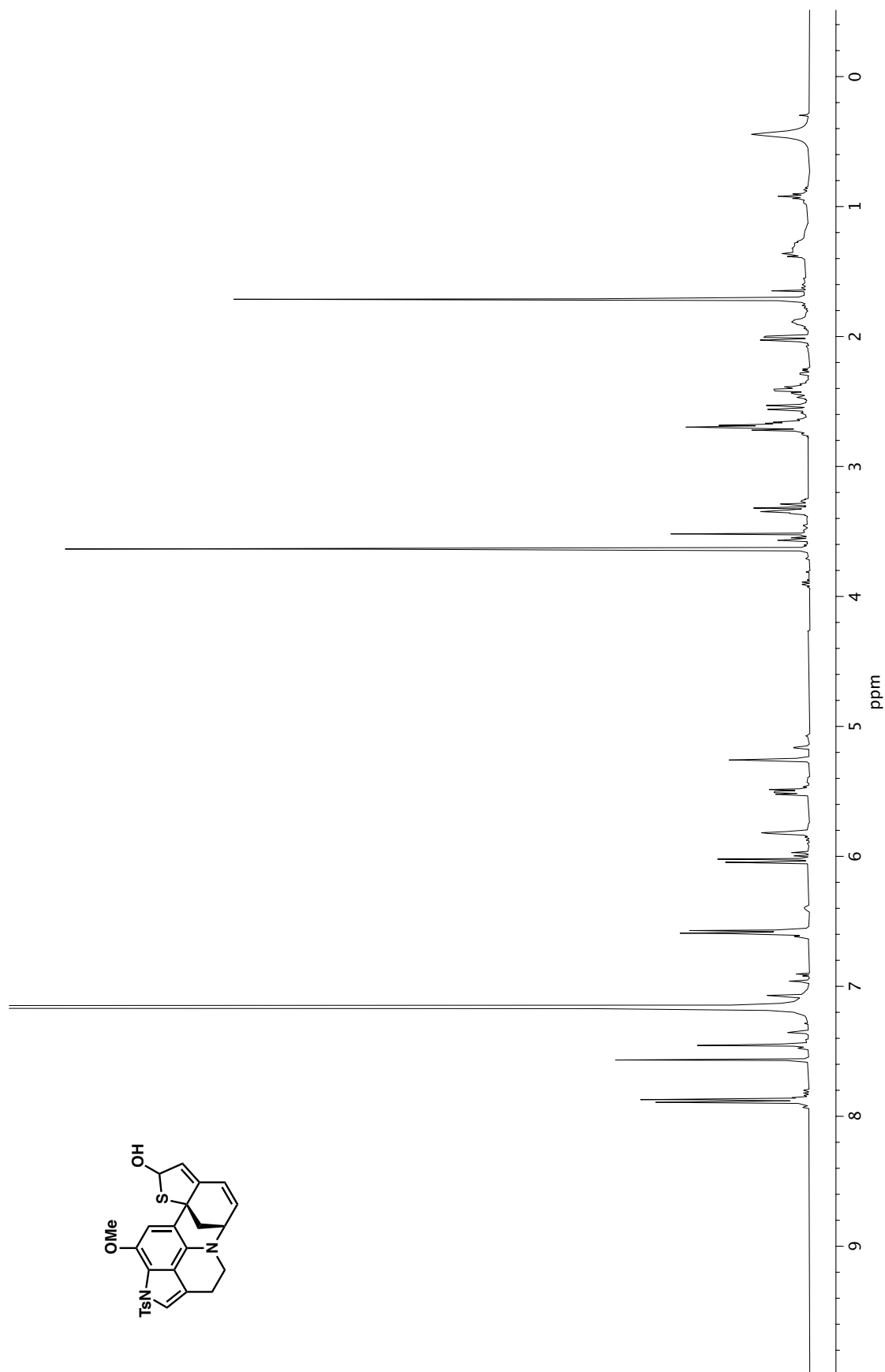


Figure A4.120. ^{19}F NMR (376 MHz, CD_3OD) of compound **206**.

Figure A4.121. ¹H NMR (400 MHz, C₆D₆) of compound 207.

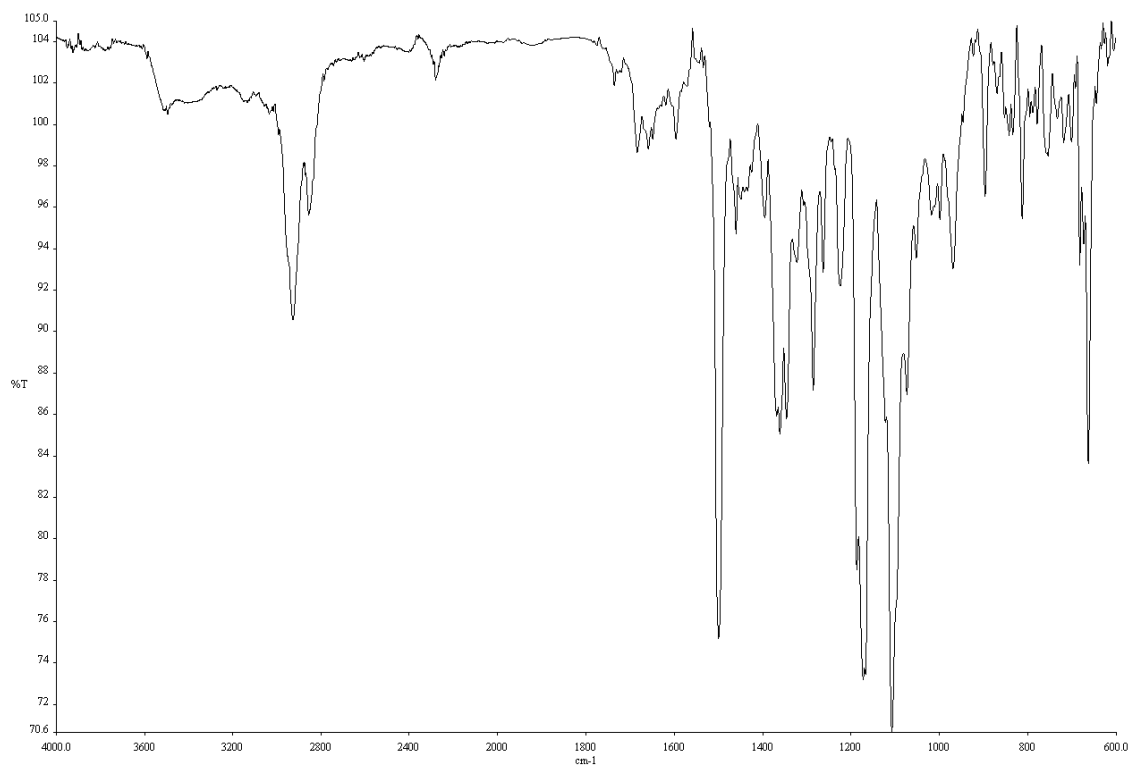


Figure A4.122. Infrared spectrum (Thin Film, NaCl) of compound **207**.

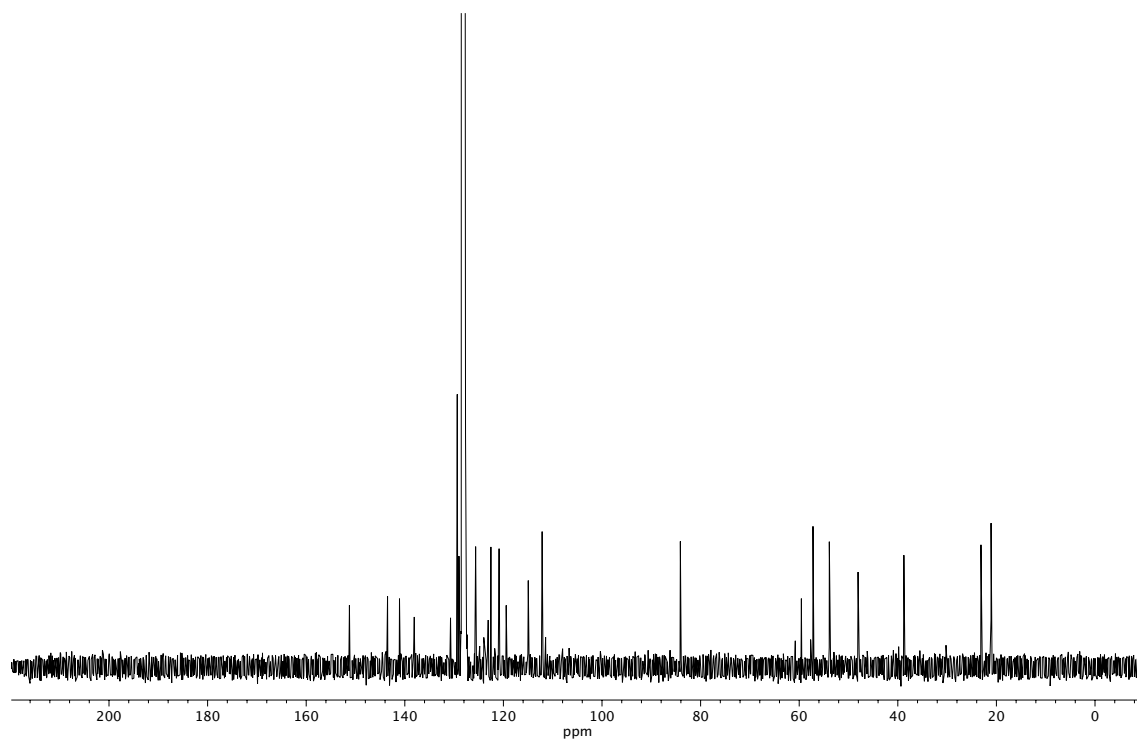


Figure A4.123. ^{13}C NMR (100 MHz, C_6D_6) of compound **207**.

APPENDIX 5

Additional Strategies and Tactics Toward the Total Synthesis of Aleutianamine[†]

A5.1 INTRODUCTION

Over the course of our synthetic studies toward aleutianamine, several strategies were briefly pursued and abandoned at a relatively early stage, and several synthetic tactics were studied in simplified systems to demonstrate their applicability prior to pursuit of a synthetic strategy. These strategies and tactics are reported in this appendix.

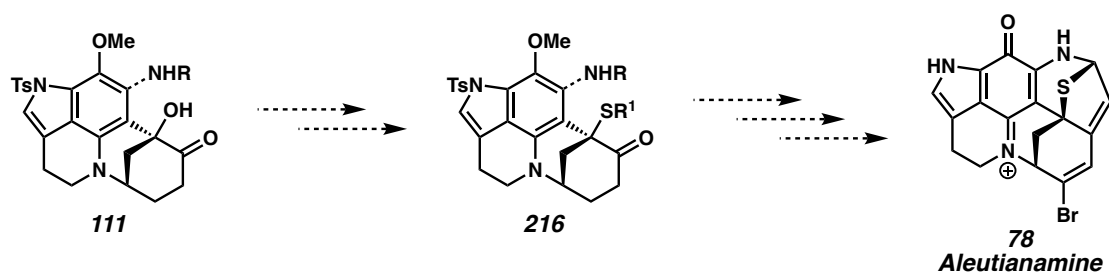
A5.2 BRIDGEHEAD SULFIDE INSTALLATION: MODEL STUDIES

Upon conceiving of our 2nd-generation retrosynthesis of aleutianamine, we recognized that installation of the bridgehead tertiary sulfide of the natural product would represent a synthetic challenge (Scheme A5.2.1). Ideally, hydroxyketone intermediate **111** would undergo a short synthetic sequence involving a substitution reaction, establishing bridgehead α -thio ketone **216** which could be advanced to the natural product. Many strategies for tertiary sulfide construction from alcohols involve either harsh, acidic conditions necessary to ionize the alcohol and effect an S_N1 reaction,¹ rely on an S_N2 reaction at the α -position of a carbonyl compound,^{2,3} or employ conjugate addition strategies.³ An S_N2 approach for the synthesis of sulfide **216** would be rendered ineffective

[†]This research was performed in collaboration with Samir Rezgui and Hao Yu and is ongoing.

by the constrained nature of the bicyclic system. We therefore planned to utilize an S_N1 -type approach employing a mild Lewis acid such as the method reported by Baba for indium-catalyzed substitution of alkyl acetates with silyl thioethers.⁴

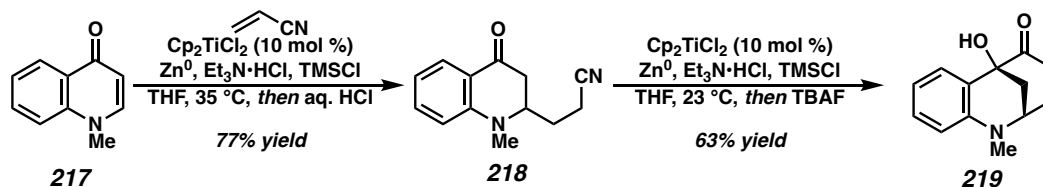
Scheme A5.2.1. Planned bridgehead sulfide installation toward aleutianamine.



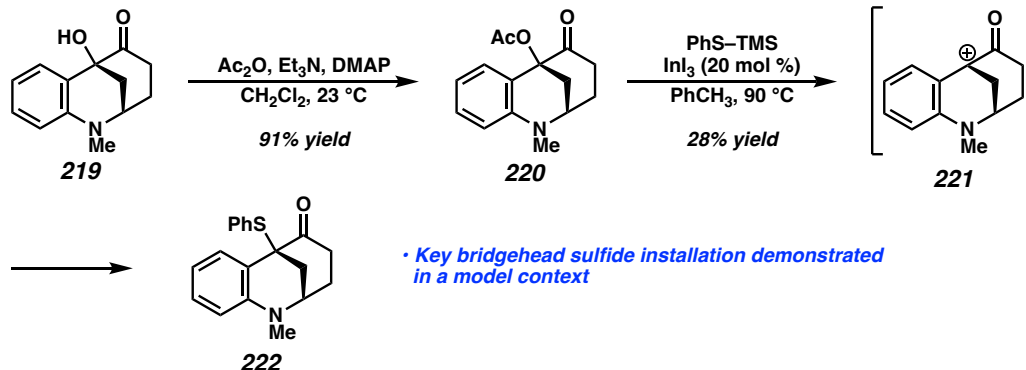
Streuff reported an elegant method for the synthesis of a relevant model system (Scheme A5.2.2A).⁵ 4-quinolone **217** (and related substrates) underwent Ti(III)-catalyzed single-electron reductive coupling with acrylonitrile to afford keto-nitrile **218**. This intermediate then underwent a related reductive coupling, now intramolecularly, to afford α -hydroxyketone **219**. After replicating Streuff's synthesis of bridgehead alcohol **219**, the alcohol was acetylated to afford ester **220** (Scheme A5.2.2B). Then, encouragingly, Baba's conditions for acetate-sulfide exchange provided desired sulfide **222**, presumably via tertiary carbocation **221**. This cation may be somewhat stabilized by resonance donation from the aniline. Although this donation would increase the ring strain of **221**, related strained bicyclo[3.3.1]octenes have been implicated as reactive intermediates.⁶

Scheme A5.2.2. A model system for bridgehead sulfide installation.

A) Reductive formal [3+3] cycloaddition between 4-quinolones and acrylonitrile (Streuff, 2015).



B) Model study for bridgehead sulfide installation.

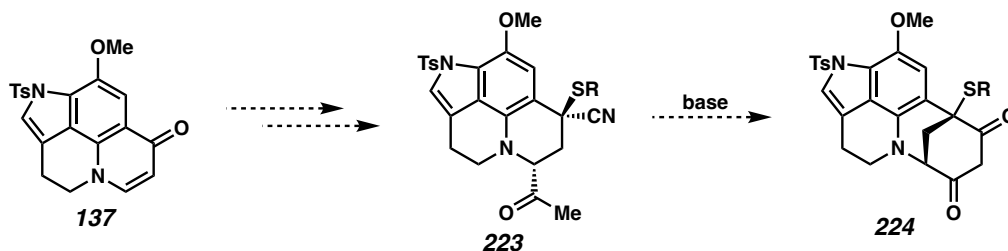


Although the yield for sulfide installation in this model system was only 28%, this proof-of-concept provided impetus to proceed with the synthesis of a bridgehead alcohol substrate in the real system. Simultaneously, however, an alternative method for sulfide installation that would obviate carbocation chemistry was briefly explored (Scheme A5.2.3A). Tetracyclic quinolone **137**, which would also be the substrate for Streuff's bicyclization method, could undergo conjugate addition of a ketone equivalent, homologation to a nitrile, and installation of the sulfide prior to bicyclization to afford ketone **223**. Bicyclization could then occur by a Dieckmann-type reaction to directly afford 1,3-diketone **224**.

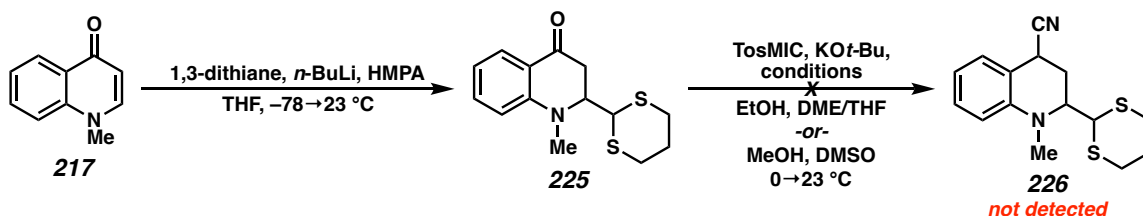
Again using 4-quinolone **217** as a model substrate, lithiated 1,3-dithiane underwent conjugate addition by a literature procedure to yield saturated ketone **225**.⁷ Unfortunately, homologation of **225** by the van Leusen reaction was unsuccessful in our hands. Ketone **226** may simply be too electron-rich to undergo the desired reaction.

Scheme A5.2.3. Alternative strategy for sulfide installation.

A) Synthetic strategy: Sulfide installation prior to bicyclization.



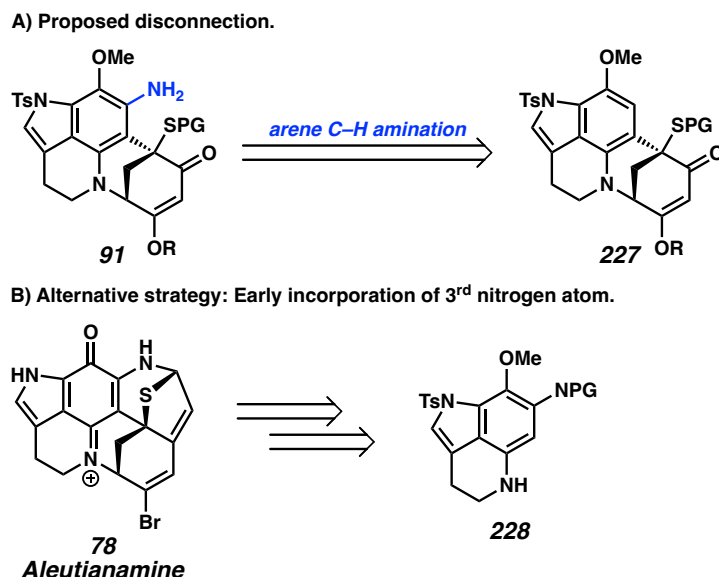
B) Synthetic strategy thwarted by unsuccessful van Leusen reaction.



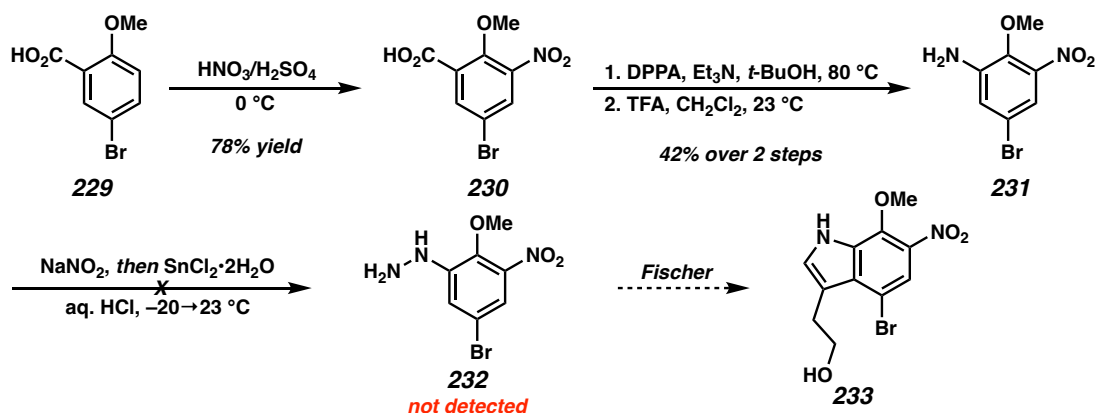
Further efforts to access nitrile **226** or derivatives thereof may be merited, but we planned to continue the synthetic sequence with the goal of utilizing Streuff's bicyclization and Baba's sulfide exchange, not yet realizing the synthetic challenge associated with accessing tetracyclic quinolone **137**.

A5.3 EARLY STRATEGIES TOWARD A TRICYCLIC AMINOINDOLE

Uncertain if the retrosynthetic disconnection of dianiline **91** to tertiary aniline **227** was indeed feasible (Scheme A5.3.1A), we invested considerable synthetic efforts into developing an alternative synthetic route that would incorporate the final nitrogen atom of the natural product at an early stage via nitrogen-rich tricycle **228** (Scheme A5.3.1B).

Scheme A5.3.1. Late-stage arene amination disconnection.

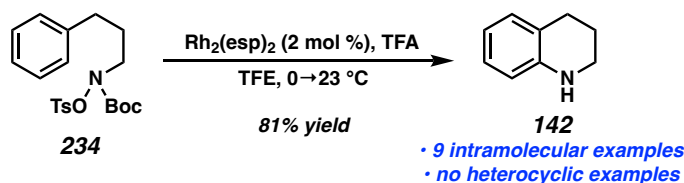
In our initial approach (Scheme A5.3.2), known brominated salicylic acid derivative **229**⁸ underwent precedented nitration to afford nitroarene **230**.⁹ DPPA-mediated Curtius rearrangement in *t*-BuOH and cleavage of the resulting *t*-butyl carbamate afforded nitroaniline **231**, an anticipated precursor to tricycle **228**. Unfortunately, attempted conversion to arylhydrazine **232** by diazotization and reduction was unsuccessful in our hands, thwarting access to necessary tryptophol **233**. The electron-poor nature of the arene may accelerate side reactions of the diazonium salt.

Scheme A5.3.2. Preparation of nitroaniline **231** and failed Fischer Indolization.

While tricycle **228** was ultimately synthesized via Larock indolization, the need for this nitrogen-rich intermediate was obviated by the discovery that late-stage formal arene C–H amination is indeed a facile process (see Chapter 2).

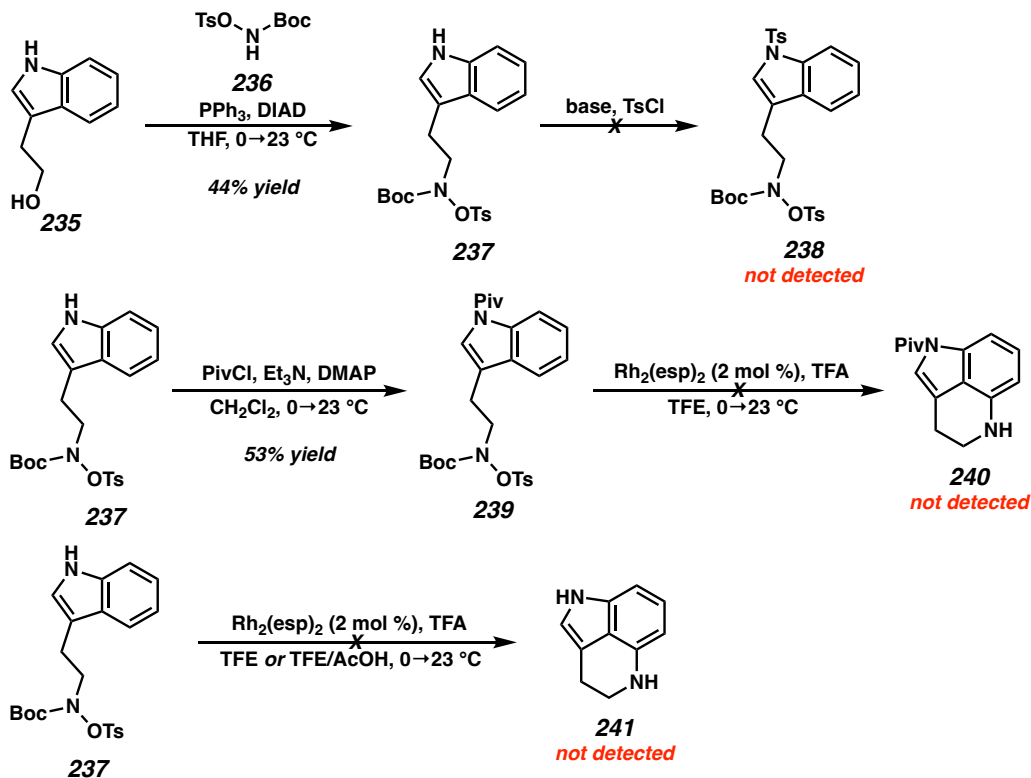
We also briefly investigated a route to simplified derivatives of this tricyclic intermediate relying on intramolecular Rh-catalyzed C–H amination. A catalytic system for this transformation was reported by Falck and found to enable both inter- and intramolecular C–N bond formation (Scheme A5.3.3).¹⁰ In the intramolecular sense, *O*-sulfonylhydroxylamines such as **234** could cyclize to afford anilines such as **142**. Falck's report did not include examples of substrates bearing heterocycles.

Scheme A5.3.3. Intramolecular aryl C–H amination (Falck, 2016).



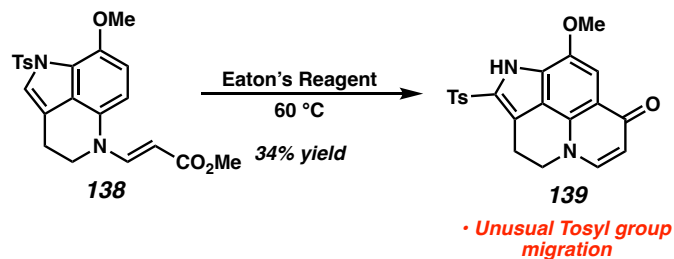
Toward an analogous indolyl system, tryptophol (**235**) underwent a Mitsunobu reaction with known hydroxycarbamate derivative **236**¹¹ to afford tryptamine **237** (Scheme A5.3.4). Subsequent tosylation was attempted but using triethylamine as a base failed to effect the reaction, and the *O*-sulfonyl hydroxycarbamate did not survive NaH. The indole was instead protected as pivaloyl amide **239**. Unfortunately, neither **239** nor free indole **237** underwent Falck's Rh-catalyzed C–H amination, instead undergoing unproductive side reactions. Following these observations, a route toward a tosyl-protected tricycle involving a Buchwald–Hartwig amination was developed (see Chapter 2).

Scheme A5.3.4. Attempts to access tricyclic aminoindoles by intramolecular C–H amination.

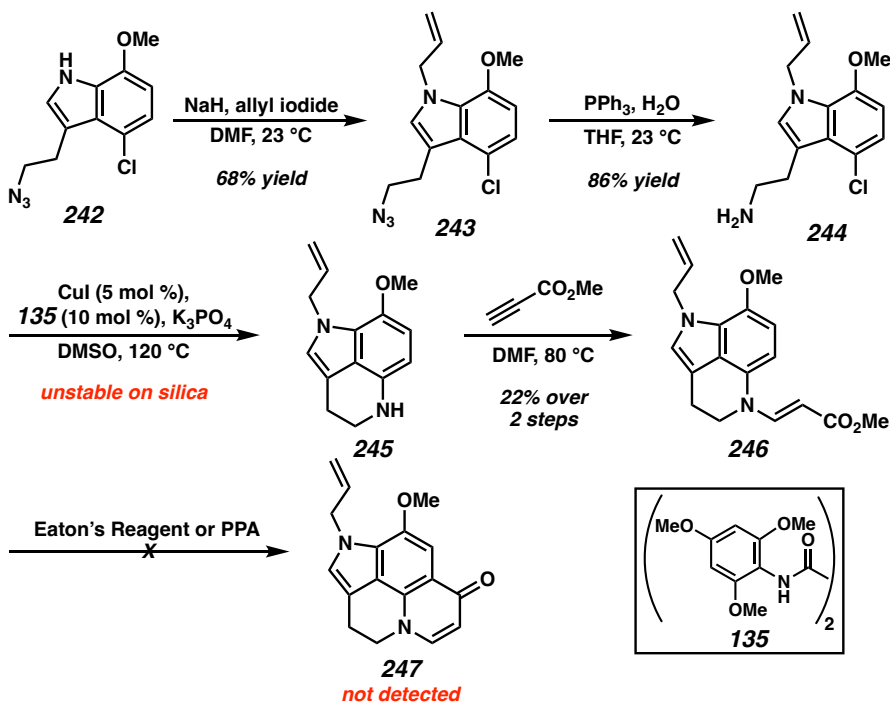


A5.4 ADDITIONAL EFFORTS TOWARD KEY TETRACYCLIC QUINOLONE

As discussed in Chapter 2, attempts to cyclize methyl ester **138** to afford a tetracyclic quinolone led to concomitant tosyl group migration, yielding unexpected product **139** (Scheme A5.4.1). Given the low yield of this cyclization, rather than incorporating additional steps to remove and reinstall the tosyl group, we evaluated alternative indole protecting groups.

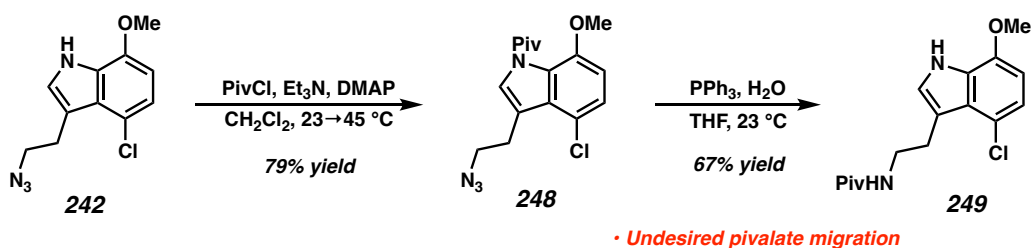
Scheme A5.4.1. Unexpected tosyl group migration during quinolone synthesis.

First, azide **242** was *N*-allylated to afford azide **243**, which underwent a Staudinger reduction to tryptamine **244** (Scheme A5.4.2). Ma's Cu-catalyzed C–N coupling employing oxalamide ligand **135** provided desired tricycle **245**, albeit in low yield.¹² This tricycle was found to be oxidatively unstable, particularly on silica gel, due to its electron-rich nature. Aza-Michael reaction with methyl propiolate afforded “push-pull” olefin **246**, but this substrate did not survive acidic conditions, likely also due to the electron-rich nature of the indole.

Scheme A5.4.2. Attempted preparation of *N*-allyl tetracycle **247**.

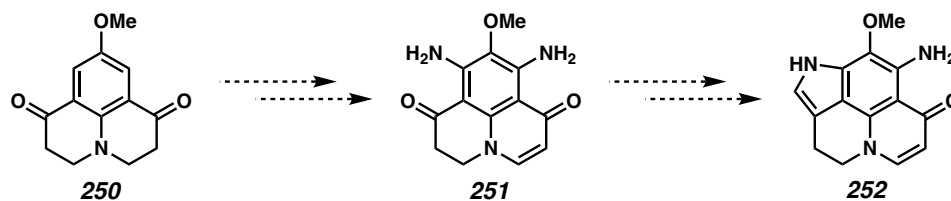
Realizing that an electron-withdrawing indole protecting group would be necessary, we evaluated the use of a Piv group (Scheme A5.4.3). Azide **242** underwent efficient pivaloylation, but subsequent Staudinger reduction of azidoindole **248** lead to concomitant migration of the Piv group from the indole to the unveiled primary amine to yield amide **249**. Following this result, the direct cyclization approach to a tetracyclic quinolone intermediate was abandoned, and a sulfonyl indole protecting group was recognized as essential.

Scheme A5.4.3. Evaluation of a pivaloyl indole protecting group.



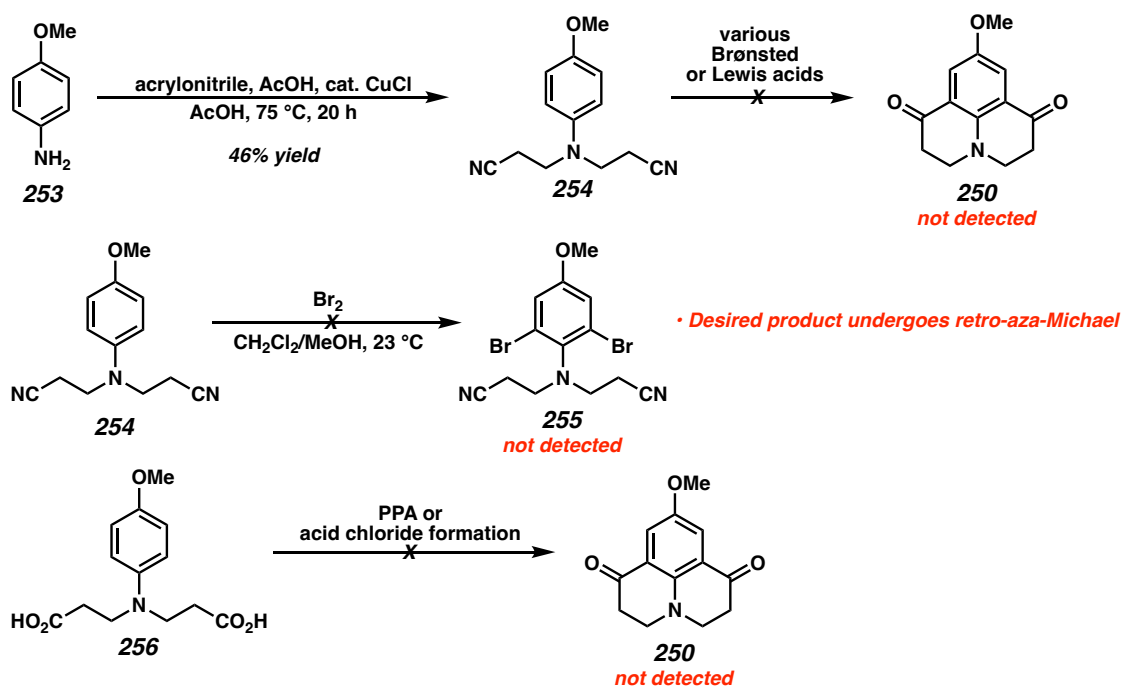
Finally, a strategically distinct approach to a tetracyclic quinolone structurally related to **139** was envisioned (Scheme A5.4.4). Diketojulolidine derivative **250** could be advanced to diaminoquinolone **251** by nitration, reduction, and desaturation. The latter transformation proceeds readily for a related compound simply by heating in the presence of Pd/C.¹³ Finally, installation of an additional methine could establish the indole moiety of **252**. This synthetic route would also have the advantage of enabling early incorporation of the final nitrogen atom of the natural product.

Scheme A5.4.4. A julolidine desymmetrization approach to quinolone **252**.



Toward the requisite diketojulolidine starting material **250**, *p*-anisidine (**253**) underwent known double aza-Michael addition into acrylonitrile to afford dinitrile **254** (Scheme A5.4.5).¹⁴ Treatment of **254** with several Brønsted and Lewis acids failed to effect the desired cyclization. Bromination was attempted in order to access **255**, a substrate for an anionic cyclization, but concomitant loss of acrylonitrile was observed. This retro-aza-Michael fragmentation was not suppressed by the addition of base. Finally, the cyclization of known diacid **256** was attempted under the conditions of Kantminene et al.¹⁵ Desired tricycle **250** was not detected, with retro-aza-Michael fragmentation again being observed. At this point, we abandoned the quinolone cyclization approach to aleutianamine, shifting our efforts instead to the intramolecular Barbier approach outlined in Chapter 2.

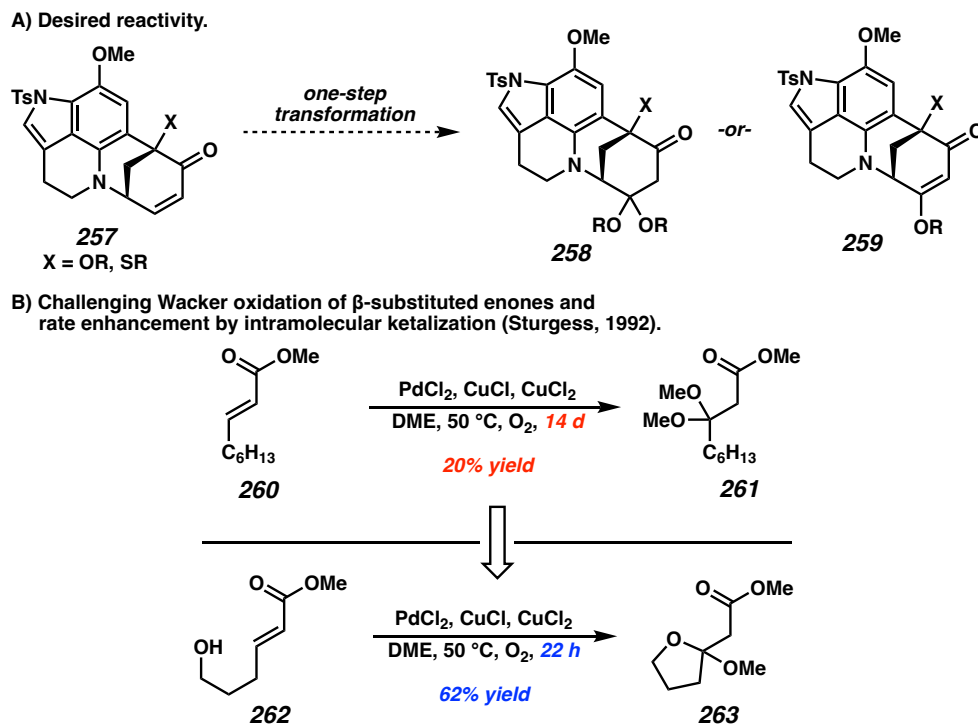
Scheme A5.4.5. Unsuccessful preparation of diketojulolidine 250.



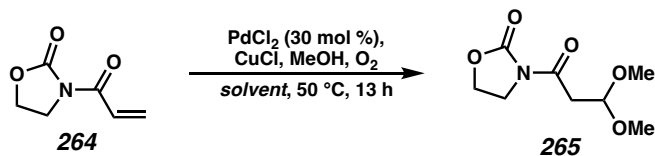
A5.5 PRELIMINARY EVALUATION OF A WACKER OXIDATION OF INTERNAL α,β -UNSATURATED CARBONYL COMPOUNDS

Toward the installation of the alkenyl bromide moiety of aleutianamine, the synthetic transformation of enone **257** or a derivative thereof to a 1,3-diketone equivalent (e.g., ketal **258** or vinylogous ester **259**) was identified as desirable (Scheme A5.5.1A). Existing methods to effect this transformation are outlined in Chapter 2, generally requiring around 3 steps. A potential alternative one-step transformation is the Wacker oxidation. While Pd-catalyzed Wacker oxidation leads to efficient oxidation of terminal α,β -unsaturated esters to acetals,¹⁶ oxidation of β -substituted unsaturated esters is typically slow and low-yielding. Interestingly, Sturgess reported that while unsaturated ester **260** undergoes Pd-catalyzed oxidative ketalization to afford **261** in only 20% yield in 14 days, substrate **262**, which bears a tethered alcohol group, undergoes Wacker oxidation to ketal **263** in improved yield in only 22 hours.¹⁷ This result suggests that the slow rate of the oxidation of β -substituted unsaturated esters is due to slow conjugate addition of the alcohol to afford an intermediate that can undergo further oxidation. We therefore hypothesized that the addition of an appropriate Lewis-acidic additive could accelerate oxa-Michael addition and promote faster oxidation of relevant substrates.

Scheme A5.5.1. Desired enone β -oxidation and challenging Wacker oxidation of internal α,β -unsaturated carbonyl compounds.



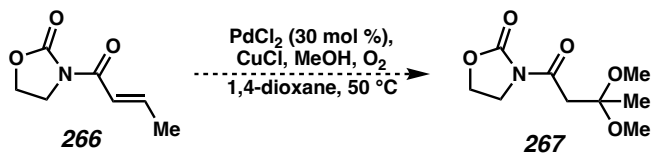
Acyl oxazolidinones were identified as a desirable substrate class for the evaluation of reaction conditions due to their crystallinity and lack of volatility. Acryloyl substrate **264** was synthesized by a reported procedure as a positive control and a brief solvent screen was conducted (Table A5.5.2).¹⁸ Among solvents tested, DME (entries 1, 2) was found to perform well, in line with previous research,^{16,17} but dioxane provided an optimal yield (entry 4). HFIP (entry 5) led to a slightly higher yield but required a longer reaction time (the reaction was conducted at a lower temperature due to the high volatility of the solvent).

Table A5.5.2. Evaluation of solvents for positive control substrate **264**.^a

entry	solvent	% yield
1	DME	52 ^b
2	DME	73
3	MeCN	56
4	1,4-dioxane	79
5	HFIP	82 ^c
6	DMA	21

[a] Reactions were conducted at 0.035 mmol scale at 0.25 M using 0.3 equiv PdCl₂, 1.0 equiv CuCl, and 25 equiv MeOH. Yields were determined by ¹H NMR analysis with 1,3,5-trimethoxybenzene as an internal standard unless otherwise noted. [b] Isolated yield on a 0.142 mmol scale with 10 mol % PdCl₂. [c] Conducted at 23 °C for 3 days.

Having validated acyloxazolidinones as a competent substrate class, β-substituted substrate **266** was also prepared and tested (Table A5.5.3). Unfortunately, all additives tested either failed to improve the reaction outcome (trace product, entry 1) or resulted in nonspecific decomposition. Indium triflate led to putative oxa-Michael addition without oxidation (entry 5).

Table A5.5.3. Evaluation of Lewis-acidic additives.^a

entry	additive ^b	result
1	—	trace (3 d)
2	+6 equiv CuCl	trace (3 d)
3	6 equiv LiCl	trace (3 d)
4	6 equiv LiI	decomp
5	In(OTf) ₃	decomp + oxa-Michael
6	Bi(OTf) ₃	decomp
7	Sc(OTf) ₃	decomp

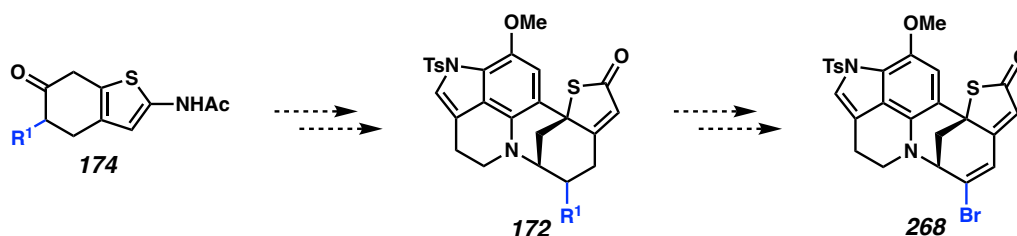
[a] Reactions were conducted at 0.035 mmol scale at 0.25 M using 0.3 equiv PdCl₂, 1.0 equiv CuCl, and 25 equiv MeOH. Reaction progress was monitored by LC-MS. [b] 2.0 equiv unless otherwise noted.

At this stage, development of the Wacker oxidation of unsaturated imide **266** was shelved in favor of development of other aspects of the total synthesis. Nevertheless, further development of the Wacker oxidation of electron-poor internal olefins could facilitate future synthetic studies.

A5.6 ALKENYL BROMIDE INSTALLATION VIA A FUNCTIONAL HANDLE

In parallel to efforts toward late-stage alkenyl bromide installation, which have thus far proved unfruitful, we have evaluated early incorporation of a functional handle R^1 into thiophene coupling fragment **174** (Scheme A5.6.1). Advancement to functionalized thiobutenolide **172** would enable installation of the alkenyl bromide moiety of **268** without selective δ -oxidation chemistry.

Scheme A5.6.1. A functional handle approach to alkenyl bromide installation.

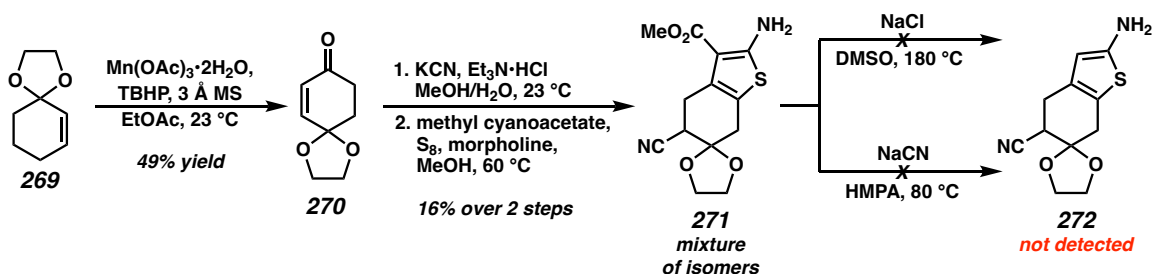


A suitable functional handle should be stable to the conditions for reductive amination and be a sufficiently poor leaving group to prevent aromatization of ketone **174**.

Given these constraints, a nitrile was first tested as a potential functional handle. Known ketal **269**¹⁹ was subjected to precedented allylic oxidation to enone **270** (Scheme A5.6.2).²⁰ Conjugate addition of cyanide in the presence of triethylamine hydrochloride led to a complex mixture of intermediates suspected to contain cyanohydrins, which underwent Gewald thiophene synthesis to afford aminothiophene **271** in low yield as a mixture of isomers. Removal of the methyl ester would be necessary to employ this

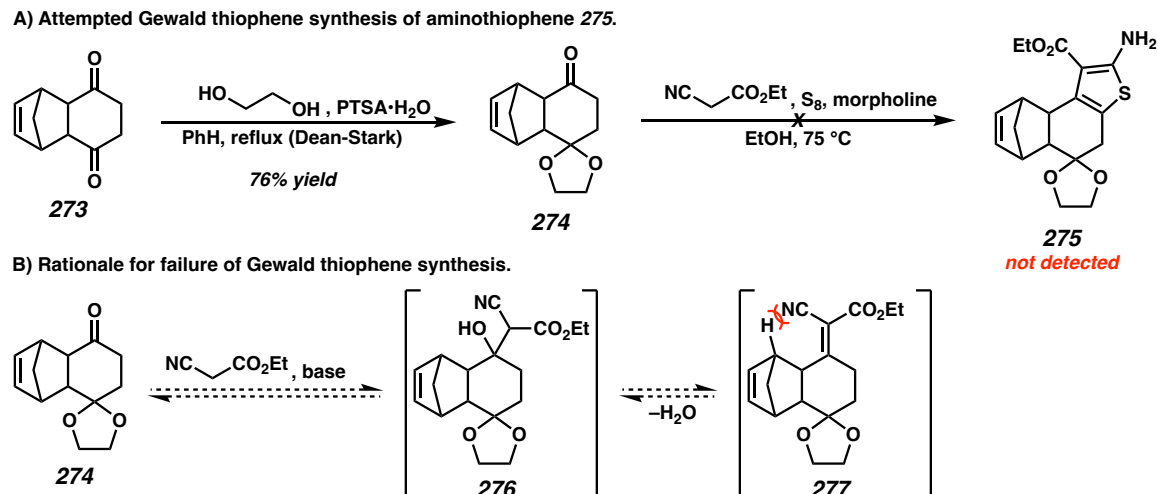
intermediate as a coupling fragment toward the synthesis of aleutianamine. Previous experiments examining the hydrolytic cleavage of the ester led to competitive hydrolysis of the nitrile, so alternative anionic decarboxylation conditions were tested. Treatment with NaCl at elevated temperature in DMSO led to nonspecific decomposition, while milder conditions employing NaCN in HMPA²¹ led to no reaction. The challenge of selective methyl ester removal coupled with the low yield and unselective synthesis of nitrile **271** led us to abandon this route.

Scheme A5.6.2. Evaluation of a cyanide functional handle.



Instead, a cyclopentadiene Diels–Alder adduct was anticipated to be a suitable removable handle, as this bulkier group could result in a more selective Gewald reaction and no potentially problematic leaving group would be present. Diketone **273** was prepared by a literature procedure²² and underwent precedented monoketalization to afford ketal **274** (Scheme A5.6.3A).²³ Unfortunately, Gewald thiophene synthesis of aminothiophene **275** could not be effected. Significant recovery of starting material was observed at 75 °C, and the desired product was not generated even at 90 °C. Likely, the initial Knoevenagel condensation of **274** with ethyl cyanoacetate is thwarted by the increase in strain of condensation product **277** relative to initial adduct **276**, as the bridgehead methine would sterically clash with the cyano group (Scheme A5.6.3B).

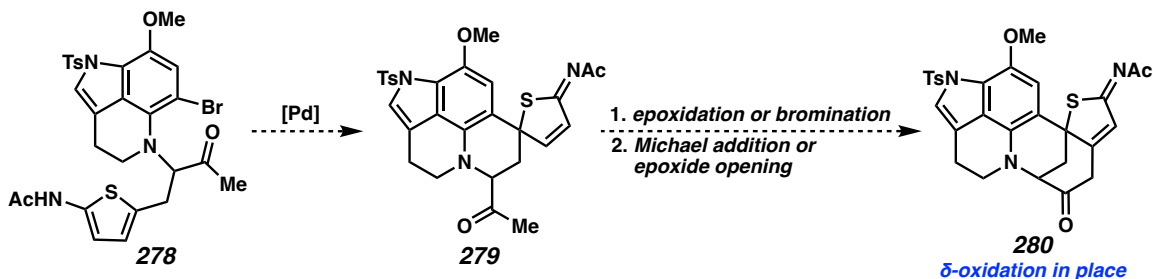
Scheme A5.6.3. Attempted Gewald reaction of a cyclopentadiene Diels–Alder adduct.



A5.7 SPIROCYCLE-FIRST APPROACH TO δ -OXIDIZED THIOIMIDATE

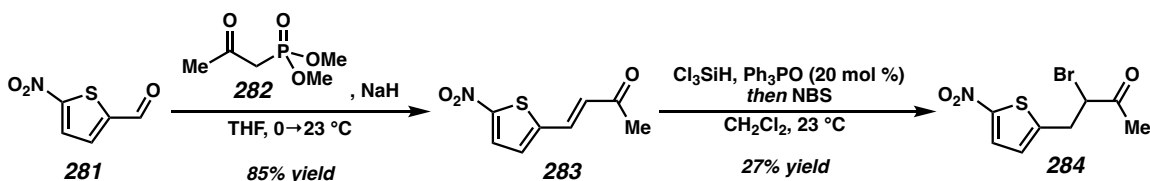
As an alternative strategy to circumvent a challenging late-stage δ -oxidation of a thiobutenolide, it was anticipated that 2-aminoketone **278** could undergo the dearomative cyclization previously developed during the course of our synthetic efforts to provide spirocyclic thioimide **279** (Scheme A5.7.1). Then, the installation of an oxidation handle such as an epoxide or vinyl bromide would enable intramolecular Michael-type addition with concomitant elimination to afford hexacycle **280** with the desired ketone in place, setting the stage for functional group interconversion to the alkenyl bromide of aleutianamine.

Scheme A5.7.1. A spirocyclization–Michael addition approach to the oxidized ring system of aleutianamine.

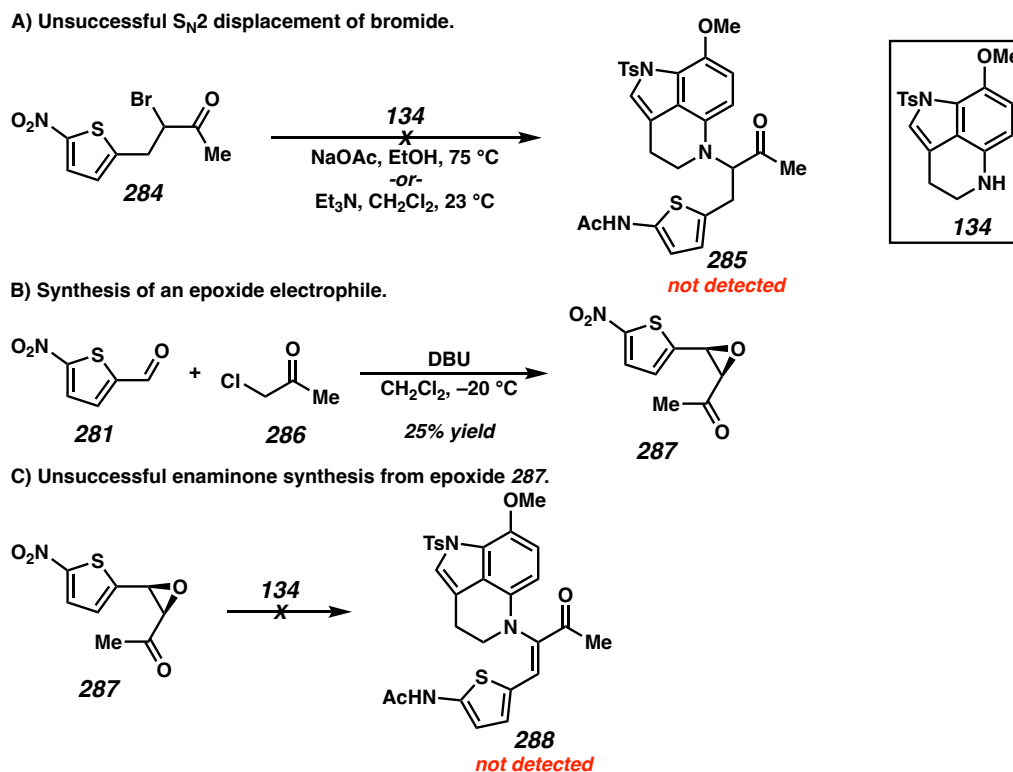


A strategy to prepare aminoketone **280** was not immediately clear due to the dissonant oxidation pattern of this species, but a potential S_N2 approach was identified. Thus, commercially available aldehyde **281** underwent Horner–Wadsworth–Emmons olefination with phosphonate **282** to afford enone **283** (Scheme A5.7.2). The hydrosilylation-bromination reaction developed by Toy afforded bromoketone electrophile **284**.²⁴

Scheme A5.7.2. Access to a 2-bromoketone electrophile.



Unfortunately, S_N2 displacement of the bromide with secondary aniline **134** could not be effected in our hands (Scheme A5.7.3A)—undesired elimination of the bromide was observed, and aminoketone **285** was not detected. As an alternative, epoxyketone **287** was prepared by a DBU-mediated Darzens reaction²⁵ between aldehyde **281** and chloroacetone (**286**) (Scheme A5.7.3B). Epoxide opening with aniline **134** to provide enamionone **288** also did not occur, however. Epoxide opening with a basic amine led to opening at the undesired benzylic position.

Scheme A5.7.3. Attempts to access a spirocyclization substrate.

The spirocyclization-first synthetic route was abandoned at this stage due to the difficulty associated with accessing aminoketone **285**.

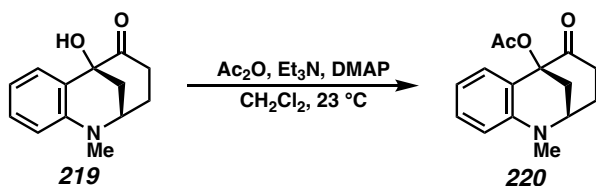
A5.8 EXPERIMENTAL SECTION

A5.8.1 MATERIALS AND METHODS

Unless otherwise stated, reactions were performed in flame-dried glassware under an argon or nitrogen atmosphere using dry, deoxygenated solvents. Solvents were dried by passage through an activated alumina column under argon.²⁶ NBS was recrystallized from boiling water prior to use and amines were distilled under nitrogen prior to use. All other reagents were purchased from commercial sources and used as received unless otherwise indicated. Reaction progress was monitored by thin-layer chromatography (TLC) or Agilent 1290 UHPLC-MS. TLC was performed using E. Merck silica gel 60 F254

precoated glass plates (0.25 mm) and visualized by UV fluorescence quenching or KMnO₄ staining. Silicycle SiliaFlash® P60 Academic Silica gel (particle size 40–63 nm) was used for flash chromatography. ¹H NMR spectra were recorded on Varian Inova 500 MHz and Bruker 400 MHz spectrometers and are reported relative to residual CHCl₃ (δ 7.26 ppm). Data for ¹H NMR are reported as follows: chemical shift (δ ppm) (multiplicity, coupling constant (Hz), integration). Multiplicities are reported as follows: s = singlet, d = doublet, t = triplet, q = quartet, p = pentet, sept = septuplet, m = multiplet, br s = broad singlet, br d = broad doublet.

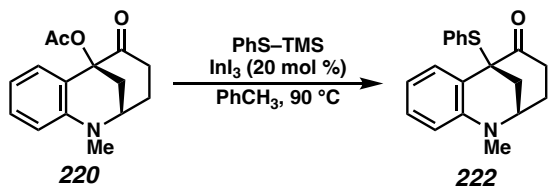
A5.8.2 EXPERIMENTAL PROCEDURES



Tertiary acetate 220

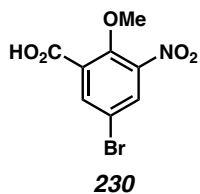
To a 1-dram glass vial under air were added tertiary alcohol **219**⁵ (25 mg, 0.115 mmol, 1.0 equiv), DMAP (1.6 mg, 0.013 mmol, 0.12 equiv), and CH₂Cl₂ (0.6 mL), followed by Et₃N (36 μL, 0.26 mmol, 2.25 equiv) and Ac₂O (24 μL, 0.26 mmol, 2.25 equiv). The reaction mixture was stirred at 23 °C for 46 h, then washed with water (2x). The combined aqueous phases were extracted once with CH₂Cl₂, and the combined organic phases were dried over Na₂SO₄ and concentrated under reduced pressure. The crude product was purified by silica gel flash chromatography (60% Et₂O/hexanes) to afford the title compound (27 mg, 0.10 mmol, 91% yield); ¹H NMR (400 MHz, CDCl₃) δ 7.36 (dd, *J* = 7.8, 1.7 Hz, 1H), 7.21 (ddd, *J* = 8.2, 7.3, 1.7 Hz, 1H), 6.72 – 6.63 (m, 2H), 3.77 (tt, *J* =

4.5, 3.1 Hz, 1H), 3.22 (dd, $J = 12.0, 2.8$ Hz, 1H), 3.09 (s, 3H), 2.52 – 2.43 (m, 1H), 2.41 – 2.35 (m, 1H), 2.35 – 2.26 (m, 1H), 2.24 (s, 3H), 2.23 – 2.19 (m, 1H), 2.05 – 1.94 (m, 1H).



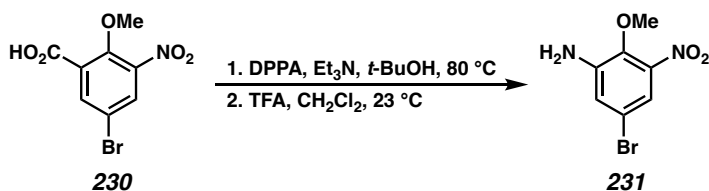
Tertiary sulfide **222**

To a 1-dram glass vial in a nitrogen-filled glovebox were added InI_3 (2 mg, 0.004 mmol, 0.2 equiv), PhCH_3 (0.2 mL), and PhSTMS (7.3 μL , 0.0386 mmol, 2.0 equiv). Then, acetate **220** (5.0 mg, 0.0193 mmol, 1.0 equiv) was added as a solution in PhCH_3 (0.25 mL), the vial was sealed with a PTFE/silicone septum and removed from the glovebox, and the reaction mixture was stirred at 90 $^\circ\text{C}$ in a metal heating block for 3 h. Then, the reaction mixture was allowed to cool to 23 $^\circ\text{C}$ and saturated aq. NaHCO_3 (1 mL) was added. The resulting suspension was extracted with Et_2O (4x0.5 mL) and the combined organic extracts were dried over Na_2SO_4 . The crude product was purified by preparative TLC on silica gel (33% EtOAc /hexanes) to afford the crude product as a brown film (1.7 mg, 0.0055 mmol, 28% yield); ^1H NMR (400 MHz, CDCl_3) δ 7.86 (dd, $J = 7.8, 1.7$ Hz, 1H), 7.37 – 7.32 (m, 2H), 7.24 – 7.13 (m, 4H), 6.69 (ddd, $J = 7.8, 7.3, 1.2$ Hz, 1H), 6.57 (dd, $J = 8.3, 1.2$ Hz, 1H), 3.53 (ddd, $J = 3.8, 2.8, 1.1$ Hz, 1H), 3.01 (s, 3H), 2.46 – 2.32 (m, 3H), 2.23 – 2.11 (m, 2H), 1.90 – 1.75 (m, 1H).



Nitroarene 230

Prepared according to the procedure of Hofmann and Sanjayan.⁹ All characterization data matched those reported in the literature.

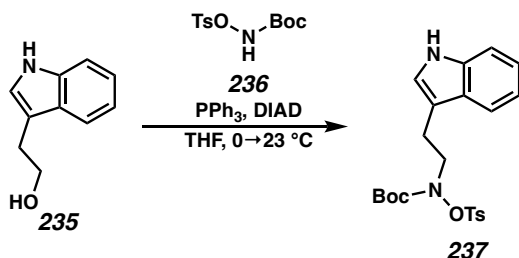


Nitroaniline 231

To a 20 mL glass vial containing nitroarene **230** under nitrogen were added *t*-BuOH (0.72 mL) and Et₃N (76 μL, 0.54 mmol, 3.0 equiv) followed by DPPA (59 μL, 0.27 mmol, 1.5 equiv). The vial was sealed with a PTFE/silicone septum and stirred at 80 °C in a metal heating block for 3 h. The reaction mixture was then cooled to 23 °C, concentrated under reduced pressure, and purified by silica gel flash chromatography (10% EtOAc/hexanes) to afford an intermediate carbamate (36 mg, 0.10 mmol, 58% yield); ¹H NMR (400 MHz, CDCl₃) δ 8.61 (d, *J* = 2.4 Hz, 1H), 7.63 (d, *J* = 2.4 Hz, 1H), 7.14 (br s, 1H), 3.91 (s, 3H), 1.54 (s, 9H).

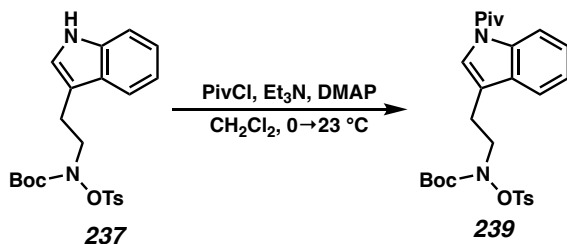
To a 1-dram glass vial were added this intermediate carbamate (20 mg, 0.0576 mmol, 1.0 equiv), CH₂Cl₂ (0.6 mL), and TFA (66 μL, 0.86 mmol, 15 equiv). The reaction mixture was stirred at 23 °C. Upon complete conversion as judged by TLC analysis, the reaction mixture was concentrated under reduced pressure and Et₃N (1 drop) was added to neutralize any remaining TFA. The crude product was purified by silica gel flash

chromatography (60% Et₂O/hexanes) to afford the title compound as a yellow film (10.4 mg, 0.0421 mmol, 73% yield); ¹H NMR (400 MHz, CDCl₃) δ 7.31 (d, *J* = 2.3 Hz, 1H), 7.06 (d, *J* = 2.3 Hz, 1H), 4.16 (br s, 2H), 3.89 (s, 3H).



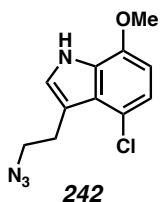
O-tosylhydroxylamine 237

To a flame-dried 20 mL vial containing PPh₃ (294 mg, 1.12 mmol, 1.2 equiv) under nitrogen was added THF (2 mL). The vial was cooled to 0 °C and DIAD (0.22 mL, 1.1 mmol, 1.2 equiv) was added dropwise, whereafter additional THF (1 mL) was added to reduce the viscosity of the heterogeneous mixture and the reaction mixture was stirred at 0 °C for 30 min. Then a solution of tryptamine (**235**, 150 mg, 0.930 mmol, 1.0 equiv) and nucleophile **236**¹¹ (322 mg, 1.12 mmol, 1.2 equiv) in THF (1.7 mL) was added dropwise and additional THF (1 mL) was used to quantitatively transfer the residual nucleophile solution. The reaction mixture was stirred at 0 °C for 1 h, then allowed to warm to 23 °C and stirred for an additional 20 h. The reaction mixture was concentrated under reduced pressure and purified twice by silica gel flash chromatography (50% Et₂O/hexanes, then CH₂Cl₂) to afford the title compound as a white foam (177 mg, 0.411 mmol, 44% yield); ¹H NMR (400 MHz, CDCl₃) δ 7.96 (br s, 1H), 7.89 – 7.85 (m, 2H), 7.60 – 7.55 (m, 1H), 7.35 – 7.29 (m, 3H), 7.18 (ddd, *J* = 8.2, 7.0, 1.3 Hz, 1H), 7.11 (ddd, *J* = 8.1, 7.1, 1.1 Hz, 1H), 7.03 (d, *J* = 2.4 Hz, 1H), 3.94 (br s, 2H), 3.10 (td, *J* = 7.5, 0.8 Hz, 2H), 2.43 (s, 3H), 1.05 (s, 9H).



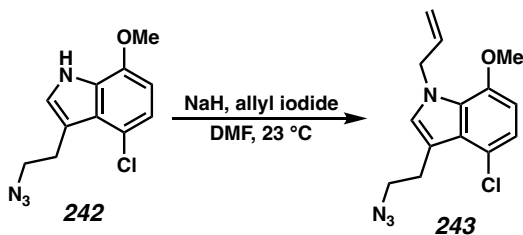
***N*-pivaloyltryptamine 239**

To a flame-dried 1-dram glass vial were added *O*-tosylhydroxylamine **237** (10 mg, 0.0232 mmol, 1.0 equiv) and DMAP (0.3 mg, 0.002 mmol, 0.1 equiv). The vial was evacuated and backfilled with nitrogen. CH₂Cl₂ (0.23 mL) and Et₃N (5.0 μL, 0.035 mmol, 1.5 equiv) were added and the vial was cooled to 0 °C. PivCl (3.4 μL, 0.028 mmol, 1.2 equiv) was added dropwise with stirring and the reaction mixture was allowed to warm to 23 °C and sealed with a PTFE-lined cap. After stirring for 15 h, the reaction mixture was warmed to 45 °C and stirring was continued. After an additional 24 h, the reaction mixture was allowed to cool to 23 °C, diluted with CH₂Cl₂ (0.5 mL), and washed once with water. The aqueous phase was extracted once with CH₂Cl₂, and the combined organic phases were dried over Na₂SO₄ and concentrated under reduced pressure. The crude product was purified by silica gel flash chromatography (15% EtOAc/hexanes) to afford the title compound as a colorless film (6.3 mg, 0.0122 mmol, 53% yield); ¹H NMR (500 MHz, CDCl₃) δ 8.48 (d, *J* = 8.4 Hz, 1H), 7.85 (d, *J* = 8.4 Hz, 2H), 7.57 (s, 1H), 7.50 (d, *J* = 7.3 Hz, 1H), 7.36 – 7.27 (m, 4H), 3.99 (br s, 2H), 3.06 (t, *J* = 7.2 Hz, 2H), 2.43 (s, 3H), 1.51 (s, 9H), 1.02 (s, 9H).



Azide 242

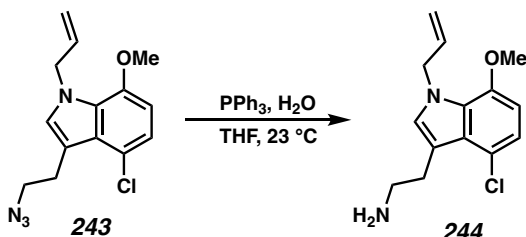
Prepared according to the procedure described in Chapter 2 for the synthesis of tryptamine **133** by a Mitsunobu reaction without subsequent tosylation and reduction. ^1H NMR (500 MHz, CDCl_3) δ 8.32 (br s, 1H), 7.06 (d, $J = 2.4$ Hz, 1H), 6.97 (d, $J = 8.2$ Hz, 1H), 6.53 (d, $J = 8.2$ Hz, 1H), 3.94 (s, 3H), 3.59 (t, $J = 7.1$ Hz, 2H), 3.27 (td, $J = 7.1, 0.8$ Hz, 2H).



N-allylindole 243

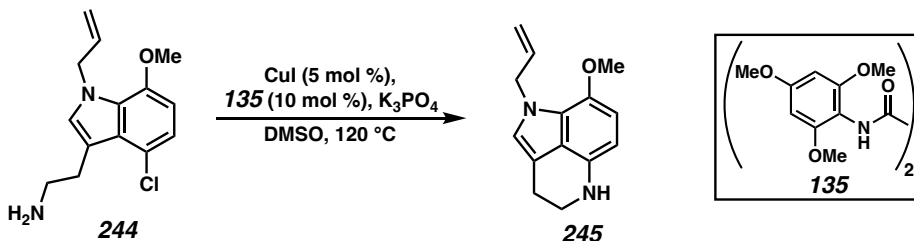
To a flame-dried 1-dram glass vial containing azide **242** (50 mg, 0.199 mmol, 1.0 equiv) under nitrogen was added DMF (1 mL) followed by NaH (60% dispersion in mineral oil, 9.6 mg, 0.24 mmol, 1.2 equiv) at 23 °C. The reaction mixture was stirred for 1 h, after which allyl iodide (22 μL , 0.24 mmol, 1.2 equiv) was added. After 4 h, the reaction mixture was diluted with saturated aq. NaHCO_3 (7 mL) and extracted with EtOAc (4x2mL). The combined organic extracts were washed twice with water, dried over Na_2SO_4 , and concentrated under reduced pressure. The crude product was purified by automated silica gel flash chromatography (Teledyne ISCO, 0 \rightarrow 20% EtOAc/hexanes) to afford the title compound (39.5 mg, 0.136 mmol, 68% yield); ^1H NMR (400 MHz, CDCl_3)

δ 6.93 (d, $J = 8.2$ Hz, 1H), 6.88 (s, 1H), 6.51 (d, $J = 8.3$ Hz, 1H), 6.07 – 5.92 (m, 1H), 5.13 – 5.07 (m, 1H), 4.99 – 4.92 (m, 3H), 3.88 (s, 3H), 3.56 (t, $J = 7.2$ Hz, 2H), 3.24 (t, $J = 7.2$ Hz, 2H).



N-allyltryptamine **244**

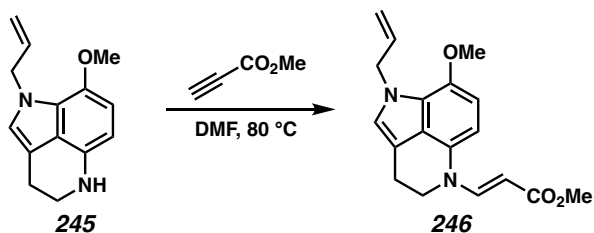
To a 1-dram vial under air were added PPh_3 (47 mg, 0.179 mmol, 1.5 equiv), THF (0.2 mL), and a solution of azide **243** (34.7 mg, 0.119 mmol, 1.0 equiv) in THF (0.6 mL) followed by H_2O (40 μL , 5% v/v). The reaction mixture was stirred at $23\text{ }^\circ\text{C}$ for 18 h, then concentrated under reduced pressure. Excess water was removed azeotropically with benzene under reduced pressure. The crude product was purified by silica gel flash chromatography (10% MeOH/ CH_2Cl_2 + 1% Et_3N) to afford the title compound (27.1 mg, 0.102 mmol, 86% yield); ^1H NMR (400 MHz, CDCl_3) δ 6.91 (d, $J = 8.2$ Hz, 1H), 6.87 (s, 1H), 6.49 (d, $J = 8.3$ Hz, 1H), 6.05 – 5.93 (m, 1H), 5.11 – 5.06 (m, 1H), 4.98 – 4.90 (m, 3H), 3.88 (s, 3H), 3.16 – 3.11 (m, 2H), 3.07 (td, $J = 6.2, 1.5$ Hz, 2H).



Secondary aniline **245**

To a $\frac{1}{2}$ -dram glass vial in a nitrogen-filled glovebox were added CuI (0.9 mg, 0.0048 mmol, 0.05 equiv), oxalamide **135**¹² (2.0 mg, 0.0048 mmol, 0.05 equiv), and K_3PO_4

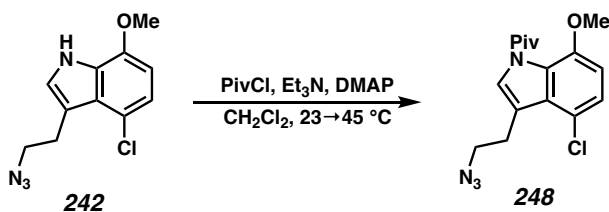
(20.3 mg, 0.0956 mmol, 1.0 equiv), followed by a solution of tryptamine **244** (25.3 mg, 0.0956 mmol, 1.0 equiv) in DMSO (0.2 mL). The vial was sealed with a PTFE-lined cap, removed from the glovebox, and heated to 120 °C in a metal heating block. After stirring for 24 h, the reaction mixture was cooled to 23 °C, diluted with EtOAc (2 mL), and washed twice with brine. The combined brine phases were extracted once with EtOAc, and the combined organic phases were dried over Na₂SO₄ and concentrated under reduced pressure. The crude product was purified by flash chromatography on basic alumina (10→20% EtOAc/hexanes) to afford the title compound as an impure, oxidatively unstable brown film (7.6 mg, NMR analysis indicates 0.025 mmol, 26% yield desired product); ¹H NMR (400 MHz, CDCl₃) δ 6.58 (s, 1H), 6.43 (d, *J* = 7.8 Hz, 1H), 6.14 – 5.92 (m, 2H), 5.13 – 5.00 (m, 2H), 4.92 (dt, *J* = 5.6, 1.7 Hz, 2H), 3.84 (s, 3H), 3.43 (t, *J* = 5.6 Hz, 2H), 2.98 – 2.93 (m, 2H).



“Push-Pull” olefin **246**

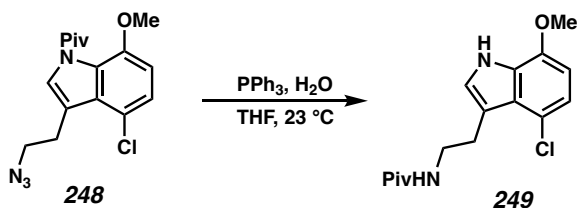
To a 1-dram vial was added impure aniline **245** (7.6 mg, 0.033 mmol assuming pure material, 1.0 equiv). Traces of water were azeotropically removed by addition of three portions of benzene followed by concentration under reduced pressure, and the vial was evacuated and backfilled with nitrogen. DMF (0.33 mL) and methyl propiolate (30 μL, 0.33 mmol, 10 equiv) were added, and the vial was sealed with a PTFE-lined cap and stirred at 80 °C in a metal heating block. After 18 h, the reaction mixture was cooled to 23 °C, diluted with water (2 mL), and extracted with EtOAc (3x0.5 mL). The combined organic

extracts were washed twice with water, dried over Na₂SO₄, and concentrated under reduced pressure. The crude product was purified by silica gel flash chromatography (20% EtOAc/hexanes) to afford the title compound as a yellow film (6.6 mg, 0.021 mmol, 22% yield over 2 steps); ¹H NMR (400 MHz, CDCl₃) δ 8.16 (d, *J* = 13.3 Hz, 1H), 6.68 (t, *J* = 1.2 Hz, 1H), 6.65 (d, *J* = 8.2 Hz, 1H), 6.54 (d, *J* = 8.2 Hz, 1H), 6.03 (ddt, *J* = 17.0, 10.1, 5.6 Hz, 1H), 5.17 (d, *J* = 13.2 Hz, 1H), 5.12 (dq, *J* = 10.3, 1.5 Hz, 1H), 5.03 (dq, *J* = 17.0, 1.6 Hz, 1H), 4.94 (dt, *J* = 5.5, 1.5 Hz, 2H), 3.89 (s, 3H), 3.75 – 3.71 (m, 5H), 3.03 (td, *J* = 6.1, 1.2 Hz, 2H).



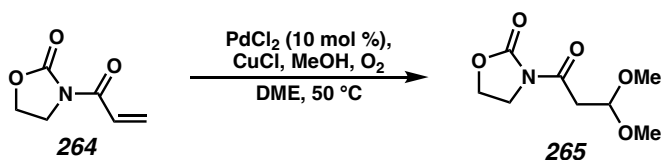
N-Pivaloyl indole **248**

To a flame-dried 1-dram glass vial were added azide **242** (50 mg, 0.199 mmol, 1.0 equiv) and DMAP (2.4 mg, 0.020 mmol, 0.1 equiv). The vial was evacuated and backfilled with nitrogen. CH₂Cl₂ (2 mL) and Et₃N (42 μL, 0.30 mmol, 1.5 equiv) were added followed by the addition of PivCl (29 μL, 0.24 mmol, 1.2 equiv). The vial was sealed with a PTFE-lined cap and stirred at 45 °C in a metal heating block. After 1 day, the reaction mixture was allowed to cool to 23 °C, washed twice with water, dried over Na₂SO₄, and concentrated under reduced pressure. The crude product was purified by automated silica gel flash chromatography (Teledyne ISCO, 0→25% EtOAc/hexanes) to afford the title compound as a white solid (52.7 mg, 0.157 mmol, 79% yield); ¹H NMR (400 MHz, CDCl₃) δ 7.18 (t, *J* = 0.9 Hz, 1H), 7.10 (d, *J* = 8.4 Hz, 1H), 6.65 (d, *J* = 8.4 Hz, 1H), 3.89 (s, 3H), 3.59 (t, *J* = 7.0 Hz, 2H), 3.23 (td, *J* = 7.0, 0.9 Hz, 2H), 1.43 (s, 9H).



Secondary amide 249

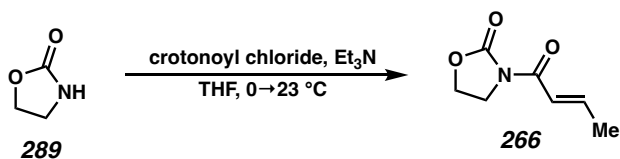
To a 1-dram glass vial under air were added PPh_3 (60 mg, 0.23 mmol, 1.5 equiv) and a solution of azide **248** (51.3 mg, 0.153 mmol, 1.0 equiv) in THF (1 mL) followed by water (50 μL). The reaction mixture was stirred at 23 $^\circ\text{C}$ for 22 h, then concentrated under reduced pressure and purified by automated silica gel flash chromatography (Teledyne ISCO, 0 \rightarrow 40 \rightarrow 100% EtOAc/hexanes) to afford the title compound as a white solid (31.5 mg, 0.102 mmol, 67% yield); ^1H NMR (400 MHz, CDCl_3) δ 8.34 (br s, 1H), 7.00 (br d, $J = 2.4$ Hz, 1H), 6.97 (d, $J = 8.3$ Hz, 1H), 6.53 (d, $J = 8.2$ Hz, 1H), 5.76 (br s, 1H), 3.93 (s, 3H), 3.60 (td, $J = 6.7, 5.6$ Hz, 2H), 3.18 (t, $J = 6.7$ Hz, 2H), 1.13 (s, 9H).



Dimethyl acetal 265

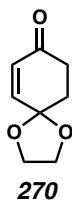
To a flame-dried 1-dram glass vial was added imide **264**¹⁸ (20 mg, 0.142 mmol, 1.0 equiv). The vial was transferred to a nitrogen-filled glovebox and PdCl_2 (2.5 mg, 0.014 mmol, 0.1 equiv), CuCl (14 mg, 0.142 mmol, 1.0 equiv), and DME (0.57 mL) were added. The vial was sealed with a PTFE/silicone septum and removed from the glovebox. MeOH (0.14 mL, 3.55 mmol, 25 equiv) was injected, whereafter the reaction mixture was sparged with O_2 , heated to 50 $^\circ\text{C}$ in a metal vial block, and stirred under a positive pressure of O_2 from a balloon. After 16 h, the reaction mixture was cooled to 23 $^\circ\text{C}$, filtered through a

plug of basic alumina with EtOAc, concentrated under reduced pressure, and purified by silica gel flash chromatography (67% EtOAc/hexanes) to afford the title compound as a white solid (14.9 mg, 0.0733 mmol, 52% yield); $^1\text{H NMR}$ (400 MHz, CDCl_3) δ 4.94 (t, $J = 5.6$ Hz, 1H), 4.41 (dd, $J = 8.7, 7.5$ Hz, 2H), 4.02 (dd, $J = 8.7, 7.5$ Hz, 2H), 3.37 (s, 6H), 3.30 (d, $J = 5.7$ Hz, 2H).



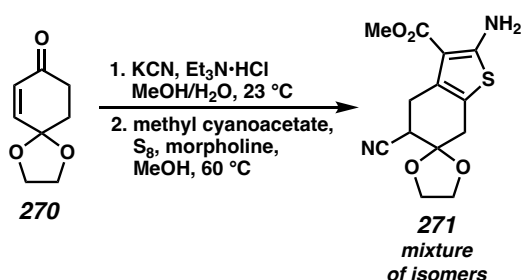
Crotonoyl imide 266

To a flame-dried 40 mL vial containing 2-oxazolidinone (**289**, 1.0 g, 11.5 mmol, 1.0 equiv) under nitrogen were added THF (20 mL) and Et_3N (4.0 mL, 28.8 mmol, 2.5 equiv). The vial was cooled to 0 °C and crotonoyl chloride (2.2 mL, 23.0 mmol, 2.0 equiv) was added dropwise with stirring. After 30 min, the reaction mixture was allowed to warm to 23 °C and stirring was continued. After 22 h, the reaction mixture was partitioned between saturated aq. NH_4Cl and CH_2Cl_2 . The layers were separated, and the aqueous phase was extracted once with CH_2Cl_2 and washed once with 1 N aq. HCl. The HCl phase was back-extracted once with CH_2Cl_2 , and the combined organic phases were dried over a mixture of NaHCO_3 and Na_2SO_4 and concentrated under reduced pressure. The crude product was purified twice by automated silica gel flash chromatography (Teledyne ISCO, 0→60% EtOAc/hexanes, then 0→80% EtOAc/hexanes) to afford the title compound as a white solid (159 mg, 1.02 mmol, 9% yield). All characterization data matched those reported in the literature.²⁷



Enone 270

Prepared according to the procedure of Shing.²⁰ All characterization data matched those reported in the literature.

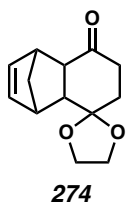


Nitrile 271

To a 2-dram glass vial were added KCN (201 mg, 3.09 mmol, 1.17 equiv), Et₃N·HCl (429 mg, 3.12 mmol, 1.18 equiv), water (0.59 mL) and methanol (0.73 mL). Enone **270** (407 mg, 2.64 mmol, 1.0 equiv) was added dropwise with stirring as a solution in methanol (1.3 mL). After 27 h, the reaction mixture was diluted with water and extracted with CH₂Cl₂ (3x). The combined organic extracts were dried over Na₂SO₄ and purified by silica gel flash chromatography (50% EtOAc/hexanes) to afford an uncharacterized complex mixture of nitrile adducts (207 mg) as a waxy substance.

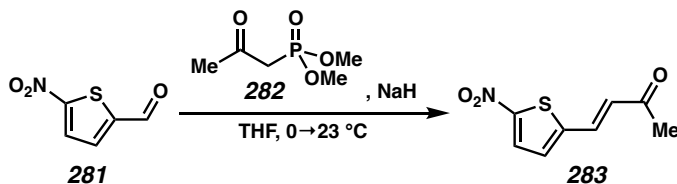
To a 20 mL glass vial were added this mixture (192 mg, 0.922 mmol, 1.0 equiv assuming mass of cyanohydrin), S₈ (30 mg, 0.115 mmol, 0.125 equiv), and MeOH (1.8 mL), followed by methyl cyanoacetate (82 μL, 0.92 mmol, 1.0 equiv) and morpholine (80 μL, 0.92 mmol, 1.0 equiv). The vial was sealed with a PTFE/silicone septum and the reaction mixture was stirred at 60 °C in a metal heating block for 20 h, resulting in a deep

red color. After 20 h, the reaction mixture was concentrated under reduced pressure and purified by automated silica gel flash chromatography (Teledyne ISCO, 0→90% EtOAc/hexanes) to afford the title compound as a mixture of constitutional isomers (117 mg, 0.398 mmol, 16% yield over 2 steps); $^1\text{H NMR}$ (400 MHz, CDCl_3) δ 4.29 – 4.21 (m, 3H), 4.16 – 3.98 (m, 5H), 3.96 – 3.85 (m, 2H), 3.81 (s, 3H), 3.36 (ddt, $J = 17.1, 5.9, 1.3$ Hz, 1H), 3.24 – 3.15 (m, 1H), 3.09 (dd, $J = 9.1, 5.8$ Hz, 1H), 2.99 – 2.89 (m, 1H), 2.87 – 2.77 (m, 2H).



Ketal 274

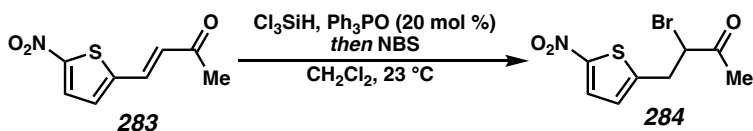
Prepared according to the procedure of Liao.²³ All characterization data matched those reported in the literature.



Enone 283

To a flame-dried 250 mL round bottom flask containing NaH (60% dispersion in mineral oil, 611 mg, 15.3 mmol, 1.2 equiv) under nitrogen was added THF (25 mL). The flask was cooled to 0 °C and phosphonate **282** (3.5 mL, 25.5 mmol, 2.0 equiv) was added rapidly with stirring. Gas evolution was accompanied by the formation of a thick white precipitate. After 15 min, aldehyde **281** (2.0 g, 12.7 mmol, 1.0 equiv) was added as a solution in THF (25 mL) by cannula, whereafter the reaction mixture was allowed to warm

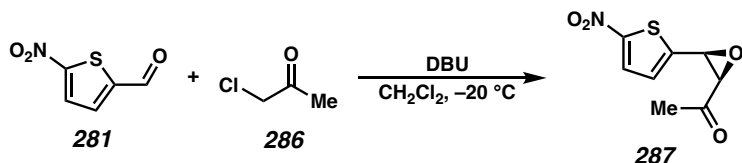
to 23 °C and stirred for 1.5 h. Then, the reaction mixture was quenched with saturated aq. NH_4Cl (100 mL), the layers were separated, and the aqueous phase was extracted with EtOAc (2x20mL). The combined organic phases were dried over Na_2SO_4 , concentrated under reduced pressure, and purified by silica gel flash chromatography (40% EtOAc/hexanes) to afford the title compound as a yellow solid (2.13 g, 10.8 mmol, 85% yield); ^1H NMR (400 MHz, CDCl_3) δ 7.86 (d, $J = 4.3$ Hz, 1H), 7.51 (dd, $J = 16.0, 0.7$ Hz, 1H), 7.22 (dt, $J = 4.3, 0.5$ Hz, 1H), 6.68 (d, $J = 16.0$ Hz, 1H), 2.38 (s, 3H).



Bromoketone 284

To a flame-dried 1-dram glass vial were added enone **283** (200 mg, 1.01 mmol, 1.0 equiv) and PPh_3O (56 mg, 0.202 mmol, 0.2 equiv). The vial was evacuated and backfilled with nitrogen, and CH_2Cl_2 (2 mL) was added followed by Cl_3SiH (0.15 mL, 1.52 mmol, 1.5 equiv). The reaction mixture was stirred at 23 °C for 7 h, then transferred by syringe into a separate 2-dram glass vial containing a suspension of NBS (270 mg, 1.52 mmol, 1.5 equiv) in CH_2Cl_2 (3 mL). The reaction mixture quickly became dark red and an exotherm occurred. After stirring for 13 h, the reaction mixture was quenched with saturated aq. Na_2CO_3 (50 mL). The resulting suspension was extracted with CH_2Cl_2 (2x20 mL), and the combined organic extracts were dried over Na_2SO_4 and concentrated under reduced pressure. The crude product was purified by automated silica gel flash chromatography (Teledyne ISCO, 0→50% EtOAc/hexanes) to afford the title compound as a thick yellow oil (75 mg, 0.27 mmol, 27% yield); ^1H NMR (400 MHz, CDCl_3) δ 7.78 (d, $J = 4.2$ Hz, 1H),

6.87 (dt, $J = 4.2, 0.9$ Hz, 1H), 4.46 (t, $J = 7.0$ Hz, 1H), 3.65 (ddd, $J = 15.5, 6.8, 1.0$ Hz, 1H), 3.38 (ddd, $J = 15.5, 7.1, 0.9$ Hz, 1H), 2.41 (s, 3H).



Epoxyketone **287**

To a flame-dried 100 mL round bottom flask under nitrogen were added CH_2Cl_2 (12.5 mL) and DBU (1.4 mL, 9.5 mmol, 3.0 equiv). The flask was cooled to -20 °C in an ice/NaCl bath. Then, a solution of aldehyde **281** (500 mg, 3.18 mmol, 1.0 equiv) and chloroacetone (**286**, 0.29 mL, 3.5 mmol, 1.1 equiv) in CH_2Cl_2 (12.5 mL) was added dropwise over 8 min with stirring, resulting in a color change to deep purple. After stirring for 1 h at -20 °C, the reaction mixture was combined with water (50 mL) and the layers were separated. The aqueous phase was extracted with CH_2Cl_2 (2x15 mL). The combined organic phases were washed with diluted brine, dried over Na_2SO_4 , and concentrated under reduced pressure. The crude product was purified by silica gel flash chromatography (33% EtOAc/hexanes) to afford the title compound as a light brown solid (169 mg, 0.793 mmol, 25% yield); ^1H NMR (400 MHz, CDCl_3) δ 7.82 (d, $J = 4.3$ Hz, 1H), 7.10 (dd, $J = 4.2, 0.6$ Hz, 1H), 4.23 (dd, $J = 1.8, 0.5$ Hz, 1H), 3.62 (d, $J = 1.8$ Hz, 1H), 2.21 (s, 3H).

A5.9 REFERENCES AND NOTES

- (1) See, for example: Ipatieff, V. N.; Pines, H.; Friedman, B. S. Reaction of Aliphatic Olefins with Thiophenol. *J. Am. Chem. Soc.* **1938**, *60*, 2731–2734.
- (2) See, for example: Blom, J.; Reyes-Rodríguez, G. J.; Tobiesen, H. N.; Lamhauge, J. N.; Iversen, M. V.; Barløse, C. L.; Hammer, N.; Rusbjerg, M.; Jørgensen, K. A. Umpolung Strategy for α -Functionalization of Aldehydes for the Addition of Thiols and other Nucleophiles. *Angew. Chem. Int. Ed.* **2019**, *58*, 17856–17862.
- (3) For a relevant review, see: Clayden, J.; MacLellan, P. Asymmetric synthesis of tertiary thiols and thioethers. *Beilstein J. Org. Chem.* **2011**, *7*, 582–595.
- (4) Nishimoto, Y.; Okita, A.; Yasuda, M.; Baba, A. Synthesis of a Wide Range of Thioethers by Indium Triiodide Catalyzed Direct Coupling between Alkyl Acetates and Thiosilanes. *Org. Lett.* **2012**, *14*, 1846–1849.
- (5) Bichovski, P.; Haas, T. M.; Kratzert, D.; Streuff, J. Synthesis of Bridged Benzazocines and Benzoxocines by a Titanium-Catalyzed Double-Reductive Umpolung Strategy. *Chem. Eur. J.* **2015**, *21*, 2339–2342.
- (6) House, H. O.; Kleschick, W. A.; Zaiko, E. J. Enones with Strained Double Bonds: The Bicyclo[3.3.1] System. *J. Org. Chem.* **1978**, *43*, 3653–3661.
- (7) Griera, R.; Rigat, L.; Alvarez, M.; Joule, J. A. Reactions of 1-Methyl-4-quinolone with 2-Lithio-1,3-dithianes. *J. Chem. Soc. Perkin Trans. I* **1992**, 1223–1227.
- (8) Nowick, J. S.; Pairish, M.; Lee, I. Q.; Holmes, D. L.; Ziller, J. W. An Extended β -Strand Mimic for a Larger Artificial β -Sheet. *J. Am. Chem. Soc.* **1997**, *119*, 5413–5424.

- (9) Baruah, P. K.; Sreedevi, N. K.; Gonnade, R.; Ravindranathan, S.; Damodaran, K.; Hofmann, H.; Sanjayan, G. J. Enforcing Periodic Secondary Structures in Hybrid Peptides: A Novel Hybrid Foldamer Containing Periodic γ -Turn Motifs. *J. Org. Chem.* **2007**, *72*, 636–639.
- (10) Paudyal, M. P.; Adebesin, A. M.; Burt, S. R.; Ess, D. H.; Ma, Z.; Kürti, L.; Falck, J. R. Dirhodium-catalyzed C-H arene amination using hydroxylamines. *Science* **2016**, *353*, 1144–1147.
- (11) Ma, X.; Hazelden, I. R.; Langer, T.; Munday, R. H.; Bower, J. F. Enantioselective Aza-Heck Cyclizations of *N*-(Tosyloxy)carbamates: Synthesis of Pyrrolidines and Piperidines. *J. Am. Chem. Soc.* **2019**, *141*, 3356–3360.
- (12) Zhou, W.; Fan, M.; Yin, J.; Jiang, Y.; Ma, D. CuI/Oxalic Diamide Catalyzed Coupling Reaction of (Hetero)Aryl Chlorides and Amines. *J. Am. Chem. Soc.* **2015**, *137*, 11942–11945.
- (13) Ittyerah, P. I.; Mann, F. G. Cyclic keto-amines. Part III. The reactions of substituted 1 : 2 : 3 : 4-tetrahydro-4-oxoquinolines and of 1 : 6-dioxojulolidines. *J. Chem. Soc.* **1958**, 467–480.
- (14) Braunholtz, J. T.; Mann, F. G. The preparation of bis-2-cyanoethyl derivatives of aromatic primary amines, and their conversion into 1 : 6-diketojulolidines. Part II. *J. Chem. Soc.* **1953**, 1817–1824.
- (15) Kantminene, K.; Mikul'skene, G.; Hormi, O.; Beresnevicius, Z. I. Synthesis of Tetrahydro-1H,7H-benzo[*ij*]quinolizine-1,7-dione Derivatives. *Chem. Heterocycl. Compd.* **2002**, *38*, 422–428.

- (16) a) Hosokawa, T.; Ohta, T.; Murahashi, S. Palladium(II)-catalysed acetalization of terminal olefins bearing electron-withdrawing substituents with 1,3- and 1,2-diols. *J. Chem. Soc., Chem. Commun.* **1983**, 848–849. b) Hosokawa, T.; Ohta, T.; Kanayama, S.; Murahashi, S. Palladium(II)-catalyzed acetalization of terminal olefins bearing electron-withdrawing substituents with optically active diols. *J. Org. Chem.* **1987**, *52*, 1758–1764.
- (17) Auclair, S. X.; Morris, M.; Sturgess, M. A. Rate Enhancement in the Wacker Oxidation of Hydroxy- α,β unsaturated Esters: A Fast Neutral Method for the Preparation of Masked β -Ketoesters. *Tetrahedron Lett.* **1992**, *33*, 7739–7742.
- (18) Li, M.; Carreras, V.; Jalba, A.; Ollevier, T. Asymmetric Diels–Alder Reaction of α,β -Unsaturated Oxazolidin-2-one Derivatives Catalyzed by a Chiral Fe(III)-Bipyridine Diol Complex. *Org. Lett.* **2018**, *20*, 995–998.
- (19) Otera, J.; Dan-oh, N.; Nozaki, H. Distannoxane-catalyzed acetalization of carbonyls. *Tetrahedron* **1992**, *48*, 1449–1456.
- (20) Shing, T. K. M.; Yeung, Y.; Su, P. L. Mild Manganese(III) Acetate Catalyzed Allylic Oxidation: Application to Simple and Complex Alkenes. *Org. Lett.* **2006**, *8*, 3149–3151.
- (21) Müller, P.; Siegfried, B. S_N2 Reactions with Carboxylic Esters. Selective cleavage of methyl esters. *Helv. Chim. Acta* **1974**, *57*, 987–994.
- (22) Oda, M.; Kawase, T.; Okada, T.; Enomoto, T. 2-Cyclohexene-1,4-dione. *Org. Synth.* **1996**, *73*, 253.

- (23) Hung, S.; Liao, C. Double Michael Additions of Lithium Enolate of 1,4-Dioxaspiro[4.5]dec-6-en-8-One to Acrylates. *J. Chin. Chem. Soc.* **1994**, *41*, 191–194.
- (24) Lao, Z.; Zhang, H.; Toy, P. H. Reductive Halogenation Reactions: Selective Synthesis of Unsymmetrical α -Haloketones. *Org. Lett.* **2019**, *21*, 8149–8152.
- (25) Luo, J.; Hu, L.; Zhang, M.; Tang, Q. An efficient Darzens reaction promoted by 1,8-diazabicyclo[5.4.0]undec-7-ene (DBU). *Tetrahedron Lett.* **2019**, *60*, 1949–1951.
- (26) Pangborn, A. M.; Giardello, M. A.; Grubbs, R. H.; Rosen, R. K.; Timmers, F. J. Safe and Convenient Procedure for Solvent Purification. *Organometallics* **1996**, *15*, 1518–1520.
- (27) Lauzon, S.; Keipour, H.; Gandon, V.; Ollevier, T. Asymmetric Fe^{II}-Catalyzed Thia-Michael Addition Reaction to α,β -Unsaturated Oxazolidin-2-one Derivatives. *Org. Lett.* **2017**, *19*, 6324–6327.

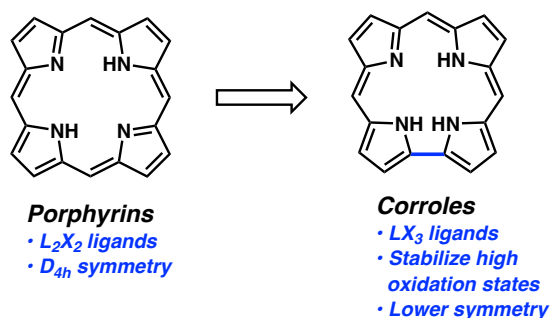
CHAPTER 3

Synthetic Strategies Toward Minimally Substituted Corroles and Azaporphyrins[†]

3.1 INTRODUCTION

Porphyrinoids and their transition metal complexes have demonstrated numerous applications in catalysis (including electrocatalysis),¹ as sensitizers for photodynamic therapy,² and as drugs.³ Corroles are a class of aromatic, ring-contracted porphyrinoid heterocycles that differ from the parent porphyrins by the absence of one *meso* carbon atom (Figure 3.1.1). The carbon skeleton of corroles is shared with the corrin moiety of vitamin B₁₂. Compared to L₂X₂ porphyrins, LX₃ corroles have been found to stabilize high metal oxidation states and often preferentially bind to trivalent metals.⁴

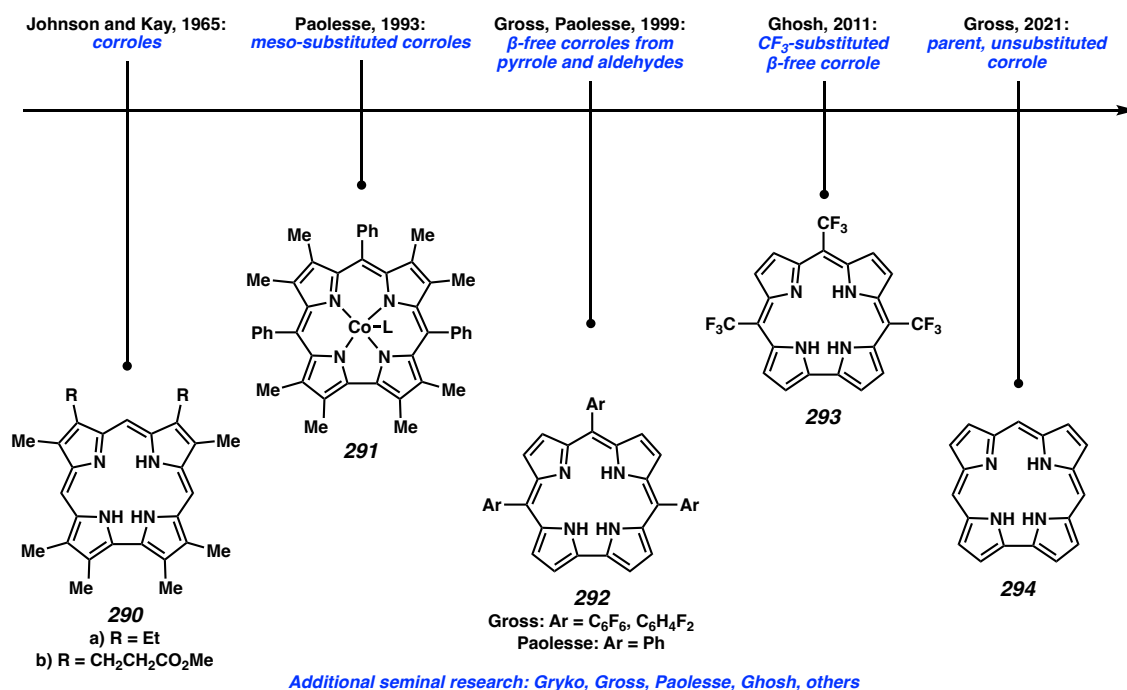
Figure 3.1.1. Introduction to the corrole ring system.



[†]This research was performed under the supervision of Prof. Zeev Gross in the Schulich Faculty of Chemistry at the Technion in collaboration with Arik Raslin, Marcelo Fernandez de la Mora, and Dr. Atif Mahammed and is unpublished.

The first corroles (**290**, Figure 3.1.2) were prepared in 1965 by Johnson and Kay.^{5,6} These compounds were unsubstituted at the *meso* positions but fully substituted at the ortho positions. Later research by Paolesse in 1993 demonstrated the synthesis of *meso*-substituted corroles such as **291**.⁷ In 1999, Gross⁸ and Paolesse⁹ simultaneously reported dramatically simplified synthetic procedures toward corroles, wherein pyrrole and an aromatic aldehyde could undergo direct condensation followed by oxidation in a modified Rothemund reaction to afford *meso*-substituted, β -unsubstituted corroles **292**. This architecture, analogous to that of *meso*-tetrasubstituted porphyrins,¹⁰ is attractive due to its smaller geometric size, electronic tunability, and potential for further functionalization.

Figure 3.1.2. Select milestones toward the synthesis of minimally substituted corroles.



The reports by Gross and Paolesse prompted a renaissance in the field of corrole synthesis and applications, and numerous syntheses of corrole derivatives and their

transition and main group metal complexes have since been reported: the “periodic table of corroles” continues to expand.¹¹

In 2011, moving toward smaller corrole derivatives, Ghosh reported the synthesis of tris(trifluoromethyl)corrole **293** from pyrrole and trifluoroacetaldehyde hydrate.¹² A single example of a rhenium complex of this corrole had previously been reported by a unique porphyrin ring contraction,¹³ but Ghosh’s report represented the first synthesis of the free base and of other metal complexes. The synthesis of this corrole was later improved upon by Gross, Gray, and Virgil.¹⁴ Corrole **293** is somewhat unique due to its small size and the fully sp³-hybridized nature of the *meso* substituents.

Most recently, in 2021, the Gross group succeeded in synthesizing corrole **294**, the fully unsubstituted parent heterocycle.¹⁵ While the electron-rich nature of the free heterocycle was found to render it unstable, several metal complexes of corrole **294** were prepared and characterized.

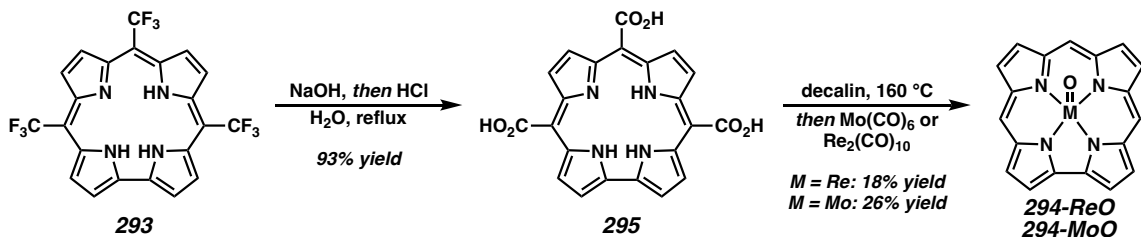
Gross’s synthesis of unsubstituted corrole **294** could proceed by two methods.¹⁵ First, tris(trifluoromethyl)corrole **293** underwent basic hydrolysis to tricarboxylate derivative **295** (Scheme 3.1.3A).¹⁶ Interestingly, esters of **295** were not competent precursors to the triacid. Thermolysis of triacid **295** in decalin led to efficient decarboxylation. The free corrole was isolated as Mo or Re oxo complexes to circumvent the unstable nature of the heterocycle.

In a more rapid fashion, complexes of **294** could be prepared by a pyrrole oligomerization approach (Scheme 3.1.3B). Similar approaches have achieved wide adoption by the community for the synthesis of *meso*-substituted corroles from pyrrole and aryl aldehydes.^{6a} Combination of excess pyrrole (**296**) with formaldehyde afforded a

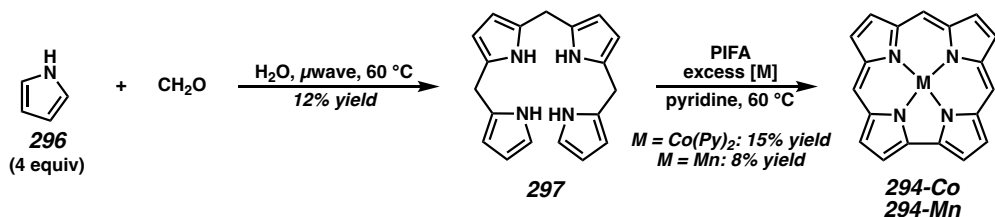
statistical mixture of oligomers, from which tetrapyrromethane (or “bilane”) **297** was isolated in 12% yield. Lastly, oxidation with PIFA in the presence of a suitable metal salt directly afforded corrole complexes **294**.

Scheme 3.1.3. Approaches to complexes of unsubstituted corrole **294** (Gross, 2021).

A) Free corrole **294** by a decarboxylative approach.



B) Free corrole **294** by a classical oligomerization-cyclization approach.



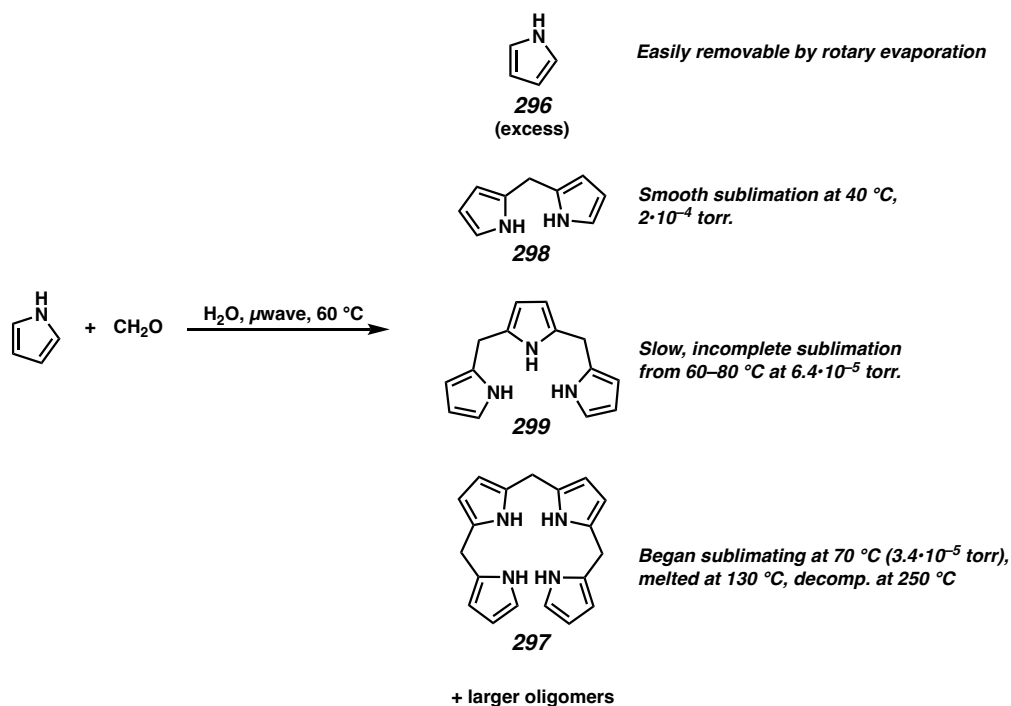
Excitingly, the $\text{Co}(\text{PPh}_3)$ complex of **294** was found to undergo sublimation at $220\text{ }^\circ\text{C}$ and 40 mTorr, a property unique among porphyrinoid metal complexes, which are generally much more challenging to sublimate. Furthermore, the molybdenum oxo complex efficiently underwent adsorption to Vulcan XC72R carbon and was shown to be an excellent electrocatalyst for proton reduction to H_2 .

Given the unique properties of corrole complexes **294**, an efficient and scalable synthetic route is desirable as it would enable further exploration of the potential applications of these complexes. Unfortunately, the cyclooligomerization approach to **294** proceeds in only up to 1.8% yield over 2 steps. We therefore set out to develop an improved procedure for the synthesis of these compounds and other minimally substituted corroles.

3.2 ATTEMPTS TO IMPROVE BILANE SYNTHESIS

The two key factors complicating the synthesis of bilane **297** are low chemical yield and a slow and laborious chromatographic separation. We first attempted to solve the latter problem, aiming to replace chromatography with sublimation. The volatilities of pyrrole (**296**) and isolated dipyrane **298**, tripyrrane **299**, and desired tetrapyrane **297**, each chromatographically isolated from a statistical oligomerization reaction of pyrrole and formaldehyde, were therefore compared (Scheme 3.2.1).

Scheme 3.2.1. Evaluation of sublimation as a means for oligopyrrane separation.

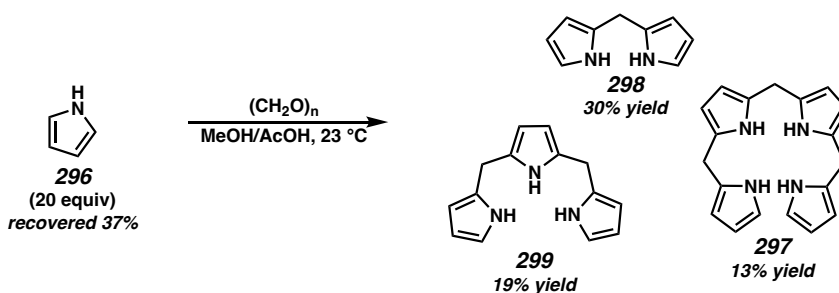


While pyrrole was readily removed by rotary evaporation and dipyrane **298** sublimated in an efficient manner, tripyrrane **299** and tetrapyrane **297** could not be separated by sublimation. The slow sublimation of the latter two compounds occurred at similar temperatures and pressures. As such, chromatography on silica gel remained the primary means of oligopyrrane isolation.

We then directed our efforts to improving the chemical process for the synthesis of bilane **297**. In addition to the low yield of **297**, the existing procedure (Scheme 3.1.3B) is inherently limited in scale as the oligomerization must be conducted in a microwave vessel to enable rapid, brief heating. The use of paraformaldehyde as a less reactive formaldehyde surrogate was envisioned as a possible method to improve the robustness and scalability of the oligomerization.

To our delight, applying a modified version of Bruce's conditions for the synthesis of dipyrromethane **298** enabled the isolation of tetrapyrromethane **297** in 13% yield (Scheme 3.2.2).¹⁷

Scheme 3.2.2. AcOH-promoted oligomerization of pyrrole and paraformaldehyde.



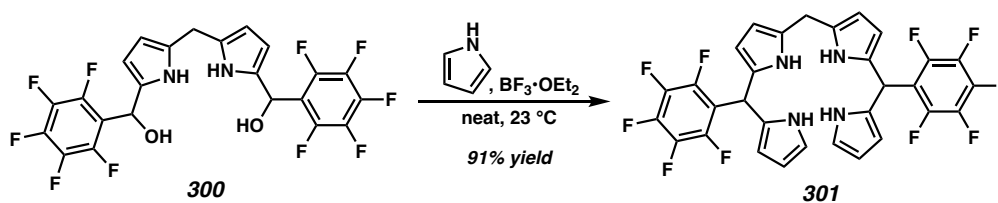
Unfortunately, the use of 20 equivalents of pyrrole were necessary to maximize the yield of the reaction. While the use of fewer equivalents was expected to favor the formation of tetrapyrane over di- and tripyrane, this appeared to simply favor the formation of putative polymeric material.

The product ratio for the oligomerization of pyrrole and aldehydes is likely biased by the increased electron-richness of the oligomers relative to free pyrrole.^{6a} For oligomerizations of pyrrole with certain aryl aldehydes, the yield can be tuned by exploiting the reduced solubility of the tetrapyrane relative to smaller oligomers. In the correct solvent mixture (typically a water/MeOH mixture), under acid catalysis,

tetrapyrane precipitates out of solution upon formation, minimizing the formation of longer oligomers.¹⁸ Unfortunately, the higher aqueous solubility of bilane **297** would prevent the use of such a method to control the oligomerization.

We instead took inspiration from well-established controlled bilane formations used to synthesize A₂B corroles. Specifically, in 2015, Tanaka and Osuka reported that diol **300**, which bears an unsubstituted *meso*-methylene linker, could undergo Lewis acid-promoted substitution with pyrrole to afford tetrapyrane **301** in excellent yield (Scheme 3.2.3).¹⁹ This compound could be oxidized to a *trans*-A₂B-type corrole.

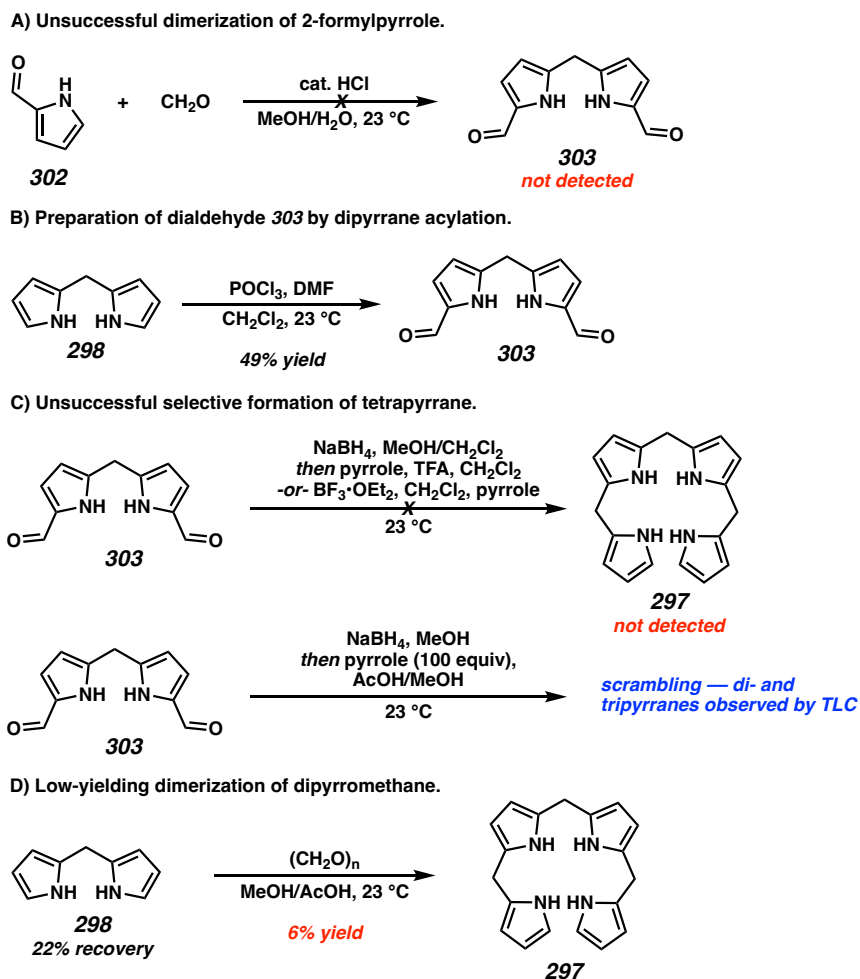
Scheme 3.2.3. A tetrapyrane from a *meso*-free dipyrane (Tanaka and Osuka, 2015).



We aimed to access dialdehyde **303** as a precursor to a *des*-aryl derivative of diol **300** (Scheme 3.2.4A). Dimerization of aldehyde **302** using formaldehyde as a linker was attempted by acid catalysis, but the electron-poor nature of the heterocycle inhibited the reaction. Instead, dipyrane **298** was formylated with the Vilsmeier reagent, providing **303** in 49% yield (Scheme 3.2.4B). NaBH₄ reduction provided a crude diol that was directly treated with pyrrole and either TFA or BF₃·Et₂O, but in either case, nonspecific decomposition was observed with no conversion to desired tetrapyrane **297**. Subjecting the crude diol to the conditions used for the mild oligomerization of pyrrole with paraformaldehyde (AcOH/MeOH) led to scrambling, as judged by TLC – both di- and tripyrranes were observed, suggesting reversible loss of formaldehyde. This phenomenon

in well-known in the porphyrin literature, occurring to a greater extent in systems with small substituents.²⁰

Scheme 3.2.4. Attempted controlled assembly of tetrapyrane **297**.



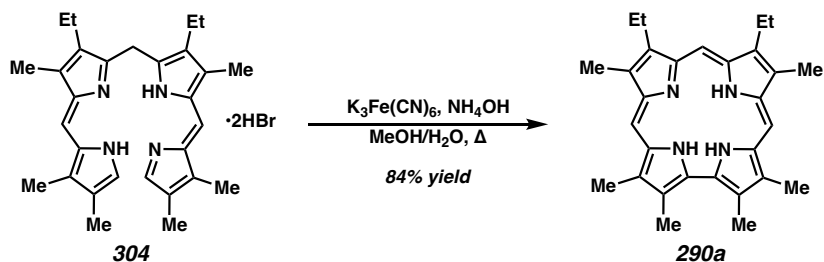
As a final resort, the dimerization of dipyrane **298** was attempted (Scheme 3.2.4D). While the standard conditions with paraformaldehyde led to formation of tetrapyrane **297**, it was only isolated in 6% yield, with the recovery of 22% of the starting material. The remainder of the mass balance appeared to consist of higher-order oligomers.

Further evaluation of reaction conditions could result in a procedure for the synthesis of tetrapyrane **297** in higher yield, but at this stage, we refocused our efforts toward the synthesis of additional minimally substituted porphyrinoids.

3.3 UNEXPECTED SYNTHESIS OF A MONOAZAPORPHYRIN

Over the course of previous synthetic efforts toward minimally substituted corroles by the Gross group, PIFA was consistently demonstrated to be the most robust oxidant for cyclization of the bilane intermediate.^{14b,15} We embarked on a campaign to evaluate further chemical oxidants, both with and without metal templating agents, in order to maximize the yields for bilane cyclization. During this campaign, our attention was drawn to an early report from the corrole literature wherein $K_3Fe(CN)_6$ was used to oxidize acyclic biladienes (e.g., **304**) to corroles (e.g., **290a**, Scheme 3.3.1).²¹

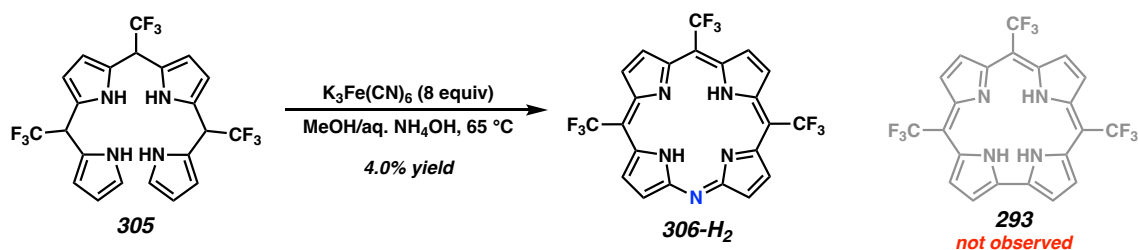
Scheme 3.3.1. Corrole synthesis by oxidation with $K_3Fe(CN)_6$ (Dolphin et al., 1966).



Using tris(trifluoromethyl)bilane **305** as a model substrate to evaluate oxidation to corroles, the $K_3Fe(CN)_6$ -mediated conditions reported by Dolphin et al., which include aqueous ammonia, were evaluated (Scheme 3.3.2). Interestingly, known free base corrole **293** was not isolated from the reaction mixture—instead, a new porphyrinoid was isolated and found to be monoazaporphyrin **306-H₂**. Replacement of NH_4OH with $NaOH$ suppressed macrocycle formation entirely. *To our knowledge, 306-H₂ is only the second*

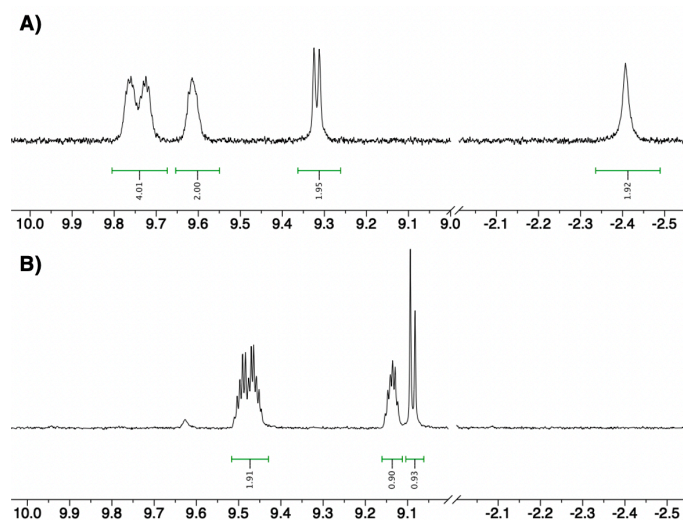
reported example of a monoazaporphyrin lacking β -substituents, and the first example of such a compound as the free base.

Scheme 3.3.2. Unexpected oxidation of a bilane to a monoazaporphyrin.



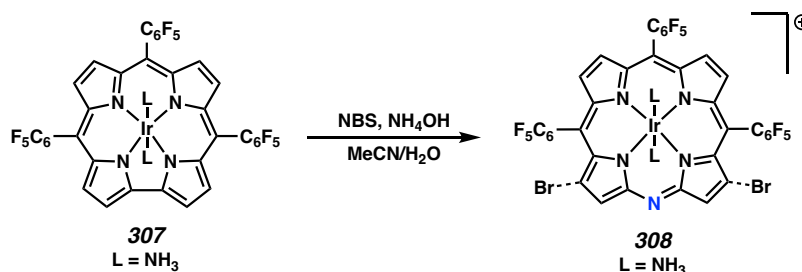
Examination of the ^1H NMR spectrum of **306-H₂** in CDCl_3 (Figure 3.3.3A) revealed the presence of 3 multiplets and one clean doublet ($J = 5.1\text{ Hz}$) in the aromatic region, consistent with the expected 2-fold symmetry of the molecule and similar to the spectra of corroles. The 2 N-H ring protons appear upfield at -2.41 ppm . Compared to the analogous corrole **293** (Figure 3.3.3B), the aryl C-H protons appear somewhat downshifted.

Figure 3.3.3. Comparison of the ^1H NMR spectra of A) azaporphyrin **306-H₂** and B) corrole **293**.



The preparation of monoazaporphyrins was reported as early as 1936,²² and since then, several targeted syntheses of these macrocycles have been developed.^{23,24} While related diazaporphyrins have been used in catalysis,²⁵ monoazaporphyrins have not found applications, and nearly all reported examples of these compounds are fully alkylated at the pyrrole β positions. Compared to porphyrins, monoazaporphyrins possess a red-shifted Q-band and a blue-shifted Soret band and their copper complexes are more prone to reduction and less prone to oxidation.²⁶ An iron(III) monoazaporphyrin complex was shown to have a different electronic ground state than the corresponding porphyrin.²⁷ In 2011, Palmer, Gross, and Gray reported the first example of a β -unsubstituted monoazaporphyrin as an iridium complex (**308**) by oxidative nitrogen insertion into a corrole ring (Scheme 3.3.4).²⁸ This compound was isolated as a mixture with mono- and dibrominated derivatives.

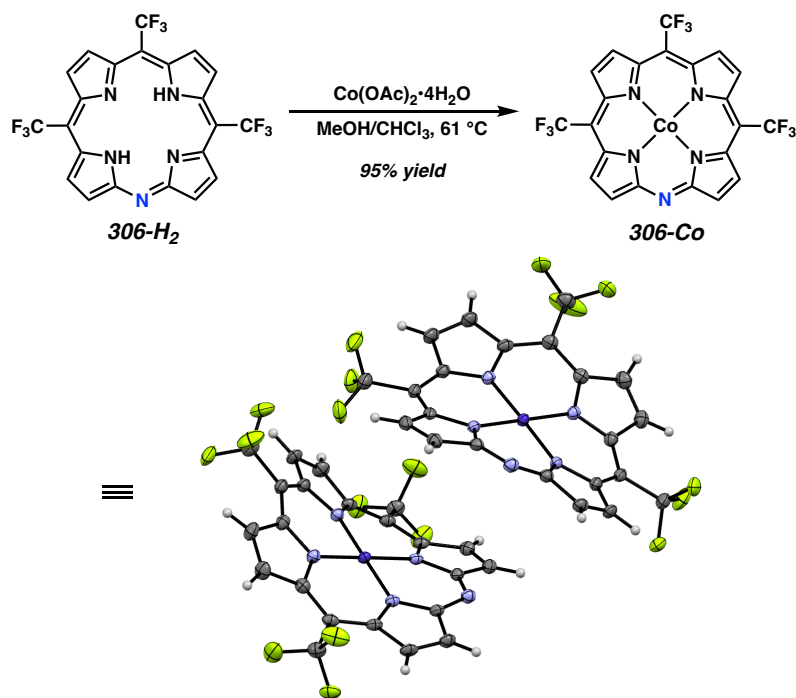
Scheme 3.3.4. Previous synthesis of a β -free monoazaporphyrin complex (Palmer, Gross, and Gray, 2011).



We were therefore thrilled to have discovered a procedure to prepare a β -free monoazaporphyrin as the free base, as access to this material would enable the preparation of metalated derivatives and their characterization and comparison with similar classic porphyrins.

Heating monoazaporphyrin **306-H₂** in methanol/chloroform solution in the presence of cobalt(II) acetate tetrahydrate led to formation of the corresponding cobalt(II) monoazaporphyrin complex **306-Co** (Scheme 3.3.5).²⁹ An x-ray quality crystal of this complex was grown by slow evaporation from a THF/heptane mixture. The crystal structure of **306-Co** revealed considerable ruffling, similar to the reported structure of an analogous 4-fold symmetric copper porphyrin. The average Co–N bond distance was 1.928 Å, compared to 1.971 Å for (octaethylporphyrinato)cobalt(II).³⁰

Scheme 3.3.5. Metallation of monoazaporphyrin **306-H₂**.



Future research will involve the synthesis of additional metal complexes of monoazaporphyrin **306**, the study of these complexes' photophysical and electrochemical properties, and the exploration of potential catalytic applications.

3.4 CONCLUSION

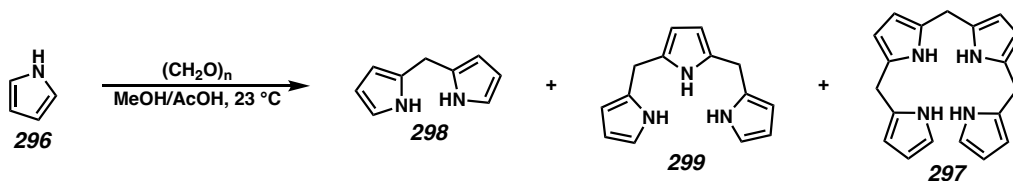
Studies toward improved syntheses of minimally substituted corrole macrocycles were performed, primarily focusing on optimization of the synthetic procedure toward bilane (tetrapyrane) macrocyclization substrates. Although the synthesis of these substrates was not substantially improved in our hands, we inadvertently prepared the first known example of a free base β -free monoazaporphyrin. The cobalt complex of this ligand was prepared and characterized by x-ray crystallography. Future studies will involve the preparation of additional metal monoazaporphyrin complexes and characterization of their photo- and electrochemical properties and potential applications in catalysis.

3.5 EXPERIMENTAL SECTION

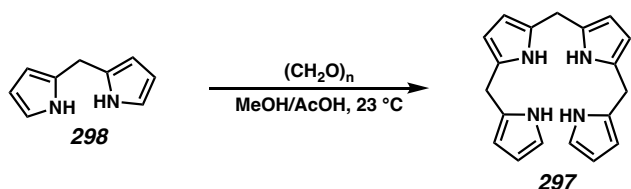
3.5.1 MATERIALS AND METHODS

Unless otherwise noted, reagents and solvents were purchased from commercial sources and used as received. Pyrrole was passed through a column of basic alumina immediately prior to use. Reaction progress was monitored by thin-layer chromatography (TLC). TLC was performed using E. Merck silica gel 60 F254 precoated glass plates (0.25 mm) and visualized by UV fluorescence quenching or Br_2 staining. Silicycle SiliaFlash® P60 Academic Silica gel (particle size 40–63 nm) was used for flash chromatography. ^1H and ^{19}F NMR spectra were recorded on Bruker Avance III 400 spectrometer (400 MHz for ^1H and 377 MHz for ^{19}F). Data for ^1H NMR are reported as follows: chemical shift (δ ppm) (multiplicity, coupling constant (Hz), integration). Multiplicities are reported as follows: s = singlet, d = doublet, t = triplet, q = quartet, p = pentet, sept = septuplet, m = multiplet, br s = broad singlet, br d = broad doublet. High-resolution mass spectra were recorded on a Bruker MaXis Impact mass spectrometer.

3.5.2 EXPERIMENTAL PROCEDURES

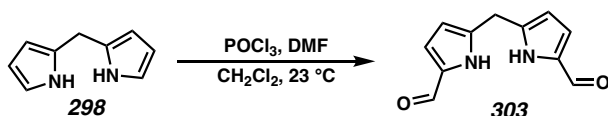
**Procedure for the oligomerization of pyrrole (296) with paraformaldehyde**

To a 250 mL round bottom flask were added paraformaldehyde (541 mg, 18.0 mmol [calculated for monomer], 1.0 equiv), pyrrole (25.0 mL, 360 mmol, 20 equiv), glacial acetic acid (75 mL), and methanol (25 mL). The reaction mixture was sparged with nitrogen for 25 min, then sealed and stirred for 17 h at 23 °C. After 17 h, the reaction mixture was diluted with CH₂Cl₂ (250 mL), washed once with water and twice with dilute aq. KOH, dried over Na₂SO₄, and concentrated under reduced pressure. Pyrrole (9.3 mL, 134 mmol, 37% recovery) was recovered by distillation under high vacuum. The residue was subjected to silica gel flash chromatography (5→10→15→20% EtOAc/hexanes) to afford dipyrane **298** (780 mg, 5.34 mmol, 30% yield), tripyrane **299** (390 mg, 1.73 mmol, 19% yield), and tetrapyrane **297** (244 mg, 0.802 mmol, 13% yield). All characterization data matched those reported in the literature.³¹

**Tetrapyrane 297 by dimerization of dipyrane 298**

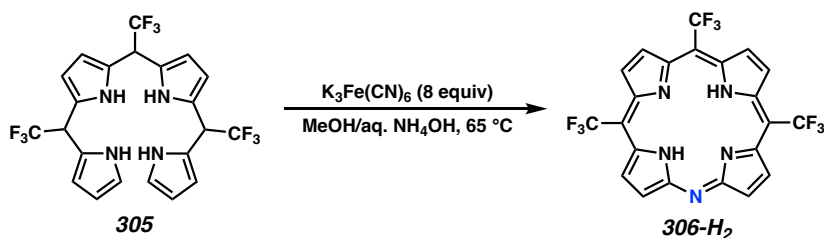
To a 2-dram glass vial were added dipyrane **298** (50 mg, 0.342 mmol, 2.0 equiv) and paraformaldehyde (5 mg, 0.171 mmol, 1.0 equiv) followed by glacial acetic acid (0.75 mL) and methanol (0.25 mL). The reaction mixture was stirred at 23 °C for 23 h, then

diluted with CH_2Cl_2 , washed with water (2x) and saturated aq. KOH (1x), and dried over Na_2SO_4 . The solution was concentrated under reduced pressure and purified by silica gel flash chromatography (10→20% EtOAc/hexanes) to afford recovered dipyrane **298** (11 mg, 0.075 mmol, 22% recovery) and tetrapyrane **297** (3.3 mg, 0.011 mmol, 6% yield). All characterization data matched those reported in the literature.³¹



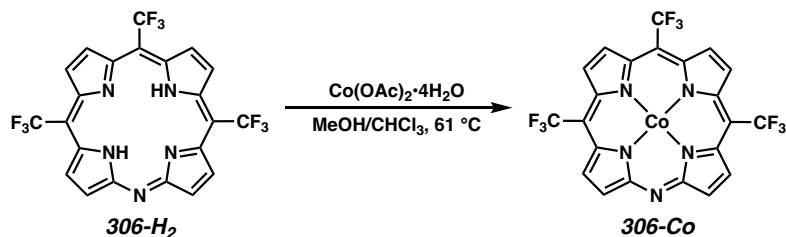
Dialdehyde 303

To a flame-dried 25 mL round bottom flask under nitrogen in an ice bath were added DMF (0.26 mL, 3.37 mmol, 9.9 equiv) and POCl_3 (0.32 mL, 3.43 mmol, 10 equiv). The ice bath was removed, and after 10 min, CH_2Cl_2 (1 mL) was added. Dipyrane **298** (50 mg, 0.342 mmol, 1.0 equiv) was added as a solution in CH_2Cl_2 (2.4 mL), and the reaction mixture was allowed to stir for 28 h. Then, the reaction mixture was quenched with 5% aq. NaOH (30 mL). The resulting biphasic suspension was stirred for 15 min at 23 °C, then diluted with water and extracted with CH_2Cl_2 (3x). The combined organic extracts were dried over Na_2SO_4 and concentrated under reduced pressure. The crude product was purified by silica gel flash chromatography (50% EtOAc/hexanes) to afford the title compound as a white solid (34 mg, 0.168 mmol, 49% yield). All characterization data matched those reported in the literature.³²



10,15,20-tris(trifluoromethyl)-5-azaporphyrin (306-H₂):

To a solution of tetrapyrromethane **305**^{14b} (247 mg, 0.486 mmol, 1.0 equiv) in methanol (49 mL) was added a solution of potassium hexacyanoferrate(III) (1.28 g, 3.89 mmol, 8.0 equiv) in 25% aq. NH₃ (99 mL) rapidly with magnetic stirring. The reaction mixture was placed in a hot water bath and heated to reflux. After 1.5 h, the reaction mixture was cooled to 23 °C, diluted with water (50 mL), extracted with dichloromethane (3x50 mL), dried over solid Na₂SO₄, and filtered. The solvent was removed by rotary evaporation and the crude product was purified by silica gel flash chromatography (10% EtOAc/hexanes, pink fractions collected) to afford monoazaporphyrin **306-H₂** as a dark brown solid (9.9 mg, 0.0192 mmol, 4.0% yield); ¹H NMR (400 MHz, CDCl₃) δ 9.81 – 9.67 (m, 4H), 9.65 – 9.55 (m, 2H), 9.32 (d, *J* = 5.1 Hz, 2H), –2.41 (s, 2H); ¹⁹F NMR (377 MHz, CDCl₃) δ –36.44 (s, 3F), –38.18 (t, *J* = 2.8 Hz, 6F); HRMS (APCI–): *m/z* calc'd for C₂₂H₁₀F₉N₅ [M[–]]: 515.0792, found 515.0802.



10,15,20-tris(trifluoromethyl)-5-azaporphyrin cobalt(II) (306-Co):

To a solution of monoazaporphyrin **306-H₂** (7.8 mg, 0.0151 mmol, 1.0 equiv.) in CHCl₃ (2.2 mL) in a 25 mL round-bottom flask was added a solution of cobalt(II) acetate

tetrahydrate (38 mg, 0.151 mmol, 10.0 equiv.) in methanol (0.3 mL) rapidly with stirring. The reaction mixture was heated to a gentle reflux and stirred for 16 h, then cooled to 23 °C. The solvent was removed under reduced pressure and the crude reaction mixture was purified by silica gel flash chromatography (CHCl₃) to afford **306-Co** as a black solid (8.2 mg, 0.0143 mmol, 95% yield); NMR data was not collected due to the paramagnetic nature of cobalt(II). HRMS (APCI⁻): *m/z* calc'd for C₂₂H₈CoF₉N₅ [M⁻]: 571.9968, found 571.9973.

3.6 REFERENCES AND NOTES

- (1) a) Barona-Castaño, J. C.; Carmona-Vargas, C. C.; Brocksom, T. J.; De Oliveira, K. T. Porphyrins as Catalysts in Scalable Organic Reactions. *Molecules* **2016**, *21*, 310.
b) Liang, Z.; Wang, H.; Zheng, H.; Zhang, W.; Cao, R. Porphyrin-based frameworks for oxygen electrocatalysis and catalytic reduction of carbon dioxide. *Chem. Soc. Rev.* **2021**, *50*, 2540–2581.
- (2) Ethirajan, M.; Chen, Y.; Joshi, P.; Pandey, R. K. The role of porphyrin chemistry in tumor imaging and photodynamic therapy. *Chem. Soc. Rev.* **2011**, *40*, 340–362.
- (3) Teo, R. D.; Hwang, J. Y.; Termini, J.; Gross, Z.; Gray, H. B. Fighting Cancer with Corroles. *Chem. Rev.* **2017**, *117*, 2711–2729.
- (4) Peters, J. C.; Thomas, J. C. Ligands, Reagents, and Methods in Organometallic Synthesis. In *Comprehensive Organometallic Chemistry III*; Mingos, D. M. P., Crabtree, R. H., Eds.; Elsevier, 2007; pp 59–92.
- (5) Johnson, A. W.; Kay, I. T. Corroles. Part I. Synthesis. *J. Chem. Soc.* **1965**, 1620–1629.
- (6) For reviews of the field of corrole synthesis, see: a) Orłowski, R.; Gryko, D.; Gryko, D. T. Synthesis of Corroles and Their Heteroanalogs. *Chem. Rev.* **2017**, *117*, 3102–3137. b) Kumar, A.; Kim, D.; Kumar, S.; Mahammed, A.; Churchill, D. G.; Gross, Z. Milestones in corrole chemistry: historical ligand syntheses and post-functionalization. *Chem. Soc. Rev.* **2023**, *52*, 573–600.

- (7) Paolesse, R.; Licoccia, S.; Fanciullo, M.; Morgante, E.; Boschi, T. Synthesis and characterization of cobalt(III) complexes of *meso*-phenyl-substituted corroles. *Inorg. Chim. Acta.* **1993**, *203*, 107–114.
- (8) a) Gross, Z.; Galili, N.; Saltsman, I. The First Direct Synthesis of Corroles from Pyrrole. *Angew. Chem. Int. Ed.* **1999**, *38*, 1427–1429. b) Gross, Z.; Galili, N.; Simkhovich, L.; Saltsman, I.; Botoshansky, M.; Bläser, D.; Boese, R.; Goldberg, I. Solvent-Free Condensation of Pyrrole and Pentafluorobenzaldehyde: A Novel Synthetic Pathway to Corrole and Oligopyrromethenes. *Org. Lett.* **1999**, *1*, 599–602.
- (9) Paolesse, R.; Jaquinod, L.; Nurco, D. J.; Mini, S.; Sagone, F.; Boschi, T.; Smith, K. M. 5,10,15-Triphenylcorrole: a product from a modified Rothmund reaction. *Chem. Commun.* **1999**, 1307–1308.
- (10) Lindsey, J. S. Synthetic Routes to *meso*-Patterned Porphyrins. *Acc. Chem. Res.* **2010**, *43*, 300–311.
- (11) Barata, J. F. B.; Neves, M. G. P. M. S.; Faustino, M. A. F.; Tomé, A. C.; Cavaleiro, J. A. S. Strategies for Corrole Functionalization. *Chem. Rev.* **2017**, *117*, 3192–3253.
- (12) Thomas, K. E.; Conradie, J.; Hansen, L. K.; Ghosh, A. Corroles Cannot Ruffle. *Inorg. Chem.* **2011**, *50*, 3247–3251.
- (13) Tse, M. K.; Zhang, Z.; Mak, T. C. W.; Chan, K. S. Synthesis of an oxorhenium(v) corrolate from porphyrin with detrifluoromethylation and ring contraction. *Chem. Commun.* **1998**, 1199–1200.

- (14) a) Chen, Q.; Soll, M.; Mizrahi, A.; Saltsman, I.; Fridman, N.; Saphier, M.; Gross, Z. One-Pot Synthesis of Contracted and Expanded Porphyrins with *meso*-CF₃ Groups. *Angew. Chem. Int. Ed.* **2018**, *57*, 1006–1010. b) Yadav, P.; Khoury, S.; Mahammed, A.; Morales, M.; Virgil, S. C.; Gray, H. B.; Gross, Z. Enhanced Synthetic Access to Tris-CF₃-Substituted Corroles. *Org. Lett.* **2020**, *22*, 3119–3122.
- (15) Kumar, A.; Yadav, P.; Majdoub, M.; Saltsman, I.; Fridman, N.; Kumar, S.; Kumar, A.; Mahammed, A.; Gross, Z. Corroles: The Hitherto Elusive Parent Macrocycle and its Metal Complexes. *Angew. Chem. Int. Ed.* **2021**, *60*, 25097–25103.
- (16) Yadav, P.; Khoury, S.; Fridman, N.; Sharma, V. K.; Kumar, A.; Majdoub, M.; Kumar, A.; Diskin-Posner, Y.; Mahammed, A.; Gross, Z. Trifluoromethyl Hydrolysis En Route to Corroles with Increased Druglikeness. *Angew. Chem. Int. Ed.* **2021**, *60*, 12829–12834.
- (17) Wang, Q. M.; Bruce, D. W. One-Step Synthesis of β , *meso*-Unsubstituted Dipyrromethane. *Synlett* **1995**, 1267–1268.
- (18) Koszarna, B.; Gryko, D. T. Efficient Synthesis of *meso*-Substituted Corroles in a H₂O-MeOH Mixture. *J. Org. Chem.* **2006**, *71*, 3707–3717.
- (19) Ooi, S.; Yoneda, T.; Tanaka, T.; Osuka, A. *meso*-Free Corroles: Syntheses, Structures, Properties, and Chemical Reactivities. *Chem. Eur. J.* **2015**, *21*, 7772–7779.

- (20) Littler, B. J.; Ciringh, Y.; Lindsey, J. S. Investigation of Conditions Giving Minimal Scrambling in the Synthesis of *trans*-Porphyrins from Dipyrromethanes and Aldehydes. *J. Org. Chem.* **1999**, *64*, 2864–2872.
- (21) Dolphin, D.; Johnson, A. W.; Leng, J.; van den Broek, P. The base-catalysed cyclisations of 1,19-dideoxybiladienes-ac. *J. Chem. Soc. C* **1966**, 880–884.
- (22) Fischer, H.; Friedrich, W. Synthese von Mono-imido-ätio- und Mono-imido-koporphyrin. II. Mitteilung über Imidoporphyrine. *Justus Liebigs Ann. Chem.* **1936**, *523*, 154–164.
- (23) Representative examples: a) Harris, R. L. N.; Johnson, A. W.; Kay, I. T. A stepwise synthesis of unsymmetrical porphyrins. *J. Chem. Soc. C* **1966**, 22–29. b) Neya, S.; Sato, T.; Hoshino, T. A concise synthesis of monoazaporphyrin from 1,19-dideoxybiladiene-ac. *Tetrahedron Lett.* **2008**, *49*, 1613–1615.
- (24) For a comprehensive review, see: Matano, Y. Synthesis of Aza-, Oxa-, and Thiaporphyrins and Related Compounds. *Chem. Rev.* **2017**, *117*, 3138–3191.
- (25) a) Nishimura, T.; Ikeue, T.; Shoji, O.; Shinokubo, H.; Miyake, Y. Iron(III) 5,15-Diazaporphyrin Catalysts for the Direct Oxidation of C(sp³)-H Bonds. *Inorg. Chem.* **2020**, *59*, 15751–15756. b) Nishimura, T.; Sakurai, T.; Shinokubo, H.; Miyake, Y. Iron hexamesityl-5,15-diazaporphyrin: synthesis, structure and catalytic use for direct oxidation of sp³ C–H bonds. *Dalton Trans.* **2021**, *50*, 6343–6348.
- (26) Ogata, H.; Fukuda, T.; Nakai, K.; Fujimura, Y.; Neya, S.; Stuzhin, P. A.; Kobayashi, N. Absorption, Magnetic Circular Dichroism, IR Spectra,

- Electrochemistry, and Molecular Orbital Calculations of Monoaza- and Opposite Diazaporphyrins. *Eur. J. Inorg. Chem.* **2004**, 1621–1629.
- (27) Nakamura, K.; Ikezaki, A.; Ohgo, Y.; Ikeue, T.; Neya, S.; Nakamura, M. Electronic Structure of Six-Coordinate Iron(III) Monoazaporphyrins. *Inorg. Chem.* **2008**, *47*, 10299–10307.
- (28) Palmer, J. H.; Brock-Nannestad, T.; Mahammed, A.; Durrell, A. C.; VanderVelde, D.; Virgil, S.; Gross, Z.; Gray, H. B. Nitrogen Insertion into a Corrole Ring: Iridium Monoazaporphyrins. *Angew. Chem. Int. Ed.* **2011**, *50*, 9433–9436.
- (29) Sonkar, P. K.; Prakash, K.; Yadav, M.; Ganesan, V.; Sankar, M.; Gupta, R.; Yadav, D. K. Co(II)-porphyrin-decorated carbon nanotubes as catalysts for oxygen reduction reactions: an approach for fuel cell improvement. *J. Mater. Chem. A* **2017**, *5*, 6263–6276.
- (30) Scheidt, W. R.; Turowska-Tyrk, I. Crystal and Molecular Structure of (Octaethylporphinato)cobalt(II). Comparison of the Structures of Four-Coordinate M(TPP) and M(OEP) Derivatives (M = Fe-Cu). Use of Area Detector Data. *Inorg. Chem.* **1994**, *33*, 1314–1318.
- (31) Saltsman, I.; Gross, Z. Microwave-assisted synthesis of non-substituted tripyrrane, tetrapyrane and pentapyrrane. *Tetrahedron Lett.* **2008**, *49*, 247–249.
- (32) de Groot, J. A.; van der Steen, R.; Fokkens, R.; Lugtenburg, J. Synthesis and photochemical reactivity of bilirubin model compounds. *Recl. Trav. Chim. Pays-Bas* **1982**, *101*, 35–40.

APPENDIX 6

Spectra Relevant to Chapter 3:

Synthetic Strategies Toward Minimally Substituted Corroles and

Azaporphyrins

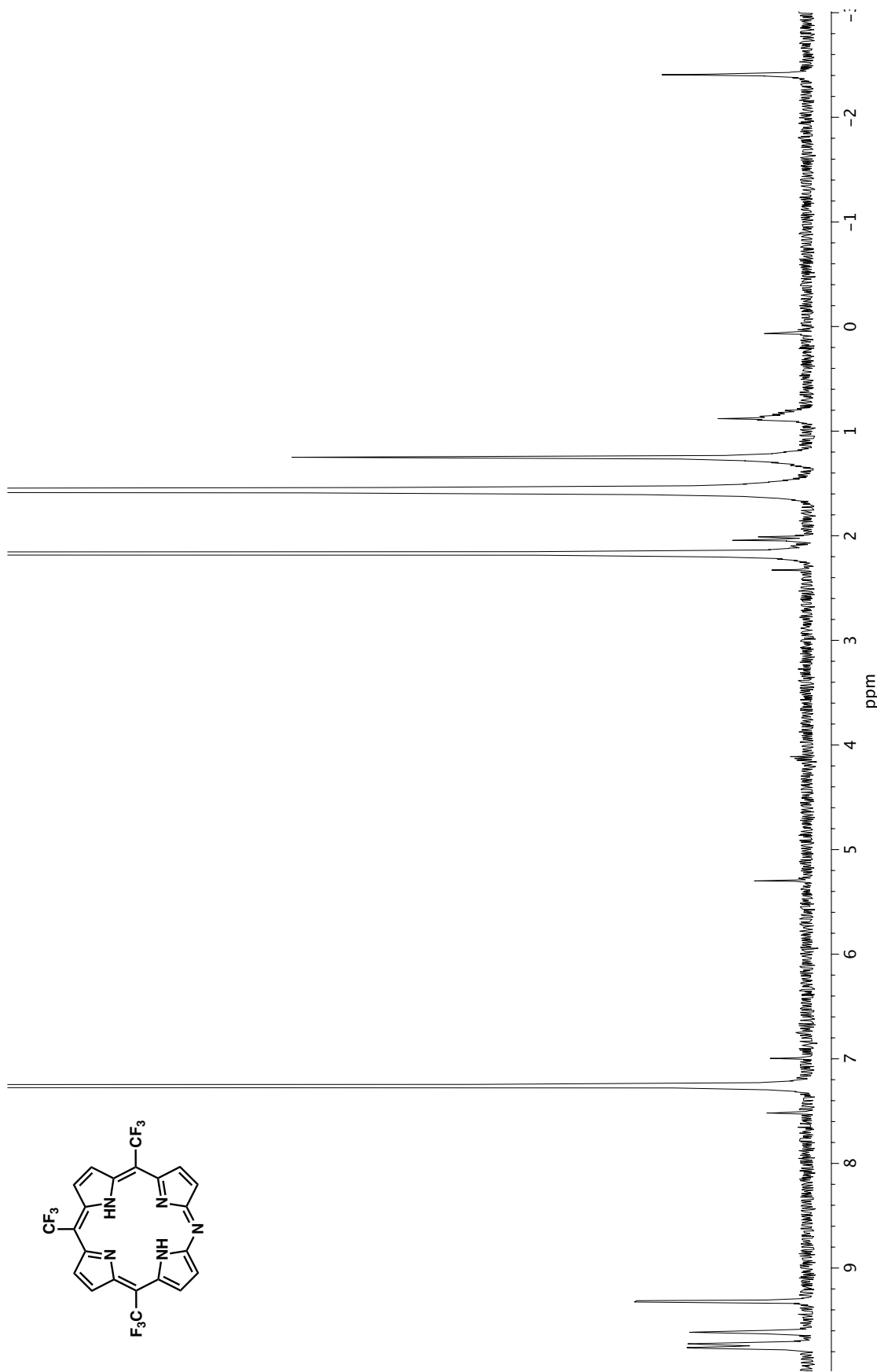


Figure A6.1. ¹H NMR (400 MHz, CDCl₃) of compound 306-H₂.

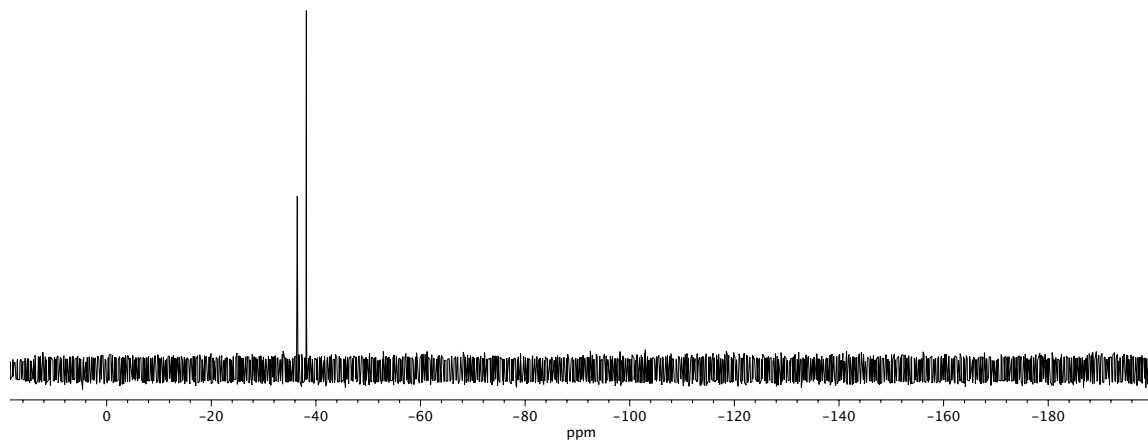


Figure A6.2. ^{19}F NMR (377 MHz, CDCl_3) of compound **306-H₂**.

APPENDIX 7

*X-Ray Crystallography Reports Relevant to Chapter 3:
Synthetic Strategies Toward Minimally Substituted Corroles and
Azaporphyrins*

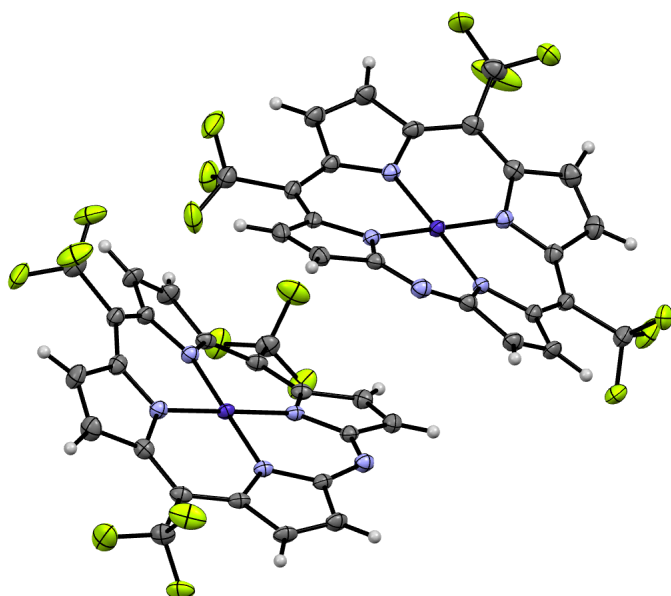
A7.1 GENERAL EXPERIMENTAL INFORMATION

A single crystal was immersed in Paratone–N oil and mounted on a Rigaku Oxford Diffraction XtaLAB Synergy-S at 100 K. Data collection was performed using monochromated Mo K α radiation, $\lambda = 0.71073 \text{ \AA}$, using φ and ω scans to cover the Ewald sphere. Accurate cell parameters were obtained with the amount of indicated reflections. Using Olex2,¹ the structure was solved with the olex2.solve² structure solution program using Charge Flipping and refined with the ShelXL³ refinement package using Least Squares minimization. All non-hydrogen atoms were refined with anisotropic displacement parameters. The hydrogen atoms were refined isotropically on calculated positions using a riding model with their U_{iso} values constrained to 1.5 times the U_{eq} of their pivot atoms for terminal sp³ carbon atoms and 1.2 times for all other carbon atoms. Software used for molecular graphics: Mercury 4.3.1.⁴

A7.2 X-RAY CRYSTAL STRUCTURE ANALYSIS OF COBALT

AZAPORPHYRIN 306-Co

Co(II) azaporphyrin **306-Co** was recrystallized by slow evaporation from THF/heptane (liquid/liquid diffusion) at 23 °C to provide suitable crystals for X-ray analysis.

Figure A7.2.1. X-ray crystal structure of azaporphyrin complex **306-Co**.**Table A7.2.2.** Crystal data and structure refinement for complex **306-Co**.

Empirical formula	C ₂₂ H ₈ CoF ₉ N ₅
Formula weight	572.26
Temperature/K	140.15
Crystal system	triclinic
Space group	P-1
a/Å	12.2205(2)
b/Å	13.5302(2)
c/Å	14.1720(3)
α/°	115.4873(18)
β/°	110.9276(18)
γ/°	90.5835(15)
Volume/Å ³	1938.02(7)
Z	4
ρ _{calc} /cm ³	1.961
μ/mm ⁻¹	0.997
F(000)	1132.0
Crystal size/mm ³	0.24 × 0.15 × 0.15
Radiation	MoKα (λ = 0.71073)
2θ range for data collection/°	4.47 to 59.468

Index ranges	$-16 \leq h \leq 16, -17 \leq k \leq 18, -18 \leq l \leq 18$
Reflections collected	28085
Independent reflections	8920 [$R_{\text{int}} = 0.0364, R_{\text{sigma}} = 0.0377$]
Data/restraints/parameters	8920/772/667
Goodness-of-fit on F^2	1.059
Final R indexes [$I \geq 2\sigma(I)$]	$R_1 = 0.0335, wR_2 = 0.0785$
Final R indexes [all data]	$R_1 = 0.0421, wR_2 = 0.0826$
Largest diff. peak/hole / $e \text{ \AA}^{-3}$	0.44/-0.41

Table A7.2.3. Fractional Atomic Coordinates ($\times 10^4$) and Equivalent Isotropic

Displacement Parameters ($\text{\AA}^2 \times 10^3$) for **306-Co**. $U(\text{eq})$ is defined as 1/3 of the trace of the orthogonalized U_{ij} tensor.

Atom	<i>x</i>	<i>y</i>	<i>z</i>	<i>U</i> (eq)
Co1	3868.3(2)	3311.6(2)	9273.0(2)	15.29(7)
F1	934.9(12)	4085.3(13)	11690.6(12)	43.6(4)
F2	1955.9(15)	5720.5(11)	12381.4(12)	42.5(4)
F3	2688.4(12)	4571.1(10)	12982.5(10)	31.0(3)
F4	-640.2(14)	1524.0(13)	5645.0(14)	57.8(5)
F5	394.3(13)	2399.6(12)	5204.8(11)	40.9(3)
F6	-353.2(14)	3309.8(13)	6376.1(12)	46.4(4)
F7	6119.8(14)	1446.3(12)	6274.2(12)	42.8(4)
F8	5259.6(12)	24.1(10)	6229.7(11)	36.1(3)
F9	6947.8(12)	941.5(11)	7566.7(11)	36.8(3)
N1	2236.7(14)	3285.3(12)	9137.1(13)	17.8(3)
N2	3359.9(14)	2295.0(12)	7670.4(13)	17.5(3)
N3	5506.6(14)	3373.8(12)	9438.4(13)	15.7(3)
N4	4416.0(14)	4313.6(12)	10879.7(13)	16.5(3)
N5	6463.2(15)	4981.2(13)	11302.8(13)	20.1(3)
C1	2558.9(18)	4225.6(15)	11154.7(16)	20.2(4)
C2	1817.9(17)	3653.2(15)	9992.0(17)	20.3(4)
C3	537.4(19)	3515.6(17)	9489.1(18)	27.0(4)
C4	199.7(19)	3139.8(17)	8363.5(18)	27.0(4)
C5	1256.8(17)	2983.6(15)	8134.1(17)	20.7(4)
C6	1292.3(17)	2529.0(15)	7054.7(16)	21.3(4)

Atom	x	y	z	U(eq)
C7	2249.7(17)	2103.9(15)	6828.2(16)	20.2(4)
C8	2234.3(19)	1347.0(16)	5731.8(17)	24.7(4)
C9	3312.5(19)	1064.5(16)	5909.1(17)	25.2(4)
C10	4036.9(18)	1690.9(15)	7117.0(15)	18.9(4)
C11	5277.2(18)	1816.4(15)	7631.2(16)	19.1(4)
C12	5978.1(17)	2691.6(15)	8691.5(16)	17.9(4)
C13	7250.5(18)	3112.7(16)	9146.3(17)	21.0(4)
C14	7530.3(18)	4044.7(16)	10131.2(17)	21.1(4)
C15	6453.0(17)	4183.1(15)	10329.7(16)	17.9(4)
C16	5528.1(17)	4976.3(14)	11561.5(15)	18.0(4)
C17	5594.1(19)	5713.7(15)	12689.3(16)	22.3(4)
C18	4530.6(19)	5475.1(15)	12694.2(16)	22.1(4)
C19	3773.3(18)	4611.4(15)	11556.6(15)	18.0(4)
C20	2023(2)	4637.5(17)	12037.5(18)	26.3(4)
C21	177.8(19)	2431.5(17)	6069.8(18)	27.8(4)
C22	5903(2)	1060.5(17)	6933.5(17)	26.3(4)
Co1A	4461.3(2)	1675.2(2)	700.9(2)	15.82(7)
F1A	75.5(11)	-906.8(10)	-2612.1(11)	31.7(3)
F2A	312.8(11)	286.2(10)	-3178.6(10)	32.2(3)
F3A	-465.4(11)	671.8(12)	-1965.3(11)	39.8(3)
F4A	2680(2)	3235.5(14)	4121.0(17)	71.8(6)
F5A	4153.1(14)	2479.5(13)	4646.4(12)	49.9(4)
F6A	2481.4(13)	1466.3(12)	3395.5(11)	39.0(3)
F7A	8250.9(12)	5113.5(10)	3871.0(12)	39.2(3)
F8A	8999.0(12)	4211.0(11)	2683.3(12)	41.2(3)
F9A	9096.9(13)	3766.4(13)	3988.3(14)	51.5(4)
N1A	2896.0(14)	1623.6(12)	733.3(13)	18.1(3)
N2A	5201.8(14)	2700.9(12)	2308.6(13)	18.1(3)
N3A	6011.3(14)	1685.8(12)	644.6(13)	16.7(3)
N4A	3754.2(14)	675.0(12)	-909.6(13)	16.6(3)
N5A	5521.5(15)	90.6(13)	-1205.2(14)	21.4(3)
C1A	1638.8(17)	663.3(15)	-1313.2(16)	20.0(4)
C2A	1793.2(17)	1217.7(15)	-163.2(17)	20.6(4)
C3A	874.9(19)	1275.0(17)	261.5(18)	26.5(4)
C4A	1424.5(19)	1641.7(17)	1393.2(19)	27.2(4)
C5A	2686.4(18)	1880.1(15)	1701.7(17)	21.3(4)
C6A	3571.4(19)	2367.2(15)	2806.3(17)	22.0(4)

Atom	x	y	z	U(eq)
C7A	4722.3(18)	2863.9(15)	3096.8(16)	21.6(4)
C8A	5557(2)	3662.7(17)	4215.4(17)	27.3(4)
C9A	6527(2)	3987.7(16)	4102.2(17)	27.0(4)
C10A	6329.6(18)	3357.4(15)	2916.3(16)	20.7(4)
C11A	7205.0(17)	3272.8(15)	2476.5(16)	21.2(4)
C12A	7086.4(17)	2406.8(15)	1439.4(16)	19.5(4)
C13A	8033.9(18)	2034.9(16)	1059.4(18)	23.4(4)
C14A	7537.5(18)	1093.3(16)	65.7(18)	23.1(4)
C15A	6279.2(17)	902.1(15)	-205.6(16)	18.9(4)
C16A	4353.7(17)	49.0(15)	-1539.0(16)	18.8(4)
C17A	3536.4(19)	-690.0(16)	-2693.5(16)	22.5(4)
C18A	2445.4(18)	-490.8(16)	-2776.3(16)	23.0(4)
C19A	2561.4(17)	339.0(15)	-1652.3(16)	19.6(4)
C20A	392.9(18)	193.4(17)	-2253.2(18)	25.3(4)
C21A	3226(2)	2401.3(17)	3743.4(18)	30.0(5)
C22A	8389(2)	4086.7(17)	3251.8(18)	28.9(5)

Table A7.2.4. Anisotropic Displacement Parameters ($\text{\AA}^2 \times 10^3$) for **306-Co**. The

Anisotropic displacement factor exponent takes the form:

$$-2\pi^2[h^2a^{*2}U_{11}+2hka^*b^*U_{12}+\dots].$$

Atom	U ₁₁	U ₂₂	U ₃₃	U ₂₃	U ₁₃	U ₁₂
Co1	16.77(13)	15.14(12)	11.42(12)	4.42(9)	5.15(10)	2.18(9)
F1	31.2(8)	67.3(10)	32.6(7)	17.8(7)	19.9(6)	3.0(7)
F2	68.6(10)	36.7(7)	44.9(8)	23.0(7)	41.2(8)	33.5(7)
F3	39.2(7)	40.0(7)	22.6(6)	17.3(6)	18.1(6)	12.1(6)
F4	38.9(9)	59.6(10)	47.5(9)	33.6(8)	-21.7(7)	-23.7(7)
F5	44.8(8)	58.1(9)	24.4(7)	24.8(7)	11.6(6)	19.9(7)
F6	43.8(9)	61.6(9)	31.7(7)	23.1(7)	10.7(7)	30.4(7)
F7	60.1(10)	46.7(8)	39.3(8)	20.9(7)	37.5(8)	18.4(7)
F8	39.2(8)	23.2(6)	31.0(7)	-1.5(5)	15.7(6)	7.8(5)
F9	30.9(7)	35.9(7)	31.6(7)	5.7(6)	11.9(6)	17.4(6)
N1	20.1(8)	15.5(7)	15.0(7)	4.8(6)	6.8(6)	2.6(6)
N2	19.6(8)	16.3(7)	15.2(7)	6.3(6)	6.7(6)	2.5(6)
N3	19.8(8)	15.1(7)	12.6(7)	6.6(6)	6.6(6)	4.2(6)

Atom	U ₁₁	U ₂₂	U ₃₃	U ₂₃	U ₁₃	U ₁₂
N4	19.1(8)	16.3(7)	14.0(7)	7.0(6)	6.5(6)	4.6(6)
N5	22.5(8)	18.9(8)	16.4(8)	6.8(6)	6.9(7)	3.0(6)
C1	26.9(10)	19.4(9)	18.8(9)	9.9(7)	12.6(8)	8.2(7)
C2	21.7(10)	19.1(9)	22.6(10)	10.1(8)	10.9(8)	6.0(7)
C3	22.1(10)	30.7(11)	27.6(11)	10.2(9)	13.3(9)	6.7(8)
C4	17.4(10)	30.9(11)	25.0(10)	8.8(9)	5.6(8)	3.3(8)
C5	19.9(10)	18.0(9)	19.8(9)	7.1(7)	5.3(8)	2.9(7)
C6	20.0(10)	19.7(9)	17.7(9)	6.9(7)	2.9(8)	0.1(7)
C7	22.3(10)	17.8(9)	15.2(9)	6.7(7)	3.3(8)	-0.5(7)
C8	25.4(11)	25.6(10)	13.2(9)	4.4(8)	3.1(8)	-1.0(8)
C9	31.1(11)	23.2(10)	15.7(9)	3.5(8)	10.2(8)	3.7(8)
C10	26.9(10)	15.5(8)	13.6(9)	5.4(7)	9.1(8)	3.2(7)
C11	24.9(10)	18.6(9)	16.3(9)	8.3(7)	10.7(8)	6.9(7)
C12	22.1(10)	17.5(8)	17.8(9)	10.0(7)	9.5(8)	8.0(7)
C13	20.5(10)	23.4(9)	22.8(10)	12.6(8)	10.1(8)	7.3(7)
C14	19.2(10)	22.5(9)	22.3(10)	11.7(8)	7.6(8)	3.5(7)
C15	20.5(9)	17.2(8)	15.7(9)	8.6(7)	5.7(7)	3.0(7)
C16	22.4(10)	16.0(8)	13.4(9)	7.0(7)	4.6(7)	3.8(7)
C17	29.2(11)	18.8(9)	13.4(9)	4.7(7)	6.3(8)	2.5(7)
C18	31.2(11)	20.6(9)	12.6(9)	6.1(7)	8.8(8)	6.8(8)
C19	25.1(10)	16.9(8)	13.6(9)	7.9(7)	8.2(8)	7.9(7)
C20	29.4(11)	28.8(10)	24.1(10)	11.8(9)	15.0(9)	10.1(8)
C21	25.5(11)	30.1(11)	21.1(10)	10.3(9)	4.2(9)	4.0(8)
C22	30.7(11)	25.7(10)	20.0(10)	6.6(8)	12.8(9)	7.5(8)
Co1A	15.88(13)	15.50(12)	12.32(12)	5.01(10)	3.49(10)	1.15(9)
F1A	27.4(7)	27.2(6)	29.0(7)	10.4(5)	2.8(5)	-8.6(5)
F2A	25.9(7)	38.6(7)	24.3(6)	18.3(5)	-2.7(5)	-2.0(5)
F3A	19.3(7)	48.2(8)	33.5(7)	10.0(6)	2.2(6)	8.3(6)
F4A	142.6(19)	53.7(10)	80.5(13)	42.2(10)	95.1(14)	58.5(11)
F5A	51.5(9)	66.3(10)	21.9(7)	21.2(7)	4.1(6)	-18.4(8)
F6A	38.5(8)	47.8(8)	32.2(7)	21.1(6)	13.1(6)	-5.8(6)
F7A	37.4(8)	22.8(6)	36.3(7)	0.8(5)	8.9(6)	-9.8(5)
F8A	33.5(8)	35.8(7)	41.3(8)	7.5(6)	14.7(6)	-13.4(6)
F9A	32.2(8)	51.0(9)	50.1(9)	30.6(8)	-14.4(7)	-8.6(6)
N1A	19.8(8)	15.7(7)	15.7(8)	5.5(6)	5.9(6)	2.5(6)
N2A	20.6(8)	14.8(7)	15.8(7)	6.2(6)	5.2(6)	2.3(6)
N3A	18.8(8)	15.1(7)	14.1(7)	7.0(6)	4.1(6)	1.4(6)

Atom	U ₁₁	U ₂₂	U ₃₃	U ₂₃	U ₁₃	U ₁₂
N4A	17.6(8)	16.3(7)	13.9(7)	7.2(6)	4.0(6)	0.3(6)
N5A	24.0(9)	20.5(8)	19.1(8)	8.5(7)	8.8(7)	4.1(6)
C1A	18.8(9)	17.9(9)	18.1(9)	8.8(7)	1.4(7)	0.3(7)
C2A	19.4(10)	19.0(9)	21.6(10)	9.1(8)	6.7(8)	3.1(7)
C3A	18.9(10)	28.5(10)	29.7(11)	12.8(9)	8.0(9)	3.8(8)
C4A	25.4(11)	30.1(11)	29.5(11)	13.1(9)	15.5(9)	7.2(8)
C5A	24.5(10)	18.0(9)	21.7(10)	8.2(8)	10.9(8)	5.3(7)
C6A	28.9(11)	17.6(9)	18.8(9)	6.1(7)	11.8(8)	5.1(7)
C7A	27.4(10)	19.4(9)	14.5(9)	6.8(7)	6.3(8)	4.2(7)
C8A	33.6(12)	24.1(10)	15.3(9)	4.9(8)	5.8(9)	-1.1(8)
C9A	32.0(12)	21.7(9)	16.2(9)	5.0(8)	2.8(8)	-2.6(8)
C10A	23.7(10)	16.9(9)	16.1(9)	6.8(7)	3.6(8)	0.6(7)
C11A	19.7(10)	18.9(9)	18.6(9)	8.8(7)	0.8(8)	-1.9(7)
C12A	17.6(9)	20.3(9)	20.3(9)	13.3(7)	2.6(7)	0.1(7)
C13A	17.7(10)	27.9(10)	28.8(11)	18.2(9)	7.3(8)	3.1(7)
C14A	21.8(10)	25.8(10)	26.8(10)	14.9(8)	11.7(8)	6.3(8)
C15A	21.7(10)	18.8(9)	18.1(9)	10.7(7)	7.5(8)	4.2(7)
C16A	23.0(10)	16.5(8)	16.7(9)	7.8(7)	7.4(8)	2.1(7)
C17A	29.5(11)	19.1(9)	14.9(9)	5.5(7)	7.8(8)	0.9(7)
C18A	25.5(11)	22.2(9)	12.9(9)	6.6(7)	1.0(8)	-3.1(7)
C19A	20.3(10)	17.4(9)	16.3(9)	7.6(7)	2.6(7)	-1.5(7)
C20A	19.1(10)	27.7(10)	23.5(10)	11.4(8)	3.1(8)	1.2(8)
C21A	40.3(13)	26.8(10)	23.9(11)	10.0(9)	16.3(10)	5.3(9)
C22A	25.6(11)	27.1(10)	24.6(11)	10.9(9)	1.5(9)	-2.9(8)

Table A7.2.5. Bond Lengths for **306-Co**.

Atom	Atom	Length/Å	Atom	Atom	Length/Å
Co1	N1	1.9319(16)	Co1A	N1A	1.9310(16)
Co1	N2	1.9293(15)	Co1A	N2A	1.9277(15)
Co1	N3	1.9273(16)	Co1A	N3A	1.9244(16)
Co1	N4	1.9253(15)	Co1A	N4A	1.9226(15)
F1	C20	1.328(3)	F1A	C20A	1.349(2)
F2	C20	1.345(2)	F2A	C20A	1.340(2)
F3	C20	1.338(2)	F3A	C20A	1.333(2)
F4	C21	1.333(3)	F4A	C21A	1.325(3)
F5	C21	1.327(3)	F5A	C21A	1.334(3)
F6	C21	1.340(2)	F6A	C21A	1.338(3)

F7	C22	1.345(2)	F7A	C22A	1.338(3)
F8	C22	1.339(2)	F8A	C22A	1.333(3)
F9	C22	1.331(3)	F9A	C22A	1.333(3)
N1	C2	1.381(2)	N1A	C2A	1.376(2)
N1	C5	1.377(2)	N1A	C5A	1.383(2)
N2	C7	1.379(2)	N2A	C7A	1.378(3)
N2	C10	1.376(2)	N2A	C10A	1.378(2)
N3	C12	1.382(2)	N3A	C12A	1.385(2)
N3	C15	1.368(2)	N3A	C15A	1.368(2)
N4	C16	1.370(2)	N4A	C16A	1.371(2)
N4	C19	1.383(2)	N4A	C19A	1.385(2)
N5	C15	1.332(2)	N5A	C15A	1.332(2)
N5	C16	1.320(3)	N5A	C16A	1.325(3)
C1	C2	1.399(3)	C1A	C2A	1.407(3)
C1	C19	1.387(3)	C1A	C19A	1.382(3)
C1	C20	1.516(3)	C1A	C20A	1.516(3)
C2	C3	1.440(3)	C2A	C3A	1.439(3)
C3	C4	1.342(3)	C3A	C4A	1.345(3)
C4	C5	1.437(3)	C4A	C5A	1.435(3)
C5	C6	1.399(3)	C5A	C6A	1.394(3)
C6	C7	1.388(3)	C6A	C7A	1.389(3)
C6	C21	1.517(3)	C6A	C21A	1.514(3)
C7	C8	1.440(3)	C7A	C8A	1.439(3)
C8	C9	1.342(3)	C8A	C9A	1.345(3)
C9	C10	1.444(3)	C9A	C10A	1.443(3)
C10	C11	1.399(3)	C10A	C11A	1.401(3)
C11	C12	1.387(3)	C11A	C12A	1.384(3)
C11	C22	1.515(3)	C11A	C22A	1.518(3)
C12	C13	1.452(3)	C12A	C13A	1.452(3)
C13	C14	1.338(3)	C13A	C14A	1.343(3)
C14	C15	1.439(3)	C14A	C15A	1.436(3)
C16	C17	1.446(3)	C16A	C17A	1.442(3)
C17	C18	1.339(3)	C17A	C18A	1.337(3)
C18	C19	1.453(3)	C18A	C19A	1.454(3)

Table A7.2.6. Bond Angles for **306-Co**.

Atom	Atom	Atom	Angle/°	Atom	Atom	Atom	Angle/°
N2	Co1	N1	91.72(7)	N2A	Co1A	N1A	91.74(7)
N3	Co1	N1	178.62(6)	N3A	Co1A	N1A	178.53(6)
N3	Co1	N2	89.48(6)	N3A	Co1A	N2A	89.33(7)
N4	Co1	N1	89.67(7)	N4A	Co1A	N1A	89.56(7)
N4	Co1	N2	178.48(7)	N4A	Co1A	N2A	178.35(7)
N4	Co1	N3	89.13(6)	N4A	Co1A	N3A	89.39(6)

Atom	Atom	Atom	Angle/°	Atom	Atom	Atom	Angle/°
C2	N1	Co1	128.67(13)	C2A	N1A	Co1A	129.02(13)
C5	N1	Co1	124.77(13)	C2A	N1A	C5A	106.09(16)
C5	N1	C2	106.27(16)	C5A	N1A	Co1A	124.47(13)
C7	N2	Co1	126.00(13)	C7A	N2A	Co1A	125.96(13)
C10	N2	Co1	127.93(13)	C7A	N2A	C10A	106.08(15)
C10	N2	C7	105.86(15)	C10A	N2A	Co1A	127.83(13)
C12	N3	Co1	129.27(13)	C12A	N3A	Co1A	129.52(13)
C15	N3	Co1	125.31(12)	C15A	N3A	Co1A	125.17(13)
C15	N3	C12	105.30(15)	C15A	N3A	C12A	105.21(16)
C16	N4	Co1	125.25(13)	C16A	N4A	Co1A	125.28(13)
C16	N4	C19	105.62(15)	C16A	N4A	C19A	105.28(15)
C19	N4	Co1	128.80(13)	C19A	N4A	Co1A	129.13(13)
C16	N5	C15	120.48(17)	C16A	N5A	C15A	120.67(16)
C2	C1	C20	120.27(18)	C2A	C1A	C20A	120.12(18)
C19	C1	C2	122.86(17)	C19A	C1A	C2A	123.32(18)
C19	C1	C20	115.98(17)	C19A	C1A	C20A	115.58(17)
N1	C2	C1	123.65(18)	N1A	C2A	C1A	123.21(18)
N1	C2	C3	109.02(17)	N1A	C2A	C3A	109.61(17)
C1	C2	C3	126.58(18)	C1A	C2A	C3A	126.33(18)
C4	C3	C2	107.72(18)	C4A	C3A	C2A	107.18(19)
C3	C4	C5	107.21(19)	C3A	C4A	C5A	107.57(19)
N1	C5	C4	109.65(17)	N1A	C5A	C4A	109.40(17)
N1	C5	C6	124.41(18)	N1A	C5A	C6A	124.37(18)
C6	C5	C4	125.82(18)	C6A	C5A	C4A	126.09(19)
C5	C6	C21	117.19(18)	C5A	C6A	C21A	117.37(18)
C7	C6	C5	123.93(18)	C7A	C6A	C5A	123.79(18)
C7	C6	C21	118.75(18)	C7A	C6A	C21A	118.76(18)
N2	C7	C6	123.20(17)	N2A	C7A	C6A	123.37(17)
N2	C7	C8	109.75(17)	N2A	C7A	C8A	109.76(18)
C6	C7	C8	126.88(18)	C6A	C7A	C8A	126.75(19)
C9	C8	C7	107.40(18)	C9A	C8A	C7A	107.28(18)
C8	C9	C10	107.08(17)	C8A	C9A	C10A	107.29(18)
N2	C10	C9	109.78(17)	N2A	C10A	C9A	109.48(17)
N2	C10	C11	124.05(16)	N2A	C10A	C11A	124.24(17)
C11	C10	C9	125.41(17)	C11A	C10A	C9A	125.46(18)
C10	C11	C22	118.42(17)	C10A	C11A	C22A	117.39(18)
C12	C11	C10	123.03(17)	C12A	C11A	C10A	122.79(17)

Atom	Atom	Atom	Angle/°	Atom	Atom	Atom	Angle/°
C12	C11	C22	117.98(18)	C12A	C11A	C22A	119.32(18)
N3	C12	C11	122.81(18)	N3A	C12A	C13A	109.64(17)
N3	C12	C13	109.50(16)	C11A	C12A	N3A	122.82(18)
C11	C12	C13	127.40(17)	C11A	C12A	C13A	127.25(18)
C14	C13	C12	107.43(17)	C14A	C13A	C12A	107.13(17)
C13	C14	C15	106.65(17)	C13A	C14A	C15A	106.81(18)
N3	C15	C14	111.02(16)	N3A	C15A	C14A	111.11(17)
N5	C15	N3	127.67(18)	N5A	C15A	N3A	127.66(18)
N5	C15	C14	121.22(17)	N5A	C15A	C14A	121.11(17)
N4	C16	C17	110.67(17)	N4A	C16A	C17A	110.84(17)
N5	C16	N4	128.15(17)	N5A	C16A	N4A	127.77(17)
N5	C16	C17	121.18(17)	N5A	C16A	C17A	121.37(17)
C18	C17	C16	106.76(17)	C18A	C17A	C16A	106.95(17)
C17	C18	C19	107.46(17)	C17A	C18A	C19A	107.30(17)
N4	C19	C1	124.05(17)	N4A	C19A	C18A	109.54(17)
N4	C19	C18	109.45(17)	C1A	C19A	N4A	123.57(17)
C1	C19	C18	126.10(17)	C1A	C19A	C18A	126.47(18)
F1	C20	F2	107.01(18)	F1A	C20A	C1A	111.06(17)
F1	C20	F3	105.57(17)	F2A	C20A	F1A	105.89(16)
F1	C20	C1	114.69(18)	F2A	C20A	C1A	112.30(17)
F2	C20	C1	111.15(17)	F3A	C20A	F1A	106.42(17)
F3	C20	F2	105.67(17)	F3A	C20A	F2A	105.68(16)
F3	C20	C1	112.16(17)	F3A	C20A	C1A	114.88(17)
F4	C21	F6	106.76(19)	F4A	C21A	F5A	107.17(19)
F4	C21	C6	112.76(17)	F4A	C21A	F6A	106.3(2)
F5	C21	F4	106.75(18)	F4A	C21A	C6A	113.23(18)
F5	C21	F6	104.62(17)	F5A	C21A	F6A	104.46(17)
F5	C21	C6	113.31(18)	F5A	C21A	C6A	113.18(19)
F6	C21	C6	112.05(17)	F6A	C21A	C6A	111.91(17)
F7	C22	C11	111.64(17)	F7A	C22A	C11A	112.32(18)
F8	C22	F7	106.39(16)	F8A	C22A	F7A	105.40(16)
F8	C22	C11	112.66(17)	F8A	C22A	F9A	107.09(19)
F9	C22	F7	106.73(18)	F8A	C22A	C11A	113.10(17)
F9	C22	F8	105.51(16)	F9A	C22A	F7A	106.74(18)
F9	C22	C11	113.40(17)	F9A	C22A	C11A	111.73(17)

Table A7.2.7. Torsion Angles for 306-Co.

A	B	C	D	Angle/°	A	B	C	D	Angle/°
Co1	N1	C2	C1	6.5(3)	Co1A	N1A	C2A	C1A	5.7(3)
Co1	N1	C2	C3	177.16(13)	Co1A	N1A	C2A	C3A	175.69(13)
Co1	N1	C5	C4	-175.78(13)	Co1A	N1A	C5A	C4A	-174.07(13)
Co1	N1	C5	C6	7.9(3)	Co1A	N1A	C5A	C6A	10.0(3)
Co1	N2	C7	C6	-8.3(3)	Co1A	N2A	C7A	C6A	-6.0(3)
Co1	N2	C7	C8	176.19(13)	Co1A	N2A	C7A	C8A	177.72(13)
Co1	N2	C10	C9	-177.94(13)	Co1A	N2A	C10A	C9A	-179.16(13)
Co1	N2	C10	C11	-7.5(3)	Co1A	N2A	C10A	C11A	-9.1(3)
Co1	N3	C12	C11	1.4(3)	Co1A	N3A	C12A	C11A	1.6(3)
Co1	N3	C12	C13	175.63(12)	Co1A	N3A	C12A	C13A	175.77(12)
Co1	N3	C15	N5	9.4(3)	Co1A	N3A	C15A	N5A	9.8(3)
Co1	N3	C15	C14	-174.02(12)	Co1A	N3A	C15A	C14A	-174.28(12)
Co1	N4	C16	N5	-7.7(3)	Co1A	N4A	C16A	N5A	-7.5(3)
Co1	N4	C16	C17	173.53(12)	Co1A	N4A	C16A	C17A	174.30(12)
Co1	N4	C19	C1	-1.2(3)	Co1A	N4A	C19A	C1A	-2.7(3)
Co1	N4	C19	C18	-174.42(12)	Co1A	N4A	C19A	C18A	-175.77(12)
N1	C2	C3	C4	-3.8(2)	N1A	C2A	C3A	C4A	-4.0(2)
N1	C5	C6	C7	14.5(3)	N1A	C5A	C6A	C7A	14.0(3)
N1	C5	C6	C21	-169.72(17)	N1A	C5A	C6A	C21A	-169.24(17)
N2	C7	C8	C9	1.3(2)	N2A	C7A	C8A	C9A	0.6(2)
N2	C10	C11	C12	-11.5(3)	N2A	C10A	C11A	C12A	-10.0(3)
N2	C10	C11	C22	177.44(17)	N2A	C10A	C11A	C22A	178.13(17)
N3	C12	C13	C14	-1.6(2)	N3A	C12A	C13A	C14A	-1.3(2)
N4	C16	C17	C18	1.5(2)	N4A	C16A	C17A	C18A	1.8(2)
N5	C16	C17	C18	-177.34(18)	N5A	C16A	C17A	C18A	-176.48(18)
C1	C2	C3	C4	166.6(2)	C1A	C2A	C3A	C4A	165.65(19)
C2	N1	C5	C4	-1.5(2)	C2A	N1A	C5A	C4A	-0.9(2)
C2	N1	C5	C6	-177.77(18)	C2A	N1A	C5A	C6A	-176.78(18)
C2	C1	C19	N4	-11.7(3)	C2A	C1A	C19A	N4A	-10.6(3)
C2	C1	C19	C18	160.39(18)	C2A	C1A	C19A	C18A	161.31(19)
C2	C1	C20	F1	24.0(3)	C2A	C1A	C20A	F1A	-97.6(2)
C2	C1	C20	F2	-97.5(2)	C2A	C1A	C20A	F2A	144.06(18)
C2	C1	C20	F3	144.45(18)	C2A	C1A	C20A	F3A	23.2(3)
C2	C3	C4	C5	2.8(2)	C2A	C3A	C4A	C5A	3.3(2)
C3	C4	C5	N1	-0.9(2)	C3A	C4A	C5A	N1A	-1.6(2)

A	B	C	D	Angle/°	A	B	C	D	Angle/°
C3	C4	C5	C6	175.36(19)	C3A	C4A	C5A	C6A	174.21(19)
C4	C5	C6	C7	-161.2(2)	C4A	C5A	C6A	C7A	-161.26(19)
C4	C5	C6	C21	14.6(3)	C4A	C5A	C6A	C21A	15.6(3)
C5	N1	C2	C1	-167.56(18)	C5A	N1A	C2A	C1A	-167.10(17)
C5	N1	C2	C3	3.1(2)	C5A	N1A	C2A	C3A	2.9(2)
C5	C6	C7	N2	-14.3(3)	C5A	C6A	C7A	N2A	-16.1(3)
C5	C6	C7	C8	160.4(2)	C5A	C6A	C7A	C8A	159.5(2)
C5	C6	C21	F4	-82.2(2)	C5A	C6A	C21A	F4A	-81.3(2)
C5	C6	C21	F5	156.37(18)	C5A	C6A	C21A	F5A	156.49(18)
C5	C6	C21	F6	38.3(3)	C5A	C6A	C21A	F6A	38.8(3)
C6	C7	C8	C9	-174.04(19)	C6A	C7A	C8A	C9A	-175.5(2)
C7	N2	C10	C9	-3.0(2)	C7A	N2A	C10A	C9A	-3.1(2)
C7	N2	C10	C11	167.45(18)	C7A	N2A	C10A	C11A	166.91(18)
C7	C6	C21	F4	93.8(2)	C7A	C6A	C21A	F4A	95.7(3)
C7	C6	C21	F5	-27.6(3)	C7A	C6A	C21A	F5A	-26.5(3)
C7	C6	C21	F6	-145.73(19)	C7A	C6A	C21A	F6A	-144.24(19)
C7	C8	C9	C10	-3.0(2)	C7A	C8A	C9A	C10A	-2.5(2)
C8	C9	C10	N2	3.9(2)	C8A	C9A	C10A	N2A	3.6(2)
C8	C9	C10	C11	-166.42(19)	C8A	C9A	C10A	C11A	-166.3(2)
C9	C10	C11	C12	157.54(19)	C9A	C10A	C11A	C12A	158.43(19)
C9	C10	C11	C22	-13.6(3)	C9A	C10A	C11A	C22A	-13.4(3)
C10	N2	C7	C6	176.67(18)	C10A	N2A	C7A	C6A	177.90(18)
C10	N2	C7	C8	1.1(2)	C10A	N2A	C7A	C8A	1.6(2)
C10	C11	C12	N3	14.5(3)	C10A	C11A	C12A	N3A	13.8(3)
C10	C11	C12	C13	-158.69(19)	C10A	C11A	C12A	C13A	-159.36(19)
C10	C11	C22	F7	83.0(2)	C10A	C11A	C22A	F7A	-39.6(3)
C10	C11	C22	F8	-36.6(3)	C10A	C11A	C22A	F8A	-158.76(18)
C10	C11	C22	F9	-156.41(18)	C10A	C11A	C22A	F9A	80.3(2)
C11	C12	C13	C14	172.34(19)	C11A	C12A	C13A	C14A	172.59(19)
C12	N3	C15	N5	-174.22(18)	C12A	N3A	C15A	N5A	-173.47(18)
C12	N3	C15	C14	2.3(2)	C12A	N3A	C15A	C14A	2.4(2)
C12	C11	C22	F7	-88.6(2)	C12A	C11A	C22A	F7A	148.28(18)
C12	C11	C22	F8	151.80(17)	C12A	C11A	C22A	F8A	29.1(3)
C12	C11	C22	F9	32.0(3)	C12A	C11A	C22A	F9A	-91.8(2)
C12	C13	C14	C15	2.9(2)	C12A	C13A	C14A	C15A	2.7(2)
C13	C14	C15	N3	-3.4(2)	C13A	C14A	C15A	N3A	-3.3(2)
C13	C14	C15	N5	173.44(17)	C13A	C14A	C15A	N5A	172.89(18)

A	B	C	D	Angle/°	A	B	C	D	Angle/°
C15	N3	C12	C11	-174.76(17)	C15A	N3A	C12A	C11A	-174.93(17)
C15	N3	C12	C13	-0.53(19)	C15A	N3A	C12A	C13A	-0.7(2)
C15	N5	C16	N4	-9.5(3)	C15A	N5A	C16A	N4A	-9.6(3)
C15	N5	C16	C17	169.11(17)	C15A	N5A	C16A	C17A	168.37(17)
C16	N4	C19	C1	172.40(17)	C16A	N4A	C19A	C1A	171.15(18)
C16	N4	C19	C18	-0.8(2)	C16A	N4A	C19A	C18A	-1.9(2)
C16	N5	C15	N3	8.6(3)	C16A	N5A	C15A	N3A	8.4(3)
C16	N5	C15	C14	-167.64(17)	C16A	N5A	C15A	C14A	-167.12(18)
C16	C17	C18	C19	-1.9(2)	C16A	C17A	C18A	C19A	-2.9(2)
C17	C18	C19	N4	1.8(2)	C17A	C18A	C19A	N4A	3.1(2)
C17	C18	C19	C1	-171.26(18)	C17A	C18A	C19A	C1A	-169.71(19)
C19	N4	C16	N5	178.37(18)	C19A	N4A	C16A	N5A	178.31(18)
C19	N4	C16	C17	-0.4(2)	C19A	N4A	C16A	C17A	0.2(2)
C19	C1	C2	N1	9.0(3)	C19A	C1A	C2A	N1A	9.1(3)
C19	C1	C2	C3	-160.02(19)	C19A	C1A	C2A	C3A	-159.24(19)
C19	C1	C20	F1	-166.47(17)	C19A	C1A	C20A	F1A	71.5(2)
C19	C1	C20	F2	72.0(2)	C19A	C1A	C20A	F2A	-46.9(2)
C19	C1	C20	F3	-46.1(2)	C19A	C1A	C20A	F3A	-167.72(17)
C20	C1	C2	N1	177.77(17)	C20A	C1A	C2A	N1A	177.24(17)
C20	C1	C2	C3	8.7(3)	C20A	C1A	C2A	C3A	8.9(3)
C20	C1	C19	N4	179.11(17)	C20A	C1A	C19A	N4A	-179.23(17)
C20	C1	C19	C18	-8.8(3)	C20A	C1A	C19A	C18A	-7.3(3)
C21	C6	C7	N2	169.99(17)	C21A	C6A	C7A	N2A	167.11(18)
C21	C6	C7	C8	-15.3(3)	C21A	C6A	C7A	C8A	-17.3(3)
C22	C11	C12	N3	-174.40(17)	C22A	C11A	C12A	N3A	-174.53(17)
C22	C11	C12	C13	12.5(3)	C22A	C11A	C12A	C13A	12.3(3)

Table A7.2.8. Hydrogen Atom Coordinates ($\text{\AA}\times 10^4$) and Isotropic Displacement

Parameters ($\text{\AA}^2\times 10^3$) for **306-Co**.

Atom	x	y	z	U(eq)
H3	24	3664	9883	32
H4	-591	3003	7820	32
H8	1581	1094	5015	30
H9	3554	550	5346	30
H13	7786	2786	8807	25

Atom	x	y	z	U(eq)
H14	8292	4522	10607	25
H17	6263	6262	13308	27
H18	4311	5809	13326	26
H3A	37	1089	-176	32
H4A	1046	1727	1897	33
H8A	5445	3914	4906	33
H9A	7214	4531	4693	32
H13A	8851	2391	1442	28
H14A	7941	641	-373	28
H17A	3735	-1218	-3283	27
H18A	1727	-829	-3445	28

A7.3 REFERENCES AND NOTES

- (1) Dolomanov, O. V.; Bourhis, L. J.; Gildea, R. J.; Howard, J. A. K.; Puschmann, H. OLEX2: a complete structure solution, refinement and analysis program. *J. Appl. Cryst.* **2009**, *42*, 339–341.
- (2) Bourhis, L. J.; Dolomanov, O. V.; Gildea, R. J.; Howard, J. A. K.; Puschmann, H. The anatomy of a comprehensive constrained, restrained refinement program for the modern computing environment – Olex2 dissected. *Acta Cryst.* **2015**, *A71*, 59–75.
- (3) Sheldrick, G. M. Crystal structure refinement with SHELXL. *Acta Cryst.* **2015**, *C71*, 3–8.
- (4) Mercury Software from CCDC: <http://www.ccdc.cam.ac.uk/Solutions/CSDSystem/Pages/Mercury.aspx>.

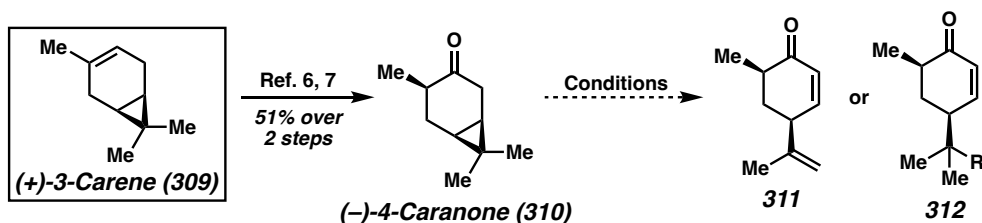
APPENDIX 8

Some Unusual Transformations of a Highly Reactive α -Bromocaranone[†]

A8.1 INTRODUCTION

The advent of asymmetric catalysis has greatly increased the number and variety of synthetically accessible chiral building blocks.¹ Nevertheless, the syntheses of many natural products and consumer commodities continue to rely on starting materials from the readily available chiral pool and derivatives thereof.^{2,3} As such, strategies for the derivatization of chiral building blocks remain vital in organic synthesis. (+)-3-Carene (**309**, Scheme A8.1.1) is one such building block: the defining dimethylcyclopropane moiety of this molecule coupled with its widespread availability and conveniently rigid structure have made it a popular chiral feedstock.^{2,4}

Scheme A8.1.1. Carene and the desired transformation.



[†]This research was conducted in collaboration with Adrian Samkian and Dr. Scott Virgil. This appendix has been modified and reproduced with permission from Samkian, A. E.; Sercel, Z. P.; Virgil, S. C.; Stoltz, B. M. *Tetrahedron Lett.* **2022**, *89*, 153496. © 2021 Published by Elsevier Ltd.

However, among the numerous syntheses beginning from **309**, most feature the presence of the intact dimethylcyclopropane moiety in the target. This is due in part to the lack of mild and selective methods for the fragmentation of the strained ring. Although such fragmentations have been performed on carene (**309**) and related dimethylcyclopropane-containing compounds, the vast majority rely on strongly acidic conditions.⁵

In the course of a total synthesis effort, we identified the fragmentation of a β -ketodimethylcyclopropane (**310**) as a valuable transformation for revealing a reactive γ -isopropenyl group (**311**) from the relatively unreactive, “protected” cyclopropane. Furthermore, we aimed to develop a method to trap the species immediately after ring fragmentation to access the challenging γ -gem-dimethyl synthon (**312**).

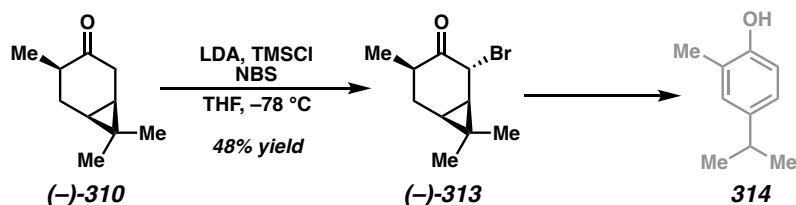
A8.2 SYNTHESIS AND FRAGMENTATIONS OF A BROMOCARANONE

We realized that in order to affect this transformation in a mild and efficient fashion, a synthetic handle would be necessary at the α -position. α -Bromocaranone **313** was selected as a promising model system to study the feasibility of this synthetic transformation due to its straightforward synthesis from carene (Scheme A8.2.1).

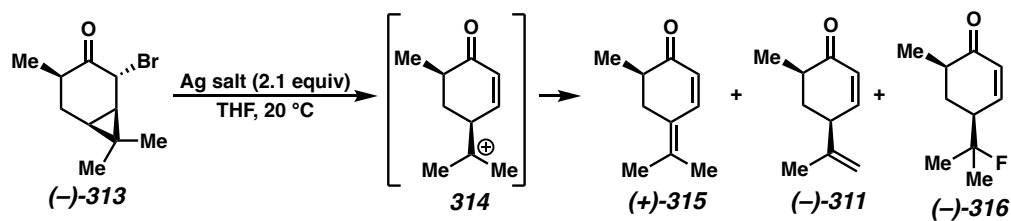
Hydroboration of commercially available (+)-3-carene (**309**) followed by oxidation afforded (–)-4-caranone (**310**) in modest yields on a >10 g scale.^{6,7} Enolization of (–)-**310** with LiHMDS and direct bromination with NBS led to the production of several inseparable side products,⁸ however, formation of the silyl enol ether with LDA and TMSCl followed by quenching with NBS led to diminished side product formation, affording (–)-**313**.⁹ Although bromide (–)-**313** decomposes rapidly on silica, purification was possible via chromatography on neutral alumina. While this compound can be stored

for at least several weeks at $-15\text{ }^{\circ}\text{C}$ as a solution in benzene, neat samples of bromide (–)-**313** stored at ambient temperature undergo spontaneous, exothermic decomposition to isocarvacrol (**314**), with the release of HBr, after several hours. Despite the unstable nature of bromide (–)-**313**, it was possible to manipulate neat samples of this intermediate for short periods of time.

Scheme A8.2.1. Synthesis of a reactive α -bromocaranone.

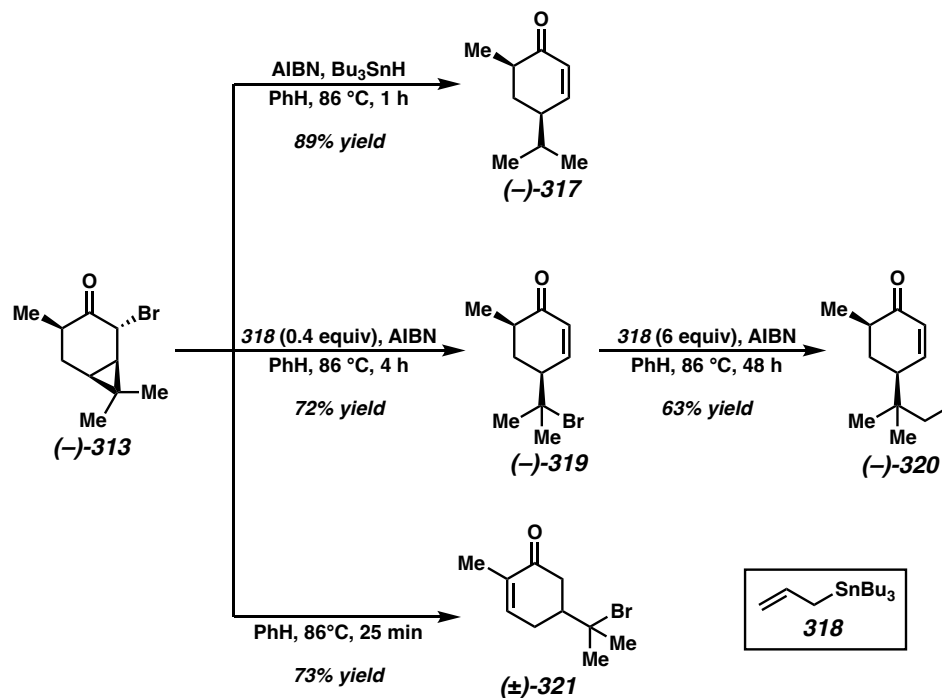


We began by treating bromide (–)-**313** with Ag^{I} reagents in order to effect a carbocation-mediated fragmentation. Treatment of (–)-**313** with AgClO_4 or AgOTf in THF afforded dienone (+)-**315** (Table A8.2.2, entries 1 and 2) in modest yields. Trace quantities of the desired compound featuring an isopropenyl group ((–)-**311**) were also observed. Attempts to favor the formation of (–)-**311** by performing the reaction in the presence of a bulky base were not successful. The rapid elimination of tertiary carbocation **314** toward (+)-**315** would appear to impede formation of (–)-**311** or trapping with nucleophiles. Despite this, we were surprised to observe tertiary fluoride (–)-**316** as the major product when AgBF_4 was used as a Ag^{I} source (entry 3).

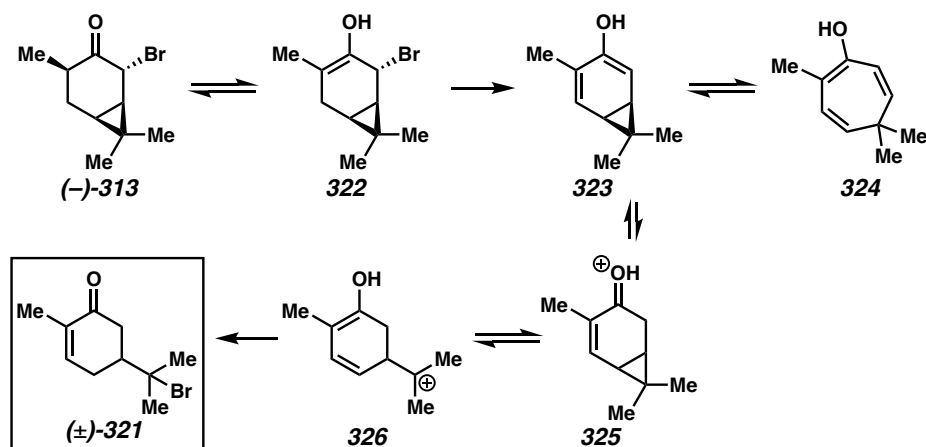
Table A8.2.2. Ag^I -mediated reactions of **313**.

entry	Ag salt	% yield 315	% yield 311	% yield 316
1	AgOTf	55	<5	—
2	AgClO ₄	67	<5	—
3	AgBF ₄	10	5	35

The lack of control observed in carbocation-mediated reactions led us to study radical-mediated fragmentations next. Treatment of (–)-**313** with AIBN and Bu₃SnH afforded isopropyl enone (–)-**317** (Scheme A8.2.3) in excellent yield. Allyltributylstannane (**318**) was used in place of Bu₃SnH in an attempt to prepare the allylated product (–)-**320**.¹⁰ Pleasingly, (–)-**320** was observed, though in moderate yields (<40%), with the tertiary bromide (–)-**319** instead being the major product. Using catalytic amounts of **318** led to high yields of (–)-**319**, which could then be isolated and subjected to similar conditions, albeit with an excess of **318**, to afford the desired allylated species (–)-**320**. It is noteworthy that treatment of dienone (+)-**315** with **318** and AIBN did not afford (–)-**320**, suggesting (+)-**315** is not an intermediate en route to (–)-**320**. The presence of catalytic stannane radicals proved vital for the production of (–)-**319**. Indeed, a control experiment performed by simply heating a solution of (–)-**313** in benzene provided racemic carvone derivative (±)-**321** in high yields, with phenol **314** being observed as a minor product. To explain this surprising divergence in reactivity between (–)-**319** and (±)-**321**, further mechanistic studies were performed.

Scheme A8.2.3. Radical-mediated cyclopropane fragmentation of **313**.

We initially suspected that the mechanism to form (±)-**321** may be radical-mediated, perhaps through the homolysis of the carbon-bromine bond followed by 1,4-HAT. However, such a mechanism would not explain a racemic product. Furthermore, DFT calculations^{11,12,13} suggested that the barriers for such a transformation are kinetically inaccessible (>31 kcal/mol). Instead, we propose a polar mechanism (Scheme A8.2.4) that, through elimination of the bromide through enol **322**, could afford diene **323**. Such a system is predestined to rapidly racemize through an electrocyclic reaction via cycloheptatriene **324**.¹⁴ Ultimately, **323** may be protonated in its keto form (**325**), eventually leading to tertiary cation **326**, which is trapped by bromide, affording (±)-**321**.

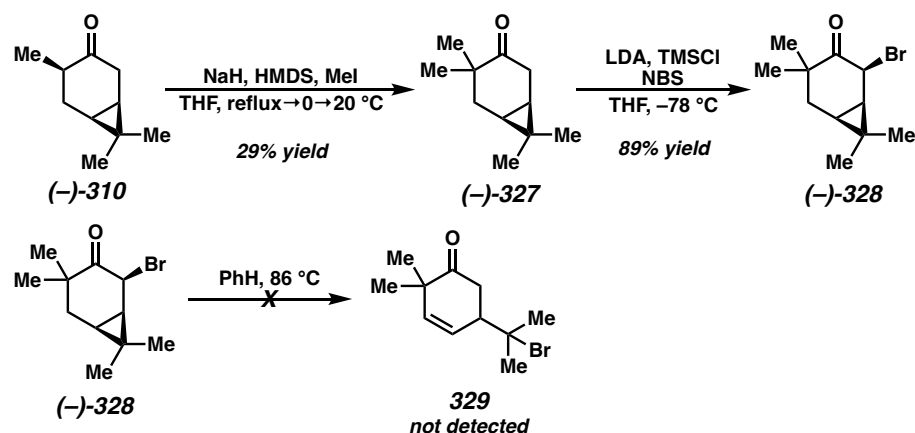
Scheme A8.2.4. Proposed mechanism for the formation of racemic **321**.

The conversion of **(-)-313** to **(±)-321** is likely catalyzed by HBr formed via the decomposition of **(-)-313** to **314**. Interestingly, despite the formation of **(-)-319** requiring longer reaction times (4 h vs. 25 min), carvone derivative **(±)-321** is not observed. Indeed, heating bromide **(-)-313** in PhH in the presence of allylstannane **318** with no radical initiator entirely suppressed the formation of **(±)-321**. We propose that this observation is due to the quenching of HBr by **318**. Another reaction performed with **(-)-313** and bis(tributylstannane), which exists in equilibrium with two tributyltin radicals,¹⁵ also suppressed the formation of **(±)-321** whilst producing **(-)-319**, albeit in lower yields. No reaction was observed when **(-)-313** was heated in hexanes, but **(±)-321** was produced rapidly in dioxane or 1,2-dichloroethane with greater quantities of phenol **314**, further implicating a polar mechanism.

Finally, control compound **(-)-328** (Scheme A8.2.5), featuring an additional *gem*-dimethyl group, was prepared in two steps from **(-)-310**. This compound was found to be significantly more stable than **(-)-313**, decomposing neither on silica nor spontaneously as a solid compound. Importantly, only clean starting material was observed when **(-)-328**

was heated in benzene for extended periods of time, providing further evidence that the reaction leading to (\pm)-**321** proceeds via the mechanism proposed in Scheme A8.2.4.

Scheme A8.2.5. Synthesis of bromide **328** and control reaction in benzene.



A8.3 CONCLUSION

Over the course of this study, readily available (+)-3-carene was derivatized into an array of useful chiral building blocks through a highly reactive α -bromocaranone as a synthetic branching point. These chiral products are expected to be useful in future synthetic efforts, and we believe that the convenient fragmentation of β -cyclopropyl ketones will also find applications outside of carene-derived systems.

A8.4 EXPERIMENTAL SECTION

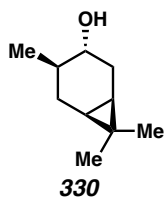
A8.4.1 MATERIALS AND METHODS

Unless otherwise stated, reactions were performed in flame-dried glassware under an argon or nitrogen atmosphere using dry, deoxygenated solvents. Solvents were dried by passage through an activated alumina column under argon.¹⁶ (+)-3-Carene was purchased from TCI and used as received, *N*-bromosuccinimide (NBS) was recrystallized from boiling water prior to use, trimethylsilyl chloride (TMSCl) was distilled under argon prior to use, all other reagents and solvents were purchased from various commercial suppliers

and used as received. Reaction progress was monitored by thin-layer chromatography (TLC) or Agilent 1290 UHPLC-MS. TLC was performed using E. Merck silica gel 60 F254 precoated glass plates (0.25 mm) and visualized by UV fluorescence quenching or *p*-anisaldehyde staining. Silicycle SiliaFlash® P60 Academic Silica gel (particle size 40–63 μm) or Sigma-Aldrich aluminum oxide (activated, neutral, Brockmann Activity I) were used for flash chromatography. Preparative HPLC was performed on an Agilent 1200 preparative HPLC system using a 9.4 x 250 mm Eclipse XDB-C18 column. A water/MeCN gradient was used as the mobile phase and the compounds were detected at 230.8 nm and 254.4 nm. Analytical SFC was performed with a Mettler SFC supercritical CO_2 analytical chromatography system utilizing a Chiralpak AD-H column (4.6 mm x 25 cm) obtained from Daicel Chemical Industries, Ltd. ^1H NMR spectra were recorded on Varian Inova 500 MHz, Varian 400 MHz, and Bruker 400 MHz spectrometers and are reported relative to residual CHCl_3 (δ 7.26 ppm). ^{13}C NMR spectra were recorded on a Varian Inova 500 MHz spectrometer (125 MHz), a Varian 400 MHz spectrometer (100 MHz), and Bruker 400 MHz spectrometers (100 MHz) and are reported relative to CHCl_3 (δ 77.16 ppm). Data for ^1H NMR are reported as follows: chemical shift (δ ppm) (multiplicity, coupling constant (Hz), integration). Multiplicities are reported as follows: s = singlet, d = doublet, t = triplet, q = quartet, p = pentet, sept = septuplet, m = multiplet, br s = broad singlet, br d = broad doublet. Data for ^{13}C NMR are reported in terms of chemical shifts (δ ppm) Some reported spectra include minor solvent impurities of water (δ 1.56 ppm), ethyl acetate (δ 4.12, 2.05, 1.26 ppm), methylene chloride (δ 5.30 ppm), acetone (δ 2.17 ppm), grease (δ 1.26, 0.86 ppm), and/or silicon grease (δ 0.07 ppm), which do not impact product assignments. IR spectra were obtained by use of a Perkin Elmer Spectrum BXII spectrometer using thin

films deposited on NaCl plates and reported in frequency of absorption (cm^{-1}). Optical rotations were measured with a Jasco P-2000 polarimeter operating on the sodium D-line (589 nm), using a 100 mm path-length cell. High-resolution mass spectrometry was performed by the Multi User Mass Spectrometry Laboratory at the California Institute of Technology using a JMS-T200 GC AccuTOF GC-Alpha mass spectrometer.

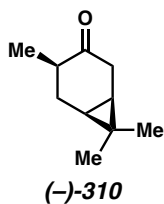
A8.4.2 EXPERIMENTAL PROCEDURES



(1R,3R,4R,6S)-4,7,7-trimethylbicyclo[4.1.0]heptan-3-ol (330)

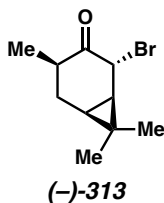
The procedure was adapted from the literature:⁶ To a dried 500 mL round bottom flask was added NaBH_4 (6.94 g, 183 mmol, 1.0 equiv), THF (60 mL), and (+)-3-carene (25 g, 180 mmol, 1.0 equiv). The reaction flask was cooled to 0 °C in an ice bath, and $\text{BF}_3 \cdot \text{OEt}_2$ (26 g, 160 mmol, 1.0 equiv) was added dropwise over 30 min. The reaction was stirred at this temperature for 4 h, after which the reaction was cooled to -10 °C and aq. NaOH (3 M, 60 mL) was added dropwise over 40 min. H_2O_2 (30 wt %, 100 mL) was then added dropwise over 1 h, and the reaction allowed to warm to 20 °C. The solution was concentrated under reduced pressure to remove THF, and the aqueous layer was extracted with CH_2Cl_2 (3 x 40 mL). The combined organic layers were washed with water (100 mL) and brine (100 mL), dried over Na_2SO_4 , and filtered. Concentration under reduced pressure afforded an oil that was distilled under vacuum (0.5 mmHg, 150 °C) to afford the title compound (22 g, 78%) as a colorless oil that solidified upon cooling. ^1H NMR (CDCl_3 , 400 MHz): δ = 3.07 (ddd, J = 10.3, 9.3, 6.6 Hz, 1H), 2.10 (ddd, J = 14.1, 6.6, 0.9 Hz, 1H),

2.01 – 1.92 (m, 1H), 1.61 – 1.51 (m, 1H), 1.29 – 1.17 (m, 1H), 0.97 (s, 3H), 0.93 (d, $J = 6.4$ Hz, 3H), 0.90 (s, 3H), 0.86 – 0.77 (m, 1H), 0.75 – 0.67 (m, 2H). Spectral data are in agreement with previously reported values.¹⁷



(1R,4R,6S)-4,7,7-trimethylbicyclo[4.1.0]heptan-3-one (310)

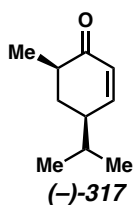
A procedure from the literature⁷ was modified as follows: To a 1 L round bottom flask was added alcohol **330** (20 g, 130 mmol, 1.0 equiv) and Et₂O (280 mL). The solution was cooled in an ice bath, and Brown–Garg (BG) reagent^{18,19} (70 mL) was added dropwise over 20 min with vigorous stirring, maintaining the reaction temperature below 20 °C. The ice bath was then removed, and the solution stirred for 1 h. Additional BG reagent (70 mL) was added slowly, and the reaction was left to stir for 18 h. The organic layer was then separated, and the aqueous layer was extracted with Et₂O (2 x 50 mL). The combined organic layers were washed with brine (100 mL), dried over Na₂SO₄, filtered, and concentrated under reduced pressure. The residual oil was distilled under vacuum (0.5 mmHg, 130 °C) to yield the title compound (12.8 g, 65%) as a fragrant, yellow oil. ¹H NMR (CDCl₃, 400 MHz): $\delta = 2.52$ (ddd, $J = 18.0, 8.4, 0.9$ Hz, 1H), 2.41 – 2.32 (m, 1H), 2.32 – 2.25 (m, 2H), 1.31 – 1.19 (m, 1H), 1.07 (m, 1H), 1.04 (s, 3H), 1.02 – 0.97 (m, 1H), 0.95 (d, $J = 6.4$ Hz, 3H), 0.84 (s, 3H). Spectral data are in agreement with previously reported values.⁷



(1R,2R,4R,6S)-2-bromo-4,7,7-trimethylbicyclo[4.1.0]heptan-3-one (313)

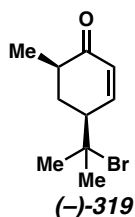
To a flame-dried 250 mL Schlenk flask was added THF (29 mL) and diisopropylamine (1.59 g, 15.8 mmol, 1.2 equiv). The solution was cooled to $-78\text{ }^{\circ}\text{C}$ and *n*-butyllithium (2.5 M in hexanes, 5.5 mL, 13.8 mmol, 1.05 equiv) was added dropwise over 8 min. After stirring for 30 min, a solution of ketone **310** (2 g, 13.1 mmol, 1.0 equiv) in THF (2 mL) was added dropwise over 5 min and the reaction mixture allowed to stir at $-78\text{ }^{\circ}\text{C}$ for 1.5 h. TMSCl (2.14 g, 19.7 mmol, 1.5 equiv) was added and the reaction was allowed to warm to $0\text{ }^{\circ}\text{C}$ in an ice bath, and further stirred at $0\text{ }^{\circ}\text{C}$ for 1 h. The reaction flask was then wrapped in Al foil to exclude light and NBS (3.5 g, 19.7 mmol, 1.5 equiv) was added in a single portion. After stirring for a further 30 min in the dark, the reaction was quenched* with saturated aq. NaHCO_3 (50 mL) and extracted with Et_2O (2 x 20 mL). The combined organic layers were washed with water (2 x 40 mL) and brine (40 mL), dried over Na_2SO_4 , and filtered. The solution was concentrated under reduced pressure to yield 2.1 g of residue. A small amount of this residue (255 mg) was purified *via* flash chromatography on neutral alumina (hexanes) to yield **313** (173 mg, extrapolated to 48% overall yield) as an unstable straw-colored oil which crystallized when pure. **313** was used immediately or stored as a frozen solution in benzene. ^1H NMR (CDCl_3 , 400 MHz): δ = 4.37 (d, J = 1.2 Hz, 1H), 3.22 (ddq, J = 13.0, 7.7, 6.5 Hz, 1H), 2.45 (ddd, J = 14.7, 9.7, 7.6 Hz, 1H), 1.52 (dd, J = 8.6, 1.3 Hz, 1H), 1.40 (ddd, J = 14.8, 13.0, 4.3 Hz, 1H), 1.18 (td, J = 8.9, 4.2 Hz, 1H), 1.07 (s, 3H), 1.00 (d, J = 6.5 Hz, 3H), 0.84 (s, 3H); $^{13}\text{C}\{^1\text{H}\}$ NMR

(CDCl₃, 100 MHz): δ = 209.7, 48.2, 36.2, 33.7, 30.7, 28.2, 22.2, 20.5, 14.7, 14.1; IR (Neat Film, NaCl) 2933, 1719, 1455, 1378, 1162, 848, 776, 622 cm⁻¹; HRMS (FI+): m/z calc'd for C₁₀H₁₅OBr [M]⁺: 230.0301 found, 230.0308; [α]_D^{22.16} -278.99 (c 1.0, CHCl₃). *Due to the light-sensitivity of the product, it is recommended to perform the work-up in the dark.



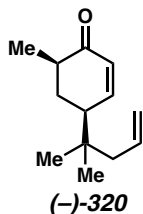
(4R,6R)-4-isopropyl-6-methylcyclohex-2-en-1-one (**317**)

AIBN (20 mg, 0.121 mmol, 0.2 equiv) was loaded into a 20 mL vial with septum cap. A solution of bromide **313** (140 mg, 0.606 mmol, 1.0 equiv) and Bu₃SnH (353 mg, 1.21 mmol, 2.0 equiv) in anhydrous benzene (6 mL) was added. The reaction mixture was stirred at 86 °C for 1 h, after which the solvent was removed under reduced pressure. The residue was purified by flash chromatography on silica (0–10% EtOAc in hexanes) to afford the title compound (82 mg, 89%) as a colorless oil. The resulting product is pure enough for most purposes, but a sample of higher purity for analysis was obtained by distillation. ¹H NMR (CDCl₃, 400 MHz): δ = 6.82 (dt, J = 10.2, 2.2 Hz, 1H), 6.01 (dd, J = 10.2, 3.0 Hz, 1H), 2.39 (m, 2H), 1.96 (dtd, J = 13.0, 4.5, 2.0 Hz, 1H), 1.80 (pd, J = 6.9, 4.8 Hz, 1H), 1.54 – 1.49 (ddd, J = 13.9, 13.0, 11.4 Hz, 1H), 1.15 (d, J = 6.6, 3H), 0.96 (d, J = 7.1, 3H), 0.94 (d, J = 6.9, 3H); ¹³C {¹H} NMR (CDCl₃, 100 MHz): δ = 202.7, 153.5, 129.7, 43.5, 41.7, 34.2, 31.8, 19.6, 19.3, 15.2; IR (Neat Film, NaCl) 2959, 2872, 1684, 1458, 1386, 1219, 803 cm⁻¹; HRMS (FI+): m/z calc'd for C₁₀H₁₆O [M]⁺: 152.1196 found, 152.1198; [α]_D^{22.31} -35.30 (c 1.0, CHCl₃).



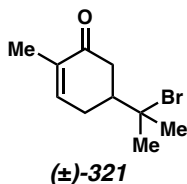
(4S,6R)-4-(2-bromopropan-2-yl)-6-methylcyclohex-2-en-1-one (319).

To a 4 mL vial was added bromide **313** (36 mg, 0.156 mmol, 1.0 equiv) in anhydrous benzene (1.5 mL). To this solution was added allyltributyltin (21 mg, 0.062 mmol, 0.4 equiv) and AIBN (5 mg, 0.03 mmol, 0.2 equiv). The vial was sealed, and the reaction mixture stirred at 86 °C for 4 h. The reaction was then allowed to cool to 20 °C and concentrated under reduced pressure. The residue was purified via flash chromatography on silica (5–10% EtOAc in hexanes) to afford the title compound (26 mg, 72%) as a colorless oil. ^1H NMR (CDCl_3 , 400 MHz): δ = 7.09 (dt, J = 10.3, 2.1 Hz, 1H), 6.09 (dd, J = 10.3, 2.8 Hz, 1H), 2.85 (dddd, J = 11.4, 4.6, 2.9, 2.0 Hz, 1H), 2.41 (dq, J = 13.4, 6.7, 4.5 Hz, 1H), 2.24 (dtd, J = 12.7, 4.4, 2.2 Hz, 1H), 1.89 (s, 3H), 1.74 (s, 3H), 1.67 – 1.58 (m, 1H), 1.17 (d, J = 6.7 Hz, 3H); $^{13}\text{C}\{^1\text{H}\}$ NMR (CDCl_3 , 100 MHz): δ = 201.3, 150.1, 130.2, 68.3, 50.5, 41.0, 34.2, 32.9, 30.9, 15.1; IR (Neat Film, NaCl) 2967, 1682, 1455, 1372, 1213, 1125, 803, 644, 601 cm^{-1} ; HRMS (FI+): m/z calc'd for $\text{C}_{10}\text{H}_{15}\text{OBr}$ $[\text{M}]^+$: 230.0301, found 230.0300; $[\alpha]_{\text{D}}^{22.13}$ -62.67 (c 1.0, CHCl_3).

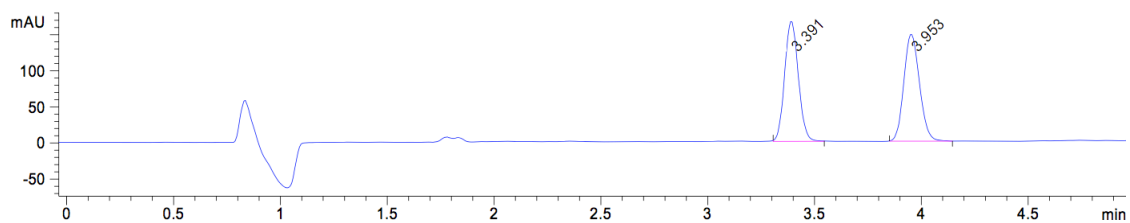


(4S,6R)-6-methyl-4-(2-methylpent-4-en-2-yl)cyclohex-2-en-1-one (320).

To a 20 mL vial was added bromide **319** (45 mg, 0.195 mmol, 1.0 equiv) in anhydrous benzene (4 mL). To this was added allyltributyltin (390 mg, 1.17 mmol, 6.0 equiv) and AIBN (6.4 mg, 0.039 mmol, 0.2 equiv). The vial was sealed, and the reaction mixture stirred at 86 °C for 48 h. The solution was concentrated under reduced pressure and the residue purified *via* flash chromatography on silica (5% EtOAc in hexanes) to afford the title compound (24 mg, 63%) as a colorless oil. The compound is pure enough for most purposes, but a sample of higher purity for analysis was obtained by preparative HPLC (60–80% MeCN in H₂O over 5 min at 12 mL/min). ¹H NMR (CDCl₃, 400 MHz): δ = 6.96 (dt, J = 10.3, 2.1 Hz, 1H), 6.03 (dd, J = 10.3, 3.0 Hz, 1H), 5.83 (ddt, J = 16.8, 10.2, 7.4 Hz, 1H), 5.13 – 5.02 (m, 2H), 2.36 (m, 2H), 2.11 – 2.06 (m, 2H), 2.03 (ddq, J = 11.0, 4.4, 2.2 Hz, 1H), 1.55 – 1.46 (m, 1H), 1.15 (d, J = 6.7 Hz, 3H), 0.95 (s, 3H), 0.92 (s, 3H); ¹³C{¹H} NMR (CDCl₃, 100 MHz): δ = 202.4, 151.7, 134.7, 130.0, 118.0, 45.7, 44.5, 41.8, 35.7, 33.1, 24.9, 24.6, 15.3; IR (Neat Film, NaCl) 2961, 1683, 1385, 1222, 914, 802 cm⁻¹; HRMS (FI+): m/z calc'd for C₁₃H₂₀O [M]⁺: 192.1509, found 192.1509; [α]_D^{22.49} –25.44 (c 0.25, CHCl₃).

**(S)-5-(2-bromopropan-2-yl)-2-methylcyclohex-2-en-1-one (321)**

To a 4 mL vial was added bromide **313** (86 mg, 0.372 mmol, 1.0 equiv) in anhydrous benzene (1.6 mL). The vial was sealed, and the reaction mixture stirred at 86 °C for 25 min. The solution was concentrated under reduced pressure and the residue was purified by flash chromatography on neutral alumina (5% EtOAc in hexanes) to afford the title compound (63 mg, 73%) as a colorless oil. ^1H NMR (CDCl_3 , 400 MHz): δ = 6.75 (ddq, J = 5.4, 2.8, 1.4 Hz, 1H), 2.74 (ddd, J = 16.0, 3.7, 1.8 Hz, 1H), 2.59 (dddt, J = 18.2, 6.2, 4.6, 1.5 Hz, 1H), 2.41 (m, 2H), 2.05 (dddd, J = 13.5, 11.1, 4.6, 3.7 Hz, 1H), 1.79 (m, 3H), 1.79 (s, 3H), 1.77 (s, 3H); $^{13}\text{C}\{^1\text{H}\}$ NMR (CDCl_3 , 100 MHz): δ = 199.2, 144.3, 135.4, 70.1, 48.3, 41.2, 32.5, 32.2, 29.2, 15.7; IR (Neat Film, NaCl) 2972, 1674, 1451, 1370, 1254, 1103, 1062, 904, 690 cm^{-1} ; HRMS (FI+): m/z calc'd for $\text{C}_{10}\text{H}_{15}\text{OBr}$ $[\text{M}]^+$: 230.0301, found 230.0302. **321** was determined to be racemic by chiral SFC analysis (AD-H, EtOH/ CO_2 = 5/95, flow rate = 3.5 mL/min, λ = 210 nm) t_{R} = 3.39, 3.95.

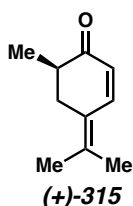


Peak #	RetTime [min]	Type	Width [min]	Area [mAU*s]	Height [mAU]	Area %
1	3.391	BB	0.0683	742.96808	165.59497	49.6580
2	3.953	BB	0.0839	753.20081	146.78207	50.3420

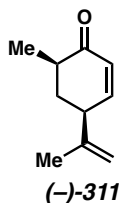
Totals : 1496.16888 312.37704

Procedure for the Ag^I-mediated fragmentation of bromide 313.

To a solution of the indicated silver salt (0.182 mmol, 2.1 equiv) in THF (0.6 mL) was added a solution of bromoketone **313** (20 mg, 0.0865 mmol, 1.0 equiv) in THF (0.3 mL, 0.1 M total concentration) dropwise over 1 min with stirring at 20 °C. In all cases, a thick precipitate immediately formed. Stirring was continued for an additional 20 min, after which the reaction mixture was quenched with saturated aq. NaHCO₃ (1 mL) and filtered through a plug of celite with EtOAc. The layers were separated and the organic layer was dried with Na₂SO₄, filtered, and concentrated under reduced pressure to provide a crude product that was purified by silica gel flash chromatography (5% EtOAc in hexanes).

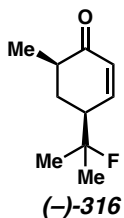
**(R)-6-methyl-4-(propan-2-ylidene)cyclohex-2-en-1-one (315)**

8.7 mg (67%) yield with AgClO₄; 7.1 mg (55%) yield with AgOTf; ¹H NMR (CDCl₃, 400 MHz): δ = 7.42 (dd, J = 10.1, 0.9 Hz, 1H), 5.80 (d, J = 10.0 Hz, 1H), 2.84 (dd, J = 14.6, 5.4 Hz, 1H), 2.48 (dq, J = 10.9, 6.8, 5.4 Hz, 1H), 2.39 – 2.27 (m, 1H), 1.93 (dd, J = 1.6, 0.8 Hz, 3H), 1.90 (s, 3H), 1.14 (d, J = 6.8 Hz, 3H); ¹³C {¹H} NMR (CDCl₃, 100 MHz): δ = 203.0, 143.1, 139.4, 126.7, 124.0, 40.9, 34.1, 21.9, 20.8, 15.9; IR (Neat Film, NaCl) 2927, 1672, 1623, 1453, 1216, 812 cm⁻¹; HRMS (FI+): m/z calc'd for C₁₀H₁₄O [M]⁺: 150.1039, found 150.1039; [α]_D^{21.95} +137.36 (c 0.5, CHCl₃).



(4S,6R)-6-methyl-4-(prop-1-en-2-yl)cyclohex-2-en-1-one (311)

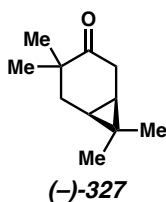
Isopropenyl enone **311** was observed in trace quantities in the Ag^I-mediated fragmentation of bromide **313**. 0.7 mg (5% yield) with AgBF₄. A sample suitable for characterization, albeit containing a minor impurity, could be obtained by automated silica gel flash chromatography (Teledyne ISCO, 0→10% EtOAc in hexanes) on a 100 mg scale. ¹H NMR (CDCl₃, 400 MHz): δ = 6.81 (dt, J = 10.1, 2.0 Hz, 1H), 6.03 (dd, J = 10.1, 3.0 Hz, 1H), 4.86 (p, J = 1.5 Hz, 1H), 4.81 (dq, J = 1.6, 0.8 Hz, 1H), 3.21 – 3.12 (m, 1H), 2.42 (dq, J = 13.5, 6.7, 4.5 Hz, 1H), 2.13 (dtd, J = 13.0, 4.5, 2.0 Hz, 1H), 1.77 (dd, J = 1.4, 0.9 Hz, 3H), 1.72 – 1.61 (m, 1H), 1.15 (d, J = 6.6 Hz, 3H); ¹³C {¹H} NMR (CDCl₃, 100 MHz): δ = 202.0, 152.5, 146.9, 129.6, 112.0, 45.2, 41.8, 37.7, 20.8, 15.1; IR (Neat Film, NaCl) 2964, 2934, 2862, 1683, 1649, 1454, 1376, 1215, 1188, 1118, 895, 804 cm⁻¹; HRMS (FI+): m/z calc'd for C₁₀H₁₄O [M]⁺: 150.1039, found 150.1030; [α]_D^{21,23} -92.59 (c 0.33, CHCl₃).



(4S,6R)-4-(2-fluoropropan-2-yl)-6-methylcyclohex-2-en-1-one (316)

6.6 mg of a 3.4:1 (w/w) mixture of fluoride **316** and dienone **315** was isolated, corresponding to a 35% yield of fluoride **316**. While this mixture was inseparable by silica gel flash chromatography, an analytical sample of **316** was isolated by reverse-phase

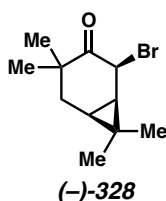
preparative HPLC (50–70% MeCN in H₂O over 3.5 min at 10 mL/min); ¹H NMR (CDCl₃, 400 MHz): δ = 6.96 (dt, J = 10.3, 2.0 Hz, 1H), 6.09 (dd, J = 10.3, 3.0 Hz, 1H), 2.88 – 2.75 (m, 1H), 2.41 (dq, J = 13.5, 6.7, 4.6 Hz, 1H), 2.08 (dtdd, J = 12.8, 4.5, 2.1, 0.9 Hz, 1H), 1.53 – 1.45 (m, 1H), 1.42 (d, J = 22.0 Hz, 3H), 1.32 (d, J = 22.0 Hz, 3H), 1.16 (d, J = 6.7 Hz, 3H); ¹³C {¹H} NMR (CDCl₃, 100 MHz): δ = 201.6, 148.9, 148.8, 130.5, 97.3, 95.6, 47.4, 47.2, 41.3, 33.4, 33.4, 25.6, 25.4, 23.7, 23.4, 15.1; IR (Neat Film, NaCl) 2930, 1682, 1453, 1376, 1219, 878, 812, 522 cm⁻¹; HRMS (FI+): m/z calc'd for C₁₀H₁₅FO [M]⁺: 170.1101, found 170.1099; [α]_D^{21.82} –37.10 (c 0.167, CHCl₃).



(1R,6S)-4,4,7,7-tetramethylbicyclo[4.1.0]heptan-3-one (327)

To a rapidly stirred suspension of NaH (60% dispersion in mineral oil, 289 mg, 7.23 mmol, 1.1 equiv) in THF (5.6 mL, 1 M final substrate concentration) in a 50 mL 2-neck flask equipped with a reflux condenser was added ketone **310** (1.00 g, 6.57 mmol, 1.0 equiv) through the top of the condenser. Additional THF (1 mL) was used to rinse the ketone into the reaction mixture. The suspension was then heated to reflux in an oil bath and stirred for 1.5 h. Then, HMDS (0.21 mL, 0.986 mmol, 0.15 equiv) was added through the top of the condenser and the reaction mixture was stirred under reflux for an additional 25 min. The flask was then cooled to 0 °C in an ice bath, and the reflux condenser was replaced with a septum. MeI (0.45 mL, 7.23 mmol, 1.1 equiv) was added dropwise, after which the ice bath was removed. After stirring at 20 °C for 17 h, the reaction mixture was quenched with H₂O (20 mL), the layers were separated, and the aqueous layer was

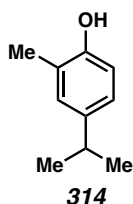
extracted with Et₂O (4x10 mL). The combined organic layers were dried over MgSO₄, concentrated under reduced pressure, and purified *via* silica gel flash chromatography (10% Et₂O in hexanes). The resulting oil was purified again by automated silica gel flash chromatography (Teledyne ISCO, 0→10% EtOAc in hexanes) to provide dimethyl ketone **327** (361 mg, 29% yield desired isomer) as a fragrant, colorless oil containing 11% of an inseparable isomeric impurity; ¹H NMR (CDCl₃, 400 MHz): δ = 2.65 – 2.52 (m, 1H), 2.19 – 2.07 (m, 1H), 1.94 (ddt, J = 14.9, 9.3, 1.4 Hz, 1H), 1.39 (ddt, J = 14.9, 6.2, 0.9 Hz, 1H), 1.22 (s, 3H), 1.11 – 1.06 (m, 1H), 1.04 (s, 3H), 0.94 (s, 3H), 0.90 – 0.80 (m, 4H); ¹³C {¹H} NMR (CDCl₃, 100 MHz): δ = 218.9, 42.4, 35.1, 34.6, 28.0, 24.8, 24.3, 22.4, 19.5, 18.2, 14.9; IR (Neat Film, NaCl) 2930, 2867, 1709, 1460, 1412, 1379, 1111, 1051, 986, 808 cm⁻¹; m/z calc'd for C₁₁H₁₈O [M]⁺: 166.1352, found 166.1358; [α]_D^{21.48} –68.91 (c 1.0, CHCl₃).



(1R,2S,6S)-2-bromo-4,4,7,7-tetramethylbicyclo[4.1.0]heptan-3-one (328)

To a solution of diisopropylamine (0.10 mL, 0.722 mmol, 1.2 equiv) in THF (1.3 mL, 0.45 M substrate concentration) was added *n*-butyllithium (2.5 M in hexanes, 0.25 mL, 0.632 mmol, 1.05 equiv) dropwise at –78 °C. The solution was allowed to warm to 0 °C and immediately cooled back to –78 °C, whereafter ketone **327** (100 mg, 0.602 mmol, 1.0 equiv) was added dropwise and the solution stirred at –78 °C for 1 h. TMSCl (0.11 mL, 0.903 mmol, 1.5 equiv) was added and the reaction was allowed to warm to 0 °C in an ice bath and stirred for an additional 45 min. The reaction was then protected from light and NBS (161 mg, 0.903 mmol, 1.5 equiv) was added in one portion. After stirring for a further

30 min in the dark, the reaction was quenched with saturated aq. NaHCO_3 (1 mL), the layers were separated, and the aqueous layer was extracted with Et_2O (1 mL). The combined organic layers were washed with water (1 mL), dried over Na_2SO_4 , and concentrated under reduced pressure. The crude product was purified *via* silica gel flash chromatography to afford α -bromoketone **328** (126 mg, 89% yield desired isomer) as a white crystalline solid containing 8% of an inseparable isomeric impurity; ^1H NMR (CDCl_3 , 400 MHz): δ = 4.23 (dd, J = 6.0, 0.8 Hz, 1H), 1.91 (ddd, J = 15.1, 8.3, 0.9 Hz, 1H), 1.44 (ddd, J = 15.0, 8.4, 0.8 Hz, 1H), 1.40 – 1.35 (m, 4H), 1.13 (s, 3H), 1.11 – 1.05 (m, 4H), 1.03 (s, 3H); $^{13}\text{C}\{^1\text{H}\}$ NMR (CDCl_3 , 100 MHz): δ = 209.2, 49.2, 44.4, 33.7, 30.4, 27.7, 26.6, 26.0, 21.8, 21.5, 14.2; IR (Neat Film, NaCl) 2954, 2869, 1721, 1462, 1376, 1244, 1054, 911, 742 cm^{-1} ; m/z calc'd for $\text{C}_{11}\text{H}_{17}\text{OBr}$ $[\text{M}]^+$: 244.0457, found 244.0459; $[\alpha]_{\text{D}}^{21.55}$ -148.50 (c 1.0, CHCl_3).



4-isopropyl-2-methylphenol (**314**)

313 (39 mg, 0.17 mmol) was left in a sealed 4 mL vial under ambient conditions for 24 h. During this time, the oil was found to spontaneously decompose with notable exotherm²⁰ and change in consistency. The blackened tar was purified via flash chromatography on silica (5% EtOAc in hexanes) to afford **314** (8 mg, 32%) as a colorless oil. ^1H NMR (CDCl_3 , 400 MHz): δ = 6.99 (d, J = 2.3 Hz, 1H), 6.94 (dd, J = 8.1, 2.2 Hz, 1H), 6.71 (d, J = 8.1 Hz, 1H), 4.62 (s, 1H), 2.83 (hept, J = 7.0 Hz, 1H), 2.26 (s, 3H), 1.23 (d, J = 6.9 Hz, 6H). Spectral data are in agreement with previously reported values.²¹

A8.5 REFERENCES AND NOTES

- (1) Nugent, W. A.; Rajanbabu, T. V.; Burk, M. J. Beyond Nature's Chiral Pool: Enantioselective Catalysis in Industry. *Science* **1993**, *259*, 479–483.
- (2) Brill, Z. G.; Condakes, M. L.; Ting, C. P.; Maimone, T. J. Navigating the Chiral Pool in the Total Synthesis of Complex Terpene Natural Products. *Chem. Rev.* **2017**, *117*, 11753–11795.
- (3) Carreira, E. M.; Yamamoto, H. *Comprehensive Chirality*; 2012.
- (4) Curlat, S. Recent studies of (+)-3-carene transformations with the retention of the native framework. *Chem. J. Mold.* **2019**, *14*, 32–55.
- (5) Ohloff, G.; Giersch, W. Säurekatalysierte Isomerisierung von α,β -Cyclopropyl-Oxiranen. *Helv. Chim. Acta* **1968**, *51*, 1328–1342.
- (6) Kilbas, B.; Azizoglu, A.; Balci, M. Incorporation of an Allene Unit into α -Pinene via β -Elimination. *Helv. Chim. Acta* **2006**, *89*, 1449–1456.
- (7) Kozioł, A.; Frątczak, J.; Grela, E.; Szczepanik, M.; Gabryś, B.; Danciewicz, K.; Lochyński, S. Synthesis and Biological Activity of New Derivatives with the Preserved Carane System. *Nat. Prod. Res.* **2020**, *34*, 1399–1403.
- (8) Zhang, X.; Cai, X.; Huang, B.; Guo, L.; Gao, Z.; Jia, Y. Enantioselective Total Syntheses of Pallambins A–D. *Angew. Chem. Int. Ed.* **2019**, *58*, 13380–13384.
- (9) Wu, K. K. Y. The Diels-Alder reaction in the synthesis of qinghaosu analogues. PhD Thesis, Hong Kong University of Science and Technology, 2002.

- (10) Bruncko, M.; Crich, D.; Samy, R. Chemistry of Cyclic Tautomers of Tryptophan: Formation of a Quaternary Center at C3a and Total Synthesis of the Marine Alkaloid (+)-Ent-Debromoflustramine B. *J. Org. Chem.* **1994**, *59*, 5543–5549.
- (11) DFT Calculations Were Carried out with the ORCA Program (See Supporting Information) at the M06-2X/Def2-TZVPP/SMD(Benzene)//M06-2X/Def2-TZVP Level of Theory.
- (12) Neese, F. The ORCA Program System. *WIREs Computational Molecular Science* **2012**, *2*, 73–78.
- (13) Neese, F. Software Update: The ORCA Program System, Version 4.0. *WIREs Computational Molecular Science* **2018**, *8*, e1327.
- (14) Marvell, E. *Thermal Electrocyclic Reactions*; Elsevier, 2012; pp 283–288.
- (15) Davies, A. G. Radical Chemistry of Tin. In *Chemistry of Tin*; Smith, P. J., Ed.; Springer Netherlands: Dordrecht, 1998; pp 265–289.
- (16) Pangborn, A. B.; Giardello, M. A.; Grubbs, R. H.; Rosen, R. K.; Timmers, F. J. Safe and Convenient Procedure for Solvent Purification. *Organometallics* **1996**, *15*, 1518–1520.
- (17) Ramachandran, P. V.; Drolet, M. P.; Kulkarni, A. S. A Non-Dissociative Open-Flask Hydroboration with Ammonia Borane: Ready Synthesis of Ammonia–Trialkylboranes and Aminodialkylboranes. *Chem. Commun.* **2016**, *52*, 11897–11900.
- (18) Brown–Garg reagent was prepared as follows: H₂SO₄ (21.2 mL) was added to Na₂Cr₂O₇ (28 g). Water was slowly added to this slurry until a final volume of 141

mL was attained. The mixture was stirred until homogeneous and used immediately.

- (19) Brown, H. C.; Garg, C. P.; Liu, K.-T. Oxidation of secondary alcohols in diethyl ether with aqueous chromic acid. Convenient procedure for the preparation of ketones in high epimeric purity. *J. Org. Chem.* **1971**, 36, 387–390.
- (20) On large scales (>200 mg) the exotherm and release of HBr can lead to dangerous pressure build up, this can be avoided by leaving the vial open to atmosphere.
- (21) Kamat, S. P.; D'Souza, A. M.; Paknikar, S. K. Sodium Metaperiodate Oxidation of Isocarvacrol. *J. Chem. Res.* **2003**, 395–397.

APPENDIX 9

Notebook Cross-Reference for New Compounds

Table A9.1. Notebook cross-reference for Chapter 1.

compound	¹ H NMR (instrument)	¹³ C NMR (instrument)	yield/procedure
20a	AWS-XII-77 (Florence)	AWS-XII-77 (Florence)	ZPS-III-115
20b	AWS-XII-65 (Florence)	AWS-XII-65 (Florence)	ZPS-III-117
20c	ZPS-I-297 (Florence)	ZPS-I-297 (Florence)	ZPS-III-119
20d	ZPS-I-279 (Florence)	ZPS-I-279 (Florence)	ZPS-I-279
20e	ZPS-II-83 (Florence)	ZPS-II-83 (Florence)	ZPS-II-83
20f	ZPS-II-13 (Florence)	ZPS-II-13 (Florence)	ZPS-II-13
20g	AWS-XIV-61 (Florence)	AWS-XIV-61 (Florence)	AWS-XIV-61
20h	ZPS-II-65 (Florence)	ZPS-II-65 (Florence)	ZPS-III-121
20i	AWS-XIV-63 (Florence)	AWS-XIV-63 (Florence)	AWS-XIV-63
20j	ZPS-II-67 (Florence)	ZPS-II-67 (Florence)	ZPS-II-67
20k	ZPS-II-69 (Florence)	ZPS-II-69 (Florence)	ZPS-II-101
20l	AWS-XIV-13 (Florence)	AWS-XIV-13 (Florence)	AWS-XIV-13
55	AWS-XII-47 (Florence)	AWS-XII-47 (Florence)	AWS-XII-47
56	ZPS-I-287 (Florence)	ZPS-I-287 (Florence)	ZPS-I-287
57	AWS-XII-287 (Florence)	AWS-XII-287 (Florence)	AWS-XII-287
18a	KY81 (Indy, zsercel2 folder)	KY81 (Indy, zsercel2 folder)	AWS-XII-49, 51, 67
18b	ZPS-I-289 (Florence)	ZPS-I-289 (Florence)	ZPS-I-289
18c	AWS-XII-289 (Florence)	AWS-XII-289 (Florence)	AWS-XII-289
19a	AWS-XII-55 (Florence)	AWS-XII-55 (Florence)	ZPS-I-241
19b	AWS-XII-53 (Florence)	AWS-XII-53 (Florence)	AWS-XII-53, 59
19c	ZPS-I-293 (Florence)	ZPS-I-293 (Florence)	ZPS-I-293
19d	AWS-XII-291 (Florence)	AWS-XII-291 (Florence)	AWS-XII-291
19e	ZPS-II-75 (Indy)	ZPS-II-75 (Indy)	ZPS-II-75
19f	ZPS-III-111 (Indy)	ZPS-III-111 (Indy)	ZPS-III-111
19g	AWS-XIV-55 (Florence)	AWS-XIV-55 (Florence)	AWS-XIV-55
19h	ZPS-II-51 (Florence)	ZPS-II-51 (Florence)	ZPS-II-51
19i	AWS-XIV-53 (Indy)	AWS-XIV-53 (Indy)	AWS-XIV-53
19j	ZPS-II-53 (Indy)	ZPS-II-53 (Indy)	ZPS-II-53
19k	ZPS-II-61 (Florence)	ZPS-II-61 (Florence)	ZPS-II-61
19l	AWS-XII-57 (Florence)	AWS-XII-57 (Florence)	AWS-XII-57
21	AWS-XIV-171 (Florence)	AWS-XIV-171 (Florence)	AWS-XIV-171

Table A9.2. Notebook cross-reference for Chapter 1 (continued).

compound	¹ H NMR (instrument)	¹³ C NMR (instrument)	yield/procedure
23	ZPS-III-127 (Florence)	ZPS-III-127 (Florence)	ZPS-III-127
25	AWS-XIV-199 (Florence)	AWS-XIV-199 (Florence)	AWS-XIV-199
35a	ZPS-III-159 (Florence)	ZPS-III-159 (Florence)	ZPS-III-159
35b	ZPS-III-69 (Florence)	ZPS-III-69 (Florence)	ZPS-III-69
35c	AWS-XIV-123 (Florence)	AWS-XIV-123 (Florence)	ZPS-IV-65
35d	ZPS-III-155 (Florence)	ZPS-III-155 (Florence)	ZPS-III-155
35e	ZPS-III-97 (Florence)	ZPS-III-97 (Florence)	ZPS-III-97
35f	ZPS-III-287 (Florence)	ZPS-III-287 (Florence)	ZPS-III-287
35g	ZPS-III-141 (Florence)	ZPS-III-141 (Florence)	ZPS-III-141
35h	ZPS-II-191 (Florence)	ZPS-II-191 (Florence)	ZPS-II-191
35i	ZPS-V-43 (Florence)	ZPS-V-43 (Florence)	ZPS-V-43
35j	ZPS-II-239 (Florence)	ZPS-II-239 (Florence)	ZPS-II-239
35k	ZPS-III-303 (Florence)	ZPS-III-303 (Florence)	ZPS-III-303
31	ZPS-III-199 (Florence)	ZPS-III-259B (Florence)	ZPS-III-285
32	AWS-XIV-23 (Florence)	AWS-XIV-23 (Florence)	ZPS-III-289
33	AWS-XIV-115 (Florence)	AWS-XIV-115 (Florence)	ZPS-IV-25
60	ZPS-V-277 (Florence)	ZPS-V-277 (Florence)	ZPS-V-277
34a	AWS-XIV-125 (Florence)	AWS-XIV-125 (Florence)	ZPS-IV-83
34b	ZPS-III-43 (Florence)	ZPS-III-43 (Florence)	ZPS-III-43
34c	AWS-XIV-85 (Florence)	AWS-XIV-85 (Florence)	AWS-XIV-85
34d	ZPS-III-79 (Florence)	ZPS-III-79 (Florence)	ZPS-III-79
34e	ZPS-II-203 (Florence)	ZPS-II-203 (Florence)	ZPS-III-45
34f	AWS-XIV-127 (Florence)	AWS-XIV-127 (Florence)	AWS-XIV-127
34g	ZPS-II-193 (Indy)	ZPS-II-193 (Indy)	ZPS-II-193
34h	ZPS-II-129 (Florence)	ZPS-II-129 (Florence)	ZPS-II-129
34i	ZPS-IV-205 (Florence)	ZPS-IV-205 (Florence)	ZPS-IV-205
34j	ZPS-II-141 (Florence)	ZPS-II-141 (Florence)	ZPS-II-141
34k	ZPS-III-163 (Florence)	ZPS-III-163 (Florence)	ZPS-III-163
52	ZPS-V-109 (Florence)	ZPS-V-109 (Florence)	ZPS-V-109
53	ZPS-V-111 (Florence)	ZPS-V-111 (Florence)	ZPS-V-111

Table A9.3. Notebook cross-reference for Chapter 2.

compound	¹ H NMR (instrument)	¹³ C NMR (instrument)	yield/procedure
96	ZPS-II-229 (Florence)	ZPS-II-229 (Florence)	ZPS-II-229
97	ZPS-VIII-251 (Florence)	ZPS-VIII-251 (Florence)	ZPS-V-203
107	ZPS-IV-215 (Florence)	ZPS-IV-215 (Florence)	ZPS-IV-231
109	ZPS-IV-243 (Florence)	ZPS-IV-243 (Florence)	ZPS-IV-243
125	ZPS-VI-13 (Florence)	ZPS-VI-13 (Florence)	ZPS-VI-13
126	ZPS-IX-127 (Florence)	ZPS-IX-127 (Florence)	ZPS-VI-89
131	ZPS-VI-169 (Florence)	ZPS-VI-169 (Florence)	ZPS-VI-169
132	ZPS-VI-113 (Florence)	ZPS-VI-113 (Florence)	ZPS-VI-125
133	ZPS-VIII-59 (Florence)	ZPS-VIII-59 (Florence)	ZPS-VIII-59 (from 132: ZPS-VI-129)
134	ZPS-IX-65 (Florence)	ZPS-IX-65 (Florence)	HY-III-213
136	ZPS-VI-153 (Florence)	ZPS-VI-153 (Florence)	ZPS-VI-153
138	ZPS-VI-193 (Florence)	ZPS-VI-193 (Florence)	ZPS-VI-211
139	ZPS-VI-261 (Florence)	ZPS-VI-261 (Florence)	ZPS-VI-261
141	ZPS-IX-117 (Florence)	ZPS-IX-117 (Florence)	ZPS-IX-117
143	ZPS-IX-115 (Florence)	ZPS-IX-115 (Florence)	ZPS-VII-69A
149	ZPS-VII-93 (Florence)	ZPS-VII-93 (Florence)	ZPS-VII-93
150	ZPS-VII-129 (Florence)	ZPS-VII-129 (Florence)	ZPS-VII-129
153	ZPS-VII-141 (Florence)	ZPS-VII-141 (Florence)	ZPS-VII-141
154	HY-I-83 (Florence, zsercel folder)	HY-I-83 (Florence, zsercel folder)	ZPS-VII-155
155	HY-I-221 (Florence, zsercel folder)	HY-I-221 (Florence, zsercel folder)	HY-I-107 (from 156: HY-I-81)
156	ZPS-VII-193 (Florence)	ZPS-VII-193 (Florence)	ZPS-VII-193
157	ZPS-VII-197 (Florence)	ZPS-VII-197 (Florence)	HY-I-121
160	HY-I-111 (Florence, zsercel folder)	HY-I-111 (Florence, zsercel folder)	HY-I-111
168	HY-I-251 (Florence, zsercel folder)	HY-I-251 (Florence, zsercel folder)	HY-I-251
169	HY-I-163 (Florence, zsercel folder)	HY-I-163 (Florence, zsercel folder)	HY-I-163
214	ZPS-VIII-301 (Florence)	ZPS-VIII-301 (Florence)	ZPS-VIII-301
177	HY-II-10 (Florence)	HY-II-10 (Florence)	HY-II-25
179	ZPS-IX-125 (Florence)	ZPS-IX-125 (Florence)	HY-II-187
184	ZPS-VIII-185 (Florence)	ZPS-VIII-185 (Florence)	HY-I-239
187	ZPS-VIII-303 (Florence)	ZPS-VIII-303 (Florence)	ZPS-VIII-303

Table A9.4. Notebook cross-reference for Chapter 2 (continued).

compound	¹ H NMR (instrument)	¹³ C NMR (instrument)	yield/procedure
215	ZPS-IX-91 (Florence)	ZPS-IX-91 (Florence)	ZPS-VIII-209
189	ZPS-IX-123 (Florence)	ZPS-IX-123 (Florence)	ZPS-VIII-215
186	HY-III-281 (Florence)	HY-III-281 (Florence)	HY-III-303
190	ZPS-VIII-199 (Florence)	ZPS-VIII-199 (Florence)	ZPS-IX-111
185	HY-V-29 (Florence)	HY-V-29 (Florence)	ZPS-IX-131
192	HY-IV-61 (Florence)	SPR-VII-17 (Florence, zsercel folder)	SPR-VII-17
198	ZPS-IX-71 (Florence)	ZPS-IX-71 (Florence)	HY-IV-243
195	HY-IV-97 (Florence)	HY-IV-97 (Florence)	ZPS-IX-73
201	HY-IV-147 (Florence)	HY-IV-147 (Florence)	HY-IV-147
206	ZPS-IX-133 (Florence)	ZPS-IX-133 (Florence)	ZPS-IX-133
207	ZPS-IX-103 (Florence)	ZPS-IX-103 (Florence)	HY-IV-271

Table A9.5. Notebook cross-reference for Appendix 2.

compound	yield/procedure	NMR instrument
62	ZPS-II-163	Indy
63	ZPS-II-167	Indy
68	ZPS-II-95	Florence
72	AWS-XIV-33	Florence
76	ZPS-II-109	Florence

Table A9.6. Notebook cross-reference for Appendix 5.

compound	yield/procedure	NMR instrument
220	ZPS-V-69	Florence
222	ZPS-V-79	Florence
231	ZPS-IV-241	Florence
237	ZPS-VI-41	Florence
239	ZPS-VI-55	Indy
243	ZPS-VI-277	Florence
244	ZPS-VI-279	Florence
245	ZPS-VI-281	Florence
246	ZPS-VI-287	Florence
248	ZPS-VI-283	Florence
249	ZPS-VI-289	Florence
265	ZPS-VII-51	Florence
271	ZPS-VIII-43	Florence
283	ZPS-VIII-97	Florence
284	ZPS-VIII-115	Florence
287	ZPS-VIII-157	Florence

INDEX

A

Allyl Cyanofornate.....	6, 21, 47–49, 248, 251
Allylic Oxidation	278, 460–461
ANDEN	14
Aniline.....	19, 246, 257, 262–265, 267, 270–276, 281–283, 288–289, 293, 448–452, 463
Aza-Michael Addition	270–274, 276, 314–315, 454, 456

B

Barbier Addition	263, 271, 274–277, 456
Bartoli Indolization	260–261
Beckmann Rearrangement.....	16–17, 249
Benzodiazepine.....	5, 244–245
BINAP.....	266–303
BrettPhos	269, 310

C

CAN	293–294, 345
-----------	--------------

D

Desaturation	275–276, 278–280, 289–292, 455
Desulfurization	20–21
Dianiline.....	264–265, 450
Diazepane.....	5–6, 9–10
Diazonium	265–266, 451
Dieckmann Condensation	449

E

Enolate.....	1, 3–4, 6–7, 12–13, 21, 244–246, 258, 261–262, 274, 290–291, 298, 525
Epoxide.....	462–464, 479

Eschenmoser's Salt..... 17–18

F

Fischer Indolization 260–261, 264–267, 451

Fluoride 9, 33–34, 260, 526, 540

G

Grignard 274

Gewald Aminothiophene Synthesis 281–282, 285, 460–462

H

Hydrogenolysis..... 12

Hydrolysis..... 279, 281–282, 284–287, 291, 334, 461, 486

Hydroxyketone 262, 323, 447–448

I

Indium 282–283, 287, 329, 333–334, 448, 459

J

Julolidine 455–456

K

KHMDS 259

L

LDA 244–245, 251, 259, 297–298, 526, 530

LiAlH₄..... 10, 62–63

LiTMP 245, 251, 290

M

Methylcyclohexane 7–9, 25–26, 40, 43

Methylation	264, 266
Mitsunobu Reaction.....	268, 452, 470

N

NBS ..	274, 276, 283, 287, 294–295, 316, 319–320, 329–330, 335, 463–464, 478, 494, 525–526, 530, 534, 542
NHK Reaction.....	274
Nitration.....	451, 455
<i>N</i> -Methylarylhydrazine	267, 305
<i>N</i> - <i>t</i> -Butylbenzenesulfinimidoyl Chloride	276, 289

P

PIFA	289, 292, 340, 357, 487, 492
Pummerer Rearrangement.....	19, 291
Pyrroloiminoquinone	254–256, 263–265, 292–294, 302, 345

Q

Quinolone	262, 270–271, 313, 448–450, 453–456
-----------------	-------------------------------------

R

Raney Nickel	20–21
Reductive Amination	12, 281–283, 286, 293

S

Silane.....	288, 329–330, 341
Sulfide	255, 258–260, 447–450, 466

T

Tetrapyrane	488–492, 496–498
Thiolactone.....	280, 284–285, 287–294, 339–340, 342–343, 345, 460, 462
Titanium	270–272, 448–449
Triethylsilane	282–283, 287, 329–330
Ty-PHOX.....	7–8, 25

W

Wacker Oxidation 457–460

X

X-Ray 495, 509–523

ABOUT THE AUTHOR

Zachary Patrick Sercel was born to Stephanie Leifer and Pete Sercel in Pasadena, California, where he was raised together with his three younger siblings. He attended elementary school at Don Benito Fundamental School and was then homeschooled for 3 years. A book given to him by his grandmother when he was 10 years old inspired his passion for chemistry. After a few years of performing experiments in his parents' garage, Zachary was accepted to the Early Entrance Program at California State University, Los Angeles in 2013.

At Cal State LA, Zachary conducted research with Professor Matthias Selke in the area of singlet oxygen chemistry as a CSULA-Penn State NSF PREM fellow. He also spent two summers conducting research in organic synthesis in the laboratory of Professor Brian Stoltz at Caltech.

After completing his B.S. in chemistry in 2018, Zachary returned to the Stoltz lab to complete his graduate studies. As a Ph.D. student, Zachary has primarily focused on the development of palladium-catalyzed decarboxylative asymmetric allylic alkylation of medicinally relevant heterocycles and the total synthesis of the marine alkaloid aleutianamine. In his fourth year of graduate school, Zachary conducted a research internship in the laboratory of Professor Zeev Gross at the Technion, where he studied the synthesis of minimally substituted porphyrinoids and their metal complexes.

After completing his Ph.D., Zachary will travel back to Israel to conduct postdoctoral research at the Technion with Professor Ilan Marek as an Azrieli and Fulbright postdoctoral fellow.